HEAT EXCHANGER DESIGN HANDBOOK

3

Thermal and hydraulic design of heat exchangers

HEDH

HEAT EXCHANGER DESIGN HANDBOOK

3

Thermal and hydraulic design of heat exchangers

Contributors

Kenneth J. Bell
D. Chisholm
Anthony Cooper
A. R. Guy
A. C. Mueller
P. Paikert
J. W. Palen
W. R. Penney
D. Reay
E. U. Schlünder
J. R. Singham
R. A. Smith
J. Taborek
J. S. Truelove
J. Dennis Usher
R. L. Webb

EDITORIAL BOARD

Ernst U. Schliinder, Editor-in-Chief
Lehrstuhl und Institut für Thermische Verfahrenstechnik der Universitat Karlsruhe TH, D-7500 Karlsruhe 1, Kaiserstrasse 12, Postfach 6380, F.R. Germany

Kenneth J. Bell
School of Chemical Engineering, Oklahoma State University, Stillwater, Oklahoma 74078, U.S.A.

Duncan Chisholm
Department of Trade and Industry, National Engineering Laboratory, East Kilbride, Glasgow G75 OQU, Scotland

Geoffrey F. Hewitt
Engineering Sciences Division, Atomic Energy Research Establishment, Harwell OX1 10RA, U.K.

Frank W. Schmidt
Mechanical Engineering Department, Pennsylvania State University, University Park, Pennsylvania 16802, U.S.A.

D. Brian Spalding
Department of Mechanical Engineering, Imperial College of Science and Technology, Exhibition Road, London SW7 2BX, U.K.

Jerry Taborek
Heat Transfer Research, Inc., 1000 South Fremont Avenue, Alhambra, California 91802, U.S.A.

Algirdas Žukauskas
The Academy of Sciences of the Lithuanian SSR, MTP-1, Lenino pr. 3, 232600 Vilnius, U.S.S.R.

V. Gnielinski, Associate Editor
Lehrstuhl und Institut für Thermische Verfahrenstechnik der Universitat Karlsruhe TH, D-7500 Karlsruhe 1, Kaiserstrasse 12, Postfach 6380, F.R. Germany

PUBLISHED UNDER THE AUSPICES OF THE INTERNATIONAL CENTRE FOR HEAT AND MASS TRANSFER

HEDH CONTENTS

1 Heat exchanger theory

Contributors xiii
General Preface xv
Part 1 Preface xvii
Nomenclature xix
International System of Units (SI): Rules, Practices, and Conversion Charts, J. Taborek xxv

1.1 DESCRIPTION OF HEAT EXCHANGER TYPES

1.1.0 Structure of the Section, D. Brian Spalding
1.1.1 Types of Flow Configuration, D. Brian Spalding
1.1.2 Types of Interactions between Streams, D. Brian Spalding
1.1.3 Types of Temperature Change Pattern, D. Brian Spalding
1.1.4 Types of Interface between Streams, D. Brian Spalding
1.1.5 Types of Heat Exchange Equipment, D. Brian Spalding
1.1.6 Unsteady Operation, D. Brian Spalding

1.2 DEFINITIONS AND QUANTITATIVE RELATIONSHIPS FOR HEAT EXCHANGERS

1.2.0 Structure of the Section, D. Brian Spalding
1.2.1 Thermodynamics: Brief Notes on Important Concepts, D. Brian Spalding
1.2.2 Flux Relationships, D. Brian Spalding
1.2.3 Transfer Coeffkient Dependences, D. Brian Spalding
1.2.4 Balance Equations Applied to Complete Equipment, D. Brian Spalding
1.2.5 The Differential Equations Governing Streams, D. Brian Spalding
1.2.6 Partial Differential Equations for Interpenetrating Continua, D. Brian Spalding

1.3 ANALYTIC SOLUTIONS TO HEAT EXCHANGER EQUATIONS

1.3.1 Uniform-Transfer-Coefficient Solutions for the No-Phase-Change Heat Exchanger, D. Brian Spalding
1.3.2 Other Analytic Solutions, D. Brian Spalding

1.4 NUMERICAL SOLUTION PROCEDURES FOR HEAT EXCHANGER EQUATIONS

1.4.1 Cases with Prescribed Flow Patterns, D. Brian Spalding

Rev. 1986

1.4.2 **Cases in Which the Flow Patterns Must Be Calculated,** D. Brian Spalding
1.4.3 **Special Applications of Numerical Solution Procedures,** D. Brian Spalding

1.5 **CHARTS FOR MEAN TEMPERATURE DIFFERENCE IN INDUSTRIAL HEAT EXCHANGER CONFIGURATIONS**

1.5.1 **Introduction,** J. Taborek
1.5.2 ***F* and θ Charts for Shell-and-Tube Exchangers,** J. Taborek
1.5.3 ***F* and θ Charts for Cross-Flow Arrangements,** J. Taborek

1.6 **EFFECTIVENESS OF MULTIPASS SHELL-AND-TUBE HEAT EXCHANGERS WITH SEGMENTAL BAFFLES (CELL METHOD)**

1.6.1 **Introduction,** E. S. Gaddis
1.6.2 **Calculation Procedure,** E. S. Gaddis
1.6.3 **Numerical Examples,** E. S. Gaddis
1.6.4 **Rules for Highest Heat Exchanger Effectiveness,** E. S. Gaddis
1.6.5 **Special Case of Two Tube Passes,** E. S. Gaddis
1.6.6 **Heat Exchangers with Longitudinal Baffles,** E. S. Gaddis
1.6.7 **Cell Effectiveness,** E. S. Gaddis
1.6.8 **Comparison of the Conventional Method and the Cell Method,** E. S. Gaddis
1.6.9 **General Remarks,** E. S. Gaddis

Index I-l

2
Fluid mechanics and heat transfer

Contributors xiii
General Preface xv
Part 2 Preface xvii
Nomenclature xix
International System of Units (SI): Rules, Practices, and Conversion Charts, J. Taborek xxv

2.1 **FUNDAMENTALS OF HEAT AND MASS TRANSFER**

2.1.0 **Introduction,** E. U. Schltinder
2.1.1 **Physical Mechanisms of Transport Phenomena,** E. U. Schltinder
2.1.2 **Industrial Applications of Heat and Mass Transfer,** E. U. Schltinder
2.1.3 **Presentation of Heat and Mass Transfer Data,** E. U. Schltinder
2.1.4 **Heat and Mass Transfer in Uniform and Nonuniform Systems,** E. U. Schltinder
2.1.5 **Analogy between Heat and Mass Transfer and Its Limitations,** E. U. Schlünder
2.1.6 **Combined Heat and Mass Transfer,** E. U. Schlünder
2.1.7 **State of the Art of Heat and Mass Transfer,** E. U. Schlünder

2.2 **SINGLE-PHASE FLUID FLOW**

2.2.1 **Introduction and Fundamentals,** K. Gersten
2.2.2 **Ducts,** K. Gersten
2.2.3 **Immersed Bodies,** K. Gersten
2.2.4 **Banks of Plain and Finned Tubes,** A. Žukauskas and R. Ulinskas
2.2.5 **Fixed Beds,** P. J. Heggs
2.2.6 **Fluidized Beds, 0.** Molerus
2.2.7 **Headers, Nozzles, and Turnarounds,** J. A. R. Henry
2.2.8 **Non-Newtonian Fluids,** Robert C . Armstrong

2.3 **MULTIPHASE FLUID FLOW AND PRESSURE DROP**

2.3.1 **Introduction and Fundamentals,** G. F. Hewitt
2.3.2 **Gas-Liquid** Flow, G. F. Hewitt
2.3.3 **Solid-Gas Flow,** M. Weber and W. Stegmaier
2.3.4 **Solid-Liquid Flow,** M. Weber and W. Stegmaier

2.4 **HEAT CONDUCTION**

2.4.1 **Basic Equations,** H. Martin
2.4.2 **Steady State,** H. Martin
2.4.3 **Transient Response to a Step Change of Temperature,** H. Martin
2.4.4 **Melting and Solidification,** H. Martin
2.4.5 **Periodic Change of Temperature,** H. Martin
2.4.6 **Thermal Contact Resistance,** T. F. Irvine, Jr.

2.5 **SINGLE-PHASE CONVECTIVE HEAT TRANSFER**

2.5.1 **Forced Convection in Ducts,** V. Gnielinski

2.5.2 **Forced Convection around Immersed Bodies,** V. Gnielinski
2.5.3 **Banks of Plain and Finned Tubes**
A. Single Rows and Tube Banks in Cross Flow, V. Gnielinski
B. Finned Tubes, A. Žukauskas and A. Skrinska
2.5.4 **Fixed Beds,** V. Gnielinski
2.5.5 **Fluid-to-Particle Heat Transfer in Fluidized Beds,** S. S. Zabrodsky with revisions by H. Martin
2.5.6 **Impinging Jets,** H. Martin
2.5.7 **Free Convection around Immersed Bodies,** S. W. Churchill
2.5.8 **Free Convection in Layers and Enclosures,** S. W. Churchill
2.5.9 **Combined Free and Forced Convection around Immersed Bodies,** S. W. Churchill
2.5.10 **Combined Free and Forced Convection in Channels,** S. W. Churchill
2.5.11 **Augmentation of Heat Transfer,** Arthur E. Bergles
2.5.12 **Heat Transfer for Non-Newtonian Fluids,** Robert C. Armstrong and H. H. Winter
2.5.13 **Heat Transfer in Liquid Metals,** V. M. Borishanski and E. V. Firsova

2.6 **CONDENSATION**

2.6.1 **General Introduction,** D. Butterworth
2.6.2 **Film Condensation of Pure Vapor,** D . Butterworth
2.6.3 **Condensation of Vapor Mixtures,** D . Butterworth
2.6.4 **Condensation of Vapor Mixtures Forming Immiscible Liquids,** R. G. Sardesai
2.6.5 **Dropwise Condensation,** P. Griffith
2.6.6 **Augmentation of Condensation,** Arthur E. Bergles
2.6.7 **Fogging,** D. Chisholm
2.6.8 **Direct-Contact Condensers,** Harold R. Jacobs

2.7 **BOILING AND EVAPORATION**

2.7.1 **Boiling of Single Component Liquids: Basic Processes,** J. G. Collier
2.7.2 **Pool Boiling,** J. G. Collier
2.7.3 **Boiling within Vertical Tubes,** J. G. Collier
2.7.4 **Convective Boiling inside Horizontal Tubes,** J. G. Collier
2.7.5 **Boiling outside Tubes and Tube Bundles,** J. G. Collier
2.7.6 **Boiling of Binary and Multicomponent Mixtures: Basic Processes,** J. G. Collier
2.7.7 **Boiling of Binary and Multicomponent Mixtures: Pool Boiling,** J. G. Collier
2.7.8 **Boiling of Binary and Multicomponent Mixtures: Forced Convection Boiling,** J. G. Collier
2.7.9 **Augmentation of Boiling and Evaporation,** Arthur E. Bergles

2.8 **HEAT TRANSFER TO GAS-SOLID SYSTEMS**

2.8.1 **Stagnant Packed Beds,** R. Bauer
2.8.2 **Packed Beds with a Gas Flowing Through,** R. Bauer
2.8.3 **Packed and Agitated Packed Beds,** E. Muchowski
2.8.4 **Fluidized Beds,** J. S. M. Botterill

2.9 **HEAT TRANSFER BY RADIATION**

2.9.1 **Introduction,** D. K. Edwards
2.9.2 **Surface Radiation Characteristics,** D. K. Edwards
2.9.3 **Radiation Transfer between Perfectly Diffuse Surfaces,** D. K. Edwards
2.9.4 **Radiation Transfer between Specular and Imperfectly Diffuse Surfaces,** D. K. Edwards
2.9.5 **Gas Radiation Properties,** D. K. Edwards
2.9.6 **Radiation Transfer with an Isothermal** Gas, D. K. Edwards
2.9.7 **Nonisothermal Gas Radiation,** D. K. Edwards
2.9.8 **Radiation Acting with Conduction or Convection,** D. K. Edwards

Index I-1

3
Thermal and hydraulic design of heat exchangers

Contributors xiii
General Preface xv
Part 3 Preface xvii
Nomenclature xix
International System of Units (SI): Rules, Practices, and Conversion Charts, J. Taborek xxv

3.1 INTRODUCTION TO HEAT EXCHANGER DESIGN

3.1.1 Fundamental Concepts, Kenneth J. Bell
3.1.2 Types of Heat Exchangers and Their Applications, Kenneth J. Bell
3.1.3 Logic of the Design Process, Kenneth J. Bell
3.1.4 Approximate Sizing of Shell-and-Tube Heat Exchangers, Kenneth J. Bell

3.2 DOUBLE-PIPE HEAT EXCHANGERS

3.2.1 Introduction, A. R. Guy
3.2.2 Applications of Double-Pipe Heat Exchangers, A. R. Guy
3.2.3 Design Parameters, A. R. Guy
3.2.4 Types Available, A. R. Guy
3.2.5 Construction/Mechanical Design, A. R. Guy
3.2.6 Operational Advantages, A. R. Guy

3.3 SHELL-AND-TUBE HEAT EXCHANGERS: SINGLE-PHASE FLOW

3.3.1 Objectives and Background, J. Taborek
3.3.2 Survey of Shell-Side Flow Correlations, J. Taborek
3.3.3 Recommended Method: Principles and Limitations, J. Taborek
3.3.4 Practices of Shell-and-Tube Heat Exchanger Design, J. Taborek
3.3.5 Input Data and Recommended Practices, J. Taborek
3.3.6 Auxiliary Calculations, J. Taborek
3.3.7 Ideal Tube Bank Correlations for Heat Transfer and Pressure Drop, J. Taborek
3.3.8 Calculation of Shell-Side Heat Transfer Coefficient and Pressure Drop, J. Taborek
3.3.9 Performance Evaluation of a Geometrically Specified Exchanger, J. Taborek
3.3.10 Design Procedures for Segmentally Baffled Heat Exchangers, J. Taborek
3.3.11 Extension of the Method to Other Shell, Baffle, and Tube Bundle Geometries, J. Taborek

3.4 CONDENSERS

3.4.1 Introduction, A. C. Mueller
3.4.2 Selection of Condenser Types, A. C. Mueller
3.4.3 Discussion of Condenser Types, A. C. Mueller
3.4.4 Mixtures, A. C. Mueller
3.4.5 Operational Problems, A. C. Mueller
3.4.6 Heat Transfer, A. C. Mueller
3.4.7 Pressure Drop, A. C. Mueller
3.4.8 Mean Temperature Difference, A. C. Mueller
3.4.9 Design Procedure, A. C. Mueller

3.5 EVAPORATORS

3.5.1 Introduction, R. A. Smith
3.5.2 Types of Evaporators, R. A. Smith
3.5.3 Arrangements, R. A. Smith
3.5.4 Design Details, R. A. Smith
3.5.5 Choice of Type, R. A. Smith
3.5.6 Estimation of Pressure Drop and Circulation Rate, R. A. Smith
3.5.7 Estimation of Heat Transfer Coefficients, R. A. Smith
3.5.8 Estimation of Surface Area, R. A. Smith

3.6 SHELL-AND-TUBE REBOILERS

3.6.1 Introduction, J. W. Palen
3.6.2 Thermal Design, J. W. Palen
3.6.3 Pressure Drop, J. W. Palen
3.6.4 Special Design Considerations, J. W. Palen
3.6.5 Calculation Procedures, J. W. Palen

3.7 PLATE HEAT EXCHANGERS

3.7.1 Construction and Operation, Anthony Cooper and J. Dennis Usher
3.7.2 Factors Governing Plate Specification, Anthony Cooper and J. Dennis Usher
3.7.3 Corrugation Design, Anthony Cooper and J. Dennis Usher
3.7.4 Friction Factor Correlations, Anthony Cooper and J. Dennis Usher
3.7.5 Heat Transfer Correlations, Anthony Cooper and J. Dennis Usher
3.7.6 Factors Affecting Plate Design, Anthony Cooper and J. Dennis Usher
3.7.7 Overall Plate Design, Anthony Cooper and J. Dennis Usher
3.7.8 Plate Arrangement and Correction Factors, Anthony Cooper and J. Dennis Usher
3.7.9 Fouling, Anthony Cooper and J. Dennis Usher
3.7.10 Methods of Surface Area Calculation, Anthony Cooper and J. Dennis Usher
3.7.11 Thermal Mixing, Anthony Cooper and J. Dennis Usher
3.7.12 Two-Phase Flow Applications, Anthony Cooper and J. Dennis Usher

3.8 AIR-COOLED HEAT EXCHANGERS

3.8.1 **Air as Coolant for Industrial Processes: Comparison to Water,** P. Paikert
3.8.2 **Custom-Built Units,** P. Paikert
3.8.3 **Fin-Tube Systems for Air Coolers,** P. Paikert
3.8.4 **Fin-Tube Bundles,** P. Paikert
3.8.5 **Thermal Rating,** P. Paikert
3.8.6 **Tube-Side Flow Arrangements,** P. Paikert
3.8.7 **Cooling Air Supply by Fans,** P. Paikert
3.8.8 **Cooling Air Supply in Natural Draft Towers,** P. Paikert
3.8.9 **Special Features of Air Coolers,** P. Paikert

3.9 COMPACT HEAT EXCHANGERS

3.9.1 **Introduction,** R. L. Webb
3.9.2 **Definition of Geometric Terms,** R. L. Webb
3.9.3 **Plate Fin Surface Geometries,** R. L. Webb
3.9.4 **Surface Performance Data,** R. L. Webb
3.9.5 **Laminar Flow Surfaces,** R. L. Webb
3.9.6 **Correlation of Heat Transfer and Friction Data,** R. L. Webb
3.9.7 **Goodness Factor Comparisons,** R. L. Webb
3.9.8 **Specification of Rating and Sizing Problems,** R. L. Webb
3.9.9 **Calculation Procedure for a Rating Problem,** R. L. Webb
3.9.10 **Pressure Drop Calculation,** R. L. Webb
3.9.11 **Procedures for the Thermal Sizing Problem,** R. L. Webb
3.9.12 **Multifluid Service,** R. L. Webb
3.9.13 **Recent Theory and Data on Vaporization and Condensation,** R. L. Webb

3.10 HEAT PIPES

3.10.1 **Introduction,** D. Chisholm
3.10.2 **Circulation and Axial Heat Transfer,** D. Chisholm
3.10.3 **Temperature Distributions and Radial Heat Transfer** Flux, D. Chisholm
3.10.4 **Axial Heat Transfer and the Operational Envelope,** D. Chisholm
3.10.5 **Selection of Working Fluid,** D. Chisholm
3.10.6 **Characteristics of Wicks,** D. Chisholm
3.10.7 **Start-up and Control,** D. Chisholm

3.11 FURNACES AND COMBUSTION CHAMBERS

3.11.1 **Introduction,** J. S. Truelove
3.11.2 **Process Heaters and Boilers,** J. S. Truelove
3.11.3 **Heat Transfer in Furnaces,** J. S. Truelove
3.11.4 **The Stirred-Reactor Furnace Model,** J. S. Truelove
3.11.5 **The Plug-Flow Furnace Model,** J. S. Truelove
3.11.6 **The Multizone Furnace Model,** J. S. Truelove
3.11.7 **Advanced Furnace Models,** J. S. Truelove

3.12 COOLING TOWERS

3.12.1 **Introduction,** J. R. Singham
3.12.2 **The Packing Region,** J. R. Singham
3.12.3 **Natural Draft Towers,** J. R. Singham
3.12.4 **Mechanical Draft Towers,** J. R. Singham
3.12.5 **Hybrid Towers,** J. R. Singham
3.12.6 **Further Topics,** J. R. Singham

3.13 DRYERS

3.13.1 **Introduction,** E. U. Schliinder
3.13.2 **Classification and Selection,** E. U. Schliinder
3.13.3 **Layout and Performance Data,** E. U. Schlünder
3.13.4 **Prediction of Drying Rates,** E. U. Schliinder
3.13.5 **Prediction of Residence Times with Prescribed Material Flow,** E. U. Schliinder
3.13.6 **Prediction of Residence Times with Nonprescribed Material Flow,** E. U. Schlünder
3.13.7 **Practical Dryer Design,** D. Reay

3.14 AGITATED VESSELS

3.14.1 **Introduction,** W. R. Penney
3.14.2 **Equipment,** W. R. Penney
3.14.3 **Heat Transfer Correlations,** W. R. Penney

3.15 REGENERATION AND THERMAL ENERGY STORAGE

3.15.0 **Introduction,** F. W. Schmidt
3.15.1 **Operation of Regenerators,** A. J. Willmott
3.15.2 **Construction of Regenerator Packing,** A. J. Willmott
3.15.3 **Internal Behavior of a Regenerator: Development of the Mathematical Model,** A. J. Willmott
3.15.4 **Heat Transfer Coefficient,** A. J. Willmott
3.15.5 **Use of Bulk or Overall Heat Transfer Coefficient,** A. J. Willmott
3.15.6 **Development of Dimensionless Parameters,** A. J. Willmott
3.15.7 **Calculation of Regenerator Thermal Performance,** A. J. Willmott

3.15.8 Effect of Longitudinal Conduction in the Packing of the Regenerator, A. J. Willmott
3.159 Dealing with Heat Losses, A. J. Willmott
3.15.10 Transient Characteristics of Regenerators, A. J. Willmott
3.1511 Explicit Design of Balanced Regenerators, B. Kulakowski
3.1512 Single-Blow Operation, F. W. Schmidt

3.16 WASTE HEAT BOILER SYSTEMS

3.16.1 Description of Typical System, P. Hinchley
3.16.2 Key Aspects of the Design and Specification of Individual Items of Plant, P. Hinchley
3.16.3 Detailed Mechanical Design and Fabrication of Equipment, P. Hinchley
3.16.4 Precommissioning of Waste Heat Boiler Systems, P. Hinchley

3.17 FOULING IN HEAT EXCHANGERS

3.17.1 Overview and Summary, James G. Knudsen
3.17.2 Types of Fouling, James G. Knudsen
3.17.3 Analysis of the Fouling Process, James G. Knudsen
3.17.4 Fouling Control Measures, James G. Knudsen
3.175 Cleaning of Heat Exchangers, James G. Knudsen
3.17.6 Measurement of Fouling Resistances, James G. Knudsen
3.17.7 Recommended Fouling Resistances for Design, James G. Knudsen

Index I-l

4
Mechanical design of heat exchangers

Contributors xiii
General Preface xv
Part 4 Preface xvii
Nomenclature xix
International System of Units (SI): Rules, Practices, and Conversion Charts, J. Taborek xxv

4.1 BASIC MECHANICAL PRINCIPLES

4.1.1 Introduction, C . Ruiz
4.1.2 Methods of Analysis, C. Ruiz
4.1.3 Shells, C. Ruiz
4.1.4 Tube Plates, C. Ruiz
4.1.5 Tubes, C. Ruiz
4.1.6 Expansion Joints, C. Ruiz
4.1.7 Flanges, C. Ruiz
4.1.8 Heads, Openings, and Branches, C. Ruiz

4.2 SHELL-AND-TUBE HEAT EXCHANGERS: ELEMENTS OF CONSTRUCTION

4.2.1 Introduction, E. A. D. Saunders
4.2.2 Design and Construction Codes, E. A. D. Saunders
4.2.3 Types of Shell-and-Tube Heat Exchangers, E. A. D. Saunders
4.2.4 Head Types, E. A. D. Saunders
4.2.5 Features Related to Thermal Design, E. A. D. Saunders
4.2.6 Features Relating to Mechanical Design and Fabrication, E. A. D. Saunders

4.3 SHELL-AND-TUBE HEAT EXCHANGERS: REVIEW OF MECHANICAL DESIGN CODES

4.3.1 Mechanical Design Codes, M. Morris
4.3.2 Index to U.S., U.K., and F.R.G. Codes, M. Morris
4.3.3 Analytic Basis of Code Rules, M. Morris
4.3.4 Comparison of Principal Codes, M. Morris
4.3.5 Guides to National Practice, M. Morris
4.3.6 Design Example: Floating-Head Heat Exchanger, TEMA Type AJS, D. Harris

4.4 MECHANICAL DESIGN: GENERAL FORMS OF HEAT EXCHANGERS

4.4.1 Mechanical Design of Air-Cooled Heat Exchangers, K. V. Shipes
4.4.2 Mechanical Design of Plate Heat Exchangers, J. Dennis Usher
4.4.3 Plate Fin Heat Exchangers, R. L. Webb
4.4.4 Other Types of Heat Exchangers, I. Murray

4.5 MATERIALS OF CONSTRUCTION AND CORROSION

4.5.1 Introduction, J . F. Lancaster
4.5.2 Materials of Construction, J. F. Lancaster
4.5.3 Corrosion and Other Types of Damage, J. J. Lancaster

4.6 FLOW-INDUCED VIBRATION

4.6.1 Introduction, J. M. Chenoweth

4.6.2 **Tube Bundle Vibration Characteristics,** J. M. Chenoweth
4.6.3 **Shell-Side Velocities in Shell-and-Tube Exchangers,** J. M. Chenoweth
4.6.4 **Flow-induced Vibration Phenomena, J . M .** Chenoweth
4.6.5 **Procedure for Vibration Predictions,** J. M. Chenoweth
4.6.6 **Design Considerations,** J. M. Chenoweth

4.7 TESTING AND INSPECTION

4.7.1 **Objectives of Inspection, Testing, and Drawing Approval,** A. Illingworth
4.7.2 **Materials,** A. Illingworth
4.7.3 **Welding,** A. Illingworth
4.7.4 **Stages of Inspection,** A. Illingworth
4.7.5 **Construction,** A. Illingworth
4.7.6 **Nondestructive Testing,** A. Illingworth
4.7.7 **Certification,** A. Illingworth
4.7.8 **Fittings,** A. Illingworth
4.7.9 **Cleanliness and Storage,** A. Illingworth
4.7.10 **Preparation and Dispatch,** A. Illingworth
4.7.11 **Quality Control and Inspection Disciplines,** R. S. M. Moffatt

4.8 COSTING OF SHELL-AND-TUBE HEAT EXCHANGERS

4.8.1 **Introduction,** D. Chisholm
4.8.2 **Costing of Shell-and-Tube Heat Exchangers,** R. C. Cowie
4.8.3 **Costing of Air Coolers, C.** North
4.8.4 **Costing of Plate Heat Exchangers,** J. Dennis Usher

4.9 SPECIFICATIONS AND TENDERS

4.9.1 **Introduction,** D. Edge
4.9.2 **Specifications, D. Edge**
4.9.3 **Tenders, D. Edge**

4.10 EXPANSION BELLOWS

4.10.1 **Introduction,** M. Morris
4.10.2 **Expansion Bellows,** M. Morris

Index I-l

5 Physical properties

Contributors xiii
General Preface xv
Part 5 Preface xvii
Nomenclature xix
International System of Units (SI): Rules, Practices, and Conversion Charts, J. Taborek xxv

5.1 PROPERTIES OF PURE FLUIDS

5.1.0 **Introduction,** M. Schunck
5.1.1 **Critical Data,** M. Schunck
5.1.2 **Specific Volume, p-$\tilde{V}$-T Correlations,** M. Schunck
5.1.3 **Thermodynamic Properties,** M. Schunck
5.1.4 **Transport Properties,** M. Schunck
5.1.5 **Surface Tension,** M. Schunck

5.2 PROPERTIES OF MIXTURES OF FLUIDS

5.2.1 **Phase Behavior of Mixtures,** R. N. Maddox
5.2.2 **Thermodynamic Properties,** R. N. Maddox
5.2.3 **Thermophysical Properties,** R. N. Maddox
5.2.4 **Interfacial Tension,** R. N. Maddox
5.2.5 **Diffuse Coeffkients,** R. N. Maddox

5.3 PROPERTIES OF RHEOLOGICALLY COMPLEX MEDIA

5.3.1 **Disperse Compositions,** Z. P. Shulman
5.3.2 **Classification of Lubricants,** Z. P. Shulman
5.3.3 **Oils,** Z. P. Shulman
5.3.4 **Plastic Lubricants,** Z. P. Shulman
5.3.5 **Lubricant-Cooling Liquids,** Z. P. Shulman
5.3.6 **Polymers,** Z. P. Shulman
5.3.7 **Oriented Polymers,** Z. P. Shulman
5.3.8 **Effect of External Electric and Magnetic Fields,** Z. P. Shulman

5.4 PROPERTIES OF SOLIDS

5.4.0 **Introduction,** M . Schunck
5.4.1 **Density of Solids,** M. Schunck
5.4.2 **Specific Heat of Solids,** M. Schunck
5.4.3 **Thermal Conductivity of Solids,** M. Schunck
5.4.4 **Emissivity of Solids,** M. Schunck
5.4.5 **Elastic Properties, S.** F. Pugh

5.5 PHYSICAL PROPERTY DATA TABLES

5.5.0 **Index to Compounds and Properties by Section,** Clive F. Beaton
5.5.1 **Properties of Saturated Fluids,** R. N. Maddox

5.5.2 Properties of Superheated Gases, R. N. Maddox
5.5.3 Steam Tables, Clive F. Beaton
5.5.4 Constants for Binary Mixtures, R. N. Maddox
5.5.5 Emissivity Data for Gases, D. K. Edwards and Robert Matavosian
5.5.6 Thermal Conductivity of Solids, P. E. Liley
5.5.7 Emissivity of Solids, P. E. Liley
5.5.8 Elastic Properties of Solids, S. F. Pugh
5.5.9 Properties of Liquid Heavy Water, G. Ulrych
5.5.10 Physical Properties of Liquids at Temperatures below Their Boiling Point, Clive F. Beaton
5.5.11 Transport Properties of Superheated Gases, G. F. Hewitt
5.5.12 Thermal and Mechanical Properties of Heat Exchanger Construction Materials, Clive F. Beaton
5.5.13 Properties of Seawater, Clive F. Beaton

Index I-1

HEAT EXCHANGER DESIGN HANDBOOK

3

Thermal and hydraulic design of heat exchangers

VDI-Verlag GmbH
Verlag des Vereins Deutscher Ingenieure • Düsseldorf
0 Hemisphere Publishing Corporation Washington New York London

Heat Exchanger Design Handbook

Copyright © 1983 by Hemisphere Publishing Corporation. All rights reserved. Printed in the United States of America. Except as permitted under the United States Copyright Act of 1976, no part of this publication may be reproduced or distributed in any form or by any means, or stored in a data base or retrieval system, without the prior permission of the publisher.

1 2 3 4 5 6 7 8 9 0 BCBC 8 9 8 7 6 5 4 3 2

This book was set in Press Roman by Hemisphere Publishing Corporation.
Editors: Brenda Munz Brienza, Judith B. Candy, and Lynne Lackenbach.
Production supervisor: Miriam Gonzalez.
Compositors: Peggy M. Rote, Sandra F. Watts, Shirley J. McNett, and Wayne Hutchins.
BookCrafters, Inc., was printer and binder.

Distribution outside the U.S.A., Canada, Mexico, U.K., and Ireland, by VDI-Verlag, Düsseldorf.

The publisher, editors, and authors have maintained the highest possible level of scientific and technical scholarship and accuracy in this work, which is not intended to supplant professional engineering design or related technical services, and/or industrial or international codes and standards of any kind. The publisher, editors, and authors assume no liability for the application of data, specifications, standards or codes published herein.

Library of Congress Cataloging in Publication Data

Main entry under title:

Thermal and hydraulic design of heat exchangers.

(Heat exchanger design handbook ; 3)
Kept up to date by supplements.
Includes index.
1. Heat exchangers-Design and construction. I. Bell, Kenneth J. II. Series.
TJ263.H38 1983 vol. 3 621.402 5s 82-9263
ISBN 3-18-41-9083-8 (VDI Part 3) [621.402'5] AACR2
ISBN 3-18-41-9080-3 (VDI set)
ISBN O-89116-125-2 (Hemisphere set)

3 Contributors

Kenneth J. Bell
School of Chemical Engineering, Oklahoma State University, Stillwater, Oklahoma 74078 U.S.A.

D. Chisholm
Department of Trade and Industry, National Engineering Laboratory, East Kilbride, Glasgow G75 OQU Scotland

Anthony Cooper
APV Company, Inc., 395 Filmore Avenue, Tonawanda, New York 14150 U.S.A.

A. R. Guy
Filtration & Transfer Ltd., Dawkins Road, Hamworthy, Pool, Dorset BH 15 4JP U.K.

A. C. Mueller
Rt. 1 Box 53J, Kennersley, Church Hill, Maryland 21623 U.S.A.

P. Paikert
GEA-Luftkiihlergesellschaft, Werk Bochum-Riemke, Rensinstrasse 11, D-4630 Bochum F.R. Germany

J. W. **Palen**
Heat Transfer Research, Inc., 1000 South Fremont Avenue, Alhambra, California 91802 U.S.A.

W. R. Penney
Monsanto Company, 800 South Lindbergh, St. Louis, Missouri 63 166 U.S.A.

D. Reay
Separation Processes Service, Bldg. 351.28, Atomic Energy Research Establishment, Harwell, Oxfordshire OX1 10RA U.K.

E. U. **Schlünder**
Lehrstuhl und Institut fur Thermische Verfahrenstechnik der Universitat Karlsruhe TH, Kaiserstrasse 12, Postfach 6380, D-7500 Karlsruhe 1 F.R. Germany

J. R. **Singham**
Department of Mechanical Engineering, Imperial College of Science and Technology, Exhibition Road, London SW7 2BX U.K.

R. A. Smith
20 Stanhope Grove, Acklam, Middlesborough TS5 7S9 U.K.

J. Taborek
Heat Transfer Research, Inc., 1000 South Fremont Avenue, Alhambra, California 9 1802 U.S.A.

J. S. **Truelove**
Department of Chemical Engineering, University of Newcastle, New South Wales 2308 Australia

J . Dennis Usher
15, Hillfield Close, Redhill, Surrey RH1 4AR U.K.

R. L. Webb
Department of Mechanical Engineering, Pennsylvania State University, University Park, Pennsylvania 16802 U.S.A.

HEDH
GENERAL PREFACE

Ernst U. Schliinder

■ The idea to create a Heat Exchanger Design Handbook originated at the seminar Recent Developments in Heat Exchangers, organized by the International Centre for Heat and Mass Transfer (ICHMT) in Trogir, Yugoslavia in 1972.

Even though much heat transfer data and correlations were available, this information was scattered throughout the open literature or buried in the files of proprietary organizations. For manufacturers, vendors, and users of heat transfer equipment it was becoming more and more difficult not only to keep up with the continually growing heat transfer information but also to compare data and correlations from various sources. In addition, these sources were often inconsistent, and it was difficult for users to decide which data and correlations would serve their own purposes best. Moreover, over the years many heat transfer publications had become more analytical and more academic, which delayed their immediate application by practicing heat transfer engineers.

Because of this situation, a group of heat transfer specialists decided to collect heat transfer information available in the existing open literature and also-as far as possible-from proprietary sources in order to create a heat transfer information base. Recommended correlations based on selected experimental material would then be provided for all heat exchanger design data.

Although there was great enthusiasm for this project, not much progress was made until 1974, at the Fifth International Heat Transfer Conference in Tokyo. The idea was formulated then of publishing the information base under the auspices of the ICHMT by Hemisphere Publishing Corporation, the publisher of the Centre. Eight representatives of universities, industry, and proprietary organizations formed the Editorial Board, which immediately started working on the scope and organization of this Handbook. As a result of these joint efforts the following five parts were planned:

Part 1 presents the theory of heat exchangers defining and explaining all parameters and concepts needed for thermal and hydraulic design and rating.

Part 2 contains recommended correlations for design and rating parameters based on evaluated available information. As far as possible experimental data are presented together with the recommended correlations in order to reveal both the consistency of the data as well as the reliability of the correlations.

Part 3 shows how to apply the material given in Parts 1 and 2 when solving actual heat exchanger design and rating problems. Because of the volume of material, it would be impossible for this part to cover all known kinds of heat exchangers. Nevertheless, most of the comtnonly used types of equipment are discussed in detail together with related installations such as cooling towers and combustion chambers.

Part 4 is devoted to the mechanical design of heat exchangers, which actually cannot be separated from thermal and hydraulic design. A useful comparison of some major national standards is included.

Part 5 contains physical property data that are needed in design calculations in the other four parts.

For each of the five parts, a member of the Editorial Board agreed to act as Lead Editor. Although each Lead Editor accepted additional administrative responsibility for his particular part, the whole Handbook has been a

cooperative effort with each editor sharing the reviewing and editorial work for all the material.

A large number of authors-well-known experts in their fields-have contributed to this Handbook. Each manuscript went through a review procedure and many of them were discussed during the regular meetings of the Editorial Board, which have been held every six months since 1975.

Nevertheless, this Handbook must be considered as a first step rather than as a final result. Though the concept was clear, the realization has not been easy and there is still room for improvement. Additionally, because new heat transfer data and correlations are published each year, a permanent updating procedure has been established to keep this Handbook current. This supplementary material will be offered regularly to the subscribers. To ensure that any future material (including personal remarks and comments) can be added easily, a loose-leaf ring binder format was chosen for the Handbook.

The users of this Handbook are urged to communicate with us about what is missing and to make suggestions for improving the contents of the book and its applicability. This kind of interaction and cooperation between users and editors not only should improve the quality of the Handbook but also should stimulate further research work guided by the requirements of heat exchanger design.

The Editorial Board wishes to thank the publisher as well as the contributing authors for their most valuable cooperation.

3 Preface

Kenneth J. Bell

■ The wide range of heat transfer services that are required in the energy, process, environmental control, and transport industries has called forth an equally wide variety of heat exchanger configurations to meet the requirements. These designs are the engineers responses to the special needs of each case, hopefully giving an optimum combination of effective performance, easy operability, and minimum capital and operational cost. All of the fluid flow and heat transfer processes discussed in Part 2 of this Handbook are encountered in one or another of the heat exchanger types and/or services included in this Part. However, now the emphasis must be upon the effect of the various construction features on the thermal-hydraulic behavior and on the thermal coupling of the two streams across a boundary.

While each of the sections has its own structure as selected by the author to best convey practical design information, most of them include the following features:

1. A description of the mechanical features of the equipment that directly impact the thermal-hydraulic performance. (A more complete description of the major types, with emphasis upon the mechanical design requirements, is given in Part 4 of this Handbook.)
2. The effect of these features upon the basic correlations presented in Part 2, generally resulting in modified correlations.
3. The integration of these correlations into a design procedure for heat transfer coefficient and pressure drop for each stream. The coefficients are combined with wall and fouling resistance terms to give an overall heat transfer coefficient and a required area or volume of the heat exchanger.
4. Special considerations in the application of the exchanger type and in the selection of design and operating parameters.

Section 3.1 presents a few of the more basic design equations, including the mean temperature difference formulation, followed by criteria for heat exchanger selection and design. The logical structure of the heat exchanger design process is described for both hand and computer methods, and an approximate design estimation procedure is given for shell-and-tube heat exchangers.

Double pipe heat exchangers are treated in Sec. 3.2, and a comprehensive description and design procedure for shell-and-tube exchangers in single phase heat transfer service (on the shell side) in Sec. 3.3.

Section 3.4 covers condenser application and design with particular reference to the shell-and-tube configuration. However, several of the procedures discussed are also applicable to other geometries.

Vapor generation equipment, basically of the shell-and-tube type, is the topic of Secs. 3.5 and 3.6. The first emphasizes evaporators and product concentrators, while the second is primarily concerned with vapor generation for the process industry.

Section 3.7 surveys plate heat exchangers, of growing interest because of their compactness and light weight. Section 3.8 deals with air-cooled heat exchangers for cooling and condensing applications, increasingly important as suitable cooling water supplies dwindle and air is used as the ultimate heat rejection sink.

Compact, or matrix, or plate fin heat exchangers are the subject of Sec. 3.9, with emphasis upon both gas-to-gas and cryogenic processing applications. Section 3.10 describes the heat pipe, a rather recent development whose full range of application has not yet been defined; a particular feature of this section is the extensive bibliography.

Furnaces, and combustion processes generally, are treated in Sec. 3.11. Cooling towers (the heat rejection solution when there is some, but not a lot of, water) are the subject of Sec. 3.12.

Section 3.13 deals with all kinds of dryers on both practical selection and analytical performance evaluation bases. And mechanically aided heat transfer equipment-often the only solution to a heat transfer problem-is described and working design correlations presented in Sec. 3.14.

The above-listed coverage, extensive as it is, does not by any means exhaust the possibilities and indeed actualities of heat transfer equipment in practice. Active efforts are under way to incorporate new sections covering these neglected areas into subsequent versions of the Handbook.

It is appropriate to close this preface with a cautionary note: The design procedures presented here are, in the opinion of each author, the best available in the open literature and within the capability of hand computation. For many-perhaps most-of these situations, better (in the sense of more accurate) design methods exist, but they are generally both proprietary and computer-based. If the absolute accuracy of the predicted result is of great importance to the user, these methods should be sought out at whatever cost. (And the user should be prepared to be disappointed, because often even the best methods have a high degree of uncertainty in the result.) But the methods presented here should be adequate for the large majority of actual cases. In the final analysis, it is mostly the understanding and attention of the user that influences the validity of the result.

NOMENCLATURE

■ The most frequently used symbols for quantities in heat and mass transfer are listed here according to the following principles:

1. Capital Roman letters (not italic) denote absolute quantities expressed in either SI basic units or derived units, e.g., N = kg m/s^2, J = N m, W = J/s.

Exceptions: Time (t), variables, coordinates (x, y, z, r), characteristic lengths in dimensionless numbers (l, d, s).

2. Lowercase Roman letters (not italic) denote the corresponding specific quantities per unit mass, mole, length, area, or volume (but not time). A dot over the symbol denotes an absolute or specific quantity per unit time.

Exception: Velocity (u, v, w).

A function will be indicated by $(\cdots)$.

Molar quantities are denoted by a tilde ($\sim$) over the symbol.

Exceptions: Gas constant ($\tilde{R}$), Loschmidt number ($\tilde{L}$), molecular weight ($\tilde{M}$), chemical potential (μ).

3. Lowercase Greek letters are used for coefficients and physical properties.

Exceptions: Overall heat transfer coefficient (U), heat capacity (c_p, c,).

Capital Greek letters refer to eddy (turbulent) quantities; e.g., A denotes eddy thermal conductivity.

4. Dimensionless variables should be denoted by a superscript $^+$ following the corresponding symbol. e.g., y^+ for a dimensionless coordinate.

5. Decimal fractions or multiples of the SI units may be denoted by the corresponding symbol preceding the SI unit, e.g. MW $=10^6$ W.

© 1983 Hemisphere Publishing Corporation

Basic Quantities

Ouantitv	Symbol	Unit
Heat rate	$\dot{Q}$	W
Heat quantity	$Q = \int \dot{Q}\, dt$	J
Heat flux	$\dot{q} = \dot{Q}/A$	W/m^2
Time	t	s
Frequency	f	1/s
Mass	M	kg
Mass flow rate	$\dot{M}$	kg/s
Mass velocity (mass flow per unit area)	$\dot{m} = \dot{M}/S$	kg/m^2 s
Mass flux	$\dot{m}_n = \dot{M}_n/A$	kg/m^2 s
Number of moles	N	mol
Molar mass flow rate	$\dot{N}$	mol/s
Molar mass velocity	$\dot{n} = \dot{N}/S$	mol/m^2 s
Molecular weight	$\widetilde{M}$	g/mol
Density	ρ	kg/m^3
Concentration	c	kg/m^3
Molar density	$\tilde{\rho}$	mol/m^3
Molar concentration	$\tilde{c}$	mol/m^3
Mass fraction	x_i, Y_i	kg$_i$/kg
Mass loading	X_i, Y_i	kg$_i$/kg$_j$
Molar mass fraction	$\tilde{x}_i, \tilde{y}_i$	mol$_i$/mol
Molar. mass loading	$\widetilde{X}_i, \widetilde{Y}_i$	mol$_i$/mol$_j$
Volume	V	m^3
Volume flow rate	$\dot{V}$	m^3/s
Velocity	u, v, w	m/s
Surface area	A	m^2
Cross-sectional area	S	m^2
Length or diameter	L, D, l, d, s	m
Coordinate	$\psi, \varphi, r, x, y, z$	
Void fraction	ϵ	–
Fraction of volume flow rate	$\dot{\epsilon}$	–
Quality	x	–
Flow quality	$\dot{x}$	–
Work	W	J

© 1983 Hemisphere Publishing Corporation

Transport coefficients

Quantity	Symbol	Unit
Heat transfer coefficient	α	$W/m^2 K$
Mass transfer coefficient	β	m/s
Overall heat transfer coefficient	U	$W/m^2 K$
Drag coefficient	ξ	
Friction factor	f	
Emissivity	ϵ	
View factor	φ_{12}	—
Thermal conductivity	λ	W/m K
Diffusivity	δ	m^2/s
Kinematic viscosity	ν	m^2/s
Dynamic (absolute) viscosity	η	kg/m s
Thermal diffusivity	$\kappa \equiv \lambda/\rho c_p$	m^2/s
Surface tension	σ	N/m
Shear stress	τ	Pa (N/m^2)
Pressure	p	Pa (N/m^2)
Pressure drop	Δp	Pa (N/m^2)

Thermodynamic quantities

Quantity	Symbol*	Unit
Enthalpy (specific)	h	J/kg
Internal energy (specific)	u	J/kg
Gibbs function free enthalpy (specific)	$g = h - T s$	J/kg
Free energy (specific)	$f = u - T s$	J/kg
Entropy (specific)	s	J/kg K
Chemical potential	μ	J/kg
Specific heat capacity	c_p, c_v	J/kg K
Temperature	T	K, °C
Mean logarithmic temperature difference	ΔT_{LM}	K, °C

*For totals, letters are capitalized, H, U.

© 1983 Hemisphere Publishing Corporation

Chemical reactions

Quantity	Symbol	unit
Reaction enthalpy; phase-change enthalpy; latent heat	Ah	J/kg
Energy of activation	AE	J/kg
Equilibrium constant	K	Various
Rate constant	k	Various
Rate of reaction	$\dot{r}$	mol/m³ s
Activity coefficient	γ_l	—
Fugacity coefficient	γ_g	—
Stoichiometric factors	ν_i	—

Physical constants

Quantity	Symbol	Unit
Gas constant	$\tilde{R}$	8.3 14 J/mol K
Loschmidt number	$\tilde{L}$	$6.0252 \cdot 10^{23}$
Avogadro number	$\tilde{L}$	1/mol
Stefan-Boltzmann constant	C_s	$5.6697 \cdot 10^{-8}$ W/m² K⁴
Acceleration of gravity	g	m/s²
Standard acceleration of gravity	$g_n = 9.8 \ldots$	m/s²

Subscripts

Quantity	Symbol
Wall	w
Bulk	b
Mean	m
Solid	s
Liquid	ℓ
Gas	g
Inlet	in
Outlet	out

© 1983 Hemisphere Publishing Corporation

Dimensionless numbers (most frequently used)

Name	Symbol and definition
Archimedes number	$Ar = gl^3\Delta\rho/\nu^2\rho = gl^3\rho\Delta\rho/\eta^2$
Biot number	$Bi = \alpha_g l/\lambda_s$ or $\alpha_l l/\lambda_s$
Effectiveness	E
Euler number	$Eu = \Delta p/(\rho u^2/2)$
Fourier number	$Fo = \kappa t/l^2 = \lambda t/\rho c_p l^2$
Froude number	$Fr = u^2/gl$
Galileo number	$Ga = l^3 g/\nu^2 = l^3 g\rho^2/\eta^2$
Grashof number	$Gr = gl^3\Delta\rho/\nu^2\rho = gl^3\rho\Delta\rho/\eta^2$
Graetz number	$Gz = ud^2/\kappa l = ud^2\rho c_p/\lambda l = Re\ Pr\ d/l$
Knudsen number	$Kn = l_0/l$, where l_0 is the molecular mean free path
Lewis number	$Le = \kappa/\delta = \lambda/\rho c_p\delta$
Mach number	$Ma = u/u_{sound}$
Number of transfer units	NTU
Nusselt number	$Nu = \alpha l/\lambda$
Péclet number	$Pe = ul/\kappa = ul\rho c_p/\lambda = Re\ Pr$
Phase change number	$Ph = c_p\Delta T/\Delta h_{gl}$
Prandtl number	$Pr = \nu/\kappa = \eta c_p/\lambda$
Rayleigh number	Ra = Gr Pr
Reynolds number	$Re = ul/\nu = ul\rho/\eta = \dot{m}l/\eta$
Schmidt number	$Sc = \nu/\delta = \eta/\rho\delta$
Sherwood number	$Sh = \beta l/\delta$
Stanton number	$St = \alpha/\rho u c_p = Nu/Re\ Pr$
Strouhal number	$Sr = fl/u$
Weber number	$We = u^2\rho l/\sigma$

Dimensionless mass transfer numbers are distinguished from dimensionless heat transfer numbers by a prime ('), e.g., Bi $=\beta l/\delta$. Exceptions: Nu $=\beta l/\delta$ = Sh and Pr $=\nu/\delta$ $=\eta/\rho\delta$ = SC

© 1983 Hemisphere Publishing Corporation

INTERNATIONAL SYSTEM OF UNITS (SI): RULES, PRACTICES, AND CONVERSION CHARTS

J. Taborek

■ HEDH is written in SI units because this system has been officially adopted by all countries and is replacing the older metric engineering system, the cgs system, as well as the U.S. customary system. In this section we shall review the basic rules for use of the SI. However, recognizing the fact that many references are written in other unit systems, comprehensive unit conversion charts are included.

A. Basic SI units

SI is absolute in the sense that there are only seven fundamental, precisely defined basic units from which all others are derived. The following five units are important to heat transfer and fluid flow.

length (meter, m): defined in terms of krypton-86 wavelength

mass (kilogram, kg): the mass of an international prototype, approximately equal to the weight of 1 liter H_2 0 at 4° C

time (second, s): defined in terms of radiation frequency of the cesium-133 atom

temperature (kelvin, K): defined in terms of the triple point of water (ice point = 273.15 K)

amount of substance (mole, mol): amount of substance that contains as many elementary entities as there are atoms in 0.012 kg of carbon-12. The elementary entities must be identified when the mole is used (atoms, molecules, ions).

B. Derived SI units with special names

Because SI is defined by the basic units only, there is a need for establishing definitions for the most frequently used composite or derived units, mainly for the purpose of simplifying unit notation. Thus, for example, newton, N, replaces kg m/s^2.

There are a number of derived units that have special names, signifying their importance: newton, joule, watt, pascal, and many others. While the unit symbols are capital letters (N, J, W, Pa), the spelled out unit names begin with lowercase letters, that is, newton, joule, watt, and pascal.

The most frequently used derived SI units with special names in the area of heat transfer and fluid flow are shown in Table 1.

Table 1 Most frequently used derived SI units

Quantity	Unit	Symbol	Dimension
Force	newton	N	kg m/s^2
Energy, work, heat (also power × time)	joule	J	N m or kg m^2/s^2 W s = J s/s
Power	watt	W	J/s = kg m^2/s^3
Pressure	pascal	Pa	N/m^2 = kg/m s^2
Frequency	hertz	Hz	1/s
Dynamic viscosity	poise	P	0.1 Pa s
	centipoise	cP	mPa s

© 1984 Hemisphere Publishing Corporation

C. Prefixes and specification rules

The magnitude of the basic units may often not fit the practice of specific applications without using a large number of decimal digits or power of ten multipliers. SI provides for this by assigning prefixes to the basic units, as shown in Table 2.

Thus, for example, to express very high pressures (stresses) in Pa, the megapascal, MPa, is used instead of 10^6 Pa. The preferred graduation is in powers of 10^3, and there are only a few exceptions to this rule, such as for units that are deeply ingrained in common use, such as centimeter. Some of these are discussed later.

(a) Punctuation and spelling rules

The following general rules should be carefully followed to maintain SI consistency.

1. Prefixes are attached directly to the base unit symbol or a derived unit symbol with a special name, such as km for kilometer or MW for megawatt.

2. Prefixed units are spelled out in text as one word, without hyphen, such as meganewton, not mega-newton.

3. The multiplication of base units can be expressed by leaving a space between the symbols, such as N s for newton X second. However, for better clarity, a center dot is often used, for example, N·s. This usage becomes especially important when the symbol m is used, which can stand for milli or for meter. Thus mN (millinewton) is clearly distinguished from m·N (meter X newton).

4. A prefix applied to a base unit constitutes a new unit. When a power is applied to such a unit, the exponent operates on the prefixed unit as an entity, i.e., mm^2 = (mm) .

5. The unit of length in SI is correctly spelled metre (French spelling). This rule will be hard to enforce in U.S. literature, however, and meter will probably be more commonly used.

Table 2 SI prefixes

Factor	Prefix	Symbol	Status
10^{12}	tera	T	Preferred
10^9	giga	G	Preferred
10^6	mega	M	Preferred
10^3	kilo	k	Preferred
10^2	hecto	h	Accepted
10	deka	da	Accepted
10^{-1}	deci	d	Accepted
10^{-2}	centi	c	Accepted
10^{-3}	milli	m	Preferred
10^{-6}	micro	μ	Preferred
10^{-9}	nano	n	Preferred
10^{-12}	pico	p	Preferred

6. Multiple prefixes are prohibited. This presents some problems with the unit kilogram (kg), where the k stands for the prefix kilo and is one of the very few inconsistencies in SI (a carryover from the older cgs system). Thus k (for kilo) cannot be used in connection with kg, as this would result in the unacceptable term kkg. Equally incorrect is the use of Mg (megagram), as gram is not a basic SI unit. Thus, the unit used is 10^3 kg or the equivalent unit, metric ton (see below).

Similarly, mkg is not an acceptable way to express 10^{-3} kg, and the more common alternate unit of gram (g) is used.

D. Alternate units and supplementary comments

There are as many derived units as the technology demands, as SI is particularly suitable for this purpose by the clearly defined unit relations. The Nomenclature of this handbook contains practically all such units used in heat transfer and fluid flow, showing the appropriate SI dimensions. Consequently, these are not repeated here.

In some cases, strict SI rules are relaxed to respect generally accepted and deeply established practices. The following list presents most frequently used exceptions, together with some additional comments to alternate units, their definition, and their usage.

length: The unit centimeter (cm) is a very practical measure for everyday usage (person s height, 6 ft≃ 183 cm), and will probably remain in perpetual use.

muss: The unit of kilogram is often too small for expressing quantities of mass experienced in many engineering applications. One of the few weaknesses of SI is the lack of a well-defined alternate unit of mass. As explained above, the prefixed units (kkg, Mg) are not acceptable. Instead, an alternate unit for large quantities of mass is introduced, designated metric ton (symbol t), t = 1000 kg. While this unit has not yet been accepted as a recognized SI unit, it is very much in common use.

In the U.S. customary lb,-based system, several definitions of a unit of mass similar in magnitude to the metric ton exist. In engineering practice, the following two definitions of the lb,-based ton are most frequently used:

short ton, which is equal to 2 000 lb, (exact) and therefore approximately = 907.2 kg

long ton, which is equal to 2 240 lb, (exact), and therefore approximately = 1 016 kg

It is important to be aware of these differences in the inconsistently defined U.S. customary system.

For small quantities of mass, gram (g) is also often used in place of 10^{-3} kg.

©1984 Hemisphere Publishing Corporation

time: The unit second (s) should be used whenever possible, as the alternates of minutes, hours, and days are nondecimal entities, and thus complicate the system.

However, to express large quantities of mass per unit of time, the unit hour (h), 3 600 seconds, or the unit day (d), 86 400 seconds, must be used sometimes. The time unit minute (min), often used in the U.S. customary system (gal/min), has no real justification, except that it is ingrained in some industrial practices. Otherwise, the differential quantity of a minute, as compared to a second, can be readily expressed by prefixes in SI units, to obtain a number with reasonable digits.

force: The newton is a very small unit of force, approximately equal to the weight of water in a small glass. Thus the more practical units of force are often the kN or MN.

volume: The liter, defined as dm^3, is a very popular unit of volume for everyday use, such as for water and gasoline. Liter (L) is accepted as a common alternate unit.

amount of substance: The frequently used units of the metric engineering system, gram-mol and kg-mol, are designated in SI as follows: 1 gram-mol = 1 mol (SI), and 1 kg-mol = 1 kmol (SI). Thus 1 mol = 6.023 X 10^{23} molecules.

pressure: The basic unit of pressure, pascal (Pa = N/m^2), is a very small quantity, equal to the pressure exerted by about O.l-mm layer of water over 1 m^2. Thus in most engineering applications kPa or MPa is more useful.

Many derived units of pressure are firmly established in various branches of engineering and will probably remain in use indefinitely. The most important metric-based units are:

bar: has exact relationship to SI (=100 kPa)

torr = 1 mmHg = 0.133 kPa: used for gas pressure measurements

mm water = 9.8067 Pa: used for very small gas pressuremeasurements

at (technical atmosphere) = kg_f/cm^3 = 98.066 kPa

atm (normal or barometric atmosphere) = 760 mmHg = 101.3 kPa

temperature: In many engineering applications it is more convenient to use degrees Celsius rather than the absolute unit kelvin. The use of Celsius is permitted as an alternate, with the relationship

$T(°C) = T(K) - 273.16$ and $\Delta T(°C) = \Delta T(°K)$

Table 3 Unit conversion

Physical quantity	Given in → / Gives ←	Multiplied by → / Divided by ←	Gives / Given in	Approximate or useful relationship
Length	ft	0.3048	m	$3\frac{1}{4}$ ft ≃ 1 m
	in	25.4 (exact)	mm	1 in ≃ 25 mm
	mil	0.0254	mm	
	yard	0.9 144	m	
	mile (mi)	1609.3	m	1 mi ≃ 1.6 km
	km	0.621388	mi	
Area	ft^2	0.092903	m^2	100 ft^2 ≃ 9 m^2
	in^2	645.16	mm^2	1 in^2 ≃ 650 mm^2
	acre	4 047.0	m^2	
Volume	ft^3	0.028317	m^3	35 ft^3 ≃ 1 m^3
	U.S. gal	0.003785	m^3	260 gal ≃ 1 m^3
	U.S. gal	3.785	liter (L)	1 gal ≃ $3\frac{3}{4}$ L
	L (liter)	0.2642	U.S. gal	1 L ≃ 0.26 gal
	Brit gal	0.004546	m^3	
	U.S. gal	0.13368	ft^3	
	barrel (U.S. pet.)	0.15898	m^3	
	barrel (U.S. pet.)	42	U.S. gal	
Velocity	ft/s[a]	0.3048	m/s	10 ft/s ≃ 3 m/s
	m/s	3.2808	ft/s	
	ft/min	0.00508	m/s	100 ft/min ≃ 0.5 m/s
	mi/h	1.6093	km/h	30 mi/h ≃ 48 km/h
	km/h	0.6214	mi/h	50 km/h ≃ 31 mi/h
	knots	1.852	km/h	

(See footnotes on page xxix.)

© 1984 Hemisphere Publishing Corporation

Table 3 Unit conversion (Continued)

Physical quantity	Given in → / Gives ←	Multiplied by → / Divided by ←	Gives → / Given in ←	Approximate or useful relationship
Mass	lb_m	0.45359	kg	1 lb, ≃ .45 kg
	kg	2.2046	lb_m	1 kg ≃ 2.2 lb,
	metric ton	2 204.6	lbm	metric ton = 10^3 kg
	ton (2 000 lb,)	907.18	kg	
Force	lb_f	4.44822	N = kg m/s^2	
	lb_f	0.45359	kg_f	1 N ≈ 0.1 kg_f
	kg_f	2.2046	lb_f	≈ 0.22 lb_f
	kg_f	9.80665	N	
	dyne	0.00001 (exact)	N	
Amount of substance	lb_m-mol	453.6	kmol	
	g-mol	1.000	mol	
	kg-mol	1.000	kmol	
	mol	1 000	kmol	
Mass flow rate	lb_m/h	0.0001260	kg/s	10^3 lb/h- .13 kg/s
	kg/s	7 936.51	lb_m/h	
	lb_m/s	0.4536	kg/s	
	lb_m/min	0.00756	kg/s	
Volume flow rate	U.S. gal/min	6.309×10^{-5}	m^3/s	
	U.S. bbl/day	0.15899	m^3 /day	
	U.S. bbl/day	1.84×10^{-6}	m^3/s	
	ft^3/s	0.02832	m^3/s	
	ft^3/min	0.000472	m^3/s	
Mass velocity (mass flux)	$lb_m/h\ ft^2$	1.356×10^{-3}	kg/s m^2	
	kg/s m^2	737.5	$lb_m/h\ ft^2$	
Energy (work) (heat)	Btu[b]	1 055.056	J = N m = W s	1 Btu ≃ 1 000 J
	Btu	0.2520	kcal	1 kcal ≃ 4 Btu
	Btu	778.28	ft lb_f	
	kcal	4 186.8	J	1 kcal ≃ 4 000 J
	ft lb_f	1.3558	J	
	W h	3600	J	
Power	Btu/h	0.2931	W = J/s	10^6 Btu/h ≃ 300 kW
	W	3.4118	Btu/h	
	kcal/h	1.163	W	
	ft lb_f/s	1.3558	W	1 000 kW ≃ 3.5 $\times 10^6$
	hp (metric)	735.5	W	Btu/h
	Btu/h	0.2520	kcal/h	
	tons refrig.	3 516.9	W	
Heat flux	Btu/h ft^2	3.1546	W/m^2	1 000 Btu/h ft^2 ≃ 3.2
	W/m^2	0.317	Btu/h ft^2	kW/m^2
	kcal/cm^2 s	41.868	W/m^2	
Heat transfer coefficient	Btu/h ft^2 °F	5.6784	W/m^2 K	1 000 Btu/h ft^2 °F ≃
	W/m^2 K	0.1761	Btu/h ft^2 °F	5 600 W/m^2 K
	kcal/cm^2 s °C	41.868	W/m^2 K	
Heat transfer resistance	(Btu/h ft °F)$^{-1}$	0.1761	(W/m^2 K)$^{-1}$	0.001 (Btu/h ft^2 °F)$^{-1}$ ≃
	(W/m* K)$^{-1}$	5.6784	(Btu/h ft^2 °F)$^{-1}$	0.000 18 (W/m* K)$^{-1}$
Pressure	lb_f/in^2 (psi)	6.8948	kN/m^2 = kPa	1 psi ≃ 7 kPa
	kPa	0.1450	psi	14.5 psi ≃ 100 kPa
	bar	100	kPa	

(See footnotes on page xxix.)

3 1984 Hemisphere Publishing Corporation

Table 3 Unit conversion (Continued)

Physical quantity	Given in → / Gives ←	Multiplied by → / Divided by ←	Gives → / Given in	Approximate or useful relationship
Pressure ***(Continued)***	lb_f/ft^2	0.0479	kPa	
	mm Hg (torr)	0.1333	kPa	1 000 kPa = 1 MPa ≃
	in Hg	3.3866	kPa	150 psi
	mm H_2O	9.8067	Pa	
	in H_2O	249.09	Pa	1 in H_2O ≃ .25 kPa
	at (kg_f/cm^2)	98.0665	kPa	
	atm (normal)	101.325	kPa	atm = 760 mmHg
Mass flux	lb_m/ft^2 s	4.8824	kg/m^2 s	
	lb_m/ft^2 h	0.001356	kg/m^2 s	
	Physical and Transport Properties			
Thermal conductivity	Btu/ft h °F	1.7308	W/m K	steel ≃ 50 W/m K
	W/m K	0.5778	Btu/ft h °F	water (20° C)≈ 0.6 W/m K
	kcal/m h °C	1.163	W/m K	air (STP) ≃ 24 mW/m K
Density	lb_m/ft^3	16.0185	kg/m^3	
	kg/m^3	0.06243	lb_m/ft^3	62.4 lb_m/ft^3 ≃ 1 000
	lb_m/U.S. gal	119.7	kg/m^3	kg/m^3
Specific heat capacity	Btu/lb_m °F	4 186.8	J/kg K	1 Btu/lb_m °F ≃ 4.2
	kcal/kg °C	4 186.8	J/kg K	kJ/kg K
Enthalpy	Btu/lb_m	2 326	J/kg	
	kcal/kg_m	4 186.8	J/kg	
Dynamic (absolute) viscosity	centipoise (cP)	0.001	kg/m s	kg/m s = N s/m^2 = P a s
	poise (P)	0.1	Pa s	
	cP	1.000	mPa s	
	cP	1 000	μPa s	water (100°C), 0.31 cP
	lb_m/ft h	0.0004134	Pa s	
	lb_m/ft h	0.4134	cP	
	cP	2.4189	lb_m/ft h	air (100°C), 0.021 cP
	lb_m/ft s	1.4482	Pa s	
Kinematic viscosity	stoke (St), cm^2 s	0.0001	m^2/s	
	centistoke (cSt)	10^{-6}	m^2/s	
	ft^2/s	0.092903	m^2/s	
Diffusivity	ft^2/s	0.092903	m^2/s	
Thermal diffusivity	m^2/h	0.0002778	m^2/s	
	ft^2/s	0.092903	m^2/s	
	ft^2/h	25.81 x 10^{-6}	m^2/s	
Surface tension	dyne/cm	0.001	N/m	
	dyne/cm	6.852 X 10^{-5}	lb_f/ft	
	lb_f/ft	14.954	N/m	

Temperature relations: $°C = \frac{5}{9}[°F - 32]$ $°C = (°F + 40)\frac{5}{9} - 40$ $\Delta T(°C) = \frac{9}{5}\Delta T(°F)$ K = °C + 273.15

$°F = \frac{9}{5}(°C) + 32$ $°F = (°C + 40)\frac{9}{5} - 40$ $\Delta T(°F) = \frac{5}{9}\Delta T(°C)$ R = °F + 459.67

Miscellaneous:

Acceleration of gravity (standard):	g = 9.806 65 m/s*
Gas constant:	R = 8 314.3 m N/K kmol
Stefan-Boltzmann constant:	5.669 7 x 10^{-8} W/m^2K^4
	1.714 X 10^{-9} Btu/ft^2 h R^4

[a] Even though the abbreviations s and h were introduced only with the SI, they are used here throughout for consistency.

[b] Note: the calorie and Btu are baaed on the International Standard Table values. The thermochemical calorie equals 4.184 J (exact) and is used in some older texts.

© 1984 Hemisphere Publishing Corporation

LENGTH: meter, m; foot, ft

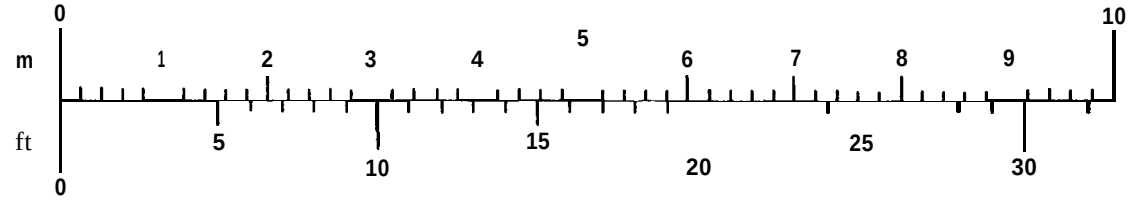

m X 3.2803 = ft
ft X 0.3048 = m

AREA: square meter, m^2; square foot, ft^2

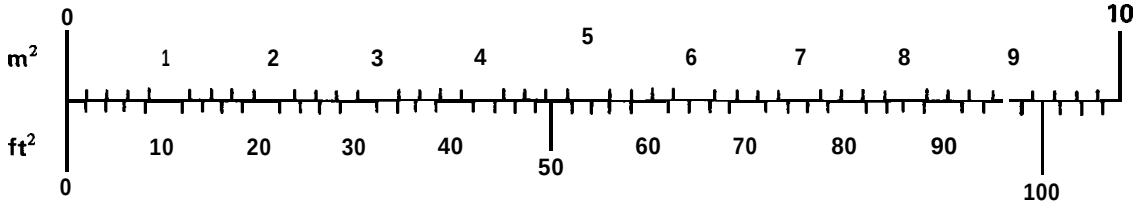

m^2 X 10.764 = ft^2
ft^2 X 0.0929 = m^2

VOLUME: cubic meter, m^3; cubic foot, ft^3

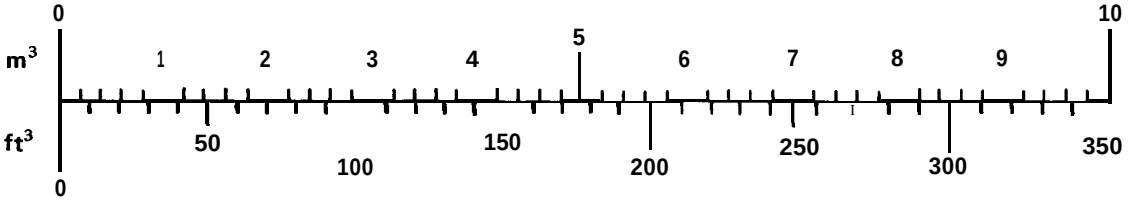

m^3 X 35.314 = ft^3
ft^3 X 0.083 = m^3

MASS: kilogram, kg; pound-mass, lb_m

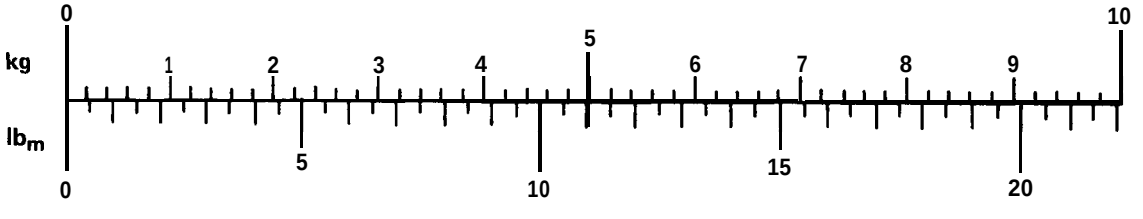

kg X 2.205 = lb_m
lb, X 0.454 = kg

© 1984 Hemisphere Publishing Corporation

VOLUME FLOW RATE: $\frac{m^3}{s}$; $\frac{gal(U.S.)}{min}$

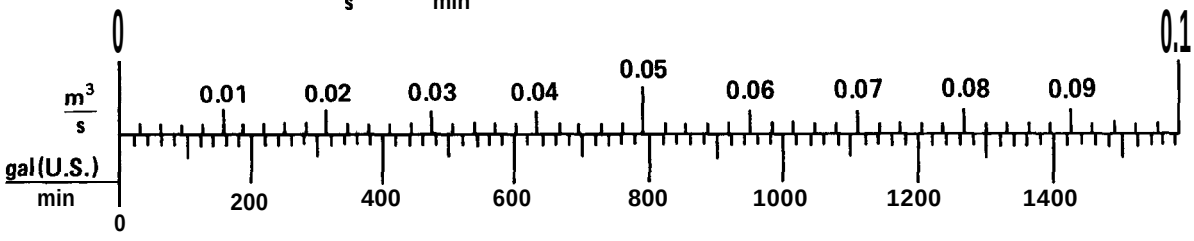

$$\frac{m^3}{s} \times 1.585(10^4) = \frac{gal(U.S.)}{min}$$

$$\frac{gal(U.S.)}{min} \times 6.31(10^{-5}) = \frac{m^3}{s}$$

VELOCITY: $\frac{m}{s}$; $\frac{ft}{s}$

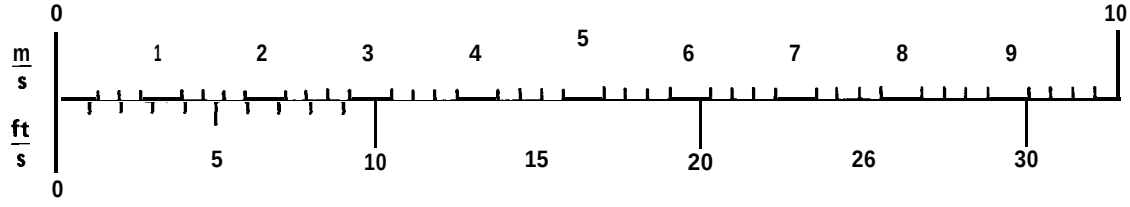

$$\frac{m}{s} \times 3.28 = \frac{ft}{s}$$

$$\frac{ft}{s} \times 0.305 = \frac{m}{s}$$

MASS VELOCITY: $\frac{kg}{s\,m^2}$; $\frac{10^3\,lb_m}{h\,ft^2}$

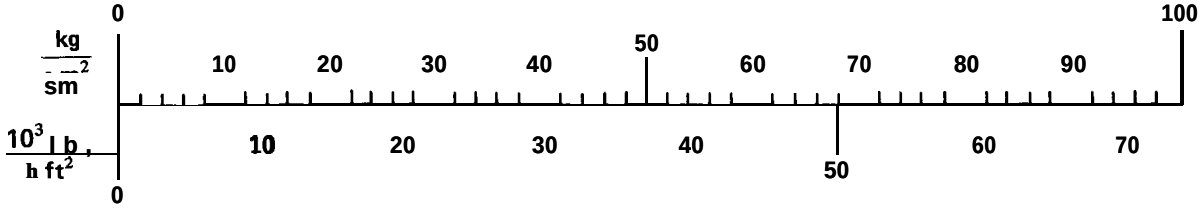

$$\frac{kg}{s\,m^2} \times 0.737 = \frac{10^3\,lb_m}{h\,ft^2}$$

$$\frac{10^3\,lb_m}{h\,ft^2} \times 1.356 = \frac{kg}{s\,m^2}$$

© 1984 Hemisphere Publishing Corporation

MASS FLOW RATE: $\frac{kg}{s}; \frac{10^3\ lb_m}{h}$

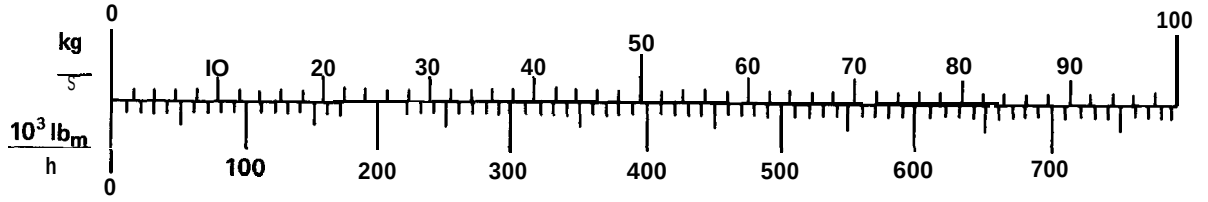

$$\frac{kg}{s} \times 7.937 = \frac{10^3\ lb_m}{h}$$

$$\frac{10^3\ lb_m}{h} \times 0.126 = \frac{kg}{s}$$

FORCE: newton, $N = \frac{kg\ m}{s^2}$; pound-force, lb_f

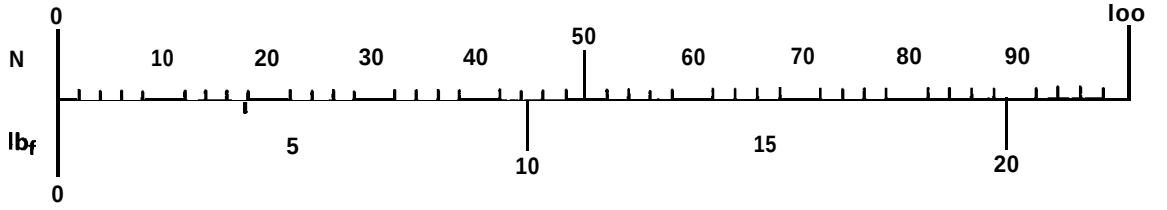

$$N \times 0.225 = lb_f$$

$$lb_f \times 4.448 = N$$

ENERGY (WORK): joule, J = N m; Btu

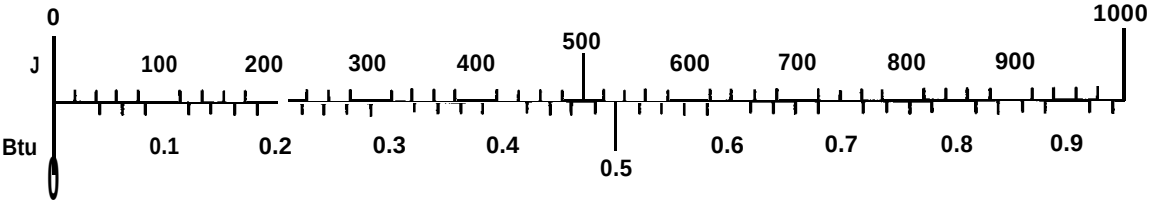

$$J \times 0.948(10^{-3}) = Btu$$

$$Btu \times 1055 = J$$

POWER OR ENERGY FLOW RATE: kilowatt, $kW = \frac{kJ}{s}$; $\frac{10^6\ Btu}{h}$

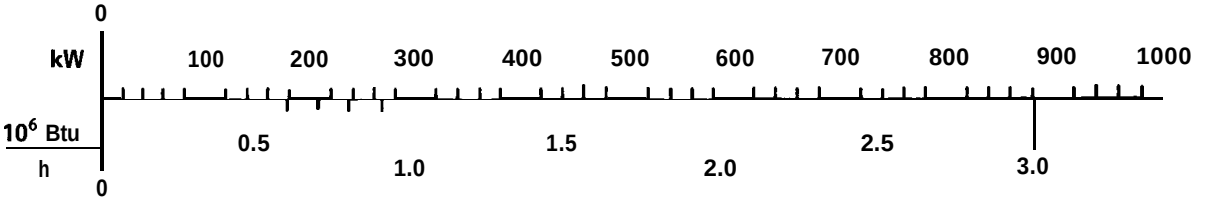

$$kW \times 3.412(10^{-3}) = \frac{10^6\ Btu}{h}$$

$$\frac{10^6\ Btu}{h} \times 293 = kW$$

©1984 Hemisphere Publishing Corporation

HEAT TRANSFER COEFFICIENT: $\frac{W}{m^2 K}$; $\frac{Btu}{h\ ft^2\ °F}$

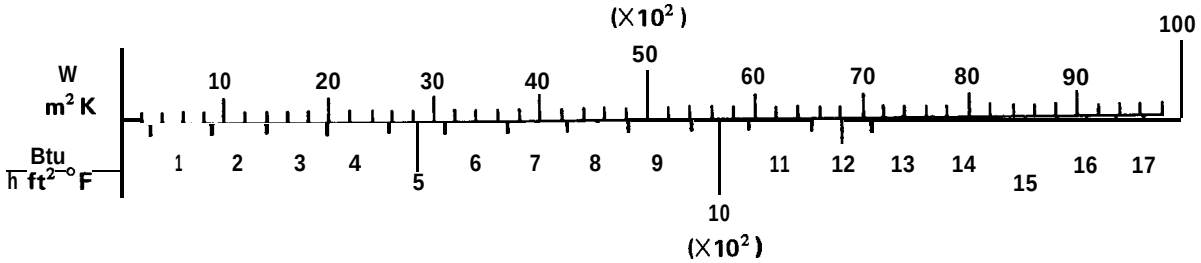

$$\frac{W}{m^2 K} \times 0.176 = \frac{Btu}{h\ ft^2\ °F}$$

$$\frac{Btu}{h\ ft^2\ °F} \times 5.68 = \frac{W}{m^2 K}$$

HEAT FLUX: $\frac{W}{m^2}$; $\frac{Btu}{h\ ft^2}$

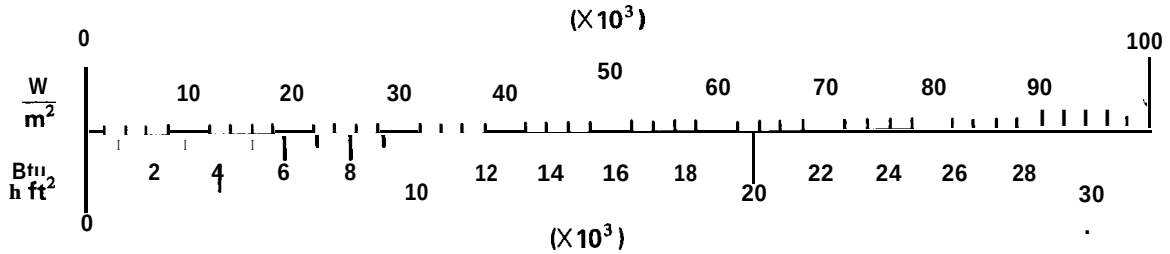

$$\frac{W}{m^2} \times 0.316 = \frac{Btu}{h\ ft^2}$$

$$\frac{Btu}{h\ ft^2} \times 3.16 = \frac{W}{m^2}$$

DENSITY: $\frac{kg}{m^3}$; $\frac{lb_m}{ft^3}$

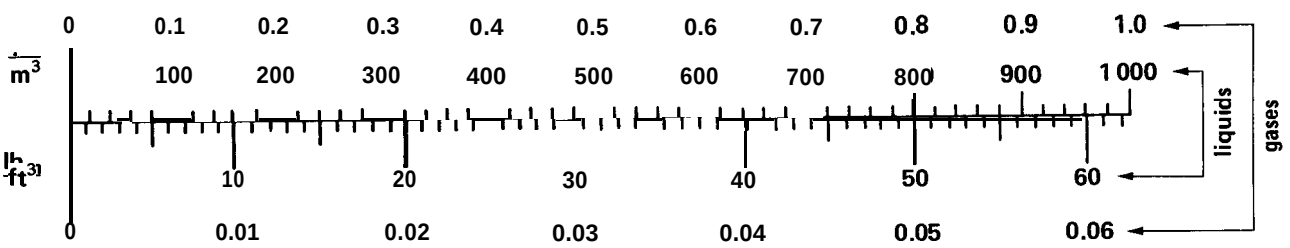

$$\frac{kg}{m^3} \times 0.0624 = \frac{lb_m}{ft^3}$$

$$\frac{lb_m}{ft^3} \times 16.02 = \frac{kg}{m^3}$$

© 1984 Hemisphere Publishing Corporation

SPECIFIC HEAT CAPACITY: $\frac{kJ}{kg\,K}$; $\frac{Btu}{lb_m\,°F}$

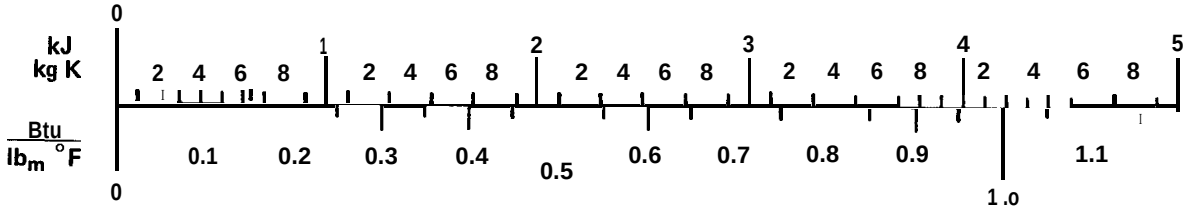

$$\frac{kJ}{kg\,K} \times 0.239 = \frac{Btu}{lb_m\,°F}$$

$$\frac{Btu}{lb_m\,°F} \times 4.187 = \frac{kJ}{kg\,K}$$

THERMAL CONDUCTIVITY: $\frac{W}{m\,K}$; $\frac{Btu}{h\,ft\,°F}$

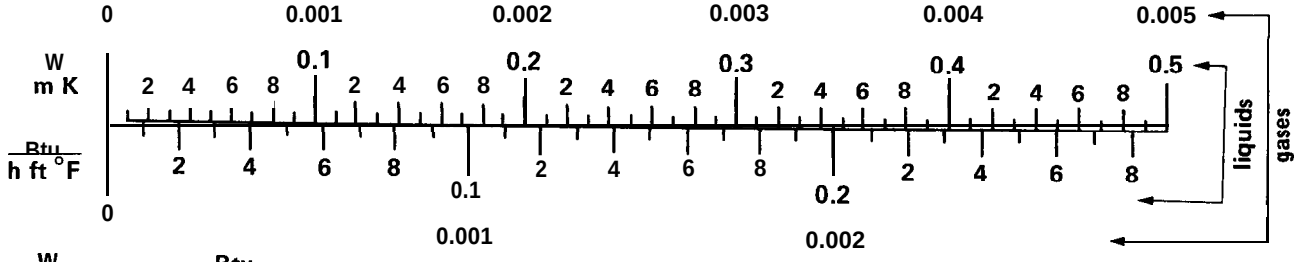

$$\frac{W}{m\,K} \times 0.578 = \frac{Btu}{h\,ft\,°F}$$

$$\frac{Btu}{h\,ft\,°F} \times 1.731 = \frac{W}{m\,K}$$

DYNAMIC (ABSOLUTE) VISCOSITY: $\frac{N\,s}{m^2}$; $\frac{lb_m}{h\,ft}$

centipoise $cP = 10^{-3}\frac{N\,s}{m^2} = mPa\,s$

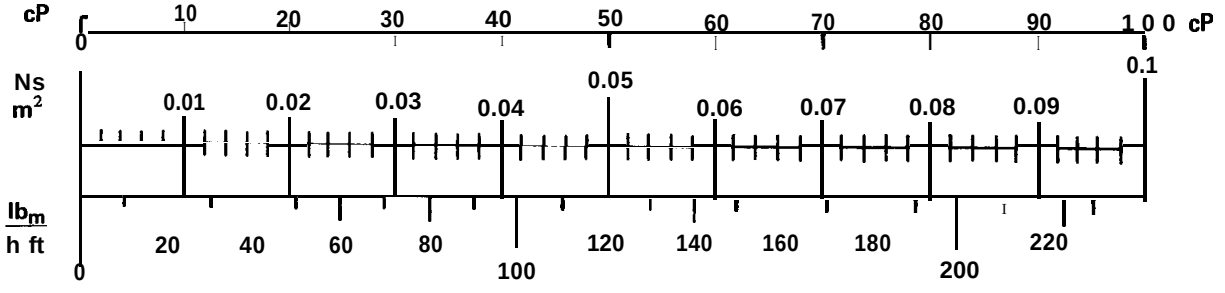

$$cP \times 2.42 = \frac{lb_m}{h\,ft}$$

$$\frac{lb_m}{h\,ft} \times 0.413 = cP$$

© 1984 Hemisphere Publishing Corporation

ENTHALPY: $\frac{kJ}{kg}$; $\frac{Btu}{lb_m}$

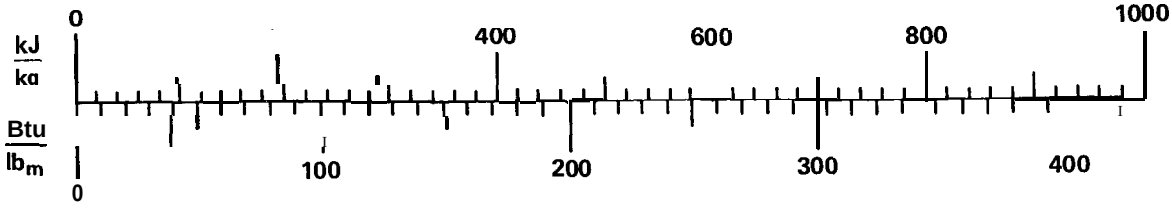

$$\frac{kJ}{kg} \times 0.430 = \frac{Btu}{lb_m}$$

$$\frac{Btu}{lb_m} \times 2.326 = \frac{kJ}{kg}$$

PRESSURE CONVERSION CHART
(top line = 1 Pa on all charts)

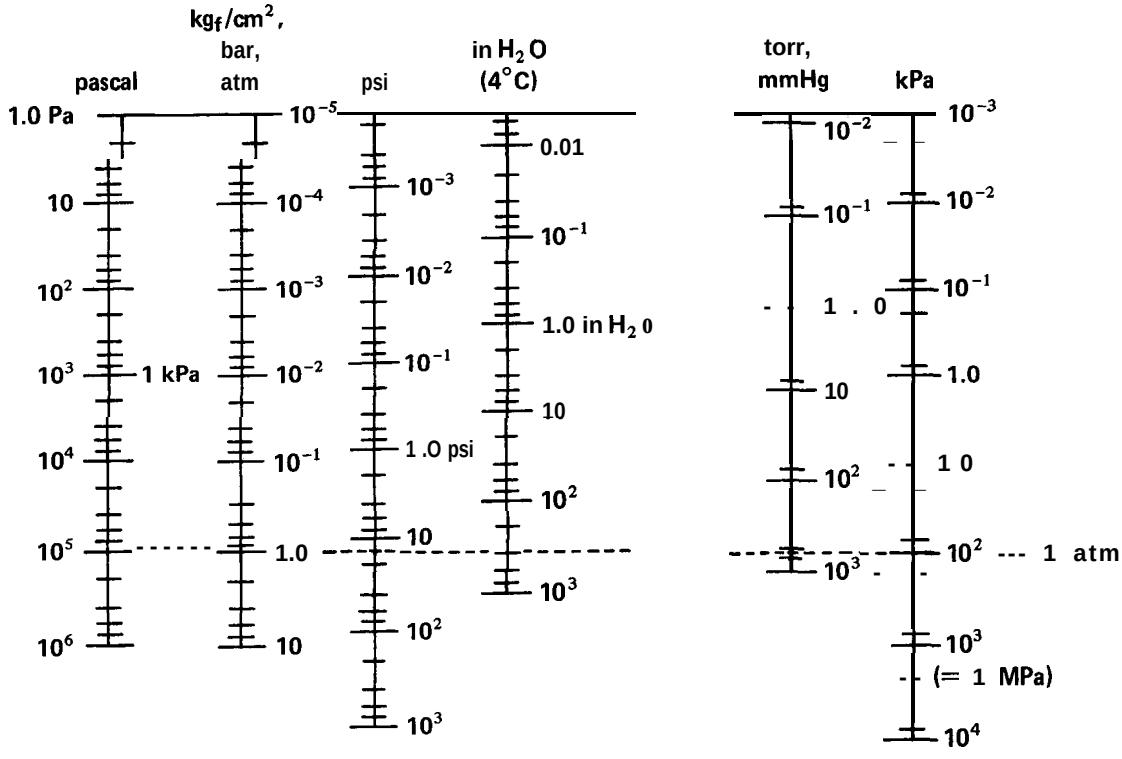

*NOTE: only bar is exact (1 bar = 10^5 Pa); however, atm and kg_f/cm^2 are within 2% accuracy (see list below).

1 atm = 1.01325 X 10^5 Pa
1 psi = 6.89476 X 10^3 Pa
1 in H_2O = 2.49082 X 10^2 Pa
1 kg_f/cm^2 = 9.80665 X 10^4 Pa
1 bar = 10^5 Pa
1 mmHg = 1.33322 X 10^2 Pa

1 Pa = 9.86923 X IO atm
1 Pa = 1.45038 X 10^{-4} psi
1 Pa = 4.01474 X 10^{-3} in H_2O
1 Pa = 1.01972 X 10^{-5} kg_f/cm^2
1 Pa = 10^{-5} bar
1 Pa = 7.50064 X 10^{-3} mmHg

© 1984 Hemisphere Publishing Corporation

TEMPERATURE COMPARISON
(NOT TO SCALE)

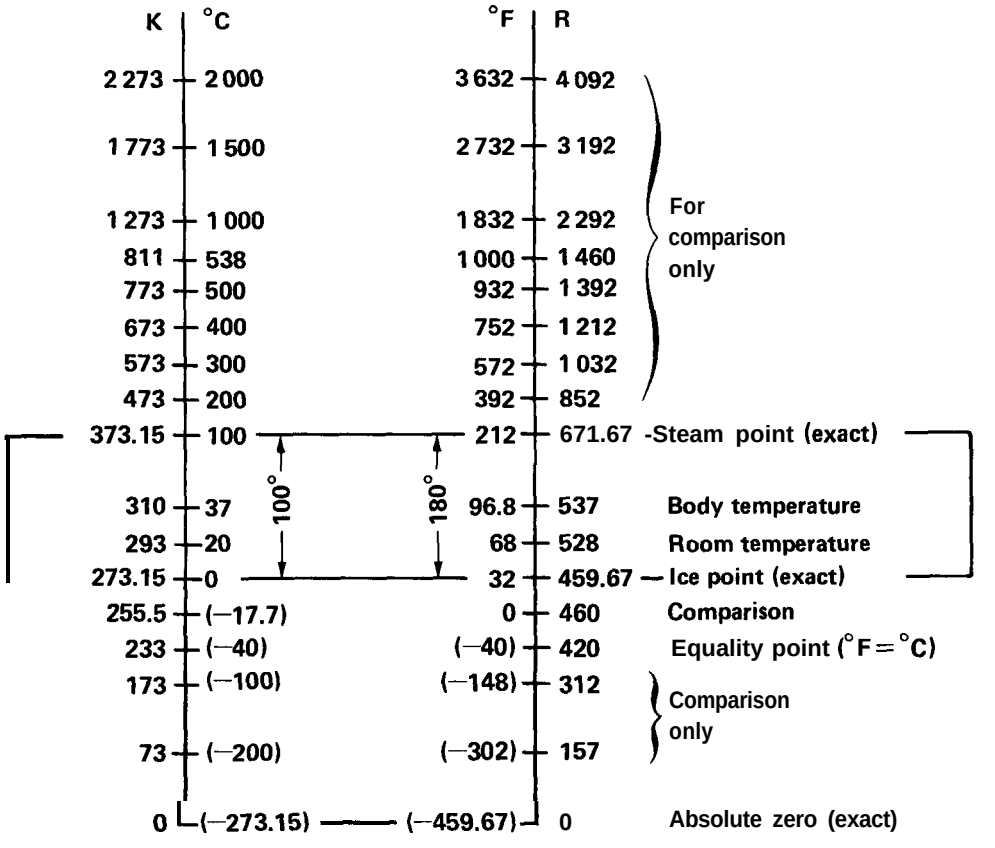

$T(°F) = (°C + 40)\frac{9}{5} - 40$ $\quad T(R) = T(°F) + 460$

$T(°C) = (°F + 40)\frac{5}{9} - 40$ $\quad T(K) = T(°C) + 273.15$

AT: $°C = \frac{5}{9}(°F)$ $\quad °F = \frac{9}{5}(°C)$

© 1984 Hemisphere Publishing Corporation

3.1
Introduction to heat exchanger design

Contents

3.1.1
FUNDAMENTAL CONCEPTS,
Kenneth. J. Bell **3.1.1-1**

A. Heat transfer coefficients 3.1.1-1
B. Basic design equation 3.1.1-2
C. Mean temperature difference concept 3.1.1-2

3.1.2
TYPES OF HEAT EXCHANGERS AND THEIR APPLICATIONS,
Kenneth J. Bell **3.1.2-l**

A. Selection of a basic type of heat exchanger 3.1.2-l
B. Double-pipe heat exchangers 3.1.2-1
C. Shell-and-tube exchangers 3.1.2-2
D. Plate heat exchangers 3.1.2-3
E. High-finned or air-cooled heat exchangers 3.1.2-4
F. Plate fin or matrix heat exchangers 3.1.2-S
G. Mechanically aided heat exchangers 3.1.2-s
H. Other types of process heat exchangers 3.1.2-6

3.1.3
LOGIC OF THE DESIGN PROCESS,
Kenneth J. Bell **3.1.3-l**

A. Criteria for a successful heat exchanger design 3.1.3-l
B. Relationship among selection, rating, and design 3.1.3-2
C. Simplified example of a design modification algorithm for a computer 3.1.3-3

Reference for Section 3.1.3 3.1.3-4

3.1.4
APPROXIMATE SIZING OF SHELL-AND-TUBE HEAT EXCHANGERS,
Kenneth J. Bell **3.1.4-l**

A. The basic design equation 3.1.4-l
B. Estimation of heat load 3.1.4-1
C. Estimation of the mean temperature difference 3.1.4-2
D. Estimation of U_o 3.1.4-3
E. Calculation of A, 3.1.4-6
F. Heat transfer area for a given shell diameter and length **3.1.4-6**
G. Extension of Fig. 2 to other shell/bundle/tube geometries 3.1.4-7
H. Example problem 3.1.4-7

© 1983 Hemisphere I blishing Corporation

3.1.1
Fundamental concepts

Kenneth J. Bell

■ This part of the handbook presents thermal-hydraulic design concepts and methods for a variety of heat exchanger configurations. The methods perforce are limited to those that can be employed by hand or on small programmable calculators, but the extension of the logic to large computer methods is introduced.

This introductory chapter sets forth a number of general concepts, facts, and philosophies that will find repeated use throughout Part 3. Some of this material is developed at greater length elsewhere in this handbook and is reproduced here only to provide coherence and a common point of reference for this part. References to the more detailed presentations are provided.

A. Heat transfer coefficients

The concept of the individual film heat transfer coefficient α, as the constant of proportionality between the heat flux $\dot{q}$ and the temperature driving force ΔT, is basic to most heat exchanger design methods. It must be understood that the heat transfer coefficient is not a fundamental quantity, but only a convenience in the formulation of the design equations. In fact, there are a number of heat transfer processes (e.g., nucleate boiling and natural convection) for which α is not independent of the temperature difference even over limited ranges, and would therefore seem to have no applicability in those cases. Nevertheless, the convenience is so great and the alternatives so formidable, at least for hand methods, that the film coefficient concept is often stretched and adapted to these cases too.

A major advantage of the use of α to quantify heat transfer rates is that individual values of α for two different fluids exchanging heat may be combined to relate the local rate of heat transfer to the local overall temperature difference between the two fluids. For the very common case of heat transfer between two fluids separated by a solid cylindrical wall with fouling deposits on each surface, the overall heat transfer coefficient U^* is related to the individual coefficients and other parameters of the system by Eq. (1):

$$U^* = 1/\{(1/\alpha_i)(A^*/A_i) + R_{fi}(A^*/A_i) + [A^* \ln(D_o/D_i)/2\pi L\lambda_w] + R_{f_o}(A^*/A_o) + (1/\alpha_o)(A^*/A_o)\} \quad (1)^\dagger$$

where subscripts i and o refer to the fluids and surfaces inside and outside the tube, respectively, and R_f is the resistance due to fouling of the heat transfer surface by dirt, corrosion products, biological growth, and so on.

A* is any convenient reference area, and U^* is the overall heat transfer coefficient based on that area. Often, the outside heat transfer surface area A, is used as the reference area; occasionally A_i is used as the reference. In either case, Eq. (1) is simplified somewhat. However, the important fact is that any area can be used as long as it and the corresponding heat transfer coefficient are clearly identified. The following relationship connects all of these areas and their corresponding overall coefficients:

$$U^*A^* = U_oA_o = U_iA_i \quad (2)$$

Other equations similar to Eq. (1) may be written to accommodate other surface geometries (including extended surfaces), composite wall materials, and so on.

†Within a three-digit section the equation, figure, and table numbers do not have the three-digit identifier; for cross-references between sections, the appropriate threedigit number will be given.

© 1983 Hemisphere Publishing Corporation

B. Basic design equation

The local rate of heat transfer is related to the local temperature difference between the two streams by

$$dQ = U^*(T_h - T_c)\, dA^* \tag{3}$$

where T_h and T_c are the local temperatures of the hot and cold streams, respectively. The asterisks are retained on U and A to indicate that these values must be on a consistent area basis and that this may be any convenient one. The differential form is used here to emphasize that a given set of values of U^*, T_h, and T_c will ordinarily be valid only at one point in the heat exchanger, and at this point an amount of heat dQ is transferred through an element of area dA^*.

Equation (3) is limited to steady-state operation; that is, conditions at any given point in the exchanger do not change as a function of time. Although this condition is seldom exactly true, during normal operation of most exchangers, the amount of heat being transferred so far exceeds the storage capacity that this is a very good approximation. Some exchangers are operated primarily in the transient mode and require a different analysis.

The usual design problem is to determine the total area in a heat exchanger required to transfer the specified total amount of heat Q_T. Equation (3) can be formally integrated to show this:

$$A^* = \int_0^{Q_T} \frac{dQ}{U^*(T_h - T_c)} \tag{4}$$

The actual evaluation of the right-hand-side of Eq. (4) can be carried out in principle by a combination of heat balance and rate equation calculations; for phase-change heat transfer, mass balances and fluid mechanics calculations are also essential in principle if not always in practice. Finally, for multicomponent phase change, detailed vapor-liquid equilibrium relationships are needed.

The computational scheme required to evaluate Eq. (4) will depend both on the nature of the heat transfer process and on the orientation of the two streams flowing through the heat exchanger. But it is safe to say that only rarely is a hand solution of Eq. (4) feasible. Small programmable calculators are somewhat more suitable, especially for frequently encountered problems. Mostly, however, integration of Eq. (4) is limited to large computers programmed with general-purpose heat exchanger rating programs. Fortunately, most heat exchangers can be adequately designed by a much simpler procedure.

C. Mean temperature difference concept

Equation (4) can be integrated analytically if a number of assumptions are made. The result, given below, is the mean temperature difference (MTD) concept. The detailed treatment is given in Sec. 1.5, but the essential features are reiterated here.

The key assumptions that need to be made are these:

1. Every element of fluid that enters the heat exchanger in a given stream has an equal opportunity to encounter heat transfer surface. That is, if any part of a stream is able to bypass heat transfer surface in passing through the exchanger, the MTD concept is inapplicable, at least in its unmodified form.
2. The heat exchanger is at steady state.
3. The specific heats of each stream are constant. An isothermal phase transition (e.g., condensation of a pure vapor with negligible pressure drop) corresponds to an infinite specific heat, which satisfies the assumption and in fact simplifies the result.
4. The overall heat transfer coefficient is constant.
5. Heat losses or gains to/from the surroundings are negligible.
6. Longitudinal heat flow is negligible.
7. The flow arrangement is either purely counter-current or purely cocurrent.

Under these assumptions, Eq. (4) may be analytically integrated (see Sec. 1.3.1) to give

$$\mathrm{AT}_{,,} = \frac{Q_T}{U^*(LMTD)} \tag{5}$$

where

$$\boldsymbol{AT}_{,,} = \frac{(T_{h,\mathrm{in}} - T_{c,\mathrm{out}}) - (T_{h,\mathrm{out}} - T_{c,\mathrm{in}})}{\ln\left[(T_{h,\mathrm{in}} - T_{c,\mathrm{out}})/(T_{h,\mathrm{out}} - T_{c,\mathrm{in}})\right]} \tag{6}$$

for counter-current flow and

$$\mathrm{AT}_{,,} = \frac{(T_{h,\mathrm{in}} - T_{c,\mathrm{in}}) - (T_{h,\mathrm{out}} - T_{c,\mathrm{out}})}{\ln\left[(T_{h,\mathrm{in}} - T_{c,\mathrm{in}})/(T_{h,\mathrm{out}} - T_{c,\mathrm{out}})\right]} \tag{7}$$

for cocurrent flow.

Most heat exchangers do not operate in either purely counter-current or purely cocurrent flow, but in some combination of the two, or in cross flow. For most of these cases, it is possible again to integrate Eq. (4) analytically or numerically to obtain

$$A^* = \frac{Q_T}{U^* F\ \mathrm{AT}_{,,}} = \frac{Q_T}{U^*\ \mathrm{AT}_{,}} \tag{8}$$

where ΔT_{LM} is defined by Eq. (6). F is a function of the flow arrangement and the parameters

$$\boldsymbol{R} = \frac{T_{h,\mathrm{in}} - T_{h,\mathrm{out}}}{T_{c,\mathrm{out}} - T_{c,\mathrm{in}}} \tag{9}$$

and

$$\boldsymbol{P} = \frac{T_{c,\mathrm{out}} - T_{c,\mathrm{in}}}{T_{h,\mathrm{in}} - T_{c,\mathrm{in}}} \tag{10}$$

© 1983 Hemisphere Publishing Corporation

Charts and equations for *Fare* presented for a number of the most important heat exchanger configurations in Sec. 1.5.

The above equations obviously offer a much simpler solution to the heat exchanger design equation than stepwise numerical integration. However, serious errors may result if the mean temperature difference is employed under conditions where the assumptions are not satisfied. Certain classes of heat exchanger problems—e.g., vertical thermosiphon reboilers, and multicomponent or partial condensers-do not satisfy the assumptions even approximately and require integration of the basic equation. Further discussion of *UAT* methods is given in Secs. 2.1.2 and2.1.3.

Nomenclature for Section 3.1.1 appears at the beginning of Part 3.

© 1983 Hemisphere Publishing Corporation

3.1.2

Types of heat exchangers and their applications

Kenneth J. Bell

A. Selection of a basic type of heat exchanger

The most important decision underlying design of a piece of heat transfer equipment is the selection of the basic type of equipment to be specified and designed for a given application. It is incumbent upon the designer, at a very early stage in the design process, to survey the range of basic equipment types available and to select the one most applicable to his or her particular process. If a clear-cut decision cannot be made, it will probably prove economically desirable to proceed with at least first-stage design on each type of equipment that may reasonably serve.

A consideration that often enters into the selection of a basic type is the availability of comprehensive and accurate design methods for that equipment. Thus, shell-and-tube exchangers, for which a generally very good design procedure is available, are often selected for a service in preference to another type that may be intrinsically preferable in the application but that lacks a comparable design method in which the designer may place confidence. There is justification for this philosophy, but it can be bought at too high a price. Most heat exchanger types have good design methods available for most applicable services, though the best methods are often proprietary to the manufacturers or to members of cooperative research organizations.

B. Double-pipe heat exchangers

A typical double-pipe heat exchanger is shown in Fig. 1. Essentially, it consists of one pipe placed concentrically inside another one of larger diameter, with appropriate end fittings on each pipe to guide the fluids from one section to the next. The inner pipe may have external longitudinal fins welded to it either internally or externally to increase the heat transfer area for the fluid with the lower heat transfer coefficient. The double-pipe sections can be connected in various series or parallel arrangements for either fluid to meet pressure-drop limitations and MTD requirements.

The major use of double-pipe exchangers is for sensible heating or cooling of the process fluid where small heat transfer areas (typically up to 50 m) are required. They may also be used for small amounts of boiling or condensation on the process fluid side. The advantages of the double-pipe exchanger are largely in the flexibility of application and piping arrangement, plus the fact that they can be erected quickly from standard components by maintenance crews. Additional surface is usually easily installed on an existing facility. They also are easily cleanable on both sides by proper selection of end fittings, and the design calculations are relatively well established and accurate. There is also the advantage of ease of controlling flow distribution in each channel of a double-pipe heat exchanger; this can be of particular importance in cooling viscous liquids, where, if necessary, one pump can be provided for each series set of exchangers. The main disadvantage

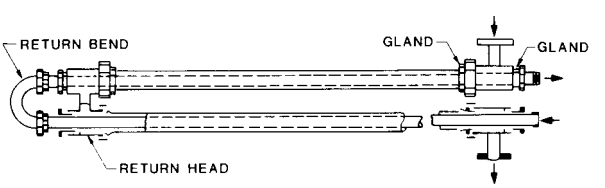

Figure 1 Double-pipe heat exchanger.

© 1983 Hemisphere I blishing Corporation

is that double-pipe exchangers are bulky and expensive per unit of heat transfer surface. The design of double-pipe exchangers is discussed in Sec. 3.2.

C. Shell-and-tube exchangers

A typical shell-and-tube exchanger is shown in Fig. 2. In their various construction modifications, they are, undoubtedly, the most commonly used basic heat exchanger configuration in the process industries. The shell-and-tube heat exchanger provides fairly large ratios of heat transfer area to volume and weight. It provides this surface in a form that is relatively easy to construct in a wide range of sizes and that is mechanically rugged enough to withstand normal shop fabrication stresses, shipping and field erection, and external and internal stresses encountered under normal operating conditions. The shell-and-tube exchanger can be cleaned reasonably easily, and those components most subject to failure—gaskets and tubes-can be easily replaced. Special construction features allow this type to meet almost any conceivable service, including extremely low and high temperatures and pressures, large temperature differentials, vaporizing and condensing services, and severely fouling and corrosive fluids. Good design methods are available, and the expertise and shop facilities for their successful design and construction are widespread. Section 4.2 describes in considerable detail the mechanical features of shell-and-tube exchangers, Sec. 3.3 the design methods for sensible heat transfer service on the shell side, Sec. 3.4 the methods for condensation on the shell side, and Secs. 3.5 and 3.6 the use and design of shell-and-tube exchangers for vaporizing and evaporation services.

The tubes are the basic component, providing the heat transfer surface between one fluid flowing inside the tubes and the other fluid flowing across the tubes. The tubes may be either plain or with low fins on the outside to increase the ratio A_o/A_i; in this case the fin outside diameter is very slightly less than the outside diameter of the unfinned ends of the tube to allow insertion of the finned tube through the holes in the tube sheets. The tubes are held in place by the tubesheets at each end (except the U-tube design, which has only one tubesheet). The tubes are either expanded into radial grooves cut into the tubesheet holes or welded to the outside of the tubesheet. In some low-pressure applications, the tubes are simply expanded into ungrooved holes in the tubesheets.

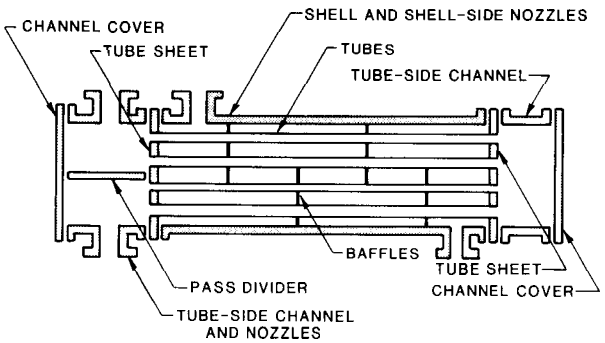

Figure 2 Diagram of a typical (fixed-tubesheet) shell-and-tube heat exchanger.

The tubesheet is a round metal plate that has been suitably drilled and grooved for the tubes and also drilled or milled for the gaskets, baffle spacer rods, and the bolt circle (if the tubesheet is bolted to the shell flange; the tubesheet may also be welded to the shell).

The shell is the cylindrical element surrounding the tubes and containing the shell-side fluid. It is commonly made by rolling a metal plate of the appropriate dimensions into a cylinder and welding the longitudinal joint. Small-diameter shells up to about 0.6 m in diameter may be made by cutting off the desired length of pipe; these pipe shells are usually more nearly round than rolled shells.

The shell-side nozzles provide the inlet and outlet ports for the shell-side fluid. Commonly the nozzles are sections of standard pipe welded to the shell, though special designs are used where low pressure drop, uniform distribution, or erosion protection is required. Impingement plates slightly larger than the cross section of the nozzle may be used inside the shell and under the inlet nozzle, especially when two-phase flows or saturated vapors are admitted to the shell side.

Tube-side channels and nozzles guide the tube-side fluid into and out of the tubes. Since the tube-side fluid is often the more corrosive, these elements may be made out of alloy materials, or out of lowcarbon steel clad with alloy by weld deposition or detonation bonding. The channel covers bolt to the channels so that the tubesheet and tubes can be exposed for inspection without disturbing the tube-side piping. Alternatively, bonnets with flanged nozzles or threaded connections for the tube-side fluid may be used.

The last major component for most exchangers is the baffle array. The baffles serve two purposes: First, and most important, the baffles support the tubes against bending and vibration; second, they guide the flow back and forth across the tube field to improve heat transfer rate (and increase pressure drop as a consequence). Segmentally cut baffles (as shown in Fig. 2) are the most common geometry, but others (described in Sec. 4.2) are used for special purposes. The main requirement is that all tubes be adequately supported, and that successive baffles overlap at least one full tube row to give the entire bundle rigidity.

Other essential construction components for some or all shell-and-tube exchangers include tie rods, spacers, sealing strips (or rods), and, of course, gaskets. Other

© 1983 Hemisphere Publishing Corporation

components are required for one or another of the major configurations discussed in Sec. 4.2.

D. Plate heat exchangers

There are at least three different configurations that fall into the category of plate heat exchangers, the common feature being that the heat transfer surface of each is constructed of thin metal plates more or less parallel to one another except as modified to prevent collapse of the channel under external pressure. One fluid flows through one set of channels and the other through the immediately adjacent channels. The three configurations are the plate-and-frame or gasketed plate exchanger (more commonly referred to simply as a plate heat exchanger), the spiral plate exchanger, and the lamella or Ramen exchanger. The first is by far the most widely used and is the subject of Sec. 3.7 in this handbook. All three are briefly discussed below.

(a) Plate-and-frame or gasketed plate exchanger

A typical exchanger of the plate-and-frame type is shown in Fig. 3. It comprises a set of formed plates held together in a frame that compresses the gaskets around the edges to prevent leakage to the outside. Gasketing around the ports controls which channels a given fluid can flow into and then across the plates. A wide range of parallel, series, and mixed flow arrangements is possible to match the flow rates, thermal capacitances, and temperature-range requirements of the two streams.

The plates are very thin and must have many points of contact with adjacent plates to withstand normal operating pressure. An embossed herringbone pattern of ridges and valleys is most commonly used to provide these multiple points of support, adjacent plates having the herringbone pattern reversed. Where the two patterns cross, a contact point is formed. The repeated contraction and expansion and change of direction of the flow results in a strongly eddying flow giving high heat transfer rates, high pressure drop, and a high shear field, which tends to suppress fouling. A rectangular pattern of embossed contact points matching those on the adjacent plates is also sometimes used.

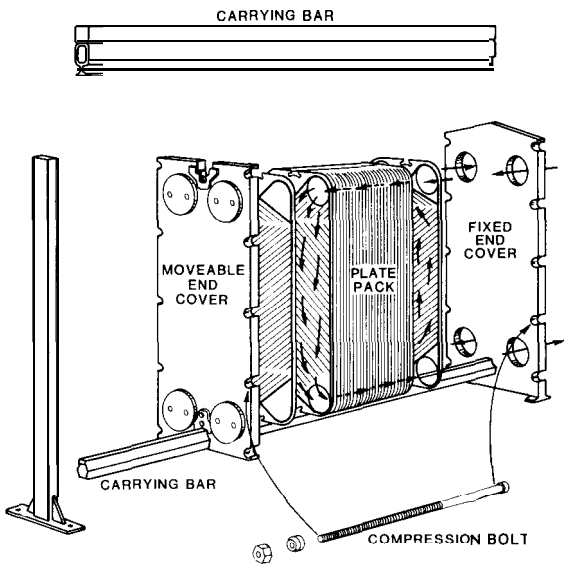

Figure 3 Exploded view of a gasketed plate heat exchanger.

These exchangers are relatively compact and lightweight heat transfer surfaces, making them attractive for use in confined or weight-sensitive locations such as on board ships and oil production platforms. The plates can be pressed from almost any metal (though low-carbon steel is almost never used because the plate exchanger is then not competitive with shell-and-tube exchangers). Pressures and temperatures are limited to comparatively low values because of the gasket materials and the construction.

Plate-and-frame heat exchangers are typically used for exchanging heat between two liquid streams in turbulent flow; even viscous liquids can be forced by the tortuous flow path into an effectively turbulent flow at low Reynolds numbers. Plate exchangers are occasionally used as condensers for fairly dense vapors (e.g., ammonia) or as vaporizers producing a lowquality vapor as for a reboiler. They are used in the food processing industry because they can be disassembled for cleaning and sterilization.

(b) Spiral plate heat exchanger

Several different versions of the spiral plate exchanger are shown in Fig. 4. This exchanger is formed by rolling two long, parallel plates into a spiral using a mandrel and then suitably welding the alternate edges of adjacent plates to form the channels. The plates are held apart by raised bosses on one of the plates. The open sides of the channels are sealed off against bypassing by cover plates (with gaskets) held in place by the bolted clamps around the periphery.

The spiral path followed by each of the fluids induces a secondary flow effective in increasing the heat transfer coefficient, especially in laminar flow, and in reducing fouling deposits. The version designed for in-column mounting with one set of channels open to the vapor is useful for condensation, providing a reflux stream without taking the vapor outside the column. Product withdrawal can be accomplished by an open trough mounted on the column wall with a drain or pump-out to product storage.

(c) Lamella (Ramen) heat exchanger

The Ramen or lamella heat exchanger, Fig. 5, consists of a set of parallel, welded thin channels placed longi-

© 1983 Hemisphere Publishing Corporation

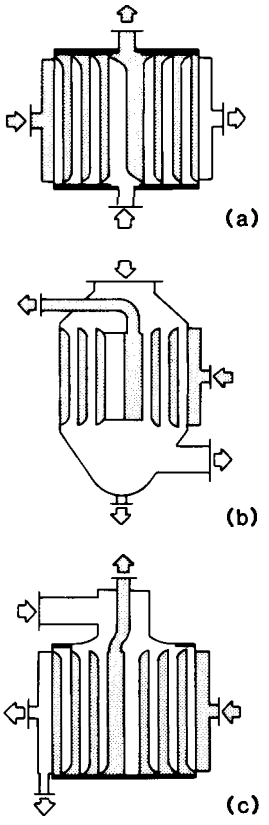

Figure 4 Schematic diagrams of three types of spiral plate heat exchangers.

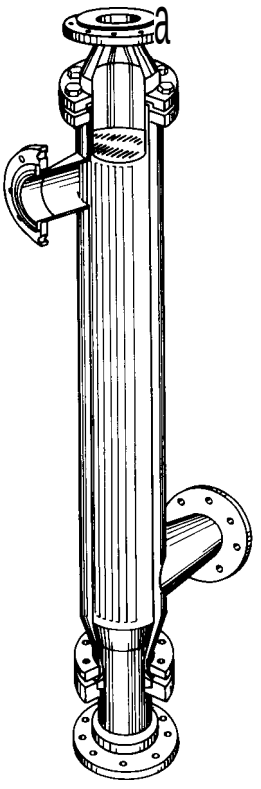

Figure 5 Ramen (lamella) plate heat exchanger.

tudinally in a shell. The channels are welded into "tube-sheets at each end and the plate bundle allowed to expand and contract independently of the shell by the use of a packing gland at the lower end. The shell-side flow is between and around the plates. The plates are supported against the pressure differential by matching longitudinal grooves rolled in each plate; these can be seam- or spot-welded together to support the plates against high internal pressures. The plate bundle can be easily removed from the shell for inspection and cleaning of the shell side.

E. High-finned or air-cooled heat exchangers

The atmosphere is being increasingly used as an ultimate heat sink, and the poor thermal-hydraulic properties of atmospheric air call forth special heat exchanger configurations for this purpose. Because of the low density, an enormous volume of air must be moved simply to satisfy the heat balance requirement. But the usual equipment for moving large quantities of air-axial-flow fans-is capable of producing only a very small pressure rise (maximum near 250 N/m^2), and this limits the air to low velocities (around 10 m/s maximum) and short flow paths. The low velocity, combined with the low density and thermal conductivity, results in low heat transfer coefficients (50-100 W/m^2 K) on the air side.

Since the heat transfer coefficient of the other fluid (on the tube side) is typically 10-200 times as great, there is very strong incentive to use a heat transfer surface with a high ratio of area in contact with the air to the area in contact with the other fluid. The high-finned tube shown in Fig. 6 meets this requirement, offering 1.5-25 times as much area on the finned surface as on the inside surface. The fins, usually aluminum, may be simply wound in tension in shallow grooves on the outside surface of the tube, which may be any metal required for corrosion resistance. This, however, leaves the tin-to-tube bond subject to deterioration by corrosion, with a possible serious loss of thermal efficiency. A better design is to wrap the fin on with an L-shaped foot providing better contact with the tube and better protection from the atmosphere.

Integral fins, where the fins are upset from a thick aluminum tube wall by successive machining steps,

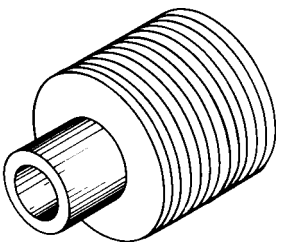

Figure 6 Typical high-finned tube used in air-cooled heat exchangers.

© 1983 Hemisphere F blishing Corporation

eliminate the atmospheric corrosion problem. A liner tube of any required metal can be provided for the tube-side fluid, with an interference fit between the liner and the finned tube. There are temperature limitations on all finned tube types, above which the bond between the fin and base tube or liner deteriorates badly producing a contact resistance. There is a fin efficiency factor that must be applied to correct for the temperature drop due to heat conduction in the fin.

The basic configuration of an air-cooled heat exchanger is a large, shallow (3-12 tube rows) bank of high-finned tubes, across which air is blown or drawn by large-diameter, relatively low-speed fans. The flow arrangement may be either forced draft, Fig. 7*a*, or induced draft, Fig. 7b.

The forced-draft arrangement has the advantage of keeping the fan and driver in cooler air, resulting in higher fan efficiency, possibly less expensive fan materials, simpler support for fan and driver, and less frequent and easier maintenance. However, the air flow across the tube bank is very nonuniform, and the low-velocity hot-an plume may be more easily recirculated back into the heat exchanger, causing a loss of temperature difference. The induced-draft arrangement gives a high-velocity, well-defined plume that is much less likely to be recirculated. The shroud also protects the tube field against physical damage and operational upsets by sudden strong rain and hail storms.

F. Plate fin or matrix heat exchangers

Plate fin or matrix heat exchangers represent about the most compact form of heat transfer surface, at least in the usual case that the fluids must be kept separated. These exchangers are constructed of multiple layers of matrix or sandwich -folded metal sheets, separated by parting sheets, as shown in Fig. 8. Fluid entry and exit into these layers is controlled by the manifolds, with a solid bar being used to prevent entry of one fluid into the channels for the other fluid. More than two fluids can be handled in a single exchanger by suitable arrangement of the manifolds.

The core of matrix, parting sheets, and side bars is laid up by hand, clamped firmly in a jig, and then brazed

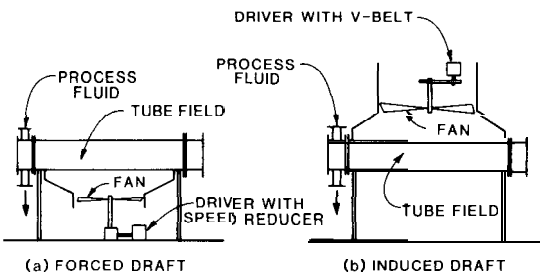

Figure 7 (a) Forced-draft and (b) induced-draft arrangements of air-cooled heat exchangers.

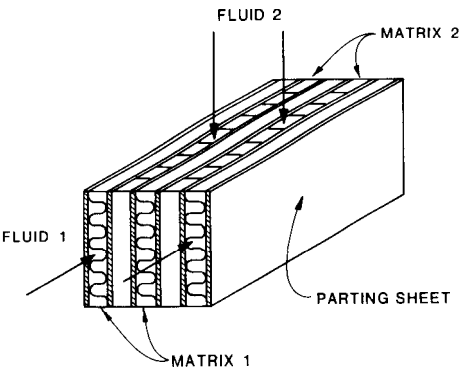

Figure 8 Section of a plate fin exchanger.

into a rigid structure, either in a molten salt bath or in a vacuum furnace. The result is a strong, rigid structure of extremely high volumetric heat transfer surface density. However, the units are limited in overall size and materials of construction (aluminum is the usual material) and cannot be cleaned mechanically. The most common area of application is in cryogenic processing such as liquefied natural gas production, hydrogen purification, and helium separation and liquefaction. Section 3.7 describes the design and construction of these units in greater detail.

G. Mechanically aided heat exchangers

Some heat transfer problems require mechanical action at or near the heat transfer surface in order to achieve reasonable heat transfer rates. This mechanical action can be achieved in two different, though related, classes of equipment: stirred-tank and scraped-surface, shown respectively in Figs. 9 and 10.

In the stirred-tank equipment, the mechanical action is imparted to the bulk of the fluid in the tank by a rotating blade or screw device usually located at the center of the tank. Anchor agitators, bladed impellers, and helical flights are among the mechanical

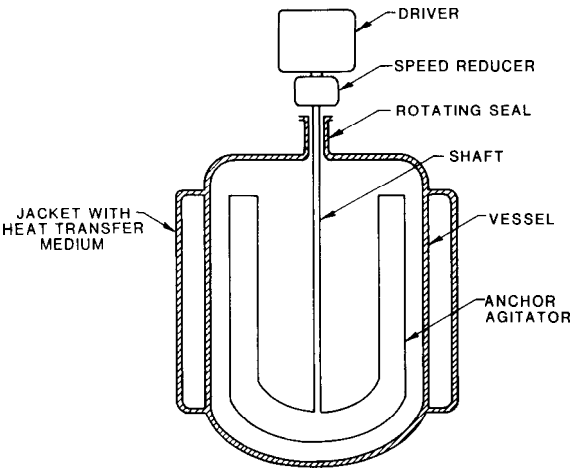

Figure 9 Diagram of a stirred tank with an anchor agitator.

© 1983 Hemisphere Publishing Corporation

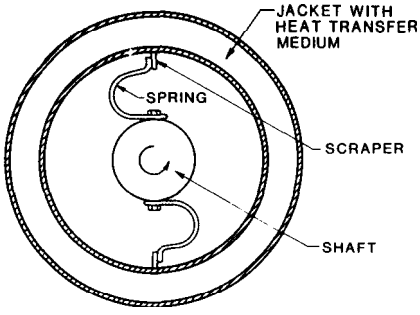

Figure 10 Cross section of a scraped-surface heat exchanger with a spring-loaded blade.

devices used. The heat transfer surface may be the inner surface of the tank, with the second fluid in a jacket or welded-on channels on the outer surface. Alternatively, the heat transfer surface may be provided inside the tank by a coiled tube, tube banks or bundles, or channeled plates, placed near the periphery of the tank. Occasionally, the heat transfer surface is provided by the agitator itself, with the second fluid flowing in channels in the agitator; the rotating seals required to get the second fluid in and out of the agitator pose some difficulties.

Stirred tanks are commonly used for carrying out chemical reactions of various kinds, including polymerization, and the main design features of the tank and agitator may be controlled more by reaction kinetics considerations than heat transfer. Nonetheless, it is usually vital to transfer heat in or out (sometimes both, at different points in the processing cycle) at the desired rates. The multiplicity of designs and applications makes it difficult to devise universally applicable design correlations, and pilot-plant testing is commonly resorted to. The problem of design is discussed further in Sec. 3.14.

Scraped-surface equipment is characterized by having the blade very close to or actually contacting the heat transfer surface, which is the inner surface of a cylindrical tank or pipe. The blade action causes intense shearing of the fluid layers immediately adjacent to the wall, resulting in locally high heat transfer rates. The blades may be fixed, spring-loaded, or hinged so that the centrifugal action forces the blade against the wall.

Scraped-surface equipment is used only for very difficult heat transfer applications: heating or cooling very viscous materials, evaporation and concentration of food products, and fractional crystallization (in which the blade function is primarily to prevent the growth of a thick layer of crystals on the wall). The equipment is heavy, bulky, expensive, and requires frequent maintenance and constant power input. It is also usually the only way to solve those heat transfer problems to which it is put. Further design considerations and methods are given in Sec. 3.14.

H. Other types of process heat exchangers

The major classes of process heat exchangers have been described above, but this listing by no means exhausts the possibilities. Many specialized configurations are commercially available, and more than one device has been jury-rigged to meet a special or urgent need. Not surprisingly, design of such equipment is in a rather uncertain state.

In those cases in which the equipment geometry is a combination of common elements such as constant-cross-section channels or tube banks, the basic correlations of Part 2 of this handbook can be used to estimate performance. In other cases, the manufacturer of the equipment has design methods and applications data that can be used. In some cases, only actual testing of scale- or full-sized equipment will allow the designer to incorporate these items into the plant with confidence.

© 1983 Hemisphere Publishing Corporation

3.1.3
Logic of the design process

Kenneth J. Bell

A. Criteria for a successful heat exchanger design

Any discussion of the design process for heat exchangers must be based on a clear understanding of the criteria by which the heat exchanger will be judged. These criteria are simple to state in broad principle, but the apparent simplicity can be very misleading when the designer or customer actually attempts to apply them to a specific case. The principles are given below in an approximate order of importance, with a few examples of how the principles must be elaborated in practice.

First, it may be pointed out that there are two broad classifications of heat exchanger application, and they call into being quite different philosophies and procedures for their design and production. Undoubtedly the greater amount of heat transfer surface in existence is in units of which there are many replicates-automotive radiators, domestic and commercial air conditioners and furnaces, engine oil coolers, and so on. For these units, production runs of thousands and even millions of nominally identical units are common. The design process for this class is modified by the opportunity– indeed, the economic compulsion-to build a number of variant candidate units and test these extensively over the range of conditions expected, ultimately selecting the best design and thenceforth attempting to build myriads more as close to the prototype as possible.

Contrast this with the typical heat exchanger found in a chemical or petroleum plant: a one-off design (duplicate items are usually intended to be used in series or parallel with one another), with no opportunity for testing until the plant becomes operational. Frequently these heat exchangers are to be used with streams whose compositions, properties, and fouling characteristics are poorly known and which, together with the flow rates and process specifications, may vary from day to day. Clearly this situation places greater demands on the design process if there is to be a high probability of success. This part of the handbook tends to emphasize design for the second case.

The first criterion that a heat exchanger should satisfy is the fulfillment of the process requirements: to accomplish the thermal change on the streams within the allowable pressure drops, and to retain the capability to do this in the presence of fouling until the next scheduled maintenance period. However, it must be recognized that the design process is fraught with uncertainties: The physical properties are seldom known to a high degree of precision, the design methods incorporate basic correlations of various degrees of experimental scatter, the exchangers are constructed only within certain dimensional limits, the actual operating conditions and process stream characteristics vary from day to day, and the fouling characteristics are little more than guesses and vary with time in any case. Therefore, meeting process requirements is at best only a matter of statistical probability. At this point, too little is known about either the statistics of individual units or their interaction in heat exchanger trains and with other process plant components to allow for a quantitative treatment. (Some indication of a possible approach to the problem is given in [1].) Hence, the designer must assure himself of a reasonable probability of success by judicious overdesign and by taking advantage of the operational flexibilities and reserve capacity inherent in the rest of the plant.

© 1983 Hemisphere Publishing Corporation

The second criterion is that the heat exchanger must withstand the service conditions of the plant environment. The immediate consideration here is the mechanical stresses, not only in normal operation but in shipping, installation, startup, shutdown, and off-specification operation caused by plant upsets and conceivable accidents. There are external mechanical stresses imposed by the piping on the exchanger by both steady state and transient flow and temperature variations of the streams. The exchanger must resist corrosion by the service and process streams and by the environment; this is mostly a matter of proper materials selection, but mechanical design does have some effect. If possible, the exchanger should resist fouling, but the designer s role here is usually limited to keeping the velocities as high as pressure drop and erosion and vibration limits allow and making sure that the fouled surfaces can be reached for cleaning.

Third, the exchanger must be maintainable, which usually means choosing a configuration that permits cleaning as required and replacement of tubes, gaskets, and any other components that are especially vulnerable to corrosion, erosion, vibration, or aging. This requirement may also place limitations on positioning the exchanger and providing clear space around it.

Fourth, and directly consequent upon the second and third criteria, the designer should consider the advantages of a multishell arrangement with flexible piping and valving provided to allow one unit to be taken out of service for maintenance without severely upsetting the rest of the plant. Condensing and cooling services in particular will benefit from an operational standpoint if one or more units can be taken off-stream in the winter, or if effluent coolant can be recycled to temper the very cold incoming coolant.

Fifth, the exchanger should cost as little as possible, consistent with the above criteria being satisfied. Balanced against possible savings in first cost, however, must always be the consideration that the cost of production lost because of an undersized or unreliable exchanger will eat up any possible savings on the exchanger first cost in a few hours or days.

Finally, there may be limitations on exchanger diameter, length, weight, and/or tube specifications due to site requirements, lifting and servicing capabilities, and maintaining an inventory of replacement tubes and gaskets.

A heat exchanger should never be designed with the idea that it can be used in other services if it doesn t work well in the design case. Most heat exchangers are intended for projects having an expected life equal to or greater than the life of the exchanger. To suggest that a heat exchanger might become available sooner implies that either the exchanger or the process is not going to work. It is far better to labor under the positive compulsion that the best hope of success for both exchanger and process is to design each item uniquely for the best performance in the task at hand.

B. Relationship among selection, rating, and design

There is a distinction to be made among the terms selection, rating, and design of a heat exchanger. Though often used interchangeably, these terms refer to quite different aspects of the heat exchanger specification problem and its solution.

Selection means choosing a heat exchanger from among a number of units already existing, or capable of being made on very short notice. Typically, these are standard units listed in catalogs of various manufacturers and available essentially off the shelf. Very few options are available, though the same design may be available in all-low-carbon steel, all-stainless, or with stainless steel tubes, tubesheets and tube-side fittings with a carbon steel shell, for example. Sufficient manufacturer s data usually exist to allow one to select a comfortably oversized exchanger with respect to both area and pressure drop. Unit cost is low because of the standardized manufacturing techniques and minimal engineering required, and delivery is fast. However, as one goes to large units (typically above 10 or 20 m^2 of surface) with special requirements, the economics moves in favor of units specifically constructed to meet the particular needs of the service, and one must talk in terms of rating and design as compared to selection.

Rating is the computational process by which one determines the thermal performance and pressure drops if two specified streams are introduced into an essentially completely defined heat exchanger. The rating procedure is drawn schematically in Fig. 1, taking the inlet flow rates and temperatures, the fluid properties (including phase equilibrium data, if phase change is involved), and the heat exchanger parameters as input. The rating program calculates either the outlet temperatures and thermal duty (if the exchanger length is specified) or the required length of the heat exchanger to accomplish the thermal change. In either case, the rating program will also calculate the pressure drop of each stream.

The rating program may be either a hand method (suitable for calculation using a slide rule or a simple electronic calculator) or a computer method (requiring a programmable computer ranging in size from one of the more sophisticated hand-held devices to the very large, extremely large-memory, high-speed scientific computers). Any hand method can be put on a large computer, but programs developed for a large computer in general cannot be considered for hand calculation.

If the exchanger configuration selected for rating gives (according to the calculations) acceptable thermal performance with pressure drops in both streams near but below the maximum allowable, this configuration

© 1983 Hemisphere Publishing Corporation

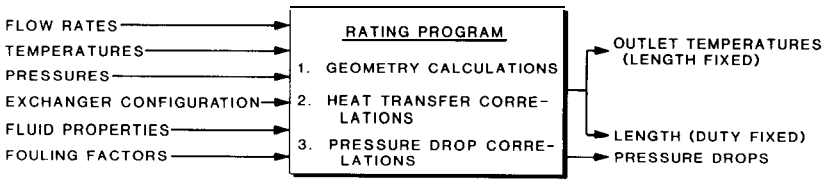

Figure 1 The rating program.

may be considered a solution to the problem. It is often possible to find a number of variant configurations that will meet these requirements; then the choice must be made on other criteria, usually first cost. (But other considerations such as reliability, maintainability, and flexibility may be much more critical, especially in the eyes of the plant operator, who is charged with getting out production.)

Usually, however, the exchanger chosen for rating is found to be deficient in one or another of the requirements, and a new design must be chosen for rating the next time around. If, for example, the pressure drops are too high, some modification must be made to reduce them, usually implying a larger exchanger. On the other hand, if the pressure drops are much too low, the design can usually be changed to increase the pressure drops ***and the heat transfer coefficients,*** resulting in a smaller and generally less costly exchanger.

The process by which one moves from one design to a more satisfactory one can be called design modification, and its relationship to the total design process is shown in Fig. 2.

The critical logical feature of the design process is the design modification program, and it assumes two quite different forms depending on whether the design is being done by hand (and head) or by computer. If by hand, the design modification is largely intuitive, as the designer s mind identifies the particular deficiencies of the previously rated configuration and sorts out, from among the many possible changes, those that will relax the deficiencies while retaining the desirable features. In this case, experience and insight into the physical processes are critical to a rapid convergence to an acceptable design.

If, however, the design process is being carried out with a fully integrated computer program (and such programs exist for most of the major heat exchanger types and applications), the success of the process is critically dependent on the skill and care with which the design modification logic has been constructed. Rapid convergence to an acceptable design is less important than that there be no gaps in the logic through which the design modification program can leak out into a completely unrealistic choice of mechanical features. It is also important that the logical structure not close off possible design options by imposing a poorly framed test that cannot be passed. Even a modest-sized design program may have 40 separate logical decisions to be made, leading to $2^{40} = 1.1 \times 10^{12}$ different paths through the logic. It is manifestly impossible to test all of these a priori, so there is no substitute for great care and conservatism in framing these decision points.

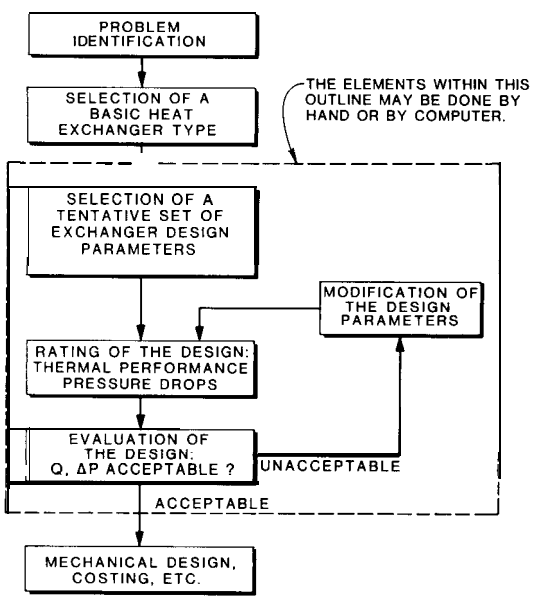

Figure 2 Basic logical structure for process heat exchanger design.

C. Simplified example of a design modification algorithm for a computer

A very simple but illustrative configuration modification program is diagrammed in Fig. 3. In this particular program, it is assumed that the duty of the exchanger has been specified and the length required for the exchanger has been calculated by the rating program. It is also assumed that the rating program has as its initial output the length of the largest diameter acceptable shell, the fewest tube passes consistent with the shell configuration, and the greatest allowable baffle spacing permitted by mechanical construction standards. (The quantities with asterisks are the maximum allowable values of that parameter as specified in the input data.) This choice results in the lowest possible pressure drops in a single-shell, thermally acceptable exchanger.

The first question that arises is this: Is the length calculated by the rating program less than the maximum allowable length of the exchanger that can be accommo-

© 1983 Hemisphere Publishing Corporation

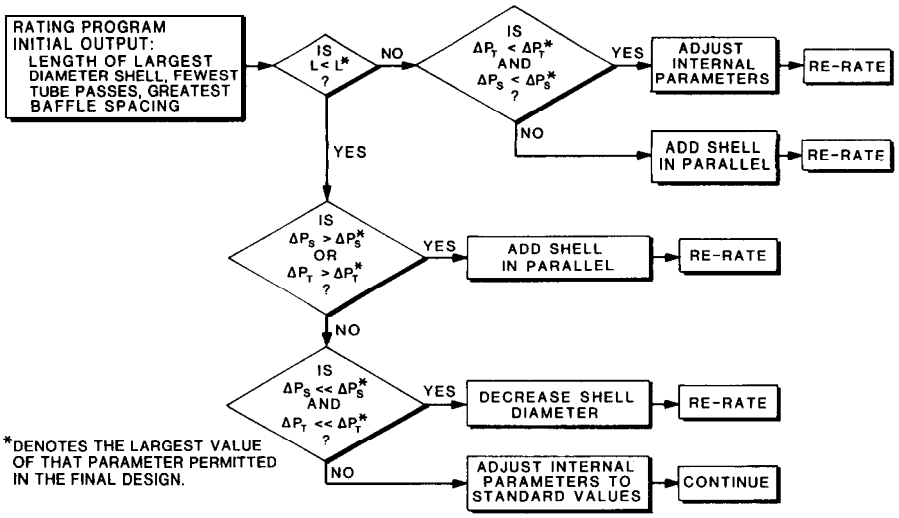

Figure 3 A schematic configuration modification program (highly simplified and truncated).

dated? If the answer to this question is no, then it is necessary either to add another shell in parallel to accommodate the flow, or to adjust internal parameters in the heat exchanger in order to increase that heat transfer coefficient and also the pressure drop. The decision between these two choices is made on the basis of the calculated pressure drops. If either pressure drop is too large, there is no alternative but to add another shell in parallel, splitting the flow and reducing the pressure drops as well as increasing heat transfer surface. Then the program must return to the rating program to compute the new length and pressure drops for the same shell with the reduced flow per shell. If at least one pressure drop is substantially below the allowable value, it may be possible to adjust one or more of the internal parameters (such as baffle spacing or number of tube side passes) to increase the overall heat transfer coefficient to a high enough value to give $L < L^*$ on a subsequent rerating. The exact choice and sequence of adjustments to try is part of the design modification subroutine alluded to above and is a very elegant piece of logic. It is of course quite possible that no choice of internal parameters will satisfy all requirements and in that case the program must default to the other leg of the decision tree and add another shell after all.

If, on the other hand, the length of the exchanger is calculated to be less than the maximum allowable length (i.e., $L < L^*$), it is necessary to determine first whether the pressure drop limitations have been exceeded. If either pressure drop limitation is exceeded, it is necessary to add a shell in parallel and rerate the new configuration. If both of the pressure drops are very much less than those allowed, it is probable that it will be possible to decrease the shell diameter one size and come up with a smaller and less expensive exchanger than the one previously rated. If the pressure drops calculated are close to but less than those allowed, then the exchanger designed is very close to the smallest acceptable exchanger (i.e., which will meet all of the operational requirements.) One then adjusts the design parameters to standard values for exchanger design and continues with the rest of the program, including mechanical design and cost estimation.

REFERENCE FOR SECTION 3.1.3

1. Al-Zakri, A. A., and Bell, K. J., Heat Transfer: Estimating Performance When Uncertainties Exist, *Chem. Eng. Prog.*, vol. 77, no. 7, pp. 39–49, 1981.

© 1983 Hemisphere I blishing Corporation

3.1.4

Approximate sizing of shell-and-tube heat exchangers

Kenneth J. Bell

■ In the previous section, the need for a preliminary estimate of the heat exchanger size and configuration was indicated. This estimate is essential for a hand design method and useful for a computer design. Additionally, there are occasions-preliminary estimates of plant cost, layout, and space requirements, for example-when a good approximate size estimate is sufficient and more quickly available than a detailed design. Eventually, if the plant is to be built, the detailed calculations will have to be done, but that task can profitably wait until the preliminary studies have ascertained if the plant looks economically promising and have given a definite idea of how the components are to be arranged.

In this section, a preliminary design method is presented in some detail. This method covers many of the usual process applications for shell-and-tube exchangers, and it can be extended with care and insight to other cases. The accuracy of the method is strongly dependent on the skill of the user in estimating or selecting appropriate heat transfer coefficient values; in this there is no substitute for experience, although Table 2 may be helpful.

A. The basic design equation

The basic design equation to be used in this section is

$$A_o = \frac{Q_T}{U_o F \Delta T_{LM}} = \frac{Q_T}{U_o \Delta T_M} \qquad 3.1.1(8)$$

where A_o is the total heat transfer area required in the exchanger, m^2 (calculated based on the outside diameter of the tube); Q_T is the heat duty of the exchanger, W or J/s; U_o is the overall heat transfer coefficient, W/m^2 K (also based on the outside diameter of the tubes); ΔT_{LM} is the logarithmic mean temperature difference calculated for countercurrent flow, K; and F is the configuration correction factor. Each of these terms will be discussed in greater detail below.

It should be noted that the validity of Eq. 3.1.1(8) is dependent on a number of assumptions, as listed in Sec. 3.1.1. These conditions are often not met exactly, and in principle, a more elaborate formulation, Eq. 3.1.1(4), is required. However, that completely defeats the purpose of this procedure, and moreover, most of these departures from ideality introduce errors smaller than the probable error in the other approximations made in the method.

B. Estimation of heat load

The heat load is calculated in the general case from

$$Q_T = M_h(h_{h,\text{in}} - h_{h,\text{out}}) = \dot{M}_c(h_{c,\text{out}} - h_{c,\text{in}}) \qquad (1)$$

where $\dot{M}_h$ and $\dot{M}_c$ are the mass flow rates (in kg/s) of the hot and cold fluids, respectively, and $h_{h,\text{in}}$, $h_{h,\text{out}}$, $h_{c,\text{in}}$, and $h_{c,\text{out}}$ are the specific enthalpies (in J/kg) of the hot and cold streams, in and out, respectively.

If both streams are transferring heat without change of phase, Eq. (1) may be written as

$$Q_T = M_h c_{ph}(T_{h,\text{in}} - T_{h,\text{out}}) = \dot{M}_c c_{pc}(T_{c,\text{out}} - T_{c,\text{in}}) \qquad (2)$$

where c_{ph} and c_{pc} are the specific heats (in J/kg K), $T_{h,\text{in}}$ and $T_{h,\text{out}}$ are the inlet and outlet temperatures of the hot stream (K), and $T_{c,\text{in}}$ and $T_{c,\text{out}}$ are the inlet and outlet temperatures of the cold stream. If one of the

© 1983 Hemisphere Publishing Corporation

streams is an isothermal phase-change stream (such as condensing steam),

$$Q_T = \dot{M}\,\Delta h \qquad (3)$$

where $\dot{M}$ is the mass of the stream changing phase per unit time (kg/s) and Ah is the latent heat of the phase change (J/kg).

More complex cases such as partial condensers require more elaborate analysis than space permits, though the present method can be applied (with care!) to obtain at least rough estimates.

C. Estimation of the mean temperature difference

The first step in calculating the mean temperature difference (ΔT_M) is to find the logarithmic mean temperature difference (ΔT_{LM}) for counter-current flow. Using the temperatures defined in the previous section,

$$\mathrm{AT}_{,,} = \frac{(T_{h,\,\mathrm{in}} - T_{c,\mathrm{out}}) - (T_{h,\,\mathrm{out}} - T_{c,\mathrm{in}})}{\ln\{(T_{h,\mathrm{in}} - T_{c,\mathrm{out}})/(T_{h,\mathrm{out}} - T_{c,\mathrm{in}})\}} \qquad 3.1.1(6)$$

For many purposes, the LMTD can be sufficiently approximated by the arithmetic mean temperature difference (AMTD), thereby avoiding the need even for a calculator:

$$\Delta T_{AM} = \tfrac{1}{2}[(T_{h,\mathrm{in}} - T_{c,\mathrm{out}}) + (T_{h,\mathrm{out}} - T_{c,\mathrm{in}})] \qquad (4)$$

ΔT_{LM} is always equal to or less than ΔT_{AM}. The difference between the LMTD and AMTD increases with decreasing ratio of the smaller temperature difference to the larger. The ratio is given in Table 1.

Values of F can be found in Sec. 1.5 for a variety of heat exchanger flow configurations. However, for estimation purposes, a reasonable estimate may often be obtained without resorting to the charts:

Table 1 Ratio of LMTD and AMTD as a function of (smaller terminal temperature difference/larger terminal temperature difference)

$(T_{h,\mathrm{in}} - T_{c,\mathrm{out}})/(T_{h,\,\mathrm{out}} - T_{c,\mathrm{in}})$	$\Delta T_{LM}/\Delta T_{AM}$
1.00	1 .ooo
0.70	0.990
0.50	0.962
0.40	0.935
0.30	0.894
0.20	0.828
0.15	0.779
0.10	0.711
0.05	0.604
0.01	0.426

[a] If $(T_{h,\,\mathrm{in}} - T_{c,\,\mathrm{out}}) < (T_{h,\mathrm{out}} - T_{c,\,\mathrm{in}})$. Otherwise, use the reciprocal.

1. For a single tube pass, purely counter-current heat exchanger, $F = 1.0$.

2. For a single shell with any even number of tube-side passes (a $1\text{-}2n$ exchanger), F may be estimated as 0.9, the average of the maximum possible value, 1.0, and the minimum recommended value, 0.8.

This value may be shaded higher if the ratio of the (counter-current) terminal temperature differences is near unity and lower if the outlet stream temperatures are similar. In the latter case-and more especially if there is a temperature cross (i.e., if the cold stream outlet temperature is higher than the hot stream outlet temperature)-the thermodynamic feasiability of the design should be checked before proceeding further. Absolute limits that may be quickly checked are

$2T_{h,\mathrm{out}} \geqslant T_{c,\mathrm{in}} + T_{c,\mathrm{out}}$ hot fluid on shell

$2T_{c,\,\mathrm{out}} \leqslant T_{h,\mathrm{in}} + T_{h,\mathrm{out}}$ cold fluid on shell

If these limits are approached, it is necessary to use multiple l -2n shells in series.

3. There is a rapid graphic technique for estimating a sufficient number of shells in series. The procedure is shown in Fig. 1 and goes as follows:

The terminal temperatures of the two streams are plotted on the ordinates of ordinary arithmetic graph paper, the hot fluid inlet temperature and the cold fluid outlet temperature on the left-hand ordinate and the hot fluid outlet and cold fluid inlet temperature on the right-hand ordinate. The distance between the ordinates is arbitrary (corresponding to the total amount of heat exchanged between the two streams) and may be chosen at the convenience of the user.

If the specific heat of each stream is constant, straight lines (operating lines) are drawn from the inlet to the outlet temperature point for each stream. If the specific heat of one or both streams varies, it is necessary to calculate the temperature of that stream as

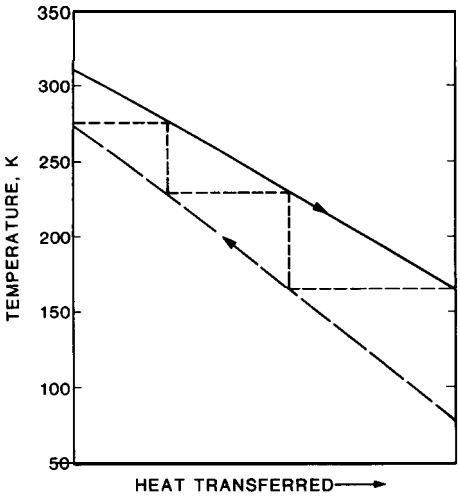

Figure 1 Estimation of required number of shells in series.

© **1983** Hemisphere **Publishing** Corporation

a function of the amount of heat added or removed by the other, resulting in one or both operating lines being curved. In this case, the procedure given here for finding a sufficient number of shells in series will still be valid. However, an additional error will be introduced into the estimation procedure for heat exchanger area, the magnitude depending on the curvature of the lines and the variation in U_o.

Starting with the cold fluid outlet temperature (275 K in Fig. 1), a horizontal line is laid off until it intercepts the hot fluid line. From that point a vertical line is dropped to the cold fluid line (reaching it in this example at a cold fluid temperature of 228 K). This operation defines a heat exchanger configuration in which the hot fluid temperature is never less than any temperature reached by the cold; that is, there is no temperature cross, and no thermodynamic difficulty can arise if this operation is carried out in one shell.

The process is repeated until a vertical line intercepts the cold fluid operating line at or below the cold fluid inlet temperature. (Alternatively, the process is continued until a horizontal line crosses the right-hand ordinate.)

The number of horizontal lines (including the one that intersects the right-hand ordinate) is equal to the number of shells in series that is clearly sufficient to perform the duty. In the case of the example problem, this number is three.

Following the above procedure will usually result in a number of shells having an overall F close to 0.8.

D. Estimation of U_o

The step with the greatest uncertainty in preliminary calculations is estimating the overall heat transfer coefficient. Tables of u s typical of various services are widespread; the drawback to their use is that, in trying to include the entire range ever encountered in practice, these tables give a spread of values so great as to be almost meaningless for reasonably close design.

A better procedure is to build up the value of U_o from the individual α values, and wall and fouling resistances, using Eq. (4):

$$U_o = 1/[(1/\alpha_0) + R_{fo} + (\Delta x_w/\lambda_w)(A_o/A_m) + (R_{fi} + 1/\alpha_i)(A_o/A_i)(1/E_f) \quad (5)$$

where Ax, is the wall thickness and A, is the effective mean wall heat transfer area, which is acceptably approximated by the arithmetic mean, using the outside and inside radii, r_o and r_i:

$$A, = \pi L(r_o + r_i) \quad (6)$$

E_f is the fin efficiency if extended surface is used, and can be calculated using the methods of Sec. 2.1 of this handbook; for most process applications, E_f will be between 0.75 for fluids with high α_o and 0.95 for fluids with low α_o.

A table of α's for various process services is included here as Table 2. The values given are for plain tubes. They can usually be used with caution for low-finned tubes if the controlling resistance is placed on the shell side; the values should be reduced by 10-30% if the shell-side fluid is of medium or high viscosity, and by 50% if the shell-side fluid is of high viscosity and is being cooled. The values given are equally valid for both tube side and shell side if optimal shell-side design practices are used, and if normal tube-side velocities (l-2 m/s for liquids, 5-10 m/s for gases) are used.

Any such table must be used with judgment. For example, the table assumes that normally allowable pressure drops are available and used (see note *b* to Table 2). If much higher or lower pressure drops are specified, the effect on α can be estimated by the following argument.

The allowable pressure drop, Δp, is approximately related to the design velocity v by

$$\Delta p \propto v^{1.6-1.8} \quad \text{(turbulent flow)} \quad (7a)$$

$$\Delta p \propto v \quad \text{(laminar flow)} \quad (7b)$$

The heat transfer coefficients are approximately related to the velocity by

$$\alpha \propto v^{0.6-0.8} \quad \text{(turbulent flow)} \quad (8a)$$

$$\alpha \propto v^{0.3} \quad \text{(laminar flow)} \quad (8b)$$

Therefore, approximately,

$$\alpha \propto \Delta p^{0.4} \quad \text{(turbulent flow)} \quad (9a)$$

$$\alpha \propto \Delta p^{0.3} \quad \text{(laminar flow)} \quad (9b)$$

Typical fouling resistance for each stream are indicated in Table 2. These values must be used with especially great care, since they vary so widely with time and exact circumstances. Higher velocities and lower temperatures will usually result in lower fouling resistances than typical, and vice versa. Fouling also depends very strongly on the specific process; for example, a freshly separated butane stream may have negligible fouling resistance, whereas the same stream on recycle from a dehydrogenation process may give very serious fouling as a result of polymerization of the unsaturated compounds.

It will generally be found that one or at most two terms will dominate the value of U_o, and attention can be focused on these controlling values. It will usually be found that the range of reasonable values is far smaller than the range of possible values. It will also prove useful to make some estimate of the basic uncertainties in each value, that is, the uncertainty in the value that would still exist even if the best available correlation and physical properties were used. This will

© 1983 Hemisphere F blishing Corporation

Table 2 Typical film heat transfer coefficients for shell-and-tube heat exchangers

Fluid conditions		a, W/m² K[a, b]	Fouling resistance, m² K/W[a]
Sensible heat transfer			
Water[c]	Liquid	5 000-7 500	1 x 10⁻⁴-2.5 x 10⁻⁴
Ammonia	Liquid	6 000-8 000	o-1 x 10⁻⁴
Light organics[d]	Liquid	1 500-2 000	1 x 10⁻⁴-2 x 10⁻⁴
Medium organics[e]	Liquid	750-l 500	1.5 x 10⁻⁴-4 x 10⁻⁴
Heavy organicsf	Liquid,		
	Heating	250-750	2 x 10⁻⁴-1 x 10⁻³
	Cooling	150-400	2.x 10⁻⁴-1 x 10-a
Very heavy organics[g]	Liquid,		
	Heating	100-300	4 x 10⁻⁴-3 x 10⁻³
	cooling	60-150	4 x 10-4-3 x 10⁻³
Gas[h]	Pressure 100-200 kN/m² abs	80-125	O-l x 10⁻⁴
Gas[h]	Pressure 1 MN/m² abs	250-400	o-1 x 10⁻⁴
Gas[h]	Pressure 10 MN/m abs	500-800	o-1 x 10⁻⁴
Condensing heat transfer			
Steam, ammonia	Pressure 10 kN/m² abs, no noncondensables[i, j]	8 000-l 2 000	o-1 x 10⁻⁴
Steam, ammonia	Pressure 10 kN/m² abs, 1% noncondensables[k]	4 000-6 000	o-1 x 10⁻⁴
Steam, ammonia	Pressure 10 kN/m² abs, 4% noncondensables[k]	2 000-3 000	O-l x 10⁻⁴
Steam, ammonia	Pressure 100 kN/m² abs, no condensables[i, j, k, l]	10 000-15 000	o-1 x 10⁻⁴
Steam, ammonia	Pressure 1 MN/m* abs, no condensables[i, j, k, l]	15 000-25 000	o-1 x 10⁻⁴
Light organics[d]	Pure component, pressure 10 kN/m² abs, no non-condensables[i]	1 500-2 000	o-1 x 10⁻⁴
Light organics[d]	Pressure 10 kN/m² abs, 4% noncondensables[k]	750-l 000	o-1 x 10⁻⁴
Light organics[d]	Pure component, pressure 100 kN/m² abs, no non-condensable&	2 000-4 000	o-1 x 10⁻⁴
Light organics[d]	Pure component, pressure 1 MN/m² abs	3 000-7 000	o-1 x 10⁻⁴
Medium organics[e]	Pure component or narrow condensing range, pressure 100 kN/m² abs[m, n]	1 500-4 000	1 x 10⁻⁴-3 x 10⁻⁴
Heavy organics	Narrow condensing range, pressure 100 kN/m² abs[m, n]	600-2 000	2 x 10⁻⁴-5 x 10⁻⁴
Light multicomponent mixtures, all condensable[d]	Medium condensing range, pressure 100 kN/m² abs[k, m, o]	1 000-2 500	o-2 x 10⁻⁴
Medium multicomponent mixtures, all condensable	Medium condensing range, pressure 100 kN/m² abs[k, m, o]	600-l 500	1 x 10⁻⁴-4 x 10⁻⁴
Heavy multicomponent mixtures, all condensable[f]	Medium condensing range, pressure 100 kN/m² abs[k, m, o]	300-600	2 x 10⁻⁴-8 x 10⁻⁴
Vaporizing heat transfer[p, q]			
Water	Pressure < 0.5 MN/m² abs, $\Delta T_{SH,max}$ = 25 K	3 000-10 000	1 x 10⁻⁴-2 x 10⁻⁴
Water	Pressure > 0.5 MN/m abs, pressure < 10 MN/m² abs, $\Delta T_{SH,max}$ = 20 K	4 000-15 000	1 x 10⁻⁴-2 x 10⁻⁴
Ammonia	Pressure < 3 MN/m² abs, $\Delta T_{SH,max}$ = 20 K	3 000-5 000	1 N 10⁻⁴-2 X 10⁻⁴

(See *footnotes on page* 3.1.4-S.)

© 1983 Hemisphere Publishing Corporation

Table 2 Typical film heat transfer coefficients for shell-and-tube heat exchangers (Continued)

Fluid conditions		α, W/m² K[a, b]	Fouling resistance, m² K/W[a]
Light organics[d]	Pure component, pressure < 2 MN/m² abs, $\Delta T_{SH,max}$ = 20 K	1 000-4 000	1 x 10^{-4}-2 x 10^{-4}
Light organics[d]	Narrow boiling range[s], pressure < 2 MN/m² abs, $\Delta T_{SH,max} \simeq 15$ K	750-3 000	1 x 10^{-4}-3 x 10^{-4}
Medium organics[e]	Pure component, pressure < 2 MN/m² abs, $\Delta T_{SH,max}$ = 20 K	1 000-3 500	1 x 10-4-3 x 10^{-4}
Medium organics[e]	Narrow boiling ranges, pressure < 2 MN/m² abs, $\Delta T_{SH,max} \simeq 15$ K	600-2 500	1 x 10-4-3 x 10^{-4}
Heavy organics[f]	Pure component, pressure < 2 MN/m* abs, $\Delta T_{SH,max}$ = 20 K	750-2 500	2 x 10^{-4}-5 x 10^{-4}
Heavy organicsg	Narrow boiling range?, pressure < 2 MN/m² abs, $\Delta T_{SH,max} \simeq 15$ K	400-l 500	2 x 10^{-4}-8 x 10^{-4}
Very heavy organics[h]	Narrow boiling range[s], pressure < 2 MN/m² abs, $\Delta T_{SH,max} \simeq 15$ K	300-l 000	2 x 10^{-4}-1 x 10-s

[a] Heat transfer coefficients and fouling resistances are based on area in contact with fluid. Ranges shown are typical, not all-encompassing. Temperatures are assumed to be in normal processing range; allowances should be made for very high or low temperatures.

Allowable pressure drops on each side are assumed to be about 50-100 kN/m² except for (1) low-pressure gas and two-phase flows, where the pressure drop is assumed to be about 5% of the absolute pressure; and (2) *very* viscous organics, where the allowable pressure drop is assumed to be about 150-250 kN/m².

[c] Aqueous solutions give approximately the same coefficients as water.

[d] "Light organics" include fluids with liquid viscosities less than about 0.5 $\times 10^{-3}$ N s/m*, such as hydrocarbons through C_8, gasoline, light alcohols and ketones, etc.

[e] "Medium organics include fluids with liquid viscosities between about 0.5 X 10^{-3} and 2.5 X 10^{-3} N s/m², such as kerosene, straw oil, hot gas oil, absorber oil, and light crudes.

[f] "Heavy organics include fluids with liquid viscosities greater than 2.5 X 10^{-3} N s/m², but not more than 50 X 10^{-3} N s/m*, such as cold gas oil, lube oils, fuel oils, and heavy and reduced crudes.

[g] "Very heavy organics include tars, asphalts, polymer melts, greases, etc., having liquid viscosities greater than about 50 X 10^{-3} N s/m². Estimation of coefficients for these materials is very uncertain and depends strongly on the temperature difference, because natural convection is often a significant contribution to heat transfer in heating, whereas congelation on the surface and particularly between fins can occur in cooling. Since many of these materials are thermally unstable, high surface temperatures can lead to extremely severe fouling.

[h] Values given for gases apply to such substances as air, nitrogen, carbon dioxide, light hydrocarbon mixtures (no condensation), etc. Because of the very high thermal conductivities and specific heats of hydrogen and helium, gas-mixtures containing appreciable fractions of these components will generally have substantially higher heat transfer coefficients.

[i] Superheat of a pure vapor is removed at the same coefficient as for condensation of the saturated vapor if the exit coolant temperature is less than the saturation temperature (at the pressure existing in the vapor phase) and if the (constant) saturation temperature is used in calculating the mean temperature difference. But see note *k* for vapor mixtures with or without noncondensable gas.

[j] Steam is not to be condensed on conventional low-finned tubes; its high surface tension causes bridging and retention of the condensate and a severe reduction of the coefficient below that of the plain tube.

[k] The coefficients cited for condensation in the presence of noncondensable gases or for multicomponent mixtures are only for very rough estimation purposes because of the presence of mass transfer resistances in the vapor (and to some extent, in the liquid) phase. Also, for these cases, the vapor-phase temperature is not constant, and the coefficient given is to be used with the mean temperature difference estimated using vapor-phase inlet and exit temperatures, together with the coolant temperatures.

[l] As a rough approximation, the same relative reduction in low-pressure condensing coefficients due to noncondensable gases can also be applied to higher pressures.

[m] Absolute pressure and noncondensables affect condensing coefficients for medium and heavy organics in approximately the same proportion as for light organics. Because of thermal degradation, fouling may become quite severe for the heavier condensates. For large fractions of noncondensable gas, interpolate between pure component condensation and gas cooling coefficients.

Narrow condensing range implies that the temperature difference between dew point and bubble point is less than the smallest temperature difference between vapor and coolant at any place in the condenser.

[o] "Medium condensing range implies that the temperature difference between dew point and bubble point is greater than the smallest temperature difference between vapor and coolant, but less than the temperature difference between inlet vapor and outlet coolant.

[p] Boiling and vaporizing heat transfer coefficients depend very strongly on the nature of the surface and *the* structure of the two-phase

© 1983 Hemisphere Publishing Corporation

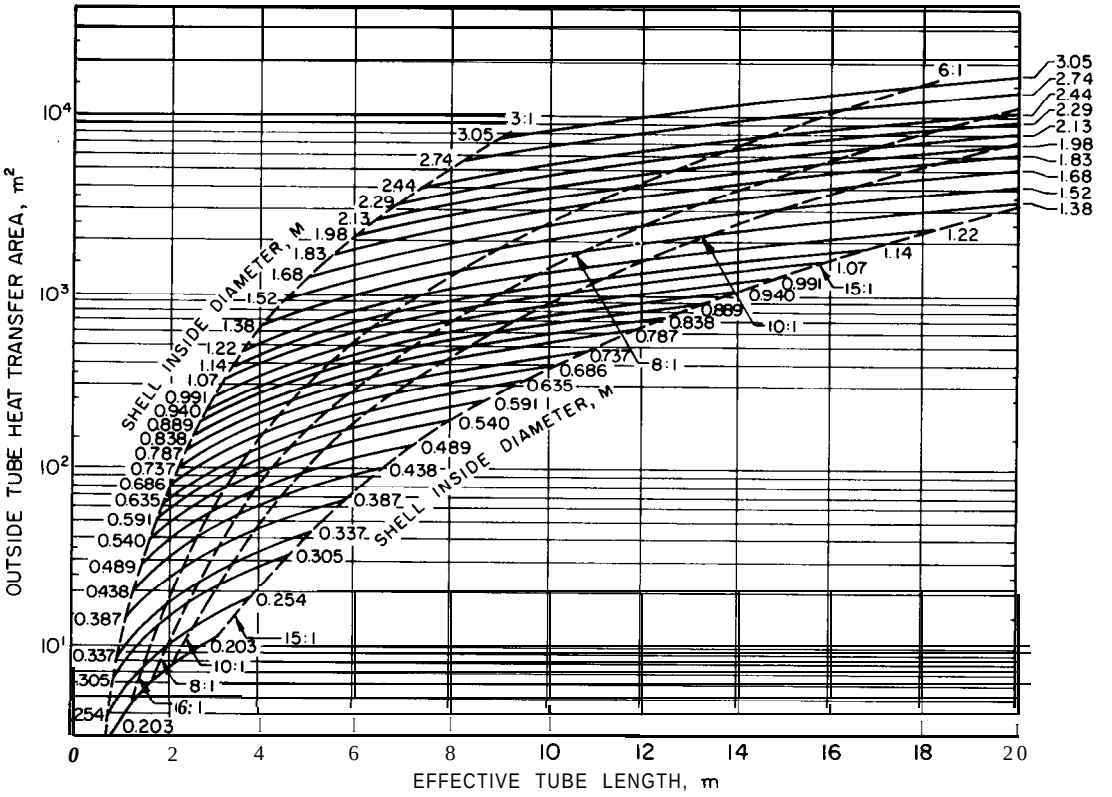

Figure 2 Heat transfer area as a function of shell inside diameter and effective tube length for $\frac{3}{4}$-in. equilateral triangular tube layout, fixed tubesheet, one tube-side pass, fully tubed shell.

often indicate clearly the futility of worrying too much about the precise value of a coefficient for preliminary design purposes.

E. Calculation of A,

Once $Q, \Delta T_M$, and U_o are known, the total outside heat transfer area (including fin area) A, is readily found from Eq. 3.1.1(8). The next question is, What set of heat exchanger dimensions will accommodate that heat transfer area? The following section presents a technique for answering that question.

F. Heat transfer area for a given shell diameter and length

Figure 2 is the key to relating the heat transfer area in a shell-and-tube exchanger to the shell inside diameter

flow past the surface in addition to all of the other variables that are significant for convective heat transfer in other modes. The flow velocity and structure are very much governed by the geometry of the equipment and its connecting piping. Also, there is a maximum heat flux from the surface that can be achieved with reasonable temperature differences between surface and saturation temperature of the boiling fluid; any attempt to exceed this maximum heat flux by increasing the surface temperature leads to partial or total coverage of the surface by a film of vapor and a ***sharp decrease*** in the heat flux.

Therefore, the heat transfer coefficients given in this table are only for very rough estimating purposes and assume the use of plain or low-finned tubes without special nucleation enhancement. $\Delta T_{SH,\max}$ is the maximum allowable temperature difference between surface and saturation temperature of the boiling surface. No attempt is made in this table to distinguish among the various types of vapor-generation equipment, since the major heat transfer distinction to be made is the propensity of the process steam to foul. Severely fouling streams will usually call for a vertical thermosiphon or a forced-convection (tube-side) reboiler for ease of cleaning.

[q] Subcooling heat load is transferred at the same coefficient as latent heat load in kettle reboilers, using the saturation temperature in the mean temperature difference. For horizontal and vertical thermosiphons, a separate calculation is required for the sensible heat transfer area, using appropriate sensible heat transfer coefficients and the liquid temperature profile for the mean temperature difference.

Aqueous solutions vaporize with nearly the same coefficient as pure water if attention is given to boiling-point elevation and if the solution does not become saturated and care is taken to avoid dry wall conditions.

[s] For boiling of mixtures, the saturation temperature (bubble point) of the final liquid phase (after the desired vaporization has taken place) is to be used to calculate the mean temperature difference. A narrow-boiling-range mixture is defined as one for which the difference between the bubble point of the incoming liquid and the bubble point of the exit liquid is less than the temperature difference between the exit hot stream and the bubble point of the exit boiling liquid. Wide-boiling-range mixtures require a case-by-case analysis and cannot be reliably estimated by these simple procedures.

© 1983 Hemisphere Publishing Corporation

and effective tube length. In this figure, the ordinate is A_o, in m^2, and the abscissa is the effective tube length (tubesheet to tubesheet for straight tube bundles, or length of a ***single*** straight section from tubesheet to tangent line for a U-tube bundle) in meters. The solid black lines in parameter are the commonly specified shell inside diameters in meters. Using standard tube count tables for 19.0-mm-OD tubes on a 23.6-mm triangular pitch for a fixed-tubesheet heat exchanger with one tube-side pass, the total outside tube heat transfer area that can be fitted into a shell has been calculated.

Therefore, once the required area A, is known, Fig. 2 shows immediately the combinations of tube length and shell diameter that will provide that area in a single shell for an exchanger of the given tube size and layout. A technique of applying Fig. 2 to other tube sizes, layouts, number of tube passes, and bundle/type will be given in the next section.

The dashed lines in parameter in Fig. 2 (marked 3: 1, 6: 1, etc.) show the approximate locus of shells having a given effective tube length-to-shell diameter ratio. Shells shorter than three times the shell diameter (3:1) may suffer from poor fluid distribution and excessive entry and exit losses, and are likely to be more expensive than a longer, smaller diameter unit of the same area, especially if the shell-side fluid is at high pressure. Shells longer than 15 times the shell diameter are likely to be difficult to handle mechanically, require a large clearway for bundle removal or retubing, and show the effect of diminishing returns on cost. Many heat exchangers fall into the 6:1 to 8:1 range, with a pronounced trend toward the higher values as pressure drop prediction procedures have improved.

G. Extension of Fig. 2 to other shell/bundle/tube geometries

Fig. 2 can be employed to estimate the required length and diameter of exchangers for other tube sizes and layouts, multiple tube-side passes, and bundle constructions. An effective area A'_o, is defined by

$$A_o = A_o F_1 F_2 F_3 \qquad (10)$$

where A'_o = the area on the ordinate of Fig. 2

A_o = the required outside area of a heat exchanger as calculated from Eq. 3.1.1(8)

F_1 = the correction factor for the unit cell tube array (= 1 .OO for 19.0-mm tubes on a 23.6-mm triangular pitch)

F_2 = the correction factor for the number of tube passes (= 1 .OO for one tube pass)

F_3 = the correction factor for the shell construction/tube bundle layout type (= 1 .00 for a fixed tubesheet)

Table 3 Values of F_1 for various tube diameters and layouts[a,b]

Tube outside diameter, mm	Tube pitch, mm	Layout	F_1
15.9	20.6	- a	0.90
15.9	20.6	→◇,□	1.04
19.0	23.8	→◁	1.00
19.0	23.8	→◇,□	1.16
19.0	25.4	- a	1.14
19.0	25.4	→◇,□	1.31
25.4	31.8	→◁	1.34
25.4	31.8	→◇,□	1.54

[a] F_1 = (heat transfer/cross-sectional area of unit cell)$_{reference}$/(heat transfer area/cross-sectional area of unit cell)$_{case}$.

[b] This table may also be used for low-finned tubing in the following way: The value stimated for U_o should be based on the total outside area (including fins) of the finned tube. This value will generally be somewhat less (10–30%) than the plain tube values given in Table 2. Then the required value of A, is based on the finned tube area, and the above values of ***F,*** are ***divided*** by the ratio of the finned tube area to the plain tube area (per unit length). Typically this value will be from 2.5 to 4.

Values of the correction factors are given in Table 3, Table 4, and Table 5. Some reiteration may be necessary because the correction factors change slightly with shell inside diameter.

It should be emphasized that use of this technique is approximate, especially for the smaller diameter shells.

H. Example problem

The use of the method can be best illustrated by an example.

High-pressure recycle gas (8.3 MN/m^2 abs with 40% hydrogen) is to be cooled from 560 to 395 K, heating a mixed liquid aromatics stream from 300 to 385 K. The gas flow rate is 48.0 kg/s, with a specific heat of 7 540 J/kg K, and the aromatic flow rate is 314 kg/s with a specific heat of 2 240 J/kg K.

Table 4 Values of F_2 for various numbers of tube-side passes

Inside shell diameter, m	Number of tube-side passes			
	2	4	6	8
up to 0.305	1.20	1.40	1.80	
0.337-0.438	1.06	1.18	1.25	1.50
0.489-0.591	1.04	1.14	1.19	1.35
0.635-0.838	1.03	1.12	1.16	1.20
0.889-1.14	1.02	1.08	1.12	1.16
1.22-1.52	1.02	1.05	1.08	1.12
Above 1.52	1.01	1.03	1.04	1.06

[a] Since U-tube bundles must always have at least two passes, use of this table is essential for U-tube bundle estimation. Most floating-head bundles ***also*** require an even number of passes.

© 1983 Hemisphere Publishing Corporation

Table 5 F_3 for various tube bundle constructions

Type of tube bundle construction	F_3 inside shell diameter, m				
	up to 0.305	0.337-0.540	0.591-0.889	0.940-1.22	Above 1.22
Fixed tubesheet (TEMA L, M, or N)	1.00	1.00	1.00	1.00	1.00
Outside-packed floating head (TEMA P)	1.30	1.15	1.09	1.06	1.04
Split backing ring (TEMA S)	1.30	1.15	1.09	1.06	1.04
Pull-through floating head (TEMA T)		1.40	1.25	1.18	1.15
U-tube (TEMA U)	1.12	1.08	1.03	1.01	1.01

[a] Since U-tube must always have at least two tube-side passes, it is essential to use Table 4 as well for this configuration.

A U-tube exchanger is to be used with the gas in the tubes. The tubes will be 301 stainless steel 25.4-mm-OD, 12-BWG (2.7-mm wall) on a 31.8-mm rotated square pitch. Typical pressure drops of about 70 kN/m² are allowed for each stream. Assume average fouling.

Estimate the effective tube length and diameter of an exchanger for this service.

Solution:

Check heat balance:

$$Q_{gas} = 48.0(7540)(560 - 395)$$

$$= 5.97 \times 10 \text{ J/s}$$

$$Q_{aro} = 314(2240)(385 - 300)$$

$$= 4.98 \times 10 \text{ J/s}$$

The mean temperature difference is

$$\Delta T_{lm} = \frac{(560 - 385) - (395 - 300)}{\ln [(560 - 385)/(395 - 300)]} = 131 \text{ K}$$

From F charts, $F = 0.85$. Therefore,

$$\Delta T_m = 0.85(131) = 111 \text{ K}$$

Estimation of U_o:

Gas: $\alpha_i = 1\,000$ W/m² K (increased over the 500-800 W/m² K shown in Table 2 to reflect the hydrogen content).

$R_{fi} = 1 \times 10^{-4}$ m² K/W

Wall: $x_w = 2.7$ mm

$\lambda_w = 17.0$ W/m K

Aromatic (probably falls at light end of medium organics"):

$\alpha_o = 1\,300$ W/m² K

$R_{fi} = 2 \times 10^{-4}$ m² K/W

Thus,

$$U_o = 1/[(1/1\,300) + (2 \times 10^{-4}) + (0.002\,7/17.0) \times (25.4/22.7) + (1 \times 10^{-4}) + (1/1000)(25.4/20.0)$$

$$= 393 \text{ W/m}^2 \text{ K}$$

Calculation of required area:

$$A_o = \frac{5.98 \times 10}{111(393)} = 1\,370 \text{ m}^2$$

This is the actual area required in the exchanger. However, in order to use Fig. 2, it is necessary to use Eq. (10) and the associated tables to find A_o':

From Table 3, for 25.4-mm tubes on a 31.8-mm rotated square layout, $F_1 = 1.54$.

From Table 4, for two tube passes and a shell diameter about 1.5 m, $F_2 = 1.02$.

From Table 5, for U-tube construction and a shell diameter of about 1.5 m, $F_3 = 1.01$.

Thus,

$$A_o' = 1\,370(1.54)(1.02)(1.01)$$

$$= 2\,170 \text{ m}^2$$

Entering Fig. 2 at 2 170 m² on the ordinate, we find that the following shell diameter/tube length combinations will provide the required area:

Shell ID, m	Effective tube length, m	Approximate shell length, m	L/D (based on tube length)
1.98	6.1	8.0	3.1
1.83	7.6	9.4	4.2
1.68	8.8	10.5	5.2
1.52	10.8	12.3	7.1
1.38	13.2	14.6	9.6
1.22	16.8	18.0	13.8

© 1983 Hemisphere Publishing Corporation

Any of these would be considered a fairly standard job by a medium- to large-size heat exchanger manufacturer. Site considerations might limit the length and tube-side velocity, and shell-side pressure drop and vibration limits would certainly play an important role in further calculations. The author would probably select the 1.38-mm-ID case for further analysis.

Nomenclature for Section 3.1.4 appears at the beginning of Part 3.

© 1983 Hemisphere Publishing Corporation

3.2
Double-pipe heat exchangers

Contents

3.2.1
INTRODUCTION, A. R. Guy **3.2.1-1**

3.2.2
APPLICATIONS OF DOUBLE-PIPE HEAT EXCHANGERS, A. R. Guy **3.2.2-l**

3.2.3
DESIGN PARAMETERS, A. R. Guy **3.2.3-l**

A. Thermal design 3.2.3-l
B. Fin geometry 3.2.3-4
C. Pressure drop 3.2.3-5

3.2.4
TYPES AVAILABLE, A. R. Guy **3.2.4-l**

A. Double pipes 3.2.4-l
B. Multitube units 3.2.4-l
C. Finned length 3.2.4-2

3.2.5
CONSTRUCTION/MECHANICAL DESIGN, A. R. Guy **3.2.5-l**

A. Finning 3.2.5-l
B. Design codes 3.2.5-l

3.2.6
OPERATIONAL ADVANTAGES, A. R. Guy **3.2.6-l**

A. Fouling 3.2.6-l
B. Flexibility 3.2.6-l
C. Low-cost standby 3.2.6-l
D. Low-cost installation 3.2.6-l
E. Maintenance 3.2.6-l
F. Tube wall thickness 3.2.6-l
G. Standardization 3.2.6-l

References for Sections 3.2.1-3.2.6 3.2.6-2

© 1983 Hemisphere Publishing Corporation

HEDH

3.2.1

Introduction

A. R. Guy

■ The simplest form of double-pipe heat exchanger is a jacketed U tube. Double-pipe exchangers with longitudinal fins were fully developed at the end of World War II, and an ASME paper [I] published in 1944 is still useful as a reference. Longitudinally finned tubes supplied by Brown Fintube, Inc., were used to heat fuel oil on the entire line of Liberty ships, thus using less of the critical tube material at a time when steel was required for other duties. Since then the range has been increased to include multitube finned bundles similar to double pipes in construction, TEMA [7] type BEU suction or line heaters, and storage tank heaters, all using longitudinal fins. Most suppliers offer a full thermal as well as mechanical guarantee, as the design methods have traditionally been proprietary. However, these sections should be useful for in-house design studies and checking suppliers designs.

The author wishes to acknowledge the help given by Filtration and Transfer, Ltd., Poole, Dorset, U.K., in the preparation of Sections 3.2.1-3.2.6. I would also like to thank Brown Fintube, Inc., Tulsa, Oklahoma, for allowing me to use some of their material. Filtration and Transfer design and manufacture double-pipe exchangers and other BFT equipment under license from Brown Fintube.

References for Section 3.2.1 appear at the end of Section 3.2.6.

© 1983 Hemisphere Publishing Corporation

HEDH

3.2.2

Applications ofdouble-pipe heat exchangers

A. R. Guy

■ The double pipe is used as an alternative to the conventional shell-and-tube heat exchanger when one or more of the following conditions are met:

1. Low shell-side film coefficient. If the ratio of tube-side to shell-side film coefficients is greater than 2.1, extended-surface tubing can be utilized. Typical examples would have gases or high-viscosity fluids on the shell side, with water, steam, or low-viscosity liquids on the tube side. The greater the ratio, the more effective will be the extended surface, hence the number and height of the fins can be increased.

2. Temperature *cross* or approach. Double pipes, because of their geometry, produce true counter-current flow, and temperature cross situations can be handled easily. Since they are of a modular construction, they can be bolted together to produce complex series/parallel combinations, with a minimum of interconnecting pipework, on common foundations.

3. High-pressure duties. For a given duty, double-pipe exchangers use much smaller shell diameters than shell-and-tube exchangers, that is, normally 50 (2-in N/B) through to 200 (8-in N/B) seamless pipes, although larger-diameter specials are available. Thus high-pressure shell sides need much lower wall thicknesses because of the smaller diameters.

4. Small duties. Double pipes are often used for small duties that do not need fin tubes, such as water/water. The same construction is utilized, except that bare inner pipes or bare tube bundles are used.

It is difficult to put a figure on the maximum duty or heat load that can be considered for double pipes because of the many combinations of film coefficients, materials of construction, pressure ranges, and so on, but anything above 1 000 kW would normally be more economical as a shell and tube.

© 1983 Hemisphere Publishing Corporation

HEDH

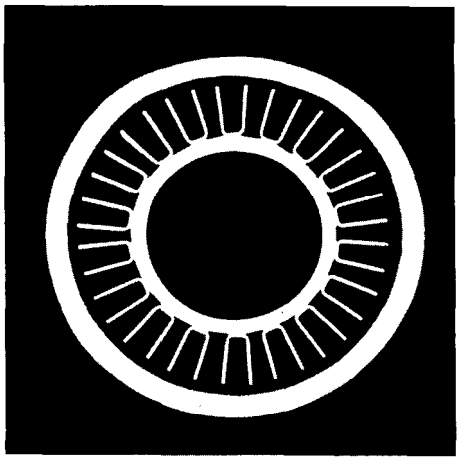

Figure 1 Fin profile, cross section.

the derivation of fin efficiency, E_f, the following assumptions are made:

1. Fin-to-tube bond offers no resistance, i.e., there is continuous fusion.
2. There is a constant cross section.
3. There is homogeneous fin metal with constant thermal conductivity.
4. The fin thickness/height ratio is so low that temperature gradients across the tin width can be ignored.
5. Shell-side fluid conditions are stable, i.e., there is uniform film coefficient and temperature.

E_f is calculated as follows:

$$E_f = \frac{\tanh H_f(\alpha f_d P_f/\lambda_f X_f)^{0.5}}{H_f(\alpha f_d P_f/\lambda_f X_f)^{0.5}} \tag{4}$$

where αf_d = fouled shell-side coefficient
λ_f = fin metal thermal conductivity
P_f = perimeter of tin (= $2L_f + 2T_f$)
X_f = cross-sectional area of fin (= $L_f T_f$)
L_f = length of fin

Since $L_f \gg T_f$,

$$\frac{P_f}{X_f} = \frac{2(L_f + T_f)}{L_f T_f} \tag{5}$$

or

$$\frac{P_f}{X_f} = \frac{2}{T_f} \tag{6}$$

then

$$E_f = \frac{\tanh H_f(2\alpha f_d/\lambda_f T_f)^{0.5}}{H_f(\alpha f_d/\lambda_f T_f)^{0.5}} \tag{7}$$

Note that

$$\tanh = \frac{e^x - e^{-x}}{e^x + e^{-x}} \tag{8}$$

E_f has to be weighted to account for the bare portion of the tube between the fins. There are two ways of approaching this problem. Kern [4] equates everything to the inside surface; that is,

$$\alpha f_{id} = (E_f A_f + A_b)\frac{\alpha f_d}{A_i} \tag{9}$$

where αf_{id} = shell-side coefficient related to the tube ID equivalent to αf_d on the outside
A_f = surface area of fins only (ignoring tip)
A_b = surface area of bare portion between tins
A_i = inside surface area

Kern then calculates an overall heat transfer coefficient, U_{id}, to be used with A_i in the rate equation.

$$Q = U_{id} A_i \text{ AT} \tag{10}$$

We prefer to relate everything to the total outside surface area, A_o:

$$A_o = A_f + A_b \tag{11}$$

The effective fin efficiency E_f' is given by

$$E_f' = \frac{A_f E_f + A_b}{A_o} = E_f \frac{A_f}{A_o} + \left(1 - \frac{A_f}{A_o}\right) \tag{12}$$

where A_f/A_o = finned area fraction
$(1 - A_f/A_o)$ = bare area fraction

The effective shell-side film coefficient, α_{od}, is given by

$$\alpha_{od} = E_f' \alpha_{fd} \tag{13}$$

Values of A_f/A_o and A_o/A_i can be found in Tables 1 and 2.

(c) Overall heat transfer coefficient

The overall heat transfer coefficient, U_{od}, is given by

$$U_{od} = \left(\frac{1}{\alpha_{od}} + \frac{1}{\alpha_{id}}\frac{A_o}{A_i} + R_m\right)^{-1} \tag{14}$$

where α_{id} = tube-side film coefficient referred to tube inside diameter, corrected for total outside surface area by multiplying by A_o/A_i
R_m = weighted tube wall resistance

and

$$R_m = \frac{d_o \ln (d_o/d_i)}{2\lambda_w}\frac{A_o}{A_i} \tag{15}$$

where d_o = tube outside diameter
d_i = tube inside diameter
λ_w = tube wall thermal conductivity, which may be different from λ_f

© 1983 Hemisphere Publishing Corporation

(d) True temperature difference

The true temperature difference equals the log mean temperature difference, or LMTD, calculated in the normal way as per Part 1, but for a single unit or number of units connected in series on both sides. The only difference from normal shell-and-tube practice occurs when more than one unit is connected in an unequal series-parallel combination. Consider two double-pipe units in series on the shell side and parallel on the tube side as shown in Fig. 2.

Half of the inner-pipe fluid enters the upper unit (2) when the shell-side (or annular) fluid is hot, whereas half the inner-pipe fluid enters the lower unit (1), in which the shell-side fluid has already been partially cooled. This results in a different amount of heat being transferred in each exchanger, and even though they are both operating in counter flow, the true temperature difference, or At, will be significantly different from the LMTD.

The simplest form of series-parallel combination is one series hot stream and n parallel cold streams or one series hot stream and n parallel cold streams. Then At can be calculated relatively easily as follows:

$$\text{At} = \nu(T_1 - t_1) \tag{16}$$

where T_1 = hot inlet (and T_2 = hot outlet)
t_1 = cold inlet (and t_2 = cold outlet)
ν is defined as follows:

1. For one series hot stream and n parallel cold streams,

$$\frac{1-P'}{\nu} = \frac{nR'}{R'-1} \ln\left[\frac{R'-1}{R'}\left(\frac{1}{P'}\right)^{1/n} + \frac{1}{R'}\right] \tag{17}$$

where

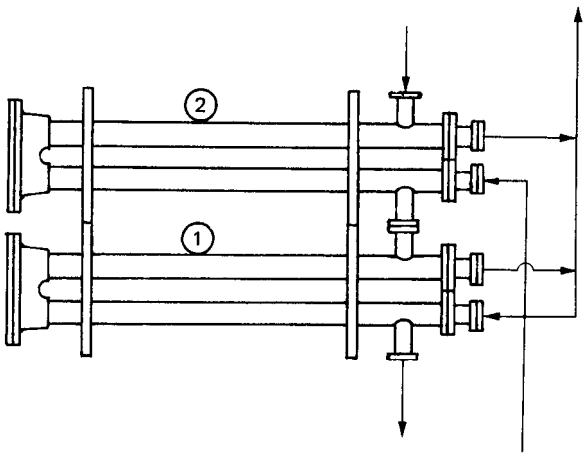

Figure 2 Parallel-series combination-true mean temperature difference.

$$P' = \frac{T_2 - t_1}{T_1 - t_1} \tag{18}$$

$$R' = \frac{T_1 - T_2}{n(t_2 - t_1)} \tag{19}$$

2. For one series cold stream and n parallel hot streams,

$$\frac{1-P''}{\nu} = \frac{n}{1-R''} \ln\left[(1-R'')\left(\frac{1}{P''}\right)^{1/n} + R''\right] \tag{20}$$

where

$$P'' = \frac{T_1 - t_2}{T_1 - t_1} \tag{21}$$

$$R'' = \frac{n(T_1 - T_2)}{t_2 - t_1} \tag{22}$$

The above relationship is derived in Kern [4] (p. 117), and similar relationships can be obtained for more complicated combinations where both sides are connected in more than one parallel path. Alternatively, one can calculate the LMTD and apply a correction factor as shown in Fig. 3. These are not the same as the LMTD correction charts used for shell-and-tube exchangers with multipass arrangements.

An important exception to the above occurs when the number of tube-side parallel paths is equal to the number of shell-side parallel paths, in which case the normal LMTD should be used. Figure 4 illustrates this point, as all three cases would be subject to a normal LMTD.

(e) Available surface area

The available surface area A is calculated as follows:

$$\text{A} = 2N_t L_f(2N_f H_f + \pi d_o) \tag{23}$$

where N_t = number of fin tubes
L_f = finned length (or effective length for bare tube units)
H_f = fin height
d_o = tube outside diameter

Note: A is the surface area per unit, that is, the total of both legs.

Values of surface area/unit length can be found in Tables 1 and 2.

B. Fin geometry

(a) Fin height

Fin height is normally the difference between the outer-pipe (or shell) ID and the inner-pipe (or tube) OD with

© 1983 Hemisphere Publishing Corporation

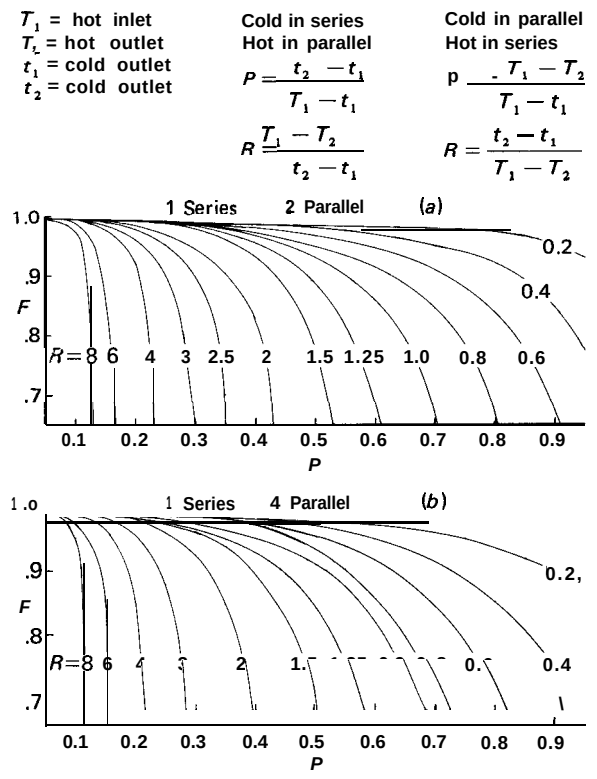

Figure 3 Mean temperature difference correction charts.

a clearance factor to allow for bundle withdrawal and pipe tolerances. Since the fins also act as tube supports, this clearance factor must be kept to a minimum. Typical geometries are given in Tables 1 and 2.

(b) Number of fins

The number of fins must be divisible by 4 because of the way in which the tin tube is produced (see Sec. 3.2.5A). The maximum number of fins is dependent on inner pipe diameter, fin thickness, and the root width of the fin channel, R_f (see Fig. 1). Weldable materials normally have a root width of 1.8-2 mm, that is, $2T_f$. Pairs of fin channels at 180° to each other are equally spaced around the inner pipe and ideally the gap between adjacent fin channels should never be less than $2T_f$ to ensure good flow distribution between the fins.

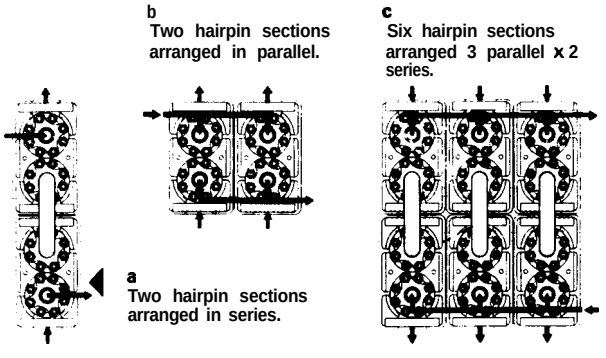

Figure 4 Parallel-series combination-normal LMTD.

C. Pressure drop

(a) Tube-side pressure drop

Tube-side pressure drop is calculated in the usual way, remembering to use an effective length for the U tubes, which can be quite significant. The double pipes, as apposed to multitubes, do not have a tubesheet, and the transition from pipework to fin tube is such that no extra pressure drop is experienced; that is, there is frictional loss only.

Multitube units do have a tubesheet with an associated channel piece, and the normal shell-and-tube methods for nozzle/channel loss will apply.

The total entrance and exit loss would not normally exceed 1.5 velocity heads based on tube velocity.

(b) Shell-side pressure drop

The following section covers shell-side pressure drop for all types, except for the large (6 and 8-in) bare multitube types with segmental baffles, which should be calculated with a shell-and-tube method.

The frictional loss is calculated using a tube-side correlation with the equivalent diameter in place of tube inside diameter. The friction factor for fin tubes can be found from Fig. 5 as a function of Reynolds number. The curves are almost identical to a tube-side plot apart from a slight difference in the transitional flow regime.

The return-bend housing will account for 0.5 velocity head based on the shell velocity. Similarly, the spider-type tube supports in the 4-in bare multitube units will cause 0.5 velocity head loss per support, again based on shell velocity. The nozzle pressure drop is often highly significant.

The cut-and-twist loss is accounted for by multiplying the frictional pressure drop by a factor, F_{ct}, defined by the following empirical relationship:

$$F_{ct} = 1.58 - 0.525 L_{ct} \qquad (24)$$

where L_{ct} = cut-and-twist length in meters. (Note: Above L_{ct} = 1.0, the factor F_{ct} = 1.O.)

© 1983 Hemisphere Publishing Corporation

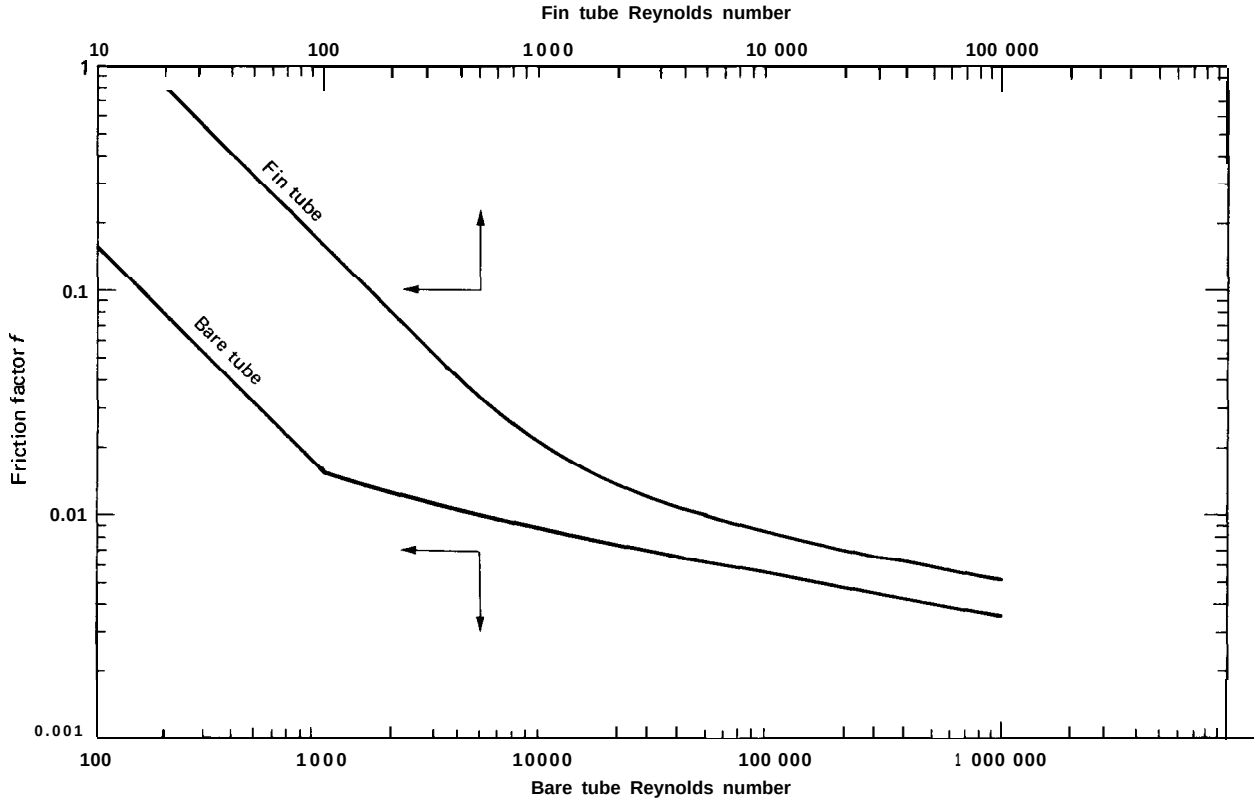

Figure 5 Shell-side friction factor.

Nomenclature for Section 3.2.3 appears at the beginning of Part 3. References appear at the end of Section 3.2.6.

© 1983 **Hemisphere Publishing Corporation**

3.2.4
Types available

A. R. Guy

■ Two main types are available, double pipes and multitube units.

A. Double pipes

Double pipes have a single pipe or tube inside a shell. Two such double pipes are joined at one end by a U bend welded to the inner pipes and a return bend housing on the shell side, which has a removable cover to allow withdrawal of the inner pipes, or element. The opposite end of the inner pipes has a closure arrangement incorporating split rings and sealing rings, which allow the tube-side connections to be removed and the inner pipes disconnected from the shells. The element can then be withdrawn from the tail end of the unit for cleaning or maintenance.

Figure 1 shows such a closure. The tube-side piece with the grooves and sealing faces is called the fin tube fitting. The sealing ring between the fin tube fitting and the shell is normally made from Armco-type soft iron. Other more suitable metals in a softened state can be used if the shell-side fluid is particularly corrosive. The tube-side connection joint uses more conventional gasket materials such as copper, metal-jacketed asbestos, spiral-wound asbestos, and so on.

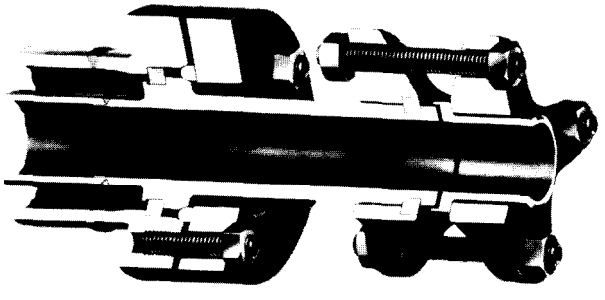

Figure 1 Tube-side closure-double pipe (Courtesy of Brown Fintube, Inc.).

Figure 2 shows a typical double-pipe or hairpin exchanger, and Table 3.2.3(1) gives the more common combinations of shell and inner pipe sizes.

B. Multitube units

Multitube units, or multis, have the same form of construction as double pipes except that the inner pipe is replaced by a bundle of U tubes. Both legs of the bundle have a separate shell welded into a return-bend housing. The tube-side closure arrangement has developed over the years into two types, uniheads and separated heads.

(a) Uniheads

In uniheads the tubesheet outer edge is used to seal both the shell side and the tube side with a common sealing ring. This type is limited to low pressures and nonstringent service, as in the event of a leak, the shell-side and tube-side fluids might mix.

(b) Separated heads

In separated heads the tubesheet has a sleeve on the back, which takes the shell-side sealing ring and split rings. The tube side has a channel-like flange bolted

© 1983 Hemisphere Publishing Corporation

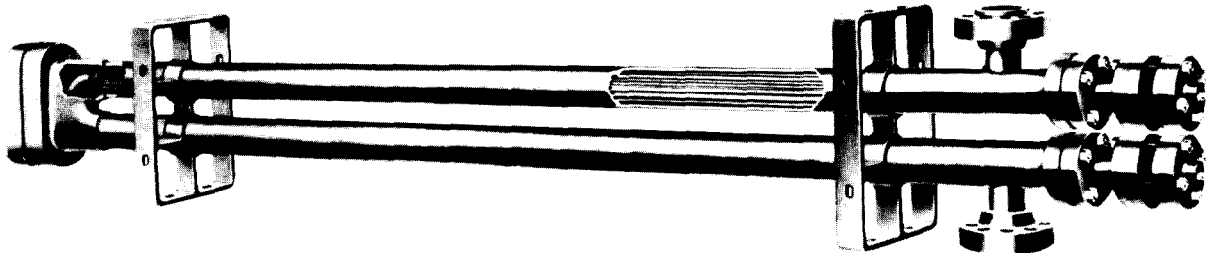

Figure 2 Double-pipe exchanger. (Courtesy of Brown Fintube, Inc.)

onto the face of the tubesheet with a conventional gasket. Thus, any leakage would be to atmosphere and not between the fluids. The tubesheet also has split rings to allow the use of a loose flange to take the channel piece bolting. Similarly, the sealing ring has a loose flange bolted onto the shell fitting flange with the sealing ring compressed in between. This somewhat complicated arrangement allows the tubesheets and bundle to be withdrawn. Figure 3 shows a typical multitube separated head closure.

Table 3.2.3(2) gives typical combinations of shell sizes and bundle types. With the unihead design it is possible to use a few more tubes or increase the fin height slightly, but this small increase in surface area is normally not worth the risk of interstream leakage.

Obviously the possibility of interstream leakage still exists via the tube to tubesheet joint, but this can easily be avoided by specifying a welded joint in place of the standard expanded joint.

C. Finned length

The finned length (or effective length in the case of bare units) is normally available from 5 ft (1 524 mm) to 25 ft (7 630 mm) in steps of 5 ft (1 524 mm). Longer units are available, and intermediate lengths can be specified to overcome special difficulties.

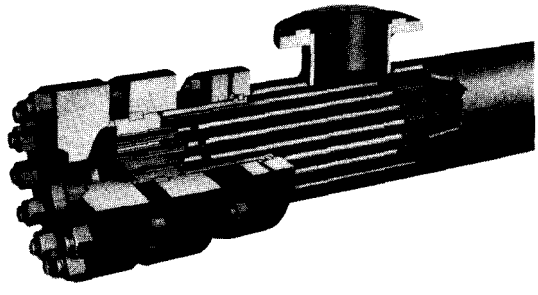

Figure 3 Tube-side closure-multitube. Tube side, 34.5 MN/m² g (5 000 psig). (Courtesy of Brown Fintube, Inc.)

© 1983 Hemisphere Publishing Corporation

3.2.5
Construction/mechanical design

A. R. Guy

A. Finning

(a) Welded fins

The fins are formed from strip into a U channel and welded onto the inner pipe using an electric resistance seam-welding technique. The U channels, two at a time, are clamped onto the pipe by circular electrodes under hydraulic pressure. A very high current is passed through the electrodes, which are also driven, thus moving the pipe through the machine. The weld takes the form of a series of spots such that complete fusion takes place between the fin root and pipe.

This technique is suitable for carbon steel, stainless steel, monel, and even titanium under controlled conditions.

Combinations of materials can also be utilized, such as a stainless steel inner pipe with carbon steel fins. This is a very useful combination, as it increases the tin efficiency by using carbon steel fin while still retaining the corrosion resistance of the inner pipe.

Distortion of the fins can occur when the tin height is more than 15 mm. This is caused by differential expansion and contraction between the fin root and tip, which gives the fins a wavy appearance. This will not detract from the performance of the fin tube; in fact, if any effect were noticeable, it would probably be beneficial because of the slight mixing effect.

(b) Soldered fins

Fins made from brass or similar materials can be soldered to copper, nickel, admiralty brass, or aluminum brass tubes. The fin is formed in the same way as above. The fins are normally 0.5 mm thick up to 12.7 mm high and 0.8 mm thick above 12.7 mm.

The maximum operating temperature is normally limited to 250° C when using soldered fins, although higher-melting-point material is available.

B. Design codes

(a) Pressure vessel codes

Since double-pipe exchangers were developed in the United States, most standard units are designed and constructed to ASME VIII, Div. 1 [5]. In the United States they can be supplied complete with a U stamp on an off-the-shelf basis.

Suppliers in other parts of the world are having to redesign some parts of the unit to comply with their local codes. This is particularly true in the U.K., where Filtration and Transfer, Ltd., is building up a set of standard calculations to BS 5.500 [6], as well as some of the other European codes.

Double pipes lend themselves to standardization, and Brown Fintube in particular has built up a range of design pressures designed to ASME. The standard

© 1983 Hemisphere I blishing Corporation

units are designed for 3 448 KN/m^2g (500 psig) both sides apart from the S-in units that are suitable for 2 069 KN/m^2g (300 psig) shell side. Design pressures up to 103.45 MN/m^2g (15 000 psig) are also available. The carbon steel units are normally offered with a corrosion allowance of 1.6 mm because of the small diameters.

(b) TEMA [7]

Strictly speaking, only the 6-in (168-mm OD) and above units should have TEMA applied to them, as anything under 6 in (168-mm OD) is excluded. However, it is possible to apply relevant parts of TEMA to all the sizes. The main difficulty is with minimum bolt size because of the compact nature of the units; for example, TEMA R specifies $\frac{3}{4}$ in (19.02 mm) as the minimum bolt size, whereas $\frac{5}{8}$ in (15.875 mm) is necessary on most of the range, and occasionally $\frac{1}{2}$ in (12.7 mm) is needed.

References for Section 3.2.5 appear at the end of Section 3.2.6.

© 1983 Hemisphere Publishing Corporation

3.2.6

Operational advantages

A. R. Guy

A. Fouling

Most fouling is dependent on temperature, and for a given duty an extended-surface exchanger has a lower tin metal temperature than the equivalent bare-tube unit, thus reducing the fouling rate. Also, the longitudinal flow means no dead areas where fouling may build up. Finally, when fouling does occur, the heat transfer rate decreases, which increases the fin efficiency, thus partially compensating for the loss in heat transfer.

B . Flexibility

Double-pipe exchangers are often supplied as multiple units connected in a series-parallel combination. Should the flow rate be changed, one can add or remove parallel streams without affecting the velocities or temperatures.

C. Low-cost standby

For critical or severe service, an extra parallel bank can easily pay for itself by allowing part of the unit to be cleaned or maintained without stopping the full performance of the unit.

D. Low-cost installation

Double-pipe exchangers are light and easily handled with a minimum of lifting equipment. They do not require large foundations and can often be bolted to existing structures or pipe racks. The standard brackets have bolt holes on all four sides, which means that multiple units can easily be bolted together. Shell sides connected in series only need a connecting gasket, and the tube side uses simple return-bend, bolt-on crossover pieces.

E. Maintenance

Simple constructions, easily reached bolting, lightweight tin tube elements, and a minimum number of parts all contribute to minimizing costs. The elements are easy to remove, and downtime can be kept to a minimum, especially if one spare element per type is available, allowing the dirty element to be cleaned while the plant is running.

F. Tube wall thickness

The true double pipes typically have 3.683-mm or 5.156-mm wall thickness, as Sch. 40 pipe is required by the finning process. The finned multitube units have a minimum wall thickness of 2.1 mm, and heavier wall thickness can be provided without unduly affecting cost or performance.

G. Standardization

The advantages of producing standard units are obvious, but the operator also benefits, as often the same type is used for different duties. Thus, spare parts can be kept to a minimum, as often one spare set of gaskets may tit a number of exchangers. Most suppliers keep stocks of standard parts, which reduces replacement time, and of course, delivery of the original unit.

© 1983 Hemisphere l ıblishing Corporation

REFERENCES FOR SECTIONS 3.2.1-3.2.6

1. De Lorenzo, B., and Anderson, E. D., Heat Transfer and Pressure Drop of Liquids in Double Pipe Fintube Exchangers, ASME 44-A-69, December 1944.
2. Sieder, E. N., and Tate, F. E., Heat Transfer and Pressure Drop in Tubes, *Ind. Eng. Chem.,* vol. 28, pp. 1429-1436, 1936.
3. Engineering Science Data Unit, Paper 67016, 1967; Paper 68007, 1968; Paper 68006 with amendment A, 1970; 4, Hamilton Place.
4. Kern, D. ***Q., Process Heat Transfer,*** McGraw-Hill, New York, 1950.
5. ASME VIII, Division 1, *ASME* ***Boiler and Pressure Vessel Code,*** American Society of Mechanical Engineers, New York, 1977.
6. BS 5500: 1976, Specification for Unfired Fusion Welded Pressure Vessels, British Standards Institution, 1976.
7. Standardsof Tubular Exchanger Manufacturers Association, 6th ed., TEMA, New York, 1978.

© 1983 Hemisphere publishing Corporation

3.3
Shell-and-tube heat exchangers: Single-phase flow

Contents

3.3.1
OBJECTIVES AND BACKGROUND, J. Taborek **3.3.1-1**

References for Section 3.3.1 3.3.1-2

3.3.2
SURVEY OF SHELL-SIDE FLOW CORRELATIONS, J. Taborek **3.3.2-1**

A. Early developments 3.3.2-1
B. Shell-side methods based on the integral approach ***3.3.2-2***
C. Shell-size methods based on the analytical approach ***3.3.2-3***

References for Section 3.3.2 ***3.3.2-6***

3.3.3
RECOMMENDED METHOD: PRINCIPLES AND LIMITATIONS, J. Taborek **3.3.3-1**

A. Method structure 3.3.3-1
B. Shell-side heat transfer equation ***3.3.3-2***
C. Shell-side pressure drop ***3.3.3-3***
D. Comparison of the recommended method with the Delaware method and probable accuracy ***3.3.3-4***

References for Section 3.3.3 ***3.3.3-s***

3.3.4
PRACTICES OF SHELL-AND-TUBE HEAT EXCHANGER DESIGN, J. Taborek **3.3.4-1**

A. Heat exchanger specification sheets 3.3.4-1
B. Rating, design, and optimization 3.3.4-1
C. Calculation method by degree of complexity ***3.3.4-3***
D. Effects and selection of constructional elements ***3.3.4-4***
E. Some other design considerations ***3.3.4-S***

References for Section 3.3.4 ***3.3.4-6***

3.3.5
INPUT DATA AND RECOMMENDED PRACTICES, J. Taborek **3.3.5-1**

A. Basic input data 3.3.5-1
B. Comments to input data (Table 1) 3.3.5-1
C. Calculations of basic correlational parameters 3.3.5-16

References for Section 3.3.5 3.3.5-17

3.3.6
AUXILIARY CALCULATIONS, J. Taborek **3.3.6-1**

A. Segmental baffle window calculations **3.3.6-1**
B. Baffle window flow areas 3.3.6-1
C. Equivalent hydraulic diameter of a segmental baffle window, D_w ***3.3.6-3***
D. Number of effective tube rows in cross flow, N_{tcc} and N_{tcw} ***3.3.6-3***
E. Number of baffles, N_b ***3.3.6-4***
F. Bundle-to-shell bypass area parameters, S_b and F_{sbp} ***3.3.6-4***

© 1983 Hemisphere Publishing Corporation

HEDH

G. Shell-to-baffle leakage area, S_{sb} (mm) 3.3.6-4
H. Tube-to-baffle hole leakage area for one baffle, S_{tb} (mm) 3.3.6-5
I. Segmented baffle window correction factor J_c (Fig. 7) 3.3.6-5
J. Correction factors for baffle leakage effects for heat transfer, J_l, and pressure drop, R_l 3.3.6-6
K. Correction factors for bundle bypass effects for heat transfer, J_b, and pressure drop, R_b 3.3.6-8
L. Heat transfer correction factor for adverse temperature gradient in laminar flow, J_r 3.3.6-Y
M. Heat transfer correction for unequal end baffle spacing at inlet and/or outlet, J_s 3.3.6-9
N. Pressure drop correction for unequal baffle spacing at inlet and/or outlet, R_s 3.3.6-l 1

References for Section 3.3.6 3.3.6-l 1

3.3.7 IDEAL TUBE BANK CORRELATIONS FOR HEAT TRANSFER AND PRESSURE DROP, J. Taborek **3.3.7-l**

A. Ideal tube bank j_i and α_i 3.3.7-l
B. Ideal tube bank-based f_i and Δ_{pi} 3.3.7-4

3.3.8 CALCULATION OF SHELL-SIDE HEAT TRANSFER COEFFICIENT AND PRESSURE DROP, J. Taborek **3.3.8-l**

A. Shell-side heat transfer coefficient, α_s 3.3.8-l
B. Shell-side pressure drop, Ap, 3.3.8-l

References for Section 3.3.8 3.3.8-3

3.3.9 **PERFORMANCE EVALUATION OF A GEOMETRICALLY SPECIFIED EXCHANGER,** J. Taborek **3.3.9-l**

A. Basic evaluation criteria 3.3.9-l
B. Performance evaluation procedure 3.3.9-2
C. Overall heat exchanger performance evaluation 3.3.9-6

3.3.10 DESIGN PROCEDURES FOR SEGMENTALLY BAFFLED HEAT EXCHANGERS, J. Taborek **3.3.10-l**

A. Computer versus manual calculations 3.3.10-l
B. Preliminary design considerations 3.3.10-2
C. First size estimation 3.3.10-3
D. Preliminary performance evaluation 3.3.10-6
E. Analysis of results 3.3.10-8

References for Section 3.3.10 3.3.10-g

3.3.11 EXTENSION OF THE METHOD TO OTHER SHELL, BAFFLE, AND TUBE BUNDLE GEOMETRIES, J. Taborek **3.3.1 l-l**

A. Divided flow, TEMA J shell 3.3.1 l-l
B. No-tubes-in-window tube bundles 3.3.1 l-l
C. Two shell pass-TEMA F shell 3.3.1 l-2
D. Double segmental or disk-and-doughnut baffles 3.3.11-2
E. Application of external low fin tubes 3.3.11-2

Nomenclature for Section 3.3.11 3.3.11-4
References for Section 3.3.11 3.3.1 **1-5**

© 1983 Hemisphere Publishing Corporation

3.3.1
Objectives and background

J. Taborek

■ The basic design of shell-and-tube exchangers was introduced in the early 1900s to fill the needs in power plants for large heat exchanger surfaces as condensers and feedwater heaters capable of operating under relatively high pressures. Both of these original applications of shell-and-tube heat exchangers continue to be used, but the designs have become highly sophisticated and specialized, subject to various specific codes and practices.

The broad industrial use of shell-and-tube heat exchangers known today also started in the 1900s to accommodate the demands of the emerging oil industry. Oil heaters and coolers, reboilers, and condensers for a variety of crude oil fraction and related organic liquids were required for rugged outdoor service, often dirty fluids, and high temperatures and pressures. Ease of cleaning and field repairs was unconditionally required.

The most serious problems in these early stages of shell-and-tube heat exchanger development appeared not to be those of heat transfer (which was crudely estimated from practice) but rather of material strength calculations for the various components, especially tubesheets. A host of other problems in the area of manufacturing techniques and practices followed, such as tube-to-tubesheet joints, flange and nozzle welding, and so on, surprisingly many being still on the list of items of continued concern and development.

During the 1920s shell-and-tube manufacturing technology became fairly well developed, mainly because of the efforts of relatively few major manufacturers. Units up to 500 m^2 (5 000 ft^2), that is, approximately 750-mm diameter and 6-m length (3 ft by 16 ft), were manufactured for the rapidly growing oil industry. In the 1930s, the shell-and-tube heat exchanger designers established many sound design principles from intuition and data emerging on ideal tube banks. Water-water and water-steam exchangers were probably designed about as well as they are today, because of the predominant effects of fouling resistances. Viscous flow was one of the most difficult problems for shell-side flow and was poorly understood until the 1960s. Shell-side pressure drop is not even mentioned in the literature until the late 1940s. Condensers and reboilers were designed purely to experience-derived values, often tightly guarded secrets of the manufacturers.

The need for mechanical design standards was equally important for reasons of safety, uniformity of tolerances, quality control, and general orderliness in competition. The first such document is the TEMA Standards of 1941 [1], presently in its sixth edition and considered a standard practice all over the world.

The steadily increasing use of shell-and-tube exchangers and greater demands on accuracy of performance prediction for a growing variety of process conditions resulted in an explosion of research activities in the 1940s and through the 1950s. These included not only shell-side flow but, equally important, calculations of true mean temperature difference and strength calculations of construction elements, in particular, tubesheets. It is also of interest to note that practically all the developments in thermohydraulic as well as mechanical design of shell-and-tube heat exchangers originated from U.S. sources, although influenced by fundamental ideas of German research [2]. The work of Colburn, Gardner, Mueller, Donohue, Kern, and Tinker are only a few examples.

© 1983 Hemisphere 1 ublishing Corporation

Shell-and-tube exchangers as they developed through the years are the most widely used type of heat exchangers because of their rugged construction and the great range of design variations and operating conditions that can be accommodated, in particular:

No phase change, condensation, and boiling in horizontal or vertical positions, both in-tube and on the shell side, depend on best operating conditions.

Pressure can range from vacuum to very high values.

Permissible pressure drop can vary within a wide range and the design can be adjusted independently for each fluid because of a variety of shell flow types and tube bundle arrangements.

Thermal stresses can be accommodated rather inexpensively.

Sizes range from very small to extremely large (5 000 m^2).

Positive separation of fluids can be obtained.

A great variety of materials can be used, accommodating demands for low construction cost as well as for corrosion resistance and high pressure/temperature requirements.

Use of a variety of enhanced surfaces, both external and internal, is readily accomplished. These include primarily finned tubes (both external and internal), various tube inserts, and special surface finishes.

Tube bundles can be removed for cleaning or repair.

However, this account of shell-and-tube exchangers flexibilities of construction should by no means deter the designer from searching for possible alternatives, especially plate, spiral, or compact exchangers, whenever the design and operating conditions appear suitable and may result in an economically preferable solution.

A brief note regarding the presentation of the correlations may be of interest. The heat transfer relations assume two forms in the various publications, one based on Nusselt number and one based on Stanton number. The basic relationship of

$$\mathrm{Nu} = C\,\mathrm{Re}^{m}\,\mathrm{Pr}^{p} \tag{1}$$

is converted for graphical representation into

$$j_{\mathrm{Nu}} = \mathrm{Nu}\,\mathrm{Pr}^{-p} = \mathrm{C}\,\mathrm{Re}^{m} \tag{2}$$

In the Stanton number form introduced by Colburn,

$$\mathrm{St} = \frac{\mathrm{Nu}}{\mathrm{Re}\,\mathrm{Pr}} = \frac{\alpha}{c_p \dot{m}} \tag{3}$$

the j_{St} becomes

$$j_{\mathrm{St}} = \mathrm{St}\,\mathrm{Pr}^{1-p} = C\,\mathrm{Re}^{m-1} \tag{4}$$

and accordingly,

$$j_{\mathrm{Nu}} = j_{\mathrm{St}}\,\mathrm{Re} \tag{5}$$

Thus the two representations in graphical form are not directly comparable by visual inspection. The Nusselt number-based representation was used up to and including Tinker s work, whereas the Delaware work used the Stanton number format. The j_{St} appears lately preferable because it permits an easy comparison to the friction factor. On the other hand, the j_{Nu} permits a closer feel for the correlation as Nu increases with Re and hence flow velocity. In this text, we shall use Colburn sj_{St} definition, consistent with the Delaware work.

The friction factor can also be presented in several forms, and the user should always ascertain that the friction factor is applied to a pressure drop equation consistent with the definition.

The process of shell-and-tube heat exchanger performance evaluation or rating will consist of calculations of heat transfer coefficient α and pressure drop Ap on both shell side and tube side. Only the methods for shell-side flow are presented here, the reader being referred to other sections for tube-side flow correlations. In some cases, such as with steam as service fluid on the shell side, the steam coefficient α will usually be specified and the rating becomes purely calculation of the tube-side flow (which in these cases will usually constitute the predominant resistance). However, the method and stepwise calculation procedures shown here allow for such cases.

In the following sections, a systematic approach to the performance rating and design of shell-and-tube exchangers is outlined. First, a survey and an evaluation of the existing methods are presented, including the justification of selecting the recommended method and its limitations. Second, the principles of rating versus design of exchanger are illustrated and comments on the aspects of optimization are given.

The remainder of Sec. 3.3 is devoted to a detailed description of the procedures to rate or design a shell-and-tube exchanger with emphasis on the shell-side flow performance analysis. The selection of constructional elements and their effects on the performance are paid particular attention. Finally, the evaluation of the results and suggested sequence of alternatives are outlined.

Nomenclature for Section 3.3. I appears at the end of Section 3.3.11.

REFERENCES FOR SECTION 3.3.1

1. ***Standards of Tubular Exchangers Manufacturers Association,*** TEMA, New York, 1941.
2. Lienhard, J., Observations on the German Origins of American Heat Transfer Pedagogy, ***Heat Transfer Eng.,*** vol. 1, no. 1, July 1979.

© 1983 Hemisphere Publishing Corporation

3.3.2

Survey of shell-side flow correlations

J. Taborek

■ It is essential that the designer of shell-and-tube exchangers becomes familiar with the principles of the various correlations and methods in numerous publications, their advantages and disadvantages, limitations, and degrees of sophistication versus probable accuracy and other related aspects. All the published methods can be logically divided into several groups:

1. The early developments based on flow over ideal tube banks or even single tubes.
2. The integral approach, which recognizes baffled cross flow modified by the presence of a window, but treats the problem on an overall basis without consideration of the modifying effects of leakage and bypass.
3. The analytical approach based on Tinker s multistream model and his simplified method.
4. The stream analysis method, which utilizes a rigorous reiterative approach based on Tinker s model.
5. The Delaware method, which uses the principles of the Tinker model but interprets them on an overall basis, that is, without reiterations.
6. Numerical prediction methods. Here an attempt is made to predict the shell-side flow pattern by solving the flow equations numerically for a mesh suitably selected to describe the shell. Applications of this method are described by Patankar and Spalding [I] and Butterworth [2]. Once the velocity is specified, the heat transfer coefficient may also be calculated on a local basis. However, although this method is promising, it is difficult to apply to complex cases and, for design purposes, it is not yet a substitute for the other methods listed.

A good review of the state of the art as of 1960 was published by Emerson [3,4]. Only the most pertinent comments to the various correlations and methods of the early and integral type are included here, mainly because some are still used in industry. The more recent methods based on Tinker s flow model will be reviewed in greater detail, as present and foreseeable future developments appear to be best handled by this approach.

A. Early developments

It was recognized in the early 1930s that baffled shell-side flow will behave similarly to flow across ideal tube banks, for which wind tunnel data were emerging. The first heat transfer correlation suggested is due to Colburn in 1933 [5] in the form

$$Nu_f = 0.33\ (Re_f)^{0.6}\ (Pr_f)^{0.33} \qquad (1)$$

where the length term in Nu and Re is the tube outside diameter and flow velocity is based on the minimum cross-sectional area at shell inside diameter (see Sec. 3.3.5). The subscript f denotes that physical properties are based on film temperature to account for noniso-thermal effects in viscous liquids. The validity was restricted to Re > 2 000 and staggered layouts. For baffled shells, where bypass and leakage streams diminish the flow effectiveness, a safety factor of 0.6 was later suggested.

Substantial new data on ideal tube banks in turbulent flow over wide ranges of tube layouts were examined by Grimison [6] in 1937, but essentially

© 1983 Hemisphere l ublishing Corporation

confirmed Colbum s correlation for the usual heat exchanger geometries. Eventually the correlation form was slightly modified to include the Sider-Tate form for nonisothermal effects, which is much easier to handle, and within the general data scatter produced equal results:

$$\mathrm{Nu} = 0.2\,\mathrm{Re}^{0.6}\,\mathrm{Pr}^{0.33}\left(\frac{\mu}{\mu_w}\right)^{0.14} \qquad (2)$$

where all properties are based on average bulk temperature except μ_w, which refers to the tube wall. The validity was restricted to turbulent flow of 2 000 < Re < 40 000.

Note that the lead constant 0.2 is the product of the original 0.33 times the baffle safety factor of 0.6. As a matter of fact, for very quick estimations, Eq. (2) may still be used, as nothing better at this level of simplicity exists.

Data in laminar flow on ideal tube banks did not for all practical purposes exist until the Delaware results of the 1950s. To suggest at least an approximate solution, McAdams [7] blended graphically a curve for laminar flow (Re < 2 000) based on experiments with air on a single tube, which attained below Re of 10 the theoretically justifiable slope of 0.33.

Prediction of pressure drop was (and still is) much more difficult and less accurate than heat transfer, because $\alpha \equiv V^{0.6}$ but $\Delta p \approx V^{1.8}$. Data on ideal tube banks were compiled by Grimison [6] for turbulent flow above Re ≈ 4 000 in the friction factor form

$$f \approx C\,\mathrm{Re}^{-n} \qquad (3)$$

where Re is again based on tube diameter and maximum flow velocity through the minimum cross-sectional area. To extend the frictional relations into the laminar region, Colburn in 1942 [8] blended graphically some data with the theoretically justifiable slope of (-1) for Re < 100.

No treatment of the flow through the baffle window turnaround was suggested either for heat transfer or pressure drop until much later. However, perceptive observations were emerging from the analysis of the meager data, characterized by Colburn [8] as follows:

> It is interesting that while the tube pitch has only a slight influence on heat transfer, it has a marked effect on friction; and other things being equal, one would want as small a pitch as possible in the turbulent flow, but a large one in the viscous.

Papers published in this period of development are too numerous to mention, but good historical reviews are in Colburn [8] and Short [9]. Significant developments in this era were made also in the field of true mean temperature difference and mechanical strength calculations.

B. Shell-side methods based on the integral approach

We use the term method rather than correlation to imply that, contrary to correlations, guidelines are given for interpretations of complex baffled flow geometries, the baffle window flow is specifically treated, and the overall format is put into terms of practical usage. The term integral pertains to the fact that the equations used are based on the overall data from actual baffled exchangers. This simplifies the calculations compared to the analytical methods, but the accuracy invariably suffers as the variations and interaction of the design parameters cannot be adequately expressed.

Furthermore, the data on baffled exchangers available in the 1940s were so limited that insufficient variations even of the basic geometry parameters (baffle spacing, baffle cut, tube layout) were represented. To overcome this deficiency the j and f curves were drawn with more than adequate safety factors.

It should be observed that overprediction of pressure drop (in all pressure drop-limited cases) results in poor heat transfer performance. This is due to the fact that the pressure drop limitation requires the use of wider baffle spacings and/or larger shell diameter, resulting in lower flow velocities than was necessary and, conversely, lower α values.

The two major methods of shell-side calculation (among several others) that qualify under the integral formulation are by Donohue and Kern.

The Donohue method was published first in 1949 [10] and later in an expanded version in 1955 [11]. It became quite popular for its simplicity while presenting more systematic treatment than anything known before. The earlier editions of the German VDI Wärmeatlas and other handbooks used this method as a recommendation.

The heat transfer correlation was, for the first time, based on a flow area that is the geometric mean between the minimum cross-flow area at the shell ID and the baffle window longitudinal flow area. The Nu equation has a form similar to Colburn s Eq.(2), except for the above-mentioned interpretation of the mass velocity, and the leading constant is converted to a weak function of the baffle-to-shell leakage area. On the other hand, the j_{Nu} curve is a single line, not reflecting the effects of tube layout configuration.

For pressure drop, a set of f curves based on Grimison s work [6] with a large safety factor was used. Again, the baffle window is for the first time accounted for, assuming the window as an orifice with a discharge coefficient of 0.7.

There is no doubt that Donohue s method represented a step in the right direction, but being based on a

© 1983 Hemisphere Publishing Corporation

nonsystematic set of data on small exchangers (some of them with unusual geometric parameters), the prediction accuracy by standards of today is rather erratic, reaching up to several hundred percent overprediction on pressure drop and scatter in heat transfer, although usually on the safe side. However, the method is simple to handle, requiring minimum data input, and is suitable for quick and rough estimations.

Kern s method, published in 1950[12], deserves special mention, as it was used as a virtual industrial standard for many years. The merits of Kern s presentations are not so much that better correlations are used, but rather in the way the overall design problem is approached as an entity, including numerous practical hints and calculated examples.

Both heat transfer and pressure drop are presented for 25% baffle cut only (a very clever selection, being reasonably close to the best design). The length term in Nu and Re is an equivalent diameter based on longitudinal flow projection (to account for tube layout variations), a concept that was later proved inferior to other methods for generalization. No account is taken for variations in the bypass or leakage areas-resulting in great simplicity of calculation-but also in rather great scatter of results. Pressure drop predictions are almost invariably on the safe side (usually more than 100%), whereas heat transfer may vary from slightly unsafe to very safe, because of the poor treatment of the bypass and leakage effects.

The prediction accuracy decreases further in laminar flow, because very few data were available at that time and the simple method is not equipped to handle the complex problem. This has been verified in an unpublished investigation in connection with [13] . Thus, although Kern s method cannot be recommended any more, many of the practical comments of design remain qualitatively valid.

C. Shell-side methods based on the analytical approach

In the late 1940s it became obvious that baffled shell-side flow is so complex that it cannot be adequately expressed on a generalized basis by the simple approach described above. Only part of the fluid takes the desirable path through the tube nest, whereas a potentially substantial portion flows through the leakage areas (baffle-to-shell and tube-to-baffle) and the bypass area between tube bundle and the shell wall. However, these clearances are inherent to the manufacturing and assembly process of shell-and-tube exchangers, and the flow distribution within the exchanger must be taken into account.

The early analysis of the shell-side flow is due to Tinker [14], who suggested a schematic flow pattern as

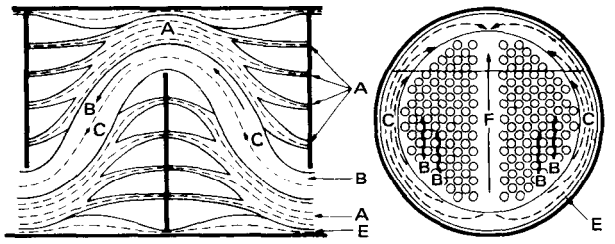

Figure 1 Schematic flow distribution diagram for baffled shell-side flow. Based on Tinker [14].

shown in Fig. 1. The shell-side flow is divided into a number of individual streams as follows (retaining Tinker s original nomenclature, which became commonly accepted in the literature).

Stream A is the leakage stream in the orifice formed by the clearance between the baffle tube hole and the tube wall (see Fig. 2).

Stream B is the main effective cross-flow stream, which can be related to flow across ideal tube banks.

Stream C is the tube bundle bypass stream in the gap between the bundle and the shell wall. (Note that the size of the gap will differ for various bundle construction types, such as fixed tubesheet, floating head, etc.).

Stream E is the leakage stream between the baffle edge and the shell wall (see Fig. 3).

Stream F is the bypass stream in flow channels due to omission of tubes in tube pass partitions. This stream has been added to the original Tinker model by Palen and Taborek [13] . It behaves similarly to stream C, but will be present only in some tube layouts.

Tinker s original analysis[14,15] is quite complex and hard to understand. In basic principle it states that the pressure drop of the cross-flow stream B will act as a driving force for the other streams, forcing part of the flow through the leakage and bypass clearances. This is demonstrated in Figs. 2 and 3.

For better understanding of the physical mechanisms, the flow distribution model of Fig. 1 was reduced

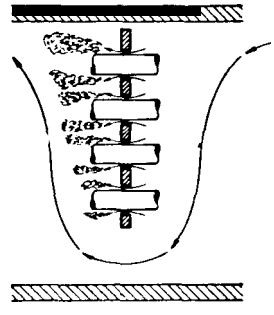

Figure 2 Schematic picture of tube-to-baffle leakage stream A.

© 1983 Hemisphere Publishing Corporation

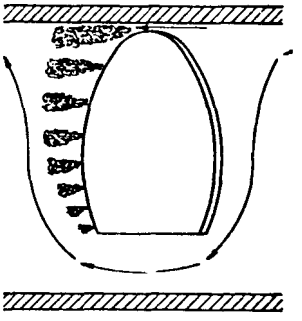

Figure 3 Schematic picture of shell-to-baffle leakage stream E.

to an equivalent piping or nodal diagram as shown in Fig. 4, with the flow streams represented by arrows and the above-defined letters, whereas the resistances to flow for each stream are represented by a valve and the letter K with proper subscript.

The cross-flow, bypass, and pass partition streams (B, C, F) are shown flowing in parallel across each baffle space, joining in the windows, and redividing at the next baffle space. The tube baffle and baffle shell leakage streams (A, E) are shown flowing in parallel from a hypothetical nodal point in one baffle space to a corresponding point in the next. Once this model is accepted, well-known piping network flow techniques can be applied to solve for the flow rate of each stream in terms of the cross-sectional area for flow and the flow resistance. The flow rates are given implicitly by the pressure drop equation:

$$\Delta p_j = CK_j \left(\frac{\dot{M}_j}{S_j}\right)^2 \tag{4}$$

where $\dot{M}_j$ = flow rate of any streamj (A, B, C, E, F)
S_j = corresponding flow area
K_j = flow resistance of stream j, particular to any flow channel geometry and Reynolds number $K_j = f(\dot{M}_j)$

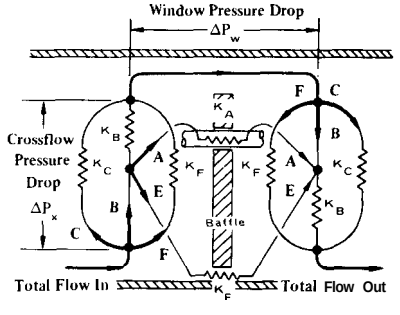

Figure 4 Schematic model of shell-side flow branches and their resistances across one baffle space. From Palen and Taborek [13].

The pressure drop relations may be expressed as follows:

$$\Delta p_C = \Delta p_F = \Delta p_B = \Delta p_X \tag{5}$$

$$\Delta p_A = \Delta p_E = \Delta p_X = \Delta p_W \tag{6}$$

where Δp_X and Δp_W are the cross-flow and window pressure drops shown in Fig. 4.

The final equation required is the mass balance of the total flow rate $\dot{M}$:

$$\dot{M} = \Sigma \dot{M}_j = \dot{M}_A + \dot{M}_B + \dot{M}_C + \dot{M}_E + \dot{M}_F \tag{7}$$

Once the representative cross-sectional flow areas S_j are defined, Eqs. (4)-(7) can be solved for the flow rates if the flow resistance terms K_j are known. Solution is somewhat simplified by rearranging the pressure drop equations into the following forms:

$$F_j = \frac{Q_j}{\Sigma Q_i} \tag{8}$$

$$Q_j = S_j \sqrt{\frac{1}{K_j}} \qquad \text{for j = B, C, F} \tag{9}$$

$$Q_j = S_j \sqrt{\frac{1+z}{K_j}} \qquad \text{for } j = \text{A or E} \tag{10}$$

$$z = \frac{\Delta p_W}{\Delta p_X} \tag{11}$$

$$\dot{M}_j = (F_j)(\dot{M}) \tag{12}$$

where F_j = flow fraction of the total stream $\dot{M}$
Q_j = relative flow stream value, introduced for simplification of the algebraic manipulations
$\Delta p_W, \Delta p_X$ = baffle window and cross-flow pressure drops, respectively

Since the K_j values are functions of Reynolds numbers, and therefore of the individual stream flow rates $\dot{M}_j$ or flow fractions F_j, the solution of the above set of equations is a reiterative one. Such time-consuming calculations were beyond the computational practicalities of the 1950s, and Tinker resorted to converting the method into a nonreiterative one, by assigning constant values for the K_j resistances and z (Eq. 11). This permitted solutions by slide rule but at a great sacrifice to the potential accuracy [13].

Notice that in this analytical method, pressure drop equations must be solved first, in order to obtain the effective flow rates for each stream. These values are then applied to the heat transfer equations. The leakage stream E is considered by Tinker to be fully heat transfer ineffective, consistent with later developments. However, Tinker also considered, apparently as a safety and simplification measure, the bypass C stream as heat transfer ineffective, which was later proven incorrect. Because of the relatively complex calculations and poor

© 1983 Hemisphere Publishing Corporation

3.3.3

Recommended method: Principles and limitations

J. Taborek

In selecting the recommended method for this handbook, the considerations summarized in Sec. 3.3.2 indicated clearly that, of all the methods surveyed, the Bell-Delaware method is in principle the most suitable one at the present. It fulfills the following requirements.

1. It is a method that can be handled readily by hand-held calculators, progressing in a stepwise manner and making use of graphical solutions of auxiliary variables. It is considered essential that the recommended method may be used in this way for educational purposes and other reasons discussed later. Even if complex computer programs are available, there is-and always will be-a need to calculate the performance of an exchanger by hand methods. Only if calculations are performed manually will the engineer develop a feel for the design process as compared to the impersonal black box calculations of a computer program.

2. The recommended method can be, however, readily programmed, possibly in parts, into even small programmable calculators, This is probably the most effective way of using the method, freeing the engineer from the time-consuming details of calculations and yet retaining the closeness of individual judgment.

3. The method is based on the principles of Tinker s flow distribution model, and thus is much superior to integral methods, such as Kern s or Donohue s. It was selected in preference to the original Tinker method, which did not have the benefit of the Delaware data. Major overhaul of Tinker s method would be necessary to achieve the same accuracy [1].

It should be clear, however, that this nonreiterative method cannot compete for accuracy with the complex stream analysis-type methods, which require relatively fast computers for their solution. Nevertheless, for a well-designed exchanger without any extremes, the results are within respectable limits of accuracy (see additional comments later in this section).

A. Method structure

The method uses ideal tube bank j_i and f_i factors and then corrects directly the resulting α_i and Δp_i for deviations caused by the various split streams. The j_i and f_i factors are defined as follows:

$$j_i = \frac{\alpha_i}{C_p \dot{m}} (\mathrm{Pr})^{2/3} (\phi)^{-r} = f(\mathrm{Re},\ \text{tube layout}) \qquad (1)$$

$$f_i = 10^3 \frac{\Delta p_i \rho}{2(\dot{m})^2\, \mathrm{N}_c} (\phi)^{r} = f(\mathrm{Re},\ \text{tube layout}) \qquad (2)$$

where ϕ is the viscosity correction factor.

The Reynolds number in the above equation is based on the minimum cross-sectional flow area at the shell diameter and the full shell-side stream. This is contrary to Tinker s method and the stream analysis-type approach, where the magnitude of the individual streams is determined. No attempt is made to express the j_i and f_i curves [Figs. 3.3.7(1)-3.3.7(3)] by a correlating equation. The designer can read the values directly from the graphs, or for computer application a set of curve-fit constants is used. The schematic diagram of the flow distribution in a baffled exchanger is shown in Fig. 3.3.2(1). The streams are designated as follows:

© 1983 Hemisphere Publishing Corporation

A = leakage in the clearance between tube and tube hole in a baffle
B = cross-flow stream in tube nest
C = bypass stream between shell wall and tube bundle
E = leakage between shell wall and baffle
F = bypass stream in tubepass partitions (if applicable)

The B stream is regarded as the essential stream in the exchanger, with the other streams exerting various modifying effects on the performance as predicted for the B stream alone.

Not all of the leakage and bypass streams have the same relative magnitude of effect and, of course, they respond differently to the various geometrical parameters of the shell side. For example, the A stream (tube-to-baffle leakage) has only a relatively small effect on the heat transfer coefficient and a moderate effect on pressure drop. The C stream has a relatively large effect, but there are mechanical ways of partially blocking this flow to minimize that effect. The E stream (shell-to-baffle leakage) has an extremely serious effect, and unfortunately there is relatively little one can do to help. Finally, the pass divider bypass stream (F stream) has a moderate effect and responds to some of the same treatments that the bundle bypass stream does.

The Delaware method does not use the actual magnitude of the streams to correct for the effective flow rate of the B stream, but rather uses a number of correction factors to modify the α_i and Δp_i values to account for decrease of the B stream due to bypass and leakage. This concept is explained later in greater detail. For further information on the development of these correction factors from the Delaware data, the reader should consult [2]. In this connection one additional note may be useful. The original presentation of the Delaware correction factors was based on the following format, for example,

$$1 - \frac{\alpha_l}{\alpha_i} = f(\text{geometry}) \tag{3}$$

where α_l is the heat transfer coefficient with leakage present. In later publications this was changed by simple rearrangement into the much-easier-to-use form of a multiplier to the ideal tube bank α_i.

$$\alpha_l = \alpha_i J_l \tag{4}$$

B. Shell-side heat transfer equation

The basic equation for calculating the effective average shell-side heat transfer coefficient is given in Eq. (5):

$$\alpha_s = \alpha_i (J_c J_l J_b J_s J_r) \tag{5}$$

where α_i is the heat transfer coefficient for pure cross flow in an ideal tube bank. This value is calculated assuming that the entire shell-side stream flows across the ideal tube bank formed by the tube array at the centerline of the exchanger. The value of α_i is obtained from the j_i curves, Sec. 3.3.7, and is defined in Eq. (1).

J_c is the correction factor for baffle cut. This factor takes into account the heat transfer in the window and calculates the overall average for the entire heat exchanger [Fig. 3.3.6(7)]. This correction factor is essentially a function of the fraction of the total tubes in the heat exchanger that are in cross flow (i.e., located between the baffle tips of adjacent baffles). This value is equal to 1.0 for a heat exchanger in which there are no tubes in the window, increases to a value as high as 1.15 for a design in which the windows are very small (and the window velocity is very high), and decreases to a value of about 0.65 for very large baffle cuts. A typical value for a well-designed heat exchanger is near 1.0, signifying that the tubular surface in the window is equally effective as in the cross-flow portion of the exchanger.

J_l is the correction factor for baffle leakage effects, including both shell-to-baffle and tube-to-baffle leakage (A and E streams). This correction factor is a function of the ratio of total leakage area per baffle to the cross-flow area between adjacent baffles and also of the ratio of the shell-to-baffle leakage area to the tube-to-baffle leakage area. J_l weights the shell-to-baffle leakage more heavily than the tube-to-baffle leakage. It is also a function of the clearances between tube and baffle and shell and baffle so that credit is given for tighter constructional practices. The correlation for J_l penalizes the design if the baffles are put too close together, leading to an excessive fraction of the flow being in the leakage streams compared to the crossflow. A typical value of J_l is in the range of 0.7 to 0.8 [see Fig. 3.3.6(9)].

J_b is the correction factor for the bundle bypass flow (C and F streams). J_b accounts for differences in construction: For the relatively small clearance between the outermost tubes and the shell for fixed tubesheet construction, $J_b \approx 0.9$, whereas for the much larger clearances required by pull-through floating-head construction, $J_b \approx 0.7$. J_b also takes into account the improvement made by sealing strips. These are typically longitudinal strips of metal between the outside of the bundle and the shell and fastened to the baffles; they periodically force the bypass flow back into the tube field, causing higher local velocities and heat transfer coefficients and mixing of the bypass stream with the main cross-flow stream. Proper use of sealing strips in a split-ring or pull-through floating head can increase J_b from 0.7 to 0.9 [see Fig. 3.3.6(10)].

J_s is the correction factor for variable baffle spacing in the inlet and outlet sections. Nozzle dimensions frequently require that the nozzles be located far enough

© 1983 Hemisphere Publishing Corporation

from the tubesheets that it may be necessary to increase the baffle spacing for the inlet and outlet sections. This correction factor allows for the change in the average shell-side coefficient caused by these locally lower velocities. J_s will usually be between 0.85 and 1.0 [see Fig. 3.3.6(13)].

J_r is the correction factor for adverse temperature gradient buildup in laminar flow. It is well known that, in laminar flow, the heat transfer coefficient decreases with increasing distance from the start of heating because of the development of an adverse temperature gradient from the conduction process. This gradient resists further transfer of heat and therefore lowers the local and the average heat transfer coefficients with increasing distance. This correction has been worked out mathematically for flow in well-defined geometries such as inside round tubes, but it is also found experimentally to exist during flow across tube banks. For large heat exchangers in deep laminar flow (Re < 20), it can result in a decrease in the average heat transfer coefficient by a factor of 2 or more compared to what would have been predicted based on flow across a 10-row tube bank, This correction factor applies only if the shell-side Reynolds number *is* less than 100 and is fully effective only in deep laminar flow characterized by Re, < 20 [see Fig. 3.3.6(12)].

The combined effect of all of these correction factors for a well-designed shell-and-tube heat exchanger is typically on the order of 0.6; that is, the effective mean shell-side heat transfer coefficient for the exchanger is 60% of that calculated if the entire flow took place across an ideal tube bank corresponding in geometry to one cross-flow section. It is interesting to observe that this value has long been used as a rule of thumb.

Notice that this method does not allow for interaction between the effects of the various parasitic streams. For example, if the bundle bypass clearance should change (such as transition from fixed tubesheet to split-ring floating-head design), only J_b will be altered. In fact, any change in any one of the streams will affect all the remaining ones. However, only the stream analysis treatment will account for such change at the expense of much more complicated calculations.

C. Shell-side pressure drop

The shell-side pressure drop is calculated as a summation of the pressure drops for the inlet and exit sections, the internal cross-flow sections, and the window sections, as explained further below. Again, the method uses the ideal tube bank friction factor f_i as a basis, as defined in Eq. (2). The correction factors (analogous to those for heat transfer) are defined as follows:

R_l is the correction factor for baffle leakage effects (A and E streams). This correction factor is different in magnitude from J_l but depends on the same ratios of total baffle leakage area to cross-flow area. Typically, $R_l \approx$ 0.4-0.5, though lower values may be found in exchangers with closely spaced baffles [see Fig. 3.3.6(8)].

R_b is the correction factor for bypass flow (C and F streams). It is also different in magnitude from J_b, but similar in form. Typically, $R_b \approx 0.5$-0.8, depending on construction type and number of sealing strips. The lower value would be typical of a pull-through floating head with only one or two pairs of sealing strips, the higher value typical of a fixed tubesheet design [see Fig. 3.3.6(11)].

R_s is the correction factor for the entrance and exit sections having a different baffle spacing than the internal sections (see Sec. 3.3.8).

Next, let us define the pressure drop in an equivalent ideal tube bank for the cross-flow section as ΔP_{bi} and for the baffle window section as Δp_{wi}. (For detailed treatment, see Sec. 3.3.8).

For an exchanger that has both bypass and leakage streams, the three pressure drop components are calculated in principle as follows:

1. The pressure drop in the interior cross-flow sections (baffle tip to baffle tip) is affected by both bypass and leakage. Therefore, the combined pressure drop of all the interior cross-flow sections is

$$\Delta p_c = \Delta p_{bi} (N_b - 1) R_l R_b \tag{6}$$

where N_b is number of baffles.

2. The pressure drop in the windows is affected by leakage but not by bypass. Therefore, the combined pressure drop of all the window sections is given by

$$\Delta p_w = \Delta p_{wi} N_b R_l \tag{7}$$

3. The pressure drop in the entrance and exit sections is affected by bypass but not by leakage. Additionally, there is an effect due to possibly larger baffle spacing. Therefore, the combined pressure drop for the entrance and exit sections is

$$\Delta p_e = \Delta p_{bi} \frac{N_c + N_{cw}}{N_c} R_b R_s \tag{8}$$

where N_c and N_{cw} are the number of tube rows crossed in the exchanger and in the baffle window, respectively. The total pressure drop over the exchanger is then

$$\Delta p_{tot} = \Delta p_c + \Delta p_w + \Delta p_e \tag{9}$$

This does not include the pressure drop in the nozzles, which is usually included in the specification. The nozzle (or other shell entry geometries) pressure drop is calculated by procedures given in Part 4).

© 1983 Hemisphere Publishing Corporation
HEDH

Although each of the correction factors can vary over quite wide ranges, depending on the configuration of the heat exchanger, the total shell-side pressure drop of a typical shell-and-tube exchanger is on the order of 20-30% of the pressure drop that would be calculated for flow through the corresponding heat exchanger without baffle leakage and without tube bundle bypass effects. In fact, this is where most of the earlier correlations for heat exchanger design failed most seriously: Not knowing the very large effects on pressure drop due to leakage and bypass, it was not uncommon for some of them to overestimate the shell-side pressure drop by a factor of 2 or even 10.

It should be noted, however, that overprediction of pressure drop may seriously affect the heat transfer design of a shell-and-tube exchanger. As is customary, the design is based on a maximum permissible value of pressure drop, mostly to comply with available pressure heads. If shell-side pressure drop is overestimated, the design is forced into large baffle spacings, larger shell diameters, or other shell geometries, all of which measures decrease shell-side flow velocity. In turn, the lower shell-side velocity results in lower heat transfer coefficients and larger units. In cases where it is applicable, fouling tendencies will also increase as a result of lower flow velocity. Thus, correct prediction of pressure drop is equally as essential as prediction of heat transfer.

D. Comparison of the recommended method with the Delaware method and probable accuracy

The method documented here is based in principle on the Delaware method (as per the latest published versions). However, a number of modifications are introduced here for the first time, as follows:

1. The correction factor curves for leakage J_l and R_l are adjusted to comply better with data and assume a theoretically correct form, approaching asymptotically rather low values at high leakage flow areas.
2. A correction factor for entry and outlet baffle spacing, based on [3], is added.
3. Treatment of the pressure drop has been put on a more understandable basis [3].
4. The method for low fin tubes has been completely modified and made systematically comparable to that for plain tubes.
5. The leakage and bypass flow areas are defined according to standard practices and experience values ***(Sec. 3.3.6).***
6. A complete data input section is included, with comments as to good design practices and limiting values.
7. A section on interpretation of results gives guidelines of evaluation of all important performance parameters.
8. A section on design gives rules on how to proceed from rating of a given exchanger to the process of establishing the dimensions of an exchanger for a given duty and pressure drop limitations.

The question is always asked as to the probable accuracy of the method. Bell [3] is deliberately cautious, basing his comments as to the possible errors on the observations by Palen and Taborek [1]. However, the data in [1] encompassed a wide variety of exchangers, some with extremes of design parameters. No method of the simplicity of the Delaware type will respond sufficiently to such cases. If the sample is limited to what may be termed a well-designed exchanger with respect to baffle spacing, baffle cut, tube layout, and all the bypass and leakage clearances, the probable accuracy of the method will improve considerably.

Superimposed on this are the effects of the temperature profile distortion due to the bypass and leakage streams (see Sec. 1.5). No published method attacks this difficult subject, and all cases with close temperature approaches should be given special consideration.

Furthermore, it is often not realized (as it is never spelled out in the pertinent texts) that even the simplest case of flow inside tubes calculated by the best available equations will result not untypically in errors of the order of magnitude of ±15% (average).

To answer the question of the probable accuracy of the recommended method for shell-side flow, the following speculation can be made, assuming a well-designed exchanger.

1. In turbulent flow heat transfer, a ±25% error must be expected, although some cases will be predicted with better accuracy. Turbulent flow pressure drop will show a scatter of about ±40% for 75% of data tested and larger, as geometry and fluid properties reach more extreme values. However, the average cases will tend to be on the safe side and have a closer error band.
2. In laminar flow, both heat transfer and pressure drop tend to be on the safe side, but scatter is too great to discern any definable trends. No safety factors appear necessary in this flow regime.

Some additional comments may be useful in the interpretation of probable accuracy. Specifications often call for rather exaggerated fouling resistances as an indirect measure of safety, and may constitute a predominant resistance. As the relative magnitude of fouling increases, the less sensitive the design becomes to errors in the overall heat transfer coefficient. Thus, the previously quoted error values ***become much smaller*** if projected into the overall coefficient. An error analysis is

© 1983 Hemisphere Publishing Corporation

indicated in all such cases. For example, if the shell-side flow constitutes about 40% of the overall resistance (not untypical), 20% error in the shell-side coefficient will amount to only about 12% error in the overall coefficient.

Allowable pressure drops are usually put on the safe side to begin with. Exceptions are compressor intercoolers and similar applications where pressure drop is a prime economic variable. Other uncertainties, primarily in physical properties, fluid composition, flow rates, and temperatures, exhibit the fortunate tendency toward compensating rather than additive errors. Thus, the question of accuracy and the need for safety factors must be left to engineering judgment, taking all the above circumstances into account. The user should be aware, however, of the general philosophy of the method, which is geared toward the average of the error band, except as noted previously.

Nomenclature** for **Section 3.3.3 appears at the end of Section 3.3.11.

REFERENCES FOR SECTION 3.3.3

1. Palen, J. W., and Taborek, J., Solution of Shellside Pressure Drop and Heat Transfer by Stream Analysis Method, ***Chem. Eng. Prog. Symp. Ser., vol. 65,*** no. 92, 1969.
2. Bell, K. J., Final Report of the Cooperative Research Program on Shell-and-Tube-Heat Exchangers, ***University of Delaware Eng. Exp. Sta. Bull. 5,*** 1963.
3. Bell, K. J., Private communications (1963–1980), and his D. Q. Kern Memorial Award Lecture at the AIChE/ASME Natl. Heat Transfer Conf., San Diego, Calif., 1979 (unpublished).
4. Chilton, C. H., and Perry, R. H., eds., ***Chemical Engineer's Handbook,*** 5th ed., sec. 10, 1973.

© 1983 Hemisphere Publishing Corporation

3.3.4

Practices of shell-and-tube heat exchanger design

J. Taborek

■ In this section we discuss briefly some of the practices and problems in shell-and-tube exchanger design that, although important, are not a direct part of the thermohydraulic calculation process.

A. Heat exchanger specification sheets

By established practice, a majority of shell-and-tube exchangers are designed by the manufacturers from specification sheets supplied by the user and partially filed out by the designer. A typical such specification sheet, taken from TEMA Standards [1], is reproduced in Fig. 1. Unfortunately, the information transferred from the user to the designer and fabricator by these forms almost never contains sufficient information for a really complete design, and the details of who is really responsible for what are rather confused. Unless there is close cooperation between the parties involved, a poor design may result.

On the other hand, the user often imposes unnecessary constraints, such as specified tube diameter and tube length, shell type and baffle type, and other design parameters, which at closer examination are found to be rather arbitrary and prevent an optimum or a good design. Specification of the maximum permissible pressure drop is probably the most sensitive of the entries, as it for all practical purposes fixes the design by inherent implications. Nevertheless, this crucial value is often based on rather arbitrary criteria. Equally so, fouling resistances are specified from experience values or are based on TEMA Standards for lack of any better sources.

The frequent practice of using high fouling resistances as safety factors is dangerous, as the amount of safety gained is relative and can be determined only after all the resistances have been established. With the exception of very common fluids, the specification of physical properties, especially for fluid mixtures, is not only a most time-consuming chore, but also is subject to potentially great errors as sources of data are scarce. More often than not, crudely estimated values are used in the absence of better answers.

Thus the practices and usage of the specification sheets is a rather sensitive problem, and the designer should make sure that input of sufficient detail but without unnecessary restrictions is available.

The recent trend, especially with large user companies, is to perform the thermohydraulic design themselves and to let the manufacturer design the details of constructional elements. This has the advantage that the user has more direct access to various aspects of the process, checks for operation at other-than-normal conditions, usually a better supply of physical properties data, and, last but not least, access to large, sophisticated computer programs. But close cooperation between the user and the manufacturers remains a very crucial element.

B. Rating, design, and optimization

The terms rating, design, and optimization have very definite meanings, but are often confused. Let us clarify what is understood under these terms in this text.

Rating an exchanger means to evaluate the thermohydraulic performance of a fully specified exchanger. The result of a rating process is a judgment as to the

© 1983 Hemisphere Publishing Corporation

HEAT EXCHANGER SPECIFICATION SHEET

							Job No.		
2	Customer						Reference No.		
3	Address						Proposal No.		
4	Plant Location						Date	Rev.	
5	Service of Unit						Item No.		
6	Size	Type	(Hor/Vert)				Connected In	Parallel	Series
7	Surf/Unit (Gross/Eff.)	Sq Ft: Shells/Unit					Surf/Shell (Gross/Eff.)		Sq Ft
8	PERFORMANCE OF ONE UNIT								
9	Fluid Allocation		Shell Side				Tube Side		
10	Fluid Name								
11	Fluid Quantity, Total	Lb/Hr							
12	Vapor (In/Out)								
13	Liquid								
14	Steam								
15	Water								
16	Noncondensable								
17	Temperature (In/Out)	°F							
18	Specific Gravity								
19	Viscosity, Liquid	Cp							
20	Molecular Weight, Vapor								
21	Molecular Weight, Noncondensable								
22	Specific Heat	Btu/Lb °F							
23	Thermal Conductivity	Btu Ft/Hr Sq Ft °F							
24	Latent Heat	Btu/Lb @ °F							
25	Inlet Pressure	Psig							
26	Velocity	Ft/S							
27	Pressure Drop, Allow./Calc.	Psi	/				/		
28	Fouling Resistance (Min.)								
29	Heat Exchanged		Btu/Hr; MTD (Corrected)						°F
30	Transfer Rate, Service		Clean						Btu/Hr Sq Ft °F
31	CONSTRUCTION OF ONE SHELL						Sketch (Bundle/Nozzle Orientation)		
32			Shell Side		Tube Side				
33	Design/Test Pressure	Psig	/		/				
34	Design Temperature	°F							
35	No. Passes per Shell								
36	Corrosion Allowance	In.							
37	Connections	In							
38	Size &	Out							
39	Rating	Intermediate							
40	Tube No.	OD	In.;Thk (Min/Avg)		In.; Length	Ft; Pitch	In. ◇ 30 △ 60 □ 90 ◇ 45		
41	Tube Type				Material				
42	Shell	ID	OD	In.	Shell Cover		(Integ.) (Remov.)		
43	Channel or Bonnet				Channel Cover				
44	Tubesheet-Stationary				Tubesheet-Floating				
45	Floating Head Cover				Impingement Protection				
46	Baffles-Cross	Type			% Cut (Diam/Area)	Spacing: c/c	Inlet	In.	
47	Baffles-Long				Seal Type				
48	Supports-Tube	U-Bend			Type				
49	Bypass Seal Arrangement				Tube-Tubesheet Joint				
50	Expansion Joint				Type				
51	ρv²-Inlet Nozzle	Bundle Entrance			Bundle Exit				
52	Gaskets-Shell Side				Tube Side				
53	-Floating Head								
54	Code Requirements						TEMA Class		
55	Weight/Shell	Filled with Water			Bundle			Lb	
56	Remarks								
57									
61									

Figure 1 Heat exchanger specification sheet [1].

ability of the unit to perform a desired duty and comply with other design conditions of operation (such as good pressure drop utilization, cleaning, thermal expansion, safety, tube vibration, etc.). Bids of manufacturers are often subjected to the rating process by the user, and a truly successful design depends on the cooperation of the two parties.

In other instances, existing exchangers can be rated for duties deviating from the original design conditions because of process changes. The so-called unknown heat balance ratings, discussed later in this section are typical of the more sophisticated possibilities.

Design is the process of determining all essential constructional dimensions of an exchanger that must perform a given heat duty and respect limitations on shell-side and tube-side pressure drop. A number of other criteria are also specified or implied, such as ease of cleaning and maintenance, minimum and maximum flow velocities, erosion, size or weight limitations, tube vibration, thermal expansion, and so on-essentially good practices of design.

The input specifications as to constructional elements should be restricted to the unconditionally required ones (such as maximum length, weight, safety, materials, etc.). Overspecification will impair the designer s freedom to choose the best combination of parameters, such as shell type, tube diameter and length, baffle type, tube layout geometry, and so on. Each design problem has a number of potential solutions, but only one will have the best combination of character-

© 1983 Hemisphere Publishing Corporation

istics, including cost, and that one should not be missed on account of overspecification.

Optimization of heat exchanger design is closely connected with the above statements. Actually, a design performed with intelligently chosen variations of construction elements is a first-degree optimization, with the objective function being the most effective overall operational performance. This type of optimization is termed the ***case study method,*** and is void of mathematical complexities and relies solely on engineering judgment for acceptance of any potential solution, be it performed by manual or computer methods.

Analytical methods were tried, but, although potentially applicable to ***specific*** solutions, they have not been successful for shell-and-tube exchangers in general, as the objective function becomes very complex and sensitive, including such hard-to-define items as cost of maintenance, reliability, and so on. Geometry constraints and step functions in the thermohydraulic equations often required in the design process are also very difficult to implement in an analytical formulation. The results of such optimization can be very misleading, and ultimately engineering judgment must prevail. A good recent survey of optimization techniques and methods for heat exchangers is by Shah et al. [2], and for specific applications to shell-and-tube exchangers by Palen et al. [3]. This latter technique is based on M. J. Box s complex method, which permits any constraints, step functions, and arbitrary calculational procedures, as it is essentially a mathematically organized case study optimization. In Fig. 2 a test case is presented from [3] showing the process of optimization from simply estimated initial cost as an objective function. It takes typically 70 to 150 individual design cases to reach a solution, and thus simplified methods must be used to guide the designer in the potentially right direction. Final detailed study and use of engineering judgment-the most reliable optimization method-is always necessary.

C. Calculation method by degree of complexity

In principle, we can distinguish three types of heat exchanger calculation methods: estimation methods, methods of intermediate complexity, and computer program methods.

(a) Estimation methods

Using simple approximations, rules of thumb, or even selected constant values for the thermohydraulic performance variables, estimation methods are extremely useful for preliminary calculations. Frequently, such estimations can identify those design variables that are the most restrictive, and thus help to focus the designer s attention on them in the early stages of the search for a better solution. Computerized versions of the estimation methods are useful as an element in an overall program for the optimization of complex systems and process loops. Such systems may contain heat transfer equipment, fractionating towers, compressors, and so on. For these applications, the exchanger design must be performed in a fraction of a second.

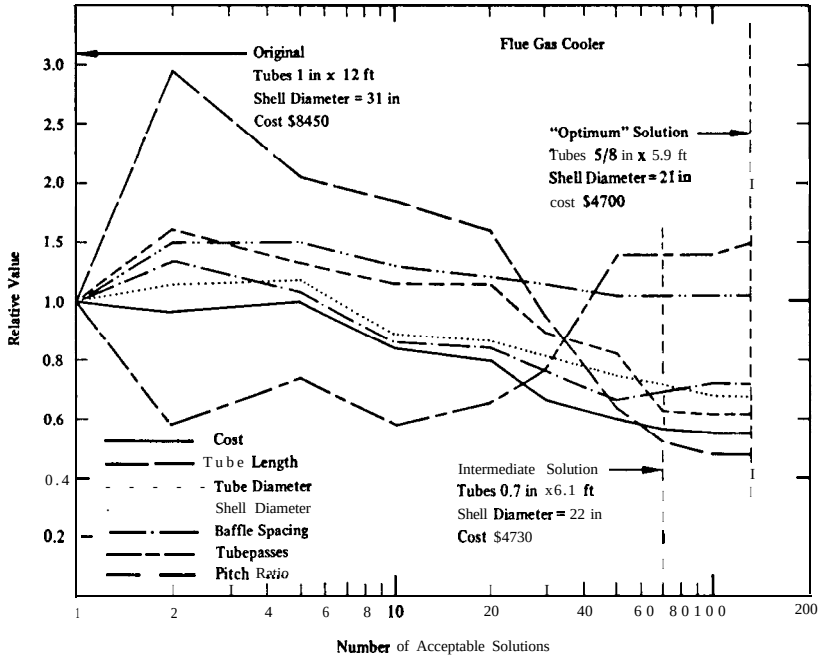

Figure 2 The process of optimization from simply estimated initial cost as an objective function [2].

© 1983 Hemisphere I blishing Corporation

(b) Methods of *intermediate complexity*

Solvable by hand-held calculators, preferably with programmable capabilities, methods of intermediate complexity must still be rather simple in terms of input variables, but should produce results of substantially increased accuracy compared to the estimation methods. A distinct characteristic of methods of this type-for example, the Delaware method for shell-side flow-is that the designer s judgment and engineering feel remain important and integral parts of the design process. This is in contrast to the frequently impersonal solutions of generalized computer programs, especially of the optimization type, where engineering judgment often disappears. Although the methods of intermediate complexity are particularly well suited for educational purposes, it is probable that their use for industrial designs will diminish in favor of the quick estimation method on the one hand and the sophisticated computer-oriented method on the other hand.

(c) Computer program methods

Under the category of computer methods we consider calculation procedures with practically no restriction on difficulty and with the main objective of accuracy, although some rational balance between complexity and probable accuracy is implied. Typically, the input to such programs is quite complex both in constructional parameters and physical properties, especially in two-phase-flow problems. Equally so, the result output is detailed and unconditionally requires careful engineering evaluation. A number of heat exchanger programs are available, but their quality varies widely with respect to the thermohydraulic methods used, flexibility of input-output, documentation, and the ease of engineer-computer interaction. The best ones are in the proprietary domain. Nevertheless, the general rule applies that no computer program is any better than the engineer-user s capability to analyze critically and to evaluate the results. As a matter of fact, an increasing danger exists that, under the cover of the seeming perfection, computer results are being accepted without the benefit of engineering judgment. Beginners in the art of heat exchanger design should be permitted access to such programs only under strict supervision of experienced practitioners of the art, to avoid potentially disastrous results.

D. Effects and selection of constructional elements

It is of utmost importance that the designer of shell-and-tube exchangers become acquainted with probable effects of elements of construction, such as:

1. Shell type
2. Tube bundle type
3. Tube diameter
4. Tube length
5. Tube layout pattern and pitch
6. Baffle type, spacing, and cut

These construction elements are described in detail in Sec. 4.2, and the serious user is urged to become familiar with these important parameters and their effects on the design and optimization of shell-and-tube exchangers. Only a summary is repeated here as a reminder and for quick reference.

(a) Shell type

The basic shell type is TEMA E, with entry and outlet nozzles at the opposite ends in single shell pass. The method documented here without further adjustments handles only this type of shell (see Sec. 3.3.11).

1. TEMA J is the so-called divided flow type, with one inlet and two outlet nozzles (thus dividing the flow in half). This results in pressure drop of approximately one-eighth that of the E type. The main use is for low-pressure applications such as gas coolers.
2. TEMA G is the so-called split flow type, with longitudinal baffle. The pressure drop is about the same as in an E shell, but the thermal effectiveness is superior. Its main use is for reboilers, but occasionally it is used for no-phase-change flow.
3. The TEMA X shell, only recently introduced as a recognized entity, has the shell-side flow in pure cross flow, without cross baffles. The result is extremely low pressure drop. It is used for gases and condensing vapors at low pressures.
4. The TEMA F shell has two shell passes because it has a longitudinal baffle. Used in applications where two shells in a series would otherwise be required, because close temperature approach and/or low shell-side flow rate precludes use of an E shell. Pressure drop is approximately eight times that for an E shell, but this is usually acceptable in the above-mentioned specific applications. It is often excluded from industrial applications because of potential leakage through the longitudinal baffle. A more detailed discussion of this problem is treated in [4] and Sec. 1.5.

(b) Tube bundle type

The tube bundle type determines mainly-as far as the thermohydraulic calculation method is concerned-the possible bundle-to-shell bypass. In mechanical design considerations, it is selected mainly on account of compatibility with thermal expansion considerations such as fixed tubesheet, various types of floating head,

© 1983 Hemisphere Publishing Corporation

and U-tube bundle, just to name the most important types. Not all combinations of baffle type, shell type, and tubepasses are possible (see Sec. 4.2).

(c) Tube diameter

Thermohydraulic considerations favor small tube diameter. Also, greater surface density within a given shell is possible with small diameter tubes. Tube cleaning practices limit tube diameters to a minimum of approximately 20 mm OD. For reboilers and condensers, other tube diameter selection considerations will apply.

(d) Tube length

In general, the longer the tube, the lower the cost of the exchangers for a given surface. This is due to the resulting smaller shell diameter, thinner tubesheets and flanges, fewer pieces to handle, and fewer holes to drill. The limitations are accommodating shell-side flow areas with reasonable baffle spacing, and practical design considerations. Usual length-to-shell diameter ratios range from about 5 to 10 for best performance.

(e) Tube layout pattern and pitch

A good practice for tube layout calls for minimum pitch of 1.25 times tube diameter and/or a minimum webb thickness between tubes of approximately 3.2 mm to assure sufficient strength for tube rolling. Generally, the smallest pitch in a triangular 30 layout is preferred for turbulent and laminar flow in clean service and 90 or 45 layout with 6.4 mm clearance for cases where mechanical cleaning is required. Exceptions may exist, however, especially if pressure drop or flow velocity must be regulated.

(f) Baffle type, spacing, and cut

The function of the cross baffle is to direct the flow across the tubefield as well as to mechanically support the tubes against sagging and possible vibration. The most common type is the segmental baffle, with a baffle cut resulting in a baffle window. Baffle spacing is subject to minimum and maximum limitations for good thermohydraulic performance and tube support [see Fig. 3.3.5(6)]. The ratio of baffle spacing to baffle cut is a crucial design parameter for efficient conversion of pressure drop to heat transfer. If very low pressure drops have to be accommodated, so-called double-segmental or disk-and-doughnut baffles will reduce the pressure drop by about 60%. Other types include triple-segmental and no-tubes-in-window, for particularly low pressure drops and prevention of tube vibration [see Fig. 4.2.5(3)].

E. Some other design considerations

The design of a shell-and-tube exchanger is a combination of proper selection of thermohydraulic elements, calculation of mechanical and strength requirements, and respect for operational practices. These demands most often call for a compromise, as the ideal combination of the elements may not be possible or practical. Some of these considerations are briefly reviewed below, but are treated in specific detail elsewhere in this handbook.

(a) Thermal expansion

Temperature differences between the shell and tube fluids cause the construction elements of the heat exchanger to expand by different amounts, and provisions must be taken to accommodate this situation. The fixed tubesheet exchanger simply absorbs these stresses either directly (at low ΔT) or with the help of a shell-side expansion joint. Special design types of tube bundles (as described in detail in Sec. 4.2) were created to absorb the thermal expansion stresses by other means. The simplest, most effective, and least expensive one is the U-tube exchanger. If not applicable because of other considerations, resort is made to the use of some type of floating-head construction.

In general, thermal stresses should not be calculated only at the operating temperature levels, but in critical cases allowances should be made for startup and during emergency conditions. Thermal stress that is not otherwise taken care of will result in straining the basic tube-to-tubesheet joint, potentially resulting in leakage, buckling of the tubes, or other rather dramatic mechanical failures.

(b) Fluid leakage

The separation of tube-side and shell-side fluid depends on:

1. Tightness of tube-to-tubesheet joints
2. In all floating-head designs, on the performance of the internal tubesheet gaskets
3. In stuffing-box designs, on the performance of the seal.

Tubes are generally rolled into tubesheets provided with two grooves about 0.4 mm ($\frac{1}{64}$ in) deep to assure tight grip. In some critical cases, tube ends are welded or brazed to the tubesheets after rolling. Even with all these precautions, leaks do develop as a result of thermal expansion (even in floating-head designs, because of differences between tube passes), and especially when tube bundles are removed for cleaning, thus imposing external stresses on the tube joints. Furthermore, tubes

© 1983 Hemisphere I blishing Corporation

may fail because of corrosion or vibration. If the process is of a nature that fluid leakage is detrimental, designs should be selected that will minimize such danger and permit plugging or replacement of defective tubes. Furthermore, if leakage may result in outright hazards, a double tubesheet design can be used, which will at least eliminate the danger resulting from mixing the fluids as a result of tube-to-tubesheet joint failures (see Sec. 4.2).

(c) Corrosion

In some cases corrosion rather than thermohydraulic considerations dominate choice of material and exchanger design features. However, because corrosion resistant materials are expensive, the corrosive fluid will be preferably placed in the tubes so that at least the shell need not be made of corrosive-resistant material. If corrosion cannot be effectively prevented but only slowed by choice of material, a design must be chosen in which corrosible components can be easily replaced. This may include the entire tube bundle, thus eliminating fixed tubesheet designs.

(d) Fouling and cleaning considerations

A majority of process fluids will deposit on the tube surface a scale or fouling layer, thus deteriorating heat transfer and making periodic cleaning necessary. The fouling characteristic of a given fluid is influenced mainly by tube wall temperature and flow velocity, and in some cases by tube material. Cooling water, as typically used in condensers and process stream coolers, is the most frequently encountered fouling fluid. Water tube-side velocities around 2 m/s (6 ft/s) should be used to obtain reasonable maintenance frequency. This will often dictate selection of an appropriate number of tube passes or baffle spacing. Shell-side flow, with its inherent eddy regions in the baffle corners, tends to foul surfaces more severely than tube-side flow, and large baffle spacings and baffle cuts are to be avoided in fouling services at all cost. Cleaning can be performed by mechanical means (rotating wire brushes on the tube side, high-velocity water jets on the shell side) or chemically (circulating a solvent). If the shell side is to be cleaned, a 45 or 90 tube layout with 6.3 mm ($\frac{1}{4}$ in) gap width is required for mechanical cleaning. In designs with expected severe fouling problem, the entire design may be dominated by features that will minimize fouling and/or facilitate cleaning.

(e) Fluid quantity

The effect of fluid quantity on proper design is extremely difficult to generalize. Tube-side flow velocity can be adjusted by the number of tube passes. Shell-side flow velocity is governed by the baffle spacing, which is subjected to practical maximum and minimum limits. In addition, the various shell flow design types allow selection from a wide range of flow arrangements, permitting further variations. As a general rule, however, it can be stated that if the two fluids have widely different flow quantities, a careful investigation as to the fluid allocation (tube side or shell side) is important, as is a careful analysis of other parameters involved, namely, tube diameter, tube length, tube layout, and pitch. The differences in design efficiency can be dramatic.

(f) *Fluid viscosity*

As a general rule, the high-viscosity fluid should be placed on the shell side, as the turbulence induced by the flow crossing the tube field will promote higher heat transfer. However, if the shell-side flow would still be laminar, then placing this fluid on the tube side should be considered.

REFERENCES FOR SECTION 3.3.4

1. ***Standards of Tubular Heat Exchanger Manufacturers Association,*** 6th ed., TEMA, New York, 1978.
2. Shah, R. K., Afimiwala, K. A., and Mayne, R. W., Heat Exchanger Optimization, ***Proc. 6th Int. Heat Transfer Conf., Toronto, 1978.***
3. Palen, J. W., Cham, T. P., and Taborek, J., Optimization of Shell-and-Tube Heat Exchangers by Case Study Method, ***Chem. Eng. Prog. Symp. Ser.,*** vol. 70, no. 138, 1974.
4. Rozenman, T. and Taborek, J., The Effect of Leakage Through the Longitudinal Baffle on the Performance of Two-Pass Shell Exchangers, ***AIChE Symp. Ser.,*** vol. 68, no. 118, 1968.

© 1983 Hemisphere Publishing Corporation

3.3.5

Input data and recommended practices

J. Taborek

■ In this section we deal with three subjects:

1. The basic set of input data as required for shell-side rating calculations, but also including those required for design of the overall exchanger, that is, including tube-side flow. These are presented in Table 1.
2. Detailed comments to the input data, to give guidance to the designer as to proper practices and standards.
3. Preliminary calculations of correlational parameters derived from the input data, as required for subsequent calculations.

A. Basic input data

We assume that the performance of a fully specified segmentally baffled exchanger is to be determined (rating) by the method recommended in Sec. 3.3.3 and described in detail in subsequent sections. Compared to some really simple estimation methods (e.g., Kern [I]), a relatively complex but still manageable set of input data is required. These include some values (such as leakage and bypass clearances) that are not readily available and usually must be estimated.

Basic data required for tube-side calculations are also included, as they must form an entity of the entire shell-and-tube exchanger rating process. Furthermore, tube-side data enter directly into shell-side flow calculations in several aspects-for example, tube wall temperature, tube count, and so on.

Because of their wide acceptance, the TEMA Standards [2] are used wherever applicable, but metric (DIN) standards are introduced wherever possible.

The set of required data is shown in Table 1.

B. Comments to input data (Table 1)

Item 1: D_s (mm), shell inside diameter. Determine from drawings if available. Tables 2-4 show suggested dimensional series for inch-based U.S. practice and for metric as per DIN 28 008 and other industrial standards. Notice that the inch-based dimensions pertain to the inside shell diameter, whereas the metric standards are based on seamless steel tubing and use the outside shell diameter as the primary dimension, therefore requiring the shell wall thickness for D_s determination.

In the inch-based series, the shells up to 21.25 in (535.75 mm) diameter are referred to as standard pipe ; however, above 12 in, shells are usually rolled and welded. There is no mandatory accepted standard, the values in Tables 2, 3, and 4 representing only a recommended series, giving approximately 10% increments in heat transfer surface. Notice that the D_s value is interpreted as a basic dimension in the sense that it does not include tolerances. For thermohydraulic calculations this is acceptable, as the only important dimension in this respect is the clearance between the shell and the baffle, item 20. For more detailed discussion, refer to Sec. 4.2.

Item 2: D_t (mm), nominal tube outside diameter. These dimensions follow generally accepted standards, both inch and metric based, as shown in Tables 5 and 6. However, several important criteria must be observed in the selection of tube diameter. Although small tube diameters are preferred because of better heat transfer effectiveness, cleaning considerations often limit the selection of tube diameter to 20 mm as a minimum. For tube-side condensation or boiling, still other criteria apply.

© 1983 Hemisphere Publishing Corporation

Table 1 Input data required for rating of segmentally **baffled shell-and-tube exchangers**

Item	Symbol	Units	Description
		Shell-side geometry data	
Tube and tube layout			
1	D_s	mm	Inside shell diameter
2	D_t	mm	Tube outside diameter
3	L_{tw}	mm	Tube wall thickness
4	D_{ti}	mm	Inside tube diameter
5	λ_{tw}	W/m K	Tube wall material thermal conductivity
6	L_{tp}	mm	Tube layout pitch
7	θ_{tp}	deg	Tube layout characteristic angle
Tube length (Refer to Fig. 2)			
8	L_{to}	mm	Overall nominal tube length
9	L_{ti}	mm	Baffled tube length
10	L_{ta}	mm	Effective tube length for heat transfer area
Baffle geometry (Fig. 7)			
11	B_c	%	Baffle cut as percent of D_s
12	L_{bc}	mm	Central baffle spacing
13a	L_{bi}	mm	Inlet baffle spacing (optional)
1 3 b	L_{bo}	mm	Outlet baffle spacing (optional)
Nozzle			
14	CN	code	Shell-side nozzle, impingement protection, annular distributor
Tube bundle geometry			
15	N_{tt}		Total number of tubes or holes in tubesheet for U tubes
16	N_{tp}		Number of tube passes
17	N_{ss}		Number of sealing strips (pairs)
18	CB	code	Tube bundle type (FX, UT, SRFH, PFH, PTFH)
19	L_{tb}	mm	Tube OD (D_t)-to-baffle hole clearance (diametral), Fig. 12
20	L_{sb}	mm	Inside shell-to-baffle clearance (diametral), Fig. 13
21	L_{bb}	mm	Inside shell-to-tube bundle bypass clearance (diametral), Fig. 14
		Temperatures	
22	T_{si}	°C	Shell-side temperature inlet
23	T_{so}	°C	Shell-side temperature outlet
24	T_{ti}	°C	Tube-side temperature inlet
25	T_{to}	°C	Tube-side temperature outlet
		Shell-side process information	
26	$\dot{M}_s$	kg/s	Shell fluid mass flow rate
At shell fluid mean temperature			
27	ρ_s	kg/m³	Density
28	λ_s	W/m K	Thermal conductivity
29	$(c_p)_s$	J/kg K	Specific heat
30	η_s	cP = mPa/s	Dynamic viscosity (may require two values)
At shell fluid mean temperature *(Continued)*			
31	$(R_f)_o$	m K/W	Shell-side fouling resistance (referred to shell-side surface)
		Tube-side process information	
32	$\dot{M}_t$	kg/s	Tube fluid mass flow rate
At tube fluid mean temperature			
33	ρ_t	kg/m³	Density
34	λ_t	W/m K	Thermal conductivity
35	$(c_p)_t$	J/kg K	Specific heat
36	η_t	cP = mPa/s	Dynamic viscosity (may require two values)
37	$(R_f)_i$	m K/W	Tube-side fouling resistance (referred to inside tube surface)
		Special information	
38	α_s	W/m² K	Shell-side heat transfer coefficient; if specified, omit items as shown in comments
39	α_t	W/m² K	Tube-side heat transfer coefficient; if specified, omit items as shown in comments
40	$(\Delta p_s)_{max}$	kPa	Maximum permissible pressure drop, shell side
41	$(\Delta p_t)_{max}$	kPa	Maximum permissible pressure drop, tube side
42	$(v_t)_{max}$	m/s	Maximum permissible tube-side flow velocity (optional)
43	$(v_t)_{min}$	m/s	Minimum acceptable tube-side flow velocity (optional)

Furthermore, the ratio of D_t to D_s must be maintained within reasonable limits. Many correlational parameter effects become increasingly erroroneous as relatively large tube diameters are used in small shells. The approximate ratio of minimum D_s to D_t should generally be about 15.

Larger ratios (that is, smaller-diameter tubes within larger shells) can be used without detriment to the method s accuracy, but cost considerations prohibit extremes, as too small tubes within a given shell would not be economically justifiable. An approximate guide to recommended combinations of tube and minimum or maximum shell diameters is shown in Fig. 1.

Item 3: L_{tw} (mm), tube wall thickness. Recom-

© 1983 Hemisphere P blishing Corporation

Table 2 Suggested inside shell diameter, dimensional series (U.S. practice, inches)

Standard pipe		Rolled shells	
in	mm (equivalent)	ill (mm equivalent)	Increment
5.047	128.19	12 (304.8)	1 in (25.4 mm)
6.065	154.05		
8.071	205.00		
10.136	257.45	22 (558.8)	2 in (50.8 mm)
12.09	307.09	·	
13.25	336.55		
15.25	387.35	60 (965.2)	3 in (76.2 mm)
17.25	438.15		
19.25	488.95	•	
21.25	539.75	102 (2 590.8)	3 in (76.2 mm)

mended dimensions are shown in Tables 5 and 6. Tube wall thickness is determined according to pressure, temperature, material strength, and possible corrosion allowance from standard practice. This dimension is required for inside tube diameter D_{ti} determination and for tube wall resistance calculations. For detailed discussion, refer to Sec. 4.2.

Item 4: D_{ti} (mm), inside tube diameter. $D_{ti} = D_t - 2(L_{tw})$. Nominal values are shown in Tables 5 and 6. For detailed discussion, refer to Sec. 4.2.

Item 5: λ_{tw} (W/m K), tube wall material thermal conductivity. This item is required for determination of the tube wall heat transfer resistance. In many cases this resistance is negligible relative to the other heat transfer resistances. The value of λ_{tw} is a function of temperature, but approximate values are given in Table 7 for most common materials at typical temperatures. For more exact values, use other references, such as TEMA Standards.

Item 6: L_{tp} (mm), tube layout pitch. The tube layout pitch, L_{tp}, determines the cross-flow area. The smaller the value, the more tubes can be accommodated within a given shell diameter. The limitation, however, is determined by a minimum necessary "webb thickness, the distance between adjacent tube holes in the tubesheet, which is required for proper tube-to-tubesheet joint. Shell-side pressure drop can be effectively adjusted by the tube layout pitch variation. If mechanical cleaning is required on the shell side, the gap between adjacent tubes should be kept to about $\frac{1}{4}$ in or 6.3 mm. For further details, refer to Sec. 4.2.

A useful characteristic value is the tube pitch-to-tube diameter ratio, referred to as tube layout pitch ratio L_{tp}/D_t, which should be kept between the values of approximately 1.25 as a minimum and 1.5 as a maximum, a compromise between the above demands. Note: The shell-side calculation method is valid only within these limits of pitch ratio.

U.S. practices of tube pitch dimension for specific tube diameters are shown in Table 8. The metric-based standards according to DIN 28 182, Rev. 1979, are shown in Table 9, where two different values of L_{tp} are shown, depending on the type of tube joint.

Item 7: θ_{tp} (deg), tube layout characteristic angle. The tube layout is defined by the characteristic angle and the corresponding definition of the tube pitch, as shown in Table 10 with θ_{tp} values of 30°, 45°, and 90 .

Table 3 Shell dimensions and inside shell diameter for fixed tubesheets (metric practice, mm)

Nominal shell diameter	Outside shell diameter	Shell wall thickness, mm[a]			Shell inside diameter D_s, mm[a]		
		(1)	(2)	(3)	(1)	(2)	(3)
150	168	4.5		4	159		160
200	219	5.9		4	207.2		211
250	273	6.3		4	260.4		265
300	324	7.1		4	309.8		316
350	355	8	6	4	339	343	347
400	406	8.8	6	4	388.4	394	398
500	508		6	4		496	500
600	600		6	5		588	590
700	700		8	5		684	690
800	800		8	5		784	790
900	900		10	6		880	888
1 000	1000		10	6		980	988
1 100	1 100		12	7		1 076	1086
1 200	1 200		12	7		1 176	1 186

[a] (1) Welded tubing, carbon steel; (2) rolled shells, carbon steel; and (3) stainless steel.

© 1983 Hemisphere Publishing Corporation

Table 4 Shell dimensions and inside shell diameter for floating-head tubesheets (metric practice, mm)

Nominal shell diameter	Outside shell diameter	Shell wall thickness, mm[a]			Shell inside diameter D_s, mm[a]		
		(1)	(2)	(3)	(1)	(2)	(3)
150	168	4		3.2	160		161.6
200	219	4.5		3.2	210		212.6
250	273	5		3.2	263		266.6
300	324	5.6	6	3.2	312.8	312	317.6
400	406	6.3	6	4	393.4	394	398
500	508	6.3	6	4	495.4	496	500
600	600		6	5		588	590
700	700		8	6		684	688
800	800		8	6		784	788
900	900		8	6		884	888
1 000	1 000		8	6		984	988
1 100	1 100		10	8		1 080	1 084
1 200	1 200		10	8		1180	1184

[a] (1) Welded tubing, carbon steel; (2) rolled shells, carbon steel; and (3) stainless steel.

Table 5 Recommended tube dimensions (inch standard)

Tube OD		Wall thickness			Tube ID		Outside surface	
in	mm	BWG gauge	in	mm	in	mm	ft^2/ft	m^2/m
0.250	6.350	22	0.028	0.711	0.194	4.928	0.066	0.020
		24	0.022	0.559	0.206	5.232		
0.375 ($\frac{3}{8}$)	9.525	18	0.049	1.245	0.277	7.036	0.098	0.030
		20	0.035	0.889	0.305	7.747		
		22	0.028	0.711	0.319	8.103		
0.500	12.700	18	0.049	1.245	0.402	10.211	0.131	0.040
		20	0.035	0.889	0.430	10.922		
0.625 ($\frac{5}{8}$)	15.875	16	0.065	1.651	0.495	12.573	0.164	0.050
		18	0.049	1.245	0.527	13.386		
		20	0.035	0.889	0.555	14.097		
0.750 ($\frac{3}{4}$)	19.050	12	0.109	2.769	0.530	13.462	0.196	0.060
		14	0.083	2.108	0.584	14.834		
		16	0.065	1.651	0.620	15,748		
		18	0.049	1.245	0.652	16.561		
		20	0.035	0.889	0.680	17.272		
0.875 ($\frac{7}{8}$)	22.225	14	0.083	2.108	0.709	18.008	0.230	0.070
		16	0.065	1.651	0.745	18.923		
		18	0.040	1.245	0.777	19.736		
		20	0.035	0.889	0.805	20.447		
1.000	25.400	12	0.109	2.769	0.782	19.863	0.230	0.070
		14	0.083	2.108	0.834	21.184		
		16	0.065	1.651	0.870	22.098		
		18	0.049	1.245	0.902	22.911		
1.250	31.750	10	0.134	3.404	0.982	24.943	0.327	0.100
		12	0.109	2.769	1.282	32.563		
		14	0.083	2.108	1.334	33.884		
		16	0.065	1.651	1.370	34.798		
2.0	50.8	12	0.109	2.769	1.782	45.26	0.523	0.16
		14	0.083	2.108	1.834	46.58		

© 1983 Hemisphere Publishing Corporation

Table 6 Recommended tube dimensions (metric standard)

Tube OD, mm	Wall thickness, mm	Tube ID, mm	Outside surface, m^2/m
6.0	0.5	5.0	0.019
8.0	1.5	5.0	0.025
10.0	1.5	7.0	0.031
(12.1)	1.5	9.0	0.038
14.0	2.0	10.0	0.044
(16.0)	2.0	12.0	0.050
18.0	2.0	14.0	0.057
20.0	2.0	16.0	0.063
(22.0)	2.5	17.0	0.069
25.0	2.5	20.0	0.079
30.0	2.5	25.0	0.094
38.0	2.5	33.0	0.119
44.5	2.5	39.5	0.139
51.0	2.5	46.0	0.160

The selection of the layouts is dictated by the following principles:

The 30 staggered layout has the highest tube density and therefore permits the largest heat transfer surface within a given shell. It also has a high effectiveness of pressure drop to heat transfer conversion. However, it produces the highest pressure drop for a given tube pitch. This layout should be considered as the prime selection, unless other considerations become predominant.

The 45 staggered layout has also a high effectiveness of pressure drop to heat transfer conversion, but permits only about 85% of tubes within a given shell, as compared to a 30 layout. For a given pitch, the pressure drop is less than for a 30 layout. It has the distinct advantage that shell-side cleaning from outside by mechanical means (water or steam jets) is possible, if sufficient clearance between tubes is allowed (approximately 7 mm).

The 90° in-line layout should be avoided in laminar shell-side flow, but it has high effectiveness of pressure drop to heat transfer conversion in turbulent flow; especially if low pressure drop is desired, it should be considered as an alternative to the 30 or 45 staggered layout. External cleaning convenience is the same as for 45 layouts.

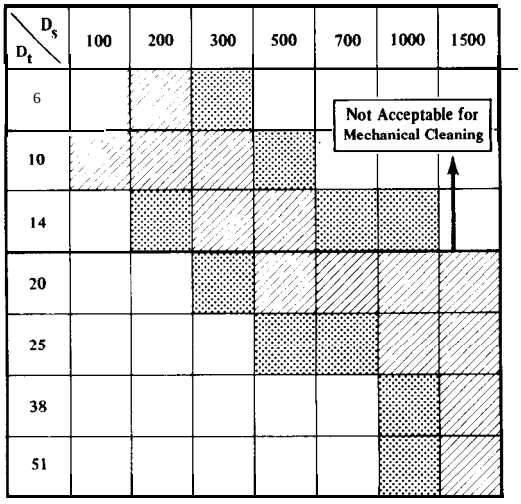

Figure 1 Recommended combinations of shell and tube diameters. Hatched areas are those preferred; dotted areas are acceptable under specific conditions. Dimensions are in millimeters.

The 60° staggered layout is not considered here or shown in Table 10. For no-phase-change flow applications, it produces lower effectiveness in pressure drop-to-heat transfer conversion and is therefore not generally recommended.

Items 8-10: L_{to}, L_{ti}, L_{ta}, tube length definitions. The tube length definitions are shown in Fig. 2. L_{to} is the nominal tube length for all bundle types except U tubes. For U-tube bundles, the tube length varies between the outer and inner rows and must be calculated by the manufacturer from tube layouts and bend radii. The designer specifies the length from the tubesheet to the tangent of the outer tube bend, as shown in Fig. 2. The last baffle should be located at that position.

L_{ti} (mm) is the length of summation of all baffle spacings. For all bundles except U tubes, this is the length between the insides of the tubesheets; for U tubes, L_{ti} is the distance between the inside of the tube sheet and the last baffle as shown in Fig. 2.

To determine L_{ti}, we must know the tubesheet thickness. If drawings are not available, the tubesheet thickness can be roughly estimated (especially for preliminary designs) as

$$L_{ts} = 0.1 D_s \quad (1)$$

Table 7 Thermal conductivities λ_{tw} of some typical tube materials

	Industrial grade			Cu-Ni				
Material	Cu	Al	Admiralty	90-10	70-30	Carbon steel	Low-alloy steel	High-alloy steel, Ti
λ_{tm} (W/m K)	310	180	120	65	40	38	30	18

© 1983 Hemisphere Publishing Corporation

Table 8 Recommended tube layout pitch dimensions by U.S. practice (inch based); pitch ratio L_{tp}/D_t

Tube OD		Pitch (L_{tp})		
in	mm	in	mm	Pitch ratio
0.250	6.350	0.312	7.938	1.250
		0.375	9.525	1.500
0.375	0.525	0.500	12.700	1.330
		0.531	13.494	1.420
0.500	12.700	0.625	15.875	1.250
		0.656	16.669	1.310
		0.688	17.462	1.380
0.625	15.875	0.781	19.844	1.250
		0.812	20.638	1.300
		0.875	22.225	1.400
0.750	19.050	0.938	12.812	1.250
		1 .ooo	25.400	1.330
		1.062	26.988	1.420
		1.125	28.575	1.500
1.000	25.400	1.250	31.750	1.250
		1.312	33.338	1.312
		1.375	34.925	1.375
1.250	31.750	1.562	39.688	1.250
1.500	38.100	1.875	47.625	1.250
2.000	50.800	2.500	63.500	1.250

with limit $L_{ts} \geqslant 25$ mm. This admittedly very simplified approach will have to suffice for most applications within the objectives of this handbook and other approximations used.

The next more accurate estimation of L_{ts} is

$$L_{ts} = 0.5 D_s \sqrt{\frac{P_s}{\sigma_{ts}}} \tag{2}$$

where P_s is the shell-side operating pressure, and σ_{ts} is the allowable strength of tubesheet material at operating temperature (in consistent units).

Elaborate procedures for tubesheet thickness calculations exist, depending on whether it is a fixed or floating-heat tubesheet (TEMA Standards and various proprietary sources), but these are outside of the objectives of this section.

By whichever method L_{ts} is determined (see Sec. 4.2 for more details), L_{ti} is calculated as

$$L_{ti} = L_{to} - 2L_{ts} \tag{3}$$

for all bundle types except U tubes, and

$$L_{ti} = L_{to} - L_{ts} \tag{4}$$

for U-tube bundles.

L_{ta} (mm), is the effective tube length for heat transfer area calculations. This length is determined for all except U-tube bundles in a straightforward manner from Fig. 2 as

$$L_{ta} = L_{ti} \tag{5}$$

For U-tube bundles, the tubular area in the U bend beyond the last baffle is estimated as an additional tube length of $0.3D_{otl}$, where D_{otl} is defined in item 21. Accordingly, from Fig. 2, for U tubes,

$$L_{ta} = L_{ti} + 0.3D_{otl} \tag{6}$$

For tube-side pressure drop calculations, the total nominal flow length of the tubes L_{tt} (mm) is required, determined as

$$L_{tt} = L_{to} \tag{7}$$

Table 9 Minimum tube layout pitch L_{tp} for various tube joint types (DIN 28 182, 1979 rev., abstracted); dimensions in mm

Joint type	Symbol	Description
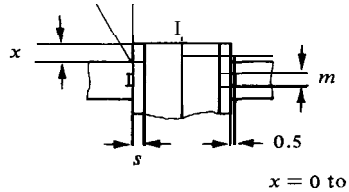	I	Rolled, with one or two grooves
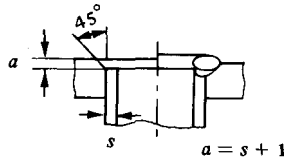	II	Welded or brazed, tube recessed
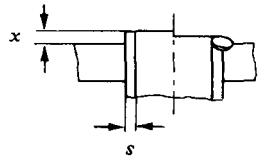	III	Welded or brazed, tube protruding

s	x
Up to 2	0 to 1
2 to 2.6	2.5 to 3

D_t	II		I and III	
mm	L_{tp}	L_{tp}/D_t	L_{tp}	L_{tp}/D_t
10	13.5	1.35	13.5	1.35
(12)	15.5	1.29	15.5	1.29
14	18	1.28	19	1.36
(16)	20	1.25	21	1.31
18	23	1.28	24	1.33
20	25	1.25	26	1.3
(22)	27	1.23	29	1.32
25	30	1.2	32	1.28
30	36	1.2	38	1.27
38	45	1.18	47	1.24
44.5	53	1.19	55	1.24

© 1983 Hemisphere Publishing Corporation

Table 10 Tube layout geometry basic parameters

Cross flow →	θ_{tp}	L_{tp}	L_{pp}
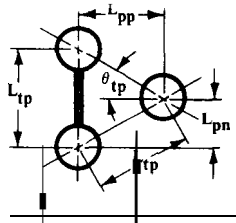	30	$0.5L_{tp}$	$0.866L_{tp}$
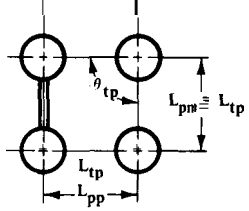	90	L_{tp}	L_{tp}
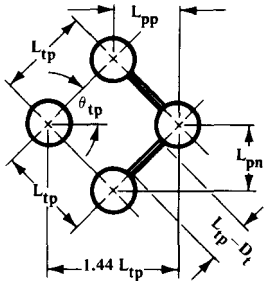	45	$0.707L_{tp}$	$0.707L_{tp}$

for all bundle types except U tubes, and for U tubes as

$$L_{tt} = L_{ta} + L_{ts} \tag{8}$$

These values must be multiplied by the number of tube passes N_{tt} to determine the effective flow length in the tubes.

Item 11: B_c(%), segmental baffle cut as percent of D_s. Assuming that the segmental baffle is centered within the shell inside diameter D_s, the baffle cut height L_{bch} (mm) is related to B_c as shown in Fig. 3 as

$$B_c = \left(\frac{L_{bch}}{D_s}\right)(100) \quad (\%) \tag{9}$$

The small difference between the shell and baffle diameter is for these purposes neglected, as the clearance L_{sb} is of importance only for leakage corrections, as explained further under item 21.

If true rating of an exchanger is desired, the value of B_c will be known. However, for design purposes and/or as a check on specified values, a chart showing the recommended practices, in the form of B_c versus the ratio of the central baffle spacing L_{bc} (item 12) and the inside shell diameter D_s is presented in Fig. 4. A sound design should not deviate substantially from the recommended values, which are based on a vast amount of practical experience as well as on studies of the shell-side flow patterns, as discussed in previous sections.

Item 12: L_{bc} (mm), central baffle spacing. This input item is called central baffle spacing to designate a uniform baffle spacing over the baffled length of the tube bundle. The deviations from this regular pattern, sometimes necessitated by the inlet and outlet regions, are described in the subsequent item 13 and Fig. 7.

The central baffle spacing is subject to two limitations, based on established practices for good flow distribution and adequate support of the tubes, as discussed below.

1. The smallest acceptable baffle spacing $L_{bc,\min}$ is required for reasons of good flow distribution, so that a steady flow pattern of the cross-flow and baffle window flow would result. Firmly established rules call for minimum baffle spacing equal to 20% of the shell diameter D_s, but not less than approximately 50 mm.

2. The maximum permissible baffle spacing $L_{bc,\max}$ is restricted by the following requirements: (a) Good flow distribution, which, in connection with the baffle window dimensioning, calls for maximum baffle spacing not exceeding the shell diameter D_s for segmental baffles, that is $L_{bc,\max} = D_s$. (b) Sufficient

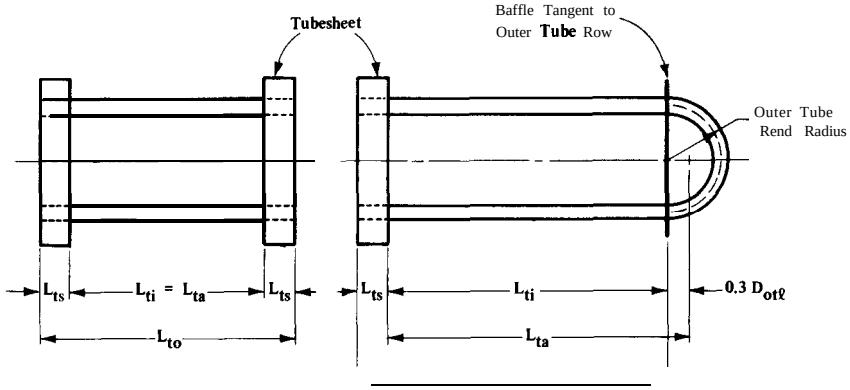

Figure 2 Tube length definitions.

© 1983 Hemisphere Publishing Corporation

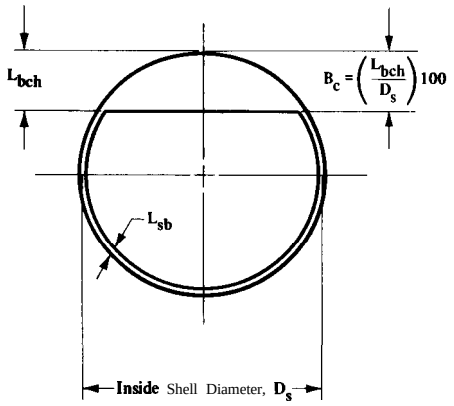

Figure 3 Segmental baffle cut height L_{bch} related to baffle cut B_c (%).

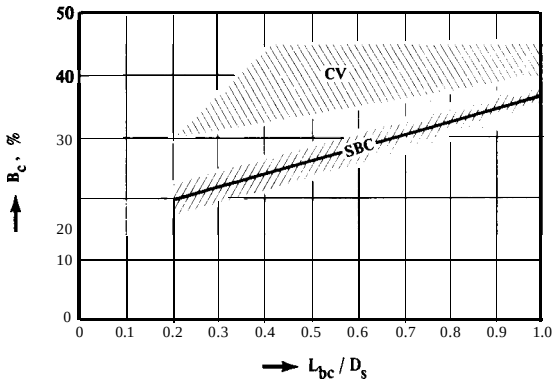

Figure 4 Recommended segmental baffle cut values B_c as a function of L_{bc}/D_s ratio. SBC, segmental baffle cuts in no-phase-change flow; CV, baffle cuts applicable to condensing vapors.

support for the tubes to prevent sagging and possible tube vibration. This dimension is defined by TEMA as the maximum unsupported span, $L_{b,\max}$.

The TEMA-recommended values of $L_{b,\max}$ for plain tubes are a function of the tube diameter and two material groups: A, steel and steel alloys; and B, aluminum and copper alloys. TEMA R type (most restrictive) specifies tube diameters between $\frac{3}{4}$ in ($\approx$19 mm) and 2 in ($\approx$51 mm). TEMA C type (less restrictive) uses the same values as the TEMA R, but extends the tube diameter to $\frac{1}{4}$ in ($\approx$6 mm). The values are shown in Fig. 5 and are represented by the following equations.

Material group A:

For D_t = 19-51 mm:

$$L_{b,\max} = 52D_t + 532 \quad \text{(mm)} \qquad (10a)$$

For D_t = 6-19 mm:

$$L_{b,\max} = 68D_t + 228 \quad (mm) \qquad (10b)$$

Material group B:

For D_t = 19-51 mm:

$$L_{b,\max} = 46D_t + 436 \quad \text{(mm)} \qquad (10c)$$

For D_t = 6-19 mm:

$$L_{b,\max} = 60D_t + 177 \quad (mm) \qquad (10d)$$

For externally finned tubes, TEMA has a rather complex formula for $L_{b,\max}$ as follows:

1. The tube diameter should be interpreted as the tin root diameter;

2. The value of $L_{b,\max}$ should be reduced in proportion to the power of 0.25 of the ratio of the weight per unit length of tube, if stripped of fins, to that of the actual finned tube.

The latter rule is not explained further and leaves some ambiguities for practical interpretation. As many parameters are involved (e.g., fin configuration, tube wall thickness, tube diameter, material), no attempt is made here at any generalized representation. As a first approximation, enter Fig. 5 with the fin root diameter instead of D_t.

Note that for the central baffle spacing, maximum unsupported length is in the baffle window and $L_{bc,\max} = 0.5L_{b,\max}$. However, the longest unsupported span can occur in the inlet or outlet baffle spacing and through the adjoining baffle window, as discussed in items 13 and 14 and shown in Fig. 7.

To put the rather confusing limitation of minimum and maximum segmental baffle spacing into perspective, Fig. 6 shows the basic relationships. The two limiting lines reflect the thermohydraulic consideration; the horizontal lines represent the TEMA upper limit on maximum unsupported spans $L_{b,\max}$ for plain tubes of tube diameters as shown and also for the two material groups A and B, as depicted in Fig. 5. For example, a

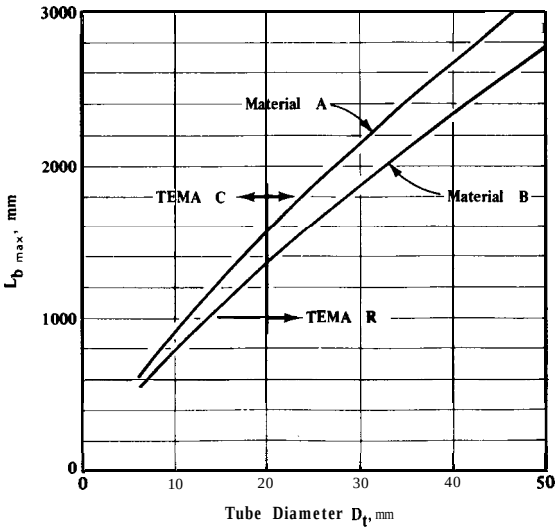

Figure 5 TEMA maximum unsupported plain tube span $L_{b,\max}$ as a function of tube diameter D_t and tube material; A = Fe and Fe alloys, B = Al, Cu alloys.

© 1983 Hemisphere I blishing Corporation

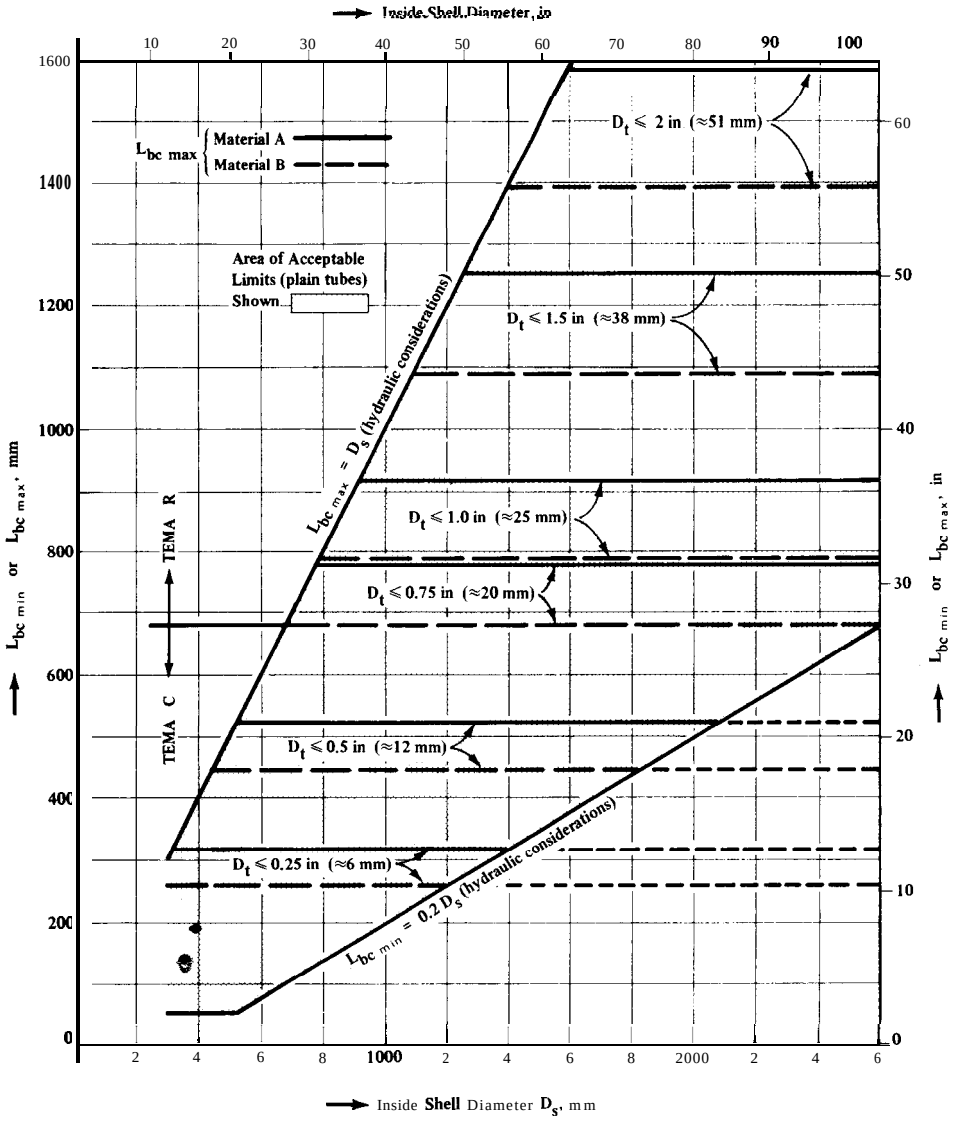

Figure 6 Maximum and minimum limitations on segmental baffle spacing from thermohydraulic and unsupported length considerations for materials **A** and B as per Fig. 5.

1 000-mm-diameter shell can have a minimum L_{bc} = 200 mm and the maximum baffle spacing can be limited by thermohydraulic considerations to $L_{bc,\max}$ = 1 000 mm, but only if the tube diameter used is at least 25 mm. For tube diameter D_t = 12 mm, $L_{bc,\max}$ is determined by the horizontal lines, with values of 520 or 440 mm, respectively, for material A or B. Finned tubes would have still lower limits.

Notice that as the tube diameter gets smaller and the shell diameter gets larger, the choice of baffle spacing diminishes, restricting the heat exchanger designer in the freedom to manipulate this variable to accommodate pressure drop and heat transfer requirements. In extreme cases this limitation may signify the need to change shell type or baffle type.

Finally, note that certain shell types (E, J, F) can be used only with odd or even numbers of baffles (hence baffle spacings):

E shell: odd or even, but nozzle orientation is then determined

J shell: only even number of baffles

F shell: only even number of baffles for standard cross-flow orientation.

Items 13a,13b: L_{bi}, L_{bo} (mm), inlet and outlet baffle spacing. If uniform baffle spacing is maintained throughout the exchanger, ignore this item. However, in some cases large inlet and outlet nozzles must be used, making it necessary to enlarge the baffle spacing adjoining the nozzles. In such cases the additional data entries of L_{bi} and L_{bo} are necessary. It should be further noted that in these cases the longest unsupported tube

© 1983 Hemisphere I blishing Corporation

span is in the baffle window adjoining the enlarged baffle space, as illustrated schematically in Fig. 7. This value must not exceed the TEMA limitation $L_{b,\max}$, as shown in Figs. 5 and 6.

The thermal performance of an exchanger having substantially larger inlet and/or outlet baffle spacings will, of course, suffer, as the shell-side flow velocities in the enlarged baffle spacings will be decreased. This effect is treated as a correction factor J_s in Sec. 3.3.6. The effect will be more pronounced as the number of baffles decreases. Frequently (such as for condensing vapors), only the inlet baffle spacing needs to be enlarged, whereas the outlet baffle spacing L_{bo} can equal the central spacing L_{bc} in Fig. 7.

Item 14: CN (Code), shell-side nozzle, impingement protection, and annular distributors. Note: This is an abbreviated version of practices for nozzle design and impingement protection. For more comprehensive detailed treatment, refer to Sec. 4.2.

The shell-side stream is discharged into the tube bundle through a nozzle. If the flow velocity through the nozzle exceeds a certain maximum, the tubes can vibrate, and can be subjected to erosion and potential damage. TEMA specifies the maximum permissible shell-side nozzle velocity $v_{ns,\max}$ in terms of limiting values of $\rho_s(v_{ns})^2$, above which an impingement protection is required. For nonabrasive liquids,

$$v_{ns,\max} = \sqrt{\frac{2\ 250}{\rho_s}} \quad \text{(m/s)} \qquad (11a)$$

or, in terms of TEMA, $\rho_s(v_{ns})^2$ = 1 500 lb/ft s^2 (2 250 kg/m s^2).

For liquids at boiling point, the TEMA value is 500 lb/ft s^2 (750 kg/m s^2) and

$$v_{ns,\max} = \sqrt{\frac{750}{\rho_s}} \quad \text{(m/s)} \qquad (11b)$$

For two-phase flow mixtures, ρ_s is calculated as the homogeneous gas-liquid density

$$\rho_s = \frac{1}{(y/\rho_{sv}) + (1-y)/\rho_{sl}} \qquad (12)$$

where ρ_{sv} is the density of the vapor or gas phase and ρ_{sl} is that of the liquid phase (kg/m^3); y is the vapor fraction.

The simplest form of impingement protection is a square or round plate located below the nozzle so that the escape flow area into the tube bundle is approximately equivalent to the nozzle area. This is illustrated schematically in Fig. 8 with the distance L_{ns} of

$$L_{ns} = 0.25D_{ns} \quad \text{(mm)} \qquad (13)$$

where D_{ns} is the inside shell nozzle diameter (mm).

An alternative impingement protection is to replace the two top tube rows below the nozzle with rods, the advantage claimed being better distribution of the flow into the tube bundle. In either case, the impingement device will reduce the number of tubes that can be placed within a shell and should be respected in tube count estimations (see Sec. 4.2.5E).

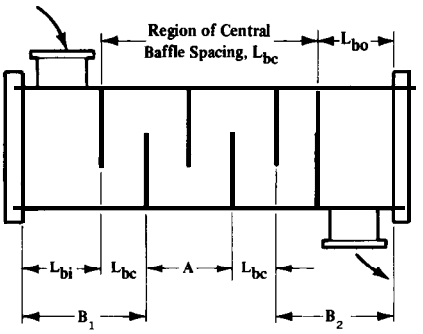

Figure 7 Schematic sketch of baffle distribution. Maximum unsupported tube span $L_{b,\max}$ in the ***Lb,*** region (A) and in the inlet/outlet region (B, and B,).

The most effective impingement protection, however, is an annular distributor, which is essentially a rectangular channel welded at the shell entry or exit, as shown schematically in Fig. 9. The annular distributor has several advantages:

The shell wall itself acts as an impingement plate, thus permitting full circular tube layout (see Sec. 4.2.5 for further details).

The shell flow entry slot can be located independently of the nozzle position, thus permitting more effective piping layout.

The flow can be introduced into the tube bundle more uniformly and at flow velocities that are low enough to prevent tube vibration.

Regular baffle spacing can be used throughout the exchanger (see item 13).

These advantages are offset by the additional cost of the distributor structure, but in all extreme cases annular distributors are the only effective solution.

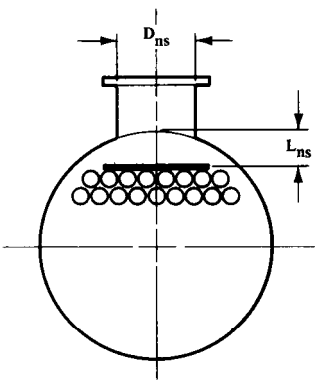

Figure 8 Schematic arrangement of shell-side impingement protection.

© 1983 Hemisphere Publishing Corporation

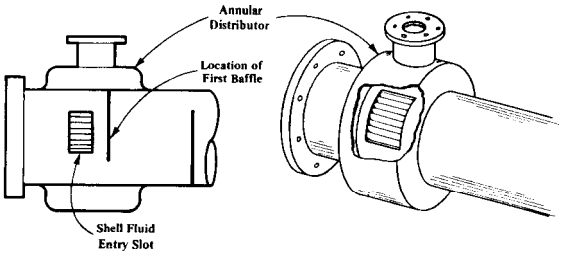

Figure 9 Annular distributor permitting the location of the first baffle below the nozzle.

Once an impingement protection has been included, the values of the maximum permissible nozzle flow velocities can be calculated with $\rho_s(v_{ns})^2$ values twice those used in Eqs. (10) and (11).

For liquids:

$$v_{ns,\max} = \sqrt{\frac{4\,500}{\rho_s}} \ (\mathrm{m/s}) \qquad (14a)$$

For two-phase flow:

$$v_{ns,\max} = \sqrt{\frac{1\,500}{\rho_s}} \ (\mathrm{m/s}) \qquad (14b)$$

For gases the permissible shell nozzle velocity is usually limited to about 20% of the acoustic velocity in the gas of density ρ_s under pressure p_s.

Finally, the minimum inside shell nozzle diameter $D_{ns,\min}$ (mm) can be determined from the recommended $v_{ns,\min}$ values and the shell-side flow rate $\dot{M}_s$ (kg/s) (input item 26) as

$$D_{ns,\min} = 10^{-3}\sqrt{\frac{M}{(\pi/4)\rho_s v_{ns,\max}}} \qquad (15)$$

Pressure drop in the nozzle and tube vibration considerations may, however, frequently require larger nozzles than those determined by Eq. (15) as the minimum values.

Item 15: N_{tt}, total number of tubes in shell, or number of holes in tubesheet for U-tube bundles. The number of tubes in a tube bundle, N_{tt}, is a function of

1. Shell diameter D_s.
2. Tube bundle type (item 18), which in turn affects the value of the tube bundle-to-shell bypass clearance L_{bb}, and determines the value of D_{ctl}, the circle diameter through the centers of the outer tube rows [see item 21 and Fig. 3.3.6(1)]. Notice that, for a given D_{ctl}, the effect of the tube bundle type on N_{tt} is eliminated.
3. Tube diameter D_t, tube pitch L_{tp}, and tube layout pattern angle, θ_{tp} (items 2, 6, and 7).
4. Number of tube passes N_{tp}, as tubes are omitted in tube pass lanes (item 16).
5. Omission of tubes due to impingement plates or no-tube-m-window designs.

For exchangers specified by drawings or otherwise, N_{tt} will be known. In most cases it is still important to know if tubes were omitted for impingement plates [Fig. (8)] or bypass partition [Fig. 3.3.6(1)], as such values enter subsequent calculations.

Because of the many parameters affecting N_{tt}, tabular information based on actual layouts and often referred to as tube count is always limited, though dependable (Sec. 4.2.5). Especially for design cases where D_s, N_{tp}, and other variables may change in the course of the calculation, an estimation procedure is important. A simple but reasonably accurate correlation (within the limitations of this method) is suggested below.

For a single tube pass, $N_{tp} = 1$:

$$N_{tt} = (N_{tt})_1 = \frac{0.78D_{ctl}^2}{C_1(L_{tp})^2} \qquad (16)$$

where D_{ctl} is determined from procedures shown in item 21, Eq. (21)

L_{tp} is tube layout pitch, input item 6

C_1 is a tube field layout constant based on input item 7, θ_{tp}, and = 0.866 for a 30 layout or = 1.000 for 45 and 90° layouts

This method will predict single-tube-pass tube count within approximately 5% accuracy if the relations of tube diameter to shell diameter are within recommended limits (see item 2). The accuracy will decrease rapidly if large tubes are used in relatively small shells.

If tubes have to be omitted to accommodate impingement plates (Fig. 8) or for reasons of shell fluid distribution, apply a correction factor based on subtracting from the area of the D_{ctl} circle in Eq. (16), $0.78D_{ctl}^2$, the area that is not occupied by tubes. Expressed in the form of a correction factor to $N_{tt,1}$,

$$N_{tt} = N_{tt,1}(1-\psi_c) \qquad (16a)$$

The correction factor ψ_c is calculated by the same principles as the baffle cut area shown in Fig. 3.3.6(1) and Eqs. 3.3.6(2) and 3.3.6(4). Substituting the values corresponding to this situation, we get

$$\theta_{ctl} = 2\cos^{-1}\left[\frac{D_s}{D_{ctl}}\left(1-2\frac{B_c^*}{100}\right)\right] \ (\mathrm{deg}) \qquad (16b)$$

$$S_c = 0.78D_{ctl}^2\left(\frac{\theta_{ctl}}{360}-\frac{\sin\theta_{ctl}}{2\pi}\right) \quad (\mathrm{mm}) \qquad (16c)$$

where S_c is the area of the cutoff from the D_{ctl} circle and B_c^* is the cut in percent of D_s between the inside shell diameter D_s and the cut line, similar to B_c in Fig. 3 or Fig. 3.3.6(1).

Then

$$B_c^* = \frac{L_{bch}^*}{D_s}\,100\ (\%) \qquad (16d)$$

© 1983 Hemisphere Publishing Corporation

with L^*_{bch} the baffle cut height.

The correction factor ψ_c is then

$$\psi_c = \frac{\theta_{ctl}}{360} - \frac{\sin\theta_{ctl}}{2\pi} \qquad (16e)$$

This applies for cut out on one side of the shell only. If the tube field on both sides of the shell is cut in the same way (such as for no-tubes-in-window designs), use $2\psi_c$ in Eq. (16*a*).

For multiple tube passes, $N_{tp} > 1$, a correction factor ψ_n must be used to account for the decrease of tube count due to tube pass partitions. This is very difficult to generalize, as it depends on several geometric parameters. A rough estimation for ψ_m is shown in Fig. 10.

$$N_{tt} = (N_{tt})_1 (1 - \psi_n) \qquad (17)$$

Expected accuracy of this method is approximately 10% on small shell diameters (D_s < 400 mm) and 5% for larger shell sizes.

Item 16: N_{tp}, number of tube passes. For typical tube pass layouts, see Sec. 4.2. Notice that pass partitions should be located as much as possible perpendicularly to the cross-flow stream, to avoid bypass flow. Tie rods are often placed into the tube pass partitions to block the flow if pass partitions are in the flow direction.

For shell-side calculations this item is used only for estimation of the tube count (item 15), as tubes are omitted on account of the pass partitions. For overall exchanger rating or design calculations, this item is used for determination of tube-side flow velocity and, in appropriate cases, for the AT,,, correction factor.

A practical maximum value of N_{tp} for a given shell diameter D_s should be observed, as otherwise too many tubes would have to be omitted from the tube field. An approximate guide to $N_{tp,max}$ as a function of D_s is shown below.

D_s (mm)	200	400-800	800-1 200	>1 200
$N_{tp,max}$	2	4-6	6-8	8-10

The large N_{tp} numbers can be used if small tube diameters are used. Another rule of thumb calls for a minimum number of tubes per tube pass of approximately 8. The accuracy of the shell-side method will decrease if the above rules are violated.

Item 17: N_{ss}, number of sealing strips (pairs) in one baffle crossing. If tube bundle-to-shell bypass clearance (L_{bb}, item 21) becomes large, such as in pull-through bundles, the bypass stream will reach considerable magnitude, resulting in decreased heat transfer efficiency. The effectiveness can be restored by allocating sealing strips, which are usually sheet metal strips attached to the baffles. These force the flow back into the tube bundle, as shown schematically in Fig. 11. As a general rule, sealing strips should be considered if the tube bundle-to-shell diameter clearance, L_{bb}, exceeds approximately a value of 30 mm. (See Fig. 14, item 21.) This means that fixed tubesheet and U-tube designs usually do not require sealing strips, but split-ring and all pull-through floating-head designs usually will.

The final judgment should be made from the calculation of the bypass correction factors (see Sec. 3.3.6), from which the effect of sealing strips can be readily estimated. Sound practice calls for the use of one sealing strip for approximately four to six tube rows crossed. See also Sec. 4.2 for additional details.

Item 18: CB (code), tube bundle construction types. The shell-side calculation method as presented here will handle the following tube bundle types (TEMA Standards). Only brief description is included here for convenience. For illustrative drawings and additional comments, see Sec. 4.2.

1. Fixed tubesheet, code FX
2. U-tube bundles, code UT
3. Split-ring floating-head bundle, code SRFH
4. Packed floating-head bundle, code PFH
5. Pull-through floating-head bundle, code PTFH

The main effect the bundle construction type has on the shell-side calculations is the bypass clearance between the shell inside diameter and the tube bundle-

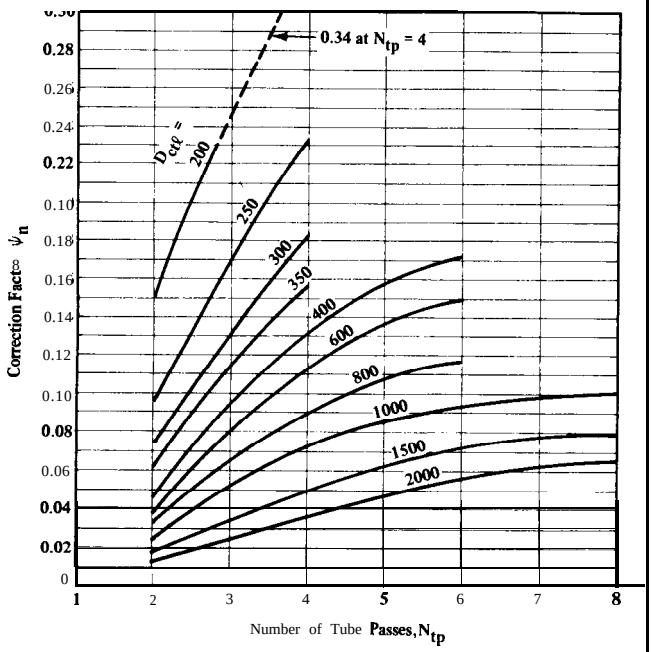

Figure 10 Correction factor ψ_n for estimation of number of tubes for tube bundles with number of tube passes N_{tp} = 2-8. Best range of application for N_t = 16-25 mm.

© 1983 Hemisphere I blishing Corporation

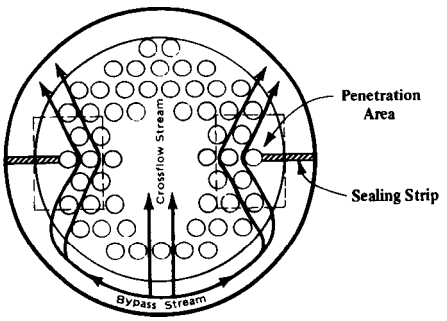

Figure **11** Typical flow pattern in bypass stream with sealing strip (N_{ss} = 1).

tube field circumscribed circle D_{otl} (see item 21). The main characteristics of the tube bundle construction types are briefly summarized below, reflecting selection from several aspects.

UT is the least expensive construction, as it needs only one tubesheet and is the best for tube expansion requirements. Only an even number of tube passes is possible. Mechanical tube-side cleaning in U bends is impractical or difficult. The tube bundle is removable, and shell-side mechanical cleaning is possible. Replacement of defective tubes cannot be made.

FX is the next least expensive construction, but it is limited by tube expansion requirements (expansion bellows); it needs two tubesheets. Only chemical cleaning of the shell side is possible. Replacement of defective tubes is easy.

SRFH is used for applications where U-tube construction is not desirable and thermal expansion excludes a fixed tubesheet. Shell-side cleaning by mechanical means is desired at infrequent intervals (complete disassembly of the rear head is necessary). More tubes per shell diameter can be accommodated than with the PTFH type; there is also much less bypass area. Defective tubes can be replaced or plugged easily.

PFH is similar to SRFH except that tubesheet packing may cause problems.

PTFH is used when frequent shell-side cleaning is necessary. It is the easiest type for pulling the bundle for shell-side cleaning, at the sacrifice of less tubes in a given shell diameter and the need for sealing strips.

Item 19: L_{tb} (mm), diametral clearance between tube outside diameter D_t and baffle hole. This dimension is required for determination of tube-to-baffle hole leakage stream, which is a correlational parameter of the shell-side method (Sec. 3.3.6). TEMA Standards specify recommended clearances in the baffle tube hole as a function of tube diameter D_t and $L_{b,\max}$, as shown in Fig. 12.

This practice is based on the ease of tube bundle assembly requirements. Notice that an uncomfortable step function exists (especially for computer calculations) for $L_{b,\max}$ = 900 mm, but nevertheless the dimensions represent a reasonable guide for lack of any better rule.

DIN Standard 28 182,4.2 presents a somewhat different recommendation:

$$L_{tb}\,(\text{mm}) = \begin{cases} D_{t,\max}\ {}^{+0.7}_{-0} - D_t \\ D_{t,\max}\ {}^{+0.4}_{-0} - D_t \end{cases} \text{ for } L_{b,\max} \begin{cases} < 1000 \text{ mm} \\ > 1000 \text{ mm} \end{cases}$$

where $D_{t,\max}$ is the maximum tube outside diameter (including tolerances), and D_t is the nominal tube outside diameter. This procedure adds the requirement for knowing $D_{t,\max}$, a frequently very cumbersome chore, depending on type of tubing material, process of manufacturing, and so on. Without specific knowledge of these values, Fig. 12 is recommended as being simpler to use.

For extruded holes, such as used for small shell and small diameter tubes, a special clearance is recommended in Fig. 12, based on practical experience.

Finally, accumulation of fouling layer thickness may partially or completely block this leakage area. If such a condition is expected, heat exchanger performance under both extreme conditions should be investigated.

Item 20: L_{sb} (mm), inside shell-to-baffle clearance (diametral). The clearance between the shell inside diameter and the baffle outside diameter provides a passage for the shell-to-baffle leakage stream, often seriously affecting the heat transfer effectiveness. To determine the leakage area, we need to establish the average diametral clearance between the shell and the baffle.

The value of D_s (mm) is a nominal dimension, subject to manufacturing tolerances as well as "out-of-roundness tolerances. The baffle outside diameter will also be subject to manufacturing tolerances. For this

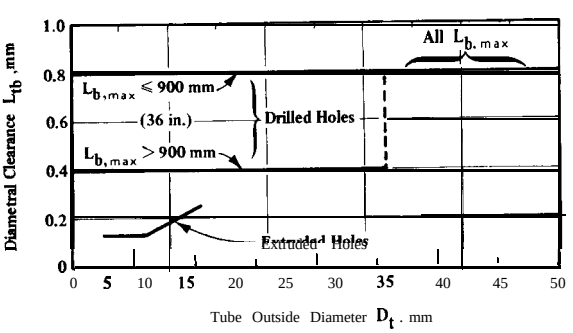

Figure 12 Diametral tube-to-baffle hole clearance L_{tb} as a function of tube diameter D_t and the maximum unsupported tube length $L_{b,\max}$, TEMA Standards and for extruded baffle holes for small-diameter shells (D_s < 350 mm).

© 1983 Hemisphere I blishing Corporation

reason, TEMA specifies only the average clearance between the shell wall and baffle, L_{sb}, as a function of the shell diameter D_s. This is shown in Fig. 13. The TEMA step values are approximated with a straight line, and curve-fitted as

$$L_{sb} = 1.6 + 0.004D_s \quad \text{(mm)} \tag{18}$$

Because of the out-of-roundness tolerances, which are not clearly defined by TEMA, an additional clearance of 1.5 mm is often added, resulting in leakage areas with a greater safety factor for heat transfer (but lower for pressure drop). This clearance is also shown in Fig. 13 and curve-fitted as

$$L_{sb} = 3.1 + 0.0040_s, \quad \text{(mm)} \tag{19}$$

Small shells (approximately up to 300 mm) are often expanded, thus permitting very close tolerances. This is shown in Fig. 13 as a separate value.

For shell-side flow applications where shell-to-baffle leakage is of no importance, L_{sb} values up to twice those in Eq. (18) can be used.

Item 21: L_{bb} (mm), inside shell diameter-to-tube bundle bypass clearance (diametral). This clearance is, for purposes of this method, defined as the distance between the inside shell wall and the circle circumscribed to the outermost tubes of the tube field, D_{otl}, as shown schematically in Fig. 3.3.6(1). For more detailed description, see Sec. 4.2. It determines the flow area for bundle bypass stream and the corresponding correction factors.

The value of L_{bb} depends mainly on the tube bundle type used. Fixed tubesheet or U-tube types require minimum clearances. Split-ring and packed floating-head designs require much larger clearances, to accommodate the rear head. Pull-through floating-head designs must accommodate bolts for the rear head and require still much larger clearances, which are also functions of shell-side design pressure. Although L_{bb} should be obtained from drawings if available, Fig. 14 shows an estimation of the values of L_{bb} based on prevailing practices.

To calculate the bypass area, we define the tube bundle-circumscribed circle, D_{otl}, as shown in Fig. 3.3.6(1) as

$$D_{otl} = D_s - L_{bb} \quad \text{(mm)} \tag{20a}$$

or, conversely,

$$L_{bb} = D_s - D_{otl} \quad \text{(mm)} \tag{20b}$$

To calculate other tube field-related parameters, the diameter of the circle through the centers of the tube located within the outermost tubes, D_{ctl}, is required:

$$D_{ctl} = D_s - (L_{bb} + D_t) = D_{otl} - D_t \quad \text{(mm)} \tag{21}$$

Items 22-25: $T_{si}, T_{so}, T_{ti}, T_{to}$ (°C), inlet and outlet temperatures for shell-side and tube-side fluid, respectively. It is assumed that all terminal temperatures are known. It is often useful to make a rough sketch of the temperatures, which will indicate possible close approaches or overlaps and thus assist the designer in selection of appropriate flow configurations, such as pure counterflow, need for multiple shells in series, and so on.

Items 26-29: Self-explanatory.

Item 30: η_s (cP = mPa/s), dynamic viscosity of shell-side fluid At least one value at approximately the average shell fluid temperature is required for liquids and gases. For calculations of the viscosity effect on α and Ap for liquids, a second value of the viscosity, at approximately the wall temperature, is required. (See comments in Sec. 3.3.7.)

Item 31: $R_{f,o}$ (mK/W), shell-side fouling resistance (referred to tube outside surface). A careful consideration should be given to assigning a value to this item, as

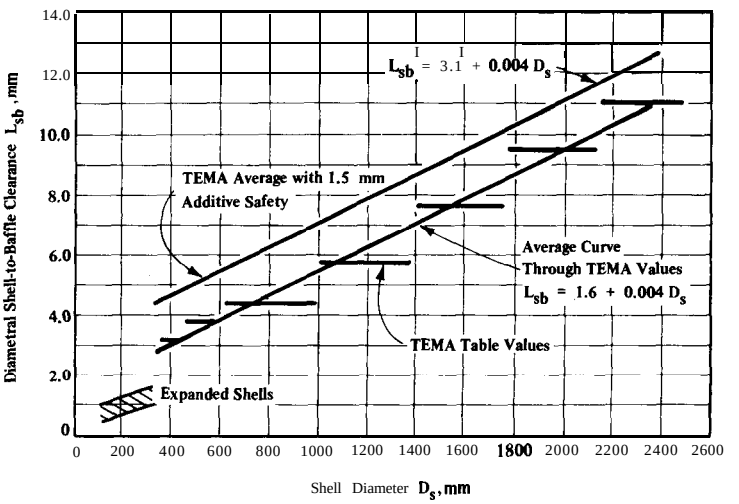

Figure 13 Diametral shell-to-baffle clearance L_{sb} as a function of shell inside diameter D_s, Eq. (19).

© 1983 Hemisphere Publishing Corporation

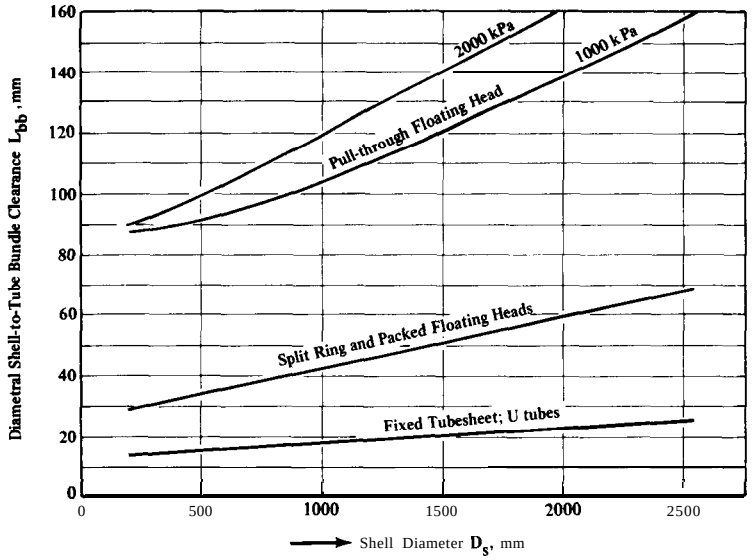

Figure 14 L_{bb} (mm), diametral shell-to-tube bundle bypass clearance.

it may substantially affect the performance of the exchanger. It is recommended that calculations also be performed for a clean exchanger, $R_{f,o} = 0$, to appreciate properly the effect of the fouling resistance assigned. If substantial fouling resistance is specified, the resulting fouling layer thickness may affect the tubular cross-flow area and the tube-to-baffle hole clearances. Engineering judgment must be employed in such cases. Also, respect carefully the flow velocity and tube wall temperature, as these may strongly affect the allocation of a fouling resistance.

Unless known from practice, guidelines for selecting the most probable values of $R_{f,o}$ for a variety of fluids are shown in TEMA Standards.

Items 32-36: same comments as to the corresponding shell-side-related items 26-30.

Item 37: $R_{f,i}$ (mK/W), tube-side fouling resistance (referred to tube-inside side surface), Similar comments apply as to shell-side fouling, item 31. However, even more careful consideration should be given to tube-side fouling resistance, as it is a strong function of flow velocity; see comments under items 31, 42, and 43.

If tube-side fouling exists on externally low-finned tubes, this resistance will be multiplied by the ratio of outside to inside tube surface (which is typically around 3) if the overall coefficient U is based (as is customary) on the outside tube surface. The effect of $R_{f,i}$ is correspondingly amplified, making application of fin tubes with high $R_{f,i}$ values questionable.

Item 38: α_s (W/m^2 K), shell-side heat transfer coefficient (specified or estimated). In some cases, the designer may want to specify the value of α_s, for example, if condensing steam is used as a heating medium ($\alpha_s \approx 8\,000$ W/m^2 K), while the controlling heat transfer resistance is on the tube side. The shell-side heat transfer calculations will, in such cases, be bypassed, and a number of the input items are not required, depending on some other requirements, such as estimation of tube count, and so on. For some cases, the shell-side pressure drop will be required even if α_s is specified. In such cases, all inputs are required. Use engineering judgment, reflecting the given circumstances.

Item 39: α_t (W/m^2 K), tube-side heat transfer coefficient (specified or estimated). Essentially same comments apply as to item 38, except that the controlling resistance is in this case on the shell side, and therefore full specifications of the shell-side flow-related data input items are required.

Note: Estimation of both α_s and α_t is useful in most cases for initial design calculation and the wall viscosity correction factor ϕ for liquids (see Sec. 3.3.8).

Items 40, 41: $\Delta p_{s,max}$, $\Delta p_{t,max}$, maximum permissible pressure drops for shell side and tube side, respectively. These values are essential for design cases, which are customarily limited by maximum permissible pressure drops. The best utilization of the allowed Δp will result in the least expensive and most efficient exchanger. Customary practices and limitations are discussed at greater detail in Sec. 3.3.10. However, even for rating cases, it is advisable to compare the resulting pressure drop to experience-based values, to avoid poor performance.

Item 42: $v_{t,max}$ (m/s), maximum permissible tube-side flow velocity. In some cases, the maximum tube-side flow velocity is specified instead of and/or in addition to the maximum pressure drop. This is mainly because of erosion effects related to tube material used and the nature of the tube-side fluid (clean or with abrasive particles present). There are no specific recommendations on this rather complex subject, but general practice

© 1983 Hemisphere Publishing Corporation

for clean fluids calls for a $v_{t,max}$ of 3 m/s for carbon steel or Cu-Ni alloys, 5 m/s for alloyed steels, and 6 m/s for titanium tubes. This is, obviously, only a very rough screening guide, subject to other considerations. The presence of abrasive particles will require the lowering of these limits, especially in U tubes. Impingement protection is always assumed.

Item 43: $v_{t,min}$ (m/s), minimum acceptable tube-side flow velocity. A minimum tube-side velocity is required primarily to prevent flow velocity-sensitive fouling. As explained in Sec. 2.10, the rate of fouling for most fluids is a strong function of the flow velocity. Consequently, the exchanger designer has to respect this restriction and eliminate design configurations that appear otherwise acceptable but that do not meet this limitation.

As an approximate guide for liquids in turbulent flow, $v_{t,min}$ should not be below about 1.0 m/s and preferably more; for cooling water, $v_{t,min}$ should be 1 m/s, but a generally accepted value based on overall cost optimizations between pumping power cost and cost of fouling in primary design and maintenance calls for $v_t \approx 2$ m/s.

C. Calculations of basic correlational parameters

Prior to calculations of correction factors and ultimately α and Δp, some basic terms, derived from the data input, must be determined.

(a) Cross-flow area S_m (mm^2) at the shell centerline within one baffle spacing L_{bc}

This is the minimum cross-flow area in the shell-side flow direction (perpendicular to the baffle cut). It is composed of two components:

1. The bypass channel between the tube bundle and shell inside diameter, L_{bb}, input item 21, with $L_{bb} = D_s - D_{otl}$, Eq. (20).
2. The minimum cross-sectional area within the tube field. Referring to Table 10, the minimum distances in cross-flow between tubes for the various layouts are shown as double lines. For 30 and 90 layouts, the minimum free cross-flow gap is simply $(L_{tp} - D_t)$ for each tube pitch L_{tp}. For the 45 staggered layout, the minimum cross-flow gap within the layout pattern is the sum of the two gaps in the triangle sides $(L_{tp} - D_t)$ in Table 10.

To generalize the above relations, a new term $L_{tp,eff}$ is introduced, which normalizes the calculational procedures. Thus

$$S_m = L_{bc}\left[L_{bb} + \frac{D_{ctl}}{L_{tp,eff}}(L_{tp} - D_t)\right] \tag{22}$$

where L_{bc} (mm) = central baffle spacing (item 12)
L_{bb} (mm) = bypass channel diametral gap (item 21)
$L_{tp,eff}$ (mm) = L_{tp} for 30 and 90 layouts
= $L_{tp}(0.707)$ for 45 staggered layout (Table 10)
D_{ctl} (mm) = defined under item 21

Consequently, within the definitions used here, the 45 rotated square layout will have 1.41 times larger cross-flow area (based on tube pitch L_{tp}) than either the 90 or the 30 layout, but the number of tube rows crossed will be 1.41 and 1.22 larger than in the 90 and 30 layouts, respectively.

(b) Average temperatures $T_{s,av}$, $T_{t,av}$

As this method is formulated primarily for manual calculation, the physical properties are evaluated at the arithmetic mean temperatures of the shell- and tube-side fluids:

$$T_{s,av} = \tfrac{1}{2}(|T_{si} + T_{so}|) \tag{23a}$$

$$T_{t,av} = \tfrac{1}{2}(|T_{ti} + T_{to}|) \tag{23b}$$

using the terminal temperatures from data input items 22-25.

However, if large variation of physical properties due to temperature change between inlet and outlet should exist, possibly causing a change from laminar to turbulent flow, the accuracy of the method will suffer. See further comments in Sec. 3.3.4.

(c) Shell-side Reynolds number Re_s

From input data, we define the maximum shell-side cross-flow mass velocity, $\dot{m}_s$ (kg/m^2 s) as

$$\dot{m}_s = \frac{M_s}{S_m}(10^6) \tag{24}$$

where $\dot{M}$ (kg/s) = shell-side flow rate from data input, item 26
S_m (mm^2) = cross-flow area, from Eq. (22)
(10^6) = adjustment factor from mm^2 to m^2

The shell-side Reynolds number Re_s is then expressed as

$$Re_s = \frac{D_t \dot{m}_s}{\eta_s} \tag{25}$$

where D_t = tube-side diameter, input item 2
$\dot{m}_s$ = defined by Eq. (24)
η_s = dynamic viscosity at average bulk temperature, input item 30

© 1983 Hemisphere I blishing Corporation

Any other consistent set of units can be used to produce Re,, as long as it is dimensionless.

(d) Shell-side Prandtl number Pr_s

By definition from input values,

$$\mathrm{Pr}_s = \frac{c_{p,s}\eta_s}{\lambda_s}(10^{-3}) \tag{26}$$

where the factor (10^{-3}) adjusts the units used in the input values. The physical properties c_p, η, and λ are referred to average shell temperature.

(e) Mean temperature difference AT,

The effective mean temperature difference is discussed in detail in Sec. 1 .5. From basic definitions,

$$\Delta T_m = T_{LM}(F) \tag{27}$$

From the input data, we can determine the terminal temperature differences in terms of hot and cold streams:

$$\Delta T_1 = T_{\mathrm{in,hot}} - T_{\mathrm{out,cold}} \tag{28a}$$

$$\Delta T_2 = T_{\mathrm{out,hot}} - T_{\mathrm{in,cold}} \tag{28b}$$

Then the log mean temperature difference

$$\Delta T_{LM} = \left.\frac{\Delta T_1 - \Delta T_2}{\ln(\Delta T_1/\Delta T_2)}\right|_{\mathrm{AT}, \neq \Delta T_2} = \left.\frac{\Delta T_1 + \Delta T_2}{2}\right|_{\mathrm{AT},-\mathrm{AT},} \tag{29}$$

The correction factor F needs to be calculated for any particular flow configuration (shell type) as determined in Sec. 1.5. For isothermally condensing fluids, such as steam-heated exchangers, $F = 1.0$. Also, for pure counter flow, $F = 1.0$. All other flow arrangements will have $F < 1.0$, but F should be kept above about 0.75-0.8, as otherwise inefficient design would result. If too low F values are encountered, the design may have to be reevaluated, adding units in series, changing bundle type, or accepting pure counter flow, as the case may be, for overall optimum performance.

(f) Effective tube length

For heat transfer area calculations, the effective tube length is specified as L_{ta}. See also comments to end zone correction factor J_r in Sec. 3.3.6, with respect to effectiveness of U-tube end zone.

For transfer calculations in the tube-side laminar flow regime, Sec. 2.5.1, the effective tube length enters as a parameter in the term d/L. The L term in these equations should be interpreted as undisturbed flow length. In all except U-tube bundles, this length should be $L = L_{ta}$; for U-tube bundles, some mixing will occur in the U bend, but as a safe assumption, $L = 2L_{ta}$.

(g) Total heat transfer surface of the exchanger, A, *(m^2)*

Determine the heat transfer-effective tubular area, pertaining to the tube length L_{ta}, input item 10. Consideration should be given to the effectiveness of the U-end baffle area.

$$A, = \pi D_t L_{ta} N_{tt} \times 10^{-6} \quad (\mathrm{m}^2) \tag{30}$$

where 10^{-6} recalculates mm^2 to m^2.

Nomenclature for Section 3.3.5 appears at the end of Section 3.3.11.

REFERENCES FOR SECTION 3.3.5

1. Kern, D. *Q., Process Heat Transfer,* McGraw-Hill, New York, 1950.
2. Standards of Tubular Exchangers Manufacturers Association, 6th ed., TEMA, New York, 1978.

© 1983 Hemisphere Publishing Corporation

3.3.6
Auxiliary calculations

J. Taborek

■ Based on the input data defined in Sec. 3.3.5, there are a number of calculations required to be able to compute the various correction factors, flow areas, surfaces, and so on, as needed for the ultimate purpose of determining the shell-side heat transfer coefficient and pressure drop. These auxiliary calculations are defined in this section.

A. Segmental baffle window calculations

Referring to Fig. 1, which illustrates the basic segmental baffle geometry in relation to the tube field, we calculate first the centri-angle of the baffle cut intersection with the inside shell wall, θ_{ds}, and the angle intersecting the diameter D_{ctl}, that is, the circle through the centers of the outermost tubes, $D_{ctl} = D_{otl} - D_t$ ***(see Sec. 3.3.5).***

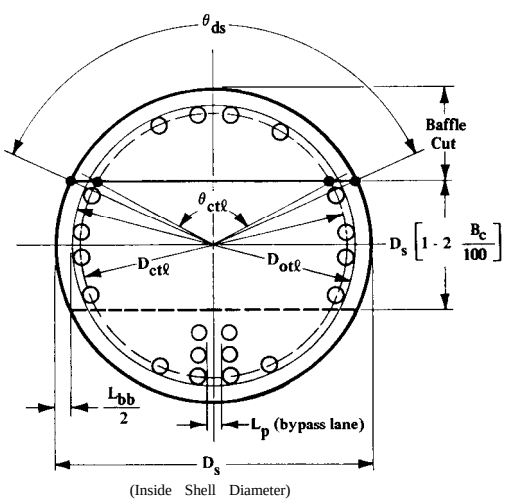

Figure 1 Basic baffle geometry relations.

$$\theta_{ds} = 2\cos^{-1}\left[1 - 2\frac{B_c}{100}\right] \quad \text{(deg)} \tag{1}$$

$$\theta_{ctl} = 2\cos^{-1}\left\{\frac{D_s}{D_{ctl}}\left[1 - 2\left(\frac{B_c}{100}\right)\right]\right\} \text{ (deg)} \tag{2}$$

In case so-called window baffles are used (see Sec. 3.3.5), that is, baffles where the area between D_s and D_{otl} is blocked, the centri-angle referred to D_{otl} is needed:

$$\theta_{otl} = 2\cos^{-1}\left\{\frac{D_s}{D_{otl}}\left[1 - 2\left(\frac{B_c}{100}\right)\right]\right\} \quad \text{(deg)} \tag{3}$$

B. Baffle window flow areas

The gross window flow area, that is, without tubes in the window, S_{wg}, is

$$S_{wg} = \frac{\pi}{4}(D_s)^2\left(\frac{\theta_{ds}}{360} - \frac{\sin\theta_{ds}}{2\pi}\right) \quad (\text{mm}^2) \tag{4}$$

The results of Eq. (4) are plotted in Fig. 2 for convenience, as a function of D_s, with B_c as a parameter. If, however, the above-mentioned window baffle is used, replace θ_{ds} in Eq. (4) with θ_{otl} from Eq. (3); Fig. 2 is no longer valid.

From the relationships in Sec. A, and Eq. (4), we can now calculate the fraction of tubes in the baffle window, F_w; and in pure cross flow, F_c, that is, between the baffle cut tips, as indicated in Fig. 1 by the distance $\{D_s[1 - 2(B_c/100)]\}$.

© 1983 Hemisphere Publishing Corporation

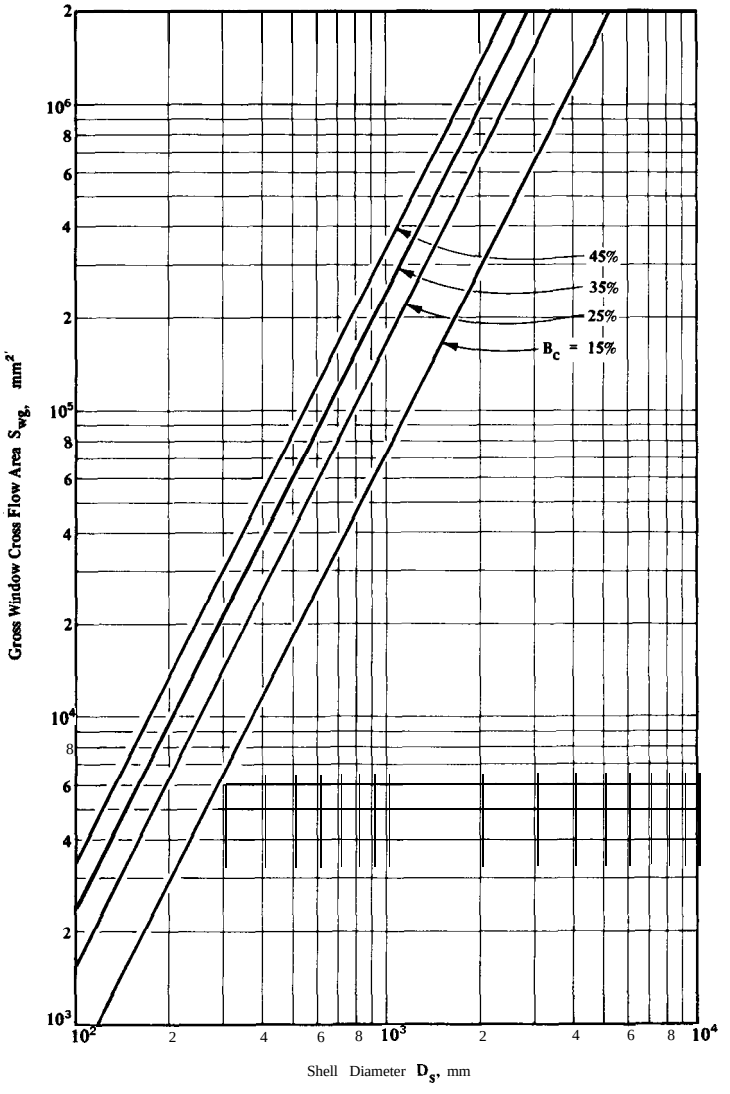

Figure 2 **Gross** segmental baffle window area (without tubes) S_{wg} as a function of inside shell diameter D_s.

These calculations assume that the tube field is uniform within the diameter D_{otl}. This premise is sometimes violated because of tube pass lanes distribution. Also, tubes are sometime omitted in the nozzle entry area to permit the placement of impingement plates. However, within the overall accuracy of the method and effects of other simplifications, this minor error must be accepted or corrected in individual cases. According to the above premises, the fraction of number of tubes in one window F_w, and the fraction of number of tubes in pure cross flow between baffle tips F_c are expressed as follows:

$$F_w = \frac{\theta_{ctl}}{360} - \frac{\sin \theta_{ctl}}{2\pi} \quad (5)$$

$$F_c = 1 - 2(F_w) \quad (6)$$

where θ_{ctl} is defined by Eq. (2).

The segmental baffle window area occupied by the tubes, S_{wt}, can be calculated as

$$S_{wt} = N_{tt} F_w \left(\frac{\pi}{4} D_t^2\right) = N_{tw} \left(\frac{\pi}{4} D_t^2\right) \quad (\text{m m} \quad) \quad (7)$$

and is presented graphically in Fig. 3. The number of tubes in the window, N_{tw}, is expressed as

$$N_{tw} = N_{tt} F_w \quad (8)$$

Finally, the net cross-flow area through one baffle window, S_w, that is, the gross flow area S_{wg}, Eq. (4), minus the area occupied by the tubes, S_{wt}, Eq. (7), is

$$S_w = S_{wg} - S_{wt} \quad (\text{mm}^2) \quad (9)$$

© 1983 Hemisphere Publishing Corporation

C. Equivalent hydraulic diameter of a segmental baffle window, D_w

The equivalent hydraulic diameter of a segmental baffle window, D_w, is required only for pressure drop calculations in laminar flow, that is, if Re, < 100. It is calculated by the classical definition of hydraulic diameter, that is, four times the window cross-flow area S_w divided by the periphery length in contact with the flow. This is expressed in the following equation (except that the baffle edge is purposefully omitted from the periphery term):

$$D_w = \frac{4S_w}{\pi D_t N_{tw} + \pi D_s \theta_{ds}/360} \quad \text{(mm)} \qquad (10)$$

D. Number of effective tube rows in cross flow, N_{tcc} and N_{tcw}

The determination of the effective number of tubes in cross flow is an essential parameter for the calculation of heat transfer coefficient and pressure drop, and the corresponding correction factors. It is a function of the tube layout and tube pitch, the same parameters as are needed for the determination of the cross-flow area S_m (Sec. 3.3.X). The pertinent values are shown in Table 3.3.5(10) for the three layouts, 30 equilateral triangular, *90"* in line, and *4.5"* staggered.

The number of effective rows crossed in one cross-flow section, that is, between the baffle tips, is

$$N_{tcc} = \frac{D_s}{L_{pp}}\left[1 - 2\left(\frac{B_c}{100}\right)\right] \qquad (11)$$

where L_{pp} is obtained from Table 3.3.5(10).

The determination of the number of effective tube rows crossed in the baffle window, N_{tcw}, is not straightforward and is subject to some interpretation of the window flow pattern. Highest flow velocity exists just below the baffle tips and then decreases rapidly, as shown schematically in Fig. 4. This was demonstrated by numerous visual experiments, such as in [1] and [2]. Ultimately, the effective distance of baffle window flow

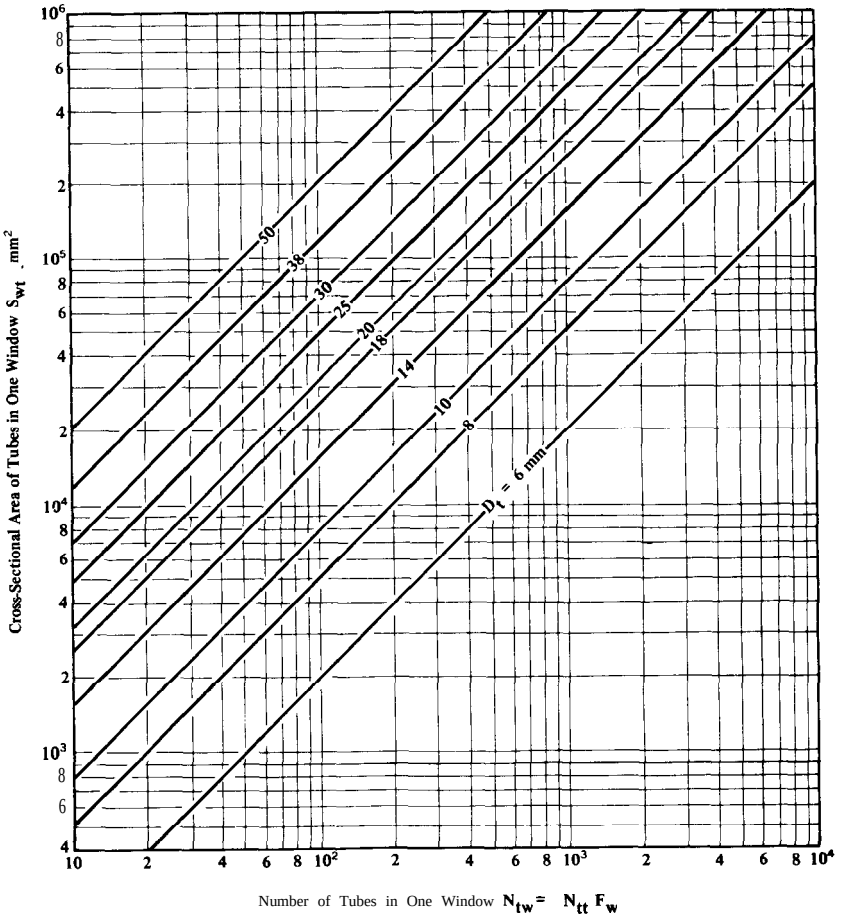

Figure 3 Cross-sectional area of tubes in one segmental baffle window S_{wt} as a function of number of tubes in the window N_{tw}.

© 1983 Hemisphere Publishing Corporation

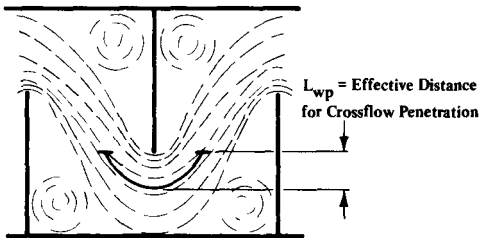

Figure 4 Schematic diagram of effective cross flow within a baffle window.

penetration, which could be considered cross flow (and includes implicitly the contribution of the longitudinal flow component), must be determined from experimental data. For more detailed discussion on this subject, see [3].

From the Delaware and other data, the effective distance of penetration, L_{wp}, was determined as 0.4 of the tubular field in the baffle window, which is the distance between the baffle cut and D_{ctl}, Fig. 4.

$$L_{wp} = 0.4\left(D_s \frac{B_c}{100} - \frac{D_s - D_{ctl}}{2}\right) \tag{12}$$

This distance is crossed twice within each window, and therefore the effective number of tube rows crossed, N_{tcw}, is

$$N_{tcw} = \frac{0.8}{L_{pp}}\left[D_s\left(\frac{B_c}{100}\right) - \frac{D_s - D_{ctl}}{2}\right] \tag{13}$$

where L_{pp}, the effective tube row distance in the flow direction, is taken from Table 3.3.5(10).

More accurate but also more elaborate interpretation of the window flow has been made [4], but the data necessary for such analysis are not in the public domain and the resulting calculations would be beyond the ease of a manual method.

E. Number of baffles, N_b

The number of baffles N_b is required for calculation of the total number of cross passes and window turnarounds. Use drawings or sketches whenever possible. If calculation is necessary, use the tube length L_{ti} as defined in Sec. 3.3.5 and notice the different interpretation for U tubes. The baffle spacing is the central one, L_{bc}, even if larger end spacings are used.

$$N_b = \frac{L_{ti}}{L_{bc}} - 1 \tag{14}$$

Notice that if end baffle spacings are the same as the central one, the value should be an integer (or close to it). If larger end spacings are used, the N_b value calculated should be rounded down. Confirm on a sketch if in doubt.

F. Bundle-to-shell bypass area parameters, S_b and F_{sbp}

The flow area between the shell wall and the tube bundle is the prime area where the flow can bypass the desirable path through the tube field. The flow in the bypass area, having a lower resistance than that through the bundle, can attain considerable magnitudes (20-30%) and decreases the efficiency of heat transfer while decreasing the pressure drop. These effects are eventually expressed in the respective correction factors J_b and R_b in Sec. 3.3.6K. These factors respect also the effect of bypass sealing strips (N_{ss} in the data input), which decrease the flow in the bypass channel.

In addition to the shell-to-bundle bypass area, there can be additional bypass flow in tube partition pass lanes. The pass lanes are, however, placed perpendicular to the cross flow whenever possible, but in some cases of multitube pass designs, it is unavoidable to place at least some of them in the flow direction. As the bypass stream in such cases touches the tube field on both sides, it is more heat transfer-effective than the peripheral bypass stream. Moreover, the bypass lanes are usually blocked by tie rods, which act similarly to the sealing strips. Within the overall accuracy of this method, the bypass lanes usually can be neglected.

Accordingly, the bypass area within one baffle, S_b, can be expressed as follows:

$$S_b = L_{bc}[(D_s - D_{otl}) + L_{pl}] \quad (\text{mm}^2) \tag{15}$$

where L_{pl} expresses the effect of the tube lane partition bypass width (between tube walls) as follows (Fig. 1):

L_{pl} = 0 for all standard calculations

L_{pl} = half of the real dimension of the tube lane partition L_p (see Fig. 1). For estimation purposes assume that $L_p = D_t$. *See Sec. 4.2* for more detail. For further refinement, engineering judgment should be used.

For calculations of the correction factors J_l and R_l, the ratio (or fraction) of the bypass area S_b to the overall cross-flow area S_m, as defined in Eq. 3.3.5(22), is required

$$F_{sbp} = \frac{S_b}{S_m} \tag{16}$$

G. Shell-to-baffle leakage area, S_{sb} (mm²)

The shell-to-baffle leakage area S_{sb} is required for calculation of the correction factors for baffle leakage effects J_l and R_l. The diametral leakage clearance between the shell diameter D_s and the baffle diameter D_b is designated as L_{sb} (mm) in the data input section. This value can be estimated by procedures outlined in

© 1983 Hemisphere Publishing Corporation

Fig. 3.3.5(13) or allocated according to individual circumstances and engineering judgment.

Assuming that L_{sb} has been determined, the shell-to-baffle leakage area within the circle segment occupied by the baffle is calculated (with acceptable approximation) as

$$S_{sb} = \pi D_s \left(\frac{L_{sb}}{2}\right)\left(\frac{360 - \theta_{ds}}{360}\right) (\text{mm}^2)$$
$$= 0.00436 D_s L_{sb} (360 - \theta_{ds}) \qquad (17)$$

This equation is represented graphically in Fig. 5 as a function of the baffle cut B_c and using values of L_{sb} as recommended in Fig. 3.3.5(13) and Eq. 3.3.5(19), that is, the TEMA values with an additional tolerance. Should the exchanger have another value of L_{sb}, S_{sb} should be calculated from Eq. (17).

H. Tube-to-baffle hole leakage area for one baffle, S_{tb} (mm²)

Similar to item G, the tube-to-baffle hole leakage area for one baffle, S_{tb}, is needed for calculation of the correction factors J_l and R_l. The diametral clearance L_{tb} is a data input item with recommended values shown in Fig. 3.3.5(12), and instructions in Sec. 3.3.5, item 19. The total tube-to-baffle leakage area within one baffle is then

$$S_{tb} = \left\{\frac{\pi}{4}\left[(D_t + L_{tb})^2 - D_t^2\right]\right\}(N_{tt})(1 - F_w) \qquad (18)$$

where F_w is related to F_c, the fraction of tubes in the baffle between baffle tips, as calculated in Eq. (6). The expression in braces in this equation represents the leakage area for one tube $(S_{tb})_1$, and is represented graphically in Fig. 6. Accordingly, Eq. (18) can be simplified to

$$S_{tb} = (S_{tb})_1 (N_{tt})(1 - F_w) \qquad (19)$$

I. Segmental baffle window correction factor J_c (Fig. 7)

The correction factor J_c is used to express the effects of the baffle window flow on the heat transfer factor j, which is based on cross flow. Postulating a number of logical assumptions on how the window flow is related to the cross flow at shell centerline, the Delaware workers developed this correction factor as shown in Fig. 7. Detailed documentation of the development is described by Bell [3] . The method, despite its simplicity, appears to hold reasonably well for the range of recommended baffle cuts and baffle spacing values.

Notice that J_c reaches the value of 1.0 for baffle cuts around 25 to 30%, and even larger than 1.0 for smaller baffle cuts. This can be explained by the fact

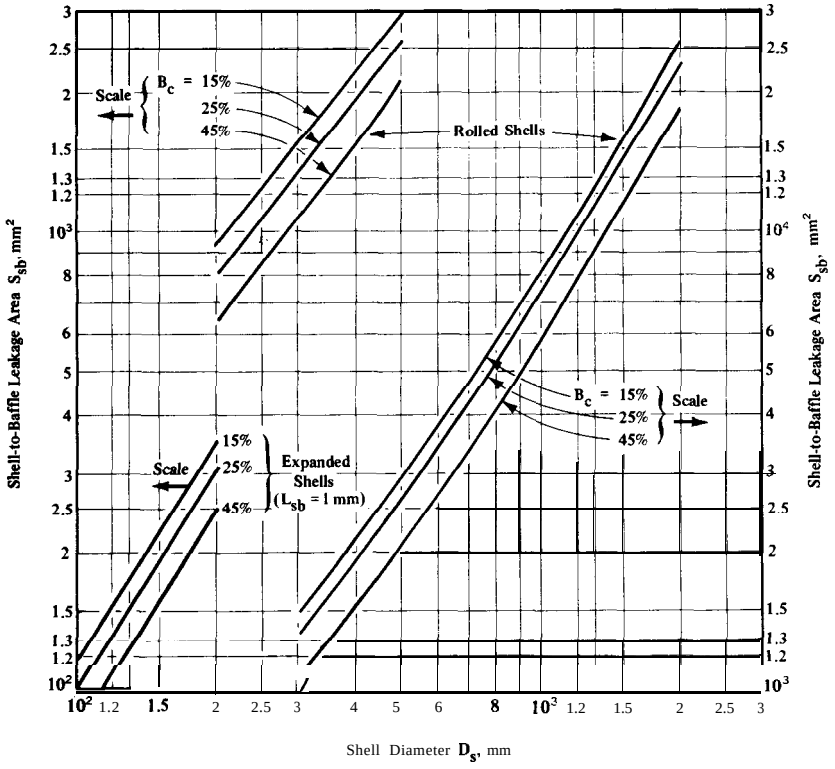

Figure 5 Shell-to-baffle leakage area as a function of D_s and baffle cut B_c, using clearance values of L_{sb} per Eq. 3.3.5(19) and Fig. 3.3.5(13).

© 1983 Hemisphere Publishing Corporation

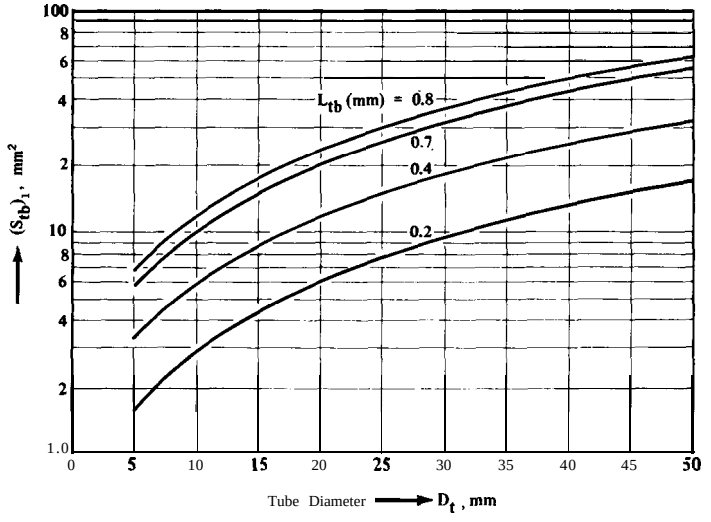

Figure 6 Tube-to-baffle leakage area for a single tube with diametral gap L_{tb} from Fig. 3.3.5(12).

that j_i is obtained at the largest cross-flow section at the center row, while much higher flow velocities will exist below the baffle cut edge, especially as the baffle cut decreases. This, in turn, is compensated by the fact that fewer tubes exist in this region. A much more complex analysis is necessary to express these interactions properly.

The factor J_c is a function of the baffle cut B_c and of the diameter D_{ctl}, as both values determine the number of tubes in the baffle window. The correlating parameter is the fraction of tubes in cross flow (between baffle tips), given as F_c in Eq. (6).

The original curve of the Delaware method is shown in Fig. 7, but for practical calculations in the range of baffle cuts 15–45%, a straight-line approximation is sufficient, expressed as

$$J_c = 0.55 + 0.72F_c \quad (20)$$

J. Correction factors for baffle leakage effects for heat transfer, J_l, and pressure drop, R_l

The pressure difference between two adjoining baffle compartments forces part of the flow to penetrate in the gap between (1) the shell and the baffle edge circumference and (2) the tube and the baffle tube holes. This decreases the effective cross-flow stream and consequently also both α_s and Ap,. The leakage streams can reach considerable magnitudes (up to 40%) and are, therefore, most important factors in the correlations.

From the two leakage streams considered, the shell-to-baffle stream is most detrimental to heat trans-

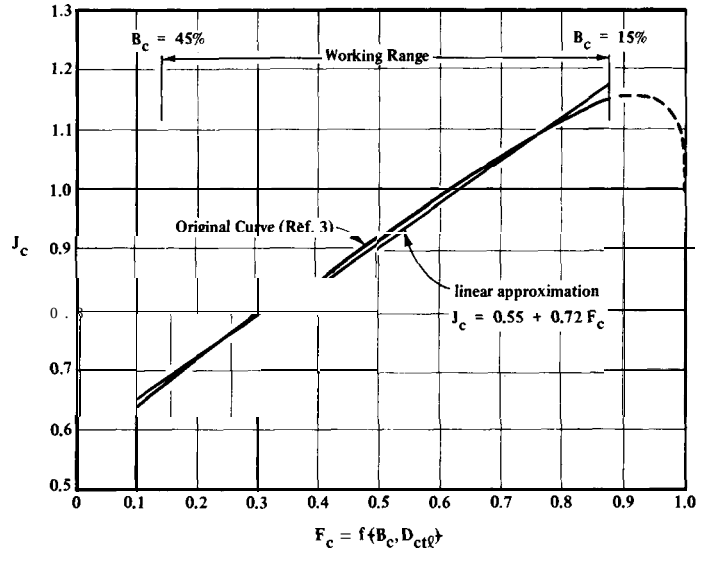

Figure 7 Segmental baffle window correction factor J_c as a function of fraction of tubes in cross flow F_c, Eq. (6).

© 1983 Hemisphere Publishing Corporation

fer, as it does not exchange heat with any tubes. On the contrary, the tube-to-baffle stream passes over the tube surface within the gap, and is consequently partially effective. Note, however, that the tube hole clearances may become plugged up by fouling deposits in some cases, and consequently this stream may decrease with time. This will increase the cross-flow stream but also the other bypass streams, with the usual effect of a relatively small change of heat transfer but usually increased pressure drop. For sensitive cases, the designer should consider performing the calculations for the initial clean condition as well as for the condition with tube clearances eliminated, $S_{tb} = 0$.

The results of the Delaware work as originally published [3] are here somewhat modified, accounting for additional data that have become available. It is assumed that the following values have been determined:

S_{sb}, shell-to-baffle leakage area, Eq. (17)
S_{tb}, tube-to-baffle hole leakage area, Eq. (19)
S_m, cross-flow area at bundle centerline, Eq. 3.3.5(22)

The correlational parameters used are

$$r_{lm} = \frac{S_{sb} + S_{tb}}{S_m} \tag{21}$$

which is the ratio of both leakage areas to the cross-flow area, and

$$r_s = \frac{S_{sb}}{S_{sb} + S_{tb}} \tag{22}$$

which is the ratio of the shell-to-baffle leakage area to the sum of both leakage areas.

The correction factors for heat transfer J_l and for pressure drop R_l are shown in Figs. 8 and 9, respectively. The following characteristics of the figures should be noted:

1. The most severe correction is for the parameter $r_s = 1$, which corresponds to the case of all leakage taking place in the shell-to-baffle area. This is in accordance with the comments above.

2. The least severe correction is for the case of all leakage in the tube baffle holes, $r_s = 0$. The effect of decreased tube-to-baffle clearance due to fouling can be readily analyzed.

3. A well-designed exchanger should have values of J_l not less than about 0.6, preferably 0.7-0.9, as otherwise too great penalty on heat transfer efficiency will exist. If low J_l values are obtained, the design should be carefully examined and possible remedial actions considered, such as: (a) Wider baffle spacing, which will increase S_m and shift r_{lm} toward higher J_l values. (b) Increasing tube pitch or changing tube layout to 90 or 45 will have similar effects (usually at the cost of

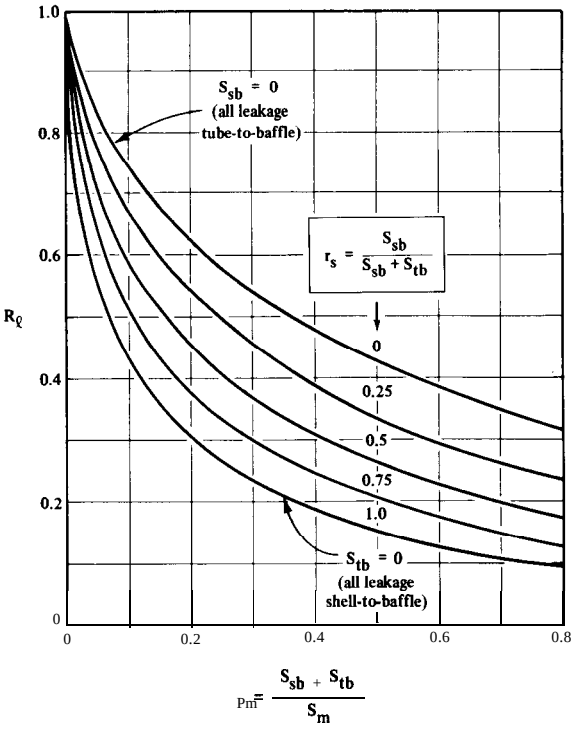

Figure 8 Baffle leakage pressure drop correction factor R_l, as a function of r_{lm}, Eq. (21), and r_s, Eq. (22).

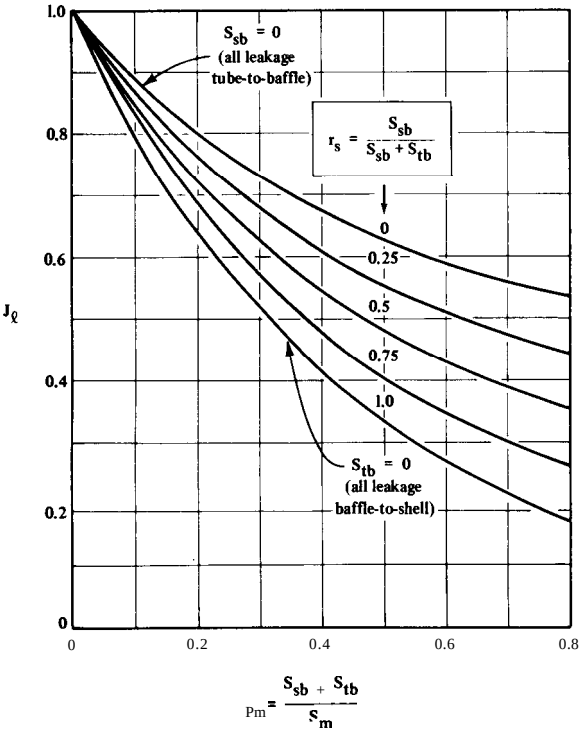

Figure 9 Baffle leakage heat transfer correction factor J_l, as a function of r_{lm}, Eq. (21), and r_s, Eq. (22).

© 1983 Hemisphere Publishing Corporation

somewhat larger surface). (c) More drastic measures include change to double- or triple-segmental baffles, TEMA J shell type, or both.

For computer applications, the correction factors are curve-fitted as follows:

$$J_l = 0.44(1 - r_s) + [1 - 0.44(1 - r_s)] \exp(-2.2 r_{lm}) \quad (23a)$$

$$R_l = \exp[-1.33(1 + r_s)(r_{lm})^p] \quad (23b)$$

where $p = [-0.15(1 + r_s) + 0.81$.

K. Correction factors for bundle bypass effects for heat transfer, J_b, and pressure drop, R_b

The flow resistance in the shell-to-bundle bypass is substantially lower than through the tube field. Consequently, part of the flow will seek this path, in proportion to the ratio of the resistances of the bypass area to the tube field cross-flow area. This stream is only partially effective for heat transfer, as it touches the tubes on one side. For fixed-tubesheet and U-tube bundles, the bypass area is usually not too large. However, for pull-through bundles, the bypass channel must be blocked by sealing strips.

To determine the J_b and R_b correction factors, the following parameters must be known:

$F_{sbp} = S_b/S_m$, the ratio of bypass to cross-flow area, Eq. (16)

If sealing strips are used, determine:

N_{ss} = number of sealing strips (pairs) in one baffle, from data input item 17

N_{tcc} = number of tube rows crossed between baffle tips in one baffle section, Eq. (11):

$$r_{ss} = \frac{N_{ss}}{N_{tcc}} \quad (24)$$

Graphic representation of the correction factors J_b and R_b is shown in Figs. 10 and 11, respectively. As can be expected, the bypass flow fraction is larger in the case of laminar flow, which for these purposes is defined as Re, < 100. The recommended range of J_b factors is indicated in Fig. 10. If lower values result, add sealing strips, which in almost all cases will remedy the problem.

The curves are curve-fitted for computer applications as follows:

$$J_b = \exp[-C_{bh} F_{sbp}(1 - \sqrt[3]{2 r_{ss}})] \quad (25)$$

with the limit of $J_b = 1$, at $r_{ss} \geq \frac{1}{2}$, and

C_{bh} = I.35 for laminar flow, Re, $\leq$ 100

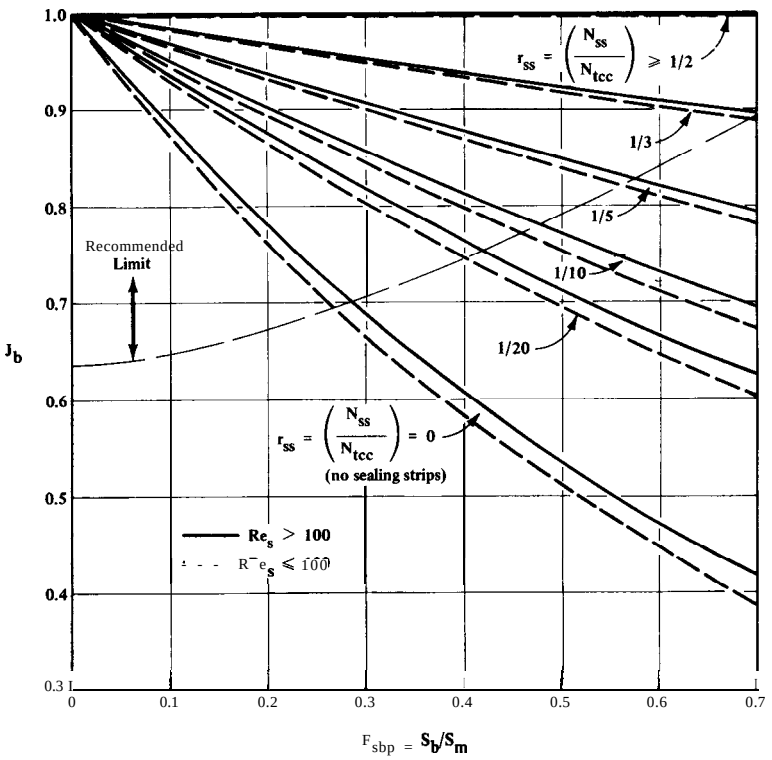

Figure 10 Heat transfer correction factor J_b for shell-to-bundle bypass as a function of F_{sbp}, Eq. (16), with effect of sealing strips per tube rows crossed, r_{ss}.

© 1983 Hemisphere Publishing Corporation

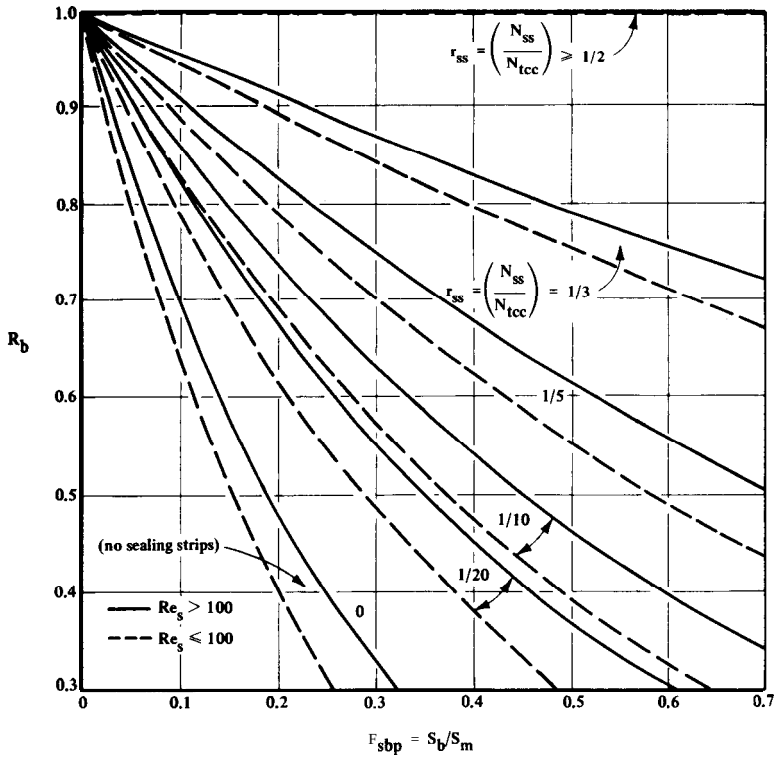

Figure **11** Pressure drop correction factor R_b for shell-to-bundle bypass as a function of F_{sbp}, Eq. (16), with effect of sealing strips per tube rows crossed, r_{ss}

C_{bh} = 1.25 for turbulent and transition flow, Re, > 100

and

$$R_b = \exp\left[-C_{bp}F_{sbp}\left(1-\sqrt[3]{2r_{ss}}\right)\right] \qquad (26)$$

with the limit $R_b = 1$, at $r_{ss} \geq \frac{1}{2}$, and

C_{bp} = 4.5 for laminar flow, Re, $\leq$ 100

C_{bp} = 3.7 for turbulent and transition flow, Re, > 100

L. Heat transfer correction factor for adverse temperature gradient in laminar flow, J_r

The Delaware data on deep laminar flow (Re, < ≈20) exhibited a large decrease of heat transfer, which was eventually postulated as an effect of adverse temperature gradient development through the boundary layer. This is similar to the well-defined effect in tube-side flow where $j \propto L^{-1/3}$. The length of flow L is interpreted in tube banks in a reasonable analogy as the number of tube rows crossed. From the Delaware data it can be concluded that for tube banks, $j \propto (N_c)^{-0.18}$, that is, the effect is somewhat weaker than for tube-side flow, due to partial distortion of the boundary layer between tube rows crossed, N_c. Above Re > 20, momentum change or inertial effects begin to disturb the laminar layer buildup and the effect decreases, until at approximately Re = 100 it disappears.

As the ideal tube bank j_i curves [Figs. 3.3.7(1)-3.3.7(3)] are based on 10 tube rows, the corresponding correction factor J_r for Re, $\leq$ 20 can be expressed as

$$J_r = (J_r)_r = \left(\frac{10}{N_c}\right)^{0.18} = \frac{1.51}{(N_c)^{0.18}} \qquad (27)$$

where N_c is the total number of tube rows crossed in the entire exchanger:

$$N_c = (N_{tcc} + N_{tcw})(N_b + 1) \qquad (28)$$

Between Re, $\leq$ 20 and Re, = 100, a linear proration is applied, resulting in

$$J_r = (J_r)_r + \left(\frac{20 - Re_s}{80}\right)[(J_r)_r - 1] \qquad (29)$$

where $(J_r)_r$ is from Eq. (27) with the limits:

$J_r = 1$ for Re, > 100

$J_r = (J_r)_r$ for Re, $\leq$ 20; $J_r \geq 0.4$

Equation (29) is represented graphically in Fig. 12.

M. Heat transfer correction for unequal baffle spacing at inlet and/or outlet, J_s

Refer to Fig. 3.3.5(7) which shows a schematic sketch of an exchanger where the inlet and outlet baffle spacing L_{bi} and L_{bo} is enlarged in comparison to the regular central

© 1983 Hemisphere Publishing Corporation

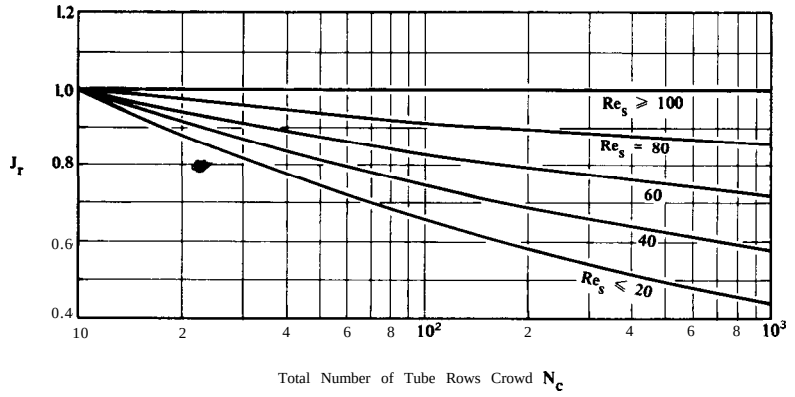

Figure 12 Heat transfer correction factor J_r for laminar flow (Re, <100), with N_c from Eq. (28).

spacing L_{bc}. Let us assume that the heat transfer coefficient α_i was calculated on the basis of the central spacing L_{bc} and that α_i is proportional to $v_{\max}^n$, where $v_{\max}$ is the cross-flow velocity based on L_{bc} and the definition of $\dot{m}_s$, Eq. 3.3.5(24).

Here n is approximately a constant, assumed to be 0.6 for turbulent flow and $\frac{1}{3}$ for laminar flow.

Assuming that the leakage and bypass flow ratios are not greatly altered by the difference between L_{bc} and L_{bi} or L_{bo} (which should be the case for well-designed exchangers where $L_{bi} \gg L_{bc}$ is not acceptable), then, from [5]

$$\alpha_i \propto v_{\max}^n \propto \left(\frac{1}{L_{bc}}\right)^n \tag{30}$$

Now, define the mean shell-side heat transfer coefficient α_s, which takes into account the different coefficients in the inlet and outlet spacing $(\alpha_s)_i$ and $(\alpha_s)_o$, coupled to the respective heat transfer areas $(A_o)_i$ and $(A_o)_o$.

$$\alpha_s A_o = (\alpha_i)_i (A_o)_i + \alpha_i [A_o - (A_o)_i - (A_o)_o] + (\alpha_i)_o (A_{o\,lo} \tag{31}$$

In the context of the method, correction factor J_s can now be defined as a multiplier to the α_i value by dividing Eq. (3 1) by the product of $\alpha_i A_o$.

$$J_s = \frac{\alpha_s}{\alpha_i} = (\alpha_i)_i \left[\frac{(A_o)_i}{A_o}\right] + \frac{A_o - (A_o)_i - (A_o)_o}{A_o} + (\alpha_i)_o \left[\frac{(A_o)_o}{A_o}\right] \tag{32}$$

Introducing the relationships

$$\frac{\alpha_i}{(\alpha_i)_i} = \left(\frac{L_{bi}}{L_{bc}}\right)^n = (L_i^*)^n \tag{33}$$

$$\frac{\alpha_i}{(\alpha_i)_o} = \left(\frac{L_{bo}}{L_{bc}}\right)^n = (L_o^*)^n \tag{34}$$

where L_o^* and L_i^* are dimensionless length ratios, it is noted that

$$\frac{A_o - (A_o)_i - (A_o)_o}{A_o} = \frac{N_b - 1}{L_i^* + (N_b - 1) + L_o^*} \tag{35}$$

Then, Eq. (32) reduces to

$$J_S = \frac{(N_b - 1) + (L_i^*)^{(1-n)} + (L_o^*)^{(1-n)}}{(N_b - 1) + (L_i^*) + (L_o^*)} \tag{36}$$

Notice that for $L_{bi} = L_{bo} = L_{bc}$ or $L^* = L_i^* = L_o^* = 1.0$, $J_s = 1.0$.

For graphical presentation, to give some feel for the magnitude of this correction, we assume that $L^* = L_i^* = L_o^*$, which is often the case. Turbulent flow results in a stronger correction, so $n = 0.6$. In Fig. 13, J_s is plotted against N_b with L^* as a parameter,

$$L^* = \frac{L_{bo}}{L_{bc}} = \frac{L_{bi}}{L_{bo}} \tag{37}$$

Values of L^* larger than 2 would be considered poor design, especially if combined with low N_b. In such cases an annular distributor or other measures should be used. Also, a low number of baffle spacings, usually less than 5, is considered generally a questionable design, as the premises of AT,,, calculations are being violated (see Sec. 1.5).

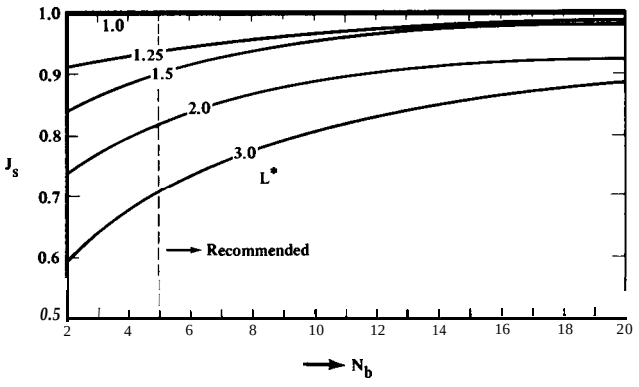

Figure 13 Unequal inlet/outlet baffle spacing correction factor J_s for heat transfer as a function of number of baffles N_b and the baffle spacing ratio L^*, Eq. (37).

© 1983 Hemisphere Publishing Corporation

For laminar flow, the correction is about halfway between 1 and J_s computed for turbulent conditions.

N. Pressure drop correction for unequal baffle spacing at inlet and/or outlet, R_s

The interpretation of the end-zone correction R_s can have several levels of sophistication. The most accurate one is to set up an equation for each end spacing, similar to Δp_{bi}, and to calculate the corresponding friction factor based on physical properties at the local temperatures. Such an elaborate procedure will be justified, within the overall accuracy of the method, only in extreme cases. The recommended method uses a similar logic as applied to the derivation of the heat transfer end zone correction J_s, but applies only to the end zone Δp_e, Eq. 3.3.8(6).

From basic equations of pressure drop,

$$\Delta p_{bi} \propto \left(\frac{1}{L_{bc}}\right)^{2-n} \tag{38}$$

where n is the slope of the friction factor curve, assuming that $n = 1$ for laminar flow, Re, < 100, and $n \approx 0.2$ for turbulent flow.

Because of the specific way pressure drop is treated in this method as shown in Figs. 3.3.8(1)-3.3.8(3), a simple geometric analogy results in

$$R_s = \left(\frac{L_{bc}}{L_{bo}}\right)^{2-n} + \left(\frac{L_{bc}}{L_{bi}}\right)^{2-n} \tag{39}$$

Refer to Sec. 3.3.8 for basic explanations. The correction factor R_s is treated here for reasons of consistency.

This development assumes that the flow regime (exponent n) is the same throughout the exchanger. The correction factor R_s has the following characteristics:

1. For $L_{bc} = L_{bo} = L_{bc}$, $R_s = 2$.
2. For the reasonably extreme case $L_{bo} = L_{bc} = 2L_{bc}$, R_s = 1.0 for laminar flow and $R_s = 0.57$ for turbulent flow.
3. For a typical U tube, $L_{bi} = L_{bc}$ and $L_{bo} = 2L_{bc}$, R_s = 1.5 for laminar flow, and R_s = 1.3 for turbulent flow.

Nomenclature for Section 3.3.6 appears at the end of Section 3.3.11.

REFERENCES FOR SECTION 3.3.6

1. Gupta, R. K., and Katz, D. L., Flow Patterns for Predicting Shell-Side Heat Transfer Coefficients for Baffled Shell-and-Tube Exchangers, *Ind. Eng. Chem.*, vol. 49, no. 6, pp. 998-999, 1957.
2. *Shell-and-Tube Heat Exchanger,* 16-mm color sound movie, originally produced by C. F. Braun Co., 1956, currently available through Heat Transfer Research, Inc. (HTRI), 1000 S. Fremont, Alhambra, Calif. 91802.
3. Bell, K. J., Final Report of the Cooperative Research Program on Shell-and-Tube Heat Exchangers, ***University of Delaware Eng. Exp. Sta. Bull. 5,*** 1963.
4. Palen, J. W., and Taborek, J., Solution of Shell Side Flow Pressure Drop and Heat Transfer by Stream Analysis Method, *Chem. Eng. Prog. Symp. Ser., vol. 65,* no. 92, 1969.
5. Bell, K. J., Private communications (1963–1980), and his D. Q. Kern Memorial Award Lecture at the AIChE/ASME Natl. Heat Transfer Conf., San Diego, Calif., 1979 (unpublished).

© 1983 Hemisphere 1 blishing Corporation

3.3.7

Ideal tube bank correlations for heat transfer and pressure drop

J. Taborek

■ The shell-side method is based on the heat transfer j_i factor and the friction factor f_i from data on ideal tube banks and then correcting these values for the non-idealistics of the flow in a baffled exchanger. Pressure drop and heat transfer in ideal tube banks are described in Secs. 2.2.4 and 2.5.3, respectively. However, the development of the Delaware method was based on a specific set of ideal tube bank data with geometric similarity to shell-and-tube heat exchanger practices. For this reason it appears preferable to use the same set of graphs as a basis. These are presented in Figs. 1-3 as functions of the layout angles and pitch ratios L_{tp}/D_t, covering the industrial range of practical values.

No attempt is made here to correlate the data, and the user is expected to read the corresponding value of j_i and f_i as functions of the Reynolds number Re, from the graphs. For possible computer application, however, a simple set of constants is given in Table 1 for a curve fit of the following form:

$$ii = (a_1)\left(\frac{1.33}{L_{tp}/D_t}\right)^a (\mathrm{Re}_s)^{a_2} \tag{1}$$

where

$$a = \frac{a_3}{1 + 0.14(\mathrm{Re}_s)^{a_4}} \tag{1a}$$

and

$$f_i = b_1\left(\frac{1.33}{L_{tp}/D_t}\right)^b (\mathrm{Re}_s)^{b_2} \tag{2}$$

where

$$b = \frac{b_3}{1 + 0.14(\mathrm{Re}_s)^{b_4}} \tag{2a}$$

Note that the j_i and f_i graphs are based on specific formulations as defined below.

A. Ideal tube bank j_i and α_i

The ideal tube bank j_i factor is defined as

$$j_i = \frac{\alpha_i}{(C_p)_s \dot{m}_s}(\mathrm{Pr}_s)^{2/3}(\Phi_s)^{-r} = f\left(\mathrm{Re}_s \frac{L_{tp}}{D_t}\right) \tag{3}$$

Using the Re, value determined in Eq. 3.3.5(25), read the corresponding value of j_i from Figs. 1-3 or calculate j_i from the equation given above. Then the heat transfer coefficient for ideal tube bank becomes α_i (W/m^2 K):

$$\alpha_i = j_i (C_p)_s \dot{m}_s (\mathrm{Pr}_s)^{-2/3}(\Phi_s)^r \tag{4}$$

where $(C_p)_s$ = shell fluid viscosity, from data input
$\dot{m}_s$ = shell-side mass velocity, Eq. 3.3.5(24)
Pr_s = shell fluid Prandtl number, Eq. 3.3.5(26)
$(\Phi_s)^r$ = correction factor that accounts for the viscosity gradient at the tube wall versus the viscosity at the average bulk fluid temperature, η_s.

The term $(\Phi_s)^r$ needs additional explanation. For liquids the relation usually employed is

$$(\Phi_s)^r = \left(\frac{\eta_s}{\eta_{s,w}}\right)^{0.14} \tag{5}$$

where $\eta_{s,w}$ is the shell fluid viscosity determined at the tube wall temperature, T_w. As the viscosity of the liquids decreases with temperature, $\Phi_s > 1.0$ for shell fluid heated, and $\Phi_s < 1.0$ for shell fluid cooled.

For gases, viscosity is a weak function of tempera-

© 1983 Hemisphere Publishing Corporation

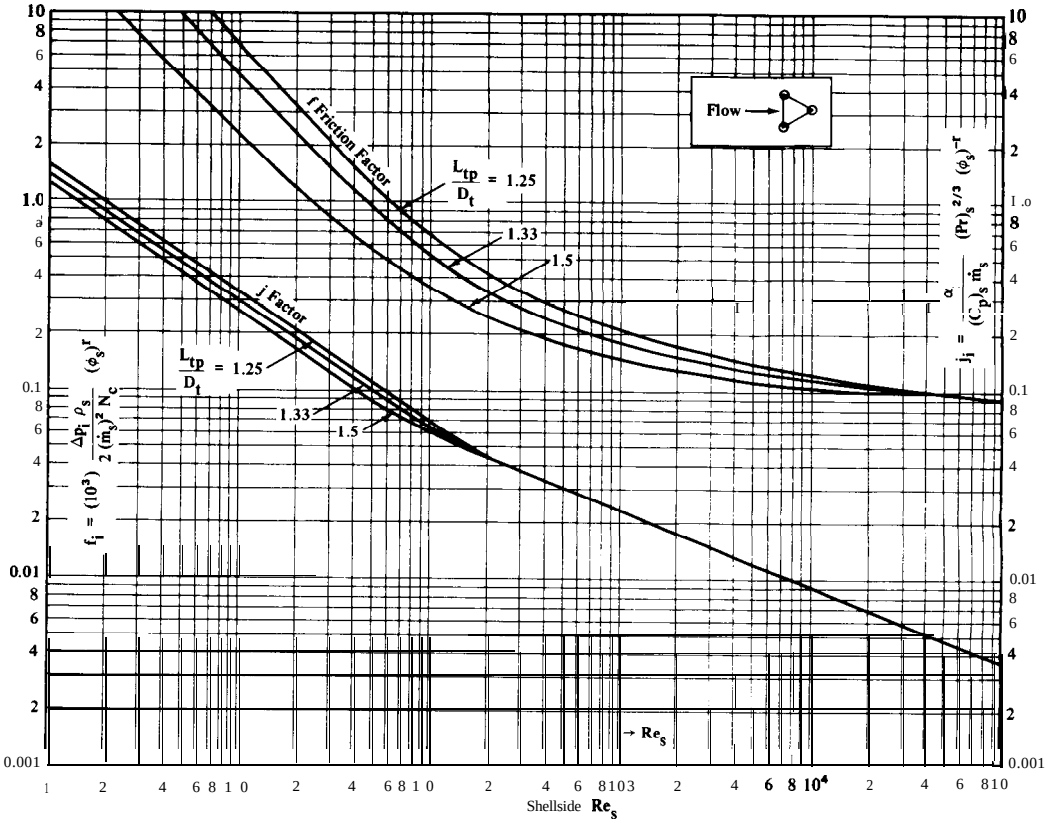

Figure 1 Ideal tube bank j_i and f_i factors for 30 staggered layout [Re, from Eq. (2.5), Sec. 3.3.5].

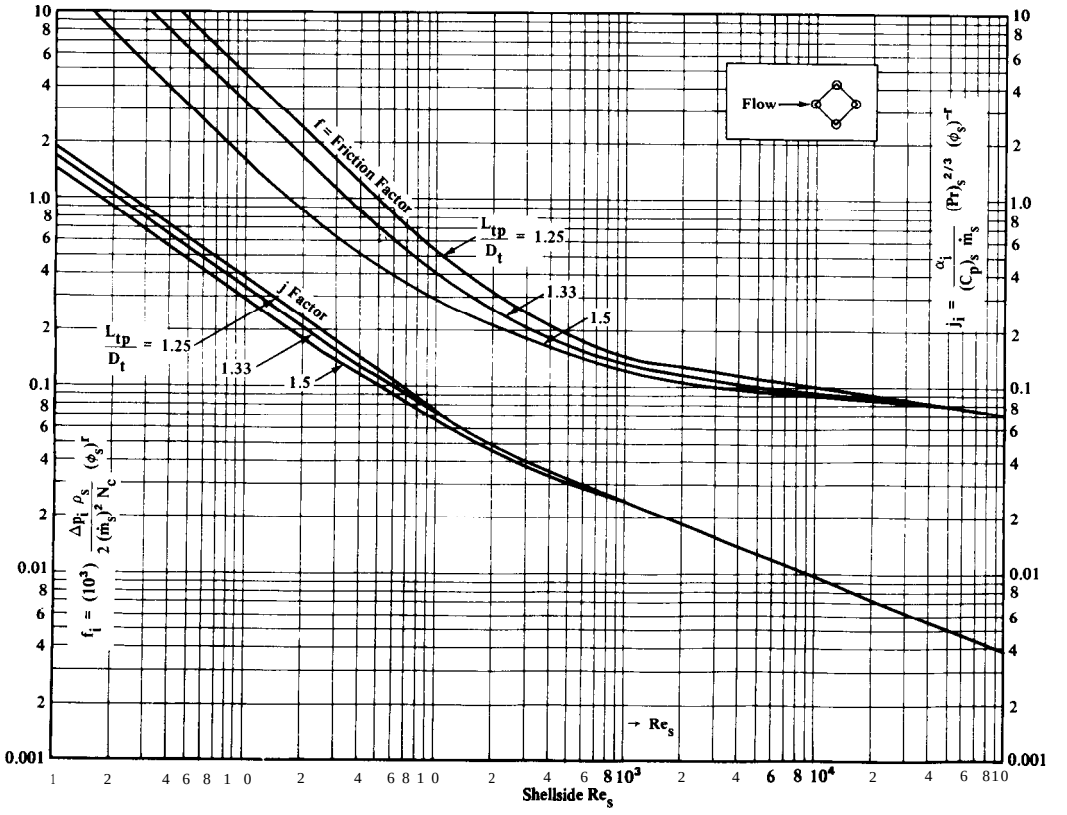

Figure 2 Ideal tube bank j_i and f_i factors for 45 staggered layout [Re, from Eq. (2.5), Sec. 3.3.5].

© 1983 Hemisphere Publishing Corporation

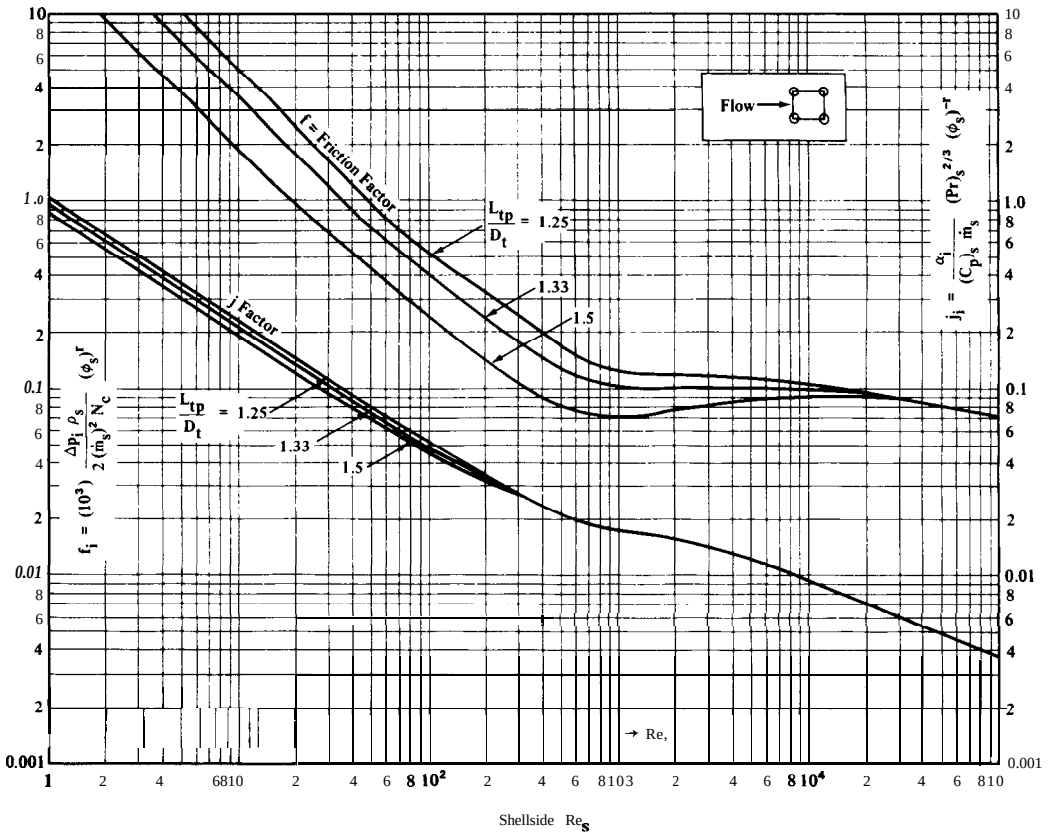

Figure 3 Ideal tube bank j_i and f_i factors for 90 in-line layout [Re, from Eq. (2.5), Sec. 3.3.5].

ture and increases with temperature. The correction factor Φ_s for gases is formulated as follows:

For gas being cooled: $(\Phi_s)^r = 1$ (6a)

For gas being heated: $(\Phi_s)^r = \left(\frac{T_{s,av} + 273}{T_w + 273}\right)^{0.25}$ (6b)

T_w for gas being heated is always larger than $T_{s,av}$, and therefore $\Phi_s < 1.0$.

The problem now is that the tube wall temperature T_w is not known a priori, as it is a function of both shell-side and tube-side heat transfer coefficients α_s and α_i, respectively, which are not known at this point of

Table 1 Correlational coefficients for j_i and f_i, Eqs. (1) and (2)

Layout angle	Reynolds number	a_1	a_2	a_3	a_4	b_1	b_2	b_3	b_4
30	10^5-10^4	0.321	−0.388	1.450	0.519	0.372	-0.123	7.00	0.500
	10^4-10^3	0.321	−0.388			0.486	−0.152		
	10^3-10^2	0.593	-0.477			4.570	-0.476		
	10^2-10	1.360	-0.657			45.100	-0.973		
	<10	1.400	-0.667			48.000	-1.000		
45	10^5-10^4	0.370	-0.396	1.930	0.500	0.303	−0.126	6.59	0.520
	10^4-10^3	0.370	AI.396			0.333	−0.136		
	10^3-10^2	0.730	-0.500			3.500	-0.476		
	10^2-10	0.498	−0.656			26.200	−0.913		
	<10	1.550	--0.667			32.000	-1.000		
90	10^5-10^4	0.370	-0.395	1.187	0.370	0.391	-0.148	6.30	0.378
	10^4-10^3	0.107	-0.266			0.0815	+0.022		
	10^3-10^2	0.408	-0.460			6.0900	-0.602		
	10^2-10	0.900	−0.631			32.1000	-0.963		
	10	0.970	-0.667			35.0000	-1.000		

© 1983 Hemisphere Publishing Corporation

the calculations. For practical calculations, proceed as follows:

1. Estimate the values of α_s and α_t from experience or using Table 3.1.4(2) for the types of fluids involved.

2. Using the average temperature $T_{s,\mathrm{av}}$ and $T_{t,\mathrm{av}}$, Eq. 3.3.5(23), calculate the estimated average tube wall temperature (neglecting tube wall resistance and fouling) as

$$T_w = T_{t,\mathrm{av}} + \left(\frac{T_{s,\mathrm{av}} - T_{t,\mathrm{av}}}{1 + (\alpha_t/\alpha_s)}\right) \tag{7}$$

Notice that the average tube wall temperature T_w will approach the average fluid temperature with the higher α value. Thus, if $\alpha_s \gg \alpha_t$, then $T_w \rightarrow T_{s,\mathrm{av}}$, and vice versa.

If the viscosity of a fluid is given at two temperatures that are different from $T_{s,\mathrm{av}}$ and T_w, an interpolation (or extrapolation, within limits) can be made using an approximation:

$$\eta = a(T^b) \tag{8}$$

where a and b are determined from the two values η_1 and η_2 at T_1 and T_2 (K). A plot on semilog paper (η log, T linear) serves the same purpose.

3. Complete calculation of $(\Phi_s)^r$ and determine the ideal tube bank-based α_i from Eq. (4).

4. After calculating the actual α_s and α_t, compare these values to the estimated ones. If substantial differences exist, estimate the effect on T_w and on Φ_s. Usually this will be negligible. However, especially with high-viscosity fluids, Φ_s may differ from the value based on estimations; in such cases, repeat calculations starting with Eq. (5).

B. Ideal tube bank-based f_i and Δp_i

The ideal tube bank friction factor f_i is defined as

$$f_i = (10^3)\frac{(\Delta p_i)\rho_s}{2(\dot{m}_s)^2 N_c}(\Phi_s)^r = f\left(\mathrm{Re}_s, \frac{L_{tp}}{D_t}\right) \tag{9}$$

where N_c is number of tube rows crossed and Δp_i is in kilopascals. This is shown graphically in Figs. 1-3. Using Re, value as determined in Eq. 3.3.5(25), find f_i from figures or calculate from the corresponding Eq. (2).

The ideal tube bank-based pressure drop Δp_i is used for the part of the flow between the baffle tips of one baffle compartment, where the number of tube rows crossed, $N_c = N_{tcc}$, is determined in Eq. 3.3.6(11). With this substitution, and designating now the pressure drop as Δp_{bi}(kPa),

$$\Delta p_{bi} = 2(10^{-3}) f_i N_{tcc} \frac{(\dot{m}_s)^2}{\rho_s}(\Phi_s)^{-r} \tag{10}$$

where $\dot{m}_s$ (kg/m^2 s) was determined in Eq. 3.3.5(24), $(\Phi_s)^{-r}$ is the tube wall viscosity gradient correction factor as defined in this section for j_i, Eq. (5) and subsequent, and (10^{-3}) is a recalculation factor to kilopascals.

Notice that the exponent on Φ is negative, that is, $\Phi_s < 1.0$ for shell-side fluid being heated and vice versa. Possible reiterative procedure on Φ_s will apply, as for heat transfer, in case the first estimated value of Φ_s results in substantial difference.

Nomenclature for Section 3.3.7 appears at the end of Section 3.3.11.

© 1983 Hemisphere Publishing Corporation

3.3.8

Calculation of shell-side heat transfer coefficient and pressure drop

J. Taborek

■ In this section we convert the ideal tube bank-based α_i and Δp_{bi} to the realistic flow conditions of a segmentally baffled exchanger.

A. Shell-side heat transfer coefficient, α_s

Based on the ideal tube bank-calculated coefficients α_i in Sec. 3.3.7, we determine now the actual shell-side coefficient α_s (W/m^{2}K), using the correction factors for nonidealities of baffled flow as determined in Sec. 3.3.6.

$$\alpha_s = \alpha_i(J_c, J_l, J_b, J_r, J_s) = \alpha_i(J_{\text{tot}}) \quad (1)$$

where J_c = the segmental baffle window correction, Eq. 3.3.6(20) or Fig. 3.3.6(7)

J_l = the baffle leakage correction factor, Eq. 3.3.6(23) or Fig. 3.3.6(9)

J_b = the bypass correction factor, tube bundle to shell, Eq. 3.3.6(25) or Fig. 3.3.6(10)

J_r = the laminar heat transfer correction factor for adverse temperature gradient, applicable for Re, < 100, Eq. 3.3.6(29) or Fig. 3.3.6(12)

J_s = the nonequal inlet/outlet baffle spacing correction factor, applicable only if such differences exist; see Eq. 3.3.6(36) or Fig. 3.3.6(13).

These correction factors may be particularly important for U-tube bundles, where larger outlet baffle spacing will always exist unless special provisions are made, such as if the outlet nozzle is located so that the U-bend area is ineffective, which is the safe procedure. Otherwise, assume that $L_{bo} = 1.20$, for calculation of J_s, because of the large bypass areas, which have not been accounted for in the calculation of α_i. Consider the total effective tube length, L_{ta}, in connection with this problem, Fig. 3.3.5(2), and use engineering judgment.

To give the heat exchanger analyst a feel for the overall effectiveness of the baffled exchanger as compared to ideal tube bank, it is considered useful to calculate J_{tot}, Eq. (1), as the product of all the correction factors. In general, J_{tot} should never be less than 0.4, and preferably $\geqslant 0.5$ for a good design. Lower values call for reevaluation of the construction geometry and remedial alternations.

B. Shell-side pressure drop, Δp_s

The shell-side pressure drop as interpreted in this method is composed of three distinct parts: in pure cross flow, Ap, ; in the baffle windows, Ap, ; and in the end zones (first and last baffle spacing), Ap, [1].

Ap, (kPa) is the pressure drop in cross flow between baffle tips. It is based on Δp_{bi}, the ideal tube bank pressure drop in one baffle compartment of central baffle spacing L_{bc}. The section of the exchanger covered by this pressure drop component is shown in Fig. 1. The number of cross passes is $(N_b - 1)$, and the ideal Δp_{bi} is corrected for both bypass and leakage effects:

$$\Delta p_c = \Delta p_{bi}(N_b - 1)(R_b)(R_l) \quad (2)$$

where Δp_{bi} is calculated in Eq. 3.3.7(10). N_b, the number of baffles, is defined in Eq. 3.3.6(14). R_b is the bypass correction factor from Eq. 3.3.6(26) or Fig. 3.3.6(11). R_l is the leakage correction factor from Eq. 3.3.6(23*b*) or Fig. 3.3.6(8).

© 1983 Hemisphere 1 blishing Corporation

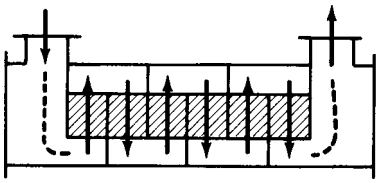

Figure 1 Region of cross flow between baffle tips in the central baffle spacing.

Δp_w (kPa) is the pressure drop in all the baffle windows crossed, which equals N_b, as shown in Fig. 2. The Delaware method offers two different correlations, one for turbulent and one for laminar flow, based for simplicity on the shell-side cross flow Re,. Both correlations employ for mass velocity calculations the geometric mean of the cross-flow area S_m [Eq. 3.3.5(22)] and the window net area S_w [Eq. 3.3.6(9)].

$$\dot{m}_w = \frac{M_s}{\sqrt{S_m S_w}} \times 10^6 \qquad (3)$$

where 10^6 recalculates mm^2 to m^2 and $\dot{m}_w$ is in kg/m^2 s.

Now we define the baffle window Ap, as follows:

For turbulent flow, Re, $\geqslant 100$, Δp_w (kPa) is

$$\Delta p_w = N_b \left[(2 + 0.6 N_{tcw}) \frac{(\dot{m}_w)^2}{2\rho_s} (10^{-3}) \right] R_l \qquad (4)$$

The factor 2 accounts for velocity heads due to the window turnaround, and 0.6 accounts for the cross-flow frictional effects over N_{tcw} tube rows crossed in the window [Eq. 3.3.6(13)].

For laminar flow, Re, < 100, Ap, (kPa), the Delaware procedure is rather complicated, accounting for the pressure loss in cross flow, in longitudinal flow, and for the turnaround. For detailed derivations refer to [2].

$$\Delta p_w = N_b \left\{ 26 \frac{(\dot{m}_w)\eta_s}{\rho_s} \left[\frac{N_{tcw}}{L_{tp} - D_t} + \frac{L_{bc}}{(D_w)^2} \right] + \left[2(10^{-3}) \frac{(\dot{m}_w)^2}{2\rho_s} \right] \right\} R_l \qquad (5)$$

The first term in brackets accounts for the cross flow and longitudinal friction, respectively; the second term in brackets represents two velocity heads for the turnaround in the window.

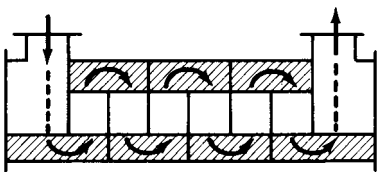

Figure 2 Flow region considered for window flow.

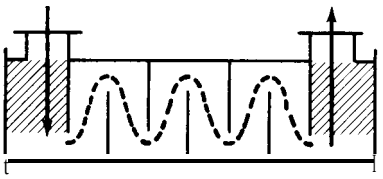

Figure 3 Flow region for the end baffle spacings.

The hydraulic diameter of the baffle window, D_w, is defined in Eq. 3.3.6(10). Notice that only the leakage correction factor R_l is applied to the baffle window Δp_w, whereas the bypass correction factor R_b is considered not applicable.

Comparing the results of Eqs. (4) and (5) at the break point of Re, = 100, we find that the values do not agree exactly, as they are based on different principles. In most cases some proration between the values may be necessary within the range of Re, = 50 to about 200, according to engineering judgment, or the larger value should be taken as a safety factor.

Ap, is the cross flow pressure drop in the end zones, the first and last baffle compartment, Fig. 3.

The flow region of the end zones differs, by definition, from the central cross flow zone, Eq. (2), in the following respects.

1. The number of tube rows crossed includes the tube rows in the entry or exit window, N_{tcw}.

2. The leakage streams have not yet developed (entry) or just joined the main stream (outlet) in the end zones, and therefore the leakage correction factor is not applicable.

3. The baffle spacing in the end zones may differ from the central spacing, especially for U-tube bundles. An end zone correction factor R_s is therefore used.

Then the pressure drop in the two end zones Ap, (kPa) is

$$\Delta p_e = (\Delta p_{bi}) \left(1 + \frac{N_{tcw}}{N_{tcc}} \right) R_b R_s \qquad (6)$$

where Δp_{bi} is calculated in Eq. 3.3.7(10,), R_b is the bypass correction factor from Fig. 3.3.6(11), and R_s is the end zone correction factor as defined in Eq. 3.3.6(39). For all baffle spacings equal, $R_s = 2$.

Finally, the total shell-side pressure drop Ap, (kPa), excluding nozzles or impingement devices, is

$$\Delta p_s = \Delta p_c + \Delta p_w + \Delta p_e \qquad (7)$$

each of the Ap terms having been defined in the text of this section.

© 1983 Hemisphere Publishing Corporation

Nomenclature for Section 3.3.8 appears at the end of Section 3.3.11.

REFERENCES FOR SECTION 3.3.8

1. Bell, K. J., Private communications (1963–1980), and his D. Q. Kern Memorial Award Lecture at the AIChE/ASME Natl. Heat Transfer Conf., San Diego, Calif., 1979 (unpublished).
2. Bell, K. J., Final Report of the Cooperative Research Program on Shell-and-Tube Heat Exchangers, *University of Delaware Eng. Exp. Sta. Bull, 5,* 1963

© 1983 Hemisphere Publishing Corporation

3.3.9

Performance evaluation of a geometrically specified exchanger

J. Taborek

■ Under performance evaluation we understand that a heat exchanger and the process conditions are fully specified. The primary questions posed to the analyst are typically as follows.

1. Does the given heat exchanger perform the heat duty required, $\dot{Q}_{req}$?
2. Does the actual heat duty $\dot{Q}_{act}$ differ from $\dot{Q}_{req}$? Is the design on the safe or unsafe side, and how can this be interpreted?
3. Is the design efficient in terms of ideal versus actual heat transfer coefficients, utilizing the available pressure drop, temperature driving force, and their combined effects?
4. Are the basic layout and construction elements well chosen?
5. How will the exchanger perform on startup (no fouling) versus fouled conditions?
6. Are the pressure drops within acceptable limits?
7. Are there any suggestions to improve or investigate an alternative design (if the exchanger is in a design stage)? If calculated performance differs substantially from the required conditions, this item becomes of utmost importance.

To demonstrate the performance evaluation procedure we shall follow an example case.

A. Basic evaluation criteria

The actual heat duty produced by an air exchanger, $\dot{Q}_{act}$ (W), is referred to tube outside surface, designated by the subscript o:

$$\dot{Q}_{act} = A_o U_o (\Delta T_{LM}) F = A_o U_o \Delta T_m \quad (1)$$

where A_o (m^2) = the heat-transferring tubular surface of the exchanger based on outside tube surface

U_o (W/m^2 K) = the overall heat transfer coefficient based on A_o

$\Delta T_m = (\Delta T_{LM})F$ = the effective mean temperature difference (or driving force) based on the fluid s temperatures and flow arrangement

Refer to the Nomenclature for all other items.

The heat duty required by the process specifications is $\dot{Q}_{req}$:

$$\dot{Q}_{req} = \dot{M}_s c_{p,s} |T_{si} - T_{so}| = M_t c_{p,t} |T_{ti} - T_{to}| \quad (2)$$

or, for isothermally condensing vapors,

$$\dot{Q}_{req} = \dot{M}\, \text{Ah} \quad (3)$$

$\dot{Q}_{req}$ can be based on the shell side or the tube side.

Only in a perfectly designed exchanger does $\dot{Q}_{act} = \dot{Q}_{req}$. In general, there is an inherent inequality between $\dot{Q}_{act}$ and $\dot{Q}_{req}$, as $\dot{Q}_{req}$ is specified by the process to be performed and $\dot{Q}_{act}$ is the actual performance of the exchanger. This inequality has to be reconciled, which is the very function of heat exchanger performance evaluation. For this purpose we write Eq. (1) in terms of resistances and compare it to Q_{req}:

$$\dot{Q}_{act} = A_o \Delta T_m \frac{1}{(\Sigma R)_o} \neq \dot{Q}_{req} \quad (4)$$

$(\Sigma R)_o$ is the sum of all resistances referred to the base surface A_o:

© 1983 Hemisphere Publishing Corporation

HEDH

$$(\Sigma R)_o = \frac{1}{\alpha_s} + \frac{1}{\alpha_t}\left(\frac{A_o}{A_i}\right) + R_{f,o} + R_{f,i}\left(\frac{A_o}{A_i}\right) + R_w \quad (5)$$

where α_s, α_t are the heat transfer coefficients, R_f is the fouling resistance on the outside or inside of the tube, and R_w is the tube wall resistance,

$$R_w = \frac{L_{tw} \times 10^{-3}}{\lambda_{tw}} \quad (\mathrm{W/m^2\ K})^{-1} \quad (6)$$

This term neglects the recalculation to the outside tube area, as it is usually insignificant for plain tubes. For correct solution, see Sec. 3.3.1.

The inequality in Eq. (4) can be restored by adjusting either or any of the three factors involved, namely, $(\Sigma R)_o, A_o$, or ΔT_m. This is the very process of heat exchanger performance evaluation and is described and commented on in the following.

(a) Differential resistance term $R_{d,o}$

Adding a differential resistance term $R_{d,o}$ to $(\Sigma R)_o$ in Eq. (4), we restore the heat transfer balance by redefining Eq. (4) as follows:

$$Q_{act} = Q_{req} = A_o\, \Delta T_m \frac{1}{(\Sigma R)_o \pm R_{d,o}} \quad (7)$$

Knowing all the values, we can determine the differential resistance $R_{d,o}$ as

$$R_{d,o} = \frac{A_o\, \Delta T_m}{Q_{req}} - (\Sigma R)_o \quad (8)$$

The minus sign implies that $\dot{Q}_{act} > \dot{Q}_{req}$; that is, there is a spare resistance $R_{d,o}$. A negative value of $R_{d,o}$ would indicate that the exchanger is underdesigned.

The resistance $R_{d,o}$ can then be applied to any of the resistances in Eq. (5). Especially useful are the following:

1. The fouling resistances $R_{f,o}$ and/or $R_{f,i}$ can be adjusted to show how much the assumed resistances can be increased (or decreased) to balance $\dot{Q}_{act}$. This procedure is especially useful if the primary calculation of $\dot{Q}_{act}$ is based on clean conditions, $R_{f,o} + R_{f,i} = 0$, and the question is what fouling resistance can be tolerated. Conversely, an exchanger designed for high fouling resistances will have a substantial overdesign under clean startup conditions, and the question is what the performance will be under clean conditions.

2. The differential resistance can be combined with the film resistance $1/\alpha_s$ or $1/\alpha_t$. This will indicate how much safety (or lack of it) is in these values. For example, if $R_{d,o}$ is calculated to be 0.000 35 ($\mathrm{m^2}$ K/W) and α_t is 1 136 ($\mathrm{W/m^2}$ K), adding $R_{d,o}$ to $1/\alpha_t$ shows that α_t can be as low as 8 12 and still produce Q_{req}.

(b) Adjustment of surface A_o

The inequality of Eq. (4) can be restored by a surface area factor, expressing the heat transfer area actually required $(A_o)_{req}$ as

$$(A_o)_{req} = \left(\frac{\dot{Q}_{req}}{\dot{Q}_{act}}\right) A_o$$

The term in parentheses is the overdesign or safety factor if <1.0, or underdesign if the term is >1.0.

(c) Adjustment of temperature difference ΔT_m

The third way to restore the heat balance of Eq. (4) is through the actual outlet temperatures of both streams, T_{so} and T_{to}. These, in turn, will affect ΔT_{LM}, F, and Q_{req}, Eq. (2). An overdesigned exchanger will produce larger temperature ranges of both streams, but this will be balanced by the simultaneously decreased ΔT_{LM} and possibly decreased correction factor F. This type of rating is often termed the unknown heat balance and requires trial-and-error calculations.

For cases with substantial fouling resistances, it may often be useful to evaluate the outlet temperatures under clean conditions, as downstream operations can be affected.

B. Performance evaluation procedure

A typical process of evaluating the performance of a fully specified exchanger will be demonstrated.

(a) General description of problem

A light oil is to be heated, flowing on the shell side, from 89.8 to 147.3°C. The heat medium is isothermal steam in two tube passes, fixed tubesheet exchangers (FX) at 178° C. The steam coefficient α_t is specified as 6 000 $\mathrm{W/m^2}$ K. This value is considered conservative, allowing for some corrosion or fouling resistance. Tube-side pressure drop is of no importance.

The shell-side fluid is assumed with no fouling, and the results of the evaluation should indicate how much shell-side fouling could be tolerated. Shell-side pressure drop should be below 25 kPa, nozzle-to-nozzle.

Note: The example is based on data from a test exchanger. Various geometry-related values have actually been measured and will differ slightly from the estimation procedures.

(b) Data input

Data input is given in Table 1. The geometry and process conditions are specified according to the items in Sec. 3.3.5. Refer to explanations for each item, if necessary.

© 1983 Hemisphere Publishing Corporation

Table 1 Data input

Item	Symbol	Value	Item	Symbol	Value
1	D_s	591 mm	13a	L_{bi}	263 mm
2	D_t	16 mm	13b	L_{bo}	263 mm
3	L_{tw}	1.24 m m	14	CN	None
4	D_{ti}	13.52 mm	15	N_{tt}	652
5	λ_{tw}	42 W/m K	16	N_{tp}	2
6	L_{tp}	20.8 mm	17	N_{ss}	0
7	θ_{tp}	30	18	CB	FX
8	Not required		19	L_{tb}	0.5 mm
9,10	$L_{ti} = L_{ta}$	2 276 m m	20	L_{sb}	5.5 mm
11	B_c	24%	21	L_{bb}	10 mm
12	L_{bc}	250 mm			
		Temperatures			
22	T_{si}	89.8°C	24	T_{ti}	178° C
23	T_{so}	147.3°C	25	T_{to}	178° C

Item	Symbol	Value	Special information
		Shell-side process information	
26	$\dot{M}_s$	22.4 kg/s	38 α_s = 1 000 W/m² K estimated only for purposes of tube wall temperature correction factor
27	ρ_s	740 kg/m³	
28	λ_s	0.105 W/m K	
29	$(c_p)_s$	2 407 J/kg K	
30	η_s	Specified at two temperatures	39 α_t = 6 000 W/m² K fixed estimation, not to be calculated
	$(\eta_s)_1$ at	90° C = 0.6cP	
	$(\eta_s)_2$ at	190° C = 0.3cP	
31	$(R_f)_O$	0	40-43 Do not apply
		Tube-side process information	
32-36			Not required in this case
37	$R_{f,i}$	0	

(c) Evaluation of critical items in data input

Item 6: L_{tp}, tube pitch. Check for tube pitch ratio, L_{tp}/D_t = 1.30; very close to recommended practice.

Item 7: $\theta_{tp} = 30°$, good selection in turbulent flow, no external cleaning required.

Item 11: B_c = 24%. Check for compatibility with baffle spacing, Fig. 3.3.5(4). L_{bc}/D_s = 250/591 = 0.42. Very efficient range.

Items 12, 13: Baffle spacing: Check against maximum unsupported length, Fig. 3.3.5(6). Well within acceptable values.

Item 15: N_{tt} = total number of tubes. A check against the estimating procedure requires the value of D_{ctl} from Eq. 3.3.5(21): D_{ctl} = 591 − (10 + 16) = 565; then, from Eq. 3.3.5(17),

$$N_{tt} = \frac{0.78(565)^2}{(0.866)(20.8)^2}(1 - 0.04) = 638$$

A very good check against 652 specified (4%).

Item 19: L_{tb} = 0.5 mm; slightly higher than recommended, but within acceptable range, Fig. 3.3.5(12).

Item 20: L_{sb} = 5.5 mm; exactly in the recommended range of TEMA value + 1.5 mm allowance, Fig. 3.3.5(13).

Item 21: L_{bb} = 10 mm; this value of bundle-to-shell clearance is lower than the estimated one from Fig. 3.3.5(14), which is -1.5 mm. However, this bundle was designed especially to tight tolerances, explaining the estimation difference.

(d) Calculation of basic parameters

Proceed with calculations as outlined in Sec. 3.3.5C.

Step 1: Calculate the cross-flow area S_m (mm*). At baffle spacing L_{bc} and using explanations to Eq. 3.3.5(22),

$$S_m = 250\left[10 + \frac{565}{20.8}(20.8 - 16)\right] = 35\ 096\ \text{mm}^2$$

Step 2: Calculate average temperatures $T_{s,av}, T_{t,av}$, Eq. 3.3.5(23).

$T_{s,av}$ = $189.8 + 147.31 = 118.6°C

$T_{t,av}$ = isothermal = 178° C

Step 3: Calculate shell-side Reynolds number Re_s, Eq. 3.3.5(25).

$$\dot{m}_s = \frac{22.4}{35\ 096} \times 10^6 = 638\ \text{kg/m}^2\ \text{s} \quad \text{from Eq. 3.3.5(24)}$$

To determine shell-side fluid viscosity, refer to data input. If viscosity is given at two temperatures, apply procedures given in Eq. 3.3.7(8), with average shell-side temperature defined in Eq. 3.3.5(23). For our example case, $(\eta_s)_1$ and $(\eta_s)_2$ are given. Employing the suggested averaging procedures, we get $\eta_{s,av}$ = 0.494 cP. Then

$$Re_s = \frac{16(638)}{0.494} = 20\ 695$$

The shell-side flow is solidly in the turbulent region.

Step 4: Calculate shell-side Prandtl number Pr_s. Refer to Eq. 3.3.5(26).

$$Pr_S = \frac{(2\ 407)(0.494\ 3)}{0.105} \times 10^{-3} = 11^{29}$$

Step 5: Calculate mean temperature difference AT,, Eq. 3.3.5(29). The terminal temperature differences are

ΔT_1 = 178 − 89.8 = 88.2°C

ΔT_2 = 178 − 147.3 = 30.7°C

The log mean temperature difference is

© 1983 Hemisphere I blishing Corporation

$$\Delta T_{LM} = \frac{88.2 - 30.7}{\ln(88.2/30.7)} = 54.5°C$$

There are two tube passes, but the tube-side fluid is an isothermal steam; therefore $F = 1.0$, and

$$\Delta T, = \Delta T_{LM} = 54.5°C$$

Step 6: Calculate effective tube length. For fixed tubesheet construction, L_{ta} applies for area calculation.

$L_{ta} = 2\ 276$ mm

Step 7: Calculate total heat transfer area A_o (m^2). From Eq. 3.3.5(30),

$A_o = \pi(16)(2\ 276)(652)(10^{-6}) = 74.6\ m^2$

(e) Auxiliary calculations

Follow procedures as outlined in Sec. 3.3.6.

Step A: Segmental baffle window, Eqs. 3.3.6(1) and 3.3.6(2).

$$\theta_{ds} = 2\cos^{-1}\left[1 - 2\left(\frac{24}{100}\right)\right] = 117.3°$$

$$\theta_{ctl} = 2\cos^{-1}\left\{\frac{591}{565}\left[1 - 2\left(\frac{24}{100}\right)\right]\right\} = 114°$$

Step B: Baffle window flow areas. Obtain gross window area S_{wg} from Fig. 3.3.6(2) or Eq. 3.3.6(4).

$$S_{wg} = \frac{\pi}{4}(591)^2\left[\frac{117.3}{360} - \frac{\sin(117.3)}{2\pi}\right] = 50\ 620\ mm^2$$

Calculate the fraction of tubes in window and cross flow, F_w and F_c, Eqs. 3.3.6(5) and 3.3.6(6).

$$F_w = \frac{114}{360} - \frac{\sin(114)}{2\pi} = 0.172$$

$F_c = 1 - 2F_w = 0.657$

Calculate window area occupied by tubes, S_{wt}, Eq. 3.3.6(7) or Fig. 3.3.6(3) with N_{tw} from Eq. 3.3.6(8).

$N_{tw} = (652)(0.172) = 112$

$$S_{wt} = (112)\left[\frac{\pi}{4}(16^2) - 1\right] = 22\ 503\ mm^2$$

$S_w = S_{wg} - S_{wt} = 28\ 117\ mm^2$

Step C: Hydraulic baffle window diameter D_w. Flow is turbulent, so this item does not apply.

Step D: Number of effective tube rows in cross flow, N_{tcc} and N_{tcw}. From Table 3.3.5(10), L_{pp} = 0.866(20.8) = 18.01 mm. Then

$N_{tcc} = 17.06$ from Eq. 3.3.6(11)

$N_{tcw} = 5.7$ from Eq. 3.3.6(13)

Step E: Number of baffles N_b. From Fig. 3.3.6(7), $N_b = 8$. Otherwise, from Eq. 3.3.6(14),

$$N_b = \frac{2\ 276}{250} - 1 = 8.1 \quad \text{rounded off to } 8$$

Step F: Bundle-to-shell bypass parameters S_b and F_{sbp}. Because of the piping arrangement, the tube pass partition is located in the cross-flow direction, that is, perpendicular to the baffle cut. The dimension L_p from Fig. 3.3.6(1) is L_p = 12.7 mm from drawings. Otherwise use Eq. 3.3.6(15) and $L_{pl} = 6.35$ mm, $D_{otl} = 581$ [Eq. 3.3.5(20*a*)], and S_b from Eq. 3.3.6(15) is

$S_b = 250[(591 - 581) + 6.35] = 4\ 088\ mm^2$

Using S_m from step 1 and Eq. 3.3.6(16),

$$F_{sbp} = \frac{4\ 088}{35\ 096} = 0.116$$

Step G: Leakage area S_{sb}. The shell-to-baffle leakage area S_{sb} from Fig. 3.3.6(5) or from Eq. 3.3.6(17), with L_{sb} from data item 20 or estimated from Fig. 3.3.5(13), $L_{sb} = 5.5$ mm is

$S_{sb} = 3\ 442\ mm^2$

Step H: Tube-to-baffle hole leakage area S_{tb}. S_{tb} is based on L_{tb} from data item 19 or estimated from Fig. 3.3.5(12); L_{tb} = 0.5 mm. Use Fig. 3.3.6(6) for $(S_{tb})_1$ and Eq. 3.3.6(19) or Eq. 3.3.6(18).

$S_{tb} = 6\ 893\ mm^2$

Step I: Baffle window correction J_c. Use Fig. 3.3.6(7) or Eq. 3.3.6(20), with F_c from Eq. 3.3.6(6).

$J_c = 1.02$

Step J: Baffle leakage correction factors J_l and R_l. Calculate auxiliary parameters r_{lm} and r_s from Eqs. 3.3.6(21) and 3.3.6(22) with S_m from step 1 and S_{sb} and S_{tb} from steps G and H.

$r_{lm} = 0.294$ $r_s = 0.333$

To determine J_l and R_l, refer to Figs. 3.3.6(8) and 3.3.6(9). Inspection of the location of J_l and R_l on the figures gives the designer a better feel for the problem. Only with computer programs use Eqs. 3.3.6(23*a*) and 3.3.6(23*b*).

$J_l = 0.665$ $R_l = 0.427$

Both values appear to be within an acceptable range.

Step K: Bypass correction factors J_b and R_b. There are no sealing strips. N_{tcc} was calculated in step D; $r_{ss} = 0$. F_{sbp} = 0.116 from step F. Lookup of Figs. 3.3.6(10) and 3.3.6(11) yields J_b = 0.865 and R_b = 0.65. The values and their locations in the figures appear to be sound.

Step L: Laminar flow correction factor J_r, Fig.

© 1983 Hemisphere Publishing Corporation

3.3.6(12). Not required for this case, flow is turbulent, Re, ⩾ 100.

Step M: Unequal end baffle spacing correction factor for heat transfer, J_s. The end baffle spacings are very close to the dimension of the central spacing L_{bc}, only 5% difference. Inspection of Fig. 3.3.6(13) shows that $J_s = 1.0$.

Step N: Unequal end baffle spacing correction factor for pressure drop, R_s. Similar comments as for Step N apply. Actual calculation yields $R_s = 1.82$ as compared to $R_s = 2.0$ for equal spacing. Within overall accuracy of this method, consider $R_s = 2.0$, which is on the safe side.

This completes the auxiliary calculations based on Sec. 3.3.6.

(f) Shell-side heat transfer coefficient α_s and pressure drop Δp_s

Item 1: Determination of ideal tube bank j_i and f_i factors. Refer to Sec. 3.3.7 for details. Using the shell-side Reynolds number Re, = 20 659, step 3 in Sec. 3.3.9B(d), and pitch ratio L_{tp}/D_t = 1.3, determine j_i and f_i from Fig. 3.3.7(1)-3.3.7(3) or, for computer calculations, from Eqs. 3.3.7(1) and 3.3.7(2). For our example, $j_i = 0.006\ 8$; $f_i = 0.11$.

Item 2: Viscosity correction Φ_s. To determine the ideal tube bank α_i and Δp_i, we need to establish the viscosity correction factor Φ_s. The shell fluid viscosity is given in the data by two points. We estimate the wall temperature from Eq. 3.3.7(7), using α_t = 6 000 W/m² K as given in the data and estimate the shell-side $\alpha_s \approx 1\,000$ W/m² K from tables such as given in Sec. 3.1 and also in the data input,

$$T_w = 178 + \left(\frac{118.6 - 178}{1 + 6\,000/1\,\mathrm{OOC}}\right) = 169^\circ\mathrm{C}$$

This is in agreement with the comment in Sec. 3.3.7 that the wall temperature will be closer to that of the fluid with higher α. The subsequent procedures such as Eq. 3.3.7(8) estimate the viscosity at 169°C as $\eta_{s,w} \approx 0.405$. According to Eq. 3.3.7(5),

$$\Phi_s = \frac{0.494}{0.405} = 1.22$$

This will result (raised to the 0.14 or -0.14 power, respectively) in rather weak correction, ≈3%, as can be expected for a light viscosity oil. Preliminary engineering judgment can often eliminate the need for Φ_s calculations for fluids with small viscosity variations.

Item 3: Determine α_i and α_s. The ideal tube bank heat transfer coefficient α_i is calculated from Eq. 3.3.7(4) as

$$\alpha_i = j_i c_{p,s} \dot{m}_s (\mathrm{Pr})_s^{-2/3} (\Phi_s)^{0.14}$$

$$= (0.006\ 8)(2406)(638)(11.29)^{-2/3} \cdot (1.22)^{0.14} = 2\ 134\ \mathrm{W/m^2\ K}$$

The shell-side heat transfer coefficient α_s is calculated from Eq. 3.3.8(1) with the correction factors J_c, J_l, J_b, J_r, and J_s, determined in steps I through M (J_r and $J_s = 1.0$).

$$\alpha_s = \alpha_i J_c J_l J_b$$

$$= 2\,134(1.02)(0.665)(0.865) = 1\,252\ \mathrm{W/m^2\ K}$$

This compares to 1 335 measured value, or about 7% on the safe side. This level of accuracy is not quite typical (see comments in Sec. 3.3.3), but within the possible range for well-designed units and average-property fluids. The product of all correction factors, $J_{tot} = 0.59$, serves as comparison against the ideal tube bank α_i. The value of around 0.6 is quite typical for well-designed exchangers, but lower values may be encountered, especially in laminar flow.

Item 4: Determine shell-side pressure drop Δp_s. Using Eq. 3.3.7(10) with N_{tcc} from step B(e, d), $\dot{m}_s$ from step B(d) and Φ_s from item B(f, 2), we get for the ideal tube bank-based single cross-flow pass Δp_{bi}:

$$\Delta p_{bi} = 2(10^{-3}) f_i (N_{tcc}) \frac{(\dot{m}_s)^2}{\rho_s} (\Phi_s)^{-0.14}$$

$$= \frac{2}{1\,000}(0.11)(17.06)\frac{(638)^2}{740}(1.22)^{-0.14} = 2.0\ \mathrm{kPa}$$

The shell-side cross-flow pressure drop between baffle tips is calculated from Eq. 3.3.8(2):

$$\Delta p_c = \Delta p_{bi} (N_b - 1) R_b R_l$$

$$= 2.0(7)(0.65)(0.427) = 3.9\ \mathrm{kPa}$$

For the baffle window Δp_w, we need to determine the window mass flow velocity $\dot{m}_w$ from Eq. 3.3.8(3).

$$\dot{m}_w = \frac{M_s}{\sqrt{S_m S_w}} \times 10^6$$

where $\dot{M}_s$ is from the data, S_m is from step B(d,1), and S_w is from step B(e):

$$\dot{m}_w = \frac{22.4 \times 10^6}{\sqrt{(35096)(28\ 117)}} = 713\ \mathrm{kg/m^2\ s}$$

The flow is turbulent, so we use Eq. 3.3.8(4):

$$\Delta p_w = N_b(2 + 0.6N_{tcw}) \frac{(\dot{m}_w)^2}{2\rho_s} \times 10^{-3} R_l$$

$$= 8\,[2 + 0.6(5.7)]\frac{(713)^2}{2(740)} \times 10^{-3} (0.427) = 6.4\ \mathrm{kPa}$$

The pressure drop in the inlet and outlet baffles is calculated from Eq. 3.3.8(6). The unequal baffle spacing correction R_s will be considered equal to 2.0,

© 1983 Hemisphere Publishing Corporation

as the difference between L_{bc} and the end spacings is negligible. Thus:

$$\Delta p_e = \Delta p_{bi}\left(1 + \frac{N_{tcw}}{N_{tcc}}\right)R_b R_s$$

$$= 2.0\left(1 + \frac{5.7}{17.06}\right)(0.65)(2) = 3.4 \text{ kPa}$$

Finally, the total shell-side pressure drop, excluding nozzles, is, from Eq. 3.3.8(7),

Ap, = Ap, + Ap, + Ap, = 3.9 + 6.4 + 3.4 = 13.7 kPa

The measured Ap, for this case was 12.5 kPa. Again, this level of accuracy is not typical. See comments in Sec. 3.3.3. Notice the relatively large Δp_e, which is due to the flow recombination and consequently $R_l = 1$ .O. The end-zone pressure drop amounts to about 25% of the total.

C. Overall heat exchanger performance evaluation

We shall now use the calculated values of the example case to perform the overall evaluation, as discussed in Sec. A.

First we calculate the heat transferred, $\dot{Q}_{\text{act}}$ (W) from Eq. (1). The summation of all resistances, Eq. (5), is

$$(\Sigma R)_o = \frac{1}{\alpha_s} + \frac{1}{\alpha_t}\left(\frac{A_o}{A_i}\right) + R_w \quad (\text{m}^2\text{ K/W}) \tag{9}$$

$$\frac{A_o}{A_i} = \frac{\pi D_t}{\pi(D_t - 2L_{tw})} = \frac{16}{16 - 2(1.24)} = 1.18 \tag{10}$$

$$R_w = \frac{L_{tw}}{\lambda_{tw}} \times 10^{-3}$$

$$= \frac{1.24}{42} \times 10^{-3} = 0.000\ 03 \text{ m}^2\text{ K/W} \tag{11}$$

$$(\Sigma R)_o = \frac{1}{1\ 252} + \frac{1.18}{6\ 000} + 0.000\ 03$$

$$= 0.000\ 790 + 0.000\ 197 + 0.000\ 03$$

$$= 0.001\ 03 \text{ Km}^2/\text{W}$$

The clean overall coefficient is then

$$U_o = \frac{1}{(\Sigma R)_o} = 971 \text{ W/m}^2\text{ K}$$

From $(\Sigma R)_o$ we can calculate that the distribution of the resistances is approximately 78% shell side, 19% tube side, and 3% tube wall, quite typical for such cases. The high shell-side resistance, combined with the low tube-side resistance, may suggest investigating the use of fin tubes as an alternative.

The heat duty (without fouling), $\dot{Q}_{\text{act}}$, is

$$\dot{Q}_{\text{act}} = A_o U_o \Delta T_{LM}(F) = (74.6)(971)(54.5)(1)$$

$$= 3\ 947\ 794 \text{ W or } 3\ 978 \text{ kW} \tag{12}$$

Next we calculate the heat duty required from process specifications (shell side), Eq. (2),

$$\dot{Q}_{\text{req}} = \dot{M}_s C_{p,s}|T_{si} - T_{so}|$$

$$= (22.4)(2407)|89.9 - 147.31 = 3\ 100\ 216 \text{ W} \tag{13}$$

The inequality of $\dot{Q}_{\text{act}}$ versus $\dot{Q}_{\text{req}}$ will be now reconciled by the methods outlined in Sec. A. The differential resistance $R_{d,o}$ can be calculated from Eq. (8) as

$$R_{do} = \frac{(74.6)(54.5)}{3\ 100\ 216} - 0.001\ 03 = 0.000\ 28 \text{ m}^2\text{ K/W} \tag{14}$$

This indicates that the exchanger has a safety factor in heat transfer performance that can be now interpreted in the ways outlined in Sec. A.

1. The first interpretation of this result is that, for example, a shell-side fouling resistance $R_{f,o} = 0.000\ 28$ K m^2/W could exist and the exchanger would still perform the duty $\dot{Q}_{\text{req}}$. This is a good practical precaution, as no fouling resistances were assumed in the specifications. Second, as the actual $\Sigma R_o = 0.001\ 03 + 0.000\ 28 = 0.001\ 31$, the overall coefficient could be only 763 W/m^2 K rather than 971 as calculated.

2. The heat transfer surface safety factor from Eq. (8) is

$$A_{o,\text{req}} = \frac{3\ 100\ 216}{3\ 947\ 794}(A_o) = 0.79A_o \tag{15}$$

that is, only 79% of the available area is used under clean conditions.

3. Adjustment of the temperature profile is a more difficult calculation. As the hot stream is isothermal and considering the cold stream entry temperature as constant, we can increase the shell stream outlet temperature. This will increase $\dot{Q}_{\text{req}}$, but decrease $\dot{Q}_{\text{act}}$ due to lowering of the ΔT_m. Effect of the changed temperature on physical properties is neglected. A first guess, that the actual shell outlet temperature T_{so} = 155° C instead of the specified 147.3°C (about 25% increase of the difference) produces a result that is within a few percent accuracy, decreasing ΔT_m to 48°C. The heat duty under these conditions is approximately 3 480 kW. This would be the performance under initial, no-fouling conditions.

Nomenclature for Section 3.3.9 appears at the end of Section 3.3.11.

© 1983 Hemisphere Publishing Corporation

3.3.10

Design procedures for segmentally baffled heat exchangers

J. Taborek

■ The process of actually designing shell-and-tube heat exchangers, from problem specifications to final product, has never before been analyzed in the literature [1] . It differs from performance evaluation or rating calculations in the following main ways:

1. The process conditions are fully specified, just as for rating cases, but limits are usually imposed on maximum allowable pressure drop and/or flow velocities, both shell side and tube side.

2. As a consequence of (1), a geometric configuration must be found that will respect these limits while performing the desired heat duty most economically. This implies the combination of initial cost, operating and maintenance cost, ease of cleaning, and potentially a number of other conditions, such as startup, safety from fluid mixing in case of mechanical failures, tube vibration, and many others.

3. It is then up to the exchanger designer (a) to select the basic construction elements such as shell type, tube size and layout, baffle type and baffle geometry, number of tube passes, etc., and (b) to find the ultimate design dimensions of shell diameter and tube length that will result in complete thermohydraulic exchanger specification.

4. The final step of converting the thermohydraulic solution into manufacturing specifications involves calculation of mechanical elements such as tubesheets, flanges, etc., compliance with various codes, and is to a large extent treated in Part 4 of this handbook.

These preliminary comments suggest that, given a minimum of restrictions, a large number of potential solutions is possible-but only a few will be truly eligible, and ultimately only one will emerge as best overall. However, frequently contradictory demands will often have to be reconciled, and several acceptable solutions may have to be considered with respect to more subtle requirements, such as standardization for replacement parts, potential construction limitations, and so on. To perform all these chores effectively is the art of heat exchanger design.

A. Computer versus manual calculations

Large numbers of heat exchangers are designed today by computer programs of grossly varying quality and sophistication. However, the heat exchanger designer must understand the art of the design process, whether it is performed by a computer or by a manual method. Actually, the condition for success in either case is identical and lies in the following:

1. Proper preliminary problem analysis, selection of design parameters, and identification of important items
2. Interpretation of results as to potential variation of design parameters and ultimate selection of the best design

Thus, the design problem is really reduced to a series of rating or *performance evaluation cases, as discussed in Sec. 3.3.9. The analyst in possession of a good computer program has the advantage of speed, but the disadvantage that input errors may pass undetected and results may be accepted without sufficient scrutiny. The analyst using manual methods has the advantage of direct engineering interpretation and a feel for the problem. By virtue of this closeness to the design, he or

© 1983 Hemisphere I :blishing Corporation

she often can minimize the computational speed handicap.

The unbeatable team is, of course, an analyst with sufficient feel for the tine points of design, who has access to a good computer program and thus can devote time to evaluation of results rather than tedious calculations. The basic problems of exchanger design, regardless of the method used, are discussed in this section.

B. Preliminary design considerations

The success of the design process is conditioned on a number of initial analysis steps, through which the main design features and some specific and/or alternative construction elements are established. All the following steps are necessary, regardless of whether a computer program or manual calculation is used.

(a) Initial problem review

Analyze the problem as specified and single out any items that may influence the selection of construction elements and other design considerations. These will typically include fouling resistances and cleaning, allowable pressure drop (especially if one is very low), a temperature profile (need for pure counter flow or multiple units in series), and possibly other items.

(b) Fluid allocation: shell side or tube side

One of the primary decisions to be made is which fluid should be placed on the shell side and the tube side. Since this decision may affect many other considerations, it should be made first. Some of the factors influencing this selection are given below.

Fluid pressure. Unless overruled by other serious considerations, high-pressure fluid (>1 000 kPa) is placed on the tube side to obtain the most economic design.

Corrosion. Since corrosion-resistant materials are invariably expensive, the corrosive fluid is preferably placed inside the tubes.

Fouling and cleaning. In many cases fouling is an inescapable consequence of the heat transfer process. It may significantly influence the exchanger design. Although the understanding of fouling in its various forms is still limited, some trends in design parameters are identifiable. Flow velocity should be kept high, as it will suppress all types of fouling. If the fouling fluid is on the shell side, the baffle design must be such as to avoid stagnant regions, that is, a well-proportioned baffle spacing/cut ratio, multisegmental baffles, or no-tubes-in-window construction. Polymerization fouling is particularly sensitive to tube wall temperature, and may increase rapidly above a certain critical temperature.

Fluid with a high tendency to fouling is preferably placed on the tube side for greater ease of cleaning; however, if chemical cleaning can be used, there is no preference between tube or shell side. For mechanical cleaning, straight tubes in a horizontal orientation are preferred. For hydraulic cleaning on the shell side, a large tube pitch must be used, which usually increases the shell size. Finned tubes should be used with caution if sludge-type fouling is anticipated on the shell side.

Fluid viscosity. As a general rule, the high-viscosity fluid should be placed on the shell side, as the induced turbulence by the flow across the tube bundle will promote higher heat transfer. However, if the flow is laminar when placed on the shell side, a switch to the tube side should be considered.

Pressure drop utilization. Different criteria influence the utilization of pressure drop on the tube side and the shell side. Tube-side velocity can be adjusted only by the number of tube passes, provided that tube diameter and tube length are considered constant. Increasing the number of tube passes from one to N increases (for the same number of tubes) the pressure drop by a factor of approximately N^3. This is usually a large step, and indicates that fine tuning of tube-side Ap utilization may be difficult and may require variations of tube length and tube diameter. On the shell side, the designer has more parameters to work with than on the tube side, namely, shell type, baffle spacing, baffle type, tube layout, and tube pitch. The possible combinations of the various parameters are numerous and require careful analysis of intermediate results.

The decision as to which fluid should be placed on the tube side or the shell side can often be made on the basis of the most effective use of the available pressure drop for the transfer of heat. Tube-side flow is generally more effective, as inherently the heat transfer-producing fluid shear occurs close to the tube wall, where effective ΔT driving force is available. Shell-side flow is generally less effective, as most of the pressure drop occurs in the eddy currents between the tubes, where temperature driving force is not present.

However, the following constraints may control the allocation of the fluid to one side or the other:

If the constraint is low maximum pressure drop for fluid with controlling heat transfer resistance, the best design will usually put that fluid on the tube side. The exception may be if tube-side flow would result in laminar flow whereas shell-side flow would be turbulent. Externally finned tubes should also be considered.

For high maximum pressure drop, tube-side flow will again be generally preferable. Design geometry restrictions such as maximum practical number of tube passes and minimum baffle spacing may, however, be the determining factors.

© 1983 Hemisphere Publishing Corporation

If the constraint is maximum heat transfer to controlling fluid with pressure drop inconsequential, the best design will generally put that fluid on the shell side, respecting again design geometry restrictions and the possible danger of tube vibration.

If the constraint is maximum pressure drop for non-controlling heat transfer resistance fluid, either fluid may be put on either side to produce the best design. Such cases should be investigated carefully.

(c) Temperature profile analysis

Temperature profile analysis should be performed at an early stage, as it may influence selection of basic construction parameters, such as straight counter flow or the need for multiple units in series. It is useful to make a temperature profile sketch (see Sec. 1.5) and calculate ΔT_{lm} and check the F correction factor to get a feel for possible problems in this respect.

(d) Construction elements selection

Refer to Sec. 3.3.5, data input. Although the items in this table describe a fully specified exchanger, in the early design stages some of the items will be, by necessity, ignored, such as the distinction of the inlet and outlet baffle spacings; others will be left floating, to be adjusted during the process of design, such as tube length, shell diameter, baffle spacing, and all the clearances, as they are functions of other, yet-to-be-determined parameters. As a guide, and referring to the general data input, Table 3.3.5(1), a similar Table 1 has been prepared for items initially required for a design case.

C. First size estimation

At this point we are ready to make the first initial estimate of the exchanger size. Proceed as follows:

1. Estimate heat transfer coefficients, α_s and α_t. Using tables such as in Sec. 3.1, estimate α_s and α_t. Use the lower values if allowable, Ap is low, and vice versa.

2. Estimate maximum pressure drop $\Delta p_{s,\max}$, $\Delta p_{t,\max}$. The design of most exchangers is governed by the specified (or assumed) maximum permissible pressure drop, as for all fluids in no-phase-change flow, α increases with Ap. Often, the required pressure drop, rather than the heat transfer, may become the limiting design consideration. However, there is no simple estimation of the probable pressure drop as there is for the heat transfer coefficients. The only resort the designer has is to check if the pressure drop, as specified, falls into a range under which the values of α_s and α_t have been estimated to begin with.

Table 1 Input items required for initial design

Item	Symbol	Description
1	D_s	Shell inside diameter. Subject of design calculations. Possible limit on maximum size.
2-7	Tube spec's.	Tube and tube layout are assumed specified, subject to careful selection. Changes possible in the course of design.
8-10	Tube length	Subject to determination in design process. Fixed values or maximum limitations can be specified.
11-13	Baffle geometry	Assume first equal baffle spacing in the range $L_{bc}/D_s \approx 0.3$ for high Δp_s and 0.6 for lower Δp_s. Subject to change in the course of design. Baffle cut from Fig. 3.3.5(4). Consider $L_{b,\max}$, Fig. 3.3.5(6).
14	CN	Nozzle and impingement protection. For initial trials, consider full tube layout. Subject to final evaluation.
15-21	Tube bundle geometry	Item 18, tube bundle type, must be assumed, based on criteria of operation. All other items in this group are derived from other assumptions and/or are subject to design process.
22-25	Temperatures	Must be specified.
26-31	Shell-side data	(1) If shell-side fluid heat transfer coefficient α_s is specified, such as for isothermal steam heating, omit all items. (2) For cases where α_s and Δp_s are to be calculated, specify all items.
32-37	Tube-side data	Same as for items 26-31.
38-39	α_s, α_t	(1) The heat transfer coefficients α_s or α_t can be specified for certain types of operation, such as steam heating or isothermally boiling liquids. This is acceptable if the specified coefficient constitutes small overall resistance. (2) It is advisable that estimates of the coefficients α_s and α_t be specified for purposes of initial sizing.
40-41	Δp	Specify each, unless the respective heat transfer coefficient α was fixed (items 38-39) and/or there is no interest in Ap.
42	$V_{t,\max}$	The maximum tube-side flow velocity may be specified instead of and/or in addition to item 41. The design should respect such limitation (erosion).
43	$V_{t,\min}$	Specify only to protect design from too low tube-side flow velocities, to suppress fouling.

The reasonable pressure drop allocation is a subject of economics and established rules and practices. Deviations are always possible, but the following guidelines apply:

© 1983 Hemisphere Publishing Corporation

For subatmospheric pressures, use 0.05 to 0.1 of the absolute fluid pressure.

For above-atmospheric liquids, Δp_{max} is proportional to the gauge pressure of the fluid, but consideration must be taken as to the effectiveness of pressure drop conversion to heat transfer (all other items being equal). Reflecting these premises, Fig. 1 shows a band of recommended values of Δp versus gauge pressure of the liquid.

The lower line should be considered for cases where the heat transfer coefficient α is not controlling and it would be therefore economically inefficient to expend higher Δp (operating cost). In some cases, however, a minimum flow velocity must be maintained to depress fouling (maintenance cost). The upper curve should be used as a maximum for cases where α is controlling and therefore decrease of the initial cost is desirable.

Most cases will be somewhere in the middle to lower range of the curves. For example, for cooling water (usually at -350 kPa), a pressure drop is determined as SO-125 kPa. As the water heat transfer resistance is usually not controlling, the low-to-medium values would apply, that is, 50-100 kPa (~7.2- 14.4 psi), which coincides well with established industrial practices. In any case, the soundness of the selected pressure drop should be checked in the design evaluation process (Sec. E).

For gases, often special criteria may exist, as the effectiveness of related process equipment may be a significant economic factor (compressors). If the specified Δp_{max} is substantially different from the suggested values, the estimates of the heat transfer coefficients may be questioned and especially careful attention must be given to both.

3. Estimate overall heat transfer coefficient U_o (W/m^2 K). Using the estimated values of α_s and α_t and the values of fouling resistances from the data input, estimate U_o from Eq. 3.3.9(5) as $1/\Sigma R$. Neglect at this point R_w and A_o/A_i, except for finned tubes.

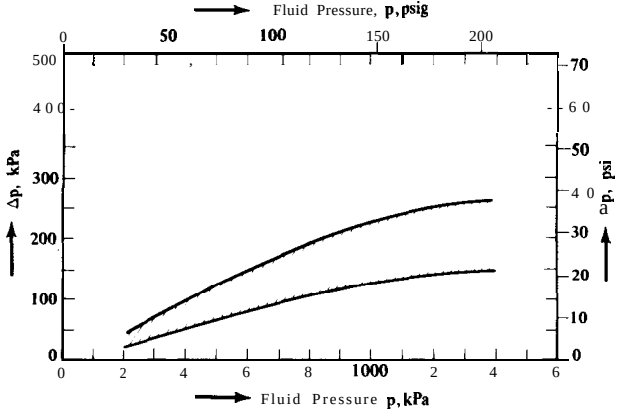

Figure 1 Range of usual pressure drop values for liquids as a function of the gauge pressure of the liquid.

4. Determine the required heat duty $\dot{Q}_{req}$ (W). From the heat balances of the two streams, calculate Q_{req} from Eq. 3.3.9(2), which becomes equal to Q_{act} for calculation purposes at this stage.

5. Estimate the heat transfer area A_o (m^2). At this point of the calculation, we know or have estimated

Mean temperature difference ΔT_m,
Overall heat transfer coefficient U_o,
Heat duty Q_{req} or Q_{act},

Consequently, from the basic heat transfer equation, the tubular (outside) area required, A_o, is calculated as

$$A_o = \frac{Q_{req}}{U_o \, \Delta T_m} \tag{1}$$

The problem now arises, how to interpret the value of A_o in terms of tube length and shell diameter, both values being still open at this point. From Eq. 3.3.5(30), the outside tube area A_o is

$$A_o = \pi D_t L_{ta} N_{tt} \times 10^{-6} \quad \text{m}^2 \tag{2}$$

and from Eq. 3.3.5(16), for estimation purposes using $(N_{tt})_1$, the tube count is

$$N_{tt} = (N_{tt})_1 = \frac{0.78}{C_1 (L_{tp})^2} \, (D_{ctl})^2 \tag{3}$$

Substituting now Eq. (3) into Eq. (2) and combining logical terms, we get

$$A_o = [10^{-6} \times \pi(0.78)] \, \frac{D_t}{C_1 (L_{tp})^2} \, [L_{ta}(D_{ctl})^2] \tag{4}$$

The first term in brackets is a pure constant; the second term reflects the tube size and tube layout geometry; the third term includes the values of tube length and shell diameter, which are the items to be determined.

Any desired heat transfer surface A_o can be obtained by various combinations of the parameters L_{ta} and D_{ctl}, for any given tube layout [the second term in Eq. (4)].

Defining a value of the tube layout density parameter as A^* (l/mm),

$$A^* = 0.78\pi \left(\frac{1}{C_1}\right) \frac{D_t}{(L_{tp})^2} \tag{5}$$

the values of A^*, for D_t = 6-50 mm and L_{tp} = 1.2-1.5, range between the extremes of 0.02 and 0.25. This is an expression of how much heat transfer surface can be packed within a given area, therefore the term tube layout density.

Thus, Eq. (4) contracts to

$$A_o = (10^{-6}) \, A^* [L_{ta}(D_{ctl})^2] \quad (\text{m}^2) \tag{6}$$

To translate the value of D_{ctl}, the tube bundle-circumscribed diameter, into terms of the inside shell diameter proper, D_s, we make use of the relations in Sec.

© 1983 Hemisphere Publishing Corporation

3.3.5, item 21, and Fig. 3.3.5(14), whichintroduces the values of $(D_s - D_{ctl})$ for various tube bundle types.

Some tube count tables include the value of surface per unit of tube length, from which the desired relationship of Eq. (4) can be readily found. If such a source is not available, the designer must assume a rational tube length L_{ta}, and calculate the corresponding diameter D_{ctl} and eventually D_s. This trial-and-error procedure can be simplified by a few rules:

(a) For usual designs of shell-and-tube exchangers, the ratio of D_{ctl}/L_{ta} should be within the limits of approximately $\frac{1}{3}$ to $\frac{1}{15}$ as extreme values. For most common cases it will be more like $\frac{1}{5}$ to $\frac{1}{10}$.

(b) A longer tube length L_{ta} is generally preferable, as it results in less expensive units. However, flow and pressure drop considerations may favor deviations from this rule, subject to engineering judgment.

(c) A fine-tuning process for L_{ta}/D_{ctl} may be necessary in some cases as described in Sec. B. This will involve pressure drop calculations, possibly on both shell and tube side. Advantages of a computer program for this purpose are obvious.

(d) For some units, where L_{ta} is specified or at least limited to a maximum, and/or the overall size of the exchanger is limited, the need will arise to employ more than one unit. These can be arranged in parallel or in series (or combination of these between tube-side and shell-side flow). If sufficient pressure drop is available, units in series are generally preferable, but there will be individual exceptions, impossible to define in common terms.

Finally, a graphic estimation method, representing Eq. (6), is shown in Fig. 2. For practical use, define parameter A^*, Eq. (5) (Table 2) and relate the desired exchanger surface $A_o\,(\mathrm{m}^2)$ to D_{ctl} (mm) for any effective tube length L_{ta}. The graph also works, of course, the other way; that is, for known D_{ctl}, A^*, and L_{ta}, the area A, can be determined.

6. Estimate baffle and tube pass specifications. With completion of item 5, the exchanger is fully specified in all external dimensions. To perform the rating calculations, we need additional estimations:

(a) Baffle spacing and baffle cut. For most cases, the interrelation as shown in Fig. 3.3.5(4) should be followed for best pressure drop-to-heat transfer conversion. If these relations do not produce the desired results, for example, because of low allowable Ap, it is generally preferable to explore other shell types (TEMA J), or to enlarge the tube pitch. Do not deviate significantly from values in Fig. 3.3.5(4), unless justified through careful analysis.

(b) Estimate the number of tube passes N_{tp}. This value is purely a function of allowable $\Delta p_{t,\max}$, which should be utilized in every case of sensible heat transfer as closely as possible. However, as noted before, Δp_t increases with $(N_{tp})^3$ and therefore is a very difficult parameter to deal with. It is also closely connected with

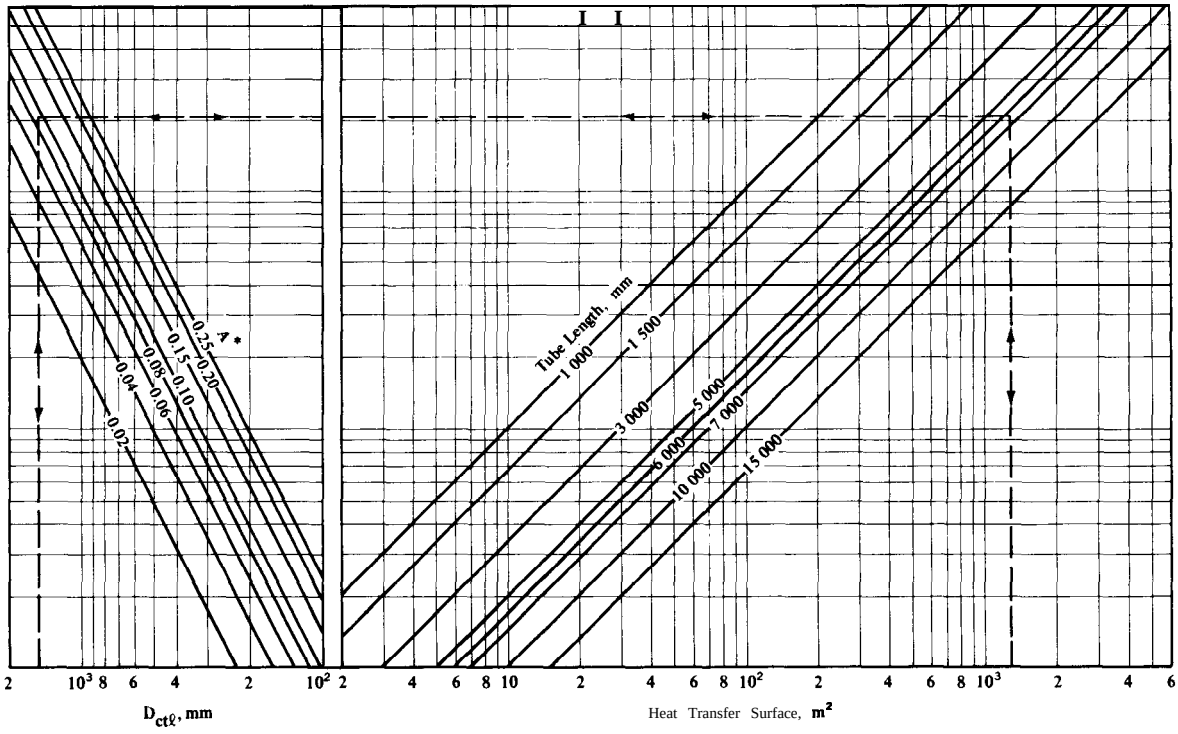

Figure 2 Heat transfer surface A as a function of D_{ctl} with A^* and tube length as parameters.

© 1983 Hemisphere Publishing Corporation

Table 2 **Values of A^* [Eq. (5)]** for selected tube layouts

D_t, mm	L_{tp}, mm	L_{tp}/D_t	A^*	
			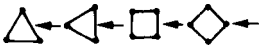	
6	9	1.5	0.211	0.183
10	13.5	1.35	0.156	0.135
12	15.5	1.29	0.142	0.123
14	18	1.29	0.123	0.106 6
	19	1.36	0.110 5	0.095 7
16	20	1.25	0.117	0.098 7
	21	1.31	0.103 4	0.089 5
18	23	1.28	0.096 9	0.084 0
	24	1.33	0.089 0	0.077 1
20	25	1.25	0.091 2	0.079 0
	26	1.3	0.084 3	0.073 0
22	27	1.23	0.086 0	0.079 5
	29	1.32	0.074 5	0.067 5
25	30	1.2	0.079 1	0.068 5
	32	1.28	0.069 6	0.060 2
30	36	1.2	0.066 0	0.057 1
	38	1.27	0.059 2	0.051 3
38	45	1.18	0.053 5	0.046 3
	47	1.24	0.490	0.042 4
44-45	53	1.19	0.045 1	0.039 1
	55	1.24	0.041 9	0.036 3

the choice of D_{ctl}/L_{ta}. If the tube-side coefficient is controlling, a thorough investigation is warranted. On the other hand, one must assure that a certain minimum tube-side flow velocity is obtained, especially in fouling-sensitive cases, and adjust other parameters accordingly. Computer programs are, again, very useful in this area.

D. Preliminary performance evaluation

Having completed all the estimations as described in Sec. C, the exchanger is now fully specified (albeit subject to later possible changes) and a rating calculation, exactly as described in Sec. 3.3.9, can be performed. The results will indicate the heat transfer and pressure drop performance. These values must be now compared to those desired or specified.

Only rarely will the initial analysis identify a unique and straightforward path to follow. More often, contradictory demands or multiple options will indicate the need for several alternative trial calculations to evaluate the complex interactions of the many design elements.

The primary evaluation can be termed identification of the limiting cases, meaning that one design parameter will usually emerge as a predominant factor. These can be grouped into four typical categories [I] : designs limited by the heat transfer coefficient, by the pressure drop, by the temperature driving force or by fouling resistance.

(a) Heat transfer coefficient-limited design

If the size of the unit has been determined by heat transfer requirements only and there will be only a small overdesign factor, the case is termed heat transfer coefficient-limited. This is generally a desirable solution, but a further check must be made to ensure that the permissible pressure drop has been utilized effectively. If there is considerable unused pressure drop, this may suggest potential further improvements. There may be cases where the permissible pressure drop was specified unrealistically high, and no further action is indicated. However, designs with inherently low heat transfer coefficients, such as laminar flow or low-pressure gases, may also reflect heat transfer coefficient limitations. They deserve special attention, as the variation of design elements may often substantially improve the final design.

(b) Pressure drop-limited design

Cases in the pressure drop-limited category are characterized by the condition that the exchanger size has been increased only to accommodate the permissible pressure drop rather than to satisfy heat transfer demands. This is a highly undesirable situation, as heat transfer surface is allocated that is not needed. By proper adjustment of the design elements, this limitation can almost always be remedied. The most common and effective actions include the following and their combinations:

Use double-segmental or multisegmental baffles.
Change the shell type to TEMA J or X.
Decrease tube length.
Increase tube pitch.
Change tube layout pattern.

The prime recognition factor for pressure drop-limited cases is a higher heat duty overdesign than would normally be acceptable. However, there will be cases where the pressure drop-limited design will not be recognized so readily. The effects of various construction elements and multiple shells in parallel and in series can conspire to obscure the normal pressure drop-limitation characteristics. This is particularly true if only the final results of computer-designed units are examined. Careful analysis of intermediate solutions will invariably permit recognition of a pressure drop-limited design.

(c) Temperature driving force-limited cases

Cases limited by temperature driving force result from severe problems associated with the effective temperature driving force. The effective mean temperature difference must reflect the corrections to the logarithmic

© 1983 Hemisphere Publishing Corporation

mean temperature difference to account for all of the potential nonidealities of the various flow arrangements. Some of the most obvious considerations are noted below.

Multi-tube-pass correction factor F for appropriate shell flow configuration (from Sec. 1.5) should always be checked to see that it does not fall into the asymptotic F-factor region. The often used criterion of $F > 0.8$ can be grossly misleading, as illustrated in Fig. 3. For more detailed discussion on this and other related items, refer to Sec. 1.5.

Counter-flow arrangement should always be considered whenever units in series have been allocated purely for reasons to counteract severe temperature profile overlap.

TEMA E shells with single tube pass are generally assumed to be in pure counter-flow operation. However, if only a few baffles (<5) are used, the exchanger actually operates as a series of elements in unmixed-unmixed cross flow. This can result in severe decrease of the effective temperature driving force compared with pure counter flow [2].

Thermal conduction through and possible fluid bypass around the edges of the longitudinal baffle for TEMA F and G shells can decrease the effective temperature driving force (see Sec. 1.5).

A most serious problem in the effective temperature difference determination arises through shell fluid bypassing and therefore ineffective exposure to heat transfer surfaces as illustrated in Fig. 4. Stream 1 is fully heat transfer effective, such as the cross-flow stream in shell-and-tube exchangers. Stream 2 is partially effective, such as the bundle bypass stream, whereas stream 3 is completely ineffective. A mixed outlet temperature is then obtained, which shows an apparent temperature difference driving force that is much larger than the one effectively present. If close temperature differences are encountered, any deviation from ideality, such as fluid bypassing, can distort the temperature profile so severely as to render the exchanger unoperational.

Problems with units showing unexpectedly low heat transfer coefficients U_o in practical application can often be tracked to the fact that they have been heavily overdesigned, thus producing a much smaller effective temperature difference (pinch) than the inlet/outlet temperatures would indicate, as shown in Fig. 5. Such cases should be analyzed with particular care and are generally recognizable from very close approach of the terminal temperature.

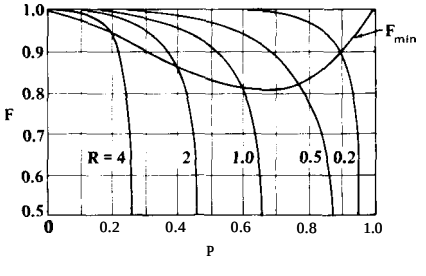

Figure 3 Schematic representation of mean temperature difference F-factor method limitations.

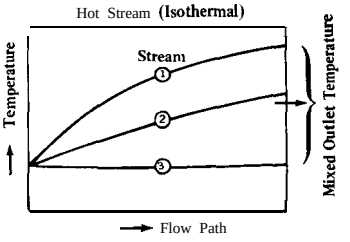

Figure 4 Effects of bypassing on mean temperature difference.

Finally, the designer should be aware of the limitations of the F-correction factor, if local coefficients vary substantially with flow path. This will occur in some cases of condensation and boiling, where both the heat transfer coefficients and temperature may change significantly from inlet to outlet. This subject is treated in other parts of this handbook, and requires the rigorous solution of the basic heat transfer equation as discussed in Part 1.

For both boiling and condensing liquids in essentially isothermal manner (linear heat release, Q versus T), the standard procedures are applicable, as long as the phase-change process takes place over the entire flow path without substantial change of the heat transfer coefficient. Steam-heated units generally qualify under this assumption.

(d) Fouling resistance-limited cases

Some design cases that operate with high heat transfer coefficients are often. allocated relatively large fouling resistances that make the design fouling limited. Efforts of the designer should then concentrate on the following items:

1. Design features that may suppress the fouling tendencies: high flow velocities; proper design of baffles

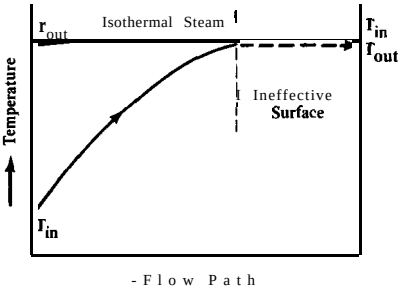

Figure 5 Temperature profile in an overdesigned exchanger.

© 1983 Hemisphere Publishing Corporation

to avoid stagnant areas; lowering tube temperatures, especially if polymerization fouling exists (use of co-current flow in some cases).

2. Design features that will promote ease of cleaning: horizontal tube-side fouling in straight tubes (not U tubes) is the easiest to clean. If chemical shell-side cleaning is not acceptable, 45 or 90 layout with approximately 6-7 mm clearance is necessary to permit mechanical cleaning.

3. It is not uncommon that unrealistically high fouling resistances are specified as a sort of safety factor. This is rather dangerous practice as the amount of safety is relative with respect to the magnitude of the heat transfer coefficients. Also, if large fouling resistances are specified, these will usually be associated with a certain fouling layer thickness, which will decrease the flow areas. This, in turn, can substantially increase the pressure drop. Such cases should be investigated under clean and fouled conditions.

E. Analysis of results

The designer must be satisfied that the results are reasonable and acceptable, compared with generally recognized practices and the demands on exchanger performance in all the above-mentioned limitations. This check will usually show any gross discrepancies, be they related to undetected input errors or to any other causes. Furthermore, the designer must question if there may be a combination of design elements that would lead to a better solution. To aid in this analysis of the final results, the following steps are suggested.

Step 1: Overall design geometry. It is a good practice to make a rough sketch of the main design dimensions, including baffle geometry. This will verify the basic rationality of the overall layout or point out areas of potential concern.

Step 2: Thermal resistances. Check distribution of the thermal resistances on the shell side, tube side, and fouling. These can be expressed in percentages of the total resistance to give the designer an overview of which resistances are dominating. If one of the resistances stands out as exceptionally large, the reasons should be analyzed and possible alternatives investigated. The possibility of switching the fluid allocations should also be considered at this point.

Step 3: Pressure drop utilization and distribution.

(a) Check how well the permissible pressure drop was utilized. If substantial unused pressure drop exists, the case may be potentially a poor design. A change of shell type, baffle type, tube length, and possibly other design elements, as well as combinations of these, should be considered. Conversely, if pressure drop was fully utilized but substantial overdesign exists, the case is pressure drop-limited and actions as described under Sec. D are called for.

(b) Next, check the pressure drop distribution. The main concern is that no excessive part of the available pressure drop be consumed in flow channels with low or zero heat transfer effectiveness, such as nozzles, which should, in general, consume not more than about 10% of the overall pressure drop (see Sec. 2.2.7).

(c) Check the magnitude of the leakage and bypass correction factors for pressure drop, R_l and R_b, and heat transfer J_l and J_b. Their relative magnitude should be reasonable, so that $J_l J_b \geqslant 0.5$. If the value is lower, especially due to baffle-to-shell leakage or bundle-to-shell bypass, the design is potentially poor. Sometimes the use of excessively high Ap, results in very narrow baffle spacing and therefore high cross-flow pressure drop, which forces more flow into bypass and leakage. In such cases, reducing pressure drop may result in increase of heat transfer.

(d) Large bypass and leakage streams, expressed in this method as low values of R_l and R_b, can also distort the temperature profile, as described in Sec. D.

(e) Compare the pressure drop in the cross-flow section (between baffle tips) Ap, with the window pressure drop Δp_w. In well-proportioned baffle geometry, Δp_w should be not more than about twice the value of Ap_c.

Step 4: Tube vibration check. If shell-side flow has a rather large pressure drop and hence flow velocity, potential danger of tube vibration may exist. This is especially true if the largest unsupported tube span approaches about 0.7 of the recommended maximum $L_{b,\max}$, Sec. 3.3.5. In such cases a tube vibration should be analyzed, as described in Sec. 4.6.

Nomenclature for Section 3.3. IO appears at the end of Section 3.3. I I.

REFERENCES FOR SECTION 3.3.10

1. Taborek, J., Evolution of Heat Exchanger Design Techniques, Donald Q. Kern Award Lecture, ***Heat Transfer Eng., vol. 1,*** no. 1, 1979.
2. Gardner, K., and Taborek, J., Mean Temperature Difference-A Reappraisal, *AIChE J.*, vol. 23, no. 6, November 1977.

© 1983 Hemisphere Publishing Corporation

3.3.11

Extension of the method to other shell, baffle, and tube bundle geometries

J. Taborek

■ The Delaware method, as originally developed and on which the method presented here is based, is more or less explicitly confined to the design of fully-tubed E-shell configurations using plain tubes. However, there are many process reasons-better balance required between the shell-side and the tube-side heat transfer coefficients, vibration problems, more effective use of available shell-side pressure drop in low-pressure-drop cases, etc.-that lead to the importance of applying the method to variant configurations.

The most important alternative geometries and how the method can be adapted to them are dealt with in this section. However, only a few can be described explicitly at this time. Others are explained only qualitatively, as additional correlational work is necessary. It is foreseen that these will be included in a forthcoming supplement.

For detailed description of the various shell and bundle geometries, refer to Sec. 4.2.

A. Divided flow, TEMA J shell

A diagramatic sketch of this arrangement is shown in Fig. 1 with a single inlet nozzle and two outlet nozzles.

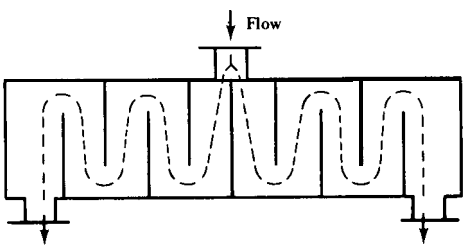

Figure 1 Schematic sketch of TEMA J shell.

The opposite arrangement can also be used. In principle, only half of the flow traverses half the length of the exchanger, resulting approximately in one-eighth of the pressure drop in turbulent flow compared to a TEMA E shell.

The adaptation of the method to a J shell is straightforward:

1. Consider one-half length of the exchanger as a Unit equivalent to an E shell. Take one-half of the flow rate M_s.
2. For pressure drop calculations, consider the flow divider partition as a tubesheet, that is, the first baffle crossing is the entry end zone to be included in Δp_e. Then proceed as for E shells.
3. Calculate the heat transfer coefficient based on the same principles as Ap and consider it valid for the entire tube length.
4. Determine the $AT_{„}$ correction factor from the charts in Sec. 1 .5.
5. Notice that only an even number of baffles can be used.

B. No-tubes-in-window tube bundles

Tubes are omitted in the window area of segmental baffles. Support plates can be used between baffles to shorten the unsupported tube span, thus minimizing tube vibration. Consequently, baffle spacings can be enlarged, often up to two shell diameters. This arrangement has the following characteristics:

1. Very low pressure drop (about one-third of segmental baffle).

© 1983 Hemisphere 1 blishing Corporation

2. Uniform shell-side flow pattern resembling that of an ideal tube bank. Consequently high α_s values and lower fouling tendency.

3. With usual baffle cuts between 10 and 25%, corresponding lower tubular surface in a given shell.

4. Very low Δp in the window (about two velocity heads), correspondingly lower bypass and leakage streams.

Based on these comments, the method can be correspondingly modified. However, as these procedures have not been tested, they are not specifically included here.

C. Two shell pass-TEMA F shell

This construction type of a TEMA F shell, Fig. 2, uses a longitudinal baffle through the exchanger with an open turnaround at the opposite end. Combined with two tube passes, it results essentially in counterflow and is used mainly for cases with close terminal temperature approaches, which would otherwise require two shells in series (at a higher cost). The number of baffles must be an even number for proper flow distribution. Pressure drop in an F shell will be approximately eight times that for an E shell of the same diameter (in turbulent flow).

The basic shell-side method can be adapted to this case under the rough assumption that the geometric parameters are modified to recognize that a segmental baffle has been split into two halves. Again, this has not been tested at present, and therefore no detailed procedures are given.

D. Double segmental or disk-and-doughnut baffles

These baffle geometries (see Sec. 4.2) are used to split the shell-side flow into two longitudinal components, each flowing through half the cross-sectional area. Thus, the pressure drop in turbulent flow is about half that for segmental baffles. The flow direction is much more longitudinal than in cross flow, and correlations are difficult. The present method cannot be easily adapted to this baffle type, as the driving forces for bypass and leakage flow are much smaller than for segmental baffles.

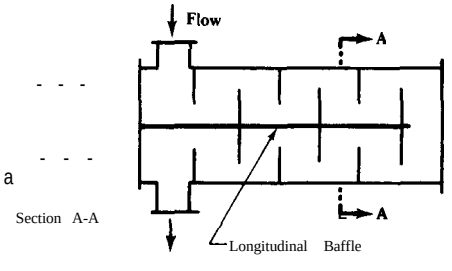

Figure 2 Schematic sketch on TEMA F shell.

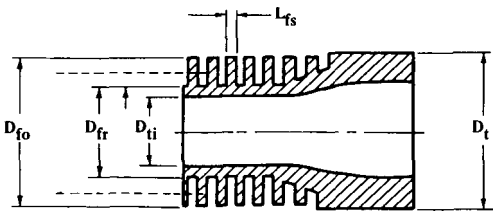

Figure 3 Geometric characteristics for external low fm tubes.

E. Application of external low fin tubes

The method for segmentally baffled E shells is relatively easy to adapt to low fin tubes. These tubes are generally classified as having 630-l 000 tins/m (16-26 fins/in), and usual fin height of about 1 to 2 mm. The tube outside surface increase ranges typically between 2 and 3 compared to a plain tube of the same diameter, whereas the heat transfer coefficient is only slightly lower. Refer to Fig. 3 for basic geometric characteristics. Such extended surface tubes are potentially very useful in applications that have the following characteristics:

1. High tube-side heat transfer coefficient, α_t and low tube-side fouling resistance.

2. Low shell-side heat transfer coefficient, typically in gas flow and in many organic streams with Re, > 1 000.

3. Shell-side fouling resistance can be tolerated as long as the deposit does not block the fin geometry with a sticky substance. Fouling in the form of a crusty deposit has been reported to be actually broken by the fin structure, thus decreasing the fouling resistances as compared to plain tubes (this is only a qualitative observation).

No specific rules for fin tube applications outside of the above mentioned premises exist, as cost factors enter into the final economic analysis. There are, however, process conditions where external low fm tubes would not be recommended:

1. In laminar flow, approximately for Re, < 1 000, a laminar boundary layer overlap develops inside the tins (function of fin density), which decreases rapidly the fm surface effectiveness.

2. Condensing steam on the fin side is ineffective, as the fin valleys fill with condensate (high surface tension of water) and do not drain readily, thus decreasing the effective surface. On the other hand, condensation of organic vapors can be very effective

© 1983 Hemisphere I blishing Corporation

(low surface tension), this subject being treated in other parts of this handbook.

The adaption of the basic shell-side method for no-phase-change flow on low fin tubes requires following a number of modifications to Secs. 3.3.5-3.3.9, as follows:

1. Section 3.3.5A, input data. Fin geometry specifications, Table 3.3.5(12): Item 2, D_t, remains unchanged, pertaining to the plain end of the tin tube. Additional tube geometry items to be included are, from Fig. 3:

Item 2a	D_{fo} (mm)	Diameter over the tins
Item 2b	D_{fr} (mm)	Fin root diameter
Item 2c	N_f (1/m)	Number of tins per unit of tube length
Item 2d	L_{fs} (mm)	Average fin thickness (assuming rectangular fin shape)
Item 2e	A_{of} (m^2/m)	Actual fin surface area per unit of tube length
Item 19	L_{tb} (mm)	Tube-to-baffle hole clearance; in determination of this value, use D_{fo} for fin tubes in place of D_t

Then, we need to define an equivalent projected diameter, D_{req}, as shown in principle in Fig. 3. This is essentially a correlational value establishing an equivalent cross-flow area as compared to a plain tube.

$$D_{req} = D_{fr} + 2L_{fh}N_fL_{fs}(10^{-3}) \quad \text{(mm)} \qquad (1)$$

where L_{fh} is the fin height, $(D_{fo} - D_{fr})/2$. Whenever the tube diameter D_t of the plain tube appears in correlational equations, it must now be interpreted in terms of the fm tube geometry.

2. Section 3.3.5C, correlational parameters.

(a) S_m calculations: Use D_{req} for D_t in Eq. 3.3.5(22).

(b) Re,, shell-side Reynolds number: Use D_{req} for D_t in Eq. 3.3.5(25).

(c) A_o, heat transfer surface: Using the input value A_{of} (m^2/m) as fin surface area per unit length, the total heat transfer surface based on the fin surface, changes Eq. 3.3.5(30) to

$$A, = A_{of}L_{ta}N_{tt} \times 10^{-3} \qquad (2)$$

3. Section 3.3.6B and 3.3.6C, baffle window. Flow area S_{wt}: In place of D_t, use D_{fo} in Eq. 3.3.6(7).

4. Section 3.3.6H, tube-to-baffle hole leakage area S_{tb}. Use D_{fo} in place of D_t to determine L_{tb}, as well as in Eq. 3.3.6(18).

5. Section 3.3.7, ideal tube bank j_i and f_i.

(a) Heat transfer factor j_i: Curves for plain tubes can be used for low fin tubes with Re, based on D_{req}, up to Re, $\geqslant$ 1 000. Below Re, = 1 000, a laminar boundary layer overlap takes place, which makes fin tubes less effective [1], and a correction factor must be applied so that

$$j_i = J_f j_{i,\text{plain tube}} \qquad (3)$$

Correction J_f, taken from [1], is shown in Fig. 4. Actually, J_f is a function of the fin height/fin spacing ratio, but data are not available in the open literature.

In calculating the ideal tube bank heat transfer coefficient α_i, a tin efficiency correction factor must be included, as described elsewhere in this handbook. For operating conditions usually favorable to fin tube application, tin efficiency is usually in the range of 0.9 or higher.

(b) Friction factor f_i. The fins present a larger frictional surface than plain tubes, and therefore it can be logically expected that the friction factor will be higher. Very few data are available, but the work of Briggs and Young [1] and other unpublished sources indicate that for the usual geometry of low fins, the following relation applies:

$$f_{i,\text{fin}} = 1.4 f_{i,\text{plain tube}} \qquad (4)$$

In other words, the f_i values for plain tubes are used and multiplied by a factor 1.4. This procedure seemingly contradicts the finding of Briggs et al. [2] where lower f values were found for fin tubes, but in this reference the friction factors are based on a baffled exchanger including the window pressure drop and are not applicable for generalized correlation based on ideal tube banks.

The methods recommended here were confirmed on test data of an industrial-size exchanger with 19 fins/in and produced results 15% and 28% on the safe side for α_s and Δp_s, respectively, which is considered a very respectable performance.

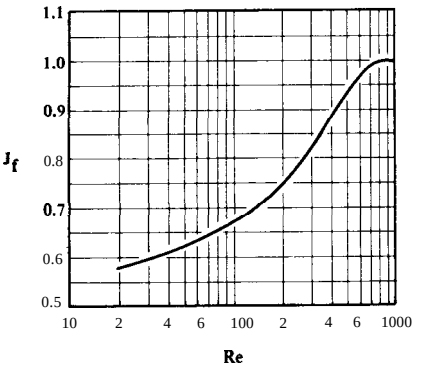

Figure 4 Correction factor of J_f for heat transfer with low tin tubes.

© 1983 Hemisphere Publishing Corporation

NOMENCLATURE FOR SECTIONS 3.3.1-3.3.11

A_o heat transfer surface based on outside tube area [Eq. 3.3.9(10)], m^2
A^* tube layout density parameter
B_c baffle cut as percent of inside shell diameter D_s (input item 11), %
B_c^* area between D_s and a tube layout cutoff line [Eq. 3.3.5(16a)], %
C_1 tube field layout constant for N_{tt} calculation [Eq. 3.3.5(16)]
CB code for tube bundle type (input item 18)
CN code for shell-side impingement (input item 14)
$C_{p,s}$ shell-side fluid specific heat at average temperature, J/kg K (input item 29)
D_{ctl} same as D_{otl}, except through the centers of the tubes, mm
D_{ns} shell-side nozzle inside diameter, mm
D_{otl} diameter of a circle circumscribed to outermost tube of a bundle [Fig. 3.3.6(1), Eq. 3.3.5(20a)], mm
D_s inside shell diameter (input item 1), mm
D_t tube outside diameter (input item 2), mm
D_{ti} tube inside diameter (input item 4), mm
$D_{t,max}$ maximum outside tube diameter including tolerances (item 19, Sec. 3.3.5), mm
D_w hydraulic diameter of baffle window [Eq. 3.3.6(10)], mm
fi friction factor for an ideal tube bank [Eq. 3.3.7(9)]
F correction factor to the ΔT_{LM} for non-counterflow systems (see Sec. 1.5)
F_{sbp} ratio of bypass to cross-flow area [Eq. 3.3.6(16)]
F_w, F_c fraction of tubes in one baffle window and in cross-flow between baffle tips, respectively [Eqs. 3.3.6(5) and (6)]
ii Colburn s heat transfer factor [Eq3.3.7(3)]
J_b bundle bypass correction factor for heat transfer [Fig. 3.3.6(10)]
J_c segmental baffle window correction factor for heat transfer [Fig. 3.3.6(7)]
J_l baffle leakage correction factor for heat transfer [Fig. 3.3.6(8)]
J_r laminar-flow heat transfer correction factor [Fig. 3.3.6(12)]
J_s heat transfer correction factor for unequal end baffle spacings (Sec. 3.3.6)
L^* ratio of outlet/inlet baffle spacing to L_{bc} [Fig. 3.3.6(13)]
L_{bb} inside shell-to-bundle bypass clearance (diametral) [input item 21 and Fig. 3.3.5(13)], mm
L_{bc}, L_{bi}, L_{bo} baffle spacing, central, inlet, outlet [see Fig. 3.5.5.(6)], mm
L_{bch} height of baffle cut [Fig. 3.3.5(2)], mm
$L_{bc,max}$ maximum permissible central baffle spacing [Fig. 3.3.5(5)], mm
$L_{b,max}$ maximum unsupported tube span [Figs. 3.5.5(5)-(6)], mm
L_{ns} nozzle flow escape distance [Fig. 3.5.5(7), Eq. 3.3.5(13)], mm
L_p tube pass lane width [Eq. 3.3.6(15), Fig. 3.3.6(1)], mm
L_p' effective pass lane partition width [Eq. 3.3.6(15)], mm
L_{pn}, L_{pp} tube layout characteristic dimensions described in Table 3.3.5(8), mm
L_{sb} inside shell-to-baffle clearance (diametral) [input item 20, also Fig. 3.3.5(12)], mm
L_{tb} tube-to-baffle hole clearance (diametral) [input item 19, also Fig. 3.3.5(11)], mm
L_{ti}, L_{ta}, L_{to} tube length [input items 8-10, see Fig. 3.3.5(1)], mm
L_{tp} tube layout pitch (input item 6), mm
L_{ts} tubesheet thickness [Eq. 3.3.5(2)], mm
L_{tt} total tube length [Eq. 3.3.5(7)], mm
L_{tw} tube wall thickness (input item 3), mm
L_{wp} baffle window flow penetration distance [Eq. 3.3.6(12)], mm
$\dot{m}$ mass velocity, kg/m^2 s
m_s shell-side cross-flow mass velocity [Eq. 3.3.5(24)], kg/m^2 s
m_w shell-side flow mass velocity through segmental baffle window [Eq. 3.3.8(3)], kg/m^2 s
$\dot{M}_s$ shell fluid mass flow rate, kg/s
$\dot{M}_t$ tube fluid mass flow rate, kg/s
N_b number of baffles [Eq. 3.3.6(14)]
N_c total number of tube rows crossed in the exchanger [Eq. 3.3.6(28)] or any number of tube rows crossed [Eq. 3.3.7(9)]
N_{ss} number of sealing strips (pairs) (input item 17)
N_{tcc} number of tube rows crossed between baffle tips of one baffle compartment [Eq. 3.3.6(11)]
N_{tcw} number of tube rows crossed in one baffle window [Eq. 3.3.6(13)]
N_{tp} number of tube passes (input item 16)
N_{tt} total number of tubes or number of holes in tubesheet for U-tube bundles [input item 15, Eq. 3.3.5(16)]
N_{tw} number of tubes in one baffle window [Eq. 3.3.6(8)]
PS shell-side operating pressure, kPa
Pr Prandtl number
Pr_s shell-side Prandtl number
$\dot{Q}_{act}$ heat duty of an exchanger actually delivered, W

© 1983 Hemisphere Publishing Corporation

$\dot{Q}_{req}$ required heat duty of an exchanger, W

r_{lm}, r_s leakage area parameters [Eq. 3.3.6(21)]

r_{ss} sealing strips correlational parameter [Eq. 3.3.6(24)]

R heat transfer resistance, referred to particular definition as designated by subscripts: o, referred to outside tube surface; f, fouling; w, tube wall; d, differential [Eq. 3.3.9(7)]; i, referred to inside tube surface, all in $(W/m^2 K)^{-1}$

R_b bundle bypass correction factor for pressure drop [Fig. 3.3.6(11)]

$R_{f,i}$ tube-side fouling resistance referred to inside tube surface (input item 37), m^2 K/W

$R_{f,o}$ shell-side fouling resistance referred to outside to the surface (input item 3 1), m^2 K/W

R_l baffle leakage correction factor for pressure drop [Fig. 3.3.6(9)]

R_s baffle end zones correction factor for pressure drop [Eq. 3.3.6(39)]

Re_s shell-side Reynolds number [Eq. 3.3.5(25)]

S_b bypass area between shell and tube bundle [Eq. 3.3.6(15)], mm^2

S_c cutoff area for calculation of tube count [Eq. 3.3.5(15c)], mm^2

S_m cross-flow area near shell centerline [Eq. 3.3.5(22)], mm^2

S_{sb} leakage area, shell to baffle [Eq. 3.5.6(17)], mm^2

S_{tb} leakage area, tube to baffle hole, for one baffle [Eq. 3.3.6(18)], mm^2

S_w net cross-flow area through one baffle window [Eq. 3.3.6(9)], mm^2

S_{wg} baffle window area without tubes [Eq. 3.3.6(4), Fig. 3.3.6(2)], mm^2

S_{wt} area occupied of tubes in one baffle window [Eq. 3.3.6(7), Fig. 3.3.6(3)], mm^2

$T_{s,av}, T_{t,av}$ average temperature of shell-side and tube-side fluid, respectively, °C

T_{si}, T_{so} shell-side temperature inlet and outlet (input items 22, 23), °C

T_{ti}, T_{to} tube-side temperature inlet and outlet [input items 24, 25], °C

T_w temperature at the tube wall [Eq. 3.3.7(7)], °C

U_o overall heat transfer coefficient based on outside tube area, W/m^2 K

v_{ns} shell nozzle flow velocity, m/s

$v_{t,max}, V_{t,min}$ maximum or minimum tube-side velocity [input items 42, 43], m/s

α_i heat transfer coefficient for ideal tube bank [Eq. 3.3.7(4)], W/m^2 K

α_s, α_i shell-side or tube-side heat transfer coefficient [input items 38, 39], W/m^2 K

Δp_{bi} pressure drop in cross flow between baffle tips, based on ideal tube bank [Eq. 3.3.7(10)], kPa

Δp_c pressure drop in cross flow between baffle tips of segmental baffles, corrected for nonidealities of flow [Eq. 3.3.8(2)], kPa

Δp_l pressure drop in end zone baffle spacings [Eq. 3.3.8(7)], kPa

Δp_i pressure drop in cross flow in ideal tube bank [Eq. 3.3.7(9)], kPa

$\Delta p_{s,max}, \Delta p_{t,max}$ maximum permissible shell-side or tube-side pressure drop [input items 40, 41], kPa

Δp_w pressure drop in window of a segmentally baffled exchanger [Eqs. 3.3.8(4), 3.3.8(5)], kPa

AT,-, ΔT_h cold and hot end terminal temperature differences [Eq. 3.3.9(9)], °C

ΔT_{LM} log mean temperature differences [Eq. 3.3.9(9) and Sec. 1.5], °C

ΔT_m effective or true mean temperature difference [Eq. 3.3.9(1) and Sec. 1.5], °C

η_s shell fluid dynamic viscosity at average temperature, cP = mPa/s

η_t tube fluid dynamic viscosity at average temperature, cP = mPa/s

e_{ctl} tube bundle baffle cut centri-angle [Fig. 3.3.6(1)], deg

θ_{ds} baffle cut centri-angle [Fig. 3.3.6(1)], deg

θ_{tp} tube layout angle [input item 7 and Table 3.3.5(8)], deg

λ_s, λ_t shell- or tube-side fluid thermal conductivity at average temperature of each fluid (input items 28, 34], W/m K

λ_{tw} thermal conductivity of tube wall material (input item 5), W/m K

ρ_s, ρ_t shell- or tube-side fluid density, respectively, at average temperature of each fluid [input items 27, 33], kg/m^3

ϕ_s viscosity correction factor for shell-side fluids, defined by Eq. 3.3.7(5)

ψ_c tube count correction factor for cutouts [Eq. 3.3.5(16*e*)]

ψ_n tube count correlation factor for multitube pass layouts [Fig. 3.3.5(10)]

REFERENCES FOR SECTION 3.3.11

1. Briggs, D. E. and Young, E. H., Convection Heat Transfer and Pressure Drop of Air Flowing Across Triangular Pitch Bank of Finned Tubes, ***CEP Symp. Ser. No.*** 41, vol. 59, Heat Transfer-Houston, pp. l-10.

2. Briggs, D. E., Katz, D. L., and Young, E. H., How to Design Finned-Tube Heat Exchangers, ***CEP,*** vol. 59, no. 11, pp. 49-59, Nov. 1963.

©1983 Hemisphere Publishing Corporation

3.5 Evaporators

Contents

3.5.1
INTRODUCTION. R. A. Smith **3.5.1-1**

3.5.2
TYPES OF EVAPORATORS,
R. A. Smith **3.5.2-1**

A. Horizontal shell-side evaporator 3.5.2-l
B. Short-tube vertical evaporator 3.5.2-l
C. Basket-type evaporator 3.5.2-1
D. Long-tube vertical evaporator 3.5.2-3
E. Climbing film evaporator 3.5.2-4
F. Falling film evaporator 3.5.2-4
G. Horizontal tube-side evaporator 3.5.2-S
H. Plate-type evaporator 3.5.2-6

3.5.3
ARRANGEMENTS, R. A. Smith **3.5.3-l**

A. Multiple-effect evaporation 3.5.3-l
B. Vapor recompression 3.5.3-2
C. Flash evaporation 3.5.3-2

3.5.4
DESIGN DETAILS. R. A. Smith **3.5.4-l**

A. Hot fluid space 3.5.4-l
B. Separators 3.5.4-l
C. Condensers 3.5.4-2
D. Desuperheaters 3.5.4-2

3.5.5
CHOICE OF TYPE, R. A. Smith **3.5.5-l**

A. Vaporization 3.5.5-l
B. Concentration 3.5.5-l
C. Crystallization **3.5.5-2**
D. Choice of tube diameter **3.5.5-2**

3.5.6
ESTIMATION OF PRESSURE DROP AND CIRCULATION RATE,
R. A. Smith **3.5.6-l**

3.5.7
ESTIMATION OF HEAT TRANSFER COEFFICIENTS. R. A. Smith **3.5.7-l**

A. Heating fluid 3.5.7-1
B. Wall 3.5.7-l
C. Dirt 3.5.7-l
D. Boiling liquid 3.5.7-2

3.5.8
ESTIMATION OF SURFACE AREA,
R. A. Smith **3.5.8-l**

References for Sections 3.5.1-3.5.8 3.5.8-2

© 1983 Hemisphere Publishiig Corporation

HEDH

3.5.1 Introduction

R.A. Smith

The function of an evaporator is to vaporize a liquid or to concentrate a solution by vaporizing part of the solvent, sometimes to the point at which crystallization occurs. The various types of equipment used for this are described in Sec. 3.5.2. The arrangements whereby these pieces of equipment may be combined with each other or with other types of equipment are described in Sec. 3.5.3. The choice of the best type and arrangement for the duties of vaporization, concentration, and crystallization is considered in Sec. 3.5.5. The design of the reboilers in the distillation plant is dealt with in Sec. 3.6. Sections 3.5.6-3.5.8 deal with the thermal design of evaporators, including the critical heat flux and pressure drop.

Many types of evaporators are in use, including shallow ponds heated by solar radiation, direct-fired open pans, coil-in-vessel evaporators, and evaporators with internal agitators. Section 3.5.2, however, deals with only the eight major types:

1. Horizontal shell-side
2. Short-tube vertical
3. Basket type
4. Long-tube vertical
5. Climbing film
6. Falling film
7. Horizontal tube-side
8. Plate type

In most cases the hot fluid is condensing steam. Except for the plate type, all are tubular heat exchangers, and in all except the horizontal shell-side type, boiling is inside the tubes.

For efficient performance, the boiling liquid must flow past the heating surface at a high velocity. To achieve this, the liquid is usually recirculated. Circulation may be natural, when produced by the differences in the densities of the boiling liquid and the returning liquid; or forced, when produced by a pump: or assisted, when both contribute to the flow. When there is no recirculation, the evaporator is described as once-through.

The pressure in an evaporator is chosen to give the required boiling temperature. Hence evaporators are often operated under vacuum so that the temperature is below the normal boiling point.

In evaporators where the liquid flows upward through vertical tubes, the boiling point of the liquid is greater at the bottom of the tube than at the top, because of the greater hydrostatic pressure. Thus, in the lower part of the tube there is no boiling and the temperature rises until the boiling point corresponding to the local pressure is reached; after that the temperature falls and boiling occurs due to both flashing and the further addition of heat. Consequently, the temperature difference is less in the middle of the tubes than at the ends, and this may lead to an appreciable loss in performance in types 2, 3, and 4.

Many of the opinions expressed in this section are based on advice given by the staff of the Agricultural and Mond Divisions of Imperial Chemical Industries Limited and on information published by Chilton and Perry [1]. The author expresses his gratitude for this help and for permission to publish it.

© 1983 Hemisphere Publishing Corporation

HEDH

In concentrating evaporators it is important to allow for the elevation in boiling point due to increased concentration.

All evaporators have devices at their outlet to separate the vapor from the liquid; see Sec. 3.5.4B. It is desirable to minimize the carryover of liquid in a concentrating evaporator because this represents a loss of product, and, if the vapor is to be used to heat a subsequent evaporator, carryover will usually lead to excessive fouling.

References for Section 3.5. I appear at the end of Section 3.5.8

© 1983 Hemisphere Publishing Corporation

3.5.2
Types of evaporators

R.A. Smith

■ The standard types of shell-and-tube heat exchanger are described in Sec. 4.2, using the nomenclature of TEMA. More elaborate designs are usually necessary for evaporators, as described in this section.

A. Horizontal shell-side evaporator

The TEMA type K (kettle reboiler) is often used as a still reboiler; it can be used as a concentrating evaporator, as shown in Fig. 1, provided that there is no danger of scaling. It may also be used as a vaporizer; the concentrate outlet can be used as a continuous purge. If the liquid to be vaporized is clean and contains no dissolved solids, the weir and purge may be omitted, but a drain connection must then be added to the bottom of the shell for occasional purging.

A simpler alternative consists of a similar horizontal U-tube bundle submerged in a half-filled, large-diameter vertical vessel.

Further information about boiling on the outside of horizontal tubes is given in Sec. 3.6.

B. Short-tube vertical evaporator

Figure 2 shows a short-tube vertical evaporator with boiling inside the tubes and an axial flow impeller to assist in the circulation of the liquid through the tubes.

Many of the opinions expressed in this section are based on advice given by the staff of the Agricultural and Mond Divisions of Imperial Chemical Industries Limited and on information published by Chilton and Perry [1]. The author expresses his gratitude for this help and for permission to publish it.

The tubes are not more than 3 m long and 25–60 mm inside diameter. The liquid starts to boil when it is nearly at the top of the tubes; for crystallization it may be preferable to arrange for boiling not to occur until the liquid has left the tubes, to avoid the deposition of solids in the top of the tubes.

It may be possible to omit the impeller and to rely on natural circulation, in which case the area of the central downcomer should be somewhat greater than the cross-sectional area of all the tubes.

When these evaporators are used for the production of crystals, it may be necessary to fit a device at the bottom of the evaporator for removing the crystals.

C. Basket-type evaporator

The basket-type evaporator is a natural-circulation, short-tube vertical evaporator, but instead of having a central downcomer (as in the short-tube vertical described above), the liquid circulates down the annular gap between the calandria and the shell, as shown in Fig. 3. The cross-sectional area of the annular gap should be greater than that of the tubes. The advantage of this arrangement is that the calandria can be removed for cleaning or repairs.

When using a natural-circulation evaporator for the production of crystals, it is important to ensure that the velocity of liquid in the tubes is high enough to recirculate crystals until they grow to the required size. In the evaporator shown in Fig. 3, liquor is recirculated through an elutriator at the bottom of the shell

© 1983 Hemisphere Publishing Corporation

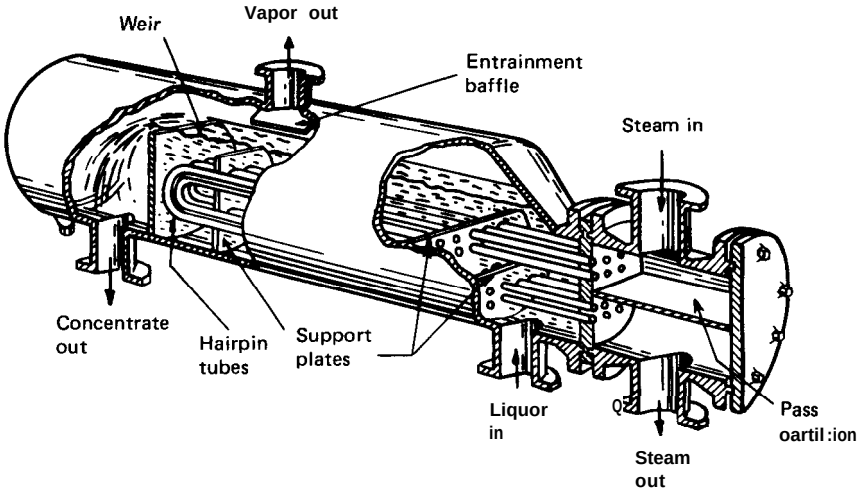

Figure 1 Horizontal shell-side evaporator with hairpin tubes. Separation of droplets by baffle.

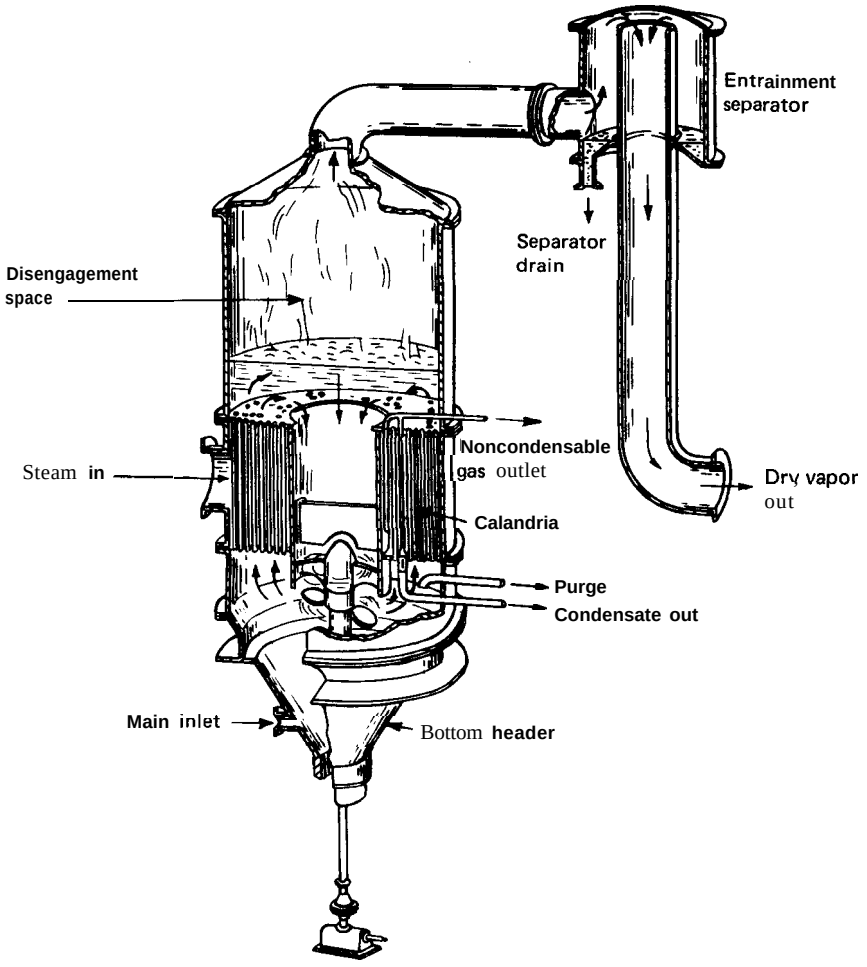

Figure 2 Short-tube vertical evaporator with assisted circulation. Separation of droplets by entrainment separator.

© 1983 Hemisphere Publishing Corporation

at such a velocity that only large crystals can leave through it, while the smaller crystals are recirculated.

With the three types of evaporator described above it is necessary to provide an adequate interfacial area between the boiling liquid and its vapor; also, there must be an adequate disengagement space above the liquid so that droplets fall back into the liquid. Further information on this is given in Sec. 3.5.4B, which also deals with the design of separators. These may be either external, as shown in Fig. 2, or internal, as shown in Fig. 3.

D. Long-tube vertical evaporator

Long-tube vertical evaporators are similar to short-tube vertical ones in that the tubes are of a similar (or somewhat smaller) diameter, but there are fewer tubes and their length is 6 m or more. The downcomer is external; circulation may be natural, but mostly it is forced, as shown in Fig. 4, to give a higher flow rate and hence a higher temperature difference, as explained below.

Compared with the short-tube type, the long-tube vertical evaporator also gives a high heat transfer coeffi-

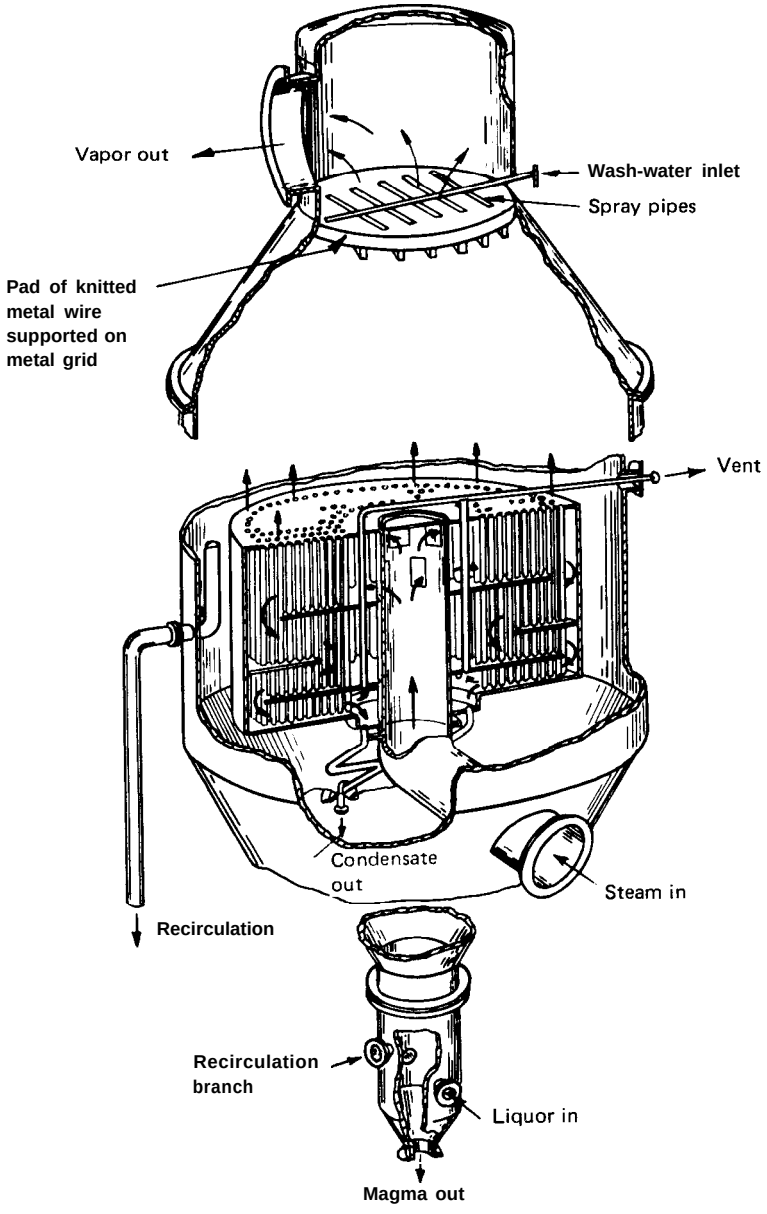

Figure 3 Basket-type short-tube evaporator with bottom steam and wire mesh separator. Spray pipes supplied with wash water are provided for intermittent washing of the wire.

© 1983 Hemisphere Publishing Corporation

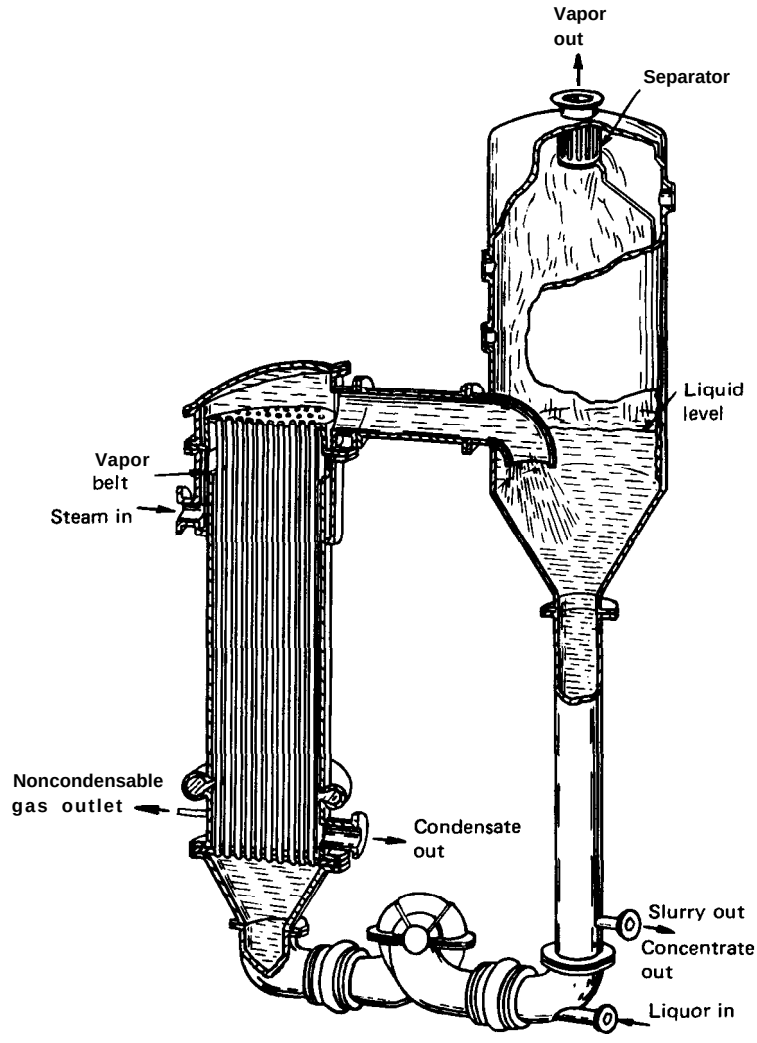

Figure 4 Long-tube vertical evaporator with forced circulation and impingement plate separator.

cient, but there is a bigger rise in temperature in the nonboiling zone because of the greater pressure at inlet; this may result in a significant reduction in temperature difference, the penalty being greater at lower operating pressures.

E. Climbing film evaporator

The climbing film evaporator is a long-tube vertical natural-circulation evaporator that differs from those described earlier in having a much lower head of liquid at the inlet. Thus boiling starts sooner, so the rise in temperature is less; also, the circulation rate is less and the quality at the outlet is higher. Compared with the long-tube vertical type, the climbing film evaporator has a higher temperature difference and a greater proportion of the length of the tubes benefits from enhancement in heat transfer coefficient resulting from boiling; however, there is a greater tendency to scaling. A typical climbing film evaporator is shown in Fig. 5.

An alternative form of the climbing film evaporator is the once-through forced-flow vaporizer, in which the liquid to be vaporized enters the bottom of the vertical tubes and is almost all vaporized as it rises through the tubes.

F. Falling film evaporator

In the falling film evaporator, liquid is fed to the top of the tubes and flows by gravity as a film of liquid on the inside surface of the tubes. The concentrated liquid is collected at the bottom. Normally the vapor that is generated flows downward (cocurrent) with the liquid. When it is required to operate below the normal boiling point but not under vacuum, a gas may be introduced

© 1983 Hemisphere Publishing Corporation

at the bottom and flow upward with the vapor countercurrent to the liquid. This type is shown in Fig. 6.

With a falling film evaporator, it is essential to have a good arrangement for distributing the incoming liquid evenly to all tubes. The simple baffle placed opposite to the inlet nozzle, as shown in Fig. 6, gives a pile-up of liquid immediately around the baffle and at the point diametrically opposite the baffle. With such an arrangement it is necessary for the tubes to project above the tubesheet by a sufficient amount for the liquid to be able to flow across the tubesheet without significant loss in head. Alternatively, with more tubes, it may be preferable to use a distributor pipe feeding several distribution troughs placed at right angles to it.

To obtain good distribution around the circumference of each tube, it is necessary to fit some form of insert in the top of each tube, or cut several weirs in each tube, as shown in Fig. 6.

When introducing a gas at the bottom of the evaporator, it is also important to ensure that the gas will be distributed evenly between tubes.

It is important for the evaporator to be set up so that the weirs are all exactly in the same horizontal plane. It is also important that the tubes be straight and vertical to within a small fraction of the diameter of the tube.

With the counter-current arrangement, the flow rates of vapor and gas must nowhere exceed the flooding rates [see Sec. 2.3.2C(d)].

G. Horizontal tube-side evaporator

The horizontal tube-side evaporator is a standard shell-and-tube heat exchanger with the steam condensing on the shell side, the calandria supplying sensible heat, and evaporation taking place in the flash vessel, as shown in Fig. 7. The calandria can be removed for cleaning or replacing the heating tubes. With this arrangement, forced circulation is needed and must be sufficient to avoid the possibility of dryout at the top of the tubes.

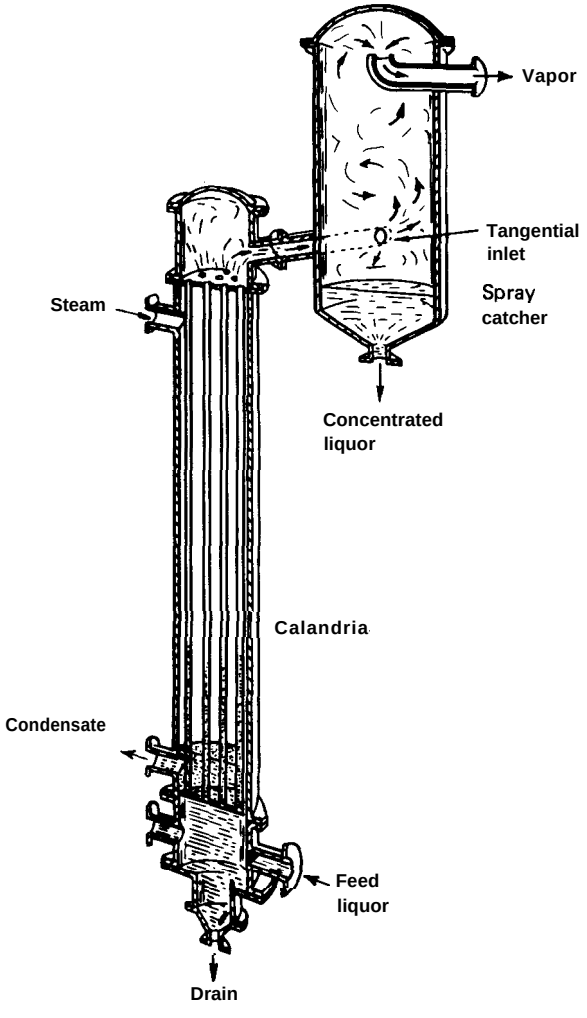

Figure 5 Climbing fiim evaporator with cyclone separator.

© 1983 Hemisphere Publishing Corporation

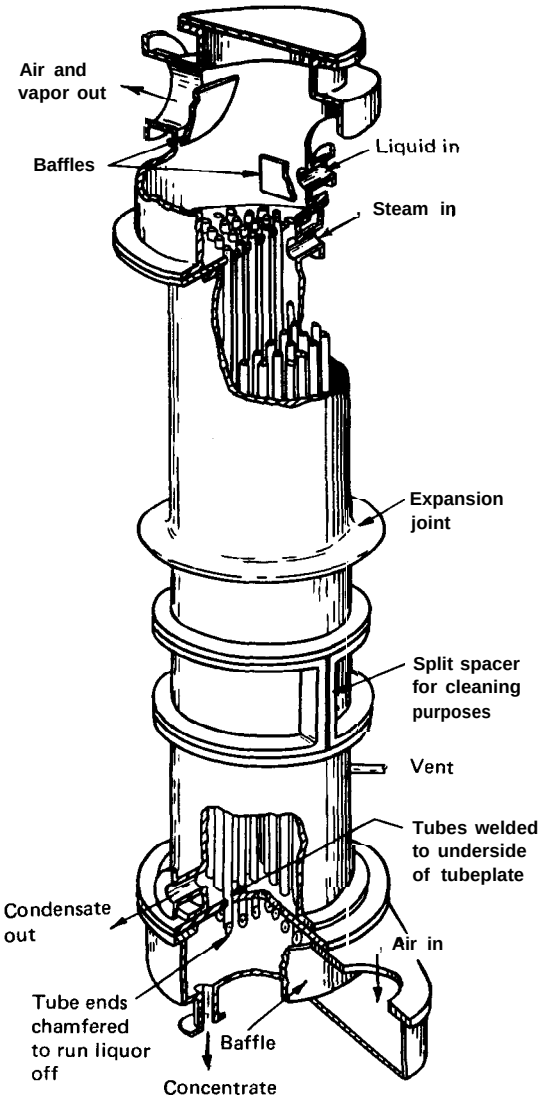

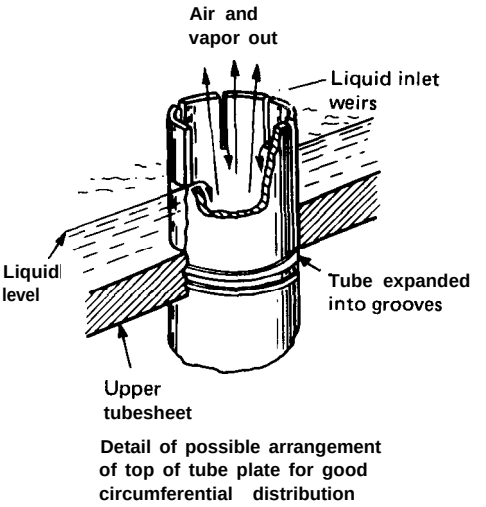

Detail of possible arrangement of top of tube plate for good circumferential distribution

Figure 6 Falling film evaporator.

H. Plate-type evaporator

The plate-type evaporator is the same in principle as the horizontal tube-side evaporator, except that a plate heat exchanger is used instead of the shell-and-tube heat exchanger as the calandria. A similar arrangement of flash vessel, separator, and circulating pump is used. Alternatively, plate-type evaporators are available that operate on either the climbing film or the falling film principle.

The advantages of plate over shell-and-tube heaters are that they cost less (for a given duty), they are less likely to foul, and they are easier to clean. A suitable material must be available for the gaskets to resist corrosion and to withstand the temperature of the hot fluid. Spiral heat exchangers and welded-plate heat exchangers are more robust developments of the normal plate heat exchanger, but the latter cannot be stripped for cleaning.

© 1983 Hemisphere Publishing Corporation

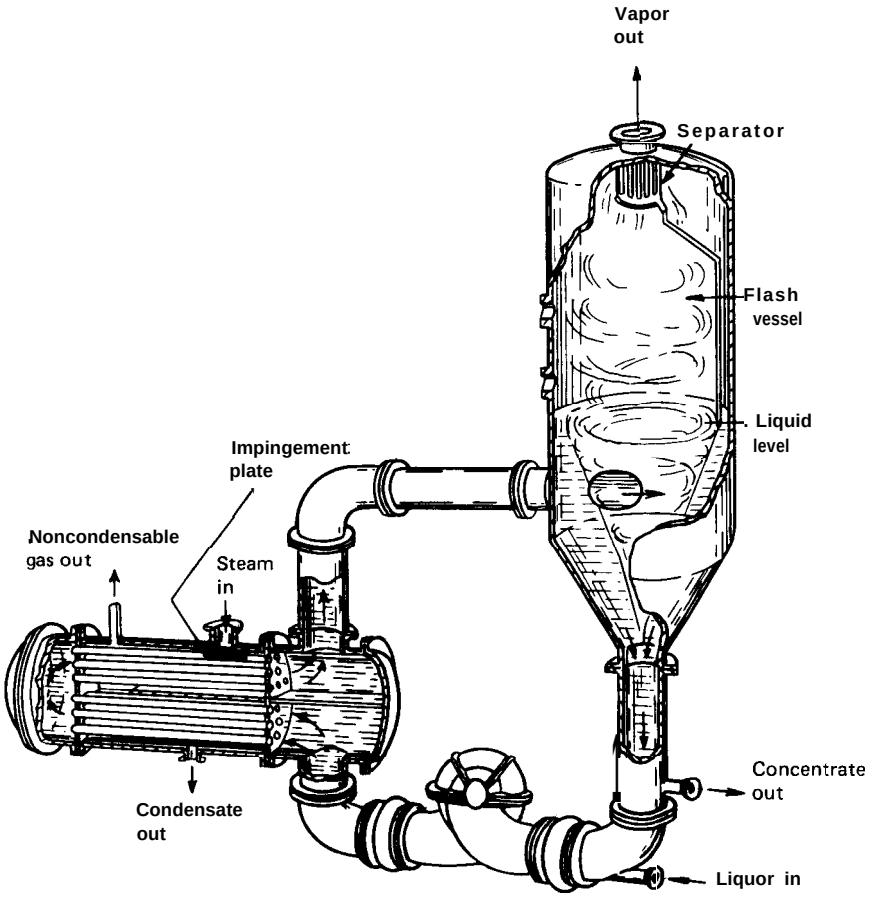

Figure 7 Horizontal-tube evaporator with heating medium outside tubes, forced circulation, and cyclone separator plus impingement plate separator.

References for Section 3.5.2 appear at the end of Section 3.5.8

© 1983 Hemisphere Publishing Corporation

3.5.3
Arrangements

R.A. Smith

This section deals with steam economy, which can be achieved either by arranging several evaporators in multiple effect, as described in Sec. A, or by vapor recompression, as described in Sec. B. Further information on these topics and the calculations needed have been published by Chilton and Perry [1] and by McCabe and Smith [2] . The advantages of flash evaporation are briefly considered in Sec. C.

A. Multipleeffect evaporation

In multiple-effect evaporation, the steam generated in the first effect is used as the heating medium for the second effect, and so on; the steam from the last effect passes to the condenser. Thus steam consumption, ideally, is reduced by a factor equal to the number of effects. In order to maintain a temperature difference, each stage must operate at a pressure lower than that in the previous stage. Consequently, the available temperature difference per effect is less with multiple- than with single-effect evaporation, so that a larger surface area is needed. Furthermore, the actual amount of steam generated in each effect is somewhat less than that in the previous effect, because a certain amount of feed heating is required and because latent heat increases with decreasing pressure. The economic number of stages can be determined by balancing the saving in fuel costs against the extra capital charges.

There are three principal feeding systems in use in multiple-effect evaporation. In forward feed, the liquor being concentrated and the vapor produced run in co-current parallel flow from each effect to the next, as shown in Fig. 1. In backward feed, the liquor and vapor are in counter-current flow, and this necessitates the installation of a liquor pump between each stage, because the liquor must rise in pressure in going from one effect to the next. In parallel feed, fresh liquor is fed to each effect, the liquor entering each effect thus being at the same concentration, but each successive effect operating at a lower temperature and pressure.

Forward feed is preferred when the feed is hot or if the maintenance of interstage pumps would be difficult. Backward feed is best when the feed is cold or viscous or when there is an appreciable elevation in boiling point with increasing concentration. Parallel feed is used where controlled crystallization is needed or where several feeds must be treated separately.

With multiple-effect evaporation, attention must be paid to the following five points: (1) the feed must be

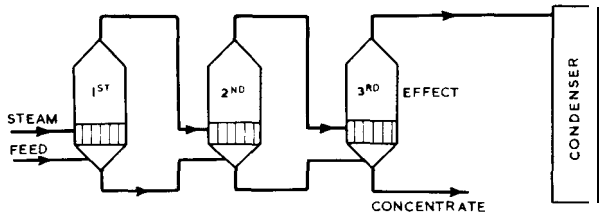

Figure 1 Triple-effect evaporator with forward feed,

Many of the opinions expressed in this section are based on advice given by the staff of the Agricultural and Mond Divisions of Imperial Chemical Industries Limited and on information published by Chilton and Perry [1]. The author expresses his gratitude for this help and for permission to publish it.

© 1983 Hemisphere Publishing Corporation

adequately preheated; (2) very efficient separators are needed (otherwise droplets of liquid carried over from one effect lead to scaling of the heating surface of the next effect); (3) steam supplied to all but the first effect may contain noncondensable gases, due either to gases coming out of solution from the liquid in the previous effect, or, in vacuum operation, to leakage of air into the steam-this must be kept to a minimum and allowed for in the heat transfer calculations, and an adequate purge must be included after the final effect; (4) liquid purge systems may be needed to avoid high concentrations of impurities in the liquor fed to the later effects; (5) the point of take-out and return of the liquid is important.

B. Vapor recompression

The most common method of steam economy is multipleeffect operation (described above) but, in countries where hydroelectric power is plentiful, mechanical recompression of the vapor has been established as the most economical method of reusing steam. Additionally, vapor recompression may be preferred when (1) it is necessary to evaporate over a narrow temperature range, thus restricting the number of effects that could be used; or (2) when the steam is available at a pressure considerably higher than that required for heating, so it can be expanded through a turbine driving the compressor. Figure 2 shows a simple arrangement. Alternatively, steam injectors may be used instead of mechanical recompression.

C. Flash evaporation

If the pressure of a preheated solution is suddenly allowed to fall to below the vapor pressure, evaporation takes place, the latent heat being supplied from a loss of sensible heat of the solution. When heat is not provided by an external source, the process continues until a new equilibrium is reached at a lower vapor pressure; this is known as flash evaporation. It can be used to obtain a solid product or to produce pure steam from an aqueous solution. Because of the high latent heat of steam, the temperature of the solution needs to fall 50 to 60° C for only 10% evaporation.

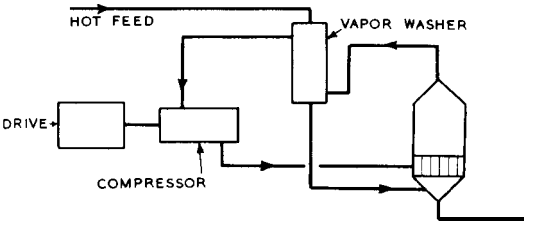

Figure 2 Evaporation with vapor recompression.

References for Section 3.5.3 appear at the end of Section 3.5.8

© 1983 Hemisphere Publishing Corporation

3.5.4
Design details

R.A. Smith

■ This section deals with miscellaneous problems in the design of evaporators and their ancillary plant.

A. Hot fluid space

When the source of heat is steam condensing on the shell side of a shell-and-tube heat exchanger, an impingement plant should be installed opposite the inlet nozzle to protect the tubes in that region from erosion; see Fig. 3.5.2(7). Alternatively, the steam may be introduced through a vapor belt; see Fig. 3.5.2(4); with this arrangement the tubes completely fill the shell, whereas without a vapor belt, some tubes must be omitted in the region of the inlet nozzle to avoid excessive pressure drop there.

Segmental baffles are fitted on the shell side to maintain an adequate velocity and to support the tubes. In the condensation of pure steam, a high velocity gives little enhancement to heat transfer, but it helps in the purging of air from the shell during start-up. When gas is present in the steam, the baffles should be progressively closer together in successive passes, as shown in Fig. 3.5.2(3).

The main function of the baffles is to support the tubes and to prevent damage due to flow-induced vibrations; see Sec. 4.2.7. This is especially important in the region of the steam inlet.

Many of the opinions expressed in this section are based on advice given by the staff of the Agricultural and Mond Divisions of Imperial Chemical Industries Limited and on information published by Chilton and Perry [1]. The author expresses his gratitude for this help and for permission to publish it.

B. Separators

The separation of droplets of liquid from the vapor leaving the evaporator can be carried out in a disengagement space above the level of the liquid or in a spray eliminator separate from the evaporator; in some cases both may be necessary. The most common types of separator are illustrated in Figs. 3.5.2(1)-3.5.2(7), but it must be realized that each separator may be used with types of evaporator other than that in the illustration.

In a horizontal shell-side evaporator, Fig. 3.5.2(1), the disengagement space should be at least 250 mm above the level of the liquid. Considerably more than this is used in large vertical tube-side evaporators, as can be seen from Figs. 3.5.2(2)-3.5.2(4). The subject has been studied by Davis [3] for marine water-tube boilers; from these experiments the following rough rule has been derived for the minimum interfacial area between liquid and vapor when bubbles are bursting:

$$A_i > \frac{0.8\dot{M}}{\sqrt{\rho_g}} \qquad (1)$$

where A_i is the interfacial area (m^2), $\dot{M}$ is the mass flow rate of vapor (kg/s), and ρ_g is the density of the vapor (kg/m^3).

The simplest type of spray separator consists of a baffle placed just in front of the vapor outlet, as seen in Figs. 3.5.2(1) and 3.5.2(6). The impingement plate separators in Figs. 3.5.2(4) and 3.5.2(7) consist of two parallel slotted plates close to each other, the slots in one plate being staggered relative to those in the other.

© 1983 Hemisphere 1 blishing Corporation

Spray separators with tangential inlets are shown in Figs. 3.5.2(5) and 3.5.2(7). If a high efficiency of separation is required, a wire mesh separator is fitted before the entry into the vapor offtake pipe, as shown in Fig. 3.5.2(3). The pad should be 100 mm thick, consisting of layers of woven metal wire; it should be above the splash zone, and it may be advisable to install washing sprays above it. The cross-sectional area, A, (m^2), should meet the following condition, other symbols being as defined above:

$$A_p > \frac{0.3\dot{M}}{\sqrt{\rho_g}} \qquad (2)$$

With the minimum flow area given by this formula, the pressure drop across the pad is approximately 250 N/m*; with larger areas, the pressure drop is reduced in inverse proportion to A_p^2.

C. Condensers

The vapor from the last effect of an evaporator usually passes to a condenser. The cheapest form is the direct contact spray condenser, as described by the Heat Exchange Institute [4] . The vapor enters a chamber containing several water sprays on a ring main; it is important to use sprays that produce well-spread droplets and to position them so that the liquid is well distributed and kept off the wall of the chamber.

When operating under vacuum, the chamber is placed at a sufficiently high level for it to be possible to remove the mixture of condensate and cooling water by gravity through a tail pipe to a hot well at ground level.

When the condensate must not be contaminated, it is necessary to use a surface condenser; the coolant may be water, air, or the cold incoming feed. The design of shell-and-tube condensers is dealt with in Sec. 3.4.

It is always necessary to have a vent on the condenser, through which gases and uncondensed vapors can be extracted. In vacuum condensers, it is important to make sure that there is adequate equipment for maintaining the vacuum; this often takes the form of a two-stage, steam-driven ejector with an interstage condenser. This must be designed for the maximum amount of air that could leak into the system plus the associated vapor. Either it must be capable of pulling the pressure down during the start-up period, or a hogging ejector of higher output but lower efficiency must be added to to cope with start-up loads.

D. Desuperheaters

It may be advisable to install a desuperheater in the incoming steam main so that the amount of superheat is reduced by direct injection of water. This has no effect on the theoretical performance, since this depends on the saturation temperature of the steam, which is a function of the pressure only (see Sec. 3.5.8). However, a high degree of superheat may lead to trouble because of (1) overheating of the shell, (2) excessive fouling in the region of the steam inlet due to the higher heat flux associated with a hot dry wall, or (3) corrosion of tubes near the steam inlet nozzle due to higher wall temperature. As these items are difficult to assess and as desuperheaters are not very expensive, they are often installed when there is some doubt about their necessity.

References for Section 3.5.4 appear at the end of Section 3.5.8

© 1983 Hemisphere Publishing Corporation

3.5.5
Choice of type

R.A. Smith

■ Some advice is given on which might be the best type of evaporator to use for a given duty. Types 1-8 refer to the eight types listed in Sec. 3.5.1.

A. Vaporization

Under the heading of vaporization are included evaporators for the revaporization of a liquefied gas and for obtaining a pure vapor from an impure liquid. For the former application, and also for the latter if the liquid is clean, the kettle type (1) is probably the best [see Fig. 3.5.2(1)] . The weir may be omitted for the former application. An alternative arrangement for revaporizing a liquefied gas is to use a short-tube vertical evaporator operating on the once-through principle, that is, having no downcomer, and keeping the level of liquid well below the top tube plate. In the region of high quality (ratio of flow rate of vapor to total flow rate), it is likely that the wall of the tube will become dry, and consequently a low heat transfer coefficient will be obtained (see Sec. 2.7.3); either the tubes must be made long enough to cope with this, or dry-wall operation must be avoided and an external separator added to remove and recirculate the droplets remaining in the vapor. The advantage of the kettle over the once-through type is that it avoids pulsating flow, but it has the disadvantage with flammable or toxic liquids of requiring a large capacity of liquid.

To obtain a pure vapor from a dirty liquid, the short-tube vertical (type 2) is often used, as shown in Fig. 3.5.2(2) but with a purge at the bottom. Alternatively, a flash system may be used, with heat being supplied at a pressure too high for boiling to occur; the calandria can be either a plate heat exchanger or a vertical or horizontal shell-and-tube heat exchanger with the heating fluid on the Shell side.

Further information on the choice of equipment for vaporization is given in Sec. 3.6.1B.

B. Concentration

Here the object is to produce a concentrate from a dilute solution. With a clean liquid, the long-tube vertical (type 4) with natural circulation is best, except when the temperature rise in the nonboiling zone is appreciable compared with the overall temperature difference. Under these circumstances, possible alternatives are to use forced circulation or to change to the climbing film type (5), or to the kettle type, in order to obtain a higher temperature difference.

With a viscous liquid, a flash system should be used at a sufficient pressure to suppress boiling in the calandria. For small rates of flow, the calandria may take the form of a helical coil with steam condensing on the outside of it; for higher rates, one of the types of calandria described at the end of the previous section may be used.

When the liquid being heated is likely to cause scal-

Many of the opinions expressed in this section are based on advice given by the staff of the Agricultural and Mond Divisions of Imperial Chemical Industries Limited and on information published by Chilton and Perry [1] The author expresses his gratitude for this help and for permission to publish it.

© 1983 Hemisphere 1 blishing Corporation
HDH

ing or fouling of the hot surface, the long-tube vertical (type 4) with forced circulation is usually preferred. Consideration should also be given to the possibility of using a plate-type heat exchanger.

With foaming liquids, the climbing film (type 5) is best. With heat-sensitive liquids, the climbing film or the falling film (type 6) should be used so that the heat is applied for only a short time with a small temperature difference. The more usual form of the falling film evaporator is with cocurrent flow of liquid and vapor, with no added gas; the arrangement shown in Fig. 3.5.2(6) is used only when it is desirable to add gas to avoid operating under vacuum. These two types of evaporator are available in the form of plate heaters, as an alternative to the shell-and-tube types shown in Figs. 3.5.2(5) and 3.5.2(6).

C. Crystallization

For crystallization the best type to use depends very much on the nature of the crystals required. A choice must be made between the short-tube vertical (type 2) as shown in Fig. 3.5.2(2), the basket (type 3) as shown in Fig. 3.5.2(3), and the long-tube vertical (type 4) as shown in Fig. 3.5.2(4). Type 4 is the most popular at present. Alternatively, it is possible to use a flash system in which heat is supplied in a shell-and-tube or plate heater (without boiling) followed by a flash vessel; the liquid then goes to a crystallizer.

Pumps may cause crystals to break down. If the crystals are sensitive to this trouble, or if they are very abrasive, it might be desirable to avoid the need for pumps by using natural circulation (and also avoiding backward-feed multiple effect).

In a crystallizing evaporator, the size of the crystals is determined by the residence time; hence control is very important and unstable flow must be avoided (see *Sec. 3.5.6).*

D. Choice of tube diameter

Normal sizes of tube (19-28 mm) may be used for shell-side boiling and for vaporization or concentration inside tubes when there is no danger of scaling or when little or no boiling occurs inside the tubes. Larger tubes (32-60 mm) are used when there is a significant amount of boiling inside the tubes, including the falling film evaporator. For evaporators where crystallization takes place inside the heated tubes, tube diameters range from 40 to 80 mm.

In designing natural circulation evaporators with limited temperature difference, the circulation rate, and hence the boiling heat transfer coefficient, can be increased by using longer tubes of smaller bore. Thus a compromise is needed between the requirements for heat transfer and the danger that the tubes will become choked if too small a bore is used.

References for Section 3.5.5 appear at the end of Section 3.5.8

© 1983 Hemisphere Publishing Corporation

3.5.6

Estimation of pressure drop and circulation rate

R.A. Smith

■ It is necessary to be able to estimate the pressure drop through the circulation loop of an evaporator. This is especially important in a natural circulation evaporator, where the circulation rate must be estimated by trial and error so that the head available from the differences between the densities in the riser and downcomer equals the loss due to friction around the circulation loop. Computer programs are normally used for this. With assisted and forced circulation it is also necessary to be able to estimate pressure drop so that the head required from the impeller can be estimated.

The estimation of pressure drop in the regions of single-phase flow presents no major problem, and the methods can be obtained from Secs. 2.2.2 and 2.2.4. The pressure drop in the boiling zone is more important because it is usually greater and always much more difficult to estimate, there being big discrepancies between the various published correlations. It is first necessary to be able to estimate the density of a two-phase mixture, for the estimation both of the pressure drop due to acceleration and of the pressure rise or drop due to gravity. Second, the pressure loss due to friction must be estimated. Correlations for two-phase density and friction are given in Sec. 2.3.2.

Two-phase fluid flows are liable to be unstable. There are several different forms of instability, and it is important to ensure that the flow in an evaporator will be steady. Unsteady flow in an evaporator can upset other items of equipment on the plant, and it has a very serious effect in a crystallizing evaporator on the size of the crystals. If the single-phase pressure drop exceeds the two-phase pressure drop, flow will be stable; otherwise see Sec. 2.3.2.

It is important when estimating the pressure drop through an evaporator to allow for the reduction in flow area due to the deposition of dirt or scale-see *Sec.* 3.5.7C.

Many of the opinions expressed in this section are based on advice given by the staff of the Agricultural and Mond Divisions of Imperial Chemical Industries Limited and on information published by Chilton and Perry [1]. The author expresses his gratitude for this help and for permission to publish it.

References for Section 3.5.6 appear at the end of Section 3.5.8

© 1983 Hemisphere Publishing Corporation

3.57 Estimation of heat transfer coefficients

R.A. Smith

■ The overall heat transfer coefficient (U) is the reciprocal of the sum of the five thermal resistances through which heat must pass: (1) the boiling liquid, (2) the dirt deposited by the boiling liquid, (3) the wall, (4) the dirt deposited by the heating fluid, and (5) the heating fluid. Each resistance is the reciprocal of the individual coefficient (α), corrected where necessary to refer to the same area, usually the outside. The estimation of these individual coefficients is dealt with below.

A. Heating fluid

Most evaporators are heated by condensing steam, which may have been generated for heating purposes or may be the exhaust from a turbine or the vapor generated in the previous effect of a series of evaporators. Whatever the source, the heat transfer coefficient may be estimated by the methods given in Sec. 2.6.2. If the source of some of the heat is a hot process fluid, the single-phase heat transfer coefficient can be estimated from Sec. 2.5.1 or 2.5.3 according to whether the hot fluid is inside or outside the tubes.

B. Wall

The heat transfer coefficient for the tube wall of a heat exchanger (referred to an area derived from the log mean of the inside and outside diameters of the tube) is given by

$$\alpha = \frac{\lambda}{Y} \qquad (1)$$

where y is the thickness of the tube wall and λ is the thermal conductivity of the material of the wall. Data on the thermal conductivity of solids can be found in Sec. 5.4.3. Materials of high thermal conductivity are desirable.

C. Dirt

Dirt is the most difficult item to assess in the design of a heat exchanger; it can only be based on past experience. On the side of the boiling fluid, the deposits result not only from the normal fouling processes but are reinforced and magnified, in many applications, by scaling from solids dissolved in the liquid. On the other hand, when evaporating a fairly corrosive liquid, the amount of fouling may be negligible. Theoretically the dirt coefficients can be calculated from Eq. (1), but in practice neither the thickness nor the thermal conductivity of the deposit can be even roughly estimated, the latter being very dependent on the composition and density of the deposit. The most useful source of information on dirt resistance is tests on existing evaporators, the estimated resistances of the wall and the two fluid films being subtracted from the measured total resistance to give the sum of the inside and outside dirt resistances. Such information will not be available for a

Many of the opinions expressed in this section are based on advice given by the staff of the Agricultural and Mond Divisions of Imperial Chemical Industries Limited and on information published by Chilton and Perry [1]. The author expresses his gratitude for this help and for permission to publish it.

© 1983 Hemisphere Publishing Corporation

new process, but advantage should be taken of any semitechnical or pilot plant, which should be planned so that data on fouling can be obtained using the same type of evaporator operating at similar temperatures. It has been found that all the information required to check a design can be obtained by carrying out a simple test on a single tube, of the same dimensions as those for the proposed full-scale design, provided with a heating jacket and fitted into equipment so that it can take a sample of the boiling process fluid. The tests should be carried out at the circulation velocity that w-ill be used in the full-scale evaporator; to achieve this with natural circulation, the vapor generation rate should equal the ultimate vapor generation rate per tube and the resistance of the external circuit should be the same as in the full-scale evaporator when expressed in terms of the velocity head in the tube. Achieved values of the boiling fouling coefficient range from 1 000 W/m^2 K for heavy scale deposits to 10 000 W/m^2 K for slight scale.

Steam from a steam main gives virtually no fouling, but a figure of 10 000 W/m^2 K may be used for safety. In multipleeffect evaporation this figure might be achieved for effects after the first provided that an efficient separator is installed; otherwise a lower figure will result from dissolved solids carried over.

D. Boiling liquid

There are five possible mechanisms of heat transfer in evaporators:

1. Single-phase liquid convection
2. Liquid falling film evaporation
3. Nucleate (pool) boiling
4. Two-phase convective boiling with subcooled or saturated liquid
5. Dry wall convection

For a given mass flow rate through an evaporator, the heat transfer coefficient is greater with mechanisms 2, 3, and 4 than with 1 and 5. The coefficient is so low with the last that this form of boiling is usually avoided.

The mechanisms are discussed below, and methods are given for estimating the heat transfer coefficient and the limits to operation in each mechanism.

(a) Single-phase liquid convection

The process is identical with that occurring in a heat exchanger in which there is no change of phase, so the same equations may be used to estimate the heat transfer coefficient, namely, those given in Sec. 2.5.1 or 2.5.3, according to whether the boiling fluid is inside or outside the tubes. This mechanism occurs in subcooled regions where the pressure of the liquid is greater than the vapor pressure, viz., in the calandria of a flash evaporator or at the inlet to vertical tubes.

There are two limits to this mechanism of boiling: either the temperature of the wall acquires a sufficient amount of superheat for nucleation to take place and the mechanism changes to type 3; or the bulk of the liquid reaches its boiling point and the mechanism then changes to type 4.

When estimating the single-phase convective heat transfer coefficient for an aqueous solution, it must be remembered that this will be less than that for water at the same temperature because the solution has a higher viscosity, a lower specific heat, and (possibly) a lower thermal conductivity. Typically the coefficient for a saturated aqueous solution of an inorganic salt will be 75-80% of that for water at the same temperature.

(b) Liquid falling film evaporation

When a film of liquid flows by gravity down a vertical heated surface, evaporation can take place from the free surface of the liquid; this is the reverse of condensation inside a vertical tube, and the same equations may be used to calculate the heat transfer coefficient (see Sec. 2.6.2).

Experimental data on the boiling heat transfer coefficient in falling film evaporators have been published by Whitt [5], Chun and Seban [6], and Chiesa et al. [7]. These experiments were carried out with clean water and single-component organic liquid without the addition of gas; they confirm the supposition that for the evaporation of falling films the heat transfer coefficients are similar to those for condensation.

When concentrating or crystallizing an aqueous solution, there is an additional resistance due to mass transfer in the liquid film. Experiments reported by Chun and Seban [8] on evaporation from falling films of water and brine (solutions of 7 and 14% initially) showed that the evaporation rates with 14% brine were about 10% less than those with water at the same flow rate and with the same temperature difference from wall to liquid. The limitations to this mechanism are that the flow rate must be sufficient to wet the wall (see Sec. 2.3.2) and the amount of superheat at the wall must be less than that for nucleation.

With upward flow of vapor and gas, flooding must be avoided (Sec. 2.3.2) and allowance must be made for the gas film resistance to mass transfer.

(c) Nucleate (pool) boiling

When the liquid in contact with a hot surface is superheated beyond a certain value, bubbles start to form; the rate increases rapidly with increasing superheat.

© 1983 Hemisphere Publishing Corporation

As these bubbles leave the surface, they convey heat rapidly from the surface. The equations for nucleate boiling are given in Sec. 2.7.2. Section 2.7.6 shows how nucleate boiling coefficients are much reduced with binary and multicomponent mixtures.

The equations for nucleate boiling are often for conditions of pool boiling, that is, for a heated surface in a stagnant liquid. In evaporators there is always a significant flow past the heated surface, in consequence of which the bubbles may be detached before they can grow fully. The estimation of the suppressed nucleate boiling coefficient is dealt with in Secs. 2.7.3, 2.7.4, and 2.7.5, according to the geometry. A simple correlation that has been found to give quite accurate predictions for the nucleate boiling of many fluids is given in Eq. 3.6.2(4).

(d) Two-phase convective boiling

The presence of bubbles in a flowing liquid increases the velocity of the liquid in contact with the heated surface and so enhances the heat transfer coefficient above that for single-phase flow, as shown in Sec. 2.7. If the wall is hot enough for nucleate boiling, the heat transfer coefficient for suppressed nucleate boiling may be added to that for two-phase convection.

Experimental data leading to the boiling heat transfer coefficient in a climbing film evaporator have been published by Doll-Steinberg [9]. Palen and Taborek [IO] have published heat transfer coefficients for hydrocarbons boiling outside tubes in horizontal kettle and internal reboilers, and have compared them with expected values for a single tube under the same conditions, thus showing the effects of the number of tubes and of their pitch. A method of predicting the bundle heat transfer coefficient is given in Eq. 3.6.2(5).

(e) Critical heat flux

As the quality of the flowing boiling liquid increases, a condition may be reached whereby liquid cannot reach the heated surface fast enough to replace the vapor formed. This is known as dryout. This is accompanied by a fall in heat transfer coefficient and possibly an increase in fouling, so it is important to find out whether this will occur and, if so, where.

Dryout occurs very suddenly in vertical in-tube boiling (see Sec. 2.7.3). Inside horizontal tubes, dryout occurs gradually as the top of the tube is alternately dried and splashed by waves in the liquid (see Sec. 2.7.4). In shell-side boiling the maximum heat flux is less than that for a single tube because tubes near the top of the bundle become starved of liquid [see Sec. 3.6.2A(f)].

(f) *Dry wall convection*

Under conditions of complete dryout, all of the liquid is in the form of mist and the heat transfer coefficient falls to roughly the value for the vapor only in single-phase flow. The vapor becomes superheated, possibly to the extent of significantly decreasing the temperature difference (see Sec. 2.7). The only type of evaporator where this mechanism of boiling should be allowed is once-through vaporizers.

References for Section 3.5.7 appear at the end of Section 3.5.8

© 1983 Hemisphere Publishing Corporation

3.5.8
Estimation of surface area

R.A. Smith

■ The required surface area of a heat exchanger is

$$A = \int \frac{d\dot{Q}}{U(T_h - T_c)} \quad (1)$$

where $\dot{Q}$ is the heat load, U is the overall heat transfer coefficient (from Sec. 3.5.7), T_h is the saturation temperature of the condensing steam, and T_c is the temperature of the boiling liquid. The steam temperature (T_h) is constant throughout an evaporator. In a heat exchanger without phase change, it can usually be assumed that U is constant and that the specific heat of the fluids is constant; thus, in a single-phase heater in which heat is supplied by isothermal condensation, the area required is

$$A = \frac{\dot{Q}}{U(T_{c,\text{out}} - T_{c,\text{in}})\log_e \left(\frac{T_h - T_{c,\text{in}}}{T_h - T_{c,\text{out}}}\right)} \quad (2)$$

If boiling is also isothermal, then with U constant the area is

$$A = \frac{Q}{U(T_h - T_c)} \quad (3)$$

In a horizontal shell-and-tube evaporator, with boiling inside or outside the tubes, or in a plate evaporator, Eq. (3) may be used, T_c being the boiling point of the liquid at the pressure on the centerline of the evaporator.

Many of the opinions expressed in this section are based on advice given by the staff of the Agricultural and Mond Divisions of Imperial Chemical Industries Limited and on information published by Chilton and Perry [1]. The author expresses his gratitude for this help and for permission to publish it.

In a vertical in-tube evaporator, U and T_c vary significantly along the tubes. Equation (2) may be applied to the preheating (lower) section of the tubes, but in the boiling (upper) section, U increases and T_c significantly decreases with increasing height, so Eq. (1) should be used. The boiling zone must be divided into sections. Equation (2) may be applied to each section; alternatively, Eq. (1) may be solved graphically by plotting $1/U(T_h - T_c)$ against Q, the area under the curve being equal to the required surface area of the evaporator.

The temperature profile in the preheating zone may be calculated from a heat balance, and it may be assumed that boiling starts when this temperature equals the boiling point corresponding to the local pressure, there being no significant superheating in commercial vaporizers and concentrators and none in crystallizers. A typical temperature profile is sketched in Fig. 1, the dashed curve showing the boiling point of the liquid in the preheating zone. It follows that a reduction in flow rate results in a more rapid initial temperature rise, a smaller temperature difference, and a smaller heat transfer coefficient before the onset of nucleate boiling; however, boiling starts sooner, so a larger proportion of the tube benefits from nucleate boiling. Similarly, lowering the head of liquid lowers the curve of boiling point and so also increases the boiling length. There is no simple way of predicting if either of these changes will improve performance.

Before attempting an accurate thermal design of an evaporator, it is advisable to carry out a rough design. Equation (3) may be used to determine the surface area *(A),* taking an approximate value of U based on pre-

© 1983 Hemisphere Publishing Corporation

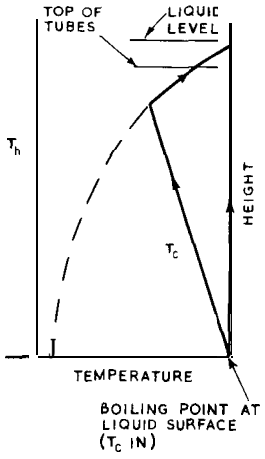

Figure 1 Variation of temperature with height inside a vertical in-tube evaporator.

vious experience. McCabe and Smith [2] give (in their Table 16-1) some typical overall heat transfer coefficients for clean water in various evaporators. Allowing for fouling and the reduced heat transfer properties of solutions, the following guidelines are suggested. For an aqueous solution in a forced-flow evaporator, U ranges from about 2 000 W/m^2 K for clean fluids down to about 700 W/m^2 K for fairly dirty fluids. The upper value may also be taken for the concentration of a clean aqueous solution in a falling film evaporator without any injection of gas. For an aqueous solution in a natural circulation evaporator, it may be assumed, for a first approximation, that U ranges from 1 000 W/m^2 K for clean fluids to 500 W/m^2 K for fairly dirty fluids, but these values depend very much on the amount of vapor generated per tube, as explained in the next paragraphs. Having decided on the length and diameter of the tubes, the number of tubes required can be calculated from the approximate value of the surface area. A more accurate procedure may then be used, based on the approximate dimensions, after which the length or number of tubes may be adjusted accordingly.

In natural circulation evaporators, design procedure is complicated by the necessity to determine the circulation rate by trial and error, as described in Sec. 3.6.5. It is important to remember that reducing the overall temperature difference reduces the natural circulation rate and so reduces the boiling heat transfer coefficient. Fouling has a similar effect.

When designing an evaporator from plant tests or research results, if U has been determined from the simple equation [Eq. (3)], this equation may be used to design the new evaporator because the errors from not calculating the correct temperature difference will cancel out at the same overall temperature difference.

Shellene et al. [11] describe tests on a highly instrumented thermosiphon reboiler of 10-m surface area with tubes of 19 mm diameter, 2.4 m long. The relationship between the heat flux and the overall temperature difference, under clean conditions, is plotted for water, several organic liquids, and some aqueous mixtures. With overall temperature differences in the range of 25 to 30°C, the achieved values of the overall heat transfer coefficient were about 3 000 W/m^2 K with water or isopropyl alcohol alone, but only 2 500 W/m^2 K with an equal mixture of the two liquids. With an equal mixture of water and glycerine, the coefficient was about 2 300 W/m^2 K; with benzene it was as low as 1 800 W/m^2 K. The coefficients fell at higher temperature differences, particularly in the presence of organic liquids, because the critical heat flux was being approached; there was evidence that the overall heat transfer coefficients would fall at lower temperature differences because of a reduction in the circulation rate.

Engelbrecht and Hunter [12] describe how they designed a climbing film evaporator for the concentration of a solution of aluminum sulfate and checked their design with a semitechnical scale evaporator, which contained two tubes of 28.5 mm bore, 6.1 m long. Operating at a pressure of 0.84 bar absolute and with a temperature difference of 75°C, the achieved heat transfer coefficient was 754 W/m^2 K.

The most important postwar advance in the design of heat exchangers has been the application of the computer to the design of reboilers and evaporators operating with natural circulation. Using the latest correlations for two-phase heat transfer and pressure drop, these programs easily perform the necessary trial-and-error calculations for the estimation of the circulation rate. The application of one of these programs has been described by Engelbrecht and Hunter [12], who used it to show that in their semitechnical evaporator (described above) fouling accounted for about half of the thermal resistance. It is urgent that future work be devoted to the testing of new evaporators before fouling has occurred, so that the correlations and computer programs can be checked, thus facilitating the estimation of achieved dirt resistance and avoiding troubles such as have occurred in the past from over- or underdesign of evaporators.

REFERENCES FOR SECTIONS 3.5.1-3.5.8

1. Chilton, C. H., and Perry, R. H., ***Chemical Engineer's Handbook,*** 5th ed., McGraw-Hill, New York, 1973.
2. McCabe, W. L., and Smith, J. ***C., Unit Operations of Chemical Engineering,*** 3d ed., McGraw-Hill, New York, 1976.

© 1983 Hemisphere Publishing Corporation

3. Davis, R. F., The Physical Aspects of Steam Generation at High Pressure and the Problem of Steam Contamination, *Proc. Inst. Mech. Eng. London,* vol. 144, pp. 198–216, 1940.
4. Heat Exchange Institute, ***Standards for Direct Contact Barometric and Low Level Condensers,*** 5th ed., New York, 1970.
5. Whitt, F. R., Performance of Falling-Film Evaporators, ***Br. Chem. Eng., vol.*** 11, pp. 1523-1525, 1966.
6. Chun, K. R., and Seban, R. A., Heat Transfer to Evaporating Liquid Films, *J. Heat Transfer*, vol. ***93,*** pp. 391-396, 1971.
7. Chiesa, C., Ciminale, A., Elias, G., and Silvestri, M., Misure sul coefficiente di scambio termico e sulle cadute di pressione di un lungo tubo verticale, ***La Termotechnica,*** vol. 28(3), pp. 140-145, 1974.
8. Chun, K. R., and Seban, R. A., Performance Prediction of Falling-Film Evaporators, *J. Heat Transfer*, vol. 94, pp. 432-436, 1972.
9. Doll-Steinberg, A., The Performance of a Climbing Film Evaporator, *Br. Chem. Eng.,* vol. 3, pp. 536-539, 1958.
10. Palen, J. W., and Taborek. J. J., Refinery Kettle Reboilers-Proposed Method for Design and Optimization, ***Chem. Eng. Prog., vol.*** 58(7), pp. 37-46, 1962.
11. Shellene, K. R., Sternling, C. V., Snyder, N. H., and Church, D. M., Experimental Study of a Vertical Thermosiphon Reboiler, *Proc. 9th Natl. Heat Transfer Conf., Seattle,* 1967.
12. Engelbrecht, A. D., and Hunter, J. B., Development of a Continuous Process for Concentration of Aluminum Sulphate Solutions in a Climbing Film Evaporator, *Conf. on Heat Transfer and the Design and Operation of Heat Exchangers, S.* Afr. Inst. Chem. Eng., 1974.

© 1983 Hemisphere Publishing Corporation

3.6
Shell-and-tube reboilers

Contents

3.6.1
INTRODUCTION, J. W. Palen **3.6.1-1**

A. General 3.6.1-1
B. Types and selection criteria 3.6.1-2

3.6.2
THERMAL DESIGN, J. W. Palen **3.6.2-l**

A. Kettle, internal, and horizontal thermosiphon reboilers 3.6.2-l
B. Axial-flow reboilers 3.6.2-6
C. Heating mediums 3.6.2-10

3.6.3
PRESSURE DROP, J. W. Palen **3.6.3-l**

A. General 3.6.3-l
B. Friction loss 3.6.3-l
C. Static head loss 3.6.3-l
D. Momentum change loss 3.6.3-l

3.6.4
SPECIAL DESIGN CONSIDERATIONS, J. W. Palen **3.6.4-l**

A. Fouling 3.6.4-l
B. Start-up and control 3.6.4-2
C. Very-wide-boiling-range mixtures 3.6.4-3
D. Operation near the critical pressure 3.6.4-3
E. Operation in deep vacuum 3.6.4-3
F. Sparging 3.6.4-3
G. Very low ΔT 3.6.4-3
H. Very high ΔT 3.6.4-4

3.6.5
CALCULATION PROCEDURES, J. W. Palen **3.6.5-l**

A. Example problem 3.6.5-l
B. Kettle reboiler 3.6.5-1
C. Horizontal thermosiphon reboiler 3.6.5-2
D. Vertical tube-side thermosiphon reboiler 3.6.5-3

Nomenclature for Sections 3.6.1-3.6.5 3.6.5-4
References for Sections 3.6.1-3.6.5 3.6.5-S

© 1983 Hemisphere Publishing Corporation

HEDH

3.6.1
Introduction

J.W. Palen

A. General

Boiling heat transfer equipment is frequently used in the process industries to supply vapors to distillation columns for separation of chemical components. In this application the heat exchangers are called reboilers, and this term is used for the equipment described in this section. Most process reboilers are of shell-and-tube construction. Boiling may take place on either the shell side (outside the tubes) or the tube side, depending on various requirements described in the next section. The heating medium is usually steam, but may also be a heat transfer service fluid or a gas, vapor, or liquid process stream. The rate of vaporization in a reboiler is sensitive to the available temperature difference because the boiling heat transfer coefficient itself is a strong function of temperature difference.

In cases where adequate ΔT is available, gross approximations in design are often made without serious consequence because vaporization can be easily adjusted to the required level by adjusting AT. However, continuing trends toward more efficient energy utilization require designs with lower AT s and less flexibility in heating medium operating conditions. This produces a requirement for better reboiler selection, much more accurate sizing of heat transfer surface, and better analysis and prediction of probable performance. Furthermore, even with adequate AT available, reboiler performance is always limited by a critical heat flux above which vapor blanketing takes place. Because of the complicated nature of the boiling process, very complex calculations are required for a comprehensive design, and use of computers has become standard practice for at least the more critical designs.

The boiling heat transfer coefficient decreases sharply with decreasing AT. Therefore, the trend toward smaller AT has prompted the use and further study of various types of enhanced boiling surfaces that provide more surface and/or more bubble nucleation sites at low AT. Use of some of these surfaces is described in later sections. One of the great unknowns in the use of enhanced surfaces and in reboiler design in general is the effect of fouling.

Because of the usually high values of heat transfer coefficients in reboilers, the fouling resistance assigned can represent a large part of the required heat transfer surface. However, it has been frequent practice in the past to assign arbitrarily high fouling factors to make up for gross simplifications in analysis of the boiling process. Actually, many process reboilers will operate with a very small amount of fouling if properly designed (e.g., see [1]) and the assigned fouling factor is often just a safety factor. When extremely large fouling factors are required, it is often a sign that the designer should investigate other reboiler geometries, higher velocities, or lower wall temperatures.

Development of adequate design techniques for reboilers has suffered in the past from a lack of data in the open literature on multitube units. Only a few articles (see for example [2–4]) have appeared presenting performance of actual process reboilers. The articles by Palen et al. [5,6] present a summary of principles of reboiler operation that have been developed from a comprehensive set of plant data. The procedures sug-

© 1983 Hemisphere I blishing Corporation

gested in this review are consistent with actual performance trends observed, and the literature methods recommended are those that are most consistent with industrial proprietary results. The next section discusses the basic types of reboilers and their applications.

B. Types and selection criteria

Reboiler types may be divided into cross-flow and axial-flow categories. Cross-flow reboilers all have boiling on the shell side. The common types are referred to as kettle, internal, and horizontal thermosiphon reboilers. Axial-flow reboilers have flow in the direction of the tube axis. The most common type is the vertical thermosiphon. If thermosiphon circulation is not adequate, a pump is used to feed the reboiler, which is then called a forced-flow reboiler and may be either vertical or horizontal. Usually, both vertical thermosiphon and forced-flow reboilers have boiling on the tube side, but shell-side boiling is also used in special applications. The following sections further describe the various reboiler types and their advantages and disadvantages.

(a) Kettle reboilers

I. Characteristics

Kettle reboilers (see Fig. 1) are characterized by an enlarged shell in which separation of the liquid and vapor phases may be achieved. Liquid level is maintained over the top of the bundle usually by a vertical baffle. Liquid draining over the baffle is taken off as the distillation column bottoms product. The vapor is taken overhead to the column. The bundle is usually two tube-pass U tubes, but may be a multitube-pass floating head.

II. Advantages

Kettle reboilers are insensitive to hydrodynamics and, therefore, relatively reliable and easy to size. The problem of how to calculate two-phase flow pressure drop is eliminated. This means highest reliability in deep vacuum and near the critical pressure where hydrodynamics are most difficult to predict and least favorable to performance. Very high heat fluxes may be obtained by sufficiently increasing tube pitch. Efficient operation is obtained at low ΔT. Integral low-finned tubes and other enhancement surfaces may be used.

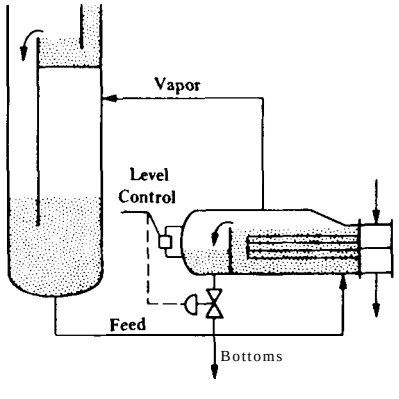

Figure 1 Schematic arrangement for a kettle reboiler [32].

III. Disadvantages

Kettle reboilers are dirt collectors and often the worst of all reboilers for fouling service. Because of the total vaporization, nonvolatiles tend to accumulate in the shell unless an adequate bottoms draw-off is maintained. This concentration effect can become a problem if the bottoms stream contains even small amounts of highly fouling or corrosive components. Because of the mixing in the shell, the temperature profile is very difficult to calculate accurately for wide-boiling-range fluids. The safest and most reliable approach is to base the effective AT on the vapor temperature, which causes a large penalty in surface for wide-boiling-range fluids at low AT. The oversized shell is, of course, expensive and often provides no advantage.

IV. Best applications

Best applications are for low-pressure, narrow-boiling-range, clean fluids at very low ΔT or at high ΔT, and for operation near critical pressure when, regardless of shell cost, reliable operation is very important.

(b) Column internal reboilers

I. Characteristics

Characteristics of column internal reboilers (see Fig. 2) are the same as for kettle reboilers except that the bundle is inserted directly into the distillation column bottoms reservoir.

II. Advantages

Advantages are the same as for kettles, with even fewer hydraulics problems. These are the least expensive of all reboilers, because the shell and connective piping are eliminated.

III. Disadvantages

Disadvantages are the same as for kettle reboilers except for the absence of the oversized shell. However,

© 1983 Hemisphere Publishing Corporation

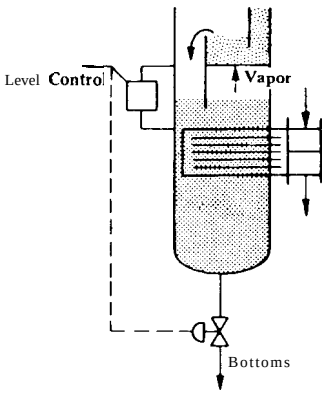

Figure 2 Schematic sketch of an internal reboiler [32].

the amount of surface area that can be installed is limited.

IV. Best application

Applications are similar to those of kettle reboilers.

(c) Horizontal thermosiphon reboilers

I. Characteristics

Horizontal thermosiphon reboilers (see Fig. 3) usually have TEMA X-, G-, or H-type shells, although E-type shells are sometimes used. The boiling fluid is on the shell side and discharges as a two-phase mixture through the exit piping into the column. The driving force for circulation is provided by the density difference between the liquid in the column reservoir and the two-phase mixture in the reboiler and exit piping. The heating medium flows on the tube side, which may be single or multipass.

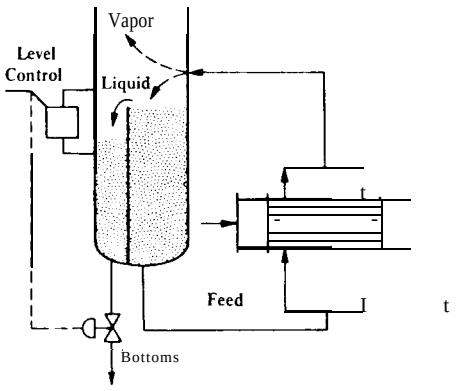

Figure 3 Typical schematic arrangement for horizontal thermosiphon reboiler [32].

II. Advantages

Because of the higher circulation rate, the effective ΔT is more favorable for boiling-range mixtures than is the case with kettle reboilers. The higher velocity and lower exit vapor fraction prevent accumulation of unwanted residual components in the reboiler and tend to decrease the fouling potential. Relatively good performance is expected for viscous fluids because of high shear and turbulent mixing. Because of the horizontal orientation and controllable flow area, a relatively low static head is required for circulation.

III. Disadvantages

Fouling, such as occurs, is on the shell side and difficult to clean. Vapor blanketing and localized dryout are possible at high heat fluxes because of the required baffling and tube supports. Multiple nozzles and expensive manifolded piping are required for good flow distribution for large units.

Wide-boiling-range fluids may require horizontal baffles (G- or H-shell construction) to prevent flashing of light components above the inlet nozzles and concentration of heavy components at the ends. Presently there are fewer data for these units than for other types. Maximum heat flux may be limited by bundle vapor blanketing or choke flow instability, but no tested design relations are presently available. Hydrodynamics problems are ill defined and could cause trouble in vacuum and at very high pressure.

IV. Best application

Best applications are for boiling-range fluids at moderate pressure with low to moderate velocity-controlled fouling tendencies, low available static head, and moderate AT. These reboilers should not be designed to high heat fluxes unless supporting data are available.

(d) Vertical tube-side thermosiphon reboiler

I. Characteristics

Boiling in vertical tube-side thermosiphon reboilers (see Fig. 4) is inside vertical tubes with the heating medium in a TEMA E-type shell. Two-phase flow is discharged through the exit piping at high velocity into the column. Because of the high exit piping velocity, the pipe diameter must be larger than is normally used for E-type exchangers and should be as short as possible. The cross-sectional flow area of the exit piping should be at least as large as the total cross-sectional area of the tubes, unless careful calculations are made to ensure that the

© 1983 Hemisphere Publishing Corporation

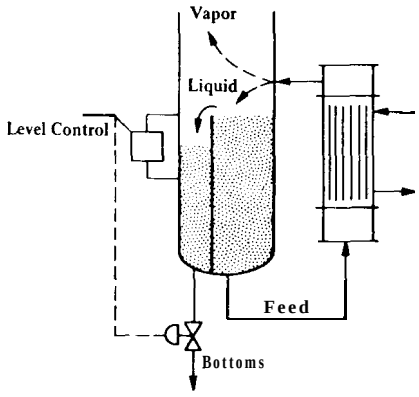

Figure 4 Typical arrangement for a vertical tube-side thermosiphon reboiler [32].

piping pressure drop is less than 30% of the total. Both long-radius elbows with axial exit nozzles and side-exit tee arrangements are used. Tests indicate that performance is not very sensitive to the type of exit piping configuration, but is very sensitive to the minimum flow area. Driving head for flow is provided by a liquid level in the column that is usually maintained at about the top of the tubesheet. For vacuum service some advantage is obtained by lowering the liquid level to about 050.8 of the length of the tubes, which decreases the effective subcooling of the liquid feed to the reboiler. A valve or orifice is sometimes used in the inlet liquid line to dampen out possible instabilities in the flow loop that can occur at low pressure and high heat flux. For best operation the exit vapor weight fraction should be in the range of about 0.10-0.35 for hydrocarbons and in the range of 0.02-0.10 for water and aqueous solutions. Proper tube diameter selection is important for adequate circulation. Tube outside diameter (at normal tube wall thickness) should be greater than 25 mm for low-pressure operation and wide-boiling mixtures, but can be as small as 19 mm for high pressures with narrow-boiling-range fluids. Tube length had been held to around 3.7 m or less in the past, but successful operation with tube lengths up to 6 m has been reported. For long tube lengths, careful design is required to assure adequate circulation to prevent dry out.

II. Advantages

Vertical tube-side thermosiphon reboilers tend to minimize fouling if well designed, as a result of high flow velocity and a relatively high heat transfer coefficient in the tubes, which lowers the wall temperature. Such fouling as does occur is on the tube side and relatively easy to brush out. However, the vertical orientation may make this operation inconvenient. The TEMA E-type shell is relatively inexpensive, as is the connecting piping if it is kept short as recommended.

The temperature profile is beneficial for wide-boiling-range mixtures, since a pure counter-flow arrangement is possible. For narrow-boiling-range mixtures with sensible heating mediums, cocurrent flow may be used to provide high vapor generation at the bottom of the tube and improve circulation.

Because of the simple flow geometry, two-phase flow distribution is less of a problem than for horizontal shell-side thermosiphons.

III. Disadvantages

These units can be very sensitive to operating conditions and are difficult to design properly in deep vacuum, at very high pressure (near the critical), and for wide-boiling-mixtures with high liquid viscosity. In such cases it is better to use a kettle-type reboiler, which is less sensitive to hydrodynamics unless a reliable, rigorous computer program is available for design. Because of the vertical orientation, the column skirt height must be higher than for other types to supply the static head, and consequently mechanical cleaning may be awkward.

Maximum heat flux is usually lower than for kettle reboilers and more difficult to predict, so design to very high heat fluxes is risky. Also, at very low heat fluxes, there may be insufficient pumping action for good circulation. For this reason and because of the inherent boiling-point elevation imposed by the large static head, these units are a poor selection for very low ***AT service.***

IV. Best applications

Best applications are for pure-component or narrow to moderately wide-boiling-range fluids with potential

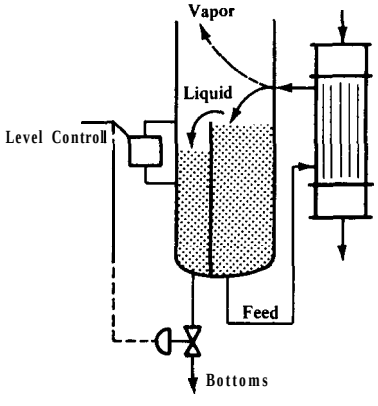

Figure 5 Typical arrangement for a vertical shell-side thermosiphon reboiler [32].

© 1983 Hemisphere Publishing Corporation

fouling tendencies in the medium-pressure range (not deep vacuum nor near critical) and at moderate AT.

(e) Vertical shell-side thermosiphon reboiler

I. Characteristics

Vertical shell-side thermosiphon reboilers (see Fig. 5) are similar to vertical tube-side thermosiphons but with boiling fluid on the shell side. Shell-side baffling should be constructed to provide as much longitudinal flow and as little flow restriction as possible. Triple-segmental baffles or rod-type tube supports are recommended to prevent tube vibration.

II. Advantages

Vertical reboilers may be used in special cases where a thermosiphon is wanted but it is impractical to put the heating medium on the shell side. An example is a waste heat boiler for which the hot fluid is corrosive or requires special metallurgy because of its temperature.

III. Disadvantages

Very careful consideration must be given to boiling-side flow distribution to avoid dead areas or recirculating areas where either vapor or high-boiling-range components may accumulate. Design information is limited. Feedback from the field indicates that most problems have to do with local overheating resulting from vapor accumulation. This can be a serious problem at the top tubesheet unless care is taken to provide for uniform high-velocity flow of the two-phase mixture past the tubesheet.

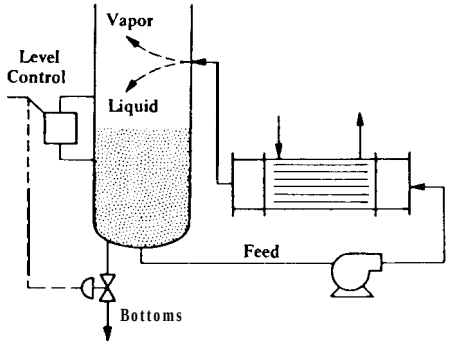

Figure 6 Schematic arrangement for forced blow reboilers [32].

N. Best application

The best application of these reboilers is for vaporization of pure components at moderate pressures and moderate **AT** where the heating medium must be on the tube side.

(f) *Forced flow reboilers*

I. Characteristics

Forced flow reboilers (Fig. 6) may be either vertical or horizontal, with boiling usually on the tube side. Flow is provided by a high-capacity pump so that vaporization is usually less than 1%, and may be suppressed completely with flashing across a valve in the exit piping.

II. Advantages

Occasionally this is the only economical way to boil severely fouling viscous fluids. Fouling can be greatly diminished if velocity is maintained high enough and vaporization low enough. However, velocities required for effective performance may be as high as 5-6 m/s.

III. Disadvantages

For effective velocities, pump cost and energy consumption are very high and must be offset by elimination of severe maintenance problems to be economical.

N. Best application

The best application of forced flow reboilers is for severely fouling or extremely viscous fluids for which no other approach is satisfactory.

(g) Selection guide

In Table 1 the four main types of reboilers are rated against certain process conditions according to rating categories. It should be clearly understood that any general recommendation for selection of reboiler type is certain to be wrong in some specific applications, and that each case should be carefully evaluated according to the specific economic and process factors which apply. However, Table 1 basically agrees with present good practice, and may be useful for initial screening of types. In Table 1, the designation Rd (risky unless carefully designed) does not necessarily mean that the reboiler is unsuitable, but rather that it requires detailed analysis to ensure that some hydrodynamics or thermal constraints are not violated.

© 1983 Hemisphere I blishing Corporation
HEDH

Table 1 Reboiler selection guide

Process conditions	Kettle or internal	Reboiler type: Horizontal shell-side thermosiphon	Reboiler type: Vertical tube-side thermosiphon	Reboiler type: Forced flow
Operating pressure				
Moderate	E	G	B	E
Near critical	B-E	R	Rd	E
Deep vacuum	B	R	Rd	E
Design ΔT				
Moderate	E	G	B	E
Large	B	R	G-Rd	E
Small (mixture)	F	F	Rd	P
Very small (pure component)	B	F	P	P
Fouling				
Clean	G	G	G	E
Moderate	Rd	G	B	E
Heavy	P	Rd	B	G
Very heavy	P	P	Rd	B
Mixture boiling range				
Pure component	G	G	G	E
Narrow	G	G	B	E
Wide	F	G	B	E
Very wide, with viscous liquid	F-P	G-Rd	P	B

[a]Category abbreviations: B, best; G, good operation; F, fair operation, but better choice is possible; Rd, risky unless carefully designed, but could be best choice in some cases; R, risky because of insufficient data; P, poor operation; E, operable but unnecessarily expensive.

References for Section 3.6.1 appear at the end of Section 3.6.5.

© 1983 Hemisphere Publishing Corporation

3.62 Thermal design

J.W. Palen

A. Kettle, internal, and horizontal thermosiphon reboilers

Kettle, internal, and horizontal thermosiphon reboilers are similar in that they have heat transfer to a vaporizing two-phase mixture flowing across a tube bundle. Nucleate boiling and convective boiling mechanisms are both effective in the boiling process. For kettle reboilers, convective circulation takes place in the enlarged shell, with mostly vapor going overhead. For the thermosiphon, a two-phase mixture is discharged from the reboiler and convective circulation involves the external piping and column liquid reservoir. Nevertheless, the heat transfer processes are similar in both types, so thermal design is covered in the same section. The following elements are important.

(a) Single-tube nucleate boiling

The nucleate boiling mechanism has considerable influence on the behavior of kettle and horizontal thermosiphon reboilers, so that a correlation for nucleate boiling on single tubes is a necessary (but not sufficient) component for design. For a more detailed discussion of nucleate boiling theory, refer to Sec. 2.7.2.

The nucleate boiling heat transfer coefficient can be described by either of the two following forms, both of which may be convenient in different types of calculations:

$$\alpha_{nb} = C_1(\Delta T_b)^{m_1} \quad (1)$$

$$\alpha_{nb} = C_2(\dot{q})^{m_2} \quad (2)$$

Usually, for typical, nonenhanced commercial tubes, the value of m, ranges roughly around 2-3. Since $q = \alpha$ AT, the corresponding value of m_2 ranges around $\frac{2}{3}$ to $\frac{3}{4}$. For a large number of published nucleate boiling correlations, α is proportional to $(\dot{q})^{0.7}$.

A simple correlation in the literature that has been found by Palen et al. [5] and by Starczewski [7] to give very reasonable results for a wide range of pure fluids is the Mostinski correlation [8], evaluated in Fig. 1.

$$\alpha_{nb1} = 0.004\,17 p_c^{0.69} \dot{q}^{0.7} F_p \quad (3)$$

where α_{nb1} = nucleate boiling heat transfer coefficient for a single tube, W/m² K
p_c = critical pressure, kPa
$\dot{q}$ = heat flux, W/m²
F_p = pressure function correction factor

The pressure function F_p is given by Mostinski as an empirical polynomial curve fit of a large amount of data over a reduced pressure range from deep vacuum to near the critical [see Eq. 2.7.2(12)].

However, the data in the range near the critical pressure are quite scattered, and the amount of uncertainty in this region may be too great for a reliable design method. A check of the overall method proposed in this section against the plant data of [2] shows that better prediction is obtained if both the second and third terms of Eq. 2.7.2(12) are omitted. In view of this and in the interest of presenting a reliable if somewhat conservative method, it is recommended that for kettle and horizontal thermosiphon reboiler design the following simplified version of F_p be used in Eq. (3), evaluated in Fig. 2.

© 1983 Hemisphere I blishing Corporation

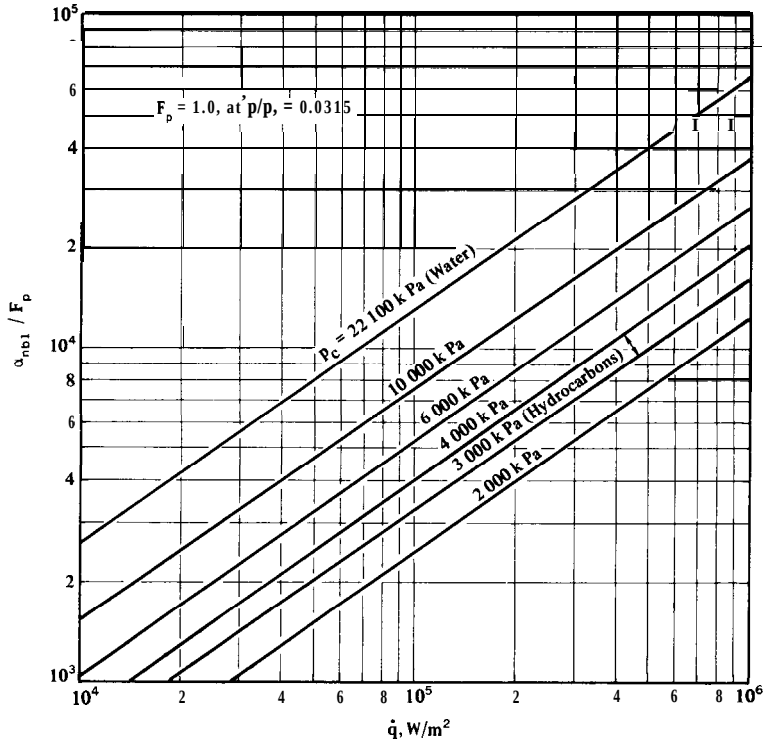

Figure 1 Nucleate boiling heat transfer coefficient, Eq. (3).

$$F_p = 1.8 \left(\frac{p}{p_c}\right)^{0.17} \tag{4}$$

Other single-tube nucleate boiling correlations are discussed in Sec. 2.7.2 and may be substituted for Eq. (3) at the decision of the designer. It is especially recommended that for refrigerants the specific University of Karlsruhe equations given in Sec. 2.7.2 be used. For other fluids also, if specific data are available, empirical equations of the form of Eq. (1) may be used. A list of these for selected fluids is given by Fair [9].

(b) Bundle-induced convection effects

Because of the presence of surrounding tubes, the effective velocity of the two-phase flow past any given tube is greater and the effective liquid film thickness is less than for a single tube. Consequently, the heat transfer coefficient for a bundle can often be considerably greater than that for boiling from a single tube under otherwise identical conditions. This is shown by Nakajima and Morimoto [10], Montgomery [11], Wallner [12], Palen et al. [5], and others and is further dis-

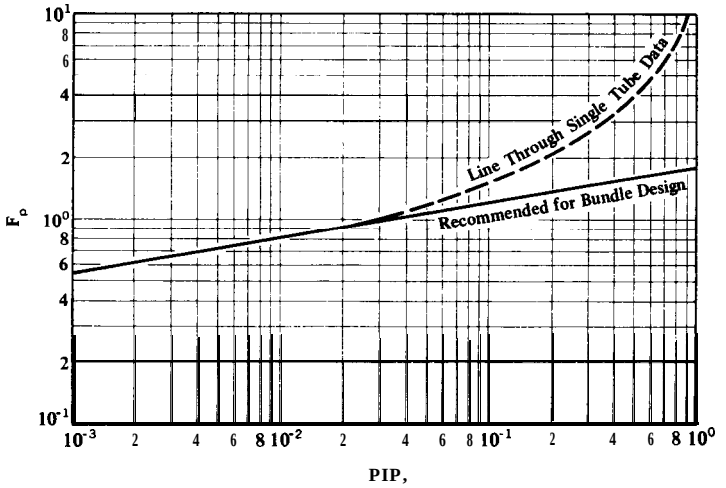

Figure 2 Pressure correction factor for nucleate boiling, Eq. (4).

© 1983 Hemisphere Publishing Corporation

cussed in Sec. 2.7.5. Unfortunately, the amount of natural circulation and hence the effective vapor velocity is very difficult to determine, especially for kettle reboilers, for which circulation is entirely in the shell. Proprietary methods are available for determining a bundle boiling heat transfer coefficient that accounts for bundle convective effects in the form

$$\alpha_b = \alpha_{nb1} F_b F_c + \alpha_{nc} \quad (5)$$

The factor F_b is a function of bundle geometry and can easily range as high as 2-3 for large bundles. However, in the absence of specific data, it is recommended to let F_b = 1.5. This will give a reasonable design that will be on the safe side, but not nearly so much so as previously used rules of thumb (for example [15]). For special low-AT refrigeration evaporators, F_b may be even greater than 3.0, and more detailed recommendations given in Sec. 2.7.5 should be followed. The factor F_c is a correction for mixture effects that is 1.0 for pure components and is discussed in Sec. (d).

The heat transfer coefficient for liquid-phase natural convection in bundles, α_{nc}, is approximately 250 W/m² K for hydrocarbons and around 1 000 W/m² K for water and does not become significant except at low ΔT (ΔT_b < 4 K). For more accuracy, a correlation is recommended in [14].

(c) Externally induced convection effects

For horizontal thermosiphon reboilers, a circulation rate through the reboiler can be obtained by a pressure balance between the available static head and the pressure drop in the reboiler and piping as shown in a later section. Once the two-phase friction pressure drop is obtained, the convective boiling heat transfer coefficient may be estimated by the general approach suggested by Taborek [13].

$$\alpha_{cb} = \left(\frac{\Delta p_{tpf}}{\Delta p_\ell}\right)^{m_3} \alpha_\ell \quad (6)$$

The coefficient α_ℓ is estimated from an ideal tube bank convective heat transfer coefficient based on liquid flow alone. The exponent m_3 ranges from about 0.4 to 0.5, and an average value of 0.45 may be used for approximation.

The presently recommended procedure for horizontal thermosiphons is to calculate α_{cb} from Eq. (6) and α_b from Eq. (5) and use the higher value for design. As a much quicker approximation on the safe side, reasonable results can be obtained by using just α_b for both horizontal thermosiphon and kettle reboilers.

(d) Mixture effects

It is now well known that the apparent heat transfer coefficient for boiling mixtures can be much lower than for single components boiling alone. A qualitative discussion of this effect is given in [5], and a detailed discussion of observations from the literature is given in Sec. 2.7.6. For many specific binary mixtures, the correction for such effects can be obtained as described in that section. For most process fluids (more than two components), a more generally applicable correction is necessary. An approximation that was tentatively proposed for reboiler design by Palen and Small [14] was later found to give reasonable results when compared with other data described in [5]. This relationship is shown in Fig. 3 and is given as follows:

$$F_c = \exp\ [-0.027\ \mathrm{BR}] \quad (7)$$

with the limit if F_c < 0.1, let F_c = 0.1, where F_c is the mixture correction factor, Eq. (5), and BR is the boiling range (difference between dew point and bubble point), K.

Although improved proprietary methods (also based on boiling range) have been developed, Eq. (7) is recommended as a reasonable published approach that can be used for multicomponent systems. It should be recognized that prediction of heat transfer to wide-

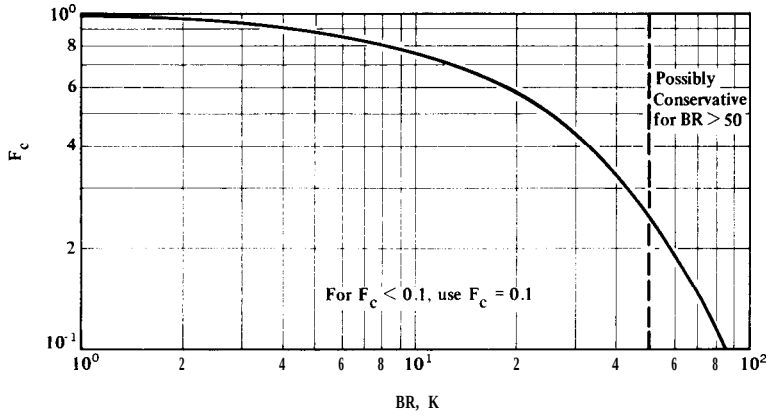

Figure 3 Mixture correction for nucleate boiling, Eq. (7).

© 1983 Hemisphere Publishing Corporation

boiling mixtures is presently in a very uncertain state and some safety factor should be applied in critical cases. An alternative approach that has been used in the past is to assign a constant value to the boiling heat transfer coefficient for hydrocarbon mixtures. Kern [15] proposed that for $\Delta T_b > 4.5$ K,

$$\alpha_b \cong 1\,700\ \mathrm{W/m^2\,K}\ (300\ \mathrm{Btu/h\,ft^2\,F}) \qquad (8)$$

A comparison with the above-recommended method indicates that Eq. (8) will not always give conservative results, especially for wide-boiling-range mixtures. Past success of this approach may have been due to arbitrary assignment of excessive fouling factors. Use of Eq. (5) with Eq. (7) should give more accurate results over a wider range of conditions.

(e) Effective mean temperature difference

For narrow-boiling-range mixtures and pure components, the boiling-side temperature is nearly constant and the log mean temperature difference is theoretically correct and recommended. If there is a significant temperature rise across the reboiler due to the boiling range of the fluid, the temperature profiles in either a kettle or horizontal thermosiphon reboilers are such that a counter-flow log mean ΔT may give too optimistic results, as explained in [5]. For the kettle reboiler, unless operating data are available, it is recommended to use a log mean temperature difference based on the ***exit vapor temperature.*** This most conservative approach gave the best results when tested against available data for wide-boiling-range mixtures in laboratory reboilers. For a horizontal thermosiphon reboiler, because of improved circulation, the above approach will be too conservative, whereas the use of a counter-flow log mean ΔT will be too optimistic. It is therefore recommended as a first conservative approximation to use a cocurrent flow log mean ΔT. As a less conservative alternative, the normal single-phase mean temperature difference corrections for cross-flow or TEMA G shells could be considered.

For large bundles and for horizontal thermosiphon reboilers with a large static head, the boiling point of the fluid will be increased because of the imposed static head. Above atmospheric pressure this is normally a negligible effect unless ΔT is very small. For vacuum reboilers, however, the boiling temperature for MTD calculation should be based on the mean pressure in the reboiler, including the imposed static head rather than on the system operating pressure.

(f) Critical heat flux and film boiling

Whenever possible, it is recommended to use a low enough AT to avoid film boiling due to the low heat transfer coefficients and corresponding high wall temperatures.

The basic phenomenon of critical heat flux is explained in Sec. 2.7.2. For tube bundles, the critical heat flux is a strong function of bundle geometry. The correlation of Palen and Small [14] is discussed in Sec. 2.7.5. This relationship can also be expressed in a more general form as follows:

$$q_{b,\max} = q_{1,\max}\phi_b \qquad (9)$$

The maximum heat flux for a single tube, $q_{1,\max}$, can be obtained from the Kutateladze-Zuber or other relationships described in Sec. 2.7.5 or can be estimated with sufficient accuracy for most design purposes from the reduced property correlation of Mostinski [8], evaluated in Fig. 4.

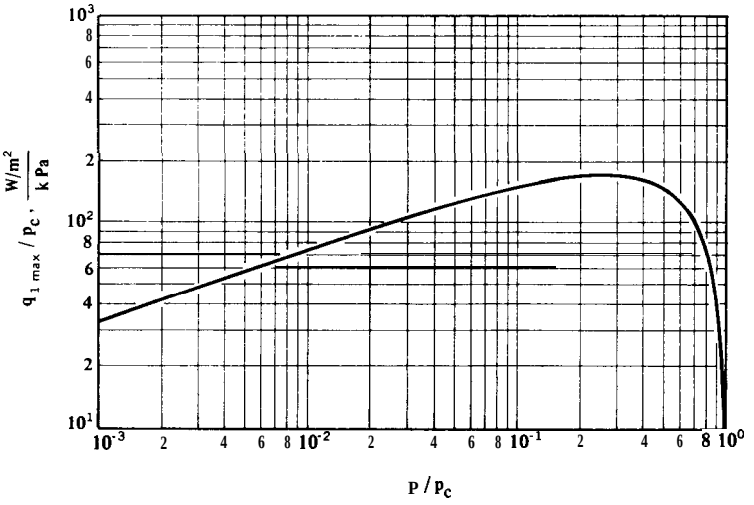

Figure 4 Maximum heat flux for boiling outside a single horizontal tube, Eq. (10).

© 1983 Hemisphere Publishing Corporation

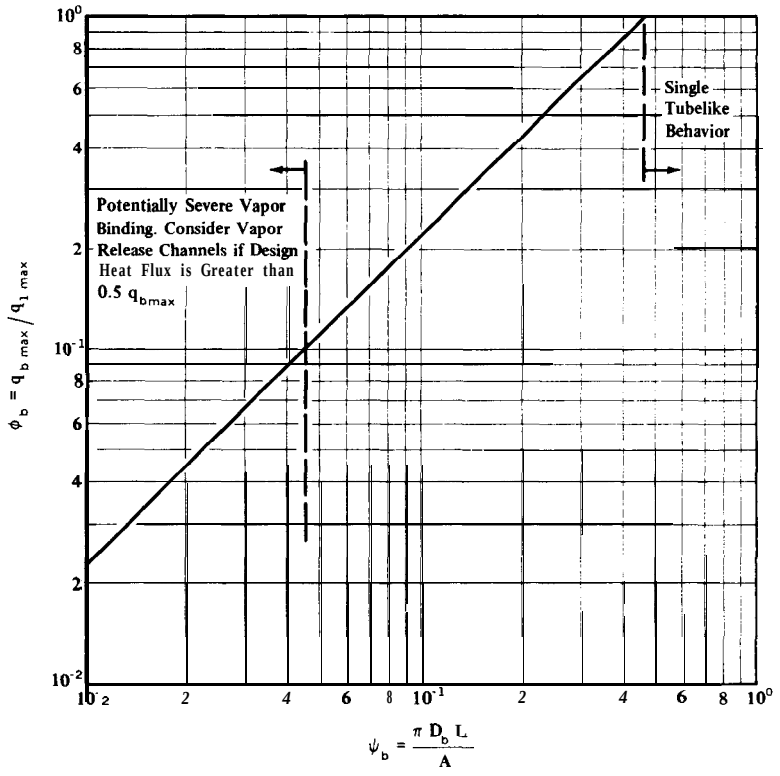

Figure 5 Bundle correction to single-tube maximum heat flux, Eq. (12).

$$q_{1,\max} = 367 p_c \left(\frac{p}{p_c}\right)^{0.35} \left(1 - \frac{p}{p_c}\right)^{0.9} \tag{10}$$

where $\dot{q}_{1,max}$ = maximum heat flux for single tube, W/m²
p = pressure, kPa
p_c = critical pressure, kPa

The bundle correction factor ϕ_b from Eq. (9) can be shown to be related to a dimensionless bundle geometry parameter,

$$\psi_b = \frac{\pi D_b L}{A} \tag{11}$$

This factor is physically equal to the perimeter of the bundle divided by the heat transfer surface contained within, and is equal to 1.0 for a single tube. The relationship between ϕ_b and ψ_b, which was determined in [14] from limited field data, was found by later proprietary studies [5] to be conservative. However, it represents a reasonable, safe design value and is recommended in lieu of better published information (see Fig. 5):

$$\phi_b = 2.2\psi_b \tag{12}$$

with the limit $\phi_b \leqslant 1.0$.

As shown by Eq. (12), for bundles with ψ_b greater than $1/2.2, \phi_b = 1.0$, and the maximum heat flux for the bundle is approximately as high as for a single tube. This is demonstrated in the classic test by Comley [16]. As tubes are placed closer together or the bundle diameter increases, the potential for vapor blanketing and liquid starvation of the bundle increases and ϕ_b decreases, producing a lower maximum heat flux. It is recommended that for $\phi_b < 0.1$, vapor release channels should be considered to promote vapor flow out of the bundles, unless design heat flux is less than $0.5\dot{q}_{b,max}$.

If the design AT is such that the design heat flux is greater than $\dot{q}_{b,max}$ from Eq. (9), the bundle design should be changed if possible by increasing bundle length and decreasing bundle diameter or by increasing tube pitch. If this is not possible and the AT cannot be decreased because of process considerations, it may be necessary to design for film boiling. This will mean a much lower heat transfer coefficient and higher wall temperature, but sometimes the economics of using an available high-temperature heating medium will require such a design. The ***AT*** should be high enough so that complete film boiling rather than transition boiling is obtained. Design in the transition boiling regime is not recommended because of reverse control characteristics (increasing AT produces decreased heat flux). Relationships for the minimum AT for film boiling and the film boiling heat transfer coefficients for single tubes as given in Sec. 2.7.5 may be applied for design for bundles and will be somewhat on the safe side.

© 1983 Hemisphere Publishing Corporation

(g) Vapor-liquid disengagement

For kettle reboilers, the shell is oversized to cause disengagement of the liquid so that vapor alone is discharged from the overhead nozzle. In practice, it is probable that some entrainment always occurs. If dry vapor is really required, as in the case of a compressor feed, additional protection, such as mechanical mist eliminators, is needed. The basic relationship used in sizing separator drums is

$$V_v = K_e \left(\frac{\rho_\ell - \rho_v}{\rho_v}\right)^{0.5} \tag{13}$$

The vapor velocity V_v, above which a certain amount of entrainment is obtained, is a function of the entrainment coefficient K_e, which usually ranges between 0.03 and 0.09 m/s and is itself a function of the maximum amount of entrainment permitted and ratio of surface tension to density.

An empirical relationship that has been used successfully in the past is

$$\mathrm{VL} = 0.064\ 5\rho_v \left(\frac{\sigma}{\rho_\ell - \rho_v}\right)^{0.5} \tag{14}$$

where VL = vapor load, kg/s m^3 (vapor rate, kg/s, divided by volume of vapor space required to prevent entrainment, m^3)

A helpful nomograph for solving Eq. (14) is given in [14].

(h) Flow distribution and hydraulics

For both kettle and horizontal thermosiphon reboilers, steps should be taken to assure adequate longitudinal flow distribution. Above a certain length-to-bundle diameter ratio, the number of liquid and vapor nozzles should be increased. As a rule of thumb, the number of pairs of nozzles (liquid and vapor) is given by

$$N_N = \frac{L}{5D_b} \quad \text{(round up)} \tag{15}$$

For kettle reboilers, the liquid and vapor piping should be sized large enough so that the liquid level in the kettle is not suppressed by flow resistance in the piping. A method for checking the liquid static head required for bundle coverage with a given kettle reboiler piping configuration is given in [14]. For a horizontal thermosiphon, hydraulic calculations are similar to those for a vertical thermosiphon and are covered in detail in a subsequent section.

(i) Finned or enhanced tubes

It was shown in [5] that low integral finned tubes are very effective for pool boiling-type reboilers at low ΔT. Not only is the finned surface fully effective, but the boiling heat transfer coefficient is also increased by as much as 50–100% because of improved nucleation capabilities provided by the manufacturing process. At high ΔT the effectiveness is lost as a result of vapor blanketing of the fin valleys and relative dominance of wall, fouling, and heating medium resistances,

Other special surfaces that produce improved nucleation capabilities can also be very effective at low ΔT. Performance of sintered surface tubes in kettle reboilers is described in [5]. For more detail on enhanced surface in boiling, see Sec. 2.7.7.

B. Axial-flow reboilers

Axial-flow reboilers have flow either in the tubes or longitudinally outside the tubes. Two-phase flow relationships for channel flow are used for design. The most common type is the vertical thermosiphon reboiler with vaporization in the tubes. Flow rate is predicted by a trial-and-error balance of available static head against pressure drop in the reboiler and piping, as described in a later section. The following considerations are necessary for design.

(a) Convective and nucleate boiling

For most designs, the flow regimes in the tube are such that both convective and nucleate boiling mechanisms are present and are combined in the following form:

$$\alpha_b = s\alpha_{nb} \quad ,\alpha_{cb} \tag{16}$$

Chen [17] gives a good description of the convective and nucleate boiling mechanisms and presents a correlation that has been popularly accepted as one of the best available. The Chen method is described more fully in Sec. 2.7.3. An earlier, very similar approach which has been used successfully for design for a number of years in the process industries was presented by Fair [9].

The nucleate boiling heat transfer coefficient correlation recommended by Chen is the Forster-Zuber correlation (see Sec. 2.7.3). Fair does not recommend a general correlation, but lists a number of specific constants from measured single-tube nucleate boiling curves. Neither author gives a recommendation for a mixture correction. For general application, a reasonable approximation can be obtained using Eq. (3) for α_{nb1} and applying F_c from Eq. (7) as follows:

$$\alpha_{nb} = \alpha_{nb1} F_c \tag{17}$$

The nucleate boiling suppression factor s may be obtained as shown in Sec. 2.7.3.

The convective boiling heat transfer coefficient can be obtained from the general relationship given in

© 1983 Hemisphere Publishing Corporation

Eq. (6). However, since the ratio $\Delta p_{tpf}/\Delta p_\ell$ is usually correlated in terms of X_{tt}, most correlations are presented as

$$\frac{\alpha_{cb}}{\alpha_\ell} = f(X_{tt}) \tag{18}$$

A curve fit of the Chen correlation, which is recommended as one of the best in the open literature, is given in Sec. 2.7.3.

At the entrance of the reboiler, the liquid is usually subcooled to some extent because of the static head imposed on it, so a subcooled boiling zone of varying length exists before the two-phase region starts. A reasonable estimation of the heat transfer coefficient in the subcooled boiling zone can be obtained by using Eq. (16) with s = $(\Delta T_b/\Delta T_0)$, $\alpha_{cb} = \alpha_\ell$, and α_{nb} based on the temperature difference between the tube wall and the *saturation* temperature of the liquid at the given local pressure, ΔT_b. The term ΔT_0 is the difference between the tube wall and the subcooled bulk temperature. For this calculation, Eq. (3) must be transformed from an Eq. (2) type to an Eq. (1) type formulation, resulting in

$$\alpha_{nb1} = 1.4 \times 10^{-8} p_c^{2.3} \Delta T_b^{2.33} F_p^{3.33} \tag{19}$$

Correspondingly, Eq. (17) evaluated at constant ΔT_b rather than constant q is obtained for the subcooled zone as

$$\alpha_{nb} = \alpha_{nb1} F_c^{3.33} \tag{20}$$

with α_{nb1} obtained from Eq. (19) and F_c obtained from Eq. (7). Above atmospheric pressure the subcooled boiling zone will normally be negligible. For vacuum, it should be checked by a reliable, rigorous method [6, 9].

(b) Heat flux limitations

The boiling curve of heat flux as a function of ΔT for axial-flow reboilers is similar to that for pool boiling [6] with the heat flux passing through a maximum value. In vertical thermosiphon reboilers, the flux limitations may be caused by several different mechanisms as explained in [6]. At low reduced pressure (p/p_c), a periodic surging instability is reached as ΔT is increased above a certain value. This phenomenon is reviewed and further discussed with regard to process reboilers by Blumenkrantz and Taborek [18]. This limitation can always be stabilized by increasing the frictional resistance in the inlet piping by using a smaller diameter or with a valve or orifice in the line. At high reduced pressure, the critical wall temperature for film boiling is reached before instability occurs and the limitation is due to film boiling.

The empirical correlation of Lee et al. [4] was found by Palen et al. [6] to do a fairly good job of predicting the observed maximum heat flux in thermosiphon reboilers. The Lee correlation is given as a nonlinear empirical plot of two-dimensional groups containing a large number of physical property parameters. The designer is referred to [6] for details.

An alternative, simpler correlation in terms of reduced properties was found to give equally good results for the existing data. These data cover a wide range of fluids, including water, alcohols, and hydrocarbons with tube diameters ranging from 19 to 50 mm and tube lengths ranging from 1.5 to 3.7 m. This correlation is similar to that presented for kettle reboilers and was given in [6] as

$$q_{\max} = 23\,660 \left(\frac{D_i^2}{L}\right)^{0.35} p_c^{0.61} \left(\frac{p}{p_c}\right)^{0.25} \left(1 - \frac{p}{p_c}\right) \tag{21}$$

where p_c = critical pressure, kPa
D_i = tube ID, m
L = tube length, m

Equation (21) is evaluated in Figs. 6 and 7. An alternative approach giving a different perspective on the problem is presented in Sec. 2.7.3. For forced flow reboilers, refer to Sec. 2.7.3.

Equation (21) does not account for the lowered

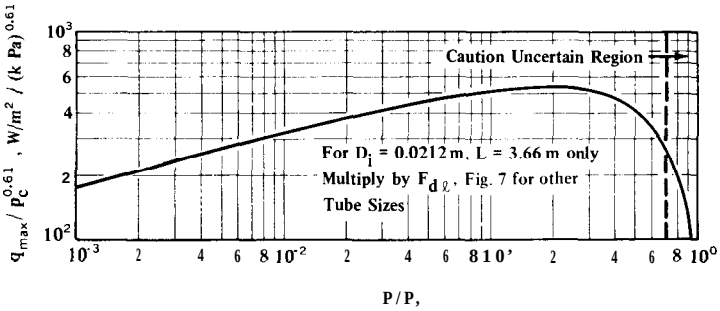

Figure 6 Maximum heat flux for natural circulation tube-side boiling in a vertical thermosiphon reboiler with 25.4 mm OD, 14 BWG, 3.66-m-long tubes.

© 1983 Hemisphere Publishing Corporation

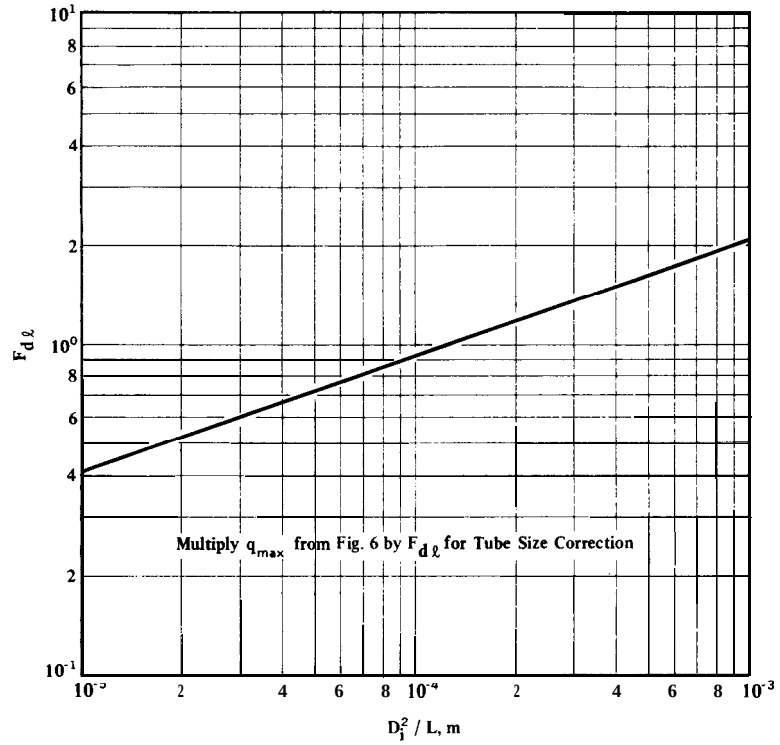

Figure 7 Tube size correction factor to thermosiphon reboiler maximum heat flux.

maximum heat flux caused by small exit piping. Small exit piping has been found to be the cause of many cases of poor operation in the field. It is recommended that the minimum exit pipe flow area be at least equal to the total cross-sectional area of the tubes. If this rule is followed, either long-radius elbow or side-exit tee piping may be used with good results. Exceptions can be made for operation at very low heat flux, but calculations should be made to ensure that the frictional pressure drop in the exit piping is less than 30% of the total reboiler pressure drop.

Equation (21) also does not predict the mist flow limitation, which is a function of vapor fraction and flow rate. For this limit, the Fair [9] flow regime map has been shown to agree with available data and is recommended. This flow map is given in Fig. 8. The

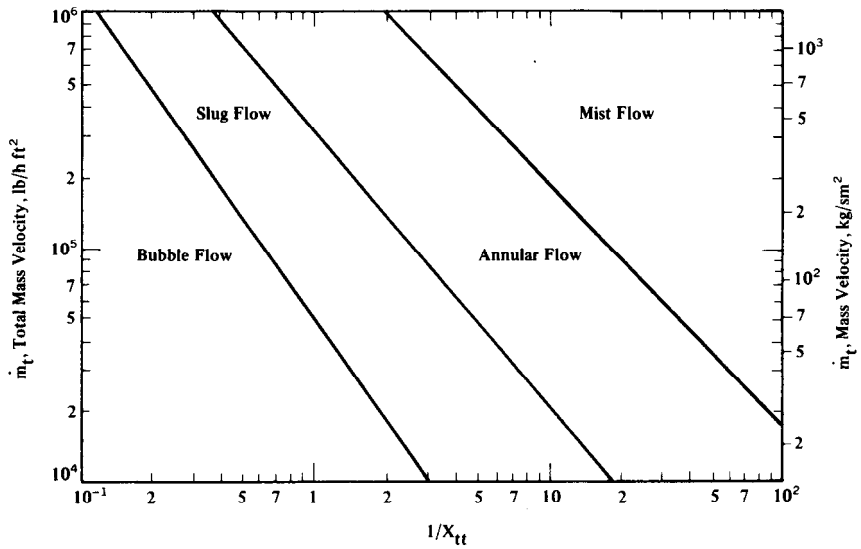

Figure 8 Flow regime map for vertical in-tube boiling, from Fair [9].

© 1983 Hemisphere Publishing Corporation

mist flow criterion from the Fair flow map may be represented as

$$\dot{m}_{mt} = 2\ 441x, \quad (22)$$

where $\dot{m}_{mt}$ is the maximum mass velocity before mist flow (kg/m s). If the total mass velocity $\dot{m}_t$ exceeds the local value $\dot{m}_{mt}$ from Eq. (22), mist flow may be expected. Other, more elaborate correlations have been obtained for the purpose of very accurate determination in specific cases, as discussed in Sec. 2.7.3. However, Eq. (22) in most cases will give adequate prediction for process reboiler design, since the objective is usually to keep velocities comfortably below the mist flow limitation. An additional recommendation is that for hydrocarbons the weight fraction vapor not exceed about 0.35 for pressurized reboilers or 0.50 for vacuum operation. For water, better operation is obtained if the weight fraction vapor is limited to less than 0.10.

(c) Film boiling

As discussed above, it is sometimes not possible or economical to provide a low enough ΔT to produce boiling in the nucleate boiling regime and a film boiling design is required. It is recommended in this case that the ΔT be high enough so that the entire tube is in film boiling. Under these conditions, operation is quite satisfactory for clean fluids. In fact, the circulation rate for thermosiphons in film boiling is higher than for nucleate boiling, since the vapor film on the wall provides much lower friction than the liquid film. The higher wall temperature required, however, may accelerate fouling, and this aspect must be carefully considered.

Methods for film boiling criteria and heat transfer are available in proprietary literature [6]. An approximate value for the AT required for film boiling may be obtained from the Cichelli-Bonilla pool boiling work [19], as given by the following equation:

$$\Delta T_{bf} = 0.555\left[52\left(1 - \frac{p}{p_c}\right) + \frac{0.04}{(p/p_c)^2}\right] \quad (23)$$

If ΔT_b is greater than ΔT_{bf}, it is estimated that film boiling will occur for narrow boiling range fluids.

The heat transfer coefficient in film boiling inside tubes may be estimated by the correlation of Glickstein and Whiteside [20], which was based on data from several rather typical industrial hydrocarbons. This correlation, however, requires calculation of the circulation rate, which is difficult for thermosiphons because no correlations are available in the open literature for two-phase pressure drop in the film boiling regime. An estimation on the safe side can be obtained from the pool boiling correlation of Frederking and Clark [21]. A modification of the Frederking-Clark equation in terms of reduced properties that may be used as a first estimate is

$$\alpha_{fb} = 105(p_c)^{0.5}\,\Delta T_b^{-0.33}\left(\frac{p}{p_c}\right)^{0.38}\left(1 - \frac{p}{p_c}\right)^{0.22} \quad (24)$$

Equation (24) is expected to give an estimate of the film boiling heat transfer coefficient in axial-flow boiling that will become increasingly conservative as velocity increases.

(d) Mist flow

It is not recommended to design reboilers to include a mist flow zone or liquid-deficient region. This can be avoided by keeping the exit vapor fraction low and the mass velocity less than the mist flow value given by Eq. (22). However, in analyzing the performance of operating units, it is useful to have a method of estimating the heat transfer coefficient in the mist flow regime. Considerable work in this area has been performed, as it is important in certain types of nuclear power systems, and a more detailed review of the available correlations is given in Sec. 2.7.3. At the level of accuracy required for reboiler design, however, a reasonable estimation is given by using the single-phase gas convective heat transfer coefficient based on the total mass velocity and on vapor properties.

(e) Temperature profiles

Vertical thermosiphon reboilers usually operate in single-pass counter flow with condensing flow from top to bottom and boiling flow from bottom to top. However, the log mean temperature difference may not always be an accurate representation of the true heat transfer temperature difference because of nonlinearities of the boiling temperature profile. Two basic types of deviation from linearity are possible. Under vacuum, a significant amount of subcooling is present in the inlet liquid as a result of imposed static head. The bulk temperature of the inlet fluid increases up to the saturation temperature and then, for pure components, decreases as the local pressure decreases in further flow up the tube. This produces a hump in the boiling fluid temperature profile and a minimum ΔT at the top of the liquid zone, which would be ignored by a calculation of log mean ΔT from end conditions. Another deviation is obtained in the case of wide-boiling-range fluids, for which the bulk temperature increases as the light material is vaporized, producing a sometimes nonlinear profile with the minimum ΔT usually at the top of the reboiler. This effect is a function of the exit vapor fraction. The effective ΔT decreases as exit vapor fraction increases, further

© 1983 Hemisphere Publishing Corporation

confirming the need to limit the exit vapor fraction for mixtures.

Because of these nonlinearities, and because the boiling heat transfer coefficients can change significantly along the tube, it is recommended that for final design, incremental calculations be performed using local ΔT's. A log mean ΔT based on end conditions should be considered only for initial estimation.

For sensible heating mediums and a narrow-boiling-range fluid, it is good practice to use cocurrent flow, which produces the highest ΔT at the bottom of the tube, effectively increasing heat transfer in the subcooled zone and improving circulation.

C. Heating mediums

The boiling-side heat transfer coefficient can be very high in some cases, and the heating-medium heat transfer coefficient is important in the overall design. For a condensing heating medium, refer to Sec. 3.4 for recommendations. If the heating medium is steam, a reasonable first approximation, which applies to all geometries, is to assume that the average condensing heat transfer coefficient α_c = 8 500 W/m^2 IS, based on the outside surface area and including fouling allowance.

For a single-phase, sensible heating medium, refer to Sec. 3.3.

Nomenclature and References for Section 3.62 appear at the end of Section 3.6.5.

© 1983 Hemisphere Publishing Corporation

3.6.3
Pressure drop

J.W. Palen

■ Two-phase pressure drop calculations are especially important for thermosiphon type reboilers because they are necessary to determine flow rates on which heat transfer calculations are based. More detailed descriptions of two-phase pressure drop correlations are covered in other sections. In this section, approximate methods that are useful in reboiler design are summarized.

A. General

Pressure drop in a vaporizing system is composed of three elements: static head Δp_{tps}, momentum Δp_{tpm}, and friction Δp_{tpf}, as follows:

$$\Delta p_{tp} = \Delta p_{tps} + \Delta p_{tpm} + \Delta p_{tpf} \quad (1)$$

Normally, the pressure drops are calculated for short-length increments, over which the vapor fraction is assumed constant, and summed. The individual pressure drop elements may be estimated as follows.

B. Friction loss

The basic separated flow formulation of Martinelli is recommended. See Sec. 2.3.2 for specific equations.

C. Static head loss

Static head loss can be an important parameter in vertical thermosiphon reboilers, especially at low design heat fluxes in the bubble flow regime for which two-phase static head may be controlling.

$$\Delta p_{tps} = \rho_{tp} g \, \Delta H \sin e \quad (2)$$

The angle θ is measured from the horizontal, so that for a vertical unit with upflow, $\sin \theta = 1.0$.

A common mistake made in predicting thermosiphon reboiler pressure drops is to calculate the two-phase density from the homogenous flow assumptions. This approximation can give very poor results on the unsafe side for most conditions, since there is usually a great amount of vapor slip and resulting liquid holdup in reboilers. This produces a much higher actual two-phase density than is obtained by homogenous flow assumptions. The density for Eq. (2) should be calculated using the true liquid volume fraction, which must be obtained from an empirical correlation.

A number of correlations are available for the liquid volume fraction, as discussed in Sec. 2.3.2.

D. Momentum change loss

Vaporization causes a momentum change that increases the pressure drop of vaporizing fluids. The momentum loss term may be theoretically derived, but results depend on the correlation used for the vapor volume fraction.

For tube-side or axial shell-side flow, the vapor volume fraction should be determined from appropriate equations in Sec. 2.3.2. For shell-side cross flow, because of the greater mixing caused by the irregular geometry, it is usually assumed that homogenous theory is more appropriate for the momentum-change term.

Nomenclature for Section 3.6.3 appears at the end of Section 3.6.5.

© 1983 Hemisphere Publishing Corporation

3.6.4
Special design considerations

J.W. Palen

■ This section summarizes certain important design considerations that apply to all reboilers. Often when a reboiler fails to operate properly, the cause is not miscalculation of the boiling heat transfer coefficient but ignorance of special conditions that fall outside the minimum required design procedures. Some of these are discussed in this section.

A. Fouling

The heat transfer resistance that must be specified to account for anticipated fouling is one of the most troublesome unknowns in the design of reboilers and one that requires the most engineering judgment. Some of the basic characteristics are summarized in [22] and [23]. For a more detailed discussion of fouling considerations, see Sec. 2.10. Since the heat transfer coefficients in reboilers are generally high, the fouling resistance specified usually accounts for an appreciable fraction of the total required surface. Yet it is doubtful if it will ever be possible to predict analytically the true fouling resistance for any particular boiling fluid with much confidence. Therefore, the only practical approach is to attempt to select equipment and operating conditions so that fouling is minimized.

A few of the most important considerations for boiling fluids with significant fouling tendencies are the following.

(a) Design for low vaporization

For many cases it is impossible to know what type of fouling is likely to occur because it may be caused by trace elements or conditions not known to the designer. However, most types of fouling tend to be decreased by designing to low exit vapor fractions. For streams with greater-than-normal fouling tendencies, the maximum local weight fraction vapor should not exceed about 0.2, as a rule of thumb. Lower vapor fraction means higher total velocity, which not only minimizes velocity-dependent fouling and vaporization-dependent fouling, but also tends to lessen temperature-dependent fouling by lowering the tube wall temperature through increase of the boiling-side heat transfer coefficient. Sometimes extra large tube diameters or tube pitches are required. Kettle reboilers are not automatically eliminated from consideration, since very high internal circulation rates may be obtained in these units with wide enough tube pitch. However, kettles are normally the last choice for fouling fluids.

(b) Design for good flow distribution

The generally detrimental effects of poor flow distribution are greatly amplified for fouling fluids. Distribution problems occur more frequently for shell-side flow and are usually due to too small tube pitch, large bypass areas, and too large or too small baffle cut. Shell-side distribution problems for single-phase flow are described in [24]. Similar effects will be obtained in two-phase flow, but the results will be more severe.

In general, any shell-side geometry that causes local regions of higher vaporization, higher wall temperature, or lower velocity will usually cause local concentrations of heavier fouling. Tube-side boiling is not immune to these problems. If shell-side distribution causes some

© 1983 Hemisphere 1 blishing Corporation

tubes to have higher wall temperatures, these tubes may begin to plug and initiate tube-side maldistribution. Tube-side nozzle orientation may also cause maldistribution. Larger tube diameters tend to minimize these effects.

(c) Use of a realistic design fouling resistance

Use of excessively high design fouling factors just to make sure is not recommended for several reasons, in addition to the obvious one of wasted surface [1]. First, excessive fouling factors may cause the unit to be so oversurfaced that the AT required for clean start-up conditions will be too small for proper operation. Smith [25] describes field observations of poor vertical thermosiphon reboiler performance resulting from excessive overdesign. A related problem is that the actual run conditions may be so different from the design conditions (which would occur only if the excess specified fouling were actually obtained) that performance analysis based on design conditions alone may be meaningless. This is not to say that fouling factors should be eliminated, but that they should be as realistic as possible. Frank and Prickett [26] indicate that a boiling-side fouling resistance of about 0.000 18 m^2 K/W gave the best average reproduction of typical plant data for nonpolymerizing fluids when using literature methods to calculate the boiling heat transfer coefficient. They recommend a minimum value of 0.000 09 m^2 K/W for fluids known to be clean and nondegrading and a value of 0.000 S-0.000 7 m^2 K/W for polymerizing materials. This is in basic agreement with the recommendations of [14], which are reproduced in Table 1.

For extreme cases, such as solvent clean-up column reboilers, for example, boiling should always be assigned to the tube side. For such cases, it probably will be necessary to provide a spare reboiler for continuous operation during frequent cleaning. Design should be for as high velocity as possible. Low pressure drop, full-open-type gate valves should be used to isolate the spare reboiler. It may be economical to provide a pump for some systems to increase velocity and thereby prolong the on-stream time. Use of high-velocity forced circulation reboilers in fouling service is discussed in [27].

Table 1 Suggested fouling resistance ranges [14] for reboilers

	Fouling resistance R_f, m^2 K/W
Boiling side	
C, -C_8 normal hydrocarbons	O-0.000 18
Heavier normal hydrocarbons	0.000 18-0.000 5
Diolefins and polymerizing hydrocarbons	0.000 5-0.000 9
Heating side	
Condensing stream	0-0.000 09
Condensing organics (without entrained heavy components)	0.000 09-0.000 18
Sensible heating, organic liquids	0.000 09-0.000 35

B. Start-up and control

All reboilers are designed with some specified fouling resistance. Therefore, on start-up with a clean unit the *AT,* surface, or heating medium heat transfer coefficient must be decreased below the design level to make up for the absence of the design fouling resistance. For reboilers heated by steam as a condensing vapor, the preferred method of controlling performance is with a valve throttling the inlet vapor. This adjusts the pressure, saturation temperature, and consequently the AT to correspond to that required to produce the needed vaporization rate. A clear discussion of the effects of this process is given in [28]. A more general discussion of the characteristics of steam heating operations is given in [29].

A reboiler designed with a high specified fouling resistance will require a much lower AT on start-up than after the specified fouling resistance has finally been reached. For some systems, especially at high pressure, *the* AT *required for film boiling in clean operation may be less than the design* AT *with specified fouling resistance.* If the clean unit is supplied with the full design ΔT, the reboiler can very possibly start boiling in the film boiling regime. For this reason, it is recommended that reboilers always be started with the minimum possible *AT* and that the heating medium temperature then be gradually increased until capacity is reached.

Another method of controlling condensing vapor-heated reboilers consists of decreasing effective reboiler surface by accumulating a level of condensate in the reboiler. This method has several disadvantages, but is still sometimes used when a very large range of capacity will be required or when it is not permissible to take control valve pressure loss from the heating medium. This method will cause a long nonboiling zone and low velocity in the part of the reboiler corresponding to the condensate flooded portion. The boiling-side fouling rate may be accelerated as a result. A worse problem occurs when the AT for clean operation exceeds the film boiling ΔT. In this case, since this method does not affect the *AT* in the nonflooded portion, that portion will certainly start up in film boiling with the high wall temperature and probably increased fouling. It is recommended that, if condensate flooding is used, it be combined with inlet vapor throttling to permit some control on the *AT.* A condensate pump may often

© 1983 Hemisphere Publishing Corporation

be used effectively if the condensate pressure falls too low [28, 29].

C. Very-wide-boiling-range mixtures

If the boiling range of the fluid is very large, additional problems may occur. The viscosity may be much higher than is normally encountered with boiling fluids because of the presence of heavy material. Nucleate boiling at the wall may be completely suppressed. Heat transfer coefficients tend to be very low for the boiling fluid because of nucleate boiling suppression plus the resistance to circulation caused by the high viscosity. Up to roughly 20 cP bulk viscosity, vertical thermosiphon reboilers can still give good operation if carefully designed by rigorous methods for as high circulation as possible (short, large-diameter tubes). For more viscous solutions, shell-side horizontal thermosiphons may give better results, as they will obtain better mixing. Care must be taken to assure even flow distribution. A longitudinal baffle is often used at the bundle centerline above the inlet nozzle (TEMA G and H shells) to prevent the more volatile components from flashing and shortcutting through the middle of the bundle. Alternatively, vertical tube-side falling film evaporators can be very effective for this type of service if properly designed for good liquid distribution.

D. Operation near the critical pressure

Very-high-pressure operation can cause problems for thermosiphon-type reboilers because as the critical pressure is approached, the vapor density approaches the liquid density and the net driving head for circulation decreases. Kettle reboilers have been found to operate well in this region, but have the economic disadvantage of the oversized high-pressure shell. Column internal reboilers potentially offer the most advantages and least difficulties if sufficient surface can be fitted into the column. If tube-side vertical thermosiphon reboilers are used, they should be carefully designed with close attention paid to physical properties.

E. Operation in deep vacuum

Heavy fluids, especially temperature-sensitive ones, are often distilled under vacuum. Special care must be taken to prevent problems in reboiler performance. Boiling heat transfer coefficients in vacuum are relatively low because of a long nonboiling zone, suppression of nucleate boiling, and low circulation rates. Since most of the vacuum problems are hydrodynamic in nature, the kettle reboiler, which is the least sensitive to hydrodynamics, is a logical choice for vacuum. However, in spite of the potential problems, the less expensive vertical tube-side thermosiphon reboiler can be quite effective and economical for vacuum if properly designed. For these units there is an optimum static head that will give sufficient circulation without excessive subcooling. This value will range from about 0.5 to 0.8 times the tube length, depending on the system.

Because of the many complex interrelated flow and heat transfer mechanisms important in vacuum design, it is not recommended to specify vertical thermosiphon reboilers for this service unless they can be checked by a reliable computer design program. If design heat fluxes are to be as high as around 30 000 W/m^2, instability is a potential problem and should be checked by a reliable method, Instability can always be stabilized by increasing frictional resistance in the inlet liquid line, and a valve in this line is good insurance in questionable cases.

F. Sparging

One way to eliminate the liquid zone of vacuum reboilers and to increase circulation for wide-boiling-range viscous fluids is to inject a small amount of noncondensable light gas or superheated steam into the reboiler feed stream. This procedure causes extra problems downstream. However, when it can be used, it will produce a significant improvement in the reboiler heat transfer rate and even greater improvement in circulation rates for low-pressure operation.

G. Very low *AT*

It is sometimes necessary because of economics or process restrictions to operate a reboiler at very low AT (less than about 4 K). This can cause several types of problems. At low AT, nucleate boiling becomes very sensitive to microscopic surface configuration. The nucleate boiling heat transfer coefficient can be very low and can change drastically from surface to surface, depending on the distribution of nucleation cavity sizes. One possible solution for clean fluids is to use one of the specially designed porous surfaces that greatly increase the nucleation potential [5, 30, 31]. Low-finned tubes also improve performance due to increased nucleation as well as increased surface [5]. However, nucleate boiling heat transfer coefficients at low *AT* are extremely difficult to predict, and experimental verification on the specific fluid surface combination is advisable where possible, before final design.

In thermosiphon reboilers, low AT causes the siphoning effect or pumping action to be greatly suppressed, resulting in low circulation rates and unpredictable performance. For vertical in-tube thermosiphon reboilers, it is advisable to have a design heat

© 1983 Hemisphere Publishing Corporation

flux of at least 5 000 W/m^2 to provide sufficient pumping action for good circulation. At lower flux levels it is usually preferable to use a kettle-type reboiler.

H. Very high *AT*

More potential problems are created by high ***AT*** than any other single condition in reboilers. On the other hand, more improvement in heat transfer can be obtained by increasing ***AT*** than by adjusting any other variable. This emphasizes the importance of being able to determine limitations resulting from high AT. The maximum heat flux may be limited by film boiling, mist flow, or instability, and the design heat flux should be checked against each of these limits. This is especially important in deep vacuum, where the instability and mist flow limits are rather low and above about 0.7 of the critical pressure where the film boiling limit can become very low.

In some cases it is economical to use a high-temperature heating medium even though the resulting ***AT*** is too high for the nucleate boiling regime in the reboiler. In this case, it is possible to design for the film boiling regime. However, it is not recommended to design a reboiler with part of the tubes in nucleate boiling and part in film boiling or mist flow. This is because operation is difficult to predict; shifts in operating condition can cause extreme shifts in performance; and because this region has a reverse control characteristic (increasing the ***AT*** results in decreasing the duty and vapor rate). Therefore, it is recommended that reboilers be designed either for complete nucleate or complete film boiling. If this cannot be accomplished under the required process conditions, it is usually possible to adjust either conditions or reboiler geometry.

References for Section 3.6.4 appear at the end of Section 3.6.5.

© 1983 Hemisphere Publishing Corporation

3.6.5
Calculation procedures

J.W. Palen

■ Thermal design of reboilers is now done largely by computer programs that make possible the stepwise calculations necessary to account accurately for the effects of the changing vapor fraction through the reboiler. Many programs are available for sale or through membership in proprietary organizations. Any computer program should be carefully reviewed with respect to internal methods used and amount of data support before trusting for final designs. This is especially true in boiling, because many empirical relationships are still necessary even in a computer-based reboiler design method. Even if detailed computer calculations are used, it is helpful to have available shortcut manual methods that can be used for preliminary estimates of reboiler size or to verify the general range of the computer-calculated heat transfer coefficients. This section gives stepwise instructions for applying the equations in Sec. 3.6.2 to obtain a shortcut initial estimate of the required reboiler heat transfer area.

A. Example problem

Vaporize a medium-wide-boiling-range hydrocarbon mixture at moderate pressure using available steam. Roughly size kettle, horizontal thermosiphon, and vertical thermosiphon reboilers for this service.

(a) General data

Duty required: 14.6 MW
Operating pressure: 1 000 kPa

(b) Boiling fluid properties at operating pressure

Bubble-point T_b = 140°C
Dew-point T_d = 180° C
Critical pressure p_c = 3 400 kPa
Latent heat Ah = 3.49 X 10^5 J/kg
Liquid viscosity η_ℓ = 4.1 X 10^{-5} kg/m s
Vapor viscosity η_v = 0.4 X 10^{-5} kg/m s
Liquid heat capacity $(C_p)_\ell$ = 2 090 J/kg K
Liquid density ρ_ℓ = 640 kg/m^3
Vapor density ρ_v = 24 kg/m^3

(c) Maximum available steam saturation temperature

T_{st} = 200°C

B. Kettle reboiler

(a) Estimated bundle geometry

Tube diameter D_o = 19 mm
Tube pitch P_t = 25.4 mm, square layout
Length L = 6.1 m
Diameter D_b = 1.42 m
Area A = 930 m^2

(b) Percentage vaporization

Bottom liquid draw-off will be about 30% of liquid feed to reboiler.
Dew point of exit vapor = 165° C.

© 1983 Hemisphere Publishing Corporation

(c) Calculation of *required heat transfer area*

Step 1: Mixture correction factor F_c from Eq. 3.6.2(7). Boiling range of reboiler feed = 40° C.

$F_c = 0.34$

Step 2: Bundle convection factor F_b. Let

$F_b = 1.5$

as suggested in Sec. 3.6.2(f)

Step 3: Natural convection heat transfer coefficient a,,. Let

$\alpha_{nc} = 250$ W/m² K

as suggested in Sec. 3.6.2(f)

Step 4: Single-tube nucleate boiling heat transfer coefficient α_{nb1}, from Eq. 3.6.2(3). Heat flux $\dot{q}$, based on estimated area = 14 600 000/930 = 15 700 W/m². Reduced pressure = 1000/3 400 = 0.294.

$\alpha_{nb1} = 1\,442$ W/m² K

Step 5: Bundle average boiling heat transfer coefficient from Eq. 3.6.2(5).

$\alpha_b = 985$ W/m²

Step 6: Calculate overall heat transfer coefficient U_o. Let steam heat transfer coefficient, including fouling resistance, α_c = 8 500 W/m² K. Let boiling-side fouling resistance R_{fb} = 0.000 35 m² K/W. Then

$$\frac{1}{U_o} = \frac{1}{\alpha_b} + \frac{1}{\alpha_c} + R_{fb}$$

(neglecting wall resistance)

$U_o = 674$ W/m² °C

Step 7: Calculate effective temperature difference ΔT_{eff}. Base on dew point of exit vapor and steam temperature. Maximum steam temperature available = 200° C. Allow 10° C for control. Design steam temperature = 190° C.

$$\text{AT,,} = 190 - 165 = 25° \text{ C} \quad (1)$$

Step 8: Calculate required area A,.

$$A,. = \frac{Q}{U_o \Delta T_{\text{eff}}} = 866 \text{ m}^2 \quad (2)$$

Assumed surface = 930 m². Therefore, assumed unit is acceptable unless design heat flux is excessive.

Step 9: Check maximum heat flux. $\dot{q}_{1,\max}$, from Eq. 3.6.2(10), is 594000 W/m². ψ_b, from Eq. 3.6.2(11), is 0.029 3. ϕ_b, from Eq. 3.6.2(12), is 0.064. Since $\phi_b < 0.1$, vapor lanes should be provided if design flux is greater than 0.5 times $\dot{q}_{b,\max}$. Now $\dot{q}_{b,\max}$, from Eq. 3.6.2(9), is 38 238 W/m². $\dot{q}$, from step 4, is 15 700 W/m². Therefore, $\dot{q}/\dot{q}_{b,\max} < 0.5$, so full tube bundle may be used.

C. Horizontal thermosiphon reboiler

Calculate as cross-flow (TEMA X shell) type.

(a) Estimated geometry

Try same as for kettle.

(b) Percentage vaporization

Try to supply head for exit vapor fraction of 0.25. Exit vapor temperature is 150° C.

Total vapor rate W_v = 41.8 kg/s
Total liquid feed rate to reboiler W_t = 167.2 kg/s

(c) Calculation of required heat transfer area

All calculations made for the bundle boiling heat transfer coefficient for the kettle reboiler apply, and the same area will be adequate. However, to determine how much additional heat transfer would be provided due to the circulation, calculate the convective two-phase heat transfer coefficient.

Step 1: Calculate the bundle cross-flow pressure drop and piping pressure drop using methods in Sec. 2.7.3. Compare calculated pressure drop to available static head. If static head is insufficient, increase tube pitch and exit piping diameter until satisfactory pressure drop is obtained. For the purpose of this example, it will be assumed that a satisfactory balance has been obtained with a 2.5-m static head, that the two-phase friction pressure drop across the tube bundle, ΔP_{tpf} = 1.5 kPa, and that the corresponding friction pressure drop for liquid flowing alone, ΔP_ℓ = 0.10 kPa. The exact values obtained for ΔP_{tpf} and ΔP_ℓ will depend on the method used, and the above values, while reasonably realistic, are for illustration only.

Step 2: Calculate the convective heat transfer coefficient for cross flow for liquid flowing alone, α_ℓ. Use methods in Sec. 3.3. For the purpose of this illustration only, assume that α_ℓ = 275 W/m² K for an average liquid weight fraction of 0.875.

Step 3: Calculate the convective two-phase heat transfer coefficient α_{cb}. Using Eq. 3.6.2(6) with m_3 = 0.45,

$$\alpha_{cb} = 275\left(\frac{1.5}{0.1}\right)^{0.45} = 930 \text{ W/m}^2 \text{ K} \quad (3)$$

Since α_{cb} is smaller than α_b as calculated from step 6 of the kettle reboiler example, nucleate boiling is domi-

© 1983 Hemisphere Publishing Corporation

nant and the use of α_b for design will be reasonable, if somewhat conservative.

Step 4: Calculate effective temperature difference ΔT_{eff}. As stated in Sec. (c) above, the effective AT for thermosiphon reboilers is improved compared to kettles because of better circulation. Since the steam temperature is constant at 190°C, the LMTD may be used for this case.

$$\Delta T_{\text{eff}} = \text{LMTD} = \frac{(190-140)-(190-150)}{\ln[(190-140)/(190-150)]}$$

$$= 44.8^\circ\text{C} \quad (4)$$

Step 5: Calculate required area A_r.

$$A_r = \frac{Q}{U_o \Delta T_{\text{eff}}} = 483 \text{ m}^2 \quad (5)$$

This is compared to 866 m^2 for the kettle case and indicates quite an advantage for the thermosiphon for the wide-boiling-range mixture case because of combined effect of the circulation and lower fraction vaporized on the effective temperature difference. Care should be taken, however, to design nozzles and baffles for flow distribution in order to realize this advantage.

D. Vertical tube-side thermosiphon reboiler

(a) Estimated bundle geometry

Number of tubes = 1 230
Tube outside diameter D_o = 25.4 mm
Tube inside diameter D_i = 21.2 mm
Tube pitch P_t = 3 1.75 mm
Tube length L = 4.9 m
Diameter D_b = 0.81 m
Area A = 480 m^2

(b) Percentage vaporization

As for the horizontal thermosiphon case, try to design for an exit vapor fraction of 0.25, which corresponds to an exit vapor temperature of 150° C.

Total vapor flow rate W_v = 41.8 kg/s
Total liquid feed rate to reboiler W_t = 167.2 kg/s

(c) Calculation of *required heat* transfer area

Step 1: Calculate the pressure drop to make sure there is enough static head for the required circulation. Use methods given in Sec. 2.3.2 to calculate ΔP_{tp}. Static head AH is then calculated as

$$\Delta H = \frac{\Delta P_{tp}}{\rho_\ell g} \quad (6)$$

If AH is less than the tube length, the above assumption of exit vapor fraction will give conservative results and may be used. If AH is greater than the tube length, the tube diameter should be increased or tube length shortened and the ΔP_{tp} recalculated.

For vacuum operation a lower static head is necessary to prevent excessive subcooling, and the net available head is less because of a significant liquid zone. Therefore, for vacuum the calculated AH should not be greater than 0.5 times the tube length. It may be necessary for vacuum to increase the design exit vapor fraction to as high as 0.5 to achieve a satisfactory pressure balance, but this value should not be exceeded. For this example case, which is at high pressure, the liquid zone length will be negligible.

Step 2: Calculate the nucleate boiling heat transfer coefficient α_{nb}. Heat flux $\dot{q}$, based on estimated area, is 14 600 000/480 = 30 400 W/m^2. From Eq. 3.6.2(3),

$$\alpha_{nb1} = 2\,290 \text{ W/m}^2 \text{ K} \quad (7)$$

From step 1 of the kettle reboiler example,

$$F_c = 0.34 \quad (8)$$

From Eq. 3.6.2(17),

$$\alpha_{nb} = 779 \text{ W/m}^2 \text{ K} \quad (9)$$

Step 3: Calculate the convective boiling heat transfer coefficient, α_{cb}. Base on mean vapor fraction of 0.125. Calculate the liquid convective heat transfer coefficient, α_ℓ, using methods given in Sec. 3.3. Assume, for the purpose of this example only, that α_ℓ = 1 100 W/m^2 K. Calculate the ratio α_{cb}/α_ℓ using the Chen method given in Sec. 2.7.3.

$$X_{tt} = \left(\frac{1-0.125}{0.125}\right)^{0.9}\left(\frac{24}{640}\right)^{0.5}\left(\frac{4.1\times10^{-5}}{0.4\times10^{-5}}\right)^{0.1} = 1.40$$

$$F = 2.35\left(\frac{1}{1.4}+0.213\right)^{0.736} = 2.22$$

$$\frac{\alpha_{cb}}{\alpha_\ell} = 2.22$$

Therefore,

α_{cb} = 1 100 X 2.22 = 2 440 W/m^2 K

Step 4: Calculate the average boiling heat transfer coefficient, using Eq. 3.6.2(16). Calculate s as shown in Sec. 2.7.3.

Vapor rate, neglecting sensible duty, is 14 600 000/(3.49 X 10^5) = 41.8 kg/s

Liquid rate at 25% vaporization = 125.4 kg/s

$$\text{Re}_\ell = \frac{W_\ell/N}{(\pi/4)D_o\eta_\ell} = \frac{125.4/1\,230}{(0.785\times0.021\,2)(4.1\times10^{-5})}$$

= 149 400

© 1983 Hemisphere Publishing Corporation

$$Re_{tp} = 149\ 400 \times 2.22^{1.25} = 404\ 800$$

$$s = \frac{1}{1 + (2.53 \times 10^{-6})(404\,800)^{1.17}} = 0.098$$

From Eq. 3.62(16),

$$\alpha_b = 2\ 516\ W/m^2\ K \quad (10)$$

Step 5: Calculate overall heat transfer coefficient U_o. Let steam heat transfer coefficient α_c = 8 500 W/m^2 K, including fouling resistance. Let boiling-side fouling resistance $R_{fb} = 0.000\ 35\ m^2$ K/W.

$$\frac{1}{U_o} = \frac{D_o}{D_i}\frac{1}{\alpha_b} + \frac{1}{\alpha_c} + R_{fb}\frac{D_o}{D_i} \quad (11)$$

(neglecting wall resistance)

$$U_o = 928\ W/m^2\ K \quad (12)$$

Step 6: Calculate effective temperature difference, ΔT_{eff}. See step 4 for horizontal thermosiphon. Since this case is at high pressure, there will be no significant liquid zone, and an LMTD will provide an approximate ΔT_{eff}.

$$\Delta T_{,,} = 44.8°C \quad (13)$$

Step 7: Calculate required area $A_{,,}$.

$$A_{,} = \frac{Q}{U_o\,\Delta T_{eff}} = 350\ m^2 \quad (14)$$

Therefore, because of both an improved ΔT_{eff} and an improved α_b caused by the high-velocity tube-side flow, the vertical thermosiphon shows considerable advantage for this case over either the kettle or the horizontal thermosiphon. This is not always true, of course, and each case must be evaluated individually. For this case it will be possible to decrease the number of tubes. However, the critical heat flux should be checked closely.

Step 8: Check the critical heat flux. A quick approximation for the design maximum heat flux for thermosiphon reboilers is obtained from Eq. 3.6.2(21). For more detail see Sec. 2.7.3. From Eq. 3.6.2(21), using an inside tube diameter of 0.02 1 2 m,

$$\dot{q}_{max} = 67\ 760\ W/m^2 \quad (15)$$

By using the tables for *n*-pentane [2.7.3(7)] in Sec. 2.7.3 and interpolating to the conditions of this example, a critical vapor fraction of about 0.6 is obtained, which gives a critical heat flux of about 87 000 W/m^2 from Eq. 2.7.3(69). This is in reasonable agreement with the design equation 3.6.2(21) for a hydrocarbon with properties similar to those of this example. The design heat flux for an area of 250 m^2 is $\dot{q}$ = 41 570 W/m^2. Therefore, design heat flux is 0.6 times the recommended design maximum, which is permissible. The number of tubes should be decreased and the design rechecked.

NOMENCLATURE FOR SECTION 3.6.1-3.6.5

A	heat transfer surface of bundle based on outside tube surface, m^2
A_r	calculated required heat transfer area, m^2
BR	boiling range; difference between dew-point temperature and bubble-point temperature, K
$(C_p)_\ell$	liquid heat capacity, J/kg K
D_b	tube bundle diameter of circle tangent to outer tubes, m
D_i	inside tube diameter or equivalent diameter for noncircular channel, m
D_o	outside tube diameter, m
F_b	tube bundle boiling correction factor
F_c	mixture correction factor
F_p	pressure correction factor for nucleate boiling
g	acceleration of gravity, m/s^2
Δh	heat of vaporization, J/kg
ΔH	vertical height increment, m
K_e	entrainment coefficient, m/s
L	length of tube bundle, m
m_{mt}	maximum total mass velocity above which mist flow is expected, kg/m^2 s
m_t	actual total mass velocity, kg/m^2 s
N_N	number of pairs (inlet plus outlet) of boiling-side nozzles for horizontal thermosiphon
P	operating pressure, kPa
P_C	critical pressure, kPa
ΔP_ℓ	friction pressure drop for liquid-phase flowing alone, kPa
P_t	tube pitch, m
ΔP_{tp}	two-phase pressure drop across a given length increment, kPa
ΔP_{tpf}	two-phase friction pressure drop, kPa
AP_{tpm}	momentum pressure drop, kPa
ΔP_{tps}	static head pressure drop, kPa
$\dot{q}$	heat flux, W/m^2
$q_{1,max}$	critical heat flux for a single tube, W/m^2
$q_{b,max}$	critical heat flux for tube bundle, W/m^2
$\dot{q}_{max}$	limiting heat flux for axial thermosiphon reboilers, W/m^2
R_{fb}	boiling-side fouling resistance, m^2 K/W
S	nucleate boiling suppression factor in axial-flow convective boiling
T_b	bubble-point temperature, °C
T_d	dew-point temperature, °C

© 1983 Hemisphere Publishing Corporation

T_{st} saturated steam temperature, °C
ΔT_0 difference between temperature of the wall and bulk temperature of the boiling fluid, K
ΔT_b difference between temperature of the tube wall and saturation temperature of the boiling fluid, kPa
ΔT_{bf} value of ΔT_b above which film boiling is expected, K
ΔT_{eff} effective mean temperature difference, K
U_o overall heat transfer coefficient based on outside area, W/m^2 K
VL vapor load parameter, kg/m^3 s
V_v vapor-phase velocity, m/s
x weight fraction vapor
X_{tt} Martinelli parameter for both phases turbulent. Square root of pressure drop for liquid phase to that for vapor phase
α_b corrected bundle boiling heat transfer coefficient for nucleate boiling mechanism, W/m^2 K
α_c condensation heat transfer coefficient, W/m^2 K
α_{cb} convective boiling heat transfer coefficient, W/m^2 K
α_{fb} heat transfer coefficient for film boiling, W/m^2 K
α_ℓ convective heat transfer coefficient for liquid-phase flowing alone, W/m^2 K
α_{nbl} single-tube nucleate boiling heat transfer coefficient for pure component, W/m^2 K
α_{nb} nucleate boiling heat transfer coefficient for boiling in axial flow, W/m^2 K
α_{nc} natural convection heat transfer coefficient, W/m^2 K
η_ℓ liquid viscosity, kg/m s
η_v vapor viscosity, kg/m s
θ orientation angle of tube axis with respect to the horizontal, deg
ρ_ℓ liquid density, kg/m^3
ρ_v vapor density, kg/m^3
ρ_{tp} two-phase density, kg/m^3
σ surface tension, N/m

REFERENCES FOR SECTION 3.6.1-3.6.5

1. Gilmour, C. H., No Fooling-No Fouling, ***Chem. Eng. Prog.***, vol. 61, no. 7, pp. 49-54, 1965.
2. Palen, J. W., and Taborek, J., Refinery Kettle Reboilers, *Chem. Eng. Prog.*, vol. 58, no. 7, pp. 37-46, 1962.
3. Shellene, K. R., Sternling, C. V., Snyder, N. H., and Church, D. M., Experimental Study of a Vertical Thermosiphon Reboiler. *Chem. Eng. Prog. Symp. Ser.,* vol. 64, no. 82, pp. 102-l 13, 1968.
4. Lee, D. C., Dorsey, J. W., Moore, G.Z., and Mayfield, F. D., Design Data for Thermosiphon Reboilers, *Chem. Eng. Prog.*, ***vol. 52,*** no. 4, p. 160, 1956.
5. Palen, J. W., Yarden, A., and Taborek, J., Characteristics of Boiling Outside Large Scale Multitube Bundles, *Chem. Eng. Prog. Symp. Ser.*, vol. 68, no. 118, pp. 50-61, 1972.
6. Palen, J. W., Shih, C. C., Yarden A., and Taborek, J., Performance Limitations in a Large Scale Thermosiphon Reboiler, *Proc. 5th Int. Heat Transfer Conf., Tokyo,* vol. 5, pp. 204-208, 1974.
7. Starczewski, J., Generalized Design of Evaporation, Heat Transfer to Boiling Liquids, ***Br. Chem. Eng., vol.*** 10, no, 8, pp. 523-530, 1965.
8. Mostinski, I. L., Application of the Rule of Corresponding States for the Calculation of Heat Transfer and Critical Heat Flux, *Teploenergetika,* vol. 4, p. 66, 1963; English Abstr., ***Br. Chem. Eng.,*** vol. 8. no. 8, p. 580, 1963.
9. Fair, J. R., What You Need to Design Thermosiphon Reboilers, *Pet. Refiner*, vol. 39, no. 2, p. 105, 1960.
10. Nakajima, K., and Morimoto, K., Boiling Heat Transfer on Outside Wall of Horizontal Tube Bundles for Freon ***11*** and ***12, Refrigeration (Japan),*** vol. 44, no. 495, pp. 3-15, 1969.
11. Montgomery, R. T., A Study of the Effect of Tube Bundle Geometry on the Nucleate Boiling Region of a Series of Hydrocarbon Liquids, Ph.D. thesis, University of Missouri at Rolla, 1969.
12. Wallner. R., Heat Transfer in Flooded Shell and Tube Evaporators, *Proc. 5th Int. Heat Transfer Conf., Tokyo,* Paper HE2.4, 1974.
13. Taborek, J., Design Methods for Heat Transfer Equipment-A Critical Survey of the State-of-the-Art, in ***Heat Exchangers: Design and Theory Sourcebook,*** ed. N. H. Afgan and E. U. Schlünder, Hemisphere, Washington, 1974.
14. Palen, J. W., and Small, W. M., A New Way to Design Kettle and Internal Reboilers, ***Hydrocarbon Process., vol. 43.*** no. 11, p. 199, 1964.
15. Kern, D. Q., ***Process Heat Transfer.*** McGraw-Hill, New York, 1950.
16. Comley, W. D., The Effect of Vapor Agitation on Boiling Coefficients, M.S. thesis, Massachusetts Institute of Technology, Cambridge, Mass., 1938.
17. Chen, J. C., Correlation for Boiling Heat Transfer to Saturated Fluids in Convective Flow, *I&EC Process* ***Design and*** *Development*, ***vol. 5.*** no. 3, pp. 322-329, July 1966.
18. Blumenkrantz, A., and Taborek, J., Application of Stability Analysis for Design of Natural Circulation Boiling Systems and Comparison with Experimental Data, *AIChE Symp. Ser.,* vol. 68, no. 118, 1971.
19. Cichelli, M. T., and Bonilla, C. F., Heat Transfer to Boiling Liquids Under Pressure, ***Trans.*** *AIChE*, ***vol. 41,*** p. 755, 1945.
20. Glickstein, M. R., and Whitesides, R. H., Jr., Forced-Convection Nucleate and Film Boiling of Several Aliphatic Hydrocarbons. ***9th Natl. Heat Transfer*** *Conf.,* ***Seattle,*** ASME Paper 67-HT-7, 1967.
21. Frederking, T. H. K., and Clark, J. A., Natural Convection Film Boiling on a Sphere, *Adv. Cryogenic* ***Eng.,*** vol. 8. p. 501, 1963.
22. Palen, J. W., and Westwater, J. W., Heat Transfer and Fouling Rates During Pool Boiling of Calcium Sulfate Solutions, *Chem. Eng. Prog. Symp. Ser.,* vol. 62, no. 64, 1966.

© 1983 Hemisphere Publishing Corporation

23. Taborek, J., Aoki, T., Ritter, R. B., Palen, J. W., and Knudsen, J. G., Fouling-The Major Unresolved Problem in Heat Transfer, *Chem. Eng. Prog.*, *vol. 68,* no. 2, pp. 59–67, 1972.
24. Palen, J. W., and Taborek, J., Solution of Shell Side Flow Pressure Drop and Heat Transfer by Stream Analysis Method, *Chem. Eng. Prog. Symp. Ser., vol. 65, no. 92,* pp. 53-63, 1969.
25. Smith, J. V., Improving the Performance of Vertical Thermosiphon Reboilers, *Chem. Eng. Prog.*, *vol. 70,* no. 7, pp. 68-70, 1974.
26. Frank, O., and Prickett, R. D., Designing Vertical Thermosiphon Reboilers, *Chem. Eng.*, vol. 80, no. 20, pp. 107-l 10, 1973.
27. Chantry, W. A., and Church, D. M., Design of High Velocity Forced Circulation Reboilers for Fouling Service, *Chem. Eng. Prog., vol.* 54, no. 10, pp. 64-67, 1958.
28. Helzner, A. E., Operating Performance of Steam-Heated Reboilers, *Chem. Eng.*, *vol. 84, no. 4,* pp. 73-76, 1977.
29. Mathur, J., Performance of Steam Heat-Exchangers, *Chem. Eng.*, vol. 80, no. 20, pp. 101-106, 1973.
30. Gottzman, C. F., O'Neill, P. S., and Minton, P. E., High Efficiency Heat Exchangers, *Chem. Eng. Prog.*, vol. 69, no. 7, pp. 69-75, 1973.
31. Arai, N., Fukushima, T., Aria, A., Nakajima, T., Fujie, K., and Nakayama, Y., Heat Transfer Tubes Enhancing Boiling and Condensation in Heat Exchangers of a Refrigerating Machine, *ASHRAE Trans.,* vol. 83, pp. 58-69, 1977.
32. Jacobs, J. K., Reboiler Selection Simplified, *Hydrocarbon Process. Pet. Refiner,* vol. 40, no. 7, pp. 189-196, 1961.

© 1983 Hemisphere Publishing Corporation

3.7 Plate heat exchangers

Contents

3.7.1
CONSTRUCTION AND OPERATION, Anthony Cooper and J. Dennis Usher **3.7.1-1**

3.7.2
FACTORS GOVERNING PLATE SPECIFICATION, Anthony Cooper and J. Dennis Usher **3.7.2-l**

3.7.3
CORRUGATION DESIGN, Anthony Cooper and J. Dennis Usher **3.7.3-l**

3.7.4
FRICTION FACTOR CORRELATIONS, Anthony Cooper and J. Dennis Usher **3.7.4-l**

3.7.5
HEAT TRANSFER CORRELATIONS, Anthony Cooper and J. Dennis Usher **3.7.5-l**

3.7.6
FACTORS AFFECTING PLATE DESIGN, Anthony Cooper and J. Dennis Usher **3.7.6-l**

A. Corrugation geometry 3.7.6-l
B. Distribution 3.7.6-2

3.7.7
OVERALL PLATE DESIGN, Anthony Cooper and J. Dennis Usher **3.7.7-l**

A. NTU rating 3.7.7-l
B. Performance characteristics 3.7.7-l
C. Design procedure 3.7.7-2

3.7.8
PLATE ARRANGEMENT AND CORRECTION FACTORS, Anthony Cooper and J. Dennis Usher **3.7.8-l**

A. Types of pass arrangement 3.7.8-l
B. Concurrency corrections for large unequal passes 3.7.8-l
C. End effect 3.7.8-2
D. Distribution along port manifolds 3.7.8-3

3.7.9
FOULING, Anthony Cooper and J. Dennis Usher 3.7.9-l

3.7.10
METHODS OF SURFACE AREA CALCULATION, Anthony Cooper and J. Dennis Usher 3.7.10-l

A. Performance limitations 3.7.10-l
B. Basic procedure 3.7.10-l
C. Approximate assessment for turbulent flow 3.7.10-2
D. Computer programs 3.7.10-4

3.7.11
THERMAL MIXING, Anthony Cooper and J. Dennis Usher **3.7.1 l-l**

© 1983 Hemisphere Publishing Corporation

HEDH

3.7.12
TWO-PHASE FLOW APPLICATIONS, Anthony Cooper and J. Dennis Usher **3.7.12-t**

Nomenclature for Sections 3.7.1-3.7.12 **3.7.12-1**
References for Sections 3.7.1-3.7.12 **3.7.12-2**

© 1983 Hemisphere Publishing Corporation

3.7.1
Construction and operation

Anthony Cooper and J. Dennis Usher

The plate heat exchanger (PHE) consists of a series of parallel plates that are corrugated both to increase turbulence and to give mechanical rigidity. Two examples of plates are shown in Fig. 1. They normally have flow ports in all four corners and are clamped together in a frame that carries bushes or nozzles lined up with the plate ports and connected to the external pipework that carries the two liquid streams.

As shown in Fig. 2, the plates are suspended in the frame from a top carrying bar and are aligned by a bottom bar. The plates are compressed against the stationary head of the frame by a movable follower, which slides along the top carrying bar. The follower and the head are clamped together by lateral bolts. Full constructional details of the PHE are given in Sec. 4.4.2.

The plates themselves are fitted with gaskets, which are shaped and located both to prevent external leakage and to direct the two liquids normally counter currently through the relatively narrow passages between alternate pairs of heat transfer plates. An exploded view of a two-pass/two-pass arrangement is shown in Fig. 3.

Most applications for plate heat exchangers are for liquid/liquid duties at operating pressures below 2,000 kN/m² and temperatures below 150°C, although some models can operate at temperatures up to 275°C. Plates can be pressed in many different metals, including stainless steel, titanium, Hastelloy alloys, nickel, Monel, and Incolloy 825. Gaskets are available in nitrile, butyl, silicone, and fluorocarbon rubbers; in addition, certain

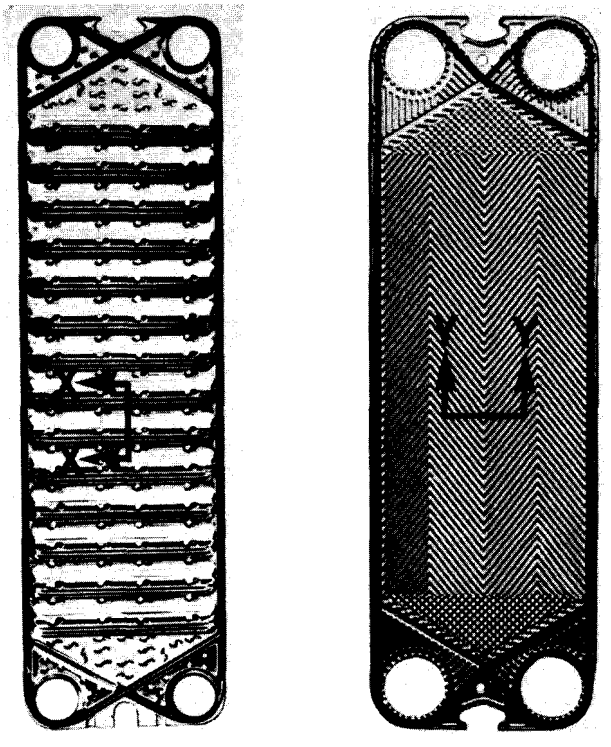

Figure 1 Typical plates showing intermating and chevron troughs.

†The authors acknowledge the directors of The APV Company, Ltd., England, for approval to publish the material in Sec. 3.7, which contains information previously proprietary to the Company.

Acknowledgments are also due to The Controller of Her Britannic Majesty s Stationery Office (HMSO) for Figs. 3.7.8(4)–3.7.8(7) and to Alfa Lava1 AB, Sweden, for Fig. 3.7.11(1).

© 1983 Hemisphere Publishing Corporation

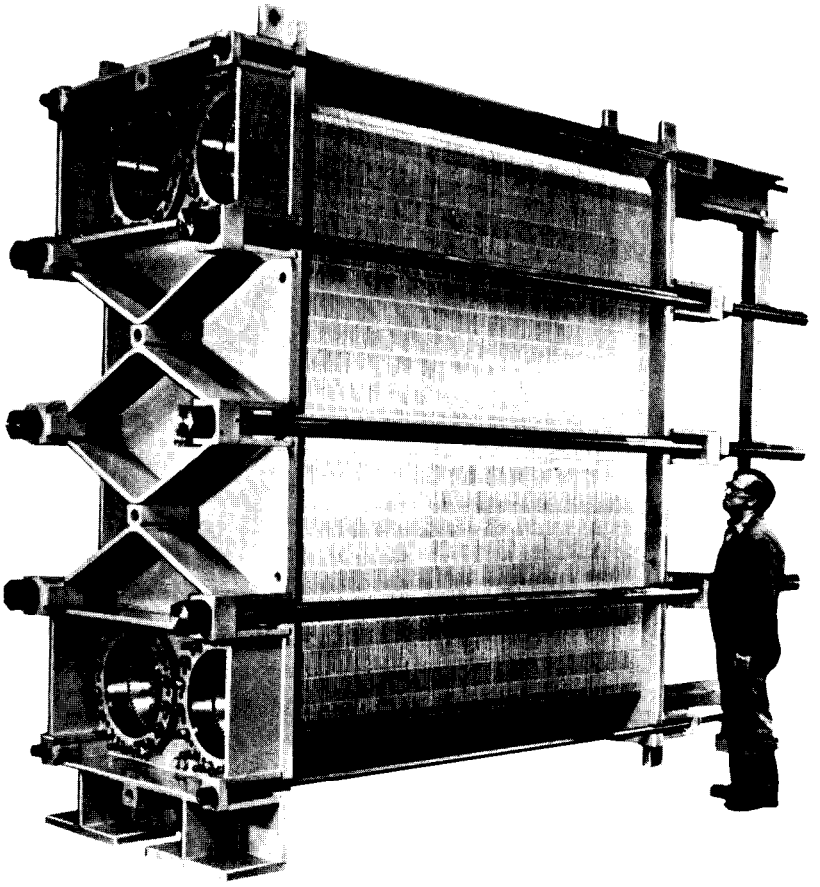

Figure 2 A large plate **heat** exchanger with all connections on the head. Photo courtesy of APV Company, Ltd., England.

plates can be supplied with gaskets of compressed asbestos fiber.

The plate heat exchanger is particularly suitable for heat recovery duties in the chemical, petroleum, food, dairy, and brewing industries.

Unlike shell-and-tube units, which can be custom built to conform to virtually any capacity and operating conditions, plates are mass produced in thicknesses ranging from 0.6 to 1 mm by complex and expensive press tools. They are therefore available only in a limited number of types and sizes, each of which has its own clearly defined specification with regard to performance and operating conditions.

There are two different aspects of PHE design, (1) the design of individual plate types so that they conform to specific performance and operational characteristics, and (2) the calculation of the number and arrangement of such plates in order to satisfy the thermal and pressure drop requirements of a particular duty as requested by a customer.

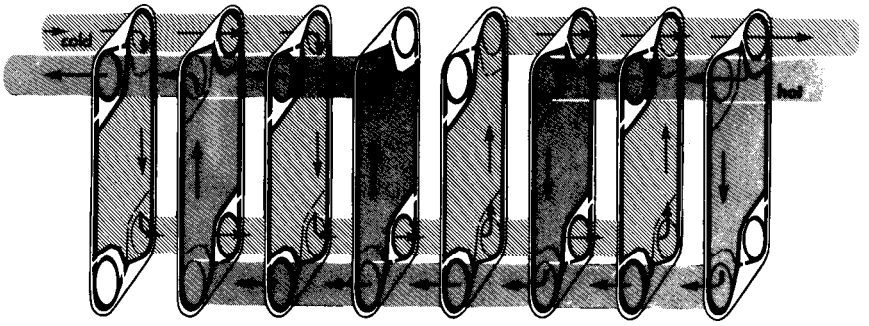

Figure 3 Flow pattern in two-pass/two-pass plate arrangement.

© 1983 Hemisphere Publishing Corporation

Because plate design varies from manufacturer to manufacturer, so does performance. Since there are more than 60 different plate types available throughout the world, it is impossible to give specific and accurate characteristics. Any data in these sections are thus only representative of plates in general.

© 1983 Hemisphere Publishing Corporation

3.7.2

Factors governing plate specification

Anthony Cooper and J. Dennis Usher

■ The two most important parameters are flow capacity and the range of NTU, the number of transfer units, defined as the temperature change of one fluid divided by the logarithmic temperature difference.

Flow capacity determines the size of the port in the four corners of the plate and, in turn, decides the overall plate dimensions. The NTU range is related to the heat transfer and pressure drop characteristics of the plate and governs the type of trough or corrugation to be adopted. The actual choice of NTU range must be considered in relation to the type of duties for which the plate is intended. Achievement of the highest possible NTU value is not necessarily representative of the optimum design; a careful investigation of the proposed market is necessary, and the range of thermal performance eventually chosen must ensure that (1) the lowest NTU duties can be handled without the heat transfer area being limited by pressure drop so that surface is wasted, and (2) the highest NTU duties can be handled without an arrangement involving too many passes so that pressure drops are unduly high.

© 1983 Hemisphere Publishing Corporation

HEDH

3.7.3
Corrugation design

Anthony Cooper and J. Dennis Usher

■ A wide range of types of corrugation is used in plate design, and the proper corrugation must be chosen from both thermal and mechanical considerations. Thermally, the corrugation function is to induce turbulence and increase the heat transfer area by amounts varying from 1.5 to 25%. The two most commonly adopted forms, illustrated in Fig. 1, can be described as the intermating type and the chevron or herringbone type. Further details are given in Sec. 4.4.2.

The intermating-type plate shown in Fig. 3.7.1(1*a*) is based on corrugations that are pressed to a depth greater than the compressed gasket depth. When the machine is closed, the corrugations fit into one another. A cross section at right angles to the flow direction is shown in Fig. la. This gives a constant change in direction and cross-sectional area in the direction of flow, so that turbulence is induced by a continuing variation in liquid velocity. The maximum flow gap ***b*** varies typically from 3 to 5 mm, with the minimum flow gap c being between 1.5 and 3 mm. Liquid velocities in the turbulent regime range from approximately 0.2 to 3 m/s depending on the pressure drop required,

Chevron troughs, shown in Fig. 3.7.1(1*b*), use parallel corrugations that are pressed in the plate to the compressed gasket depth. These corrugations run obliquely across the plates, with the angle of obliquity reversed on adjacent plates. The cross-sectional area in the direction of flow is constant, as shown in Figs. lb and 1*c*, but the change in shape of the flow passage induces turbulence by a continual change in direction.

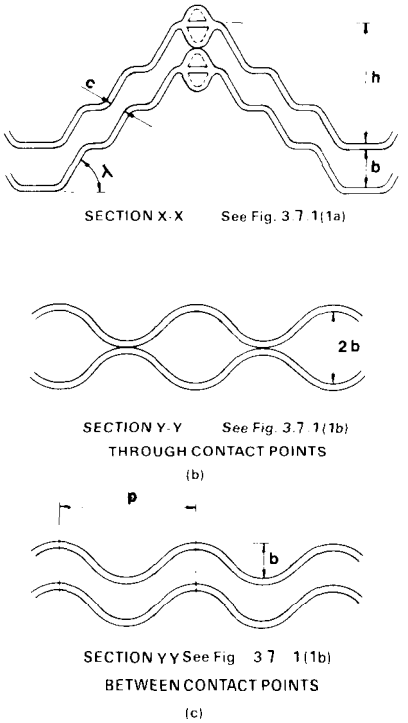

Figure **1** Sections through intermating and chevron troughs.

The corrugation depths on typical plates vary from about 3 to 5 mm. Velocities in the turbulent regime vary from about 0.1 to 1 m/s.

The intermating and chevron forms are examples of two- and three-dimensional troughs, respectively. The performance of a wide variety of trough types can be correlated by using a hydraulic mean diameter

© 1983 Hemisphere I blishing Corporation

derived from the expression

$$d_e = \frac{4 \times \text{volume between plates}}{\text{wetted surface between plates}} \quad (1)$$

which gives

$$d_e = \frac{2b}{r} \quad (2)$$

Nomenclature for Section 3.7.3 appears at the end of Section 3.7.12.

© 1983 Hemisphere Publishing Corporation

3.7.4
Friction factor correlations

Anthony Cooper and J. Dennis Usher

■ Although the performance of the many different corrugation forms can vary considerably, the pressure loss in a plate heat exchanger can always be calculated from a friction factor type of equation:

$$\Delta p = \frac{2fLG^2}{\rho d_e} \quad (1)$$

For a typical small plate heat exchanger with intermating plates, Fig. 3.7.1(1*a*), the friction factor would be predicted from the following equations:

$$f = \frac{1.22}{\mathrm{Re}^{0.252}} \quad \text{or} \quad f = \frac{38}{\mathrm{Re}} \quad (2)$$

In turbulent flow In laminar flow

In the transition regime, the friction factor relationship can be determined by interpolating between the boundaries of the turbulent and laminar flow regimes. However, with the intermating trough plate, the friction factor is also a function of liquid viscosity as well as Reynolds number (Fig. 1).

The Reynolds number at which the transition between the three flow regimes can occur varies considerably between plates. As a general rule, all types of plate heat exchangers will operate in fully turbulent flow at Reynolds numbers over 1 000 and will be in laminar flow at Reynolds numbers below 10. In between lies a range of duties that is difficult to predict

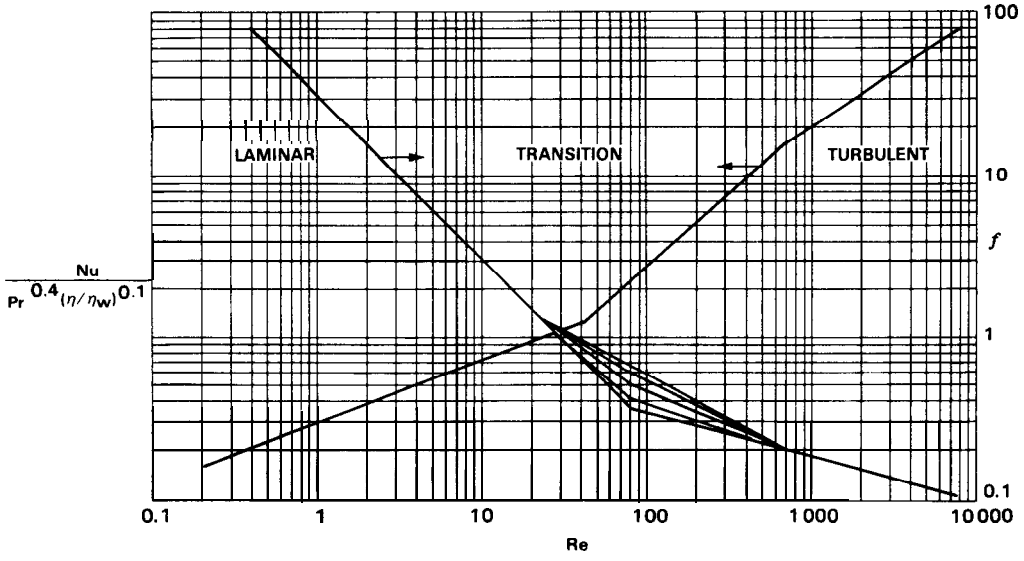

Figure 1 Performance characteristics of a small intermating-trough plate heat exchanger.

© 1983 Hemisphere Publishing Corporation

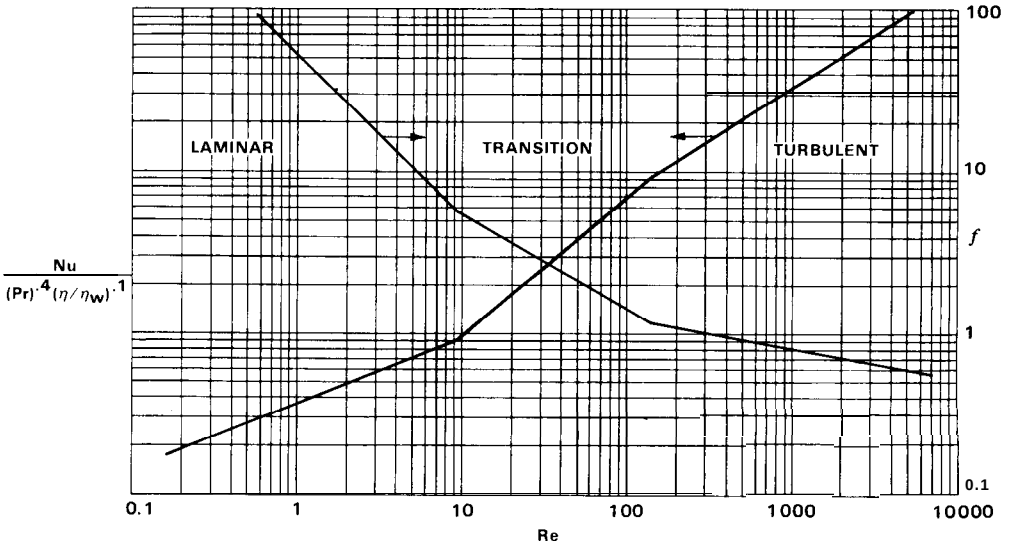

Figure 2 Performance characteristics of a small chevron-trough plate heat exchanger.

without accurate test work on the individual exchanger types.

For a typical small plate heat exchanger with chevron corrugations, the transition regime would range approximately from Reynolds numbers of 10 to 150 (Fig. 2).

From Figs. 1 and 2, it is obvious that with plate heat exchangers the friction factors are much higher than for equivalent Reynolds numbers in tubes. However, velocities in plates are much lower and usually range from 0.1 to 3 m/s depending on the type of plate and application. Also, the length of plate required to achieve a given NTU is much less than with a tube, so the pressure drop in Eq. (2) is often less than that in tubes for equivalent heat transfer performance.

In laminar flow applications, the plate heat exchanger is also an effective heat transfer device, particularly for those pseudoplastic non-Newtonian fluids where an increase in shear rate causes a decrease in viscosity. Prediction of pressure drop is, however, extremely difficult. Some success has been obtained by Parrott [1], who combined Wilkinson s generalized Reynolds number [2] with flat-plate theory. Currently, however, these correlations are still academic and not very applicable to practical use.

From the viscosity/shear rate/temperature relationship and knowledge of the shear rate in the exchanger, the user can generally make a good design using conventional Newtonian equations. For particularly difficult fluids that are highly sensitive to shear and temperature, most manufacturers offer a loan service so that a test can be carried out in the field on an actual heat exchanger.

Nomenclature and References for Section 3.7.4 appear at the end of Section 3.7.12.

© 1983 Hemisphere Publishing Corporation

3.7.5
Heat transfer correlations

Anthony Cooper and J. Dennis Usher

■ The heat transfer performance of plate-type units is also calculated from typical dimensionless heat transfer equations with the appropriate exponents and constants for each specific type of exchanger. A number of references [3-5] have reported correlations.

For a small intermating heat exchanger, Figs. 3.7.1(1*a*) and 3.7.4(1), the heat transfer equations would be

Turbulent flow $$Nu = 0.2(Re)^{0.67}Pr^{0.4}\left(\frac{\eta}{\eta_w}\right)^{0.1} \quad (1)$$

Laminar $$Nu = 1.68\left(Re\ Pr\frac{d_e}{L}\right)^{0.4}\left(\frac{\eta}{\eta_w}\right)^{0.1} \quad (2)$$

In the transition regime, the heat transfer relationship can usually be determined by interpolating between the boundaries of the turbulent and laminar regimes, Figs. 3.7.4(1) and 3.7.4(2).

It is impracticable in any study such as this to give specific, accurate performance equations. Since individual plate performance varies greatly, the equations given here and in Sec. 3.7.4 can be regarded as typical and can be used only to estimate approximate surface area requirements for duties when the flow is fully turbulent or completely laminar.

To employ the equations in these sections, the reader is advised to use values of L in the range 0.7-2 m and values of d_e in the range of 4 mm for the smaller plates. This rises to 5-7 mm for the larger plates. A typical length/width ratio for many plates is 2. The plate gap can be taken as one-half the equivalent diameter d_e for budget calculations.

Calculation methods including two simple examples are given in Sec. 3.7.10 for the estimation of surface areas based on correlations similar to those described.

The effect of non-Newtonian characteristics on heat transfer is less than on pressure drop and usually less significant than the effect of temperature on viscosity. Calculation procedures for Newtonian fluids are generally used that, for a typical pseudoplastic non-Newtonian fluid, will give conservative designs.

By far the most important design problem with viscous fluids, whether they are Newtonian or non-Newtonian, occurs with cooling duties, where a basically unstable system can develop. If the fluids are poorly distributed either over the plate area or along the plate pack, overcooling of the fluid can occur. This increases the viscosity, lowers the velocity, and causes further cooling. Channeling of the fluid is increased, and this makes large areas of the plate virtually ineffective. This does not occur on heating duties, where the effect of maldistribution or channeling is self-balancing, or in turbulent flow, when the pressure drop characteristics help to establish better distribution.

Nomenclature and References for Section 3.7.5 appear at the end of Section 3.7.12.

© 1983 Hemisphere Publishing Corporation

3.7.6

Factors affecting plate design

Anthony Cooper and J. Dennis Usher

A. Corrugation geometry

Much of the published information on corrugation performance is based on specific shapes and relates to pressure drop rather than heat transfer. The majority of corrugations, however, give approximately the same relation between these two quantities if they are expressed as (1) film heat transfer coefficient (HTC) α and energy loss per unit area of developed surface E, Fig. 1 [3], or (2) film HTC α and specific pressure drop J, expressed as pressure drop per NTU, Fig. 2 [3]. These correlations allow therefore an estimate of heat transfer performance to be made from an assessment of pressure drop.

Experimental work carried out on different corrugations indicates the following:

(a) Intermating troughs

Tests [6,7] on a wide range of corrugation types shows that the $Nu/Pr^{0.4}$ value increases and the film HTC α decreases with increase in plate spacing b at constant Re values. Pressure drop likewise increases, a simple corrugation giving the approximate relation

$$\frac{\Delta p}{L} \propto \frac{1}{(d_e)^3} \qquad (1)$$

Other work has confirmed the influence of spacing on pressure drop, which also increases both with corrugation height h and with the base angle λ [8-10].

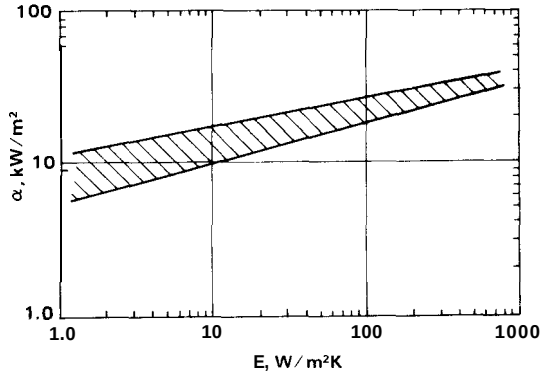

Figure 1 Film coefficient/energy per unit area.

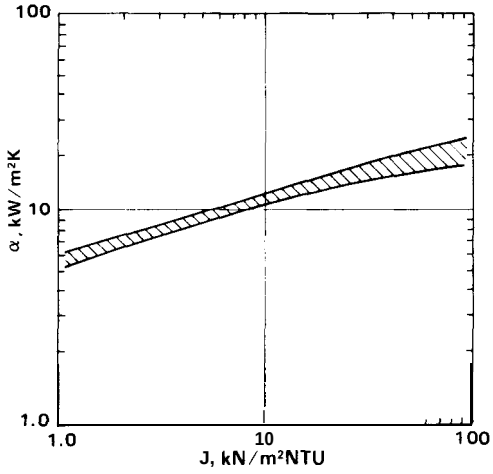

Figure 2 Film coefficient/specific pressure drop.

© 1983 Hemisphere 1 blishing Corporation

(b) Chevron troughs

Graphs of $Nu/Pr^{0.4}$ and $\Delta p/L$ plotted against Re show that both quantities increase as the angle of obliquity β is increased from 30 to 120 [6]. Mass transfer studies using the Chilton-Colburn analogy give the same general relationship [11].

The effect of increase in trough pitch p from 8 to 15 mm with a constant corrugation depth b of 4 mm is to halve the pressure drop per unit length, whereas $Nu/Pr^{0.4}$ is unaffected [6].

B. Distribution

Since the diameter of the entry port at either end of the plate is small compared with the width of the main heat transfer area, transverse distribution of flow across the plate can be adversely affected. The most important factors are port arrangement, aspect ratio, and plate entry losses.

(a) Port arrangement

Ports can be arranged either in diagonal flow (entry and exit at opposite corners of the plate) or vertical flow (entry or exit on the same side of the plate) as shown in Figs. 3.7.1(1*a*) and 3.7.1(1*b*), respectively, and discussed in Sec. 4.4.2. The resulting difference in flow distribution has some effect on the transverse temperature profile, as shown in Fig. 3. This compares diagonal and vertical downward-flowing plates at an identical Reynolds number of 8 280 [12].

The effectiveness of air removal is important, particularly in downward-flowing plates where the liquid velocity must be high enough to ensure that the plates run full [13]. For practical purposes this can normally be achieved by ensuring that the pressure loss down the plate is not significantly less than the static head corresponding to the vertical distance between the ports.

(b) Aspect ratio

The effects of poor distribution can be accentuated by low aspect ratio (i.e., mean heat transfer length/flow width). No positive recommendations appear to be available for this factor, but on most commercial plates the aspect ratio does not fall much below a value of 1.8.

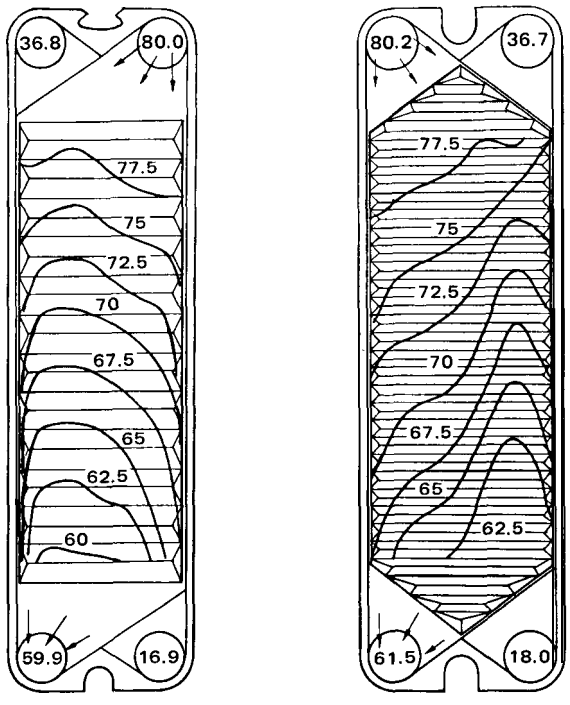

Figure 3 Temperature distribution (°C) on vertical- and diagonal-flow plates.

(c) Plate entry losses

Extraneous pressure losses must be minimized at the plate entry area by avoiding any undue restriction. Since this entrance region of the plate is the most mechanically weak area of the entire plate, the mutual support between adjacent plates adds to the restriction and therefore requires very careful design. The lower the thermal and pressure drop performance of the plate, the greater will be the proportional effect of these extraneous losses.

Nomenclature and References for Section 3.7.6 appear at the end of Section 3.7.12.

© 1983 Hemisphere Publishing Corporation

3.7.7
Over all plate design

Anthony Cooper and J. Dennis Usher

A. NTU rating

A heat exchanger plate can be regarded as a module of known characteristics that can be defined by the NTU range covered by a single plate. For such a plate operating under unit flow ratio conditions,

$MC_p \phi = Ua$ A T

so that

$$\text{NTU} = \frac{\phi}{A} = \frac{Ua}{MC_p} \tag{1}$$

For n active plates, the total area is na. The total flow passages for each liquid are $(n+1)/2$. Hence,

$$\text{NTU} = \frac{2n}{n+1}\frac{Ua}{MC_p}$$

and when n is infinite,

$$\text{NTU} = \frac{2Ua}{MC_p} \tag{2}$$

Because plates are normally arranged in large packs, it is customary to define the NTU value of a plate by the expression given in Eq. (2) for $n = \infty$.

B. Performance characteristics

Figure 1 plots overall HTC U and overall pressure drop Ap against flow rate for a typical plate in 0.6 mm stainless steel, whereas Fig. 2 plots NTU directly against pressure drop.

If as a rough approximation the following laws are assumed:

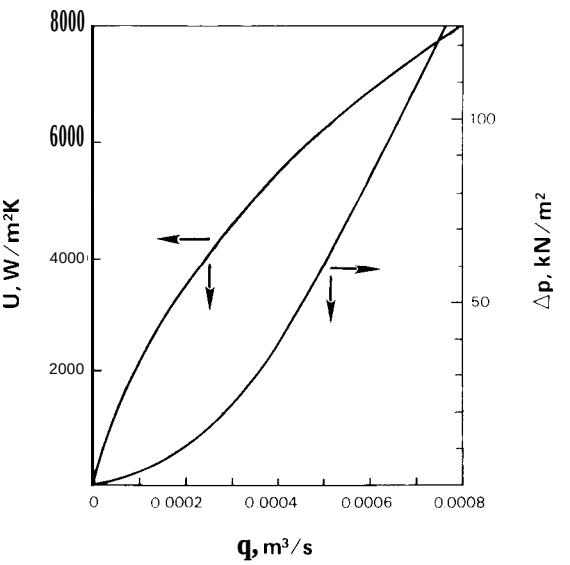

Figure 1 Overall HTC and pressure drop/plate flow rate.

$$U \text{ a } V^{2/3} \quad \text{and} \quad \text{Ap} \propto V^{5/3} \tag{3}$$

we find that

$$U \text{ a } \Delta p^{2/5} \quad \text{and} \quad \text{NTU a } V^{-1/3} \text{ a } \Delta p^{1/5} \tag{4}$$

The actual indices depend on the corrugation design, but these expressions give the order of the relationship between the different quantities involved. Since the lowest feasible plate flow rate is that corresponding to a pressure drop approximately equal to the static head between the ports, it will be seen that this condition determines the maximum NTU value, which has already been fixed by the plate specification.

© 1983 Hemisphere Publishing Corporation

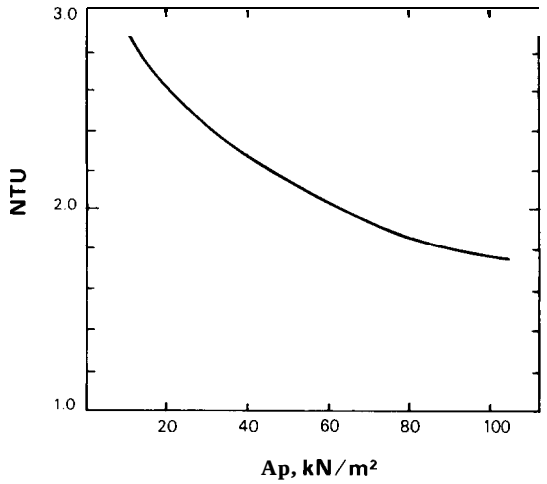

Figure 2 NTU/pressure drop curve for typical plate.

C. Design procedure

From a design specification that defines the maximum flow rate and NTU value, the stages in developing a particular plate are as follows:

1. From the maximum flow rate that the PHE has to handle, determine the port size. Excessive velocities along the manifold comprised by the plate ports can give rise to significant extraneous pressure losses, the allowance for which is discussed later. Port sizing on the basis of a maximum velocity of about 6 m/s is normal practice.

2. The largest size of flange is selected to meet the specified operating pressure and code requirements. Allowing for adequate clearance, the center distance between ports can then be determined and from this the width of the plate.

3. The length can now be determined from considerations of the aspect ratio. This leads to both the developed and projected heat transfer areas (the ratio r normally lies between 1.15 and 1.25, depending on the shape of the corrugation).

4. Knowing the maximum NTU value, the corresponding pressure drop, and the plate area, the parameters are available to allow a suitable corrugation to be selected to conform to these conditions.

Nomenclature for Section 3.7.7 appears at the end of Section 3.7.12.

© 1983 Hemisphere publishing Corporation

3.7.8

Plate arrangement and correction factors

Anthony Cooper and J. Dennis Usher

■ The preceding sections cover the design of individual plates. This is mainly the concern of the plate manufacturer, who defines the performance of each type of plate in terms of its thermal and pressure drop characteristics. These are then used in calculations in order to determine the number and arrangement of plates to meet any specified duty. The basis for these calculations is explained in the remaining sections of this chapter .

A. Types of pass arrangement

There are three fundamental ways in which plates can be arranged: single pass, multipass with equal passes, and multipass with unequal passes.

(a) Single pass

Both liquids flow countercurrently through parallel passages that make up a single pass as shown in Fig. 1.

(b) Multipass with equal passes

When NTU values greater than those given by a single plate are required, multipass arrangements can be obtained by blanking off the correct flow port at P and Q to define the end of each pass. Figure 2 shows a two-pass (2/2) arrangement.

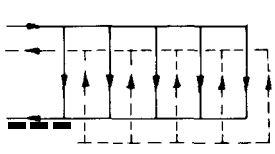

Figure 1 Single-pass plate arrangement.

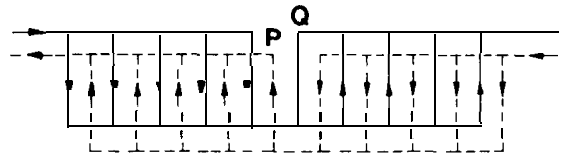

Figure 2 Two-pass/two-pass plate arrangement.

(c) Multipass with unequal passes

When flow ratios are high or there is some other reason for minimizing the pressure drop on one side, unequal passes can be used with fewer passes on the low-pressure-drop side. Figure 3 shows a two-pass/one-pass (2/1) arrangement.

B. Concurrency corrections for large unequal passes

Where the number of passes for each liquid is unequal, concurrency occurs as shown by Fig. 3. Depending on the NTU value and flow rates, this will reduce the effectiveness of any particular arrangement. If T_i is the

Figure 3 Two-pass/one-pass plate arrangement.

© 1983 Hemisphere Publishing Corporation

inlet and T_o the outlet temperature of one fluid and T_i' and T_o' the inlet and outlet temperatures of the second fluid, then for a basically countercurrent arrangement with these temperatures,

$$M_1 C_{p1}(T_i - T_o) = M_2 C_{p2}(T_o' - T_i') \quad (1)$$

$$\text{Ratio } R = \frac{T_o' - T_i'}{T_i - T_o} \quad (2)$$

$$\text{NTU} = \frac{T_o' - T_i'}{\Delta T} \qquad \text{Ratio Z} = \frac{T_o' - T_i'}{T_i - T_o'} \quad (3)$$

$$\text{Effectiveness} = \frac{T_o' - T_i'\ M_1 C_{p1}}{T_i - T_i'\ (M\ C_p)_{\min}} \quad (4)$$

Effectiveness/NTU charts for shell-and-tube units are based on the assumption that the transverse temperature across the shell is uniform. In the case of a PHE, the degree of correction is less severe, since the flow passages are segregated by plates so that the cross flow that occurs in a shell-and-tube unit is avoided.

Information for a number of different plate arrangements has been published in terms of the correction factor F to be applied to the LMTD (where $F = \Delta T_x/\Delta T$) as a function of the parameter Z [14]. The graphs relating to infinite passes of 2/1, 3/1, and 4/1 for values of R from 1 to 10 are shown in Figs. 4, 5, and 6. T_i, T_o, T_i', and T_o' can be determined from the relevant Z and R values. This leads to the corresponding figures for effectiveness and NTU.

C. End effect

The concurrency corrections given above assume that the size of the passes is infinite. For small platages, however, certain additional factors become important.

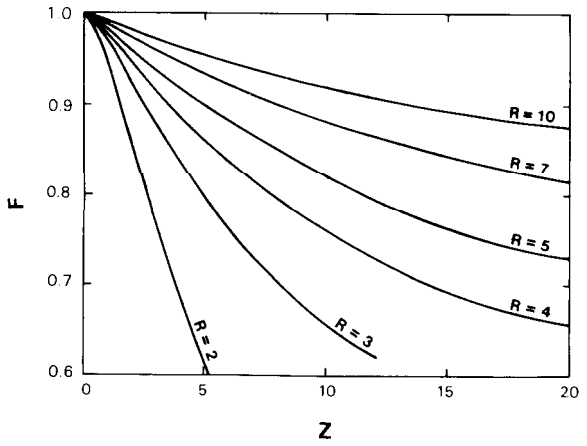

Figure 4 Concurrency factors, two-pass/one-pass arrangement.

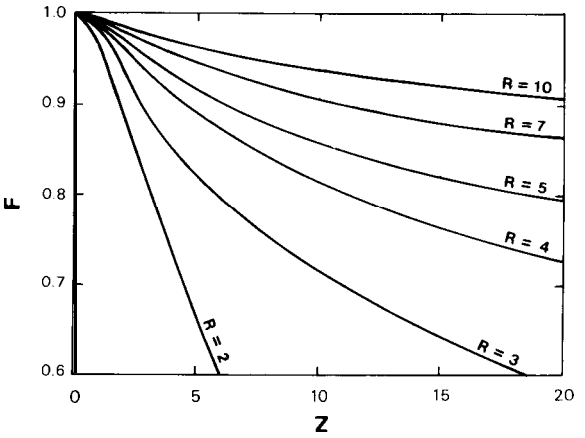

Figure 5 Concurrency factors, three-pass/one-pass arrangement.

(a) End passages

In all plate arrangements, every passage transfers heat in both directions except the end passages, which transfer heat in one direction only.

(b) Equal number of *passes*

From Fig. 2 it will be seen that although the flows are basically counter current, the plate that separates passages PQ at the end of each pass is subject to concurrent flow,

(c) Unequal passes

The two-pass/one-pass system in Fig. 3 has eight concurrent and seven countercurrent plates. This inequality, which applies to all pass arrangements, must be taken into account.

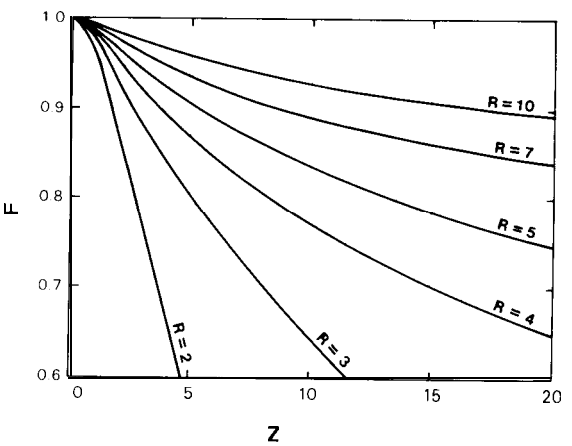

Figure 6 Concurrency factors, four-pass/one-pass arrangement.

© 1983 Hemisphere Publishing Corporation

These factors can be denoted as end effects, because they result from passages at the end of each pass. Their magnitude increases with the following parameters:

1. Increase in plate NTU
2. Decrease in size of pass
3. Increase in number of passes

Some published information [23] about these factors presents them in terms of looped flow, (i.e., number of passes of single passages, rarely encountered in practice), series flow (i.e., single passes), or complex flow (i.e., multiple passes). Another analysis [14] has investigated the effect of pass size on 2/1 and 3/1 pass arrangements. An F/Z plot for a 2/1 pass arrangement for $R = 5$ is given from three thermal plates to infinity in Fig. 7. This shows that with about 20 or more plates, the end effect is not serious.

D. Distribution along port manifolds

On small plate packs, the effect of pressure drop down the port manifold can be ignored and calculations can be based on the assumption of equal flow rates down each plate in a pass. On large plate packs, distribution effects can become significant, depending on the relative magnitudes of the plate and manifold pressure drops. This will reduce the effective LMTD.

The two factors that affect the port pressure drop are (1) the frictional loss along the manifold, and (2) the momentum change due to the variation in liquid velocity.

Distinction must be made between two port arrangements [15].

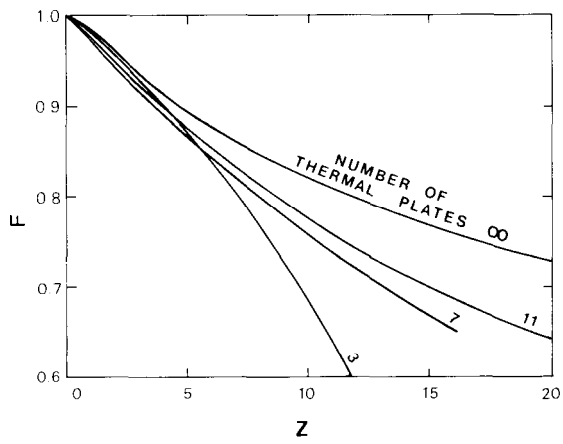

Figure 7 Concurrency factors, two-pass/one-pass of different sizes.

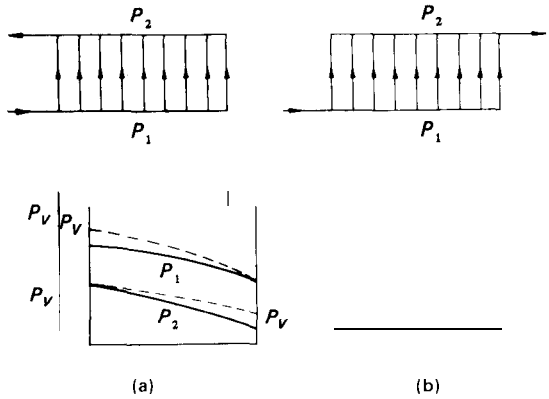

Figure 8 Pressure distribution along port manifolds.

(a) U connections

On U connections the inlet and outlet connections are made to the head of the machine only, so that this system is restricted to single-pass arrangements. The combination of frictional loss and velocity head P_v shown in Fig. 8*a* results in maximum pressure drop across the plate adjacent to the head and minimum against the follower.

(b) Z *connections*

On Z connections the inlet and outlet connections are on the head and follower, respectively. This arrange-

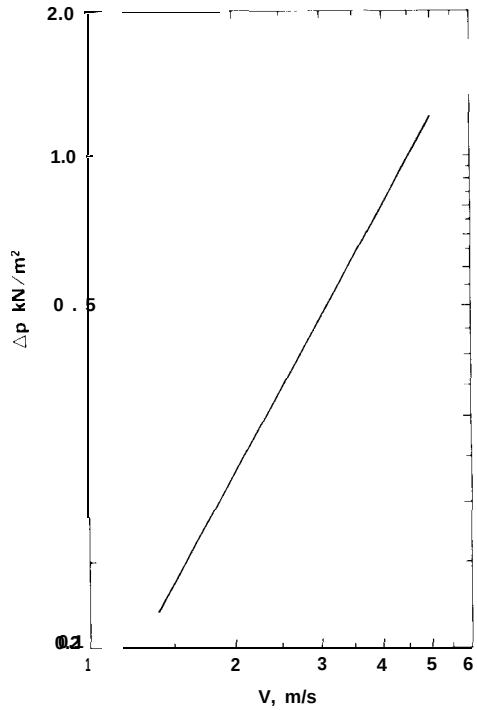

Figure 9 Pressure drop/velocity curve for port manifold.

© 1983 Hemisphere Publishing Corporation

ment, shown in Fig. 8*b*, also applies to each pass of a multipass system. The combination of frictional loss and velocity head P_v usually gives a variation in pressure drop across the plate pack that is less than with the U arrangement.

(c) Performance analysis

The friction factor as a function of the number of plates can be obtained by measuring the pressure drop down a port manifold operating with a constant flow rate from end to end (i.e., not withdrawing any liquid down the plates), and a typical pressure drop/velocity curve for 100 plates (50 passages) is shown in Fig. 9. These data, in conjunction with the plate pressure drop characteristics, can be used as a basis for an iterative program to determine the pressure drop down the manifold.

Nomenclature and References for Section 3.7.8 appear at the end of Section 3.7.12.

© 1983 Hemisphere Publishing Corporation

3.7.9
Fouling

Anthony Cooper and J. Dennis Usher

■ Often termed the most unresolved problem in heat transfer, fouling is usually handled better in plate heat exchangers than in most other types of exchanger. The high induced turbulence between the plates minimizes the build up of most types of fouling. The high turbulence also enhances the effect of in-place cleaning methods. Should the extent of fouling require manual cleaning, this type of exchanger is easily opened, cleaned, and closed.

Experimental data have been obtained by Heat Transfer Research Inc. (Alhambra, CA) on fouling with cooling tower water in plate and tubular heat exchangers [16]. These tests showed that the fouling resistance on the plates was less than half that in the tubular exchangers. Data from one of the tests are shown in Fig. 1. The fouling resistance in the plate heat exchanger was only 25% of that recommended by TEMA for cooling tower water.

These tests were performed on chevron plates with a gap of 3 mm. This type of plate gives higher turbulence than the intermating design, so fouling on some types of scaling liquids is less severe. The chevron design, however, usually has more contact points between the plates, so when the liquid carries discrete solids in suspension, it can be more prone to blockage.

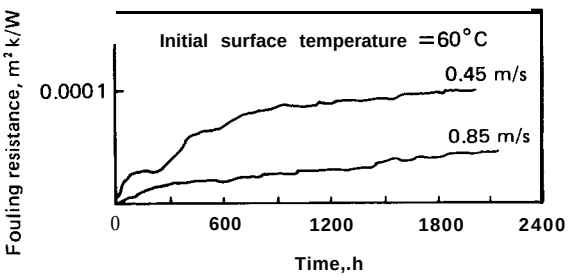

Figure 1 Fouling resistances at two different plate velocities.

Nonetheless, because of the high turbulence within the plates, the PHE is particularly good at minimizing sedimentation fouling. Slurries, for example, can be easily processed, since the particles are maintained in suspension. However, because of the narrow gap, it is essential where possible to ensure that all particles over 2 mm in size are removed by screening before the heat exchanger.

Because PHE heat transfer coefficients are much higher than for tubular units, the use of tubular fouling resistances is unrealistic. For design purposes, it is recommended that values of not greater than one-fifth of the published tubular figures [17] be used.

References for Section 3.7.9 appear at the end of Section 3.7.12.

© 1983 Hemisphere Publishing Corporation

3.7.10

Methodofface area calculation

Anthony Cooper and J. Dennis Usher

A. Performance limitations

The previous sections have shown the principles underlying the design and performance of plates, both individually and arranged in a heat exchanger. Assessment of the suitability for a particular duty must be based on the fact that the world-wide range of plates operating in a single pass at unity flow ratio on aqueous liquids cover the following range of parameters:

Area	Up to 2.5 m^2 approx.
NTU	**0.3-3.5** approx.
Maximum operating pressure	2 000 kN/m^2 approx.
Maximum viscosity	5 kg/m s
Port diameter	Up to 400 mm
Maximum flow rate	**2** 500 m^3/h

A quick assessment of the PHE suitability can be made by comparing the above figures with the actual flow rate and duty NTU required, that is, the NTU based on LMTD corrected to allow for physical properties, fouling, and so on, from which the number of passes required can be derived. NTU values in excess of 12 are normally avoided, because the increase in temperature change and pressure drop rarely justify the additional area required.

B. Basic procedure

The actual calculation method is based on the following procedure, which indicates the iterative process involved. The object is to establish the number of plates n and of passes H **to** conform to the specified heat transfer and pressure drop requirements.

Consider a duty of M kg/s of an aqueous liquid with similar flow rates on each side and with a LMTD of AT. The required temperature change is ϕ and the permissible pressure drop Δp. The passages per pass is $n/2H$, so the plate flow rate is $2MH/n$.

The overall HTC is a function of plate flow rate, fouling, and physical properties, so

$$U = f_1\left(\frac{MH}{n}, x\right) \tag{1}$$

Allowing for end effect, concurrency, and port losses, which depend on the plate arrangement,

$$\text{Actual LMTD AT} = \text{AT} f_2(n,H) \tag{2}$$

thus from

$$Q = UA\ \Delta T$$

we have

$$MC_p\phi = f_1\left(\frac{MH}{n}, x\right) na\ \Delta T\ f_2(n, H) \tag{3}$$

Allowing for port losses, the available pressure drop is Ap $f_3(n,H)$, and this is also a function of plate rate, fouling, and physical properties, that is,

$$\Delta p\ f_3(n, H) = f_4\left(\frac{MH}{n}, y\right) \tag{4}$$

If the functions f_1, f_2, f_3, and f_4 are known, n and H can be obtained from the complex relationships given in Eqs. (3) and (4), suitably modified where necessary

© 1983 Hemisphere I blishing Corporation

for variations such as unequal flow rates. Manual calculations can be based on either the so-called LMTD method or the effectiveness-NTU method [18], whereas a very approximate estimate of surface area can be made by the method given below for aqueous liquids.

C. Approximate assessment for turbulent flow

This method, based on data representative of PHEs in general, can be used to obtain an approximate estimate of the heat transfer area required for a particular duty within the following limitations:

Turbulent flow conditions (i.e., viscosity not exceeding 4 X 10^{-3} kg/m s)

Volumetric flow ratio not exceeding 3:1

However, for any degree of accuracy, plate manufacturers must be approached for quotations based on their own data.

Three basic curves for water/water at unity flow ratio are employed:

1. Area/flow rate curve that relates the individual plate heat transfer area to the total flow the PHE can handle. See Fig. 1.
2. $\alpha/\Delta p$ curve representative of plates in general, where α in this case is equal to $2U$, thereby incorporating an approximate allowance for metal resistance. See Fig. 2.
3. Typical Δp/plate flow rate curves for plates of different areas between 2 m^2 and 0.1 m^2. See Fig. 3.

These curves apply to water at 313 K, for which the following physical properties can be assumed:

Density = 1 000 kg/m^3
Specific heat = 4.2 kJ/kg K
Thermal conductivity = 0.63 W/m K
Viscosity = 0.65 X 10^{-3} kg/m s

The procedure is then as follows:

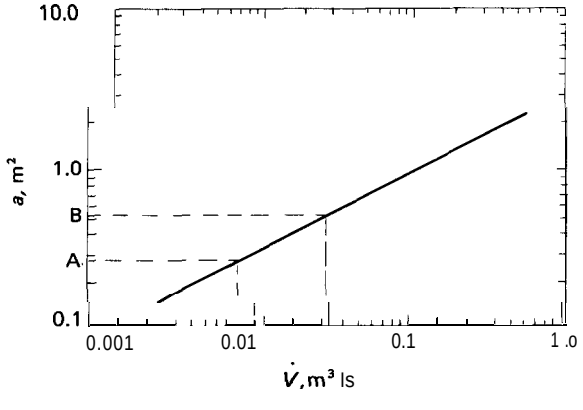

Figure **1** Plate area/total flow rate.

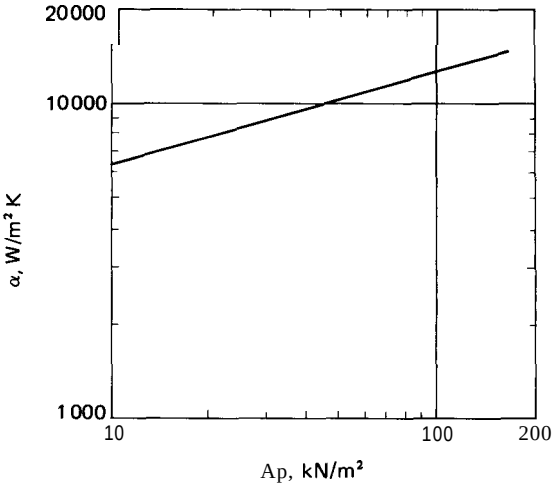

Figure 2 Film HTC/pressure drop for typical plates on water.

Step 1. Select from the plate area/flow rate graph, Fig. 1, the approximate area a of the plate to be used, based on the higher of the two liquid flow rates.

Step 2. Modify the $\alpha/\Delta p$ curve, Fig. 2, for each liquid by correcting the α ordinate in each case to allow for fouling and physical properties in relation to those of water using the correlations in Sec. 3.75.

Step 3. The two curves in Fig. 2, already revised in step 2, should be further modified by adjusting the Ap ordinates to allow for fouling and physical properties of the liquids in relation to water by using the correlations for friction factor and pressure drop in Sec. 3.7.4.

Step 4. Similarly modify the two curves in Fig. 3 by factoring the Δp ordinates to allow for fouling and physical properties in relation to those of water using the correlations given in Sec. 3.7.4.

Step 5. To find the number of plates n and the number of passes H on each side to comply with the required duty:

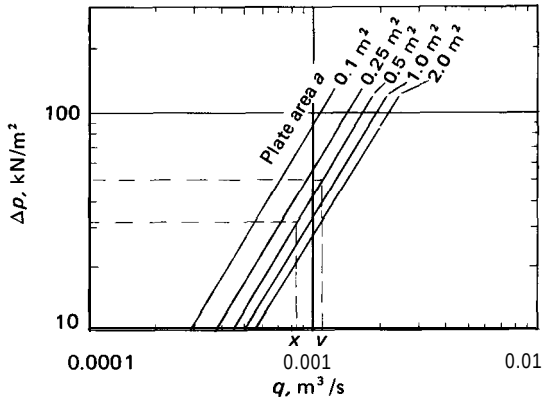

Figure 3 Pressure drop/plate flow rate for different plate areas on water.

© 1983 Hemisphere Publishing Corporation

(a) Select a whole number of passes H and determine the available pressure drop per pass on each side as given by

$$\Delta p = \frac{\text{allowable pressure drop}}{H}$$

(b) From modified Fig. 2 in step 3, select the α values corresponding to Ap values for each side.

(c) Using the reciprocal equation and incorporating any fouling allowance, but excluding metal resistance, combine the two α values obtained above to give the overall U value.

(d) From the modified curves in Fig. 3, determine the q values corresponding to the allowable pressure drop per pass on each side and select the higher of the two values.

(e) Calculate $n = 2H\dot{V}/q$, where $\dot{V}$ is the higher of the two liquid flow rates and q is the higher value given in (d).

(f) Calculate $Una\,AT$ and compare with the required heat transfer rate; if necessary, repeat with different values of H until optimum agreement is reached.

The value of na will give a very approximate idea of the area required, but for the correct plate arrangement, proper calculations must be used.

(a) Example I

Duty: To heat 7.78 kg/s of wash oil by regeneration from 331 K to 371 K using hot feed at 383 K. The allowable pressure loss = 130 kN/m^2 each side.

Physical properties:

Density = 880 kg/m^3
Specific heat = 1.926 kJ/kg K
Thermal conductivity = 0.125 W/m K
Viscosity = 3 $\times 10^{-3}$ kg/m s

Solution: From heat balance,

ϕ = 40 K and AT = 12 K

Required heat rate $\dot{Q} = MC_p\phi$ = 600 kW

1. Plate area from Fig. 1: The volumetric rate is

$\dot{V} = 8.8 \times 10^{-3}\ m^3/s$

and the corresponding plate area is

$a = 0.27\ m^2$

See point A in the figure.

2. Modification of the α ordinates in Fig. 2: From Eq. 3.7.5(1) relating physical properties to heat transfer, the film coefficient α is proportional to

$$k^{0.6}\rho^{0.67}C_p^{0.4}\eta^{-0.27}$$

ignoring the factor $(\eta/\eta_w)^{0.1}$.

Using the data already given for wash oil and water, the correction factor for α becomes 0.17, and this must be applied to the α ordinate in Fig. 2. See curve C in Fig. 4.

3. Modification of Ap ordinates in Figs. 2 and 3: From Eqs. 3.7.5(1) and 3.7.5(2) for turbulent flow, the pressure drop is related to physical properties by the expression

$$\Delta P \propto \eta^{0.252}\rho^{0.748}$$

Using the data already given, the correction factor for Ap in relation to water becomes 1.34, which must be applied to the Δp ordinates of the curve in Fig. 2 already modified as in step 1 (see curve ***D,*** Fig. 4) and to the Ap ordinates of Fig. 3. This being a regenerative arrangement with the same liquids on both sides, only one curve is necessary for each figure, but if dissimilar liquids were involved, corrected curves for both sides would be required in each case.

4. Selection of pass arrangement:

(a) Try H = 8. Then

Pressure drop per pass = $\frac{130}{8}$ = 16.25 kN/m^2

(b) and (c) The modified $\alpha/\Delta p$ curve ***D*** in Fig. 4 shows that this corresponds to an α value of 1 200 W/m^2 K at point E and, as conditions on both sides of the plate are the same, this can be halved ***to*** give the value of U so that

$$U = 600$$

Where conditions are not the same, follow the treatment given in Example 2.

(d) In Fig. 3 the curve for a = 0.27 m^2, with Δp ordinates factored by 1.34, gives

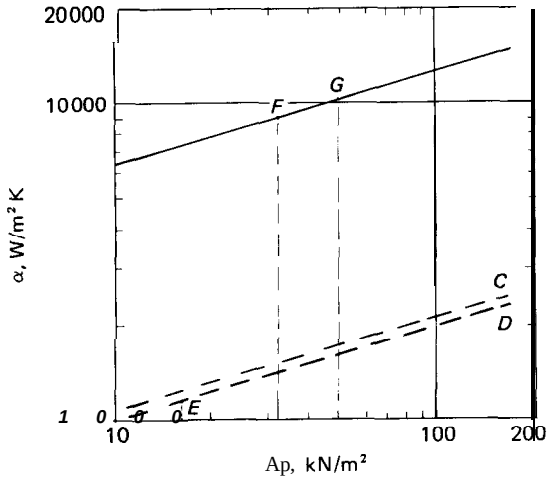

Figure 4 Modified Fig. 2 corrected for physical properties.

© 1983 Hemisphere Publishing Corporation

q = 0.44 X 10^{-3} m^3/s when Ap = 16.25 kN/m^2

(e) Therefore,

$$n = \frac{2 \text{ X } 8 \text{ X } 8.8 \text{ X } 10^{-3}}{0.44 \text{ x } 10^{-3}} = 320$$

(f) As already stated, for a regenerative arrangement,

$$U = \frac{\alpha}{2} = 600 \text{ W/m}^2 \text{ K}$$

which gives a heat transfer rate of

600 X 320 X 0.27 X 12 X 10^{-3} = 622 kW

This is sufficiently close to the specified figure of 600 kW to be an acceptable solution, so that

Total area = ***na = 86.4*** m^2

Where different liquids or flow rates are involved, α values for each side would be required from the two modified versions of Fig. 2, using the two Δp values relating to the two sides, and they would then be combined by the reciprocal equation.

Example 2

Duty: To heat 22.7 kg/s of water from 283 K to 361 K by 34 kg/s of hot water at 368 K. The allowable pressure drops are 100 kN/m^2 and 150 kN/m^2, respectively.

Solution: Let suffixes 1 and 2 denote the primary and secondary flows. From the heat balance,

ϕ = 78 K and ***A T*** = 16.77 K

Required heat rate $\dot{Q} = M_1 C_p \phi$
= 22.7 X 4.2 X 78
= 7 437 kW

Volumetric flow rate $\dot{V}_1$ = 22.7 X 10^{-3} m^3/s
$\dot{V}_2$ = ***34*** X 10^{-3} m^3/s

1. ***Plate area from Fig. 1:*** Based on the higher flow rate $\dot{V}_2$,

a = 0.52 m^2

See point ***B*** in the figure.

2, 3. Modification of α and ***AP ordinates:*** For water at the given temperatures, the overall corrections for physical properties would be small and may be ignored.

4. Selection of pass arrangements:

(a) Try ***H*** = 3, which gives pressure drops per pass:

$$\Delta p_1 = \frac{100}{3} = 33.3 \text{ kN/m}^2$$

$$\Delta p_2 = \frac{150}{3} = 50 \text{ kN/m}^2$$

(b) Figure 2 shows that the corresponding values are

α_1 = ***9 000*** W/m^2 K

α_2 = 10200 W/m^2 K

See points ***F*** and *G* in Fig. 4.

(c) Using the reciprocal equation, we find

U = 4780 W/m^2 K

(d) Figure 3 gives, for Δp_1 and Δp_2,

q_1 = ***0.85*** X 10^{-3} m^3/s

q_2 = 1.1 X 10^{-3} m^3/s

See points ***X*** and Y in the figure.

(e) Therefore,

$$n = \frac{2H\dot{V}_2}{q_2} = \frac{2 \text{ x } 3 \text{ x } 34 \text{ x } 10^{-3}}{1.1 \text{ x } 10^{-3}} = 185$$

as q_2 has the higher of the two values.

(f)

Rate of heat transfer achieved = ***Una*** AT

= 4 780 X 185 X 0.52 X 16.77 X 10^{-3} kW

= 7 710 kW

This is sufficiently close to the specified figure of 7 437 kW to be an acceptable solution, so that

Total area = *na* = 185 X 0.52 m^2 = 96.2 m^2.

D. Computer programs

As already explained, the correlations given in Secs. 3.7.4 and 3.7.5 are merely typical of a wide range of plates whose performance characteristics vary considerably. The presentation of specific correlations in this book, therefore, is impossible. To combat this problem certain manufacturers make computer programs available so that customers can size and budget price plate heat exchangers [19].

Nomenclature and References for Section 3.7.10 appear at the end of Section 3.7.12.

© 1983 Hemisphere I blishing Corporation

3.7.11
Thermal mixing

Anthony Cooper and J. Dennis Usher

■ Single rather than multipass operation is often desirable on large industrial PHEs because the U arrangement of inlet and outlet flow enables follower connections to be avoided and the machine to be opened easily for plate accessibility. However, a single pass of any particular plate type gives a single finite relationship between NTU and pressure drop. It is, therefore, not always possible to conform exactly to any specified thermal and pressure drop requirement. This problem has been overcome by utilizing the phenomenon that the NTU value of a chevron plate type is dependent to a large extent on the angle at which the corrugations cross [20].

By using two different angled troughed plates as shown in Fig. 1 that are mechanically compatible, it is possible to form three different thermal characteristics as is shown in Fig. 2. This gives a high, medium, and low NTU passage. In addition, by mixing a batch of one type with a batch of different NTU plates in one frame, it is possible to vary the combined NTU performance of the exchanger between the extremes of the two mixed plates. The advantage of this technique is that it is possible to match more closely a single-pass design to the required duty, within the limits of the NTU range of two types of plate.

The different combinations are set out as an NTU/Δp relationship in Fig. 3, where it will be seen that, by mixing the plates to vary the passages:

H passages alone can cover duties along *AB*
L passages alone can cover duties along *CD*
H, L, and *H/L* passages in different proportions can cover duties in the area *ABCD,* each set of passages heating the liquid to different temperatures which, when mixed, give the required outlet value.

Below *CD,* oversurfacing is necessary to meet pressure drop requirements, whereas above *AB,* more than one pass must be used. In any case, multipass arrangements are much more acceptable on small machines, where the follower connections can be uncoupled easily for inspection.

© 1983 Hemisphere I blishing Corporation

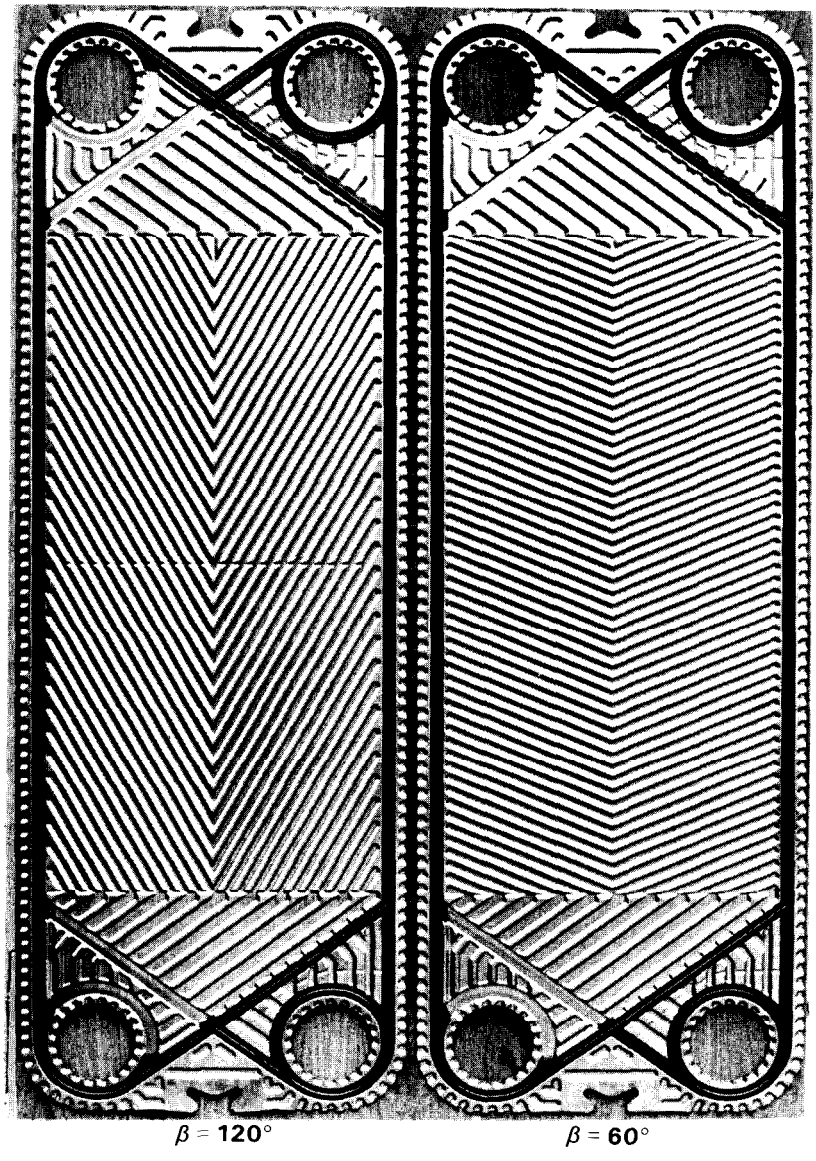

Figure **1** Typical plates that can be used in mixed formation. Photo courtesy of Alfa-Laval AB, Sweden.

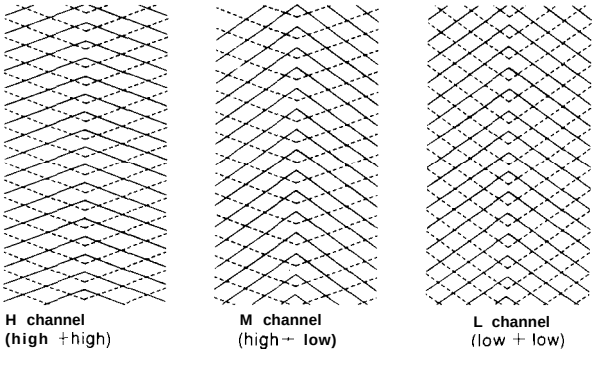

Figure 2 Schematic representation of mixed plates.

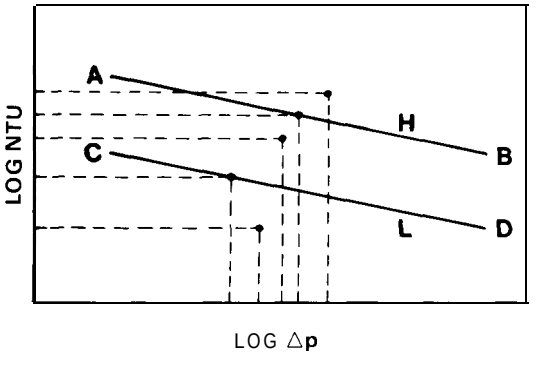

Figure 3 NTU/Δp for mixing plates.

References for Section 3.7.11 appear at the end of Section 3.7.12

© 1983 Hemisphere Publishing Corporation

3.7.12
Two-phase flow applications

Anthony Cooper and J. Dennis Usher

■ Although almost all plate heat exchanger types have been specifically designed for liquid/liquid duties, many units operate on boiling and condensing duties. In particular, these exchangers are often used to evaporate liquids with viscosities up to 0.5 kg/m s.

Plate heat exchangers are also used to cool mixtures of gases and water vapor where a close temperature approach to the cooling water is required.

For many condensing duties, this exchanger can be highly efficient, particularly where the heat fluxes involved are low due to either a low temperature difference or poor thermal properties of the fluids. However, since the port sizes of the plates are fixed for each type and the plate gaps are small, pressure drop is often the controlling parameter in condenser design. If a very low vapor pressure drop is available, the plate will only operate for a fraction of its length and the efficiency will be reduced.

There are many applications in the above areas, but the most common duty is for heating process fluids with steam. Often the available pressure drop is over 2 kN/m^2, and efficient designs can be achieved.

For designs with low pressure or vacuum steam, the main design requirement is to predict the pressure loss accurately, since the pressure drop can significantly affect the condensing temperature of the steam, and therefore the available temperature difference [21].

The pressure drop of the steam is a function not only of flow rate but also of the temperature profile down the plate. In the case of the process fluid being in counter-current flow, the steam pressure drop at a given steam flow rate is higher than when the flow is concurrent at the same steam flow rate. This occurs since in concurrent flow most of the condensation takes place in the top half of the plate, which gives a lower average steam velocity in the entire plate.

The steam pressure drop is therefore a function of steam flow rate, pressure, and the temperature difference profile along the plate. Since the pressure drop affects the steam condensation temperature, the temperature difference is also a function of the pressure drop.

Although the steam pressure drop can be predicted for known conditions by the application of conventional two-phase pressure drop techniques to the normal single-phase PHE pressure drop correlation [22], the calculation procedures are so complex that they can only be carried out by a computer.

A further complication is that when the process fluid takes more than one pass through the exchanger, the steam passages are not loaded equally [21] This complicates the rating, since the pressure loss down all the steam passages has to be balanced. For ail but the most simple applications, the rating of a PHE for these duties should be left to the manufacturers, who have the necessary computer programs.

NOMENCLATURE FOR SECTIONS 3.7.1-3.7.12

a	individual plate heat transfer area, m^2	*b*	plate spacing, m
A	total heat transfer area, m^2	c	maximum plate gap (intermating corrugation), m

© 1983 Hemisphere Publishing Corporation

C_p specific heat
d_e effective diameter, m
E energy per unit area, W/m^2
f fanning friction factor
F concurrency factor
G mass velocity, kg/m^2 s
h height of corrugation, m
H number of passes for each liquid
J specific pressure drop, kN/m^2 NTU
L length, m
$M_1 M_2$ maximum flow rate, kg/s
n number of thermal plates
Nu Nusselt number
P corrugation pitch, m
P_v velocity head, KN/m^2
Pr Prandtl number
4 volumetric flow rate per passage (plate rate), m^3/s
$\dot{Q}$ heat rate, W
r (developed heat transfer area)/(projected heat transfer area)
R $(T_o' - T_i')/(T_i - T_o)$
Re Reynolds number
T_i, T_o, T_i', T_o' temperatures, K
U overall heat transfer coefficient, W/m^2 K
v velocity, m/s
$\dot{V}$ volumetric flow rate, m^3/s
x function of physical properties relating to heat transfer
Y function of physical properties relating to pressure drop
Z $T_o' - T_i'/T_i - T_o'$
α film heat transfer coefficient, W/m^2 K
β angle of trough obliquity
Ap pressure drop, kN/m^2
ΔT, AT LMTD, K
ΔT_x concurrent LMTD, K
η bulk dynamic viscosity, kg/m s
η_w wall dynamic viscosity, kg/m s
λ base angle of corrugation
ρ density, kg/m^3
ϕ temperature change, K

REFERENCES FOR SECTIONS 3.7.1-3.7.12

1. Parrott, D. L., Heat Transfer in Plate Heat Exchangers at Low Reynolds Numbers, *14th Natl. Heat Transfer Conf., Atlanta,* Preprint 5, 1973.
2. Wilkinson, W. L., *Non-Newtonian Fluids,* Pergamon, London, 1960.
3. Marriott, J., Where and How to Use Plate Heat Exchangers, *Chem. Eng., vol. 78,* no. 8, pp. 127-134, 1971.
4. Usher, J. D., Evaluating Plate Heat Exchangers, *Chem. Eng.,* vol. 77, no. 4, pp. 90-94, 1970.
5. Jackson, B., and Troupe, R., Laminar Flow in Plate Heat Exchangers, *Chem. Eng. Prog.,* vol. 60, no. 7, pp. 62-65, 1964.
6. Okada, K., et al., Design and Heat Transfer Characteristics of a New Plate Heat Exchanger, *Heat Transfer Jpn. Res.,* vol. **1, no. 1, pp. 90-95, 1972.**
7. Okada, K., et al., Studies on the Heat Transfer and Pressure Drop of Several Kinds of Plate Heat Exchangers, *Kagaku Kogaku,* vol. 32, no. 11, pp. 89-94, 1968.
8. Maslov, A., Calculation of the Heat Exchange of Plate Apparatus on the Basis of a Diagram, *Kholdoilhaya Tekhnika,* no. 6, pp. 25-29, 1965.
9. Maslov, A., Diagram for the Determination of Resistances in Plate Heat Exchangers, *Molochnaya Promyshlennost vol. 26, no. 3,* pp. 23-24, 1965.
10. Maslov, A., The Hydraulic Resistance in Channels between the Plates of a Heat Exchanger, *Izvestiya VUZ Pishchevaya Tekhnologiya, vol. 42,* no. 5, pp. 143-147, 1964.
11. Rosenblad, G., and Kullendorf, A., Estimating Heat Transfer Rates from Mass Transfer Studies on Plate Heat Exchanger Surfaces, *Wärme und Stoffübertragung, vol. 8,* no. 3, pp. 187-191, 1975.
12. Okada, K., et al., Temperature Distribution of Fluids in Plate Type Heat Exchangers, *Kagaku Kogaku,* vol. 34, no. 1, pp. 93-95, 1970.
13. Watson, E. L., et al., Plate Heat Exchangers, Flow Characteristics, *Ind. Eng. Chem.,* vol. 52, no. 9, pp. 733-740, 1960.
14. Foote, M. R., Effective Mean Temperature Differences in Multipass Heat Exchangers, NEL Rept. 303, 1969.
15. Wilkinson, W. L., Flow Distribution in Plate Heat Exchangers, *Chem. Eng., no. 285,* pp. 289-293, May 1974.
16. Cooper, A., Suitor, J. W., and Usher, J. D., Cooling Water Fouling in Plate Heat Exchangers, *6th Int. Heat Transfer Conf., Toronto,* 1978.
17. Kern, D. *Q., Process Heat Transfer,* p. 85, McGraw-Hill, New York, 1950.
18. Edwards, M. F., and Wilkinson, W. L., Plate Heat Exchangers, HTFS Design Rept. 36, pp. 58-61, 94-97, January 1975 (available to HTFS sponsors only).
19. Cooper, A., Recover More Heat with Plate Heat Exchangers, *Chem. Eng.,* no. 285, pp. 280-284, May 1974.
20. Marriott, J., Performance of an Alfaflex Plate Heat Exchanger, *Chem. Eng. Prog.,* vol. 73, no. 2, pp. 73-78, 1977.
21. Cooper, A., Condensation of steam in Plate Heat Exchangers, *AIChE Symp. Ser.,* vol. 70, no. 138, pp. 172-177, 1974.
22. Martinelli, R. C., and Nelson, D. B., Prediction of Pressure Drop During Forced Circulation Boiling of Water, *J.* Heat Transfer, vol. 70, pp. 695-702, 1948.
23. Jackson, B. W., and Troupe, R. A., Plate Heat Exchanger Design by E-NTU Method. *Chem. Eng. Prog. Symp. Ser.,* vol. 62, no. 64, pp. 185-190, 1966.

© 1983 Hemisphere Publishing Corporation

3.8
Air-cooled heat exchangers

Contents

3.8.1
AIR AS COOLANT FOR INDUSTRIAL PROCESSES: COMPARISON TO WATER,
P. Paikert **3.8.1-1**

3.8.2
CUSTOM-BUILT UNITS, P. Paikert 3.8.2-1

A. Mechanical draft fan coolers 3.8.2-1
B. Natural draft heat exchangers 3.8.2-1

3.8.3
FIN-TUBE SYSTEMS FOR AIR COOLERS, P. Paikert 3.8.3-1

A. Applications of common fin tubes 3.8.3-2
B. Fin efficiency and temperature distribution in fin tubes 3.8.3-3

3.8.4
FIN-TUBE BUNDLES, P. Paikert 3.8.4-1

3.8.5
THERMAL RATING, P. Paikert 3.8.5-1

A. Estimation of the tube-side heat transfer coefficients α_i 3.851
B. Selection of fin tubes 3.8.5-1
C. Selection of the cooling air velocity u 3.8.5-1
D. Overall heat transfer coefficient U 3.852
E. Number of tube rows n_R **3.8.5-2**
F. Product thermal number Φ_{prod} 3.852
G. Coolant design number κ 3.8.5-2
H. NTU number 3.852
I. Coolant thermal number Φ_c **3.8.5-3**
J. Effective mean temperature difference EMTD 3.8.5-4
K. Surface area A **3.8.5-4**
L. Face area S **3.8.5-5**

References for Section 3.8.5 **3.8.5-5**

3.8.6
TUBE-SIDE FLOW ARRANGEMENT.
P. Paikert 3.8.6-1

3.8.7
COOLING AIR SUPPLY BY FANS,
P. Paikert 3.8.7-1

A. Selection of fan type and size 3.8.7-1
B. Power consumption of fans 3.8.7-1
C. Fan drive design 3.8.7-2
D. Air design temperature 3.8.7-2
E. Economic operation and control of the cooling air flow 3.8.7-3
F. Exchange rate during flow outages 3.8.7-3

3.8.8
COOLING AIR SUPPLY IN NATURAL DRAFT TOWERS,
P. Paikert 3.8.8-1

© 1983 Hemisphere Publishing Corporation

HEDH

3.8.9
SPECIAL FEATURES OF AIR COOLERS, P. Paikert **3.8.9-l**

A. Sound power and sound pressure levels 3.8.9-l
B. Vacuum condensers **3.8.9-2**
C. Air-cooled exhaust steam condensers **3.8.9-2**
D. Gas/vapor mixtures with a nonlinear $t/\dot{Q}$ curve **3.8.9-2**

© 1983 Hemisphere Publishing Corporation

3.8.1

Air as coolant for industrial processes: Comparison to water

P. Paikert

■ In many industrial processes a large amount of heat is developed, which must be removed by cooling systems. In the past, cooling was done only by water. However, with growing industrialization the large quantities of water needed for cooling can no longer be procured economically, so that atmospheric air is now often used as coolant.

In spite of its relatively bad cooling properties, air has been successfully introduced as an economical coolant in many fields of industrial cooling by the use of suitable heat exchangers.

The poor cooling properties of air are compensated for by a number of advantages that air has over water, namely:

Availability in unlimited quantities

Higher purity, uniform over the entire year

No scale, calcerous, salt, or mud deposits, no formation of algae or growth of other biological substances in the cooling system

Fewer corrosion and cleaning problems

No permanent supervision of quality required, no treatment or retreatment with chemicals

No costs for procurement and waste disposal

Little impact on the environment.

© 1983 Hemisphere Publishing Corporation

HEDH

3.8.3

Fin-tube systems for air coolers

P. Paikert

■ The relatively low heat transfer coefficients of flowing cooling air as compared to those of the products to be cooled or condensed may be partly compensated by a surface extension on the air side. This is realized by fin-tube heat exchanger bundles.

By finning the tubes, the heat exchange surface may be extended to 10 to 2.5 times the bare tube surface. The surface extension is optimized on the basis of considerations of economy and manufacture.

One criterion for the optimization is the specific performance increase in the heat transfer attainable per cost unit C, which first grows with increasing surface extension A/A_i but decreases after having reached the optimum value (Fig. 1). The vertex of this function indicates the optimum surface extension, which grows with increasing tube-side heat transfer coefficient.

In the optimization coefficient $UA/S/C$, according to Fig. 1, both A/S and U depend on the surface extension. The parameter A/S, the surface area in contact with air per square meter of face area, is merely a geometric factor and can be determined easily according to Fig. 2 on the basis of the selected fin-tube type.

The quantity U, the heat transfer coefficient, however, is very complex. According to Eq. (1), it depends on a large number of parameters in addition to the surface extension A/A_i.

$$\frac{1}{UA} = \frac{1}{\eta_F \alpha_O A A} + \frac{1}{\alpha_i A_i} + R_j \qquad (1)$$

where α_O = mean value of the locally varying air-side heat transfer coefficient (W/m^2 K). It also depends on the following characteristics:

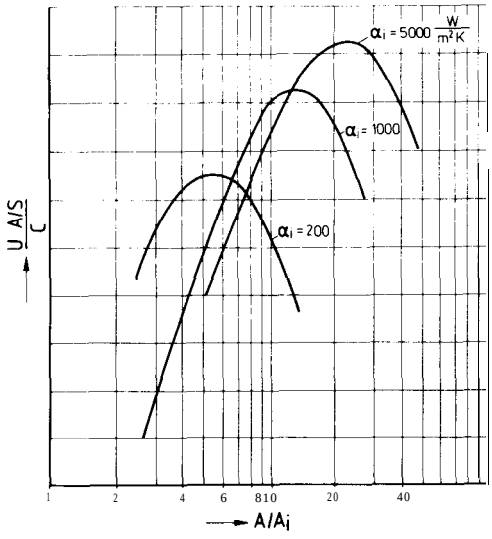

Figure 1 Optimum surface extension of fin tubes.

Cooling air velocity
Spacing between the fins
Geometric shape of the fins (round, elliptical, rectangular)
Degree of turbulence of the cooling air
Artificial turbulence intensifiers on the surface

η_F = fin efficiency as defined by Eq. (2) below and Fig. 3, depending on
The fin geometry (height, thickness, cross-sectional shape)
The fin material (thermal conductivity coefficient)
The heat transfer coefficient.

© 1983 Hemisphere Publishing Corporation

HEDH

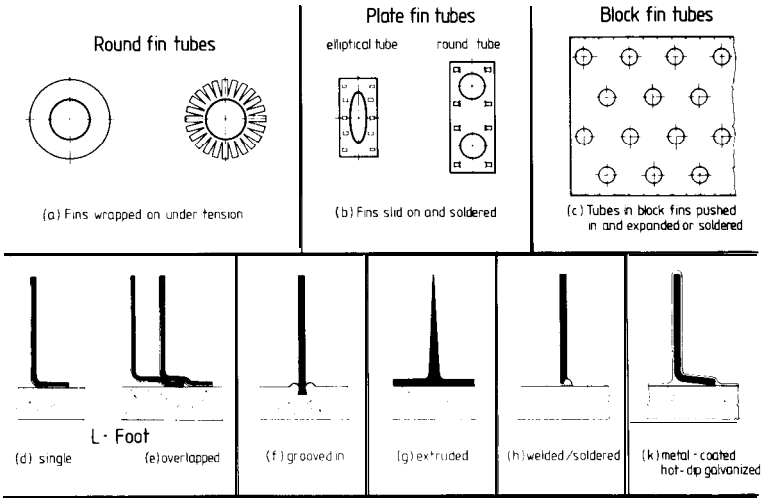

Figure 2 Customary fin-tube systems of varying geometry and with various fin-to-tube connections.

α_i = product-side heat transfer coefficient of the fluid in the tubes (W/m^2 K).

R_j = further heat transfer resistances from the cooling air side up to the product side (m^2 K/W), in which the contact resistance between fin and bare tube as well as the tube-side fouling may be essential quantities, whereas the thermal conductivity resistance of the tube wall and the fouling on the air side, which are also contained in R_j, mostly play a minor role.

A = reference area for the overall heat transfer coefficient U. This reference area is arbitrary and may be any real or assumed surface, e.g., the internal tube surface, the external tube surface, the total surface area, or a combination of various surfaces. Consequently, the quantity of the overall heat transfer coefficient U is no standard of valuation. It is only admissible for a comparison of various fin tubes where the reference area A in Eq. (1) is identical.

A. Applications of common fin tubes

Figure 2 shows a selection of typical fin tubes for air-cooled heat exchangers and various methods of fixing the fins on the bare tube. Although a general evaluation is not possible, the various systems have their typical fields of application.

The contact resistance at the base of the fin is decisive for the maximum operating of the fin tubes.

Round fin tubes: Aluminum fins wrapped on steel tubes under tension according to Fig. 2, a and *d*, have a high contact resistance which quickly increases with the operating temperature so that their application is limited to temperatures of 100° C or less, since otherwise the tension would be reduced until the fins loosen due to the higher thermal expansion of aluminum.

Fins mounted in a groove and back filled as shown in Fig. 2*f* are usable up to a temperature of approximately 350° C but require a bare-tube wall thickness increased by the groove depth.

Fins extruded from a thick-walled aluminum sleeve as shown in Fig. 2*g* provide good contact properties even when thin-walled, high-quality core tubes are used so that operating temperatures up to 250° C are admissible.

Metallic fin-to-bare tube connections such as shown in Fig. 2, *b, h,* and *k,* have a minor contact resistance and are applicable up to the solder melting temperature.

Plate fin tubes as shown in Fig. *2b* allow the use of any type of tube section and any fin shape and size.

Elliptical tubes with rectangular fins are widely used, especially in Europe, for compact units with low flow resistance.

Plate-type fins permit the mounting of turbulators to increase the air-side heat transfer while maintaining low cooling air velocities and low pressure drops.

By hot-dip galvanization, the fin tubes receive a uniform metal coat, which also serves as additional protection against corrosion.

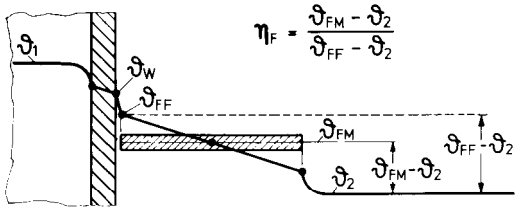

Figure 3 Temperature distribution in a fin tube (definition of fin efficiency).

© 1983 Hemisphere Publishing Corporation

3.8.2
Custom-built units

P. Paikert

■ Air-cooled heat exchangers are constructed either as mechanical draft fan coolers or as natural draft cooling towers.

A. Mechanical draft fan coolers

With mechanical draft fan coolers, the cooling air may be pushed (forced draft) or pulled (induced draft) through the heat exchanger. With a forced draft arrangement, the fan always supplies cooling air at ambient temperature, whereas with induced draft, heated air is discharged by the fan (Fig. 1).

Consequently, when both types of fans supply the same air volume, a higher cooling air mass flow and a better cooling efficiency are obtained by forced draft units. To reach the same cooling efficiency (i.e., the same cooling air mass flow) as in the forced draft fan, the induced draft fan must deliver a higher air volume and thus requires more horsepower.

In spite of these thermodynamic disadvantages, the induced draft arrangement is often chosen for other advantages, such as

More even distribution of air across the bundle

Protection of the heat exchange surface against damage under extreme climatic conditions, e.g., sleet, hail, heavy rainfall, snow, and sun rays.

B. Natural draft heat exchangers

Air coolers of the natural draft type always pull the cooling air through the heat exchangers, the cooling air supply being assured by the draft effect in a 100- or 150-m-high tower, which is due to the difference in density between the heated air in the tower and the ambient air.

With high towers and a high rise in air temperature, the draft may grow considerably, so that a

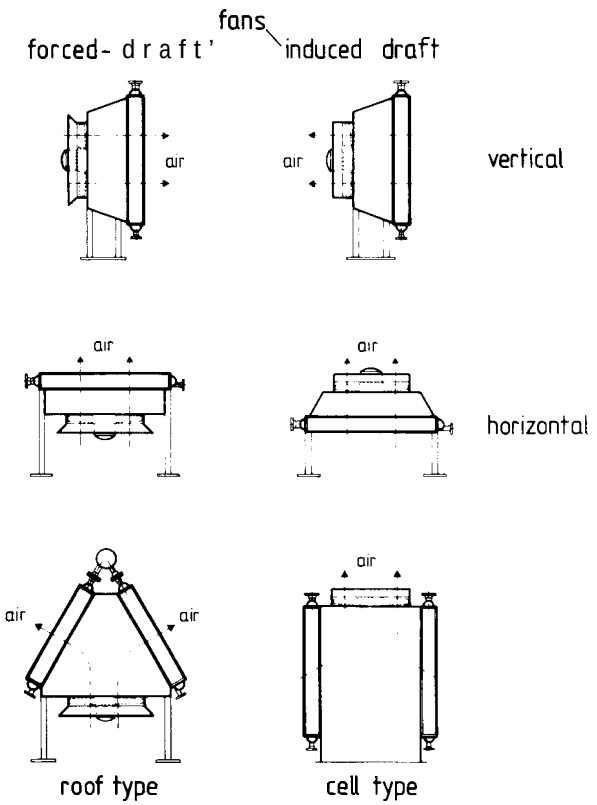

Figure 1 Arrangement of air-cooled heat exchangers.

© 1983 Hemisphere l ıblishing Corporation

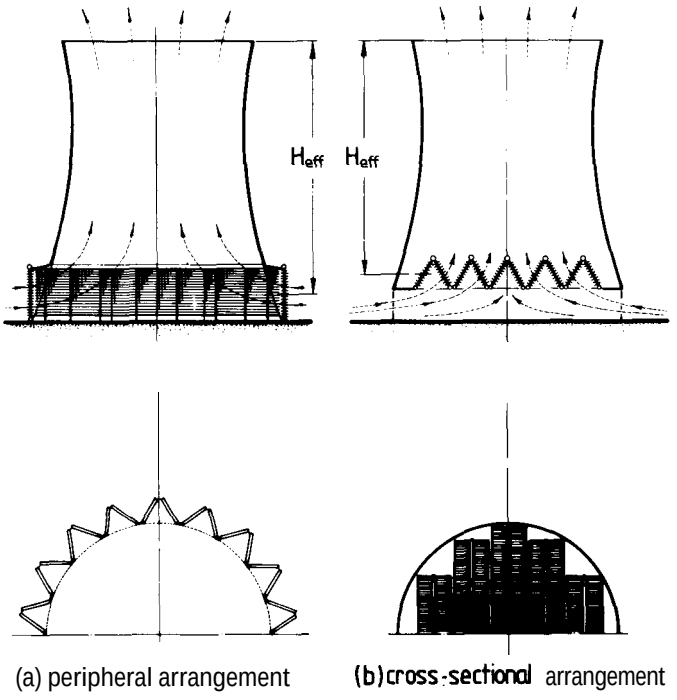

Figure 2 Arrangement of cooling bundles in natural draft dry cooling towers.

cooling air velocity in the heat exchanger, that is, a cooling air supply rate, may be obtained that equals that in a fan-cooled air cooler.

The types of natural draft heat exchangers depend on the shape and size of the towers. Towers with smaller diameters may be more conveniently equipped with heat exchangers at the tower periphery, where a zigzag arrangement is possible which would increase the air inlet cross section (Fig. 2). Towers with large diameters for higher heat duties are usually equipped with heat exchangers over their entire cross section. The exchangers may be arranged horizontally or zigzag and on one plane or in the form of stairs within the tower cross section (Fig. 2*b*).

© 1983 Hemisphere Publishing Corporation

Welded fins as shown in Fig. ***2h*** are used where high temperatures (over 400° C) are involved and where fin tubes described above cannot be used.

B. Fin efficiency and temperature distribution in fin tubes

The thermodynamic quality of a fin tube is expressed by the fin efficiency, which indicates the temperature loss in the fin and is defined as follows:

$$\eta_F = \frac{\text{effective temperature difference between fin center and atmospheric air}}{\text{temperature difference between fin base and atmospheric air}}$$

$$\eta_F = \frac{\vartheta_{FM} - \vartheta_2}{\vartheta_{FF} - \vartheta_2} \qquad (2)$$

according to Fig. 3. For most fin types there is no definite mathematical solution for η_F.

The known solution for the specific case of the flat fin of constant thickness

$$\eta_F = \frac{\tanh X}{X} \qquad (3)$$

where

$$X = h\left(\frac{2\alpha_o}{\lambda_F \cdot \delta_F}\right)^{1/2} \qquad (4)$$

These factors are

h = fin height (m); often not constant (e.g., Fig. ***2b)***

α_O = external heat transfer coefficient (W/m^2 K); varying locally over the entire fin

λ_F = thermal conductivity coefficient of the fin material (W/m K); with galvanized plate fins, a value combined from fin sheet and zinc layer

δ_F = fin thickness (m); often not constant

Figure 3 illustrates the typical temperature curve through a tin tube. The temperature variation is proportional to the heat flow resistance.

Nomenclature for Section 3.8.3 appears at the beginning of Part 3.

© 1983 Hemisphere Publishing Corporation

3.8.4
Fin-tubebundles

P. Paikert

■ The fin tubes selected for an actual requirement are arranged in rectangular cooler bundles up to 3 m in width and 15 m in length, mostly with four to eight tube rows. The arrangement substantially influences the cooler bundle performance.

With in-line arrangement of the fin tubes, the pressure loss is up to 60% lower and the heat transfer coefficients approximately 30% lower than with the staggered arrangement, which is most commonly used because of its compactness.

The mean heat transfer coefficient decreases as more rows are installed. Heat transfer coefficients often relate to six-row systems. Correction values for units with much more or less than six rows and with in-line or special tube arrangements must be defined by the fin-tube manufacturer.

Fin-tube bundles must be designed with consideration of the fan diameter and number. Within certain limits, longer tube bundles are less expensive than short ones, since fewer tubes and fewer tube-to-tubesheet welds are needed.

Product distribution headers may be welded or bolted onto the tube plates (Fig. 1).

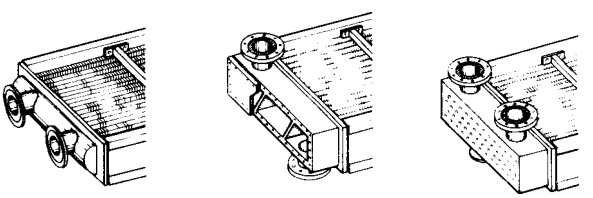

Figure 1 Product distributing and collecting headers.

All-welded headers assure good air-tight sealing but make mechanical cleaning of the tubes impossible.

Bolted headers must be provided in case the tubes require regular cleaning from product-side deposits. Typical solutions are removable cover plates or plugs (Fig. 1, *b* and c). The thermal expansion of the tubes must be accounted for by a floating tube plate. Large variations in the temperature of the product to be cooled make additional measures necessary-for example, the splitting of the headers.

Figure 2 shows a typical fin-tube bundle structure.

© 1983 Hemisphere l blishing Corporation

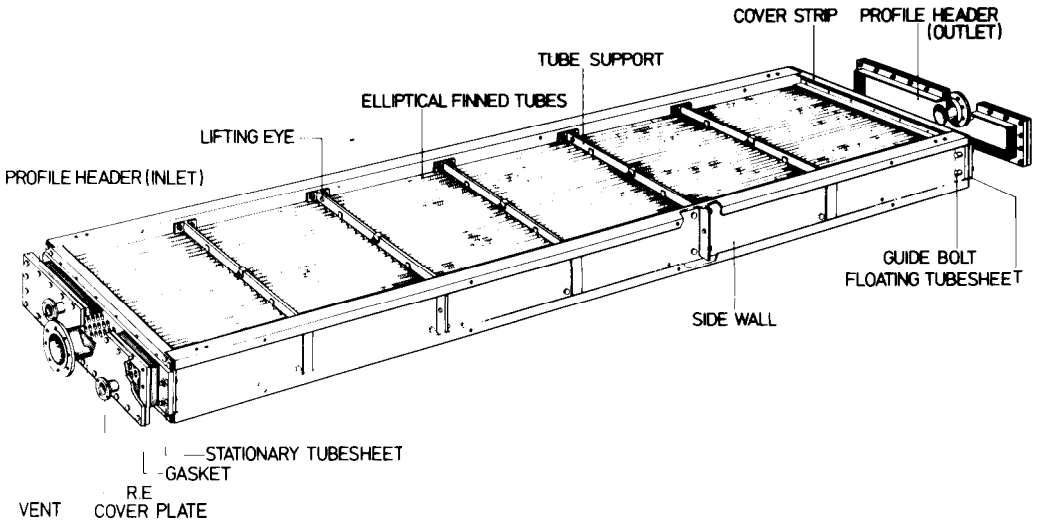

Figure 2 Fin-tube bundle of GEA air-cooled heat exchanger.

© 1983 Hemisphere Publishing Corporation

3.8.5
Thermal rating

P. Paikert

■ The thermal rating first requires a reasonable adaptation of the means to be selected to the specified requirement. This implies a certain experience. Shape, size, finning, and fin-tube material must be suitable for the fluid to be cooled or condensed and must be adapted to its physical properties. The rating is then carried out by the following step-by-step method.

A. Estimation of the tube-side heat transfer coefficients α_i

On the basis of the specified task, an initial guess of the expected α_i values may be made by means of Tables 1 and 2 or Fig. 1. The indicated values refer to typical conditions of air coolers and air condensers.

When the tube-side conditions such as flow velocity and temperature of the streaming fluids or the temperature difference of condensing or evaporating fluids are specified or known, the tube-side heat transfer coefficients may be determined more exactly-for example, in accordance with Part 2 of this handbook.

Table 1 Estimated heat transfer coefficients of flowing liquids inside tubes (fluid velocity about 1 m/s, service values)

Liquid	α_i, W/m² K
Cooling water	2 000-4 000
Paraffins (C_6H_{14}-$C_{11}H_{24}$)	800-1 200
Benzene/toluene	1 000-I 500
Methanol	1 400-1 700
Ethanol	1 100-1 500
Hexanol	600-800
Octanol	400-600

Table 2 Estimated heat transfer coefficients of condensing vapor

Condensing vapor	α_i, w/m K
Steam	3 000-5 000
Paraffins	800-1 600
Benzene/toluene	1 400-1 800
Ethanol	1 500-2 000
Methanol	1 600-2 200
Ammonia	2 500-3 000
Refrigerant R 12	1000-1 500

B. Selection of fin tubes

The estimated heat transfer coefficient gives a first idea of the required and expedient surface area ratio A/A_i of the fin tube to be chosen according to Fig. 3.8.3(1). The thermal and hydraulic data of the selected fin tube should be available as a function of the cooling air velocity u, as shown in Fig. 2 or according to Eq. 3.8.3(1) (obtained from the fin-tube manufacturer).

C. Selection of the cooling air velocity u

The cooling air velocity is fixed within rather narrow limits, since the increase of the air-side pressure drop with growing velocity is almost square and due to the low static pressure of 100 to 200 Pa developed by conventional fans. It ranges mostly from 2 to 4 m/s,

© 1983 Hemisphere Publishing Corporation

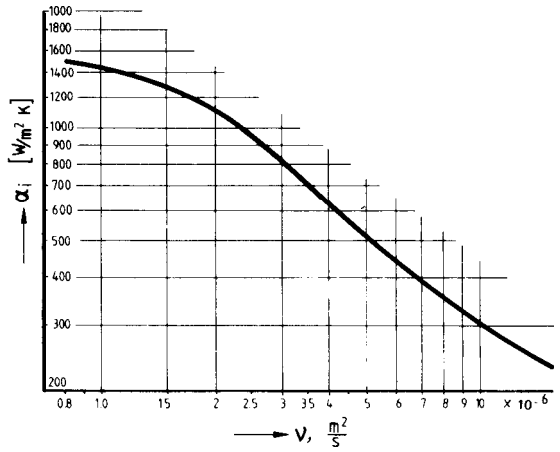

Figure 1 Mean heat transfer coefficient of flowing mineral oils (estimate).

depending on the face area, the number of tube rows n, and on the admissible and feasible temperature rise of the cooling air.

D. Overall heat transfer coefficient U

After the α_i value and the cooling air velocity have been determined, the overall heat transfer coefficient for a selected fin-tube system may be obtained from Fig. 2 or Eq. 3.8.3(1). When an additional product-side fouling r_{foul} needs to be taken into account, the actual service value α_{iserv} is first determined. Then:

$$\frac{1}{\alpha_{iserv}} = \frac{1}{\alpha_i} + r_{foul} \tag{1}$$

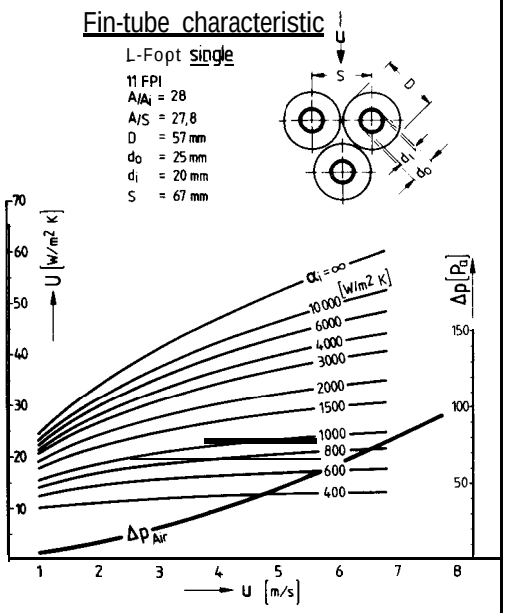

Figure 2 Overall heat transfer coefficient U and air-side pressure drop ΔP_{air} as function of air velocity u.

The fouling resistance r_{foul} may be taken from pertinent manuals or gotten from experience.

Generally, air-side fouling need not be considered for the U value. Although relatively high air-side fouling may adversely affect the air flow through the unit and thus decrease the effective temperature difference, it scarcely influences the U value because of the relatively small air-side heat flux.

E. Number of tube rows n_R

The number of tube rows needed depends on both the specific requirement and the efficiency of the selected fin-tube system. Roughly estimated, these two factors can be expressed by a quantity a, which includes the temperature difference between product and cooling air inlet as well as the value $U(A/S)$ of the fin tube (Fig. 3).

$$a = \frac{t_{prod,\,in} - t_{air,\,in}}{U\,A/S} = \frac{\Delta\vartheta_O}{U\,A/S} \tag{2}$$

$$n_R = C_1\ a^{C_2} \tag{3}$$

where $C_1 = 24$ for fin tubes of the kind according to Fig. 2

$C_2 = 0.49$

F. Product thermal number Φ_{prod}

One auxiliary term for the further thermal rating is the dimensionless number

$$\Phi_{prod} = \frac{\Delta t_{prod}}{\Delta\vartheta_O} = \frac{t_{prod,\,in} - t_{prod,\,out}}{t_{prod,\,in} - t_{air,\,in}} \tag{4}$$

It is used later to determine the effective mean temperature difference (EMTD) and the surface area needed.

G. Coolant design number κ

The dimensionless design number applicable for one tube row is now calculated on the basis of the available results.

$$\kappa = \frac{U\,A/S}{u\,\rho\,c_p} \tag{5}$$

where c_p is the specific heat of air at constant pressure.

H. NTU number

The dimensionless NTU number (number of transfer units) is obtained by the product of the coolant design number and the number of tube rows:

© 1983 Hemisphere Publishing Corporation

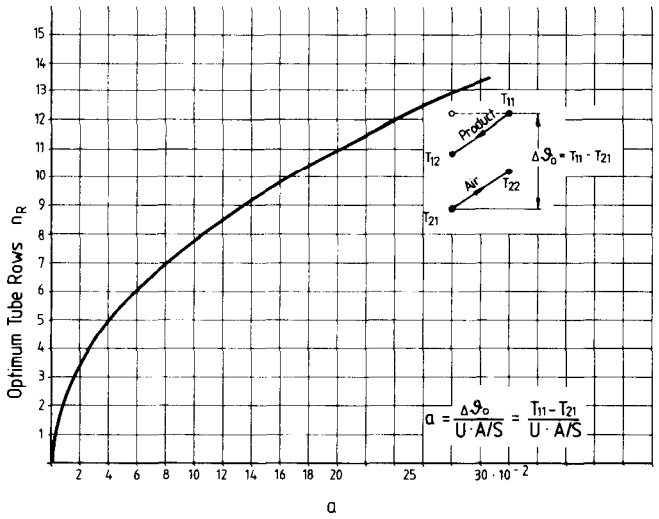

Figure 3 Optimum tube rows for air coolers.

$$NTU = n_{R\,K} = \frac{\Delta t_{air}}{EMTD} \tag{6}$$

For optimum design it normally lies in the range of $0.8 < NTU < 1.5$. This quantity already represents a control value for the available quantities u and n_R.

I. Coolant thermal number Φ_{air}

The dimensionless value $\Phi_{air} = \Delta t_{air}/\Delta\vartheta_O$ for various types of flow in air coolers is given in [1,2]. For three typical flow arrangements with air coolers (1, cross flow; 2, cross-counter flow return bend; 3, counter flow), Φ_{air} is given by Eqs. (7), (8), and (10) or may be obtained from Figs. 4-6. Besides the known quantity NTU, the equations also contain the quantity $\tau = \Delta t_{prod}/\Delta t_{air}$, which must first be estimated in order to obtain Φ_{air}. τ generally lies between 0 and 1, but may also be higher.

For isothermal condensation, $\Delta t_{prod} = 0$ and $\tau = 0$, so the same Φ_{air} is obtained for all flow types.

Arrangement I: cross flow

On the tube side, one or more passes, side by side:

$$\Phi_{air} = \frac{1 - \exp\,[-\tau(1 - e^{-NTU})]}{\tau} \tag{7}$$

Arrangement 2: cross-counter-flow return bend

On the tube side two passes in the counter-flow direction to the air flow:

$$\Phi_{air} = \frac{1}{\tau}\left[1 - \frac{1}{1 + (1 - \varphi_o/2)(e^{2\tau\varphi_o} - 1)}\right] \tag{8}$$

with

$$\varphi_o = 1 - e^{NTU/2} \tag{9}$$

Arrangement 3: counter flow

On the tube side four or more passes in the counter-flow direction to the air flow:

$$\Phi_{air} = \frac{1 - e^{-(1-\tau)NTU}}{1 - \tau e^{-(1-\tau)NTU}} \tag{10}$$

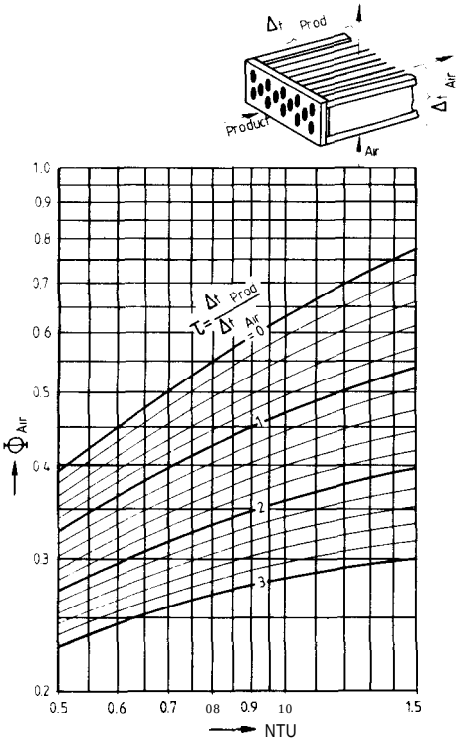

Figure 4 Coolant thermal number Φ_{air} for cross flow.

© 1983 Hemisphere Publishing Corporation

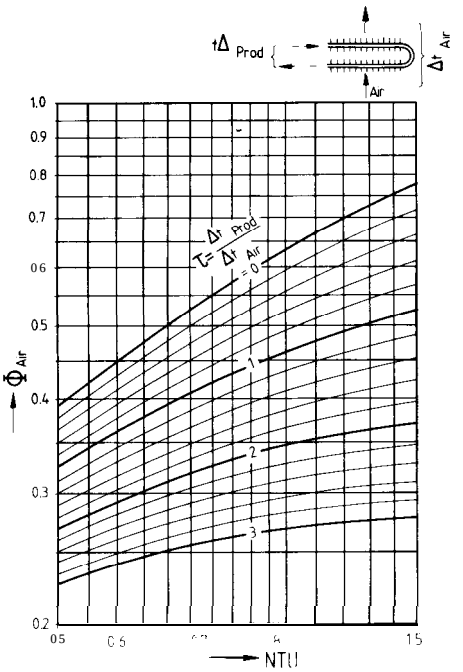

Figure 5 Coolant thermal number Φ_{air} for counter-flow return bend.

The flow arrangements are selected according to the product volume to be cooled or condensed and the temperature difference between the product and the cooling air. Arrangement 1 applies when large product volumes are to be cooled or condensed or when high temperature differences are involved. Arrangement 2 applies to liquid coolers with small volumes and low temperature differences. Arrangement 3 applies to high-pressure coolers or coolers where the temperatures of the two flows approach or overlap each other.

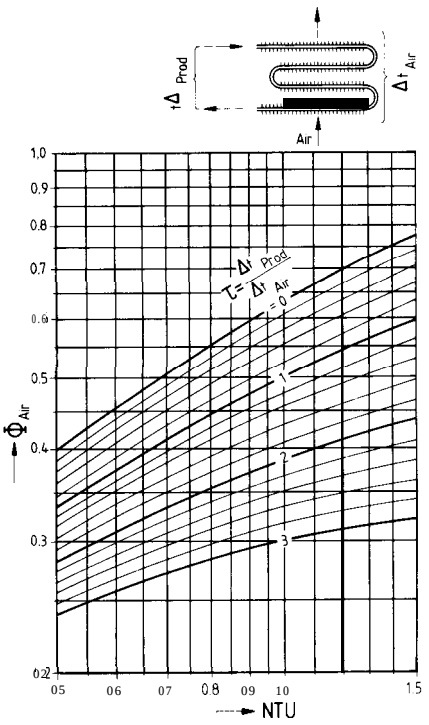

Figure 6 Coolant thermal number Φ_{air} for counter flow.

J. Effective mean temperature difference EMTD

The EMTD is obtained from the definition of NTU according to Eq. (6) as follows:

$$\text{EMTD} = \frac{\Delta t_{air}}{\text{NTU}} = \frac{\Phi_{air}\,\Delta\vartheta_O}{\text{NTU}} \tag{11}$$

In order to simplify the calculation and avoid a trial-and-error procedure, Eqs. (7)-(10) can be rearranged to get the expression

$$\frac{\text{EMTD}}{\Delta\vartheta_O} = \frac{\Phi_{air}}{\text{NTU}} \tag{12}$$

which can be solved graphically as a function of Δt_{prod} and NTU. This is shown in Figs. 7-9 for the three arrangements.

K. Surface area A

The surface area needed is

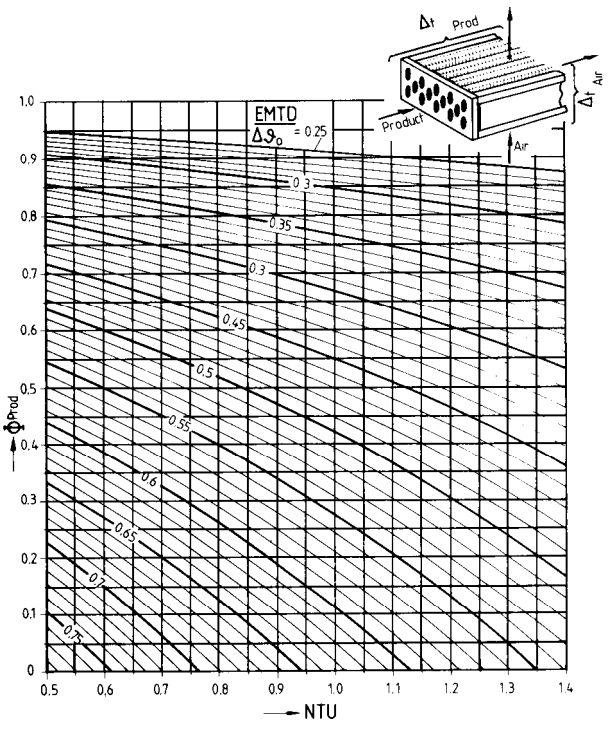

Figure 7 Effective mean temperature difference (EMTD) for cross flow.

© 1983 Hemisphere Publishing Corporation

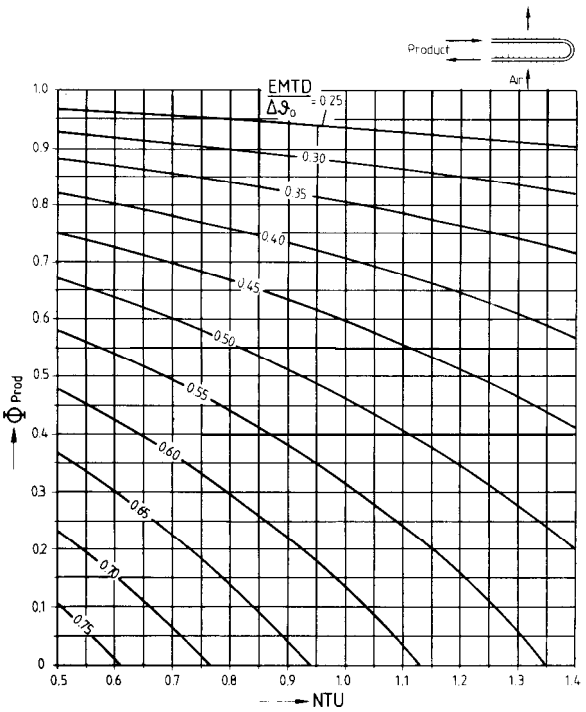

Figure 8 Effective mean temperature difference (EMTD) for counter-flow return bend.

$$A = \frac{\dot{Q}}{U\ \mathrm{EMTD}} \tag{13}$$

in which $\dot{Q}$ is the total heat transferred in the exchanger.

L. Face area S

The coolant-side face area needed is obtained from the expression

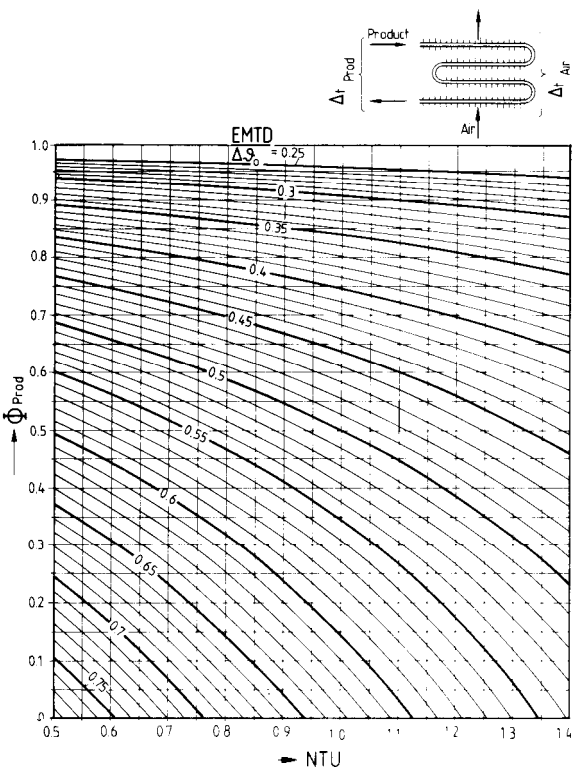

Figure 9 Effective mean temperature difference (EMTD) for counter flow.

$$S = \frac{A}{A/S\ n_R} \tag{14}$$

This face area is so apportioned to length and width that reasonable bundle dimensions are obtained.

Nomenclature** for **Section 3.8.5 appears at the beginning** of **Part 3.

REFERENCES FOR SECTION 3.8.5

1. Bosnjakovic, F., VDI-Forschungsheft 432. Deutscher Inp. Verlag, Diisseldorf, Band 17.
2. Bosnjakovic, F., Quersinnig gekoppelte Wärmeaustauscher CIT, 2.5 (1953), Nr. 11.

© 1983 Hemisphere Publishing Corporation

3.8.6

Tube-side flow arrangement

P. Paikert

■ To determine the tube-side flow arrangement, carry out the following steps.

1. Calculate the tube-side heat transfer coefficient α_i. This may require correction of the initial guesses.

2. Determine the tube-side pressure loss as a function of the product velocity, the fluid properties, and the geometric characteristics of the cooler bundle, according to Part 2 of this handbook.

3. Calculate the air-side static pressure loss of heat exchangers for the volume of the cooling air flow and the cooling air velocity. The pressure loss is obtained from the fin-tube characteristic and the number of tube rows as follows:

$$\Delta p_{st} = \Delta p_{\text{air}}\, n_R\, c_n \qquad (1)$$

where c_n is a correction factor that must be defined by the fin-tube manufacturer and that accounts for the fact that due *to* the losses at the inlet and outlet the pressure drop is not directly proportional to the number of tube rows.

Nomenclature for Section 3.8.6 appears at the beginning of Part 3.

© 1983 Hemisphere Publishing Corporation

3.8.7

Cooling air supply by fans

P. Paikert

A. Selection of fan type and size

To supply cooling air, axial-flow fans are used that can handle large volumes at low pressure. To assure good air distribution, the following ratio between face area S and cross-sectional area of the fan S_v should be observed:

$$1.8 < \frac{S}{S_v} < 2.6 \qquad (1)$$

Usually, axial-flow fans are provided with four to eight blades. Both the fan cost and the air volume supplied at the given fan speed increase with increasing blade number.

When the air volume remains unchanged, the rpm can be reduced with increasing blade number. This has the favorable effect of reducing noise and increasing efficiency.

B. Power consumption of fans

The energy consumption of axial-flow fans often accounts for 1% to 3% of the cooling capacity. Roughly estimated, the following result is obtained from the volume supplied and the pressure difference:

$$N = \frac{\dot{V}(\Delta p_{stat} + \Delta p_{dyn})}{1\,000\eta_v}\ \text{kW} \qquad (2)$$

where $\dot{V}$ = cooling air rate (m^3/s)
Δp_{stat} = static pressure difference (Pa)
Δp_{dyn} = dynamic pressure difference over the fan cross section (Pa) to be calculated from fan charts or from the air flow and the effective fan cross section S_{VE}; and

$$\Delta p_{dyn} = \left(\frac{\dot{V}}{S_{VE}}\right)^2 \frac{\rho}{2}\ \text{Pa} \qquad (3)$$

Δp_{dyn} = 40-60 Pa
η_v = fan efficiency (often, η_v = 0.6-0.7)

when reading the fan power from fan charts, it must be noted that these charts apply only to a certain temperature and that the power must be converted to the air temperature over the fan cross section. Figure 1

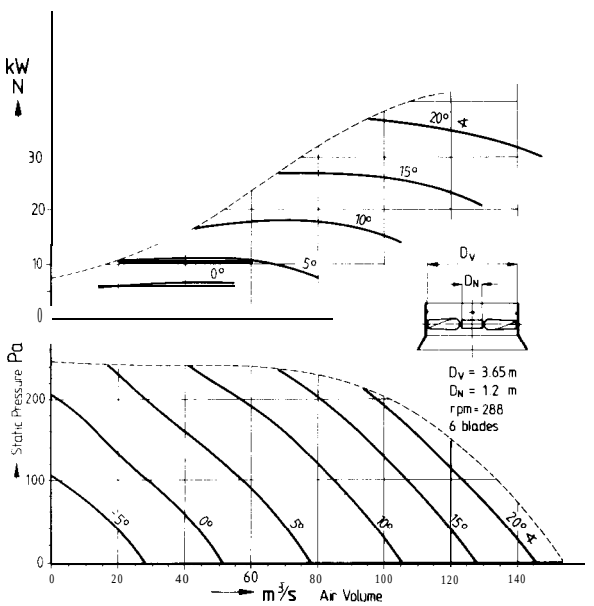

Figure **1** Fan chart: air volume, static pressure, and power consumption at fan shaft.

© 1983 Hemisphere Publishing Corporation

shows a typical fan chart for an axial-flow fan. To minimize the calculation work, in such a chart the fan efficiency and the dynamic pressure are already included and one needs only the static pressure and the air volume to get the blade angle from the lower part of the diagram and then get from the upper part the power consumption of the fan out of the blade angle and the air volume.

C. Fan drive design

Fans and drives should be low cost, solid, and reliable. Therefore, fans up to a diameter of 1.5 m are often mounted directly on the motor shaft. When fans with larger diameters are used, the fan rpm must be reduced to avoid the development of noise growing with the tip velocity. The cheapest solution for speed reduction is a V-belt drive mounted between the motor and fan. V belts are used up to driving powers of 30-40 kW. For higher driving powers, various types of reduction gears are used. These may be installed on the ground with an extended fan shaft or on a supporting structure directly on the fan hub (Fig. 2).

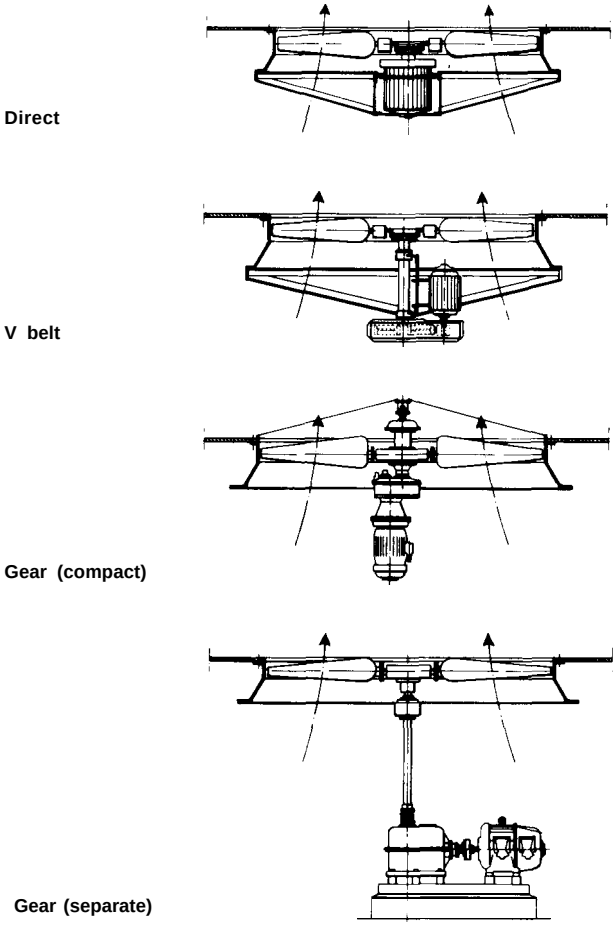

Figure 2 Normal fan drives.

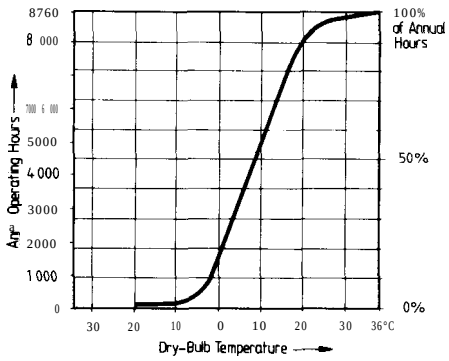

Figure 3 Temperature distribution of outside air.

Since a fan always supplies a constant air volume, an increase in driving power is required at low air temperature, especially in winter, because of higher air density. This must be taken into account when rating the driving motor for fans that are not autovariable. In this case the motor must be oversized by 25-30%. For fans where the blades are mechanically adjusted for summer and winter operation the motor must be 15% oversized.

D. Air design temperature

The cooling air design temperature t_{air} is of great importance for cooler design and thus for investment cost, since the temperature difference between product and coolant inlet is directly proportional to the surface area needed. Because of seasonal temperature variations in atmospheric air, a design temperature must be chosen that is at the tolerable limit for the cooling process and still appears reasonable for the investment cost. In general, this temperature is not the statistical maximum air temperature at the plant location but often the temperature that is not exceeded during 94-96% of the annual operating hours.

By renouncing the full cooling capacity for the remaining 4-6% of the annual operating hours, it is possible to reduce the air design temperature by 12-14° C and the investment cost by 50-60%, for example, when the temperature of the product to be cooled is 60° C and a typical air temperature chart as shown in Fig. 3 applies. These annual air temperature charts are available for many places or may be obtained from meteorological stations. Unless a reduction of the cooling capacity is allowable for the few hours per year or in case the product temperatures are still lower, the capacity may be increased by humidifying the air and thus cooling it down to almost its wet-bulb temperature. For example, the wet-bulb temperature of atmospheric air of 32° C is approximately 20-24°C, depending on the relative humidity.

© 1983 Hemisphere Publishing corporation
HEDH

Air humidification should be practiced over short periods only, and should be confined to special cases since otherwise problems may arise by corrosion attack or deposits on the fin tubes.

E. Economic operation and control of the cooling air flow

Because of the variations in the atmospheric air temperature, a fan without control supplies too much cooling air most of the year and thus often has the unwanted effect of subcooling the product. Furthermore, the horsepower consumption of the fan supplying the full air volume is unnecessarily high.

By adapting the cooler air volume to the actual requirements, much power may be saved since the latter goes with the third power of the air volume. The air volume may be reduced by the following measures:

1. Shutdown of individual fans (expedient only when more than three fans are installed)
2. Pole-changing driving motors. (By throttling the speed to two-thirds of the rated rpm, the driving power may be reduced by approximately 70%.)
3. Autovariable blades (These fans automatically adjust pitch in response to a preset product outlet temperature.)

The annual saving in energy achieved by the three measures still depends on the difference between product and air design temperature and on the number of fans installed. The amount of energy saved varies with each specific case and must always be investigated separately. Savings of 20–80% of the rated horsepower are possible.

F. Exchange rate during fan outages

In case of fan failure, the air in the cooler bundles first heats up considerably and then leaves the bundle by free convection so that ambient air can flow in. The height of the horizontal cooler bundle and, with an induced draft arrangement, the height of the plenum chamber, forms a chimneylike unit filled with hot air with corresponding draft. Calculation of the air flow through the unit and thus of the exchange rate can proceed according to Sec. 3.8.8.

Nomenclature for Section 3.8.7 appears at the beginning of Part 3.

© 1983 Hemisphere Publishing Corporation

3.8.8

Cooling air supply in natural draft towers

P. Paikert

■ When exchange rates above 100 MW are to be handled, the energy consumption for the cooling air supply by fans becomes so important that natural draft towers are more economical in most cases.

The air flow rate in a natural draft tower is determined by the hot air draft in a tower of height ***H.*** The draft equals the resistance of the tower plus the resistance of the cooling bundles:

$$\Delta p = \Delta p_{tow} + \Delta p_{stat} = H_{eff}\,\Delta\rho\, g \qquad (1)$$

where $\Delta\rho$ = difference in density between the atmospheric air and the hot air in the tower (kg/m^3)

g = acceleration due to gravity (m/s^2)

H_{eff} = effective height of tower (m)
= difference in height between the center of the cooling bundle and the tower outlet

Δp_{tow} = pressure losses in the tower including the pressure caused by the air supply, turn, and outlet (Pa)

It often reaches the same value as the static pressure difference of the cooler bundle.

Nomenclature for Section 3.8.8 appears at the beginning of Part 3.

© 1983 Hemisphere 1 ublishing Corporation

3.8.9

Special features of air coolers

P. Paikert

A. Sound power and sound pressure levels

Definitions:

Sound power level: objective quantity; the total sound emitted by a system to the environment. It is identical to the sound pressure level related to a reduced surface of 1 m^2.

Sound pressure level: subjective quantity; the measured sound pressure related to a fixed value, largely depending on the distance from the noise source.

The sound power emitted to the environment by air-cooled heat exchangers originates almost entirely from the fans and drives. The fan drive-motor and gear unit-often accounts for as much sound power as the fan itself, a fact that should not be neglected.

The noise developing in the fan by interruptions of the air flow and by air turbulence has a low basic frequency resulting from the product of the number of blades and the rpm, and therefore is resented less with decreasing basic frequency. All measures likely to reduce the turbulent vortex within the range of the fan help decrease the noise and increase the fan efficiency. This applies particularly to the air inlet.

Approximate equation for the sound power:

$$L_w = c + 30 \log w + 10 \log \frac{\Delta p_{stat}\, \dot{V}}{1\,000} - 5 \log D \text{ dB(A)} \quad (1)$$

where c = specific basic level; 44 dB(A), normal design; 37 dB(A), low-noise design

w = tip velocity (m/s)

Δp_{stat} = static pressure rise (Pa)

$\dot{V}$ = air quantity (m^3/s)

D = fan diameter (m)

The sound pressure level at a distance R (m) from the fan is approximately

$$L_P = L_W - 10 \log 2\pi R^2 \text{ dB(A)} \quad (2)$$

If n identical fans are installed in a plant, the total noise is obtained by the expression

$$(L_W)_n = L_W + 10 \log n \text{ dB(A)} \quad (3)$$

A reliable prediction of the sound power of the electric motors and fan drives is not possible. The sound power of these units is near the following values:

Electric motors	up to 50 kW	60–70 dB(A)
	SO-100 kW	70-80 dB(A)
V belts	20–40 kW	60–65 dB(A)
Gear boxes	40-60 kW	70-80 dB(A)
	60-100 kW	80-100 dB(A)

With a larger number of smaller fans and drives, the increased sound power must always be taken into account by the summation according to Eq. (3). This may result in a considerable additional impact on the environment.

In natural draft towers, noise may develop to a minor extent by air vibrations in the exchanger bundle at high air velocities.

© 1983 Hemisphere Publishing Corporation

B. Vacuum condensers

Air-cooled condensers with the product flowing inside the tubes are usually provided with long tubes for economic reasons. For calculating these units, not only the condensation heat to be removed but also the product-side pressure loss must be taken into account. In vacuum condensers with a pressure below 30 torr, the change in pressure often is of the same order of magnitude as the absolute pressure, which has the effect of considerably increasing the volume coupled with a still higher pressure loss. This may cause a quick approach to the maximum flow limit of a condenser, which is reached when the fluid flows at sonic velocity at the tube inlet.

In many cases this maximum flow, not the heat amount to be removed, is the dominant factor for the rating of a condenser. Furthermore, pressure losses occurring before the fluid enters the tubes as a consequence of acceleration and of the entry into the headers must be taken into consideration. For sharp-edged tubes, the absorption limits may be as low as 50–60% of the sound velocity of the vapor to be condensed, related to the geometric tube cross section so that short tubes of 1.0 or 2.0 m must be used.

C. Air-cooled exhaust steam condensers

The direct condensation of the turbine exhaust steam of power stations often causes specific problems at low ambient temperatures during the winter season. The plant must be designed for full load at the maximum summer temperature of the cooling air and is thus oversized for operation under partial load, which may become necessary at low winter temperatures. In this case subcooling of the condensate and freezing must be feared unless special provisions are made. Figure 1 shows a schematic of a properly built exhaust steam condenser. The exhaust stream from the turbine flows through the exhaust steam piping first into the upper collecting headers of the condensers and is cooled and partly condensed when flowing down the tubes. The remaining steam enters the succeeding condenser bundles, where the steam rises and continuously heats the down-streaming condensate and thus prevents freezing.

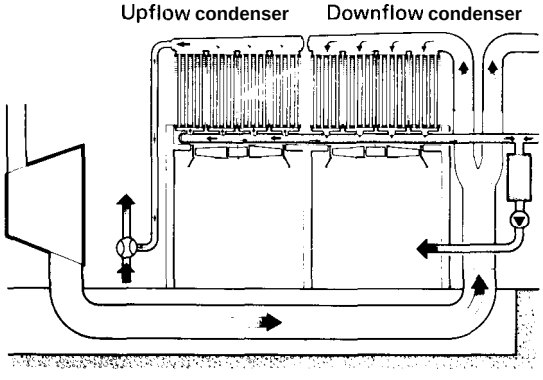

Figure 1 Air-cooled condenser for power stations.

However, if the steam is not properly distributed between the downflow and upflow units, flooding may be caused at the tube inlet of the upflow unit by excess vapor velocity so that the performance is considerably reduced, and the tubes blocked by the condensate may freeze. The shares of the downflow and upflow units in the plant may be varied by means of control valves in the distribution piping.

The tube portions of the upflow unit that are not used for condensation contain inert gas (air), which must be permanently removed by a vacuum pump in order to maintain the condensation performance. The moisture contained in the air may freeze on the tubes until they are blocked.

D. Gas/vapor mixtures with a nonlinear $t/\dot{Q}$ curve

When gas/vapor mixtures are cooled or condensed, the EMTD cannot be determined as defined in Sec. 3.8.5J, where the determination of the EMTD is based on a linear temperature curve plotted against the heat load ($t/\dot{Q}$ curve). This applies only to the cooling and condensation of pure fluids (Fig. 2, a and b). For gas/vapor mixtures with heavily curved temperature/heat load curves similar to Fig. 2*c*, the EMTD and the exchanger surface must be calculated in several steps after the $t/\dot{Q}$ curve has been linearized. Because of the

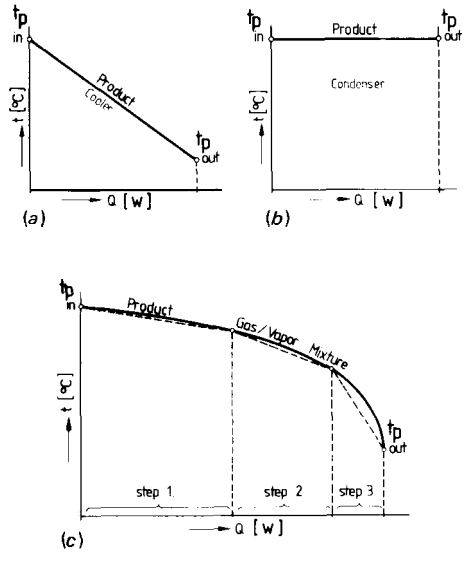

Figure 2 Temperature distribution for cooling and condensing pure fluids and gas/vapor mixtures. (*a*) Cooling product with constant specific heat. (*b*) Condensing pure vapor with negligible pressure loss. (*c*) Condensing gas/vapor mixture.

© 1983 Hemisphere Publishing Corporation

varying α_i values in the individual sections, which decrease with increasing curvature (= increasing gas content), the following expression must be used:

$$A_{tot} = \sum_{i=1}^{j} A_i = \sum_{i=1}^{j} \left(\frac{\dot{Q}}{U \, \mathrm{EMTD}} \right)_i \qquad (4)$$

Problem: An air-cooled water recooler has to be designed for a closed-cycle process.

Heat load $\dot{Q} = 5 \times 10^3$ kW

Water inlet $t_p = 55°$ C

Water outlet $t_p = 45°$ C

Ambient air $t_{air} = 25°$C

Determine size, power consumption, noise power, and noise pressure level at a distance of 300 m from the air cooler.

Solution: For a closed-cycle cooling process and low temperature level, a design with induced draft and horizontal cooler bundles similar to Fig. 3.8.2(1) and an L-foot fin tube as in Fig. 3.8.3(2*a, d*) has been chosen. Fin-tube characteristics are given in Fig. 3.8.5(2).

Air velocity (chosen):

$u = 3.0$ m/s

$\Delta p_{air} = 21$ Pa Fig. 3.8.5(2)

$\alpha_i = 4\,000$ W/m² K Table 3.8.5(1)

$U = 33$ W/m² K Fig. 3.8.5(2)

Number of tube rows:

$a = 0.032$ Eq. 3.8.5(2)

$n_R = 4$ Eq. 3.8.5(3)

Product thermal number:

$\Phi_{prod} = 0.33$ Eq. 3.8.5(4)

Effective mean temperature difference:

NTU = 1.06 { Eq. 3.8.5(5) / Eq. 3.8.5(6)

$\frac{\mathrm{EMTD}}{\Delta\vartheta_O} = 0.53$ Fig. 3.8.5(8)

EMTD = 15.9 K

Surface area:

$A = 9\,530$ m² Eq. 3.8.5(13)

Face area:

$S = 86$ m² Eq. 3.8.5(14)

Chosen dimensions:

Four bundles, each 10 m long, 2.2 m width
Size of aircooler: 11 m X 9.2 m overall
Number of tubes per bundle: $n_{TB} = 128$
Number of tubes per flow pass: $n_P = 256$ (cross-counter-flow return bend)

Water flow in tubes:

$$\dot{m}_w = \frac{\dot{Q}}{\Delta t_w \, c_w} = 120 \text{ kg/s}$$

Water velocity in tubes:

$$u_w = \frac{m_w}{\rho_w \, n_P \, d_i^2 \, \pi/4} = 1.49 \text{ m/s}$$

and therefore $\alpha_i = 4\,000$ W/m² K from Table 8.5(1) is justified.

Fan selection and power consumption:

Air temperature rise:

$\Delta t_{air} = \mathrm{NTU}\ \mathrm{EMTD} = 16.8$ K Eq. 3.8.5(8)

Cooling air volume:

$$\dot{V}_{air} = (SU) \frac{273 + t_{air} + \Delta t_{air}}{273 + t_{air}} = 272 \text{ m}^3/\text{s}$$

Chosen: four fans, each 68 m³/s air volume capacity

$D_V = 3.65$ m
$D_N = 1.2$ m } Fig. 3.8.7(1)

rpm = 288

V-belt drive Fig. 3.8.7(2)

Static pressure:

Cooler bundle: 4 X 21 Pa = 84 Pa

Entrance losses (estimated) = 26 Pa

$\Delta p_{stat} = 110$ Pa

Power consumption:

$N = 15$ kW at 7.5 fan blade angle Fig. 3.8.7(1)

or

$$N = \frac{68\,(110 + 30)}{10^3 \times 0.65} = 14.7 \text{ kW} \quad \text{Eq. 3.8.7(2)}$$

Motor size:

$N_{mot} = 20$ kW

Sound power level:

$$L_w = 44 + 30 \log 55 + 10 \log \frac{110 \times 68}{1\,000} - 5 \log 3.65 = 102 \text{ dB(A)} \quad \text{Eq. 3.8.9(1)}$$

© 1983 Hemisphere Publishing Corporation

With four fans:

L_{W4} = 102 + 10 X 0.6 = 108 dB(A) Eq. 3.8.9(3)

Sound pressure at 300-m distance:

L_P = 108 — 10 X 5.75 = 50 dB(A) Eq. (2)

Nomenclature for Section 3.8.9 appears at the beginning of Part 3.

© 1983 Hemisphere Publishing Corporation

3.9
Compact heat exchangers

Contents

3.9.1
INTRODUCTION, R. L. Webb **3.9.1-1**

3.9.2
DEFINITION OF GEOMETRIC TERMS, R. L. Webb **3.9.2-l**

3.9.3
PLATE FIN SURFACE GEOMETRIES, R. L. Webb **3.9.3-l**

3.9.4
SURFACE PERFORMANCE DATA, R. L. Webb **3.9.4-l**

3.9.5
LAMINAR FLOW SURFACES, R. L. Webb **3.951**

3.9.6
CORRELATION OF HEAT TRANSFER AND FRICTION DATA, R. L. Webb **3.9.6-l**

3.9.7
GOODNESS FACTOR COMPARISONS, R. L. Webb **3.9.7-l**

3.9.8
SPECIFICATION OF RATING AND SIZING PROBLEMS, R. L. Webb **3.9.8-l**

3.9.9
CALCULATION PROCEDURE FOR A RATING PROBLEM, R. L. Webb **3.9.9-1**

3.9.10
PRESSURE DROP CALCULATION, R. L. Webb **3.9.10-l**

3.9.11
PROCEDURES FOR THE THERMAL SIZING PROBLEM, R. L. Webb 3.9.1 **l-l**

3.9.12
MULTIFLUID SERVICE, R. L. Webb **3.9.12-1**

3.9.13
RECENT THEORY AND DATA ON VAPORIZATION AND CONDENSATION, R. L. Webb **3.9.13-1**

Nomenclature for Sections 3.9.1-3.9.13 3.9.13-2
References for Sections 3.9.1-3.9.13 3.9.13-3

© 1983 Hemisphere Publishing Corporation

HEDH

3.9.1 Introduction

R. L. Webb

■ A brazed plate fin heat exchanger is used primarily for gas-to-gas, gas-to-liquid, or two-phase service. It was initially developed for gas-to-gas and gas-to-liquid aircraft and mobile applications. Here, compactness and low weight were valued. This favored aluminum construction. Next, development focused on regenerative heat exchangers for gas turbines, which also valued compactness. Because of high gas turbine exhaust temperatures, stainless steel was used for construction. The brazed aluminum concept has found wide acceptance for gas processing applications (separation and liquefaction). This includes gas-to-gas and two-phase service. Such heat exchangers may be made up of cores 1 X 1 X 6 m in size, manifolded into large batteries. Small brazed aluminum designs are used for air-to-liquid or oil coolers, and as automotive refrigeration evaporators. More recent applications include heat recovery from combustion products, heating ovens, and for recovery of heat from building ventilation air. Because of the compactness possible, the brazed aluminum design is also being considered for large dry cooling towers of multimegawatt capacity. Many other applications are possible.

Primary construction materials are aluminum for temperatures below 250° C and stainless steel for temperatures up to 650° C. Although plate fin construction is usually employed for pressures less than 2 000 kN/m^2, designs have been developed for pressures as high as 5 000 kN/m^2. With clean fluids, fin densities of 5-8 fins/cm are common. When dirty gases are involved, 2-5 fins/cm are more common. Illustrations of heat exchanger design for the various duties are shown and discussed in Sec. 4.4.3. In this section we consider the construction details of the heat exchanger as it influences its thermal and hydraulic performance.

Brazed plate fin heat exchangers normally employ a sandwich-type construction, as illustrated in Fig. 1. The space between the parting sheets is filled with fins that are stamped and folded in an accordion pattern. The fins are bonded to the parting sheets by brazing. Kays and London [1] have termed this construction a compact heat exchanger. Based on parting sheet or prime surface area, the compact heat exchanger will yield a very high heat transfer coefficient. Three basic principles are employed to obtain high heat transfer rates per unit volume for heat transfer to gases: (1) use of extended surface, (2) small hydraulic diameter passages, and (3) augmented or special fin surface geometries.

In addition to a compact, low-weight design, the plate fin construction offers other advantages. The heat transfer surface for each stream may be independently selected. This allows one to select the optimum surface

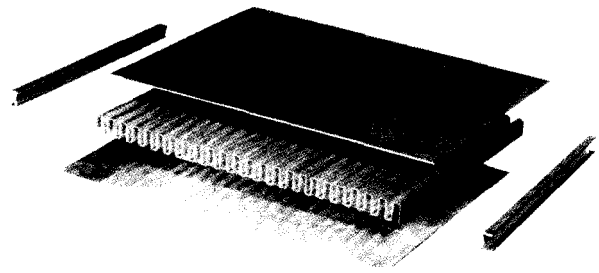

Figure 1 Illustration of plate fin assembly

© 1983 Hemisphere Publishing Corporation

HEDH

geometry and flow area for each fluid stream. The design concept also allows one to employ multiple fluid streams in a single heat exchanger. A plate fin heat exchanger may be designed for any flow arrangement-counter flow, cross flow, and so on. Major limitations of the plate fin design include difficulty in cleaning the fin passages. The use of special augmented surface geometries and flow distributor fins render mechanical cleaning virtually impossible. Mechanical cleaning may be possible for a simple cross-flow design without distributor fins. Therefore, most plate fin exchangers are normally limited to the use of relatively clean, nonfouling fluids. Since the sandwich construction must also function as a pressure vessel, design pressures are limited to moderate values, for example, 2 000 kN/m^2. If higher design pressures are of interest, the possible selection of fin geometries is more limited and thicker fins must be employed.

References for Section 3.9.1 appear at the end of Section 3.9.13.

© 1983 Hemisphere I blishing Corporation

3.9.2
Definition of geometric terms

R. L. Webb

■ The design of a plate fin heat exchanger requires the use of a special terminology. First, a terminology is required to define the geometric characteristics of a particular surface geometry. Second, certain relations are required to define the geometry of the heat exchanger. The geometric factors needed to specify the fin geometry are (1) the basic surface description, (2) plate spacing b, (3) hydraulic radius r_h, (4) fin thickness δ, (5) surface area per unit volume between parting sheets β, and (6) fraction of total surface area formed by the fins A_f/A. These factors will be provided with the test data for each fin surface geometry. Other geometric factors are required to define the flow and heat transfer surface geometry for each stream of the heat exchanger. The geometric factors that must be specified for each of the exchanger streams are A, A_{fr}, L, γ, and σ. The thickness of the parting sheets is a, and the total heat exchanger volume is V. Table 1 defines the surface and core geometric relations for side 1 of the core. The terminology is defined in the Nomenclature at the end of Sec. 3.9.13.

Table 1 Compact heat exchangers: surface and core geometric relations

$$r_h = L\frac{A_c}{A}$$

$$\sigma_1 = \left(\frac{A_c}{A_{fr}}\right)_1 = \left(\frac{Ar_h}{LA_{fr}}\right)_1 = \frac{(Ar_h)_1}{V} = (\gamma r_h)_1$$

$$\sigma_1 = \frac{b_1\beta_1 r_{h1}}{b_1 + b_2 + 2a}$$

$$\gamma_1 = \frac{A_1}{V} = \left(\frac{A}{LA_{fr}}\right)_1 = \left(\frac{\sigma}{r_h}\right)_1$$

$$\gamma_1 = \frac{b_1\beta_1}{b_1 + b_2 + 2a}$$

$$A_{c1} = (\sigma A_{fr})_1 = \left(\frac{Ar_h}{L}\right)_1 = \left(\frac{A\sigma}{L\gamma}\right)_1$$

$$\left(\frac{r_h}{L}\right)_1 = \left(\frac{A_c}{A}\right)_1 = \left(\frac{\sigma}{L\gamma}\right)_1$$

$$A_1 = (\gamma LA_{fr})_1 = \gamma_1 V$$

Nomenclature for Section 3.9.2 appears at the end of Section 3.9.13.

© 1983 Hemisphere Publishing Corporation

3.9.3

Plate fin surface geometries

R. L. Webb

■ Figure 1 shows typical surface geometries used for heat transfer to gases. The figure shows seven basic types of surface geometry, and defines the geometric variables associated with each type. By varying the basic geometric variables for each type of surface, it is possible to obtain a wide variety of specific surface geometries. Although typical fin spacings are 5-8 fins/cm, applications may exist for as many as 16 fins/cm. Fin thicknesses of 0.1 to 0.25 mm are common. Fin heights may range from 0.25 to 2 cm. A plate fin exchanger with 6 fins/cm provides about 1 300 m^2 of heat transfer surface per cubic meter of volume. Such a heat exchanger would contain 10 times as much heat transfer surface per unit volume as in a typical shell-and-tube heat exchanger having 19-mm-diameter tubes. Operated at a frontal velocity of 3 m/s, the heat transfer coefficient based on prime surface area would be on the order of 1 800 W/m^2 K.

The rectangular and triangular fins are simple geometries that offer increased heat transfer because of their small hydraulic radius. The addition of perforations or holes in the fin surface provides some heat transfer increase as a result of wake mixing that occurs in the hole regions. The wavy fins yield increased heat transfer because of secondary flows established by the wavy channel. The offset strip fin, louvered, and pin fins all provide heat transfer augmentation via the repeated growth of laminar boundary layers, followed by dissipation in the wake regions. The offset fin provides heat transfer coefficients two to three times higher than a plain fin geometry having the same fin spacing.

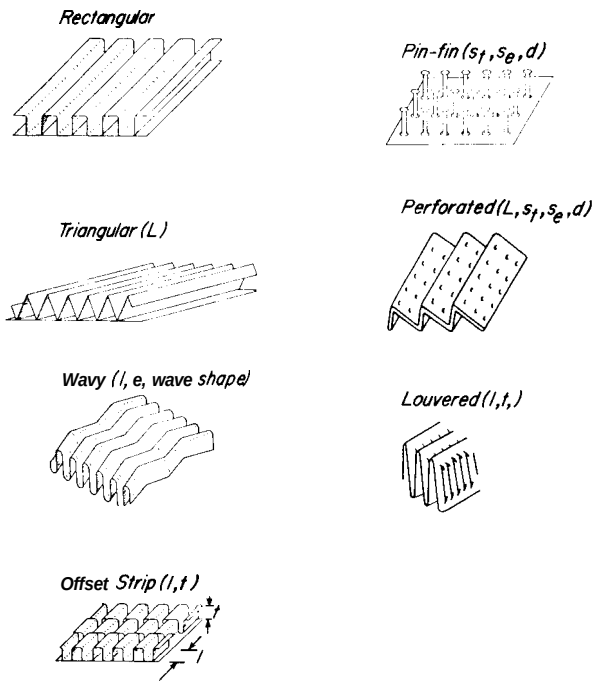

Figure 1 Plate fin surface geometries.

© 1983 Hemisphere Publishing Corporation

3.9.4
Surface performance data

R. L. Webb

■ The heat transfer and friction data are normally presented in the form $j \equiv \mathrm{St}\,\mathrm{Pr}^{2/3}$, and f versus a Reynolds number (Re) based on the hydraulic diameter. This approach is somewhat arbitrary, since several variations of one basic type of surface geometry will generally not correlate on the j and f versus Re basis. This is because geometric variables, other than the hydraulic diameter, may have a significant effect on surface performance. For example, in laminar duct flows, j and f are influenced by the channel shape, or aspect ratio. Because the values of j, f, and Re are dimensionless, the test data are applicable to surfaces of any hydraulic diameter, provided that geometric similarity is maintained.

A standard reference for the heat transfer and friction data of plate fin heat exchanger surfaces is the book by Kays and London, ***Compact Heat Exchangers*** [1]. This book presents j and f versus Reynolds number plots for 52 different plate fin surface geometries. Similar data are also included for tube banks, fin-tube heat exchangers, and crossed-rod matrices. Creswick et al. [2] present a very complete report of existing data as of 1964. Since the publication of the Kays and London book in 1964, additional performance data have been published. Recent additions include:

1. Perforated surfaces [3-7]
2. Offset strip fins [8-12]
3. Louvered fins [11, 13, 14]
4. Pin fins [15]

A compilation of f and j versus Re plots is not presented, because of space limitations. Such data are readily available in the book by Kays and London and the above references. Figures 1 and 2 show the j and f versus Reynolds number characteristics for two surface geometries: a plain rectangular tin, and a high-performance offset strip fin. Surface 101, from [8], has 9.84 fins/cm X 0.1 mm tin thickness; and surface 10-27, from [I], has 4.37 fins/cm X 0.2 mm fin thickness. If the dimensions of surface 10-27 are scaled down to 9.84 fins/cm, the plate spacing and thickness are 5.35 mm and 0.089 mm, respectively. The corresponding hydraulic diameters are 1.49 mm (surface 101) and

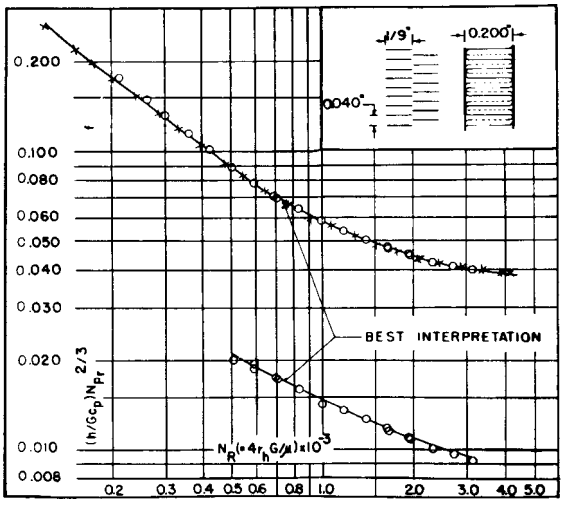

Figure 1 Plot of j and f versus Re for surface 101. Fin pitch = 25.01/in. Plate spacing b = 0.200 in. Flow passage hydraulic diameter $4r_h$ = 0.004 905 ft. Fin metal thickness = **0.004** in., aluminum. Total transfer area/volume between plates β = 719.4 $\mathrm{ft}^2/\mathrm{ft}^3$. Fin area/total area = 0.881.

© 1983 Hemisphere Publishing Corporation

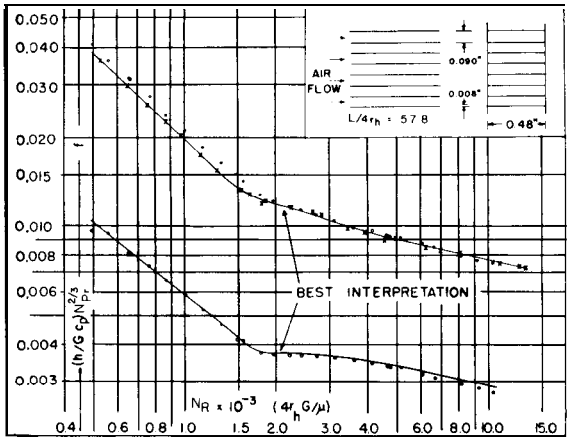

Figure 2 Plot of j and f versus Re for surface 10-27. Fin pitch = 11.11/in. Plate spacing b = 0.48 in. Flow passage hydraulic diameter $4r_h$ = 0.0115 3 ft. Fin metal thickness = 0.008 in., copper. Total transfer area/volume between plates β = 312 ft^2/ft^3. Fin area/total area = 0.854.

1.61 mm (surface 10-27). Thus, the scaled-down dimensions of surface 10-27 are approximately equal to those of surface 101. Comparison of the two figures shows the offset strip fin has considerably higher heat transfer and friction characteristics. At Re = 2 000, the j factor of the offset strip fin is 2.9 times higher than the rectangular fin, and the relative friction factor increase is 3.66. Considering the j/f ratio as an efficiency index between heat transfer and friction, the offset strip fin yields a 190% increased heat transfer coefficient with a heat transfer-to-friction ratio (j/f) 80% as high as the plain rectangular fin. The steep slope of the plain rectangular fin at low Reynolds numbers indicates that the surface is operating in the laminar flow regime. As the Reynolds number increases, the flow passes through a transition regime and then into the turbulent region, where it exhibits a lower slope.

The channel hydraulic diameter is small because of the closely spaced fins. Operation with low-density gases requires excessive friction power, unless the gas velocity in the heat exchanger channels is low. These factors usually imply operational Reynolds numbers in the range 500-I 500. Typically, the operating point may be in the transition region between the laminar and turbulent flow regions. As the hydraulic diameter is reduced, the Reynolds number is forced to yet smaller values. As a result, very compact surfaces may operate in the laminar flow regime. Small hydraulic diameter alone, without a special fin surface geometry, will provide high heat transfer coefficients compared to the flow through circular tubes. For example, an 8 fin/cm plain fin geometry in the laminar flow regime would provide the same heat transfer coefficient as a 19-mm-diameter tube operated at Re = 25 000. If the plain fin geometry is replaced by the offset strip fin, the resulting heat transfer coefficients may be 2.5 times higher. Thus, the combination of small hydraulic diameters, large surface area per unit volume, and specially augmented surface geometries can yield very high heat transfer rates per unit volume. When liquids are used on one side of the heat exchanger, a fin geometry different from that used for gases may be desirable. For a thermally balanced design, we desire $\eta\alpha A$ to be equal for both streams. For liquids having high heat transfer coefficients, the resulting low fin efficiency would render high fins impractical. Thus, it is reasonable to use shorter fins and a larger fin spacing. For high-viscosity oils, it may be advantageous to use turbulator strips on the oil side. These may be viewed as very short offset strip fins oriented 90 to the direction used for gas flow.

Although the fins of Fig. 3.9.3(1) were developed for gases, they have also been used in boiling and condensing applications. Parting sheet materials especially designed for reboiler service have also been developed. Several U.S. patents [16-18] illustrate special nucleate boiling surfaces. At high vapor velocities and high vapor qualities, the offset strip fin has proved to be a good choice for forced convection vaporization. The liquid-vapor mixing induced in the fin channels causes good wetting of the fin surface, and allows heat to be transferred by evaporation across thin liquid films. Milton s patent[16] also suggests the use of the fluted Gregorig condensing surface. However, this requires vertical orientation of the flow channels for best performance. In the vertical orientation, a simple rectangular or triangular fin also serves to draw condensate to the base of the fins, and thus provides drainage and thin films for condensation. Although liquids and two-phase flows may allow a larger fin spacing for thermal performance, a certain maximum fin spacing may be permitted to meet the mechanical strength requirements (dictated by design pressure).

References for Section 3.9.4 appear at the end of Section 3.9.13.

© 1983 Hemisphere Publishing Corporation

3.9.5
Laminar flow surfaces

R. L. Webb

■ We have previously noted that very compact surfaces (small hydraulic diameter) may operate at Reynolds numbers well within the laminar flow region. In the laminar regime, surface geometries designed to produce boundary layer interruptions may be of little benefit. Therefore, plain fin surfaces are likely candidates for very compact designs operating in the laminar regime. Laminar-flow plate fin geometries are also used in rotary regenerators, discussed in Sec. 3.10. For fully developed laminar flow, Nu and f Re are independent of Reynolds number. But Nu and f Re are dependent on the cross-sectional shape of the flow channel. Because of the small hydraulic diameter of the flow channels, their L/D_h may be sufficiently large that fully developed laminar flow solutions are applicable. For most channel shapes the mean Nusselt number and friction factor will be within 10% of the fully developed value if L/D_h > 0.2 Re. If the heat exchanger flow length is short (L/D_h < 0.2 Re), it will be necessary to use analytical solutions that account for the developing flow. In the developing flow region, Nu and f are greater than the fully developed values. Considerable information exists on analytical solutions for channel shapes commonly used on compact heat exchangers. Shah and London [19] present an excellent compilation of analytical solutions for heat transfer and friction of 21 basic cross-sectional shapes. The results include information on the entry length required for fully developed flow and some results for developing flow. Solutions are given for wide range of aspect ratios for each basic channel shape, for example, triangular and rectangular channels.

Table 1 gives fully developed laminar flow solutions for 11 channel shapes of interest in compact heat exchanger design. The tables gives Nu_H (constant heat input per unit length with uniform peripheral temperature), and Nu_T (constant wall temperature). The ratio j/f (for Pr = 0.7) is proportional to the required flow channel frontal area for specified αA and friction power. The hydraulic entrance length $L^+_{hy} = X/D_h$ Re is the dimensionless length required for the centerline velocity to attain 99% of its fully developed value. The constant $K(\infty)$ defines the pressure drop increment to be added to account for the increased friction in the flow development region. The pressure drop, accounting for the flow development region, is

$$\Delta P = \left(\frac{4 f_{fd} L}{D_h} + K(\infty) \right) \frac{G^2}{2\rho} \tag{1}$$

Table 1 lists the channel shapes in order of decreasing Nu. Low aspect ratio rectangular channels are superior to circular or square tubes and triangular channels. High j/f is also associated with high Nu. Thus, increasing channel frontal area would be required for equal αA and friction power, as one moves down the table. The high-aspect-ratio channels not only require less surface area to do the same job, but also require smaller frontal area. Also, notice that the hydraulic entrance length usually increases as one moves down the table.

If the channel length is sufficiently short, it may be necessary to use entrance length solutions to predict the mean Nu and f over the flow length. The parameter $X^* = x/D_h \mathrm{RePr}$ is a dimensionless length for the

© 1983 Hemisphere I blishing Corporation

Table 1 Fully developed laminar flow solutions[a]

Geometry	Nu_H	Nu_T	f Re	$K(\infty)$	j_H/f	j_T/f	L^+_{hy}
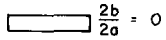 $\frac{2b}{2a} = 0$	8.235	7.541	24	0.686	0.386	0.354	0.005 6
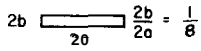 $\frac{2b}{2a} = \frac{1}{8}$	6.490	5.597	20.585	0.879	0.355	0.306	0.009 4
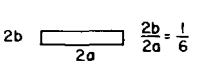 $\frac{2b}{2a} = \frac{1}{6}$	6.049	5.137	19.702	0.945	0.346	0.294	0.011 0
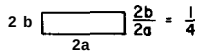 $\frac{2b}{2a} = \frac{1}{4}$	5.331	4.439	18.233	1.076	0.329	0.274	0.014 7
	4.364	3.657	16.00	1.24	0.307	0.258	0.038
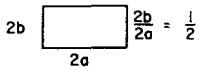 $\frac{2b}{2a} = \frac{1}{2}$	4.123	3.391	15.548	1.383	0.299	0.245	0.025 5
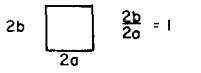 $\frac{2b}{2a} = 1$	3.608	3.091	14.227	1.552	0.286	0.236	0.032 4
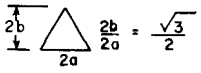 $\frac{2b}{2a} = \frac{\sqrt{3}}{2}$	3.111	2.47	13.333	1.818	0.263	0.209	0.039 8
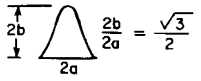 $\frac{2b}{2a} = \frac{\sqrt{3}}{2}$	3.014	2.39	12.630	1.739	0.269	0.214	0.040 8
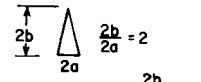 $\frac{2b}{2a} = 2$	2.88	2.22	13.026	1.991	0.249	0.192	0.044 3
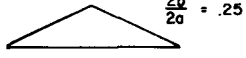 $\frac{2b}{2a} = .25$	2.60	**1.99**	12.622	2.236	0.232	0.178	0.051 5

[a] j_H and j_T for Pr = 0.7. $T \approx$ constant temperature. $H \approx$ heat flux, $\approx$ heat flux with uniform peripheral temperature.

entrance region. For circular tubes, the local Nusselt number will attain its fully developed value within about $X^* \cong 0.1$ for gases. But the value of the mean Nusselt number over the developing flow region (Nu_m) would be about 35% higher than Nu_{fd}. Therefore, it is important to know when L/D_h is sufficient to use the Nu_{fd} for the heat exchanger design. Figure 1 shows the ratio Nu_m/Nu_{fd} for several channel geometries, having a constant wall temperature boundary condition [19] . If X* < 0.2, it appears that the entrance region solutions are required for rectangular and circular channels. Triangular channels have a longer entrance region. Figure 2 gives the pressure drop increment $K(x)/K(\infty)$ of the entrance region for several duct shapes. Equation (1) applies to the entrance region with $K(\infty)$ replaced by K from Fig. 2 at the appropriate X/D_h Re.

Mondt and Siegla [3] and Kays [20] give test results of several laminar flow geometries. They compare their experimental results to the laminar flow analytical solutions and show good agreement, including one case for developing flow.

© 1983 Hemisphere Publishing Corporation

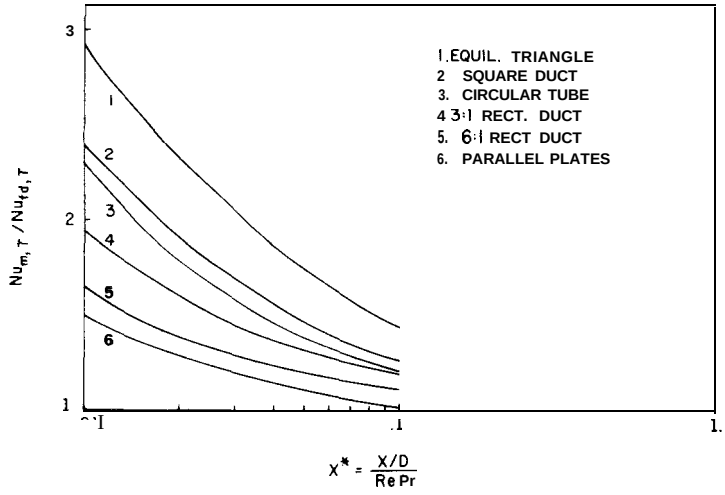

Figure 1 Plot of Nu_m/Nu_{fd} for different channel shapes.

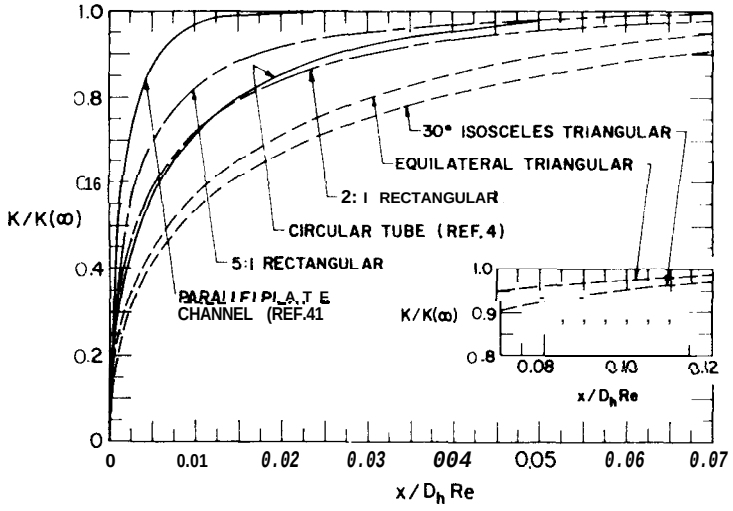

Figure 2 Plot of $K/K(\infty)$ for different channel shapes. $K(\infty)$ channel: 0.65, parallel plates; 0.96, 5:1 rectangular; 1.24 circular tube; 1.46, 2:1 rectangular; 1.67, equilateral triangle; 1.85, 30° isosceles triangular.

Nomenclature and References for Section 3.9.5 appear at the end of Section 3.9.13.

© 1983 Hemisphere Publishing Corporation

3.9.6

Correlation of heat transfer and friction data

R. L. Webb

■ Although performance data are normally presented on a surface-by-surface basis, some progress has been made in prediction or correlation of surface performance. Analytical solutions exist for most possible plain fin geometries in laminar flow regions as discussed in Sec. 3.9.5. In the turbulent flow region, the hydraulic diameter is the significant dimension. One may predict the turbulent region j and f characteristics of plain fin geometries using the hydraulic diameter. This will generally give good results, except for isosceles triangular channels having a very small apex angle.

No specific correlations or prediction methods exist for the j and f values of wavy or herringbone tins. However, several studies of wavy channel geometries used in plate-type heat exchangers [21,22] are applicable, using the principle of geometrical similarity. These studies relate specifically to small-aspect-ratio channels, where the aspect ratio in a typical compact heat exchanger is on the order of 1: 8.

No general correlations have been developed that accurately correlate the performance of the offset strip fin geometry. In addition to fin spacing, the major variables are the fin thickness and the length of the fin strip in the flow direction. The situation is complicated by burrs formed on the leading and trailing fin edges during the manufacturing operation. Wieting [23] established an empirical correlation of f and j versus Re for 22 offset strip fin geometries with $0.7 < X/D_h < 2.7$. Although 85% of the data are within ±10% for j and ±15% for f, the maximum deviation is ±30%. The deviation is probably influenced by burrs on the fin leading and trailing edges, whose effect is not considered. The Wieting correlation is given by Eqs. (1) and (2).

$$f = 7.66\left(\frac{X}{D_h}\right)^{-0.38}(\alpha^*)^{0.09}\mathrm{Re}^{-0.71} \qquad (\mathrm{Re} < 1\,000)$$

$$j = 0.48\left(\frac{X}{D_h}\right)^{-0.16}(\alpha^*)^{0.18}\mathrm{Re}^{-0.54} \qquad (1)$$

$$f = 1.14\left(\frac{X}{D_h}\right)^{-0.78}\left(\frac{t}{D_h}\right)^{0.53}\mathrm{Re}^{-0.2} \qquad (\mathrm{Re} > 1\,000)$$

$$j = 0.24\left(\frac{X}{D_h}\right)^{-0.32}\left(\frac{t}{D_h}\right)^{0.09}\mathrm{Re}^{-0.37} \qquad (2)$$

Sparrow [9] provides a numerical solution for laminar flow in a matrix, which approximates the offset strip fin geometry. His analysis is for zero-thickness fins, and for an infinite aspect ratio.

The offset strip fin is the most widely used augmented fin geometry, because of its high performance. A basic understanding of its heat transfer mechanism is possible. This is discussed in Sec. 3.9.7.

The pin fins may be considered as tube banks having very-small-diameter tubes. As such, low Reynolds number tube bank correlations may provide a first-order prediction of the j and f characteristics of the pin fin geometry. Theoclitus [15] measured the performance of pin fin surfaces with in-line square pin spacings of $2 < s/d < 12$. He compared the experimental results with predictions using tube bank correlations. The friction factor results bracketed the tube

© 1983 Hemisphere 1 blishing Corporation

bank correlations. However, the heat transfer results were 20% lower than predicted by the tube bank correlations.

Attempts to correlate surface data other than plain fins must recognize that end effects exist. Approximately 5–15% of the total surface area is associated with the smooth parting sheets. These end effects were not accounted for by Wietang and Theoclitus. LaHaye et al. [24] have been moderately successful in developing an empirical first-order correlation for all possible surface geometries in the turbulent flow region. Their data for a variety of surface geometries correlated within ±20% when plotted in a form of j Re and $f\,\mathrm{Re}^3$ versus x/D_h. Essentially, this method plots $\alpha A/V$ and P/V for equal D_h versus X/D_h. If the correlation is restricted to variations of one specific type of surface geometry, such as offset fins, the scatter of the data is reduced to the ±10% range. In this correlation method, the length X in the term X/D_h is defined as the flow length between major boundary layer disturbances.

The offset strip fin provides augmented heat transfer by the repeated growth and destruction of laminar boundary layers. Figure 1 illustrates the boundary layer over the short strip length, followed by its destruction in the wake region between the strips. A typical strip length is 3.2 mm. If a Reynolds number based on the strip length is calculated, it will be well within that of a stable laminar boundary layer. Kays [20, 25] has shown that j and f may be approximated using the Polhausen laminar boundary equations for a flat plate. His results are

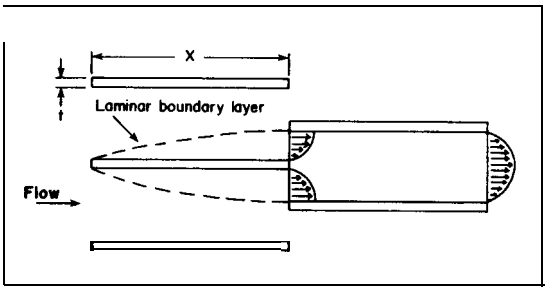

Figure 1 Heat transfer mechanism of offset strip fin.

$$j = 0.664\ \mathrm{Re}_x^{-0.5} \tag{3}$$

$$f = \frac{C_D t}{2x} + 1.328\ \mathrm{Re}_x^{-0.5} \tag{4}$$

This model assumes that the thermal and hydraulic boundary layers are destroyed in the wake region. The first term in the friction equation accounts for the form drag on the plate. Kays suggests use of C_D = 0.88, based on potential flow normal to a thin plate.

The friction factor increases with fin thickness as a result of increased form drag. For Re, = 2 000 and 3.18-mm strip lengths, the form drag contribution is 32% for O.lO-mm fin thickness and increases to 54% with 0.25mm fin thickness. Usually, the experimental friction factor exceeds that of Eq. (4). This is due to burrs that may exist on the leading and trailing edges of the fins. The burr increases the effective plate thickness, causing increased form drag.

Nomenclature and References for Section 3.9.6 appear at the end of Section 3.9.13.

© 1983 Hemisphere 1 blishing Corporation

3.9.7
Goodness factor comparisons

R. L. Webb

■ Surface geometries must be selected for each fluid stream before the heat exchanger design can be undertaken. This selection will depend on mechanical design and thermal performance considerations. On a thermal performance basis alone, one desires a surface geometry that meets the required cost, size, and friction power limitations. Several goodness factors have been proposed to allow comparison of surface performance characteristics in this regard [26-29]. These methods compare the thermal performance of two surfaces on a friction power basis. By writing the heat transfer coefficient (α) and the friction power (P) as functions of j, f, Re, and D_h, one obtains Eqs. (1) and (2).

$$h = \frac{c_p \eta}{\mathrm{Pr}^{2/3}} \frac{j\,\mathrm{Re}}{D_h} \tag{1}$$

$$\frac{P}{A} = \frac{\eta^3}{2\rho^2} f \frac{\mathrm{Re}^3}{D_h^3} \tag{2}$$

The thermal performance of two surfaces may be compared by plotting j Re/D_h versus $f(\mathrm{Re}/D_h)^3$, which compares the heat transfer coefficients for equal friction power per unit surface area. For equal ***P/A,*** or $f(\mathrm{Re}/D_h)^3$, the surface having the largest value of j Re/D_h will require the least heat transfer surface area for equal thermal effectiveness. Alternatively, one may modify Eqs. (1) and (2) to allow comparison on a volume basis. Multiplying each equation by $\beta = A/V = 4\sigma/D_h$ allows comparison of $\alpha A/V$ versus ***P/V.*** Thus, for equal friction power per unit volume ***(P/V),*** one compares the heat exchanger volumes for equal thermal effectiveness.

The application of Eqs. (1) and (2) are illustrated in Fig. 1. This figure shows the performance of the surfaces of Figs. 3.9.4(1) and 3.9.4(2) on a surface area goodness factor basis. The graph is prepared for the case of equal hydraulic diameter. Figure 1 shows that the offset strip fin yields significantly higher heat transfer coefficients for equal ***P/A.*** As the Reynolds number is reduced to small values, associated with laminar flow, the offset fin loses some of its advantage.

Similar goodness factor comparisons may be made with other surface geometries shown in Fig. 3.9.3(1). We would find that the rectangular fin is superior to the triangular fin, and the offset fin is superior to the wavy fin. The pin fin would be competitive with the offset fin, but it contains less surface per unit volume, so a pin fin heat exchanger will require a larger volume for the same αA.

The goodness factor comparison method illustrated in Fig. 1 provides only qualitative information. A more realistic comparison would be to specify flow rate ($\dot{M}$) and friction power ***(P),*** and determine the relative αA offered by the two surfaces under consideration. Or, to specify flow rate ($\dot{M}$) and the αA required, and calculate the friction power ***(P)*** required by the two surfaces. An expression relating the quantities may be obtained by dividing Eq. (1) by Eq. (2) and solving for the ratio j/f. The result is

$$\frac{j}{f} = \frac{\nu^2\,\mathrm{Pr}^{2/3}}{2c_p} \frac{\alpha A}{P} \frac{\mathrm{Re}^2}{D_h^2} \tag{3}$$

Substituting Re = $D_h\dot{M}/\eta A_c$, we obtain

© 1983 Hemisphere Publishing Corporation

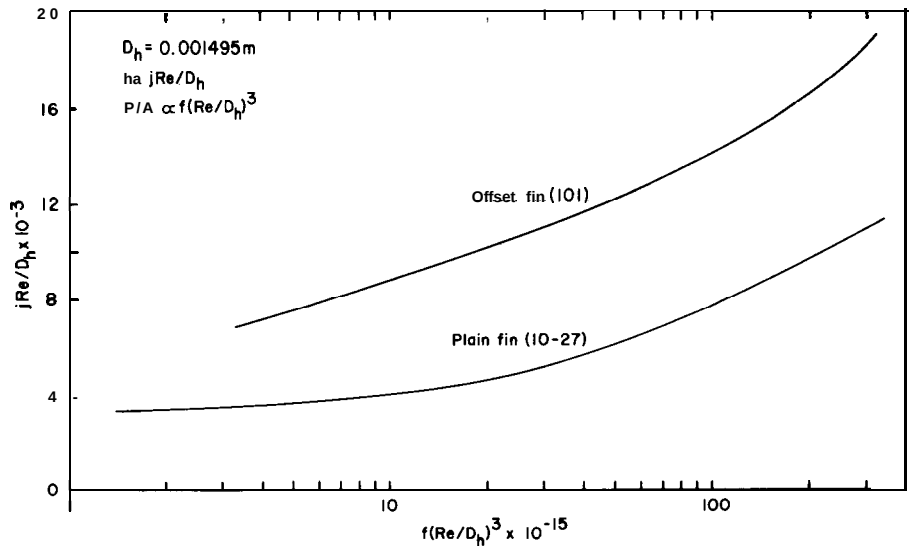

Figure 1 Area goodness factor comparisons for surfaces 10-27 and 101.

$$\frac{j}{f} = \frac{\mathrm{Pr}^{2/3}}{2c_p\rho^2}\,\frac{\alpha A}{P}\,\frac{\dot{M}^2}{A_c^2} \qquad (4)$$

This equation provides a third goodness factor. It allows definition of the frontal area required for two surfaces operating at the same duty (equal $\dot{M}$, P, and A). If frontal area is important, the designer may choose a smoother surface, having a higher value of j/f.

Equations (1), (2), and (4) are particularly useful to compare the relative performance of two surface geometries for equal duty. Assume that the heat exchanger flow rate ($\dot{M}$) is specified. Three possible cases of interest are defined in Table 1.

Example 1: Compare the relative performance, of rectangular and triangular fin geometries, both designed for equal αA, and operating at the same frontal velocity. Air at 27° C and u_{fr} = 4 m/s enters the flow channels. For case 2, calculate the relative friction power (P) and the total surface area (A). Also, determine the relative channel lengths. Figure 2 shows the two surface geometries. Fluid properties are ρ = 1.177 kg/m^3, c_p = 1.00 kJ/kg°C, η = 1.983 X 10^{-5} kg m/s, k = 0.026 2 W/m C. Subscripts T and R refer to the triangular and rectangular fins, respectively. Table 2 gives the calculated results for each surface geometry.

Table 1 Cases for performance comparison

Case	Specify	Calculate
1	αA, P	A, A_{fr}, V, L
2	αA, A_{fr}	P, A, V, L
3	P, A_{fr}	αA, A, V, L

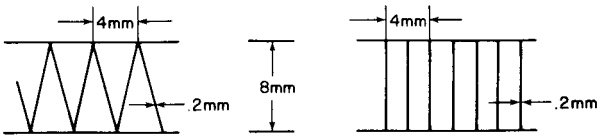

D_h = 2.962 x 10^{-3}m
β = 1215 m^2/m^3
σ = 0.900

D_h = 2.939 x 6 %
β = 1225 m^2/m^3
σ = .900
a* = .225

Figure 2 Triangular and rectangular fin geometries for Example 1.

For αA = constant,

$$\frac{A_T}{A_R} = \frac{\alpha_R}{\alpha_T} = \frac{41.45}{19.64} = 2.11$$

$$\frac{P_T}{P_R} = \frac{f_T}{f_R}\,\frac{A_T}{A_R}\left(\frac{D_{hR}}{D_{hT}}\right)^3\left(\frac{\mathrm{Re}_T}{\mathrm{Re}_R}\right)^3 = 0.652$$

$$= 0.669 \times 2.11\left(\frac{2.94}{2.96}\right)^3\left(\frac{781}{776}\right)^3 = 1.41$$

$$\frac{V_T}{V_R} = \frac{A_T}{A_R}\,\frac{\beta_R}{\beta_T} = 2.11 \times \frac{1\,225}{1215} = 2.13$$

$$\frac{L_T}{L_R} = 2.13 \text{ (since } A_{fr} \text{ is fixed)}$$

Table 2 Calculated results for example

	Triangular	Rectangular
Re = $D_h G_{fr}/\sigma\eta$	781	***776***
f Re from Table 3.9.5(1)	13.026	18.67
Nu$_T$ from Table 3.9.5(1) (by interpolation)	***2.22***	***4.65***
$\alpha = Nu\,k/D_h$	19.64	41.45

© 1983 Hemisphere. I blishing Corporation

Conclusion: For the same frontal area, flow rate, αA, and P, the triangular fin requires 111% more surface area and 40% higher friction power. The triangular flow channel must be twice the depth and volume of the rectangular channel.

Nomenclature and References for Section 3.9.7 appear at the end of Section 3.9.13.

© 1983 Hemisphere Publishing Corporation

3.9.8

Specification of rating and sizing problems

R. L. Webb

● There are two basic types of thermal design problems: rating and sizing. In a rating problem, the geometry and size of the heat exchanger are fully specified. Entering flow rates and fluid temperatures are known. The job is to calculate the thermal effectiveness (heat transferred) and pressure drop of each stream. This is a quite straightforward problem, with one exception. Since the exit stream temperatures are not known, the average temperatures at which fluid properties are evaluated are not known.

In a sizing problem, the heat exchange requirement is specified and the designer must calculate the heat exchanger size. Normally pressure drop limits are given for each fluid stream. Since the entering flow rates, temperatures, and pressures are given, and the heat duty (or leaving temperatures) is specified, the ϵ and NTU (number of transfer units) are directly calculable. A true sizing problem is considerably more complex than the rating problem. A number of decisions must be made prior to making the thermal performance calculations. These include the selection

1. Heat exchanger flow arrangement, e.g., counter flow, cross flow.

2. Heat exchanger materials, as influenced by fluid temperatures and corrosion potential.

3. Fin geometry and fin thickness, as influenced by design pressure requirements.

4. The type of surface geometry and fin spacing and height. Fouling considerations influence the type of surface geometry and fin spacing that may be selected. Fin height is influenced by the desired fin efficiency.

5. Heat exchanger frontal area. This key decision establishes the Reynolds number for each flow stream. The pressure losses are directly dependent on this decision. Use of high-performance surfaces (high j characteristics) will tend to require larger frontal area and less core depth (and less core volume) for a specified pressure drop. If a small frontal area is preferred, surfaces having a high value of j/f will support this need. However, such a selection will likely require greater core volume, and heat exchanger material.

The specification of the above five items is quite complex, and cannot be completed by a step-by-step rational decision path. The main complicating factor is the choice of available surface geometries. Since several candidates are likely, a number of heat exchanger designs that meet the specified thermal and pressure drop performance are possible. Identification of the optimum design requires considerably more effort. First, the designer must establish what variables are to be optimized: first cost, operating cost, or size. Design optimization is discussed by Shah et al. [30] and Palen et al. [31].

Aside from the optimization question, the first crucial element of a design problem is selection of the surface geometries for which the heat exchanger size will be calculated. The second crucial element is selection of the flow frontal areas (or velocities) on which the pressure drops depend. Methods for selecting the

© 1983 Hemisphere Publishing Corporation

fluid velocities are discussed in Sec. 3.9.11. Once the surface geometry and flow velocities have been specified, the thermal design calculation is relatively straightforward. The calculation steps are basically the same as for a rating problem.

Pressure drop calculations are normally performed after completion of the thermal rating (or sizing) calculations. Given the fluid velocities and flow length, the pressure drop calculation follows a straightforward procedure.

In the next sections, we discuss step-by-step procedures for performing sizing and rating calculations.

Nomenclature and References for Section 3.9.8 appear at the end of Section 3.9.13.

© 1983 Hemisphere Publishing Corporation

3.9.9

Calculation procedure for a rating problem

R. L. Webb

■ This section outlines a step-by-step procedure for the thermal calculations involved in a rating problem. Steps 4-9 are required for each fluid stream.

1. Surface geometry parameters: Given $\beta, A_f/A, D_h$. Calculate γ, σ, for each stream.

2. Using the given heat exchanger size, calculate the frontal mass velocity (G_{fr}) for each stream. Then calculate G_c using $G_c = G_{fr}/\sigma$.

3. Estimate ϵ to allow calculation of the average fluid temperature for each stream. This may be based on an outright guess, or a preliminary calculation following steps 4-l 2.

4. Evaluate fluid properties (ρ_m, η_m, c_{pm}) at the estimated average fluid temperature.

5. Calculate Re = $D_h G_c/\eta_m$.

6. Determine f and j (or Nu) from j and f versus Re plots for the surface, or from tabled laminar flow solutions, where appropriate.

7. Calculate $\alpha = jG_c c_{pm} \mathrm{Pr}^{-2/3}$ or α = Nu k/D_h.

8. Calculate fin efficiency. With $ml = (2\alpha/k\delta)^{1/2} l$ calculated, the fin efficiency (η_f) is determined from the appropriate fin efficiency chart or equation.

9. Calculate surface efficiency, $\eta_0 = 1 - (1 - \eta_f)(A_f/A)$.

10. Calculate heat transfer surface areas and determine UA. A simpler approach is to use the given heat exchanger volume (V) and calculate UA from

$$\frac{V}{UA} = \left(\frac{1}{\eta_0 \alpha \gamma}\right)_1 + \left(\frac{1}{\eta_0 \alpha \gamma}\right)_2 \tag{1}$$

11. Calculate $C_{\min}/C_{\max}$ and NTU $= UA/C_{\min}$.

12. Using the parameters in step 1 1, determine ϵ from the ϵ-NTU chart (or equation) for the given heat exchanger flow arrangement.

13. Compare calculated ϵ with estimated ϵ. Repeat steps 4-12 as necessary to obtain desired accuracy.

Nomenclature for Section 3.9.9 appears at the end of Section 3.9.13.

© 1983 Hemisphere Publishing Corporation

3.9.10

Pressure drop calculation

R. L. Webb

■ After the heat exchanger geometry is fixed, the pressure loss may be calculated. The pressure loss for each stream through the heat exchanger finned passages is calculated by

$$\Delta P = \frac{G_c^2}{2}\left[\frac{(K_c + 1 - \sigma^2)}{\rho_1} + 2\left(\frac{1}{\rho_2} - \frac{1}{\rho_1}\right) + \frac{f}{\rho_m}\frac{A}{A_c} - \frac{(1 - \sigma^2 - K_e)}{\rho_2}\right] \quad (1)$$

The terms of Eq. (1) are entrance loss, flow acceleration loss, core friction, and exit loss, respectively. The K_c and K_e values depend on the cross-sectional flow geometry, σ, and Re. Figure 1 gives K_c and K_e for a 1: 1 ratio channel [1] . Kays and London [1] give similar curves for two other channel geometries (parallel-plate channel and triangular channel). The entrance and exit losses are normally less than 10% of the total core loss, so the data of Fig. 1 will cover most situations with adequate accuracy. The differences due to other channel configurations should cause only a second-order effect for most situations. Figure 1 is based on a uniform velocity entering the heat exchanger and fully developed flow in the core, and at the exit. This assumption is not valid for interrupted fin surfaces. In this case, Kays and London [I] recommend use of the Re = ∞ curves to evaluate K_c and K_e. In this case, all channel configurations have the same K_c and K_e values for Re = ∞. The calculation steps for the core pressure loss requires the information developed through step 6 of the rating calculation procedure. After calculation of the K_c, K_e, values and the densities entering and leaving the core (ρ_1, ρ_2), the core AP may be calculated using Eq. (1).

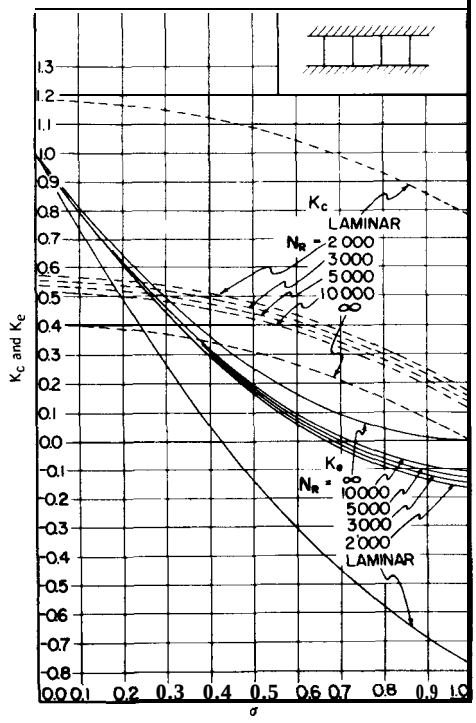

Figure 1 Entrance and exit loss coefficients for multiple square channels with abrupt contraction entrance and abrupt expansion exit.

If the heat exchanger construction contains manifolds and flow distributor fins, one must also account for these losses. These losses may be a significant fraction of the total pressure loss.

© 1983 Hemisphere Publishing Corporation

Kays and London [1] recommend calculation of the losses for each stream in the form $\Delta P/P_1$, where P_1 is the inlet pressure. This defines the fraction of the inlet flow energy dissipated as flow losses. In a balanced gas-to-gas design, one desires approximately equal values of $\Delta P/P$ for each stream.

Nomenclature and References for Section 3.9.10 appear at the end of Section 3.9.13.

© 1983 Hemisphere Publishing Corporation

3.9.11

Procedures fthehermal sizing problem

R. L. Webb

■ The sizing problem was introduced in Sec. 3.9.8. Assume that the factors discussed in that section have led to the selection of surface geometries for each fluid stream. Then, it is necessary to size the heat exchanger for the required thermal duty and fluid temperature and pressure conditions. The remaining unspecified variables are the velocities for each flow stream. The heat exchanger will require minimum surface area if the velocity is chosen to use all of the allowed pressure drop. Two approaches are possible.

The simplest method is to compute designs for a series of velocities that yield pressure losses above and below the allowable value. Each design meets the required ϵ. Then, a graph of the calculated pressure drops versus the frontal velocity permits selection of the design velocity. This approach is ideally suited for a digital computer design program. In essence, the design for each velocity is a rating problem calculation. Since the required thermal duty is known, the average fluid temperature of each stream is known, and the properties are evaluated at these average temperatures. The calculation procedure for a counter-flow or parallel-flow heat exchanger is as follows:

1. From the required ϵ and given $C_{\min}/C_{\max}$, calculate the required NTU.
2. Calculated the required $UA =$ NTU $C_{\min}$.
3. Follow steps 1, 2, and 4-9 of the rating problem (Sec. 3.9.9).
4. Using the equation given in step 10 of the rating problem, calculate the required heat exchanger volume.
5. Calculate heat exchanger length by $L = V/A_{fr}$. The frontal area (A_{fr}) is directly calculable, since the frontal velocity was initially specified for each stream.
6. Calculate the pressure drop following Sec. 3.9.10. This procedure is not applicable to a cross-flow design.

In this case, independent specification of each velocity fixes the heat exchanger size. Adaptation of this procedure to cross flow requires setting the velocity for stream 1, and applying the procedure to a range of velocities for stream 2. Then repeat this procedure with a new velocity for stream 1. This will require an extensive number of calculations. However, they may be done quickly using a digital computer.

The second procedure uses the coupled heat transfer and pressure drop Eq. 3.9.7(4) for each channel (1). This equation is solved for the velocity that satisfies both the thermal effectiveness (E) and pressure drop limits. This should define the design velocity within 10% for most cases. The core friction term is usually the dominant term in the pressure drop equation 3.9.1 0(10). Because the entrance and exit losses are opposite in sign, their effects tend to cancel. For gases, the flow acceleration loss should be less than 10% of the total core friction loss. One may approximately specify the allowable core friction loss as 90% of the total core pressure loss. The design equation to select the approximate G_c for stream 1 is developed in Eqs. (1), (2), and (3).

Let $R_1 = C_{\min}/C_1$ and $F_1 = (U/\eta_0\alpha)_1$, where U_1 is based on A_1 and j = St $\mathrm{Pr}^{2/3}$. The NTU may be expressed as

© 1983 Hemisphere I blishing Corporation

$$\mathrm{NTU} = \frac{1}{R_1}\left(\frac{Fj\eta_0 A}{\mathrm{Pr}^{2/3} A_c}\right)_1 \quad (1)$$

Solve Eq. (1) for (A/A_c), and substitute in the pressure drop equation, (2), yielding Eq. (3).

$$\Delta P_1 = \left(\frac{fA}{A_c}\frac{G_c^2}{2\rho_m}\right)_1 \quad (2)$$

$$G_{c1} = \left[\frac{\mathrm{Pr}^{-2/3}}{\mathrm{NTU}\,R_1}\,\frac{j}{f}_{0}(2\rho_m\ \Delta P\ \eta_0 F)_1\right]^{1/2} \quad (3)$$

Equation (3) is to be solved for the required mass velocity, G_{c1}. The known quantities in Eq. (3) are NTU, R_1, ΔP, and ρ_{m1}. Approximate values must be established for $(j/f)_1$, η_{01}, and F_1. The recommended procedure is as follows:

1. Estimate, or specify the desired value for F_1 (0.5) and estimate the surface efficiency, $\eta_{01}(\eta_0 \cong 0.8)$.
2. Plot $(j/f)_1$ versus Re for surface 1. This value will probably vary no more than 15% over the Re of interest. Select an approximate value for $(j/f)_1$.
3. Using the estimated values of F_1, η_{01}, and $(j/f)_1$, calculate G_{c1} from Eq. (3).
4. Repeat steps 1-3 for stream 2.

Once the approximate values of G_{c1} and G_{c2} are fixed, the procedure initially described may be used for the final design calculations. The preliminary design procedure is of considerable value in establishing a reasonably close starting point for the design. It is particularly useful for a cross-flow heat exchanger. This procedure will define the approximate design velocity for each stream of the cross-flow exchanger.

Ideally, a two-fluid heat exchanger should have equal thermal resistance values for each stream. Thus, $(\eta_0 \alpha A)_1 = (\eta_0 \alpha A)_2$. And, for gas-to-gas designs we may equally desire $\Delta P_1/P_1 = \Delta P_2/P_2$. Both of these criteria are virtually impossible to achieve for a limited choice of surface geometries. The design is biased toward minimum material content if the thermal resistances are equal.

Nomenclature for Section 3.9.11 appears at the end of Section 3.9.13.

© 1983 Hemisphere Publishing Corporation

3.9.12
Multifluid service

R. L. Webb

■ Plate fm heat exchangers are frequently used in applications involving three or more separate fluid streams. Important applications include the liquefaction or separation of gas mixtures. The brazed aluminum exchanger is ideally suited for this service. Its compact design yields minimum size and surface area for environmental heat leaks. The heat transfer and pressure drop requirements for each stream are satisfied by varying the fm geometry (type, fin spacing, and height), and the number of flow channels apportioned to each fluid stream. Further, barriers can be provided within the channel stack to allocate one channel to more than one fluid over the length of the exchanger. Headers and flow distributors are located on the core, as required, to accommodate the number of fluids involved. Within a single core, heat may be transferred between boiling, condensing, or sensible streams. Figure 1 illustrates a brazed aluminum design for three fluid service.

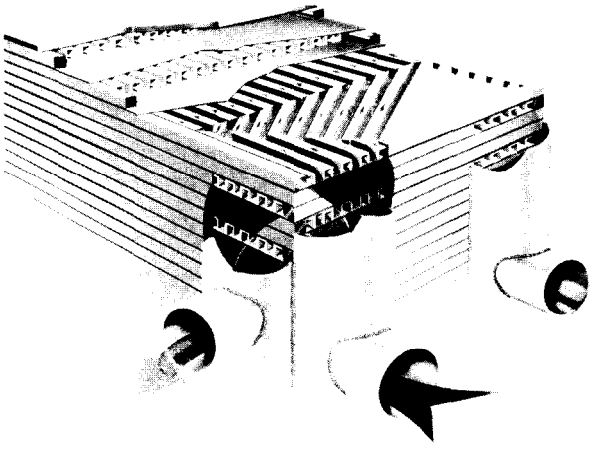

Figure 1 Brazed aluminum heat exchanger for three-fluid service.

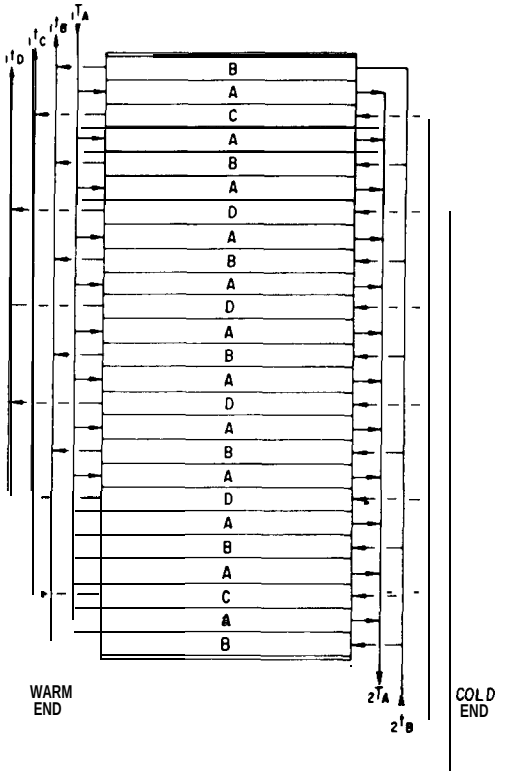

Figure 2 Plate stacking pattern for four-fluid exchanger.

Multifluid designs consist of a large number of passages stacked in a repeating pattern. Figure 2 illus-

© 1983 Hemisphere Pu lishing Corporation

trates one possible stacking arrangement for a four-fluid exchanger [32]. Fan [32] discusses the thermodynamic advantages of different plate stacking arrangements for up to four-fluid service. Depending on the number of fluids, the core may contain several different repeating patterns. The design problem involves analysis of the heat transfer process in each of the repeating patterns, and then scaling the results to satisfy the total flow requirements. The thermal effectiveness of a two-fluid exchanger is expressed as a function of two variables $(NTU, C_{min}/C_{max})$. In the three-fluid case, two thermal effectiveness values must be calculated, each of which depends on five variables (an inlet temperature ratio, two capacity rate ratios, and two NTUs). Sorlie [33], Willis and Chapman [34], and Chato et al. [35] have developed modifications of the effectiveness-NTU method for three-fluid exchangers. They assume that two fluids exchange heat with a third, but not with each other. Sorlie considers parallel- and counter-flow problems, Willis and Chapman a cross-flow problem, and Chato et al. a parallel-flow problem. Demetri and Platt [36] extend the procedure to account for heat exchange among nonadjacent fluids, due to conduction through the fins of intervening passages. Because of the number of variables involved, these design methods must be performed by computer, and it is not possible to draw generalized performance charts for each flow arrangement.

Demetri and Platt describe a generalized design procedure based on the analogy between heat transfer paths and electric circuits. They present results for parallel flow, cross flow and counter flow. Their results agree well with Sorlie and Willis and Chapman for the case of negligible fin conduction.

Nomenclature and References for Section 3.9.12 appear at the end of Section 3.9.13.

© 1983 Hemisphere Publishing Corporation

3.9.13

Recent theory and data on vaporization and condensation

R. L. Webb

■ In recent years, several important studies dealing with vaporization and condensation in plate-fin channels have been completed. Haseler [1] condensed nitrogen in a plain-fin channel having 709 fins/m. The measurements defined the local condensation coefficient as a function of vapor quality. Figure 1 compares the ability of several existing correlations to predict the experimental condensation coefficient. The Nusselt equation (N) clearly underpredicts the data. Although the Shah (S) and Boyko-Kruzhilin (B) correlations predict the 58.5 kg/m² s data of Fig. 1 well, Haseler shows that these correlations underpredict the lower mass flux (30.6 kg/m² s) data on the order of 40%. Yung et al. [38] condensed ammonia in a "serrated-fin" geometry (see Fig. 1 in Sec. 3.9.3). They develop an analytical model, which assumes the condensate flows in an uninterrupted sheet in the wake region between the fin segments. The net effect is to reduce the film thickness 50%, compared to a plain-fin geometry. Their model also includes the effect of interfacial shear. Their predicted overall heat transfer coefficients agree within 20% of the experimental values.

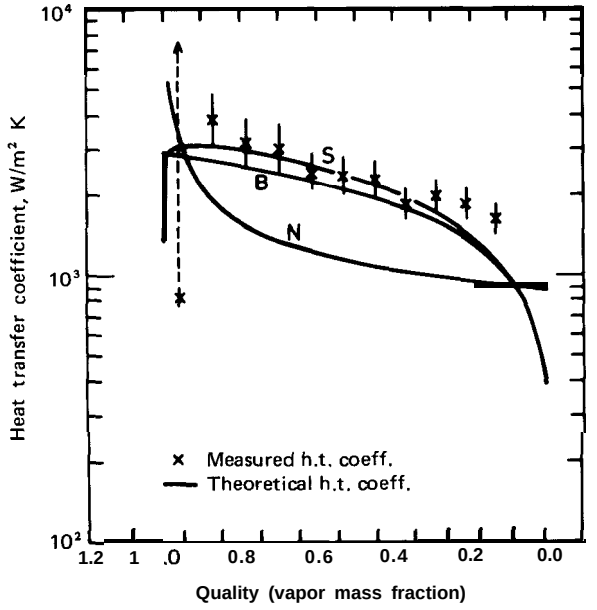

Figure 1 Condensation heat transfer coefficient for nitrogen as a function of vapor quality. Pressure (337 kPa), mass flux (58.5 kg/m s), heat flux (8.26 kW/m²).

Robertson and Lovegrave [39] have measured heat transfer coefficients for vaporization of nitrogen [39] and R-l 1 [40] in a serrated-fin geometry having 591 fins/m. Figure 2 shows the measured heat transfer coefficients vs. $\mathrm{Re}_L (D_h G/\eta_L)$ with vapor quality as the parameter. They conclude that nucleate boiling was not present, so convective boiling was the dominant heat transfer mechanism. For $800 < \mathrm{Re}_L < 1600$, the heat transfer coefficient is independent of Reynolds number. Above the transition Reynolds number, the coefficient is proportional to the 0.8 power of Re_L. The boiling nitrogen data showed essentially the same transition Reynolds number range as that for R-l 1.

Yung et al. [38] vaporized ammonia in the previously described serrated-fin geometry. Their analytical condensation model is also assumed to apply to the convective vaporization data, e.g., evaporation from a thin liquid film. Their overall heat transfer coefficients are predicted within ±5% by this model. Since the

© 1983 Hemisphere. I blishing Corporation

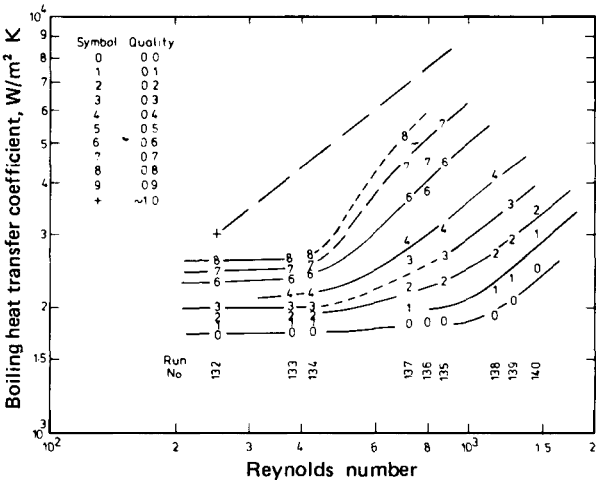

Figure 2 Boiling heat transfer coefficient vs. Reynolds number $(D_h G/\eta_L)$ for R-l 1.

model assumes no liquid entrainment, its validity is limited to a critical Reynolds number, at which entrainment will occur. They argue that entrainment is expected for $\mathrm{Re}_L \cong 1\,000$. Their model does a very good job of predicting the boiling coefficient of the Robertson and Lovegrave data [39].

NOMENCLATURE FOR SECTIONS 3.9.1-3.9.13

a	plate thickness
a	short side of a rectangular flow passage
A	exchanger total heat transfer area on one side
A_c	exchanger minimum free-flow area
A_f	exchanger total fin area on one side
A_{fr}	exchanger total frontal area
b	plate spacing
b	long side of a rectangular flow passage
c_p	specific heat at constant pressure
c	flow stream capacity rate $(\dot{M}c_p)$
C_c	flow stream capacity rate of cold-side fluid
C_h	flow stream capacity rate of hot-side fluid
$C_{\min}$	minimum of C_c or C_h
$C_{\max}$	maximum of C_c or C_h
d	diameter of pin fin
D_h	hydraulic diameter of any internal passage $(D_h = 4r_h = 4A_cL/A)$
f	mean friction factor, defined on the basis of mean surface shear stress
G	exchange flow stream mass velocity $(\dot{M}/A_c)$, $G_c = \dot{M}/A_c, G_{fr} = \dot{M}/A_{fr}$
k	unit thermal conductivity
K_c	contraction loss coefficient for flow at heat exchanger entrance
K_e	expansion loss coefficient for flow at heat exchanger exit
ℓ	fin length from root to center
L	total heat exchanger flow length; also, flow length of uninterrupted fin
m	a fin effectiveness parameter $\sqrt{2\alpha/k\delta}$
$\dot{M}$	mass flow rate
NTU	number of heat transfer units of an exchanger, a heat transfer parameter $(AU/C_{\min})$
Nu	Nusselt number $(\alpha D_h/k)$
AP	pressure drop
P	friction power expended per unit of surface heat transfer area [see Eq. 3.9.7(2)]
Pr	Prandtl number $(\eta c_p/k)$
4	heat transfer rate, W/m
r_h	hydraulic radius (A_cL/A)
R	flow stream capacity rate ratio $[(\dot{M}c_p)_{\min}/(\dot{M}c_p)_{\max}$ 1
Re	Reynolds number $(D_h G/\eta)$
s	center-to-center spacing for pin fins
St	Stanton number (α/Gc_p)
T	temperature to any arbitrary scale
t_c	cold-fluid-side temperature
t_h	hot-fluid-side temperature
U	unit overall thermal conductance
u	velocity
V	volume
X	axial flow coordinate
α	convection heat transfer coefficient
a*	aspect ratio of a rectangular flow passage (b/a), dimensionless
β	ratio of total heat transfer area on one side of a plate fin heat exchanger to the volume between the plates on that side
γ	ratio of total transfer area on one side of the exchanger to total volume for the exchanger
δ	fin thickness
A	denotes difference
ϵ	exchanger effectiveness, dimensionless
η	dynamic viscosity
ν	kinematic viscosity
η_F	fin efficiency, dimensionless

© 1983 Hemisphere Publishing Corporation

η_0 total surface temperature effectiveness, dimensionless
ρ density
α ratio of free-flow area to frontal area, A_c/A_{fr}, dimensionless
τ_0 unit surface shear stress

Subscripts

fd fully developed condition
m mean conditions, defined as used
1, 2 indicates different sides of the heat exchanger; inlet and outlet conditions
max maximum
min minimum

REFERENCES FOR SECTIONS 3.9.1-3.9.13

1. Kays, W. M., and London, A. L., ***Compact Heat Exchangers,*** 2d ed., McGraw-Hill, New York, 1964.
2. Creswick, F. A., Talbert, S. G., and Bloemer, J. W., Compact Heat-Exchanger Study, Final Technical Rept., DA-44-009, AML-313(X), March 31, 1964.
3. Mondt, J. R., and Siegla, D. C., Performance of Perforated Heat-Exchanger Surfaces, ***J. Eng. Power,*** vol. 96, pp. 81-86, 1974.
4. Shah, R. K., Perforated Heat Exchanger Studies, Part 1, Flow Phenomena, Noise and Vibration, ASME Paper 75-WA/HT-8.
5. Shah, R. K., Perforated Heat Exchanger Studies, Part 2, Heat Transfer and Flow Friction Characteristics, ASME Paper 75-WA/HT-9.
6. Liang, C. Y., and Yang, W. J., Heat Transfer and Friction Loss Performance of Perforated Heat Exchanger Surfaces, ***J. Heat Transfer,*** vol. 97, pp. 9-15, 1975.
7. Pucci, P. F., Howard, C. P., and Piersall, C. H., Jr., The Single Blow Transient Testing Technique for Compact Heat Exchanger Surfaces, ***J. Eng. Power,*** vol. 89, pp. 29-39, 1967.
8. London, A. L., and Shah, R. K., Offset Rectangular Plate-Fin Surfaces-Heat Transfer and Flow Friction Characteristics, ***J. Eng. Power,*** vol. 90, pp. 218-288, 1968.
9. Sparrow, E. M., Baliga, R. R., and Patankar, S. V., Heat Transfer and Fluid Flow Analysis of Interrupted-Wall Channels, with Application to Heat Exchangers, ***J. Heat Transfer,*** vol. 99, pp. 4-11, February 1977.
10. Mochizuki, S., and Yagi, Y., Heat Transfer and Friction Characteristics of Strip Fins, ***Heat Transfer Jpn. Res.,*** vol. 6, pp. 36-59, 1977.
11. Dubrovskii, E. V., and Fedotva, A. I., Investigation of Heat Exchanger Surfaces with Plate Fins, ***Heat Transfer Sov. Res.,*** vol. 4, pp. 75-79, 1972.
12. Shah, R. K., and London, A. L., Influence of Brazing on Very Compact Heat Exchanger Surfaces, ASME Paper 71-HT-29, 1971.
13. Smith, M. C., Performance Analysis and Model Experiments for Louvered Fin Evaporator Core Development, SAE Paper 720078, 1972.
14. Wong, L. T., and Smith, M. C., Airflow Phenomena in the Louvered-Fin Heat Exchanger, SAE Paper 730237, 1966.
15. Theoclitus, G., Heat Transfer and Flow-Friction Characteristics in Nine Pin-Fin Surfaces, ***J. Heat Transfer,*** vol. 85, pp. 383-390, 1966.
16. Milton, R. M., Heat Exchange System, U.S. Patent 3,384,154, May 1968.
17. Theophilus, N. P., and Wang, D., Multiple Passage Heat Exchanger Utilizing Nucleate Boiling, U.S. Patent 3,457,990, July 1969.
18. Milton, R. M., Heat Exchange System with Porous Boiling Layer, U.S. Patent 3,587,730, June 1971.
19. Shah, R. K., and London, A. L., ***Laminar Flow Forced Convection in Ducts,*** Academic, New York, 1978.
20. Kays, W. M., Compact Heat Exchangers, ***AGARD Lecture Ser., #57 on Heat Exchangers,*** ed. J. J. Ginoux, AGARD-LS-57-72, January 1972.
21. Rosenblad, G., and Kullendorf, A., Estimating Heat Transfer Rates from Mass Transfer Studies on Plate Heat Exchanger Surfaces, ***Wärme S'toffbertrag.,*** vol. 8, pp. 187-191, 1975.
22. Okada, K., Ono, M., Tomimura, T., Okuma, T., Konno, H., and Ohtani, S., Design and Heat Transfer Characteristics of New Plate Type Heat Exchanger, ***Heat Transfer Jpn. Res., vol.*** 1, pp. 90-95, 1972.
23. Wietang, A. R., Empirical Correlations for Heat Transfer and Flow Friction Characteristics of Rectangular Offset-Fin Plate-Fin Heat Exchangers, ***J. Heat Transfer,*** vol. 97, pp. 488-490, 1975.
24. LaHaye, P. G., Neugebauer, F. J., and Sakhuja, R. K., A Generalized Prediction of Heat Transfer Surface Performance and Exchanger Optimization, ***J. Heat Transfer,*** vol. 96, pp. 511-517, 1974.
25. Kays, W. M., and London, A. L., Remarks ***on*** the Behavior and Applications of Compact High-Performance Heat Transfer Surfaces, ***General Discussion on Heat Transfer,*** 195 1.
26. Cox, B., and Jallouk, P. A., Methods for Evaluating the Performance of Compact Heat Transfer Surfaces, ***J. Heat Transfer,*** vol. 95, pp. 464–469, 1973.
27. Bergles, A. E., Bunn, R. L., and Junkhan, G. H., Extended Performance Evaluation Criteria for Enhanced Heat Transfer Surfaces, ***Left. Heat Mass Transfer,*** vol. 1, pp. 113-120, 1974.
28. Soland, J. G., Mack, W. M., and Rohsenow, W. M., Performance Ranking of Plate-Fin Heat Exchanger Surfaces, ASME Paper 76-WA/HT-31, 1976.
29. Shah, R. K., Heat Exchanger Surface Selection, *Proc. 6th Int. Heat Transfer Conf.,*
30. Shah, R. K., Atimiwala, K. A., and Mayne, R. W., Heat Exchanger Optimization, *Proc. 6th Int. Heat Transfer Conf.,*
31. Palen, 3. W., Cham, T. P., and Taborek, J., Optimization of Shell and Tube Heat Exchangers by Case Study Method, ***Chem. Eng. Prog. Symp. Ser.,*** vol. 70, no. 138, 1974.
32. Fan, Y. N., How to Design Plate-Fin Exchangers, ***Hydrocarbon Process.,*** vol. 45, no. 11, pp. 211-217, 1966.

© 1983 Hemisphere Publishing Corporation

33. Sorlie, T., Three Fluid Heat Exchanger Design Theory, Counter and Parallel Flow, Tech. Rept. 54, August 1962, Dept Mech. Eng., Stanford University, Stanford, Calif.
34. Willis, N. C., Jr., and Chapman, D. J., Analysis of Three Fluid, Crossflow Heat Exchangers, ***J. Heat Transfer, vol. 90,*** pp. 333-339, 1963.
35. Chato, J. C., Laverman, R. J., and Shah, J. M., Analysis of Parallel Flow, Multi-Stream Heat Exchangers, ***Int. J. Heat Mass Transfer,*** vol. 14, pp. 1691-1703, 1971.
36. Demetri, E. P., and Platt, M., A General Method for the Analysis of Compact Multifluid Heat Exchangers, ASME Paper 72-HT-14, 1976.
37. Haseler, L., Condensation of Nitrogen in Brazed Aluminum Plate-Fin Heat Exchangers, ASME Paper 80-HT-57, 1980.
38. Yung, D., Lorenz, J. J., and Panchal, C., Convective Vaporization and Condensation in Serrated-Fin Channels, in ***Heat Transfer of Ocean Thermal Energy Conversion (OTEC) Systems,*** ed. W. L. Owens, ASME Symp. vol. HTD-vol. 12, pp. 29-38, 1980.
39. Robertson, J. M., and Lovegrave, P. C., Boiling Heat Transfer with Freon-11 in Brazed-Aluminum Plate-Fin Heat Exchangers, ASME Paper 80-HT-58, 1980.
40. Robertson, J. M., Review of Boiling, Condensing, and Other Aspects of Two-Phase Flow in Plate-Fin Heat Exchangers, in ***Compact Heat Exchangers,*** eds. R. K. Shah, C. F. McDonald, and C. P. Howard. ASME Symp., vol. HTD-vol. 10, pp. 17-27, 1980.

© 1983 Hemisphere Publishing Corporation

3.10.1
Introduction

D. Chisholm

■ The heat pipe (Fig. la) is a self-contained system that transfers heat by boiling a fluid at one point and condensing it at another; the liquid is transferred back to the boiling area by capillary action through a wick structure. It is the use of the capillary action that is the unique characteristic of the heat pipe.

The heat pipe is closely related to the two-phase thermosiphon (Fig. lb). In the thermosiphon the condensate returns from the evaporator to the condenser under the action of gravitational forces, rather than under the action of capillary forces as in the heat pipe. For this reason, in the thermosiphon the evaporator must always be below the condenser, as illustrated in Fig. 1, whereas the evaporator of the heat pipe can be in any orientation in relation to the condenser; in the heat pipe it is possible to transfer heat downward.

Provided that the pressure gradient in the vapor is kept small, the axial temperature gradient along the heat pipe can be small, resulting in a device of a very high thermal conductivity. The effective thermal conductivity of the device can be more than 1 000 times that of a solid copper rod of similar dimensions. Heat fluxes as high as 15 kW/cm^2 have been measured with lithium as the working fluid at temperatures of 1 500° C. Against gravity, with existing wicks, the maximum length of heat pipe that can be used is about 40 cm.

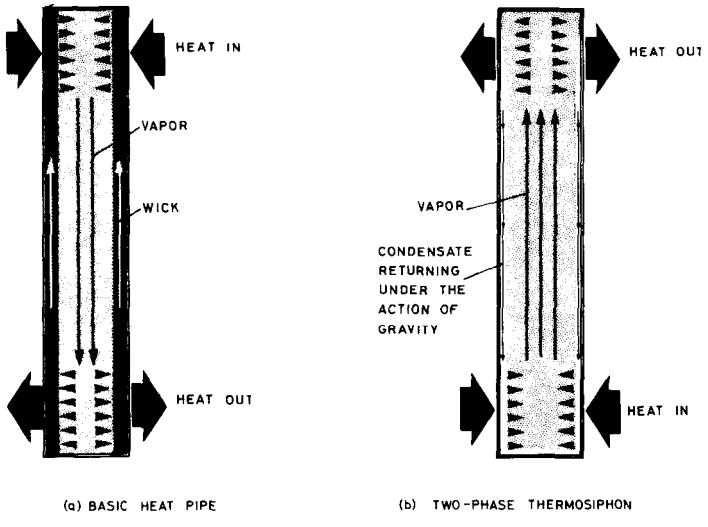

Figure 1 A heat pipe and thermosiphon.

© 1983 Hemisphere Publishing Corporation

R. S. Gaugler filed the first heat pipe patent (U.S. Patent 2 350 348) in 1942, the proposed application relating to the cooling of the interior of an icebox. In U.S. Patent 2 448 261, filed in 1945, he outlined the desirable arrangement of wick as one with large pores at the condenser with the smallest pores occurring in the evaporator where the capillary pull is exerted. Gaugler wrote, It is the object of my invention to provide a secondary heat transferring circuit which is capable of transferring heat downwardly and which can be bent and formed as desired. Prior to his 1942 patent, Gaugler filed in 1941 U.S. Patent 2 350 347, in which wicks were used to spread liquid over the evaporating surfaces of refrigerating equipment. U.S. Patent 2 517 654, filed by Gaugler in 1946, relates to a similar application, with more detailed descriptions of the methods of inserting wicks in tubes.

G. M. Grover, working at Los Alamos on heat transfer problems in spacecraft, reinvented the heat pipe in U.S. Patent 3 229 759, entitled "Evaporation-Condensation Heat Transfer Device, filed in 1963. The performance of heat pipes is, of course, greatly improved in the absence of gravity, and wicks then become an ideal method of ensuring that the liquid remains on the hot surfaces. Grover s patent begins: this invention relates to structures of very high thermal conductance and, more particularly, to devices for the transfer of a large amount of heat with a small temperature drop, thereby being equivalent to a material having a thermal conductivity exceeding that of any known metal by a very large factor. It continues: The condensate must be returned to the evaporator. . . . This function is accomplished by a wick of suitable capillary structure. Devices of this general class will hereinafter be referred to as heat pipes although it should be kept in mind that the shape of the devices is not a matter of concern. As far as the writer is aware, this was the first use of the term heat pipe.

Grover, Cotter, and Erikson [1] published the first technical paper on the heat pipe in 1964. When this author wrote a text [2] on the heat pipe in 1970, I was able to collect 152 relevant articles. There must now be more than a thousand articles on the subject, and there are two further texts [3, 4].

In addition to its high effective thermal conductivity the heat pipe has the following features:

1. It is flexible.
2. It is controllable.
3. It can act as a thermal diode.
4. It can act as a heat flux transformer.
5. It has isothermal surfaces.

The heat pipe is therefore being used in a wide range of industrial applications as shown in Table 1.

Table 1 Heat pipe applications

Application	References
Battery temperature control	[5]
Biological	[6, 71
Brakes	[8]
Coal gasification	[9, 10]
Cooking pm	[11]
Cooling electronic equipment	[12-14]
Cryosurgery	[15]
Deicing	[16-18]
Die casting/molds	[19, 20]
Domestic uses	[21]
Drying	1221
Electric motors	[23, 24]
Energy storage and conversion	[25-28]
Fiber drying	[29]
Fluidized beds	[10, 301
Food industry	[11, 311
Fuel preparation	[32, 33]
Gas turbines	[34, 35]
Geothermal	[36]
Glass industry	[37, 38]
Heat recovery	[22, 39]
Instrumentation	[40]
Easers	[41]
Nuclear:	
Reactors	[42-45]
Experiments	[46]
Steel making	[47]
Ovens	[48-50]
Permafrost stabilization	[51-53]
Plasma torches	[54]
Recuperators	[55, 56]
Rocket engine cooling	[57]
Space	[58-60]
Stirling engine	[30, 61]
Solar collectors	[62-65]
Thermal drills	[66]
Thermionic applications	[67]
Tropical applications	[68]
Ventilation and air conditioning	[22, 69]
Waste heat recovery	[70-72]

References for Section 3.10.1 *appear at the end of Section 3.10.7.*

© 1983 Hemisphere Publishing Corporation

3.10.2

Circulation and axial heat transfer

D. Chisholm

■ At all points along the length of the heat pipe, at the interface between the vapor and the liquid, the difference in the static pressures of the phases is balanced by the local capillary pressure difference. The equilibrium condition is expressed as

$$p_v - p_l = \frac{2\sigma \cos \alpha}{r} \tag{1}$$

The interface adjusts its location within the wick pore structure such that there is an equilibrium condition; the interface finds the pore radius r, which satisfies Eq. (1).

Figure 1 illustrates the variation of pressure and mass flow rate along the heat pipe and also the associated interfacial distribution. Maximum circulation will occur when there is no pressure difference between the phases at one point (in the case illustrated at the end of the condenser), whereas at the end of the evaporator the liquid interface is at the plane where the pore radius is smallest. The capillary pressure difference over the heat pipe length *is* then

$$\Delta p_\sigma = \frac{2\sigma \cos \alpha}{r_\sigma} \tag{2}$$

If the capillary pressure difference is not zero at the condenser end of the pipe, then the pressure difference created by capillary forces is

$$\Delta p_\sigma = 2\sigma\left(\frac{\cos \alpha_\sigma}{r_\sigma} - \frac{\cos \alpha_c}{r_c}\right) \tag{3}$$

The capillary pressure difference in steady-state operation balances the friction, momentum, and gravitational pressure differences in the phases. This can be expressed simply as

$$-\Delta p_\sigma = \Delta p_v + \Delta p_l \tag{4}$$

Ap indicates a pressure rise in the direction of the flow

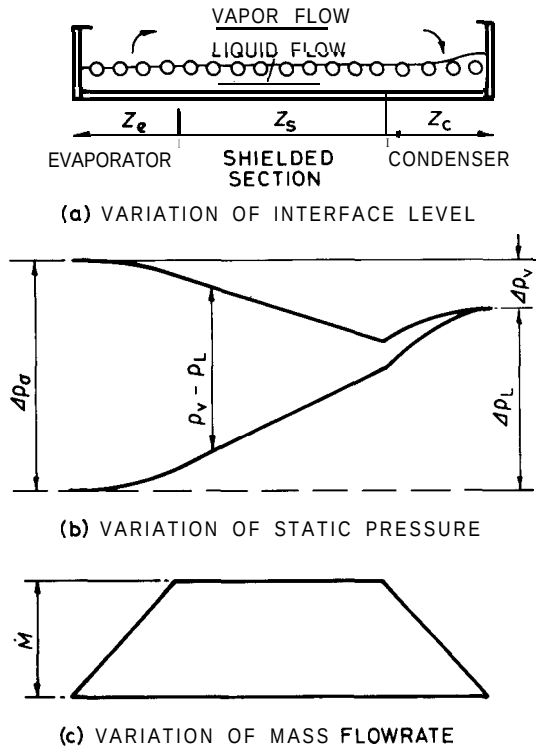

Figure 1 Variation of interface level, static pressure, and mass flow rate along length of heat pipe.

© 1983 Hemisphere Publishing Corporation

HEDH

of the phase (over the total length of the heat pipe unless otherwise indicated).

The static pressure difference in the liquid can be written as

$$\Delta p_l = \Delta p_{fl} + \Delta p_g \tag{5}$$

The pressure difference due to momentum changes can be neglected in the case of the liquid. The pressure difference due to friction during laminar flow in a wick of porous material can be expressed as

$$\Delta p_{fl} = -\frac{\eta_l \dot{M} Z_{\text{eff}}}{\rho_l K A} \tag{6}$$

Because of the small pore size in wicks, the flow is usually laminar. It should be noted that Z_{eff}, the effective length, is used here; this is to allow for the variation in mass flow in both the evaporating and condensing sections (see Fig. 1). On the assumption that the rate of evaporation is uniform in both the evaporating section and the condensing section, it can be shown that the effective length is

$$Z_{\text{eff}} = Z_s + \tfrac{1}{2}(Z_e + Z_c) \tag{7}$$

The pressure difference due to gravity is

$$\Delta p_g = -g \rho_l Z \sin\theta \tag{8}$$

The angle of the tube to the horizontal θ is between 0 and 180 when the liquid is flowing upward, that is, when the evaporator is above the condenser.

From Eqs. (5), (6), and (8),

$$\Delta p_l = -\frac{\eta_l \dot{M} Z_{\text{eff}}}{\rho_l K A} - g \rho_l Z \sin\theta \tag{9}$$

If the pressure drop in the vapor is neglected, then from Eqs. (2), (4), and (9), the maximum circulation is

$$\dot{M} = \frac{\sigma \rho_l \cos\alpha}{\eta_l} \frac{KA}{Z_{\text{eff}}} \left(\frac{2}{r_\sigma} - \frac{g \rho_l Z \sin\theta}{\sigma \cos\alpha} \right) \tag{10}$$

The rate of heat transfer along the heat pipe is

$$Q = \dot{M} \Delta h_v \tag{11}$$

In the absence of gravity and with the usual assumption that there is perfect wetting ($\cos\alpha = 1$), this reduces, using Eq. (10), to

$$Q = 2 \frac{\sigma \rho_l \Delta h_v}{\eta_l} \frac{KA}{r_\sigma Z_{\text{eff}}} \tag{12}$$

It should be noted that the first group on the right-hand side is a characteristic of the fluid only, whereas the second is a characteristic of the wick. This is relevant to the selection of working fluids and wicks, which is discussed later.

In practice, the capillary pressure difference is obtained frequently by measuring the so-called capillary rise:

$$Z_r = \frac{\Delta p_\sigma}{\rho_l g} \tag{13}$$

This is the height the liquid will rise up the wick, against gravity, in the absence of friction gradient. In terms of capillary rise, Eq. (10) can be written as

$$Q = \frac{g \rho_l^2 \Delta h_v K A}{\eta_l Z_{\text{eff}}} (Z_r - Z \sin 19) \tag{14}$$

and Eq. (12) as

$$Q = \frac{g \rho_l^2 \Delta h_v K A Z_r}{\eta_l Z_{\text{eff}}} \tag{15}$$

Figure 2 has been constructed for the case where $\Delta p_{lc} > -\Delta p_{vc}$, that is, where the pressure recovery in the vapor flow direction is less than the pressure drop in the liquid flow direction in the condenser.

If $\Delta p_{vc} > -\Delta p_{lc}$ and the point of zero coverage of the interface occurred at the end of the condenser, the pressure distribution would be as shown in Fig. 2*a*. At the vapor entrance to the condensing section, p_l is greater than p_v, hence at that point it would be necessary for a convex surface to occur as shown in Fig. 2*a*. This will not occur under normal wetting conditions of the surface, and the equilibrium distribution will be

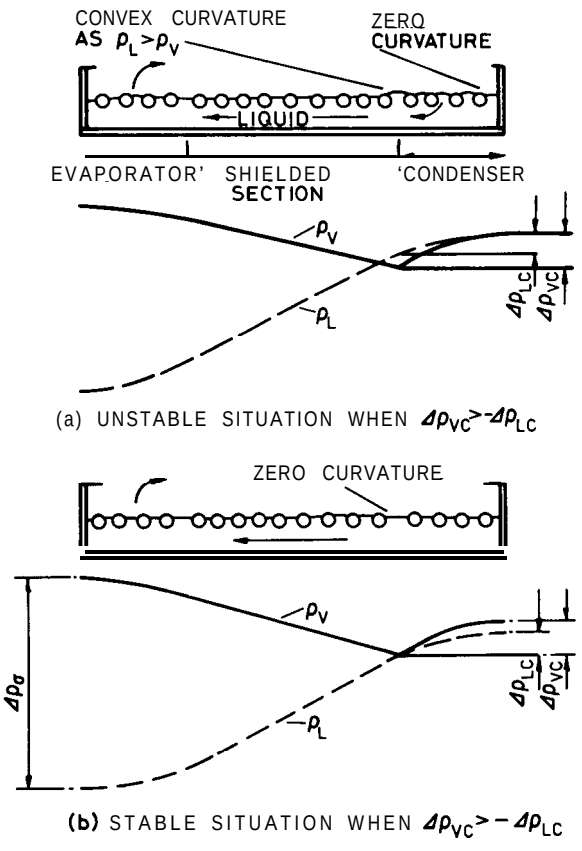

Figure 2 Variation of static pressure and interface level when $\Delta p_{vc} > -\Delta p_{lc}$

© 1983 Hemisphere Publishing Corporation

[73] as shown in Fig. 2b. In this case the capillary pressure difference balances the pressure drops in the evaporator and shielded section; other things being equal, the circulation will be greater in this case.

Table 1 gives references to more detailed calculation procedures.

Table 1 Index to references

Topic	References
1. Introduction	
Texts and general	[2-4, 74, 75]
2. Circulation and axial heat transfer	
Entrainment of liquid in vapor	[76]
Flooding	177,781
Interfacial shear	179,801
Partially saturated wick	[81]
Supersonic flow	[82]
Two-phase Mach number	1831
Vapor choking	1841
Vapor pressure drop	[85-88]
3. Temperature distributions and radial heat transfer flux	
Condensation	[89, 90]
Dryout	[91, 92]
Effective conductivity of wicks	[93-95]
Evaporation	[84, 96-102]
Nonuniform heating	[103, 104]
Temperature distribution	[105, 106]
4. Axial heat transfer and the operational envelope	
Design of heat pipes	[107-110]
Effect of filling ratio	[111-117]
General	[73, 87, 118-120]
Minimum limits	[121]
Nonsteady state	[122-126]
Operational envelope	[127-129]
Optimization	[117, 130]
Rotation	[131, 132]
5. Selection of working fluid	
Angles of contact	[133]
General	[134, 135]
High temperature	[41, 136, 137]
Low temperature	[133]
Wetting agents	[138]
6. Characteristics of wicks	
Arteries: bubble formation	[139, 140]
general	[141-146]
venting	[147]
Capillary forces	[148, 149]
General	[150-153]
Geometric arrangement	[154, 155]
Graded porosity	[156]
Grooves	[128, 157]
Partial saturation	[81]
Resistance to liquid flow	[81, 150, 158-160]
Two-phase arteries	[25, 161-163]
7. start-up	
General	[164-170]
8. Control	
Constant temperature	[5, 71, 171, 172]
Devices	I1731
Diode	[174, 175]
Electrical feedback	[176, 177]
Gas control	[71, 109, 178-184]
General	[185, 186]
Heat pipe heat exchangers	[56, 185]
Thermal switch	[173, 187
Two components	[188, 189]
9. Development, manufacture, and life	
Compatibility	[190-193]
Ceramic heat pipe	[194]
Conformable wall	[195]
Development,	[146, 196]
Explosion	[197]
Flexible	[154]
Gas evolution	[198]
General	[135]
High temperature	[41, 136, 137]
Life	[10, 190, 199, 200]
Low temperature	[133]
Manufacture	[201-204]
Material selection	[9, 27, 191, 205, 206]
10. Related topics	
Heat pipe heat exchangers	[22, 55, 56, 194, 207-209]
Heat recovery	135,721
Inverse thermosiphons	[210, 211]
Jet pump-assisted heat pipes	[212]
Liquid fins	[213]
Osmotic heat pipes	[214, 215]
Photochemical heat pipes	[216]
Rotating heat pipes: general	[131, 217]
low speed	[29]
Thermosiphons	[51, 185, 218, 219]

Nomenclature and References for Section 3. IO.2 appear at the end of Section 3.10. 7.

© 1983 Hemisphere Publishing Corporation

3.10.3

Temper&distributions and radial heat transfer flux

D. Chisholm

■ Figure 1 illustrates diagrammatically the variation of temperature of the fluid as it circulates around the heat pipe. Starting at the end of the condenser and following the direction of flow, the temperature of the liquid at the wall falls until the liquid reaches the exit from the condenser. In the shielded section, the liquid temperature rises as a result of heat transfer from the vapor. In the evaporator, the liquid temperature rises quickly with heat transfer from the wall, until the liquid temperature is above the vapor temperature. As the pressure of the liquid in the evaporator is below that of the vapor, because of capillary forces, the saturation temperature of the liquid is below the vapor saturation temperature; thus in the evaporator the liquid is at a temperature above its saturation temperature. Boiling is suppressed because of surface tension forces on the nucleation sites, provided that the temperature difference over the wick is less than

$$T_{wp} - T_{wv} = \frac{T_v}{\Delta h_v \rho_v}\left(\frac{2\sigma}{r_n} - \frac{2\sigma}{r_e}\right) \quad (1)$$

Following now the vapor flow from the end of the evaporator, the temperature drops along the flow path with falling pressure and heat transfer to the liquid, a small part of the vapor condensing in certain circumstances, until the inlet to the condenser is reached. In the condensing section there can be a slight temperature recovery associated with the pressure rise in the vapor.

As the pressure change along the vapor path is normally small, the temperature gradient in the vapor phase is also normally small in absolute terms (less than 2 K) and also in relation to the temperature differences

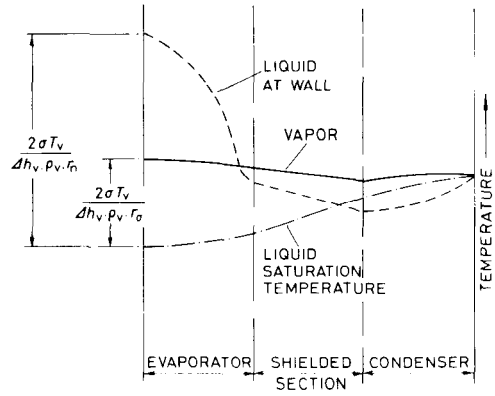

Figure 1 Fluid temperature distribution.

Table I Effective thermal conductivity of wicks[a]

Wick structure	λ_e
Wick and liquid in series	$\frac{\lambda_l \lambda_w}{\epsilon\lambda_w + (1-\epsilon)\lambda_l}$
Wick and liquid in parallel	$\epsilon\lambda_l + (1-\epsilon)\lambda_w$
Wrapped screen	$\frac{\lambda_l[\lambda_l + \lambda_w - (1-\epsilon)(\lambda_l - \lambda_w)]}{(\lambda_l + \lambda_w) + (1-\epsilon)(\lambda_l - \mathrm{A},)}$
Packed spheres	$\frac{\lambda_l[(2\lambda_l + \lambda_w) - 2(1-\epsilon)(\lambda_l - \lambda_w)]}{(2\lambda_l + \mathrm{A},) + (1-\epsilon)(\lambda_l - \lambda_w)}$
Rectangular grooves	$\frac{(w_f \lambda_l \lambda_w \delta + w\lambda_l)(0.185 w_f \lambda_w + \delta\lambda_l)}{(\mathrm{w} + w_f)(0.185 w_f \lambda_f + \delta\lambda_l)}$

Source: Chi[3].

© 1983 Hemisphere Publishing Corporation

that can occur over the wick and wall in both the evaporator and condenser.

The effective thermal conductivity of a number of saturated wick structures is given in Table 1. The radial heat flux in the evaporator is then

$$4 = \lambda_e(T_{wp} - T_{wv}) \tag{2}$$

A similar equation is obtained in the condenser, but with opposite signs. From Eqs. (1) and (2), the maximum heat flux to avoid evaporation in the wick is

$$q = \frac{\lambda_e T_v}{\Delta h_v \rho_v}\left(\frac{2\sigma}{r_n} - \frac{2\sigma}{r_e}\right) \tag{3}$$

In many wick structures this value can be exceeded, the surface of the evaporation receding into the wick, effectively reducing the thickness of the structure. This, however, has the disadvantage of reducing the liquid flow area in the wick, reducing circulation.

Nomenclature and References for Section 3.10.3 appear at the end of Section 3.10. 7.

© 1983 Hemisphere Publishing Corporation

3.10.4

Axial heat transfer and the operational envelope

D. Chisholm

■ The output from a heat pipe can be limited by a number of considerations: The velocity of the vapor cannot exceed the sonic or choking velocities; entrainment of liquid by the vapor must be avoided, or the evaporator will be starved of liquid; boiling in the wick must be avoided; and the final limitation is the rate of circulation of the fluid obtainable. Figure 1 illustrates [108] diagrammatically how these four factors combine to give the operational envelope for a given design of heat pipe. At low pressures the sonic velocity may be the limiting factor as the gas density will be low; this is region l-2 in the diagram. In region 2-3, the heat flow is limited by entrainment. In region 3-4 the restriction on output is due to limitations of the capillary action. In region 4-5 the axial heat flow is limited by the onset of boiling within the wick. In practice the design point is made within region 3-4.

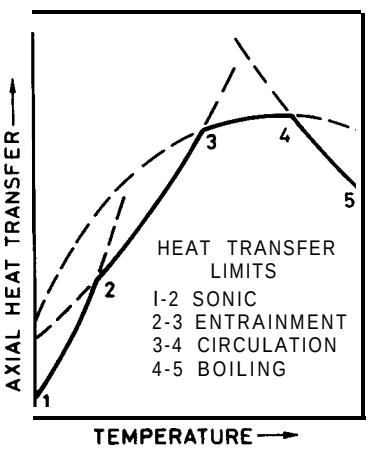

Figure 1 Operational envelope: maximum heat transfer capacity as a function of operating temperature.

References for Section 3.10.4 appear at the end of Section 3. IO. 7.

© 1983 Hemisphere Publishing Corporation

3.10.5

Selection of working fluid

D. Chisholm

■ The working fluid should possess the following properties:

1. High surface tension to provide satisfactory capillary pumping
2. Good wetting characteristics for the same reason
3. Low viscosity to aid pumping
4. High latent heat of vaporization to aid axial heat transfer
5. High thermal conductivity to aid heat transfer between fluid wall and wick
6. Freezing and boiling points compatible with the range of operation
7. High density to reduce flow resistance
8. Compatibility in relation to corrosion with container wall and wick
9. Chemical stability

Equation 3.10.2(12) contains a fluid property group that can be referred to as the liquid transport factor [107], as the higher its value, the higher the circulation rate in the heat pipe. The liquid transport factor

$$N = \frac{\sigma \rho_l \Delta h_v}{\eta_l}$$

$$= \frac{\text{[surface tension] [latent heat per unit volume]}}{\text{dynamic (absolute) viscosity}} \quad (1)$$

Table 1 shows the most commonly used working fluids, their liquid transport factor, and some other relevant features.

©1983 Hemisphere Publishing Corporation

Table 1 Working fluids and relevant characteristics

Normal operating temperature range, °C	Working fluid	Properties at atmospheric pressure: Boiling point, °C	Properties at atmospheric pressure: Liquid transport factor, kW/m²	Suitable material for shell and wick
-200 to -170	Nitrogen	-196	9×10^6	Stainless steel
-70 to +50	Ammonia	-33	1×10^8	Stainless steel, nickel, aluminum
−60 to +40	Freon 12	-30	1×10^7	Stainless steel, copper
-30 to +100	Methanol	65	5×10	Copper
+10 to +200	Water	100	5×10^8	Copper, nickel
190 to 500	Mercury	356	2×10^9	Stainless steel
400 to 800	Potassium	760	5×10^8	Stainless steel
500 to 900	Sodium	883	2×10^9	Stainless steel
900 to 1 500	Lithium	1 330	8×10^9	Tantalum, TZM

Nomenclature and References for Section 3.10.5 appear at the end of Section 3. IO. 7.

© 1983 Hemisphere Publishing Corporation

3.10.6
Characteristics of wicks

D. Chisholm

■ The original wick structures used in heat pipes were materials such as woven cloth, glass fiber, porous metal, and wire mesh. These wicks will be referred to as homogeneous wicks, to distinguish them from wicks made up of combinations of these materials, which will be referred to as composite wicks.

Figure ***la*** illustrates diagrammatically the use of homogeneous wicks. The wick is attached to the wall of the heat pipe in such a manner as to ensure good contact between the wick and the wall in the regions where heat transfer occurs. Good contact helps to maintain satisfactory heat transfer rates from and to the heat pipe wall. Channels in the wall, as illustrated in Fig. lb, have also been used; a further development is to cover the channel with a fine screen as illustrated in Fig. lc. One advantage of this arrangement is that it reduces entrainment of the liquid flowing in the wick by the vapor flowing from the evaporator section of the heat pipe to the condensing section. More important, the screen can be of very small pore size to give high capillary driving pressure without significantly increasing the flow resistance in the channels. Kemme [196] tested the arrangements shown in Figs. lb and lc and found a threefold improvement in the performance of the heat pipe with the latter arrangement.

Some other arrangements of wick are shown in Fig. 1, ***d-h.*** Figure lh is an example of a wick with an artery; the artery provides low-resistance flow paths to reduce the pressure drop in the liquid. Figure 1, e-g, also provides low-resistance flow paths for the liquid.

In Fig. 1, ***e-h,*** the low-resistance flow path or artery is adjacent to the wall, which can have the disadvantage that boiling may occur within it. Figure 2 illustrates in cross-section some arrangements [144] of arterial heat pipes that avoid this problem.

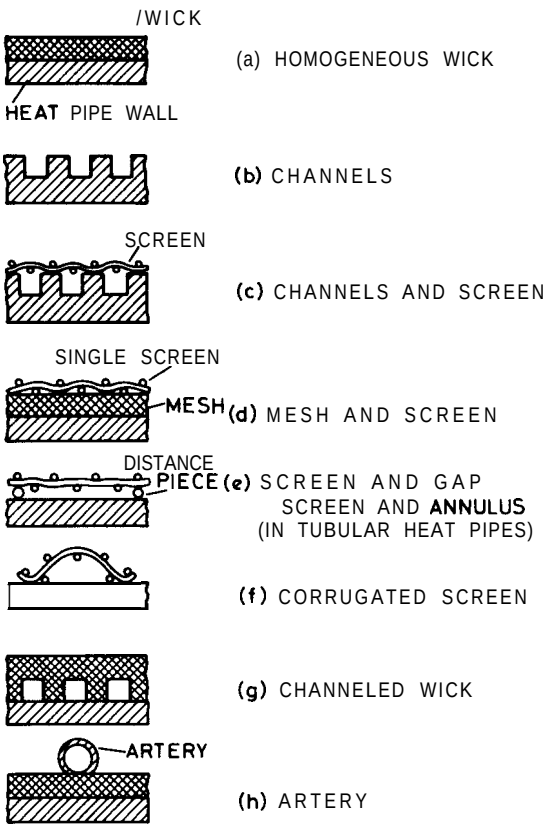

Figure 1 Geometric arrangement of wicks.

Figure 3 illustrates an alternative form [142] of artery. It is important, as is apparent from this figure,

© 1983 Hemisphere Publishing Corporation

that at all points the artery be sealed from the vapor space. In that event the artery can be primed by a number of mechanisms:

1. Capillary forces
2. Condensing the vapor in the artery
3. Raising the pressure in the vapor space by heating, causing the vapor to be compressed in the artery and replaced by liquid, the residue vapor being located by design away from heated surfaces

Any gases in the artery will tend to go into solution [140].

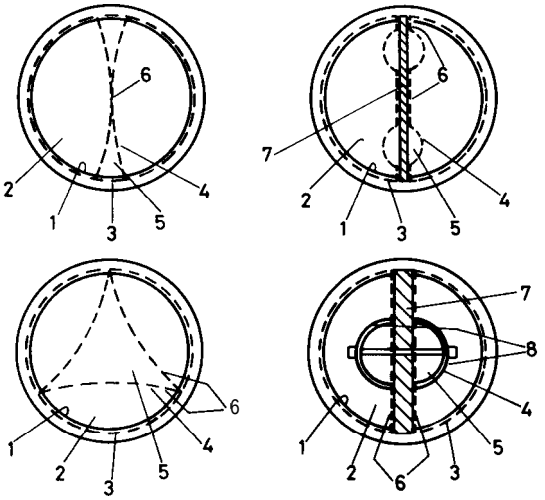

Figure 2 Heat pipes with arteries [144]. Key: 1, internal wall surface; 2, vapor space; 3 grooves; 4, mesh; 5, liquid artery; 6, mesh (cross piece); 7, supporting structure; 8, slit tube (without capillaries).

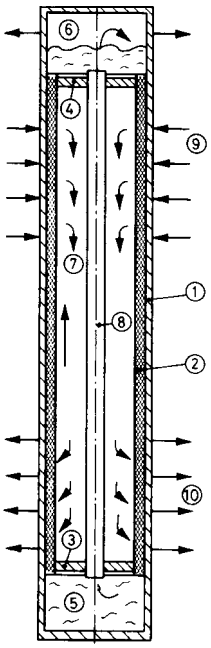

Figure 3 Heat pipe with header and artery system. Key: 1, pipe wall; 2, wick; 3 and 4, header plate; 5 and 6, headers; 7, vapor space; 8, artery; 9, evaporator; 10, condenser.

In Figure 3, the pressure in the artery will be below that of the vapor space. Creating a hole in the artery surface will allow vapor to enter the artery and form a two-phase mixture there. For operation against gravity, this will add natural-circulation driving forces to the capillary forces acting with a single-phase artery [25, 161].

References for Section 3.10.6 *appear at the end of Section 3.10. 7.*

© 1983 Hemisphere Publishing Corporation

3.4 0.7
Start-up and control

D. Chisholm

■ It is important to appreciate that it may not be possible to attain the design point simply by heating the evaporator or cooling the condenser; the heat pipe may not start.

Cotter [165] uses the terms uniform start-up and frontal start-up. In uniform start-up the temperature along the heat pipe is practically uniform during the start-up process; this is obtained where initially the vapor density is not too low.

In frontal start-up there is a considerable temperature variation along the pipe, and it is only gradually that a relatively uniform axial temperature variation is obtained.

When the density of the vapor is initially very low, I it is possible for sonic flow to occur. This will start first at the outlet from the evaporator, or at the outlet from the isothermal length. Cotter s treatment has now been found to be inadequate in the light of work with lithium heat pipes carried out by Sockol and Forman [169]. They present the equations for predicting the rate at which the sonic front will move along the heat pipe to the condenser.

Downstream of the sonic front, supersonic flow may occur, followed by a shock wave.

Sockol and Forman [169] had three thermocouples 13 mm apart along the axis of the condenser. At one moment during start-up there was a 400 K temperature difference between the readings from these thermocouples; presumably at that moment the sonic front was passing the thermocouples.

Dryout may occur during start-up for a number of reasons:

1. Higher heat fluxes can be obtained initially if the temperature differences between source and sink are greater than for steady-state conditions. Circulation may not be adequate for this heat flux.
2. Vaporization may occur in the wick due to high initial temperature differences between wall and vapor.
3. There may be inadequate circulation, hence dryout, due to high pressure drops in the vapor where there is initially a low vapor density.
4. There may be inadequate circulation due to entrainment of the liquid in the vapor associated with the low vapor density and therefore high vapor velocity.
5. There may be inadequate circulation due to the condenser being initially frozen.

Where a heat pipe will not start (i.e., approach a uniform temperature in the vapor), either insulate the condenser from the sink, or heat the condenser. One method of doing the latter is to build into the heat pipe a small-diameter auxiliary heat pipe to transfer heat from the evaporator to the condenser; the auxiliary heat pipe must of course have a different fluid from the principal heat pipe.

A. Control

In addition to its ability to transfer high heat fluxes with small temperature gradients, the heat pipe has the following advantages:

1. As a transformer it allows the heat to be absorbed as a high heat flux (i.e., over small area) and

© 1983 Hemisphere Publishing Corporation

transferred from the heat pipe with a low heat flux (i.e., over a large area).

2. It serves as a control device. By a number of methods it is possible to arrange the device to operate at an approximately constant temperature.

3. It can be arranged to transfer heat only when required (the thermal switch).

4. It can be designed as a heat pipe diode, allowing heat to flow in one direction only.

5. It can be arranged to transmit a maximum power.

6. It can be arranged to have a condenser with two temperature zones (the two-component heat pipe).

One method of control is to use an inert gas in the vapor. As the vapor moves along the condenser, the inert gas is swept before it, accumulating at the end of the condenser, where it blankets off heat transfer. If, for example, the source temperature decreases, the vapor temperature in the heat pipe will also tend to drop. This will cause a fall in the vapor pressure, which will cause the noncondensable gas to expand, reducing the rate of heat transfer from the condenser. Figure 1 illustrates the arrangement; with a suitably sized reservoir of inert gas, an almost constant vapor temperature can be maintained for large variations in axial heat transfer. Units have operated successfully with as much as an eightfold variation in axial heat flux.

The gas-controlled heat pipe is sometimes referred to as the constant-temperature or variable-conductance heat pipe. It has been studied by, among others, Marcus and Fleischman [183]. They show the importance of providing a porous plug at the inlet to the gas reservoir to prevent liquid entering it. They also show the very slow response that can occur following a power surge; the power surge compresses the gas, allowing an excess of vapor to enter the reservoir.

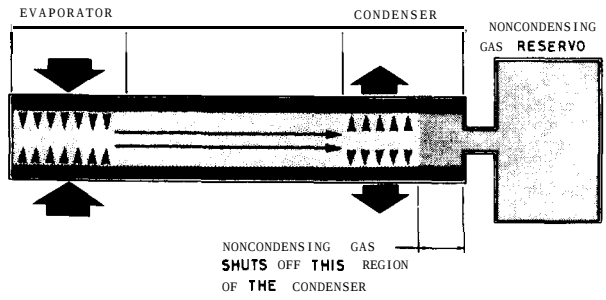

Figure 1 Heat pipe with noncondensable gas control.

Bienert [176] describes feedback-controlled variable conductance heat pipes. This is in effect a heat pipe with a wet gas reservoir, the term wet indicating that there is a liquid present. The reservoir is electrically heated, which varies the partial pressure of the vapor, thus varying also the partial pressure of the gas in the reservoir; this in turn varies the amount of gas in the condenser. Bienert demonstrates the use of the device to obtain a constant source temperature with a varying rate of heat transmission.

Basiulis and Filler [173] and Chisholm [185] describe a variety of methods of controlling heat pipes. Methods particularly suitable for controlling banks of heat pipes are discussed in the latter reference, and also *in* [56].

B. Conclusions

The above is essentially an introduction to the heat pipe. Table 3.10.2(1), is intended to serve as an index to the references, which give access to more detailed information. Finally, remember that the heat pipe is a sealed pressure vessel with no safety valve, and if abused may reach dangerously high pressures [197].

NOMENCLATURE FOR SECTIONS 3.10.2-3.10.7

A	cross section of wick, m^2	Δp_v	total pressure difference in vapor, N/m^2
g	gravitational acceleration, m/s^2	Δp_{vc}	total pressure difference in condenser, N/m^2
Δh_v	latent heat of vaporization, J/kg	Δp_σ	pressure difference due to capillary forces, N/m^2
K	permeability [Eq. 3.10.2(6)], m^2	4	radial heat transfer rate, kW
$\dot{M}$	mass flow or circulation rate, kg/s	Q	axial heat transfer rate, kW
N	liquid transport factor, kW/m^2	r	pore radius, m
p_l	pressure of liquid, N/m^2	r_e	capillary radius in evaporator, m
p_v	pressure of vapor, N/m^2	r_n	radius of nucleation site, m
Δp_{fl}	pressure difference due to friction in liquid, N/m^2	r_σ	minimum capillary radius, m
Δp_g	pressure difference due to gravity, N/m^2	T_v	vapor temperature, K
Δp_l	total pressure difference in liquid, N/m^2	T_{wp}	wick temperature at pipe wall, K
Δp_{lc}	total pressure difference in liquid condenser, N/m^2	T_{wv}	wick temperature at vapor interface, K
		w	groove width, m
		W_f	width of groove fin, m

© 1983 Hemisphere Publishing corporation

Z	length of heat pipe, m
Z_c	length of condenser, m
Z_e	length of evaporator, m
Z_{eff}	effective length of heat pipe, m
Z_r	capillary rise, m
α	contact angle
δ	groove depth, m
ϵ	wick porosity
η_l	dynamic (absolute) viscosity of liquid, N s/m^2
θ	inclination to horizontal, deg
λ_e	effective thermal conductivity of wick, W/m K
λ_f	thermal conductivity of fin, W/m K
λ_l	thermal conductivity of liquid, W/m K
λ_w	thermal conductivity of wick material, W/m K
ρ_l	density of liquid, kg/m^3
ρ_v	density of vapor, kg/m^3
σ	surface tension, N/m

REFERENCES FOR SECTIONS 3.10.1-3.10.7

1. Grover, G. M., Cotter, T. P., and Erikson, G. F., Structures of Very High Thermal Conductance, ***J. Appl. Phys.,*** vol. 35, pp. 1990–1991, 1964.
2. Chisholm, D. The ***Heat Pipe,*** Mills and Boon, London, 197 1.
3. Chi, ***S.*** W. ***Heat Pipe Theory and Practice. A Source Book.*** Hemisphere, Washington, D.C., 1976.
4. Dunn, P. D., and Reay, D. A., ***Heat Pipes,*** 2d ed., Pergamon, Oxford, 1978.
5. Edelstein, F., and Flieger, H., Satellite Battery Temperature Control, ***3d Int. Heat Pipe Conf., Palo Alto, Calif., May 22-24, 1978,*** CP784, Paper 78-448, pp. 360-366, American Institute of Aeronautics and Astronautics, New York, 1978.
6. Osterle, J. F., and McGowan, J. G., The Bionic Relationship Between Transpiration in Vascular Plants and the Heat Pipe, ***Math. Biosci.,*** vol. 14, pp. 317-323.
7. Thiele, F. A. J., and Reay, D. A., Heat Transfer Across the Skin: The Application of Heat Pipe Theory to Predict Resting Sweat Gland Performance. ***2d Znt. Heat Pipe Conf., Bologna, March 31-April*** 2, 1976, Paper I-18, Instituto di Fisica Tecnica, Bologna, Italy, 1976.
8. Firkin, E., Internally Cooled Motion Control System, U.S. Patent 3 481 439, 1969.
9. Ewell, G. J., and Basiulis, A, Heat Pipe Materials Unique Requirements for Coal Gasification Processes. ***Diversity-Technology Explosion, 22d Natl. Symp. and Exhibition, San Diego, Calif., April 26-28, 1977, Proceedings,*** pp. 454-465, Society for the Advancement of Material and Process Engineering, Azusa, Calif., 1977.
10. Mei, J. S., and Keddy, E. S., Heat Pipes for Fluid-Bed Gasification of Coal. Metallurgical Condition of Heat Pipes After Tests in Process Environment, ***11th Intersoc. Energy Conversion Eng. Conf., State Line, Nev., September 12-17, 1976, vol.*** 1, pp. 883-886, American Institute of Chemical Engineers, New York, 1976.
11. Energy Conversions Systems, Inc., Food Container, British Patent 1 275 846, 1972.
12. Basiulis, A., and Dixon, J. C., Heat Pipe Design for Electron Tube Cooling, ASME Paper 69-HT-25, 1969.
13. Graves, J. R., Use of Heat Pipes in Electronic Hardware, NASA-CP-2019, ***Proc. ASPE/MSFC Symp. 'Engineering and Productivity Gains from Space Technology, Huntsville, Ala., May 11-12, 1977,*** pp. 249-255, NASA, Marshall Space Flight Center, Huntsville, Ala., 1977.
14. Haros, J. L., Heat Pipe Cooling of Airborne Phased Array Radar, PAT-APPL-604530/GA, AD-DO01 451/4, filed Aug. 14, 1975, National Technical Information Service, Springfield, Va., 1975.
15. Midwest Research Institute, Heat Pipes, NASACR-250, 1975.
16. Ferrara, A., and Brinkman, P., Applying Heat Pipes to Avoid the Preferential Freezing of Highway Bridge Decks, ASME Paper 76-ENAs-25, 1976.
17. Larkin, B. S., and Dubuc, S., Self-De-Icing Navigation Buoys Using Heat Pipes, ***2d Int. Heat Pipe Conf., Bologna, March 31-April 2, 1976,*** Paper I-1 1, Instituto di Fisica Tecnica, Bologna, Italy, 1976.
18. Suelau, H. J., Kroliczek, E. J., and Brinkman, C. P., Application of Heat Pipes to De-Icing Systems, ***2d Int. Heat Pipe Conf., Bologna, March 31-April 2,*** 1976, Paper I-IO, Instituto di Fisica Tecnica, Bologna, Italy, 1976.
19. Hahn, D. R., Cooling Aluminium Molds Using Heat Pipes. Final Report, BDX-613-2039, Contract EY-76-C-04-0613, Bendix Corporation, Kansas City, Mo., Dec. 1978.
20. Reay, D. A., The Use of Heat Pipes in Pressure Die-Casting. ***3d Int. Heat Pipe Conf., Palo Alto, Calif., May 22-24, 1978,*** CP784, Paper 78-401, pp. 434-439, American Institute of Aeronautics and Astronautics, New York, 1978.
21. Brown, A., and Morris, K. J., Heat Pipes for Domestic Use, ***1st Int. Heat Pipe Conf., Stuttgart, October 15-17, 1973,*** Preprint 11-2.
22. Paikert, P., The Heat Pipe in Heat Recovery, Air Conditioning and Drying, ***Rev. Prat. Froid Condit. Air,*** vol. 30, pp. 35-40, 1977 (in French).
23. Groll, M., Krahling, H., and Munzel, W. D., Heat Pipes for Cooling of an Electric Motor, ***3d Int. Heat Pipe Conf., Palo Alto, Calif., May 22-24, 1978,*** CP784, Paper 78-466, pp. 354-359, American Institute of Aeronautics and Astronautics, New York, 1978.
24. Oslejsek, O., and Polasek, F., Cooling of Electrical Machines by Heat Pipes, ***2d Int. Heat Pipe Conf., Bologna, March 31-April 2,*** 1976, Paper I-6, Instituto de Fisica Tecnica, Bologna, Italy, 1976.
25. Basiulis, A., VBP Heat Pipes for Energy Storage, ***11th Intersoc. Energy Conversion Eng. Conf., State Line, Nev., September 12-l 7,*** 1976, vol. 1, pp. 901-904, American Institute of Chemical Engineers, New York, 1976.
26. Hanneman, R. E., Vakil, H., and Wentorf, R. H., Jr., Closed Loop Chemical Systems for Energy Transmission, Conversion and Storage, ***9th Intersoc. Energy Conversion Eng. Conf., San Francisco, Calif., Aug. 26-30, 1974,*** pp. 435–441, American Society of Mechanical Engineers, New York, 1974.
27. Jacobson, D. L., Material Selection Considerations for Fluoride Thermal Energy Storage Containment in a Sodium Heat Pipe Environment. Final Report, June l-August 1976, AFAPL-TR-77-9, Purdue University, Lafayette, Ind., May 1977.

© 1983 Hemisphere Publishing Corporation

28. Yang, W. J., and Lee, C. P., Modelling of a Heat-Pipe-Operated Thermal Storage Device, *ASHRAE Trans.,* vol. 82, pp. 634-643, 1976.
29. Finlay, I. C., Heat Pipes and Two-Phase Thermosiphons, *Chart. Mech. Eng.,* vol. 22, no. 3, pp. 59-63, 1975.
30. Dunn, P. D., Rice, G., and Thring, R. H., Hydraulic and Rotary Drive Stirling Engines with Fluidized Bed Combustion/Heat Pipe System, *10th Intersoc. Energy Conversion Eng. Conf., Newark, Del., August 18-22, 1975,* pp. 942-947. Institute of Electrical and Electronics Engineers, New York, 1975.
31. Elson, C. R., The Heat Pipe and Its Possible Applications in the Food Industry. Scientific and Technical Surveys, No. 89. The British Food Manufacturing Industries, Leatherhead, Surrey, U.K.
32. Harned, J. L., Early Fuel Evaporation Using Heat Pipes, *SAE Fuels and Lubricants/Powerplant Meet., Chase Park Plaza, St. Louis, Mo., June 7-10, 1976,* SAE Paper 760565, Society of Automotive Engineers, Warrendale, Pa., 1976.
33. Harrow, G. A., Mills, W. D., Thomas, A., et al., The Vapipe-A Practical System for Producing Homogeneous Gasoline-Air Mixtures, SAE Paper *760564, SAE Fuels and Lubricants/Powerplant Meet., Chase Park Plaza, St. Louis, Mo., June 7-10, 1976,* Society of Automotive Engineers, Warrendale, Pa., 1976.
34. Edwards, J. P., Liquid and Vapour Cooling System for Gas Turbines, ARC-CP-1127, Her Majesty s Stationery Office, London, 1970.
35. Shchukin, V. K., Mosin, I. I., Lokai, N. V., et al., Study of a Heat Exchanger with Heat Pipes Within the System of a Small-Scale Gas-Turbine Engine, *Aviatsion. Tekh.,* vol. 21, no. 3, pp. 127-132, 1978 (in Russian).
36. Green, J. Salt Domes, Pit Craters, and Dry Steam Fields. Heat Pipe Applications, *Energy Delta: Supply v. Demand; Proc. Energy Symp., San Francisco, Calif., February* 25-27, 1974, pp. 455-487, American Astronautical Society, Tarzana, Calif., 1975.
37. Haye, H. Control of the Temperature of Tools for Glass-Forming Machines, British Patent 1 309 911, 1973.
38. Schubert, K. P., Application of Heat Pipes to the Glass Industry, CZ. *Chem-Tech.,* vol. 3, no. 1, pp. 5-8, 1974 (in German).
39. Ptacek, J. Heat Pipes and Heat Recovery Equipment, *L'Installateur,* vol. 41, pp. 5-8, 1976 (in French).
40. Finlay, I. C., and Green, D. B. Heat Pipes and Their Instrument Applications, *J. Phys. E: Sci. Instrum.,* vol. 9, pp. 1026-1035, 1976.
41. Deverall, J. E., and York, G. W., Sodium Vapour Heat Pipe Laser *Cell, 3d Int. Heat Pipe Conf., Palo Alto, Calif., May 22-24, 1978,* CP784, Paper 78-392, pp. 71-75, American Institute of Aeronautics and Astronautics, New York, 1978 (LA-UR-78-532, Contract W-7405-eng-36, Los Alamos Scientific Laboratory, Los Alamos, N.M., May 22, 1978).
42. Beghi, G., Busse, C. A., Casini, G., et al., A Modular Fusion Reactor Blanket System with Heat Pipes and Helium Cooling, *EURATOM/CEA 7th Symp. Fusion Technology, Grenoble, October* 24-27, 1972, pp. 113-124, EURATOM Centre for Information and Documentation (EUR 4938e), Luxembourg, December 1972.
43. Dunckel, T. L., Emergency Heat Removal System for a Nuclear Reactor, U.S. Patent 3 935 063, 1976.
44. Hitzschke, U., A Study of the Possible Application of Heat Pipes in Steam Generators of Sodium-Cooled Reactors, **EURFNR-1069, KFK-1664,** Nuclear Research Center, Karlsruhe, F.R. Germany, December 1972.
45. Koenig, D. R., and Ranken, W. A., Heat Pipe Nuclear Reactors for Space Applications, *3d Znt. Heat Pipe Conf, Palo Alto, Calif., May* 22-24, 1978, CP784, Paper 78454, pp. 391-397, American Institute of Aeronautics and Astronautics, New York, 1978.
46. Deverall, J. E., and Watson, H. E., Temperature Control of Irradiation Experiments with Gas-Controlled Heat Pipes, Thesis, University of California, Los Alamos, N.M., 1973. *Irradiat. Exp. Fast Reactors, Proc., Amer. Nucl. Soc. Top Meet., 1973,* pp. 267-278, American Nuclear Society, Hinsdale, Ill., 1973.
47. Ando, M. Application of Heat Pipes to Nuclear Steel Making, *Nucl. Eng. Znt.,* vol. 21, pp. 38-39, 1976.
48. Asselman, G. A. A., and Green, D. B., Heat Pipes, *Philips Tech. Rev.,* vol. 33, pp. 104-148, 1973.
49. Finlay, I. C., Cree, D. G., and Blundell, D. J., Performance of a Prototype Isothermal Oven for Use with an X -Band Microwave Noise Standard, *2d Int. Heat Pipe Conf., Bologna, March 31-April 2,* 1976, Paper 1-13, Instituto di Fisica Tecnica, Bologna, Italy, 1976.
50. Stadelmann, M., Gas-Heated Heat Pipe Vacuum Furnace, *Schweiz. Tech.* Z., vol. 71, pp. 40-43, 1974 (in German).
51. Reid, R. L., Tennant, J. S., and Childs, K. W., The Modelling of a Thermosiphon Type Permafrost Protection Device, *J. Heat Transfer,* vol. 97, pp. 382-386, 1975.
52. Vasil ev, L. L., Grakovich, L. P., and Pylilo, L. E., Application of Heat Pipes for Freezing Grounds, *3d Int. Heat Pipe Conf., Palo Alto, Calif., May* 22-24, 1978, CP784, Paper 78-400, pp. 109-113, American Institute of Aeronautics and Astronautics, New York, 1978.
53. Waters, E. D., Heat Pipes for the Trans-Alaska Pipeline, *CNR Proc. 2d Int. Heat Pipe Conf., Bologna, March 31-April 2, 1976,* **ESA-SP-112,** vol. 2, Paper I-19, pp. 803-814, European Space Agency, Paris, 1976.
54. Dyos, T. G., Improvements in or Relating to Heat Pipes in Plasma Torches, British Patent 1 328 576, 1973.
55. Brisbane, T. Are Heat Pipes Under Control? *Process Eng.,* PE Heat Transfer Survey, pp. 70-71, 1976.
56. Q-Dot Corporation, Heat Exchange System, British Patent 1 255 114, 1971.
57. Holmgren, J. S., Stephanou, S. E., and Ward, T. E., Application of Heat Pipe Technology to Rocket Engine *Cooling, American Institute of Aeronautics and Astronautics, Propulsion Joint Specialist Conf., 5th U.S. Air Force Academy, Colorado Springs, Colo., June* 9-13, 1969, AIAA Paper 69-582, American Institute of Aeronautics and Astronautics, New York, 1969.
58. Carter, R. P., Croke, E. J., Norco, J. E., et al., A Heat Pipe Cooled Fast Reactor Space Power Supply, ANL-7422, Contract W-31-109-eng-38, Argonne National Laboratory, Argonne, Ill., June 1968.
59. Chato, J. C., and Hertig, B. A., Physiological and Engineering Study of Advanced Thermoregulatory Systems for Extravehicular Space Suits. Final Report, NASA-CR-130811, ME-FR-400, Illinois University, Urbana, Ill., August 1972.
60. Katzoff, S., Heat Pipes and Vapor Chambers for Thermal Control of Spacecraft, *AIAA Thermophysics Specialist Conf., New Orleans, La., April 17-20,* 1967, Paper 67-310, American Institute of Aeronautics and Astronautics, New York, 1967.
61. Meir, R. J., Prospects of the Stirling Engine for Vehicular Propulsion, *Philips Tech. Rev.,* vol. 31, no. 5/6, pp. 169-186, 1970.
62. Bienert, W. B., and Wolf, D. A., Heat Pipes in Flat Plate Solar Collectors, ASME Paper 76-WA/SOL-12, 1976.

© 1983 Hemisphere Publishing Corporation

63. Ernst, D. M., and Eastman, G. Y., Cost Effective Solar Collectors Using Heat Pipes, *13th Zntersoc. Energy Conversion Eng. Conf., San Diego, Calif., August* 20-25, 1978, vol. 2, pp. 1050-1055, Society of Automotive Engineers, Warrendale, Pa., 1978.
64. Gehrke, G. A Solar House with Heat Pipe Collectors, *Energie-wirtschaftliche Tagesfragen*, vol. 26, pp. 726-728, 1976 (in German).
65. Swet, C. J., A Universal Solar Kitchen, *7th Intersoc. Energy Conversion Eng. Conf., San Diego, Calif., September 25-29, 1972,* pp. 720-726, American Chemical Society, Washington, D.C., 1972.
66. Fisher, H. N., Thermal Analysis of Some Subterrene Penetrators, *J. Heat Transfer,* vol. 98, pp. 485-490, 1976.
67. Ernst, D. M., and Shefsiek, P. K., Heat Pipe Development for Thermionic Applications, *4th Zntersoc. Energy Conversion Eng. Conf., Washington, D.C., September* 22-26, 1969, pp. 879-887, American Institute of Chemical Engineers, New York, 1969.
68. Brossard, L. F., Use of Heat Pipes Under Tropical Climate Conditions, *Cadena Frig. Cubano,* vol. 1, pp. 29-38, 1975 (in Spanish).
69. Richter, W. Using the Heat Pipe in Ventilation and Air Conditioning, *Luft. Kaltetech.,* vol. 13, pp. 197-203, 1977 (in German).
70. Basiulis, A., and Plost, M., Waste Heat Utilization Through the Use of Heat Pipes, ASME Paper 75-WA/HT-48, 1975.
71. Bassani, C., and Loens, J., Precision Temperature Control with Gas Buffered Water Heat Pipes, *3d Znt. Heat Pipe Conf., Palo Alto, Calif., May* 22-24, *1978,* CP784, Paper 78-4-14, pp. 162-166, American Institute of Aeronautics and Astronautics, New York, 1978.
72. Bernier, J., Optimization of Heat Recovery from Exhaust Air by a Multi-stage Heat Pump Combined with a Heat Pipe, *Rev. Prat. Froid Condit. Air,* vol. 29, pp. 43-47, 1976 (in French).
73. Bohdansky, J., Strub, H., and Van Andel, E., Heat Transfer Measurements Using a Sodium Heat Pipe Working at Low Vapour Pressure, *IEE-Thermionic Conversion Specialist Conf., Houston, Tex., November 3-4, 1966,* pp. 144-188.
74. Duminil, M., Heat Pipes, *Rev. Gen. Froid,* vol. 68, pp. 119-133, 1977 (in French).
75. National Engineering Laboratory, Fluids Group, Applied Heat Transfer Division, The Heat Pipe Forum, Papers Presented at a Meeting at NEL, March 18, 1975, NEL Rept. 607, National Engineering Laboratory, East Kilbride, Glasgow, 1976.
76. Tien, C. L., and Chung, K. S., Entrainment Limits in Heat Pipes, *3d Int. Heat Pipe Conf., Palo Alto, Calif., May 22-24, 1978,* CP784, Paper 78-382, pp. 36-40, American Institute of Aeronautics and Astronautics, New York, 1978.
77. Ewald, R., and Perroud, P., The Flooding Phenomenon in a Cryogenic Heat Pipe with Vertical Countercurrent Two-Phase Flow, *Proc. 3d Int. Cryo. Eng. Conf.,* 1970, pp. 136-139.
78. Sakhuja, R. K., Flooding Constraint in Wickless Heat Pipes-Axial Heat Flux Limitations, ASME Paper 73-WA/HT-7, 1973.
79. Feldman, K. T., Jr., and Thupvongsa, C., Investigation of Counterflow Shear Effects in Heat Pipes, AIAA Paper 77-749, *12th Thermophysics Conf., Albuquerque, N.M., June* 27-29, 1977, AIAA Paper 77-749, American Institute of Aeronautics and Astronautics, New York, 1977.
80. Hufschmidt, W., Burck, E., DiCola, G., et al., The Shearing Effect of Vapour Flow on Laminar Liquid Flow in Capillaries of Heat Pipes, *Wärme Stoffubertrag,* vol. 2, pp. 222-229, 1969 (in German).
81. Eninger, J. E., and Marcus, B. D., Capillary Flow Through Partially Saturated Fibrous Wicks. Final report, TRW-21160-6005-RU-00, Contract N00019-72-C-0340, TRW Systems Group, Redondo Beach, Calif., June 15, 1973 (AD 763 427).
82. Bystrov, P. I., and Popov, A. N., The Supersonic Flow of Vapour in the Condensation Zone of High Temperature Heat Pipes, *3d Int. Heat Pipe Conf., Palo Alto, Calif., May* 22-24, 1978, CP784, Paper 78-379, pp. 21-26, American Institute of Aeronautics and Astronautics, New York, 1978.
83. Bursik, J. W., Two-Phase Mach Numbers in Heat Pipe Analysis, *AIAA J., vol.* 11, p. 781, 1973.
84. Ivanovsky, M. N., Prosvetov, V. V., Sorokin, V. P., et al., Evaporation and Sonic Limits in Sodium Heat Pipes, *Inzh.-Fiz. Zh.,* vol. 33, pp. 832-837, 1977 (in Russian).
85. Bankston, C. A., and Smith, H. J., Vapour Flow in Cylindrical Heat Pipes, *J. Heat Transfer,* vol. 95, pp. 371-376, 1973.
86. Kemme, J. E., Vapor Flow Considerations in Conventional and Gravity-Assist Heat Pipes, *2d Znt. Heat Pipe Conf., Bologna, March 31-April 2,* 1976, Paper A-2, Instituto de Fisica Tecnica, Bologna, Italy, 1976.
87. Shevchuk, E. N., and Chistophanova, N. V., Investigation of the Flow and the Temperature Distribution in the Vapour Duct of a High-Temperature Heat Pipe, *Teplofiz. i. Teplotekh.,* no. 32, pp. 75-81, 1977 (in Russian).
88. Tien, C. L., and Rohani, A. R., Analysis of the Effects of Vapour Pressure Drop on Heat Pipe Performance, *Int. J. Heat Mass Transfer,* vol. 17, pp. 61-67, 1974.
89. Annand, D. K., Dybbs, A. Z., and Jenkins, R. E., Effects of Condenser Parameters on Heat Pipe Performance, *J. Spacecraft Rockets,* vol. 4, pp. 695-696, 1976.
90. Kamotani, Y., Analysis of Axially Grooved Heat-Pipe Condensers, *Prog. Astronaut. Aeronaut.,* vol. 56, pp. 37-55, 1977.
91. Busse, C. A., and Kemme, J. E., The Dry-out Limits of Gravity-Assist Heat Pipes with Capillary Flow, *3d Int. Heat Pipe Conf., Palo Alto, Calif., May* 22-24, *1978,* CP784, Paper 78-383, pp. 41-48, American Institute of Aeronautics and Astronautics, New York, 1978.
92. Chun, K. R. Some Experiments on Screen Wick Dry-out Limits, *J. Heat Transfer, vol. 94(C),* pp. 46-5 1, 1972.
93. Semena, M. G., and Zaripov, V. K., Influence of the Diameter and Length of Fibres on Material Heat Transfer of Metal-Fibre Wicks of Heat Pipes, *Thermal Eng.,* vol. 24, no. 4, pp. 69-72, 1977.
94. Singh, B. S., Dybbs, A., and Lyman, F. A., Experimental Study of the Effective Thermal Conductivity of Liquid Saturated Sintered Fibre Metal Wicks, *Znt. J. Heat Mass Transfer,* vol. 16, pp. 145-155, 1973.
95. Van Sant, J. H., and Malet, J. R., Thermal Conductivity of Some Heat Pipe Wicks, *Lett. Heat Mass Transfer,* vol. 2, pp. 199-206, 1975.
96. Abhat, A., and Seban, R. A., Boiling and Evaporation from Heat Pipe Wicks with Water and Acetone, *J. Heat Transfer,* vol. 96, pp. 331-337, 1974.
97. Alleavitch, J., and Ferrell, J. K., Vaporization Heat Transfer in Capillary Wick Structures, *Chem. Eng. Prog., Symp. Ser.,* no. 102, pp. 82-91, 1970.

© 1983 Hemisphere Publishing Corporation

98. Bezrodnyi, M. K., and Alekseenko, D. V., Intensity of Heat Transfer in the Boiling Section of Evaporative Thermosiphons, *Teploenergetiku,* No. 7, pp. 83-85, 1977 (in Russian).
99. Gorman, J. C., and Walmet, G. E., Vaporization from Capillary Wick Structures, ASME Preprint 72-HT-35, 1972.
100. Cornwell, K., Nair, B. G., and Patten, T. D., Observation of Boiling in Porous Media, *Int. J. Heat Mass Transfer, vol.* 19, pp. 236-238, 1976.
101. Davis, W. R., and Ferrell, J. K., Evaporative Heat Transfer of Liquid Potassium in Porous Media, *Prog. Astronaut. Aeronaut.,* vol. 39, pp. 187-199, 1975.
102. Ferrell, J. R., Davis, R., and Winston, H., Vaporization Heat Transfer in Heat Pipe Wick Materials, *1st Int. Heat Pipe Conf., Stuttgart, October 15-1* 7, 1973, Preprint 6-4.
103. Kamenetskii, B. la., Heat-Transfer Characteristics of a Non-uniformly Circumferentially Heated Pipe, *High Temp., vol.* 13, pp. 613-616, 1975.
104. Kamotani, Y., Effects of One-Sided Heat Input and Removal on Axially Grooved Heat Pipe Performance, *15th Aerospace Sciences Meet., 15th, Los Angeles, Calif., January* 24-26, 1977, AIAA Paper 77-191, American Institute of Aeronautics and Astronautics, New York, 1977.
105. Fox, R. D., Carothers, K. G., and Thomson, W. J., Internal Temperature Distributions in an Operational Heat Pipe, vol. 10, pp. 859-860, 1972.
106. Kimura, H., and Kuriyama, Y., Theoretical Study of Heat Pipe-Temperature Distribution Prediction by Finite Element Method, *10th Int. Symp. on Space Technology and Science, Tokyo, September 3-8, 1973,* pp. 587-593, AGNE, Tokyo, 1973.
107. Feldman, K. T., Scott Heat Pipe Analysis, Design and Experiments, Publication 9 068, Scott Engineering Sciences, Pompano Beach, Fla., 1968.
108. Kemme, J. E., Heat Pipe Design Considerations, USAEC Rept. LA-4221, Contract W-7405-eng-36, Los Alamos Scientific Laboratory, University of California, Los Alamos, N.M., August 1, 1969.
109. Shimoji, S., Kimura, H., and Matsushita, T., Prediction of Evaporator Temperature of a Gas Loaded Heat Pipe by the Diffuse Front Model, *3d Int. Heat Pipe Conf., Palo Alto, Calif., May* 22-24, *1978,* CP784, Paper 78-410, pp. 155-161, American Institute of Aeronautics and Astronautics, New York, 1978.
110. Vasil ev, L. L., and Kiselyov, V. G., Simplified Analytical Model of Vertical Arterial Heat Pipes, *Hear Transfer, 1974, Proc. 5th Znt. Heat Transfer Conf., Keidanrenkaikan Building, Tokyo, September 3-7,* 1974, vol. 5, Paper He2.3, pp. 209-213, Japan Society of Mechanical Engineers and Society of Chemical Engineers, Tokyo, 1974.
111. Chi, H. N., and Abhat, A., Performance Evaluation of Gravity-Assisted Copper-Water Heat Pipes with Liquid Overfill, *3d Int. Heat Pipe Conf., Palo Alto, Calif., May* 22-24, 1978, CP784, Paper 78-385, pp. 49-58, American Institute of Aeronautics and Astronautics, New York, 1978.
112. Eninger, J. E., and Edwards, D. K., Excess Liquid in Heat Pipe Vapor Spaces, *12th Thermophysics Conf., Albuquerque, N.M., June* 27-29, 1977, AIAA Paper 77-748, American Institute of Aeronautics and Astronautics, New York, 1977.
113. Ivanovsky, M. N., Sorokin, V. P., and Privezentsev, V. V., Effect of Quantity of Heat Carrier on the Operation of Heat Pipes with Inhomogeneous Capillary Structure in the Absence of Mass Forces, *Teplofiz. Vys. Temp.,* vol. 15, pp. 873-878, 1977 (in Russian). (English tr.: *High Temp.,* vol. 15, pp. 736-741, 1978).
114. Konovalov, A. S., Experimental Study of a Co-Axial Heat Pipe with Excess Liquid, in *Intensif. Protsessov Perenosa Energ. Veshchestva Poristykh Sredakh Nizk. Temp.,* 1975, ed. G. I. Bobrova, S. A. Tanaeva, and V. A. Krivonos, pp. 51-55, USSR: Akad. Nauk B. SSR, Inst. Templo-Massoobmena, Minsk, 1975 (in Russian).
115. Rice, G., and Jennings, J. D., Heat Pipe Filling, *1st Int. Heat Pipe Conf., Stuttgart, October 15-1* 7, 1973, Preprint 3-3.
116. Srivastava, R. M., Varma, H. K., and Sharma, R. C. Deterioration in Heat Pipe Performance with Excess Wetting Fluid, *Lett. Heat Mass Transfer,* vol. 3, pp. 387-402, 1976.
117. Strel tsov, A. I., Theoretical and Experimental Investigation of Optimum Filling for Heat Pipes, *Heat Transfer-Sov. Res.,* vol. 7, pp. 23-27, 1975.
118. Hage, M., Ikepipe-A Programme for the Calculation of Heat Pipes, IKE-5-201, Stuttgart University, Inst. fur Kernenergetik, Stuttgart, July 1976 (in German).
119. Prager, R. C., and Sun, T. H., The Analysis of Heat Transfer with and without Condensation in a Heat Pipe Exchanger, ASME Paper 78-WA/HT-59, 1978.
120. Sun, K. H., and Tien, C. L., Thermal Performance Characteristics of Heat Pipes, *Int. J. Heat Mass Transfer,* vol. 18, pp. 363-380, 1975.
121. Rohani, A. R., and Tien, C. L., Minimum Heat-Flux Limit in Simple and Gas-Loaded Optimal Heat Pipes, *1st Znt. Heat Pipe Conf., Stuttgart, October 15-1* 7, *1973,* Preprint l-3.
122. Ivanovsky, M. N., Ilyin, Yu. A., Korneev, V. I., et al., Investigations of Non-steady State Processes at Cryogenic Heat Pipe Operation, *2d Int. Heat Pipe Conf., Bologna, March 31-April 2,* 1976, Paper D-l, Instituto di Fisica Tecnica, Bologna, Italy, 1976.
123. Nestler, J., and Tzivelekas, I., Stationary and Dynamic Behaviour of Heat Pipes, *Wissenschaft. Ber. AEG-Telefunken,* vol. 51, pp. 25-29, 1978 (in German).
124. Oshima, K., Transient Flow Phenomena Observed in Heat Pipes, *14th Congr. Int. Union Theor. Appl. Mech., Delft, August 30-September 4, 19 76.*
125. Rajakumar, A., and Krishnaswamy, P. R., Experimental Frequency Domain Dynamics of Heat Pipes, *Int. J. Heat Mass Transfer,* vol. 21, pp. 1333-1340, 1978.
126. Rice, G., and Azad, E., Dynamic Characteristics of Heat Pipes, *2d Int. Heat Pipe Conf., Bologna, March 31-April 2,* 1976, Paper D-4, Instituto di Fisica Tecnica, Bologna, Italy, 1976.
127. Busse, C. A., Theory of the Ultimate Heat Transfer Limit of Cylindrical Heat Pipes, *Int. J. Heat Mass Transfer, vol.* 16, pp. 169-186, 1973.
128. Feldman, K. T., Investigation of Performance Limits in Axial Groove Heat Pipes, NASA-CR-137912: UNM-TR-ME-70 (76)NASA-365-1, July 1976, N77-13340.

© 1983 Hemisphere Publishing Corporation

129. Mojtabi, A., Limiting Axial Power of Vertical Gravity-Assisted Water-Filled Heat Pipes, ***Lett. Heat Mass Transfer,*** vol. 5, pp. 141-148, 1978 (in French, English abstract).
130. Cotter, T. P., and Frank, T. G., Optimal Heat Pipes, ***1st Int. Heat Pipe Conf., Stuttgart, October 15-17, 1973,*** Preprint l-l.
131. Daniels, T. C., and Al-Baharnah, N. S., Temperature and Heat Load Distribution in Rotating Heat Pipes, ***3d Int. Heat Pipe Conf., Palo Alto, Calif., May 22-24, 1978,*** CP784, Paper 78-416, pp. 170-176, American Institute of Aeronautics and Astronautics, New York, 1978.
132. Hwangbo, H., Eby, R. J., and Rovinski, R. S., Performance of Heat Pipe Rotating About the Vertical Axis and Its Application to a Spinning Spacecraft, ***2d Int. Heat Pipe Conf., Bologna, March 31-April 2, 1976,*** Paper F-4, Instituto di Fisica Tecnica, Bologna, Italy, 1976.
133. Semena, M. G., Kostornov, A. G., Gershuni, A. N., et al., Investigation of the Angles of Contact of Wicks in Low-Temperature Heat Pipes, ***Inzh.-Fiz. Zh.,*** vol. 28, pp. 217-222, 1975 (in Russian).
134. Reale, F., Wetting and Surface Properties of Refrigerants to Be Used in Heat Pipes, ***2d Int. Heat Pipe Conf., Bologna, March 31-April 2, 1976,*** Paper G-2, Instituto di Fisica Tecnica, Bologna, Italy, 1976.
135. Saaski, E. W., and Tower, L., Two-phase Working Fluids for the Temperature Range 100-350°C, ***12th Thermophysics Conf., Albuquerque, N.M., June 27-29, 1977,*** AIAA Paper 77-753, American Institute of Aeronautics and Astronautics, New York, 1977.
136. Busse, C. A., Geiger, F., Strub, H., et al., High Temperature Lithium Heat Pipes, ***Proc. 2d Int. Conf. on Thermionic Electrical Power Generation, Stresa, Italy, May 1968,*** pp. 495-506, EURATOM Centre for Information and Documentation (EUR No. 4210 f,e), Luxembourg, 1969.
137. Deverall, J. E., Mercury as a Heat Pipe Fluid, ***Space Systems and Thermal Technology for the 70s, Proc. ASME Space Technology and Heat Transfer Conf., Los Angeles, June*** 21-24, ***1970,*** pt. 2, American Society of Mechanical Engineers, New York, 1970.
138. Brown, Boveri, and Cie Aktiengesellschaft, Heat Pipe (Wetting Agent), British Patent 1 281 272, 1972.
139. Abhat, A., Groll, M., and Hage, M., Bubble Formation in Arteries of Gas-Controlled Heat Pipes, ***Prog. Astronaut. Aeronaut., vol.*** 49, pp. 461-483, 1976.
140. Saaski, E. W., Arterial Gas Occlusions in Operating Heat Pipes, ***10th Thermophysics Conf.***, Denver, Colo., May 27-29, 1975, AIAA Paper 75-657, American Institute of Aeronautics and Astronautics, New York, 1975.
141. Chaikovsky, V., Smirnov, G., Burdo, O., et al., Complex Investigation of Characteristics and Processes in Artery-Grooved Heat Pipes, ***3d Int. Heat Pipe Conf., Palo Alto, Calif., May*** 22-24. 1978, CP784, Paper 78-460, pp. 426-433, American Institute of Aeronautics and Astronautics, New York, 1978.
142. Chisholm, D., Heat Pipes with Header and Artery Systems, ***Int. J. Heat Mass Transfer,*** vol. 21, pp. 1207-1212, 1978.
143. Dolgirev, Yu. E., Gerasimov, Yu. F., Maidanik, Yu. F., et al., Design Calculation of a Heat Pipe with Separate Channels for Steam and Liquid, ***Inzh.-Fiz. Zh.,*** vol. 34, pp. 988-993 (in Russian). (English tr., ***J. Eng. Phys., vol. 34,*** pp. 661-665, 1978.)
144. Junkers-Flugzeug-und Motorenwerke GmbH, Apparatus for the Conduction or Exchange of Heat, British Patent 1 275 946, 1972.
145. National Engineering Laboratory, Fluids Group, Applied Heat Transfer Division, The Heat Pipe, Papers presented at a meeting at NEL, November 25, 1970, NEL Rept. No. 491, National Engineering Laboratory, East Kilbride, Glasgow, 1971.
146. Savage, C. J., Development of Artery Heat Pipes in Europe Under ESA Sponsorship, ***2d Int. Heat Pipe Conf., Bologna, March 31-April 2,*** 1976, Paper G6, Instituto di Fisica Tecnica, Bologna, Italy, 1976.
147. Eninger, J. E., Priming Foils for Venting Non-condensable Gas from Heat-Pipe Arteries, ***Prog. Astronaut. Aeronaut.,*** vol. 39, pp. 235-243, 1975.
148. Uhlemann, H., Marks, C. J. A. Th., and Spigt, C. L., Capillary Pressure in Screen Wick Structures, ***1st Int. Heat Pipe Conf., Stuttgart, October 15-17*** 7, 1973. Preprint 6-2.
149. Wayner, P. C., Jr., Effect of Interline Heat Transfer on Meniscus Profile and Capillary Pressure, ***3d Int. Heat Pipe Conf., Palo Alto, Calif., May*** 22-24, 1978, CP784, Paper 78-403, pp. 123-127, American Institute of Aeronautics and Astronautics, New York, 1978.
150. Birnbrieer, H., and Gammel, G., Measurement of the Effective Capillary Radius and the Permeability of Different Capillary Structures, ***1st Int. Heat Pipe Conf., Stuttgart, October 15-17, 1973,*** Preprint 5-4.
151. Hinderman, J. D., and Phillips, E. C., Determination of Properties of Capillary Media Useful in Heat Pipe Design, ASME Paper 69-HT-18, 1969.
152. Keser, D., Experimental Determination of Properties of Saturated Sintered Wicks, ***1st Int. Heat Pipe Conf., Stuttgart, October 15-17, 1973,*** Preprint 6-l.
153. Matveev, V. M., Filippov, Yu. N., Silaev, A. F., et al., Study of Heat Pipe with Capillary Structure Made from Powered Material, ***Teplofiz. Vys. Temp.,*** vol. 16, pp. 1054-1059 (in Russian).
154. Radio Corporation of America, Flexible Heat Pipe, British Patent 1 322 276, 1973.
155. Saaski, E. W., Investigation of an Inverted Meniscus Heat Pipe Wick Concept, NASA CR-l 37 724, Army Research Centre, Moffet Field, Calif., August 1975.
156. Eninger, J. E., Graded-Porosity Heat Pipe Wicks, AIAA Paper ***76-480, 11th Thermophysics Conf., San Diego, Calif., July 14-16,*** 1976, AIAA Paper 76-480, American Institute of Aeronautics and Astronautics, New York, 1976.
157. Hermann, E., Koch, H., Kreeb, H., et al., Handbook of Grooved Heat Pipes, BMFT-FB-W-76-17, Dornier-System, Friedrichshafen, F. R., December 1976 (in German, English summary).
158. Hoogendoorn, C. J., Nio, S. G., and Hardy, H. J. J., Permeability Studies on Wire Screens and Grooves, ***1st Int. Heat Pipe Conf., Stuttgart, October*** 15-I 7, 1973, Preprint 5-3.
159. Katzoff, S., A Siphon Method of Determining Resistivities of Thin Heat Pipe Wicks, NASA-TP-1304, October 1978.
160. Uhlemann, H., Marks, C. J. A. Th., and Spigt, C. L., Flow Resistance in Screen Wick Structures, ***1st Int. Heat Pipe Conf., Stuttgart, October 15-17, 1973,*** Preprint 6-3.
161. Chisholm, D., Heat Pipes with Headers and Single and Two-phase Artery Systems, NEL Rept. 656, National Engineering Laboratory, East Kilbride, Glasgow, 1978.

© 1983 Hemisphere publishing Corporation

162. Roberts, C. C., Jr., A Zero g Variable Conductance Heat Pipe Using Bubble Pump Injection, 12th *Thermophysics Conf., Albuquerque, N.M., June 27-29, 1977,* AIAA Paper 77-752, American Institute of Aeronautics and Astronautics, New York, 1977.

163. Vasil ev, L. L., Heat Pipes and Their Use in Technology, *Inzh.-Fiz. Zh.,* vol. 31, pp. 905-930, 1976 (in Russian). (English tr., *J. Eng. Phys., vol.* 31, pp. 1356-1375, 1976.)

164. Brost, O., Krahling, H., and Maier, R., Theoretical and Experimental Investigation of the Start-up Behaviour of Alkali-Metal Heat Pipes, *2d Int. Heat Pipe Conf., Bologna, March 31-April 2, 1976,* abstract only, pp. 54-55, Instituto di Fisica Tecnica, Bologna, Italy, 1976.

165. Cotter, T. P., Heat Pipe Start-up Dynamics, USAEC Ref. LA-DC-9026, Conf., -671045-2, Los Alamos Scientific Laboratories, Univ. of Calif., Los Alamos, N.M., 1967.

166. Ivanovsky, M. N., Sorokin, V. P., Subbotin, V. I., et al., Some Features of Start-up of Alkali Metal Heat Pipes, *2d Int. Heat Pipe Conf., Bologna, March 31-April 2,* 1976, Paper C-7, Instituto di Fisica Tecnica, Bologna, Italy, 1976.

167. Mironenko, Y. P., Smirnov, G. S., and Gnilichenko, V. I., Experimental and Theoretical Analysis of Water Heat Pipes. Start-up from the Frozen State., *2d Int. Heat Pipe Conf., Bologna, March 31-April 2,1976,* Paper D-2, Instituto di Fisica Tecnica, Bologna, Italy, 1976.

168. Semena, M. G., Baturkin, V. M., and Rassamakin, B. M., Steady and Start-up Characteristics of a Heat Pipe with Wickless Tank, *Inzh.-Fiz. Zh.,* vol. 33, pp. 381-387, 1977 (in Russian). (English tr., *J. Eng. Phys.,* vol. 33, pp. 999-1003, 1978.)

169. Sockol, P. M., and Forman, R., Reexamination of Heat Pipe Start-up, *IEEE-1970 Thermionic Conversion Specialist Conference, Miami Beach, Fla., October* 26-29, 1970, pp. 571-573, American Institute of Electrical and Electronic Engineers, New York, 1970.

170. Tolubinsky, V. I., Shevchuk, E. N., and Stambrovsky, V. D., Study of Liquid-Metal Heat Pipe Characteristics at Start-up and Operation Under Gravitation, *3d Int. Heat* Pipe *Conf., Palo Alto, Calif., May* 22-24, 1978, CP784, Paper 78-434, pp. 274-282, American Institute of Aeronautics and Astronautics, New York, 1978.

171. Shlosinger, A. P., Multi-chamber Controllable Heat Pipe, U.S. Patent 3 543 839, NASA-Case-ARC-10199, 1970.

172. Steele, W. H., and McKee, H. B., A Precise Satellite Thermal Control System Using Cascaded Heat Pipes, *12th Thermophysics Conf., Albuquerque, N.M., June* 27-29, *1977,* AIAA Paper 77-777, American Institute of Aeronautics and Astronautics, New York, 1977.

173. Basiulis, A., and Filler, M., Characteristics of Six Novel Heat Pipes for Thermal Control Applications, ASME Paper 71-AV-29, 1971.

174. Kosson, R. L., Quadrini, J. A., and Kirkpatrick, J., Development of a Blocking Orifice Thermal Diode Heat Pipe, *Prog. Astronaut. Aeronaut.,* vol. 39, pp. 245-258, 1975.

175. Williams, R. J., Investigation of a Cryogenic Thermal Diode, *3d Int. Heat Pipe Conf., Palo Alto, Calif., May 22-24, 1978,* CP784, Paper 78-417, pp. 177-183, American Institute of Aeronautics and Astronautics, New York, 1978.

176. Bienert, W. B., Development of Electrical Feedback Controlled Heat Pipes and the Advanced Thermal Control Flight Experiment, NASA-CR-l 1475 1, DTM-74-2, Contract NASA-6227, Dynatherm Corp., Cockeysville, Md., May 1974.

177. Groll, M., Hage, M., Munzel, W. D., et al., An Electrical Feedback Controlled High Capability Variable Conductance Heat Pipe for Satellite Application, *1st Znt. Heat Pipe Conf., Stuttgart, October 1.5-l* 7, 1973, Preprint 8-l.

178. Barsukov, V. V., Study of Gas-Controlled Heat Pipes with Constant and Variable Volume Containers, *Inzh.-Fiz. Zh.,* vol. 31, pp. 587-593, 1976 (in Russian).

179. Busse, C. A., Labrande, J. P., and Bassani, C., Gas-Controlled Heat Pipe. Temperature-Pressure Transducer, *Inst. Phys. Conf. Ser.,* vol. 26, pp. 428-438, 1975.

180. Casarosa, C., and Latrofa, E., Heat Pipes at the Range of Moderate Temperatures with Gas Presence, *2d Int. Heat Pipe Conf., Bologna, March 31-April 2,* 1976, Paper E-5, Instituto di Fisica Tecnica, Bologna, Italy, 1976.

181. Deverall, J. E., Gas Interface Studies in Large Horizontal Heat Pipes, USAEC Rept. LA-6646-MS, Contract W-7405-eng-36, Los Alamos Scientific Laboratory, Los Alamos, N.M., 1977.

182. Galaktionov, V. V., and Shalia, 0. M., Heat and Mass Transfer at the Region of the Vapor-Gas Front in Gas-Controlled Heat Pipes, *2d Int. Heat Pipe Conf., Bologna, March 31-April 2,1976,* Paper E-6, Instituto di Fisica Tecnica, Bologna, Italy, 1976.

183. Marcus, D. B., and Fleischman, G. L., Steady-State and Transient Performance of Hot Reservoir Gas-Controlled Heat Pipes, ASME Paper 70-HT/SpT-11, 1970.

184. Vasil ev, L. L., Makarov, V. I., and Konovalov, A. S., A Gas Controlled Thermostat, *3d Int. Heat Pipe Conf., Palo Alto, Calif., May* 22-24, *1978,* CP784, Paper 78-415, pp. 167-169, American Institute of Aeronautics and Astronautics, New York, 1978.

185. Chisholm, D., Control of Heat Pipes and Thermosiphons, Heat Pipe Forum, pp. 30-37. NEL Rept. 607, National Engineering Laboratory, East Kilbride, Glasgow, 1976.

186. Westinghouse Electric Corporation, Heat Pipe Amplifier Apparatus (Comprises Two Heat Pipes Employing Working Fluids of Different Vapour Pressures), German Patent 2 832 669, 1979 (in German). (English tr., British Patent 2 001 427.)

187. Altoz, F. E., and Porter, R. F., Thermal Switch, U.S. Patent 3 957 107, 1976.

188. Baum, Ya. M., Sorokin, V. P., and Yurov, S. S., Experimental Study of Specific Features of Heat and Mass Transfer in the Two-Component Low-Temperature Heat Pipe, *Inzh.-Fiz. Zh., vol. 35,* pp. 1034–1043, 1978 (in Russian).

189. Brommer, H. J., Theoretical and Experimental Investigation of Two-Component Heat Pipes, *AIAA and ASME Thermophysics and Heat Transfer Conf., Boston, July 15-1* 7, *1974,* AIAA Paper 74-720, American Institute of Aeronautics and Astronautics, New York, 1974.

190. Basiulis, A., Prager, R. C., and Lamp, T. R., Life Tests and Compatibility of Heat Pipe Materials, *2d Int. Heat Pipe Conf., Bologna, March 31-April 2,* 1976, Paper G5, Instituto di Fisica Tecnica, Bologna, Italy, 1976.

191. Eninger, J. E., Fleischman, G. L., and Luedke, E. E., Heat Pipe Materials Compatibility, NASA-CR-135069: TRW-26148-6004-RU-00, Contract NAS3-19128, TRW Systems Group, Redondo Beach, Calif., January 1976.

© 1983 Hemisphere Publishing Corporation

192. King, P. P., and Waters, E. D., Compatibility Evaluation of an Ammonia-Aluminium-Stainless Steel Heat Pipe, ASME Paper 70-HT/SpT-15, 1970.
193. Munzel, W. D., Compatibility Tests of Various Heat Pipe Working Fluids and Structural Materials at Different Temperatures, *3d Int. Heat Pipe Conf, Palo Alto, Calif., May 22-24,* 1978, CP784, Paper 78-398, pp. 96-101, American Institute of Aeronautics and Astronautics, New York, 1978.
194. Ranken, W. A., Ceramic Heat Pipe Heat Exchangers, LA-6514MS, Contract W-7405-eng-36, Los Alamos Scientific Laboratory, Los Alamos, N.M., September 1976.
195. Rosenbaum, H. M., and Goodacre, J. B., Improvements in or Relating to Heat Pipes, British Patent 1 327 794, 1973.
196. Kemme, J. E., Heat Pipe Capability Experiment, USAEC Ref. LA-3585-MS, Contract W-7405-eng-36, Los Alamos Scientific Laboratory, Los Alamos, N.M., 1966.
197. Moorhouse, W. E., Investigation into the Reasons Causing Explosion in Steam Tubes of Bakers Ovens, *Proc. Inst. Mech. Eng., vol.* 174, pp. 561-574, 1960.
198. Anderson, W. T., Hydrogen Evolution in Nickel-Water Heat Pipes, *8th Thermophysics Conf., Palm Springs, Calif., July 16-18, 1973,* AIAA Paper 73-726, American Institute of Aeronautics and Astronautics, New York, 1973.
199. Kreeb, H., Groll, M., and Zimmermann, P., Life Test Investigations with Low Temperature Heat Pipes, *1st Int. Heat Pipe Conf., Stuttgart, October 15-1* 7, 1973, Preprint 4-1.
200. Munzel, W. D., and Savage, C. J., Life Tests of Artery Heat Pipes for Low Temperature Range, *2d Int. Heat Pipe Conf., Bologna, March 31-April 2, 1976,* Paper G7, Instituto di Fisica Tecnica, Bologna, Italy, 1976.
201. Arcella, F. G., Phillips, E. C., and Sprecace, R. P., Method of Forming a Wick for a Heat Pipe, NASA-Case-NPO-13391-1, U.S. Patent Appl. SK446567, 1974.
202. Kirchner, G., and Cappelletti, C., A Method for Securing a Metal Grid on a Surface of a Metal Plate, British Patent 1 228 103, 1971.
203. Piffl, L., and Scheidegger, R., Method for the Production of Bodies with Capillaries, Swiss Patent 531 050, 1973 (in German).
204. Uhlemann, H., Marks, C. J. A. Th., and Spigt, C. L., Design and Construction of Wick Structures, *1st Znt. Heat Pipe Conf., Stuttgart, October 15-1* 7, 1973, Preprint 5-5.
205. Busse, C. A., Material Problems for High Temperature Heat Pipes, *Forsch. Zngenieurw.,* vol. 37, no. 2, pp. 38-43, 1971 (in German).
206. Pittinato, G. F., Elimination or Control of Material Problems in Water Heat Pipes. Final Report, January 1, 1974-March 31, 1976, MDC-95481-F, NSF/RA-761643, PB-291 467, McDonnell Douglas Astronautics Co., West Huntington Beach, Calif., March 31, 1976.
207. Feldman, K. T., Jr., Simplified Design of Heat Pipe Heat Exchangers, *2d Znt. Heat Pipe Conf., Bologna, March 31-April 2, 1976,* Paper I-2, Instituto di Fisica Tecnica, Bologna, Italy, 1976.
208. Lee, Y., and Bedrossian, A., The Characteristics of Heat Exchangers Using Heat Pipes or Thermosiphons, *Int. J. Heat Mass Transfer,* vol. 21, pp. 221-229, 1978.
209. Wakiyama, Y., Harada, K., Inoue, S., et al., Heat Transfer Characteristics of a Gas-to-Gas Heat Exchanger Using Heat Pipes, *Heat Transfer Jpn. Res.,* vol. 7, pp. 23-29, 1978.
210. Chisholm, D., Grant, I. D. R., and Duncan, P. J., Condenser Operated Inverse Thermosiphons, *6th Int. Heat Transfer Conf., Toronto, August 7-11, 1978,* vol. 3, Paper M-11, pp. 117-122, Hemisphere, Washington, D.C., 1978.
211. Grant, I. D. R., Inverse Thermosiphons, Heat Pipe Forum, NEL Rept. 607, pp. 38-42, National Engineering Laboratory, East Kilbride, Glasgow, 1976.
212. Bienert, W. B., Ducao, A. S., and Trimmer, D. S., Jet Pump Assisted Arterial Heat Pipe, *3d Int. Heat Pipe Conf., Palo Alto, Calif., May* 22-24, *1978,* CP784, Paper 78443, pp. 335-345, American Institute of Aeronautics and Astronautics, New York, 1978.
213. Madejski, J., and Mikielewicy, J., Liquid Fin-A New Device for Heat Transfer Equipment, *Int. J. Heat Mass Transfer,* vol. 14, pp. 357-363, 1971.
214. Doshi, M. R., and Eastman, G. Y., Osmotic Heat Pipe-Problems and Promises, *Lett. Heat Mass Transfer,* vol. 4, pp. 429-436, 1977.
215. Minning, C. P., Fleischman, G. L., and Giants, T. W., Development of an Osmotic Heat Pipe, *3d Int. Heat Pipe Conf., Palo Alto, Calif., May* 22-24, *1978,* CP784, Paper 78-442, pp. 327-334, American Institute of Aeronautics and Astronautics, New York, 1978.
216. Carlsson, B., and Wettermark, G., The Photochemical Heat Pipe, *Sol. Energy, vol.* 21, no. 2, pp. 87-92, 1978.
217. Marto, P. J., and Wagenseil, L. L., Augmenting the Condenser Heat Transfer Performance of Rotating Heat Pipes, *3d Int. Heat Pipe Conf., Palo Alto, Calif., May 22-24, 1978,* CP784, Paper 78-409, pp. 147-154, American Institute of Aeronautics and Astronautics, New York, 1978.
218. Gelperin, N. I., Solopenkov, K. H., and Lianin, V. V., Circulation Velocity of Fluids in Vertical Thermosiphons, *CHISA'75. 5th Int. Cong. of Chem. Eng., Chem. Equipment Design and Automation, Prague, August* 25-29, 1975, Paper E5.8.
219. Japikse, D., Advances in Thermosiphon Technology, *Adv. Heat Transfers,* vol. 9, pp. 1-1 11, 1973.

© 1983 Hemisphere Publishing Corporation

3.11 Furnaces and combustion chambers

Contents

3.11.1 INTRODUCTION, J. S. Truelove **3.11.1-l**

3.11.2 PROCESS HEATERS AND BOILERS, J. S. Truelove **3.11.2-l**

A. Process heaters 3.11.2-1
B. Boilers 3.11.2-2

3.11.3 HEAT TRANSFER IN FURNACES, J. S. Truelove **3.11.3-l**

A. Heat source 3.11.3-l
B. Heat sink 3.11.3-3
C. Refractory surfaces **3.11.3-6**
D. Heat transfer to the sink 3.11.3-6

3.11.4 THE STIRRED-REACTOR FURNACE MODEL. J. S. Truelove **3.11.4-l**

A. Basis of model 3.11.4-1
B. Model formulation 3.11.4-1
C. Sample calculation 3.11.4-S

3.11.5 THE PLUG-FLOW FURNACE MODEL. J. S. Truelove **3.1151**

A. Basis of model 3.11.5-1
B. Model formulation 3.11.5-l
C. Sample calculation 3.11.5-2

3.11.6 THE MULTIZONE FURNACE MODEL, J. S. Truelove **3.11.6-l**

A. Basis of model 3.11.6-1
B. Model formulation 3.11.6-l
C. Sample calculation 3.11.6-3

3.11.7 ADVANCED FURNACE MODELS, J. S. Truelove **3.11.7-1**

A. Basis of model 3.11.7-1
B. Model formulation 3.11.7-l

References for Sections 3.11.1-3.11.7 3.11.7-5

© 1983 Hemisphere Publishing Corporation

HEDH

3.11.1 Introduction

J. S. Truelove

■ A furnace is an insulated chamber in which heat is transferred from a high-temperature source to a sink. The types of furnaces used are numerous and depend on the requirements of the heating process. Sections 3.11.1-3 .1 1.7 are concerned with fuel-fired furnaces, in which the heat is supplied by combustion of a fuel within the furnace chamber and transferred to the sink by a combination of radiative and convective heat transfer processes. The most important applications of fuel-fired furnaces are encountered in petrochemical process heaters and steam-generating boilers.

The design of a furnace and the prediction of its performance still owes as much to art, past experience, and empiricism as it does to sound scientific theory. This situation is a consequence of two related problems: first, the many factors in addition to the heat transfer calculation that must enter into the basic design of a furnace, such as, for example, the permissible heat fluxes, peak-to-mean flux ratios, heat sink arrangement, combustion volume, and burner size and placement; and second, the formidable difficulties of developing a general unified theory for predicting the performance of all furnaces. Nevertheless, a number of theoretical models for furnace calculations have been developed, and it is the purpose of these sections to present some of these and to indicate their application to combustion chamber design.

The material is arranged as follows. A brief description of the types of process heaters and boilers currently in use is given in Sec. 3.11.2. General aspects of heat transfer in furnaces are discussed in Sec. 3.11.3. This is followed by four sections in which various furnace models are described, starting with the simple stirred-reactor model and progressing through to advanced models based on numerical solution of the equations governing a turbulent, chemically reacting flow in a furnace chamber.

© 1983 Hemisphere I blishing Corporation

3.11.2

Process heaters and boilers

A. Process heaters

Process heaters are used in the petrochemical industry to heat petroleum feedstock for fractionation, thermal cracking, and high-temperature processing. The feedstock, or process fluid, flows through tubes within the heater and must receive a specified amount of heat, without local overheating of the fluid or structural components. Operating temperatures within the tubes may be as high as 900°C, and at a combination of pressure and temperature as severe as 20 000 kPa at 450°C. Process heater size is defined in terms of its design heat absorption, or duty. The majority of units fall within the range of 3 to 100 MW, although very large steam hydrocarbon reformers may run to 300 MW. Oil and gas fuels are used exclusively in these heaters.

There are many variations in the layout, design, and detailed construction of process heaters [1, 2]. A typical process heater arrangement is shown in Fig. 1. It consists of a bottom-fired vertical cylindrical furnace chamber, also known as the firebox or radiant section, within which the fuel is burned. The walls, roof, and floor of the chamber are generally constructed from refractory material. The chamber contains heat-absorbing tubes arranged vertically along the walls, which remove a part of the heat from the flame gases before they flow to the convection section. With this arrangement, all the tubes are equidistant from the burners, ensuring good circumferential heat distribution, although the heat flux may vary considerably along the length of the tubes. Heat transfer within the radiant section is principally by radiation, although convection may contribute some 10% or so. Typical peak heat fluxes in the radiant section are about 50 kW/m² of tube surface. The convection section tubes are arranged as a horizontal bank of tubes positioned above the combustion chamber, and they recover additional heat from the furnace gases at a lower temperature level than do the radiant section tubes. In the convection section the principal mode of heat transfer is convection. Fins and other types of extended surface are frequently used

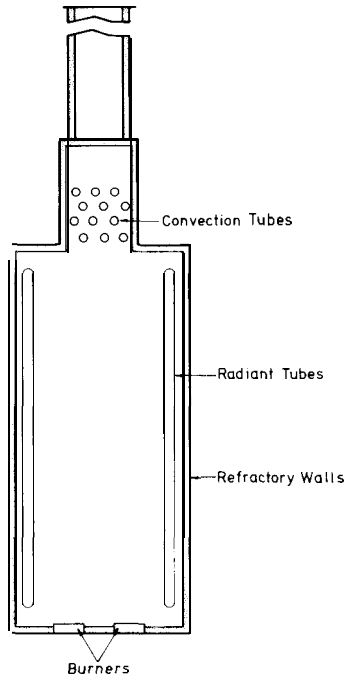

Figure 1 Vertical cylindrical heater with cross-flow convection section.

© 1983 Hemisphere Publishing Corporation

to enhance convective heat transfer. However, the first row or two of tubes in the convection section, known as shock or shield tubes, also receive significant heat by radiation from the radiant section. Extended surfaces are not used on the shock tubes because of the severe effect of radiation on the extremities of the surface extensions. The process heater configuration shown in Fig. 1 provides an economical high-efficiency design, and the majority of new, vertical-tube process heater installations fall into this category. The typical duty range is 3-60 MW.

Another typical arrangement-the horizontal-tube cabin-is shown in Fig. 2. The radiant section tubes are arranged horizontally so as to line the side walls of the combustion chamber and the sloping roof. The convection section tubes are positioned as a horizontal bank of tubes above the combustion chamber. These units are usually fired vertically from the floor, but they can also be fired horizontally by sidewall-mounted burners located below the tubes. This design is economical, of high efficiency, and is used in the majority of new, horizontal-tube process heater installations. Typical duties run from 3 to 60 MW.

A third arrangement-the horizontal-tube double-fired heater-is shown in Fig. 3. The horizontal radiant tubes are arranged in a single row and are fired from both sides to achieve a uniform distribution of heat transfer around the tube circumference. These heaters are normally fired vertically from the floor. The burners may also be arranged to fire against refractory walls so as to enhance radiant heat transfer by wall reradiation.

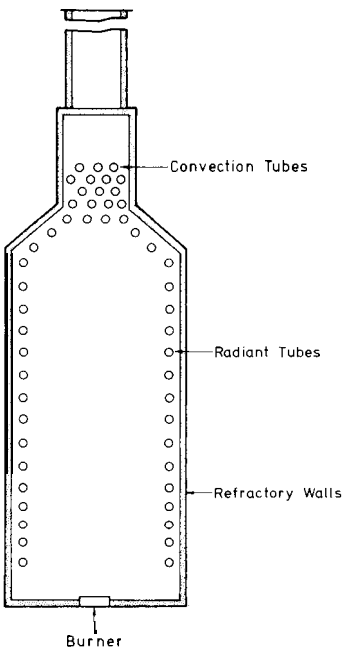

Figure 2 Horizontal-tube cabin heater with top-mounted convection section.

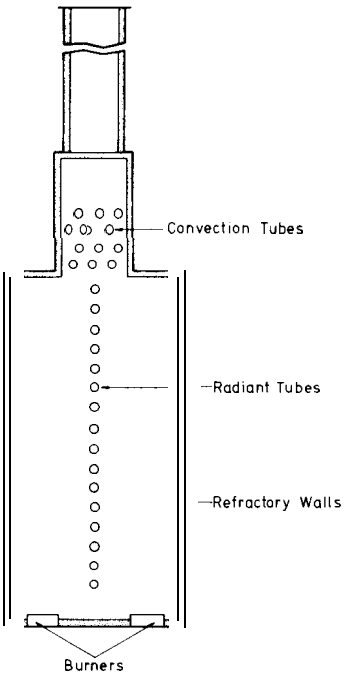

Figure 3 Horizontal-tube, double-fired heater.

These heaters are often chosen for critical reactor-feed heating. A typical duty range in each cell of this design is about 5-15 MW.

B. Boilers

There are two general classes of steam-generating boilers: the fire-tube boiler and the water-tube boiler [3].

Fire-tube boilers are used widely for industrial and commercial steam and hot water generation. Modern fire-tube boilers can produce steam at pressures up to 2 500 kPa and throughputs up to about 8 kg/s. Some boilers are equipped with superheating tubes and thus can be used for small-scale power generation. Fire-tube boilers can be fired on gas, oil, or solid fuel. A typical tire-tube boiler is shown in Fig. 4. It consists of a cylindrical vessel containing tubes that are completely immersed in water and through which hot combustion gases pass. The hot gases are produced in a combustion chamber, or fire tube, which also forms the first pass of the boiler. From the fire tube, the hot combustion gases flow through a reversal chamber and then through small-diameter tubes forming the second pass, and finally through a second bundle of tubes forming the third pass. In some boiler configurations the third pass is not included. The combustion chamber in some boilers consists of two fire tubes. The combustion chamber can also be outside the boiler shell. The principal mode of heat transfer in the tubes is convection. However, in the tire tube, radiative heat transfer is sig-

© 1983 Hemisphere F blishing Corporation

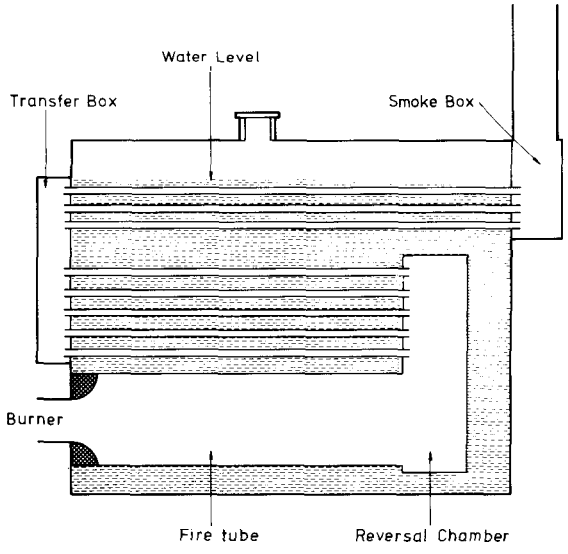

Figure 4 Fire-tube boiler with three passes.

nificant. Peak heat fluxes within the fire tube may be as high as 400 kW/m^2.

Water-tube boilers offer advantages over fire-tube boilers for pressures above 2 000 kPa and throughputs in excess of about 5 kg/s. Water-tube boilers are used in large process plants and power stations for generating high-pressure steam. They may be fired on gas, oil, or solid fuel. A typical power-generation water-tube boiler is shown in Fig. 5. Boiler tubes carrying water cover the entire wall surface of the combustion chamber, forming a so-called water wall. The boiler is fired by burners mounted in rows on the front wall. Heat transfer to the boiler tubes in the combustion chamber is principally by radiation. Further heat transfer is accomplished by arranging the flow of hot combustion gases over a convective superheater tube bank. The combustion gases may also be used to preheat the combustion air, thereby increasing the efficiency of the boiler. Power-generation boilers are generally fired on oil or pulverized coal.

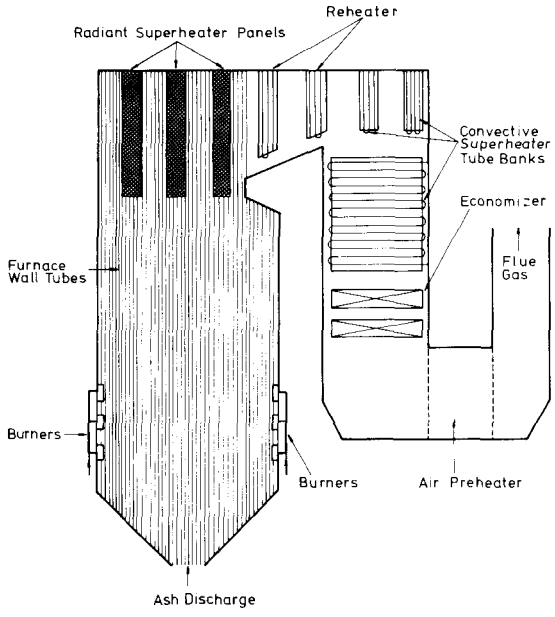

Figure 5 Pulverized coal-fired power-generation water-tube boiler.

References for Section 3.11.2 appear at the end of Section 3.11.7.

© 1983 Hemisphere I blishing Corporation

3.11.3
Heat transfer in furnaces

J. S. Truelove

■ A fuel-fired furnace may be visualized as a gaseous heat source (the flame and furnace gases), a sink, and a refractory enclosure. Heat is transferred to the sink surface by radiation and convection from the furnace gases and radiation from refractory surfaces. The dominant mode of heat transfer is radiation. The roles of the heat source, sink, and refractory in the heat transfer process are described in the following sections.

A. Heat source

The heat to a fuel-fired furnace is provided primarily by the combustion reaction. The heat liberated by the combustion of a unit mass of fuel is given by the heat of reaction, or calorific value, of the fuel. For fuels containing hydrogen, two caloritic values are reported: the gross calorific value, determined by assuming that all the water vapor produced during the combustion process is condensed and cooled to 288 K; and the net calorific value, determined assuming that the water vapor formed during combustion remains in the vapor phase. The source of oxygen for combustion is generally air. An excess of air above the stoichiometric requirement is used to ensure complete combustion of the fuel. Typical excess air requirements are 10% for gaseous fuels, IS-20% for liquid fuels, and 20% or more for pulverized solid fuels. Tables 1 and 2 give the compositions, calorific values, and air requirements for the components of most industrial gaseous fuels, and for typical liquid and solid fuels.

Gaseous fuels generally bum with nonluminous flames, whereas oil fuels can be tired to produce flames of varying degrees of luminosity. Pulverized coal burns with a highly luminous flame due to the presence of hot solid particles suspended in the flame.

The principal sources of radiation from nonluminous flames are the gases carbon dioxide and water vapor, which are present in the furnace gases as products of combustion. The total radiation from a gas mass depends on the temperature and volume of the gas, and the radiative properties of the emitting gas species. For engineering heat transfer purposes, the radiative properties of gases are usually defined in terms of the total emissivity and total absorptivity. These terms are defined in Sec. 2.9.5D. The total emissivity of a gas depends on the gas temperature T_g, the partial pressure-path length product pL, and to a small extent on the total pressure; it is denoted by $\epsilon_g(T_g, pL)$. The total absorptivity depends on the same parameters and in addition the source temperature of the radiation being absorbed, T_s; it is denoted by $\alpha_g(T_g, T_s, pL)$. Total emissivity charts for carbon dioxide and water vapor are given in Sec. 2.9.5D. The total absorptivity may be estimated from the total emissivity as

$$\alpha_g(T_g, T_s, pL) \cong \left(\frac{T_g}{T_s}\right)^m \epsilon_g\left(T_s, pL\left(\frac{T_s}{T_g}\right)^n\right) \qquad (1)$$

where the exponents m and n are empirically determined for each gas. For carbon dioxide, $m = 0.65$ and $n = 1.0$; for water vapor, $m = 0.45$ and $n = 1.0$. When carbon dioxide and water vapor are present together, the total emissivities are additive, although a small correction is necessary to allow for spectral overlap. The same type of correction applies to calculating the

© 1983 Hemisphere Publishing Corporation

Table 1 Properties of selected gaseous fuels[a]

Fuel	Composition (% by volume)												Calorific value, MJ/kg		Combustion air, kg/kg
	co,	N_2	co	H_2	CH_4	C_2H_6	C_3H_8	C_4H_{10}	C_5H_{12}	C_2H_4	C_3H_6	C_4H_8	Gross	Net	
Pure gases															
Carbon monoxide			100										10.10	10.10	2.46
Hydrogen				100									142.0	120.0	34.27
Methane					100								55.48	49.95	17.20
Ethane						100							51.88	47.45	15.90
Propane							100						50.35	46.33	15.25
n-Butane								100					49.55	45.73	14.98
n-Pentane									100				49.02	45.33	15.32
Ethylene										100			50.28	47.11	14.81
Propylene											100		48.91	45.75	14.8 1
Butylene												100	48.46	45.30	14.81
Fuel gases															
North Sea gas	0.2	1.5			94.5	3.0	0.5	0.2	0.1				53.5	48.2	16.6
Gröningen gas	0.9	14.0			81.8	2.7	0.4	0.1	0.1				42.3	38.1	13.1
Synthetic natural gas	2.0		0.1	0.7	95.2		2.0						52.3	47.2	16.2
Commercial propane						1.5	91.0	2.5			5.0		50.3	46.3	15.2
Commercial butane					0.1	0.5	1.2	88.0			4.2		49.6	45.8	15.0
Water gas	4.1	4.5	41.0	49.0	0.8								16.5	15.1	4.0
Blast furnace gas	17.5	56.0	24.0	2.5									2.49	2.45	0.61
Coal gas	4.0	6.6	18.0	49.4	20.0							2.0	30.3	27.2	8.4
Producer gas	5.0	54.5	29.0	11.0	0.5								4.55	4.34	1.12
Lurgi crude gas	25.6	1.8	24.4	31.3	10.3					0.3	0.3		13.1	11.8	3.5
Lean reformer gas	16.7		2.2	46.4	34.1								30.9	27.3	8.9
Rich reformer gas	21.0		1.0	17.0	61.0								30.2	27.1	9.2

[a]Taken from data published by Rose and Cooper [4].

© 1983 Hemisphere Publishing Corporation

Table 2 Properties of selected liquid and solid fuels

Fuel	Composition (% by mass, as fired)							Calorific value, MJ/kg		Combustion air, kg/kg
	C	H	0	S	N	Ash	Moisture	Gross	Net	
Liquids										
Kerosene	85.8	14.1		0.1				46.5	43.5	14.7
Gas oil	86.1	13.2		0.7				45.6	42.8	14.4
Light fuel oil	85.6	11.7	0.1	2.5	0.08	0.02		43.5	41.1	14.0
Medium fuel oil	85.6	11.5	0.15	2.6	0.12	0.03		43.1	40.8	**13.9**
Heavy fuel oil	85.4	11.4	0.2	2.8	0.15	0.05		42.9	40.5	13.8
Methanol	37.5	12.5	50.0					22.1	19.9	6.5
Ethanol	52.2	13.0	34.8					30.2	27.2	**9.1**
Solids (coals)										
Anthracite	*18.2*	2.4	1.5	1.0	0.9	8.0	8.0	29.1	28.9	9.8
Low volatile bituminous	17.4	3.4	2.0	1.0	1.2	8.0	7.0	30.6	29.7	10.1
Medium volatile bituminous	75.8	4.1	2.6	1.2	1.3	8.0	7.0	30.8	29.8	10.2
High volatile bituminous	71.6	4.3	3.8	1.7	1.6	8.0	9.0	29.5	28.4	9.7
Lignite	56.0	4.0	18.4	0.6	1.0	5.0	15.0	21.5	20.2	7.1

[a] Taken from data published by Rose and Cooper [4] and Bell [5].

total absorptivity. Effective use can often be made of the fact that, in the products of combustion, carbon dioxide and water vapor are found in fixed proportions; for example, the partial pressure ratio p_{H_2O}/p_{CO_2} is equal to 1 .O for the products of combustion of $(CH_2)_x$, and 2.0 for products of combustion of CH_4. This range brackets most industrial hydrocarbon fuels, with oils lying at the lower end and gases at the upper end. Figures 1 and 2, constructed on this basis by Hadvig [6] from the data in Hottel and Sarofim s charts[7], give the total emissivity of mixtures with partial pressure ratios of 1 and 2. The use of $(p_{CO_2} + p_{H_2O})L$ as a correlating parameter reduces the effect on the emissivity of departures of the partial pressure ratio from the fixed values of 1 and 2.

The calculation of radiation from luminous flames requires a knowledge of the concentration distribution of soot and other particulates within the flame, and their radiative properties.

When calculations of the total flame emission are to be based on a mean flame temperature and gas emissivity, it is generally sufficient to make an approximate allowance for soot emission by adding 0.05 to the nonluminous emissivity if the flame is bright but not intensely luminous and 0.1 if the flame is quite bright [7]. These small additions reflect the fact that the luminous flame occupies only a small fraction of the total furnace volume. Allowance for radiation by large particulates, such as ash and char, is discussed in [8].

The radiative properties of the furnace gas can be conveniently incorporated into a furnace calculation using the so-called mixed gray gas model [7] The total emissivity and total absorptivity are written as

$$\epsilon_g = \sum_n a_{g,n}(T_g)\,(1 - e^{-k_{a,n}L}) \tag{2}$$

$$\alpha_g = \sum_n a_{s,n}(T_s)\,(1 - e^{-k_{a,n}L}) \tag{3}$$

where $k_{a,n}$ is the absorption coefficient of the nth gray gas component, and $a_{g,n}$ and $a_{s,n}$ are the corresponding weighting factors. The weighting factors and absorption coefficients are determined by fitting Eqs. (2) and (3) to the observed emissivity and absorptivity of the furnace gas over a range of path lengths and temperatures. A clear gas component with $k_a = 0$ is included to represent the nonabsorbing regions, or windows, in the gas absorption spectrum. The weighting factors for the clear gas are determined by the requirement that the weighting factors in each expansion sum to unity. A three-term expansion, or one clear, two gray gas model, is adequate for most applications. In practice, little error is incurred if $a_{s,n}(T_s)$ is taken equal to $a_{g,n}$ evaluated at temperature T_s.

B. Heat sink

The heat sink in most fired heaters is in the form of a single or double row of tubes in front of a refractory wall. This arrangement increases the effectiveness of the tube as an absorber of heat because a greater part of the tube circumference is irradiated. The radiation not intercepted by the tubes passes to the refractory, from which it is reradiated. In general, the heat flux distribution on the tube circumference is not uniform. In the case of a single row of refractory-backed tubes,

© 1983 Hemisphere Publishing Corporation

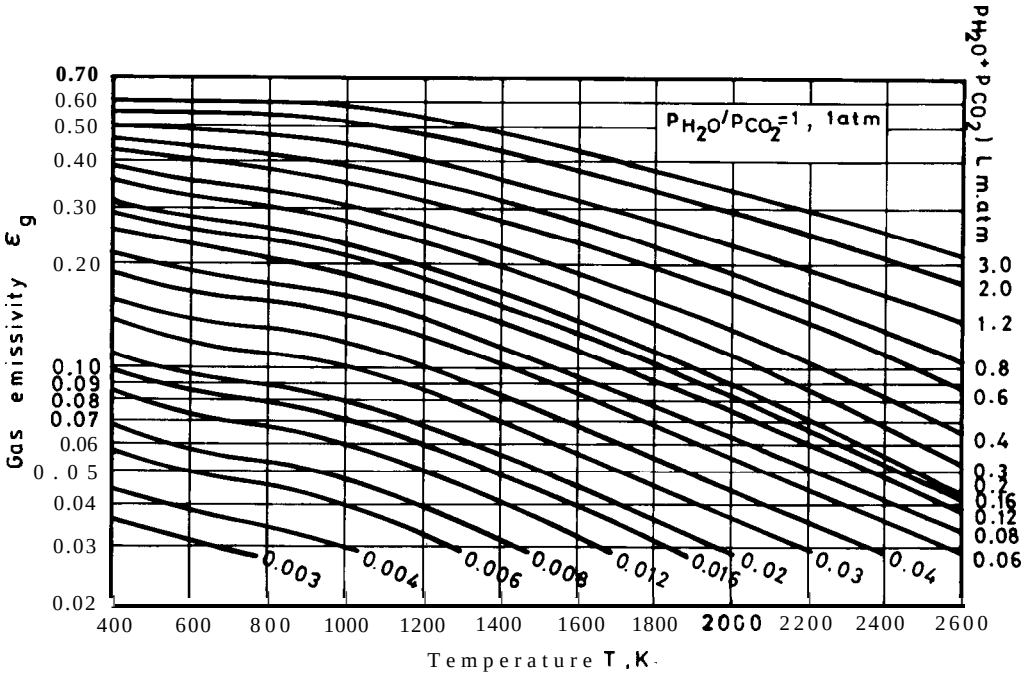

Figure 1 Total emissivity for carbon dioxide and water vapor mixture with $p_{H_2O}/p_{CO_2} = 1$ and a total pressure of 1 atm. Adapted from Hadvig [6].

there will be a peak at the front face of the tube due to direct radiation from the furnace gases, and to a lesser extent at the back face of the tube due to reflection and reradiation from the hot refractory wall. The ratio of peak to mean heat fluxes can be controlled by varying the tube-to-tube spacing, as illustrated in Fig. 3. For a normal tube spacing of about two times the outer diameter, the ratio is about 1.8. As the tube spacing is increased, the ratio approaches unity. In the case of a refractory-backed double row of tubes, the back row

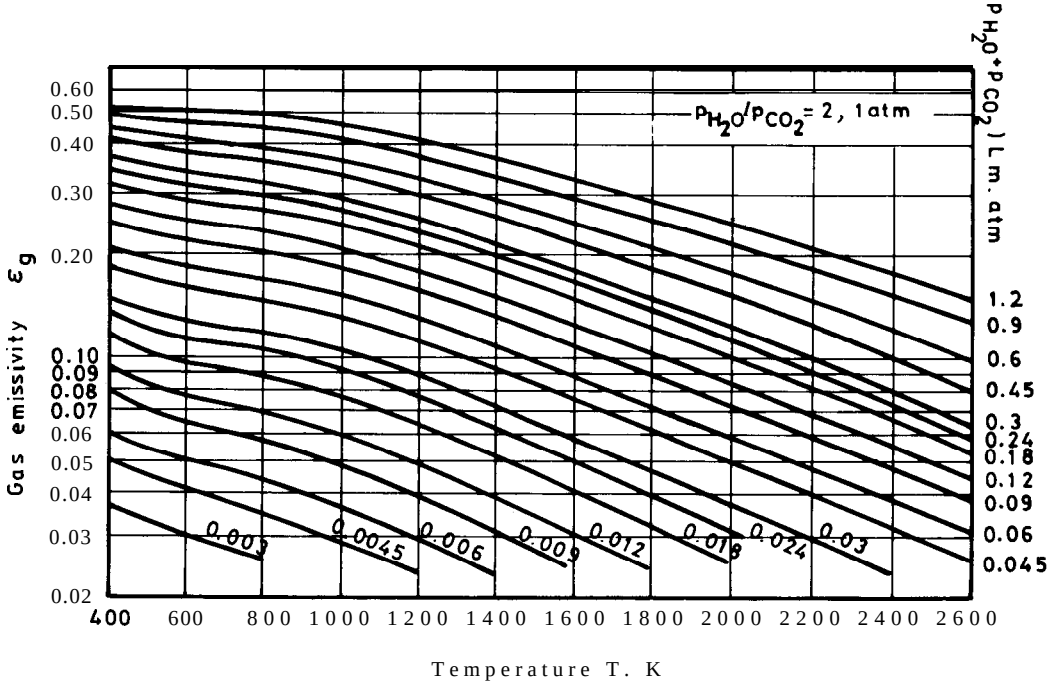

Figure 2 Total emissivity for carbon dioxide and water vapor mixture with $p_{H_2O}/p_{CO_2} = 2$ and a total pressure of 1 atm. Adapted from Hadvig [6].

© 1983 Hemisphere. Publishing Corporation

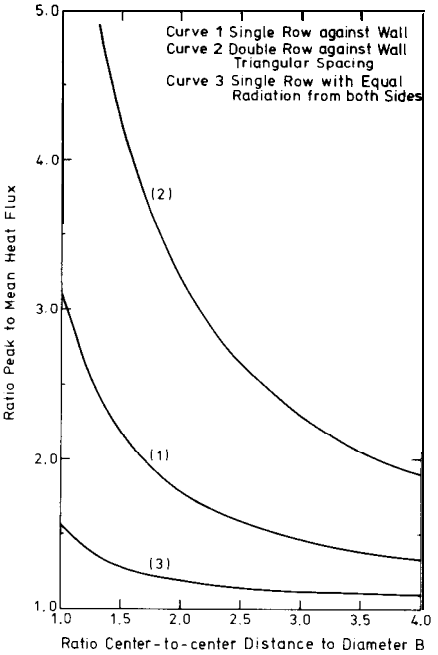

Figure 3 Ratio of peak heat flux to mean heat flux around the tube for various arrangements of (black) tubes.

receives about one-quarter of the total heat transfer. The peak-to-mean (circumferential) flux ratio for both rows of tubes is much worse than for a single row due to the effect of tube shielding.

For the purpose of radiative heat transfer in the furnace chamber, the refractory-backed tubes behave like a plane surface of area equal to the total area of refractory covered by tubes--not just the projected area-as illustrated in Fig. 4. If the refractory is assumed to be radiatively adiabatic, then the effective emissivity of the equivalent plane surface is

$$\epsilon_{\text{eff}} = \frac{1}{[1/F(2-F)] + (B/\pi)[(1/\epsilon_t) - 1]} \qquad (4)$$

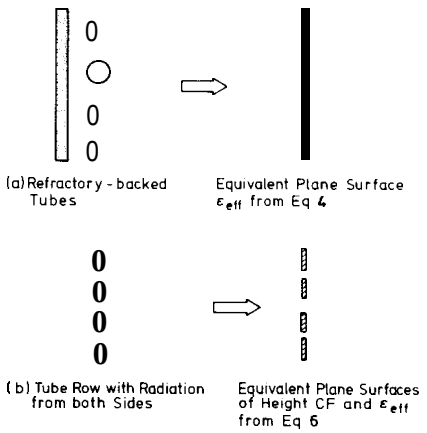

Figure 4 Representation of tubular heat sinks by equivalent plane surfaces.

where B is the ratio of tube center-to-center distance to diameter, F is the fraction of radiation incident on the tube plane that is intercepted by the tubes, and ϵ_t is the true emissivity of the tubes (about 0.85). The effective temperature of the equivalent surface is equal to the true temperature of the tubes. For isotropic radiation incident on a single row of tubes,

$$F = 1 - \frac{1}{B}\left[(B^2-1)^{1/2} - \cos^{-1}\left(\frac{1}{B}\right)\right] \qquad (5)$$

Any deviations from isotropy can almost always be ignored. If the heat sink consists of a double row of tubes, then the only change is the increase in value of the interception factor F. The interception factors for single and double rows of tubes are shown in Fig. 5.

Another common tubular heat sink arrangement is in the form of horizontal tubes mounted in a vertical plane and centered between refractory walls. This arrangement is used for critical applications where a uniform circumferential heat flux is needed. For a typical tube spacing of two times the outer diameter, the ratio of peak to mean heat fluxes is about 1.2. A rigorous treatment of this configuration presents problems. A plausible approach suggested by Hottel [9] is to replace each tube by a plane vertical surface that intercepts the same radiation as would the tube, as illustrated in Fig. 4. The height of each surface is equal to the center-to-center spacing C, multiplied by the interception factor F of Eq. (5). The effective emissivity of the plane surfaces replacing the tubes is greater than the true emissivity of the tube, due to internal reflections in the tube bank, and is given by

$$\epsilon_{\text{eff}} = \frac{1}{1 + (2BF/\pi)[(1/\epsilon_t) - 1]} \qquad (6)$$

If there are several equally spaced tube banks, with

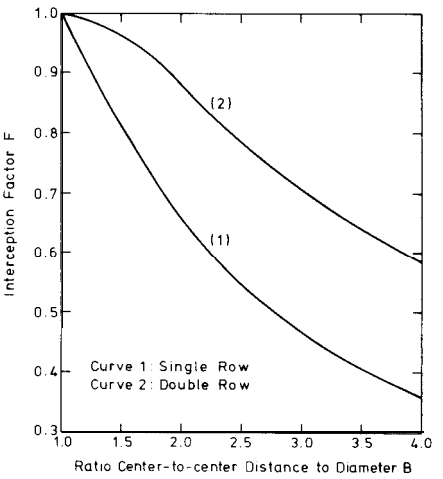

Figure 5 Interception factors for single and double (triangular-spaced) rows of tubes.

© 1983 Hemisphere Publishing Corporation

firing between each pair, then one zone of the system can be reduced to the above case by taking advantage of the fact that a plane of symmetry can be approximately replaced by a surface that reflects diffusely and completely.

Table 3 gives some typical values for the emissivities of sink surfaces.

C. Refractory surfaces

The refractory has an important role in the transfer of heat from the furnace gases to the sink. Some of the radiation from the furnace gases is directed toward refractory surfaces, at which it is reflected or absorbed and reemitted, and some of this radiation is directed toward the sink. A rigorous analysis of the effect of the refractory is complicated by, among other things, the different spectral characteristics of the reflected and reradiated energy. The furnace gases are more transparent to the reradiation than to the reflection, since the spectral characteristics. of the former depend on the characteristics of the refractory, whereas those of the latter are the same as the gas. Thus, a fraction of the radiant energy leaving the refractory surface passes through the windows in the gas absorption spectrum directly to the sink. The net effect of the refractory is to enhance radiation heat transfer from the furnace gases to the sink.

The heat loss through the refractory walls depends on the furnace design-its size, operating temperature, and construction-and is usually between 1% and 10% of the net heat release. Wall losses can be neglected for many furnace types. However, in high-temperature furnaces, particularly those with large areas of refractory, wall losses may become significant.

D. Heat transfer to the sink

From the results of Sec. 2.9.6H, the rate of heat transfer from a gaseous source to a sink surface i by radiation and convection is given by

$$\dot{Q}_i = \sum_j g_{j-i}\sigma(T_j^4 - T_i^4) + \alpha_i A_i(T_k - T_i) \qquad (7)$$

where σ is the Stefan-Boltzmann constant, equal to $5.67 \times 10^{-8}\ \mathrm{W/m^2 K^4}$; T_i is the absolute temperature of the surface i; T_j is the absolute temperature of the surface or volume j; g_{j-i} is the total transfer factor for radiation from j to i; α_i is the convective heat transfer coefficient from the furnace gases to the surface i; A_i is the area of the surface i; and T_k is the temperature of the furnace gases adjacent to the surface i. The j summation runs over all surfaces and volumes within the furnace chamber. The factor g_{j-i} allows for multiple reflections at all surfaces. The convective heat transfer term in Eq. (7) is usually small relative to the radiative heat transfer term.

The calculation of $\dot{Q}_i$ from Eq. (7) is exceedingly complex when the total number of surfaces and volumes is large. Clearly, the application of Eq. (7) to practical furnaces must incorporate simplifications and assumptions. These form the subject of the following sections on furnace models.

Table 3 Normal total emissivities of selected surfaces

Surface	Temperature, °C	Emissivity
A. Metals and their oxides		
Aluminum:		
Polished	100	0.095
Commercial sheet	100	0.09
Heavily oxidized	95-505	0.20-0.31
Iron and steel (not stainless):		
Iron, polished	425-1 02.5	0.14-0.38
Steel, polished	100	0.066
Cast iron, polished	200	0.21
Iron plate, oxidized	20	0.69
Steel, oxidized at 600° C	200-600	0.79
Cast iron, oxidized at 600° C	200-600	0.64-0.78
Cast iron, molten	1 300-l 400	0.29
Mild steel, molten	1600-l 800	0.28
Stainless steels:		
Type 304 (8 Cr; 18 Ni)		
Polished	100	0.074
After heating	215-490	0.44-0.36
After 42 h at 525° C	215-525	0.62-0.73
Type 310 (25 Cr; 20 Ni)		
Oxidized from furnace service	215-525	0.90-0.97
B. Refractories		
Alumina	1 010-l 565	0.50-0.18
Alumina-silica	1010-l 565	0.78-0.43
Brick:		
Red, rough	20	0.93
Building	1000	0.45
Fireclay	1000	0.75
Carbon:		
Graphitized	100-320	0.76-0.75
Graphitized	320-500	0.75-0.71
Thin layer on iron plate	20	0.93
Thick layer	20	0.97
Magnesite refractory brick	1000	0.38
Silica	1010-l 565	0.62-0.33

[a] Taken from data published by Hottel and Sarofii [7].

Nomenclature for Section 3.11.3 appears at the beginning of Part 3. References appear at the end of Section 3.11.7.

© 1983 Hemisphere Publishing Corporation

3.11.4

The stirred-reactor furnace model

J. S. Truelove

■ The simple model to be described in this section is found to make substantially correct predictions of the overall heat transfer performance for a wide range of furnace types. The model is quite general and can therefore be applied, in principle, to any combustion chamber configuration and to all fuels. The generality, relative simplicity, and predictive potential of the model have led to its extensive use for preliminary design of radiant sections of process heaters and boilers. The model may be readily used to estimate the effect on furnace performance of changes in furnace operational variables such as, for example, fuel flow rate, air preheat, and excess air factor.

A. Basis of model

The furnace chamber is modeled using three zones: a single gas zone to represent the flame and combustion products within the chamber and two surface zones to represent the heat sink and refractory, respectively. It is assumed that the gas can be assigned a mean radiating temperature T_g; the heat sink surface is gray and at a specified temperature T_1; and the refractory surface is radiatively adiabatic. Radiation losses through openings in the furnace walls are neglected.

B. Model formulation

(a) Heat transfer from furnace gases

With these assumptions, the net rate of heat transfer from the combustion gases to the heat sink by radiation and convection is

$$\dot{Q}_1 = g_{g-1,r}\sigma(T_g^4 - T_1^4) + \alpha_1 A_{1,c}(T_g - T_1) \quad (1)$$

where σ is the Stefan-Boltzmann constant, equal to $5.67 \times 10^{-8}\ \mathrm{W/m^2K^4}$, α_1 is the convective heat transfer coefficient from the gas to the sink, $A_{1,c}$ is the area of the sink receiving heat by convection, and $g_{g-1,r}$ is the total transfer factor for radiation from the gas to the heat sink. $g_{g-1,r}$ allows for multiple reflections at all surfaces ***and*** reradiation from the refractory; its evaluation is discussed in Sec. B(d). Equation (1) may be simplified by approximating the convective heat transfer term. Linearization in T^4 yields

$$\alpha_1 A_{1,c}(T_g - T_1) = \frac{\alpha_1 A_{1,c}}{4\sigma T_{g1}^3}\sigma(T_g^4 - T_1^4) \quad (2)$$

where T_{g1} may be approximated as the arithmetic mean of T_g and T_1 The net rate of heat transfer to the heat sink then becomes

$$Q_1 = g_{g-1,r,c}\sigma(T_g^4 \text{ --- } T_1^4) \quad (3)$$

where

$$g_{g-1,r,c} = g_{g-1,r} + \frac{\alpha_1 A_{1,c}}{4\sigma T_{g1}^3} \quad (4)$$

The net rate of heat transfer from the furnace gases, $\dot{Q}_g$, is the sum of the heat transfer rates to the sink and through the furnace walls by conduction:

$$\dot{Q}_g \equiv \dot{Q}_1 + \dot{Q}_r = g_{g-1,r,c}\sigma(T_g^4 - T_1^4) + U_r A_r(T_g - T_e) \quad (5)$$

© 1983 Hemisphere Publishing Corporation

HEDH

where A, is the area of refractory, T_e is the external temperature, and U_r is an overall coefficient of heat transfer from the furnace gases to the external surroundings.

(b) Heat balance

The heat balance on the furnace chamber is

$$\dot{Q}_g = \dot{m}_g(h_{g,i} - h_{g,o}) \tag{6}$$

where $\dot{m}_g$ is the mass flow rate of gases through the furnace chamber, $h_{g,i}$ is the specific enthalpy of the inlet gases including heats of reaction, and $h_{g,o}$ is the specific enthalpy of the gases leaving the outlet of the furnace. Because of imperfect stirring within the furnace chamber, the mean enthalpy temperature of the gases leaving the furnace is lower than the mean radiating temperature of the gases within the furnace by ΔT_g. The leaving gas specific enthalpy may be written as

$$h_{g,o} = \bar{c}_{p,g}(T_g - \Delta T_g - T_o) \tag{7}$$

where $\bar{c}_{p,g}$ is the mean specific heat of the furnace gases over the temperature interval from the enthalpy base temperature, T_o, to $T_g - \Delta T_g$. The same mean specific heat may be used to define a fictitious gas temperature $T_{g,f}$, associated with the inlet gas specific enthalpy :

$$T_{g,f} = T_o + \frac{h_{g,i}}{\bar{c}_{p,g}} \tag{8}$$

By substituting Eqs. (7) and (8) into (6), the heat balance equation becomes

$$\dot{Q}_g = \dot{m}_g\bar{c}_{p,g}(T_{g,f} - T_g + \Delta T_g) \tag{9}$$

(c) Thermal performance

The thermal performance of the furnace, that is, $\dot{Q}_1$, is obtained by solving Eqs. (5) and (9). The final solution is simplified by rewriting the equations in dimensionless form as [9]

$$Q\ D = (T_g'^4 - T_1'^4) + L_r'(T_g' - T_e') \tag{10}$$

$$Q' = 1 - T_g' + \Delta T; \tag{11}$$

where

$$Q' = \frac{\dot{Q}_g(1 - T_o')}{\dot{m}_g h_{g,i}} \tag{12}$$

$$D' = \frac{\dot{m}_g h_{g,i}}{g_{g-1,r,c}\sigma T_{g,f}^4(1 - T_o')} \tag{13}$$

$$L_r' = \frac{U_r A_r}{g_{g-1,r,c}\sigma T_{g,f}^3} \tag{14}$$

and primes on the temperatures denote dimensionless ratios to $T_{g,f}$. The quantity Q' is known as the reduced furnace efficiency, D' as the reduced tiring density, and L_r' as the refractory loss factor.

The temperature drop that allows for the effect of imperfect stirring must be estimated. Values of ΔT_g in the range 1 10°-170°C are found to correlate the data from heavily fired cracking coils and marine boilers [10]. For box-type heaters having approximately square cross section and no areas of refractory with direct flame impingement, the temperature drop is negligible. In the opposite extreme of a high-temperature heater with a tall, narrow combustion chamber and wall-mounted radiant burners, ΔT_g may be 100°-150°C. Other types, such as narrow, bottom-fired vertical cylindrical heaters, fall somewhere in between [11]. For a wide range of furnace types and operating conditions the dimensionless temperature drop, $\Delta T_g'$, is found to be approximately proportional to Q [9]. It is convenient to assume that

$$\Delta T = \left(1 - \right)Q' \tag{15}$$

A tentative value of $d = 1.2$ is recommended. The case of perfect stirring ($\Delta T_g = 0$) is obtained by setting $d = 1$.

Substituting $\Delta T_g'$ from Eq. (15) into Eq. (11), and then eliminating T_g' between Eqs. (10) and (11) yields the performance equation

$$\frac{Q'}{d}D'd = \left(1 - \frac{Q'}{d}\right)^4 - T_1'^4 + L_r'\left(1 - \frac{Q'}{d} - T_e'\right) \tag{16}$$

When this equation has been solved for Q', the thermal efficiency of the furnace for transfer of useful heat to the sink is calculated from

$$\eta \equiv \frac{Q_1}{\dot{m}_g h_{g,i}} = \frac{\dot{Q}_g - U_r A_r(T_g - T_e)}{\dot{m}_g h_{g,i}} = \frac{Q' - (L_r'/D')[1 - (Q'/d) - T_e']}{1 - T_o'} \tag{17}$$

and the furnace gas temperature from

$$T_g = \left(1 - \frac{Q'}{d}\right)T_{g,f} \tag{18}$$

When wall losses are neglected, Eq. (16) gives the thermal performance of the furnace as a function of the two dimensionless groups $D'd$ and T_1'. The reduced tiring density D' makes allowance for any operating variables such as fuel type or excess air or air preheat that affect flame temperature or gas emissivity, for fractional occupancy of the walls by sink surfaces, and for wall emissivlty. The relationship among Q'/d, $D'd$, and T_1' is shown graphically in Fig. 1. The range of practical

© 1983 Hemisphere Publishing Corporation

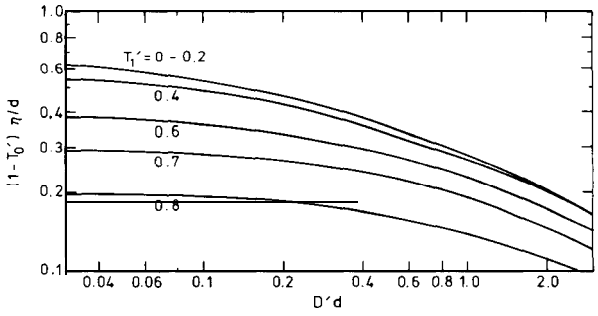

Figure 1 Performance curves for stirred-reactor furnace with negligible wall losses.

interest is $0.1 < D' < 2$. Some consequences of the relationship are noteworthy:

1. At low firing density the efficiency increases with decreasing firing density approaching a limiting value of $1 - T_1'$ (this behavior is modified when wall losses are included).
2. At high firing density the efficiency is inversely proportional to D'.
3. Changes in the sink temperature have little effect if $T_1' < 0.3$.

The effect of refractory wall losses on furnace performance is illustrated in Fig. 2, which shows the reduced furnace efficiency, $(1 - T_0')\eta/d$, as a function of $D'd$ and T_1' for the case L_r' = 0.02 and T_e' = 0.125. The reduction in furnace efficiency as a result of wall losses is seen clearly by comparing the curves in Fig. 2 with the corresponding curves in Fig. 1. At very high firing rates the efficiency is low and the wall loss is small compared with the heat transfer rate to the sink. As the firing rate is decreased the efficiency increases, passes through a maximum, and then falls to zero when the heat transfer from the gas is balanced by the heat loss through the wall.

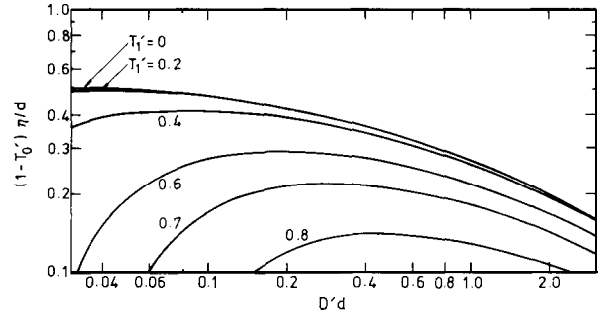

Figure 2 Performance curves for stirred-reactor furnace with wall losses: L_r' = 0.02, T_e' = 0.125.

(d) Transfer factor

The total transfer factor, $g_{g-1,r}$, accounts for the geometric complexities of the furnace chamber, including multiple reflections at all surfaces and absorption and reemission by the refractory. It may be determined most easily from the radiation network for the stirred-reactor model.

The radiation network for the stirred-reactor model may be derived from the results of Sec. 2.9.6. It is shown in Fig. 3 with the gas as a source of potential σT_g^4 connected to the sink and refractory by resistances R_{g-1} and R_{g-r}, and the refractory to the sink by a resistance R_{r-1}. The resistance to transfer at the sink due to surface reflection is shown by a resistance R_1. The refractory potential is represented by a floating node, since the refractory is assumed to be radiatively adiabatic.

Using the radiation network, the general expression for the total transfer factor is obtained as

$$g_{g-1,r} = \frac{1}{R_1 + 1/[(1/R_{g-1}) + 1/(R_{g-r} + R_{r-1})]} \tag{19}$$

where

$$\frac{1}{R_{g-1}} = A_1 \epsilon_{g,g-1} \tag{20}$$

$$\frac{1}{R_{g-r}} = A_r \epsilon_{g,g-r} \tag{21}$$

$$\frac{1}{R_{r-1}} = A_r F_{r-1}(1 - \epsilon_{g,r-1}) \tag{22}$$

$$\frac{1}{R_1} = \frac{A_1 \epsilon_1}{1 - \epsilon_1} \tag{23}$$

where $\epsilon_{g,g-1}$, $\epsilon_{g,g-r}$, and $\epsilon_{g,r-1}$ are the gas emissivities evaluated at the mean beam lengths for radiation from gas to sink, gas to refractory, and refractory to sink

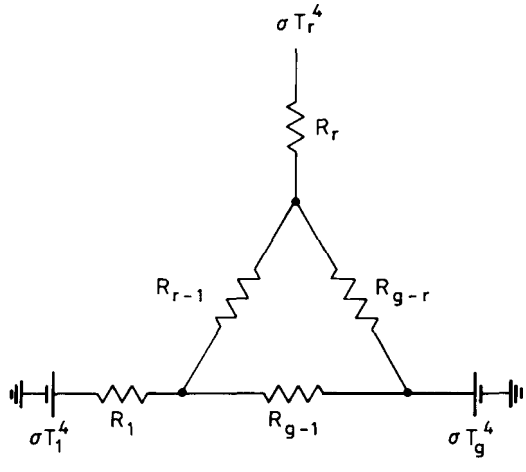

Figure 3 Radiation network for stirred-reactor furnace model,

© 1983 Hemisphere Publishing Corporation

respectively, ϵ_1 is the emissivity of the sink surface, and F_{r-1} is the view factor from refractory to sink. F_{r-1} depends on the arrangement of refractory and sink surfaces within the furnace chamber. A rigorous evaluation of F_{r-1} is usually not possible. However, several cases can be identified that yield relatively simple expressions for the total transfer factor.

Consider a planar heat sink surface. If the small differences between the gas emissivities associated with the various resistances are neglected, then the total transfer factor becomes

$$g_{g-1,r} = 1/([(1-\epsilon_1)/A_1\epsilon_1] + 1/\epsilon_g\{A_1 + A_r/[1+\epsilon_g/(1-\epsilon_g)F_{r-1}]\}) \quad (24)$$

where ϵ_g is the average gas emissivity evaluated at a beam length equal to the mean beam length for the entire furnace chamber ($\cong 3.5\,V/A_T$, where V is the chamber volume and A_T is the bounding area), and a temperature T_g. The view factor F_{r-1} can be readily evaluated for three limiting cases.

First, when the sink and refractory surfaces are intimately mixed within the chamber-the so-called speckled wall condition-then $F_{r-1} = A_1/(A_1 + A_r)$ and Eq. (24) simplifies to

$$g_{g-1,r} = \frac{A_T}{(1/C_1\epsilon_1) + (1/\epsilon_g) - 1} \quad (25)$$

where $A_T(\equiv A_1 + A_r)$ is the total area of the furnace chamber and C_1 is the fraction of the total area covered by the heat sink. The fraction C_1 is bounded by $0 < C_1 < 1$.

Second, when the heat sink and refractory surfaces are segregated with the sink lying in a single plane, then $F_{r-1} = A_1/A_r, C_1 < \frac{1}{2}$, and the total transfer factor is

$$g_{g-1,r} = \frac{A_T}{(1/C_1\epsilon_1) + [(1-\epsilon_g)/(1-C_1\epsilon_g)][(1/\epsilon_g)-1]} \quad (26)$$

Third, when the refractory surface is in a single plane, then $F_{r-1} = 1$, $C_1 > \frac{1}{2}$, and the total transfer factor is

$$g_{g-1,r} = A_T/((1/C_1\epsilon_1) + \{[1-(1/C_1-1)\epsilon_g]/[1-(1-C_1)\epsilon_g]\} \times [(1/\epsilon_g)-1]) \quad (27)$$

For most practical furnaces the total transfer factor may be calculated with reasonable precision from the speckled wall expression, Eq. (25). For typical values of ϵ_1 and ϵ_g ($\epsilon_1 = 0.85$ and $\epsilon_g = 0.3$), the maximum difference between the transfer factors calculated using the speckled wall assumption and the segregated wall assumption is about 10% at $C_1 \cong 0.4$.

For refractory-backed tubular heat sinks, the total transfer factor can be calculated from the expressions for the planar heat sink by taking A_1 as the total area of refractory covered by tubes and ϵ_1 as the effective emissivity calculated from Eq. 3.11.3(4).

For horizontal tubes mounted in a vertical plane centered between refractory walls, the effective sink area and emissivity are determined as described in Sec. 3.11.3B, and the total transfer factor is then calculated from Eq. (19) by substituting the resistance values determined from gas emissivities evaluated at the appropriate mean beam lengths [9]. This gives

$$g_{g-1,r} = \frac{A_T}{(1/C_1\epsilon_1) + [1/(1-C_1)][(1/\epsilon_g)-1]} \quad (28)$$

where the gas emissivity ϵ_g is evaluated using a mean beam length based on the *full* width of the furnace.

Approximate allowance for the effect of nongray gas radiation may be made within the framework of the stirred-reactor model using a clear-plus-gray-gas model of the real furnace gases. With this simple model the total transfer factor for the speckled wall condition becomes [9]

$$g_{g-1,r} = A_T/\{(1/C_1\epsilon_1) + (1/\epsilon_g) - (1/a_g) + [(1/a_g)-1]/[C_1\epsilon_1 + (1-C_1)\epsilon_r]\} \quad (29)$$

where a_g is the weighting factor for the gray gas in the clear-plus-gray-gas mixture and ϵ_r is the emissivity of the refractory. The value of a_g is calculated from ϵ_g evaluated at the mean beam length L_m and at $2L_m$:

$$a_g = \frac{(\epsilon_g(L_m))^2}{2\epsilon_g(L_m) - \epsilon_g(2L_m)} \quad (30)$$

The presence of the refractory emissivity in Eq. (29) allows for the spectral redistribution of radiant energy during the process of absorption and reemission from the refractory. Very often, almost nothing is known about the refractory emissivity. If the refractory walls are assumed to be perfectly reflecting ($\epsilon_r = 0$), then Eq. (29) simplifies to

$$g_{g-1,r} = \frac{a_g A_T}{(1/C_1\epsilon_1) + (a_g/\epsilon_g) - 1} \quad (31)$$

In general, $g_{g-1,r}$ for the clear-plus-gray-gas model with $\epsilon_r = 0$ is equal to a_g times $g_{g-1,r}$ based on a gray gas of emissivity ϵ_g/a_g. Equation (31) is a special case of this general relation. The value of $g_{g-1,r}$ for the clear-plus-gray-gas model with nonzero ϵ_r (~0.5) may be approximated as the mean of values calculated using the gray-gas model and the clear-plus-gray-gas model with $\epsilon_r = 0$. This method of allowing for nonzero ϵ_r can be used for cases other than the speckled wall furnace, which are generally too complex to formulate rigorously. Strictly,

© 1983 Hemisphere Publishing Corporation

the evaluation of the net radiative transfer between a nongray gas and a sink involves two values of the transfer factor: one ($g_{g\to 1,r}$) multiplying σT_g^4 to represent gas-to-sink radiation, and based on ϵ_g, the other ($g_{1\to g,r}$) multiplying σT_1^4 to represent sink-to-gas radiation, and based on gas absorptivity α_g. However, the difference between the two values can be ignored if T_1 is less than one-half of T_g.

C. Sample calculation

A vertical cylindrical process heater with a convection section is to be designed for a total duty of 3.3 MW. The design flue gas temperature at the outlet of the convection section is 600 K. The radiant section average flux is 29 kW/m^2. The radiant tubes are 0.14 m outer diameter on 0.25 m centers in a single row. The tube surface emissivity is 0.85, and the average skin temperature in the radiant section is estimated to be 650 K. Fuel oil (88% carbon, 12% hydrogen by mass) with a net calorific value of 41 MJ/kg is to be fired with 25% excess air (corresponding to 18.6 kg air/kg fuel), which is dry and preheated to 480 K. Steam for atomizing the fuel is at the rate of 0.25 kg/kg oil. The problem is to design the radiant section of the furnace.

For simplicity, the furnace gases are assumed to be gray and wall losses are neglected. The mean specific heat of the furnace gases is assumed to be constant at 1 200 J/kg K. The convective heat transfer coefficient to the tubes is taken as 10 W/m^2 K, and the parameter d in Eq. (15) is set to 1.2.

The first step is to determine the overall efficiency and the fuel consumption.

Neglecting the small steam contribution to the input-stream enthalpy and assuming a base temperature T_o of 288 K and a mean air specific heat of 1 020 J/kg K gives

Input-stream enthalpy = 2.25 MJ/kg
Fictitious inlet-gas temperature = 2 163 K
Flue gas enthalpy (at 600 K) = 0.37 MJ/kg
Heat available = 2.25 − 0.37 = 1.88 MJ/kg
Percent heat extracted = (1.88/2.25) X 100 = 84%
Heat fired = 3.3/0.84 = 3.93 MW
Furnace gas flow rate = 3.93/2.25 = 1.75 kg/s
Fuel flow rate = 0.088 kg/s

The second step is to determine the split between the radiant section duty and the convection section duty. The duty split is a function of the gas temperature at the outlet of the radiant section. This temperature must be estimated initially, then checked against the trial design, and finally corrected if necessary and the iterative cycle repeated. A good initial estimate of the furnace gas radiating temperature may be obtained using Eq. (1) and the design average heat flux, and neglecting the convective heat transfer contribution to the total heat transfer. The speckled wall condition is assumed and ϵ_g is estimated as 0.3 and C_1 as 0.85. This value of C_1 is obtained assuming a ratio of effective tube length to tube circle diameter equal to 3. With these assumptions, T_g is estimated as 1 320 K. Using Eqs. (11) and (15) yields an outlet gas temperature, $T_g - AT$,, of 1 150 K. Thus:

Fraction of heat extracted that is absorbed in the radiant section = (2 163 − 1 150)/(2 163 − 600) = 0.65
Radiant section heat absorption = 0.65 X 3.3 = 2.15 MW

The final step in the initial design is to determine the number of tubes required:

Tube surface area = 2.15 X 10^6/29 000 = 74 m^2
Total tube length = 74/(π X 0.14) = 168 m

Assuming that there are 28 tubes, then the exposed length of each tube is 6.0 m, the tube circle diameter is 2.23 m, and a ratio of tube length to tube circle diameter is 2.7.

The total transfer factor can now be calculated and the design checked. The effective heat sink area A_1 is 42.0 m^2, the total area of the combustion chamber A_T is 49.8 m^2, the heat sink fraction C_1 is 0.84, and the effective emissivity of the heat sink ϵ_1 is 0.84 [from Eq. 3.11.3(4)]. From the analysis of the fuel, the steam quantity, and excess air, the partial pressures of carbon dioxide and water vapor in the furnace gases are 0.106 and 0.107, respectively. The mean beam length calculated from the expression 3.5 V/A_T is 1.64 m. Using the chart in Sec. 3.11.3A, the nonluminous emissivity is found to be 0.23. Assuming a soot contribution of about 0.05 gives ϵ_g = 0.28. Substituting these values into Eq. (25) gives $g_{g-1,r}$ = 12.5 m^2. Equation (4) gives $g_{g-1,r,c}$ = 15.9 m^2. Equation (13) gives D' = 0.23. Solving Eq. (16) yields Q' = 0.49. Finally, the outlet-gas temperature, $T_g - AT$,, is 1 100 K, the radiant section duty, $\dot{Q}_1$, is 2.24 MW, and the average flux in the radiant section is 30.3 kW/m^2. The radiant section efficiency based on the heat input is 57%. The design check indicates that the radiant section duty is slightly higher than assumed-2.24 MW compared with 2.15 MW-but for all practical purposes this difference is not significant. The effect of wall losses on heater performance may be estimated by assuming a wall conductance U_r of 1 W/m^2 K. This gives a loss in efficiency of about 1%.

The stirred-reactor model may also be used to estimate the effect of changes in the heater operating conditions. For example, if the combustion air is not

© 1983 Hemisphere Publishing Corporation

preheated to 480 K, the radiant section efficiency falls from the design value of 57% to 54%, and the duty performed in the radiant section falls from 2.24 to 1.95 MW. The temperature at the outlet of the radiant section falls by about 10 K, and consequently the performance of the convection section is also degraded. Changing the excess air also has a significant effect on the furnace efficiency. If the burner is operated with only 20% excess air, then the radiant section efficiency increases from 57% to 59%.

Nomenclature for Section 3.11.4 appears at the beginning of Part 3. References appear at the end of Section 3.11.7.

© 1983 Hemisphere Publishing Corporation

3.11.5

The plug--flow furnace model

J. S. Truelove

■ The stirred-reactor furnace model described in the previous section predicts the overall heat transfer performance of furnaces, but it gives no information on the distribution of heat flux within the furnace and it cannot account for some important design parameters, for example, the burner heat release pattern. These limitations can be serious when the furnace is long compared with its mean hydraulic radius, for example, fire-tube boilers, tunnel kilns, and metal reheating furnaces. For these cases, the plug-flow, or long-furnace, model is more appropriate.

A. Basis of model

The gas at any flow cross-section is assumed to have a reasonably uniform velocity and to be characterized by a single temperature. When combustion occurs, heat is released in such a way that the gas temperature over the furnace cross section remains reasonably uniform. Further, it is assumed that the net radiative flux in the flow direction is negligible, that all surfaces are gray, and that the refractory surfaces are in radiative equilibrium. Radiation losses through openings are neglected.

B. Model formulation

(a) Heat transfer from furnace gases

With these assumptions, the net heat flux to the sink surface at the downstream distance x can be expressed in terms of the local gas and surface temperatures as

$$\dot{q}_1 = \frac{g_{g-1,r}}{A_1}\sigma(T_g^4 - T_1^4) + \alpha_1 \frac{A_{1,c}}{A_1}(T_g - T_1) \qquad (1)$$

where $g_{g-1,r}$ is given by Eq. 3.11.4(19) evaluated as for a two-dimensional system that is infinite in the flow direction.

The net heat flux through the refractory wall is

$$\dot{q}_r = U_r(T_g - T_e) \qquad (2)$$

(b) Heat balance

A heat balance on the furnace gases between x and ***x + dx gives***

$$\dot{q}' \, dx - \dot{q}_1 P_1 \, dx - \dot{q}_r P_r \, dx = \dot{m}_g c_{p,g} \, dT_g \qquad (3)$$

where $\dot{q}'$ is the heat release rate per unit length due to combustion, P_1 is the perimeter occupied by sink surface, and P_r is the perimeter occupied by refractory surface.

(c) Thermal performance

The heat balance may be rewritten in the form of a differential equation as

$$\frac{dT_g}{dx} + \frac{\dot{q}_1 P_1 + \dot{q}_r P_r - \dot{q}'}{m_g c_{p,g}} = 0 \qquad (4)$$

This equation may be integrated numerically to obtain the distribution of gas temperature in the flow direction. Note that $\dot{q}_1, \dot{q}_r$, and $c_{p,g}$ depend on the local value of T_g. The surface temperature, T_1, may be prescribed or calculated from an auxiliary relation, such

© 1983 Hemisphere Publishing Corporation

as a conduction equation linking T_1 to an external temperature.

When there is no heat release due to combustion, or when all heat release takes place upstream of x = 0, then $\dot{q}' = 0$ and Eq. (3) can be rearranged and integrated to find the furnace length X, from inlet, to cool the furnace gases from $T_g(0)$ to $T_g(X)$:

$$X = \int_{T_g(0)}^{T_g(X)} \frac{-\dot{m}_g c_{p\,g}}{\dot{q}_1 P_1 + \dot{q}_r P_r}\, dT_g \qquad (5)$$

The integral may be evaluated numerically or graphically from a plot of the integrand as a function of T_g.

When the gas temperature distribution has been calculated from Eq. (4) or (5), then the distribution of heat flux to the sink may be calculated using Eq. (1), and the wall loss using Eq. (2).

C. Sample calculation

The application of the plug-flow furnace model is illustrated using the example of Sec. 3.11.4C. The plug-flow model is appropriate when the heater is bottom-fired with multiple burners. The heat release rate due to combustion is assumed to vary exponentially with axial distance from the burner, and the flame length, defined as the axial distance at which combustion is 99% complete, is taken as 2.9 m. This gives $\dot{q}' = 5.74e^{-1.59x}$ MW/m. Note that the integral of $\dot{q}'$ between x = 0 and x = ∞ yields the total heat release-3.61 MW. The furnace gas temperature is calculated by numerical integration of Eq. (4), and the heat flux distribution is found from Eq. (1). The heat flux distribution to the tubes is shown in Fig. 1. The average heat flux is 32.5 kW/m², the total absorption is 2.41 MW, and the furnace efficiency is 61%. It is seen that the plug-flow model predicts a higher efficiency than the stirred-reactor model. Somewhat more realistic predictions of heat flux may be obtained from a plug-flow model with allowance for radial temperature gradients and axial radiation. Some results are presented in the next section.

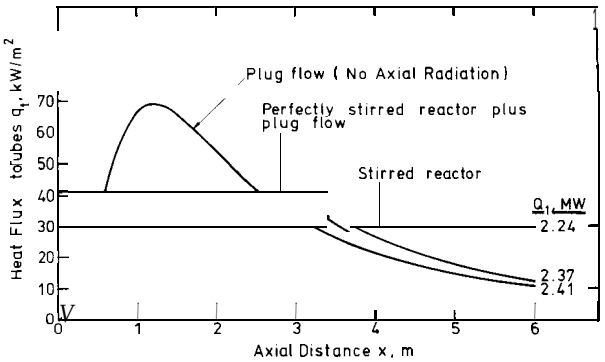

Figure 1 Heat flux distributions calculated using plug-flow and perfectly stirred-reactor-plus-plug-flow furnace models.

When the heater is fired with a single burner from the center of the base, a combination of perfectly stirred-reactor and plug-flow models may be more appropriate. Close to the burner, the turbulent mixing between the fuel and air and the external recirculation between the flame and the wall of the chamber result in a region in which the furnace gases are well stirred. This region may be modeled as a perfectly stirred reactor. The length of the perfectly stirred region is estimated from a knowledge of the flame length and flow pattern within the chamber. Beyond the perfectly stirred region, the plug-flow model is used. The results obtained using a stirred-reactor and plug-flow model with a perfectly stirred region of length 3.4 m are also shown in Fig. 1. As expected, the large peak in the heat flux distribution near the burner is flattened, and a more nearly uniform heat flux profile is predicted.

Nomenclature for Section 3.1 I.5 appears at the beginning of Part 3.

© 1983 Hemisphere Publishing Corporation

3.11.6

The multizone furnace model

J. S. Truelove

The restrictions of gas temperature uniformity imposed in the stirred-reactor model and of a one-dimensional temperature field imposed in the plug-flow model severely limit the usefulness of these models when applied to furnaces where there are significant gradients in temperature. Allowance for gradients in temperature, and other properties, may be made using the multizone model to be described in this section. Furthermore, the model may be used to examine the effect on heat flux distribution of complex factors such as recirculatory flow and combustion pattern.

A. Basis of model

The volume of the furnace chamber is subdivided (conceptually) into small zones in which the temperature, composition, and other physical properties can be assumed to be uniform. Similarly, thesurfaces within the furnace chamber are subdivided into small surface zones that are assumed to have uniform temperature and emissivity and over which the incident and leaving fluxes can be considered to be uniform. The surfaces are assumed to be gray and to emit and reflect radiation diffusely. The geometric arrangement of zones is determined by the furnace shape and the ease with which radiation transfer factors between zones can be evaluated.

The stirred-reactor furnace model is a special case of the multizone model with one gas zone and two surface zones.

B. Model formulation

(a) Radiation transfer between zones

For a gray gas, the net rate of heat transfer by radiation between zones i and j is

$$\dot{Q}_{i-j} = g_{i-j}\sigma(T_i^4 - T_j^4) \tag{1}$$

where g_{i-j} is the total transfer factor for the zone pair i-j. The notation used here is the same as that adopted in Sec. 2.9.6 and does not distinguish explicitly between a volume and a surface zone. It is assumed that the furnace is subdivided into N surface zones and M volume zones and that indices $i = 1, \ldots, N$ denote surface zones, whereas indices $i = N+1, \ldots, N+M$ denote volume zones. The evaluation of total transfer factors is described in Sec. B(d).

Allowance for the effect of nongray gas radiation may be made using a mixed gray gas representation of the real furnace gas-see Sec. 3.11.3A. When Eqs. 3.11.3(2) and 3.11.3(3) are used to determine ϵ_g and α_g, the radiant heat transfer between two zones in a furnace chamber containing a real gas is calculated as the weighted sum of the independent contributions from gray gases of different absorption coefficients. For example, the net rate of heat transfer between gas zone i and surface zone j is

© 1983 Hemisphere Publishing Corporation

HEDH

$$\dot{Q}_{i-j} = \left[\sum_n a_{g,n}(T_i)(g_{i-j})_n\right]\sigma T_i^4 - \left[\sum_n a_{s,n}(T_j)(g_{i-j})_n\right]\sigma T_j^4 \quad (2)$$

where $(g_{i-j})_n$ is the total transfer factor for the gray gas component with absorption coefficient $k_{a,n}$. The terms in brackets are the directed flux factors, so called because they depend on the temperature of the emitting zone. The directed flux factors are designated by $g_{i\to j}$, with the arrow pointing in the direction of the flux. The general expression for the net rate of heat transfer between two zones i and j is

$$\dot{Q}_{i-j} = g_{i\to j}\sigma T_i^4 - g_{j\to i}\sigma T_j^4 \quad (3)$$

where for a surface zone emitter,

$$g_{i\to j} = \sum_n a_{s,n}(T_i)(g_{i-j})_n \qquad i = 1, \ldots, N \quad (4)$$

and for a gas zone emitter,

$$g_{i\to j} = \sum_n a_{g,n}(T_i)(g_{i-j})_n \qquad i = N+1, \ldots, N+M \quad (5)$$

(b) Heat balances

Heat balances are formulated on all surface and gas zones of unknown temperature.

A heat balance on surface zone *i gives*

$$\sum_{j=1}^{N+M} g_{j\to i}\sigma T_j^4 - \sum_{j=1}^{N+M} g_{i\to j}\sigma T_i^4 + \alpha_i A_i(T_k - T_i) = \dot{Q}_i \quad (6)$$

where α_i is the convective heat transfer coefficient at surface zone i and T_k is the temperature of the gas zone k adjacent to the surface. $\dot{Q}_i$ is the net flux to the surface, which must be specified by a supplementary boundary condition, such as a wall conduction equation. For an adiabatic zone, $\dot{Q}_i = 0$. Similarly, a heat balance on gas zone *i gives*

$$\sum_{j=1}^{N+M} g_{j\to i}\sigma T_j^4 - \sum_{j=1}^{N+M} g_{i\to j}\sigma T_i^4 - \alpha_k A_k(T_i - T_k) + \dot{Q}_{h,i} = 0 \quad (7)$$

where α_k is the heat transfer coefficient for convection to an adjacent surface zone at temperature T_k (if any), and $\dot{Q}_{h,i}$ is the net total enthalpy flux (sensible plus chemical) into zone i across its boundaries. The term $\dot{Q}_{h,i}$ allows for any heat release due to combustion in the zone.

(c) Thermal performance

Equations (6) and (7) constitute a system of nonlinear algebraic equations for the unknown gas and surface temperatures. When these are solved and the temperature distribution has been determined, the heat flux distribution at the surfaces may be calculated from heat balance equations similar to Eq. (6).

(d) Transfer factors

The total transfer factors are determined from a radiosity irradiation formulation at each surface zone. The leaving flux, or radiosity, at surface zone i is

$$q_i^+ = (1-\epsilon_i)q_i^- + \epsilon_i B_i \quad (8)$$

where q_i^- is the incident flux, ϵ_i is the surface emissivity, and B_i denotes the blackbody emissive power σT_i^4. The incident flux, or irradiation, at surface zone i is the sum of the products of leaving flux and direct transfer factor for all zones in the furnace, and is given by

$$A_i q_i^- = \sum_{j=1}^{N} g_{i-j}q_j^+ + \sum_{j=N+1}^{N+M} g_{i-j}B_j \quad (9)$$

where g_{i-j} is the direct transfer factor for the zone pair i-j. From the results of Sec. 2.9.6D, the direct transfer factor for surface-to-surface radiation is given by

$$g_{i-j} = \int_{A_i}\int_{A_j} \tau_{i-j}\frac{\cos\theta_i \cos\theta_j}{\pi r_{i-j}^2}\,dA_j\,dA_i$$

$$i, j = 1, \ldots, N \quad (10)$$

where θ_i and θ_j are the angles between the normals to the differential areas dA_i and dA_j and the line joining dA_i to dA_j, r_{i-j}, is the distance between dA_i and dA_j, and τ_{i-j} is the transmissivity of the gas between dA_i and dA_j,

$$\tau_{i-j} = \exp(-\int k_a\,dr) \quad (11)$$

where k_a is the gas absorption coefficient and the path integral is taken along the line joining dA_i to dA_j. If the absorption coefficient is independent of spatial location in the furnace chamber, then τ_{i-j} simplifies to $\exp(-k_a r_{i-j})$. It can be seen that g_{i-j} is essentially the product $A_i F_{i-j}$, where F_{i-j} is the view factor from surface i to surface j, but with a correction to allow for absorption by the gas between the two zones. Similarly, the direct transfer factors for surface-to-gas and gas-to-gas radiation are given by

© 1983 Hemisphere I blishing Corporation

$$g_{i-j} = \int_{A_i}\int_{V_j} \tau_{i-j} \frac{k_{a,j}\cos\theta_i}{\pi r_{i-j}^2}\, dV_j\, dA_i$$

$$\begin{cases} i = 1, \ldots, \mathrm{N} \\ j = N+1, \ldots, N+M \end{cases} \qquad (12)$$

$$g_{i-j} = \int_{V_i}\int_{V_j} \tau_{i-j} \frac{k_{a,i}k_{a,j}}{\pi r_{i-j}^2}\, dV_j dV_i$$

$$i, j = N+1, \ldots, N+M \qquad (13)$$

where $k_{a,i}$ is the gas absorption coefficient in volume zone i. It follows from the above definitions that the direct transfer factors satisfy the reciprocity relation $g_{i-j} = g_{j-i}$, and from energy conservation considerations that the sum rules are

$$\sum_{j=1}^{N+M} g_{i-j} = A_i \qquad i = 1, \ldots, N$$

$$= 4k_{a,i}V_i \qquad i = N+1, \ldots, N+M \qquad (14)$$

Direct transfer factors are available in graphic or tabular form for many systems of practical importance, for example, rectangular and axisymmetric cylindrical geometries [7]. Substituting q_i^+ from Eq. (8) into Eq. (9) and rearranging the resulting expression yields

$$\sum_{j=1}^{\mathrm{N}} [A_i\delta_{ij} - (1-\epsilon_j)g_{i-j}]\, q_j^- = \sum_{j=1}^{\mathrm{N}} g_{i-j}\epsilon_j B_j + \sum_{j=N+1}^{N+M} g_{i-j}B_j \qquad (15)$$

where δ_{ij} is the Kronecker delta function. When Eq. (1.5) is applied to each surface zone in the furnace, the result is a system of N simultaneous linear equations for the incident fluxes q_i^- ($i = 1, \ldots, \mathrm{N}$). The linearity of the governing equations for the radiant heat flow enables the powerful superposition principle to be used to determine the parameters that describe the system for any set of temperatures, namely, the transfer factors g_{i-j}. From Eq. (1), it can be seen that the net heat transfer into surface zone i, when B_j is set equal to unity and all other B_i are set equal to zero, is g_{i-j}. For the same conditions, Eq. (8) may be used to express the net heat transfer in terms of the incident flux at surface zone i. Equating these two expressions yields

$$g_{i-j} = A_i\epsilon_{i\,j}q_i^- \qquad \begin{cases} i = 1, \ldots, N \\ j = 1, \ldots, N+M \end{cases} \qquad (16)$$

where ${}_jq_i^-$ is the flux incident on surface zone i due to emission by zone j. Note that zone j may be a surface or volume zone. The flux ${}_jq_i^-$ is obtained from the solution of Eq. (15) with the appropriate right-hand side, viz., $g_{i-j}\epsilon_j$ for $1 \leqslant j \leqslant N$ or g_{i-j} for $N+1 \leqslant j \leqslant N+M$. Equation (16) gives the total transfer factors for surface-to-surface and gas-to-surface radiation. The surface-to-gas factor may be obtained using the reciprocity relation $g_{i-j} = g_{j-i}$. The total transfer factor for gas-to-gas radiation may be found by considering the radiation incident at gas zone i due to original emission by gas zone j. This yields

$$g_{i-j} = g_{i-j} + \sum_{k=1}^{\mathrm{N}} (1-\epsilon_k)_j q_k^- g_{k-i}$$

$$i, j = N+1, \ldots, N+M \qquad (17)$$

From energy conservation considerations it may be shown that the total transfer factors satisfy the sum rules

$$\sum_{j=1}^{N+M} g_{i-j} = \epsilon_i A_i \qquad i = 1, \ldots, N$$

$$= 4k_{a,i}V_i \qquad i = N+1, \ldots, N+M \qquad (18)$$

Equation (18) is a useful check on computed values of the total transfer factors. Note that the self-transfer factor g_{i-i} is required for the sum rules but not for the calculation of net radiative heat transfer.

(e) Flow and combustion patterns

The enthalpy fluxes $\dot{Q}_{h,i}$ that appear in the heat balance equation are calculated from the mass flow rates across the zone boundaries and the specific enthalpies of gas evaluated at the temperature of the zone from which the gas flows.

The mass flow rates and combustion pattern must be specified. These may be obtained in one of three ways: from a physical model; from a simple mathematical model of confined turbulent jet flames [12,13]; or from a detailed mathematical model based on the equations for conservation of mass, momentum, chemical species, and energy. The further development of the zone model as a useful tool for furnace design will greatly depend on the progress in predicting flow and combustion patterns in furnaces from input and design parameters. This topic is discussed further in Sec. 3.11.7.

C. Sample calculation

The application of the multizone furnace model is also illustrated using the fired-heater example of Sec.

© 1983 Hemisphere Publishing Corporation

3.11.4C. The combustion chamber is subdivided into zones of radial and axial dimension 0.373 m, giving three zones in the radial direction and 16 zones in the axial direction. This subdivision gives a total of 48 gas zones, 16 cylindrical sink zones, and six adiabatic refractory zones. The gas within the furnace chamber is assumed to be gray, and the absorption coefficient is chosen to reproduce the gas emissivity used for the stirred-reactor calculation. This gives $k_a = 0.2\ \mathrm{m}^{-1}$. Two flow patterns are considered: a plug-flow typical of multiburner firing; and a recirculating jet flow typical of that formed by a single high-momentum burner axially fired into a cylindrical furnace. Figure 1 shows the streamline pattern for the jet flow. The mass flow rates across the zone boundaries may be readily calculated from the mass flow stream function values indicated on the streamlines. The axial distribution of heat release due to combustion is assumed to follow an exponential relationship. For the plug flow, the heat release is distributed radially in the same proportion as the mass flowrate of gas. For the jet flow, all combustion takes place in the central row of zones and is distributed axially according to the pattern shown in Fig. 1.

The calculated heat flux distributions to the tubes are shown in Fig. 2, together with the results obtained using the stirred-reactor and plug-flow models. The total heat absorption is indicated for each curve. It can be seen that the furnaces with plug flow have higher efficiencies than the stirred-reactor and jet-flow furnaces. The jet-flow furnace has the lowest efficiency because the high-temperature flame zone is of small volume and consequently not a very effective radiator, and is surrounded by much cooler combustion products. However, it should be noted that in the calculations the gas is assumed to have a constant mean absorption coefficient chosen to reproduce the emissivity of the radiating gases and soot, whereas in practice the flame region contains most of the soot and has an absorption coefficient higher than the mean, and the gases surrounding the flame have an absorption coefficient lower than the mean. This effect makes the jet-flow furnace efficiency somewhat too low. Of course, the local soot radiation from the flame can easily be included in the zoning method, provided that the soot concentration distribution and soot radiative properties are known [14, 15].

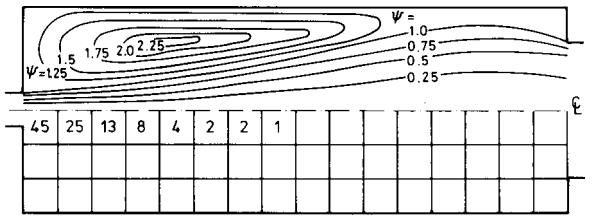

Figure 1 Mean streamline pattern and percentage of fuel burned in each zone for the enclosed jet flow.

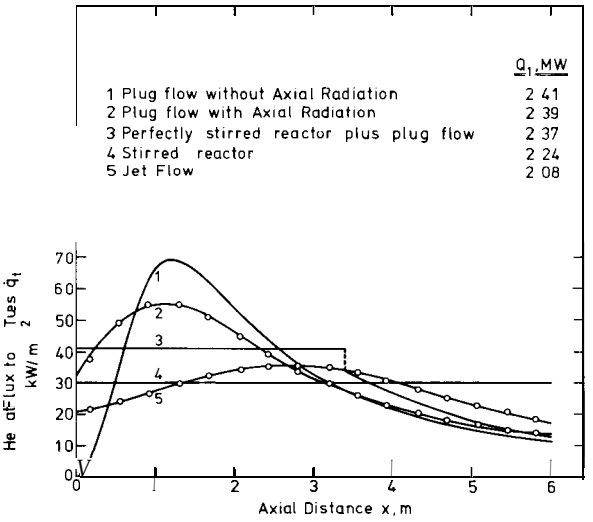

Figure 2 Heat flux distributions calculated using different flow patterns and furnace models.

Nomenclature for Section 3.11.6 appears at the beginning of Part 3. References appear at the end of Section 3.11.7.

© 1983 Hemisphere Publishing Corporation

3.11.7
Advanced furnace models

J. S. Truelove

■ The multizone model described in the previous section provides a solution for the radiation component of the overall furnace heat transfer problem. However, some additional means must be provided to obtain the other components in the heat balance, such as convection and heat generation due to combustion. In principle, these may be calculated by solving the equations governing conservation of mass, momentum, chemical species, and energy in a turbulent, chemically reacting flow. In practice, there are many unresolved difficulties in formulating and applying models of this nature. The complexities of turbulent, recirculating, reacting, two-phase flows are not yet fully understood. Universal parameters for turbulence models have not been established. The interaction of turbulence and chemical reaction, and the effect of gas turbulence on the motion of entrained drops and particles, are both poorly understood. Finally, the task of solving the set of coupled governing conservation equations is formidable, and only recently have reliable and accurate numerical methods for the computation of recirculating flows been developed. The extent of model evaluation by comparison of predictions with measurements is limited, with few (if any) comparisons for full-scale combustion chambers. Despite the difficulties and complexities of the problem, the development of models for turbulent flow and combustion is steadily advancing. A complete discussion of the topic is well outside the scope of this section, and, therefore, the present discussion is restricted to the case of heat transfer in a gas-fueled furnace. The modeling of oil spray and pulverized coal flames is described in [16-18] . The modeling of pollutant formation is discussed in [19,201 .

A. Basis of model

Equations are formulated for the conservation of mass, momentum, chemical species, and energy, together with appropriate boundary conditions. To these are added equations to model various physical processes, such as turbulent transport and radiation. The need to introduce additional physical models arises because many of the processes that occur in the furnace are far too complex to be handled at a fundamental level. The resulting system of coupled, nonlinear, elliptic, partial differential equations is solved numerically by finite difference techniques.

B. Model formulation

(a) Conservation equations

It is assumed that no external body forces act on the system; that species diffusion follows Fick s law; that the Lewis number for each chemical species is unity; that kinetic heating terms in the energy equation are negligible; and that the gas follows the ideal gas equation of state. With these assumptions, the equations for conservation of mass, momentum, chemical species, and energy may be written as follows [21]:

Mass conservation:

$$\nabla \cdot (\rho \mathbf{u}) = 0 \qquad (1)$$

Momentum conservation:

$$\nabla \cdot (\rho \mathbf{u}\mathbf{u}) = -\nabla p + \nabla \cdot \boldsymbol{\tau} \qquad (2)$$

© 1983 Hemisphere Publishing Corporation

Species conservation :

$$\mathbf{v} \cdot (\rho \mathbf{u} m_j) = \mathbf{v} \cdot (\rho \delta_j \nabla m_j) + R_j \tag{3}$$

Enthalpy conservation:

$$\nabla \cdot (\rho \mathbf{u} h) = \nabla \cdot (\rho \kappa \nabla h) - \nabla \cdot \mathbf{q}_r \tag{4}$$

where ρ is the density, $\mathbf{u}$ the velocity, p the pressure, $\boldsymbol{\tau}$ the stress tensor,

$$\boldsymbol{\tau} = \eta(\nabla \mathbf{u} + \nabla \mathbf{u}^T) - \tfrac{2}{3}\eta(\nabla \cdot \mathbf{u})\mathbf{I} \tag{5}$$

η is the molecular viscosity, m_j the mass fraction of species j, δ_j the diffusivity of species j, R_j the volumetric rate of formation of species j, h the specific enthalpy, κ the thermal diffusivity, and $\mathbf{q}_r$ the radiation heat flux. The enthalpy includes the contribution due to chemical enthalpy :

$$h = \sum_j m_j \left(\int_{T_o}^{T} c_{p,j}\, dT + h_{f,j} \right) \tag{6}$$

where $c_{p,j}$ is the constant-pressure specific heat of species j and $h_{f,j}$ is the heat of formation of species j. It should be noted that the $\mathbf{v} \cdot ( )$ terms in the momentum equation are not simple divergences because of the tensor nature of uu and $\boldsymbol{\tau}$. The superscript T denotes the transpose of the tensor, and I is the idemfactor.

The above conservation equations are correct at any instant of time. In a laminar flow, the equations may be solved for the instantaneous values of the dependent variables. However, for turbulent flow, solution of the instantaneous equations is neither feasible, due to the very rapid turbulent fluctuations in the values of the dependent variables, nor necessary, since interest is principally in the time-average values of the dependent variables.

The instantaneous equations may be transformed to yield equations for the time-average variables using a procedure known as Reynolds decomposition, whereby the instantaneous value of any variable ϕ, say, is expressed as the sum of a time-average term $\bar{\phi}$ and an instantaneous fluctuating term ϕ', as

$$\phi = \bar{\phi} + \phi' \tag{7}$$

By definition, $\overline{\phi'} = 0$. Substituting the Reynolds-decomposed expressions for $\mathbf{u}, p, m_j$, and h into the instantaneous conservation equations, ignoring fluctuations in density, transport properties, and radiation, and time-averaging the resulting equations yields the conservation equations for the time-average variables as follows:

$$\nabla \cdot (\rho \bar{\mathbf{u}}) = 0 \tag{8}$$

$$\nabla \cdot (\rho \bar{\mathbf{u}} \bar{\mathbf{u}} + \rho \mathbf{u}'\mathbf{u}') = -\nabla \bar{p} + \nabla \cdot \bar{\boldsymbol{\tau}} \tag{9}$$

$$\mathbf{v} \cdot (\rho \bar{\mathbf{u}} \bar{m}_j + \rho \mathbf{u}' m_j') = \mathbf{v} \cdot (\rho \delta_j \nabla \bar{m}_j) + \bar{R}_j \tag{10}$$

$$\nabla \cdot (\rho \bar{\mathbf{u}} \bar{h} + \rho \mathbf{u}' h') = \nabla \cdot (\rho \kappa \nabla \bar{h}) - \nabla \cdot \mathbf{q}_r \tag{11}$$

where the overbars denote time-averaged quantities. These equations are similar to the instantaneous equations, with time-average values replacing instantaneous values and the addition of new terms $\rho \overline{u' u'}$, $\rho \overline{u' m_j'}$, and $\rho \overline{u' h'}$ to account for turbulent transport of momentum, chemical species, and enthalpy, respectively. These terms cannot be readily evaluated. Further application of Reynolds decomposition leads to higher-order correlation terms. This difficulty is referred to as the closure problem. It is necessary to resort to turbulence models to obtain expressions for these terms and so close the equations.

(b) Turbulence model

In the momentum conservation equation, turbulent transport is given by the term $-\rho \overline{\mathbf{u}'\mathbf{u}'}$, called the Reynolds stress. The conventional approach to the closure problem is to relate the turbulent Reynolds stresses to the mean strain rate, by analogy with Newton s linear relation between viscous stresses and strain rate given by Eq. (5). The Reynolds stresses are written as

$$\bar{\boldsymbol{\tau}}_t \equiv -\rho \overline{\mathbf{u}'\mathbf{u}'} = \eta_t(\nabla \bar{\mathbf{u}} + \nabla \bar{\mathbf{u}}^T) - \tfrac{2}{3}(\eta_t\, \mathbf{v} \cdot \mathbf{ii} + \rho k)\mathbf{I} \tag{12}$$

where η_t is the turbulent or eddy viscosity and k is the kinetic energy of turbulence,

$$k = \tfrac{1}{2}\overline{\mathbf{u}' \cdot \mathbf{u}'} \tag{13}$$

Equation (12) is known as the Boussinesq approximation. The Boussinesq approximation is convenient but is not strictly correct, since the turbulent viscosity is known to be anisotropic and should be represented by a tensor with several components, rather than as an isotropic scalar. This deficiency of the Boussinesq approximation is apparent in certain complex flows, for example, strongly swirling flows. Substituting Eq. (12) into (9) yields the time-averaged momentum conservation equation

$$\mathbf{v} \cdot (p\mathbf{iii}) = -\nabla p_{\text{eff}} + \mathbf{v} \cdot [\eta_{\text{eff}}(\nabla \bar{\mathbf{u}} + \nabla \bar{\mathbf{u}}^T) - \tfrac{2}{3}\eta_{\text{eff}}(\nabla \cdot \bar{\mathbf{u}})\mathbf{I}] \tag{14}$$

where

$$p_{\text{eff}} = \bar{p} + \tfrac{2}{3}\rho k \tag{15}$$

$$\eta_{\text{eff}} = \eta + \eta_t \tag{16}$$

Equation (14) has exactly the same form as the instantaneous conservation equation, Eq. (2), but with p replaced by $\bar{p} + \frac{2}{3}\rho k$ and η replaced by $\eta + \eta_t$. In effect, turbulent flow is treated as quasi-iaminar flow, with the molecular viscosity replaced by an effective turbulent

© 1983 Hemisphere F blishing Corporation

viscosity in the momentum conservation equation. In general, $\eta_t \gg \eta$.

The turbulent viscosity is related to properties of the mean flow field. If the turbulence is characterized by the kinetic energy of turbulence, k, and its dissipation rate, ϵ,

$$\epsilon = \frac{\eta}{\rho} \overline{\nabla \mathbf{u}' : \mathrm{vu}} \tag{17}$$

then by dimensional analysis,

$$\eta_t = \frac{C_\eta \rho k^2}{\epsilon} \tag{18}$$

where C_η is a constant. This closure scheme is known as a two-equation mode[22], so called because k and ϵ are calculated from transport equations. An exact equation for the turbulent kinetic energy k may be derived from the instantaneous momentum conservation equation [23]. Similarly, an exact equation for ϵ may be derived. When the unknown correlations appearing in these equations are related to the mean flow variables, the resulting modeled k and ϵ equations are

$$\nabla \cdot (\rho \bar{\mathbf{u}} k) = \nabla \cdot \left[\left(\eta + \frac{\eta_t}{\sigma_k} \right) \nabla k \right] + G - \rho \epsilon \tag{19}$$

$$\nabla \cdot (\rho \bar{\mathbf{u}} \epsilon) = \nabla \cdot \left[\left(\eta + \frac{\eta_t}{\sigma_\epsilon} \right) \nabla \epsilon \right] + (C_1 G - C_2 \rho \epsilon) \frac{\epsilon}{k} \tag{20}$$

where

$$G = \bar{\tau}_t : \mathrm{VU} \tag{21}$$

σ_k and σ_ϵ are turbulent Prandtl-Schmidt numbers for transport of k and ϵ, respectively, and C_1 and C_2 are constants. The five constants, $C_\eta, \sigma_k, \sigma_\epsilon, C_1$, and C_2 must be specified by comparisons of predictions with measured data. The recommended values are

$$C_\eta = 0.09 \quad \sigma_k = 1.0 \quad \sigma_\epsilon = 1.217 \quad C_1 = 1.44$$
$$C_2 = 1.92$$

Unfortunately, these constants are not universal, and therefore not the optimum set for all flow conditions.

Turbulent transport of chemical species and enthalpy involve correlations $\rho \mathbf{u}' m_j'$ and $\rho \mathbf{u}' h'$, respectively. These terms may be modeled using the Boussinesq approximation to relate the turbulent fluxes to mean flow property gradients via a turbulent exchange coefficient. Since the transport of species, enthalpy, and momentum occur by similar turbulent exchange processes, the turbulent exchange coefficients for species and enthalpy can be presumed proportional to the turbulent viscosity. Thus,

$$-\rho \overline{\mathbf{u}' m_j'} = \frac{\eta_t}{\sigma_{m_j,\mathrm{t}}} \nabla \bar{m}_j \tag{22}$$

$$-\rho \overline{\mathbf{u}' h'} = \frac{\eta_t}{\sigma_{h,t}} \nabla \bar{h} \tag{23}$$

where $\sigma_{m_j,t}$ and $\sigma_{h,t}$ are the turbulent Schmidt and Prandtl numbers. These numbers are additional empirical constants; for typical furnace flows they may be taken as 0.9. Substituting Eq. (22) into Eq. (10) and Eq. (23) into Eq. (11) yields the mean conservation equations

$$\nabla \cdot (\rho \bar{\mathbf{u}} \bar{m}_j) = \nabla \cdot (\rho \delta_{j,\mathrm{eff}} \nabla \bar{m}_j) + \bar{R}_j \tag{24}$$

$$\nabla \cdot (\rho \bar{\mathbf{u}} \bar{h}) = \nabla \cdot (\rho \kappa_{\mathrm{eff}} \nabla \bar{h}) - \nabla \cdot \mathbf{q}_r \tag{25}$$

where $\delta_{j,\mathrm{eff}}$ and κ_{eff} are effective diffusivities given by

$$\rho \delta_{j,\mathrm{eff}} = \rho \delta_j + \frac{\eta_t}{\sigma_{m_j,t}} \tag{26}$$

$$\rho \kappa_{\mathrm{eff}} = \rho \kappa + \frac{\eta_t}{\sigma_{h.t}} \tag{27}$$

(c) Turbulent combustion model

The fuel and oxidant are presumed to enter through separate inlet streams. For the purpose of calculating heat transfer, it is sufficient to assume a global, single-step irreversible chemical reaction between fuel and oxidant,

$$\mathrm{FU} + i\ \mathrm{OX} \rightarrow (1 + i)\ \mathrm{PR}$$

where 1 kg of fuel reacts with i kg of oxidant to produce $(1 + i)$ kg of products. Thus, in the species conservation equation, j stands for FU, OX, and PR. The principal problem is the determination of the time-average reaction rates $\bar{R}_{\mathrm{FU}}$, and so on. A considerable simplification may be introduced by assuming equal diffusivities for all species. With these assumptions, the quantity

$$\chi = m_{\mathrm{FU}} - \frac{m_{\mathrm{OX}}}{i} \tag{28}$$

is a conserved scalar under the chemical reaction. It is convenient to work with a dimensionless χ, known as the mixture fraction, defined by

$$f = \frac{\chi - \chi_{\mathrm{OX}}}{\chi_{\mathrm{FU}} - \chi_{\mathrm{OX}}} \tag{29}$$

where χ_{FU} and χ_{OX} are the values of χ in the fuel and oxidant streams, respectively. The bounds on ***fare*** zero in the oxidant stream and unity in the fuel stream. With the additional assumption of infinitely fast chemistry, the instantaneous species mass fractions are completely determined by the mixture fraction as

© 1983 Hemisphere I blishing Corporation

$$0 \leqslant f \leqslant f_{st}: \quad m_{FU} = 0 \quad m_{OX} = 1 - \frac{f}{f_{st}} \quad m_{PR} = 1 - m_{OX} \tag{30}$$

$$f_{st} \leqslant f \leqslant 1: \quad m_{FU} = \frac{f - f_{st}}{1 - f_{st}} \quad m_{OX} = 0 \quad m_{PR} = 1 - m_{FU} \tag{31}$$

where f_{st} is the stoichiometric value of the mixture fraction, that is, the value off for $\chi = 0$.

The time-average species mass fractions may be obtained by weighting the instantaneous values by the probability density function for $f, p_f(f)$, defined so that $p_f(f)\,df$ is the fractional time during which the mixture fraction is in the range $(f, f + df)$. The local time-average values of the species mass fractions are given by

$$\bar{m}_j = \int_0^1 m_j(f)\, p_f(f)\, df \tag{32}$$

where j = FU, OX, PR.

The probability density function is specified in terms of the mean and variance, which are defined as

$$\bar{f} = \int_0^1 f\, p_f(f)\, df \tag{33}$$

$$g = \int_0^1 (f - \bar{f})^2 p_f(f)\, df \tag{34}$$

The variables f and g are determined from modeled transport equations derived from the instantaneous species conservation equations [24]:

$$\nabla \cdot (\rho \bar{u} \bar{f}) = \nabla \cdot (\rho \delta_{f,\text{eff}} \nabla \bar{f}) \tag{35}$$

$$\nabla \cdot (\rho \bar{u} g) = \nabla \cdot (\rho \delta_{g,\text{eff}} \nabla g) + 2 \frac{\eta_t}{\sigma_{g,t}} \nabla \bar{f} \cdot \nabla \bar{f} - C_g \rho \frac{\epsilon}{k} g \tag{36}$$

where $\delta_{f,\text{eff}}$ and $\delta_{g,\text{eff}}$ are the effective diffusivities for f and g, $\sigma_{g,t}$ is the turbulent Prandtl-Schmidt number for g and C_g is a constant. The recommended values of these parameters are

$$\delta_{f,\text{eff}} = \delta_{g,\text{eff}} = \delta_{j,\text{eff}} \qquad \sigma_{g,t} = \sigma_{m_j,t} = 0.9 \qquad C_g = 2.0$$

The shape of $p_f(f)$ must be specified. A detailed discussion of various shapes is given in [25]. Fortunately, calculations of turbulent chemically reacting flows do not seem to be very sensitive to the precise form of the probability density function. A top hat distribution is recommended.

The formulation described above allows the time-average values of the species mass fractions to be calculated without the need to know the time-average reaction rates. An expression for the time-average reaction rate for the fuel may be calculated by weighting the instantaneous reaction rate,

$$R_{FU} = -\rho \delta_{FU} \nabla f \cdot \nabla f \frac{\delta(f - f_{st})}{1 - f_{st}} \tag{37}$$

by the probability density function $p_f(f)$. The result is [26]

$$\bar{R}_{FU} \cong -\frac{\rho(\epsilon/k) g^{1/2}}{1 - f_{st}} p_{\hat{f}}(\hat{f}_{st}) \tag{38}$$

where $\hat{f}$ is the dimensionless variable $f/g^{1/2}$, and $p_f(f_{st}) \cong 0.3$ if f_{st} is not too far from $\bar{f}$. This expression for the mean reaction rate is very similar to the eddy breakup model [27]:

$$\bar{R}_{FU} = -C_{ebu} \rho \frac{\epsilon}{k} g^{1/2} \tag{39}$$

(d) Radiation model

Thermal radiation enters as a source term in the enthalpy equation (11). Thermal radiation is governed by an integro-differential equation. The integral nature of the governing equation means that the local radiation source at a point is given by an integral over the whole flow domain. In finite-difference terminology, every point on the computational mesh is linked with every other point. In principle, the radiation equation may be solved using the zone method, as described in Sec. 3.11.6. In practice, however, this would be an exceedingly complex procedure, involving a coupling of the integral equations of the zone method to the differential equations for the flow, chemical reaction, and heat transfer. A simpler method is to replace the integro-differential equation by a system of differential equations using a flux method of approximation [28]. These equations can be solved easily together with the equations for the flow and chemical reaction.

For simplicity, the furnace gas is assumed to be a gray, nonscattering medium. The equation of radiation transfer in the direction of the unit vector $\boldsymbol{\Omega}$ is given by (see Sec. 2.9.7)

$$\boldsymbol{\Omega} \cdot \nabla I = -k_a I + k_a I_b \tag{40}$$

where I is the total radiation intensity, $I_b (\equiv \sigma T_g^4/\pi)$ is the blackbody intensity at the gas temperature T_g, and k_a is the absorption coefficient of the furnace gases. The intensity $I(\equiv I(\mathbf{r}, \boldsymbol{\Omega}))$ is a function of position $\mathbf{r}$ and direction $\boldsymbol{\Omega}$. The left-hand side of Eq. (40) is to be interpreted as a directional derivative in the $\boldsymbol{\Omega}$ direction [29].

The basis of the flux method is an analytic approxi-

© 1983 Hemisphere Publishing Corporation

mation to the directional dependence of the intensity, which reduces Eq. (40) to a system of coupled differential equations in the space variable only. The most general methods are the spherical harmonic and discrete ordinate approximations [29]. The flux method described here is a first-order spherical harmonic, or Eddington, approximation. The intensity may be formally expanded in a series as

$$I(\mathbf{r}, \Omega) = I_0(\mathbf{r}) + \mathbf{I}_1(\mathbf{r}) \cdot \Omega + \mathbf{I}_2(\mathbf{r}) : \Omega\Omega + \ldots \tag{41}$$

where $I_0, \mathbf{I}_1, \mathbf{I}_2, \ldots,$ are the expansion coefficients. In practice, the series expansion must be truncated; the simplest useful model is obtained by retaining the first two terms of the series. Equations for the expansion coefficients I_0 and $\mathbf{I}_1$ are obtained by substituting the truncated expansion (41) into the equation of transfer, Eq. (40), and forming the first two angular moments. This gives

$$\nabla \cdot \mathbf{I}_1 = -3k_a(I_0 - I_b) \tag{42}$$

$$\mathbf{I}_1 = -\frac{1}{k_a} \nabla I_0 \tag{43}$$

Substituting $\mathbf{I}_1$ from Eq. (43) into Eq. (42) leads to a single second-order differential equation for I_0:

$$\nabla \cdot \left(\frac{1}{k_a} \nabla I_0 \right) = 3k_a(I_0 - I_b) \tag{44}$$

The radiative heat flux $\mathbf{q}_r$ is given in terms of the intensity Z as

$$\mathbf{q}_r = \int_{4\pi} \Omega I \, d\Omega \tag{45}$$

Substituting the truncated expansion for the intensity into this equation gives

$$\mathbf{q}_r = \frac{4\pi}{3} \mathbf{I}_1 \tag{46}$$

The radiation source term in the enthalpy equation is

$$\nabla \cdot \mathbf{q}_r = \frac{4\pi}{3} \nabla \cdot \mathbf{I}_1 = 4\pi k_a (I_b - I_0) \tag{47}$$

(e) Numerical solution of *equations*

The basic transport equations to be solved can be written in terms of a general scalar variable ϕ as follows:

$$\nabla \cdot (\rho \bar{\mathbf{u}} \phi - \Gamma_{\phi,\text{eff}} \nabla \phi) + S_\phi = 0 \tag{48}$$

where S_ϕ denotes the source term in the equation. The differential equations are then converted into a system of algebraic finite-difference equations by any one of several possible methods [30]. For example, in the control volume method, Eq. (48) is integrated over the volume V_P of a typical cell (centered on node P) to yield

$$\int_{A_p} (\rho \bar{\mathbf{u}} \phi - \Gamma_{\phi,\text{eff}} \nabla \phi) \, d\mathbf{A} + \int_{V_P} S_\phi \, dV = 0 \tag{49}$$

The first term represents the total transport across the cell boundary by convection and diffusion, and may be expressed in terms of the mass flow rates across the boundary, and the values of ϕ at the nodal point P and at relevant neighboring locations. The integral of the source term may be expressed in linearized form as $S_0 + S_P \phi_P$. The resultant difference equation has the form

$$(a_P - S_P)\phi_P = \sum_n a_n \phi_n + S_0 \tag{50}$$

where the a_n's are coefficients involving mass flow rates and diffusion coefficients, Σ_n denotes summation over the relevant neighboring nodes, and $a_P \equiv \Sigma_n a_n$. An equation similar to Eq. (50) may be written for each variable at every grid node of the finite-difference mesh. The system of coupled, nonlinear algebraic equations is generally solved using an iterative technique: a full description of the method is beyond the scope of this section, and the reader is referred to [30-32] for a discussion of the numerical solution procedure.

Nomenclature** for **Section** 3.11.7 **appears at the beginning** of **Part 3.

REFERENCES FOR SECTIONS 3.11 .1-3.11.7

1. Berman, H. L., Fired Heaters-I. Finding the Basic Design for Your Application, *Chem. **Eng.,*** vol. 85, pp. 99-104, 1978.
2. Evans, F. L., ***Equipment Design Handbook for Refineries and Chemical Plants,*** vol. 2, chap. 1 (Fired Heaters and Boilers), Gulf Publishing Company, Houston, 1974.
3. Shields, ***C.*** D., ***Boilers-Types, Characteristics and Functions,*** McGraw-Hill, New York, 1961.
4. Rose, J. W., and Cooper, J. R., ***Technical Data*** on ***Fuel,*** chap. 5, British National Committee, World Energy Conference, London, 1977.
5. Bell, P. ***C., Industrial Fuels,*** Macmillan, Basingstoke, Hampshire, 1971.
6. Hadvig, S., Gas Emissivity and Absorptivity: A Thermodynamic Study, *J. **Inst. Fuel,*** vol. 43, pp. 129-135, 1970.
7. Hottel, H. C., and Sarofim, A. F., ***Radiative Transfer,*** McGraw-Hill, New York, 1967.

© 1983 Hemisphere Publishing Corporation

8. Sarofim, A. F., and Hottel, H. C., Radiative Transfer in Combustion Chambers: Influence of Alternative Fuels, *Proc. 6th* ***Int. Heat Transfer*** *Conf.*, ***Toronto, August 7-11, 1978,*** vol. **6,** pp. 199-217, 1978.
9. Hottel, H. C., First Estimates of Industrial Furnace Performance-The One-Gas-Zone Model Reexamined, in ***Heat Transfer in Flames,*** eds. N. H. Afgan and J. M. Beer, chap. 1, pp. S-28, Wiley, New York, 1974.
10. Hottel, H. C., Heat Transmission by Radiation, ***in Chemical Engineers Handbook,*** ed. R. H. Perry and C. H. Chilton, chap. 10, pp. 48-64, McGraw-Hill, New York, 1973.
11. Wimpress, N., Generalized Method Predicts Fired-Heater Performance, ***Chem. Eng.***, vol. 85, pp. 95-102, 1978.
12. Thring, M. W., and Newby, M. P., Combustion Length of Enclosed Turbulent Jet Flames, *Proc.* ***4th Symp.*** *(Int.)* ***Combustion, Baltimore,*** pp. 789-796, 1953.
13. Barchilon, M., and Curtet, R., Some Details of the Structure of an Axisymmetric Confined Jet with Backflow, ***.I. Basic Eng., vol.*** 86D, pp. 777-787, 1964.
14. Johnson, T. R., and Beer, J. M., The Zone Method Analysis of Radiant Heat Transfer: A Model for Luminous Radiation, *J.* ***Inst. Fuel, vol. 46,*** pp. 301-309, 1973.
15. Johnson, T. R., Lowes, T. M., and Beér, J. M., Comparison of Calculated Temperatures and Heat Flux Distributions with Measurements in the IJmuiden Furnace, ***J. Inst. Fuel,*** vol. 47, pp. 39-5 1, 1974.
16. ***Soo, S. I., Fluid Dynamics of Multiphase Systems,*** Blaisdell, Waltham, Mass., 1967.
17. Crowe, C. T., Conservation Equations for Vapour-Droplet Flows, *Proc.* ***1976 Heat Transfer and Fluid Mechanics Institute, Davis, Calif.***, ed. A. A. McKillop, J. W. Baughn, and H. A. Dwyer, chap. 13, pp. 214-228, Stanford University Press, Stanford, Calif., 1976.
18. Smoot, L. D., and Pratt, D. T., ***Pulverized-Coal Combustion and Gasification,*** Plenum, New York, 1979.
19. Caretto, L. S., Mathematical Modelling of Pollutant Formation, *Prog.* ***Energy Combust. Sci.***, vol. 1, pp. 47-71, 1976.
20. Lilley, D. G., and Wendt, J. 0. L., Modelling Pollutant Formation in Coal Combustion, *Proc.* ***1976 Heat Transfer and Fluid Mechanics Institute, Davis, Calif.***, eds. A. A. McKillop, J. W. Baughn, and H. A. Dwyer, chap. 12, pp. 196-213, Stanford University Press, Stanford, Calif., 1976.
21. Bird, R. B., Stewart, W. E., and Lightfoot, E. ***N., Transport Phenomena,*** Wiley, New York, 1960.
22. Launder, B. E., and Spalding, D. B., *Mathematical Models* ***of Turbulence,*** Academic, New York, 1972.
23. Tennekes, H., and Lumley, J. L., ***A First Course in Turbulence,*** M.I.T. Press, Cambridge, Mass., 1972.
24. Spalding, D. B., Concentration Fluctuations in a Round Turbulent Free Jet, ***Chem. Eng. Sci., vol. 26,*** pp. 95-107, 1971.
25. Pratt, D. T., Mixing and Chemical Reaction in Continuous Combustion, ***Prog. Energy Combust. Sci.,*** vol. 1, pp. 73-86, 1976.
26. Bilger, R. W., The Structure of Diffusion Flames, ***Comb. Sci. Technol.***, vol. 13, pp. 155-170, 1976.
27. Spalding, D. B., Mixing and Chemical Reaction in Steady Confined Turbulent Flames, *Proc.* ***13th Symp.*** *(Int.)* ***Combustion,*** Utah pp. 649-657, 1971.
28. Siddall, R. G., Flux Methods for the Analysis of Radiant Heat Transfer, ***J. Inst. Fuel,*** vol. 47, pp. 101-109, 1974.
29. Pomraning, ***G. C., The Equations of Radiation Hydrodynamics,*** Pergamon, New York, 1973.
30. Roache, P. J., ***Computational Fluid Dynamics,*** Hermosa, Albuquerque, N.M., 1972.
31. McDonald, H., Combustion Modelling in Two and Three Dimensions-Some Numerical Considerations, ***Prog. Energy Combust. Sci.,*** vol. 5, pp. 97-122, 1979.
32. Gosman, A. D., Pun, W. M., Runchal, A. K., Spalding, D. B., and Wolfshtein, M., ***Heat and Mass Transfer in Recirculating Flows,*** Academic, London, 1969.

© 1983 Hemisphere Publishing Corporation

3.12
Cooling towers

Contents

3.12.1
INTRODUCTION, J. R. Singham **3.12.1-1**

A. The need for cooling towers 3.12.1-1
B. Types of cooling towers 3.12.1-1
C. Structure of following sections 3.12.1-2

3.12.2
THE PACKING REGION, J. R. Singham **3.12.2-l**

A. The basis of thermal design 3.12.2-1
B. Theory of thermal design 3.12.2-3
C. The packing 3.12.2-8
D. State of air leaving packing 3.12.2-11
E. Departures from uniform counter flow 3.12.2-12

3.12.3
NATURAL DRAFT TOWERS, J. R. Singham 3.12.3-l

A. Outline of main features 3.12.3-1
B. Thermal performance and design 3.12.3-2
C. Some remarks on structural design 3.12.3-6

3.12.4
MECHANICAL DRAFT TOWERS, J. R. Singham **3.12.4-1**

A. Outline of main features 3.12.4-1
B. Thermal performance and design 3.12.4-2

3.12.5
HYBRID TOWERS, J. R. Singham **3.12.5-l**

A. Dry towers 3.1251
B. Wet-dry towers **3.12.5-2**
C. Assisted draft towers **3.12.5-3**
D. Closed-circuit evaporative coolers 3.12.5-4

3.12.6
FURTHER TOPICS, J. R. Singham **3.12.6-1**

A. Testing and acceptance 3.12.6-1
B. Water loss 3.12.6-2
C. Variation of atmospheric pressure 3.12.6-2

Nomenclature for Sections 3.12.1-3.12.6 3.12.6-3
References for Sections 3.12.1-3.12.6 3.12.6-3

© 1983 Hemisphere 1 ublishing Corporation

HEDH

3.12.1
Introduction

J. R. Singham

A. The need for cooling towers

In a great many industries it is essential to transfer heat from certain parts of the plant in order to prevent the local temperature from rising. Sometimes heat can be transferred directly to the atmosphere by natural or forced convection, but more frequently water cooling is either necessary or more economical. Where cold water is abundant, the supply can be taken from a river, lake, or estuary and returned directly at a somewhat higher temperature. But in many circumstances this is not possible, either because the supply at the preferred site is insufficient, or because the water temperature has already been raised as high as is allowable. In such cases, the plant cooling water is continuously recirculated through a cooling tower in which heat is transferred from the cooling water to the atmosphere. This, then, is the essential purpose of a cooling tower: to enable heat to be transferred conveniently and economically from plant to atmosphere, usually by means of a stream of recirculating water (though not always: In dry towers, the process fluid itself may flow through the tower-Sec. 3.12.5A).

A large demand for cooling comes from the electricity supply industry. In a 2 000-MW station that uses cooling towers, cooling water for the steam condensers circulates at a rate of more than 60 m^3/s; and about 34 liters of water from a fresh source are needed for every kilowatt-hour generated to replace water lost from the cooling towers by evaporation and to keep the circulating water acceptably pure. Cooling towers are also used extensively in many other industries, in sizes that cover a range of water flow rates of about 5 000 to 1. Among these industries are petrochemicals, steel making, food processing, industrial refrigeration, air conditioning, the chemical industry, plastics, the dairy industry, breweries, and distilleries.

The generous assistance of Visco, who provided information and drawings for mechanical draft towers, is gratefully acknowledged. Thanks are also expressed to Film Cooling Towers (1925) Ltd., who kindly supplied information about their range of products.

B. Types of cooling towers

Most cooling towers perform the same function as an automobile radiator, which is to transfer heat from warm circulating water to the atmosphere; but car radiators are regarded as heat exchangers, not cooling towers.

There is in fact no hard-and-fast distinction between the two. The spectrum of cooling tower design is very wide: at one end it includes designs that could equally well be regarded as heat exchangers; and at the other there are towering structures in which water and air are in direct contact with no heat exchanger walls separating them. The structures just referred to are the concrete shells of the large natural draft cooling towers that are part of the industrial landscape of Europe and increasingly of other parts of the world. In these towers it is the natural buoyancy of the warmed air that causes it to flow upward through the tower, as with the flue gases in a chimney. Most of them are wet towers, the water and air being in direct contact as the water trickles or

© 1983 Hemisphere Publishing Corporation

splashes over a grid of bars or plates, known as the packing. Some, though very few, are dry towers; they rely on natural draft and have a similar external appearance to their wet counterparts, but the packing is replaced by heat exchangers and there is no direct contact between water and air.

In mechanical draft towers the air is circulated by means of electrically driven fans. These towers are more numerous but less conspicuous, since the buoyancy effect of a tall chimney is no longer necessary; they cover a much wider range of sizes than natural draft towers. Again, most of them provide for direct contact in a packing and hence are wet, but dry mechanical draft towers are also widely used. It is at this part of the spectrum that cooling towers merge with heat exchangers: a small, dry, mechanical draft tower, with an axial-flow fan placed close to the heat exchanger surfaces, with no tower or chimney, and with a minimum of surrounding ducting, has become, as it were, a car radiator.

As with heat exchangers, the relative directions of flow of the water and air provide another basis of classification. The water always flows downward through the packing, but the air can flow upward (counter flow) or horizontally (cross flow). For obvious reasons, the air never flows downward (unless unintentionally), and so parallel-flow designs do not occur. Mixed flow, however, intentional and unintentional, is quite common, the air changing direction from horizontal to vertical as it flows through the packing.

The desire to combine the advantages of natural and mechanical draft has led to the design of assisted draft towers, which have both a shell to provide natural draft and an array of fans around the base of the shell to provide mechanical draft. The result is a very high-capacity cooling tower, which can perform the function of several conventional natural draft towers of the same height.

A similar desire to combine the advantages of wet and dry towers had led to the design of wet-dry towers, which make use of both direct and indirect contact between water and air in different parts of the tower. These designs are usually based on mechanical draft.

Another design variation, but one of long standing, is the closed-circuit evaporative cooler, in which the primary circulating water (or other fluid) is confined in tubes while secondary water trickles, or is sprayed, over the tubes as over a conventional cooling tower packing. Thus there is indirect contact with regard to the primary circulating water and direct contact between the secondary water and the air.

C. Structure of following sections

The performance of most cooling towers is governed by the processes that take place in the packing, and this region is crucial to the theory and practice of thermal design, whether the tower has natural or mechanical draft. The packing region is therefore discussed in general terms before attention is given to particular types of towers. The discussion is based on the important case of uniform counter flow; departures from uniform counter flow (including cross flow) are examined in a separate section. After that, natural and mechanical draft towers are discussed in turn. Then, under the heading Hybrid towers, the various special types of tower that have been referred to above are discussed in more detail. We conclude with some remarks on certain general topics: testing and acceptance; water loss; and variation of atmospheric pressure.

© 1983 Hemisphere Publishing Corporation

3.12.2
The packing region

J. R. Singham

A. The basis of thermal design

(a) Specification of cooling requirement

A cooling tower is required to cool water at a certain rate between stated inlet and exit temperatures under prescribed atmospheric conditions. A suitable list of the quantities that need to be specified is

$\dot{M}_w$, the water mass-flow rate
$T_{w,\text{in}}$, the water inlet temperature (hot)
$T_{w,\text{out}}$, the water exit temperature (cold)
T_{WB}, the atmospheric wet-bulb temperature
T_{DB}, the atmospheric dry-bulb temperature
p_a, the atmospheric pressure

Usually p_a is taken as 1 atm, and this value is to be understood throughout Sec. 3.12 unless otherwise stated. For the theory of thermal design presented in Sec. B, knowledge of T_{DB} is not required. It is needed in the case of natural draft towers for the accurate determination of the density of the entering air (Sec. 3.12.3); and in the comparatively rare cases where it is necessary to calculate the humidity of the air leaving the packing (Sec. D).

As a matter of terminology, the water temperatures may be specified as the ***cooling range,*** AT,, and either $T_{w,\text{in}}$ or $T_{w,\text{out}}$, where AT, is defined as $(T_{w,\text{in}} - T_{w,\text{out}})$. The water exit temperature is often referred to as the *recooled* ***water temperature.*** The wet-bulb depression, ΔT_{WB}, defined as $(T_{DB} - T_{WB})$, may be given as an alternative to T_{WB}. ***Also,*** the ***approach*** temperature difference $(T_{w,\text{out}} - T_{WB})$, may be specified in place of $T_{w,\text{out}}$.

(b) Importance of water-to-air mass flow ratio

Once the value of the water-to-air mass flow ratio $\dot{M}_w/\dot{M}_g$ is known, the mass flow rate of air $\dot{M}_g$ can be found, since $\dot{M}_w$ is already known from the design point specification. The designer of a mechanical draft tower can then estimate the fan requirements and tower dimensions (Sec. 3.12.4); and the designer of a natural draft tower can estimate the air pressure loss and relate it to the air buoyancy driving force, for any trial set of tower dimensions (Sec. 3.12.3). $\dot{M}_w/\dot{M}_g$ can be determined from the specification quantities and data for the packing region alone, independently of, say, the fan power for a mechanical draft tower, or of the height, say, of a natural draft tower. Thus $\dot{M}_w/\dot{M}_g$ is an important quantity that can and must be determined at an early stage of design. For both mechanical draft and natural draft towers, its value in uniform counter flow is found from the simultaneous solution of three relations,

1. Merkel s equation
2. A packing relationship
3. The enthalpy balance equation

as discussed in Sec. B. In cross-flow towers, it is found by an analogous, though somewhat more complicated procedure (Sec. E).

(c) The heat and mass transfer processes

I. Heat transfer

In a wet cooling tower, the water and air in the packing region are in direct contact at the interface between

© 1983 Hemisphere Publishing Corporation

them; Fig. 1 is a diagram of a small part of this interface. The water near the interface may be part of a film of water flowing over the packing, or it may be part of a droplet in the spray.

The local heat flux $\dot{q}$, from water to air across the interface normal to the surface, is known to depend on the difference in specific enthalpy between the air at the surface and air in the bulk stream. (The reader may wish to refer to Sec. 1.2.2C for a related discussion of this point.) For the purpose of cooling tower analysis it is safe to assume that:

1. The temperature of the air at the interface is equal to the local bulk temperature of the water.
2. The air at the interface is saturated.
3. The local heat flux $\dot{q}$ is given by

$$\dot{q} = \gamma(h_s - h_g) \tag{1}$$

where h_s = the specific enthalpy of the air at the surface
h_g = the specific enthalpy of the bulk of the air locally
γ = an empirical coefficient with the units kg/m^2 s

In accordance with assumptions 1 and 2, h_s may be taken as the specific enthalpy of saturated air at the local bulk temperature of the water. (As stated in Sec. 1.2.2, the equation is valid when the specific enthalpies of both air and water are defined to be zero at 0° C. Use of other bases may lead to unacceptable error.)

Equation (1) may be compared with the equation that would be written for heat transfer from a dry surface to the air:

$$\dot{q} = \alpha(T_s - T_g) \tag{2}$$

where T_s = the surface temperature
T_g = the temperature of the bulk of the air near the surface
α = the surface heat transfer coefficient

It may be noted that whereas dry heat transfer is proportional to the ***temperature*** difference, wet heat transfer is proportional to the ***specific enthalpy*** difference. Indeed, heat transfer can occur in a cooling tower even where the local bulk temperatures of the water and air are equal, because the bulk of the air may be less than saturated locally, so that $h_s > h_g$.

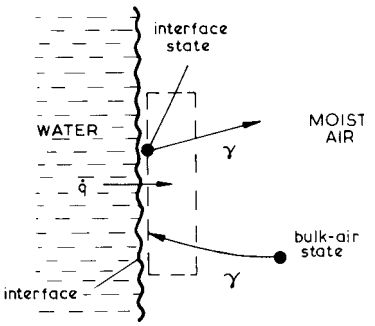

Figure 1 Reynolds flux model of local heat transfer at interface between water and air.

The coefficient γ is seen to have the units of a mass flux. Useful insight into the nature of γ can be gained by consideration of a Reynolds model of the flow [1]. According to this model, the heat transfer process on the air side of the interface may be accounted for by:

1. Flow of air, possessing the properties of the bulk air stream, from that stream to the interface, at a mass flow rate γ_R per unit area of interface
2. An equal flow of air, possessing the properties of air at the interface, from the interface to the bulk of the air stream

Application of the first law of thermodynamics to a control volume on the air side of the interface, Fig. 1, yields

$$\dot{q} = \gamma_R(h_s - h_g) \tag{3}$$

The flux γ_R may be called the Reynolds flux (following [1]). The similarity of Eq. (3) to Eq. (1) may be noted, γ_R taking the place of γ. Hence the empirical coefficient γ can be interpreted as the Reynolds flux, γ_R:

$$\gamma = \gamma_R \tag{4}$$

A similar model can be used to represent dry heat transfer for the same flow geometry, but in this case the specific enthalpy h is replaced by the product of the specific heat capacity of air at constant pressure, c_p, and air temperature, T:

$$\dot{q} \approx \gamma_R c_p(T_s - T_g) \tag{5}$$

The approximation sign is used in recognition of the fact that γ_R might not have precisely the same value in the wet and dry cases. Comparison now of Eq. (5) with Eq. (2), and use of Eq. (4) to replace γ_R, results in

$$\gamma \approx \frac{\alpha}{c_p} \tag{6}$$

Thus the coefficient γ in Eq. (1) is expected to equal (α/c_p) to a certain degree of approximation, where α is the surface heat transfer coefficient in a dry flow that is similar geometrically and in other respects. And, in the absence of more reliable information, we could use heat transfer formulas for α to obtain estimates for y. Naturally, caution is needed in making use of such estimates, partly because the Reynolds model is only an approximation to reality, and partly because the dry flow is unlikely to be closely similar geometrically to a flow that includes water films and droplets.

II. Mass transfer

Mass transfer of water vapor from the water to the air occurs simultaneously with the heat transfer. Neverthe-

© 1983 Hemisphere Publishing Corporation

less, the heat transfer can be calculated independently from Eq. (1), and usually there is no need to consider the local mass transfer process in similar detail. In most circumstances, it is safe to assume that the air leaving the packing region is saturated and to calculate its density and water content, when required, from its specific enthalpy, known from the heat transfer calculations. If, however, the exit air is thought to be unsaturated, its complete exit state cannot be determined without considering the mass transfer process (Sec. D).

B. Theory of thermal design

(a) Merkel's equation

Merkel s equation relates quantities associated with the specified cooling requirement to quantities associated with the heat transfer performance of the packing (Merkel s original paper is commented upon briefly in Sec. 1.2.2C). To obtain the equation, reference is made to a small element of the packing region in counter flow, as illustrated in Fig. 2. The heat transfer rate from water to air occurring within the element $d\dot{Q}$ is given by

$$d\dot{Q} = \dot{q} A_i \, dV \tag{7}$$

where A_i = the area of the water-air interface per unit volume
dV = the volume of the element
$\dot{q}$ = the local heat flux at the interface, given by Eq. (1)

Application of the first law to the stream of moist air flowing through the element yields

$$d\dot{Q} = (\dot{m}_g \, dA) \, dh_g \tag{8}$$

where $\dot{m}_g$ = the mass flow rate of air per unit plan area
dA = the plan area of the element
dh_g = the increase in specific enthalpy of the stream of moist air in the direction of air flow

[Strictly, Eq. (8) should be written as an approximation; but it is a good one, subject to the same warning concerning enthalpy bases as was appended to Eq. (1).]

Equating the right-hand sides of Eqs. (7) and (8), substituting for $\dot{q}$ from Eq. (1), and equating dV to $dA\,dz$ yields, upon rearrangement,

$$\frac{dh}{h_s - h_g} = \frac{\gamma}{\dot{m}_g} A_i \, dz \tag{9}$$

where dz is the length of the element in the direction of air flow.

Before integration of this equation, use is made of the enthalpy balance equation [Sec. (c)] ,

$$\dot{m}_g \, dh_g = \dot{m}_w \, dh , \tag{10}$$

to eliminate dh_g from the left-hand side; the water mass

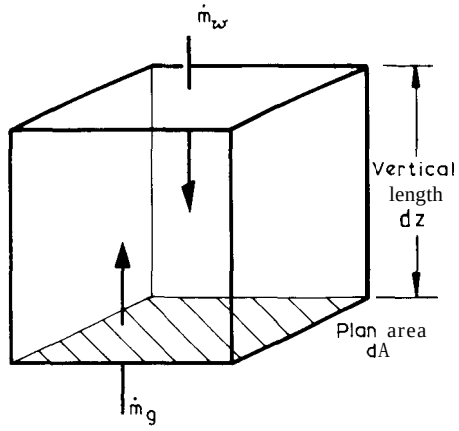

Figure 2 Counter flow through an element of the packing region. Element volume dV; interface area A_i per unit volume.

flux $\dot{m}_w$ is replaced by $\dot{M}_w/A$. After rearrangement, there results

$$\frac{dh_w}{h_s - h_g} = \frac{\gamma A_i}{\dot{M}_w} A \, dz \tag{11}$$

This equation is now integrated across the packing region from air entry to air exit:

$$\int_{h_{w,out}}^{h_{w,in}} \frac{dh_w}{h_s - h_g} = \int_{z_1}^{z_2} \frac{\gamma A_i}{\dot{M}_w} A \, dz$$

or

$$I_M = z_p \tag{12}$$

where I_M and z_p stand identically for the left-hand and right-hand sides of the upper of the two equations. Equation (12) will be taken as the basic statement of Merkel s equation. Some alternative expressions for z_p are discussed in Secs. (b) and (c). The left-hand side, I_M, can be determined (by a suitable numerical integration procedure) without knowledge of the characteristics of the packing; whereas the right-hand side, I_P, can be determined without knowledge of the properties of the air and water at entry to and exit from the tower. The designer s task is to ensure equality of the two sides of the equation [Sec. (d)] .

(b) The packing relationship

The value of the integral z_p on the right-hand side of Merkel s equation, Eq. (12), has to be determined for a particular type and depth of packing, and for particular characteristics of the associated water spray. The contribution of the spray will be overlooked for the time being; it is discussed in Sec. C(b). The quantity I_P is usually obtained from empirical data in the form of a graph or formula, which will be referred to here as the

© 1983 Hemisphere I blishing Corporation

packing relationship. The expected form of this relationship will first be stated, and then discussed.

$$I_P = f\left(\frac{\dot{m}_w}{\dot{m}_g}, \mathrm{Re}_g\right) \tag{13}$$

is the expected form where, on the right-hand side, $\dot{m}_w/\dot{m}_g$ is the water-to-air mass flux ratio and Re_g is a Reynolds number for the air stream (which could be replaced by a Reynolds number for the water stream).

Functions of this kind are in fact obtainable for particular types and depths of packing, and particular data will be discussed in Sec. C. For the moment, attention is given to clarifying the nature of the relationship expressed by Eq. (12). First, $\dot{M}_w$, in the integrand of I_P, is replaced by $(\dot{m}_w/\dot{m}_g)\dot{M}_g$, and then $\dot{m}_g$ is substituted for $\dot{M}_g/A$, with the result:

$$I_P = \frac{\dot{m}_g}{\dot{m}_w}\int_{z_1}^{z_2}\frac{\gamma}{\dot{m}_g}A_i\,dz \tag{14}$$

the ratio $\dot{m}_g/\dot{m}_w$ having been treated as a constant and taken outside the integral sign.

Since, from Sec. A(c),

$$\gamma \approx \frac{\alpha}{c_p} \tag{6}$$

Eq. (14) can be written as

$$I_P \approx \frac{\dot{m}_g}{\dot{m}_w}\int_{z_1}^{z_2}\left(\frac{\alpha}{c_p\dot{m}_g}\right)A_i\,dz \tag{15}$$

The quantity in parentheses in the integrand is of course the Stanton number for heat transfer and is a function of Reynolds number. Thus the expectation expressed by Eq. (13) is confnmed by Eq. (15).

Because $\gamma/\dot{m}_g$ in Eq. (14) is now seen to be a form of Stanton number, it might be thought necessary to seek correlations for $\gamma/\dot{m}_g$ in the way that it is done for dry Stanton numbers. In fact, it is neither necessary nor desirable to do so. Equation (14) clearly shows that it is the product of $\gamma/\dot{m}_g$ and A_i that is needed, where A_i has been defined as the surface area of the water-air interface per unit volume of packing. Since A_i includes not only the wetted surface area of the packing (usually itself fairly complex in shape), but also the surface area of the water droplets within the packing, it is better to treat $(\gamma/\dot{m}_g)A_i$ as a group of quantities. Equation (14) is now integrated, with this group treated as constant (much as the Stanton number might be treated as uniform in a heat exchanger):

$$I_P = \frac{\dot{m}_g}{\dot{m}_w}\left[\left(\frac{\gamma}{\dot{m}_g}\right)A_i(z_2 - z_1)\right] \tag{16}$$

Either the quantity z_P or the bracketed quantity can be regarded as the quantity that needs to be determined experimentally and expressed empirically as a function of dimensionless flow rates or ratios. Both practices are in use, and there are some differences in terminology that need to be clarified. These matters are discussed in the following section.

(c) Remarks on terminology

The expression for z_P in Eq. (16) can be handled for practical purposes in two closely related but different ways. Since both practices are in common use, it is desirable to discuss them both and to relate one to the other. The first to be discussed expresses the performance of the packing as the number of transfer units NTU, whereas the second expresses the performance as a packing characteristic quantity, KaV/L. Both quantities are dimensionless and bear a very simple relationship to each other, which is given below.

According to the first practice, the bracketed quantity in Eq. (16) is taken as the measure of performance of the packing and designated as the number of transfer units NTU. The product $A_i(z_2 - z_1)$ within the same brackets is equal to the surface area of the water-air interface per unit plan area of packing, a_i. Hence NTU can be defined by

$$\mathrm{NTU} \equiv \frac{\gamma}{\dot{m}_g}a_i \tag{17}$$

Thus NTU can be regarded as the product of a Stanton number and a geometric feature of the packing, a_i. All three of these quantities are obviously dimensionless. Since a_i is proportional to the depth of the packing in the flow direction, NTU may also be expected to be proportional to the packing depth, $z_2 - z_1$. Hence it is often convenient to make use of the number of transfer units per unit length NTU :

$$\mathrm{NTU}' \equiv \frac{\mathrm{NTU}}{z_2 - z_1} \tag{18}$$

Substitution of NTU for the quantity in square brackets in Eq. (16) leads to

$$I_P = \frac{m_g}{\dot{m}_w}\,\mathrm{NTU} \tag{19}$$

And substitution of this expression for z_P in Eq. (12) leads to an alternative statement of Merkel s equation:

$$\int_{h_{w,\mathrm{out}}}^{h_{w,\mathrm{in}}}\frac{dh_w}{h_s - h_g} = \frac{\dot{m}_g}{\dot{m}_w}\,\mathrm{NTU} \tag{20}$$

Since z_P is a function of $\dot{m}_w/\dot{m}_g$ and Re_g, it is evident from Eq. (19) that NTU is also a function of these two quantities:

© 1983 Hemisphere I blishing Corporation

$$\text{NTU} = f\left(\frac{\dot{m}_w}{\dot{m}_g}, \text{Re}_g\right) \tag{21}$$

According to the second practice, the quantity Zp is taken as the measure of performance of the packing. In Eq. (16), $\dot{m}_g$ is canceled in the right-hand side, with the result that

$$I_P = \frac{\gamma A_i (z_2 - z_1)}{\dot{m}_w} \tag{22}$$

Also, different symbols are used: γ is replaced by K, A_i by a, and $\dot{m}_w$ by L, the meanings being the same. Further, $z_2 - z_1$ is replaced by V, defined as the effective packed volume per unit plan area of packing. Thus, for the second practice, we have a further version of Merkel s equation:

$$\int_{h_{w,\text{out}}}^{h_{w,\text{in}}} \frac{dh_w}{h_s - h_g} = \frac{KaV}{L} \tag{23}$$

Like NTU, the group KaV/L is to be treated as an entity and as a function of $\dot{m}_w/\dot{m}_g$:

$$\frac{KaV}{L} = f\left(\frac{\dot{m}_w}{\dot{m}_g}, \text{Re}_g\right) \tag{24}$$

Evidently the two practices are very closely related, and the packing relationship can be expressed equally well by either Eq. (21) or Eq. (24). The first practice has the advantage that the measure of performance of the packing, NTU, is recognizable as a form of Stanton number, with some conceptual advantage to those familiar with dry heat transfer. The second practice has the advantage of eliminating the ratio $\dot{m}_w/\dot{m}_g$ from Merkel s equation. Comparison of Eq. (20) and Eq. (23) shows the relation between the two measures to be

$$\frac{KaV}{L} = \frac{m_g}{\dot{m}_w}\,\text{NTU} \tag{25}$$

(d) The enthalpy balance equation

The third of the three relations needed for calculating the water-to-air flow ratio is the enthalpy balance equation (in both differential and overall forms). For a thin element taken horizontally across unit plan area of the packing region at an arbitrary level, the heat transfer rate $d\dot{Q}$ from water to air in counter flow may be written in terms of the increases in specific enthalpy of the air and water streams in the direction of air flow:

$$d\dot{Q} = \dot{m}_g\, dh_g = \dot{m}_w\, dh_w \tag{26}$$

Integration of the equation over the whole of the packing region yields

$$\dot{m}_g (h_{g,\text{out}} - h_{g,\text{in}}) = \dot{m}_w (h_{w,\text{in}} - h_{w,\text{out}}) \tag{27}$$

These are the two forms of the required equation. [As pointed out in Sec. 1.2.4, the enthalpy balance equation written in the form of Eq. (27) is approximate; so, it may be added, is Eq. (26). Provided that the specific enthalpies of both air and water are defined to be zero at 0°C, the errors due to the approximations are acceptably small.]

(e) Determination of water-to-air mass flo w ratio

The three relations required for determining the water-to-air flow ratio have now been assembled and the method of determination can now be described. Three steps are required:

1. Determination of the quantity I_M in Merkel s equation from

$$\int_{h_{w,\text{out}}}^{h_{w,\text{in}}} \frac{dh_w}{h_s - h_g} = I_M \tag{28}$$

at values of $\dot{m}_w/\dot{m}_g$ within the likely range of this variable

2. Determination of Zp from the packing relationship, again at different values of $\dot{m}_w/\dot{m}_g$

3. Finding the value of $\dot{m}_w/\dot{m}_g$ for which $I_M = Zp$

Step 1

The method of determining I_M from Eq. (28) can conveniently be explained by referring to a graph on which h_s and h_g are plotted against h_w, as sketched in Fig. 3. The scale for water temperature, T_w, is also indicated, since T_w rather than h_w is usually given in the specification. It will be recalled that h_s is the specific enthalpy of saturated air. The h_s–h_w curve and the T_w–h_w scale sketched can be drawn with adequate accuracy from the data in Table 1.

The values of $h_{w,\text{out}}$ and $h_{w,\text{in}}$ marked on the

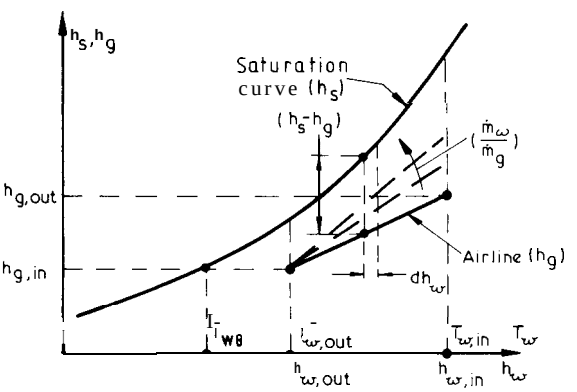

Figure 3 Evaluation of $I_M = \int_{h_{w,\text{out}}}^{h_{w,\text{in}}} (dh_w)/(h_s - h_g)$. The saturation curve h_s can be constructed from data in Table 1.

© 1983 Hemisphere I blishing Corporation

Table 1 Properties of water substance, dry air, and saturated air[a]

Temperature, °C	Saturated water substance: Saturation pressure, kN/m²	Saturated water substance: Specific enthalpy, kJ/kg: Water	Saturated water substance: Specific enthalpy, kJ/kg: Steam	Saturated water substance: Specific volume, steam, m³/kg	Dry air: Specific enthalpy, kJ/kg	Dry air: Density, kg/m³	Saturated air (p = 1 atm): Specific enthalpy, kJ/kg	Saturated air (p = 1 atm): Density, kg/m³	Saturated air (p = 1 atm): Mass fraction humidity, kg/kg
0	0.61	0.0	2 501.6	206.2	0.0	1.293	9.4	1.289	0.003 76
2	0.71	8.4	2 505.2	179.9	2.0	1.283	12.9	1.280	0.004 34
4	0.81	16.8	2 508.9	157.3	4.0	1.274	16.6	1.270	0.005 00
6	0.93	25.2	2 512.6	137.8	6.0	1.265	20.5	1.260	0.005 76
8	1.07	33.6	2 516.2	121.0	8.0	1.256	24.6	1.251	0.006 61
10	1.23	42.0	2 519.9	106.4	10.0	1.247	29.0	1.241	0.007 57
12	1.40	50.4	2 523.6	93.8	12.1	1.238	33.8	1.232	0.008 65
14	1.60	58.8	2 527.2	82.9	14.1	1.229	38.9	1.222	0.009 87
16	1.82	67.1	2 530.9	73.4	16.1	1.221	44.3	1.213	0.011 24
18	2.06	75.5	2 534.5	65.1	18.1	1.212	50.2	1.203	0.012 77
20	2.34	83.9	2 538.2	57.8	20.1	1.204	56.6	1.194	0.014 49
22	2.64	92.2	2 541.8	51.5	22.1	1.196	63.4	1.184	0.016 40
24	2.98	100.6	2 545.5	45.9	24.1	1.188	70.8	1.175	0.018 54
26	3.36	108.9	2 549.1	41.0	26.1	1.180	78.9	1.165	0.020 91
28	3.78	117.3	2 552.7	36.7	28.1	1.172	87.6	1.156	0.023 56
30	4.24	125.7	2 556.4	32.9	30.1	1.165	97.1	1.146	0.026 50
32	4.75	134.0	2 560.0	29.6	32.1	1.157	107.3	1.136	0.029 76
34	5.32	142.4	2 563.6	26.6	34.1	1.149	118.5	1.127	0.033 37
36	5.94	150.7	2 567.2	24.0	36.1	1.142	130.7	1.117	0.037 36
38	6.62	159.1	2 570.8	21.6	38.2	1.135	144.0	1.107	0.041 78
40	7.38	167.5	2 574.4	19.55	40.2	1.127	158.4	1.096	0.046 66
42	8.20	175.8	2 577.9	17.69	42.2	1.120	174.1	1.086	0.052 04
44	9.10	184.2	2 518.5	16.04	44.2	1.113	191.3	1.076	0.057 97
46	10.09	192.5	2 585.1	14.56	46.2	1.106	210.0	1.065	0.064 5 1
48	11.16	200.9	2 588.6	13.23	48.2	1.099	230.4	1.054	0.071 70
50	12.33	209.3	2 592.2	12.05	50.2	1.093	252.6	1.042	0.079 62

[a] The properties of saturated air are referred to the mass of moist air. The table can be used to find the properties of nonsaturated air of known relative humidity, ϕ, from those of dry air (ϕ = 0) and saturated air (ϕ = 1) at the same temperature by linear interpolation.

diagram are obtained from the water inlet and exit temperatures, $T_{w,\text{in}}$ and $T_{w,\text{out}}$, given in the specification.

The specific enthalpy of the air at entry to the packing region, $h_{g,\text{in}}$, is equal to the specific enthalpy of saturated air at a temperature equal to the atmospheric wet-bulb temperature, T_{WB}, given in the specification (since the specific enthalpy of moist air at atmospheric pressure is a function of wet-bulb temperature alone, for defined zero specific enthalpies of air and water at 0° C).

The value of $h_{g,\text{out}}$ at any assumed value of $\dot{m}_w/\dot{m}_g$ is found from the enthalpy balance equation, Eq. (27). Equation (26) shows that the slope of the h_g-h_w line, dh_g/dh_w, is constant and equal to $\dot{m}_w/\dot{m}_g$: Intermediate values of h_g can therefore be interpolated linearly.

The value of the integral I_M in Eq. (28) can now be evaluated from a graph like that sketched in Fig. 3, or from a table of values or formula for h_s, by any convenient numerical procedure. The simplest method is the original one proposed by Merkel: $h_s - h_g$ is taken as equal to $\bar{h}_s - \bar{h}_g$, where the bars denote means of the entry and exit values of the quantity. Since the h_s-h_w curve is concave facing upward, a little thought reveals that the value of I_M obtained by Merkel s approximation is too small, though the method does have the advantages of simplicity and therefore of lending itself to analytical development. But the ready availability of electronic calculators and computers nowadays renders such approximation unnecessary and undesirable.

A much more accurate but still fairly simple approximation is the use of a four-point quadrature formula: $h_s - h_g$ is taken as the mean of its values at 0.1, 0.4, 0.6, and 0.9 of the distance along the horizontal axis h_w between $h_{w,\text{out}}$ and $h_{w,\text{in}}$[2].

As the value of $\dot{m}_w/\dot{m}_g$ increases, the slope of the h_g-h_w line increases proportionately, the line pivoting anticlockwise about its left-hand end toward the h_s-h_w curve. Clearly, therefore, the value of the integral I_M increases with $\dot{m}_w/\dot{m}_g$. Moreover, as the h_g-h_w line approaches contact with the h_s-h_w line, the integral tends to infinity. Thus there exists a limiting value of $\dot{m}_w/\dot{m}_g$ at and above which the tower cannot meet the specified cooling requirement (however much packing is employed). Obviously the designer will avoid using

© 1983 Hemisphere Publishing Corporation

water-to-air flow ratios anywhere near as high as this limiting value. A curve showing the variation of the integral is sketched in Fig. 4.

Step 2

The quantity I_P must next be evaluated from the right-hand side of Merkel s equation, by means of Eq. (21) or of Eq. (24), for the same range of values of $\dot{m}_w/\dot{m}_g$ as in step 1. This requires the selection of the type and depth of packing to be used and assembly of the corresponding performance data. These data may take the form of graphs or formulas for NTU or KaV/L as functions of $\dot{m}_w/\dot{m}_g$ and Re_g, as represented by Eq. (21) and Eq. (24). The main discussion of such data is deferred until Sec. C. For the moment it suffices to say that the influence of Re_g as a variable is frequently unknown and therefore ignored; and that NTU increases with $\dot{m}_w/\dot{m}_g$ and KaV/L decreases, in the manner sketched in Fig. 5. To obtain I_P from NTU, NTU must be divided by $\dot{m}_w/\dot{m}_g$ as required by Eq. (19).

Step 3

I_M, the right-hand side of Merkel s equation, and I_P, the left-hand side, have now been found at a number of values of $\dot{m}_w/\dot{m}_g$. The two sides are equal at only one value of $\dot{m}_w/\dot{m}_g$, which can be found from the point of intersection of the I_M-$(\dot{m}_w/\dot{m}_g)$ and I_P-$(\dot{m}_w/\dot{m}_g)$ curves, as sketched in Fig. 6, or by other means.

The value of the water-to-air mass flux ratio has now been determined for the specified cooling requirement and the selected type and depth of packing. The water-to-air mass flow ratio is also known, since it is equal to the mass flux ratio.

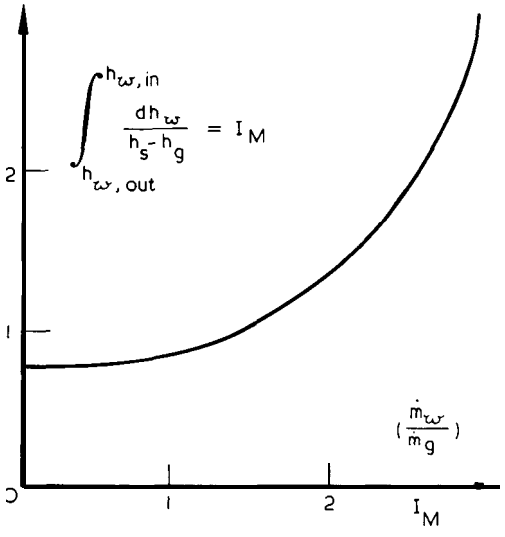

Figure 4 Variation of the integral I_M in Merkel s equation with water-to-air mass flux ratio for a specified cooling requirement (diagrammatic).

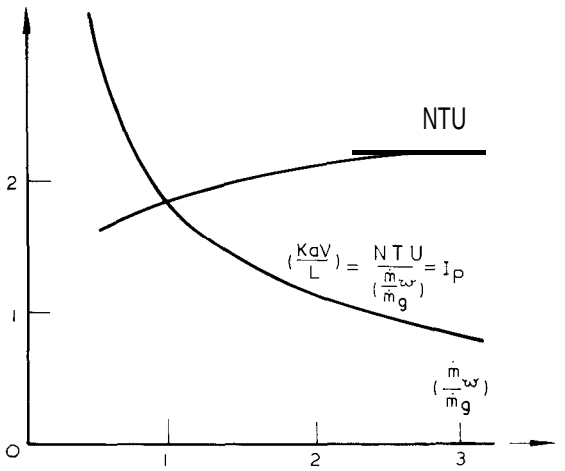

Figure 5 Variation with water-to-air mass flux ratio of packing heat transfer performance (diagrammatic).

(f) *The remaining task*

With the water-to-air mass flow ratio $\dot{M}_w/\dot{M}_g$ now known, the mass flow rate of the air stream $\dot{M}_g$ can be calculated from

$$\dot{M}_g = \frac{M_w}{\dot{M}_w/\dot{M}_g} \tag{29}$$

$\dot{M}_w$ being known from the specification.

The designer of a natural draft tower can now estimate the pressure loss through the tower for any trial set of dimensions and adjust the dimensions to ensure that the pressure loss is balanced by the available buoyancy driving force (Sec. 3.12.3). Similarly, the designer of a mechanical draft tower can estimate the pressure loss and fan size and power for any trial value of the plan cross-sectional area of the tower (Sec.

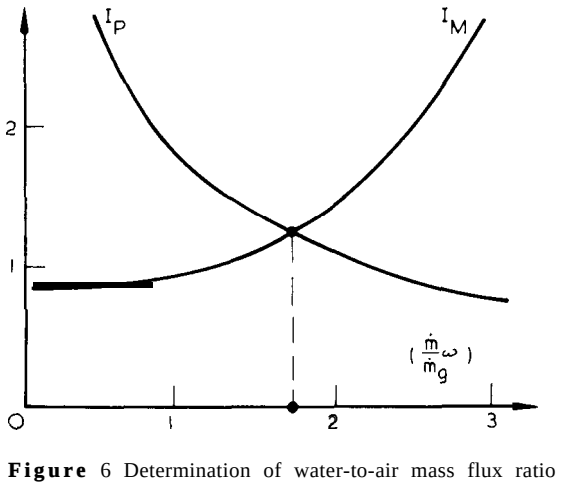

Figure 6 Determination of water-to-air mass flux ratio from intersection of curves for I_M (obtained from tower cooling requirement) and I_P (obtained from packing characteristics) (diagrammatic).

© 1983 Hemisphere 1 blishing Corporation

3.12.4). In both cases, there are an infinite number of possible sets of dimensions that will satisfy the specified cooling requirement at the calculated air flow. The designer will therefore look for the set corresponding to minimum total cost.

C. The packing

(a) Choice of *packing*

The purpose of the packing is to arrest the falling water in such a way as to create a large surface area of contact between the water and air streams. This can be achieved in two principal ways: by causing the water to trickle over a grid of horizontal splash bars, or by causing it to form a thin film over the surface of the packing material. A given type of packing may rely primarily on splash or on film, or make significant use of both. In principle, the packing material is not essential-the water can be supplied as a freely falling spray to an empty region through which the air passes; Lowe and Christie [3] discuss some experimental work in this field. However, to date virtually all cooling towers use some kind of packing material to control the water, probably because of the difficulty of maintaining a stable spray in an empty space. Nevertheless, spray-filled space above and below a packing can make a significant contribution to the total water-to-air interface area and to the heat transfer.

Packings can be made from a variety of materials, including wooden or plastic laths, corrugated asbestos-cement sheets, formed plastic sheets and sheets of galvanized steel, resin-impregnated paper or glass fiber. Some of the packings tested by Lowe and Christie are illustrated in Fig. 7. Wooden laths are the most widely used, usually in the form of splash bars, but laths of suitable geometry can also support a high proportion of film surface. Corrugated asbestos-cement sheets have been found durable and effective in large towers and have been used to about the same extent as timber laths in natural draft towers built in recent years for the Central Electricity Generating Board [4]. But this type of sheet is heavy, requires careful handling, and is less suitable in small or medium-sized mechanical draft towers, for which splash bars or specially formed plastic sheet packings are more suitable.

The factors influencing the choice of packing are heat transfer performance, pressure loss, total packing cost, and durability. Durability, including freedom from maintenance, is specially important in electrical power generation and other applications where the cooling towers represent a very small part of the total plant cost, since a shutdown for cooling tower maintenance is very expensive. In comparing the costs of different packings, account must be taken of associated costs such as the cost of the support structure (high for a heavy material), cost of water pumping (high for a tall packing), and cost of installation (higher for site assembly than for factory-built modules).

Obviously, a packing that has lower cost, higher heat transfer performance, and lower pressure loss than other packings is one to be preferred. But the problem of selection becomes more difficult when a packing is better in one or two respects and worse in the remainder. Thus a particular packing might be very cheap and have a high heat transfer performance but still be unsuitable because of its high pressure loss. The problem has been discussed in some detail by Lieberam [5], who displays the relative merits of different packings for natural draft cooling towers as points on a graph in which log R_p is plotted against log C_p, where R_p is the ratio of the pressure drop to heat transfer performance, taken as the number of dynamic pressures lost per unit length divided by the number of transfer units per unit length; and where C_p is the cost per unit cross-sectional area of a transfer unit for a particular packing. Symbolically,

$$R_p \equiv \frac{N'_{v,p}}{\mathrm{NTU}} \tag{30}$$

and

$$C_p \equiv \frac{c_p}{\mathrm{NTU}'} \tag{31}$$

where $N'_{v,p}$ = number of dynamic pressures lost per unit length

NTU = number of transfer units per unit length

c_p = cost of unit volume of packing

[The number of transfer units, NTU and NTU , were defined and discussed in Sec. B(c). It may be recalled that NTU is a form of Stanton number and is proportional to KaV/L at a fixed water-to-air mass flux ratio.] The graph is shown diagramatically in Fig. 8. Each point represents the cost performance of a packing (at the same water and air mass fluxes, for strict comparability). Points near the vertical and horizontal axes are good. Unfortunately, one point may lie nearer to the vertical axis than another that lies nearer to the horizontal axis. Lieberam resolves this difficulty by plotting lines of constant total cost for an optimized tower on the same axes, thus providing a basis of discrimination between such points. Although the method is applied only to natural draft towers, its extension to mechanical draft towers is discussed.

In the majority of cases it would be neither practicable nor profitable to follow through a full rational procedure of optimization for both the tower as a whole and the type of packing, since the time needed and the associated cost would offset the possible gain, Such a procedure is justified for a large project with high

© 1983 Hemisphere Publishing Corporation

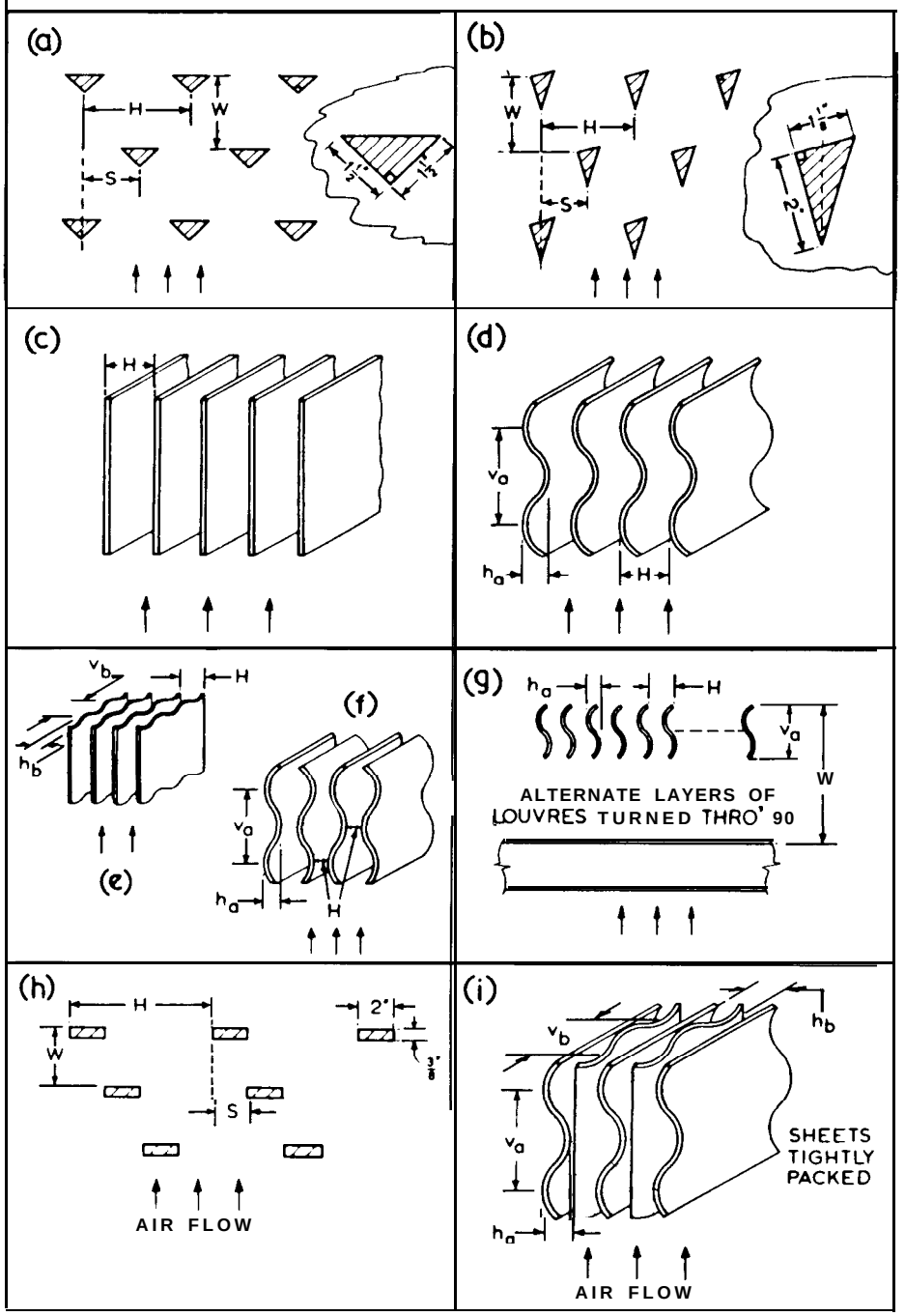

Figure 7 Geometry of packings tested by Lowe and Christie [3].

potential cost savings; otherwise cost comparison of a number of trial designs is more appropirate.

(b) Heat transfer data

As stated in Sec. B(b), two measures of the heat transfer performance of a given depth of the packing are in common use, namely, the number of transfer units NTU and the group KaV/L, which is identically equal to NTU divided by the water-to-air mass flux ratio $\dot{m}_w/\dot{m}_g$. For the presentation of data, it is more convenient to refer to unit depth of packing and to discuss NTU , the number of transfer units per unit length, or Ka/L, which is identically equal to $\mathrm{NTU}'/(\dot{m}_w/\dot{m}_g)$. Both NTU and Ka/L can be presented as analytical, graphical, or tabular functions of $\dot{m}_w/\dot{m}_g$ and, if the data warrant it, of another flow variable, usually $\dot{m}_w$ or $\dot{m}_g$, but alternatively a corresponding Reynolds number. Lowe and

© 1983 Hemisphere Publishing Corporation

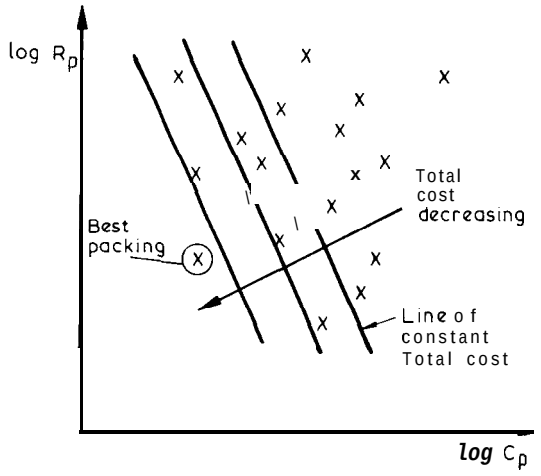

Figure 8 Selection of best packing [5].

Christie [3] found that almost all their results could be represented in the form

$$\frac{Ka}{L}\frac{m_w}{\dot{m}_g} \equiv \mathrm{NTU}' = \lambda\left(\frac{\dot{m}_w}{\dot{m}_g}\right)^{1-n} \qquad (32)$$

with neither $\dot{m}_w$ nor $\dot{m}_g$ necessary as a separate variable. For a splash bar packing with the geometry of Fig. 7*a*, with $H = W = 152.4$ mm and $S = 76.2$ mm, they found that $\lambda = 0.309\ \mathrm{m}^{-1}$ and $n = 0.5$. For corrugated asbestos-cement sheets with geometry (*d*), and with $h_a = 54.0$ mm, $v_a = 146.0$ mm, and $H = 44.5$ mm, they found that $\lambda = 0.691\ \mathrm{m}^{-1}$ and $n = 0.69$. The data were obtained from tests in an experimental tower $1.216\ \mathrm{m}^2$ with packing depths of about 1.2-2.4 m and pure counter flow.

Lieberam [5], however, using a smaller cross section, $0.456\ \mathrm{m}^2$, found it necessary to include $\dot{m}_w$ as a variable in order to correlate his data adequately. Lieberam also carried out dry heat transfer tests on corrugated sheet packings and compared the results with data for wet tests on packings of similar geometry. The agreement between the two sets of data, when expressed in the comparable form of (Stanton number)–(Reynolds number) was quite close, providing support both for the interpretation of NTU as a form of Stanton number and for the use of the Reynolds flow model for deducing wet from dry da[Secs. A(c) and B(c)].

Tezuka [6] reports data obtained in an experimental counter-flow tower, $0.6\ \mathrm{m}^2$, for film packings with smooth honeycomb passages formed by resin-impregnated paper, and with plate-and-corrugated fin passages formed from plastic sheet. He is able to correlate these data for several geometries and over ranges of water and air flow rates by a single, simple, power law, dimensionless equation.

For cross-flow packings, the same form can be used for the presentation of heat transfer data (though the manner in which the data are used in design is necessarily different-Sec. E). However, several different forms are used, and the user of such data needs to be careful in their interpretation. The data are to be found more readily in manufacturers publications than in the open literature. In cross flow the air flows horizontally instead of vertically and at right angles to the direction of water flow. But since NTU (or Ka/L) is a kind of heat transfer coefficient, its value is likely to depend more on the geometry of the passage through which the air flows and to follow the same trend as data for counter flow with a similar passage geometry. Such data as are available confirm these expectations. For example, data for wooden splash bars, issued by a manufacturer in graphic form, can be recast in the form of Eq. (32), with $\lambda = 0.44\ \mathrm{m}^{-1}$ and $n = 0.59$ for a particular geometry. Hayashi et al. [7] correlate data for a film packing of plastic (PVC) plates of eliminator shape with a power law equation for a Nusselt number in terms of the air and water Reynolds numbers. Expressed in the form of Eq. (32), n would have a value of 0.42, whereas λ would be weakly dependent on $\dot{m}_g$ (to the power -0.09).

When evaluating the heat transfer performance of a tower from packing data, it is important to consider the contribution of the spray insofar as it is not already accounted for in the packing data. For a spray in counter flow, Lowe and Christie [3] suggest a value of λ in Eq. (32) in the range 0.033-0.066 m^{-1} with n about 0.5. In a counter-flow design the value of NTU for the spray is simply added to the NTU value for the pack. In a film-packed natural draft tower, the allowance for the spray might be about a quarter of the total [8, 9]. The eliminator louvers may also be expected to make a contribution, though a smaller one.

Data obtained from tests on full-scale towers are preferable to data from small-scale experiments, and there should be a logical correspondence between the design procedures and those used in obtaining the data. For example, the procedures used for evaluating the integral I_M in Merkel s equation, Eq.(12), should be equivalent.

(c) Pressure drop

The pressure drop data for the packing can be expressed by the value of $N'_{v,p}$, the number of dynamic pressures lost per unit length in the direction of air flow. As a rough approximation, $N'_{v,p}$ may be taken as constant for a given packing geometry, but usually its value falls with air mass flux $\dot{m}_g$ and rises with water mass flux $\dot{m}_w$. Data for the packings illustrated in Fig. 7 are presented by Lowe and Christie [3]. For the splash bar packing of geometry *(a)*, for which heat transfer data and dimensions were quoted in Sec. (b), the value of $N'_{v,p}$ was

© 1983 Hemisphere Publishing Corporation

12.17 m^{-1} for a water mass flux of 1.365 kg/s m^2 at an air velocity of 0.912 m/s; this value fell to 10.85 when the air velocity was doubled, and rose to 15.79 when the water mass flux was doubled. The corresponding three values of $N'_{v,p}$ for the corrugated asbestos-cement packing with geometry (*d*) referred to in Sec. (c) were 10.53, 8.88, and 12.50. Tezuka [6] gives pressure drop data for the plastic film packs referred to in the same section, but in a dimensional form.

When the contribution of the spray to heat transfer is large, there is likely to be an associated pressure drop. Some data are provided by Lowe and Christie [3], but with cautionary remarks concerning their accuracy. Rish [8] based his estimate for spray pressure drop on Eq. 3.12.3(10) for the film-packed natural draft tower to be referred to in Sec. 3.12.3B(b).

D. State of air leaving packing

The specific enthalpy of the air at exit from the packing, $h_{g,\text{out}}$, is known as a by-product of the determination of the water-to-air mass flux ratio. However, this is insufficient to fix the state completely. Further knowledge of the state is likely to be needed for two purposes: first, in order to calculate the amount of water carried away by the air; and second, for natural draft towers, to provide a good estimate of the change in density. In most circumstances, the air leaving the packing region is close to saturation and can safely be assumed saturated: its state is then defined by its known specific enthalpy alone, and its corresponding mass fraction humidity and density can be found, for example, from Table 1.

The circumstances in which the exit state of the air may be significantly different from the saturation state are hot, dry ambient air; high mean water temperature; or short depth of packing. If the ambient air is close to saturation, the air will remain so as it flows through the packing; otherwise, any combination of these three conditions may result in a significant degree of non-saturation at exit.

To find the humidity at exit, it is necessary to follow its variation through the packing. Several kinds of humidity can be defined, and the one most convenient for the present purpose is the mass of moisture per unit mass of moist air, which may be called the mass fraction humidity and denoted by f. A Reynolds model, similar to that used for the analysis of heat transfer (Sec. A) and sketched in Fig. 1, may be used to analyze the process of mass transfer of water vapor from the water-air interface to the air. The equation representing mass conservation of water is then

$$w = \gamma_w \frac{f_s - f_g}{1 - f_s} \tag{33}$$

where $\dot{w}$ = the mass transfer rate of water per unit area of interface

f_g = the mass fraction humidity of the bulk of the air near the interface

f_s = the mass fraction humidity of the air at the interface

γ_w = the Reynolds flux for mass transfer, units kg/m^2 s

An equation for the change in humidity of the bulk air stream in the flow direction may be obtained by application of the principle of mass conservation of water to the bulk air stream:

$$\dot{m}_g \, df_g = \dot{w} A_i \, dz \tag{34}$$

where $\dot{m}_g$ = the mass flow rate of air per unit plan area of packing

A_i = the area of the water-air interface per unit volume

dz = an element of distance in the direction of air flow

$\dot{w}$ may now be eliminated, with the result that

$$\frac{df_g}{f_s - f_g}(1 - f_s) = \left(\frac{\gamma_w}{\dot{m}_g} A_i\right) dz \tag{35}$$

Reference to Eq. (9) reveals that the right-hand side of the last equation may be replaced by $dh_g/(h_s - h_g)$, provided that the Reynolds flux for mass transfer, γ_w, may be equated to the Reynolds flux for heat transfer, γ. This equation ($\gamma_w = \gamma$) may be made with acceptable accuracy when the Lewis number for the mixture approximates to unity, and this is so for moist air [1]. The following equation may therefore be written:

$$\frac{df_g}{f_s - f_g}(1 - f_s) = \frac{\dot{m}_w}{\dot{m}_g} \frac{dh_w}{h_s - h_g} \tag{36}$$

where dh_g has been replaced by $(\dot{m}_w/\dot{m}_g)\,dh_w$, by use of Eq. (26).

Equation (36) provides the means whereby the variation of f_g through the packing region may be determined by a step-by-step numerical procedure (Fig. 9). The h_s and h_g lines and the ratio $\dot{m}_w/\dot{m}_g$ are obtained by procedures already described. The f_s–h_w line may be drawn by making use of Table 1, with the assumption [made also in Sec. A(c)I] that the air at the water-air interface is saturated. The initial values of h_s, h_g, f_s, and f_g are either known or readily determined. The increments in f_g, Δf_g, may therefore be evaluated for finite increments in h_w, Ah,, by treating Eq. (36) as a finite-difference equation. Thus the true exit value of the mass fraction humidity of the air stream can be found. This value and the known specific enthalpy fix the exit state of the air.

© 1983 Hemisphere Publishing Corporation

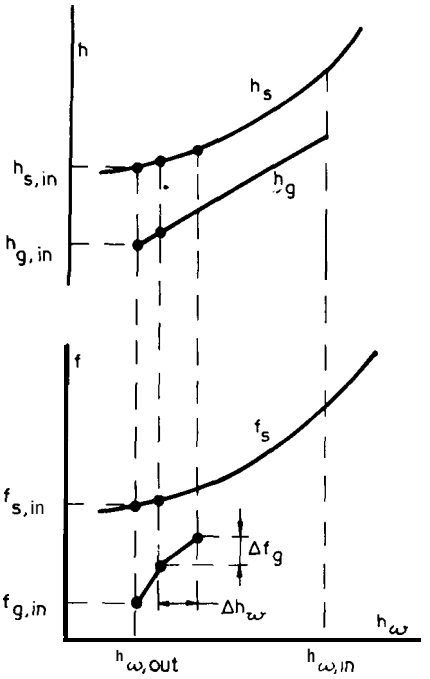

Figure 9 Determination of variation of mass fraction humidity f_g by finitedifference calculation, using Eq. (36).

E. Departures from uniform counter flow

Throughout this discussion it is usually assumed that flow through the tower is uniform, one-dimensional counter flow, that is, that the water and air flow parallel to one another in opposite directions and that the velocities, specific enthalpies, and other properties of the two streams vary only in the direction of motion. Two important departures from such conditions will now be discussed briefly:

1. Nonuniform counter flow
2. Cross flow

(a) Nonuniform counter flow

In both natural and mechanical draft counter-flow towers, the air changes its direction through a right angle as it enters the packing region. It is therefore to be expected that conditions in the packing will deviate appreciably from uniformity. Full-scale test data tend to confirm this expectation. For a natural draft tower, designed ostensibly for radial uniformity, Rish [8] obtained measurements of air velocity above the packing that varied from about 0.5 m/s on the axis to more than 1.2 m/s near the wall; and measurements of wet-bulb temperature above the packing varying from 36.7°C on the axis to 35.1°C at the wall. Measurements of this kind are difficult to carry out and subject to unavoidable error; nevertheless, there is little doubt that considerable nonuniformity can exist even when wind effects are absent. In forced draft towers the fans are likely to add to the nonuniformity of conditions below the packing, while in induced draft towers the fans tend to draw more air from the region directly below and less from the sides. However, towers can be designed adequately on a one-dimensional basis, provided that care is taken to ensure that the design procedure correctly predicts the test performance of towers of similar design [9]. One alternative is to resort to a two- or three-dimensional, computer-aided numerical analysis. Another, simpler alternative, is to assume a shape for the velocity profile of the air across the packing, normal to the direction of flow, basing it on test data or on rational expectation. This profile would then be used in calculating the mean water-to-air mass flow ratio and the mean pressure drop across the packing.

(b) Cross flow

As is well known, cross-flow heat exchangers can be designed by using counter-flow theory with the application of a correction factor; and in some circumstances the correction factor is near to unity and can, as an approximation, be ignored. A similar approach can be applied to cross-flow cooling towers, but the problem is more difficult because of the nonlinear relation between the specific enthalpy of saturated air and of water at the same temperature. However, with the availability of computers and electronic calculators, there is no reason to evade the real two-dimensionality of the problem, except perhaps for preliminary approximate calculations. The problem can be set up as one to be solved by a numerical, finite-difference procedure. If necessary, the specific enthalpies and the mass fluxes can be solved for, but in most cases it is sufficient to treat the mass fluxes as known. Thus the water mass flux might be taken as uniform, whereas the air mass flux could be taken as uniform in the direction of flow and conforming to an assumed profile normal to the flow. The problem then becomes a comparatively simple one, whose solution may be outlined in the following terms.

Figure 10 represents a rectangular element of the packing with air flowing horizontally in the z direction from left to right and with water l-lowing vertically downward in the y direction. The element has unit thickness normal to the yz plane. By an analysis similar to that used to obtain Eq. (11) for an element in counter flow, the following approximate equations can be derived.

$$\delta h_g = (h_s - h_g)\mathrm{NTU}'\,\delta z \tag{37}$$

and

$$\delta h_w = \frac{\dot{m}_g}{\dot{m}_w}\frac{\delta y}{\delta z}\,\delta h_g \tag{38}$$

© 1983 Hemisphere Publishing Corporation

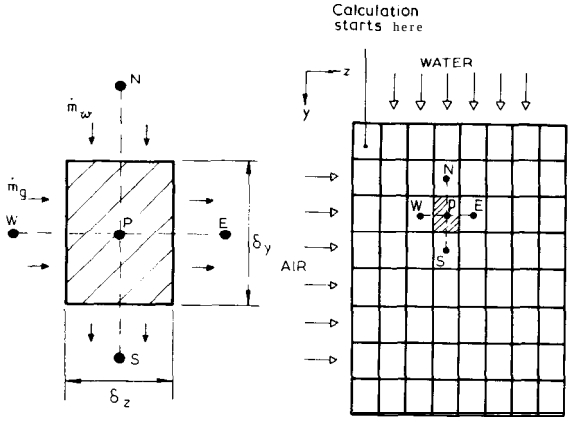

Figure 10 A rectangular element of a cross-flow packing.

where δh_g = increase in specific enthalpy of air through element

δh_w = decrease in specific enthalpy of water through element

h_s = specific enthalpy of saturated air at P

h_g = specific enthalpy of bulk air at P

$\dot{m}_g$ and $\dot{m}_w$ are known (specified) for all elements, and NTU is known from packing heat transfer data. (NTU' is identically equal to the product of Ka/L and $\dot{m}_w/\dot{m}_g$.)

The packing is divided into a network of such elements and, starting in the top left corner (according to the convention of Fig. 10, δh_g is calculated from Eq. (37) and then δh_w from Eq. (38). To avoid iteration, h_s can be based on the known value of h_w at point N and h_g can be taken as the value of h_g at W, for the purpose of finding the difference $(h_s - h_g)$ for use in Eq. (37).

The values of h_g at point E and of h_w at point S are then found from

$$h_{g,E} = h_{g,\,W} + \delta h_g \tag{39}$$

and

$$h_{w,S} = h_{w,N} - \delta h_w \tag{40}$$

The calculation is repeated systematically, cell by cell and row by row (or column by column), until the whole grid has been covered. The mean specific enthalpies of the water and air at exit can then be evaluated. As pointed out by Zivi and Brand [IO], the results of the calculation are valid for any partial rectangular block of the packing that has its top left-hand corner coincident with the top left-hand cell. Thus it is possible to examine simultaneously a range of overall dimensions of packing and to select dimensions that result in the specified mean water exit temperature. Examples of cross-flow calculations are presented by Zivi and Brand [IO] and Baker and Shryock [11].

Nomenclature and References for Section 3.12.2 appear at the end of Section 3.12 6.

© 1983 Hemisphere Publishing Corporation

3.12.3
Natural draft towers

J. R. Singham

A. Outline of main features

Natural draft towers can be designed for direct contact between the water and air (wet towers); or for indirect contact, with heat transfer taking place through a separating wall (dry towers); or for a combination of direct and indirect contact (wet-dry towers). But a large majority of natural draft towers are of the wet type, and attention usually will be confined to these in the present section. Dry and wet-dry towers are discussed in Sec. 3.12.5.

For most towers, the main structure consists of a large concrete shell, roughly cylindrical in form with a vertical axis, but tapering inward and outward to form a throat that is located near the top. The packing is confined to a comparatively thin horizontal layer at the base of the shell, and is usually either a grid of timber splash bars or a film packing formed by corrugated sheets of asbestos-cement of the type commonly used for simple roofing. The shell is supported by columns above a large pond or basin, leaving a circumferential gap below the base of the shell through which air from the atmosphere enters. Figure 1 is a photograph of a group of large, direct-contact, natural draft cooling towers; the packing is completely enclosed within the shell. Figure 2 shows diagrammatically the essential features of such a tower.

The air has to turn through a right angle in order to flow vertically upward through the packing, so the velocity profile along a radius above the packing may be somewhat nonuniform. This difficulty apart, the water to be cooled is distributed as uniformly as possible over the cross section of the tower above the packing and flows or splashes downward through the packing to the basin below. Splash bar packings usually extend below the base of the shell into the air entry space between the shell base and the water surface, whereas film packings usually terminate at the base of the shell. Natural draft, wet towers have also been built in which the packing is located in a circumferential ring outside the main shell. The water is distributed through the ring-shaped flat roof over the packing and the flow is essentially cross flow.

Heat transfer takes place between the water and air both within the packing and in the spray above and below the packing. To prevent the smaller droplets from being carried away by the air, a water eliminator is placed across the whole cross section of the tower above the water distribution level (Sec. 3.12.6B). The heat transfer to the air reduces its density, and in a natural draft tower it is the resulting buoyancy alone that causes the air to flow. Evidently, the higher the tower, the greater is the air flow. Also, other things being equal, the larger the tower diameter, the greater the air flow, since pressure losses fall as the cross-sectional area increases. So for a fixed water-to-air mass flow ratio, the water mass flow rate cooled in the tower increases with both tower height and tower diameter. As the cost of the tower increases less rapidly with these variables than the water mass flow rate, large natural draft towers have an economic advantage over small ones. Tall towers have the further advantages of discharging their warm moisture-laden air at a high level where it causes least inconvenience, and of being less prone to "recirculation"—the drawing in of warm moist air that has passed through the tower. Consequently, although there is a

© 1983 Hemisphere Publishing Corporation

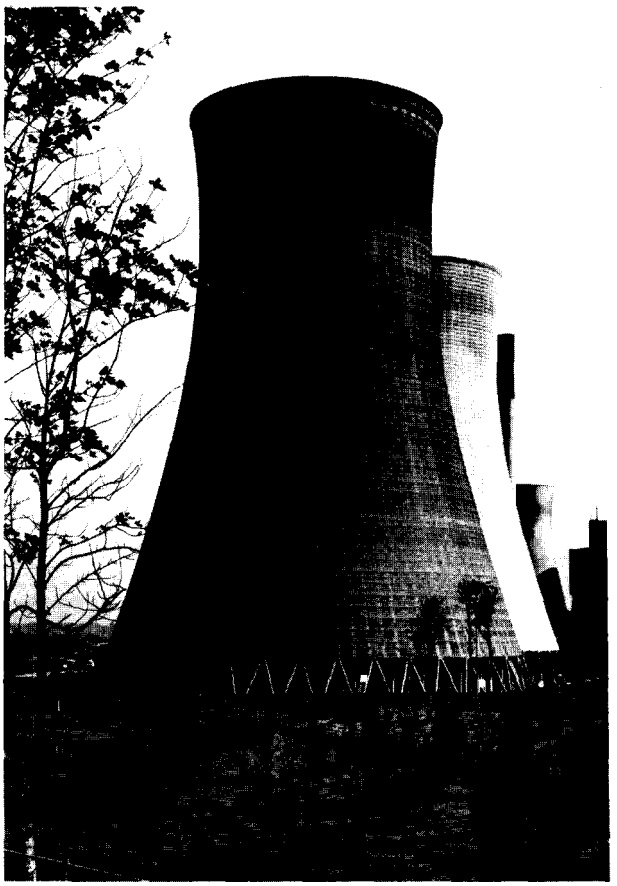

Figure 1 Natural draft coolings towers, 114 m high, at West Burton power station in Nottinghamshire. Two towers are employed for each of the four 500-MW turbo generators.

lower height limit of perhaps 20 m below which natural draft towers are uneconomical and unsuitable, the upper limit is imposed principally by environmental (visual) considerations. Several power stations in the United Kingdom use a pair of 375-ft (114.3-m) towers to serve one 500-MW turbo generator.

The ratio of base diameter to height usually lies in the range 0.75-0.85; the ratio of throat diameter to base diameter is in the range 0.55-0.65; and the ratio of vertical depth of air opening to base diameter lies in the range 0.10-0.12. A low value of the last ratio tends to restrict the entry of the air to the tower, whereas a high value increases the head of water and hence the pumping cost.

The mean water-to-air mass flow ratio usually lies in the range 0.5-3.0, although nonuniformity of the water and air flows may cause considerable local departures from the mean. The air velocity through the packing is quite low, about l-2 m/s. The water flow rate is typically equivalent to a rainfall over the packing of 5-15 cm/min. In very cold weather, there may be a danger of icing up around the entry; to prevent this, additional warm water may be distributed to the periphery of the packing.

Jones [4] discusses the use of large cooling towers for power stations and gives the life of such towers as no less than the station life of 30 years, whether the pack is made of timber or asbestos-cement. Timber packs, however, need to be treated initially with a suitable preservative; and concrete, rather than timber, is required for the pack support columns.

B. Thermal performance and design

(a) The thermal design equation

As stated in Sec. 2.12.2A, the water-to-air mass flow ratio, $\dot{M}_w/\dot{M}_g$, can be determined from the specification of the cooling requirement and data for the packing region alone. Thus $\dot{M}_w/\dot{M}_g$ can, and indeed must, be determined before suitable values for the principal dimensions of the tower are selected. The procedures given in Sec. 3.12.2 may be used for the determination of $\dot{M}_w/\dot{M}_g$. The designer then has to find values for the tower s height, base diameter, depth of air opening, and throat diameter that will produce a mass flow of air through the tower, $\dot{M}_g$, corresponding to this value of $\dot{M}_w/\dot{M}_g$ at the specified mass flow rate of cooling water, $\dot{M}_w$. A steady flow of air through the tower takes place when :

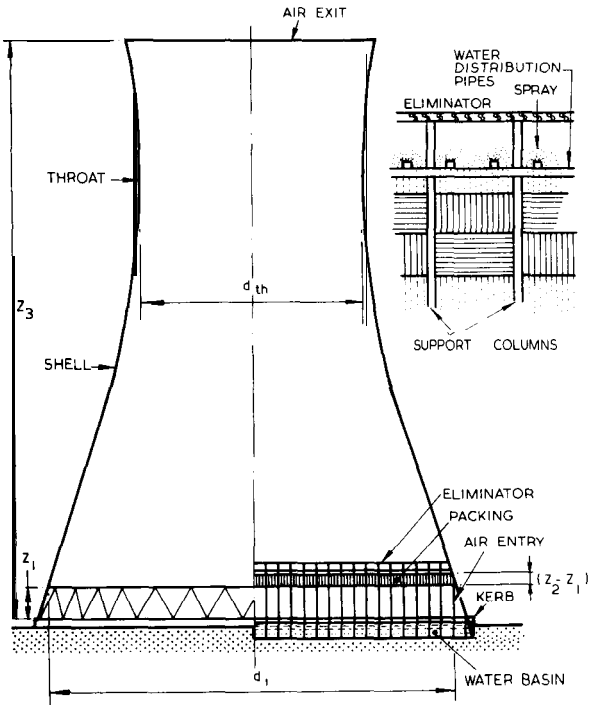

Figure 2 Components of a natural-draught direct-contact cooling tower.

© 1983 Hemisphere Publishing Corporation

The hydrostatic pressure difference, caused by the difference of density between the warm, moist air inside the tower and the cooler, dryer air outside is equal to the pressure loss that would be experienced by the air stream flowing through the tower in the absence of hydrostatic pressure differences [9].

This statement may be expressed symbolically to yield the ***buoyancy equation:***

$$g(z_3 - z_1 \text{ x\&ii-- P\&}_{ou}t) = N_v\left[\frac{1}{2\rho_{g,in}}\left(\frac{\dot{M}_g}{\pi d_1^2/4}\right)^2\right] \quad (1)$$

where g = gravitational acceleration
z_3 = height of top of tower above water basin curb
z_1 = height of top of air opening above water basin curb
$\rho_{g,in}$ = density of atmospheric air
$\rho_{g,out}$ = density of air leaving packing region
N_v = total number of air dynamic pressures lost, based on cross-sectional area of shell corresponding to d_1
$\dot{M}_g$ = air mass flow rate
d_1 = internal diameter of shell at top of air opening

The equation is based, of course, on the assumption of one-dimensional flow, that is, that quantities vary only in the direction of flow. The left-hand side represents the driving force of buoyancy. The right-hand side represents the resistance to flow of air through the tower and is the product of one dynamic pressure of air (the quantity within the outer brackets), and the number of such dynamic pressures lost in the various parts of the tower. The evaluation of N_v is discussed in Sec. (b).

The value of $\dot{M}_g$ is not normally given, and it is therefore convenient to replace it by the product of $\dot{M}_w$, known from the specification, and the reciprocal of the water-to-air mass flow ratio, $1/(\dot{M}_w/\dot{M}_g)$, known from calculation procedures described in Sec. 3.12.2. Before making this change, however, a general observation should be made concerning the validity of Eq. (1). Although presented here as an equation to be used for design purposes, the equation ought to be equally applicable to test data for an existing tower. However, when the measured quantities are inserted in the equation, its two sides rarely balance. This is partly due to the inadequacy of the theory, especially its one dimensionality, and partly to the inaccuracy of the design and test data. Whatever the reason, it is desirable to insert an empirical correction factor k into the equation. With a little rearrangement, the following equation results:

$$\frac{d_1^4(z_3 - z_1)}{N_v} = \frac{1}{k}\frac{8}{\pi^2 a}\frac{(\dot{M}_w)^2}{\rho_{g,in}(\rho_{g,in} - \rho_{g,out})(\dot{M}_w/\dot{M}_g)^2} \quad (2)$$

The value of k to be used in design needs to be obtained from full-scale test data on existing towers, similar in type to the tower to be designed. Little is published concerning the value of k, or on alternative procedures for ensuring balance of the two sides of the equation, due perhaps to the high commercial value of the information. Singham [9] analyzed the data published by Rish [8] for a medium-sized tower and obtained values of k ranging from 0.666 to 0.964, with an average value for the 23 tests of 0.799. He also found that k could be expressed as a linear function of the smoothed test data variables (water and air temperatures and water flow rate) with a standard deviation of k of 0.017 5. However, it must be repeated that the designer of a new tower needs to make use of test data for an existing tower of as similar design as possible.

Equation (2) provides the basis of thermal design for wet, natural draft cooling towers and may be termed the ***thermal design equation.*** For a specified cooling requirement and a given type and depth of packing, its right-hand side can be evaluated. The designer is then free to vary the geometry of the tower, provided that the resulting value of the left-hand side equals the now known value of the right-hand side, as discussed further in Sec. (c).

The form of design theory presented above treats the determination of the water-to-air mass flow ratio and of the tower dimensions as separate matters. Early theories of natural draft towers, including Chilton s [12], introduce Merkel s approximation [referred to in Sec. 3.12.2B(e)] in order to relate these two matters analytically, but as remarked earlier [also in Sec. 3.12.2B(e)], there is no longer need for such approximation now that excellent computational facilities are so readily available. Further comparison of these theories is given in [9] and [13].

(b) Pressure losses

Before use can be made of the thermal design equation, Eq. (2), expressions are needed for the individual components of the total number of dynamic pressures lost, N_v. Following [8], N_v is expressed as the sum of six terms:

$$N_v = N_{v,in} + N_{v,out} + N_{v,p} + N_{v,elim} + N_{v,sp} + N_{v,col} \quad (3)$$

where $N_{v,in}$ = losses in air entry
$N_{v,out}$ = losses at air exit

© 1983 Hemisphere Publishing Corporation

$N_{v,p}$ = losses in packing
$N_{v,\text{elim}}$ = losses in eliminator
$N_{v,sp}$ = losses in spray
$N_{v,\text{col}}$ = losses due to support columns, pipes, etc.

all expressed in numbers of air dynamic pressures, based on the cross-sectional area of the shell at the top of the air opening (where d_1 is measured). Each of these components will now be discussed briefly.

$N_{v,\text{in}}$: The cross-sectional area of the circumferential air entry, $\pi d_1 z_1$, is very much less than the cross section of the tower at the base of the shell, $\pi d_1^2/4$, on which the dynamic pressure is based. The ratio of the air entry velocity to the vertical air velocity based on d_1 is, from the continuity equation, equal to $d_1/4z_1$; so the ratio of the air entry dynamic pressure to the vertical dynamic pressure based on d_1 is equal to $(d_1/z_1)^2/16$. The ratio d_1/z_1 usually has a value of about 10; so, on this basis, the air entry dynamic pressure is about six times the base value. If the whole of this was lost in the bend, then $N_{v,\text{in}}$ would have a value of 6.

Unfortunately, the evaluation of $N_{v,\text{in}}$ is a great deal more difficult than this for several reasons, the principal ones being as follows: First, as in any sudden contraction, a vena contracta forms in the air entry, and the air entry velocity is correspondingly increased; second, it is oversimplifying matters to say that the air turns through a right angle at the entry and loses the whole of the dynamic pressure in doing so; third, the distribution of air flow over the cross section of the tower is not really uniform; and fourth, with splash bar packings, the packing occupies part of the air entry space and therefore influences the flow.

Nevertheless, it is reasonable to expect that $N_{v,\text{in}}$ will vary linearly with the ratio $(d_1/z_1)^2$ and to postulate a relation of the form

$$N_{v,\text{in}} = C_1 + C_2 r^{-2} \tag{4}$$

where $r \equiv z_1/d_1$, and C_1 and C_2 are empirical constants, whose values depend on the particular design details. Ioannides [14] found that relations like Eq. (4) could be used to correlate the results of tests of models of cooling tower entries. For the Staythorpe tower tested by Rish [8], values of C_1 and C_2 equal to 2 and 0.036 have been considered appropriate [9].

$N_{v,\text{out}}$: The dynamic pressure of the air at exit is lost," so the value of $N_{v,\text{out}}$ is simply this loss expressed in terms of the base dynamic pressure. From the tower throat to the top of the tower, the shell diverges like a diffuser; however, the divergence is usually small and the pressure recovery uncertain, so the exit dynamic pressure may reasonably be equated to its value at the tower throat. With this assumption, $N_{v,\text{out}}$ can be expressed by

$$N_{v,\text{out}} = C_3 s^{-4} \tag{5}$$

where $s \equiv (d_{\text{th}}/d_1)$, with d_{th} being the internal diameter of the tower throat, and C_3 an empirical constant, which, in the absence of other information, may be taken as equal to unity.

$N_{v,p}$: The value of $N_{v,p}$ is proportional to $N'_{v,p}$, the number of dynamic pressures lost per unit packing depth for the particular packing at the particular water and air mass fluxes. Data for $N'_{v,p}$ are discussed in Sec. 3.12.2C(c). $N_{v,p}$ is also proportional to the vertical depth of packing $(z_2 - z_1)$. And there is a further variable that should be taken into account. The cross-sectional area of the tower at packing level is seldom fully packed: there may be vertical water ducts, horizontal walkways, and difficult corner areas that it is easier to blank. Moreover, it may be economical to blank an even larger proportion of the cross section (because of the high cost of the packing, its support columns, and the associated water distribution system). It is therefore useful to introduce a geometric quantity t, defined by

$$t \equiv \frac{\text{total packed volume}}{(z_2 - z_1)(\pi/4)d_1^2} \tag{6}$$

For a fully packed tower, t equals unity; for a tower packed as completely as is reasonably convenient, t might be 0.96; and, depending on the cost data for the particular circumstances, t could have a somewhat lower value for a fully optimized design. The velocity of the air through the packing varies inversely as t, and the dynamic pressure inversely as t^2. So $N_{v,p}$ can be expressed by

$$N_{v,p} = C_4 t^{-2} \tag{7}$$

where

$$C_4 \equiv N_{v,p}(z_2 - z_1) \tag{8}$$

$N_{v,\text{elim}}$: If the tower is fully packed $(t \approx 1)$, then $N_{v,\text{elim}}$ is simply the number of dynamic pressures lost across the eliminator, as obtained from wind tunnel tests or other data. If, however, a substantial part of the cross section was left unpacked, there would be no need to provide eliminator over this part: the air would flow through the same reduced area of eliminator as for the packing, and the eliminator loss would also vary inversely as t^2. For generality, then, it is desirable to express the loss by

$$N_{v,\text{elim}} = C_5 t^{-2} \tag{9}$$

where C_5 equals the number of dynamic pressures lost in the eliminator, based on the local air velocity, and obtained from test or other data. Values in the range 2–4 may be expected.

© 1983 Hemisphere Publishing Corporation

$N_{v,sp}$: The contribution of the spray to the total pressure loss is clearly dependent on the particular design features of the packing region, and it is difficult to lay down rules in the present context of a general one-dimensional procedure. It may, however, be helpful to quote a relation that was adopted for the analysis of a small tower with an asbestos-cement film packing [8, 93]:

$$N_{v,sp} = 0.526(z_1 + 1.22)\left(\frac{\dot{M}_f}{\dot{M}_g}\right)^{1.32} \quad (10)$$

with z_1 in meters.

For the particular tower, at a water-to-air mass flow ratio of 2, the equation yielded a value for $N_{v,sp}$ of 9.6.

$N_{v,col}$: The value to be assigned to $N_{v,col}$ depends on the particular design details, and also on the extent to which the losses due to support columns, pipes, and so on, may already be accounted for in the other terms. (Thus the loss associated with the diagonal columns that support the shell could be included in $N_{v,in}$.) A value in the range 2-6 may be thought suitable after such considerations.

In the light of this discussion of the individual terms on the right-hand side of Eq. (3), the equation may be recast in the following form:

$$N_v = a_1 r^{-2} + a_2 s^{-4} + a_3 t^{-2} + a_4 \quad (11)$$

where $a_1 \equiv C_2$, introduced in Eq. (4)
$a_2 \equiv C_3$, introduced in Eq. (5)
$a_3 \equiv C_4 + C_5$, C_4 having been introduced in Eq. (7) and C_5 in Eq. (9)
$a_4 \equiv C_1 + N_{v,sp} + N_{v,col}$, C_1 having been introduced in Eq. (4)

For illustration, the value of N_v will be calculated for particular values of the constants and variables on the right-hand side of Eq. (11):

Constants: $C_1 = 2$ $C_2 = 0.036$ $c_3 = 1$

$C_4 = 35$ (for a particular type and depth of packing)

$C_5 = 3$ $N_{v,sp} = 10$ $N_{v,col} = 4$

Hence,

$a_1 = 0.036$ $a_2 = 1$ $a_3 = 38$ $a_4 = 16$

Variables: $r = 0.09$ $s = 0.65$ $t = 0.95$

Hence,

$$N_v = 0.036(0.09)^{-2} + (0.65)^{-4} + 38(0.95)^{-2} + 16$$
$$= 4.4 + 5.6 + 42.1 + 16$$

giving

$N_v = 68.1$

(c) Design and optimization

The first stage in thermal design is the evaluation of the right-hand side of the thermal design equation, Eq. (2). This may be achieved by the following steps:

1. Select the type and vertical depth of packing.
2. Evaluate the water-to-air mass flow ratio, $\dot{M}_w/\dot{M}_g$, for the specified cooling requirement, by the procedure described in Sec. 3.12.2B(e).
3. Evaluate the density change of the air across the packing region, normally by assuming the air to be saturated at exit from the region.
4. Evaluate the right-hand side of Eq. (2), taking a value for the correction factor k based on test data for the tower most similar to the one proposed.

If the right-hand side of the thermal design equation is denoted by K, the equation may now be rewritten as

$$\frac{d_1^4(z_3 - z_1)}{N_v} = K \quad (12)$$

with K known and constant for the given cooling requirement and the selected type and depth of packing.

The next stage is to evaluate N_v from Eq. (11) for trial values of the tower geometric ratios r, s, and t, which express dimensionlessly the vertical depth of the air opening, the diameter of the throat, and the proportion of the total available cross section that is occupied by the packing, respectively.

The value of the product $d_1^4(z_3 - z_1)$ can now be evaluated. Any pair of values of the base diameter d_1 and the shell depth $z_3 - z_1$ that give this product, satisfy the thermal design equation and may be selected. Having selected a suitable pair of values, the water mass flux $\dot{m}_w$ and depth of air opening z_1 corresponding to d_1 should be calculated and the value of N_v checked, since the pressure losses of the packing and spray may be thought to depend on the water mass flux, and the spray pressure loss may also depend on z_1. But the dependence is weak, and not more than one stage of iteration is likely to be needed.

By following this procedure, any number of sets of values of $d_1, (z_3 - z_1), r$ (or z_1), s (or d_{th}) and t may be found to satisfy the cooling requirement with a given type and vertical depth of packing. There may, of course, be nonthermal constraints to be taken into account, such as a maximum value for the tower height z_3; or a maximum allowable pumping head, imposing, in effect, a maximum value on z_1; or a desired visual appearance, imposing limits on the throat-to-base diameter ratio s. Even with such constraints, however, there is likely to remain some freedom for these variables, and the final choice of values will be made in a way that minimizes total cost.

The total initial capital cost of a cooling tower, C,

© 1983 Hemisphere Publishing Corporation

depends mainly on three items: the cost of the shell, C_{sh}, the cost of the packing and water distribution system, C_p, and the capitalized operating and maintenance cost, C_{op}:

$$c = C_{sh} + C_p + C_{op} \tag{13}$$

C_{sh} depends mainly on the values of $d_1, z_3 - z_1$, and s (or d_{th}). For a given type of packing, C_p depends mainly on $d_1, z_2 - z_1$, and t. And C_{op} depends mainly on the pumping head, and so on r (or z_1). Hence Cwill be a function of all these variables:

$$C = C(d_1, (z_3 - z_1), r, s, t, (z_2 - z_1)) \tag{14}$$

The aim of the designer should be to find the values of these six variables that give a value of C near to the minimum value of the function, C_{min}, while satisfying the thermal design equation, as expressed by Eq. (12), and any other constraints.

It may be that a value of C sufficiently close to C_{min} can be found by a series of trial calculations, but systematic search procedures, used in conjunction with a computer program, are likely to save both time and money. In [9], it is shown that for a fixed preliminary choice of packing depth, $z_2 - z_1$, the optimum values of the remaining five variables may be found from simultaneous solution of Eqs. (11) and (12) and the following five equations:

$$\begin{aligned}
-\lambda &= \frac{d_1}{4}\frac{\partial C}{\partial d_1} && (a)\\
&= (z_3 - z_1)\frac{\partial C}{\partial (z_3 - z_1)} && (b)\\
&= \frac{N_v r^3}{2a_1}\frac{\partial C}{\partial r} && (c)\\
&= \frac{N_v s^5}{4a_2}\frac{\partial C}{\partial s} && (d)\\
&= \frac{N_v t^3}{2a_3}\frac{\partial C}{\partial t} && (e)
\end{aligned} \tag{15}$$

Thus there are seven equations containing seven unknowns, namely, $d_1, (z_3 - z_1), r$, s, t, N_v, and λ (λ having only a mathematical significance as the Lagrange multiplier for the system of equations). The five cost derivatives, $\partial C/\partial d_1$, and so on, which are partial derivatives of the cost function, Eq. (14), have to be obtained from the manufacturer s cost data and information concerning the cost of pumping. The equations must then be solved iteratively, but their form is such that convergence is very rapid and, although a computer program is convenient, manual solution with a small electronic calculator is not difficult. If any of the five geometric variables is to be held to an assigned value, the corresponding equation of the set Eq. (15) is dropped and the remaining equations are solved for the remaining free variables.

(d) Performance away from design point

A tower of given design will rarely, if ever, operate at the design point values of the independent variables. It is required to operate over ranges of values of these variables, and a procedure is needed for predicting the performance of the tower for any combination of these variables. The basis of the procedure is, of course, the solution of the same equations as are used for design, viz., Eq. (2), Eq. (1 1), and the relations needed for determining the water-to-air mass flow ratio by the procedure described in Sec. 3.12.2B(e). With the tower design dimensions and packing characteristics known, these equations permit the calculation of the water exit temperature, $T_{w,out}$, for any set of assumed values of $\dot{M}_w, T_{w,in}, T_{WB}, T_{DB}$, and p_a. (There is no difficulty in handling variation of the atmospheric pressure p_a, provided that data for the properties of moist air at the correct pressure are used.) The calculation is more laborious than a corresponding design calculation, because $T_{w,out}$ is unknown and the calculation of the water-to-air mass flow ratio requires knowledge of both $T_{w,in}$ and $T_{w,out}$. Consequently, trial is required, and use of a computer is desirable. Using a suitable program, it is a simple matter to explore the whole range of the variables. If desired, the tower performance can then be summarized by expressing $T_{w,out}$ as a linearized function of the five independent variables, $\dot{M}_w, T_{w,in}, T_{WB}$, T_{DB}, and p_a [9].

C. Some remarks on structural design

Whereas the height and base diameter of the concrete shell of a cooling tower are determined mainly by thermal considerations, the shape of the shell is determined more by considerations of strength and cost. The required thermal performance could be achieved with a cylindrical or conical shell, but these would be more expensive and less strong than the conventional shape of tower with a throat near the top and a hyperbolic profile. As noted in Sec. B(b), the introduction of a throat increases the pressure loss, but for a large tower the increase in cost associated with this loss is more than offset by the reduction in material needed for the tower with a throat. Nevertheless, small cylindrical towers . . . have been common in some countries, notably Germany. For such smaller units, the economy of materials in hyperboloidal towers can be outweighed by the speed of construction that can be achieved in cylindrical towers using sliding formwork [4].

Very large towers are subject to wind forces, which can give rise to vibration, buckling, and even to superimposed tensile stresses that exceed the compressive stresses from the dead weight of the structure [15, 16]. According to Jones [4] : Prior to 1965 tower

© 1983 Hemisphere Publishing Corporation

shells had a general thickness of about 120 mm, which incidentally was almost as thin as practical considerations of construction would permit. However, in 1965 three out of eight newly built cooling towers [114 m tall] at Ferrybridge collapsed in strong winds, and as a result of subsequent investigations it was concluded that the towers had been subjected by the wind to uplift forces greater than those assumed in design. The wind loading was intensified by dynamic loading effects which were magnified by the layout of the groups of towers. As a result of the Inquiry, shell thickness is increased to about 200 mm. . . ."

The maximum size of natural draft towers continues to increase, especially for dry towers, and alternatives to the conventional hyperbolic concrete shell are being tried. A completely new kind of cable network structure was used at Schmehausen in Germany for a 181 -m-high dry cooling tower for a nuclear power plant. According to Zerna and Mungan[17], the structure consists of (1) a vertical central reinforced concrete pylon with foundation; (2) a compression ring near the top, attached to the central pylon by radial spokes; (3) two similarly attached rings at intermediate levels between the top and the ground; (4) a network of cables criss-crossed and stretched over the outside of the rings; and (5) cladding to enable the structure to channel the air without its escape. The cables are attached to the central pylon at the top and to a ring foundation at the ground. The cladding is made from an aluminum alloy. Zerna and Mungan suggest that the cost of cable network towers increases less rapidly with height than that of conventional towers and that the crossover point, though uncertain, may be around 200 m.

A less radical alternative to the conventional reinforced concrete shell of smoothly changing wall thickness is a concrete shell equipped with circumferential stiffening rings. Above a certain size, such a shell requires a smaller volume of reinforced concrete and offers greater resistance to vibration and buckling. The advantage may be apparent at a height of 1.50 m and increases with height [17].

Nomenclature and References for Section 3.12.3 appear at the end of Section 3.12.6.

© 1983 Hemisphere Publishing Corporation

3.12.4
Mechanical draft towers

J. R. Singham

A. Outline of main features

In a mechanical draft tower the air is made to flow through the tower by means of one or more fans. With forced draft, the fans are placed at ground level and blow the air through the packing (Fig. ***la),*** whereas in induced draft towers the fan is located above the packing and sucks the air through the tower (Fig. 1, ***b*** and c). The type of flow may be wholly counter flow, partly counter flow and partly cross flow, or wholly cross flow; all three cases are illustrated diagrammatically in Fig. 1. Cross-flow packings are raked at an angle to take account of the influence of the air stream on the line of fall of the water.

Mechanical draft towers cover a much wider range of size than natural draft towers, from a size capable of being loaded on a small truck, to banks of towers capable of cooling the circulating water of a large power station. Large towers tend to use axial-flow fans and induced draft, whereas small towers often use forced draft provided by either a centrifugal or an axial fan. According to Marriott [18], centrifugal fans are considered to be quieter than equivalent axials but may be more expensive.

Packings may consist of wooden splash bars or plastic sheeting formed into passages of various shapes. Timber may have to be used if the water temperature exceeds the safe operating value for the particular plastic, for example, about 70° C for PVC, which is commonly used. Plastic packings can be made as lightweight modules that are easy to assemble on site. The surrounding cladding of the tower may be formed by sheets of galvanized steel, corrugated asbestos-cement, or PVC. According to the National Fire Protection Association [19], fire can be a serious danger with cooling towers, especially with the induced draft type. Fires occur during construction and shutdown periods, but can also happen during full operation if parts of the packing and structure are insufficiently wetted.

A typical water loading is 2.3 $kg/m^2 s$, plus or minus 20%, depending on the type and depth of packing [2], equivalent to a rainfall over the packing of about 14 cm/mm. Air velocities commonly fall within the range of 1.5-4 m/s, and the mean water-to-air mass flow ratio falls within the range 0.5-2.5.

The relative merits of mechanical and natural draft towers are discussed in [2] and by Kunesch [20]. The latter considers a cooling requirement for the generation of electric power of 100 MW: 6.1 m^3/s with a cooling range (change in water temperature) of 8.5°C, an approach (difference between water exit and ambient wet-bulb temperatures) of 10°C, and an ambient wet-bulb temperature of 17° C. He estimates the capital cost of the natural draft tower at £1 200 000 and that of the mechanical draft at £750 000 (paper published in 1978). But the mechanical draft tower would require a fan power of 775 kW, and the natural draft tower none.

The water pumping costs are excluded, since they are approximately the same in the two cases. Depending on the cost of electrical power, the two systems appear to be fairly evenly balanced economically (the annual cost of the fan power would be about £70 000 for every £0.01/kWh of fan energy), but with the advantage moving toward natural draft. Kunesch remarks that greater allowance for the harmful effect of air recirculation would put up the capital and fan costs for the

© 1983 Hemisphere Publishing Corporation

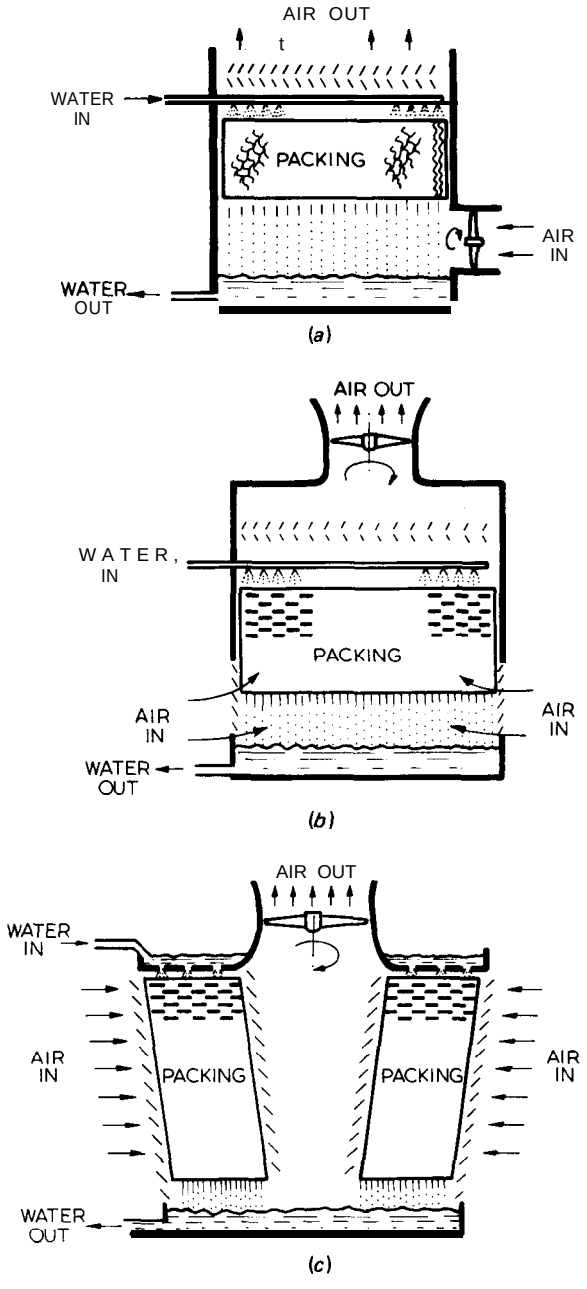

Figure 1 Some layouts for mechanical draft cooling towers. (a) Forced draft counter flow. (*b*) Induced draft mixed flow. (*c*) Induced draft cross flow.

mechanical draft plant by 15%. It may be noted, however, that natural draft towers become relatively less competitive as size decreases and are probably uneconomical at water flow rates below 1.25 m^3/s[2].

A perspective drawing of a forced draft tower, equipped with two centrifugal fans, is shown in Fig. 2. A drawing of a much larger, induced draft tower, with a single axial fan, is shown in Fig. 3. Both towers have plastic counter-flow film-type packings and have timber-louver drift eliminators. The induced draft tower could be fitted with a wooden splash bar packing instead; this would introduce a degree of cross flow.

B. Thermal performance and design

As with a natural draft tower, the first stage in the thermal design of a mechanical draft tower is the evaluation of the water-to-air mass flow ratio for the specified cooling requirement and for a particular type and quantity of packing, according to the procedures of Sec. 3.12.2B. In this case, however, the atmospheric dry-bulb temperature is not normally required, since accurate evaluation of the air density is necessary only when density differences are important, as in natural draft towers. For a mechanical draft tower, the atmospheric wet-bulb temperature and pressure suffice to characterize the state of the atmosphere.

However, there is an important extra factor that may have to be taken into account with mechanical draft towers above a certain size, namely, the possible recirculation of moist air from the tower exit to its entry. According to [2], the recirculation increases with the size of tower and may amount to as much as 20% with large towers under certain conditions of wind velocity. To take account of recirculation, an upward correction, ΔT_{WB}, has to be made to the design ambient wet-bulb temperature. The correction is a function of four variables: water mass flow rate $\dot{M}_f$, design ambient wet-bulb temperature T_{WB}, approach of water exit temperature to wet-bulb temperature $T_{w,\text{out}} - T_{WB}$, and water cooling range $T_{w,\text{in}} - T_{w,\text{out}}$. To allow for the fact that recirculation is at its worst for only a short proportion of total working time, BS 4485 [2] recommends that the correction be based on a recirculation of 60% of the estimated maximum. The following sample values of ΔT_{WB} are based on these recommendations, but are rounded to the nearest tenth of a degree:

$\dot{M}_w$, m^3/s	0.5	1.0	2.0	4.0	6.0
ΔT_{WB}, °C	0.2	0.3	0.5	0.8	0.9

for $T_{WB} = 17°C$, $T_{w,\text{out}} - T_{WB} = 8.5°C$, $T_{w,\text{in}} - T_{w,\text{out}} = 8°C$.

The recommended correction increases with all three of these quantities. For example, at $T_{WB} = 20°C$, $T_{w,\text{out}} - T_{WB} = 12°C$, and $T_{w,\text{in}} - T_{w,\text{out}} = 15°C$, the above values of ΔT_{WB} have to be multiplied by a factor of about 2.

Having determined the ratio $\dot{M}_w/\dot{M}_g$, the air mass flow rate $\dot{M}_g$ can at once be found, since the water mass flow rate $\dot{M}_w$ is known from the specified cooling requirement. The aim of the designer is now to choose a cross-sectional area for the packing (normal to the

© 1983 Hemisphere Publishing Corporation

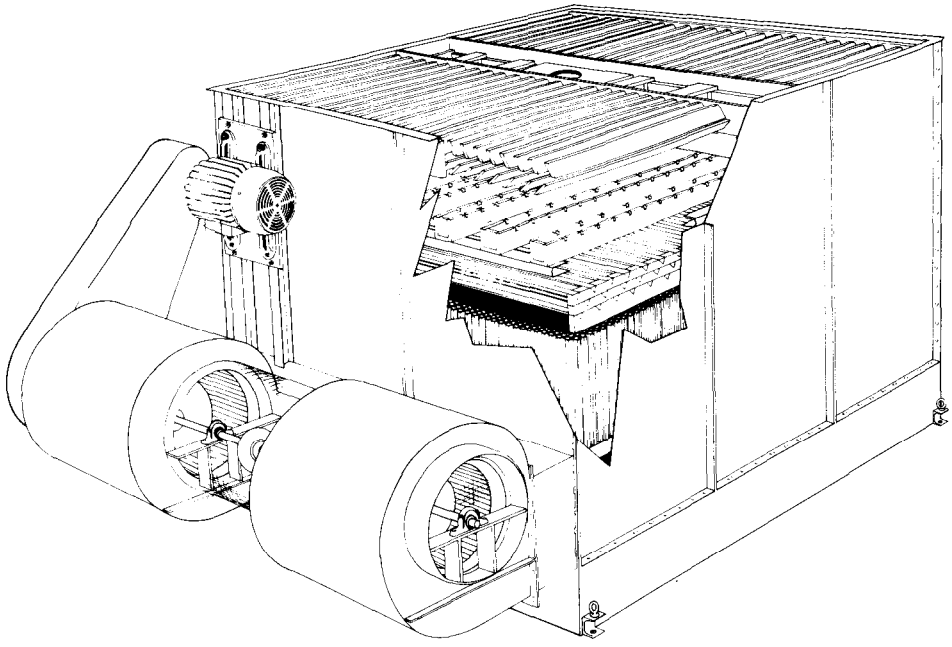

Figure 2 Forced draft tower with twin centrifugal fans. The tower is 2.6 m high and cools 30 kg/s of water for a total power of 11 **kW** (numbers approximate). Drawing courtesy of Visco.

direction of air flow) and to select a fan, or a number of fans, that will force or induce air through the tower at the calculated rate, and at the total pressure loss that results with that cross-sectional area. If the fan and the fan power seem unduly large, the designer can try a larger cross-sectional area, eventually arriving at a combination of tower size and fan size and power that yield a total cost near to the minimum.

Before this last stage of the design can be carried out, the designer must decide whether to use forced or induced draft, and whether to use a centrifugal or an axial fan. A further choice is whether to use counter

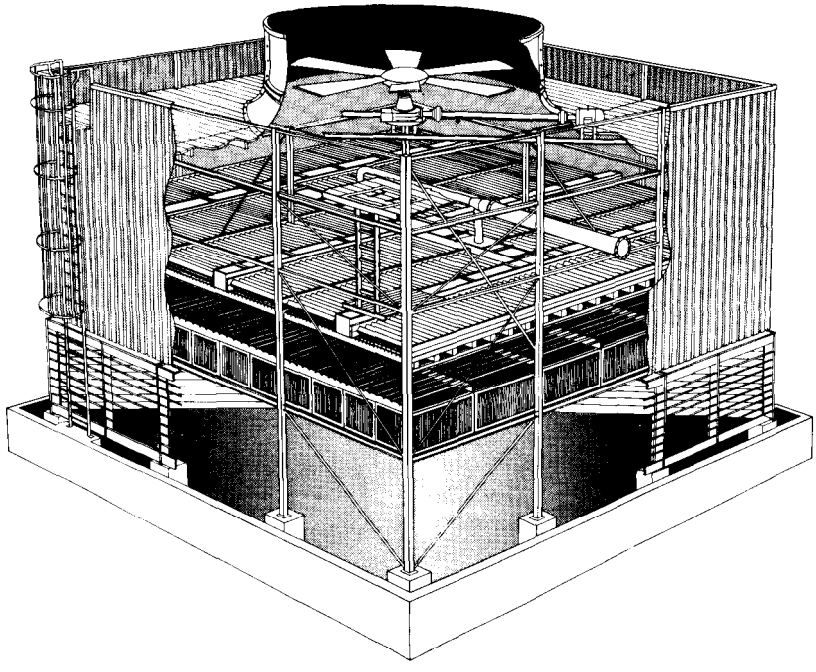

Figure 3 Induced draft tower with axial fan. The tower is 6 m high and cools 250 kg/s of water for a power of 30 **kW;** the fan rotor diameter is 4.5 m (numbers approximate). Drawing courtesy of Visco.

© 1983 Hemisphere Publishing Corporation

flow, cross flow, or mixed flow. In most cases, all of these choices will probably have been made at the outset from the designer s experience of what is likely to prove most satisfactory in the particular circumstances; and from knowledge of where the designer sexpertise and that of the organization are greatest. If doubt arises as to the correct choice, then of course the correct procedure, time permitting, is to investigate two or more possibilities before deciding which choice is best.

The characteristics of fans are usually given as the rise in total or static pressure across the fan as a graphic function of volumetric flow rate and fan rotational speed. For present purposes, it is the rise in total pressure that is required, but this is equal to the static rise when the fan entry and exit areas are equal, as is often the case with axial fans. In order to match the tower s pressure loss to the fan s pressure rise, it is convenient to calculate the air volumetric flow rate $\dot{V}_g$ from the known mass flow rate and the appropriate air density and to locate this value on the graph of the fan characteristic, as shown diagrammatically in Fig. 4. The total pressure drop through the tower, Δp_{tower}, may be expressed as the sum of three terms:

$$\Delta p_{\text{tower}} = \Delta p_{\text{pack}} + n_{\text{ex}}\,\Delta p_{\text{ex}} + \Delta p_{\text{misc}} \qquad (1)$$

where Δp_{pack} = pressure loss in packing
Δp_{ex} = dynamic pressure at fan exit
Δp_{misc} = sum of miscellaneous pressure losses, e.g., in eliminator, entry to fan (if not otherwise accounted for), etc.
n_{ex} = a numerical factor of unity or less

Δp_{pack} can be determined from the value of $N_{v,p}$, the number of dynamic pressures lost across the packing, known from packing data (Sec. 3.12.2C) and the air dynamic pressure based on the packing cross-sectional area normal to the air flow.

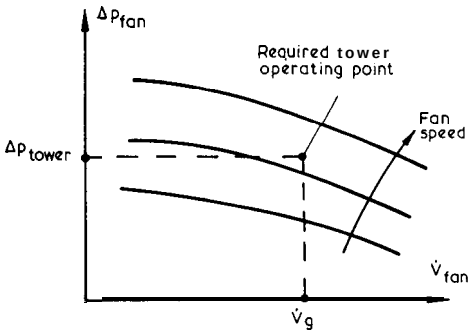

Figure 4 Locating the tower operating point on the fan characteristics.

The term $n_{\text{ex}}\,\Delta p_{\text{ex}}$ accounts for the loss of all or part of the dynamic pressure at the fan exit which takes place in both forced and induced draft towers; thus n_{ex} lies between 0 and 1. If there is no diffuser after the fan exit, then n_{ex} will be 1 for an induced draft tower, since the whole of the exit dynamic pressure is fhrown away ; n_{ex} will be near to unity for forced draft since the dynamic pressure is unlikely to be recovered in the unguided flow below the packing. Use of a diffuser, however, can reduce the value of n_{ex} to 0.5 or less. The value of Δp_{ex} is given by

$$\Delta p_{\text{ex}} = \frac{1}{2\rho_g}\left(\frac{\dot{M}_g}{n_f A_{f,\text{ex}}}\right)^2 \qquad (2)$$

where $\dot{M}_g$ = air mass flow rate
ρ_g = air density
nf = number of fans
$A_{f,\text{ex}}$ = cross-sectional area at exit from fan

The term Δp_{misc} is normally small compared with the other two terms-a few dynamic pressures, based on the packing cross-sectional area normal to the air flow.

Δp_{tower} and $\dot{V}_g$ having been evaluated, the tower operating point can be located on the fan characteristics. Provided that the fan efficiency is about 75% or more at this point of the characteristics, then this combination of tower and fan size may be acceptable. But, as noted earlier in this section, several different cross-sectional areas need to be tried to ensure that a combination is found near to that corresponding to minimum total cost (sum of initial costs of tower structure, packing, and fan, and capitalized cost of fan power) for the particular type and depth of packing.

Predicting the performance of the tower away from the design point amounts to finding the value of $T_{w,\text{out}}$ for given values of $\dot{M}_w$, $T_{w,\text{in}}$, T_{WB}, and p_a, and for a particular fan speed, if this is variable. As with a natural draft tower, the calculation is by trial when $T_{w,\text{out}}$ is unknown. In the present case, the values of ΔP_{tower} and $\dot{V}_g$ can be calculated for any assumed value of $T_{w,\text{out}}$, *in* the same way as for the design point. The locus of the tower operating point, as $T_{w,\text{out}}$ is varied, can then be marked on the fan characteristics, the solution being at the intersection of the locus with the correct fan speed characteristic.

Nomenclature and References for Section 3.12.4 appear at the end of Section 3.12.6.

© 1983 Hemisphere Publishing Corporation

3.12.5
Hybrid towers

J. R. Singham

A. Dry towers

A dry tower is a tower in which no direct contact between the air and water is allowed, the packing of the conventional wet tower being replaced by heat exchangers not unlike automobile radiators. Wet towers require an external supply of water amounting to about 3% of the total flow, 1% for evaporation, and 2% for keeping the concentration of salts at an acceptable level, equivalent to a requirement of about 4 liters/kWh; dry towers require none. Consequently, dry towers can operate on many sites where wet towers are impossible due to the unavailability of the necessary external water supply. As the number of suitable sites for wet towers on rivers, lakes, and estuaries decreases with the expansion of industrialization, so dry towers become increasingly attractive. For nuclear power stations, the greater freedom of site choice is especially advantageous. Dry towers are also free from troublesome vapor plumes. Dry towers may be built for mechanical and natural draft; but in the present section attention will be confined to natural draft, since dry mechanical draft towers are considered nearer to heat exchangers than cooling towers for our purposes.

The cost of a dry tower for a given cooling requirement is much greater than the cost of a wet tower. Jones [4] gives the cost of a dry tower built at Rugeley [21] for a 120-MW turbogenerator as about double that of a wet tower. Moreover, for a given duty, the dry tower has to be larger, and this is an environmental disadvantage. Part of the extra cost can be attributed to the heat exchangers that replace the comparatively inexpensive wet packing system, and part to the need for a larger tower.

This need arises from the fact that a dry tower requires a much larger air flow than a wet tower performing the same duty. The larger air flow is made necessary by the fact that the change in specific enthalpy of the air in a dry tower is necessarily much less than in a wet tower where water evaporates into the air stream. A numerical example may serve to illustrate the point :

Data from cooling requirement:

Atmospheric wet-bulb temperature $T_{WB} = 10°C$

Entry temperature of water $T_{w,\text{in}} = 32°C$

Exit temperature of water $T_{w,\text{out}} = 20°C$

Aim of calculation:

To find the ratio R_g of the air mass flow rate for a dry tower, $\dot{M}_{g,\text{dry}}$, to that for a wet tower, $M_{g,\text{wet}}$, when the airstream for each tower experiences its maximum possible change in specific enthalpy.

Evaluation of R_g:

For equal water flow rates, the heat transfers are equal in the two cases:

$$M_{g,\text{dry}}\, c_p (T_{g,\text{out}} - T_{g,\text{in}})_{\text{dry}} = M_{g,\text{wet}} (h_{g,\text{out}} - h_{g,\text{in}})_{\text{wet}}$$

and therefore

$$R_g = \frac{(h_{g,\text{out}} - h_{g,\text{in}})_{\text{wet}}}{c_p (T_{g,\text{out}} - T_{g,\text{in}})_{\text{dry}}}$$

© 1983 Hemisphere Publishing Corporation

HEDH

In accordance with the aim of the calculation, $h_{g,out}$ is taken as the specific enthalpy of saturated air at temperature $T_{w,in}$, the best that can be achieved in a wet tower; and $T_{g,out}$ is taken as equal to $T_{w,in}$, the best that can be achieved in a dry tower. The values of $h_{g,out}$ and $h_{g,in}$ are read from Table 3.12.2(1), $h_{g,in}$ being based on T_{WB}. The specific heat capacity of air c_p may be taken as 1.010 kJ/kg K.

The remaining quantity required for the calculation is the value of $T_{g,in}$. The lowest value is when the atmospheric air is saturated, when $T_{g,in}$ equals T_{WB}; this condition is the one most favorable to the dry tower. With these assumptions,

$$R_g = \frac{107.3 - 29.04}{1.01(32 - 10)} \approx 3.5$$

Thus, in the above example, the dry tower requires 3.5 times the air mass flow rate of the wet tower, and the ratio would be higher if the atmospheric air was less than saturated. The influence of a high air mass flow rate on the tower dimensions can be seen from Eq. 3.12.3(1), which will be rearranged for the present purpose:

$$d_1^4(z_3 - z_1) = \frac{B\dot{M}_g^2}{\rho_{g,in} - \rho_{g,out}} \quad (1)$$

where $$B \equiv \frac{8N_v}{\pi^2 g \rho_{g,in}}$$

The value of B is proportional to N_v, the total number of dynamic pressures lost, and therefore depends on the design of the heat exchangers and on the tower geometry. Nevertheless, B may be treated as constant while endeavoring to discern the main trends. The influence of the density difference in the denominator will also, for the moment, be ignored.

For a tower of fixed proportions, both the base diameter d_1 and the vertical shell depth $(z_3 - z_1)$ are proportional to the overall height z_3. So, for such a tower, from Eq. (1),

$$z_3 \propto (\dot{M}_g)^{2/5}$$

Thus, for a dry tower to achieve the same duty as a wet tower of similar proportions, the height must be increased in the ratio of the relative air flow raised to the power 2/5. In the above numerical example, the dry tower was found to require 3.5 times the air flow of the wet tower. Its height and other dimensions would therefore need to be $(3.5)^{2/5}$ times greater, that is, a ratio of 1.65.

The dry tower also suffers some disadvantage from the fact that the density of air at a given temperature is greater for dry air than for moist air. The air leaving the heat exchangers in a dry tower is far from saturation, whereas the air leaving a cooling tower packing is usually very close to saturation. Consequently, for a given water entry temperature, the density difference in Eq. (1) is significantly less for a dry than for a wet tower. If the atmospheric dry-bulb temperature is high, then the density of the ah at entry, $\rho_{g,in}$ will be low, and the disadvantage of lower density difference will be even more marked in the dry tower.

The tower at Rugeley, England [21], has all-aluminum tube-and-fin heat exchangers arranged in a zigzag formation around the base of the tower, outside the shell; the fins are louvered plates. The tower at Grootvlei, South Africa [22], has externally galvanized steel tubes with spirally wound aluminum fins for its heat exchangers, which are mounted above ground within the shell. The use of fins in the heat exchangers is necessitated by the low surface heat transfer coefficient on the air side. Dry cooling towers allow the circulating water to be kept pure, and the water from both of these towers is used directly in spray steam condensers. As noted in Sec. 3.12.3C, the nuclear power plant at Schemausen, Germany, uses a dry tower with a cable network structure 18 1 m high.

At both Rugeley and Grootvlei, the performance of the towers has been found to decrease with increasing wind velocity. At Rugeley, the cause appeared to be associated with the zigzag layout of the heat exchangers at those positions where the wind was tangential to the circular base; the air flow through the heat exchangers facing downwind was found to be very low. At Grootvlei, the cause was thought to be connected with a tendency for the wind to reverse the flow at the tower exit. Russell et al. [23] report model tests on air flow in dry cooling towers with various heat exchanger layouts; they tentatively favor layouts resembling Grootvlei s in which the heat exchangers are mounted within the shell.

B. Wet-dry towers

Wet-dry (or dry-wet) towers have dry heat exchanger sections where heat transfer takes place by indirect contact between the water and air streams, and wet packing sections where the two streams are in direct contact. The dry section serves to reduce the demand for makeup water and to reduce or eliminate the nuisance of water plumes and local precipitation, while the wet section, being more cost-effective, makes the cost of the wet-dry tower significantly less than that of an all-dry tower. If there was no shortage of sites with plentiful makeup water and no need for environmental considerations to be taken into account, wet towers would always be preferred to both dry and wet-dry towers. But such is increasingly not the case, and there is a great deal of interest in the wet-dry compromise.

Some possible arrangements of wet and dry cooling are reviewed by Croley et al. [24], and Fig. 1 is reproduced from their paper. All the schemes illustrated

© 1983 Hemisphere Publishing Corporation

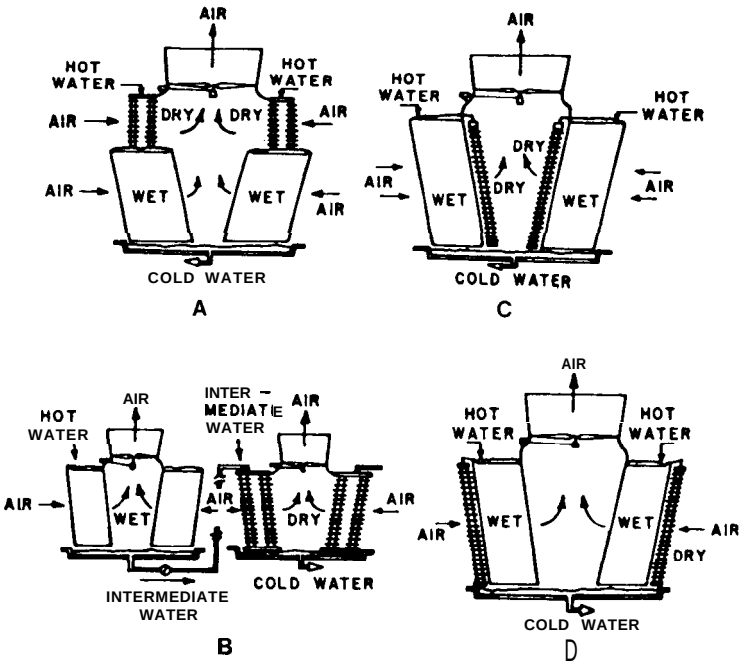

Figure 1 Some possible arrangements for wet-dry towers. From Croley et al[24].

use induced draft and cross flow and are for large water flow rates, since it is under these conditions that the wet-dry combination looks most practical and economic. In scheme B, the wet and dry sections are in fact separate towers handling the same circulating water. According to the authors, schemes somewhat similar to A have been offered by two manufactuers in the United States. The air flows through the wet and dry sections in parallel, with the advantage that the cross-sectional area normal to the flow is increased and the pressure drop correspondingly reduced; also, both sections receive the air at its coldest, direct from the atmosphere. But the flow needs to be divided correctly between the two sections, and adequate mixing of the two streams of air ensured. Clearly, there is scope for much analysis, experiment, and cost optimization before the best design of a given scheme can be developed and before the relative advantages of different schemes can be properly assessed, and work of this kind is proceeding [25].

A rather different approach to wet-dry cooling has been adopted by Bentley et al. [26]. They have developed and tested a packing plate made of aluminum and carrying vertical grooves that channel the water. The grooves are spaced at horizontal intervals of 76 mm, and the plates are inclined at an angle of 10 to the vertical, with the grooves on the upper side. The air flows horizontally through a stack of such plates in cross flow. The aluminum sheeting between the grooves acts as a dry cooling fin, transferring heat from the water in the grooves to the air; the water in the grooves is in direct, but limited, contact with the air. The system appears to be closer to dry cooling than to wet, but the plates should be cheaper than the tubes and fins in a conventional dry tower. If the system is essentially dry, however, it must suffer the other disadvantage of dry towers discussed in Sec. A, namely, the need for a much higher air flow than in a wet tower. Moreover, in a larger tower there would be formidable difficulties in ensuring even distribution of water to the many grooves in the plates.

C. Assisted draft towers

In an assisted draft tower, the resistance of the tower to the flow of air is overcome partly by fans at the base of the tower and partly by the natural draft created by the tower. For a given cooling requirement, the size of the tower can be greatly reduced. The cost of the structure is similarly reduced, but this is offset by the cost of the fans. There is, however, a net reduction in initial capital cost, but this is more than outweighed by the capitalized running cost of the fans, so that the total capital cost is greater than for a plain natural draft tower. The main advantage is the fact that the tower is smaller for a given duty, or that a single assisted draft tower can perform the same duty as three natural draft towers of similar size [4].

Figure 2 from Jones [4], illustrates the design of the Central Electricity Generating Board s assisted draft tower for the 1 OOO-MW (electrical) Ince B power station. The tower is 117 m tall and has a shell base diameter of 86 m. The roofed structure that surrounds

© 1983 Hemisphere Publishing Corporation

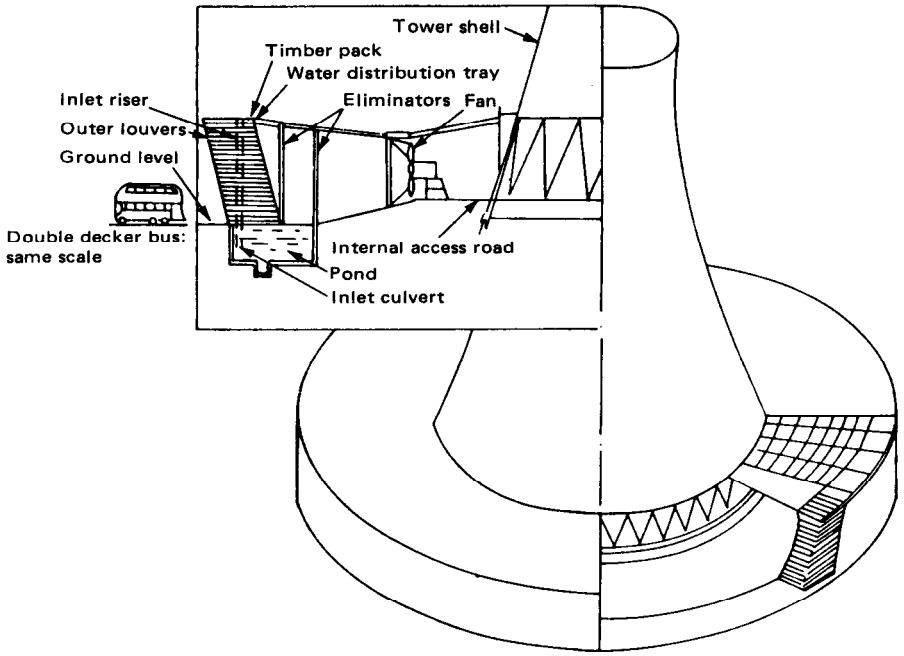

Figure 2 An assisted draft tower for a 1 OOO-MW power station. The tower is 117 m high with an outside base diameter of 172 m. From Jones [4].

the base and houses the cross-flow packing and 35 fans is 172 m in outside diameter; the fans consume 6 MW at the design point, 0.6% of the station output. Gardner [27] reports the development of this tower in some detail. Consideration was given to location of the fans upstream of the packing, where they would be readily accessible and dry, but construction costs favored a downstream location, with the further advantage that the fan blades would be protected from fluctuating stresses caused by cross winds. Accessibility is obtained by providing 36 fan cells around the base (instead of 35) and leaving the extra cell unoccupied. The packing consists of a prefabricated design of timber-lath splash bars. Two arrays of corrugated asbestos-cement louvers are necessary to cope with the high air and water mass fluxes of an assisted draft tower. Compared with the usual design, the trailing edges of the louvers are slightly extended to ensure a close approach to axial flow at the fan entry.

D. Closed-circuit evaporative coolers

The function of wet and dry cooling towers is usually to provide the means whereby heat is transferred from a primary fluid, usually condensing steam, to the atmosphere. In wet towers, low-quality cooling water is used as an intermediate fluid: as the water flows through the tubes of the heat exchanger or condenser, its temperature increases; then, as it flows through the packing of the cooling tower, its temperature falls. In a closed-circuit evaporative cooler, the heat exchanger or condenser tube bundle is placed inside the cooling tower, and the primary fluid flows within the tubes. The tube bundle can then be used as a conventional cooling tower packing, with the cooling water recirculated over the packing, without having to be ducted to an external heat exchanger or condenser, and with air ducted into and out of the tower, usually by means of a fan. As in a dry tower, the primary fluid is kept pure in a closed circuit and the packing is eliminated; but the advantage of a wet tower over a dry tower (higher change in specific enthalpy of the air stream, as discussed in Sec. A) is retained, as are its disadvantages, namely, its need for makeup water and the discharge of a possibly troublesome stream of warm, moist air. A diagram of such a cooler is presented in Fig. 3. Several other design layouts are possible, including ones using finned tubes,

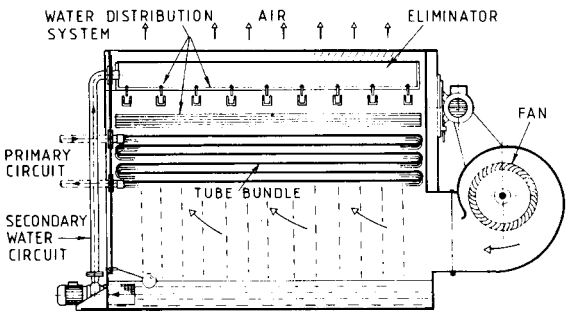

Figure 3 A closed-circuit evaporative cooler. Based on drawing supplied by Visco.

© 1983 Hemisphere Publishing Corporation

as discussed by Finlay and Grant [28]. This type of cooling tower is used for low to medium rates of heat dissipation in the process industries and for air conditioning plant rather than for electrical power generation, but it may be that the principle can be applied economically in that field as well.

The design of evaporative coolers has to take into account the simultaneous heat transfer from the tube fluid to the circulating water and heat and mass transfer between the circulating water and the air. Thus the enthalpy changes of three fluids have to be considered, compared with two in the case of wet or dry cooling towers. Parker and Treybal [29] have described a basis of analysis for design purposes. Both they and Finlay and Grant [28] discuss empirical relationships for the transfer coefficients on the outside of the tubes.

Nomenclature and References for Section 3.12.5 appear at the end of Section 3.12.6.

© 1983 Hemisphere Publishing Corporation

3.42.6
Further topics

J. R. Singham

A. Testing and acceptance

One reason for testing a cooling tower is to obtain empirical data for the design of future towers. The heat transfer and pressure drop performance of the packing are especially important in design, yet too often it is necessary to rely on data obtained in small-scale tests, which may not adequately represent the full-size behavior. Also, measurements of the distribution of water and air flow over the packing are needed so that departures from uniformity can be taken into account, either by allowing for them in design or if necessary changing the design in future to avoid them. Test data of this kind are valuable both scientifically and commercially, and it is to be hoped that more will be published in the future than have been in the past, though it has to be recognized that their very commercial value is inevitably, and not always reasonably, a deterrent to publication.

An equally important reason for testing is to enable the manufacturer and purchaser to agree on whether the tower performs the purchaser s specified cooling requirement. In this case such details as the distribution and even the magnitude of the air flow are unimportant. What matters is the values of the specified quantities and the differences between their design and test values, a matter that can give rise to considerable disagreement unless fully anticipated and catered for in the agreement at the outset. Probably the best solution to the problem is for the manufacturer to state the performance of the tower over ranges of the specified quantities [see, for example, Sec. 3.12.3B(d)]. Then the test and specified values of a suitable variable, say, the mean water exit temperature, can be compared for equal test and stated values of the remaining quantities [listed in Sec. 3.12.2A(a)].

However, this simple procedure is not always followed. It then becomes necessary to deduce from the test data the extent to which the tower would have satisfied the specified cooling requirement if it had been tested under the design conditions. This can be done only by recourse to a theory of performance or to some agreed procedure of calculation (for example, [2]). For both natural and mechanical draft towers, Sec. 3.12.2B(e) provides a basis for determining the water-to-air mass flow ratio in counter-flow towers, and it is usual for the same procedure to be used for cross-flow towers without modification. The intersection of the manufacturer s performance line for the packing, I_P In Fig. 3.12.2(6), with the curve I_M calculated for the test data, gives the value of $\dot{M}_w/\dot{M}_g$ for the test conditions.

For a natural draft tower, the procedure next to be followed can be based on Eq. 3.12.3(2), which, for a fixed design of tower and ignoring the weak dependence of N_v on the flow ratio, may be written as

$$\dot{M}_w = C\frac{M_w}{\dot{M}_g}\,[\rho_{g,1}(\rho_{g,1} - \rho_{g,2})]^{1/2} \qquad (1)$$

where C is a constant for the tower which can be determined by inserting the test values of the other quantities in the equation. Using this value of C, the same equation can now be used to predict the value of the water mass flow rate $\dot{M}_w$ that the tower is capable of cooling under design conditions, by inserting design

© 1983 Hemisphere Publishing Corporation

values on the right-hand side of the equation. This value of $\dot{M}_w$ can then be compared with the required design value.

For a mechanical draft tower, the fan controls the air mass flow rate, and fan power is one of the measured quantities. The value of the water mass flow rate under design conditions can be predicted from the test data with the aid of the following identity:

$$\dot{M}_w \equiv R_{wg}\dot{M}_g \tag{2}$$

where $R_{wg} \equiv \dot{M}_w/\dot{M}_g$, the water-to-air mass flow ratio.

This identity is applied to both the design and test values and the first identity divided by the second:

$$\frac{\dot{M}_{w,d}}{\dot{M}_{w,t}} = \frac{R_{wg,d}}{R_{wg,t}}\left(\frac{\dot{M}_{g,d}}{\dot{M}_{g,t}}\right) \tag{3}$$

where d and t are used to denote design and test values, respectively. The test mass flow rate is not usually measured but, on the assumption that $\dot{M}_g$ varies with fan power P to the power one-third (a common assumption), $\dot{M}_g$ can be eliminated:

$$\frac{\dot{M}_{w,d}}{\dot{M}_{w,t}} = \frac{R_{wg,d}}{R_{wg,t}}\left(\frac{P_d}{P_t}\right)^{1/3} \tag{4}$$

This equation enables the value of $\dot{M}_w$ at the design point, $\dot{M}_{w,d}$, to be predicted from the test values $R_{wg,t}$, $\dot{M}_{w,t}$, and P_t and the design values $R_{wg,d}$ and P_d. Again, this value of $M_{w,d}$ can be compared with the required design value.

B. Water loss

The loss of water from a cooling tower by evaporation amounts to about 1% of the rate of flow of the circulating water. If, as is nearly always the case, the air leaving the tower is close to saturation, the. magnitude of the loss may be found from

$$w = \frac{f_{g,\text{out}} - f_{g,\text{in}}}{\dot{M}_w/\dot{M}_g} \tag{5}$$

where w = rate of water loss, expressed as a fraction of the rate of flow of the circulating water

f_g = mass fraction humidity of the air stream, tabulated in Table 3.12.2(1) for saturated air, out and in denoting values at tower exit and entry, respectively

$\dot{M}_w/\dot{M}_g$ = water-to-air mass flow ratio

The value of $\dot{M}_w/\dot{M}_g$ is found by the procedure described in Sec. 3.12.2B(e). $f_{g,\text{out}}$ can be found from the specific enthalpy of the air at exit, $h_{g,\text{out}}$, calculated from Eq. 3.12.2(27), by assuming the exit air to be saturated and reading the corresponding value from Table 3.12.2(1). $f_{g,\text{in}}$ can be found from the same table by linear interpolation based on the relative humidity (determined from the dry- and wet-bulb temperatures, if not otherwise known).

A pair of natural draft cooling towers serving a 500-MW turbo generator have a combined circulating rate of about 17 m^3/s. A loss by evaporation of 1% is therefore equivalent to about 1.2 liters/kWh.

Water can also escape with the air in the form of fine droplets. To minimize this loss, called drift, eliminators are usually fitted at exit from the packing, and these intercept the larger droplets. The eliminators may consist of two rows of timber laths arranged as louvers; or a single row of louvers of corrugated asbestos cement, each louver consisting of about a single pitch cut from a large sheet; or of a more intricate design formed from plastic sheeting. Such eliminators are found to be very effective. Nevertheless, some drift loss occurs, and the stream of saturated warm air leaving the tower and carrying very fine droplets of water can give rise to a visible plume 500 m or more in length and even to very fine precipitation [20].

If makeup water were supplied at a rate just equal to the loss of water due to evaporation and drift, impurities would accumulate steadily in the circulating water. Eventually, the whole stock of circulating water would have to be changed, by which time it might be difficult to dispose of safely. Consequently, makeup water is supplied at several times the rate of loss, and water is purged from the system at a corresponding rate. The circulating water requires chlorination or other suitable treatment to suppress biological fouling.

C. Variation of atmospheric pressure

Most cooling tower design procedures employ empirical data that apply strictly only at standard atmospheric pressure. At a fixed low-altitude site the actual pressure can vary by about ±5%, but the effect on performance is small and usually ignored. If, however, the tower is built at an altitude of 5 000 ft, say (about 1 500 m), the atmospheric pressure is about 15% below the sea-level value, and the effect of this difference cannot be ignored. Pressure affects the performance of towers in two principal ways: first by its effect on the air density and hence on the air mass flow; and second by its effect on the specific enthalpies of moist air. The heat transfer performance of the packing is also likely to be somewhat pressure dependent.

The reduction in density brought about by a reduction in pressure tends to spoil the performance of both natural and forced draft towers, but the effect is more marked with natural draft since differences of density provide the driving force. On the other hand, performance tends to be improved by the changes in specific enthalpies of the air that result from a lower

© 1983 Hemisphere 1 blishing Corporation

pressure. [The h_s-h_w saturation line in Fig. 3.12.2(3) moves upwards as pressure falls since, at fixed temperature, the partial pressure of steam is constant and the mass fraction of steam in saturated air increases; steam has a higher specific enthalpy than dry air at the same temperature, and so h_s increases. For a given wet-bulb temperature, the value of $h_{g,\text{in}}$ also rises, but to a lesser extent. Consequently, the value of the integral I_M, which expresses the cooling requirement, falls at any value of $\dot{m}_w/\dot{m}_g$.] The net effect of a reduction in pressure appears to be unfavorable to natural draft and favorable to mechanical draft. However, this generalization needs to be treated with caution and proper calculations made in each particular instance.

The methods discussed for calculating the performance of cooling towers apply equally to atmospheric pressures other than standard, provided that the properties of the air are evaluated at the different pressure. (Strictly, it should be added: and provided that the effect of pressure on the heat transfer performance data for the packing is taken into account. But it is unlikely that adequate information will be available, and the effect is probably small enough to be ignored.) Thus, all that is necessary is to take the required properties from a table like Table 3.12.2(1), but for the required operating pressure. Unfortunately, tables that take pressure as an argument are not readily available, and particular correction procedures are sometimes used as an alternative.

NOMENCLATURE FOR SECTIONS 3.12.1-3.12.6

Most symbols in Sec. 3.12 are used in accordance with the overall nomenclature of this handbook. These, and all other symbols, are defined in the text at the point of their introduction. Some of the additional symbols occur in more than one subsection or are of special importance, and these are defined below.

A plan area of packing, m^2
A_i area of water-air interface per unit volume, m^2/m^3
d tower internal diameter, m
f mass fraction humidity (mass of moisture per unit mass of moist air), kg/kg
g gravitational acceleration, m/s^2
I_M integral on left-hand side of Eq. 3.12.2(12)
I_P integral on right-hand side of Eq. 3.12.2(12)
k an empirical correction factor, introduced in Eq. 3.12.3(2)
K introduced in Eq. 3.12.3(12) to replace right-hand side of Eq. 3.12.3(2), m^5 [also a component of the group KaV/L, from which it is never separated; see Sec. 3.12.2B(c)]
Ka/L introduced in Eq. 3.12.2(32); see also Sec. 3.12.2B(c), m^{-1}
KaV/L a dimensionless measure of heat transfer performance of packing; see Sec. 3.12.2B(c)
NTU the number of transfer units, a dimensionless measure of heat transfer performance of packing; see Sec. 3.12.2B(c)
NTU the number of transfer units per unit length in the direction of air flow, m^{-1}
N'_v number of dynamic pressures lost per unit length in the direction of air flow, m^{-1}
r, s, t variables of tower geometry defined following Eq. 3.12.3(4) and Eq. 3.12.3(5) and by Eq. 3.12.3(6), respectively
γ an empirical coefficient, introduced in Eq. 3.12.2(1), kg/m^2 s
γ_R the Reynolds flux for heat transfer, introduced in Eq. 3.12.2(3); approximated by γ in Eq. 3.12.2(4), kg/m^2 s
γ_w the Reynolds flux for mass transfer of water vapor, introduced in Eq. 3.12.2(33), kg/m^2 s

Subscripts

a atmospheric (pressure)
DB atmospheric dry-bulb (temperature)
g air (moist)
P packing
S air at water-air interface (considered saturated)
w water
WB atmospheric wet-bulb (temperature)
in entry to tower
out exit from tower
1 bottom of packing; bottom of shell of tower
2 top of packing
3 top of tower
th throat of tower

REFERENCES FOR SECTIONS 3.12.1-3.12.6

1. Spalding, D. B., ***Convective Heat and Mass Transfer,*** Arnold, London, 1963.
2. British Standard ***4485, Specification for Water Cooling Towers,*** Part ***1, Glossary of Terms,*** 1969; Part ***2, Methods of Test and***

© 1983 Hemisphere Publishing Corporation

Acceptance Testing, 1969; Part ***3, Thermal and Functional Design of Cooling Towers, 1977***; Part ***4, Structural Design of Cooling Towers,*** 1975, British Standards Institution, London.

3. Lowe, H. J., and Christie, D. G., Heat Transfer and Pressure Drop Data on Cooling Tower Packings and Model Studies of the Resistance of Natural-Draught Towers to Airflow, ***Proc. 1961 Int. Heat Transfer Conf., Colorado,*** Part V, pp. 933-950, 1961.
4. Jones, W. G., Cooling Water for Power Stations, ***Proc. Inst. Civ. Eng. London,*** vol. 62, pp. 373-398, 1977.
5. Lieberam, A., Heat Transfer in Corrugated Passages, Ph.D. thesis, Imperial College, University of London, 1967.
6. Tezuka, S., Performance of Aqueous-Film-Type Packing of Cooling **Tower, *Heat Transfer Jpn Res.,*** vol. 2, no. 3, pp. 40-52, 1973.
7. Hayashi, Y., Hirai, E., and Okubo, M., Volumetric Film Coefficients in Cross-Flow Cooling Towers, ***Heat Transfer Jpn. Res,*** vol. 2, no. 2, pp. 1-6, 1973.
8. Rish, R. F., The Design of a Natural Draught Cooling Tower, ***Proc. 1961 Int. Heat Transfer Conf., Colorado,*** **Part V,** pp. 951-958, 1961.
9. Singham, J. R., The Thermal Performance of Natural-Draught Cooling Towers, MED Rept. ED/R/C/l, Imperial College, London, 1967.
10. Zivi, S. M., and Brand, B. B., An Analysis of the Cross-Flow Cooling Tower, ***Refrigerating Eng.,*** vol. 64, pp. 31-34, 90-92, 1956.
11. Baker, D. R., and Shryock, H. A., A Comprehensive Approach to the Analysis of Cooling Tower Performance, ***J. Heat Transfer,*** vol. 83, pp. 339-349, 1961.
12. Chilton, H., Performance of Natural-Draught Water-Cooling Towers, ***Proc. Inst. Elec. Eng. London,*** vol. 99, pp. 440-452, 1952.
13. Singham, J. R., and Spalding, D. B., The Performance of Natural-Draught Cooling Towers: Comparison of Theory with Experiment, ***II Int. Congr. Chem Eng., Chem Equipment and Automation, Marienbad, Czechoslovakia,*** 1965. (Reprinted by Department of Mechanical Engineering, Imperial College, London, 1965, German translation published in Chemische Technik, July 1966.)
14. Ioannides, J. P., Resistance to Air Flow through Natural-Draught Cooling Towers, Ph.D. thesis, Imperial College, University of London, 1965.
15. Gurtinkel, G., and Wolser, A., Analysis and Design of Hyperbolic Cooling Towers, ***Trans. Am. Soc. Civil Eng., J. Power Div., vol. 98,*** pp. 133-152, 1972.
16. Diver, M., and Paterson, A. C., Large Cooling Towers-the Present Trend, ***Proc. Inst. Struct. Eng. London, Structural Eng., vol. 55,*** pp. 431-445, 1977.
17. Zerna, W., and Mungan, I., Construction and Design of Large Cooling Towers, ***Trans. Am Soc. Civil Eng., J. Struct. Div.,*** vol. 106, pp. 531-544, 1980.
18. Marriott, K. E., Noise in Mechanical Draught ***Cooling*** Towers, ***Heating and Air Conditioning J.,*** London, vol. 48, pp. 12-18, 38-45, 1978.
19. National Fire Protection Association, Pamphlet 214, ***Water Cooling Towers*** 1977, Boston, 1977.
20. Kunesch, A., Mechanical and Environmental Considerations of Cooling Tower Selection, Process ***Eng.,*** Sept., pp. 164-167, Nov., pp. 86-91, 1978.
21. Christopher, P. J., and Forster, V. T., Rugeley Dry Cooling Tower System, ***Proc. Inst. Mech. Eng. London,*** vol. 184, pp. 197-211, 1969-1970.
22. Van der Walt, N. T., West, L. A., Sheer, T. J., and Kuball, D., The Design and Operation of a Dry Cooling System for a 200 MW Turbo-Generator at Grootvlei Power Station, South Africa, ***S. Afr. Mech. Eng.,*** vol. 26, pp. 498-507, 1976.
23. Russell, C. M. B., McChesney, H. R., Holder, D. W., and Verlinden, M., Cross Wind and Internal Flow Characteristics of Dry Cooling Towers, ***Combustion,*** vol. 49, no. 11, pp. 20-24, 1978.
24. Croley, T. E., Patel, V. C., and Cheng, M.-S., Economics of Dry-Wet Cooling Towers, ***Trans. Am Soc. Civil Eng., J. Power Div.,*** **vol.** 102, pp. 147-163, 1976.
25. Larinoff, M. W., and Forster, L. L., Dry and Wet-Peaking Tower Cooling Systems for Power Plant Application, ***J. Eng. Power (Trans. ASME),*** vol. 98, pp. 335-348, 1976.
26. Bentley, J. M., Snyder, T. K., Glicksman, L. R., and Rohsenow, W. M., An Experimental and Analytical Study of a Unique Wet/Dry Surface for Cooling Towers, ***J. Heat Transfer,*** **vol. 100,** pp. 520-526, 1978.
27. Gardner, B. R., The Development of the Assisted-Draught Cooling Tower, ***Combustion, vol. 48,*** pp. 15-22, 1976.
28. Finlay, I. ***C.,*** and Grant, W. D., ***Thermal Design of Evaporative*** Coolers, part of NEL Rept. 534, National Engineering Laboratory, Glasgow, 1972.
29. Parker, R. O., and Treybal, R. E., The Heat, Mass Transfer Characteristics of Evaporative Coolers, ***Chem. Eng. Prog. Symp. Ser.,*** vol. 57, pp. 138-149, 1961.

© 1983 Hemisphere Publishing Corporation

3.13 Dryers

Contents

3.13.1
INTRODUCTION, E. U. Schliinder **3.13.1-1**

3.13.2
CLASSIFICATION AND SELECTION, E. U. Schliinder **3.13.2-1**

3.13.3
LAYOUT AND PERFORMANCE DATA, E. U. Schliinder **3.13.3-1**

A. The Mollier chart 3.13.3-1
B. Energy and mass balances 3.13.3-1
C. The wet-bulb temperature 3.13.3-2
D. Description of drying processes in the Mollier chart 3.13.3-4

3.13.4
PREDICTION OF DRYING RATES, E. U. Schliinder **3.13.4-1**

3.13.5
PREDICTION OF RESIDENCE TIMES WITH PRESCRIBED MATERIAL FLOW, E. U. Schliinder **3.13.5-l**

A. Example: drying of bricks 3.1352

3.13.6
PREDICTION OF RESIDENCE TIMES WITH NONPRESCRIBED MATERIAL FLOW, E. U. Schliinder **3.13.6-1**

3.13.7
PRACTICAL DRYER DESIGN, D. Raey **3.13.7-1**

A. Band dryers 3.13.7-1
B. Fluid-bed dryers 3.13.7-2
C. Rotary dryers 3.13.7-2
D. Pneumatic conveying dryers 3.13.7-2
E. Spray dryers 3.13.7-2

Nomenclature for Sections 3.13.1-3.13.7 **3.13.7-3**
References for Sections 3.13.1-3.13.7 3.13.7-3

© 1983 Hemisphere Publishing Corporation

HEDH

3.13.1 Introduction

E. U. Schliinder

■ Dryers are used to remove water or solvents from solid material by evaporation. The solid material usually has a rigid structure. However, pastes, slurries, and liquid solutions are also handled in dryers. In this case the formation of the rigid structure of the solid material occurs during the drying process itself. The effect of drying on the quality of the dried product depends on the drying conditions. The use of fast drying at high temperatures reduces the size of dryer required; however, it may also destroy the solid product by shrinking it too fast and by formation of fissures or by denaturing and other forms of deterioration of the constituents. The selection of drying conditions is usually a compromise between these two requirements-minimizing the size of the drying equipment and optimizing the product quality. Also, energy consumption has to be taken into account.

Dryers are designed in many different ways in order to serve various requirements, such as high- or low-temperature drying at normal pressure, or at vacuum with air or nitrogen or superheated vapor as the drying agent.

Other requirements result from whether the product is a liquid, a slurry, or a solid. Solid material may be in the form of large pieces, sheets, threads, granules, powder, or other.

Another aspect is the required residence time of the product in the dryer, which may vary from a fraction of a second up to several days. This leads to different concepts of dryer design.

The heat necessary to evaporate the moisture may be supplied by convection through the drying agent, by radiation, by direct contact conduction, or by microwaves. This again leads to different concepts of dryer design. The majority of dryers, however, are furnished with convective heat supply. A classification of types of dryers must take into account all these aspects in order to provide a good tool for the selection of a proper type with respect to the nature of the product.

Once the type of dryer has been selected, the next step is to determine the layout of the drying process and the performance data as well as the size of the dryer.

Layout and performance data result from overall and partial energy and mass balances. A very useful tool in the case of convective drying is the Mollier chart, which depicts the correlations among enthalpy, humidity, and temperature of the drying agent.

The prediction of the size of the dryer is based on the so-called drying rate function, which correlates the drying rate $\dot{M}$ (kg/m^2 s) with the product moisture content Y (kg liquid/kg dry product). The drying rate is the amount of vapor in kilograms escaping from the product surface in square meters per unit time in seconds. Usually the drying rate function must be determined through laboratory-scale experiments with a sample of the particular product. Many attempts have been made to predict drying rate functions by the application of heat and mass transfer fundamentals. These attempts, however, have been only partially successful. Usually the parameters that appear in these theoretical analyses are not available. Therefore, a well-balanced combination of laboratory tests and theoretical approaches is the fastest and most reliable way to determine drying rate functions.

Knowing the drying rate function, the remaining question is the residence time and the residence time

© 1983 Hemisphere Publishing Corporation

distribution in the large-scale dryer. In many cases this question is easy to answer, for example, for batch dryers or in continuous dryers with a well-defined path for the product, as in a belt dryer. In spray dryers, fluidized-bed dryers, pneumatic conveyance dryers, rotary dryers, and others, the residence time distribution is difficult to predict and is therefore subject to more or less rough guesses. In view of what has been pointed out so far, the subsequent sections are organized as follows:

Classification and selection of dryers
Layout and performance data of dryers
Rating of dryers

© 1983 Hemisphere Publishing Corporation

3.13.2
Classification and selection

E. U. Schliinder

■ Among the various requirements that determine the design concept of a dryer, the transportation of the product through the dryer may be very important, since it is closely related to the residence time. Second, the initial state of the product (liquid, paste, solid, powder, granular, sheet, etc.) also influences the design concept to a great extent. Therefore a matrix is presented in Table 1 that correlates the residence time and the initial state of the product (liquid to solid).

A brief description of various types of dryers, including some indication of the specific energy consumption per kilogram of evaporated water, is also given in Table 2.

© 1983 Hemisphere Publishing Corporation

Table 1 Classification of dryers with respect to the physical state of the product and the residence time of the product in the dryer

Residence time	Wet, moist material					
			Solid			
	Liquid	Paste	Powdery	Granular	Clumpy	Sheet
Short (<1 min)	Spray dryer Drum dryer (Agitated film dryer)	Spray dryer Drum dryer (Agitated fii dryer)	Flash dryer	Flash dryer Grinding dryer	Flash dryer (Grinding dryer)	Cylindrical dryer
Moderate (1 min-1 h)			Screw conveyer dryer Paddle dryer Horizontal cylindrical dryer	Continuous band dryer Roto louver dryer Vibrating dryer	Continuous band dryer	
		(Kneading dryer)	Vibrating dryer	Fluidized-bed dryer	Kneading dryer	
		Rotating shelf dryer	Rotating shelf dryer	Rotating shelf dryer Pan dryer Plate dryer	Rotating shelf dryer	
		(Paddle dryer) Horizontal cylindrical dryer		Paddle dryer Horizontal cylindrical dryer Steam-tube rotary dryer	Paddle dryer Horizontal cylindrical dryer Steam-tube rotary dryer	
		Rotary dryer (with lifters)		Rotary dryer (with lifters)	Rotary dryer (with lifters)	
Long (>1h)		Tray dryer Truck dryer Tunnel dryer	Tray dryer Truck dryer Tunnel dryer	Tray dryer Truck dryer Tunnel dryer	Tray dryer Truck dryer Tunnel dryer Continuous band dryer	

© 1983 Hemisphere Publishing Corporation

Table 2 Capacity and energy consumption for various types of dryers

Figure[a]	Type	Evaporation rate, kg H_2O/h per m^2 or per m^3	Energy consumption, kJ/kg evaporated H_2O
1	Drying loft	20/m^2	5 000–6 000
2	Compartment dryer (normal pressure)	0.1–15/m^2	5 000-13 000
3	Compartment dryer (vacuum)	0.1–1/m^2	3 000-5 000
4	Tunnel dryer		5 500-6 500
5	Band dryer		4 000-6 000
6	Jet impingement dryer	50/m*	5 000-7 000
7	Shelf dryer	4–8/m^2	3 500–9 000
8	Rotary dryer	30–80/m^2	4 600–9 200
9	Centrifugal dryer	90/m^3	3 000-4 000
10	Fluidized-bed dryer		
11	Pneumatic bed dryer	Particle diameter d_p = 0.5 mm: 100/m^3 d_p = 1 mm: 20/m^3 d_p = 5 mm: 4/m	4 600–9 200
12	Spiral-tube dryer	500/m^3	3 500
13	Spray dryer	1–50/m^3	4600-11500
14	Drum dryer for pasty materials	7–25/m^2	3 200-6 500
15	Holoflite dryer	5–15/m^2 (0.5-2.5 low moisture content)	3 700-6 500

[a]Figures 1-15 show more or less schematically the design of the various types of dryers in common use.

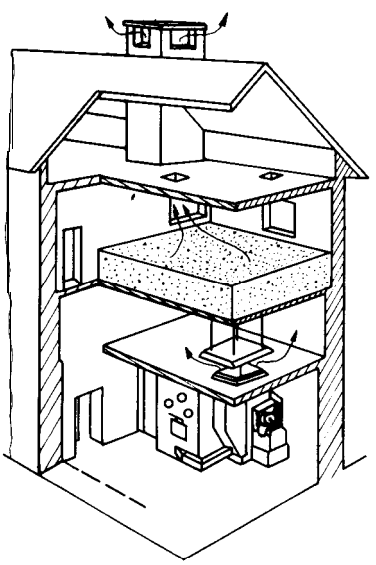

Figure 1 Drying loft.

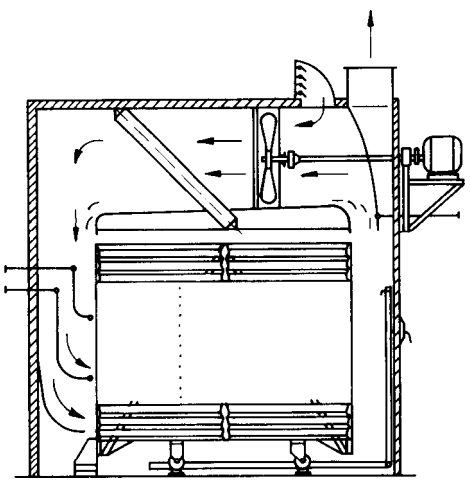

F & e 2 Compartment dryer (normal pressure).

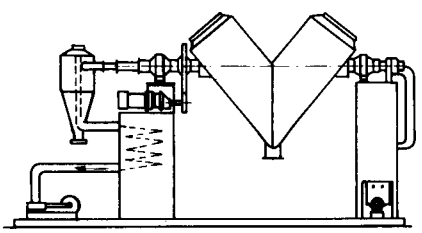

Figure 3 Compartment dryer (vacuum).

© 1983 Hemisphere I blishing Corporation

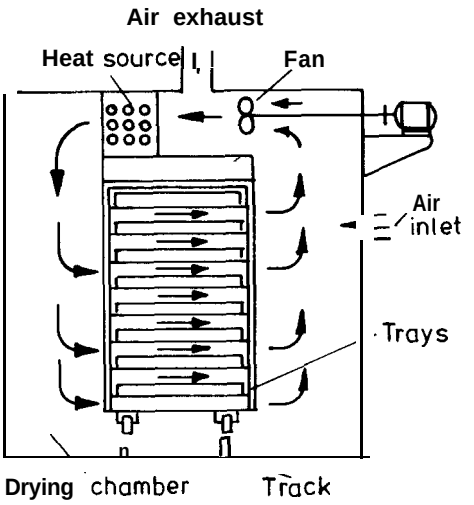

Figure 4 Tunnel dryer.

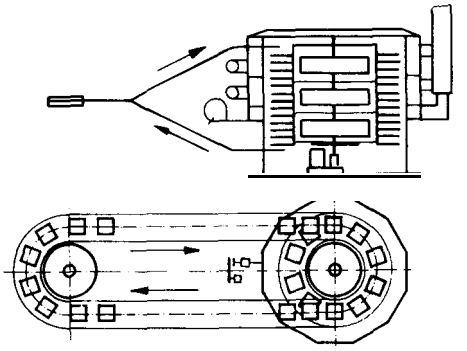

Figure 5 Band dryer

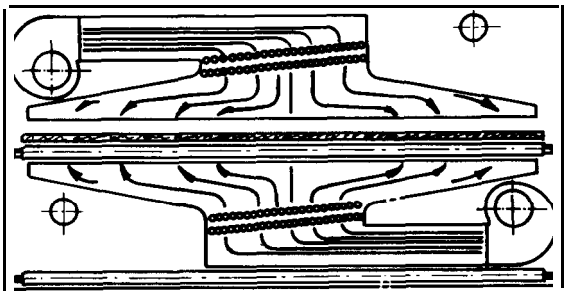

Figure 6 Jet impingement dryer.

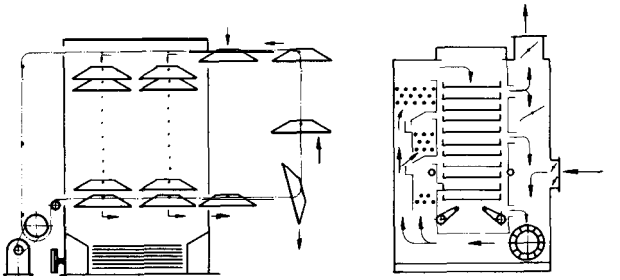

Figure 7 Shelf dryer.

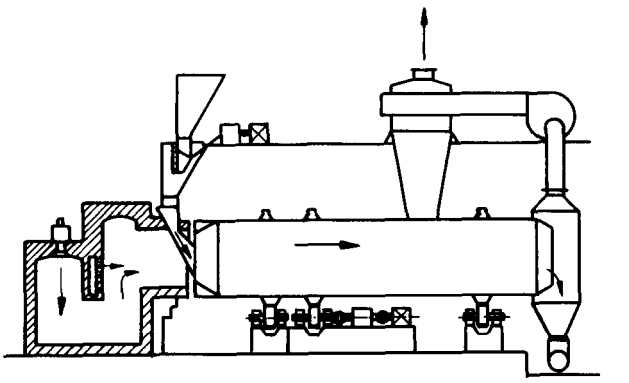

Figure 8 Rotary dryer.

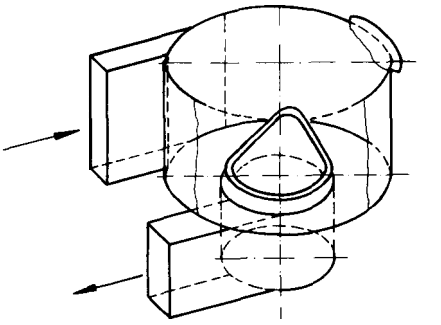

Figure 9 Centrifugal dryer.

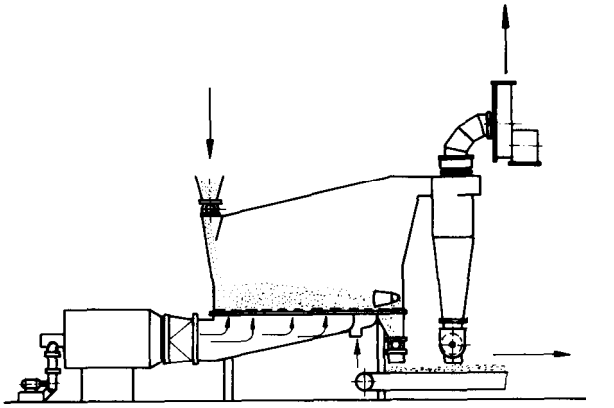

Figure 10 Fluidied-bed dryer.

© 1983 Hemisphere Publishing Corporation

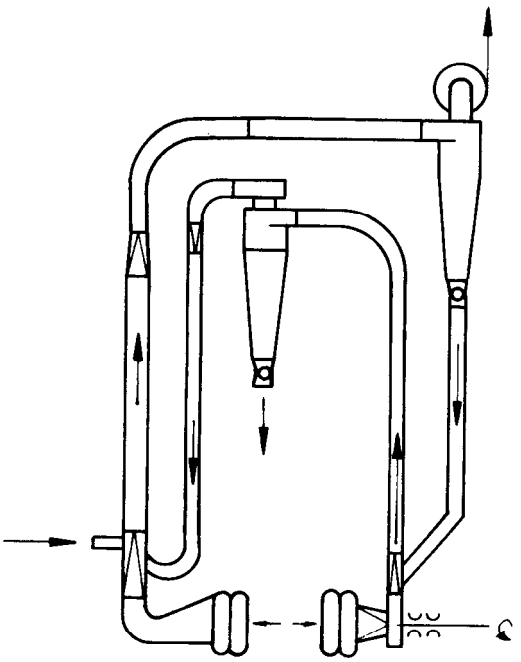

Figure 11 Pneumatic bed dryer.

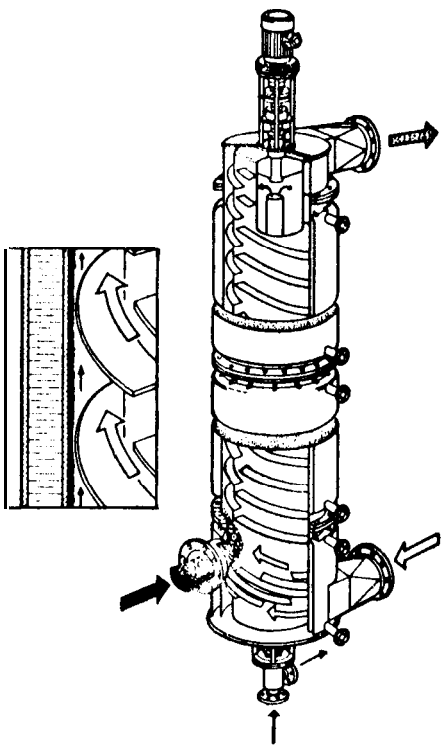

Figure 12 Spiral-tube dryer.

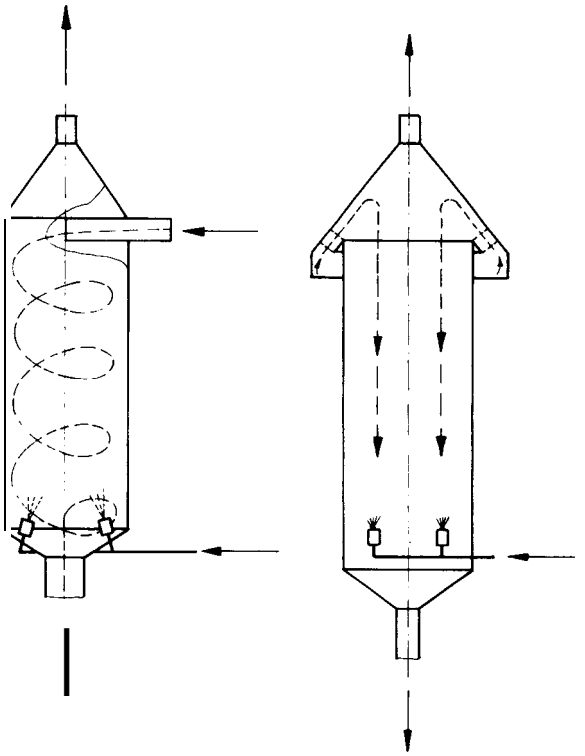

Figure 13 Spray dryer.

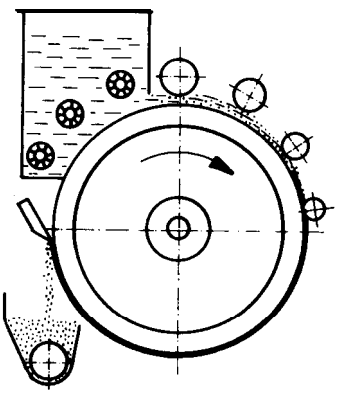

Figure 14 Drum dryer for pasty materials.

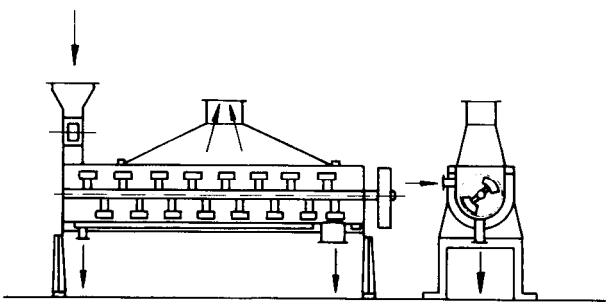

Figure 15 Holofiite dryer.

© 1983 Hemisphere Publishing Corporation

3.13.3
Layout and performance data

E. U. Schliinder

A. The Mollier chart

In most cases the drying agent is air. During the drying process, heat is transferred from the air to the product while vapor is transferred from the product to the air. This combined transfer process of heat and mass leads to a change of enthalpy as well as of the vapor concentration of the drying agent. It is convenient to depict those changes in an enthalpy concentration chart for the drying agent, the so-called Mollier chart for humid air as shown in Fig. 1 (see also Krischer and Kast [1]). The enthalpy of the humid air is defined as

$$h = c_{p,\text{air}} T + X(\Delta h_v^0 + c_{p,\text{vapor}} T) \qquad (1)$$

$c_{p,\text{air}}$ (in J/kg dry air K) is the specific enthalpy of the dry air, $c_{p,\text{vapor}}$ is that of the pure vapor. Δh_v^0, in joules per kilogram, is the standard latent heat of vaporization at 0°C, X is the vapor content in kilograms vapor/kilogram dry air or the absolute humidity, T is the temperature in degrees Celsius, and h is the enthalpy of the *humid* air in joules per kilogram *dry* air. φ in Fig. 1 is the relative humidity, which is equal to the ratio of the partial vapor pressure p_v to the saturation vapor pressure at a given temperature $p_v^*(T)$. The absolute humidity can be calculated from the partial vapor pressure p_v and the total pressure p:

$$X = 0.622 \frac{p_v}{p - p_v} \qquad (2)$$

In this equation the factor 0.622 is the ratio of the gas constants $R_{\text{air}}/R_{\text{vapor}}$. Both Eqs. (1) and (2) are based on the assumption that air and vapor can be considered as ideal gases. When the partial vapor pressure p_v is equal to the saturation vapor pressure p_v^*, the air is saturated with vapor or the relative humidity φ equals unity. The corresponding saturation values of enthalpy and absolute humidity are $h^*(T)$ and X*(T).

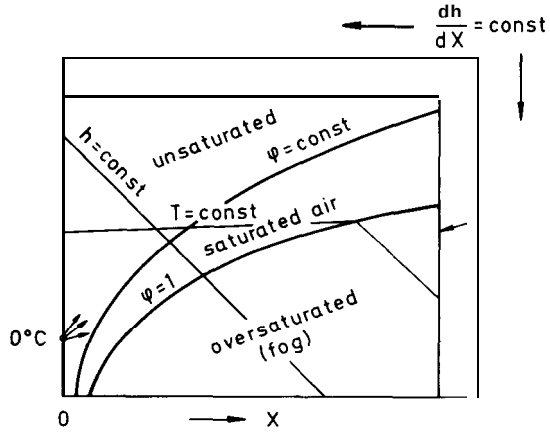

Figure 1 Mollier chart for humid air at constant total pressure [1].

B. Energy and mass balances

The Mollier chart permits the tracing of the change of state of the drying agent during a convective drying process and also the determination of the temperature of the moist product in a simple, graphic manner. Figure 2 shows schematically a convective dryer. Hot and dry air with temperature T_{in}, humidity X_{in}, and enthalpy h_{in} enters the dryer. At the outlet at position L, these

© 1983 Hemisphere Publishing Corporation

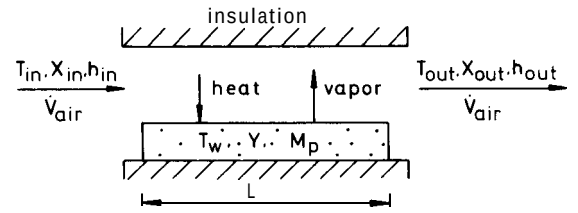

Figure 2 Drying of porous material with hot air.

quantities have been changed to $T_{out}, X_{out}, h_{out}$. The temperature of the moist product is T_w, and the moisture content is Y in kilograms liquid per kilogram dry substance. The energy balance for this dryer yields

$$\rho_{air}\dot{V}_{air}(h_{in} - h_{out})\, dt = -M_p\, dh, \qquad (3)$$

where $(\rho\dot{V})_{air}$ is the air mass flow rate in kilograms dry air per second, dt is the incremental time difference, M_p is the mass of the dry product, and dh, is the incremental change of the product enthalpy, which is defined by

$$h_p = (c_{p,product} + Yc_{p,liquid})T_w \qquad (4)$$

where Y is the free liquid content of the product. The mass balance can be written

$$\text{Pair}\ \dot{V}_{air}(X_{in} - X_{out})\, dt = -M_p\, dY \qquad (5)$$

If the product temperature T_w is constant during the drying process, then Eq. (3) gives

$$dh_p = -c_{p,liquid}T_w\, dY \qquad (6)$$

In this case one obtains, by combining the energy and the mass balance,

$$\frac{h_{in} - h_{out}}{X_{in} - X_{out}} = c_{p,liquid}T_w \qquad (7)$$

Assuming the dryer to be infinitely long, h_{out} and X_{out} approach the saturation data $h_w^*(T_w)$ and $X_w^*(T_w)$. This means also that

$$\frac{h_{in} - h_w^*(T_w)}{X_{in} - X_w^*(T_w)} = c_{p,liquid}T_w \qquad (8)$$

is valid. This equation is formally identical with the equation describing the fog isotherm in the Mollier chart. Figure 3 shows that, for a given entrance condition of the drying agent T_1, X_1, h_1, the product temperature T_w can be found by selecting that fog isotherm which intersects the point representing the entrance condition when prolonged backward into the unsaturated region. These prolonged fog isotherms are called lines of constant wet-bulb temperature, because a thermometer stuck into a wetted bulb and exposed to an air stream having T_1 and X_1, or T_2 and X_2, or any T and X along this line, will measure the temperature T_w.

C. The wet-bulb temperature

The determination of the temperature T_w of the moist product through energy and mass balances applies as long as the product temperature remains constant with respect to both the time and the position in the dryer. This is true in fact as long as the moisture evaporates at the surface of the product, and as long as the ratio of the heat transfer coefficient α between the drying agent and the product surface and the respective mass transfer coefficient β is equal to the heat capacity of the humid air $\rho_g c_{pg}$ per unit volume:

$$\frac{\alpha}{\beta} = \rho_g c_{pg} \qquad (9)$$

Equation (9) is called the Lewis law. Furthermore, the drying rate must not be too high. This restriction is discussed below.

The Lewis law applies fairly well for air-water vapor mixtures. From the analogy between heat and mass transfer, one can derive the expression for the α/β ratio,

$$\frac{\alpha}{\beta} = \rho_g c_{pg}\, \mathrm{Le}^m \qquad (10)$$

with m between 0.6 and 0.7. Le is the Lewis number, defined by $\mathrm{Le} = \kappa/\delta$, where κ is the thermal and δ the mass diffusivity. This number is close to unity for air-water vapor, so Eq. (9) applies. For other solvents that evaporate into air, for example, organic substances, Le lies approximately between 2 and 5. In these cases the lines of constant wet-bulb temperature in the Mollier chart are no longer straight, and the product temperature increases slightly downstream within the dryer. In practical calculations, however, this variation of the product temperature is often neglected.

Actually, the fact that the product temperature during the drying process is practically stationary as

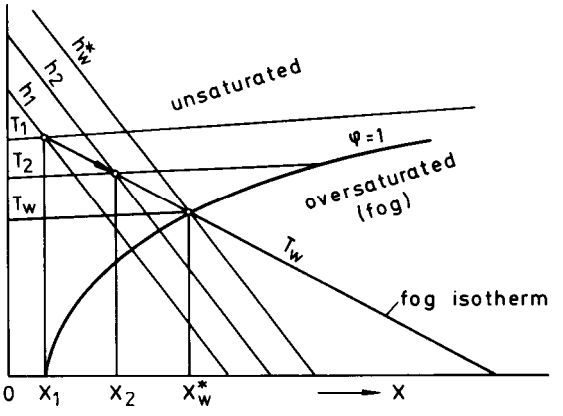

Figure 3 Lines of constant wet-bulb temperature in the Mollier chart.

© 1983 Hemisphere Publishing Corporation

long as the evaporation of the moisture takes place at the product surface results from a steady-state balance of heat and mass transfer. Therefore, the general expression for the prediction of the wet-bulb temperature T_w must be derived by starting with the basic laws of heat and mass transfer. This derivation is presented in the following paragraphs. The result of this more general approach explains the above-mentioned restrictions on the application of Eqs. (7) and (8), which are derived from energy and mass balances only.

The heat $\dot{q}$ transferred from the drying agent to the surface of the product is given by

$$\dot{q} = \alpha(T - T_w) \tag{11}$$

whereas the vapor transferred from the surface into the drying agent follows from

$$\dot{N}_{\text{vapor}} = \tilde{\rho}_g \beta(\tilde{x}_w - \tilde{x}) \tag{12}$$

where $\tilde{\rho}$ is the molar density of the humid air ($\tilde{\rho} = p/\tilde{R}T$), $\dot{N}_{\text{vapor}}$ is the molecular flux of the vapor, and $\tilde{x}$ is the mole fraction of vapor in the drying agent. Both Eqs. (11) and (12) apply if the mole fractions x_w and $\tilde{x}$ are low, that is, $\tilde{x} < \tilde{x}_w \ll 1$. The energy balance at the surface yields

$$\dot{q} = \dot{N}_{\text{vapor}} \Delta\tilde{h}_v(T_w) \tag{13}$$

where $\Delta\tilde{h}_v(T_w)$ at surface temperature T_w follows from the standard heat of vaporization by

$$\Delta\tilde{h}_v = \Delta\tilde{h}_v^0 - (\tilde{c}_{p,\text{liquid}} - \tilde{c}_{p,\text{vapor}})T_w \tag{14}$$

Assuming thermodynamic equilibrium at the product surface, so that $\tilde{x}_w = \tilde{x}_w^*(T_w)$, one obtains from the energy balance

$$\alpha(T - T_w) = \tilde{\rho}_g \beta(\tilde{x}_w^* - \tilde{x}) \times [\Delta\tilde{h}_v^0 - (\tilde{c}_{p,\text{liquid}} - \tilde{c}_{p,\text{vapor}})T_w] \tag{15}$$

Putting

$$\frac{\alpha}{\tilde{\rho}_g \beta} = \tilde{c}_{pg} = (1 - \tilde{x})\tilde{c}_{p,\text{air}} + \tilde{x}\tilde{c}_{p,\text{vapor}} \tag{16}$$

according to the Lewis law, Eq. (15) becomes

$$\tilde{c}_{p,\text{air}} T + \frac{\tilde{x}}{1-\tilde{x}}(\Delta\tilde{h}_v^0 + \tilde{c}_{p,\text{vapor}} T) - \left[\tilde{c}_{p,\text{air}} T_w + \frac{\tilde{x}_w^*}{1-\tilde{x}}(\Delta\tilde{h}_v^0 + \tilde{c}_{p,\text{vapor}} T_w)\right] = \left(\frac{\tilde{x}}{1-\tilde{x}} - \frac{\tilde{x}_w^*}{1-\tilde{x}}\right)\tilde{c}_{p,\text{liquid}} T_w \tag{17}$$

For $\tilde{x} < \tilde{x}_w \ll 1$, the mole fractions may be replaced by the absolute humidity:

$$\frac{\tilde{x}_w^*}{1-\tilde{x}} \cong \frac{\tilde{M}_{\text{vapor}}}{\tilde{M}_{\text{air}}} X_w^*$$

$$\frac{\tilde{x}}{1-\tilde{x}} = \frac{\tilde{M}_{\text{vapor}}}{\tilde{M}_{\text{air}}} X$$

Further, $\tilde{M}_{\text{air}}\tilde{c}_{p,\text{air}} = c_{p,\text{air}}$, $\tilde{M}_{\text{vapor}}\tilde{c}_{p,\text{vapor}} = c_{p,\text{vapor}}$ and $\tilde{M}_{\text{vapor}}\,\Delta\tilde{h}_v^0 = \Delta h_v^0$. Thus Eq. (17) transforms into

$$c_{p,\text{air}} T + X(\Delta h_v^0 + c_{p,\text{vapor}} T) - [c_{p,\text{air}} T_w + X_w^*(\Delta h_v^0 + c_{p,\text{vapor}} T_w)] = (X - X_w^*)c_{p,\text{liquid}} T_w \tag{18}$$

Replacing the left-hand side of this equation by the enthalpy h and h_w^*, respectively, according to Eq. (1), gives

$$h - h_w^* = (X - X_w^*)c_{p,\text{liquid}} T_w \tag{19}$$

which is identical with Eq. (8). Thus it has been shown that the more general approach, starting from the basic laws of heat and mass transfer, leads to the same expression for the wet-bulb temperature as the special approach, starting from the energy and mass balances, as long as the Lewis law applies and the mole fractions $\tilde{x}$ are small compared with unity.

Also, under these conditions the effect of additional heat transfer by radiation $\dot{q}_r$ on the wet-bulb temperature can be taken into account in a simple way. In this case the energy balance at the product surface gives

$$\alpha(T - T_w) + \dot{q}_r = \dot{N}_{\text{vapor}} \Delta\tilde{h}_v(T_w) \tag{20}$$

Defining an apparent temperature T_{app} of the drying agent by

$$T_{\text{app}} = T + \frac{\dot{q}_r}{\alpha} \tag{21}$$

Eq. (20) becomes

$$\alpha(T_{\text{app}} - T_w) = \dot{N}_{\text{vapor}} \Delta\tilde{h}_v(T_w) \tag{22}$$

which is formally identical with Eq. (13) and therefore leads to the same result,

$$T_w = T_w(T_{\text{app}}, X)$$

as shown in Fig. 4.

However, one should not forget that T_{app} is a fictitious temperature that depends on the heat transfer coefficient α, which is always very large at the leading edge of the product and decreases downstream. Therefore, the product temperature is close to the adiabatic wet-bulb temperature T_w and increases downstream. The downstream change of the properties T, h, and X of the drying agent must be computed stepwise by numerical methods.

If the drying rate is very high because the tem-

© 1983 Hemisphere Publishing Corporation

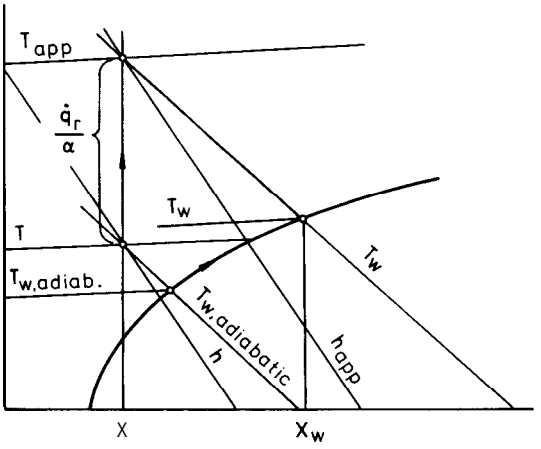

Figure 4 Effect of radiation on the wet-bulb temperature.

perature of the drying agent is very high, and the mole fraction $\tilde{x}_w^*$ is no longer much less than unity, the wet-bulb temperature is calculated by the formula

$$T - T_w = \left\{ \frac{\Delta \tilde{h}_v}{\tilde{c}_{p,\text{vapor}}} + \frac{\dot{q}_r}{\alpha} \frac{1}{\ln\left[1 + (\tilde{x}_w^* - \tilde{x})/(1 - \tilde{x}_w^*)\right]^{\mu}} \right\} \times \left[\left(1 + \frac{\tilde{x}_w^* - \tilde{x}}{1 - \tilde{x}_w^*} \right)^{\mu} - 1 \right] \quad (23)$$

with

$$\mu = \frac{\tilde{p}_g \tilde{c}_{p,\text{vapor}} \beta}{\alpha} \quad (24)$$

or, with Eq. (10),

$$\mu = \frac{\tilde{c}_{p,\text{vapor}}}{(1-\tilde{x})\tilde{c}_{p,\text{air}} + \tilde{x}\tilde{c}_{p,\text{vapor}}} \quad h\text{-}0.65 \quad (25)$$

Evaluation of Eq. (23) has shown that μ is almost independent of temperature T and humidity X of the drying agent. For the system air-water vapor, μ is equal to -1.3. For air-decane vapor, μ is equal to 3.8; see [2].

D. Description of drying processes in the Mollier chart

A very common type of dryer is the tunnel dryer, as shown schematically in Fig. 5. The mass balance for the volatile component yields

$$\dot{M}_{\text{prod}} Y_{\text{in}} + \dot{M}_{\text{air}} X_{\text{in}} = \dot{M}_{\text{prod}} Y_{\text{out}} + \dot{M}_{\text{air}} X_{\text{out}} \quad (26)$$

The energy balance gives

$$\dot{Q}_h + \dot{M}_{\text{prod}} h_{p,\text{in}} + \dot{M}_{\text{air}} h_\infty = \dot{Q}_{\text{trans}} + \dot{M}_{\text{prod}} h_{p,\text{out}} + \dot{M}_{\text{air}} h_{\text{out}} \quad (27)$$

The enthalpy of the drying agent h has been defined by Eq. (1) and the product enthalpy h_p by Eq. (4),

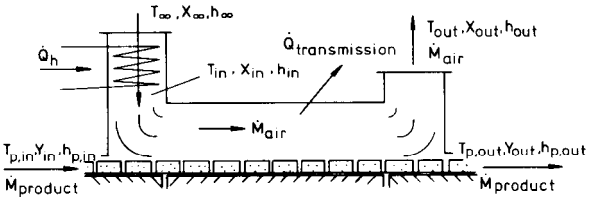

Figure 5 Tunnel dryer, schematically.

which applies, however, only if Y indicates the free moisture content. For strongly hygroscopic materials, the sorption energy must be added.

Figure 6 shows the mass and energy balances in a Mollier chart. The ambient air having $T_\infty, X_\infty, h_\infty$ is heated in the preheater by $\dot{Q}_h$ up to $T_{\text{in}}, h_{\text{in}}$ while X remains constant, so that $X_{\text{in}} = X$,. If the product temperature is constant, that is, $T_{w,\text{out}} = T_{w,\text{in}}$, and if no sorption energy is involved, and if there were no heat losses, that is, $\dot{Q}_{\text{trans}} = 0$, the state of the air would change along the line $(dh/dX)_{\text{adiabatic}}$, and the product temperature would be $T_{w,\text{in}}$ all the way downstream. Usually, however, $T_{w,\text{out}}$ is different from $T_{w,\text{in}}$. Also, some amount of sorption energy is involved, and heat losses $\dot{Q}_{\text{trans}}$ are unavoidable. Therefore, the state of the air changes along the line $(dh/dX)_{\text{prod+trans}}$ and the product temperature changes from $T_{w,\text{in}}$ to $T_{w,\text{out}}$ and may eventually come close to the temperature of the exhaust air T_{out}.

The energy consumption $\dot{Q}_h$ of this drying process per unit mass of evaporated liquid is

$$\frac{\dot{Q}_h}{\dot{M}_{\text{vapor}}} = \left(\frac{dh}{dX}\right)_{\text{exh}} + \frac{\dot{Q}_{\text{trans}} + \dot{M}_p(h_{p,\text{out}} - h_{p,\text{in}})}{\dot{M}_{\text{vapor}}} \quad (28)$$

where $(dh/dX)_{\text{exh}}$ is the specific energy consumption per unit mass of evaporated liquid due to the change

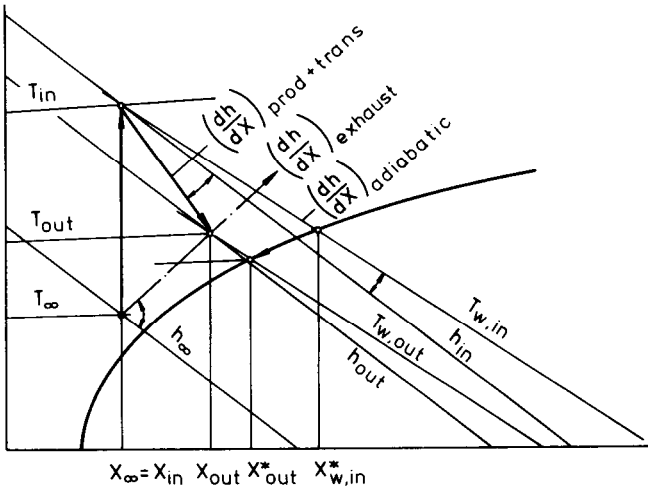

Figure6 Mass and energy balances for a dryer, depicted in a Mollier chart.

© 1983 Hemisphere Publishing Corporation

of enthalpy of the drying agent, and

$$\frac{\dot{Q}_{\text{trans}} + \dot{M}_p(h_{p,\text{out}} - h_{p,\text{in}})}{\dot{M}_{\text{vapor}}} = -\left(\frac{dh}{dX}\right)_{\text{prod + trans}} \quad (29)$$

that is, the specific energy consumption due to the change of enthalpy of the product plus the heat losses by transmission. Table 1 contains some data of specific energy consumption for both $\dot{Q}_h/\dot{M}_{\text{vapor}}$ and $-(dh/dX)_{\text{prod + trans}}$ for several types of dryers.

Table 1 Specific energy consumption for various types of dryers[a]

Type of dryer	$\dot{Q}_h/\dot{M}_{\text{vapor}}$, total specific energy consumption, kJ/kg H_2 0	$-(dh/dX)_{\text{prod+trans}}$, specific energy consumption by product transmission heat losses, kJ/kg H_2 0
Tunnel dryer	5 500–6 500	1800-2 700
Rotary dryer	4 600–9 200	800-5 500
Pneumatic dryer	4 600–9 200	800-S 500
Spray dryer	4600-11500	800-8 000
Drum dryer	3 200–6 500	
	3 700–6 500	

[a]These data indicate that the total energy consumption of a dryer is two to three times as much as is required to evaporate the water.

Nomenclature and References for Section 3.13.3 appear at the end of Section 3.13.7.

© 1983 Hemisphere Publishing Corporation

3.13.4
Prediction of drying rates

E. U. Schlünder

■ The drying rate $-dY/dt$ depends primarily on the moisture content Y of the product. Figure 1 shows a typical drying rate function $-(M_s/A)(dY/dt) = \dot{M}_v = f(Y)$ for constant drying conditions such as temperature T_∞, humidity X_∞, pressure P, and mass transfer coefficient β_g between the surface of the product and the drying agent (air). M_s is the amount of dry product, and A is the interfacial area. Starting the drying process from the initial moisture content Y_0, the drying rate remains constant until the so-called critical moisture content Y_{cc} is reached. Within this constant rate period -regime I-the liquid evaporates directly at the external surface area A of the product. The capillary suction of the liquid-filled pores is strong enough to replace the liquid being evaporated at the surface. The temperature of the product in the steady state is identical with the wet-bulb temperature T_{WB} as derived in the aforegoing section.

At the critical moisture content Y_{cc}, the moisture

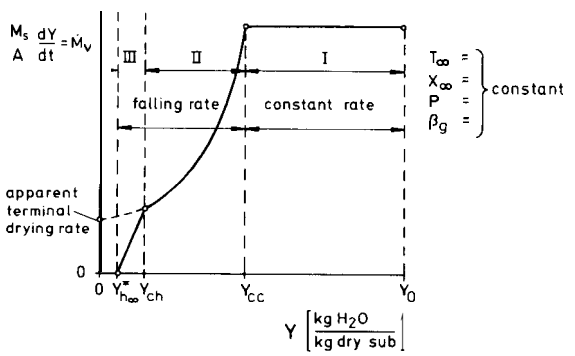

Figure 1 Drying rate function of a porous slab.

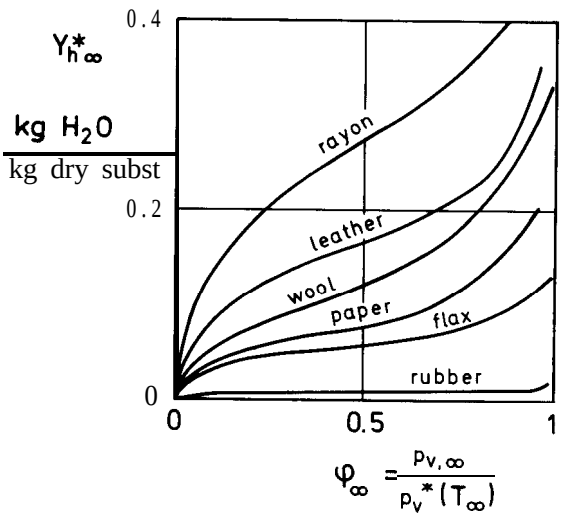

Figure 2 Sorption isotherms for various materials at 20°C.

level starts to retreat. The capillary forces are no longer sufficient to transport the liquid to the surface. Thus a layer of dry material forms with additional heat and mass transfer resistances, which lowers the drying rate in regime II.

At low moisture contents a second critical moisture content Y_{ch} emerges due to sorptive bonds of the product, which lower the vapor pressure of the liquid. This additional effect brings the drying rate down to zero at the hygroscopic equilibrium moisture content $Y_{h\infty}(T_\infty, \varphi_\infty(X_\infty), P)$, which depends on the temperature T_∞, the humidity $\varphi_\infty(X_\infty)$, and the pressure P of the drying agent according to the so-called sorption isotherms as shown in Fig. 2 ($\varphi_\infty = p_{v\infty}/p^*_{v\infty}(T_\infty) =$

© 1983 Hemisphere Publishing Corporation

$\tilde{x}_\infty/\tilde{x}^*_\infty(T_\infty)$ = relative humidity at T_∞). Regime III is called the hygroscopic one. As the hygroscopic bonds vanish, one observes an apparent terminal drying rate, provided that the sample is a slab (e.g., not a sphere).

In practice, one does not always observe all three regimes. The initial moisture content can be less than Y_{cc} as well as less than Y_{ch}. Also, Y_{ch} might be so large that the product dries only in the hygroscopic regime (e.g., soap).

To predict the drying rate for the constant rate period (regime I), one has to apply the following equation :

$$\dot{M}_{v,I} = \tilde{M}_{\text{vapor}}\tilde{\rho}_g\beta_g \ln\frac{1-\tilde{x}_\infty}{1-\tilde{x}^*_{WB}(T_{WB})} \tag{1}$$

$\tilde{M}_{\text{vapor}}$ is the molecular mass of the vaporized liquid (usually water, $\tilde{M}_{\text{vapor}}$ = 18 kg/kmol); $\tilde{\rho}_g$ is the molar density of the drying agent, $\tilde{\rho}_g = P/\tilde{R}T_{\text{av}}$; and $\tilde{x}^*_{WB}(T_{WB})$ is the mole fraction of the vapor at wet-bulb temperature, $\tilde{x}^*_{WB} = p^*_v(T_{WB})/P$ with $p^*_v(T_{WB})$ as the vapor pressure at the wet bulb temperature; β_g is the mass transfer coefficient between the external surface area A and the drying agent to be determined from the correlations given in Part 2 of this handbook.

If the mole fraction $\tilde{x}^*_{WB}(T_{WB})$ is small ($\ll$ I), Eq. (1) reduces to

$$\dot{M}_{v,I} \doteq \tilde{M}_{\text{vapor}}\tilde{\rho}_g\beta_g(\tilde{x}^*_{WB}(T_{WB}) - \tilde{x}_\infty) \tag{1a}$$

or

$$\dot{M}_{v,I} \cong \tilde{M}_{\text{air}}\tilde{\rho}_g\beta_g(X^*_{WB}(T_{WB})^* - X_\infty) \tag{1b}$$

The drying rate in the falling rate period (regimes II and III) must be found by experiment. Many attempts have been made to predict the drying rate in those regimes, but the fundamental parameters, such as diffusivities and conductivities (which depend on temperature and moisture content), are usually not available, particularly for natural products.

In general, there are two types of drying rate functions. Type A refers to very hygroscopic material, such as shown in Fig. 3 for a woolen textile material, which has been dried in a so-called through-air-drying process. Parameters are the air throughput $\dot{M}_{\text{air}}$ and the air temperature T_E. Normalizing those functions by introducing a normalized drying rate

$$\dot{\nu} = \frac{\dot{M}_v}{\dot{M}_{v,I}(T_\infty, X_\infty)} \tag{2}$$

and a normalized moisture content

$$\eta = \frac{Y - Y_{h\infty}}{Y_{cc} - Y_{h\infty}} \tag{3}$$

one finds that the resulting curves depend neither on the temperature nor on the air throughput as shown in Fig. 4 (see [3-5]). This is a very simple result and also very convenient for dryer design and rating.

Type B refers to less hygroscopic material, as shown in Fig. 5 for spherical particles of aluminum silicate dried in a fluidized bed. The normalized drying rate functions show a significant influence of the air temperature, in particular at lower moisture contents. In this range the normalized drying rate is always lower for lower temperatures. This result agrees in principle with the predictions of the so-called shrinking core model; see [2]. Therefore, it may be stated that drying rate functions obtained with low temperatures and then extrapolated to high-temperature drying are always conservative, provided that the original structure of the dry material does not undergo considerable change.

The drying rate functions both of type A and of type B can be interpolated between an upper and a lower temperature, if for those limiting temperatures the drying rate functions are known through experiments. The concept of the interpolation procedure is based mainly on the introduction of a moisture diffusivity depending on the temperature and the moisture content of the product (see [6, 7]).

The critical moisture content Y_{cc} is in many cases almost constant. It may vary, however, in a way such that Y_{cc} increases with increasing drying rates $\dot{M}_{v,I}$ (see [7, 8]).

© 1983 Hemisphere Publishing Corporation

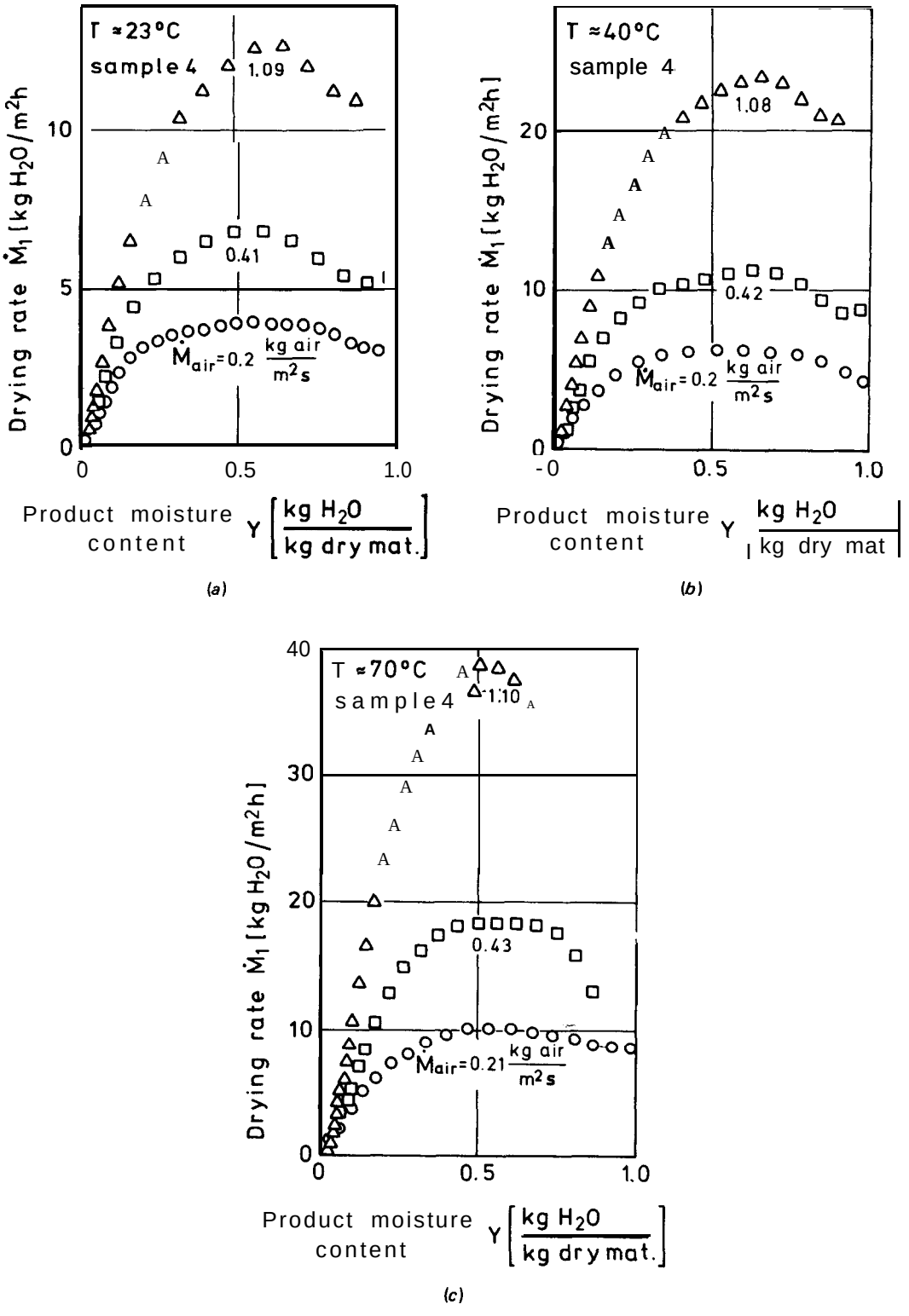

Figure 3 Drying rate $\dot{M}_v(Y)$ for a woolen textile material at various air throughputs $\dot{M}_{air}$. (*a*) At 23° C. (*b*) At 40° C. (*c*) At 70°C, Type A.

© 1983 Hemisphere publishing Corporation

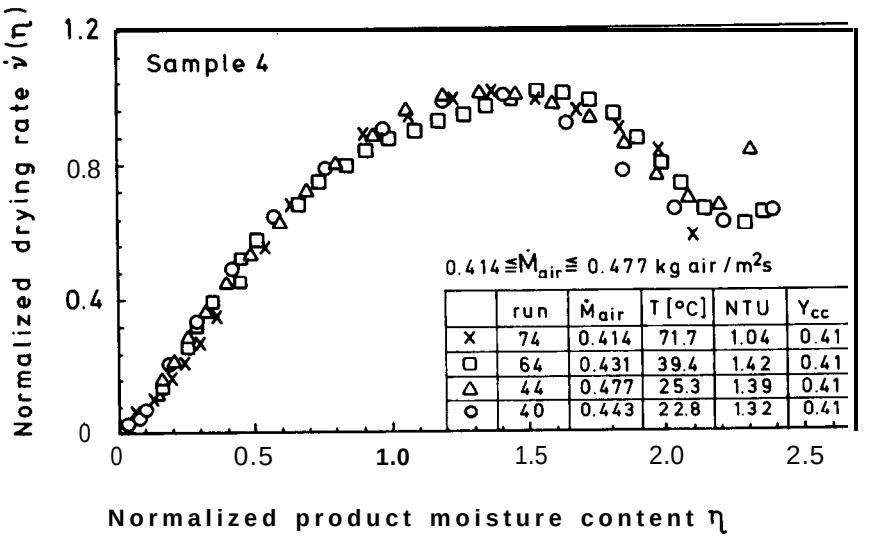

	run	$\dot{M}_{air}$	T [°C]	NTU	Y_{cc}
×	74	0.414	71.7	1.04	0.41
□	64	0.431	39.4	1.42	0.41
△	44	0.477	25.3	1.39	0.41
○	40	0.443	22.8	1.32	0.41

(a)

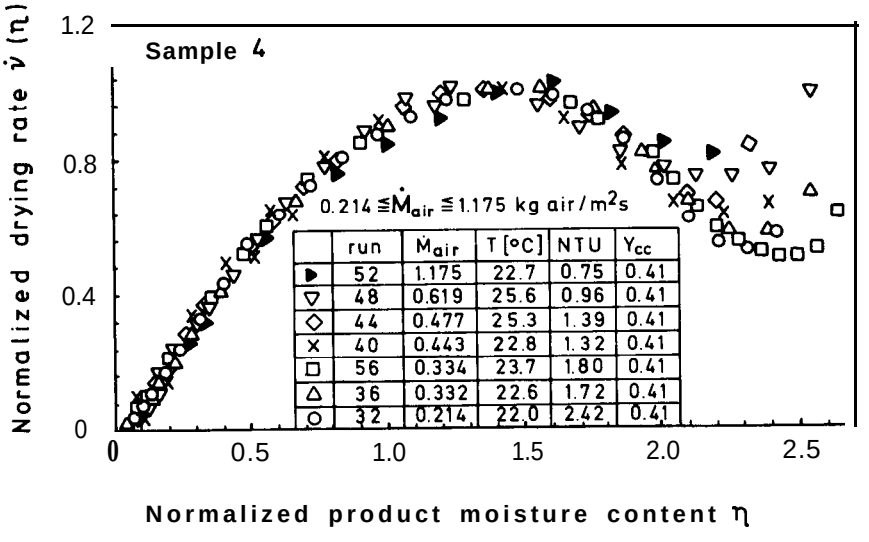

	run	$\dot{M}_{air}$	T [°C]	NTU	Y_{cc}
▶	52	1.175	22.7	0.75	0.41
▽	48	0.619	25.6	0.96	0.41
◇	44	0.477	25.3	1.39	0.41
×	40	0.443	22.8	1.32	0.41
□	56	0.334	23.7	1.80	0.41
△	36	0.332	22.6	1.72	0.41
○	32	0.214	22.0	2.42	0.41

(b)

Figure 4 Normalized drying rate function $\dot{\nu}(\eta)$ for a woolen textile material at (a) various air inlet temperatures and (*b*) at various air throughputs $\dot{M}_{air}$, Type B.

© 1983 Hemisphere Publishing Corporation

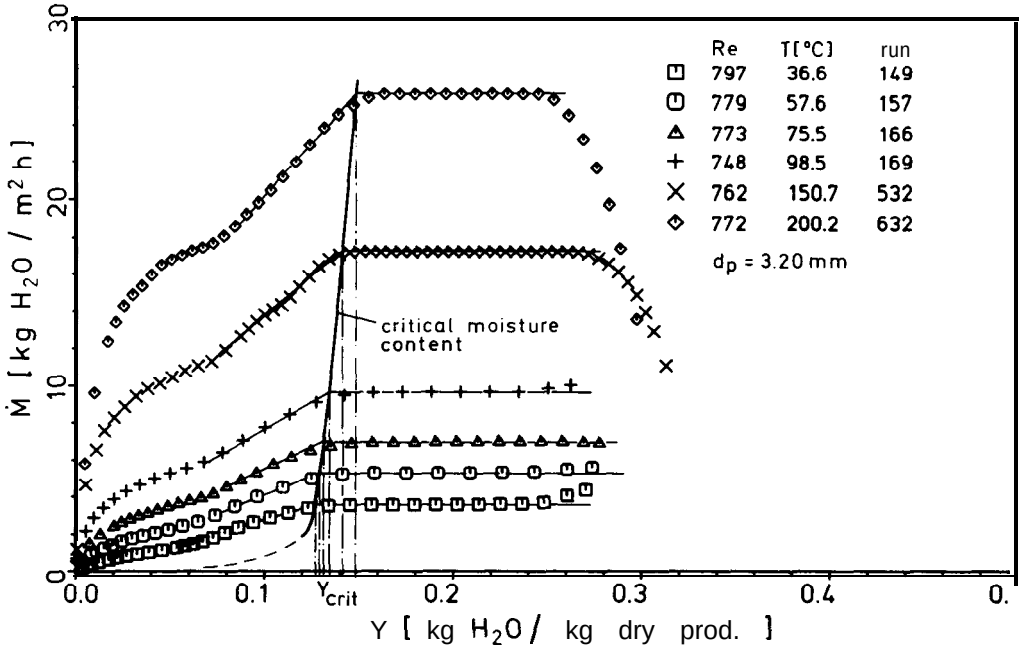

(a)

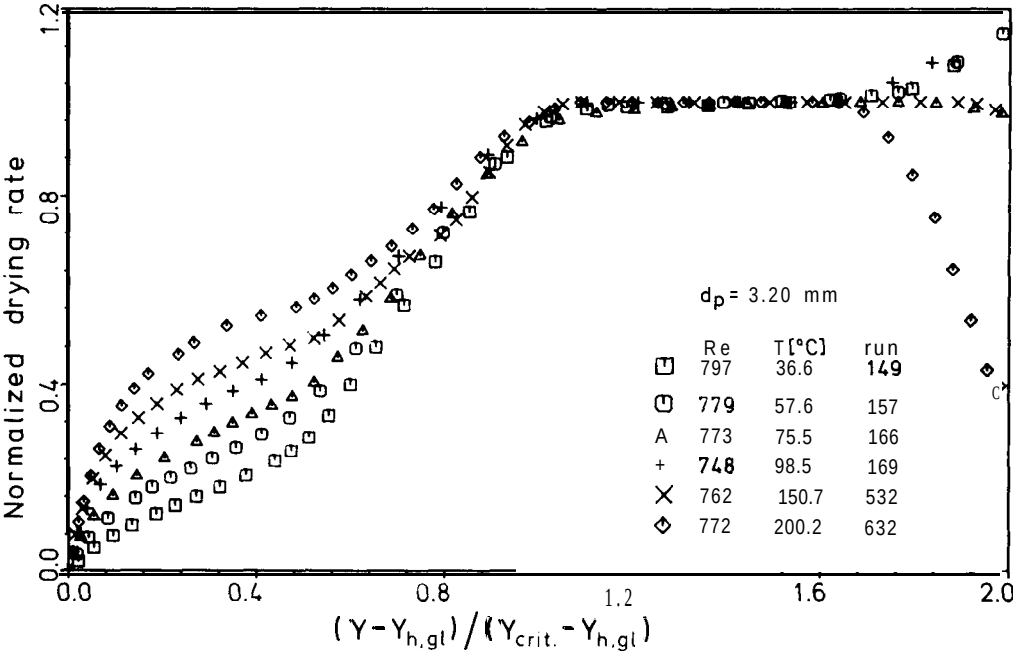

(b)

Figure 5 (a) Drying rate for spherical particles of aluminum silicate at various air inlet temperatures. (b) Normalized drying rate function 3(q) for spherical particles of aluminum silicate at various air inlet temperatures.

Nomencla ***ture and References*** *for* ***Section 3.13.4 appear at the end of Section 3.13.7.***

© 1983 Hemisphere Publishing Corporation

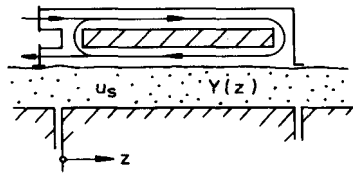

X=const and Y=Y(z)

Figure 5 Continuous dryer with large air recirculation.

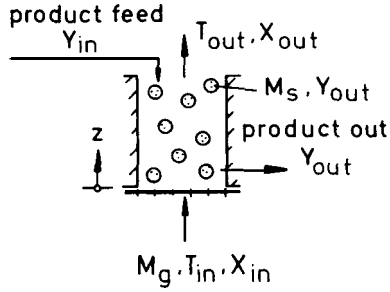

Figure 6 Continuous dryer with large product recirculation.

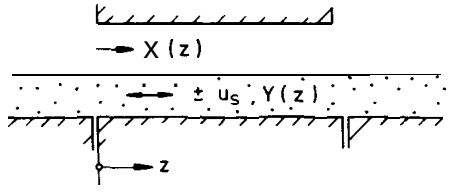

X=X(z) and Y=Y(z)

Figure 7 Continuous dryer with low air recirculation.

Class III. Batch dryers with large product recirculation, but no air recirculation

Figure 8 shows a fluidized-bed batch dryer, which falls into this class of dryers. The product is assumed to be perfectly mixed, while for the air flow no back mixing seems to be closer to reality than any other assumption. Because of the mass balances,

$$M_s \frac{dY}{dt} + M_g(X_{out}(t) - X_{in}) = 0 \tag{11}$$

and

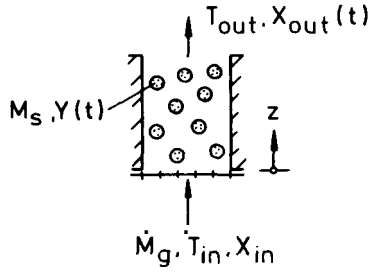

Figure 8 Batch dryer with large product recirculation.

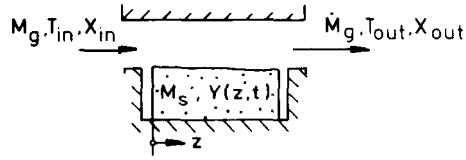

Figure 9 Batch dryer, no product recirculation and no air recirculation.

$$\dot{M}_g \frac{\partial X}{\partial z} dz = \dot{M}_{v,I} \dot{\nu}(\eta)\, dA(z) \tag{12}$$

it follows that Y = $Y(t)$ and X = $X(z,t)$.

The problem is one dimensional with respect to Y and two dimensional with respect to X.

Class IV. (a) Batch dryers without (or low) air and product recirculation

(b) Continuous dryers with cross flow of product and drying agent (air)

(a) In this case (see Fig. 9) the mass balances for the evaporating liquid are

$$\dot{M}_g \frac{\partial X}{\partial z} dz + dM_s \frac{\partial Y}{\partial t} = 0 \tag{13}$$

$$\dot{M}_g \frac{\partial X}{\partial z} dz = \dot{M}_{v,I} \dot{\nu}(\eta)\, dA(z) \tag{14}$$

Both X and Y depend on z and t, respectively: X = $X(z,t)$ and Y = $Y(z,t)$.

The problem is two dimensional with respect to both X and Y.

(b) Figure 10 shows a belt dryer for granular material. The drying agent (air) is blown in cross flow through the moving packed bed of particles. If the coordinate system on the belt is fixed so that it moves with the belt velocity u_s, then the coordinate l can be replaced by the residence time of the particles in the dryer :

$$t = u_s l \tag{15}$$

It is obvious that the cross-flow drying problem (b) then becomes identical with the batch drying problem (a).

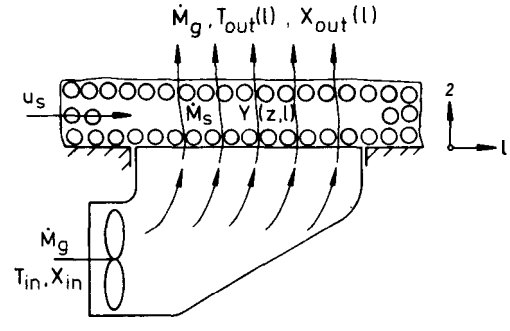

Figure 10 Continuous dryer with cross flow of product and drying agent (air).

© 1983 Hemisphere I blishing Corporation

In the following sections the basic differential equations for the above four classes of dryers are given together with their solutions for the most simple type of drying rate function.

$$\dot{\nu}(\eta) = 1 \quad \text{for } \eta \geqslant 1 \tag{16}$$

$$\dot{\nu}(\eta) = \eta \quad \text{for } 0 \leqslant \eta \leqslant 1 \tag{17}$$

In addition to the definitions of the normalized product moisture content η [Eq. 3.13.4(3)] and the dimensionless time τ [Eq. (4)], we introduce a normalized humidity of the drying agent (air),

$$\xi = \frac{X^*_{WB} - X}{X^*_{WB} - X_{\text{in}}} \quad \text{or} \quad \xi = \frac{X^*_{WB} - X}{X^*_{WB} - X_{\infty}} \tag{18}$$

and a dimensionless length coordinate,

$$\zeta = \frac{\beta_g A}{\dot{V}_g} \frac{z}{L} = \text{NTU}_g \frac{z}{l} \tag{19}$$

where $\dot{V}_g$ is the volumetric flow rate of the dry drying agent (air), and L is the total length of the dryer in the z direction.

Furthermore, it is assumed that the drying rate during the constant rate period (regime I) can be calculated according to Eq. 3.13.4(1*b*).

η_0 is the initial or inlet product moisture content, whereas η_{end} is the final one. η_{end} may be always less than unity.

Class I:

(a, b) X = const and Y = $Y(t)$

$$\frac{d\eta}{d\tau} + \dot{\nu}(\eta) = 0 \tag{20}$$

$$\tau_{\text{end}} = \eta_0 - 1 + \ln \frac{1}{\eta_{\text{end}}} \tag{21}$$

(c) X = $X(z)$ and Y = Y_{out} = const

$$\zeta_{\text{out}} = \frac{1}{\dot{\nu}(\eta_{\text{out}}) \ln (1/\xi_{\text{out}})} \tag{22}$$

where

$$\zeta_{\text{out}} = \frac{\beta_g A}{\dot{V}_g} \equiv \text{NTU}_g$$

$$\eta_{\text{out}} = \frac{Y_{\text{out}} - Y_{h\infty}}{Y_{cc} - Y_{h\infty}}$$

$$\xi_{\text{out}} = \frac{X^*_{WB} - X_{\text{out}}}{X^*_{WB} - X_{\text{in}}}$$

Class II:

(a, b) X = $X(z)$ and Y = $Y(z)$

(a) Cocurrent operation

$$\frac{d\eta}{d\tau} + \xi\dot{\nu}(\eta) = 0 \tag{23}$$

$$\xi = 1 - \dot{K}(\eta_0 - \eta) \tag{24}$$

$$\dot{K} = \left| \frac{\dot{M}_s(Y_{cc} - Y_{h\infty})}{\dot{M}_g(X^*_{WB} - X_{\text{in}})} \right| \tag{25}$$

$$\tau_{\text{end}} = -\frac{1}{\dot{K}} \ln [1 - \dot{K}(\eta_0 - 1)] + \frac{1}{1 - \dot{K}\eta_0} \ln \frac{1 - \dot{K}(\eta_0 - \eta_{\text{end}})}{\eta_{\text{end}}[1 - \dot{K}(\eta_0 - 1)]} \tag{26}$$

(b) Counter-current operation

$$-\frac{d\eta}{d\tau} + \xi\dot{\nu}(\eta) = 0 \tag{27}$$

$$\xi = 1 + \dot{K}(\eta_{\text{end}} - \eta) \tag{28}$$

$\dot{K}$ as in Eq. (25)

$$\tau_{\text{end}} = -\frac{1}{\dot{K}} \ln \frac{1 + \dot{K}(\eta_{\text{end}} - \eta_0)}{1 + \dot{K}(\eta_{\text{end}} - 1)} - \frac{1}{1 + \dot{K}\eta_{\text{end}}} \ln \eta_{\text{end}} [1 + \dot{K}(\eta_{\text{end}} - 1)] \tag{29}$$

Example: $\dot{K} = 0.40$

$\eta_0 = 2.0$

$\eta_{\text{end}} = 0.10$

(a) Cocurrent: $\tau_{\text{end}} = 1.3 + 7.0 = 8.3$

(b) Counter-current: $\tau_{\text{end}} = 2.5$ k2.6 = 5.1

Cocurrent operation requires more residence time, because both ξ and 3 are low in the falling rate period, whereas in counter-current operation large ξ and low $\dot{\nu}$ in the falling rate period and large 3 and low ξ in the constant rate period (regime I) give a more uniform drying rate in the whole dryer, which always leads to shorter required residence times.

Class III: X = $X(z,t)$ and Y = $Y(t)$

$$\frac{d\eta}{d\tau} = \frac{\xi_{\text{out}} - 1}{\zeta_{\text{out}}} \tag{30}$$

$$\frac{\partial\xi}{\partial\zeta} + \xi\dot{\nu}(\eta) = 0 \tag{31}$$

$$\tau_{\text{end}} = \frac{\zeta_{\text{out}}}{1 - \exp(-\zeta_{\text{out}})}(\eta_0 - 1) + \zeta_{\text{out}}(1 - \eta_{\text{end}}) + \ln \frac{1 - \exp(-\zeta_{\text{out}})}{1 - \exp(-\zeta_{\text{out}}\eta_{\text{end}})} \tag{32}$$

Class IV: X = $X(z,t)$ and Y = $Y(z,t)$

© 1983 Hemisphere Publishing Corporation

3.13.5

Prediction of residence times with prescribed material flow

E. U. Schliinder

■ Prediction of the residence time required for drying a product from an initial moisture content Y_0 to some final moisture content Y_e is based on the normalized drying rate function

$$\dot{M}_v = \dot{M}_{v,I}(T_\infty, X_\infty, \beta_g)\dot{\nu}(\eta) \tag{1}$$

where $\dot{M}_{v,I}$ is the drying rate in the constant rate period [regime I in Fig. 3.13.4(1)] and depends on the external mass transfer coefficient β_g and is to be predicted by Eq. 3.13.4(1) or (la, lb), respectively, whereas $\dot{\nu}(\eta)$ usually follows from laboratory-scale experiments.

The basic rate equation (1) is combined with the respective conservation law for the evaporating liquid (e.g., water),

$$M_v A = -M_s \frac{\partial Y}{\partial t} \tag{2}$$

which gives

$$\frac{\partial \eta}{\partial \tau} + \dot{\nu}(\eta) = 0 \tag{3}$$

where the normalized product moisture content η is defined by Eq. 3.13.4(3), and the dimensionless drying time τ is defined by

$$\tau = \frac{\dot{M}_{v,I} A}{M_s (Y_{cc} - Y_{h\infty})} t \tag{4}$$

The group $M_s(Y_{cc} - Y_{h\infty})/\dot{M}_{v,I}A = t_{OM}$ is the time required for drying the product in the falling rate period from Y_{cc} down to $Y_{h\infty}$ with constant drying rate $\dot{M}_{v,I}$. Since the actual drying rate $\dot{M}_v$ is always less than $\dot{M}_{v,I}$, the actual drying time in the falling rate period is always longer than t_{OM}. Nevertheless, t_{OM} gives an idea of the order of magnitude of the drying time (e.g., seconds or weeks).

Equation (3) applies to dryers where $\dot{M}_{v,I}$ is constant, that is, does not vary with time and position. Consequently, η does not vary with respect to the position in the dryer, but only with time. This type of dryer is realized in the case of large recirculation of the drying agent, as shown in Fig. 1. The external (air-side) drying conditions can be depicted in a Mollier diagram, Fig. 2.

The ambient air $(\dot{M}_F, T_A, X_A)$ is mixed with the recirculated air $(\dot{M}_R, T_\infty, X_\infty)$, giving T_{mix} and X_{mix}:

$$\frac{M_F}{M_R} = \frac{X_\infty - X_{mix}}{X_\infty - X_A} = \frac{h_\infty - h_{mix}}{h_\infty - h_A} \tag{5}$$

If $\dot{M}_F/\dot{M}_R \to 0$, then $h_\infty = h_{mix}$, $X_\infty = X_{mix}$, and $T_\infty = T_{mix} = T_H$. In this case the external drying conditions (T_∞, X_∞) and the drying rate in the constant rate period [regime I in Fig. 3.13.4(1)] are constant along the interface A. Therefore, the required drying time for a

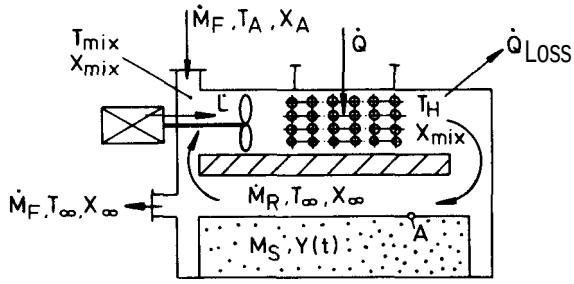

Figure 1 Batch dryer with air circulation.

© 1983 Hemisphere I blishing Corporation

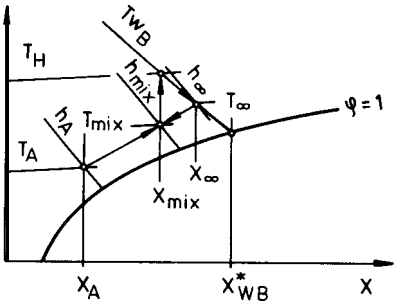

Figure 2 Mollier chart showing the external drying conditions in a batch dryer with air recirculation,

product to be dried in a batch dryer with large air recirculation is found by integration of Eq. (3):

$$\tau = -\int_{\eta_0}^{\eta_e} \frac{d\eta}{\dot{\nu}(\eta)} \tag{6}$$

Assuming that $\dot{\nu}(\eta) = \eta$ for $0 < \eta < 1$ (which is often quite a good guess, at least for a first approximation), the solution of Eq. (6) is

$$\tau_e = \eta_0 - 1 + \ln \frac{1}{Be} \tag{7}$$

The same solution applies if $\dot{\nu}(\eta)$ can be represented by a sequence of straight lines:

$$\dot{\nu}(\eta) = a_j + b_j\eta \qquad j = 1, 2, \ldots, n \tag{8}$$

Equation (6) yields, in this case,

$$\tau_e = \eta_0 - 1 + \frac{1}{b_1} \ln \frac{a_1 + b_1}{a_1 + b_1\eta_{12}} + \frac{1}{b_2} \ln \frac{a_2 + b_2}{a_2 + b_2\eta_{23}} + \frac{1}{b_3} \ln \frac{a_3 + b_3}{a_3 + b_3\eta_e} \tag{9}$$

with

$$\eta_{12} = \frac{a_1 - a_2}{b_2 - b_1} \quad \text{and} \quad \eta_{23} = \frac{a_2 - a_3}{b_3 - b_2}$$

A. Example: drying of bricks

The drying rate function $\dot{M}_v = \dot{M}_v(Y)$ may be given as in [I] and represented here in the normalized form as shown in Fig. 3. For $\eta_e = \eta_{23} = 0.07\,1$, Eq. (9) gives $\tau_e = 12.8$.

In general, both the humidity of the drying agent X and the moisture of the product Y may vary with time and position in the dryer. Then the prediction of drying times is somewhat more complicated than in the case of a batch dryer with large air recirculation. The following list gives a classification of dryers with respect to the variation of X and Y under steady-state operating conditions :

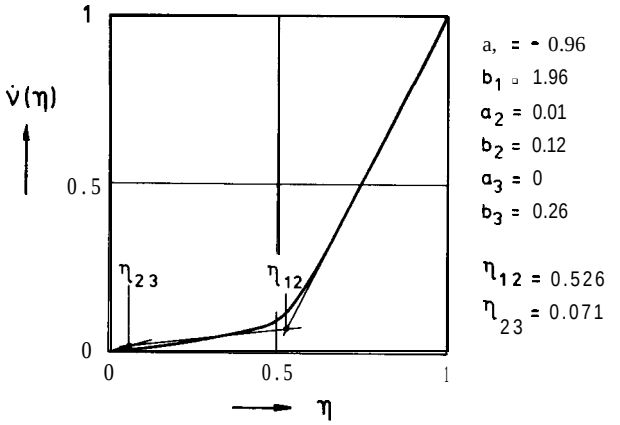

Figure 3 Normalized drying rate function i(q) for a brick.

Class I. (a) Batch dryers with large air recirculation (Fig. 4)

(b) Continuous dryers with large air recirculation (Fig. 5)

(c) Continuous dryers with large product recirculation

(a, b) Replacing the length z by

$$z = u_s t \tag{10}$$

shows that problem (b) is identical with problem (a). Dryers belonging to class I are zero dimensional with respect to X and one dimensional with respect to Y; that is, X = const and Y = $Y(t)$ or Y = $Y(z)$, respectively.

(c) Figure 6 shows a continuous fluidized-bed dryer. The product within the dryer can be assumed to be perfectly mixed, so that $Y = Y_{out}$ = const, whereas the air may be assumed to pass through the dryer without any back mixing. Therefore, $X = X(z)$. The problem is zero dimensional with respect to Y and one dimensional with respect to X = $X(z)$.

Class II. Continuous dryers with low air recirculation (Fig. 7)

(a) Cocurrent operation

(b) Counter-current operation

In this case we have X = $X(z)$ and Y = $Y(z)$. The problem is one dimensional with respect to both X and Y.

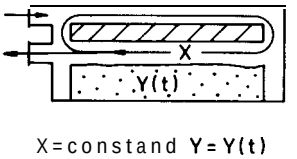

Figure 4 Batch dryer with large air recirculation.

© 1983 Hemisphere Publishing Corporation

$$\frac{\partial \eta}{\partial \tau} + \xi \dot{\nu}(\eta) = 0 \tag{33}$$

$$\frac{\partial \eta}{\partial \tau} = \frac{\partial \xi}{\partial \zeta} \tag{34}$$

Separation of the variables yields

$$\frac{\partial^2 \eta}{\partial \tau \, \partial \zeta} - \frac{1}{\dot{\nu}(\eta)} \frac{d\dot{\nu}}{d\eta} \frac{\partial \eta}{\partial \zeta} \frac{\partial \eta}{\partial \tau} + \dot{\nu}(\eta) \frac{\partial \eta}{\partial \tau} = 0 \tag{35}$$

Integration with respect to τ yields

$$\frac{1}{\dot{\nu}(\eta)} \frac{\partial \eta}{\partial \zeta} + \eta = \eta(\zeta, \tau = 0) = \eta_0 \tag{36}$$

Integration with respect to ζ yields

$$\int_1 \frac{d\eta}{(\eta_0 - \eta)\dot{\nu}(\eta)} = \zeta - \zeta_{cc}(\tau) \tag{37}$$

where $\zeta_{cc}(\tau)$ is the time-dependent position of the critical moisture content in the dryer. The type of solution according to Eq. (37) is

$$F(\eta) = \zeta - \zeta_{cc}(\tau) \tag{38}$$

or

$$\eta = G[\zeta - \zeta_{cc}(\tau)] \tag{39}$$

Putting

$$\zeta - \zeta_{cc}(\tau) = \zeta^* \tag{40}$$

yields

$$\eta = G(\zeta^*) \tag{41}$$

which means that the moisture distribution in the batch dryer follows a unique function G, which does not vary with time but only shifts through the dryer with a varying velocity, which is given by the moisture content at the dryer inlet,

$$\frac{d\zeta_{cc}}{d\tau} = \frac{\mathrm{I}}{\eta_0 - \eta(0, \tau)} \tag{42}$$

Figure 11 shows the unique moisture distribution $\eta = G[\zeta - \zeta_{cc}(\tau)]$ at various times τ corresponding to various positions ζ_{cc} of the critical moisture content $\eta_{cc} = 1$. Of course, $\zeta_{cc} < 0$ and $\zeta_{cc} > \zeta_{out}$ have only a formal and no physical meaning. The function G moves from $-\infty$ to $+\infty$ with infinite initial and finite terminal velocity through the dryer.

Evaluation of the basic equations again for $\dot{\nu}(\eta) = 1$ for $\eta \geq 1$ and $\dot{\nu}(\eta) = \eta$ for $0 \leq \eta \leq 1$ gives for $\eta(0,\tau) = 1$

$$\eta_0 - 1 = \tau_{cc} \tag{43}$$

Within the region $\zeta > \zeta_{cc}$ and $0 < (\tau/\tau_{cc}) < \infty$, one obtains

$$\eta(\zeta - \zeta_{cc}) = \eta_0 - (\eta_0 - 1) \exp[-(\zeta - \zeta_{cc})] \tag{44}$$

and within the region $\zeta < \zeta_{cc}$ and $0 < (\tau/\tau_{cc}) < \infty$,

$$\eta(\zeta - \zeta_{cc}) = \frac{\eta_0}{1 + (\eta_0 - 1) \exp[-\eta_0(\zeta - \zeta_{cc})]} \tag{45}$$

Further, for $(\tau/\tau_{cc}) \leq 1$,

$$\zeta_{cc} = \ln \frac{\tau}{\tau_{cc}} \tag{46}$$

and for $(\tau/\tau_{cc}) \geq 1$,

$$\zeta_{cc} = \frac{1}{\eta_0} \ln \frac{\eta_0 \exp\{(\eta_0 - 1)[(\tau/\tau_{cc}) - 1]\} - 1}{\eta_0 - 1} \tag{47}$$

By these five equations, (43)-(47), the moisture distribution $\eta(\zeta, \tau)$ with respect to position ζ and time τ is determined.

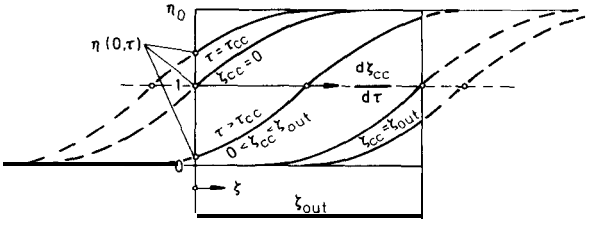

Figure 11 Product moisture distribution in a batch dryer without product and air recirculation.

Nomenclature and References for Section 3.13.5 appear at the end of Section 3.13.7.

© 1983 Hemisphere Publishing Corporation

3.13.7
Practical dryer design

D. Reay

The information presented in the preceding sections gives the reader an idea of how to set about estimating the required product residence time under idealized conditions. The designer must now derive the equipment dimensions required to give this residence time. If there are significant deviations from the idealized conditions, for example nonuniform distribution of air and solids or partial back mixing, the designer must also correct the calculated residence time to allow for these nonidealities.

These aspects of dryer design need a knowledge of particle transport mechanisms and velocities and gas flow patterns. Such aspects are impossible to discuss in general terms, since each dryer type is an individual case having little in common with other dryer types as far as these aspects are concerned. Sometimes they are also very complex and impossible to model theoretically. In such cases, dryer design is based on empirical scale-up from pilot-plant tests using the dryer manufacturer s previous experience as a guide. In other cases, however, they are not so complex, and at least a preliminary design can be made based on laboratory-scale tests allied to the foregoing theory. These considerations will now be illustrated by reference to some important types of continuous industrial dryers.

A. Band dryers

In band dryers, air is blown in cross flow either up or down through a shallow moving bed of particles [Fig. 3.13.5(10)]. A real dryer will consist of a number of sections in series, each of which may have a different air temperature, humidity, and velocity. The bed moves at a constant speed on a perforated belt from one section to the next, so the particle transport is well defined. The design problem is *to* calculate the required length of dryer for a given band speed, that is, a given bed thickness, and a given profile of air conditions in the series of sections. Repeated calculations can be made for different band speeds and different profiles to obtain an optimal design.

Each section can be considered as a class IV dryer. A simple laboratory experiment can be performed in which air is blown through a layer of material on a static perforated tray and a drying rate curve can be obtained. This curve can be used for two purposes:

1. From the drying rate in the constant rate period, a mass transfer coefficient can be calculated and compared with that predicted by available correlations for this gas-solids contacting situation.
2. From the falling rate portion, the drying rate function $\dot{v}(\eta)$ characteristic of the material can be obtained.

It is now possible to simulate the section using the class IV equation, and a computer program could easily be written to simulate a series of such sections using the same basic information. Thus, the design problem can be solved.

In this case, the particle transport velocity is known with certainty and there is no particle back mixing. There is also no air back mixing within the bed. There is usually some air recirculation in each section to control the humidity of the air approaching the bed, but this is an independent variable controlled by damper

© 1983 Hemisphere Publishing Corporation

settings. The only real uncertainties are the degree of nonuniformity of air flow over the band area, the extent of air bypassing round the edges of the band, and any local variations in the layer thickness and permeability. These effects will cause a reduction in performance, so the designer must multiply the calculated band length by a correction factor greater than unity. The correction factor will depend on the detailed construction of the dryer and must be determined by operating experience with a particular type of design.

B. Fluid-bed dryers

Continuous fluid-bed dryers may have either a long, shallow, usually rectangular bed in which the objective is a more or less close approach to plug flow of the particles, or a deep circular or rectangular bed in which the residence time distribution of the particles approaches perfect mixing. The first type is a class IV cross-flow dryer, and the second type is a class I dryer with large product recirculation. Fluid-bed dryers with an intermediate residence time distribution may be modeled as a series of perfectly mixed dryers.

A batch drying curve obtained in a laboratory fluid bed will yield the mass transfer coefficient and the drying rate function characteristic of the material. The required bed area can then be calculated from either the class IV equations or the class I(c) equations. It should be noted that to simulate conditions in the bed, the batch drying curve should be obtained at constant air inlet temperature for a plug-flow bed and at constant bed temperature for a perfectly mixed bed. The latter is difficult to achieve accurately in practice, which may give rise to some uncertainty in the design, so in this case a confirmatory continuous pilot-plant test is recommended. A pilot-plant test may be needed in any case if there is a potential material-handling problem with the wet feed.

C. Rotary dryers

In rotary dryers the material progresses along a sloping rotating cylinder through being repeatedly lifted up by flights on the inside surface of the cylinder and dropped down in curtains through a hot air stream moving either cocurrently with the solids or counter currently to them. There is no air recirculation and comparatively little product back mixing. Therefore, the class II equations apply.

Unfortunately, it is not possible to make practical use of these equations for the following reasons.

1. There is no reliable equation for predicting the mass transfer coefficient for this gas-solids contacting situation.

2. No bench-scale test has yet been devised for measuring the mass transfer coefficient experimentally in this situation.

3. There is no reliable equation relating the residence time to equipment design parameters such as drum diameter, slope and rotational speed, number and shape of lifting flights, and gas velocity. Therefore, even if the required residence time could be calculated by the class II equations, there is no way in which this could be converted into an equipment design.

Consequently, the design of rotary dryers is an empirical art based largely on the previous experience of the dryer manufacturer supplemented by pilot-plant tests on the material in question.

D. Pneumatic conveying dryers

Pneumatic conveying dryers consist of a vertical tube in which the particles and gas flow upward cocurrently. Therefore, the class II(a) equations apply. In theory, it should be possible to use these equations for dryer design since procedures are available for calculating the mass transfer coefficient and velocity of particles suspended in an air stream and the drying rate function of the material could be determined in a bench-scale fluidized bed.

However, there are certain practical difficulties.

1. The tube length calculated by such a procedure will be critically dependent on the particle size, and this is rarely known accurately. The feed particles are usually agglomerated because of surface moisture; the agglomerate size will be known only very roughly and will depend very much on how the feed is prepared and dispersed in the air stream. Moreover, these agglomerates tend to break up as they move up the tube, so the particle size changes in an unpredictable manner.

2. In large diameter tubes the feed is not usually dispersed uniformly over the cross section of the tube.

3. Turbulence in the air stream introduces considerable uncertainty into calculations of the mass transfer coefficient and particle velocity even if the particle size is known.

Consequently, design of pneumatic conveying dryers is based on pilot-plant tests with scale-up according to empirical rules derived by the plant manufacturer from previous experience.

E. Spray dryers

In spray dryers a slurry or solution is atomized into a chamber through which hot air is passing either in the same direction as the droplets or in the opposite direction. There are many different gas flow patterns depend-

© 1983 Hemisphere Publishing Corporation

3.13.6

Prediction of residence times with nonprescribed material flow

E. U. Schlünder

■ In some cases the product flow through the dryer is more or less nonuniform. This is true for the continuous fluidized-bed dryer as described in Sec. 3.13.5, class II(c). As a consequence of the perfect product back mixing, there is a residence time distribution of the individual particles between zero and infinity with a most probable residence time $\bar{t}_R$ of the order of

$$\bar{t}_R = \frac{V_s}{\dot{V}_s} \tag{1}$$

where V_s is the solid holdup of the fluid bed and $\dot{V}_s$ is the solid throughput. Some particles will leave the dryer still entirely wet and some others will already be overdried. There is a moisture distribution among the particles leaving the dryer according to the residence time distribution. The nonuniform drying occurring as a result of the nonuniform residence time is a principal disadvantage of those types of dryers. One method to reduce this nonuniformity is to split the whole dryer into a number of stages.

In a spray dryer, as near as possible, uniform droplet size should be arranged, whereas in a rotary dryer, back mixing should be avoided as far as possible. In general, each type of dryer has its own residence time distribution, which must be determined in individual large-scale experiments.

Nomenclature for Section 3.13.6 appears at the end of Section 3.13.7.

© 1983 Hemisphere Publishing Corporation

HEMISPHERE

ing on the design of the chamber, the air dispersion arrangement, and the type and position of the atomizer. Gas back mixing is usually intense in the region of the atomizer, but may be quite small in regions well away from the atomizer. The chamber must be wide enough to prevent appreciable deposition of particles on the wall and tall enough to provide sufficient residence time for drying of the particles.

None of the equations presented in the preceding sections is of much help in simulating this situation. Furthermore, no bench-scale test has yet been devised for obtaining batch drying curves for very small droplets under conditions of rapid drying. The residence time of particles in these chambers is not known, but it will not be greater than the gas residence time, which is normally in the range of 5-60 s.

Design of spray dryers is based on pilot-plant tests in which the atomization system, operating conditions, and gas residence time are varied until an acceptable product is obtained. The search for an acceptable operation is largely empirical, and the time taken to achieve an acceptable operation depends very much on the experience and intuition of the plant manufacturer. The full-scale dryer is usually designed to operate with the same gas inlet and outlet temperatures and the same gas-to-feed ratio as the successful pilot-plant test. The full-scale chamber will have the same general shape as the pilot plant and will be sized to give a gas residence time similar to that in the successful test, multiplied by an empirical correction factor based on the manufacturer s previous experience with scale-up of the particular type of spray dryer.

NOMENCLATURE FOR SECTIONS 3.13.1-3.13.7

c_p	specific heat capacity, J/kg K
h	enthalpy, kJ/kg
L	dryer length, m
M	mass of dry product, kg
$\tilde{M}$	molecular weight, kg/kmol
Le	Lewis number
$\dot{M}$	mass flow rate, kg/s
$\dot{N}$	molar mass flow rate, kmol/s
p	pressure, bar
$\dot{q}$	heat flux, W/m^2
$\dot{Q}$	heat rate, W
R	gas constant, J/kg K
t	drying time, s, h
T	temperature, K, °C
$\dot{V}$	volume flow rate, m^3/s
X	vapor content of air, kg H_2O/kg dry air
Y	moisture content of product, kg H_2O/kg dry product
α	heat transfer coefficient, W/m^2 K
β	mass transfer coefficient, m/s
δ	mass diffusivity, m^2/s
ζ	dimensionless length
η	dimensionless moisture content of product
κ	thermal diffusivity, m^2/s
ν	drying rate function
ξ	dimensionless humidity of air
ρ	density, kg/m^3
τ	dimensionless drying time
φ	relative humidity

Subscripts

cc	critical
g	gas
in	inlet
out	outlet
P	product
r	radiation
v	vapor
w	wet

Superscripts

0	standard conditions
*	equilibrium

REFERENCES FOR SECTIONS 3.13.1-3.13.7

1. Krischer, O., and Kast, W., ***Die wissenschaftlichen Grundlagen der Trocknungstechnik,*** Berlin, Heidelberg, New York, 1978.
2. Schlünder, E. U., *Hochschulkurs* ***Trochnungstechnik*** 1975, Institut für Thermische Verfahrenstechnik, Universitat Karlsruhe.
3. Gummel, P., Experimentelle Bestimmung und Analyse der Trocknungsgeschwindigkeit und des Druckverlustes luftdurchstromter Textilien und Papiere, Dissertation, Universitat Karlsruhe (TH), 1977.
4. Gummel, P., and Schliinder, E. U., Through Air Drying of Textiles and Paper, in ***Drying*** 80, vol. 1, ed. A. S. Mujumdar, ***Developments in Drying,*** pp. 357-366, Hemisphere, Washington, D.C., 1980.
5. Gummel, P., and Schlünder, E. U., Durchströmungstrocknung von Textilien und Papieren, Teil 1, ***"vt" verfahrenstechnik,*** vol. 11, pp. *743-747,* 1977; Teil 2, *"vt" verfahrenstechnik*, vol. 12, pp. 21-25, 1978.
6. Zabeschek, G., Experimentelle Beschreibung und analytische Beschreibung der Trocknungsgeschwindigkeit rieselfähiger, kapillarporöser Güter in der Wirbelschicht, Dissertation, Universitat Karlsruhe, 1977.
7. Härtling, M., Messung und Analyse von Trocknungsverlaufskurven als Grundlage zur Vorausberechnung von Trocknungsprozessen, Dissertation, Universitat Karlsruhe, (TH), 1978.
8. Hartling, M., Prediction of Drying Rates, in ***Drying '80,*** vol. 1, ed. A. S. Mujumdar, pp. 88-98, Hemisphere, Washington, D.C., 1980.

© 1983 Hemisphere Publishing Corporation

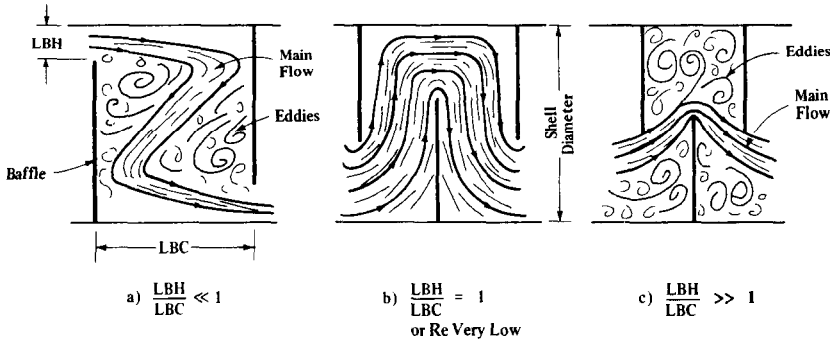

Figure 5 Schematic flow pattern through baffled tube bundles. Effects of baffle cut to baffle spacing ratio, LBH/LBC.

clarity of presentation, Tinker s method never became widely accepted, despite its imaginative approach.

It was not until computers became widely available that the real potential of Tinker s approach could be put to proper use. Furthermore, two additional factors contributed to much better understanding of shell-side flow.

1. Flow visualization studies in baffled flow [16-18] dramatically demonstrated the widely varying effectiveness of the various streams. The results are illustrated schematically in Fig. 5. It became obvious that effectiveness factors must be introduced to properly adjust the heat transfer performance. Vice versa, conclusions could be drawn as to sound design practices.

2. The results of extensive research at the University of Delaware [19] supplied (a) values for the A and E stream orifice resistance coefficients, indispensable to proper calculation of the flow fractions, (b) a massive data set on small-scale baffled exchangers with reasonably systematic variation of many parameters, and (c) data on ideal tube banks in laminar and transition flow.

The first direct result of this progress was the formulation of the Delaware method by Bell [19, 20]. Searching for a nonreiterative type of method suitable for manual calculations, Bell could not take full advantage of Tinker s flow model. Instead, a new type of method emerged that may be best termed "semi-analytical, as it is based on ideal tube bank flow and respects the effects of leakage and bypass streams, but not the interaction between them. Other calculational refinements have also been added as compared to any previous method, such as effect of baffle cut and adverse temperature gradient buildup in laminar flow. The method became very popular and was used in several handbooks. It will be not further analyzed in this survey, as it has been selected as the recommended method of this handbook and is described in great detail in subsequent sections.

The next development was the rigorous application of Tinker s flow principles in a reiterative system of calculations. This was made possible through both availability of digital computers and the data of the Delaware project. To distinguish this method from the nonreiterative one, it is termed the stream analysis method, as documented in [13]. In addition to the Delaware data, a very extensive data set on commercial-size exchangers [13] was necessary for the formulation of the crucial correlations of the K values for the various streams as functions of the geometry parameters and Reynolds numbers. The calculational process by trial and error proceeds as follows:

1. Initial values of K_j and z are assumed. The flow areas S_j are known from specified geometry.
2. This permits solution of Eqs. (8)-(12) for F_j and hi,,.
3. Having now the values of the individual stream flow rates $\dot{M}_j, K_j$ are determined from correlations.
4. Cross-flow and window pressure drops are calculated, permitting the determination of z.
5. The previous values of F_j are compared, and until within certain limits (usually ±0.5%), the calculations are repeated from step 2, substituting the last calculated values of F_j and z or other convergency method.

Convergence is not very sensitive to initial guesses and is usually quite fast. The number of trials required for 0.5% flow fraction accuracy ranges from a minimum of about three in turbulent to a maximum of about 15 in laminar flow.

Having completed the flow stream calculations, the heat transfer calculations are performed. The basis, as in all the analytical methods, is the cross-flow stream B, which is referred to ideal tube banks. The effectiveness of the other streams was determined empirically from best fit of the data. It is of interest to see the typical flow fractions of the various streams. For well-designed geometry configurations (baffle spacing/baffle cut, normal industrial clearances, bypass streams blocked by sealing strip whenever necessary), the flow fractions calculated for industrial size exchangers from the Heat Transfer Research, Inc. data bank were as follows.

© 1983 Hemisphere Publishing Corporation

Stream	Turbulent	Laminar
Main cross flow (B)	40–70%	25–50%
Bundle bypass (C + F)	15–20%	20–30%
Shell-to-baffle leakage (E)	6-20%	6-40%
Tube-to-baffle leakage (A)	9–20%	4-10%

This method also recognizes for the first time the effects of the bypass and leakage streams on distortion of the temperature profile. The temperature of these streams is altered much less than that of the cross-flow stream B, which is in direct contact with heat transfer surface. Mixing will occur to some extent between baffles and ultimately at the outlet. However, the incompleteness of mixing, especially in laminar flow, will result in distortion of the assumed temperature profile for purposes of calculations of the mean temperature difference (see Sec. 1.5 for more details). This is particularly dangerous when close temperature approach is encountered and with large leakage stream E, which is considered highly ineffective and does not readily mix with other streams. From all the unresolved problems in shell-side flow, the temperature profile distortion is probably the most serious one, and it will take a concentrated effort to resolve it on the same level of confidence as the flow correlations themselves.

In conclusion, we can summarize our findings as follows.

1. All the integral methods, such as those of Donohue and Kern, cannot be recommended, as the resulting errors are potentially very high and the Delaware method, with only incrementally more complicated calculation, will be much more precise.

2. Although Tinker s flow model is accepted as a valid basis, its full usefulness is realized only in the rigorous reiterative form, suitable for digital computers. Even so, the crucial correlations of the flow resistance K values are not in the public domain.

3. For manual calculations, the Bell Delaware method appears to be the best available and the most suitable fox general engineering applications.

Subsequent sections deal with the Delaware method in detail, and a somewhat modified and supplemented version is presented as the recommended method in this handbook for shell-side calculations.

Nomenclature for Section 3.3.2 appears at the end of Section 3.3.11.

REFERENCESFORSECTION 3.3.2

1. Patankar, S. V., and Spalding, D. B., A Calculation Procedure for the Transient and Steady-State Behavior of Shell-and-Tube Heat Exchangers, ***Heat Exchangers: Design and Theory Sourcebook,*** eds. N. Afgan and E. U. Schlünder, Hemisphere, Washington, D.C., 1974.
2. Butterworth, D., A Model for Heat Transfer During Three-Dimensional Flow in Tube Bundles, *Proc. 6th Int. Heat Transfer Conf.,* ***Toronto,*** 1978.
3. Emerson, W. H., National Engineering Laboratory Report No. 45, Glasgow, August 1962 (Abstract in [4]).
4. Emerson, W. H., Shell-Side Pressure Drop and Heat Transfer with Turbulent Flow in Segmentally Baffled Shell-and-Tube Heat Exchangers, *Int. J. Heat Mass Transfer,* vol. 6, pp. 649-668, 1963.
5. Colburn, A. P., A Method of Correlating Forced Convection Heat Transfer Data and Comparison with Fluid Friction, ***Trans.*** *AIChE,* vol. 29, pp. 174-210, 1933.
6. Grimison, E. D., Correlation and Utilization of New Data of Flow Resistance and Heat Transfer for Cross-Flow of Gases over Tube Banks, ***J. Heat Transfer,*** vol. 59, no. 7, pp. 583-594, 1937.
7. McAdams, W. H., ***Heat Transmission,*** 2d ed., McGraw-Hill, New York, 1942.
8. Colbum, A. P., Heat Transfer by Natural and Forced Convection, ***Purdue University*** *Eng.* ***Exp. Sta. Bull. 84,*** 1942.
9. Short, B. E., Heat Transfer and Pressure Drop in Heat Exchangers, ***University of Texas Bull. 4324,*** 1943.
10. Donohue, D. A., *Ind. Eng. Chem.,* vol. 41, no. 11, pp. 2499-2511, 1949.
11. Donohue, D. A., ***Pet. Refiner,*** Part 1, August 1955; Part 2, October 1955; Part 3, November 1955; Part 4, January 1956.
12. Kern, D. ***Q., Process Heat*** *Transfer,* McGraw-Hill, ***New*** York, 1950.
13. Palen, J. W., and Taborek, J., Solution of Shell Side Flow Pressure Drop and Heat Transfer by Stream Analysis Method, ***Chem. Eng. Prog. Symp. Ser.,*** vol. 65, no. 92, 1969.
14. Tinker, T., *J. Heat Transfer,* vol. 80, pp. 36-52, 1958.
15. Tinker, T., Shell Side Characteristics of Shell and Tube Heat Exchangers, ***Parts I, II, and HZ, General Discussion of Heat Transfer,*** *Proc.* ***Znstitution of Mechanical Engineers,*** London, 1951.
16. Kopp, S., Sennstrom, H. R., and Gunter, A. Y., A Study of Flow Patterns in Baffled Heat Exchangers, ASME Paper 47-A-103, 1947.
17. Gupta, R. K., and Katz, D. L., Flow Patterns for Predicting Shell-Side Heat Transfer Coefficients for Baffled Shell-and-Tube Exchangers, ***Znd.*** *Eng. Chem.,* vol. 49, no. 6, pp. 998-999, 1957.
18. ***Shell-and-Tube Heat Exchanger,*** 16-mm color sound movie, originally produced by C. F. Braun Co., 1956, currently available through Heat Transfer Research, Inc. (HTRI), 1000 S. Fremont, Alhambra, Calif., 9 1802.
19. Bell, K. J., Final Report of the Cooperative Research Program on Shell-and-Tube Heat Exchangers, ***University of Delaware Eng. Exp. Sta. Bull. 5,*** 1963.
20. Bell, K. J., Exchangers Design Based on the Delaware Research Program, ***Pet. Eng.,*** vol. 32, no. 11, pp. C26-36, C40a–C40c, 1960.

© 1983 Hemisphere Publishing Corporation

3.10
Heat pipes

Contents

3.10.1
INTRODUCTION, D. Chisholm **3.10.1-l**

3.10.2
CIRCULATION AND AXIAL HEAT TRANSFER, D. Chisholm **3.10.2-l**

3.10.3
TEMPERATURE DISTRIBUTIONS AND RADIAL HEAT TRANSFER FLUX, D. Chisholm **3.10.3-l**

3.10.4
AXIAL HEAT TRANSFER AND THE OPERATIONAL ENVELOPE,
D. Chisholm **3.10.4-l**

3.105
SELECTION OF WORKING FLUID,
D. Chisholm **3.10.5-l**

3.10.6
CHARACTERISTICS OF WICKS,
D. Chisholm **3.10.6-l**

3.10.7
START-UP AND CONTROL,
D. Chisholm **3.10.7-l**

A. Control **3.10.7-l**
B. Conclusions **3.10.7-2**

Nomenclature for Sections 3.10.2-3.10.7 **3.10.7-2**
References for Sections 3.10.1-3.10.7 **3.10.7-3**

© 1983 Hemisphere Publishing Corporation

HEDH

3.14.1 Introduction

W. R. Penney

Heat transfer in agitated vessels has been extensively researched. Comprehensive coverage is beyond the scope of this work; only the most useful and general information will be summarized and presented here. Books by Sterbacek and Tausk [1], Holland and Chapman [2], Uhl and Gray [3], and Nagata [4] present comprehensive coverages. Parker [5], Jordan [6], Edwards and Wilkinson [7], and Kase [8] present less comprehensive coverage.

The following steps are required to design an agitated vessel to satisfy certain heat transfer requirements:

Select the agitator and vessel geometry.
Select the vessel internals.
Size the agitator and heat transfer surfaces.

Only the most commonly used equipment will be covered here. The intent is to provide sufficient information to enable the designer to get close to the economically optimum system. It is advised that one obtain quotes from agitation equipment vendors before finalizing design.

The most important parameters affecting the design of an agitated vessel for heat transfer are

The process results, other than heat transfer, to be achieved
The amount of heat to be transferred
The fluid physical properties (primarily viscosity)
The vessel volume

For low to moderate viscosities (η < 10, i.e., 100 poise), in industrial-size vessels, high impeller pumping rates, producing turbulent motion, are possible, and nonproximity impellers (propellers and turbines) are used. For higher viscosities, proximity impellers (anchors, helical ribbons, etc.) are used.

For low to moderate heat duties, the vessel jacket is usually adequate to provide the required heat transfer surface. As heat duty increases, internal heat transfer surface (helical coils, baffle pipes, or plate coils) is required. For some systems with very high heat duties, adequate heat exchange capability is not possible with internal heat transfer surface-external, pumped-through heat exchangers or vaporization within the vessel followed by condensation in an external exchanger is used. Design techniques for the latter situations are covered elsewhere in this handbook.

A special problem exists for heat removal applications. Because agitator power requirements (which always add heat to the vessel contents) are much more strongly dependent on agitator speed than are heat transfer coefficients, a maximum heat removal capability exists for any particular agitated vessel. This phenomenon is of particular importance for heat removel in high-viscosity systems. Refer to Penney and Koopman [9] for recommendations concerning optimum design.

References for Section 3.14.1 appear at the end of Section 3.14.3.

© 1983 Hemisphere Publishing Corporation

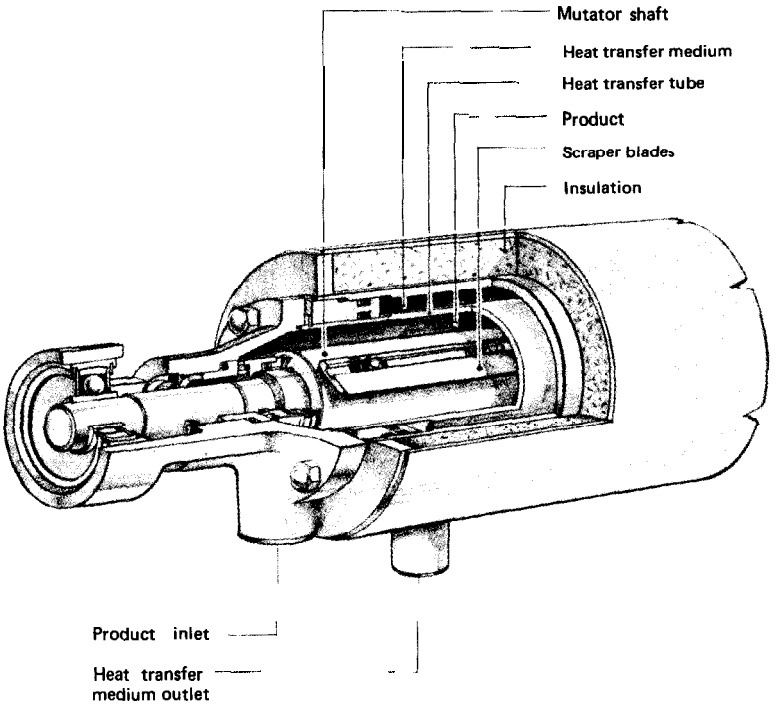

Figure 3 The Votator scraped-wall unit. Courtesy Chemetron Corp., Louisville, Ky.

tween pipes in a helix need not be great and if $\eta < 0.5$ the clearance between layers may be as little as one-third pipe diameter. Unfortunately, insufficient quantative information is available to allow recommendation of any other geometry. For cases where the geometry of Fig. 5 will provide insufficient heat duty, an equipment manufacturer should be contacted. Manufacturers often have additional information that allows selection of a more economical geometry. For example, for some situations a second and a third coil [13, 14] may be economical, although the heat transfer coefficients will be reduced for the middle and outer coils-to about 60% and 40% of the inner coil, according to Marshall and Yazdani [14] .

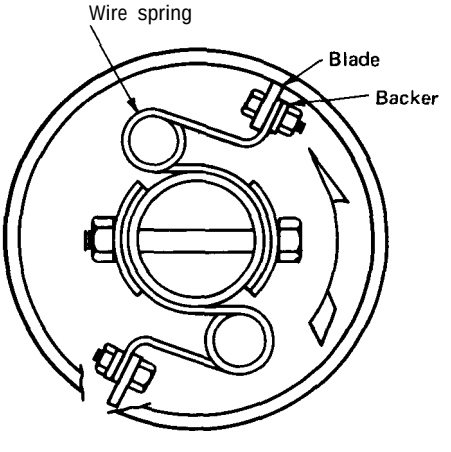

Figure 4 Spring-loaded wall scraper unit. Courtesy R. M. Armstrong Co., West Chester, Pa.

(c) Baffle pipes and plate coil baffles

The recommended geometries are presented in Fig. 6. The baffle pipes can either be placed radially across the

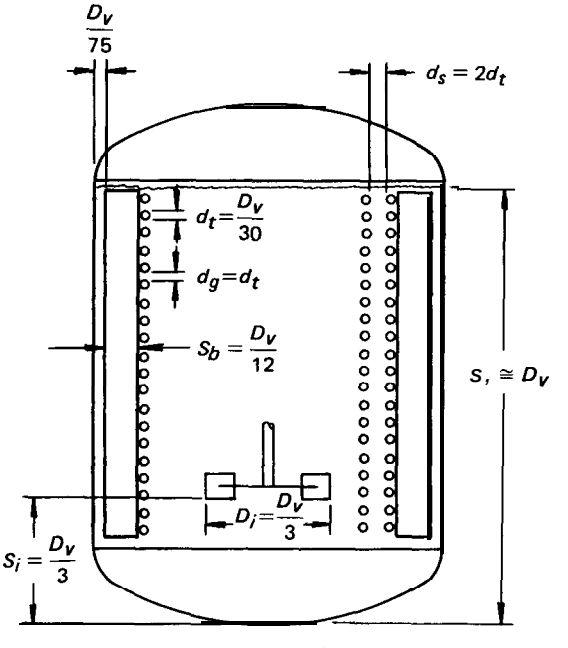

Figure 5 Recommended geometries for wall baffles and helical coils.

© 1983 Hemisphere 1 iblishing Corporation

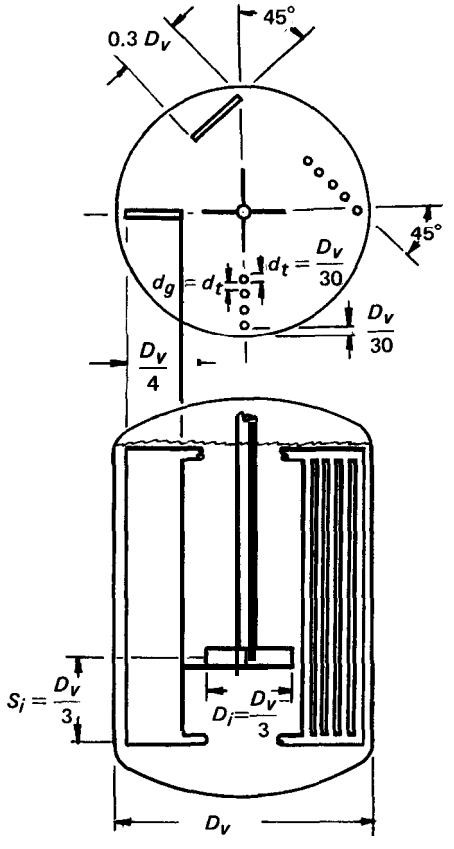

Figure 6 Recommended geometry for vertical tube baffles and plate coils.

vessel or at an angle of 45 with the vessel radius. With radial positioning, four pipes per baffle are recommended; and with angled positioning, five pipes per baffle are recommended. The experimental work discussed later was done with four baffles. **More than** four baffles, especially when using plate coils, are often installed. Probably six baffles would have Little effect on the heat transfer coefficient. For more than six baffles, a manufacturer of plate coils should be consulted.

Nomenclature and References for Section 3.14.2 appear at the end of Section 3.14.3.

© 1983 Hemisphere Publishing Corporation
HEDH

3.14.2 Equipment

W. R. Penney

■ The vessel, vessel internals, and an agitation source are the components of the typical installation. Mechanical agitators (consisting of a drive, a drive shaft, and an impeller) are most often used to provide agitation; however, gas sparging and liquid jets entering the vessel (primarily from recirculation through a pump) are also used to provide agitation.

A. Mechanical agitators

The most commonly used agitators will be discussed and preliminary selection criteria will be given. Figures l-4 present visuals of commonly used mechanical agitators.

(a) Nonproximity

Propeller: Applicability Re, > 300, $\eta < 2$, $V < 6.0$, all applications except gas dispersion. Not normally used for $V > 6.0\ m^3$ (except for side-entering units in large storage tanks), because the weight of large propellers makes them more expensive than lighter turbines.

Disk flat-blade turbine: Applicability Re, > 50, $\eta < 20$, gas dispersion only.

Flat-blade turbine: Applicability Re, > 50, $\eta < 20$, primarily liquid-liquid dispersions or applications requiring the impeller to be located < ***D/2*** off the vessel bottom.

Pitched-blade turbine: Applicability Re, > 100, $\eta < 10$, all single-phase and solid-liquid operations.

Glass-coated turbines: Applicability Re, > 50, $\eta < 20$, all applications where glass is needed for economical corrosion protection; inefficient for gas dispersion; consequently, high-alloy metal agitators are sometimes used in glass-lined vessels.

(b) Proximity

Anchors: Applicability Re, > 50, $20 < \eta < 100$, all applications.

Helical ribbons: Applicability Re, < 50, $100 < \eta < 1\ 000$, all applications, except for highly non-Newtonian liquids, which tend to rotate with the impeller and are sheared only near the vessel wall.

Double motion: Applicability is high viscosity, non-Newtonian liquids.

Votator: Applicability $\eta < 100$ for concentric floating blades, $100 < \eta < 300$ for eccentric floating blades, and $300 < \eta < 1\ 000$ for oval-tube floating blades, per Chemetron Corp. Bulletin V300R1-5-1072. They are used extensively in the food processing industry.

Scraped-wall pipe: Applicability $\eta < 100$ routinely, $100 < \eta < 1\ 000$ with special designs (consult a manufacturer) for high viscosity.

B. Gas sparging

For bubble columns with height/diameter > 5, a simple open pipe sparger at the bottom of the column is adequate. For height/diameter < 5, a ring or finger-style sparger is desirable to obtain uniform radial distribution of the gas and prevent excessive channeling of the gas.

© 1983 Hemisphere Publishing corporation

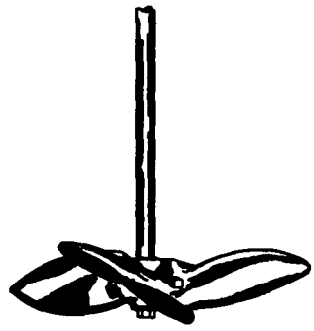

Propeller

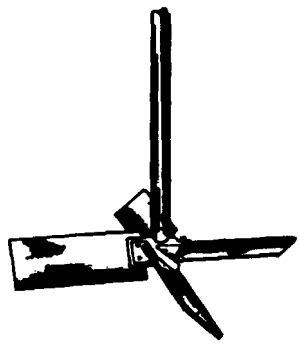

Axial flow turbine

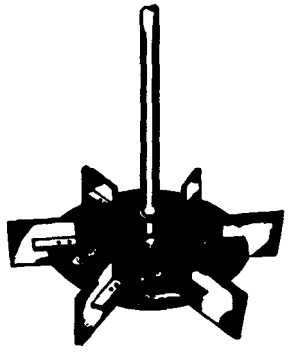

Disk turbine

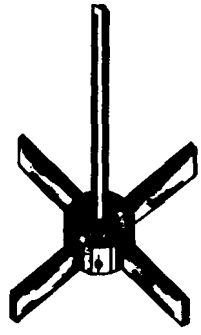

Flat blade turbine

Figure 1 Typical nonproximity impellers. Courtesy Mixing Equipment Co., Rochester, N.Y.

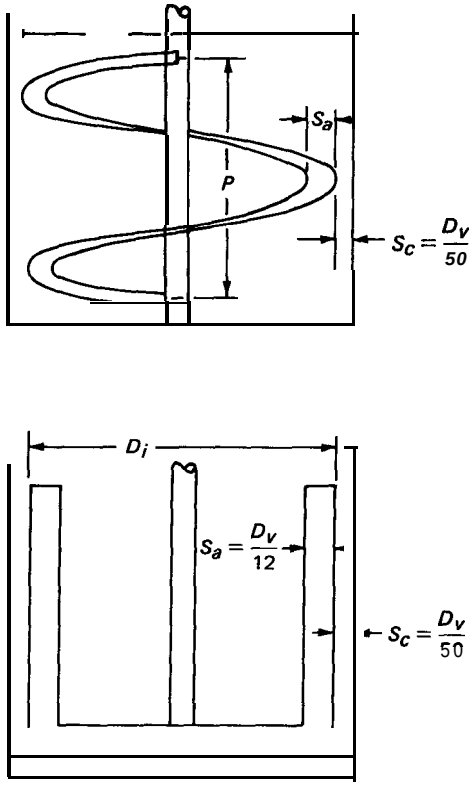

Figure 2 Anchor and helical-ribbon proximity impellers.

C. Vessel internals

With nonproximity agitators, baffles are commonly used to prevent swirl and vortexing and to increase top-to-bottom motion and turbulence. Helical coils, pipe baffles, and plate coil baffles are the most common heat transfer surfaces within the vessel.

(a) Wall baffles

Figure 5 shows the recommended geometry. Small propeller units (<7.5 kW) are often mounted angled, off-center [10, 11, 3, pp. 153-156] to prevent swirl and vortexing. Sometimes vortexing is desirable, such as when wetting powders. Brennan [12] gives predictive methods for vortex depth (as a first approximation, $S_{vo}/D_i = 4\ \mathrm{Fr}_a$). A cylindrical probe ($d_p/D_v = 1/17$) and a helical coil both decrease the vortex depth ≅ 50%.

(b) Helical coils

Figure 5 presents the recommended geometry. Rushton [IO], Parker [5], and Hicks and Gates [13] give recommendations concerning coil geometry. This geometry is not the economical optimum for all cases; for example, Rushton [IO] recommends: clearance be-

© 1983 Hemisphere Publishing Corporation

3.14
Agitated vessels

Contents

3.14.1
INTRODUCTION, W. R. Penney **3.14.1-1**

3.14.2
EQUIPMENT, W. R. Penney **3.14.2-1**

A. Mechanical agitators 3.14.2-1
B. Gas sparging 3.14.2-1
C. Vessel internals 3.14.2-2

3.14.3
HEAT TRANSFER CORRELATIONS, W. R. Penney **3.14.3-1**

A. Nonproximity mechanical agitators 3.14.3-1
B. Gas sparged vessels 3.14.3-3
C. Anchors and helical ribbons 3.14.3-3
D. Scraped-wall pipe equipment 3.14.3-4
E. Other equipment having proximity agitators 3.14.3-5

Nomenclature for Sections 3.14.1-3.14.3 **3.14.3-6**
References for Sections 3.14.1-3.14.3 3.14.3-7

© 1983 Hemisphere Publishing Corporation

HEDH

3.14.3

Heat transfer correlations

W. R. Penney

A. Nonproximity mechanical agitators

The recommended correlations are presented as Table 1. All correlations are of the form:

$$\mathrm{Nu} = K\ \mathrm{Re}_a^a\ \mathrm{Pr}^b \left(\frac{\eta_b}{0\eta_w}\right)^c \times (\text{geometric corrections}) \qquad (1)$$

Geometric corrections have been changed from the original references and in several cases additional geometric corrections have all been ratioed to a standard geometry. In most cases this changes the value of K from the original reference, but the correlations remain the same. This practice makes it much easier to directly compare various correlations. Before finalizing a design, one should consult the original sources.

The characteristic length (l) in the Nusselt number (Nu) is D_v for the vessel wall, d_t for helical coils or baffle pipes, and [S_{pc}/(number of internal passes)] for plate coils.

(a) Vessel wall

Flat, disk, and pitched-blade turbines-no baffles: For the standard geometry the correlations of Nagata et al. [15] are recommended; except the geometric corrections have been changed.

Flat, disk, and pitched-blade turbines-baffles: For the standard geometry, the correlations of Strek [17], Brooks and Su [16], and Chapman et al. [18] agree. Some of the geometry corrections suggested by Nagata et al. [15] and Chapman et al. [18] appear to be unreasonable; recommended geometric corrections are given.

Propeller-no baffles: Nagata et al.'s [20] correlation is recommended, although the dependence of α on D_v is obviously incorrect. The correlation presented by Kupcik [21] predicts lower (by 30–40%) values. Also, Kupcik found that wall baffles lower (by about 10%) the wall heat transfer coefficient; however, Strek et al.'s [22] coefficients with baffles are higher than Nagata et al.'s [20] coefficients without baffles.

Propeller-baffles: Strek et al.'s [22] correlation is recommended.

Glass-coated three-bladed impeller-one glassed baffle: The correlation of Ackley [19] is recommended.

(b) Helical coils

Flat, disk, and pitched-blade turbines-no baffles: Nagata et al.'s [20] correlation is recommended, except the geometric corrections are changed.

Flat, disk, and pitched-blade turbines-baffles: Oldshue and Gretton s [23] correlation is recommended for the standard geometry.

Propeller-no baffles: Ackley's [19] correlation is recommended for the standard geometry, except K = 0.05 rather than 0.078 is recommended. Geometric corrections are suggested.

Propeller-baffles: Oldshue s [24] correlation is recommended for the standard geometry. The correction for d_t is taken from [3].

© 1983 Hemisphere Publishing Corporation

HEDH

Table 1 Heat transfer correlations for nonproximity agitators

Investigators	Impeller(s)	Heat transfer surfaces	Standard geometry								K	Exponents of:			Recommended geometric corrections
			S_l/D_v	S_i/S_l	D_i/D_v	L_i/D_i	d_t/D_v	d_g/d_t	N_{bl}	Baffles		Re_a	Pr	η_b/η_w	
Nagata et al. [15]; Brooks and Su [16]	Various turbines: disk, flat, and pitched blades	Vessel wall	1.0	1/3	1/3	1/5			6	No	0.54	213	1/3	0.14	$\left(\frac{L_i/D_i}{1/5}\right)^{0.15}\left(\frac{N_{bl}}{6}\right)^{0.15}[\sin(\theta)]^{0.5}$
Brooks and Su [16]; Strek [17]; Chapman et al. [18]	Various turbines: disk, flat, and pitched blades	Vessel wall	1.0	1/3	1/3	1/5			6	Yes	0.74	2/3	1/3	0.14	$\left(\frac{L_i/D_i}{1/5}\right)^{0.2}\left(\frac{N_{bl}}{6}\right)^{0.2}[\sin(\theta)]^{0.5}$
Ackley [19]; Nagata et al. [20]	Propeller	Vessel wall	1.0	1/3	1/3	$P/D_i = 1$			3	No	0.37	213	1/3	0.14	$\left(\frac{D_v/D_i}{3}\right)^{0.25}\left(\frac{S_i}{S_l}\right)^{0.15}$
Strek et al. [22]	Propeller	Vessel wall	1.0	1/3	1/3	$P/D_i = 1$			3	Yes	0.5	2/3	1/3	0.14	$\left(\frac{1.29P/D_i}{0.29 + P/D_i}\right)$
Ackley [19]	Three glass-coated retreating blades	Vessel wall	?	?	?	?			3	Yes	0.33	0.67	0.33	0.14	
Nagata et al. [20]	Various turbines: disk, flat, and pitched blades	Helical coils	1.0	1/3	1/3	1/5	0.064	1.0	6	No	0.08	0.56	1/3	0.14	$\left(\frac{L_i/D_i}{1/5}\right)^{0.15}\left(\frac{d_t/D_v}{0.064}\right)^{0.5}$
Nagata et al. [20]; Oldshue and Gretton 1231	Various turbines. disk, flat, and pitched blades	Helical coils	1.0	1/3	1/3	1/5	0.04	1.0	6	Yes	0.03	0.67	1/3	0.14	$\left(\frac{L_i/D_i}{1/5}\right)^{0.2}\left(\frac{d_t/D_v}{0.04}\right)^{0.5}\left(\frac{D_v}{S_l}\right)^{0.15}\times\left(\frac{N_{bl}}{6}\right)^{0.2}[\sin(\theta)]^{0.5}$
Ackley [19]; Nagata et al. [20]	Propeller	Helical coils	1.0	1/3	1/3	$P/D_i = 1$	0.03?	1.0	3	No	0.078[a]	0.62	1/3	0.14	$\left(\frac{d_t/D_v}{0.03}\right)^{0.5}\left(\frac{D_v/D_i}{3}\right)^{0.2}$
Oldshue [24]; Skelland et al. [25]	Propeller	Helical coils	1.0	1/3	1/3	$P/D_i = 1$	0.04	1.0	3	Yes	0.016	0.67	0.37	0.14	$\left(\frac{D_i/D_v}{1/3}\right)^{0.1}\left(\frac{d_t/D_v}{0.04}\right)^{0.5}$
Dunlap and Rushton [26]	Four-bladed disk turbine	Vertical tube baffle	1.0	1/2	1/3	1/5	0.04	1.0	2	Three tubes	0.06[b]	0.65	0.3	0.4[c]	$\left(\frac{L_i/D_i}{1/5}\right)^{0.2}\left(\frac{d_t/D_v}{0.04}\right)^{0.5}\left(\frac{D_v}{S_l}\right)^{0.15}\times\left(\frac{2}{\text{no. baffles}}\right)^{0.2}$
Gentry and Small [27]	Two six-bladed, flat-blade turbines	Vertical baffle coil at 45 to radius	2.0	1/4, 3/4	1/3	1/8	0.04	0.7	4	Four tubes	0.021	0.67	0.4	0.27	$\left(\frac{L_i/D_i}{1/8}\right)^{0.2}\left(\frac{d_t/D_v}{0.04}\right)^{0.5}$
Petree and Small [28]	Two six-bladed, flat-blade turbines	Plate coils	2.0	1/4, 3/4	1/3	1/8	$S_{pc}/D_v = 0.3$		4	Yes	0.031	0.66	0.33	0.5[d]	$\left(\frac{L_i/D_i}{1/8}\right)^{0.2}$

[a] This value appears unreasonably high compared to other correlations. A value of 0.05 is recommended.

[b] This value appears unreasonably high compared to Gentry and Small s[27] correlation. A value of 0.04 is recommended.

[c] Dunlap and Rushton [26] and Petree and Small [28] used the ratio of the bulk viscosity to the film viscosity. It is recommended that one use the wall viscosity instead and use $(\eta_b/\eta_w)^{0.14}$.

[d] For the vessel wall, $Nu_y = \alpha D_v/\lambda$, for helical and vertical tube baffles, Nu, = $\alpha d_t/\lambda$; for the plate coil, $Nu_{pc} = \alpha(S_{pc}/\text{no. of passes})/\lambda$. For Petree and Small s[28] work, there were four internal passages in the plate coil: therefore, $Nu_{pc} = \alpha S_{pc}/4\lambda$, for their work.

© 1983 Hemisphere Publishing Corporation

HEMISPHERE

Four-bladed disk turbines-vertical baffle coil: Dunlop and Rushton s correlation is recommended with appropriate geometric corrections added. The value of K seems high. A value of 0.04 rather than 0.06 is recommended.

Two six-bladed disk turbines-vertical tube baffles: Gentry and Small s[27] correlation is recommended with correction added for L_i/D_i and d_t/D_v.

(c) Plate coils

Two six-bladed disk turbines-vertical plate coils: Petree and Small s[28] correlation is recommended.

B. Gas sparged vessels

Hart [29], Nagata et al. [30], Tamari and Nishikawa [31], and Steiff and Weinspach [32] have done the latest work and summarized earlier work. Hart s correlation is recommended.

$$\frac{a!}{c_p v_s \rho} = 0.125 \left(\frac{v_s^3 \rho}{\eta g}\right)^{-0.25} \mathrm{Pr}^{-0.6} \qquad (2)$$

C. Anchors and helical ribbons

Uhl [33], Harry and Uhl [34], and Nishikawa et al. [35] have well summarized all previous work. lshibashi et al. [36] and Rautenbach and Bollenrath [37] have published the latest works. Coyle et al. [38] have presented very useful experimental data. Nagata et al. [39] and Mitsuishi and Miyairi [40] are of interest.

(a) Recommended geometry

Figure 3.14.2(2) presents the recommended geometries.

(b) Heat transfer correlations

Harry and Uhl [34] have presented the most reliable correlations for the geometries that they tested. Pertinent geometric parameters for their tests are given below.

Geometric ratios	Anchor	Helical ribbon[a]
P/D_v	∞	0.082 1/2
S_a/D_v	0.082	
S_c/D_v	0.02	0.02
D_i/D_v	0.96	0.96

[a] Single-helix.

For these geometries the correlations were of the form

$$\mathrm{Nu}_a = K\, \mathrm{Re}_a^a\, \mathrm{Pr}^b \left(\frac{\eta_b}{\eta_w}\right)^c \qquad (3)$$

The values of the parameters a, b, c, and K are as follows: $b = 1/3$, c = 0.14, and a and K varied with Re, and geometry as follows:

Anchor					
$\mathrm{Re}_a < 12$		$12 < \mathrm{Re}_a < 100$		$\mathrm{Re}_a > 100$	
K	a	K	a	K	a
1.05	1/3	0.69	1/2	0.32	2/3
Helical ribbon					
$P/D_v = 1/4$ $\mathrm{Re}_a < 9$		$9 < \mathrm{Re}_a < 135$		$\mathrm{Re}_a > 135$	
K	a	K	a	K	a
0.98	1/3	0.68	1/2	0.3	2/3
$P/D_v = 1/2$ $\mathrm{Re}_a < 13$		$13 < \mathrm{Re}_a < 210$		$\mathrm{Re}_a > 210$	
K	a	K	a	K	a
0.94	1/3	0.61	1/2	0.25	213

These correlations agree reasonably well (≅±30%) with the data and correlations of other workers, with the exception of the work by Nishikawa et al. [35]. For Re, > 1 000, Nishikawa et al. obtained correlational results up to 10% higher than the above correlations; and for Re, < 10, with their helical ribbon impeller, up to 40% greater. Nishikawa et al. tested a double-helix, helical ribbon impeller, and they tested five different values of S_c/D_v, but their range of S_c/D_v bracketed the S_c/D_v tested by Harry and Uhl. The double helix versus the single helix is probably the only significant geometric difference between the two investigations for equal values of S_c/D_v. This difference would not be expected to cause the great differences in correlational results; and, in fact, Mitsuishi and Miyairi [40] obtained correlational results with a double-helix, helical ribbon impeller that agree very well with the results of Harry and Uhl. This evidence, plus the fact that the correlations of Nishikawa et al. overpredict the experimental data of Coyle et al. [38] by up to 400%, indicates strongly that the data of Nishikawa et al. are in error on the high side. For the anchor and both single-helix and double-helix helical ribbon impellers, the correlations of Harry and Uhl [34] presented above are recommended for the indi-

© 1983 Hemisphere Publishing Corporation

cated ratio of clearance to impeller diameter (S_c/D_v). The effect of clearance between impeller tip and vessel wall will be discussed later.

The correlations above indicate that the anchor is slightly superior to the helical ribbon impeller over the entire range of Re,. For Re_a > 500, these results are probably correct and, in this Re, range, undoubtedly the anchor is the economical choice because it is significantly less expensive than the helical ribbon. As Re, decreases from 500 to 50, the mixing produced by the anchor becomes progressively worse than the mixing produced by the helical ribbon. Consequently, temperature gradients become progressively greater for the anchor-agitated vessel than for the helical ribbon-agitated vessel, and the experimental determination of an accurate heat transfer coefficient becomes increasingly difficult for the anchor. All investigators have noticed much greater thermal gradients in an anchor-agitated vessel than in a helical ribbon-agitated vessel at low Re,. The thermal gradients are so great for an anchor for Re, < 50 and the scatter in the correlated data so great that the recommended correlation for the anchor should not be trusted below Re, = 50 and should be used conservatively and with caution for 50 < Re, < 500. Essentially all investigators agree that the helical ribbon impeller is the appropriate choice for Re, < 50 because of its superior mixing performance.

Now the effect of clearance between the impeller tip and the vessel wall, in particular, and geometry in general will be considered. In the fully turbulent regime (Re_a > 500), geometry has little effect; consequently, the least expensive impeller should be used; in fact, in this range the nonproximity impellers (turbines, propellers, etc.) should be considered. As Re, decreases from 500 to 50, geometry becomes progressively more important, until for Re, < 50, geometry significantly affects heat transfer performance. The effects of P/D, (Note that for an anchor, P/D, = ∞.) have already been discussed. Other than the pitch of the impeller arms, the clearance between the impeller tip and the vessel wall is about the only other significant geometric variable. There is much disagreement about its effect: Coyle et al. [38] found for two vessels (0.38 m, S_c/D_v = 0.035 and 0.74 m, S_c/D_v = 0.015) with viscous organic liquids that wall scrapers increased both heat transfer coefficient and agitator power about 100%; whereas Nishikawa et al. [35] found less than a 30% increase in heat transfer coefficient for the same range of S_c/D_v. In light of these basic disagreements, it appears that available methods do not give reasonable accuracy for predicting the effect of clearance. Figure 1 presents the method recommended here to predict the effect of clearance. This recommendation is based on the judgment of this author, taking into consideration the results of all investigations.

D. Scraped-wall pipe equipment

Votator style [Fig. 3.14.2(3)] and spring-loaded scraper style [Fig. 3.14.2(4)] are the most common scraped-wall pipe equipment types. Their construction and uses have been well described by Uhl [33]. These equipment types have greater L/D, ratios than anchor- and helical ribbon-agitated equipment and, for this reason, they are used almost exclusively for continuous processing. The long lengths reduce the effect of back mixing, thereby increasing the mean temperature difference (MTD) between the process and utility streams above that obtained in well-mixed vessels. To design this equipment accurately, predictive methods are needed for (1) heat transfer coefficient and (2) MTD.

(a) Local heat transfer coefficient

As for anchors and helical ribbon impellers, the agitator geometry has little effect on the heat transfer coefficient in the turbulent regime. However, as Re, decreases below 200, the fluid flow patterns become progressively more streamlined and agitator geometries that produce

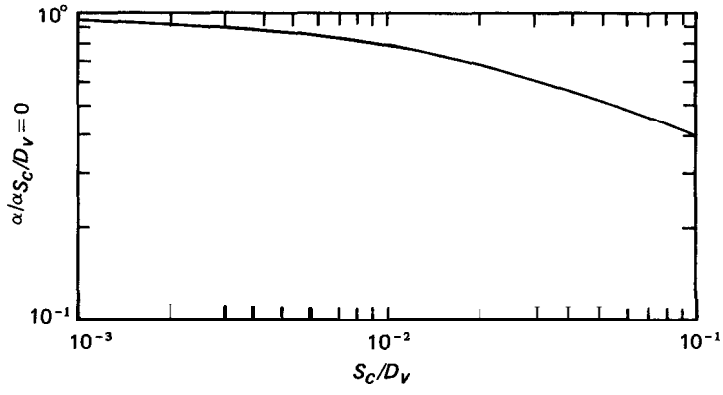

Figure 1 Effect of impeller tip to vessel wall clearance on the heat transfer coefficient for helical ribbon impellers.

© 1983 Hemisphere Publishing Corporation

recirculating regions that never migrate to the vessel wall produce poor radial mixing and thereby large radial temperature gradients, which are detrimental to heat transfer. The large observed temporal temperature fluctuations observed by Penney [41] indicate that the thin, flat blade used (this agitator geometry does produce recirculating regions that never migrate to the vessel wall) produces poor radial mixing in the laminar regime. Industrial equipment manufacturers have long recognized the need for equipment that provides adequate radial mixing for high fluid viscosities. Votator offers a rotor with eccentric floating blades or an oval tube, and the spring-loaded scraper rotors [Fig. 3.14.2(4)] often have segmented blades with alternate sections rotated 90 . All these designs produce good radial mixing.

Uhl [33] discusses previous efforts to develop correlations to predict heat transfer coefficients for this equipment. None of the previous correlations is acceptable. The predictive method recommended here is based on the correlation of Harry and Uhl [34] for the helical ribbon impeller with P/D, = 1/4 and S_c/D_v = 0.02. In the turbulent regime their correlation is recommended as is, and in the laminar regime their correlation is adjusted for the effect of scrapers per Fig. 1. In the transition regime, judgment should be used to estimate the increased effect of wall scrapers. The recommended correlation is

$$\mathrm{Nu}, = K\,\mathrm{Re}_a^a\,\mathrm{Pr}^b\left(\frac{\eta_b}{\eta_w}\right)^c \qquad (4)$$

where b = 1/3, c = 0.14, and K and a vary with Re, as follows:

$\mathrm{Re}_a < 30$		$30 < \mathrm{Re}_a < 520$		$\mathrm{Re}_a > 520$	
K	a	K	a	K	a
1.5	1/3	0.85	1/2	0.3	2/3

Equipment manufacturers probably have more accurate and reliable correlations, and they should be consulted before finalizing design.

(b) Mean temperature difference and heat transfer capacity

Penney and Bell [42] have presented a method for predicting the effect of axial mixing on the MTD and, consequently, on the heat transfer capability. The dispersion model is used to predict the effects of back-mixing. The step-by-step computational procedures for applying the method are presented below (refer to [42] for details).

1. $\mathrm{Pe}_a = 33\,\mathrm{Re}_{ae}^{0.17}\,(\mathrm{Re}_{ae} > 100)^{\dagger}$
2. $\mathrm{Pe}_f = \mathrm{Pe}_a(vL/v_t D_e)$
3. Compute α from heat transfer coefficient correlations.
4. Compute U.
5. $B = UA/\dot{M}c_p$.
6. Determine E from Fig. 2 for the case of constant-utility fluid temperature (refer to [42] for other cases).
7. $Q = UA(\mathrm{LMTD})(E)$.

Table 2 presents the results of an example case. The apparatus is a Votator style with $D_v = D_i = 3/4$ m, L = 4 m, N = 3.33 rps (Artisan Industries, Waltham, Massachusetts, manufactures a similar unit). The fluid properties are the same as ambient water except that the fluid viscosity is 50 poise. Also, assume that $D_e = 0.611D_v$, $U = \alpha$, utility stream temperature = 100°C, and inlet process stream temperature = 20°C.

Note that the greatest relative effect of back mixing on the outlet fluid process temperature (T_{out}) is for the lowest flow rate; in fact, as $\dot{M} \to 0$, the temperature is constant along the axial length of the vessel. Also, as $\dot{M} \to \infty$, there is no effect of back mixing.

It should be noted that the equipment and conditions selected were intended to illustrate worst-case conditions; consequently, the performance of most industrial equipment will probably be less affected by back mixing than the equipment of this example, especially for equipment with a length-to-diameter ratio greater than the value of 5 used here.

E. Other equipment having proximity agitators

Most of the remaining equipment is used primarily for highly non-Newtonian (especially pseudoplastic) materials and/or for extremely high viscosities, exceeding 1 000 poise. A major portion of this equipment (double-motion scraper, double-shaft units, e.g., Sigma and Helicone, the Porcupine Processor) is discussed by Uhl [33]. Extruders are an important class of equipment not discussed by Uhl. The correlations presented here for the helical ribbon with scrapers are suggested for predicting performance of the double-motion agitator. No general predictive methods are available for the equipment used for extremely high viscosities. Correlational work is complicated for this equipment because of the great amount of heat generated within the clearance region between the impeller tip and the wall. As a minimum,

†For Re_a < 100, the dispersion model does not well represent experimental data. Consult the manufacturer and/or do experimental work; although normally for Re_a < 100 back mixing is not expected to affect performance significantly.

© 1983 Hemisphere I blishing Corporation

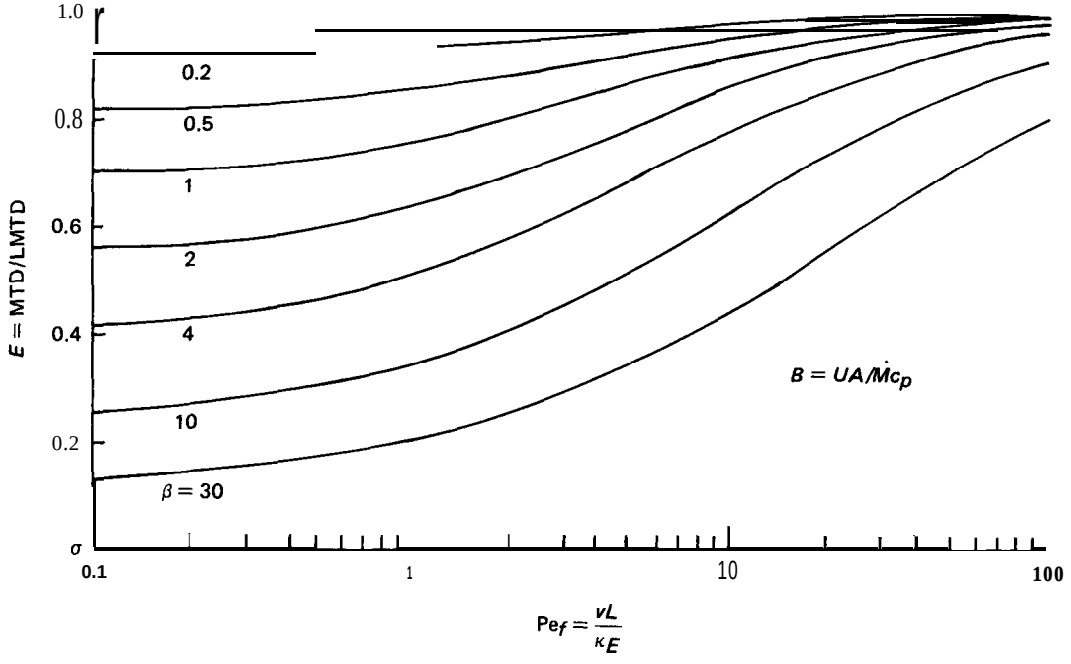

Figure 2 Effect of back mixing on MTD agitated pipe style equipment operating in the turbulent regime for the case of constant-utility fluid temperature. For variable utility fluid temperature see [42].

Table 2 Effect of back mixing on process **fluid outlet** temperature for a particular **votator** apparatus

$\dot{M}$ (kg/h)	500	1 000	2 000
Re_a	372	372	372
Re_{ae}	713	713	713
Pe_a	0.01	0.01	0.01
Pe_f	0.04	0.07	0.14
B = MTD/LMTD	0.35	0.45	0.63
T_{out} (no back mixing)	99.9	96.6	83.5
T_{out} (with back mixing)	91.2	82.5	70.0

the high-intensity equipment will probably always perform better than the correlations for helical ribbon agitators would predict. Uhl [33] has well summarized the status of predictive methods for double-shaft units,

intense mixing devices such as the Helicone and intermeshing double-blade batch mixers such as the Sigma mixer for Re, < 30 should provide a value of α several times that attainable for the anchor and helical ribbon. This is due to the recognized better transport from the wall to the bulk and return, but also results from the generation in the clearance space of much if not all the heat removed.

NOMENCLATURE FOR SECTIONS 3.14.1-3.14.3

- A heat transfer area, m^2
- c_p heat capacity, J/kg K
- d_g width of gap between successive tubes in a helical coil or tube bank, m
- d_p diameter of vertical probe in vessel, m
- d_t outside diameter of tubes used as internal vessel heat transfer surfaces, m
- D_e equivalent hydraulic diameter of flow channel = 4(flow area)/(total wetted length normal to flow direction), m
- D_i impeller diameter, m
- D_v vessel inside diameter, m
- E ratio of actual mean temperature difference to logarithmic mean temperature difference
- Fr_a agitation Froude number, N^2D_i/g
- g acceleration due to gravity, m/s^2
- K geometry-dependent constant in Eq. 3.14.3(1)
- l characteristic length (see Sec. A)
- L length of flow channel for pipe-style agitated equipment, m
- L_i height of impeller blade parallel to axis of rotation, m
- LMTD logarithmic mean temperature difference, °C
- MTD true or actual integrated mean temperature between a process stream and a utility stream, °C
- $\dot{M}$ mass flow rate, kg/s
- N impeller rotational speed, rev/s
- N_{ba} number of baffles in the vessel
- N_{bl} number of blades on an impeller
- Nu Nusselt number, = $\alpha l/\lambda$

© 1983 Hemisphere Publishing Corporation

N_i number of impellers
Nu_v Nusselt number based on vessel diameter, $= \alpha D_v/\lambda$
Nu_t Nusselt number based on outside tube diameter, $= \alpha D_t/\lambda$
P pitch of propeller or helical ribbon impeller, m
Pr Prandtl number, $= \nu/\kappa$
Pe_a effective Péclet number based on agitation parameters, $= v_t D_e/\kappa_E$
Pe_f effective Péclet number based on flow channel parameters, $= vL/\kappa_E$
Q overall rate of heat transfer, W
Re_a agitation Reynolds number, $= ND_i^2/\nu$
Re_{ae} rotational Reynolds number based on v_t and D_e as characteristic velocity and length, respectively, $= v_t D_e/\nu$
S_a width of the impeller blade arm in a radial direction for anchors and helical ribbon impellers, m
S_b baffle width, m
S_c clearance between the impeller blade tip and the vessel wall, m
S_i height of impeller off vessel bottom, m
S_l depth of liquid in vessel, m
S_{pc} width of plate coil, m
S_{vo} depth of vortex from free liquid surface (at rest) to bottom of vortex, m
T temperature, °C
U overall heat transfer coefficient, W m^2/K
v fluid velocity along a flow channel, m/s
v_s sparged gas superficial velocity, m/s
v_t impeller tip speed, $= \pi ND_i$, m/s
V vessel volume, m^3
$a!$ heat transfer coefficient, W m^2/K
η dynamic viscosity, kg/m s
η_b dynamic viscosity at the average vessel temperature, kg/m s
η_w dynamic viscosity at the temperature of the heat transfer surface, kg/m s
θ angle between a pitched blade on an impeller and a plane normal to the axis of rotation, deg
K thermal diffusivity, $= \lambda/\rho c_p$, m^2/s
κ_E effective axial thermal diffusivity along a flow channel due to all mechanisms of thermal transport, i.e., molecular, flow and turbulence, m^2/s
λ thermal conductivity, W/m K
V kinematic viscosity, m^2/s
P density, kg/m^3

REFERENCES FOR SECTIONS 3.14.1-3.14.3

1. Sterbacek, Z., and Tausk, P., ***Mixing in the Chemical Industry,*** Pergamon, London, 1965.
2. Holland, F. A., and Chapman, F. ***S., Liquid Mixing and Processing in Stirred Tanks,*** Reinhold, New York, 1966.
3. Uhl, V. W., and Gray, J. B. ***(eds.),Mixing-Theory and Practice,*** vols. I and II, Academic, New York, 1966.
4. Nagata, ***N., Mixing-Principles and Applications,*** Wiley, New York, 1975.
5. Parker, N. H., Mixing-Modern Theory and Practice on the Universal Operation, ***Chem. Eng.***, June 8, 1964, pp. 165-220.
6. Jordan, D. ***G., Chemical Process Development,*** pt. 1, chap. 3, pp. 111-174, Interscience, New York, 1968.
7. Edwards, M. F., and Wilkinson, M. A., Heat Transfer in Agitated Vessels: Part I-Newtonian Fluids, and Part II-Non-Newtonian Fluids, ***The Chemical Engineer,*** pt. I, pp. 310-319, August, and pt. II, pp. 328-335, September 1972.
8. Kase, H. ***F., Chemical Reactor Design for Process Plants, Volume One: Principles and Techniques,*** chap. 8, pp. 331-392, Wiley, New York, 1971.
9. Penney, W. R., and Koopman, R. N., Prediction of New Heat Removal for Agitated Vessels (and Pumped-Through Heat Exchangers), AIChE Preprint No. 10, 12th National Heat Transfer Conference, AIChE-ASME, Tulsa, Oklahoma, 1971.
10. Rushton, J. H., Design and Utilization of Internal Fittings for Mixing Vessels, ***Chem. Eng. Prog.,*** vol. 43, pp. 649-657, December 1974.
11. Weber, A. P., Selecting Propeller Mixers, ***Chem. Eng.,*** September 2, 1963, pp. 91-98.
12. Brennan, D. J., Vortex Geometry in Unbaffles Vessels with Impeller Agitation, ***Trans. Inst. Chem. Eng.,*** vol. 54, pp. 209-217, 1976.
13. Hicks, R. W., and Gates, L. E., Fluid Agitation in Polymer Reactors, ***Chem. Eng. Prog.***, vol. 71, pp. 74-79, August 1975.
14. Marshall, V. C., and Yazdani, N., Design of Agitated, Coil-in-Tank Coolers, ***Chem.*** Process ***Eng.,*** April 1970, pp. 89-101.
15. Nagata, S., et al., Turbulent Heat Transfer from the Wall of a Jacketed Tank, ***Heat Transfer Jpn. Res., vol. 1,*** no. 1, pp. 66-74, 1972.
16. Brooks, G., and Su, G. J., Heat Transfer in Agitated Vessels, ***Chem. Eng. Prog.***, vol. 55, no. 10, pp. 54-57, 1959.
17. Strek, F., Heat Transfer in Liquid Mixer-Study of a Turbine Agitator with Six Flat Blades, ***Int. Chem. Eng.,*** vol. 3, no. 4, pp. 533-556, 1963.
18. Chapman, F. S., et al., Heat Transfer in Baffled, Jacketed Agitated Vessels, ***Trans. Inst. Chem. Eng.,*** vol. 42, pp. T398-T406, 1964.
19. Ackley, E. J., Film Coefficients of Heat Transfer for Agitated Process Vessels, ***Chem. Eng.***, August 22, 1960, pp. 133-140.
20. Nagata, S., et al., Turbulent Heat Transfer from Helical Cooling Coils in Agitated Vessels, ***Heat Transfer Jpn. Res.,*** vol. 1, no. 2, pp. 44-56, 1972.
21. Kupcik, F., Heat Transfer at the Bottom and at the Walls of Agitated Vessels, ***Int. Chem. Eng.,*** vol. 16, no. 1, pp. 91-96, January 1976.
22. Strek, F., et al., Heat Transfer in Mixers for Liquids (Studies of Propeller Agitators), ***Int. Chem. Eng.,*** vol. 5, no. 4, pp. 695-710, 1965.

© 1983 Hemisphere Publishing Corporation

23. Oldshue, J. Y., and Gretton, A. T., Helical Coil Heat Transfer in Mixing Vessels, *Chem. Eng.* frog., vol. 50, pp. 615-621, December 1954.
24. Oldshue, J. Y., Fluid Mixing, Heat Transfer and Scale-up, *Chem.* Process *Eng.*, April 1966, pp. 183-188.
25. Skelland, A. H. P., et al., Heat Transfer to Coils in Propeller-Agitated Vessels, *AIChE J.*, vol. 11, no. 5, pp. 95 l-954, 1965.
26. Dunlap, I. R., and Rushton, J. H., Heat-Transfer Coefficients in Liquid Mixing Using Vertical-Tube Baffles, *Chem. Eng. Prog. Symp.* Ser. 5, vol. 49, pp. 137-151, 1953.
27. Gentry, C. L., and Small, W. M., Heat Transfer and Power Expenditure for Agitated Vessels Having Bare and Finned, Vertical Tube Baffles, *Proc. 6th Int. Heat Transfer Conf.*, vol. 4, pp. 13-18, 1978.
28. Petree, D. K., and Small, W. M., Heat Transfer and Power Consumption for Agitated Vessels with Vertical Plate *Coils, AIChE Symp. Series 174,* vol. 74, pp. 53-59, 1978.
29. Hart, W. F., Heat Transfer in Bubble-Agitated Systems. A General Correlation, *Ind. Eng. Chem., Process Des. Dev.,* vol. 15, no. 1, pp. 109-114, 1976.
30. Nagata, S., et al., Study of Heat Transfer for Aerated Mixing Vessel and Aerated Tower, *Heat Transfer Jpn. Res.,* vol. 5, no. 4, pp. 75-83, 1976.
31. Tamari, M., and Nishikawa, K., The Stirring Effect of Bubbles upon Heat Transfer to Liquids, *Heat Transfer Jpn. Res.,* vol. 5, no. 1, pp. 31-44, 1976.
32. Steiff, A., and Weinspach, P. M., Heat Transfer in Stirred and Non-Stirred Gas-Liquid Reactors, Ger. Chem. *Eng.*, vol. 1, pp. 150-161, 1978.
33. Uhl, V. W., Mechanically Aided Heat Transfer to Viscous Materials, *Symposium: Augmentation of Convective Heat and Mass Transfer, ASME Winter Annual Meeting, New York,* pp. 109-117, December 1970.
34. Harry, F. P., and Uhl, V. W., Heat Transfer to Viscous Materials in a Vessel with a Helical Ribbon Impeller, Paper presented at the 74 National AIChE Meeting, New Orleans, March 1973.
35. Nishikawa, M., Kamata, N., and Nagata, S., Heat Transfer for Highly Viscous Liquids in Mixing Vessels, *Heat Transfer Jpn. Res.,* vol. 5, no. 4, pp. 84-92, 1975.
36. Ishibashi, K., et al., Heat Transfer in Agitated Vessels with Special Types of Impellers, *J. Chem. Eng. Jpn.,* vol. 12, no. 3, pp. 230-235, 1979.
37. Rautenbach, R., and Bollenrath, F. M., Heat Transfer in Stirred Vessels to High-Viscosity Newtonian and Non-Newtonian Substances, *Ger. Chem. Eng.,* vol. 2, pp. 18-24, 1979.
38. Coyle, C. K., et al., Heat Transfer to Jackets with Close Clearance Impellers in Viscous Liquids, *Can. J. Chem. Eng.,* vol. 48, pp. 275-278, June 1970.
39. Nagata, S., Nishikawa, M., and Kayama, T., Heat Transfer to Vessel Wall by Helical Ribbon Impeller in Highly Viscous Liquids, *J. Chem. Eng. Jpn.,* vol. 5, no. 1, pp. 83-85, 1972.
40. Mitsuishi, N., and Miyairi, Y., Heat Transfer to Non-Newtonian Fluids in an Agitated Vessel, *J. Chem. Eng. Jpn.,* vol. 6, no. 5, pp. 415-420, 1973.
41. Penney, W. R., Heat Transfer and Agitator Power Requirements in Mechanically-Agitated Thermal Processors with Fixed-Clearance Agitators, Ph.D. thesis, Oklahoma State University, Stillwater, Oklahoma, 1968.
42. Penney, W. R., and Bell, K. J., The Effect of Backmixing on the Mean Temperature Difference in an Agitated Heat Exchanger, *AIChE Symp. Ser. No. 92,* vol. 65, pp. 21-33, 1969.

© 1983 Hemisphere Publishing Corporation

3.15

Regeneration and thermal energy storage

Contents

3.150
INTRODUCTION, F. W. Schmidt **3.15.0-l**

A. Basic concept of energy storage devices 3.15.0-l
B. Classification of thermal energy storage devices 3.15.0-2
C. Thermal storage materials 3.15.0-3
D. Design considerations 3.15.0-4

References for Section 3.15.0 3.15.0-S

3.15.1
OPERATION OF REGENERATORS,
A. J. Willmott **3.15.1-1**

3.15.2
CONSTRUCTION OF REGENERATOR PACKING,
A. J. Willmott **3.15.2-1**

A. Packing for high temperature operation 3.15.2-1
B. Moderate temperature packings 3.15.2-2
C. Lower temperature packings 3.15.2-3

3.15.3
INTERNAL BEHAVIOR OF A REGENERATOR: DEVELOPMENT OF THE MATHEMATICAL MODEL,
A. J. Willmott **3.15.3-l**

A. Entrance gas temperature conditions 3.15.3-l
B. Counter-flow and parallel flow operation 3.15.3-1
C. Heat transfer in counter-flow mode 3.15.3-1
D. Simplification of the model 3.15.3-2

3.15.4
HEAT TRANSFER COEFFICIENT,
A. J. Willmott **3.15.4-1**

3.15.5
USE OF BULK OR OVERALL HEAT TRANSFER COEFFICIENT,
A. J. Willmott **3.15.5-l**

3.15.6
DEVELOPMENT OF DIMENSIONLESS PARAMETERS,
A. J. Willmott **3.15.6-1**

3.15.7
CALCULATION OF REGENERATOR THERMAL PERFORMANCE,
A. J. Willmott **3.15.7-1**

A. Relationship between symmetric and nonsymmetric regenerators 3.15.7-1
B. Method I of regenerator calculation 3.15.7-2
C. Method II of regenerator calculation 3.15.7-3
D. Computational note 3.15.7-4
E. Complete calculation using method II 3.15.7-4
F. Precise methods for the calculation of regenerators 3.15.7-6

Peter J. Heggs, Chemical Engineering Department, Leeds University, United Kingdom, served as the consulting editor for Sections 3.15.0-3.15.10.

© 1984 Hemisphere Publishing Corporation

HEDH

G. Method III (Nahavandi and Weinstein, 1961): Closed 3.15.7-6
H. Method IV (Willmott, 1964): Open 3.15.7-7

3.15.8
EFFECT OF LONGITUDINAL CONDUCTION IN THE PACKING OF THE REGENERATOR,
A. J. Willmott **3.15.8-1**

3.15.9
DEALING WITH HEAT LOSSES,
A. J. Willmott **3.15.9-1**

A. Example of heat loss calculation 3.15.9-2

3.15.10
TRANSIENT CHARACTERISTICS OF REGENERATORS,
A. J. Willmott **3.15.10-l**

A. Example calculation 3.15.10-l
B. Worked example 3.15.10-4
C. Further worked example 3.15.10-S
D. Conclusions 3.15.10-S

Nomenclature for Sections 3.15.3-3.15.10 **3.15.10-6**
References for Sections 3.15.3–3.15.10 **3.15.10-6**

© 1984 Hemisphere Publishing Corporation

3.15.0
Introduction

F. W. Schmidt

A. Basic concept of energy storage devices

An energy storage device transfers thermal energy between hot and cold fluid streams indirectly by the utilization of a third substance for the temporary storage of energy. This substance may be a solid, liquid, or a material that is undergoing a change in phase. The substance comes into physical contact with both the hot and cold fluid streams in an alternating fashion during the storage process.

There are two major areas where energy storage devices are currently used. In many situations the availability of a source of energy does not coincide time-wise with the demands for the energy. The capacity to store and retrieve energy at different times thus adds an important capability to an energy management system. It also allows alternative sources of energy, such as solar energy, to be used to meet conventional energy demands.

The second area involves the use of a thermal storage device in place of a standard recuperator to exchange thermal energy between two fluid streams whose inlet fluid temperatures and fluid flow rates are relatively time invariant. The following lists some major advantages of a thermal storage device under these conditions.

A high heat transfer surface area per unit volume is obtainable.

Only one set of flow channels are needed since the fluids flow through the same channels alternatively.

There is an even distribution of pressure within the regenerator.

Counterflow of the two fluid streams can give a cleaning action, thereby reducing fouling.

Vapors that are condensed during the heat retrieval process may be vaporized during the heating process and carried away with the hot fluid stream.

When the stream passing through the flow passages of the heat storage device is changed, some residual fluid is left in the passages and is mixed with the incoming fluid stream. A slight decrease in the performance of the unit may result. If the two streams react or if the contamination of the streams is undesirable, thermal storage devices should not be used.

A study on the potential benefits to be obtained using energy storage devices has indicated that the following factors must be considered:

Storage capacity
Storage/retrieval rate
Replacement lifetime
Weight, volume and other physical limits
Critical safety parameters
Environmental standards
Acceptable capital and operating costs

It was also indicated that the areas where storage devices could be used were so varied that no specific type of storage device could be expected to have proper operating characteristics for all possible applications.

© 1984 Hemisphere Publishing Corporation

B. Classification of thermal energy storage devices

The physical locations of sources of energy and the device or process requiring energy seldom coincide, and one must be concerned with the transport of energy from one location to another as well as with storage of energy. The ideal situation occurs when the energy transporting fluid also serves as the storage medium. There are many examples of these types of systems. Hot water storage is used in most residential and commercial units for domestic water service. A large number of solar units use hot water for storage. Units using a fluid as both the transport and storage media are, however, restricted to low-temperature applications.

Thermal energy storage devices employing steam or hot water accumulators have been used in industry in Europe for many years. A complete discussion of these systems has been presented by Goldstern [1]. The first of these units developed were essentially high-pressure steam or water tanks from which the fluid was expanded as required to a lower pressure for the generation of power or for use in an industrial process. Reay [2] describes new units which can be used for both steam generation and storage. These are called thermal storage boilers.

A general classification system for thermal storage devices has been presented by Schmidt [3].

(a) Regenerator

The regenerator is a thermal energy storage device in which the heat storage and heat retrieval processes are repeated in a periodic fashion. Only one of the fluid streams is in contact with the storage material at any instant of time, so both the hot and cold fluids can use the same flow channels. When both the hot and cold fluid streams are flowing continuously it may be necessary to have two or more regenerators arranged to transfer the heat continuously from the hot fluid stream to the cold fluid stream. The system of regenerators can thus be used in place of a recuperator.

Identical fluid passages are used during the heat storage and retrieval processes. The hot and cold fluids usually flow in opposite directions (counter-flow operation). Two types of regenerators are in common use. A rotary regenerator is a unit in which the storage material moves physically from one fluid stream to the other in a periodic fashion. A regenerator in which the storage material is stationary and a series of valves and ducts are used to alternately direct the hot and cold streams through the storage material is called a fixed bed or fixed matrix regenerator. In nearly all current applications using regenerators, the hot and cold fluids are gases.

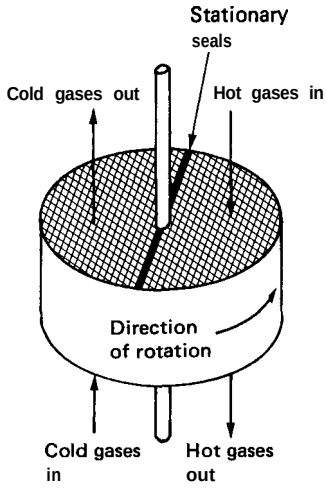

Figure 1 Rotary regenerator.

Rotary regenerators are used extensively in electrical power generating stations for air preheating. They are also used in vehicular gas turbine power plants, in cryogenic refrigeration units, and in the food dehydration industry. A schematic sketch of a rotary regenerator is shown in Fig. 1. Major problems encountered in the design of rotary regenerators are: the sealing off of hot and cold gas streams; thermal stresses encountered during start up and shut down; gas contamination and localized burnout of storage material due to in situ combustion or blocked passages in the regenerator matrix.

Fixed bed or fixed matrix regenerators are used extensively in the metallurgical, glassmaking, and chemical processing industries. A diagram of a fixed bed regenerator is shown in Fig. 2. If the hot and cold fluid streams are continuous, at least two fixed-bed regenerators must be used so that hot gases can pass through one regenerator while the cold gases are passing through the other regenerator. The fluid streams are then peri-

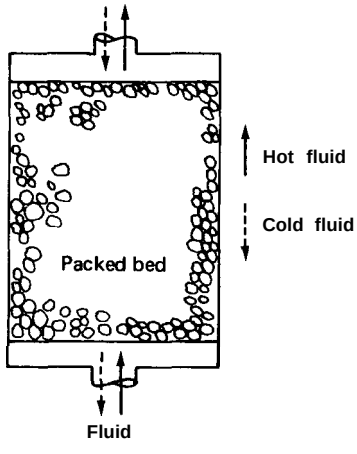

Figure 2 Fixed-bed regenerator.

© 1984 Hemisphere Publishing Corporation

odically switched from one regenerator to the other. If a constant outlet temperature is required during the heat retrieval process series-parallel or staggered-parallel arrangements of two or more regenerators are required [4]. When the hot and cold streams are not flowing at the same time, a single fixed regenerator can be used. The temperature of the cold air stream can be regulated using a bypass arrangement during the retrieval period of operation [5].

(b) Heat storage unit

A heat storage unit is a thermal energy storage device in which there is no periodic pattern to the storage and retrieval processes. Only one stationary storage unit is used and the hot and cold fluid streams pass through the same flow channels. The mass flow rates, inlet fluid temperatures, and duration of flow for the hot and cold fluid streams vary in an arbitrary timewise fashion. There may even be periods of time when neither fluid stream is passing through the storage unit. A typical heat storage unit is diagramed in Fig. 3.

A heat storage unit is a necessary component in most active solar energy systems. The energy is collected during the daytime and is transported from the collector to the storage unit. If the transporting fluid is air, sensible heat or phase change materials will be used as the energy storage material. If the transporting fluid is water, it will probably be used as the energy storage material.

Many industries wish to use the waste energy produced by batch-type process in order to reduce the amount of energy that must be purchased. Heat storage units are used to match in a timewise fashion the availability and demands for the energy. There are many other applications in waste heat recovery where energy storage units are utilized to improve the operating characteristics of the system.

(c) Heat storage exchangers

A heat storage exchanger is a device in which two or more fluid streams may be simultaneously in contact with the storage material. A portion of the heat removed from the hot fluid stream is transferred directly to the cold fluid stream while the remaining energy is stored in the storage material. Figure 4 shows a sketch of a heat storage exchanger. This type of a storage unit is essentially a thick-wall heat exchanger.

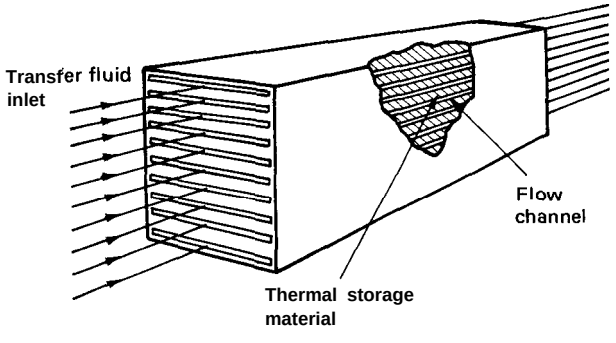

Figure. 3 Heat storage unit.

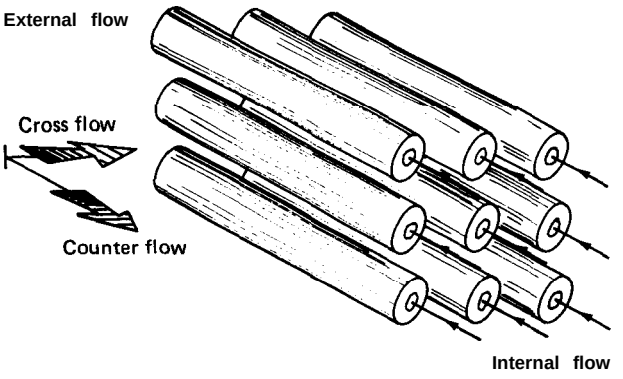

Figure 4 Heat storage exchanger.

C. Thermal storage materials

Many factors must be considered when selecting storage material. A set of desirable characteristics would include the following:

High specific heat
High density
High thermal diffusivity
Reversible heating and cooling
Chemical and geometric stability
Noncombustible, noncorrosive, and nontoxic
Low vapor pressure to reduce the cost of containment
Low cost for material and containment
Sufficient mechanical strength to support the stacking of the storage core
Proper operating temperature range
Long operating life

At present there are three major groups of heat storage media utilized for thermal energy storage: nonmetals, metals, and phase change materials.

(a) Nonmetals

Firebricks formed from clay, olivine, chrome, magnesite, and various mixtures of these represent an important group of nonmetals used in storage devices operating at high temperatures. In an effort to obtain a material having a high volume heat capacity, feolite, composed of ferric oxide, Fe_2O_3, was developed. The commercial material, called Tenemax, utilizes low cost enriched iron

© 1984 Hemisphere Publishing Corporation

ores and uses virtually standard brick making manufacturing processes.

Concrete is another nonmetal that is attracting considerable attention as a sensible heat storage material. Although its thermal storage capabilities are marginal, its cost and the fact that the unit can be fabricated on site are attractive factors. Architects are using concrete and other construction material in the design of buildings for passive storage of solar energy.

The last nonmetal to be noted is gravel. This is used primarily in packed beds for low temperature solar energy storage.

(b) Metals

Castable metals, including gray cast irons and cast irons containing alloying ingredients such as silicon and aluminum, have been used in storage devices in the past. Their advantage offered by having a very high heat storage capacity per unit volume is more than offset by their high cost. As a result, most storage devices using these materials are no longer economically practical. The only exceptions are rotary regenerators, which are fabricated using metallic matrices. The matrices are constructed using very thin metal strips and are designed to give a very large surface to volume ratio. The material which is used depends to a large extent on the application. Stainless steel is used where the atmosphere is corrosive.

(c) Phase change materials

Storage devices utilizing the phase change properties of the storage material (PCM) are receiving considerable attention. These units are of interest because they have a small temperature swing as one cycles from storage to retrieval, since the major portion of the energy is stored or removed while the material is at a nearly uniform temperature. The major advantage of these units, however, is that they utilize the high heat of fusion of the storage material and thus have a very high heat capacity per unit volume or weight. The mean storage temperature can be controlled to a large extent by the selection of the storage material. A set of criteria for phase change storage materials has been presented by Lorsch et al. [6]. Typical storage materials of this type are sodium sulfate decahydrate ($Na_2SO_4 \cdot 10H_2O$) and paraffin waxes.

D. Design considerations

A number of items must be considered in the design of thermal energy storage units. They will, to a large extent, be dependent upon the specific application that the storage device is to be used for.

(a) Storage material

The importance of this item in the design of a thermal energy storage device has been properly emphasized by the discussion presented in the previous section. This item is listed only for completeness of factors that must be considered in the design of storage devices.

(b) Pressure drop

The allowable pressure drop across the storage device will depend strongly on the application for which the device is intended. In many cases this is not a critical item in the design of the storage device, while in other applications it represents a severe design limitation. Pressure drop is related to the properties of the fluid, the mass velocity of the fluids flowing through the channels in the storage device, the geometry of the fluid flow passages, and the length of the flow channels. The magnitude of the convective heat transfer coefficient is also dependent on many of these same factors. A compromise is required since the designer ideally desires to obtain a high film coefficient and a low pressure drop. To facilitate making a decision, an understanding of the influence of the convective heat transfer coefficient on the performance of the thermal storage device is required.

(c) Configuration

The need to design a device with realistic dimensions in obvious. Special restrictions, however, are frequently imposed because of the physical location of the device or the particular system in which the storage device is to be used. The restraints usually involve the length, breadth, weight, or volume of the device.

(d) Amount of available energy stored

In many installations, particularly those involving heat storage units, the hot stream is discharged to the surroundings immediately after it leaves the storage unit. Design consideration can include the maximization of the amount of energy removed from the hot stream, however, care must be taken or an extremely long unit will result.

(e) Utilization of storage material

This is another item that may be of considerable concern to the designer of a heat storage device. A criterion that might be used for the assessment of the performance of a storage unit could be the total amount of heat stored when the mean temperature of the storage material is equal to the temperature of the fluid entering the

© 1984 Hemisphere Publishing Corporation

storage unit. Basing the design only on obtaining the maximum energy storage per unit volume is not recommended, since, during the latter part of the storage process, little energy is removed from the hot fluid stream. The amount of the energy available in the hot streams that is stored is thus very small.

(f) *Operating characteristics*

Although there are many operating characteristics that may affect the design of the storage device, most of these are contained within the parameters used to calculate the performance of the device. They in a sense act as independent variables. An operating characteristic that is of the dependent variable type is the temperature of the cold stream leaving the storage device. A minimum acceptable temperature is usually established by the device or process that uses the retrieved energy. In many systems where heat storage devices are used, it is necessary to maintain the heated fluid at a constant temperature. Since the temperature of the cold fluid leaving a storage device during the retrieval process will decrease as the duration of retrieval increases, a combination of several storage devices or a bypass arrangement is necessary to ensure the availability of a constant temperature.

REFERENCES FOR SECTION 3.15.0

1. Goldstern, W., ***Steam Storage Installations,*** Pergamon Press, Oxford, 1970.
2. Reay, D. A., ***Industrial Energy Conservation,*** Pergamon Press, Oxford, 1977.
3. Schmidt, F. W., Thermal Energy Storage and Regeneration, ***in Heat Exchangers: Theory and Practice,*** eds. J. Taborek, G. F. Hewitt, and N. H. Afgan, Hemisphere, Washington, D.C., 1983.
4. Shah, R. K., Thermal Design Theory for Regenerators, in ***Heat Exchangers: Thermohydraulic Fundamentals and Design,*** eds. S. Kakac, A. E. Bergles, and F. Mayinger, Hemisphere, Washington, D.C., 1981.
5. Kulakowski, B. T., and F. W. Schmidt, Design of Packed Bed Regenerators with By-Pass, ***Heat Transfer Engineering,*** vol. 4, no. 1, pp. 17–23, 1983.
6. Lorsch, H. G., Kauffman, K. W., and Denton, J. C., Thermal Energy Storage for Heating and Air Conditioning, in ***Future Energy Production Systems,*** eds. J. C. Denton and N. H. Afgan, vol. 1, p. 69. Hemisphere, Washington, D.C., 1976.

© 1984 Hemisphere Publishing Corporation

3.15.1

Operation of regenerators

A. J. Willmott

■ Thermal regenerators of regenerative heat exchangers are devices that effect the transfer of heat between two fluids (usually gases) by temporarily storing heat from the hotter gas, in a permeable packing, and subsequently passing this thermal energy to the cooler gas. All the surface area of the regenerator packing or checkerwork is washed by the hot gas for the duration of the hot period in which time sensible heat is stored in the packing. At the end of this period, a reversal takes place at which the hot gas is switched off and the cooler gas starts to flow through the same channels in the packing over the whole surface area. During the cold period thermal energy is recovered by the cold gas at the end of which occurs another reversal.

Regenerators appear in two distinct forms, the fixed-bed regenerator and the rotary regenerator. The reversals in the fixed-bed system are effected by the closing and opening of the relevant valves, shutting off the hot/cold gas and allowing the start of the flow of the cold/hot gas through the packing. In order to provide an almost continuous exchange of heat between the two gases, at least two fixed-bed regenerators must be used, one of which at any instant will be preheating the cold gas.

The Ljungström or rotary regenerator consists of a cylindrical packing through which the hot and cold gases pass simultaneously (Fig. 1). Heat temporarily stored in this packing from the hot gas is physically moved into the cold gas stream by steadily rotating the cylindrical body of the checkerwork, whose axis of rotation is parallel to the gas flow. Considerable attention must be paid to providing gas seals that minimize the leakage between hot and cold gases at the gas entrance/exit faces of the packing. As a section of the packing rotates between the gas seals from one gas stream to the other, it experiences what is the equivalent of a reversal in the fixed-bed system. The time taken for this section to pass through the hot/cold gas stream corresponds to the hot/cold period.

Regenerators are commonly operated in counter-flow mode; that is, the hot gas passes through the checkerwork in a direction opposite to the cold gas. If the gases pass through the packing in the same direction, regenerator operation is said to be in parallel flow mode.

The choice between fixed-bed and rotary regenerators is largely determined by the conditions under which the energy recovery system is required to operate. In a fixed-bed system consisting of two or more regenerators, the hot and cold gas streams are completely isolated. Such a system can be constructed to accommodate high inlet gas temperatures for the hot gas stream and/or severe pressure differences between the

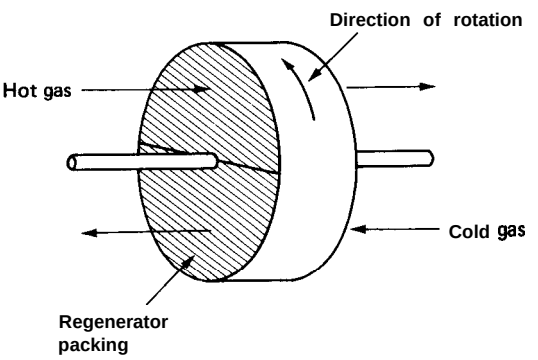

Figure 1 Rotary regenerator.

© 1984 Hemisphere Publishing Corporation

HEDH

two gas streams. Cowper stoves or hot blast stoves (Fig. 2) are used to preheat the blast for the iron-making furnace and are required to deliver preheated air at a temperature of 800°-1 200° C. The pressure difference between the hot and cold gas streams can be as large as 5 atm. Regenerators are constructed as part and parcel of the Siemens-Martin furnace and the glass furnace and must be able to withstand inlet gas temperatures of up to 1 600° C. In these applications the checkerwork is made of ceramic material; this material must be able to withstand the corrosive effects of material entrained in the hot gas stream, such as the carryover of material from the glass-making furnace.

Figure 3 illustrates the construction of a large, modern, three hot-blast stoves installation. Each stove is over 30 m high and about 7 m in diameter and transfers heat from the cornbusted waste gas from the iron-making process to the wind for the blast furnace. The chimney to the left of the three stoves is the exit for waste gas once the heat has been recovered by its passage through the packing of a stove. Solidified or liquified gases residing in the channels of the regenerator in one period of operation are naturally purged from the packing by the passage of gas through the system in the opposite period. Similarly dust or other carryover material entrained in the gas entering the regenerator in the hot period of a high temperature regenerator may be

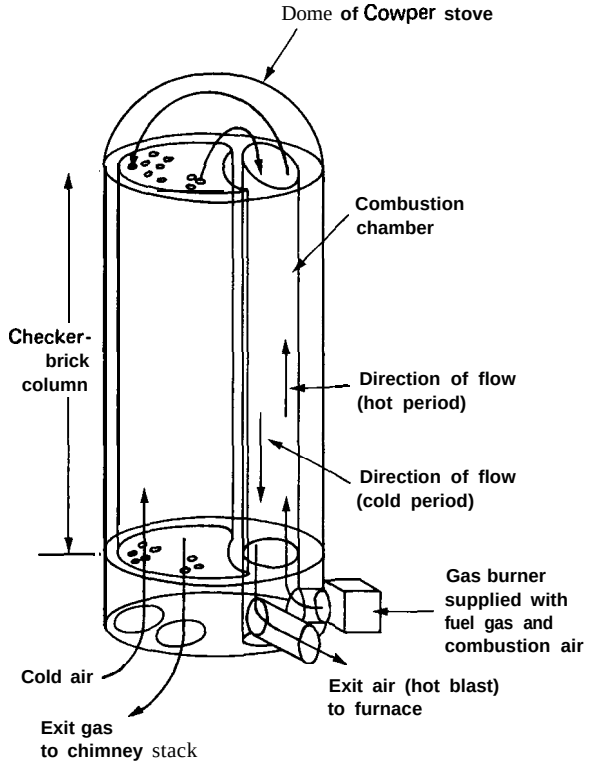

Figure 2 Hot blast stove or Cowper stove for metal reduction furnaces. Approximate height, 35 m; approximate diameter, 1.5 m.

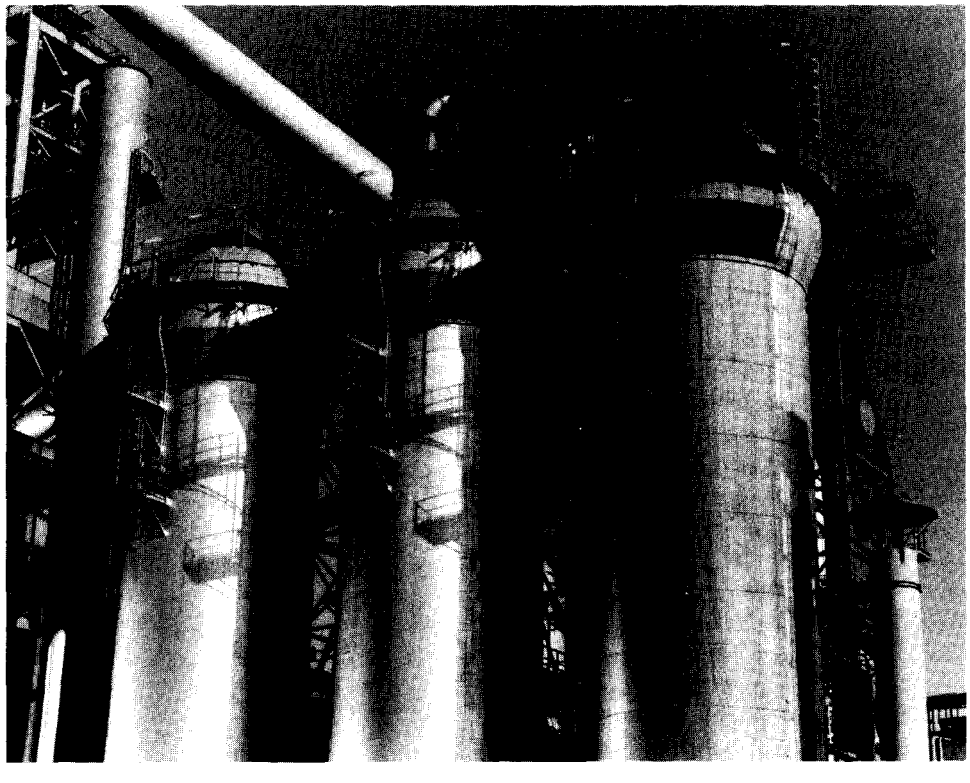

Figure 3 A modern hot blast stove installation. Courtesy of Davy Ashmore International Ltd., Stockton-on-Tees, Cleveland, U.K.

© 1984 Hemisphere Publishing Corporation

removed by the self-cleaning action of the gas passing through the regenerator in the cold period.

Rotary regenerators are commonly used in areas of application including air conditioning systems and the waste heat recovery from boilers and drying processes where operating conditions are much less severe. The packing of the Ljungström regenerator is often constructed of metal or plastic-like materials and this immediately restricts possible operating temperatures. On the other hand, these rotary regenerators are extremely compact and their mode of operation precludes the need of two or more units for continuous operation in contrast to the fixed-bed system.

© 1984 Hemisphere Publishing Corporation

3.15.2

Construction of regenerator packing

A. J. Willmott

■ The packing or checker-work of a regenerator varies considerably from one type of application to another. The selection of this heat storing mass is determined by a number of factors, in particular, the temperature conditions under which the regenerator is required to operate, the potentially corrosive contents of the gases, whether the channels are likely to be blocked by material entrained in one of the gas streams and the maximum pressure drop down the length of the packing that is acceptable for a particular application.

In a later section it will be seen that the efficiency of a regenerator with a chosen available heating surface area A for particular gas flow rates in the hot and cold periods is limited by the product of the cycle time and the heating surface area to heat capacity ratio of the packing. The larger this ratio of area to mass, the shorter must be the cycle time. In fixed-bed regenerators, the time taken to effect a regenerator reversal, as long as 10 min for Cowper stoves, forces a minimum cycle time to be adopted, as much as between 1 and 3 h. Smooth and effective running of a glass furnace or an air conditioning system involves running the accompanying fixed-bed regenerators with a minimum cycle time of between 30 and 50 min. This means that the heat capacity of the packing supporting a given heating surface area must be larger for such fixed systems compared with rotary regenerators where the speed of rotation is usually several revolutions per minute, implying a cycle time of operation of 1 min or less. Rotary regenerators are sometimes called ***compact*** regenerative heat exchangers, reflecting the fact that the short cycle times facilitate a very high area to heat capacity ratio and hence a compactness in the checkerwork.

A. Packing for high temperature operation

Regenerators of the fixed-bed type operating at high temperatures are constructed of fireproof refractories or of special quality ceramic material where the hot gas entrains especially corrosive material. The checkerwork is frequently zoned with packings of different materials; at the top of the regenerator silica checkers are sometimes used because of their ability to withstand high temperatures and large compressive loads. Lower down the regenerator, different silica-alumina refractories are used, which provide high mechanical strength and good volume stability together with a resistance to the effects of the swings in temperature that occur at the position in the regenerator where the checkers are located. In glass furnace regenerators, high alumina checkers are often used in order to withstand the corrosive effects of lime, sodium sulfate, potash, silica, and vanadium, which are carried over from the furnace into the regenerative chambers.

The geometric arrangements of such refractory material vary. Where the checkerwork must accommodate the passage of carryover material to avoid the blocking of the passage, square chimney or closed basket weave settings are commonly used as are the open basket weave and staggered open basket weave checkerwork arrangements (Fig. 1). The channel width is approximately 200 mm. Where the gases are much cleaner, as in Cowper stoves, the so-called Freyn checker is often used (Fig. 2). This is a hexagonal brick with vertical passage, 5 cm wide, both in the body and at the corners of the checker. Freyn checkers are arranged layer upon layer in such a way that the heat storing mass

©1984 Hemisphere Publishing Corporation

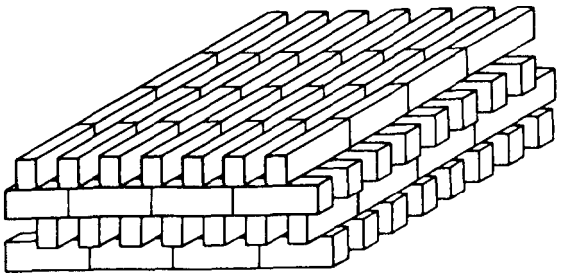

Figure 1 Schematic representation of basket weave checkerwork arrangements.

provides a bundle of channels for the clear passage of the gases from entrance to exit of the regenerator. Under these severe high temperature conditions, the thickness of the packing is as much as 200 mm. With regenerators used at lower temperatures in the chemical industry, thinner (about 50 mm) refractory bricks can be used.

B. Moderate temperature packings

At more moderate temperatures, the rotary regenerative air preheater is commonly used to recover heat from the waste gases at 400°–500°C from boilers, for example, in chemical plants or aboard ships as well as in electrical power stations. The heat is transferred to the combustion air for the firing of the boiler. Here the packing consists of thin steel sheets notched to form a large number of undulated passages, which facilitate the turbulent flow of hot and cold gases through the regenerator. The sheets are arranged in removable units and lie on the radii from the axis of rotation (Fig. 3). Where the waste gases are corrosive with a high sulfur content, a vitreous enamelled heating surface area may be used which protects the steel packing at operating temperatures below the acid dew point of the gases.

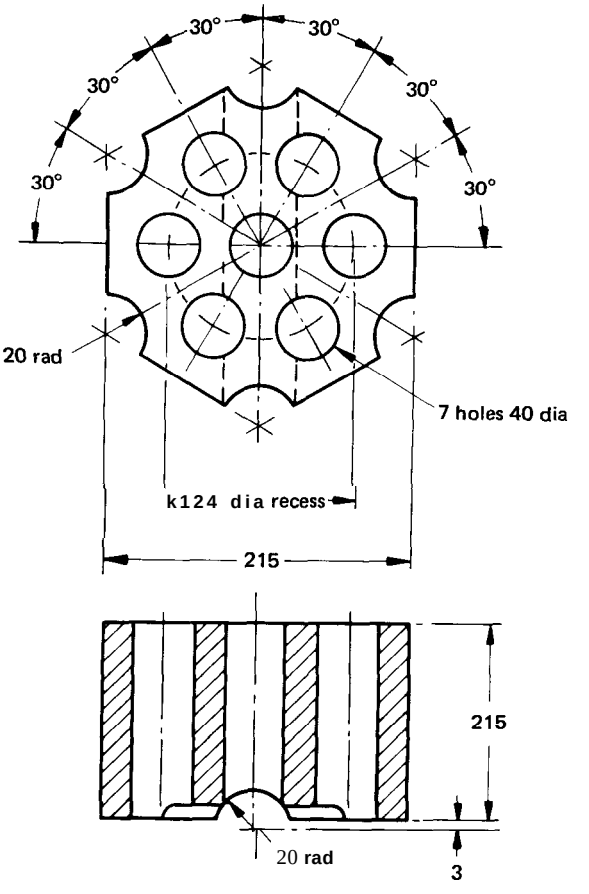

Figure 2 Typical design of a hot blast stove checkerwork brick (all measurements in millimeters).

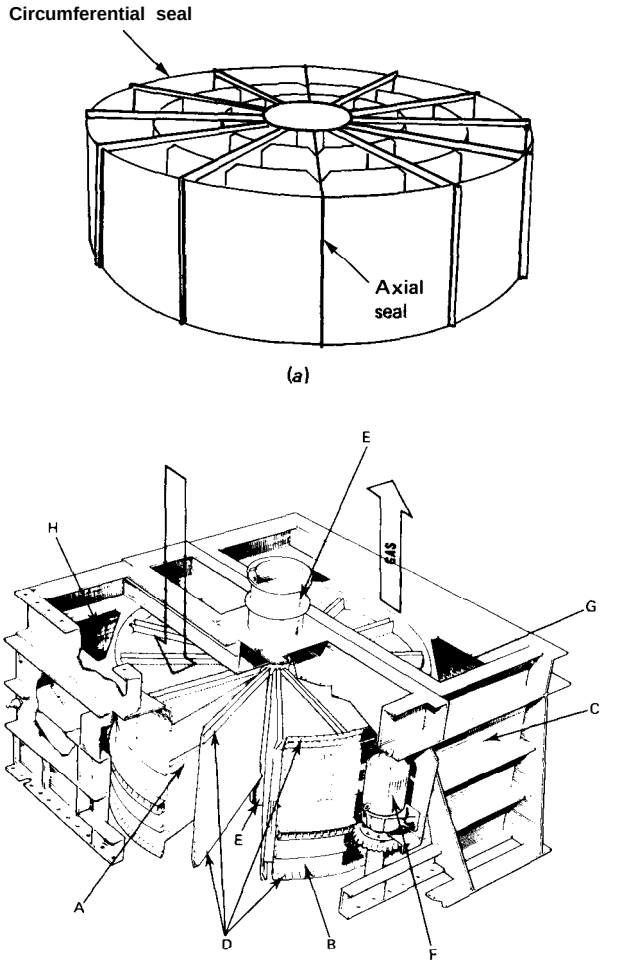

Figure 3 Possible arrangements of rotary regenerator plate packing. *(a)* Plates arranged in concentric cylinders, as suggested by Ljungström. *(b)* Plates arranged along the radii of the regenerator. A, Heating surface elements. B, Rotor in which the elements are packed. C, Housing in which the rotor rotates D, Seals and sealing surfaces. E, Support and guide bearing assemblies. F, Drive mechanism. G, Gas by-pass. H, Air by-pass. Courtesy of James Howden & Co., Glasgow, Scotland.

3 1984 Hemisphere P dishing Corporation

C. Lower temperature packings

At lower working temperatures, a variety of packings for rotary regenerators are in common use and include knitted corrugated wire mesh, approximately 100 mm wide, a polyethylene terephthalate film which is wound around and around the spindle of the rotor (to yield heat wheels 1 250, 1 750, 2 000, and 2 500 mm in diameter) (Fig. 4) and corrugated aluminum sheets and honeycomb arrangements.

Recently, regenerators have been developed to recover both latent heat and specific heat from warm, moist gas streams. Here the packings are made of nonmetallic fibrous material that can absorb moisture on the one hand but is inert to bacterial contamination and therefore cannot contaminate ventilation air that may be preheated by the regenerator.

The fixed-bed regenerators commonly used in low temperature technology are sometimes packed with corrugated aluminum sheets that are laid on each other with the corrugation running in alternating directions so that fine intersecting channels are formed. This is very costly and has been superseded for some applications by beds of flint or basalt chips or gravel.

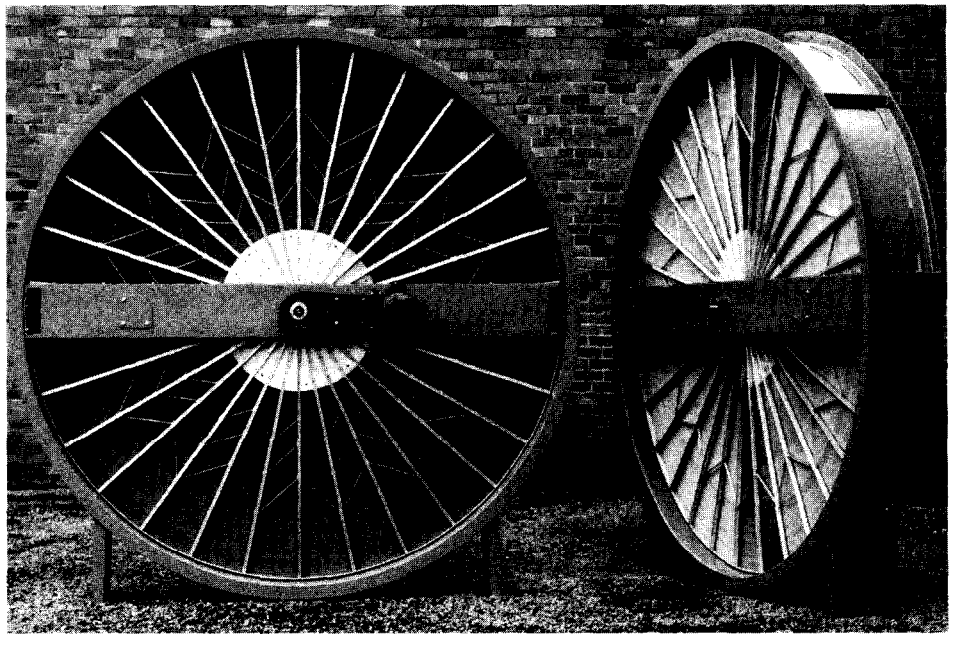

Figure 4 Typical rotary regenerators or heat wheels, showing a polyethylene terephthalate film wound around the spindle of the rotor. Courtesy of Rotary Heat Exchangers Pty. Ltd., Bayswater, Victoria, Australia.

© 1984 Hemisphere Publishing Corporation

3.15.3

Internal behavior of a regenerator: Development of the mathematical model

A. J. Willmott

A. Entrance gas temperature conditions

The gas enters the regenerator during the hot period at what is usually a constant temperature. In some applications, the entrance temperature varies with time. This may occur as a function of the operation of the industrial process from which it is desired to recover waste heat. It may also occur as a result of a regenerator operating policy, typically where it is required to supply as high an inlet gas temperature as possible until such time during the hot period that the solid temperature reaches a permissible maximum when the gas temperature is lowered, so that no temperature difference then exists between gas and solid at the regenerator entrance. However, it is usually assumed in regenerator theory that the entrance gas temperature can be treated as not varying with time, and, where it is not, the chronological mean is used as a constant inlet gas temperature.

The gas enters at the opposite end of the regenerator in counterflow mode at what is almost always a constant inlet temperature, which is either the ambient temperature or the temperature after the gas, usually air, has been compressed by the blower attached to the regenerator system.

B. Counter-flow and parallel flow operation

Counter-flow regenerator operation is far more thermally effective than parallel flow. This can be concluded from the observation that at the end of a hot period of operation, the temperature of the solid packing steadily decreases from the entrance to the exit of the gas. In the cold period that follows, the gas encounters, in counter-flow mode, a continuously increasing solid temperature and, thus, the temperature of the gas rises steadily as it passes through the packing.

However, in parallel flow operation where the hot and cold gases flow alternately in the same direction from the same entry position, the cold gas is exposed initially to a relatively high temperature difference with the solid, but then proceeds to encounter decreasing solid temperatures. It is thus possible for the rate at which heat is transferred to the gas to decrease so rapidly down the length of the regenerator that by the time the gas is approaching the exit, it is losing heat to the packing rather than rising in temperature. Under these circumstances, the gas transports heat from the hot to the cold end of the regenerator, and comparatively little heat is exchanged between the hot and the cold gases. The occurrence of this possible phenomenon in parallel flow operation is particularly sensitive to the cycle time.

C. Heat transfer in counter-flow mode

Here attention is focused upon the more usual counter-flow mode of operation.

The rate of transfer of heat between the gas and solid surface is represented by the equation

$$\bar{\alpha}A(t_s - t_f) = \dot{M}_f C_f L \left(\frac{\partial t_f}{\partial x} + \frac{1}{v} \frac{\partial t_f}{\partial \tau} \right) \tag{1}$$

while the following equation represents the rate at which heat is given up or absorbed from the gas.

$$\bar{\alpha}A(t_f - t_s) = M_s C_s \frac{\partial t_s}{\partial \tau} \tag{2}$$

© 1984 Hemisphere Publishing Corporation

The equations can be derived by detailed consideration [1] of the exchange of heat between gas and solid in a single channel of the packing. It is then assumed that all the channels behave in an identical manner, and thus that no maldistribution of flow occurs across the cross section of the regenerator at any position down the length of the packing.

Application of these equations for successive hot and cold periods of regenerator operation is possible provided the necessary boundary conditions are defined. It is assumed, as discussed above, that the entrance gas temperature does not vary in either hot or cold periods. The direction x down the length of the regenerator is assumed to be measured from the gas entrance. Bearing this in mind, the other boundary condition, which specifies that the solid temperature distribution at the beginning of the hot/cold period is the same as that at the end of the previous cold/hot period, is expressed mathematically in the following manner

$$t_s'(x, 0) = t_s''(L - x, P'') \tag{3}$$

$$t_s''(x, 0) = t_s'(L - x, P') \tag{4}$$

Equations (1) and (2) assume that there is no longitudinal conduction of heat in the direction of gas flow, either in the solid or in the gas. Certain other assumptions are embodied in the use of the bulk heat transfer coefficient $\bar{\alpha}$, and these are discussed in Sec. 3.15.5.

D. Simplification of the model

A drastic simplification of the model is facilitated if it is further assumed that the heat transfer coefficients and the thermophysical properties of both gas and solid vary neither spatially nor chronologically in either the hot or cold period, although the parameter values employed for the hot period can be different from those for the cold period. This assumption enables the use of simple and rapid methods for approximate calculation of regenerator thermal performance. Where such approximations are not acceptable, methods for solving Eqs. (1) and (2), such as those described by Schmidt and Willmott [2], must be used. Needless to say, computer simulation is required for such cases, and the fewer the assumptions made in the model, the longer the calculation time on the computer.

This apparently drastic simplification of the model is employed here and rapid methods of regenerator calculation are proposed. While it is true that for some applications it is important to take note of the temperature dependence of the gas specific heat, for example, these rapid methods do enable rather better than first approximations to be provided of likely regenerator behavior.

Nomenclature and References for Section 3.15.3 appear at the end of Section 3.15. IO.

© 1984 Hemisphere Publishing Corporation

3.15.4

Heat transfer coefficient

A. J. Willmott

■ The form of the packing and the arrangement of the flues through which the gases pass in both the hot and cold periods are so varied from one type of regenerator to another that it is impossible to make anything more than general recommendations about the heat transfer coefficients appropriate to regenerators.

Where the regenerator packing consists of plates, the correlations suggested in Sec. 2.5.2 may be applicable, although some thermal regenerator manufacturers try to enhance the likelihood of turbulent heat transfer by including ripples, grooves, or notches on the plates. The manufacturer will often provide commercially confidential heat transfer correlations for such modified plates which have been determined experimentally.

If it is proposed that a regenerator packing consist of a packed bed of either regularly (for example, spheres) or irregularly (for example, gravel) shaped pieces of heat storing material, then the correlations set out in Sec. 2.5.4 may be appropriate.

Section 2.5.3A deals with convective heat transfer in tube banks and it might be interesting to compare with these the correlations proposed by Boehm [3] for laminar flow and turbulent flow in high temperature regenerator packings consisting of refractory material embodying circular ducts [see Fig. 3.15.2(2)]. In a similar way, the heat transfer coefficient for cross flow in tube banks may be similar to that for basket weave arrangements [see Fig. 3.15.2(1)] of regenerator packings. Correlations for such geometries have been proposed by Kistner [4] and Langhans [5].

For some regenerator packing geometries, the heat transfer coefficients are either unknown and the regenerators are designed on very much an empirical basis, or the correlations have been determined experimentally but are concealed under the cloak of industrial secrecy, and are therefore not generally available.

In certain higher temperature regenerators of both the rotary and fixed-bed types, radiative heat transfer between carbon dioxide and water vapor and the surface of the regenerator packing may be important. Reference should be made to Secs. 2.9.6 and 2.9.8 of this handbook. Mention is also made of this aspect by Schmidt and Willmott [2], while Hausen [1] makes proposals for approximations in the calculation of average radiative heat transfer effects which are appropriate to regenerators.

References for Section 3.15.4 appear at the end of Section 3.15. IO.

© 1984 Hemisphere Publishing Corporation

3.15.5

Use of bulk or overall heat transfer coefficient

A. J. Willmott

● Equations 3.15.3(1) and 3.15.3(2) are derived on the assumption that the thermal conductivity of the packing material is infinite in a direction perpendicular to gas flow (and zero in a direction parallel to gas flow). This implies that, at any level in the regenerator, the solid material is isothermal in a direction perpendicular to gas flow, and this may be true or approximately true where the packing is thin or is made of materials of high conductivity.

Thus this assumption will probably be acceptable if the regenerator packing is made of metal plates, metal gauze, or sheets of polyethylene terephthalate film for example. In this case, the coefficient $\bar{\alpha}$ is simply the surface heat transfer coefficient, usually a convective coefficient to which may be added a radiative component.

However if the packing of the regenerator is constructed of material of low thermal conductivity and/or the thickness of packing around the channels through which the gases flow is comparatively large, then it is necessary to incorporate the resistances to heat transfer at the solid surface and within the solid into a bulk, lumped, or overall heat transfer coefficient.

Hausen [6] proposed that this coefficient should take the form as follows:

$$\frac{1}{\bar{\alpha}} = \frac{1}{\alpha} + \frac{d}{2(n+2)\mathrm{X}}\,\phi_H \qquad (1)$$

where n = 1 for slabs (plane walls) of thickness d
n = 2 for solid cylinders of diameter d
n = 3 for spheres of diameter *d*

The resistance to heat transfer within the regenerator packing is represented by the term $d\phi_H/[2(n+2)\lambda]$.

If y is the direction perpendicular to the direction, x, of gas flow and $t(x, y, \tau)$ is the solid temperature at time τ at position (x, y) in the packing, the temperature t_s used in Eqs. 3.15.3(1) and 3.15.3(2) is a space mean at level x and time τ and can be defined by Eq. (2)

$$t_s(x, \tau) = \frac{n}{d^n} \int_0^d y^{n-1}\, t(x, y, \tau)\, dy \qquad (2)$$

The Hausen factor ϕ_H attempts to account for the inversion of the temperature profile inside the packing, which occurs after each reversal in regenerator operation. Hausen developed a simple form for ϕ_H, namely,

$$\phi_H = 1 - \frac{d^2}{4[(n+3)^2 - 1]\,\kappa}\left(\frac{1}{P'} + \frac{1}{P''}\right) \qquad (3)$$

$$\text{for } \frac{d^2}{4\kappa}\left(\frac{1}{P'} + \frac{1}{P''}\right) \leqslant 5\frac{n+1}{2}$$

For other values of $1/P'$ and $1/P''$

$$\phi_H = \frac{2.142(n+2)}{\sqrt{\epsilon + (18d^2/\kappa)(1/P' + 1/P'')}} \qquad (4)$$

where ϵ = 2.7 for plates, 9.9 for cylinders, and 27.0 for spheres.

Razelos [7] developed a form ϕ_H for hollow cylinders. This is necessarily quite complicated since two parameters are involved, namely the internal and the external diameters of the hollow cylinder, whereas only one parameter, the diameter, is required for spheres, for example.

This and other complicated geometries are used in

© 1984 Hemisphere Publishing Corporation

practice for regenerator packings, especially where the solid is shaped either to withstand physical stress at high temperatures or corrugated to encourage turbulence in the gas flow, and thereby improve the conditions for convective heat transfer between gas and solid surface.

Hausen has proposed that in such cases, the plane wall approximation should be used, the thickness d of which plane wall should be computed using the equation

$$d = \frac{V}{F} + \frac{d_{ch}}{2} \tag{5}$$

where V/F is the volume to surface area ratio of the packing and d_{ch}, its characteristic thickness, which Hausen does not define.

It turns out that in the majority of cases, the bulk heat transfer coefficient $\bar{\alpha}$ can be used with confidence for regenerator calculations. The circumstances where it cannot be used or should be modified are discussed by Willmott [8] and Hinchcliffe and Willmott [9] as are the underlying assumptions behind the development of the bulk heat transfer coefficient.

Nomenclature and References for Section 3.15.5 appear at the end of Section 3.15.10.

© 1984 Hemisphere Publishing Corporation

3.15.6

Development of dimensionless parameters

A. J. Willmott

■ If the dimensionless variables

$$\xi = \frac{\bar{\alpha}Ax}{\dot{M}_f C_f L} \tag{1}$$

$$\eta = \frac{\bar{\alpha}A}{M_s C_s}\left(\tau - \frac{x}{v}\right) \tag{2}$$

are introduced, Eqs. 3.15.3(1) and 3.15.3(2) are simplified into nondimensionless form, namely,

$$\frac{\partial t_f}{\partial \xi} = \xi - t_f \tag{3}$$

$$\frac{\partial t_s}{\partial \eta} = t_f - t_s \tag{4}$$

These variables allow a natural set of design parameters to be evolved which correspond to the values of ξ and η for x = L and τ = P, for both the hot and cold periods. These design parameters were called by Hausen [10] the reduced length Λ and the reduced period II. They can be tabulated in the following way:

Hot period:

$$\Lambda' = \frac{\bar{\alpha}'A}{\dot{M}'_f C'_f} \qquad \Pi' = \frac{\bar{\alpha}'A(P' - L/v')}{M_s C_s}$$

Cold period:

$$\Lambda'' = \frac{\bar{\alpha}''A}{\dot{M}''_f C''_f} \qquad \Pi'' = \frac{\bar{\alpha}''A(P'' - 1/v\ )}{M_s C_s}$$

where prime refers to the hot period; double prime refers to the cold period.

Noting that t'_{fi} and t''_{fi} are the hot and cold period inlet gas temperatures respectively, a nondimensional [0, 1] temperature scale can be employed. We define the nondimensional temperatures T_f and T_s by the following equations:

$$T_f = \frac{t_f - t''_{fi}}{t'_{fi} - t''_{fi}} \tag{5}$$

$$T_s = \frac{t_s - t''_{fi}}{t'_{fi} - t''_{fi}} \tag{6}$$

in which case Eqs. (3) and (4) are modified simply and become

$$\frac{\partial T_f}{\partial \xi} = T_s - T_f \tag{7}$$

$$\frac{\partial T_s}{\partial \eta} = T_f - T_s \tag{8}$$

with $T'_{fi} = 1$ and $T''_{fi} = 0$.

The reversal conditions, which represent counterflow operation [see Eqs. 3.15.2(3) and 3.15.2(4)], can now be written

$$T'_s(\xi', 0) = T'_s\left[\frac{\Lambda''(\Lambda' - \xi')}{\Lambda'}, \Pi''\right] \tag{9}$$

$$T''_s(\xi'', 0) = T'_s\left[\frac{\Lambda'(\Lambda'' - \xi'')}{\Lambda''}, \Pi'\right] \tag{10}$$

Not only do the reduced lengths A and A and the reduced periods II and II form a natural set of parameters, in the sense they are evolved easily and directly from the descriptive differential equations 3.15.3(1) and 3.15.3(2), these parameters separate conveniently the distinct mechanisms of the transfer of heat

© 1984 Hemisphere Publishing Corporation

to the gases passing through the packing, reduced length, and of the storage of heat in the packing, reduced period.

There is little doubt that an appreciation of the meaning of these parameters throws much light, for the engineer, upon the mechanisms that govern thermal regenerator performance.

It is sufficient here to say that the reduced length provides a measure of the thermal size ($\bar{\alpha}'A$, hot period; $\bar{\alpha}''A$, cold period) of the regenerator relative to the loads ($\dot{M}_f'C_f'$, hot period; $\dot{M}_f''C_f''$, cold period) imposed during cyclic operation.

On the other hand, the reduced period illustrates clearly the relationship between the ratio of the thermal size to the heat capacity M_sC_s of the packing on one hand, and the duration of the hot and cold periods on the other hand. It is well known that the smaller the reduced period, the more thermally effective is regenerator operation. It follows that if the ratio $\bar{\alpha}A/M_sC_s$ is large, this must be matched by a small period length. Hence in rotary regenerators, the packing of which is constructed of wire mesh or thin metal plates, the area to mass ratio is so large that it must be matched by small cycle times; indeed, the packing revolves at several revolutions per minute yielding period lengths measured in seconds. On the other hand, in glass furnace regenerators, the overall consideration is that the packing must be thick and strong enough and made of refractory material to be able to withstand the hostile conditions of temperature, stress, and corrosion. Here the area to mass ratio is low and period lengths of 20 min or more can easily be accommodated. The same considerations apply to hot blast stoves, and period lengths between 20 and 90 min can be employed.

The effectiveness of regenerator behavior may be measured in terms of the thermal ratios, η'_{REG} and η''_{REG}. Ideally, the exit gas temperature in hot or cold period should be equal to the inlet gas temperature in the opposite period. The thermal ratios, which are defined below, measure the degree to which this ideal is achieved.

$$\eta'_{REG} = \frac{t'_{fi} - t'_{fo}}{t'_{fi} - t''_{fi}} = 1 - T'_{fo} \tag{11}$$

$$\eta''_{REG} = \frac{t''_{fo} - t''_{fi}}{t'_{fi} - t''_{fi}} = T''_{fo} \tag{12}$$

The term thermal ratio can be misleading in the sense that it is not always a measure of efficiency, and perhaps the term temperature ratio might be more appropriate.

In fixed-bed regenerators, the exit gas temperatures vary with time. The chronological average exit temperatures are therefore computed. This corresponds in the case of the rotary regenerator to the temperature of the exit gas, which consists of a mixture of gases coming simultaneously from the several sectors of the rotating packing. These average exit gas temperatures are denoted by $t'_{fo}(T'_{fo})$ and $t''_{fo}(T''_{fo})$ and incorporated within Eqs. (11) and (12), above.

As might be expected, the larger the reduced length, the greater the thermal ratio. For the symmetric regenerator (A = A = Λ'', II = II = II , and η_{REG} = η'_{REG} = η''_{REG}), an estimate of the thermal ratio is given by

$$\eta_{REG} = \frac{A}{\Lambda + 2}$$

This estimate becomes exact for infinitely small cycle times and is called the ideal thermal ratio. By solving Eqs. (3) and (4) for counter-flow regenerator operation, Hausen [1] evaluated η_{REG} for symmetric regenerators for a whole range of values of A and II and these are presented in graphic form in Fig. 1.

From considerations of a heat balance, once cyclic equilibrium is attained-that is, the thermal performance in the current cycle remains unaltered from the previous cycle for the same operating conditions-it can be concluded that

$$\dot{M}_f'C_f'P'(t'_{fi} - t'_{fo}) = \dot{M}_f''C_f''P''(t''_{fo} - t''_{fi}) \tag{13}$$

Dividing throughout by $(t'_{fi} - t''_{fi})$, this reduces to

$$\dot{M}_f'C_f'P'\eta'_{REG} = \dot{M}_f''C_f''P''\eta''_{REG} \tag{14}$$

If $\dot{M}_f'C_f'P' = \dot{M}_f''C_f''P''$, the regenerator is said to be balanced and $\eta'_{REG} = \eta''_{REG}$. Multiplying the numerator and denominator of the left-hand side by $\bar{\alpha}'A$, the right-hand side by $\bar{\alpha}''A$ of Eq. (14) and then multiplying both sides by M_sC_s, this equation becomes

$$\frac{\Pi'}{\Lambda'}\eta'_{REG} = \frac{\Pi''}{\Lambda''}\eta''_{REG} \tag{15}$$

Hence if $\Pi'/\Lambda' = \Pi''/\Lambda''$, the regenerator is balanced. In general, a regenerator is balanced if

$$\frac{II}{I'I''} = \frac{A}{A''} = k \tag{16}$$

The special case, to which reference has been made previously, is the one where $k = 1$, in which case the regenerator is said to be symmetric. The first equation in (16) can be rewritten

$$\frac{\Pi'}{A'}\frac{A}{I'I''} = \gamma \tag{17}$$

with 7 = 1 when the regenerator is balanced. When $\dot{M}_f'C_f'P' \neq \dot{M}_f''C_f''P''$, this corresponds to the most general case where $7 \neq 1$, $\eta'_{REG} \neq \eta''_{REG}$ and the regenerator is said to be unbalanced. A summary of these classifications is presented in Table 1.

Hausen [6] proposed the performance of a balanced regenerator can be accurately estimated using a sym-

©1984 Hemisphere Publishing Corporation

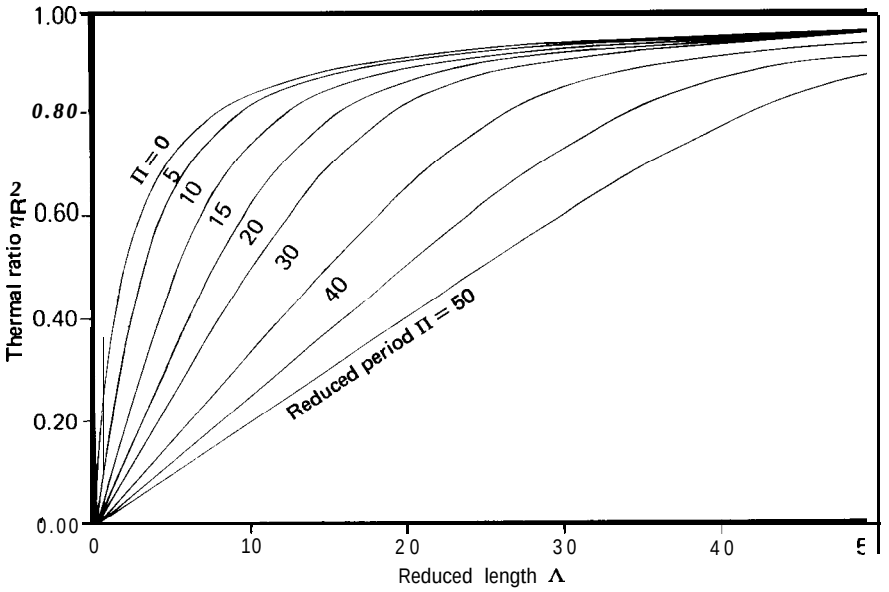

Figure 1 Thermal ratio as a function of reduced length and reduced period for symmetric counterflow regenerators. From Schmidt and Willmott [2].

metric regenerator model employing the reduced length Λ_H and the reduced period Π_H in both the hot and cold periods. If A , A Π', and Π'' are the parameters of the original balanced but unsymmetric regenerator, then Λ_H and Π_H are computed as harmonic means

$$\frac{2}{\Lambda_H} = \frac{1}{\mathrm{A}} + \frac{1}{\mathrm{A}} \tag{18}$$

$$\frac{2}{\Pi_H} = \frac{1}{\Pi'} + \frac{1}{\Pi''} \tag{19}$$

This proposal was verified as acceptable by Iliffe [11] and its applicability was extended to unbalanced regenerators by Razelos [12].

For this most general case, the kernel of the problem is that symmetric regenerator approximation will generate equal hot and cold period thermal ratios, whereas for unbalanced regenerators, the thermal ratios are unequal.

Razelos redefined Eq. (14) in terms of 7:

$$\eta''_{\mathrm{REG}} = \gamma \eta'_{\mathrm{REG}} \tag{20}$$

He then proposed to relate the thermal ratio η_{REG} computed using the symmetric model approximation, using harmonic mean reduced lengths Λ_H and reduced periods Π_H, to the thermal ratios η'_{REG} and η''_{REG} of the unbalanced regenerator whose values are sought. The exact way this is done is described in Sec. 3.15.7 where two illustrative examples are included.

Table 1 Summary of regenerator types

		Nonsymmetric	
	Symmetric	Balanced	Unbalanced
Parameters	Λ, Π	A , A Π', Π''	A , A Π', Π''
Relations	$\Lambda = \Lambda' = \Lambda''$ $\Pi = \Pi' = \Pi''$	$\frac{\Pi'}{\Pi''} = \frac{\mathrm{A}'}{\mathrm{A}''} = k \neq 1$	$\frac{\Pi'}{\Pi''} \neq \frac{\Lambda'}{\Lambda''}$
Thermal ratios	$\eta_{\mathrm{REG}} = \eta'_{\mathrm{REG}} = \eta''_{\mathrm{REG}}$	$\eta'_{\mathrm{REG}} = \eta''_{\mathrm{REG}}$	$\eta'_{\mathrm{REG}} \neq \eta''_{\mathrm{REG}}$
γ	1	1	$\neq 1$

Nomenclature and References for Section 3.15.6 appear at the end of Section 3.15.10.

©1984 Hemisphere Publishing Corporation

3.15.7

Calculation of regenerator thermal performance

A. J. Willmott

■ Several methods of calculation are presented. The overall performance of a regenerator is conveniently measured in terms of the thermal ratios η'_{REG} and η''_{REG} at cyclic equilibrium, as defined by Eqs. 3.15.6(11) and 3.15.6(12). The simpler and more approximate methods are used to evaluate estimates of the thermal ratios. A more detailed method is outlined whereby the spatial and chronological variations of gas and packing temperature can be computed. It will be assumed at this juncture that the dimensionless groups A , A Π', and IT can be calculated.

A. Relationship between symmetric and nonsymmetric regenerators

The basis of the methods of calculation described here is the proposal of Hausen [6], as confirmed and extended by Iliffe [1 1] and Razelos [12] that the performance of a nonsymmetric regenerator, with dimensionless parameters A , A Π', and Π'' can be satisfactorily approximated by a symmetric regenerator whose hot and cold period reduced length and reduced period are Λ_H and Π_H. The harmonic mean reduced period Π_H is defined by Eq. 3.15.6(19). The reduced length Λ_H is defined by

$$\frac{2}{\Lambda_H} = \frac{1}{\Pi_H}\left(\frac{\Pi'}{\Lambda'} + \frac{\Pi''}{\Lambda''}\right) \tag{1}$$

When Π' is approximately equal to Π'', this reduces to the form of Eq. 3.15.6(18).

For the balanced regenerator, η'_{REG} is equal to η''_{REG} , so that the thermal ratio of the equivalent (A_H, Π_H) symmetric regenerator can be used directly as a good approximation of η'_{REG} and η''_{REG} for such a balanced regenerator. How can one deal with an unbalanced regenerator where η'_{REG} does not equal η''_{REG} ? The relationship between η'_{REG} and η''_{REG} is shown in Eq. 3.15.6(20).

Hausen [6] suggested that a factor K/K_0 (the original purpose of which does not concern us here) is a function only of Λ_H and Π_H together with the thermal ratio η^H_{REG} of the (A_H, Π_H) symmetric regenerator and independent of the degree of unbalance, γ, as defined by Eq. 3.15.6(17). This has been verified recently in an important paper by Razelos [12].

The variation of K/K_0 is displayed in Fig. 1 as a function Λ_H and Π_H. Any particular value of K/K_0 can be computed using Eq. (2)

$$\frac{K}{K_0} = \frac{2\eta^H_{REG}}{\Lambda_H(1 - \eta^H_{REG})} \tag{2}$$

Razelos [12] shows that K/K_0 is related to η'_{REG} (the hot side thermal ratio of a regenerator with degree of unbalance, γ) by

$$\frac{K}{K_0} = \frac{4\gamma}{\Lambda_H(1-\gamma^2)} \ln\frac{1 - \gamma\eta'_{REG}}{1 - \eta'_{REG}} \tag{3}$$

This equation has been rearranged by Hilton (198 1, private communication) into the form

$$\eta_{REG} = \frac{1 - k :}{\gamma - e^F} \tag{4}$$

where

$$F = \frac{K}{K_0}\frac{\Lambda_H(1-\gamma^2)}{47} \tag{5}$$

or, using η^H_{REG} from Eq. (2),

© 1984 Hemisphere I ublishing Corporation

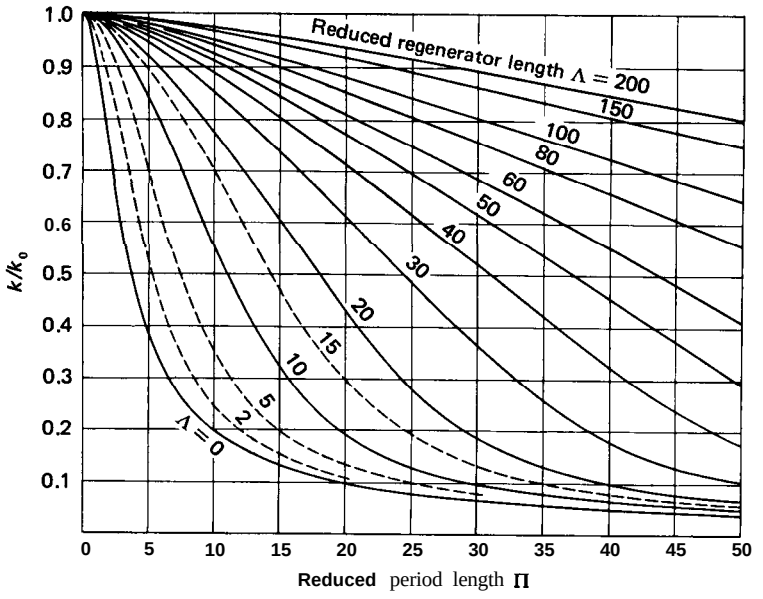

Figure 1 Graphic representation of the relationship between the ***K/K,,*** factor and the dimensionless parameters ***AH*** and Π_H. After Hausen [1].

$$F = \frac{\eta^H_{\mathrm{REG}}(1-\gamma^2)}{2\gamma(1-\eta^H_{\mathrm{REG}})} \tag{6}$$

The procedure can be summarized:

1. Compute η^H_{REG} using Λ_H and Π_H (methods for doing this will be described shortly)
2. Compute Fusing Eq. (6)
3. Compute η'_{REG} using Eq. (4)
4. Compute η''_{REG} using Eq. 3.15.6(20)

B. Method I of regenerator calculation

The simplest method of calculation is based on the assumption that the reduced period is sufficiently small so that the thermal ratio based on zero cycle time (sometimes called ***ideal thermal ratio)*** can be used. In general this will be approximately true if $\Lambda_H/\Pi_H \geqslant 8.0$ and $\Pi_H \leqslant 2.0$.

(a) Symmetric regenerator

$$\Lambda' = \Lambda'' = \Lambda = 10.0$$

$$\Pi' = \Pi'' = \Pi = 1.0$$

The ideal thermal ratio η_{REG} is evaluated employing the ratio

$$\eta_{\mathrm{REG}} = \frac{\mathrm{A}}{\mathrm{A}+2} = \frac{10.0}{12.0} = 0.833$$

By way of comparison, the thermal ratios calculated by an exact method and published by Schmidt and Willmott [2] are compared with this ideal thermal ratio. The acceptability of this simple approach can be concluded for higher reduced lengths by inspection of Fig. 3.15.6(1).

Reduced length	Thermal ratio: Exact value for n = 1	Thermal ratio: Exact value for n = 2	Thermal ratio: Ideal Λ/(Λ + 2)
8.0	0.798 4	0.793 6	0.8
9.0	0.816 9	0.812 9	0.818 2
10.0	0.832 2	0.828 9	0.833 3

(b) Balanced regenerator

$\mathrm{A} = 10.0 \qquad \Pi' = 0.5$

$\Lambda'' = 20.0 \qquad \Pi'' = 1.0$

$$\frac{\mathrm{A}}{\Pi'} = \frac{\mathrm{A}}{\Pi''} = 20.0$$

Compute the harmonic mean reduced period

$$\frac{1}{\Pi_H} = \frac{1}{2}\left(\frac{1}{1.0} + \frac{1}{0.5}\right) = \frac{3}{2}$$

$$\Pi_H = \frac{2.0}{3.0}$$

Compute the mean reduced length

© 1984 Hemisphere Publishing Corporation

$$\frac{2}{\Lambda_H} = \frac{1}{\Pi_H}\left(\frac{\Pi'}{\Lambda'} + \frac{\Pi''}{\Lambda''}\right) = \frac{3.0}{2.0}\left(\frac{0.5}{10.0} + \frac{1.0}{20.0}\right) = \frac{3.0}{20.0} \quad (1)$$

$$\Lambda_H = 13.333$$

The ideal thermal ratio can now be found and used as an estimate of η^H_{REG}

$$\eta^H_{REG} \approx \eta_{REG} = \frac{\Lambda_H}{2 + \Lambda_H} = \frac{13.333}{15.333} = 0.870$$

(c) Unbalanced regenerator

A = 10.0 Π' = 0.5

A = 20.0 Π'' = 1.5

The unbalanced factory can be computed

$$\gamma = \frac{\Pi}{\Lambda'}\frac{\Lambda''}{\Pi''} = \frac{0.5}{10.0}\frac{20.0}{1.5} = \frac{2}{3}$$

Calculate the harmonic mean Π_H

$$\frac{1}{\Pi_H} = \frac{1}{2}\left(\frac{1}{0.5} + \frac{1}{1.5}\right) = \frac{4.0}{3.0}$$

$$\Pi_H = \frac{3.0}{4.0}$$

Next calculate the value of Λ_H using Eq. (1)

$$\frac{2}{\Lambda_H} = \frac{1}{\Pi_H}\left(\frac{\Pi'}{\Lambda'} + \frac{\Pi''}{\Lambda''}\right) = \frac{4.0}{3.0}\left(\frac{0.5}{10.0} + \frac{1.5}{20.0}\right) = \frac{1}{6}$$

Λ_H = 12.0

The ideal thermal ratio, denoted here as η^H_{REG} is calculated

$$\eta^H_{REG} = \frac{\Lambda_H}{\Lambda_H + 2} = \frac{12.0}{14.0} = 0.857\ 1$$

The value of F is calculated using Eq. (6)

$$F = \frac{\eta^H_{REG}(1-\gamma^2)}{2\gamma(1-\eta^H_{REG})} = \frac{0.857\ 1\ [1+(2/3)^2]}{2(2/3)(1-0.857\ 1)}$$

$$= \frac{(0.857\ 1)(0.555\ 6)}{(4/3)(0.142\ 9)} = 2.499\ 2$$

e^F = 12.172 8

Employing Eq. (4), the value of η'_{REG} for the original unbalanced regenerator is calculated

$$\eta'_{REG} = \frac{1-e^F}{\gamma - e^F} = \frac{12.172\ 8 - 1.0}{12.172\ 8 - 0.666\ 6}$$

$$= \frac{11.172\ 8}{11.506} = 0.971\ 0$$

Finally η''_{REG} is evaluated using Eq. 3.15.6(20)

$$\eta''_{REG} = \gamma\eta'_{REG} = \tfrac{2}{3}(0.971\ 0) = 0.647\ 4$$

C. Method II of regenerator calculation

The second method presented here was developed by Tipler [13] in 1947 and although it has been long neglected by many workers in the field, it provides values of η_{REG} for symmetric regenerators, with an absolute error of less than 0.05 when Π < 10.0, and for II < 5.0, the error is less than 0.01. These error values relate to reduced lengths A > 5. This means of course a much wider field of possible application of method 11 in comparison with method I.

Tipler proposed that the thermal ratio for a symmetric regenerator, and it is suggested here that the method be applied to the general (A_H, Π_H) regenerator, by the following formula:

$$\eta^H_{REG} = \frac{\Lambda_H}{\Pi_H}\tanh\frac{\Pi_H}{2 + \Lambda_H} \quad (7)$$

where tanh is the hyperbolic tangent defined by

$$\tanh x = \frac{e^x - e^{-x}}{e^x + e^{-x}}$$

It is further suggested that this method be applied to unbalanced regenerators using Eqs. (6), (4), and 3.15.6(19), once the thermal ratio η^H_{REG} has been evaluated using Eq. (7).

Tipler presents in his original paper a graphic comparison between the thermal ratios computed using Eq. (7) and more precise values, originally computed by Hausen in 1929 [10]. This comparison is offered here as Fig. 2.

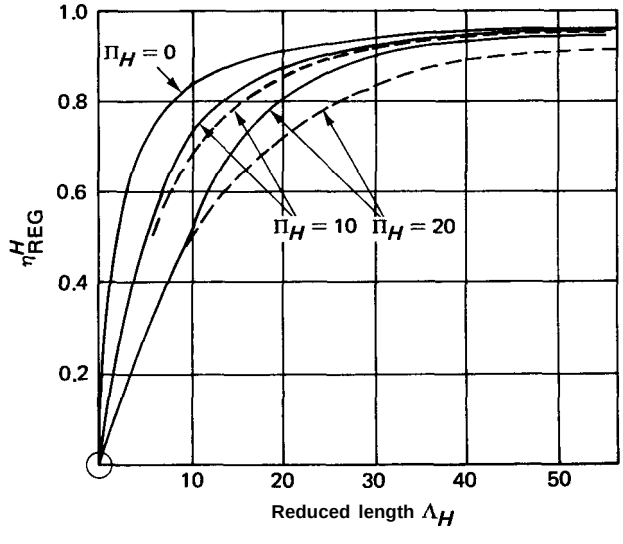

Figure 2 Tipler [13] comparison between thermal ratio calculated accurately by Hausen [10] and calculated using Eq. (7). — Hausen s 1929 results; – – – Tipler s approximation. [Note: Eq. (7) reduces to $\Lambda/(\Lambda + 2)$ for $\Pi = 0$.]

© 1984 Hemisphere Publishing Corporation

(a) Symmetric and balanced regenemtors

We consider the case where

$\Lambda_H = 10.0 \qquad \Pi_H = 10.0$

(the mean values Λ_H and Π_H having been evaluated from $\mathbf{A}$,A ,Π', and Π'' in the manner described previously).

$$\eta^H_{REG} = \frac{\Lambda_H}{\Pi_H} \tanh \frac{\Pi_H}{2 + \Lambda_H} = \frac{10.0}{10.0} \tanh \frac{10.0}{12.0}$$

$$= \tanh \frac{5}{6} = 0.682\ 3$$

Schmidt and Wilhnott [2] quote a value of η^H_{REG} = 0.738 for this case. The error is thus 0.738 − 0.6823 = 0.056. This constitutes a limiting case for the applicability of this method. We therefore present the following additional cases:

1. $\Lambda_H = 25.0 \qquad \Pi_H = 10.0$

Now we have

$$\eta^H_{REG} = \frac{25.0}{10.0} \tanh \frac{10.0}{2.0 + 25.0} = 2.5 \tanh 0.370\ 4$$

$$= 0.885\ 8$$

Here Schmidt and Willmott [2] specify a value of 0.911 and thus the error is 0.025.

2. $\Lambda_H = 10.0 \qquad \Pi_H = 3.0$

$$\eta^{II}_{REG} = \frac{10.0}{3.0} \tanh \frac{3.0}{2.0 + 10.0} = \frac{10}{3} \tanh 0.25$$

$$= 0.816\ 4$$

The Schmidt and Willmott [2] value is 0.8238 and the error is 7.4 X 10^{-3}.

(b) Unbalanced regenemtors

$\mathbf{A}$ =A = 10.0

Π' = 1.26 II = 1.88 γ = 0.67

(This data might approximate that for a small hot blast stove or a large rotary regenerator.)

The harmonic mean Π_H is first calculated:

$$\frac{1}{\Pi_H} = \frac{1}{2}\left(\frac{1}{1.26} + \frac{1}{1.88}\right) = 0.662\ 8$$

Π_H = 1.509

Next is computed the mean Λ_H

$$\frac{2}{\Lambda_H} = \frac{1}{\Pi_H}\left(\frac{\Pi'}{\Lambda'} + \frac{\Pi''}{\Lambda''}\right)$$

$$\frac{2}{\Lambda_H} = 0.662\ 8\left(\frac{1.26}{10.0} + \frac{1.88}{10.0}\right) = 0.208\ 1$$

Λ_H = 9.609 9

The Tipler formula for thermal ratio is applied.

$$\eta^H_{REG} = \frac{\Lambda_H}{\Pi_H} \tanh \frac{\Pi_H}{2.0 + \Lambda_H} = \frac{9.609\ 9}{1.509} \tanh \frac{1.509}{11.609\ 9}$$

$$= 6.368 \tanh 0.13 = (6.368)(0.129\ 2)$$

$$= 0.823\ 1$$

The value of F is now computed using Eq. (6)

$$F = \frac{\eta^H_{REG}(1 + \gamma^2)}{2\gamma(1 - \eta^H_{REG})} = \frac{0.823\ 1(1 + 0.67^2)}{2(0.67)(1 - 0.823\ 1)}$$

$$= \frac{(0.823\ 1)(0.551\ 0.453}{(1.34)(0.176\ 9)\ 0.237\ 0} \quad 1.913^{6}$$

e^F = 6.777 4

Again, applying Eq. (4), the value η'_{REG} for the original unbalanced regenerator is found

$$\eta'_{REG} = \frac{1 - e^F}{\gamma - e^F} = \frac{6.777\ 4 - 1.0}{6.777\ 4 - 0.67} = \frac{5.777\ 4}{6.107\ 4} = 0.946$$

Finally we find η''_{REG}

$$\eta''_{REG} = \gamma\eta'_{REG} = (0.67)(0.946) = 0.634$$

Schmidt and Willmott [2] present values of η'_{REG} = 0.947 and η''_{REG} = 0.635, which have been computed using a much more precise method. This points to the usefulness of the Tipler method in these and similar circumstances.

D. Computational note

Simple methods of regenerator calculation have been deliberately presented here. They are amenable to computation using a pocket calculator and can be readily programmed for the type of programmable calculator that is readily available on the market. Needless to say, the methods can be programmed for the smallest microcomputers now available for scientific calculations.

E. Complete calculation using method II

This example was set up by Hausen [14] and relates to a regenerator in which air is preheated by a waste flue gas. The heating storing mass consists of sheets of thickness d = 0.05 m where the thermophysical properties are

Density ρ_s = 1 800 kg/m³
Specific heat C_s = 1 200 J/kg K
Thermal conductivity λ_s = 1 W/m K
Thermal diffusivity κ_s = 0.463 X 10^{-6} m²/s

The other geometric features of the checkerwork are:

© 1984 Hemisphere Publishing Corporation

Heating surface area A = 10 000 m²
Volume V_s = 90 m³

It can be deduced that:

Checkerwork mass $M_s = \rho_s V_s$ = 162 000 kg.

The operating characteristics are as follows.

	Hot period	Cold period	Units
Duration	1800.0	1 800.0	s
Entrance gas temperature, t_{fi}	1 250.0	100.0	°C
Gas mass flow rate, $\dot{M}_f$	18.0	20.0	kg/s
Gas specific heat, C_f	1 000.0	1040.0	J/kg K
Heat transfer coefficient, α	31.0	26.0	W/m² K

We first compute the Hausen factor ϕ_H for a plane wall [n = 1, Eq. 3.15.5(3)]

$$Z\ (\text{say}) = \frac{\alpha^2}{4\kappa_s}\left(\frac{1}{P'} + \frac{1}{P''}\right)$$

$$= \frac{0.05^2}{(4)(0.463)(10^{-6})}\left(\frac{1}{1\,800} + \frac{1}{1\,800}\right)$$

$$= \frac{(2.5)(10^{-3})}{(4)(0.463)(10^{-6})}\left(\frac{1}{900}\right) = 1.5 < 5$$

$$\phi_H = 1 - \frac{Z}{15} = 1 - \frac{1.5}{15} = 0.9$$

The value of $d\phi_H/(6\lambda_s)$ can next be computed.

$$\frac{6\lambda_s}{} = \frac{(6.0)(1.0)}{} = 0.007\,5 \text{ m}^2 \text{ K/W}$$

The bulk heat transfer coefficients $\bar{\alpha}'$ and $\bar{\alpha}''$ can now be computed.

$$\frac{1}{\bar{\alpha}'} = \frac{1}{\alpha'} + \frac{d\phi_H}{6\lambda_s} = \frac{1}{31.0} + 0.007\,5 = 0.039\,76 \text{ m}^2 \text{ K/W}$$

$$\bar{\alpha}' = 25.152 \text{ W/m}^2 \text{ K}$$

Similarly

$$\bar{\alpha}'' = 21.757 \text{ W/m}^2 \text{ K}$$

We now compute the dimensionless parameters reduced length and reduced period.

$$\Lambda' = \frac{\bar{\alpha}' A}{\dot{M}_f' C_f'} = \frac{(25.152)(10\,000)}{(18.0)(1\quad 000)} = 13.97$$

$$\Lambda'' = \frac{\bar{\alpha}'' A}{\dot{M}_f'' C_f''} = \frac{(21.757)(10\,000)}{(20)(1\quad 040)} = 10.46$$

$$\Pi' = \frac{\bar{\alpha}' A P'}{M_s C_s} = \frac{(25.152)(10\,000)(1\,800)}{(162\,000)(1\,200)} = 2.329$$

$$\text{l-l} = \frac{\bar{\alpha}'' A P''}{M_s C_s} = (21.757)(0.092\,59) = 2.015$$

The calculation now proceeds as previously. The harmonic mean reduced period Π_H:

$$\frac{1}{\Pi_H} = \frac{1}{2}\left(\frac{1}{2.329} + \frac{1}{2.015}\right) = 0.4628$$

$$\Pi_H = 2.161$$

The mean reduced length Λ_H is now evaluated.

$$\frac{2}{\Lambda_H} = \frac{1}{\Pi_H}\left(\frac{\Pi'}{\Lambda'} + \frac{\Pi''}{\Lambda''}\right) = \frac{1}{2.161}\left(\frac{2.329}{13.97} + \frac{2.015}{10.46}\right)$$

$$= 0.166\,3$$

$$\Lambda_H = 12.027$$

The imbalance factor γ is found using

$$\gamma = \frac{\Pi'}{\Lambda'}\frac{A}{\Pi''} = \frac{(2.329)(10.46)}{(13.97)(2.015)}$$

and hence

$$\gamma = 0.865$$

The Tipler thermal ratio η_{REG}^H comes next.

$$\eta_{REG}^H = \frac{\Lambda_H}{\Pi_H} \tanh \frac{\Pi_H}{\Lambda_H + 2} = \frac{12.027}{2.161} \tanh \frac{2.161}{14.027}$$

$$= 5.565 \tanh 0.154\,1 = 0.850\,7$$

The value of F is determined.

$$F = \frac{\eta_{REG}^H(1-\gamma^2)}{2\gamma(1-\eta_{REG}^H)} = \frac{(0.850\,7)[1.0-(0.865)^2]}{(2)(0.865)(0.149\,3)}$$

$$= \frac{(0.850\,7)(0.251\,78)}{(1.73)(0.149\,3)} = 0.829^3$$

$$e^F = 2.291\,63$$

It is now possible to compute η_{REG}' for the original regenerator configuration.

$$\eta_{REG}' = \frac{1-e^F}{\gamma - e^F} = \frac{2.291\,63-1.0}{2.291\,63-0.865} = 0.905\,4$$

$$\eta_{REG}'' = \gamma\eta_{REG}' = (0.865)(0.905\,4) = 0.783\,1$$

It is only at this stage that the time mean exit gas temperatures t_{fo}' and t_{fo}'' are computed.

We note from Eq. 3.15.6(11) that

$$\eta_{REG}' = \frac{t_{fi}' - t_{fo}'}{t_{fi}' - t_{fi}''} = 0.905\,4$$

Thus

$$\frac{1\,250 - t_{fo}'}{1\,250 - 100} = 0.905\,4$$

and

$$t_{fo}' = 1\,250.0 - (1\,150.0)(0.905\,4) = 208.8°\text{C}$$

Again from Eq. 3.15.6(12) we note

© 1984 Hemisphere I blishing Corporation

$$\eta''_{REG} = \frac{t''_{fo} - t''_{fi}}{t'_{fi} - t''_{fi}} = 0.783\ 1$$

and

$$\frac{t''_{fo} - 100}{1\ 250 - 100} = 0.783\ 1$$

Thus

$$t''_{fo} = (1\ 150.0)(0.783\ 1) + 100.0 = 1000.6°C$$

Hausen finds

$$t'_{fo} = 204°C$$

$$t''_{fo} = 1\ 003°\ C$$

by a different method which involves reading off values of K/K_n from the graph in Fig. 1. From a practical point of view, it must be concluded that the two sets of results are consistent.

F. Precise methods for the calculation of regenerators

The solution of the differential Eqs. 3.15.6(3) or 3.15.6(7) and 3.15.6(4) or 3.15.6(8) subject to the reversal conditions Eqs. 3.15.6(9) and 3.15.6(10) with $T'_{fi} = 1$ and $T''_{fi} = 0$, provides the most precise method of regenerator calculation (unless it is required to represent in some way other than the bulk heat transfer coefficient $\bar{\alpha}$, the intra-conduction effects within the packing, as mentioned in Sec. 3.15.5). Many methods of solution of these equations have been proposed. These fall into two distinct classes: closed and open.

In the open methods, the gas and solid temperatures are evaluated by solving the differential equations over successive cycles of regenerator operation. An arbitrary solid temperature distribution is imposed for the start of the first cycle. Once cyclic equilibrium has been achieved, the thermal ratio can be calculated.

On the other hand, the closed methods are those in which the reversal conditions Eqs. 3.15.6(9) and 3.15.6(10) are imposed at the outset in formulating the mathematical model. In this way the steady-state performance is calculated directly without the consideration of any previous cycles.

The great advantage of these methods is that they can provide the gas and solid temperature variations, both in distance down the length of the regenerator and with time. Their disadvantage lies in the fact that they are only practicable if programmed for a computer. Needless to say, however, it is not necessary to use the (A_H, Π_H) symmetric regenerator approximation, and the performance of general unbalanced regenerators can be computed directly.

In this handbook, no attempt is made to review the very many methods, both open and closed, that have been published. Reference should be made to the texts by Hausen [1] and Schmidt and Willmott [2]. Instead, a concise description of just one closed and one open method is provided.

G. Method III (Nahavandi and Weinstein, 196 1) : Closed

Many of the closed methods are based upon the solution of a pair of integral equations. It is convenient to start by specifying that $F'(\xi')$ is the spatial solid temperature distribution at the start of the hot period at cyclic equilibrium, and that $F''(\xi'')$ is the corresponding temperature distribution in the cold period.

It can be shown that the differential Eqs. 3.15.6(7) and 3.15.6(8) can be transformed into two integral equations, one relating to the hot period, the other to the cold.

Hot period:

$$1 - F''\left[\Lambda''\left(1 - \frac{\xi'}{\Lambda'}\right)\right] = e^{-\Pi'}[1 - F'(\xi')] + \int_0^{\xi'} K'(\xi' - \epsilon)[1 - F(\epsilon)]\, d\epsilon \tag{8}$$

Cold period:

$$F'\left[\Lambda'\left(1 - \frac{\xi''}{\Lambda''}\right)\right] = e^{-\Pi''}F''(\xi'') + \int_0^{\xi''} K''(\xi'' - \epsilon)F''(\epsilon)\, d\epsilon \tag{9}$$

These equations embody the reversal conditions. The function K is defined in the following way:

$$K(\xi - \epsilon) = \frac{iJ_1(2i\sqrt{\Pi(\xi - \epsilon)})}{\sqrt{\Pi(\xi - \epsilon)}}\, e^{\Pi - (\xi - \epsilon)} \tag{10}$$

Within a computer program, the first-order Bessel function J_1 with imaginary argument, can be evaluated using a standard library subprogram. If one is not available, Iliffe [1 1] suggests J_1 be evaluated using a series expansion. Alternatively it is useful to note that

$$iJ_1(2i\Pi x) = \frac{1}{\Pi}\int_0^{\Pi} e^{-2x\Pi\cos t}\cos t\, dt \tag{11}$$

and thus

$$K(x) = \frac{-1}{\Pi}\int_0^{\Pi}\sqrt{\frac{\Gamma}{x}}\, e^{-2\sqrt{\Pi x}\cos(t - x - \Pi)}\cos t\, dt \tag{12}$$

© 1984 Hemisphere Publishing Corporation

This last integral can be evaluated numerically, and it is recommended that a IO-point Gaussian quadrature method be used. Such a method of numerical integration is again commonly available in scientific computer program libraries.

It can be demonstrated that

$$\lim_{x \to 0} \mathrm{K}(x) = \Pi e^{-\Pi}$$

and it recommended this limit be used for $0 \leqslant x \leqslant 10^{-4}$ and for $\Pi < 5$.

Nahavandi and Weinstein proposed that the temperature distributions F' and F'' be represented in polynomial form

$$F'(\xi') = \sum_{j=0}^{n} a_j (\xi')^j \tag{13}$$

$$F''(\xi'') = \sum_{j=0}^{n} b_j (\xi'')^j \tag{14}$$

The cold period equation now becomes

$$\sum_{j=0}^{n} a_j \left[\Lambda' \left(1 - \frac{\xi''}{\Lambda''}\right)\right]^j = e^{-\Pi''} \sum_{j=0}^{n} b_j (\xi'')^j + \int_0^{\xi''} K''(\xi'' - \epsilon) \sum_{j=0}^{n} b_j \epsilon^j \, d\epsilon \tag{15}$$

An exactly equivalent equation can be developed for the hot period.

These two equations are applied to $2n + 2$ distinct data points $\xi_i (i = 0, 1, 2, \ldots, 2n + 1)$ and this yields a set of $2n + 2$ simultaneous linear equations in the $2n + 2$ coefficients $a_0, a_1, a_2, \ldots, a_n, b_0, b_1, b_2, \ldots, b_n$. In fact the essential problem in programming this method for a digital computer is to plant the correct elements in the matrix on the left-hand side and the column vector on the right-hand side of the equations. Usually, the solution of the resultant linear equations can be left to another library program and in this way the $2n + 2$ coefficients can be evaluated.

The regenerator thermal ratio can be computed using the form developed by Iliffe [11].

$$\eta'_{\mathrm{REG}} = \frac{\Lambda'}{\Pi'} \left[\frac{1}{\Lambda''} \int_0^{\Lambda''} F''(\xi'') \, d\xi'' - \frac{1}{\Lambda'} \int_0^{\Lambda'} F'(\xi') \, d\xi'\right] \tag{16}$$

This can be rewritten

$$\eta'_{\mathrm{REG}} = \frac{\Lambda'}{\Pi'} \left[\sum_{j=0}^{n} b_j \frac{(\Lambda'')^j}{j+1} - \sum_{j=0}^{n} a_j \frac{(\Lambda')^j}{j+1}\right]$$

$$= \frac{\Lambda'}{\Pi'} \sum_{j=0}^{n} \frac{b_j (\Lambda'')^j - a_j (\Lambda')^j}{j+1}$$

Finally

$$\eta''_{\mathrm{REG}} = \gamma \eta'_{\mathrm{REG}}$$

where

$$\gamma = \frac{\mathrm{A}}{\Pi''} \frac{\mathrm{II}}{\Lambda'}$$

It is recommended that the so-called Chebyshev values be used for the data points (see [2]).

$$\xi'_i = \frac{\Lambda'}{2} \left(1 - \cos \frac{2n i \pi}{2n + 1}\right)$$

$$\xi''_i = \frac{\Lambda''}{2} \left(1 - \cos \frac{2n i \pi}{2n + 1}\right)$$

both for $i = 0, 1, 2, \ldots, 2n + 1$.

The thermal ratios of a regenerator of specified reduced length A and A and reduced period II and II is first computed with the degree of the polynomials for $F'(\xi')$ and $F''(\xi'')$ equal to 1 or 2. The calculation is repeated using successively higher degrees of the polynomials. This iterative process is said to have converged when the absolute value of the difference between two successive evaluations of η'_{REG} (or η''_{REG}) is less than some prescribed level, say 10^{-4} or 10^{-5}.

This method should not be used for large reduced lengths and an upper value of $\Lambda_H < 30$ is recommended. For most practical applications of regenerators, this restriction is not prohibitive.

H. Method IV (Willmott, 1964): Open

In this method, the differential equations 3.15.6(7) and 3.15.6(8) are solved numerically. The gas and solid temperatures are evaluated over a mesh in the hot period, that is at the gas entrance and exit and at a number of equally spaced positions, $\Delta\xi' = \Lambda'/m$ apart and at the start and end of the hot period, and at a number of equally spaced time intervals, $\Delta\eta' = \Pi'/p'$ apart. In a similar way, the temperatures are computed at positions $\Delta\xi'' = \Lambda''/m$ apart and at time intervals An $= \Pi''/p''$ apart in the cold period.

At the start of the hot period, the solid temperatures are either set arbitrarily (usually equal to 0.5) for the first cycle, or equal to the temperatures at the end of the previous cold period.

We denote $T_f(r, s)$ and $T_s(r, s)$ to be the gas and solid temperatures respectively at position $r \Delta\xi'$ from the gas entrance and at the position in time s An from the start of the hot period.

At the beginning of the hot period, given the solid

© 1984 Hemisphere Publishing Corporation

temperature distribution, the corresponding gas temperatures are computed by solving Eq. 3.15.6(7) using

$$T_f(r+1, 0) = A_1 T_f(r, 0) + A_2 [T_s(r+1, 0) + T_s(r, 0)] \quad (17)$$

where

$$A_1 = \frac{2 - \Delta\xi'}{2 + \Delta\xi'}$$

$$A_2 = \frac{\Delta\xi'}{2 + \Delta\xi'}$$

$T_f(0, s) = 1$ (inlet gas temperature on dimensionless scale)

$s = 0, 1, 2, \ldots, p'$

Thereafter at any instant $s\,\Delta\eta'$, the gas and solid temperatures will have been computed at all positions down the length of the regenerator and it is then required to compute these temperatures at time $(s+1)\Delta\eta'$. This is done at the entrance by applying Eq. 3.15.6(8) in the form

$$T_s(0, s+1) = B_1 T_s(0, s) + 2B_2 \quad (18)$$

where

$$B_1 = \frac{2 - \Delta\eta'}{2 + \Delta\eta'}$$

$$B_2 = \frac{\Delta\eta'}{2 + \Delta\eta'}$$

The remaining temperatures down the length of the regenerator are computed by applying the equation

$$T_s(r+1, s+1) = K_1 T_s(r+1, s) + K_2 T_f(r+1, s) + K_3 T_s(r, s+1) + K_4 T_f(r, s+1) \quad (19)$$

followed by the equation

$$T_f(r+1, s+1) = A_1 T_f(r, s+1) + A_2 [T_s(r+1, s+1) + T_s(r, s+1)] \quad (20)$$

at successive positions $r = 0, 1, 2, \ldots, m-1$. Note that

$$K_1 = \frac{B_1}{X} \quad K_2 = \frac{B_2}{X} \quad K_3 = \frac{A_2 B_2}{X} \quad K_4 = \frac{A_1 B_2}{X}$$

$$X = 1 - A_2 B_2$$

This procedure can then be applied to the cold period provided note is taken of the counterflow operation of the regenerator (this can be the most difficult part of the method to program for a computer) and that the inlet temperature $T_{fi}'' = 0$.

The regenerator is then simulated over successive cycles until equilibrium is achieved. There are a number of practical details about which care should be taken, in particular how to control the error associated with the numerical method and how to determine whether cyclic equilibrium has been reached by the simulation. The reader is directed to [2] for further information about these matters.

The advantages of this method are that the full spatial and chronological variation of gas and solid temperature is computed and that, as far as the author knows, there are no restrictions on the range of dimensionless parameters to which the method can be applied. It is possible to compute the initial temperature distribution using the Nahavandi and Weinstein method described previously. In this way, the repeated cycling of the model is avoided but the full chronological as well as spatial variation of temperature at cyclic equilibrium is calculated.

This method has been modified [15] to be able to cope with, for example, temperature-dependent thermophysical properties of gas or solid and time varying flow rate. However, this matter is outside the scope of this text ([1] and [2] deal with this matter in detail).

Nomenclature and References for Section 3.15.7 appear at the end of Section 3.15.10.

© 1984 Hemisphere Publishing Corporation

3.15.8

Effect of longitudinal conduction in the packing of the regenerator

A. J. Willmott

■ Bahnke and Howard [16] proposed a conduction factor that we shall denote β. It essentially measures the rate of longitudinal (that is, parallel to the direction of gas flow) conduction relative to the rate at which heat is input from the gas in the hot period or extracted by the gas in the cold period.

$$\beta' = \frac{Ad\,\lambda_s}{2\dot{M}_f' C_f' L^2} \tag{1}$$

$$\beta'' = \frac{Ad\,\lambda_s}{2\dot{M}_f'' C_f'' L^2} \tag{2}$$

where L is the length of the regenerator packing.

Schmidt and Willmott [2] show that the descriptive differential equations embodying longitudinal conduction are

$$\frac{\partial T_s}{\partial \eta} = T_f - T_s + \beta\Lambda \frac{\partial^2 T_s}{\partial \xi^2} \tag{3}$$

$$\frac{\partial T_f}{\partial \xi} = T_s - T_f \tag{4}$$

with the appropriate values of β and A set for the hot and cold periods, respectively. The last term in Eq. (3) represents the conduction effect and it will be seen that for small values of reduced length A or A , or the conduction factor β' or β'', this effect is negligible. It turns out that β' and β'' have the dominating effect unless the reduced lengths are very large.

For many practical applications, β' and β'' are indeed very small; for hot blast stoves, the values are significantly less than 10^{-4} while for many rotary regenerators they are 10^{-3} or less. Bahnke and Howard specify the effect is negligible if β' and $\beta'' \leqslant 10^{-2}$. Examination of Eqs. (1) and (2), shows that tall and narrow regenerators are unlikely to be affected by longitudinal conductivity. However, metallic regenerators, whose packings have a high thermal conductivity, can be subject to the effect of longitudinal conduction when the walls between the passages carrying the flow of gas are relatively thick, and when the regenerators are broad and squat, and operate at low flow rates.

It is a simple procedure to evaluate β' (or β'') for a typical regenerator. If its value is 10^{-2} or less, for $\Lambda_H < 50$, it is recommended to forget this problem. This is usually the case.

However, there are new rotary regenerators being developed which are small in height L, but very broad in cross section. If constructed of packings with a sufficiently great thermal conductivity, such regenerators may require this longitudinal effect to be recognized. The means for solving Eqs. (3) and (4) are outlined in [2].

Nomenclature and References for Section 3.15.8 appear at the end of Section 3.1510.

© 1984 Hemisphere Publishing Corporation

3.15.9

Dealing with heat losses

A. J. Willmott

■ It is first necessary to define what is meant by heat losses in regenerator operation. Here it is understood that the loss of heat or cold to the surroundings is through the outer casing and end sections of the thermal regenerator (for example the shell and dome of a hot blast stove).

Hausen [1] mentions the exhaust gas or flue gas losses caused by the unavoidable thermodynamic inefficiency of the heat exchanger. These of course are accounted for, implicitly, in the calculation of the thermal ratio for the hot period in regenerator calculations. Hausen also includes longitudinal conduction effects (see Sec. 3.15.8) as a possible source of heat loss. However, as has already been stated, consideration is restricted here to heat losses to the surroundings.

The basic assumption built into most published methods is that the heat losses from the shell can be averaged out across the whole cross section of the regenerator, and that each channel through which the gas flows experiences the same if small heat loss effect. No attempt is made to represent the situation in practice where heat losses are greater in channels near the shell of the regenerator, and probably zero in the middle of the regenerator cross section.

One approach is to modify the differential equation 3.15.3(2) so that the rate at which heat is given up (or absorbed from) by the gas is equated to the sum of the heat loss rate $\dot{Q}_{\text{loss}}$ and the rate at which heat is taken up by the packing. In this case, the differential equation becomes

$$\bar{\alpha}A(t_f - t_s) = M_s C_s \frac{\partial t_s}{\partial \tau} + \dot{Q}_{\text{loss}} \tag{1}$$

This can be rewritten

$$\frac{\partial t_s}{\partial \tau} = \frac{\bar{\alpha}A}{M_s C_s}(t_f - t_s) - \frac{Q_{\text{loss}}}{M_s C_s} \tag{2}$$

Applying the transformation (which ignores the effect of gas resident in the channels at the reversal, which can usually be neglected)

$$\eta = \frac{\bar{\alpha}A}{M_s C_s}\tau \tag{3}$$

we obtain the differential equation

$$\frac{\partial t_s}{\partial \eta} = t_f - t_s - \dot{q}_{\text{loss}} \tag{4}$$

where

$$\dot{q}_{\text{loss}} = \frac{\dot{Q}_{\text{loss}}}{\bar{\alpha}A} \tag{5}$$

Equation (4) together with Eq. (3) can now be solved in a suitably but simply modified form of the open method IV described above.

How important will be the effect of $\dot{Q}_{\text{loss}}$ depends on many factors including the thickness and quality of the thermal insulation in the shell of the regenerator and the ambient temperature and air flow conditions in which the regenerator is located.

Hausen [2] describes the approach of Nesselman [17] to this problem in which some estimation of the rate of heat loss is attempted as a function of the packing temperature of the regenerator and the temperature of the ambient air surrounding the shell of the heat exchanger.

©1984 Hemisphere Publishing Corporation

The effect of heat losses is to cause decreases $\Delta t'_{fo}$ and $\Delta t''_{fo}$ in the average exit gas temperature from the regenerator. Hausen suggests that for blast furnace stoves, these decreases can be of order of magnitude 10°C, whereas in low temperature technology regenerators that are well insulated, the figure is much smaller and close to 0.1°C. In this latter case, cold losses occur and increases $\Delta t'_{fo}$ and $\Delta t''_{fo}$ are observed. In conclusion, one basic relationship must be recorded:

$$\dot{Q}_{loss}(P' + P'') = \dot{M}'_f C'_f P' \Delta t'_{fo} + \dot{M}''_f C''_f P'' \Delta t''_{fo} \qquad (6)$$

This is essentially a heat balance between the total loss of heat in a cycle and the heat losses in the hot and cold periods respectively.

A. Example of heat loss calculation

We extend the example calculation presented previously in Section 3.15.7 and use the equation

$$\dot{Q}_{loss}(P' + P'') = \dot{M}'_f C'_f P' \Delta t'_{fo} + \dot{M}''_f C''_f P'' \Delta t''_{fo} \qquad (7)$$

in order to estimate a heat loss rate necessary to generate a particular difference in outlet gas temperatures between those computed with and without heat losses. In the example we have $P' = P'' = 1\,800$ s; we assume in making this estimate that $\Delta t''_{fo} \approx \Delta t'_{fo}$. The heat loss equation takes the form

$$Q_{loss} = \tfrac{1}{2}(\dot{M}'_f C'_f + \dot{M}''_f C''_f)\Delta t'_{fo}$$

$$\dot{M}' C'_f = 18\,000 \text{ J/s K}$$

$$\dot{M}'' C''_f = 20\,800 \text{ J/s K}$$

and hence

$$\dot{Q}_{loss} = 1.94 \times 10^4 \Delta t'_{fo} \text{ J/s}$$

Recalling the values of

$$\bar{\alpha}'_1 = 25.152 \text{ W/m}^2 \text{ K}$$

$$\bar{\alpha}''_2 = 21.757 \text{ W/m}^2 \text{ K}$$

and a heating surface area $A = 10^4$ m^2, we can establish values for $\dot{q}'$ and $\dot{q}''$

$$\dot{q}'_{loss} = \frac{\dot{Q}_{loss}}{\bar{\alpha}' A} = \frac{(1.94)(10^4)}{(25.152)(10^4)} \Delta t'_{fo} = 0.077\ 1\ \Delta t'_{fo}$$

$$\dot{q}''_{loss} = \frac{\dot{Q}_{loss}}{\bar{\alpha}'' A} = \frac{1.94}{21.757} \Delta t'_{fo} = 0.089\ \Delta t'_{fo}$$

Upon submitting this data to a computer program developed by the author for the solution of the differential equations (4) and 3.15.6(3), employing the method indicated, the results were obtained that are given in Table 1.

The values computed for $\dot{q}'_{loss} = \dot{q}''_{loss} = 0$ correspond closely to the results calculated using the Tipler method (see Sec. 3.15.7).

Table 1 Calculated time mean exit gas temperatures

Reduced length Λ			Reduced period Π				
Hot period 13.97	Cold period 10.46		Hot period 2.329	Cold period 2.015			
Hot inlet gas temperature 1250° C							
Cold inlet gas temperature 100° C							
$\dot{Q}_{loss} \times 10^4$, J/s	$\dot{q}'_{loss}$	$\dot{q}''_{loss}$	$\dot{q}'_{loss}$ and $\dot{q}''_{loss}$ based on $\Delta t'_{fo}$, estimate	Hot period t'_{fo}, °C	Actual $\Delta t'_{fo}$	Cold period t''_{fo}	Actual $\Delta t''_{fo}$
0.0	0.0	0.0	0.0	205.5	0.0	1003.9	0.0
9.7	0.385	0.445	5.0	201.0	4.5	998.5	5.4
19.4	0.77	0.89	10.0	196.5	9.0	993.1	10.8
29.1	1.155	1.335	15.0	192.0	13.5	987.7	16.2

Nomenclature and References for Section 3.158 appear at the end of Section 3.15.10.

© 1984 Hemisphere Publishing Corporation

3.15.10

Transient characteristics of regenerators

A. J. Willmott

■ The temporary storage of heat in the packing implies that the regenerator must possess a thermal capacity and, with this capacity, an inertia whereby alterations in operating conditions do not result immediately in corresponding changes in thermal performance. Instead the regenerator operates through a number of non-equilibrium cycles and, if the operating conditions are not changed again, the regenerator eventually reaches cyclic equilibrium. The time lag in this response can be of considerable magnitude and may last over very many cycles, so many indeed that the lag may be measured in days, rather than hours.

The dimensionless parameters reduced length A and A and reduced period II andΠ'' turn out to be as important in describing the nonstationary performance as they are for cyclic equilibrium. Such transient responses can be studied theoretically, in which case the time to equilibrium, consisting of the sum of the several cycles of hot and cold periods, is a function of the convergence criteria. From a practical point of view, however, it is pretty well impossible to measure the time to equilibrium since the operating conditions, from one cycle to the next can never be so exactly the same, even in an experimental or pilot plant environment. It follows that the more conventional time constant provides a better measure of regenerator inertia.

Willmott and Burns [18] demonstrated that for a step change in inlet gas temperature, the time to equilibrium Θ, in dimensionless terms could be represented by the equation

$$\Theta = \sim(0.622\ \Lambda_H^2 + 4.144\ \Lambda_H + 4.464) \qquad (1)$$

for $\Lambda_H \leqslant 40$, employing a convergence Of $\epsilon = 10^{-4}$. The exact meaning of this convergence criteria will be explained in the example below. Note that

$$\mu = (1 + k)\left(1 + \frac{1}{k}\right) \qquad (2)$$

where $\Lambda'/\Lambda'' = \Pi'/\Pi'' = k$, that is, Eq. (1) relates to unsymmetric but balanced regenerators.

A. Example calculation

We modify the example given by Hausen [14] and set out in Sec. 3.15.7. The regenerator configuration remains the same but the operating conditions are altered so that the regenerator is balanced, that is,

$$\dot{M}_f' C_f' P' = \dot{M}_f'' C_f'' P''$$

The operating characteristics are then as given in Table 1.

It is necessary to *recompute* ϕ_H.

$$Z = \frac{0.05^2}{(4)(0.463)10^{-6}}\left(\frac{1}{1\ 800} + \frac{1}{1\ 5.58}\right)$$

$$= \frac{(2.5)(10^{-3})}{(4)(0.463)10^{-3}}\ (1.197\ 4)(10^{-3}) = 1.616 < 5$$

$$\phi_H = 1 - \frac{Z}{15} = 1 - \frac{1.616}{15} = 0.892$$

The value of $d\phi_H/(6\lambda_s)$ is little altered to 0.007 44 from 0.007 5 in Hausen s original data. The change irϕ_H due to the change in cold period duration from 1 800 to 1 558 s is therefore ignored.

Both reduced lengths remain unaltered as does the hot reduced period. However the cold reduced period becomes

© 1984 Hemisphere Publishing Corporation

Table 1 Operating characteristics for example calculation

Parameter, units	Hot period	Cold period
Duration, s	1800.0	1558
Entrance gas temperature after step change, °C	1 250.0	100.0
Gas mass flow rate, kg/s	18.0	20.0
Gas specific heat, J/kg s	1 000.0	1 040.0
Heat transfer coefficient, W/m² K	31.0	26.0

$$\Pi'' = \frac{(2.015)(1\ 558)}{1\quad 800} = 1.744\ 1$$

The mean reduced length can be computed using

$$\frac{1}{\Lambda_H} = \frac{1}{2}\left(\frac{1}{\Lambda'} + \frac{1}{\Lambda''}\right)$$

for a balanced regenerator

$$\frac{1}{\Lambda_H} = \frac{1}{2}\left(\frac{1}{13.97} + \frac{1}{10.46}\right)$$

Thus

$$\Lambda_H = 11.96$$

The value of

$$k = \frac{\Lambda'}{\Lambda''} = 1.335$$

and

$$\mu = (1 + k)\left(+ \frac{1}{k}\right) = 4.084$$

The total time to equilibrium is given by

$$\Theta = \mu(0.622\,\Lambda_H^2 + 4.144\,\Lambda_H + 4.464)$$
$$= 4.084[0.622(11.96)^2 + 4.144(11.96) + (4.464)] = 584.0$$

$$\Pi' + \text{II} = 2.329 + 1.7441 = 4.073\ 1$$

Hence number of cycles to reach equilibrium is equal to 584.0/4.073 1 = 144. (We must round up from 143.4 to 144 since part of a cycle has little meaning). The total cycle time is 1 800 + 1 558 = 3 358 s. Hence, total actual time to reestablish cycle equilibrium = [(3 558) (144)]/[(3 600)(24)] = 5.93 days.

In other words, the regenerator configuration specified in the example in Sec. 3.9.7 would take almost a week to reestablish cyclic equilibrium for the convergence $\epsilon = 10^{-4}$.

What does this mean? The simulation is regarded as having attained equilibrium if the difference At between the exit gas temperatures at the very end of the hot (or cold) period in successive cycles, measured on the dimensionless scale specified by Eq. 3.9.6(5), is less than 10^{-4}, i.e.,

$$\frac{\text{At}}{t'_{fi} - t''_{fi}} \leqslant 10^{-4}$$

Hence $t'_{fi} - t''_{fi} = 1250 - 100$ and $At = 1\ 150 \times 10^{-4} \approx 0.1°C$. Note t'_{fi} refers to inlet temperature *after* the step change. If we consider equilibrium to have been attained if At = 5°C, we require that the stopping factor should be $E = 4.35 \times 10^{-3}$.

Willmott and Burns specify that the time to equilibrium Θ_E, estimated with stopping criteria E is related to the time to reestablish equilibrium using stopping criterion ϵ by the equation

$$\Theta_E = \frac{\Theta \log_e E}{\log_e \epsilon} \tag{3}$$

Since Θ is related to the *real* time (in days) by a linear transformation, we can compute the time to equilibrium with At = 5° C to be

$$\frac{5.93 \log_e(4.35 \times 10^{-3})}{\log_e(10^{-4})} = (5.93)(0.590\ 4) \approx 3\tfrac{1}{2} \text{ days}$$

This example calculation is introduced at this early stage of this section, not just to explain how to estimate the time taken for a regenerator to attain equilibrium, but also to emphasize how very long are the time periods involved.

If a disturbance in operating conditions were applied on a Friday afternoon to the Hausen example regenerator, operating in balanced mode, the regenerator would *not* have regained cyclic equilibrium by the Monday morning, even if it were run with unchanging operating conditions over the entire weekend!

What this implies of course, is that many industrial regenerators never have the chance to reach cyclic equilibrium, unless the operating conditions are very steady and are changed very infrequently.

An important implication emerges for any attempt to correlate experimental data collected from an industrial regenerator (operating with cycle times of 0.5 h or more), with theoretical predictions of regenerator thermal performance at cyclic equilibrium. Unless one can be sure the experimental data relates to performance after at least *1 week* of unchanging operation, the theoretical model may predict temperatures by as much as 20° C or more, higher or lower than the observed temperatures collected from the industrial plant. Whether they are higher or lower will depend upon previous operating conditions.

This problem is exacerbated by the fact that if a step change is made on the hot side of regenerator operation, in either the inlet gas temperature or the gas flow rate, the response by the hot side exit gas

© 1984 Hemisphere Publishing Corporation

temperature lags behind the response of the cold side exit gas temperature.

London et al. [19] illustrated the responses to changes in operating conditions by the dimensionless temperatures $\epsilon f_1(\tau)$ and $\epsilon f_2(\tau)$ which are defined by

$$\epsilon f_1(\tau) = \frac{t'_{fo}(\tau) - t'_{fo}(0)}{t'_{fo}(\infty) - t'_{fo}(0)} \tag{4}$$

$$\epsilon f_2(\tau) = \frac{t''_{fo}(\tau) - t''_{fo}(0)}{t''_{fo}(\infty) - t''_{fo}(0)} \tag{5}$$

At cyclic equilibrium, immediately before the step change, $\tau = 0$ and $\epsilon f_1(0) = \epsilon f_2(0) = 0$. Once cyclic equilibrium has been restored at $\tau = \infty$, then $\epsilon f_1(\infty) = \epsilon f_2(\infty) = 1$. Either real time τ (seconds) or dimensionless time can be employed as the time variable in ϵf_1 and ϵf_2. London et al. [19] restricted their considerations to symmetric regenerators, and to the cases where $\Lambda/\Pi > 100$. Willmott and Burns [18] illustrated the lag of the hot side response behind that of the cold side response for step changes in inlet gas temperature on the hot side (see Fig. 1).

That is the response increases with reduced length A and is illustrated by Fig. 2. Here only the hot side responses are displayed for clarity in graphic presentation.

The response ϵf_1 is better described as the ***same side response,*** that is the response of the exit temperature on the hot/cold side to a step change in the inlet temperature on the same side of regenerator operation, hot or cold. Similarly ϵf_2 is often described as the ***opposite side response.***

That ϵf_1 lags behind ϵf_2 is a direct consequence of counterflow regenerator operation. Consider a step change in cold inlet temperature. The impact of such a change is felt immediately and recorded by the temperature changes in the packing in the cold gas inlet region of the regenerator. When a reversal takes place, hot gas encounters the effects of these changes at what has become the hot gas exit. Consequently, the opposite side response begins immediately whereas the long-term effects of cold inlet gas step change only become manifest on the same side as the heat or cold front gradually penetrates the regenerator packing over successive cycles.

Willmott and Burns [18] demonstrate that the

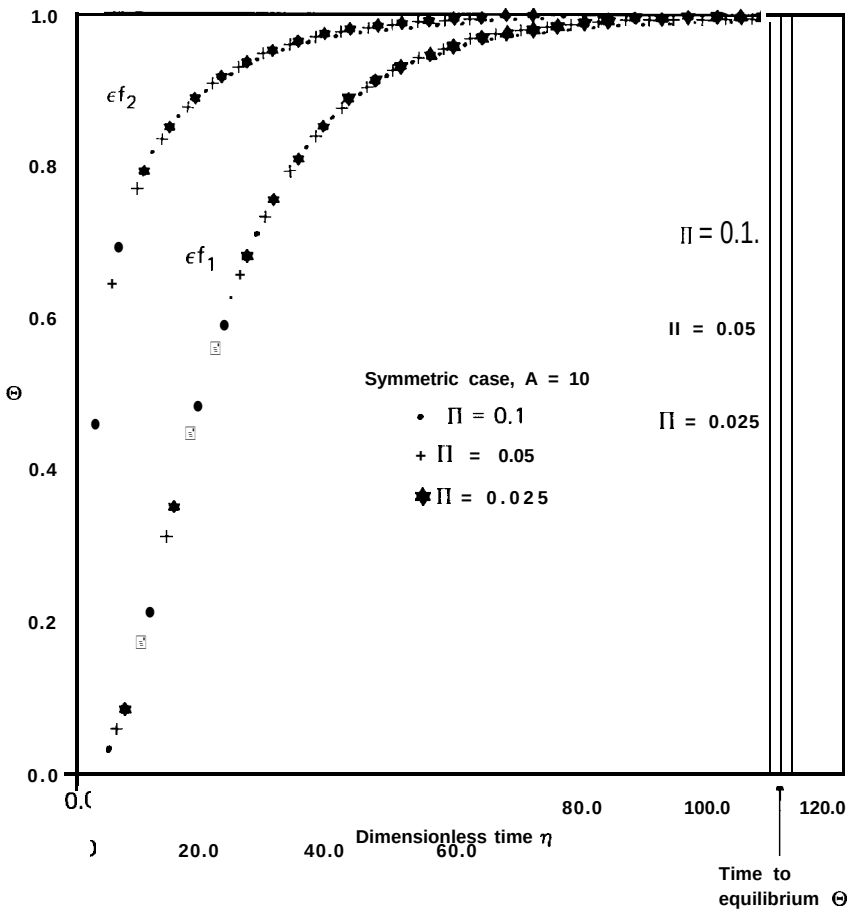

Figure 1 The responses ϵf_1 and ϵf_2 for a step change in hot inlet gas temperature for $\Lambda/\Pi > 100$ in the case of a symmetric regenerator. From Schmidt and Willmott [2].

© 1984 Hemisphere Publishing Corporation

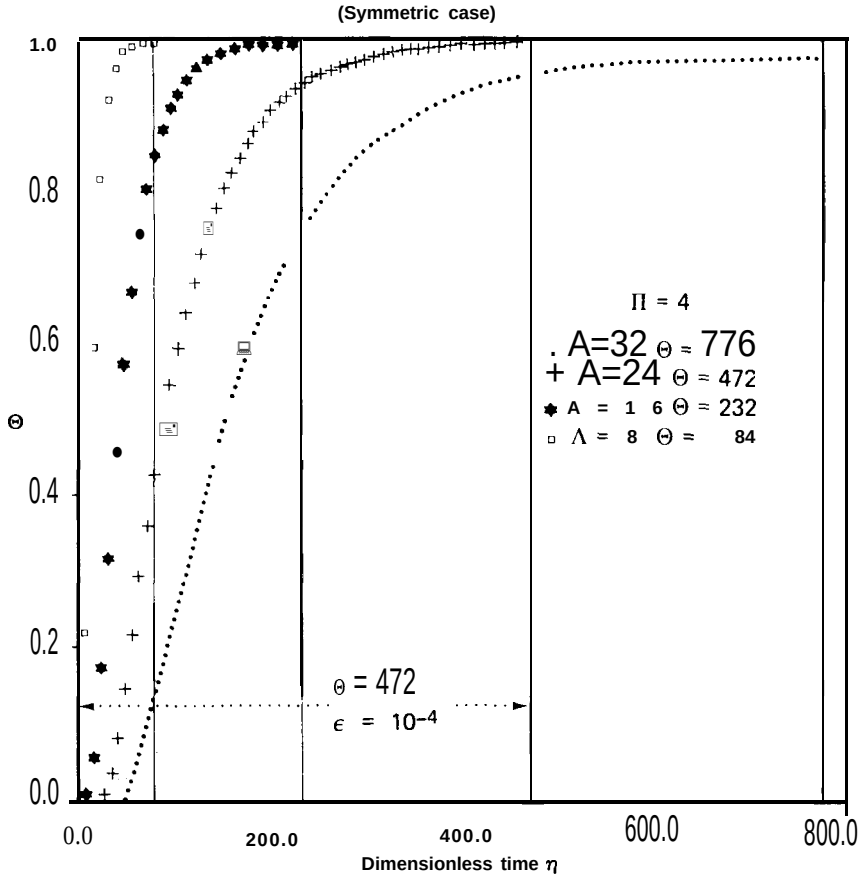

Figure 2 The hot side response ϵf_1 for a step change in hot inlet gas temperature and the dimensionless time to equilibrium Θ as a function of reduced length A. From Schmidt and Wilhnott [2].

analysis for symmetric regenerators can be extended to unsymmetric but balanced regenerators using the Λ_H, Π_H symmetric regenerator approximation described in Sec. 3.15.7 and this analysis is exploited in the worked example earlier in this section. In the unbalanced case, the duration of the response is reduced by degree of unbalance, γ, as defined by Eq. 3.15.6(17). They illustrate this effect graphically and their representation appears in Fig. 3.

The effect of changes in gas flow rate is more complicated but readers are referred to Chap. 10 of the Schmidt and Willmott text [2].

It was mentioned earlier in this section that a representation, better than the time to regain cyclic equilibrium, is the conventional time constant. This is probably more applicable to the analysis of experimental results.

The response ϵf_1 and ϵf_2 can be represented approximately by the equations

$$\epsilon f_1 \approx 1 - \exp\left(-\frac{\eta_H - C_1}{\eta_c}\right) \tag{6}$$

$$\epsilon f_2 \approx 1 - \exp\left(-\frac{\eta_H + C_2}{\eta_c}\right) \tag{7}$$

where η_H is on the harmonic mean reduced period time scale.

Willmott and Burns show from their theoretical studies that ϵf_1 and ϵf_2 share a common time constant η_c and that for balanced regenerators

$$\eta_c \approx 0.092\ 2\ \Lambda_H^2 + 0.489\ \Lambda_H + 0.928 \tag{8}$$

B. Worked example

For the Hausen modified example regenerator discussed earlier in this section $\Lambda_H = 11.96$

$$\eta_c \approx 0.092\ 2(11.96)^2 + 0.489(11.96) + 0.928 = 19.96$$

The cycle time is $2\Pi_H = 2(1.995) = 3.989$. Now

$$\frac{1\eta_c)}{2\Pi_H} \doteq \frac{9\ 6}{3.989} = 5$$

corresponds to the number of cycles comprising the time constant. Since the total cycle time is 3 350 s, the time constant η_c in realtime is $[5(3\,350)]/(3\ 600) = 4.66$ h.

The lag between same side and opposite side responses can be measured in terms of the constants C_1 and C_2 and represented by the simple equation

©1984 Hemisphere Publishing Corporation

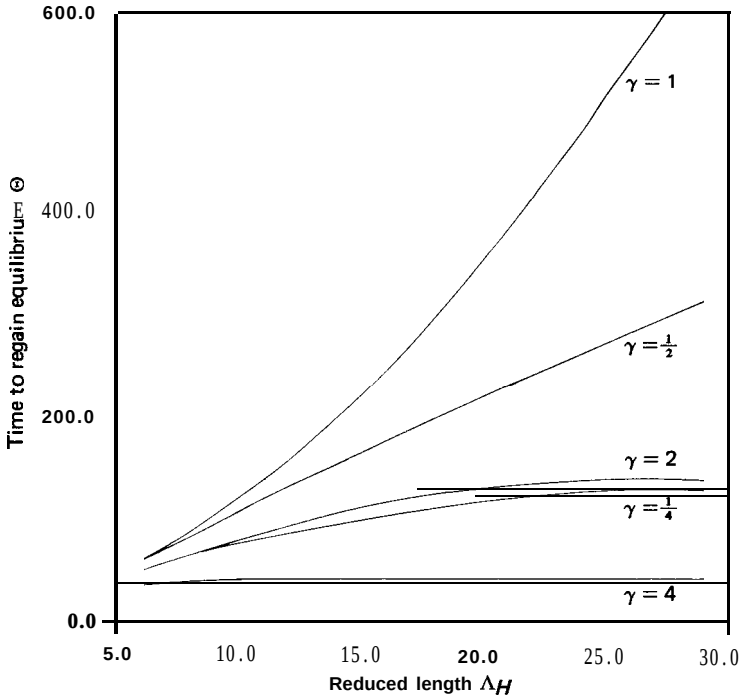

Figure 3 Dependence of time to reestablish cyclic equilibrium as a function of the mean reduced length Λ_H and the degree of unbalance γ. The convergence criterion is $\epsilon = 10^{-4}$. From Schmidt and Willmott [2].

$$\text{lag}_H = C_1 + C_2 \tag{9}$$

For balanced regenerators, Willmott and Burns [20] displayed lag_H, together with η_c, C_1, and C_2 as functions of reduced length Λ_H. This is shown in Fig. 4.

C. Further worked example

For a reduced length $\Lambda_H \simeq 12$, (for the Hausen example), it would appear from Fig. 4 that $\text{lag}_H \approx 25$. This corresponds to a real time lag which is equal to

$$\frac{(25)(P' + P'')}{(3\ 600)(2\Pi_H)} = \frac{(25)(3\ 358)}{(3\ 600)(2 \times 1.995)} = 5.8 \text{ h}$$

Finally, the degree of unbalance λ does reduce the time constant as one might expect. The way this does vary is shown in Fig. 5.

D. Conclusions

It is most difficult to cover all the material relating to regenerator transient behavior. It has been regarded as

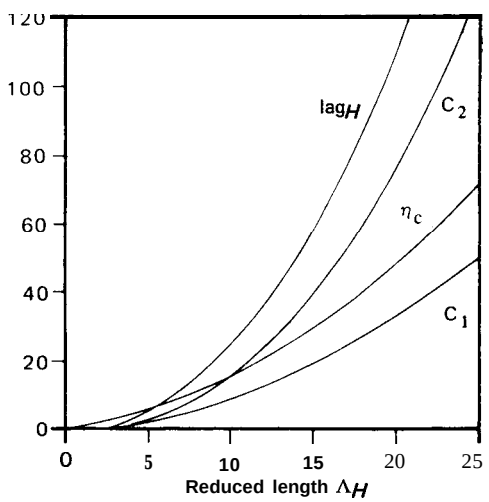

Figure 4 Graphic of the dependence of lag_H, η_c, C, , and C_2 on reduced length Λ_H. From Schmidt and Willmott [2].

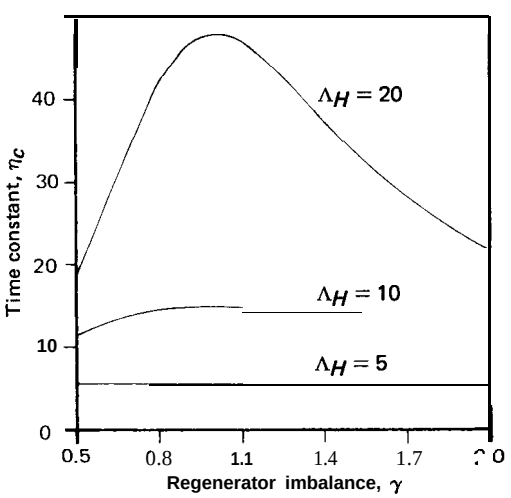

Figure 5 Relationship between regenerator unbalance and the time constant. From Schmidt and Willmott [2].

© 1984 Hemisphere Publishing Corporation

sufficient here to present what are probably the most important conclusions and to illustrate the importance of this topic by reference to a worked example. Readers are encouraged to inspect the scientific literature in order to pursue this matter further.

NOMENCLATURE FOR SECTIONS 3.15.3-3.15.10

A	heating surface area, m^2
C	specific heat, J/kg K
	characteristic thickness of heat storing mass, m
H	dimensionless time to equilibrium [Fig. 3.15.10 (2)]
L	length of regenerator, m
	number of spatial increments (Sec. 3.15.7)
a	mass flow rate, kg/s
M	mass of packing, kg
n	parameter characterizing the packing geometry [Eq. 3.15.5(1)]
p	number of time increments (Sec. 3.15.7)
P	duration of period, s
Q_{loss}	rate of heat loss, W
q_{loss}	dimensionless rate of heat loss, K
t	temperature, K or °C†
T	dimensionless temperature?
x	distance from gas entrance in direction from gas entrance in direction of gas flow, m
Y	distance from surface of packing, perpendicular to gas flow, m
r	denotes spatial position on finite difference grid
s	denotes time position on finite difference grid
v	interstitial velocity, m/s
α	heat transfer coefficient, W/m^2 K
$\bar{\alpha}$	lumped heat transfer coefficient, W/m^2 K [Eq. 3.15.5(1)]
β	longitudinal conduction factor (Sec. 3.15.8)
γ	degree imbalance [Eq. 3.15.6(17)
ϵ	convergence factor
ξ	dimensionless distance [Eq. 3.15.6(1)]
η	dimensionless time [Eq. 3.15.6(2)]
η_{REG}	thermal ratio [Eqs. 3.15.6(11) and (12)]
Θ	dimensionless time to equilibrium [Fig. 3.15.10 (2)]
κ	packing thermal diffusivity, m^2/s
λ	packing thermal conductivity, W/m^2 K
Λ	reduced length
ν	viscosity
Π	reduced period
ϕ_H	Hausen correction factor [Eqs. 3.15.5(3) and (4)]
τ	time, s†

†*Note:* t is used to denote temperature while τ is employed to denote time. This is done to enable T to be used to denote dimensionless temperature.

Superscripts

$'$	refers to hot period
$''$	refers to cold period

Subscripts

f	refers to gas/liquid
s	refers to regenerator packing
H	mean, in connection with reduced length and reduced period
i	refers to inlet
o	refers to outlet, chronological mean

REFERENCES FOR SECTIONS 3.15.3–3.15.10

1. Hausen, H., ***Heat Transfer in Counterflow, Parallel*** Flow ***and Cross*** Flow, McGraw-Hill, New York, 1983.
2. Schmidt, F. W., and Willmott, A. J., ***Thermal Energy Storage and Regeneration,*** Hemisphere, Washington, D.C., 1981.
3. Boehm, H. H., Versuche zur Ermittling der Konvektiven Wärmeübergangszahlen an gemauerten engen Kanälen, Arch. ***Eisenhiittenwes.,*** vol. 6, pp. 423-431, 1932/3.
4. Kistner, H., Bestimmung der Wärmeübergangszahlen und Druckverluste bei doppelt versetzter und nicht versetzter Rost packung, ***Arch. Eisenhiittenwes.,*** vol. 3, pp. 751-768, 1929/30.
5. Langhans, W. U., Wärmeübergang und Druckverlust in Regeneratoren mit rostgitterartiger Speichermasse, ***Arch. Eisenhiittenwes,*** vol. 33, pp. 347–353, 441–451, 1962.
6. Hausen, H., Vervollständigte Berechnung des Wärmeaustausches in Regeneratorcn, ***Z. Ver. Deutsch. Ing., Beiheft Verftk No. 2,*** pp. 31-43, 1942/3.
7. Razelos, P., and Lazaridis, A., A Lumped Heat Transfer Coefficient for Periodically Heated Hollow Cylinders, ***Int. J. Heat Mass Transfer,*** vol. 10, pp. 1373-1387, 1967.
8. Willmott, A. J., The Regenerative Heat Exchanger Computer Representation, ***Int. J. Heat Mass Transfer,*** vol. 12, pp. 997-1014, 1969.
9. Hinchcliffe, C., and Willmott, A. J., Lumped Heat Transfer Coefficients for Thermal Regenerators, ***Int. J. Heat Mass Transfer,*** vol. 24, pp. 1229–1236, 1981.

© 1984 Hemisphere Publishing Corporation

10. Hausen, H., Uber die Theorie des Wärmeaustausches in Regeneratoren, *Z. Angew. Math. Mech.*, *vol. 9,* pp. 173-200, 1929.
11. Illiffe, C. E., Thermal Analysis of Counterflow Regenerative Heat Exchanger, *J. Inst. Mech. Eng.,* vol. 159, (war emergency issue no. 44), pp. 363-372, 1948.
12. Razelos, P., An Analytic Solution to the Electric Analog Simulation of the Regenerative Heat Exchanger with Time-Varying Fluid Inlet Temperatures, *Wärme Stoffübertrag.,* vol. 12, pp. 59-71, 1979.
13. Tipler, W., A Simple Theory of the Heat Exchanger, Shell Tech. Rept. ICT/14, London, 1947.
14. Hausen, H., *Periodische Wärmeübertragung in Regeneratoren,* 2d ed., pp. l-9, VDI-Wärmeatlas, Dusseldorf, 1974.
15. Wiimott, A. J., Simulation of a Thermal Regenerator under Conditions of Variable Mass *Flow, Int. J. Heat Mass Transfer,* vol. 11, pp. 1105-1116, 1968.
16. Bahnke, G. D., and Howard, C. P., The Effect of Longitudinal Heat Conduction on Periodic-Flow Heat Exchanger Performance, *J. Eng. Power,* pp. 105-120, April 1964.
17. Nesselmann, K., Der Einflusse der Wärmeverluste auf Doppelrohrwlrmeaustauscher, Z. *Gesamte Kälte Ind., vol. 35,* p. 62, 1928.
18. Willmott, A. J., and Burns, A., Transient Response of Periodic-Flow Regenerators, *Int. J. Heat Mass Transfer,* vol. 20, pp. 7.53-761, 1977.
19. London, A. L., Samsell, P. F., and McGowan, J. G., The Transient Response of Gas Turbine Plant Heat Exchangers-Additional Solutions for Regenerators of the Periodic-Flow and Direct Transfer Type, *J. Eng. Prog.,* vol. 86A, pp. 127-135, 1964.
20. Willmott, A. J., and Bums, A., Periodic-Flow Regenerators: Parameter Identification for Transient Performance, *Heat Transfer* 1978, vol. 4, pp. 297-302, Hemisphere, Washington, D.C., 1978.

© 1984 Hemisphere Publishing Corporation

3.16
Waste heat boiler systems

Contents

3.16.1
DESCRIPTION OF TYPICAL SYSTEM, P. Hinchley **3.16.1-1**

A. Introduction **3.16.1-1**
B. Typical waste heat boiler system **3.16.1-1**

3.16.2
KEY ASPECTS OF THE DESIGN AND SPECIFICATION OF INDIVIDUAL ITEMS OF PLANT,
P. Hinchley **3.16.2-1**

A. Boiler feedwater treatment plant **3.16.2-1**
B. Undeaerated boiler feedwater heaters **3.16.2-1**
C. Deaerators **3.16.2-2**
D. Boiler feedwater pumps **3.16.2-2**
E. Boiler feedwater heaters/economizers 3.16.2-3
F. Boilers/evaporators 3.16.2-3
G. Steam drums 3.16.2-8
H. Superheaters and attemperators 3.16.2-12
I. Combustion air heaters 3.16.2-13
J. Forced and induced draft fans 3.16.2-15

3.16.3
DETAILED DESIGN AND FABRICATION OF EQUIPMENT,
P. Hinchley **3.16.3-1**

3.16.4
PRECOMMISSIONING OF WASTE HEAT BOILER SYSTEMS,
P. Hinchley **3.16.4-1**

A. Objective 3.16.4-1
B. Provision for cleaning at the design stage 3.16.4-1
C. Cleanliness during manufacture and construction 3.16.4-1
D. Planning the chemical cleaning procedure 3.16.4-l
E. Cleaning operations 3.16.4-2
F. Storage 3.16.4-2

References for Sections 3.16.1-3.16.4 3.16.4-2

© 1984 Hemisphere Publishing Corporation

HEDH

3.16.1

Description of typical system

P . Hinchley

A. Introduction

The economics of many processes depend on the generation of steam from their waste heat. Such processes are those in which the required chemical reactions take place at elevated temperatures. Waste heat is available in the process gases and in the flue gas leaving the furnace which is often used to supply the heat required for endothermic reactions.

The scale of a waste heat recovery system varies over a wide range; thus a small acid plant may produce 5 t (metric tons)/h of steam at 15 atm and 300°C whereas a large single-stream ammonia plant may produce up to 300 t/h of steam at up to 150 atm and 530° C.

In some cases the steam is exported to a factory, where it may be used for heating purposes only, whereas in others it may be used in large turbines that drive the main compressors, pumps, and fans, with the exhaust being used in the process and for heating, thus making the plant self-sufficient in power. Nevertheless, there are several features that are common to most plants generating steam from waste heat, and these are covered in Sec. B.

However, before proceeding further it is important to stress the need for considering reliability when designing and selecting the equipment. A number of authors have described problems that have occurred in waste heat boilers and have emphasized the huge losses that resulted from some of these failures [1-4].

B. Typical waste heat boiler system

Figure 1 shows the basic elements in a waste heat boiler installation. The water entering the unit has to pass through a water treatment plant into an on-plot treated water storage tank from which it is pumped into a deaerator, frequently preceded by an undeaerated boiler feedwater heater. The deaerated water, after treatment by injected chemicals, passes through boiler feedwater pumps which generate enough head to force the water through the boiler feedwater heaters/economizers and into the steam drum. Steam is generated in waste heat

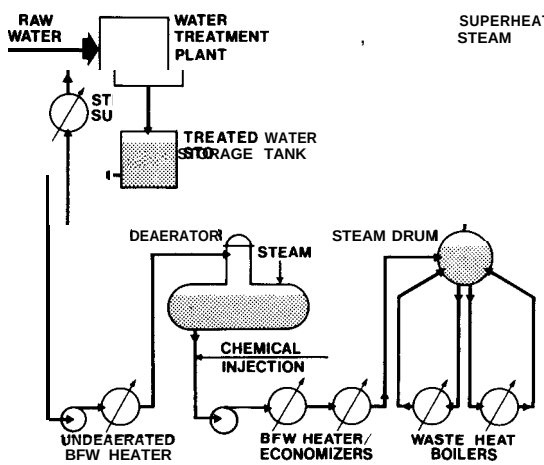

Figure 1 Typical arrangement of waste heat boiler system and its associated equipment.

© 1984 Hemisphere Publishing Corporation

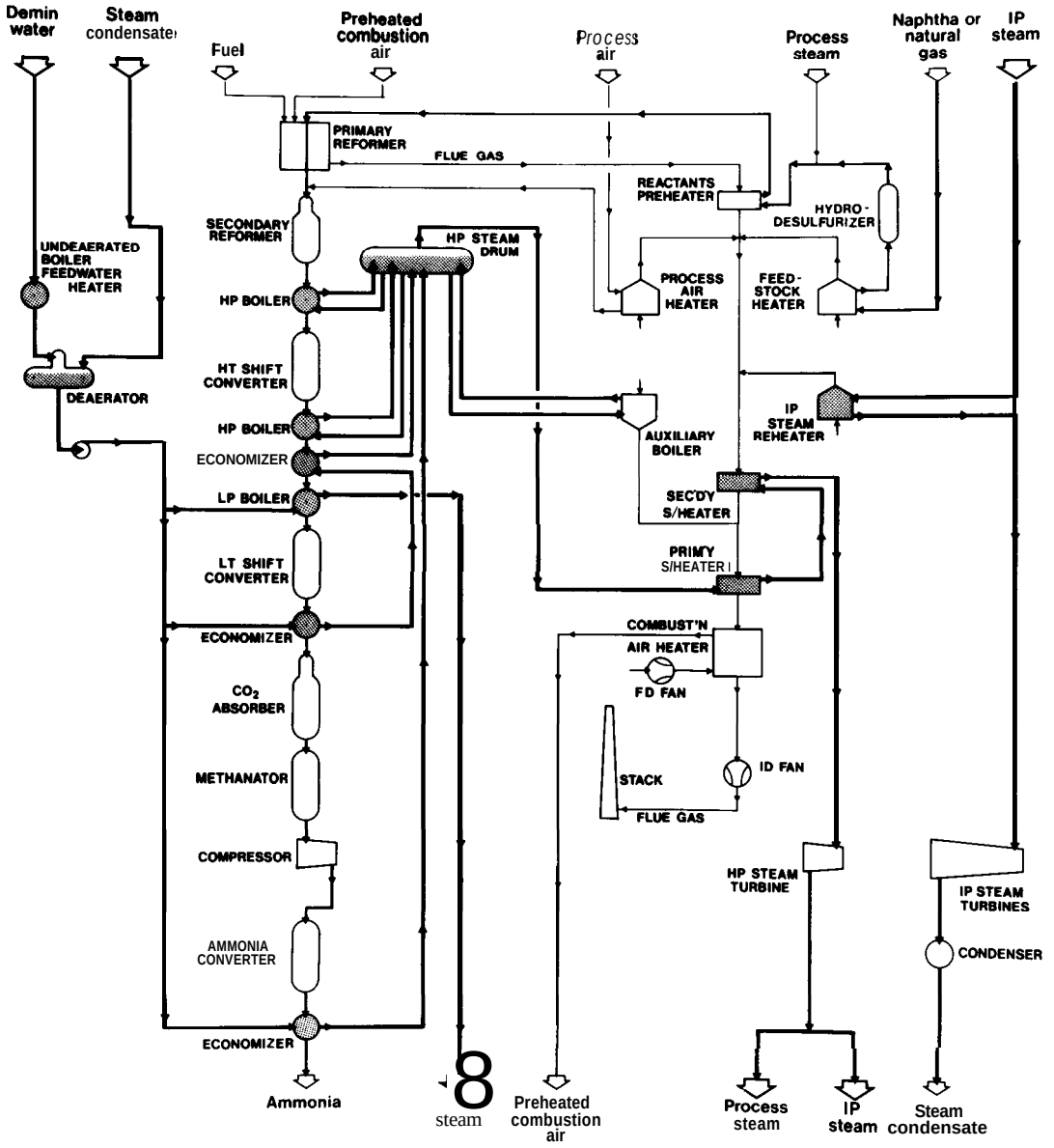

Figure 2 Steam generation flow diagram for a typical ammonia plant.

boilers that are connected to the steam drum by downcomer and riser pipes. There is a continuous circulation through these pipes with water flowing from the steam drum into the boilers and a mixture of steam and water leaving the boiler and entering the steam drum. This flow is maintained either by forced circulation using boiler circulating pumps or by natural circulation using the driving head arising from the difference in density between the water in the downcomer pipes and the steam/water mixture in the riser pipes. The steam is separated from the water in the steam drum, passes through a superheater and is then available for internal consumption or export. In Fig. 1 arrows indicate where heat is supplied, since it may come from the process gases or from flue gases depending on the particular process and flowsheet.

The way in which a waste heat boiler system may be integrated into a process is illustrated in Fig. 2, which shows the steam generation flow diagram for a typical ammonia plant.

References for Section 3.16.1 appear at the end of Section 3.16.4.

©1984 Hemisphere Publishing Corporation

3.16.2

Key aspects of the design and specification of individual items of plant

P. Hinchley

■ While the flowsheets that are developed for different processes vary enormously, they frequently contain items of equipment that are common to most waste heat boiler systems. This section highlights areas of importance in those items of equipment that have general application. It does not aim to deal in detail with special features or designs that have been developed purely for one process. The items are discussed in the order in which they occur in the process of producing steam rather than in order of difficulty.

A. Boiler feedwater treatment plant

The type of water treatment plant depends on the quality of the raw water, the steam generation pressure, and the heat flux at the steam generation surface of the boilers. The subject is very complex but useful background is given by Strauss [5] and quantitative standards are laid down by the VGB [6]. Nevertheless, the importance of the water treatment cannot be stressed too highly since a major proportion of boiler failures is linked with water problems. It is vital that the correct treatment processes are selected and that the plant management is provided, at an early date, with all information that is required for them to operate the plant correctly.

Allowable working ranges should be agreed on for key measurements such as pH, conductivity, and phosphate level, and provision should be made in the design for the continuous monitoring of these properties.

The experience of many companies is that it is not uncommon for acid or alkali breakthrough to occur. A frequent cause, in demineralization plants, is the failure to carry out an adequate final rinse at the end of the regeneration cycle of any of the ion exchange units.

There is some evidence to show that the risk of breakthrough is greater with manually operated plants and for this reason automated plants are preferred. In either case, an instrument should be installed in the treated water line which continuously measures the conductivity and which actuates a trip should the reading exceed a pre-set level. This trip should either dump the water to drain or trip the transfer pump thus ensuring that contaminated water never enters the treated water tank. The capacity of this tank should be generous, in order to allow time for locating and rectifying faults without shutting down the whole process.

Another common problem is the contamination of the return steam condensate, for example, by cooling water, as a result of leakage in the vacuum condensers. Provision should be made for the continuous monitoring of the conductivity of this and other return condensates and automatic dump facilities should be provided.

B. Undeaerated boiler feedwater heaters

Such heat exchangers are used on some plants to achieve maximum heat recovery by preheating the water that is fed to the deaerator, thus minimizing the use of low-pressure steam in the latter. Three features are of particular importance. The first is that care should be taken with their sizing and with their control system, in order to ensure that the water does not reach too high a temperature. If it approaches the saturation temperature of the water in the deaerator, then the normal pressure

© 1984 Hemisphere Publishing Corporation

control system of the latter will cut off or reduce the supply of steam to the deaerator and this will cause the performance of the latter to fall. If the deaerator is to operate at, say, 1 10°C, then the control system should bypass some of the heating gas, to ensure that the water entering the deaerator does not exceed, say, 85° C. This is particularly important at start-up or reduced load operation and these conditions must be carefully studied at the design stage.

The other item of importance is the choice of tubing for the exchanger. Carbon steel suffers serious corrosion pitting when subject to oxygen at the temperatures that occur in this type of exchanger. Copper is suitable from the point of view of waterside corrosion, but it might be attacked by the process gas. Stainless steel is another possibility but it is necessary to consider the risk of chloride stress-corrosion cracking. Clearly, each case requires separate consideration and sometimes the solution might be bimetallic or a stress-corrosion-resistant stainless steel.

The heating fluid should be at a lower pressure than the feedwater, since leakage of the former could introduce harmful chemicals into the boiler.

C. Deaerators

Deaerators are installed to reduce the level of oxygen in the boiler feedwater to a very low level, e.g., 0.005 ppm for a 100 bar boiler. A number of boiler feedwater heaters/economizers and boilers fail as a result of oxygen pitting [4]. Careful and thorough checking has shown that many proprietary deaerators fail to achieve their specified duties. In some cases this has been due to insufficient steam for oxygen stripping because the water supplied to the deaerator has been too hot for the reasons described above.

In other cases vacuum deaerators have been supplied and air has been pulled into the deaerator or its extraction pumps. Experience has shown that it is extremely difficult to prevent this ingress and for this reason pressure deaerators are preferred. On other occasions even pressure deaerators have not worked until improved means were adopted for stripping the oxygen from the water by the steam. Leading suppliers of deaerators to power stations have supplied similar designs for process plants and failed to recognize that the former have nearly 100% return condensate with little raw make-up water containing oxygen, whereas in the case of the latter the situation is nearly reversed. When subsequently they have recognized the problem, the required performance has sometimes been achieved by fitting a scrubbing section in the storage part of the deaerator which supplements the sprays, or sprays and trays, in the deaerator dome. A typical deaerator is shown in Fig. 1. The spray head, trays, and scrubber

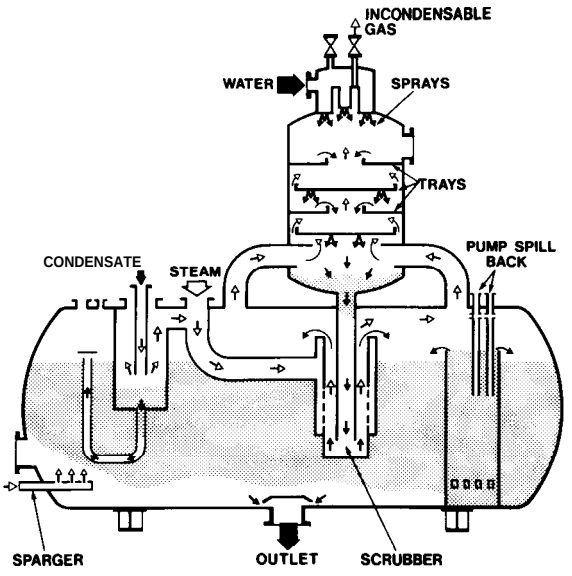

Figure 1 Deaerator.

should be made of stainless steel, but in the case of the upper pressure vessel it is often more economical to use epoxy-coated carbon steel. The storage vessel may not require such protection.

Careful design of the nozzles can minimize the vibration arising from the introduction of sparge steam during start-up and from the steam that flashes off from hot return condensate. Nevertheless, it is prudent to design a stiff support structure that is capable of absorbing any loads that arise from within the deaerator.

Clearly, care is required in the selection of the deaerator and it should be supplied with all-welded stainless steel sample lines which are used as soon as the plant goes into operation. Thus any shortcomings can be attended to before the pitting of other equipment becomes serious.

D. Boiler feedwater pumps

These, somewhat surprisingly, are rarely a cause of trouble. A number of manufacturers can supply reliable multistage pumps and their main stipulation is that the deaerator height and the water inlet system are chosen to avoid cavitation in the suction of the pump. Normally, at least two and sometimes three pumps are provided. Alternative sources of power are used. Frequently one pump is motor driven and the others are driven by turbine(s) supplied with steam generated in the boilers they serve. The standby pump should start-up automatically if the flow, or pressure, in the feedwater line falls below a pre-set figure. Each pump must be fitted with a leak-off system, back to the deaerator, to ensure that the pump is guaranteed a minimum flowrate, because at low or no

© 1984 Hemisphere Publishing Corporation

flow, a multistage high-head pump easily generates excessive pressure and heat, which would lead to rapid failure.

An important consideration for operational reliability is the stability of pumps running in parallel. Generally this leads to a requirement for the pumps to have a steep head-flow characteristic, e.g., a rise in head of 20% from normal to minimum flow.

E. Boiler feedwater heaters/economizers

These may take the form of a tube-in-shell exchanger in which the water is heated by process gas, or a tubular bundle over which flue gas or process gas passes. They are not a common cause of trouble unless corrosion takes place on the gas side as a result of the tube wall temperature dropping below the acid dew point. This can be avoided at the design stage by careful selection of tube material or by introducing a small heat exchanger which, by automatic control, ensures that the temperature of the water entering the boiler feedwater heater is above the acid dew point. Thus, for example, in a sulfuric acid plant it is possible to insert such an exchanger in the water space of the steam drum and an automatic three-way valve can divert sufficient water through this bundle to ensure that the temperature of the water entering the boiler feedwater heater is not less than, say, 130° C (Fig. 2).

The only general type of fault that can occur is when boiling takes place in an economizer not designed to generate steam. This can cause water hammer, vibration, and general disturbance to the boiler system. At the process flowsheet stage it is usually possible to avoid this risk by not aiming for too close an approach to saturation temperature in the economizer. If for any reason this is considered desirable to generate steam then a steaming economizer can be designed in which the steam/water mixture is arranged to flow upward through the bundle and into the steam drum, thus avoiding any high pockets where the steam can separate and give rise to hydraulic disturbance (see Fig. 2).

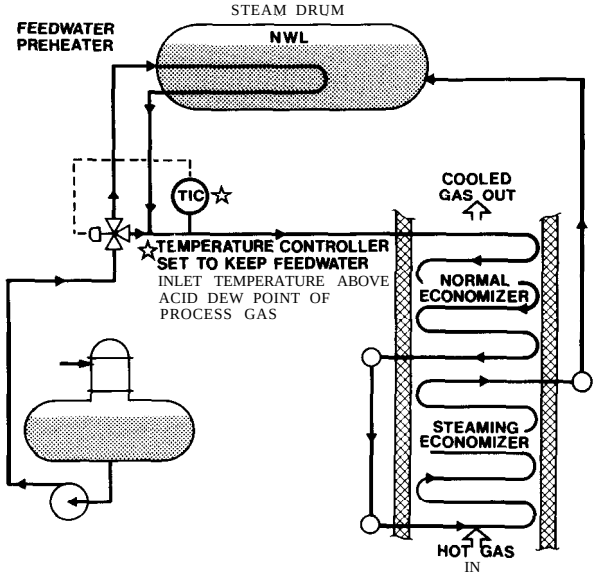

Figure 2 Arrangement of economizer.

F. Boilers/evaporators

Boilers or evaporators can be broadly split into two categories: watertube, in which the water/steam mixture is inside the tubes, and firetube, in which the heating gas in inside the tubes. In either case the boilers can be designed to operate on the forced or natural circulation modes described in the introduction. It is clear from my surveys [I, 4] that the boilers are potentially the most vulnerable items in waste heat boiler systems.

(a) Boilers heated by flue gas

When the heating fluid is flue gas, a watertube boiler is nearly always adopted since it is cheaper to keep the steam, which is at pressure, within small diameter tubes and contain the flue gas, which is normally slightly below atmospheric pressure inside a large refractory-lined or water-cooled enclosure. Two basic types of flue gas boiler are common. The one usually adopted by process contractors or vendors of fired heaters consists of large horizontal tubes through which the boiler water is pumped (Fig. 3). The tubes are typically 3-4 in nominal diameter (88.9-l 14.3 mm OD) and usually have extended-surface fins to enhance the heat transfer coefficient on the gas side, although in cases where the boiler is subject to direct radiation the first few rows of tubes are without fins. The other type is that usually adopted when the equipment is supplied by a boiler vendor. The evaporation usually takes place in relatively small diameter vertical tubes through which the steam/water mixture flows upward by natural circulation. The tubes are typically $1\frac{1}{2}$ in nominal diameter (48.3 mm OD) and are often attached to each other by flat strips to give a membrane wall construction that avoids the need for refractory lining of the radiant chamber. The installation shown in Fig. 4 consists of an auxiliary boiler whose exhaust flue gases join those from the furnace before passing over a superheater and an air preheater.

Vertical natural-circulation boilers are intrinsically more reliable than forced-circulation horizontal boilers. Nevertheless, the vast majority of horizontal boilers are reliable but there is a potential risk of dry-out which can cause severe corrosion of the crown of the tubes, if harmful chemicals are present in the boiler water or

© 1984 Hemisphere Publishing Corporation

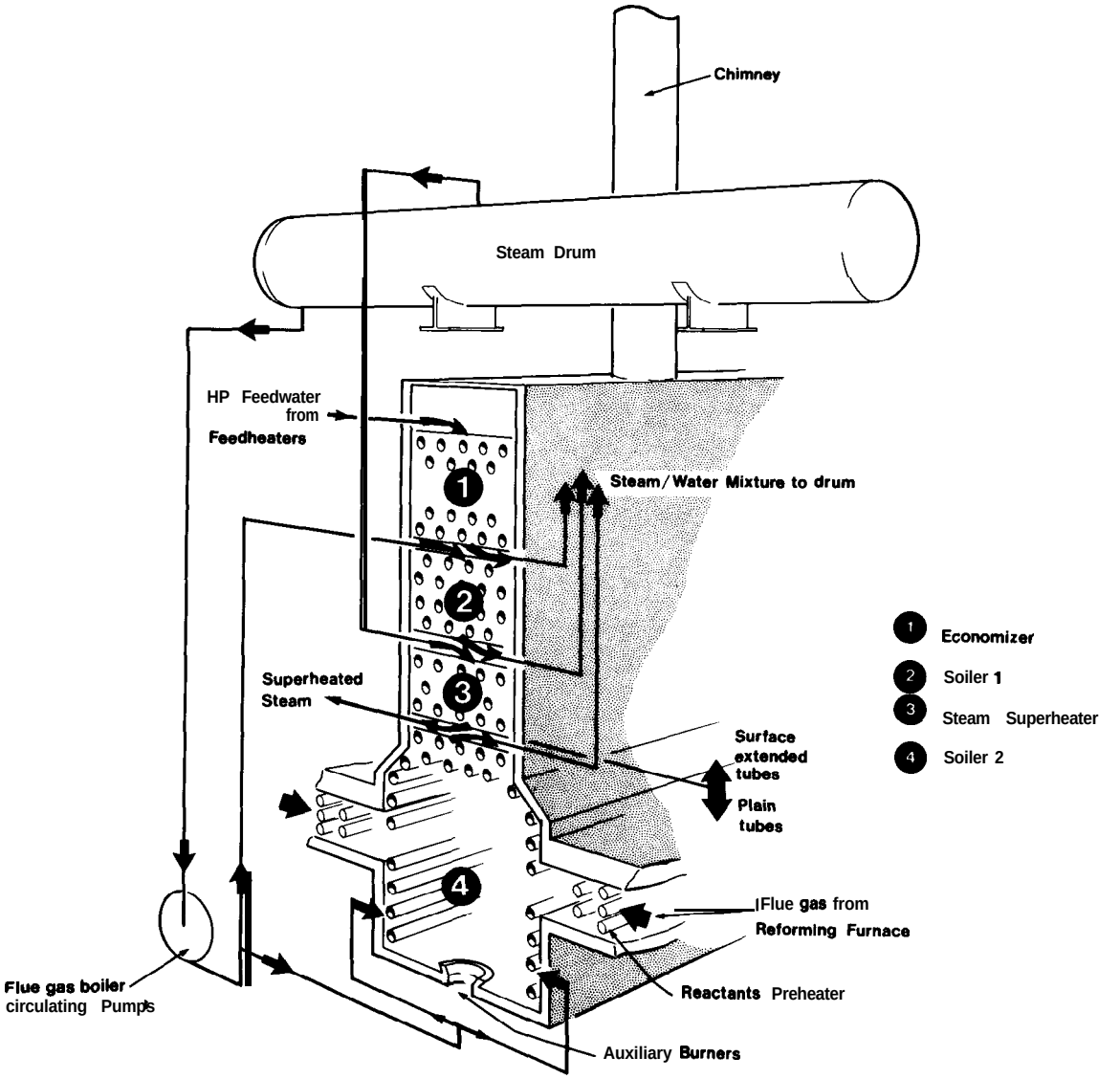

Figure 3 Horizontal forced-circulation boiler heated by flue gas.

overheating if the heat flux is enough. The subject has been covered in detail [4].

(b) Boilers heated by process gas

The design of boilers heated by process gas has attracted the interest of many clever engineers and there are many ingenious designs of boiler in operation on various processes [7-12]. The description and evaluation of these boilers is beyond the scope of this section. Nevertheless, it is appropriate to devote some space to them because they are potentially the most vulnerable items of equipment in the whole system.

In some cases the design of boiler has evolved with the process and is virtually standard (for example, the flat pancake watertube boilers used in nitric acid plants) (Figs. 5 and 6). Such boilers have raised as much as 50 t/h of steam at up to 60 bar and 450° C. Boilermakers new to this field have sometimes developed quite different designs but have experienced problems because of a lack of knowledge of the process. For example, the inclusion of porous insulation in the design has provided a site for the collection of humid oxides of nitrogen, which have turned into acid at plant shut-downs and caused corrosion of the inner liner leading to the ultimate failure of the shell and to corrosion of some evaporator tubes. Another example has been the nitrate stress-corrosion cracking that has occurred when the shell has not been fully stress-relieved.

In the oil gasification process a design of boiler that has become well-established is the submerged helical-coil smoke-tube boiler, which is capable of cooling high-pressure process gases from temperatures as high as 1500° C (Fig. 7).

© 1984 Hemisphere Publishing Corporation

In ethylene plants, there is a need to quench as quickly as possible the low-pressure high-temperature process gases leaving the cracking furnace. This is done in quench boilers, which operate at very high steam pressures (up to 100 atm) in order to maintain high tube-temperatures and thereby reduce the amount of deposition from the process gas. **Two** of the most common proprietary designs are the double-tube type described in [12] and shown in Figs. 8 and 9, and the special thin ribbed tubesheet design described in [10] and shown in Figs. 10 and 11.

The position is less clear with regard to the reformed gas boilers on plants that produce town gas, methanol, ammonia, and hydrogen. The importance of these can be judged from the fact that these boilers cool gas at pressures of around 30 bar from temperatures of up to 1000° C and that the largest of these generate 233 t/h of steam at 140 bar in a single vessel. Here there is a divergence of opinion: some of the plants currently being built incorporate fire-tube boilers whereas others incorporate one of the many types of watertube boilers that are available.

The typical arrangement of a large natural circulation fire-tube reformed gas boiler, generating steam at pressures in excess of 100 bar, is shown in Fig. 12. In order to reduce the stresses that arise due to the differential expansion between tube and shell, these boilers are often built in two compartments. This also has the advantage of easing the duty on the valves which are required in cases where the temperature entering the

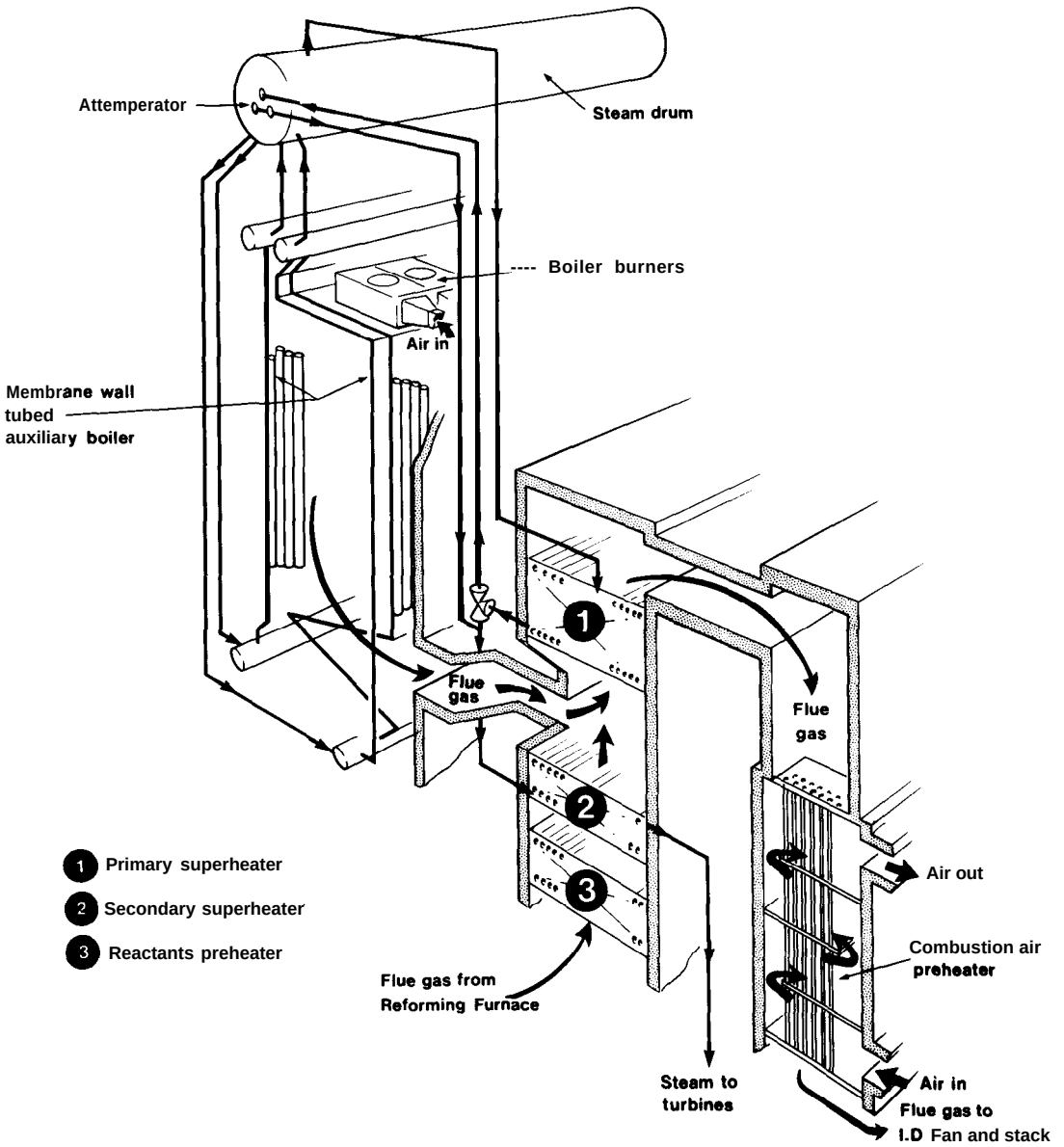

Figure 4 Vertical natural circulation auxiliary boiler associated with reformer convection section.

© 1984 Hemisphere Publishing Corporation

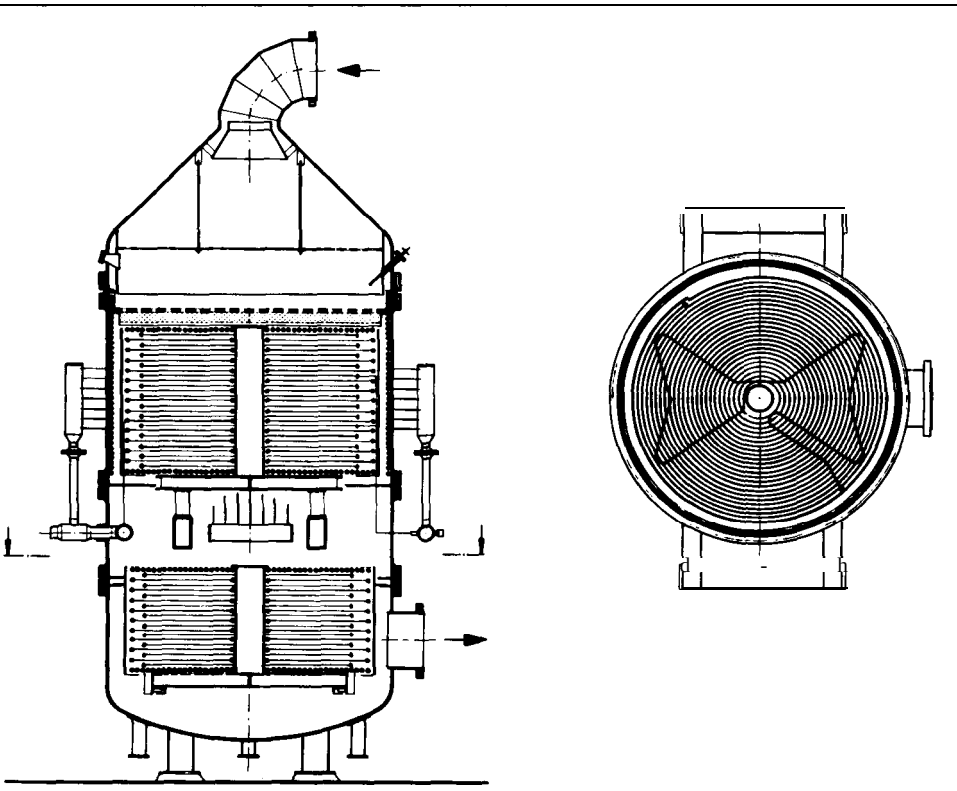

Figure 5 Arrangement of typical nitric acid plant waste heat boiler. Courtesy ofSteinmuller.

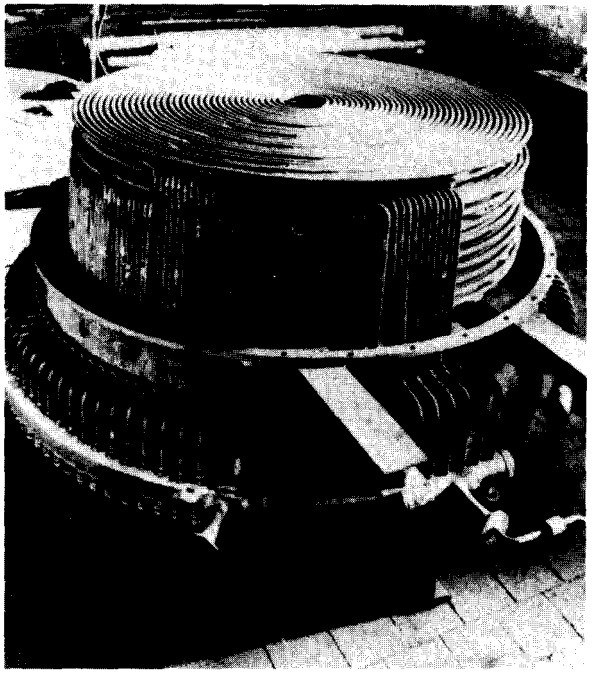

Figure 6 Typical elements of nitric acid plant boiler. Courtesy of Oschatz.

next reaction stage has to be controlled. Thus, the bypass valve, which may be internal or external to the boiler, has to contend with a gas temperature of only 600-650°C instead of 1000° C. Figure 13 shows one of the largest boilers of the two-compartment design so far built. The stiffened tubesheet design developed for quench boilers has now been widely accepted for reformed gas boilers. It is supplied in a single compartment.

The keys to success with fire-tube boilers are the adoption of a maximum heat flux which is reasonable having regard to the geometry and hydraulics of the boiler, the thorough understanding of the stresses in all parts of the boiler, the thermal protection of inlet tubesheet, the methods of attaching the tube to the tubesheet, and the tubesheet to the shell and the channel. Figure 14 shows one successful design for dealing with the last three points but various manufacturers have their own preferred ways of handling them. The author has a strong preference for the fire-tube boiler design since it is far less sensitive to dirt or debris left in the system or released from the walls of the system during plant upsets. The presence of a 100-150 mm thick layer of refractory inside the inlet channel results in a large untubed annulus on the shell side. Thus a large amount of dirt or debris could accumulate in the base of the boiler without building up on the heat transfer surface and without interfering with

©1984 Hemisphere Publishing Corporation

boiler circulation. This advantage disappears completely if the boiler is mounted vertically and the author is strongly opposed to the use of vertical firetube boilers even if, as in some cases, they have attractions from the point of view of plant layout.

Of the watertube reformed gas boilers that are built, the most common is the natural-circulation bayonet tube. This should not be taken as implying that it is the best boiler; it happens to be the design favored by the world s largest supplier of ammonia plants. The principal features of this type of boiler are shown in Fig. 15. The water from the steam drum enters the upper chamber and passes through the false tubesheet containing the bayonet tubes and at the bottom reverses and flows up through the annulus between the bayonet and scabbard tubes. The hot gas enters at the bottom of the vessel and flows across baffles and leaves at the top. The proponents of this design point out that the central downcomer tube is not heated and that the steam bubbles that are generated are required to flow upward only. This is basically a sound argument, although the

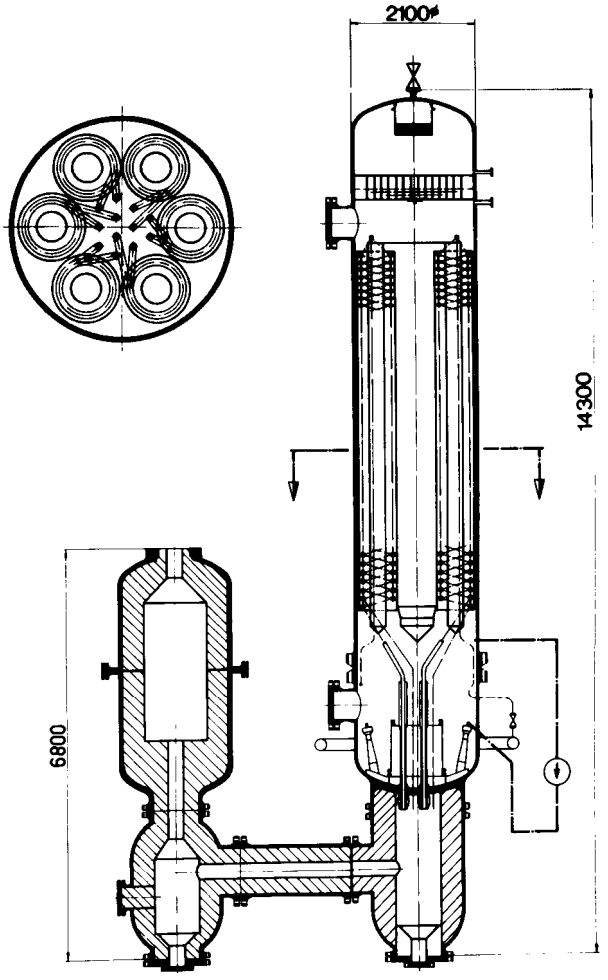

Figure 7 Arrangement of typical helical fire-tube boiler for gasification process. Courtesy of Steinmuller.

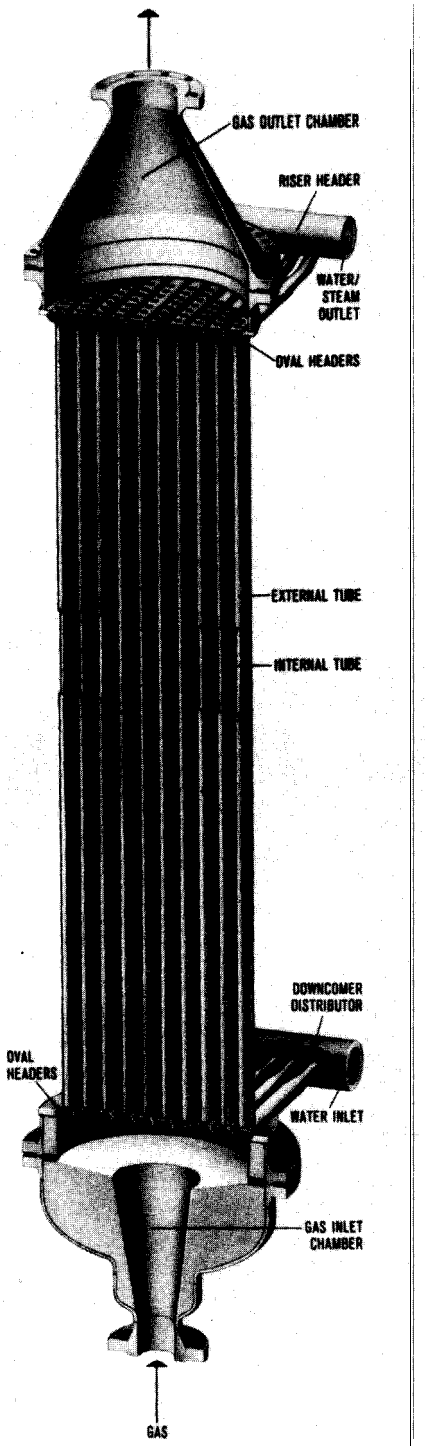

Figure 8 Arrangement of doubletube quench boiler for ethylene process. Courtesy of SHG.

details on some plants have caused reverse circulation to occur under certain circumstances and this has sometimes led to failures, There are others who argue that the vertical U-tube boiler used on many plants is equally satisfactory, particularly when circulation is ensured by

©1984 Hemisphere Publishing Corporation

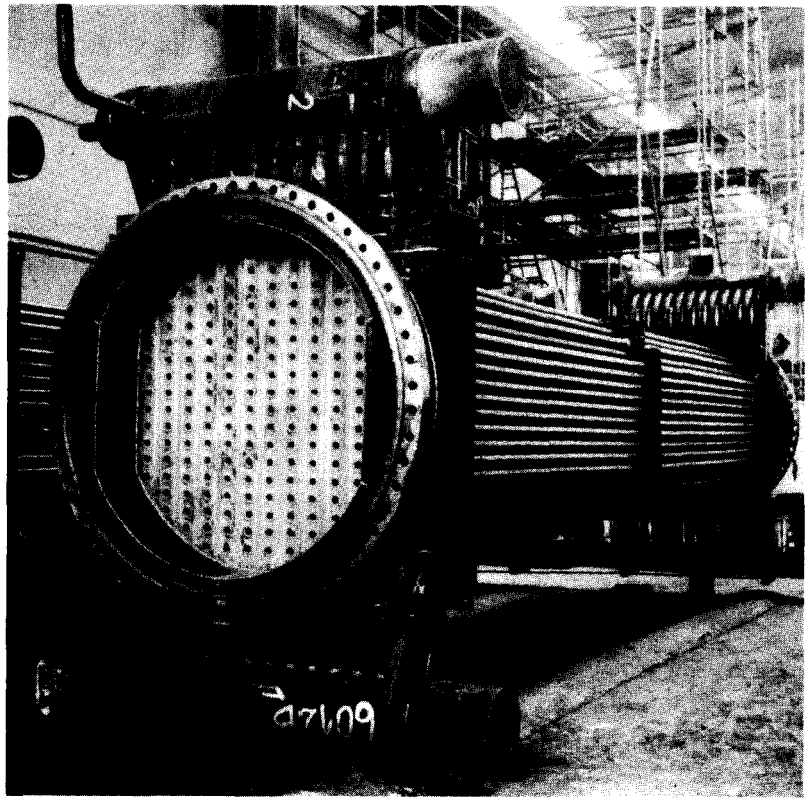

Figure 9 Double-tube quench boiler. Courtesy of SHG.

the use of forced circulation pumps. They also argue that the whole boiler duty can be achieved in a single exchanger whereas in the other design the bayonet-tube boiler is followed by a fire-tube boiler. Several boiler-makers have made two or three of their own designs of water-tube reformed gas boilers incorporating features which have special merit but which often add to the cost and complexity of the units.

Perhaps the boiler of most technical interest is the monotube boiler installed on a 1000 te/d ammonia plant in France shown in Figs. 16 and 17. This generates 137 t/h of steam at 152 bar in a single vessel. The installation is the most striking that the author has seen. The main reasons are that there is no large steam drum and associated structure, only a vertical separator which is little more than a pipe attached to the boiler; there are no risers or downcomers and there are no circulating pumps. Furthermore the whole duty is handled inside one shell; and temperature control is achieved by an internal arrangement thus avoiding hot gas piping. Further details are given by Silberring [11]. The fact that this boiler operated without trouble for many years does not imply that it is the most reliable water-tube boiler; it is more a tribute to the quality of control of the plant and particularly of the water.

Nevertheless, most of the water-tube reformed gas boilers have low points, where any debris can collect, in the zones of highest heat flux thus giving rise to the risk of corrosion or overheating of the type described in [4]. Furthermore, they are all likely to fail if poor pre-commissioning or a plant upset causes a significant blockage to flow at the inlet of one or more tubes. Notwithstanding these potential risks some users obtain reliable service from water-tube boilers. There is a significant point in favor of most designs of water-tube boilers: inadequate water treatment can lead to the rapid failure of the tubes of either a water-tube or a fire-tube boiler, and if a large number of tubes fail then a spare water-tube bundle can be fitted in quite a short time, whereas a fire-tube boiler would require a long time to retube or replace. Such major failures are rare, and if only a few tubes are affected they can be readily plugged off in either design.

G. Steam drums

The main purpose of a steam drum is to separate the steam from the steam/water mixtures that return from boilers but it also provides hold-up capacity of water to feed the boilers. In forced circulation water-tube boilers, the ratio of quantity of water circulating to that which is converted into steam may be as low as 4:1 whereas in a

© 1984 Hemisphere Publishing Corporation

natural circulation fire-tube boiler it is normally between 10: 1 and 20: 1. Thus the primary stage of separation is the coarse one of removing the bulk of the water from the steam. The second stage is the removal of water droplets from the steam. This stage is of vital importance if the steam is subsequently superheated and used in turbines. The dissolved solids in the feedwater concentrate up to a 100-fold in the boiler water, depending on the amount of blowdown or purge from the system, and as a result any boiler water carried over in the steam carries a high level of dissolved solids. The solids will be deposited in the superheater and some will build up on the heat transfer surfaces resulting in overheating and, in the limit, creep rupture failure. Some may deposit in the turbine and cause a lowering of efficiency. The most serious event that can occur is priming of the steam drum when there is bulk carryover of water due to a plant upset or loss of control. Not only does this have a severe effect *on* the superheaters but it can lead to failure of the steam turbines.

A common design aim in many boiler specifications is that the steam drum shall have a separation efficiency of 99%. This has little meaning, cannot be measured, and even if it were achieved it would be completely inadequate for most high-pressure boilers fitted with superheaters. It is better to state that the steam leaving the drum shall have a solids content of less than, say, 0.01 ppm of sodium. An isokinetic sample point should be provided in the steam line from the drum. This should be connected to a continuous analyzer fitted with high level alarms. The purity levels can usually only be achieved in the complex steam drums developed by leading boilermakers. Figure 18 shows such a drum, in which the primary separation is carried out in a large number of small cyclones and the final separation in packs of chevron pads. Knitted wiremesh pads are sometimes used and these are equally acceptable but the author is very suspicious of those who claim that the guaranteed purity can be achieved with simple baffles inside an ordinary pressure vessel.

Additional advantages accrue from the use of a steam drum from a specialist boilermaker. He usually has developed special designs for the uniform distribution of chemicals for water treatment, for the uniform removal

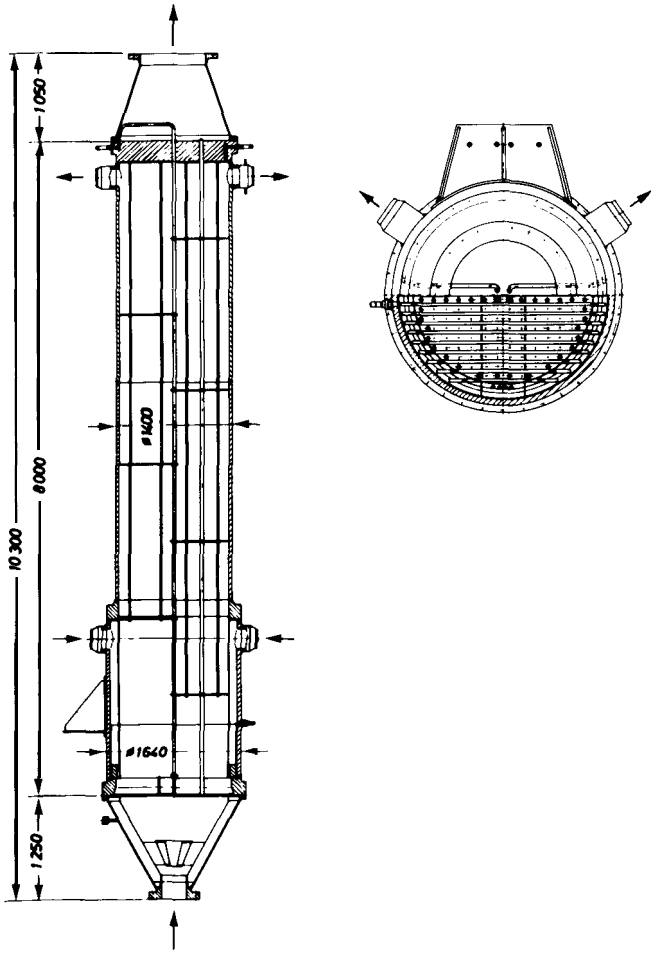

Figure 10 Arrangement of special thin tub&sheet quench boiler for ethylene process. **Courtesy** of Borsig.

©1984 Hemisphere Publishing Corporation
HEDH

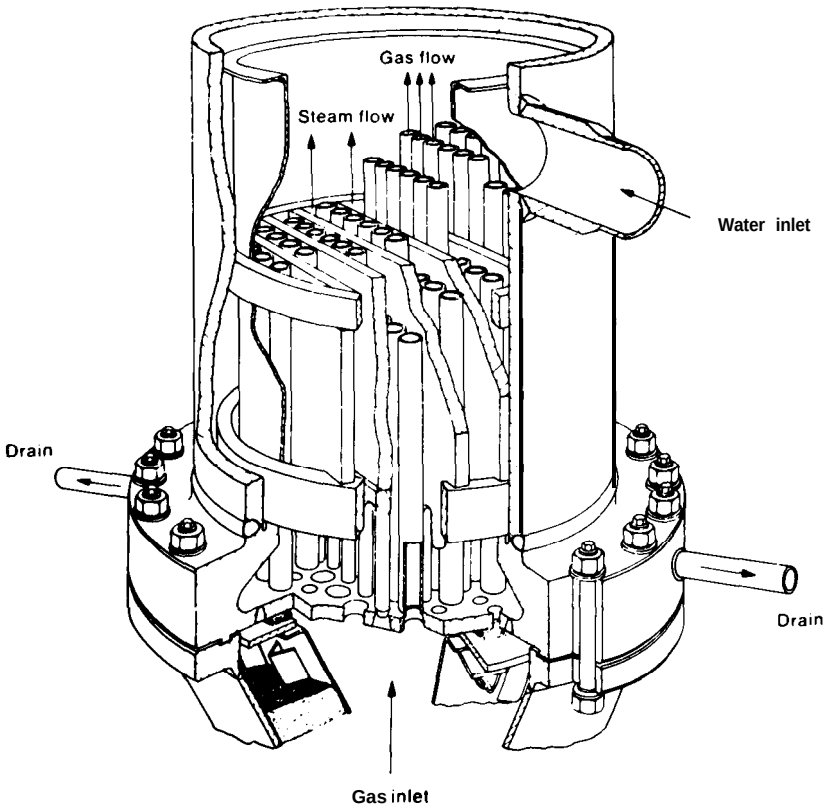

Figure 11 Arrangement of special stiffened design of thin tubssheet boiler. Courtesy of Borsig.

of blowdown water, and for the design of the downcomers to ensure that there is no underflow of the steam that could upset the circulation of the system or cause cavitation in boiler circulation pumps Nevertheless, experience shows that close liaison is necessary with the boilermaker to ensure that the standard design is modified, where necessary, to take account of any differences that arise in process waste heat boiler systems. In one particular case the boilermaker had selected the number of cyclones appropriate to the evaporation rate of his water-tube boilers and had completely overlooked the fact that with the natural circulation fire-tube boilers the quantity of water returning with the steam was several times greater. Not only were the cyclones seriously overloaded but the chambers enclosing the riser outlets were damaged, nuts came loose, and carry-over occurred on a massive scale. Another problem that has occurred, and caused failures, is reverse circulation in one or more boilers sharing a common steam drum. This arose because one of the boilers in the process was brought on load earlier than the others. The normal practice of allowing all risers to enter a common equalized chamber had been followed and the hydraulic head generated in the operating boiler had been sufficient to initiate reverse circulation in the cold boiler. This incident should not be taken as a reason for not continuing with the highly desirable practice of one common drum. The boilermaker, when made aware of the circumstances, can arrange the baffles to avoid the problem, albeit at the expense of some extra cyclones.

The final aspect of the steam drum concerns the maintenance of drum water level. If the size of the steam drum is arrived at on the basis of providing adequate space for the steam purifying equipment, then the hold-up capacity between the normal drum level and that of drum empty (i.e., exposed downcomer entry) may be only 1 or 2 min. This is probably inadequate when one bears in mind the many factors that demand the attention of the plant operators during the upset of a complex process plant. On nitric acid plants this is not a serious problem since the unit can be automatically tripped out before the level becomes dangerously low. However, on reforming plants, there is large heat capacity in the system, and flow through the reformers must continue in order to protect the catalyst. In these cases more hold-up capacity is desirable and process contractors usually provide at least 3 min capacity; users who have suffered boiler failures caused by loss of level sometimes specify 5 min. The cost of this extra capacity is not insignificant in large plants. An instrument for indicating water level which has recently become available is worthy of special mention, since it provides the

© 1984 Hemisphere Publishing Corporation

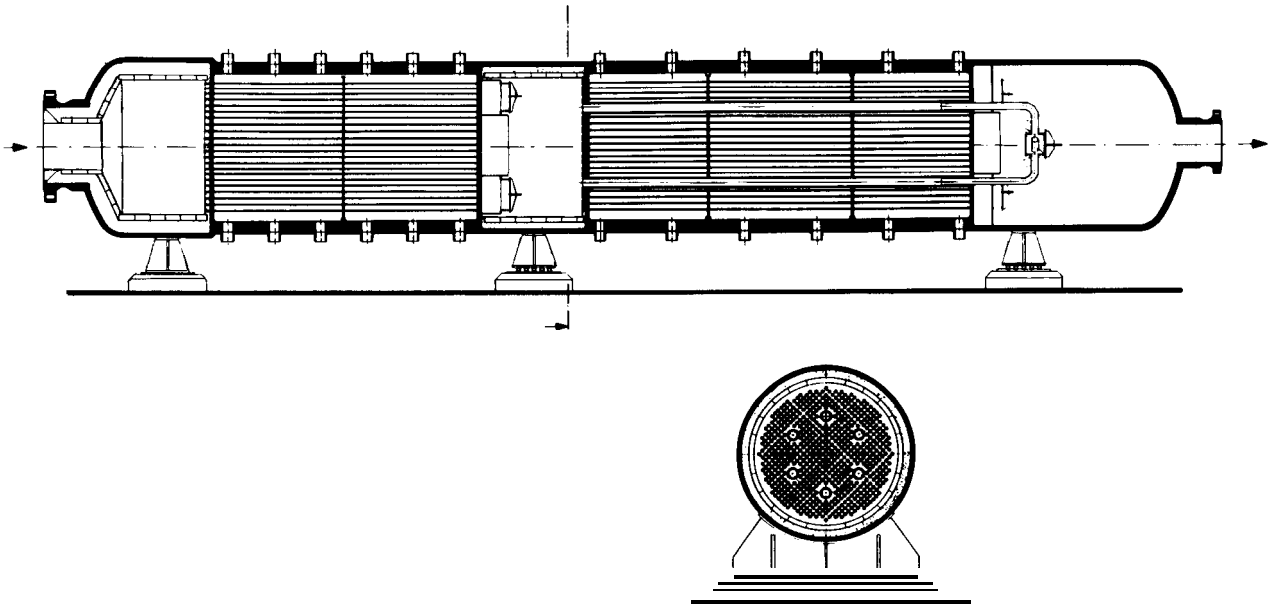

Figure 12 Arrangement of high pressure tired tube-sheet twin compartment reformed gas boiler. Courtesy of Steinmuller.

operators in the control room with such a vivid indication of the steam drum level that they are unlikely to overlook it, no matter how serious the nature of the process problems they are faced with. The device uses a stack of electrical conductivity cells that detect the difference in conductivity between steam and water [13]. The control room display has a similar stack of 20-mm square lights for each cell, glowing red for steam and green for water. The level should, of course, be controlled automatically, preferably with a three-element system with the primary control being of feedwater flow, reset by steam flow and drum level.

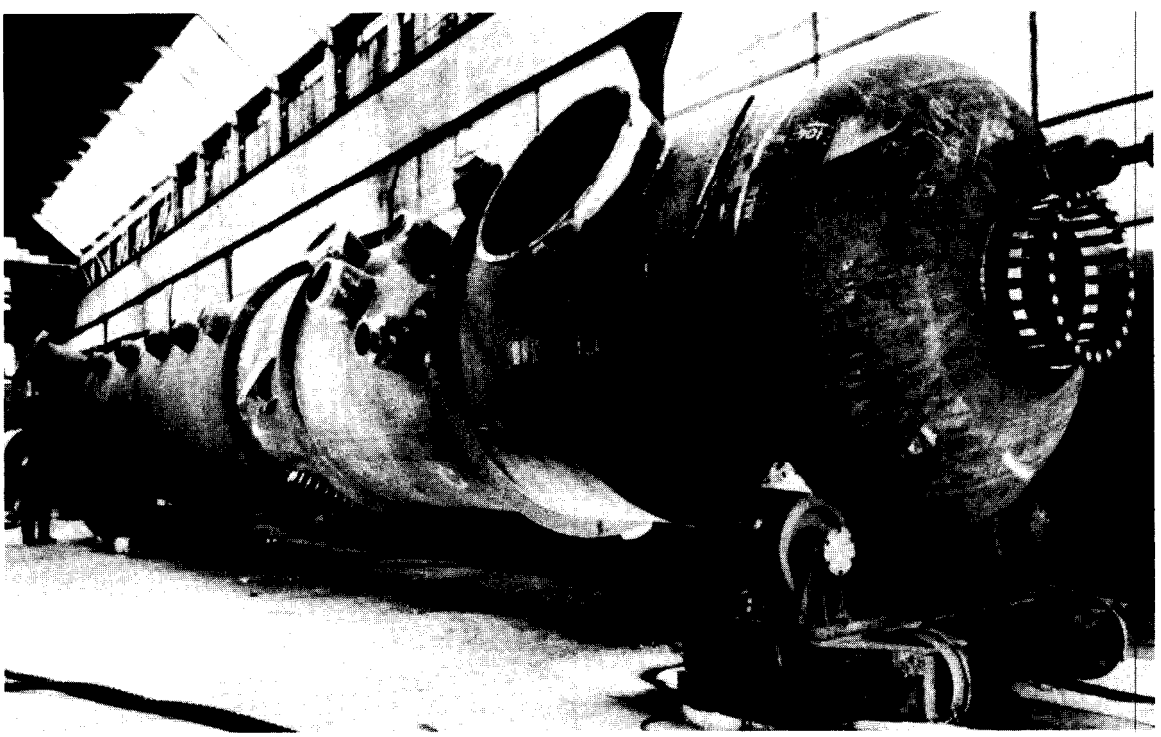

Figure 13 Fabricated twin compartment reformed gas boiler. Courtesy of Struthers-Wells.

©1984 Hemisphere Publishing Corporation

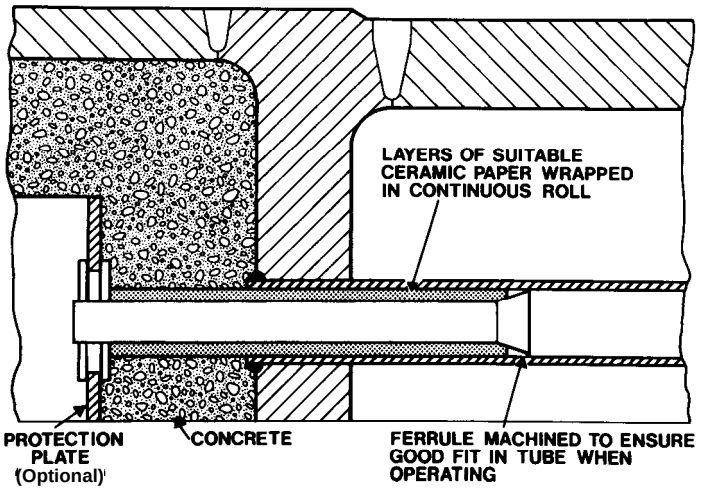

Figure 14 Some key features of a fiietube boiler.

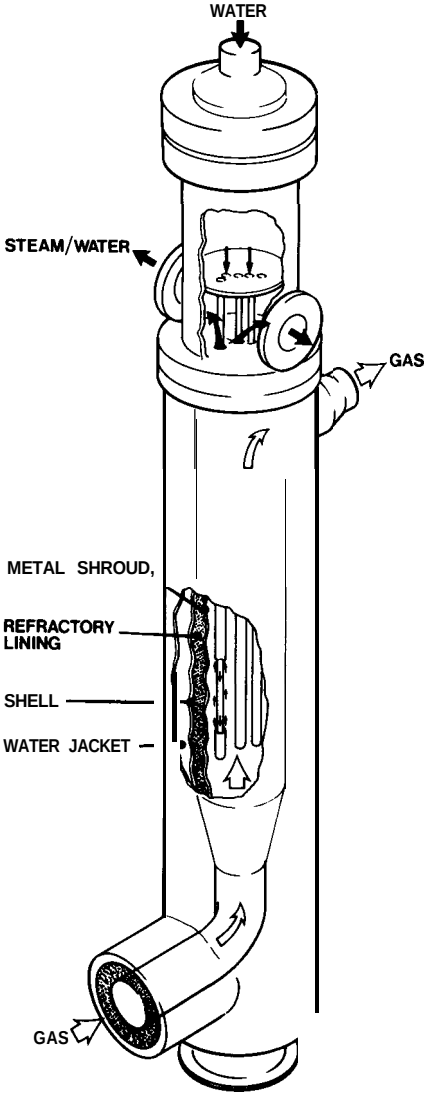

Figure 15 Bayonet-tube reformer gas boiler.

H. Superheaters and attemperators

Steam is usually superheated by contact with flue gas although it can be heated by process gases in plants that do not have any flue gas. In virtually all cases the steam flows inside tubes. In plants which are designed by boilermakers the tubes are usually typically $1\frac{1}{2}$ in diameter (48.3 mm OD) and in those designed by furnace vendors the tubes are more usually 3-4 in diameter (88.9 to 114.3 mm OD) and frequently have extended surfaces to enhance the outside heat transfer coefficient (see Fig. 3). The steam that leaves the drum at saturation temperature is heated up to temperatures as low as 300° C and as high as 540°C, with 460–480°C a more common figure. As can be expected, the smallest heat transfer area is obtained by heating the steam in counterflow with the hottest gases from the furnace or the reactor. This results in progressively higher metal temperatures in the superheaters and subjects the final rows to very severe conditions, particularly the final two which are likely to receive heat by radiation as well as by convection. The tubes in such a superheater are potentially vulnerable to creep rupture failure due to overheating if the gases are hotter than expected or if the steam flow is less than expected or if there are transient operational modes in which there is a mismatch between the flue gas rate and the rate of steam production. In some designs an attempt is made to minimize these effects by the insertion of one or two rows of evaporator tubes to shield the superheater. A more sophisticated approach for plants, in which the risks described above are real, is shown in Fig. 19. The superheating duty is divided between a primary superheater and secondary superheater. The former, which heats the saturated steam from the drum is in normal counterflow. The secondary superheater is in co-current flow with the

© 1984 Hemisphere Publishing Corporation

hotter flue gas. In cases where calculations show that the steam temperature would still vary excessively under certain operating conditions, then an attemperator can be installed to control the steam outlet temperature by cooling part of the steam from the primary superheater

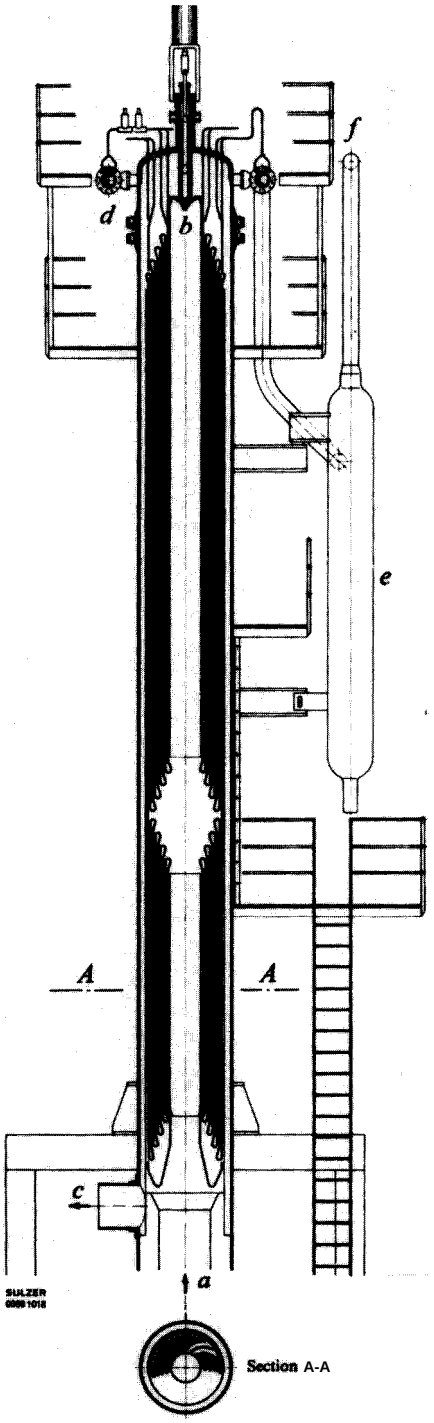

Figure 16 Arrangement of monotube reformed gas boiler. (a) Gas inlet; (b) gas temperature control valve; (c) gas outlet; (*d*) feedwater inlet; (e) water separator; (*f*) saturated steam outlet. Courtesy of CCM-SULZER.

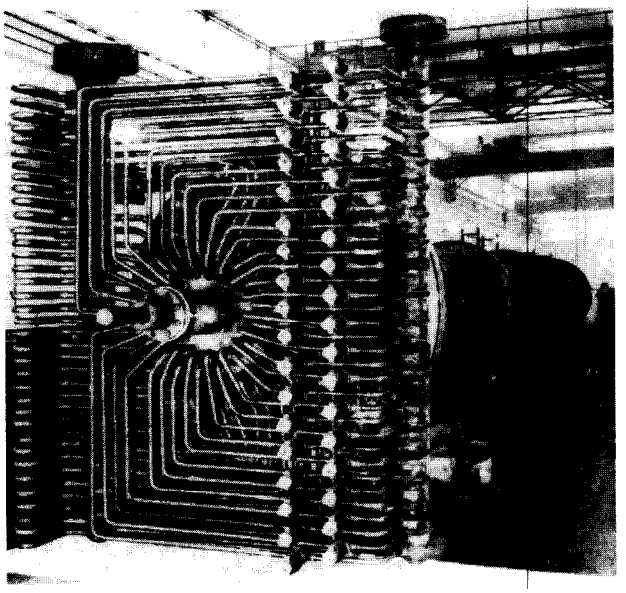

Figure 17 Fabricated tube bundle of monotube boiler. Courtesy of CCM-SULZER.

in the manner shown in Fig. 19. This is most easily accomplished in a drum attemperator which consists of heat exchanger bundles situated in the water space of the steam drum. A controlled amount of steam is cooled by evaporating water in the drum.

As well as the above precautions, for design purposes an additional margin of say 50° C should be provided on top of the predicted long-term metal temperatures in order to cover unforeseen happenings such as solids carry-over from the drum, stratification of hot gas and some of the happenings described in Sec. G. This margin is not sacrosanct and should be reviewed if, for example, it leads to a very large increase in cost because it requires a change from ferritic to austenitic steel in the tube bundle.

This general approach to the design of superheaters should also be applied to any process heaters that are included in the flue gas duct.

I. Combustion air heaters

Brief mention must be made of combustion-au heaters, since they are a common feature of flue-gas streams of waste-heat-boiler systems. If the fuel is natural gas, then no problems should be expected, and the user can install an air preheater of the type shown in Fig. 4. \$or large plants, the capital cost of the air preheater can be reduced significantly by using the rotary type, but this saving has to be balanced against the slightly increased risk of unreliability brought about by the introduction of moving parts and the additional running costs arising from air leakage across the seals. Another alternative

©1984 Hemisphere Publishing Corporation

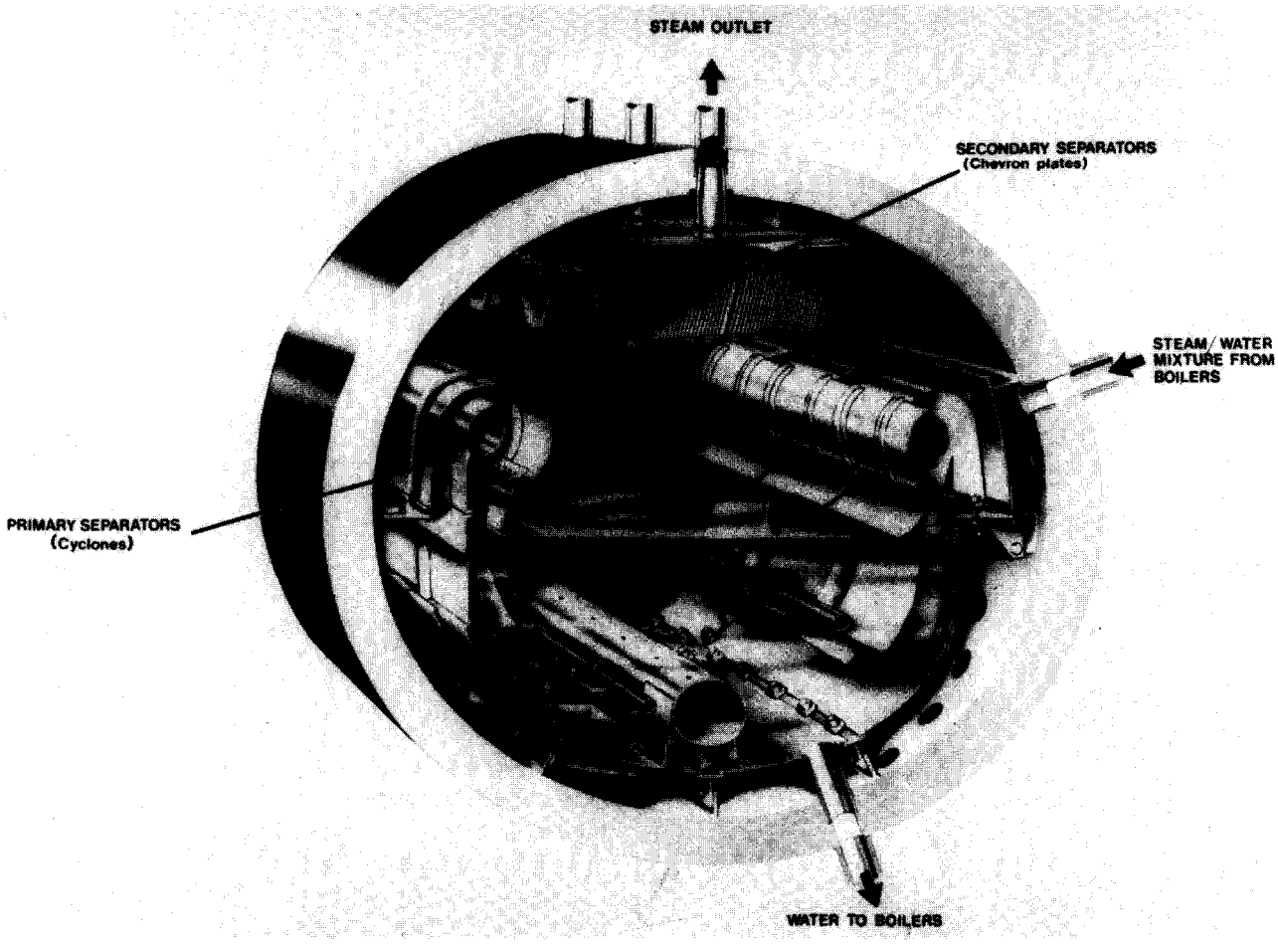

Figure 18 Internals of a steam drum designed to produce steam of high purity. Courtesy of Foster Wheeler.

that warrants an economic evaluation is a design that uses internally and externally finned cast-iron tubes. The various alternatives are described. illustrated and discussed in [14].

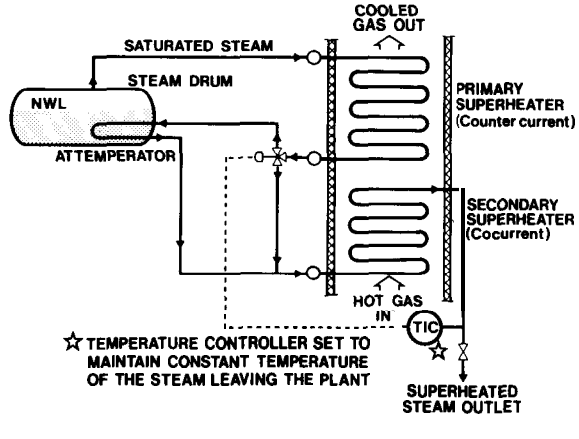

Figure **19** Arrangement of superheater system that maintains constant outlet steam temperature while minimizing metal temperatures.

If the fuel contains sulfur then more care is required. Glass tube has been successfully used in the coldest passes of tubular air heaters. In the case of rotary air heaters a small steam-heated section is often used to preheat the inlet air by the amount necessary to keep the main heater above the acid dew point.

J. Forced and induced draft fans

An induced-draft fan is installed on virtually all modern furnaces. In many cases, in order to achieve maximum heat recovery, the combustion air is preheated by the flue gas and a forced-draft fan is required to overcome the pressure losses in the combustion air preheater and in the burner windbox.

Many of the earlier plants incorporating such equipment had their outputs limited by the capacity of the forced-draft or induced-draft fans. The burners may have required more air to achieve their duty and furthermore that duty may have been underestimated and consequently the forced draft fan could not supply that amount of air without being increased in size.

©1984 Hemisphere Publishing Corporation

The problem was often worse in the case of the induced-draft fan because the additional quantity of flue gas was increased still further by air leakage into the furnace and its convection section. Clearly it is desirable to introduce some margins and suggested figures are 10–20% on the forced-draft fan rate and 15–25% on the induced-draft fan rate. It is important when specifying the fan duty to ensure that this increased flow is achieved with pressure losses appropriate to the increased flow. This, of course, leads to a much larger driver and it may be economic to supply a variable-speed drive or inlet guide vanes on the fans to minimize the power consumption should the plant be found not to need the margins built into them.

Obviously the introduction of the fans could lead to a decrease in reliability of the plant. In the opinion of the author the desired reliability is best obtained by installing one high-quality fan rather than by duplicating basic fans.

References for Section 3.16.2 appear at the end of Section 3.16.4.

© 1984 Hemisphere Publishing Corporation

3.16.3

Detailed mechanical design and fabrication of equipment

P . Hinchley

■ It is inappropriate to discuss the detailed mechanical design and fabrication of each of the many items of equipment in a complex waste heat boiler system, but their importance should not be underestimated. The author [1, 4] has highlighted costly failures that have arisen as a result of poor detailed design and bad workmanship. Frequently companies use their best engineers to perform the conceptual and basic design and pass on the execution of the contract without managing to convey the importance to and requirement of the plant for special quality. The client should take steps to ensure that this does not happen and prior to the order the main contractor should lay down protedures for submission for approval of detailed designs, Welding procedures, quality control schedules, manufacturing procedures, protection, and shipping instructions and should arrange to supplement the internal inspection by external inspectors as appropriate. These comments apply equally well to site fabrication where there is probably even greater need for continuous close scrutiny of the quality of workmanship including, in particular, the welding.

References for Section 3.16.3 appear at the end of Section 3.16.4.

©1984 Hemisphere Publishing Corporation

3.16.4

Precommissioning of waste heat boiler systems

P . Hinchley

A. Objective

The object of the precommissioning is to ensure that when the boiler system goes into service it is free from debris, scale, and corrosive products and that all the metal surfaces are covered in a uniform tightly adhered layer of magnetite. It is desirable to have the feedwater system cleaned in a similar manner to prevent the carriage of scale and debris into the steam-generation circuits.

B. Provision for cleaning at the design stage

The general approach to the cleaning processes should be established at a very early stage so that the design of the equipment and piping that are to be cleaned incorporates the required piping connections and access for inspection and physical removal of debris. All too often this is not the case and late and costly alterations are made to the piping and undesirable compromises are accepted.

Piping connections should be provided and sized to achieve an optimum cleaning velocity over the heat transfer surfaces (e.g., about 0.3 m/s for 5% hydrochloric acid solution). Where there are several boilers in parallel, provision may need to be made for cleaning each boiler separately.

The total system to be cleaned should be critically examined to establish where dirt and debris will collect during cleaning and provisions should be made for its physical removal. In the case of fire-tube boilers the blowdown pipes in the bottom annulus can be attached to a removable pad and in the case of some water-tube boilers a mud pot can be provided on the bottom of the distribution manifolds.

C. Cleanliness during manufacture and construction

Equipment should be supplied in a clean dry condition and in some cases should be shipped under a blanket of nitrogen. Those involved in construction should be made aware of the need to take special care over cleanliness and should be warned that if they were to leave behind only one foreign body, then in operation it could restrict the flow of water and cause a boiler failure, particularly if it is of water-tube design. Prefabricated sections of piping for the system should be cleaned mechanically to remove millscale. Wire-brushing even by power tools is seldom a satisfactory method of descaling but high pressure water jets can remove a significant proportion of the scale. Alternatively, grit blasting can be used.

Cleanliness is an important aspect of inspection of equipment prior to dispatch from the manufacturer s works, after its receipt on site, and of the inspection of the whole assembled system prior to hand-over to the commissioning staff.

D. Planning the chemical cleaning procedure

A detailed plan of the cleaning procedure must be drawn up and agreed to between the cleaning contractor and client, and there must be supervisors from both parties who know every detail of the program. A careful check should be made to ensure the pumps that the contractor proposes to use are capable of achieving the rate

© 1984 Hemisphere Publishing Corporation

corresponding to the optimum cleaning velocity, taking into account the resistance in the circuits. A suitable spare pump must always be available.

E. Cleaning operations

A typical procedure for the chemical cleaning of an important system operating under arduous conditions is outlined below.

Stage 1. Flush out to remove loose material at a water velocity equal to or greater than that which will occur in service.

Stage 2. Alkaline degrease for 24 h at 95-100°C using 1 000- 1500 ppm by weight of trisodium phosphate and a suitable detergent.

Stage 3. Acid clean using 5% inhibited hydrochloric acid at 75-85°C. This continues until the total iron content in the circulating system has reached a definite plateau, typically 0.3-0.4 g/l.

Stage 4. Citric acid flush using a 0.2% solution.

Stage 5. Passivate using ammoniated hydrazine solution at 95-100°C for 24 h.

Stage 6. Drain system and dry thoroughly.

In the case of the plant illustrated in Fig. 4, a special step was introduced between Stages 2 and 3. For a period of nearly 2 d water was circulated while tests were carried out to check, by contact flowmeter [15], that each of the membrane tubes in the auxiliary boiler had a similar flow rate and that in particular none was blocked.

F. Storage

If the boiler system is not held under the correct conditions after cleaning then much of the passivation can be lost within a few days. The system can be stored wet if filled with ammoniated hydrazine solution, or dry using dehumidified air or nitrogen. The use of dehumidified air allows access to the system for further work or inspection, without costly, time-consuming purging, and drying.

REFERENCES FOR SECTIONS 3.16.1-3.16.4

1. Hinchley, P., How to Avoid Problems of Waste Heat Boilers, *Chem. Eng.*, vol. 82, pp. 94-98, Sept. 1, 1975.
2. Appl, P., and Feind, K., Troubles with Thin Tube Sheet Waste Heat Boilers, *AIChE, Ammonia Plant Safety,* vol. 18, pp. 113-121, 1975.
3. Sawyer, J. G., and Williams, G. P., Causes of Shut Downs in Ammonia Plants, *AIChE Safety in Air and Ammonia Plants,* vol. 14, pp. 62-68, 1971; What Causes Ammonia Plant Shut Downs, *AIChE Safety in Air and Ammonia Plants,* vol. 16, pp. 4-9, 1973.
4. Hinchley, P., Waste Heat Boilers: Problems and Solutions, *Chem Eng. Prog.,* vol. 86, pp. 90-96, 1977.
5. Strauss, S. D., Water Treatment, *Power,* pp. Sl-S24, June 1973.
6. Neue Richtlinien fur das Kesselspeisewasser und das Kesselwasser von Dampferzeugern, VGB *Kraftwerkstechnik,* no. 2-52, pp. 167-172, Apr. 1972.
7. Becker, J., Examples for the Design of Heat Exchangers in Chemical Plant, *Verfahrenstechnik,* vol. 3, no. 8, pp. 335-350, 1969.
8. Kummel, V. J., Abhitze und Sonderkessel in der chemischen und petrochemischen Industrie, *Chem. Ing. Tech.,* vol. 49, nos. 6-5, pp. 475-479, 1977.
9. Capitaine, D., and Stoffels, J., Der Einsatz von Abhitzekesseln und einige Konstructionsmerksmale, *Mitt. VGB,* vol. 49, no. 3, pp. 165-173, 1969.
10. Deuse, K. H., Waste Heat Boilers in Large Plants, *Het Ingenieursblad,* 40E Jahrgang, no. 21, 1971.
11. Silberring, L., Waste Heat Recovery in Ammonia Plants, CPE-Heat Transfer Survey 1969, and Energetische Probleme der Ammoniak-Erzeugung, *Chem. Ing. Tech., vol. 43,* no. 12, pp. 71 l-720, 1971.
12. Knulle, H. R., Problems with Exchangers in Ethylene Plants, *Chem Eng. Prog.,* vol. 68, no. 7, pp. 53-56, 1972.
13. Hasler, E. F., and Martin, R. E., Hydrastep: A 'Fail Operative Gauge System to replace Visual Boiler Water Level Gauges, *Meas.* Control, vol. 4, pp. 366-371, Dec. 197 1.
14. Berman, H. L., Fired Heaters-IV: How to reduce your fuel bill, *Chem. Eng.,* vol. 85, pp. 165-169, Sept. 11, 1978.
15. Roughton, J. E., Detection of Boiler Tube Blockages. Experience with CERL Contract Flowmeter, *CEBG Digest,* pp. 7-10, May 1973.

© 1984 Hemisphere Publishing Corporation

3.17
Fouling in heat exchangers

Contents

3.17.1
OVERVIEW AND SUMMARY, James G. Knudsen **3.17.1-1**

A. Definitions 3.17.1-1
B. Importance of fouling 3.17.1-3
C. Preview of chapter 3.17.1-5

3.17.2
TYPES OF FOULING, James G. Knudsen **3.17.2-1**

A. Types of fouling according to mechanism 3.17.2-1
B. Types of fouling by process type 3.17.2-3
C. Types of fouling by industry 3.17.2-4

3.17.3
ANALYSIS OF THE FOULING PROCESS, James G. Knudsen **3.17.3-1**

A. Processes involved in fouling 3.17.3-1
B. Mechanism of deposition and removal 3.17.3-l
C. Variables influencing fouling 3.17.3-2

3.17.4
FOULING CONTROL MEASURES, James G. Knudsen **3.17.4-1**

A. Introduction 3.17.4-1
B. Fouling control measures: Design and operation 3.17.4-1
C. Fouling control measures: Fluids treatment 3.17.4-3

3.17.5
CLEANING OF HEAT EXCHANGERS, James G. Knudsen 3.17.5-1

A. Mechanical cleaning 3.17.5-1
B. Chemical cleaning 3.17.5-2

3.17.6
MEASUREMENT OF FOULING RESISTANCES, James G. Knudsen **3.17.6-1**

A. Constant heat flux devices 3.17.6-2
B. Constant wall temperature devices 3.17.6-2
C. Liquid-liquid devices X17.6-2

3.17.7
RECOMMENDED FOULING RESISTANCES FOR DESIGN, James G. Knudsen **3.17.7-1**

A. Recommended fouling resistances 3.17.7-2
B. TEMA fouling resistance 3.17.7-5

References for Sections 3.17.1-3.17.7 3.17.7-6

© 1984 Hemisphere Publishing Corporation

HEDH

3.17.1
Overview and summary

James G. Knudsen

A. Definitions

The term fouling refers to the deposition of material on a heat transfer surface, usually resulting in an increase in the resistance to heat transfer and a subsequent loss of thermal exchange capacity of the heat transfer equipment. In practice, some fouling usually occurs in most heat exchangers, and in some it becomes a predominant resistance. It is therefore necessary for the designer to estimate the probable magnitude of the fouling resistance as well as means by which it may be reduced. Once fouling is accepted as unavoidable, design steps must be taken to provide for periodic shutdown and cleaning of the equipment. In some cases, provisions for cleaning may be the dominating factors in heat exchanger design.

Since 1960 considerable progress has been made in understanding the fouling process; however, this has not resulted in significant improvement in the ability of the designer to predict fouling resistances. Evidence of increased interest is noted in the rapidly expanding literature on fouling and the number of conferences and reviews on the subject. Sources of information on fouling include the pioneering papers of Taborek et al. [1, 2] and Epstein [3, 4] as well as those of Hasson [5] and Knudsen and Roy [6] and the proceedings of several conferences and seminars devoted to the subject [7–39]. These references constitute an excellent source of the extensive literature on fouling that has appeared in the past 20 yr. In addition, the quarterly journal ***Fouling Prevention Research Digest*** began publication in 1979 [40–43] and is available by subscription.

(a) Fouling resistance

Sizing of heat exchangers is based on the heat duty and the temperatures, properties, and flow rates of the hot and cold streams. This information is used to determine the individual heat transfer coefficients in the equation for the overall heat transfer coefficient:

$$\frac{1}{U_1} = \frac{1}{\alpha_1} + R_{f1} + \frac{x}{\lambda_w}\frac{A_w}{A_2} + \left(\frac{1}{\alpha_2} + R_{f2}\right)\frac{A_1}{A_2} \qquad (1)$$

The overall heat transfer coefficient is used in the heat exchanger equation to determine the required surface area:

$$\dot{Q} = UA\ \mathrm{AT},,, \qquad (2)$$

where $\dot{Q}$ = heat transfer rate

A = surface area on which U is based

AT, = log mean temperature difference between sides 1 and 2

Equation (1) defines the ***fouling resistance.*** The quantities R_{f1} and R_{f2} are thermal resistances, which are included in series along with all the other resistances encountered as heat flows through a heat exchanger wall from a hot fluid to a cold fluid. Fouling may occur on either or both sides of the heat transfer surface. It is usually not possible to determine the individual values of R_{f1} and R_{f2}, even under conditions of known local heat flux, wall temperature, and known values of α_1 and α_2. Therefore fouling resistances for operating heat exchangers are reported as a single value $R_f (=R_{f1}+R_{f2})$. Usually, the fouling characteristics of the fluids are

© 1984 Hemisphere Publishing Corporation

HEDH

known, and often only one fluid is the major contributor to the fouling resistance. The fouling resistance R_f is frequently called the fouling factor. However, this is misleading, since R_f is not a factor by which something is multiplied but is a resistance to heat transfer with appropriate units of m^2 K/W (h ft^2°F/Btu).

(b) Deposition and removal rate

The process of fouling of a heat transfer surface involves the deposition of material onto the surface. Such deposition causes an increase in the resistance to heat transfer and often causes a significant increase in friction loss as well. As the deposit becomes thicker, and depending on its physical strength, a certain amount of material may be removed from the surface and re-entrained in the flowing stream. The following equation expresses the rate of change of the fouling resistance as a function of the deposition rate ϕ_d and the removal rate ϕ_r (m^2 K/sW) (ft^2 °F/Btu).

$$\frac{dR_f}{dt} = \phi_d - \phi_r \tag{3}$$

Fouling is a dynamic process. The fouling resistance changes with time in a manner determined by the deposition rate and the removal rate.

(c) Fouling resistance-time curves

Equation (3) can be represented as a fouling resistance-time curve, as shown in Fig. 1. The shape of the curve is indicative of the phenomena occurring during the fouling process.

A linear relationship is generally characteristic of tough, hard, adherent deposits and indicates that the deposition rate is constant and there is no removal or that the deposition rate minus the removal rate is constant. A falling rate or asymptotic curve may be obtained even though there is no removal, due to retardation forces that increase as the deposit builds up.

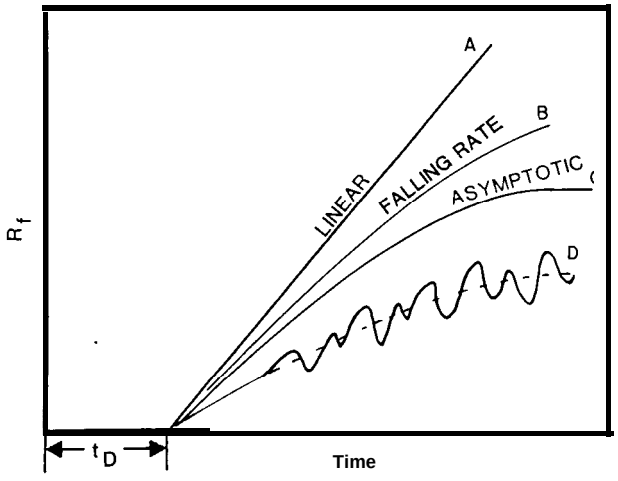

Figure 1 Typical fouling resistancetime curves.

An asymptotic curve is generally characteristic of soft or fragile deposits, which flake off easily due to the shearing force of the fluid flowing past them. This behavior can be obtained if the deposition rate is constant and the removal rate is proportional to the thickness of the deposit. This assumption leads to a simple exponential equation.

However, asymptotic behavior may result from other variations of the deposition and removal rates. The deposition rate may decrease with increasing deposit thickness to the point where essentially no deposition occurs.

The falling rate behavior shown by the intermediate curve in Fig. 1 may result from a falling deposition rate or from a falling deposition rate and an increasing removal rate. While the fouling resistance-time curve may be of great value to the designer, one must be careful in interpreting the curves with respect to describing the mechanisms that occur. The fouling curve is the result of a combination of deposition and removal, which are very complex and often interrelated processes.

Curve D is occasionally observed with commercial cooling tower water [1, 2] and seawater. The sawtooth configuration is brought about by periodic changes of conditions (such as periodic treatment) and occurs when a buildup of the deposit is suddenly removed. The cycle continues, resulting in the sawtooth pattern.

Occasionally, particularly with new surfaces, a delay time t_D is observed before deposition occurs. During this time nuclei are forming on the surface; as their population grows, gross deposition occurs and creates resistance to heat transfer. During this period, an enhancement of heat transfer is frequently observed due to increased roughness of the surface as nucleus formation proceeds.

(d) Cleanliness factor

The amount of fouling that has occurred in a heat exchanger that has operated for a period of time is often expressed in the power industry in terms of a cleanliness factor. This factor represents the ratio of the overall heat transfer coefficient U_F for the fouled condition to that for the clean condition, U_C. Thus if CF is the cleanliness factor

$$\text{CF} = \frac{U_F}{U_C} \tag{4}$$

CF is a function of the same parameters as R_f.

The overall coefficients U_F and U_C must be compared with each other at constant conditions of flow

© 1984 Hemisphere Publishing Corporation

and temperature; that is, the individual coefficients α_1, α_2, and x/λ_w making up the overall coefficients must be the same in both cases. These are often difficult conditions to meet in industrial environments; therefore, at least the liquid fluid flow rates should be the same for U_F as for U_C. If U_F and U_C are compared for condensers or reboilers, the condensing temperature and/or boiling temperature must be the same for U_F and U_C.

From Eq. (1) it may be shown that for the same α_1, α_2, and x/λ_w

$$R_{f1} + R_{f2} = R_f = \frac{1}{U_F} - \frac{1}{U_C} \tag{5}$$

Combining Eqs. (4) and (5),

$$R_f = \frac{1}{U_C}\left(\frac{1}{\mathrm{CF}} - 1\right) = \frac{1-\mathrm{CF}}{U_C(\mathrm{CF})} \tag{6}$$

For a clean heat exchanger, CF is, of course, unity.

B. Importance of fouling

(a) Design and operation

The incentive for the increased attention to fouling of heat exchangers over the past two decades is certainly economic. In an era of inexpensive energy and material, the crude method of estimating fouling resistance was satisfactory even though considerable excess surface was specified in the exchanger.

Fouling deposits are usually poor conductors of heat, and as they accumulate on the heat transfer surface there is a reduction in the performance and efficiency of the heat exchanger. The designer of a heat exchanger must specify sufficient surface to accomplish the desired heat transfer, using a certain fouling factor. The practice is to incorporate the fouling resistances as part of the overall coefficient. To show the effect of fouling, expressions can be developed relating the total fouling resistance R_f and the overall heat transfer coefficient for the clean exchanger, U_C, to the surface area A, the temperature difference AT, or the heat duty $\dot{Q}$. Usually the designer is given temperatures and heat duty. Holding these constant and varying the fouling resistance has the following impact on surface area:

$$\frac{A_F}{A_C} - 1 = U_C R_f \tag{7}$$

where A_C = area required for a clean exchanger

A_F = area required for an exchanger with a fouling resistance of $R_f (=R_{f1}+R_{f2})$

Equation (7) is plotted in Fig. 2.

After the exchanger has been designed and built, the area cannot be changed. The mode of operation determines the effect that fouling will have. If the mode of operation is with a constant temperature difference, then as fouling deposits occur the heat duty will decrease according to:

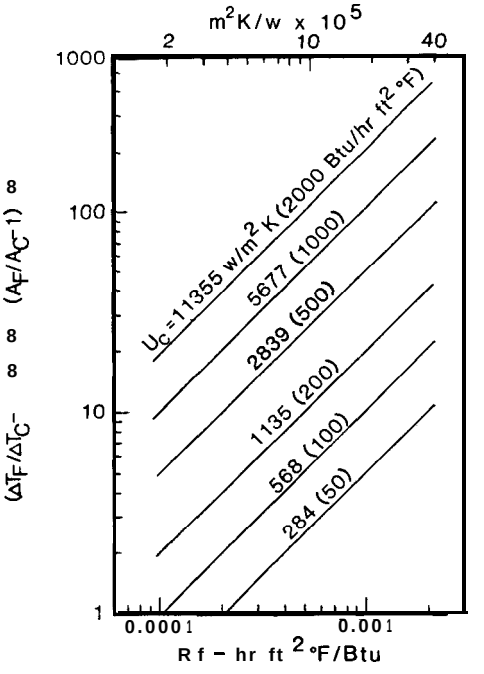

Figure 2 Effect of fouling resistance on surface area (design) and temperature driving force (operation at constant heat duty).

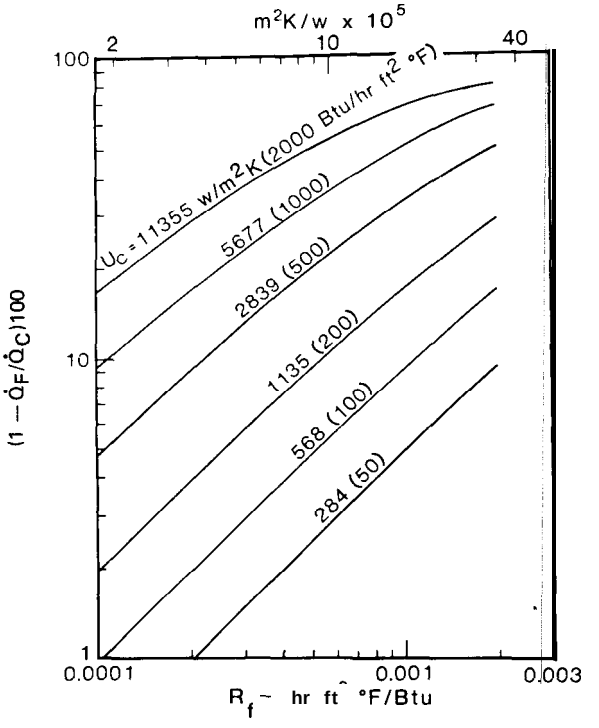

Figure 3 Effect of fouling resistance on heat duty (operation at constant temperature driving force).

© 1984 Hemisphere Publishing Corporation

$$1 - \frac{\dot{Q}_F}{\dot{Q}_C} = U_C R_f (1 + U_C R_f) \quad (8)$$

where $\dot{Q}_C$ = heat duty of the clean exchanger

$\dot{Q}_F$ = heat duty when the fouling factor is R_f

Equation (8) is plotted in Fig. 3. A second mode of operation is with a constant heat flux, such as would occur in nuclear reactors and electrically heated heat exchangers, As fouling occurs in this mode of operation, the overall temperature difference increases according to:

$$\frac{\Delta T_F}{\Delta T_C} - 1 = U_C R_f \quad (9)$$

where ΔT_C = temperature difference for the clean exchanger

ΔT_F = temperature difference for the exchanger with a fouling resistance of R_f

Equation (9) is plotted in Fig. 2.

As the overall coefficient becomes larger the effect of fouling becomes more significant. Table 1 shows typical values of the effect of fouling resistance for several applications.

Example

A typical overhead condenser has the following individual coefficients:

Cooling water inside tubes:

$\alpha_i = 2\ 840\ \mathrm{W/m^2\ K}$ (500 $\mathrm{Btu/h\ ft^{2\circ}F}$)

Condensing hydrocarbon outside tubes:

$\alpha_o = 2\ 840\ \mathrm{W/m^2\ K}$ (500 $\mathrm{Btu/h\ ft^{2\circ}F}$)

The tubes are mild steel, 0.019 1 m OD, 0.001 65 m wall (0.75 in OD, 16 BWG wall). There is no fouling on the condensing side, but the water-side fouling resistance is considered likely to become 0.000 35 $\mathrm{m^2}$ K/W (0.002 $\mathrm{h\ ft^{2\circ}F/Btu}$). Determine the overall coefficient for the exchanger based on the outside area and the percentage of the total resistance assignable to each resistance. The thermal conductivity of mild steel is 45 W/m K (26 $\mathrm{Btu/h\ ft\ ^\circ F}$).

From the information above,

$$\frac{A_o}{A_i} = \frac{0.019\ 1}{0.019\ 1 - 2(0.001\ 65)} = \frac{0.019\ 1}{0.015\ 8} = 1.21$$

$$A_w = \frac{0.019\ 1}{0.5(0.019\ 1 + 0.015\ 8)} = 1.09$$

(A_w = average of inside and outside areas for thin-walled tube)

Substituting into Eq. (1)

$$\frac{1}{U_o} = \frac{1}{2\ 840} + \left(\frac{0.001\ 65}{45}\right) 1.09 + (0.000\ 35)(1.21) + \frac{1}{2\ 840}(1.21) = (3.52)(10^{-4}) + (4.00)(10^{-5}) + (4.26)(10^{-4}) + (4.26)(10^{-4}) = (1.24)(10^{-3})\ \mathrm{m^2\ K/W}$$

Thus U_o = 804 $\mathrm{W/m^2\ K}$ (142 $\mathrm{Btu/h\ ft^{2\circ}F}$)

The resistances are allocated as follows:

Outside coefficient	3.52×10^{-4}	28.3%
Wall	4.00×10^{-5}	3.3%
Fouling resistance	4.26×10^{-4}	34.2%
Inside coefficient	4.26×10^{-4}	34.2%
Overall coefficient	1.24×10^{-3}	100%

The fouling resistance is 34% of the total resistance.

(b) Cost of fouling

The quantitative effects described above are reflected in additional materials, fabrication, installation, and energy costs. Lost production and cleaning are additional costs involved when plant shutdown is required for cleaning of fouled heat exchangers.

Table 1 Effect of fouling resistance on heat exchangers for a fouling resistance of 0.000 528 $\mathrm{m^2}$ K/W (0.003 h $\mathrm{ft^{2\circ}F/Btu}$)

Typical application	Overall coefficient for clean exchanger, W/m* K ($\mathrm{Btu/h\ ft^{2\circ}F}$)	Percent change in area or temperature difference, $(A_F/A_C - 1)\ 100$ or $(\Delta T_F/\Delta T_C - 1)\ 100$	Percent change in heat duty, $(1 - \dot{Q}_F/\dot{Q}_C)100$
Gas-gas exchanger	57 (10)	3	2.9
Liquid-gas exchangers	170 (30)	9	8.3
Water-cooled overhead condensers	1420 (250)	75	42.8
Water-cooled steam condensers	4 260 (750)	225	69.2
Ocean thermal energy conversion (OTEC) condensers	8 520 (1500)	450	81.8

© 1984 Hemisphere Publishing Corporation

There have been estimates of the economic cost of fouling. Thackery [7] placed the overall annual cost of fouling in the United Kingdom at 300 to 500 million pounds (approximately $1 billion). In a study based on the case histories of specific refinery units, Van Nostrand et al. [10] estimated fouling-related costs for the United States to be $1.4 billion annually.

Clearly, the cost of fouling is significant. A thorough economic analysis is not possible in either the design phase or the operational phase unless the fouling resistance-time relation is known. Crittenden and Khater [11] showed that, if the fouling transient can be predicted, the optimum number of plant shutdowns per year may be determined by balancing investment costs against plant cleaning costs and loss of revenue during shutdown. Epstein [12] derived an analytic expression for maximum production, minimum cost evaporation cycles based on the Hasson-Reitzer scale formation equation. The analytic relations are complicated but can be replaced by a simple graphic procedure.

Fouling also has a significant effect on power plant design and economics. The effect of a given fouling resistance on the heat transfer duty of a condenser is relatively easy to determine. However, in a power plant the output capability and thermal efficiency are strongly dependent on the performance of heat exchange equipment. Curlett and Impagliazzo [34] made a detailed analysis of a power plant and determined the effect of condenser tube fouling on the performance of the plant. Parameters such as water temperature rise, approach temperature, and water velocity were considered. The differential evaluated cost of the heat rejection system was $5 million (1978 present worth of revenue requirements) for a 600-MW hypothetical coal-fired power plant when the fouling resistance increased from a base value of 4.4×10^{-5} to 1.8×10^{-4} m² K/W (0.000 25 to 0.001 h ft² °F/Btu). Differential costs of $12 million were estimated when the fouling resistance reached 3.5×10^{-4} to 4.4×10^{-4} m² K/W (0.002 to 0.002 5 h ft² °F/Btu).

C. Preview of Sections 3.17.2-3.17.4

The following Sections (3.17.2-3.17.4) are devoted to a detailed discussion of the fouling phenomenon, fouling control measures, cleaning of heat exchangers, measurement of fouling resistances, and recommended fouling resistances for design. Generic types of fouling are discussed as well as types encountered in various processes and industries. Fouling is analyzed according to the processes that bring about deposition onto and removal from a heat transfer surface. Fouling control measures that can be exercised during the design and construction phase are discussed, as well as those that can be used during on-line operation (fluid treatment) or off-line periods (cleaning during shutdown). A section is devoted to the techniques used to measure fouling resistances. The final section is a discussion of some recommended fouling resistances and of what is available to the designer.

Nomenclature for Section 3. I 7. I appears at the beginning of Part 3. References appear at the end of Section 3.17.7.

© 1984 Hemisphere Publishing Corporation

3.17.2
Types of fouling

James G. Knudsen

A. Types of fouling according to mechanism

(a) Precipitation (crystallization) fouling

This type of fouling involves crystallization of dissolved material in the flowing fluid and occurs whenever the fluid becomes supersaturated with respect to the depositing material. Inorganic salts can show normal solubility (solubility increasing with temperature) or inverse solubility (solubility decreasing with temperature). Figure 1 shows the solubility of calcium sulfate with both inverse and normal solubility behavior. If a liquid containing an inverse solubility salt is in contact with a heated surface at such a temperature that it becomes supersaturated, crystallization will occur on the surface. Nuclei will form and a deposit of the inverse solubility salt will occur. Under these conditions the deposit (particularly if it is a pure material) will be hard and adherent. Occasionally, the bulk temperature of the flowing liquid is such that the liquid is supersaturated. Crystallization will then occur throughout the bulk liquid, and deposition will occur on the surface both by crystallization and by deposition of crystal nuclei from the flowing stream. In this instance, the deposit may be softer and more friable.

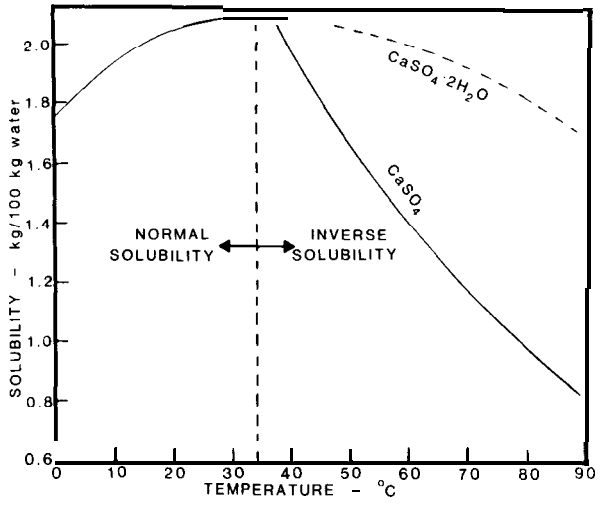

Figure 1 Solubility of calcium sulfate [45].

When precipitation fouling involves the deposition of inorganic salts from water it is called *scaling*. This type of fouling mostly involves sparingly soluble inverse solubility salts such as calcium carbonate, calcium sulfate, various forms of calcium phosphate, calcium and magnesium silicate, calcium and magnesium hydroxide, sodium sulfate, and lithium sulfate and carbonate in water [4]. Reviews of precipitation fouling have been given by Epstein [4], Troup and Richardson [44], Hasson [13], and Bridgewater [8].

Fouling by normal solubility salts is not as common as fouling by inverse solubility salts, but it does occur. Deposits high in silica (which occur in geothermal brines) will precipitate on a cold surface [4]. Nucleation and deposition will occur for any normal solubility salt when it is in contact with a surface that is sufficiently cold to bring about supersaturation of the solution.

Precipitation fouling can occur in cooling water systems, desalination systems, boilers, geothermal systems, food processing systems, and black, liquor evaporators.

© 1984 Hemisphere Publishing Corporation

(b) Freezing fouling

Freezing fouling is the solidification of a pure liquid in contact with a subcooled heat transfer surface or the deposition of a high-melting-point constituent of a liquid in contact with a cold heat transfer surface. A vapor may also deposit in solid form on a surface without passing through the liquid phase. The deposit is often of low density and provides a high resistance to heat transfer. Bott [14] reviewed freezing fouling and classified the overall problem of freezing into three main areas: (1) cooling and subsequent freezing of boiling liquids, (2) cooling of mixtures of related substances such as a wide range of paraffin hydrocarbons, and (3) cooling of gaseous mixtures, some components of which will condense and freeze (humid air).

Freezing fouling is a complex process, particularly in complicated geometries. In simple geometries it can be subjected to mathematical analysis and the extent of fouling can be predicted. Deposits can be removed by increasing the temperature of the heat transfer surface to a value above the melting temperature of the deposit, although it is not always convenient or possible to do this.

(c) Particulate fouling

Particulate fouling is the accumulation of particles from a fluid containing suspended solids. A comprehensive review of this mode of fouling has been presented by Gudmundsson [15]. Particulate fouling occurs in a variety of processes. Boiler waters and reactor coolants contain corrosion products. Cooling tower waters contain particles carried into them by air and corrosion products (iron oxides and hydroxides). Gaseous streams are often heavily laden with dust particles, which deposit out on heat transfer surfaces. Particles in the form of inorganic salts can be present due to supersaturation of the liquid somewhere in the circulation system.

(d) Chemical reaction fouling

This type of fouling occurs when chemical reactions take place at a heat transfer surface and the solid products of reaction are deposited on the surface. The reaction is often polymerization and results in the formation of high-molecular-weight materials. Chemical reaction fouling can occur in any streams that are prone to react at a heated surface. Corrosion fouling may be catalyzed by some solid surfaces or corrosion products. Petroleum hydrocarbon streams and food product streams are outstanding examples of streams susceptible to chemical reaction fouling.

Froment [16] reviewed fouling of heat transfer surfaces by coke formation in petrochemical reactors and discussed thermal cracking of heavy hydrocarbons. Lund and Sandu [17] presented a thorough review of the chemical reaction fouling of streams encountered in food processing.

(e) Corrosion fouling

Corrosion fouling is due to the chemical reaction of containment materials (including heat transfer surfaces) with the circulating process stream. Somerscales [35] distinguishes between two types of corrosion product fouling. In one type the fouling is a result of corrosion products formed at locations remote from the heat transfer surface and transported to and deposited on the heat transfer surface. This type is more appropriately classed as particulate fouling or ex situ corrosion fouling. Lister [18] has reviewed aspects of this type of corrosion fouling. The second type, in situ corrosion fouling, is due to corrosion products that form and remain at the heat transfer surface.

(f) Biofouling

Biofouling (biological fouling) results from the development on the heat transfer surface of an organic film consisting of microorganisms (microbial biofouling) and their products, or from the deposition and growth of macroorganisms such as barnacles (macrobial biofouling). Biofouling can usually be controlled with proper treatment in cooling systems, but its control in once-through seawater or river systems is much more difficult. There is considerable interest in biofouling. The Condenser Biofouling Control Conference [25, 26] was concerned with control of biofouling under new effluent guidelines that mandated lower concentrations of residual chlorine in effluent streams. There is always a tendency for biofouling to occur, since bacteria are ubiquitous in cooling tower waters and oceans, rivers, and lakes.

Epstein [4] stated that some 2 000 species of organisms have been recorded as a fouling nuisance. Macroorganisms in their early life forms pass easily through water strainers. Microorganisms such as bacteria on the heat transfer surface produce slimes, which are the initial stages of formation of a more complicated fouling deposit that can contain suspended solids and corrosion products. Conditions in heat exchangers are often suitable for the promotion of biofouling.

Biofouling has been reviewed by Characklis [19] and Bott [9].

(g) Combined fouling

It is convenient to classify fouling of heat transfer surfaces into several clearly definable types, especially

©1984 Hemisphere Publishing Corporation

since research workers tend to investigate individual or isolated types. However, most deposits that occur on heat transfer surfaces are the result of two or more of the types described. In cooling water systems, the deposits can be the result of crystalline, particulate, in situ corrosion, and biofouling. In the initial stage of deposit formation, one particular type of fouling may predominate, and this can accelerate deposition by other types. The process is very complicated, and while some progress has been made in understanding individual types of fouling, only speculations exist about the interaction between fouling types when they occur simultaneously on a heat transfer surface.

B. Types of fouling by process type

(a) No phase change

Virtually all types of fouling can occur during the heating of flowing fluids when no phase change occurs. Water is the most common cooling fluid in industry and contains dissolved solids, particulate materials, and microorganisms, each of which can contribute to fouling. Hydrocarbon liquids tend to polymerize or deposit coke during heating. Air used as a cooling medium can be contaminated with particulate materials, traces of polymerization-prone constituents, and microorganisms. Combustion gases produced in furnaces usually contain ash particles and condensible acids, both of which can cause significant fouling problems, particularly when they are present simultaneously. In general, process fluids often react chemically or polymerize when heated, contributing to potential fouling problems.

In cooling operations, such as crystallization, fouling can occur whenever a solution is cooled below its saturation temperature. Streams encountered in food processing have a tendency to react chemically when heated under conditions such that there is no phase change. Crystallization fouling is also a problem in some food product streams; an example is the deposition of calcium salts during pasteurization of milk.

Table 1 Fouling of heat transfer surfaces in industry groups

Industry group	Type of fouling that occurs in heat exchange equipment	Usual extent of problem
Food and kindred products	Chemical reaction	Major
	Crystallization (milk processing)	Major
	Biofouling	Medium
	Particulate (gas side) (spray drying)	Minor/major
	Corrosion	Minor
Textile milt products	Particulate (cooling water)	
	Biofouling (cooling water)	
Lumber and wood products including paper and allied products	Crystallization (liquor, cooling water)	Major
	Particulate (process side, cooling water)	Minor
	Biofouling (cooling water)	Minor
	Chemical reaction (process side)	Minor
	Corrosion	Medium
Chemical and allied	Crystallization (process side, cooling water)	Medium
	Particulate (cooling water) (gas side)	Minor/medium
	Biofouling (cooling water)	Medium
	Chemical reaction (process side)	Minor/major
	Corrosion	Medium
Petroleum refining and related industries	Chemical reaction (process side)	Major
	Crystallization (cooling water)	Medium
	Particulate (cooling water, gas side)	Minor/medium
	Biofouling (cooling water)	Medium
	Corrosion (process side)	Medium
Stone, clay, glass, and concrete products	Particulate (gas side) (heat recovery)	Minor/major
Electric power production	Biofouling (cooling water)	Major
	Crystallization (cooling water, boiler water)	Medium
	Particulate (furnace side)	Major
	Freezing (furnace-side slag formation)	Major
	Corrosion (air-cooled condensers)	Minor

From Fassbender [48] and Garrett-Price et al. [49]

© 1984 Hemisphere Publishing Corporation

(b) Boiling and evaporation

When liquids are boiled or evaporated, saturated and supersaturated solutions may be produced from which salts will precipitate and deposit on heat transfer surfaces. Water-soluble sulfate-carbonate scales form during the evaporation of alkaline black liquor [46, 47]. Fouling often occurs on the water side of utility and power boilers, even though the water used has a low total dissolved solids content. Traces of oxygen in boiler waters can lead to significant corrosion. The rate of deposition of crystals during boiling is proportional to a power of the difference in concentration between the bulk liquid and the liquid at the heat transfer surface. Values of the power of the concentration difference are discussed by Epstein [4].

(c) Condensation

In the absence of polymerization or other chemical reactions, most condensing liquids are clean and relatively pure, so that fouling is not a significant problem during condensation operations. Traces of high-boiling-point constituents in condensate, such as compressor oil in refrigerant, have a potential for fouling. Condensation in the presence of acidic gases such as CO_2 can cause corrosion problems. Likewise, vapor condensation assists in depositing any particles that are present.

C. Types of fouling by industry

In virtually every industry in which heat transfer is a major operation, and heat exchange equipment is a major capital investment, it is important to be cognizant of fouling and of how it affects the processes involved and their design and maintenance. Table 1 is a list of major industry groups and the types of fouling that occur frequently in heat transfer equipment.

References for Section 3.17.2 appear at the end of Section 3.17.7.

© 1984 Hemisphere Publishing Corporation

3.17.3

Analysis of the fouling process

James G. Knudsen

A. Processes involved in fouling

Fouling of heat transfer surfaces is made up of at least five distinct processes, each of which may be subjected to analysis [20]. These are:

1. Processes in the body of the fluid.
2. Transport to the heat transfer surface.
3. Attachment or formation of the deposit at the heat transfer surface.
4. Removal of material from the heat transfer surface by dissolution (material leaves in ionic form), erosion or reentrainment (material leaves in particulate form), or spalling or sloughing (material leaves as a large mass).
5. Transport of removed material into the body of the flowing fluid.

Epstein [50] classified the processes in five main categories-initiation, transport, attachment, removal, and aging-and combined these in a 5 X 5 matrix that includes the five main types of fouling. Figure 1 shows the matrix and the areas that have received the most and least attention from the standpoint of research. A research goal should be to fill in our knowledge in all 25 spaces of the matrix.

Clearly, a fundamental knowledge of the processes described above would permit the development of models with which fouling could be predicted. However, such complete fundamental knowledge is not available at present.

The outcome of the processes listed above is net deposition of material on the heat transfer surface. The results can be represented as a fouling resistance-time curve, examples of which are shown in Fig. 3.17.1(1) and discussed in Sec. 3.17.1A(c).

B. Mechanism of deposition and removal

In the formulation of mathematical models to describe the curves shown in Fig. 3.17.1(1) the usual starting point is the rate equation

$$\frac{dR_f}{dt} = \phi_d - \phi_r \tag{1}$$

where dR_f/dt = rate of change of fouling resistance with respect to time

ϕ_d = deposition rate

ϕ_r = removal rate

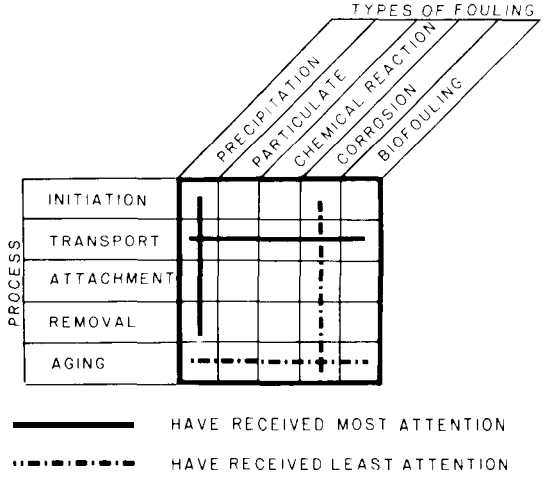

Figure 1 The 5 x 5 fouling matrix. From Epstein [SO].

© 1984 Hemisphere Publishing Corporation

HEDH

It should be noted that, while this fundamental model applies to many types of fouling, there are examples in which the rate of fouling decreases and ultimately becomes zero even though there is no removal.

Integration of Eq. (1) at constant heat flux and constant surface temperature to give R_f as a function of time requires a knowledge of ϕ_d and ϕ_r. A classical model was developed by Kern and Seaton [51, 52], who assumed ϕ_d to be constant and ϕ_r to be proportional to shear stress on the surface of the deposit. The result is an exponential relation between fouling resistance and time, giving a curve corresponding to curve C in Fig. 3.17.1(1).

A significant improvement in the Kern-Seaton model was made by Taborek et al. [1, 2], who expressed the deposition and removal functions more generally in terms of the basic quantities that control fouling. Developed specifically for water, the deposition rate is expressed as

$$\phi_d = C_1 P_d \Omega^n \exp\left(\frac{-E}{\tilde{R}T_s}\right) \tag{2}$$

where C_1 = const
P_d = deposition probability factor related to velocity and the stickiness or adhesion characteristics of the deposit
Ω^n = water quality factor
$\exp(-E/\tilde{R}T_s)$ = Arrhenius reaction rate function
E = activation energy
$\tilde{R}$ = gas constant
T_s = absolute temperature at the surface of the deposit

The removal function is

$$\phi_r = C_2 \tau \frac{x}{\psi} \tag{3}$$

where C_2 = const
τ = shear stress exerted on the surface of the deposit
x = thickness of the deposit
ψ = strength or removal resistance of the deposit

Equations (9) and (10) are a conceptual representation of factors that influence fouling, but numerical values of C_1, C_2, P_d, Ω^n, and ψ are not known.

Substitution of Eqs. (2) and (3) in Eq. 3.17.1(1) results, upon integration, in the relation

$$R_f = \frac{C_1 P_d \Omega^n}{C_2 \tau \lambda_f/\psi} \exp\left(\frac{-E}{\tilde{R}T_s}\right)\left[1 - \exp\left(\frac{-C_2 \tau \lambda_f t}{\psi}\right)\right] \tag{4}$$

where λ_f = thermal conductivity of the scale.

As time t becomes large, the expression for the asymptotic fouling factor R_f^* is

$$R_f^* = \frac{C_1 P_d \Omega^n}{C_2 \tau \lambda_f/\psi} \exp\left(\frac{-E}{\tilde{R}T_s}\right) \tag{5}$$

The integration assumes that T_s, P_d, Ω^n, τ, and ψ are constant and therefore applies to one scale, one water quality, and one set of flow conditions. Thus Eq. (4) may be used to show the effect of the variables above as they are changed. Equation (4) is exponential in time, and the time constant t_c—that is, the time required for the fouling resistance to reach 63% of the asymptotic value-is given by

$$t_c = \frac{\psi}{C_2 \lambda_f t} \tag{6}$$

In three time constants, the fouling resistance has attained 95% of the asymptotic value. Morse and Knudsen [53] obtained preliminary data relating t_c to scale composition. The time constant decreased significantly as the concentration of non-calcium carbonate components in the deposit increased with all other variables held constant. The results indicated that as the scale composition approached that of pure calcium carbonate (higher scale strength), the time constant became infinite, suggesting a type of fouling resistance-time relationship similar to that of curve A in Fig. 3.17.1(1).

Other models have been formulated to describe the fouling resistance-time relationship. Pinheiro [30, 54] developed a generalized model that incorporates the major features of several previous models for particulate deposition, precipitation fouling, and chemical reaction fouling. It is based on fundamental mechanisms that occur during fouling, but it cannot be applied until more knowledge of the processes involved becomes available. Epstein [4] gave an excellent summary of deposition and removal models for various types of fouling. These models may be included in Eq. (1), which can then be integrated to obtain a relationship between fouling resistance and time.

From a practical standpoint, Eqs. (4) and (5) provide a suitable basis for determining the effect of the several fundamental variables on fouling. Based on experience or known fouling resistances, the model may be adjusted as variables are changed.

C. Variables influencing fouling

On the basis of Eqs. (4) and (5), the effects of several variables on fouling resistance are described below. The qualitative effects of these variables are shown in Table 1. These qualitative effects are generally applicable to cooling water fouling and may not be completely applicable to all types of fouling.

© 1984 Hemisphere Publishing Corporation

Table 1 Effect of various parameters on fouling resistance

Parameter (increasing)	Rate of deposition	Rate of removal	Asymptotic fouling resistance
Stickiness and adherence	Increases	Decreases	Increases
Heat transfer surface temperature	Increases	Depends on character of deposit	increases
Strength and removal resistance	Probably slight	Decreases	Increases
Surface roughness	Possibly increases	Possibly increases	Possibly no effect
Ex situ corrosion	Increases	Probably no effect	Increases
In situ corrosion	Increases	Depends on product formed	Increases
Velocity	Decreases (almost always)	Increases (always)	Decreases

(a) Deposition probability P_d (effect of velocity and stickiness)

Deposition probability increases as velocity decreases, since a particle or crystal will have a longer residence time at the surface at a lower velocity. Deposition probability is also related to the stickiness or adhesion of the deposit. As stickiness increases, the deposition probability and the fouling resistance increase. The deposition probability is a complex quantity. Mass transport to the surface increases with increasing velocity. Stickiness may or may not be a function of velocity, depending on the properties of the surface and how they are affected by shear stress. This complexity indicates the need for basic studies of the fundamental variables that affect fouling.

(b) Water quality Ω^n

Water quality is related to the scaling characteristics, mainly of treated cooling water. It is generally based on some index related to the calcium hardness of the water. Indices commonly used are the Langelier index [55] and the Ryznar index [56]. Water is considered to have a scaling tendency if the Langelier index is greater than 1 or the Ryznar index is less than 6.

Bodnar [57] developed a criterion for estimating the scaling tendency of cooling water which is also based on the solubility of calcium carbonate. He defined a crystallization head as a function of the amounts of dissolved calcium carbonate, carbonic acid, and free carbon dioxide and the pH of the water. A plot is used to determine the crystallization head from the values of these parameters. When the crystallization head is unity the water is saturated; when it is negative the water is unsaturated.

It is important to note that all the criteria above are based only on calcium carbonate-bicarbonate equilibria; interaction with other ions in solution is not considered.

Computer programs have been developed for predicting which species will precipitate from a solution that contains a large number of dissolved mineral salts [58]. These programs consider the interactions between various ions as well as the solubility products of sparingly soluble constituents. They need to be much more refined and tested against experimental data. They should provide a more reliable means of predicting scaling tendencies of cooling water. It is doubtful, however, that any criterion will predict the amount or rate of scaling (and hence the fouling resistance) for any cooling water. Such predictions will, no doubt, be based on experimental fouling data obtained on a real-time basis.

(c) Surface temperature

Equation (4) indicates that as the temperature at a heat transfer surface increases, fouling resistance due to crystallization fouling by inverse solubility salts increases. However, under boiling conditions the increase of fouling with surface temperature may hold for all salts. The same is true of biofouling up to a certain surface temperature limit, usually about 35° C (95° F). For crystallization fouling by calcium carbonate, magnesium silicate, and their mixtures, Knudsen and Lahm [33] reported values of the activation energy E in the range 4.65 X 10 to 9.3 X 10 J/kmol (20 000 to 40 000 Btu/lb mol). This gives some basis for calculating the effect of surface temperature on crystallization fouling.

Temperature affects particulate deposition through thermophoresis, which acts in the direction of the temperature gradient and is enhanced by cooling rather than heating surfaces [4]. Chemical reaction fouling is enhanced by increasing temperature according to the temperature function shown in Eqs. (4) and (5).

(d) Shear stress (velocity)

According to Eq. (4), fouling resistance decreases with increasing shear stress. The mechanism of deposit re-

© 1984 Hemisphere Publishing Corporation

moval by the action of shear stress is described by two theories. According to one theory, the shear stress exerted by the adjacent laminar sublayer is sufficient to fracture the upper layers of the deposit and remove material. The other theory is based on the fine structure of the laminar sublayer in which sudden random eruptions of fluid normal to the wall occur. These so-called turbulent bursts are thought to influence both deposition and removal of material from the surface; a model of this process is described by Wright [40]. With either theory, increasing velocity means increasing shear stress (or turbulent bursts) and removal of the deposit is enhanced, particularly if the deposit consists of mixed crystals or has weak fault lines.

(e) Deposit strength or "'removal resistance" of deposit, ψ

The effects of velocity and associated shear stress are closely linked to the strength or removal resistance of the deposit. According to Eqs. (4) and (5), fouling resistance is proportional to a strength factor ψ. A hard, adherent deposit such as pure calcium carbonate follows a linear fouling resistance-time relationship similar to curve A in Fig. 3.17.1(1). As the strength factor is reduced by the presence of other types of crystals or by weakening crystalline structure, the fouling resistance is reduced and curve C is more representative of the time behavior.

(f) Surface material

The effect of the material of the heat transfer surface is not included in Eqs. (4) and (5). There are several ways in which materials may influence fouling. Biofouling is generally retarded by copper-containing materials. Ritter et al. [28] compared copper alloys and titanium for biofouling in seawater. Biofouling occurred on both surfaces, and it appeared that the toxicity of copper had a significant effect at lower velocities. At higher velocities the difference between the two materials was much less significant. Copper and copper alloys can be effective in reducing biofouling only if they slowly corrode so that copper ions are released.

Baier [59] studied the effect of surface free energy on biofouling and showed that through appropriate surface treatment biofouling can be reduced. Minimum biofouling was found at a surface free energy of about 0.02 N/m (20 dyne/cm).

Surface charges can also effect fouling rate. Bowen and Epstein [60] showed that asymptotic behavior of the fouling resistance-time curve [curve C of Fig. 3.17.1(1)] could be obtained without appreciable removal but by changing surface forces and geometry as deposition proceeded.

For crystalline and particulate fouling, the material of the surface may have an effect on the induction period during which the surface is being covered with nuclei. This is a stochastic process and not easily predictable. As soon as enough nucleation sites have formed on the surface, the fouling resistance will follow one of the curves shown in Fig. 3.17.1(1) (that is, at times greater than t_D). In this period of deposition the surface material appears to have no effect on the fouling resistance, except for the case in which corrosion is enhanced at the deposit-metal interface when the surface is completely covered by deposit.

(g) Surface roughness

Rough surfaces are thought to enhance deposition of materials, especially in the incipient stages. However, there has been no systematic investigation of the fouling characteristics of rough surfaces. Grocki and Westergren [61] indicate that scaling can be minimized in alkaline evaporator service by using tubes of high surface finish made by a special process. Enhanced heat transfer surfaces have not been used extensively in services where fouling liquids are used. It is possible that turbulence created by the geometry of enhanced heat transfer surfaces could contribute to the removal of any fouling deposit that is formed. Watkinson et al. [62] studied the scaling of plain, internally longitudinally finned, and spirally indented tubes. The finned tubes showed fouling resistances 15-35% greater than those of plain tubes. At 1 m/s the fouling resistances of the spirally indented tubes were 25-50% below those of the plain tubes. Knudsen and Roy [63] reported identical fouling resistances for a spirally corrugated tube and a plain tube. Moore [64] described several applications in which radial finned tubes had distinct advantages over plain tubes under fouling conditions. He contended that irregular thermal expansion on the fins tends to produce a looser scale which is easier to remove. Because of the advantage of using enhanced heat transfer surfaces, information on their fouling characteristics is needed.

Plate exchangers have a very complicated flow geometry and develop high levels of turbulence and shear. Plant experiences indicate that plate heat exchangers have lower fouling rates than tubular exchangers because of the turbulence induced by the corrugations on the plate. Cooper et al. [65] studied the fouling of plate heat exchangers and confirmed that they showed considerably lower fouling resistances than a circular tube under similar operating conditions with cooling tower water.

© 1984 Hemisphere Publishing Corporation

(b) Corrosion

In situ corrosion has been discussed as one type of fouling. Corrosion occurs quite frequently with other types of fouling when the heat transfer surface reacts with the flowing process fluid. In these cases corrosion does not appear to affect other types of fouling that occur simultaneously [6]. However, corrosion can also occur under a deposit of crystals, particles, or biological material even when it would not normally occur with the material directly in contact with the flowing fluid. In any case, corrosion results in additional thermal resistance to heat transfer.

Nomenclature for Section 3. I 7.3 appears at the beginning of Part 3. References appear at the end of Section 3.1 7.7.

© 1984 Hemisphere Publishing Corporation

3.17.4
Fouling control measures

James G. Knudsen

A. Introduction

The process by which key decisions are made in selecting, specifying, designing, manufacturing, and operating heat exchangers typically follows the pattern:

1. A fouling factor is specified to the designer by the potential customer.
2. The heat exchanger is designed as part of an architect-engineer function.
3. A contract is let to the lowest bidder for fabrication to the specifications provided.
4. The heat exchanger is installed and may or may not be put into operation by the prime contractor.
5. The heat exchanger is operated by the customer, after acceptance, with appropriate fluid treatment and/or periodic cleaning to maintain desired capacity.

In this total process, there are several opportunities to mitigate potential fouling problems. The ultimate decision to select one or several mitigation techniques depends on the apparent effectiveness of the technique, the type of fouling, and various economic parameters. The major efforts to mitigate fouling are made during operation and during shutdown of the exchanger. Mitigation of fouling needs to be addressed during the four phases in the life of a heat exchanger:

1. Design phase
2. Construction phase
3. Operation phase (on line)
4. Shutdown phase (off line)

Table 1 shows these four phases and some of the items to be considered during each of them [49].

B. Fouling control measures: Design and operation

(a) Economic considerations

As seen from Table 3.17.2(1), fouling problems of various types can arise in most industries. Designers of heat exchange equipment should be aware that any potential fouling problem must be considered with at least as much attention as heat transfer coefficients or any other design aspect. However, fouling problems cannot be avoided in many heat exchanger operations, and it is then necessary to introduce defensive measures to minimize fouling and the cost of cleaning. Often operating conditions and fluid compositions change after the exchanger has been in service.

The fouling control measures used during either design or operation must be subjected to a thorough economic analysis, taking into consideration all the costs of the fouling control measures and their projected benefits in reducing costs due to fouling. The TEMA [66] fouling resistances are not asymptotic ones but rather reflect design practices that lead to a reasonable time between cleaning periods.

Under some conditions, nearly asymptotic fouling resistances can be attained, and this suggests a somewhat different approach to the economics. If, through proper design and process modification, the ideal case of nearly asymptotic fouling resistance could be obtained during continued service, then the amount of heat exchange surface could be specified so that cleaning would be almost never necessary. On the other hand, if it is expected that fouling resistances will be great (regardless

© 1984 Hemisphere I ublishing Corporation

Table 1 Spectrum of fouling mitigation strategies

Design phase	Construction/installation phase	Operation (on-line) phase	Shutdown (scheduled/ unscheduled) phase
Heat exchanger type	Manufacturing quality control	Maintaining appropriate temperature operating range	Disassembly and manual cleaning[b]
Heat exchanger geometry and configuration	Protection in transport and storage	Maintaining appropriate flow operating range	Mechanical removal[b] Drilling Scraping
Operating conditions Temperature Flow rate	Preoperation cleaning and passivation	Fluids pretreatment[b]	Lances Liquid jet Steam Air jet
		Use and control by appropriate additive8 Inhibitors Antiscalants Dispersants Acids	Chemical cleaning[b]
		On-line cleaning[b] Amertap (sponge balls) MAN (brushes) Sonic horns Soot blowers Chains and scrapers Thermal shock	

[a] From Garrett-Price et al. [49].
[b] Strategies that are commonly used by industry.

of measures taken to reduce them), then the fouling resistance-time curve becomes important in determining the optimum service time between shutdowns for cleaning.

(b) Design measures

In the past two decades the design of heat transfer equipment has become very sophisticated. Use of computer programs permits the investigation of a wide range of design variables to determine their effect on pressure drop, heat transfer, and costs. This gives the designer the opportunity to consider configurations and modes of operation that will mitigate fouling of the heat transfer surface. As a rule, however, the user gives the designer fouling resistances to be used in a specific design, so that the designer has little opportunity to explore geometries that might mitigate fouling.

Overestimation of fouling resistance can lead to specifying an excessive amount of surface in the heat exchanger, which can cause problems during initial operation, when the fouling resistance is zero. Overcapacity of the exchanger leads to reduction of flow rates to the extent that fouling is enhanced, so that the estimated fouling resistance used in design becomes virtually a self-fulfilling prophecy.

Several good references give suggestions for steps that the designer can take to mitigate fouling [5, 41, 67, 68]. These suggestions can serve as a guide to possible approaches. Data are not available for quantifying the steps taken. Without such quantitative information the designer is not likely to make design modifications, since their possible advantages cannot be demonstrated.

Cousins and Pritchard [41] discuss various factors that can be considered during the design phase in order to reduce fouling. These factors include exchanger geometry, materials of construction, wall temperature, velocity, and nature of the fluids.

Significant changes in the traditional configuration of the shell-and-tube heat exchanger have been proposed, not only to improve heat transfer but to mitigate fouling. One promising configuration is the ROD baffle heat exchanger [69, 70]. Various special heat exchangers have been patented for handling fouling fluids [49]. These are more expensive than the conventional shell-and-tube heat exchanger, and their use must be justified on economic grounds.

It has been mentioned that plate exchangers have considerably lower fouling resistance than circular tubes [65]. Novak [32] presented a summary of the design of plate heat exchangers from the standpoint of fouling reduction.

For severe fouling conditions, Klaren [31] proposed a fluidized bed heat exchanger consisting of a large number of parallel heat exchanger tubes in which small solid particles are maintained in a stationary fluidized

© 1984 Hemisphere Publishing Corporation

state by liquid passing up the tubes. Heat transfer coefficients obtained are three to five times the coefficient for single-phase flow in the tubes. Klaren summarized results for a variety of experimental fluidized-bed exchangers in which the liquid fluidizing media all demonstrated severe fouling tendencies in conventional heat exchangers but showed no such fouling in the fluidized-bed exchangers. The fluidized-bed heat exchanger has some disadvantages, including larger space requirements, uneven distribution of particles among the tubes, and wear of the tube and particle materials. The concept is in the developmental stage.

(c) Construction, operation, and maintenance

Construction of plants can extend over considerable periods of time, and heat exchange surfaces can be exposed to a variety of adverse environmental conditions. Fouling problems can be initiated during fabrication when pressure testing is carried out with poor-quality water and the equipment is not subsequently washed out with clean water and purged with nitrogen. Heat exchange surfaces should be protected from environments that will initiate corrosion or result in deposits on the surface [42].

Often the manner in which a system is operated can lead to significant fouling problems. Initially, because of the specification of a certain fouling resistance in the design, the heat exchanger is usually underutilized. This often results in use of lower velocities and higher wall temperatures, both of which can lead to fouling. Many fouling problems are initiated during start-up. Every effort should be made at the outset to operate at least at design velocity, and to use corrosion control and antifouling treatment for water so that fouling is not started or is maintained at an acceptably low asymptotic value.

All heat exchangers should be well instrumented with flow and temperature sensors so that the progress of fouling can be monitored.

If cleaning is required, provision should be made to accomplish this maintenance operation conveniently and effectively. Pipework should be accessible and of a configuration that is easily cleaned. If tube bundles must be removed, exchanger orientation and placement should be such that removal and cleaning are accomplished without undue difficulty.

In the happy circumstance that a heat exchanger does not need cleaning, there will be times when it is not operating. It should be left in a shutdown condition such that fouling does not start during this period. Not only excessive corrosion but biofouling can be initiated during this period.

(d) Process modification

If severe fouling problems occur, it is often necessary to consider a major modification in the process [5]. Some modifications that can be helpful are:

1. Replace tubular evaporator with submerged combustion evaporator.
2. Replace multistage evaporation process with multiflash evaporation process.
3. Use processes requiring lower temperatures.

C. Fouling control measures: Fluids treatment

Although the design engineer can mitigate fouling through proper design and knowledge of the fluids being processed, this does not reduce the need for treatment of the fluids. In fact, trouble-free operation of a well-designed heat exchanger is dependent on a well-organized, well-controlled treatment program.

There is a large amount of information available on the effectiveness of various treatment chemicals and treatment techniques in reducing or preventing fouling. Not all such references can be covered here, but the general aspects of the subject will be presented. The following discussion concerns the three fluids that are responsible for most heat exchanger fouling: water, gases, and hydrocarbons.

(a) Well, river, and lake water (fresh water)

The category fresh water pertains to waters that occur naturally but contain a certain amount of scale-forming minerals (typically 1000 ppm or less). They are not classified as brackish waters or seawaters, which contain several times as much minerals (approximately 3.5%) as fresh waters. Table 2, from Krisher [71], is reproduced here to show the common impurities found in fresh water.

Fresh water is used extensively for cooling. In many cases it is used in once-through cooling, in which it passes through the heat exchangers and is returned to the environment slightly heated. As water becomes scarcer and more costly, however, evaporative cooling towers are being used in which the heated water is cooled by direct contact with air and returned to the plant. The water becomes more concentrated in minerals to a level dependent on the number of concentration cycles at which the cooling tower is operated. The number of concentration cycles is determined by the rate of evaporation in the cooling tower and the amount of water discharged from the system. The cooling tower and associated circulating system (including the plant heat exchangers) provide an excellent environment for biofouling, scaling, and particulate deposition.

© 1984 Hemisphere Publishing Corporation

Table 2 Common impurities in fresh water, problems caused and treatment

Constituent	Chemical formula	Difficulties caused	Means of treatment
Turbidity	None-expressed in analysis as units	Imparts unsightly appearance to water. Deposits in water lines, process equip ment, etc. Interferes with most process uses.	Coagulation, settling, and filtration.
Color	None-expressed in analysis as units	May cause foaming in boilers Hinders precipitation methods such as iron removal and softening. Can stain product in process use.	Coagulation and filtration. Chlorination. Adsorption by activated carbon.
Hardness	Calcium and magnesium salts expressed as $CaCO_3$	Chief source of scale in heat exchange equipment, boilers, pipelines, etc. Forms curds with soap, interferes with dyeing, etc.	Softening- Demineralization. Internal-boiler water treatment. Surface active agents.
Alkalinity	Bicarbonate (HCO_3^-) carbonate (CO_3^{2-}), and hydrate (OH-), expressed as $CaCO_3$	Foaming and carryover of solids with steam. Embrittlement of boiler steel. Bicarbonate and carbonate produce CO, in steam, a source of corrosion in condensate lines.	Lime and lime-soda softening. Acid treatment. Hydrogen zeolite softening. Demineralization. Dealkalization by anion exchange.
Free mineral acid	H_2SO_4, HCl, etc., expressed as $CaCO_3$	Corrosion.	Neutralization with alkalies.
Carbon dioxide	CO_2	Corrosion in water lines and particularly steam and condensate lines.	Aeration. Deaeration Neutralization with alkalies.
pH	Hydrogen ion concentration, defined as $pH = \log [1/(H^+)]$	pH varies according to acidic or alkaline solids in water. Most natural waters have a pH of 6.0–8.0.	pH can be increased by alkalies and decreased by acids.
Sulfate	SO_4^-	Adds to solids content of water but in itself is not usually significant. Combines with calcium to form calcium sulfate scale.	Demineralization.
Chloride	Cl^-	Adds to solids content and increases corrosive character of water.	Demineralization.
Nitrate	NO_3^-	Adds to solids content but is not usually significant industrially. Useful for control of boiler-metal embrittlement.	Demineralization.
Silica	SiO_2	Scale in boilers and cooling water systems. Insoluble turbine blade deposits due to silica vaporization.	Hot-process removal with magnesium salts. Adsorption by highly basic anion exchange resins, in conjunction with demineralization.
Iron	Fe^{2+} (ferrous) Fe^{3+} (ferric)	Discolors water on precipitation. Source of deposits in water lines, boilers, etc. Interferes with dyeing, tanning, paper-making, etc.	Aeration. Coagulation and filtration. Lime softening. Cation exchange. Contact filtration. Surface-active agents for iron retention.
Manganese	Mn^{2+}	Same as iron.	Same as iron
Oxygen	O_2	Corrosion of water lines, heat exchange equipment, boilers, return lines, etc.	Deaeration. Sodium sulfite. Corrosion inhibitors.
Hydrogen sulfide	H_2S	Cause of rotten egg odor. Corrosion.	Aeration. Clorination. Highly basic anion exchange.
Ammonia	NH_3	Corrosion of copper and zinc alloys by formation of complex soluble ion.	Cation exchange with hydrogen zeolite. Chlorination. Deaeration.
Dissolved solids	None	Dissolved solids is measure of total amount of dissolved matter, determined by evaporation. High concentrations of dissolved solids are objectionable because of process interference and as a cause of foaming in boilers.	Various softening processes, such as lime softening and cation exchange by hydrogen zeolite, will reduce dissolved solids. Demineralization.

(See footnote on p. 3.17.4-X)

© 1984 Hemisphere Publishing Corporation

Table 2 Common impurities in fresh water, problems caused and treatment (Continued)

Constituent	Chemical formula	Difficulties caused	Means of treatment
Suspended solids	None	Suspended solids is the measure of undissolved matter determined gravimetrically. Suspended solids cause deposits in heat exchange equipment, boilers, water lines, etc.	Subsidence. Filtration, usually preceded by coagulation and settling.
Total solids	None	Total solids is the sum of dissolved and suspended solids, determined gravimetrically.	See Dissolved solids and Suspended solids.

Excerpted by special permission from *Chemical Engineering,* August 28, 1978. Copyright © 1978 by McGraw-Hill, Inc., New York, N.Y. 10020.

In regions where water is very scarce, evaporative cooling towers may be too extravagant in water consumption and dry cooling towers may be used. In this case, the plant water system is a closed system and air cooling with an extended surface heat exchanger is used. This cooling is limited by the temperature of the air, whereas in a direct contact cooling tower it is limited by the wet-bulb temperature of the air. With a dry cooling tower system, the plant water supply may be maintained in a relatively constant state in a closed circuit such that fouling is minimal. In locations where air temperatures can become high, additional cooling is accomplished through evaporation by occasionally deluging the heat transfer surfaces with water in a wet-dry or hybrid cooling tower. A certain amount of fouling then occurs on the outside of the extended heat transfer surface.

Several practical guides to water treatment are available [45, 72,731.

(i) Scale control. Because of environmental regulations, there is a tendency to reduce the amount of water discharged from a cooling system. Systems are then operating at a higher number of concentration cycles and attempts are made to eliminate any liquid discharge from the system except for liquid carried out by entrainment in the effluent plume from the cooling tower.

There are a number of ways to mitigate or prevent scale deposition due to high concentrations of scale-forming ions (Ca^{2+}, Mg^{2+}, CO_3^{2-}, SO_4^{2-}, PO_4^{3-}, SiO_3^{2-}) [5, 43, 74]. Other constituents that contribute to fouling are organics, clays, silts, and metal oxides in untreated surface waters, corrosion products from the cooling system, oil, process fluid from leaks, and atmospheric pollutants such as dust, pollen, insects, and gases [75].

1. Removal of scaling species. Scaling species can be removed by ion exchange and lime soda treatments. Both ion exchange systems and lime soda systems have high capital and operating costs.

2. Mechanical prevention. This method is related to the design measures described previously, in which geometric configuration and process variables are selected to mitigate scaling. There are proprietary devices based on continuous passage of sponge balls or frequent passage of nylon brushes at predetermined intervals through the tubes. These devices prevent buildup of scale, but should be used at the outset and not after scale is deposited. They require a high capital cost but have modest operating costs and reduce cleaning and down time costs.

3. pH control. The solubility of scale-forming constituents increases with decreasing pH. Many treatment programs involve addition of acid (H_2SO_4) to the system to maintain pH in the range 6.5 to 7.5. If the system contains corrosion-resistant materials, a pH may be selected at which no scaling will occur.

In all-steel systems, one treatment method is to reduce pH such that RSI $-$ 0.5 = 2 $pH_s - pH -$ 0.5, where pH_s is the saturation pH defined by Langelier [55]. Under these conditions the water is slightly corrosive and a corrosion inhibitor must be added. The corrosion inhibitor itself adds minerals to the water and can result in precipitation fouling. Care is needed when using pH control to ensure that malfunction of the acid injection system does not cause low values of pH, which can bring about very corrosive conditions in the system. Frequently, such malfunctions are the beginning of fouling problems. Figures 1 and 2 were presented by Schieber [76] to demonstrate the effect of pH.

4. Scale inhibitors. A large number of proprietary compounds are available for scale control [43]. They include:

a. Compounds that modify crystal habit and reduce cohesive strength.

b. Threshold agents, which retard precipitation of scale-forming salts while they remain in the system.

c. Dispersants, which impart like charges to the heat exchanger surface and the particles of scale in suspension. They control particle scaling.

d. Chelating agents, which complex strongly with scaling cations.

© 1984 Hemisphere I blishing Corporation

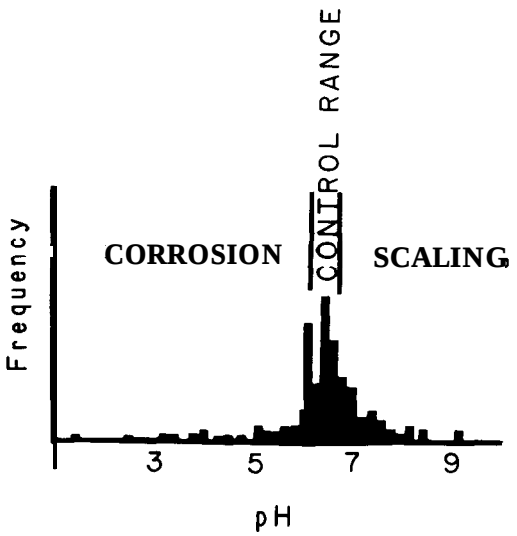

Figure 1 Variation of pH in a cooling tower system. From Schieber [76].

These additives can be as effective in reducing or preventing fouling as pH control, and they do not carry the risk of corrosion. Table 3 shows antiscalants that are commonly used. The presence of an antiscalant has the most direct effect on the scale strength factor or removal resistance in Eqs. 3.17.3(4) and 3.17.3(5).

Often, combination treatments are used in which pH is controlled such that $RSI + 2 = 2\ pH_s - pH + 2$ and an additive that is a corrosion inhibitor is applied.

Although various antifoulant additives are used

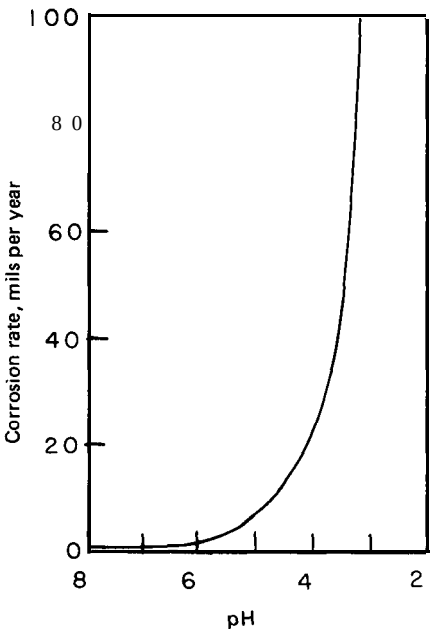

Figure 2 Effect of pH on corrosion of mild steel in a cooling system. From Schieber [76].

Table 3 Antiscalants

Natural organics	Organic acids, starch, tannin
Mineral sequestrant	Polyphosphate
Synthetic organics	Polyelectrolytes-ionic, phosphonates, polyacrylates
Functional groups	Crystal distortion, adsorbants, dispersants, flocculants, chelants, emulsifiers

mainly to reduce or prevent calcium carbonate fouling, they are effective in inhibiting deposition of calcium carbonate and colloidal silica. Midkiff and Foyt [77] reported that the hard, tenacious scale formed by a combination of calcium carbonate and colloidal silica can be avoided by any technique that prevents formation of calcium carbonate. This includes chemical treatment, softening, or pH control. Midkiff and Foyt reported successful operation of a cooling water system containing 216 mg/kg silica and approximately 120 mg/kg hardness.

(ii) Biofouling control. The environment in cooling towers and cooling systems is particularly conducive to growth of microorganisms in the water and on the surfaces. Power plant condensers in which the heat transfer surface is at a temperature in the range 35-50°C (95-120°F) are subject to biofouling. The biofilm deposited not only adds to the resistance to heat transfer but often has a structure such that a significant increase in pumping power is observed as well.

Biological growths can be controlled by destroying microorganisms with biocides. However, biocides do not necessarily remove the film or the fouling resistance. An effective biofouling control program should be initiated at the beginning of operation of a new heat exchanger. Biocides are effective only if they reach the bacteria deposited on the heat transfer surfaces. Microorganisms that are attached to and growing on surfaces produce polysaccharides, which increase the sticking probability of particles and crystals that come in contact with heat transfer surfaces. Baier et al. [21, 29, 36, 59] investigated the early events leading to biofilm development. They found that layers of natural organic films grow spontaneously to submicrometer thickness on all solids in contact with aqueous fluids. These films appear to be the precursors for subsequent adhesion of living and dead particulate material. Baier and co-workers developed techniques for characterizing these precursor films on the substrate material.

Of major importance in any biofouling control program is the environmental impact of control measures. Biocides that are effective in biofouling control may have an adverse impact on organisms in the environment into which water is discharged. Chlorine has been the biocide most widely used to control

© 1984 Hemisphere Publishing Corporation

biofouling. However, it reacts with ammonia and organics to form products that are potentially hazardous in the environment. Chloramine has been found to be more toxic to warm-water fish than free chlorine [75]. Because of these potential environmental hazards, the U.S. Environmental Protection Agency is attempting to reduce the amount of free available chlorine (FAC) discharged into bodies of water. In 1979 the daily average amount in cooling tower discharges was not to exceed 0.2 mg/l or a maximum daily rate of 0.5 mg/l. It was further required that FAC or total residual chlorine should not be discharged for more than 2 h per day from each unit and that no more than one unit should be chlorinated at a time if there are multiple units in a plant [25]. Efforts are being made to reduce discharge of chlorine even further, which raises the question of whether it is possible to effectively control biofouling with chlorine. Therefore, biocides such as halogenated organic compounds, which can be neutralized and made harmless to fish life when discharged, are being developed.

A variety of alternatives are available to control biofouling in cooling systems. Table 4, from Waite and Fagan [26], shows a wide range of chemical alternatives for biofouling control. The organic biocides are non-oxidizing toxicants. Some of the more popular organics are listed below [45]:

Chlorinated phenolics
Organotin compounds
Quaternary ammonium salts
Organosulfur compounds
Acrolein

The method of biofouling control selected by a plant operator will ultimately be based on economics and environmental regulations. Biofouling should be controlled from the beginning of operation of the equipment. The fact that coupon tests indicate a very low level of microorganisms in the bulk circulating fluid does not necessarily mean that biofouling is absent from the system. Stagnant regions in the system can be highly active in microbiological activity, even when a biocide is used. The point of injection of the biocide is critical for effective control.

Table 4 Evaluation of chemical alternatives for biofouling control

Property	Chlorine (Cl,, HOCl, OCl^-)	Chlorine dioxide	Ozone	Bromine (Br, , HOBr, OBr^-)	Bromine chloride	Iodine (I_2, HOI, OI^-)	Permanganate
Biocidal capacity							
Suspended bacteria	Good	Good	Excellent	Good	Good	Fair	Fair[b]
Biological films	Good	Unknown	Fair	Unknown	Good	Unknown	Unknown
Engineering considerations							
Storage facilities	Base	May be excessive	<Base	Base	Base	Base	<Base
Handling hazards	Dangerous	Dangerous	Dangerous	Severe	Dangerous	Dangerous	Minor
Application equipment	Common	Critical	Critical	Specialized	Common	Common	Common
Monitoring of residuals	Routine	Needs refinement	Needs refinement	Routine	Routine	Routine	Routine
Corrosion or scaling problems	Minor	Unknown	Probable[b]	Unknown	Unknown	Unknown	Unknown
Commercial considerations							
Availability	Some problems	Some problems	Limitless	Restricted	Questionable	Restricted	Questionable
Transportation	Some restrictions[b]	Generated on site	Generated on site	Severe restrictions	Some restrictions[b]	Some restrictions[b]	Routine
Projected cost	Low	High	High	Excessive	High	Excessive	High
Environmental considerations							
Direct toxicity	High	High	Medium	High	High	High	Low
Formation of toxins	High	Probable high	High in salt water	High	Probable high	Unknown	Probable low
Probable application							
Once through	Yes	Yes	Yes	No	Yes	No	No
Closed cycle	Yes	Yes	Yes	Yes	Yes	Yes	Yes

(See footnotes on p. 3.17.4-8.)

© 1984 Hemisphere Publishing Corporation

Table 4 Evaluation of chemical alternatives for biofouling control[a] (Continued)

Property	Ferrate	Peroxide	Mixed halogen	Dechlorination (sulfur)	Dechlorination (activated carbon)	Organics
Biocidal capacity						
Suspended bacteria	Good	Poor	Good	–	–	Good
Biological films	Unknown	Unknown	Probable good	–	–	Good aid
Engineering considerations						
Storage facilities	<Base	Base	Unknown	> Base	≫ Base	> Base
Handling hazards	Minor	Minor	Severe	Dangerous	Dangerous	May be severe[b]
Application equipment	Common	Common	May be problem	Common	Common	Common
Monitoring of residuals	Routine	Needs refinement	Dependent on mixture	Routine	Routine	Requires special equipment
Corrosion or scaling problems	Unknown	Minor	Unknown	Minor	Minor	Minor
Commercial considerations						
Availability	Currently not produced	Adequate	Restricted	Some problems	Some problems	Restricted
Transportation	Routine	Minor restrictions	Some restrictions[b]	Some restrictions[b]	Some restrictions[b]	Some restrictions[b]
Projected cost	Probable medium high	Medium high	Excessive	High	Excessive	High
Environmental considerations						
Direct toxicity	Low	Medium	High	Low	Low	High
Formation of toxins	Probable low	Probable high	High	High	Probable high	Unknown
Probable application						
Once through	Possible	**Yes**	**No**	**Yes**	**Yes**	**No**
Closed cycle	Yes	**Yes**	**Yes**	**No**	**No**	**Yes**

[a] From Waite and Fagan [26].
[b] Constraint in certain instances.

Biofouling control is used mainly to prevent growth on heat transfer surfaces that reduces heat transfer capacity and increases pumping power. Biocides such as chlorine are very effective in controlling the microorganism population in the bulk fluid, but they are dissipated so fast that they often have no effect on the population at the heat transfer surface. For this reason, slow-release biocides are often more effective in combating biofouling on heat transfer surfaces. The effectiveness of a biofouling program is best determined by monitoring the heat transfer and pressure drop of the heat exchangers being treated.

Copper-bearing materials in heat transfer surfaces provide a toxic base on which microorganisms are deposited. They are effective in reducing biofouling, but microorganisms can also adapt to the environment. The effect of tube material is discussed in the following section on seawater. Copper salts can be used for biofouling control, but their use is limited because of their toxicity to environmental organisms.

(iii) Corrosion control. Corrosion control is needed if the material of the cooling system is reactive with water under the conditions of the system. When pH control is used to limit scaling, it is necessary to protect the system with a corrosion inhibitor. Corrosion inhibitors with a chromate base have long been used. In chromate-acid treatment, acid is added to reduce pH and a chromate compound is added to inhibit corrosion. The chromate is a highly efficient inhibitor and is cost-effective. However, the environmental toxicity of chromates has led to restriction of their use and to the development of other corrosion inhibitors. Zinc is an effective corrosion inhibitor, but it is also toxic to organisms in the

© 1984 Hemisphere Publishing Corporation

Table 5 Comparison of cooling water treatments

Treatment	Kumar index
Chromate-zinc base corrosion inhibitor plus organic phosphate sequestrant	0.45
Aminophosphonate plus polyacrylamide	1.37
Polyphosphate plus organic phosphate sequestrant	1.44
Alkaline thiosulfate plus phosphate ester plus zinc	1.84
Zinc-based corrosion inhibitor plus organic polyelectrolyte	2.20
Alkaline organiobased inhibitor	2.72
Polyester corrosion control agent plus dispersant	2.78
Organic polymer	3.69

Excerpted by special permission from *Chemical Engineering,* April 26, 1976. Copyright © 1976 by McGraw-Hill, Inc., New York, N.Y. 10020.

environment. A usual chromate-zinc treatment is maintained at a level of 20-30 ppm (as CrO_4) chromate and 1-5 ppm zinc [75].

An alternative to the high-chromate treatment is a low-chromate treatment, using 5-10 ppm CrO_4, a pH range of 7.5 to 9.0, and organic phosphorus compounds such as aminomethylene phosphoric acid [75]. Organic (nonchromate) compounds are being investigated as corrosion inhibitors. These are used in conjunction with antiscalants and consist of polyphosphates, silicates, or lignosulfonates, for example. Kumar and Fairfax [78] compared various cooling water treatments on the basis of a cost index developed by Kumar. This index is a figure of merit that weighs the influence of scaling tendency, corrosion rate, and treatment cost. A low value of the index is desirable. The results are shown in Table 5 for one specific water composition. It is expected that different indices will be obtained for different water compositions, and thus each situation must be addressed separately.

(b) Boiler water

Boilers operate over a wide range of pressures and temperatures, and there are limits on the composition of boiler water so that scaling and corrosion are minimized. Recommended limits for industrial boilers are shown in Table 6. These guidelines [79] were issued in 1975 by the ASME Committee for Water in Thermal Power Systems and are an extension and modification of guidelines issued in 1932 by the American Boiler Manufacturers Association. Boiler waters are subjected to various pretreatments to remove excess concentrations of unwanted species. Table 7 shows a list of various pretreatment processes that was presented by Herman [80].

In the preboiler section of the system no phase changes take place, and fouling and corrosion must be avoided through the various treatments discussed above. Orthophosphates should be avoided in this section, since they have a tendency to form calcium phosphate, which is slightly soluble. Also, sodium hydroxide should not be fed into the preboiler section because scaling could result.

In the boiler itself, deposits on the water side of the tubes can reduce the rate of heat transfer, cause high metal temperatures, and frequently can rupture the tubes.

Two treatment techniques used to prevent fouling on the tube side of boilers are the phosphate and chelate treatments [80], which are described below.

(i) Phosphate treatment. Calcium ions are precipitated by adding phosphate and alkali to the water. Magnesium ions are precipitated by alkali and silicates. The precipitates form a sludge of calcium hydroxyapatite $[3Ca_3(PO_4)_2 \cdot Ca(OH)_2]$ and serpentine $[2MgSiO_3 \cdot Mg(OH)_2 \cdot H_2O]$. The sludge settles into a mud drum and is removed periodically. Sludge conditioners con-

Table 6 Guidelines for water quality in modem industrial water tube boilers

	Feedwater			Boiler water		
Operating pressure, psig	Iron, ppm	Copper, ppm	Total hardness, ppm $CaCO_3$	SiO_2, ppm	Total alkalinity, ppm $CaCO_3$	Specific conductivity, micromho/cm³
O-300	0.100	0.050	0.300	150	700	7 000
301-450	0.050	0.025	0.300	90	600	6 000
451-600	0.030	0.020	0.200	40	500	5 000
601-750	0.025	0.020	0.200	30	400	4 000
75 l-900	0.020	0.015	0.100	20	300	3 000
901-l 000	0.020	0.015	0.050	8	200	2 000
1001-l 500	0.010	0.010	0.000	2	0	150
1501-2 000	0.010	0.010	0.000	1	0	100

From Simon [79].

© 1984 Hemisphere Publishing Corporation

Table 7 External treatment systems for boiler water

Treatment	Effect
1. Aeration	Reduce iron, manganese, hydrogen sulfide, carbon dioxide.
2. Prechlorination	Reduce organic matter and microorganisms.
3. Clarification	Reduce color and suspended matter.
4. Cold process softening	Reduce suspended matter, iron, calcium, magnesium, bicarbonate, and maybe some silica.
5. Cation exchange, sodium cycle	Reduce calcium and magnesium.
6. Split stream cation exchangers, sodium and hydrogen cycles with degasifier	Reduce calcium, magnesium, sodium, and bicarbonate.
7. Cation exchanger, sodium cycle followed by anion exchanger, chloride cycle for dealkalizing or hydroxide cycle for dealkalizing and desilicizing	Reduce calcium, magnesium, bicarbonate, and, if needed, silica.
8. Hot lime followed by filters and cation exchanger, sodium cycle	Reduce suspended matter, iron, calcium, magnesium, bicarbonate, and silica.
9. Demineralization	Reduce all cations, anions, and silica to very low concentrations.

From Herman [80].

taining polymers, organics, sequestrants, iron-sequestrant-dispersant, and antifoamants are used to retard deposition by dispersing boiler sludge so that it will be less adherent to the tube walls.

(ii) Chelate treatment. Chelation is a scale prevention treatment by which soluble, heat-stable complexes are formed. The most common chelating agents are ethylenediamine tetraacetic acid (EDTA) and the trisodium salt of nitrite triacetic acid (NTA). The chelant concentration must be well controlled, as an excess can cause corrosion and a deficiency can cause scaling. Oxygen must be completely removed from the system.

(iii) Control of iron oxide. Iron oxide is particularly troublesome in many boilers. It acts as a binder for the boiler sludge, which in turn is deposited on the tube wall. The source of the iron oxide is corrosion in other parts of the system. The problem can be mitigated by inhibiting the corrosion at its source, removing the iron oxide by filtration, and treating the iron oxide to minimize its deposition [81]. Use of an iron oxide dispersant along with other organic compounds has been found effective in controlling iron oxide deposition.

(ii) Boiler corrosion control. Corrosion in boilers is promoted by the presence of oxygen. Oxygen is effectively removed by deaeration of the feedwater followed by addition of an oxygen scavenger to the boiler water. Sodium sulfite and hydrazine are two common oxygen scavengers. Proprietary formulations of these chemicals are available which contain a catalyst [80].

(c) Seawater

(i) General considerations. Although seawater is used extensively as a coolant medium, it has two main disadvantages. It has a high concentration of corrosive and scaling salts, and it has a high level of macrobial and microbial activity. Ship condensers use seawater continuously on a once-through basis. Temperatures in these condensers are normally in a range that promotes biofouling rather than scaling. Under these conditions copper-bearing alloys are used to withstand corrosion and to mitigate the biofouling. If necessary, biofouling control measures can be used to limit the growth of microorganisms in the condenser.

Ritter et al, [28] showed that a 90-10 CuNi surface at 27° C (80° F) exposed to seawater flowing at a velocity of 1.8-2.4 m/s (6-8 ft/s) fouled at the same rate as a titanium surface, but after a short period deposits were lost when the binding organism died. At the same temperature and a velocity of 0.6 m/s (2 ft/s) titanium showed a fouling rate about three times that of the copper-based alloy. Fouling resistances on the 90-10 CuNi surface ranged from 1.76 X 10^{-4} to 3.52 X 10^{-4} m^2 K/W (0.001-0.002 h ft^2 °F/Btu). It was observed that the titanium surface was susceptible to biofouling, which bound silt to the surface. The 90-10 CuNi surface was less susceptible to biofouling but was susceptible to corrosion fouling.

Two types of scales can form in heat exchangers with seawater: alkaline scales (calcium carbonate and magnesium hydroxide) and calcium sulfate [82]. In the temperature range 60-85°C (140-185°F) deposition of calcium carbonate predominates and the form normally found is aragonite. Above 80° C (185°F), increasing proportions of magnesium hydroxide are deposited. For calcium sulfate, litte deposit occurs if operating temperatures are below 93-120° C (200-250°F), depending on brine concentration.

(ii) Proposed OTEC plants. Scaling, biofouling, and corrosion are significant factors in the efficient operation of proposed ocean thermal energy conversion (OTEC) plants. Biofouling is the most serious problem and probably can be attacked most effectively through the use of in situ mechanical cleaning devices such as sponge balls or nylon brushes. Corrosion can be eliminated by use of titanium; however, because of the

© 1984 Hemisphere Publishing Corporation

extensive heat transfer surface needed for an OTEC plant, this scarce metal would be too expensive. Aluminum alloy is the main candidate material, but its corrosion resistance must still be proved. As far as scaling is concerned, it appears probable that the warm-water heat exchangers will encounter seawater supersaturated with respect to calcium carbonate at some locations on the ocean surface [83].

(iii) Desalination plants. The most serious scaling problems with seawater occur during its evaporation in the production of fresh water. The main scale control methods in multistage flash (MSF) plants are polyphosphate dosing, acid dosing, and use of organic polymers [84, 85].

Polyphosphates retard the formation of hard alkaline scales at temperatures up to about 90°C (195°F). Brine velocity should be maintained above 1.8 m/s (6 ft/s). This does not completely eliminate scaling but allows operating times of 3-4 mo between cleanings. Fouling resistances of 1.5 X 10^{-4} m^2 K/W (0.000 85 h ft^2 °F/Btu) are attained before cleaning. Close control of the polyphosphate concentration is necessary so that calcium orthophosphate does not form.

Acid dosing (pH control) is used to attain higher temperatures in the system. Its main drawback is the risk of corrosion due to malfunction of acid injection equipment. It is necessary to maintain the pH within the narrow range 7.7-8.0. Typical fouling resistances for acid-dosed plants are 8.0 X 10^{-5} m^2 K/W (0.000 43 h ft^2 °F/Btu).

A variety of polyelectrolytes can be used for scale control. Examples are polyacrylic acid, polymethacrylic acid, copolymers of maleic anhydride with monomers such as methyl vinyl ether, styrene, vinyl acetate, and hydrolyzed polyacrylamide [85]. Polymers that are effective have a molecular weight less than 10 000 and are thought to act as threshold inhibitors or lattice structure distorters. They have been shown to control alkaline scale formation as well as calcium sulfate without the need for acid treatment.

(d) Geothermal brines

Steam and hot water from underground reservoirs contain many impurities, which precipitate as the temperature and pressure of the fluid are decreased. The result is deposition mainly of silicates and carbonates on surfaces exposed to the brines. Such deposition is almost inevitable when geothermal brines are used in geothermal power plants [86].

The presence of gases such as carbon dioxide and hydrogen sulfide along with chloride and sulfate ions also makes corrosion virtually inevitable in geothermal plants.

Because of the variability in composition of geothermal brines, prediction of their behavior is not possible. Scaling and corrosion behavior must be studied with suitable test equipment at the site where the geothermal brine is to be utilized.

(e) Pulping liquors

Sodium carbonate-sodium sulfate scale and calcium scale are the two most common scales formed during evaporation of black alkaline pulping liquor [46, 47]. The growth of soluble scales appears to be governed by solubility conditions in the bulk liquor. Scaling can be minimized by reducing the solids content of liquor discharged from the evaporator, reducing the amount of sulfate and carbonate in the liquor, providing entrained solids to encourage precipitation in the bulk liquor, and maintaining stable operation.

The calcium content of the liquor is the most important factor in calcium scaling and it appears to be affected by wood supply.

Calcium scales appear to be the most serious problem in the evaporation of black alkaline liquors, with fouling resistances in the range 7.0 X 10^{-4} to 1.4 X 10^{-3} m^2 K/w (0.004-0.008 h ft^2 °F/Btu).

(f) Hydrocarbons

(i) Fouling by hydrocarbon streams. In hydrocarbon processing operations fouling deposits are formed which consist of carbon-rich organic polymers [5]. Autooxidation is considered to be the mechanism of formation. Important factors include inorganic salts; the presence of oxygen or mercaptans; and traces of copper, cobalt, manganese, iron, nickel, and chromium, which catalyze the reaction.

Froment [16] concluded that

1. Relatively little is known about the reaction under process conditions.
2. The process operates under severe conditions and direct observations are difficult.
3. The severity of the conditions and chemical nature of the feedstock are critical factors in the fouling process.
4. There appears to be little hope of reducing fouling unless the severity of operation can be decreased.
5. The use of additives reduces fouling but not to the point that periodic cleaning can be avoided.

Duggan et al. [87] reported a technique for determining the fouling tendency of hydrocarbon streams. They stated that additives are being used successfully in refineries and chemical plants to control hydrocarbon fouling in a variety of process equipment. Escalating fuel costs have made the use of such additives

©1984 Hemisphere Publishing Corporation

more economically attractive. Significant decreases in fouling rates were obtained in several plant cases, including the preheat exchanger system of a crude unit, a hydrodesulfurization unit, reformer feed-effluent exchangers, and a naphtha hydrotreater. A proprietary additive was used. In some cases constant overall heat transfer coefficients were obtained, and in others the on-stream time between shutdowns for cleaning was at least doubled.

Fouling in crude unit preheat exchangers caused by the presence of salt water in the crude oil was described by Van der Wee and Tritsmans [88], who listed several procedures for minimizing fouling due to the presence of salt water.

(ii) Corrosion by hydrocarbon streams. Most of the corrosion problems in refinery and petrochemical plant streams [89] are caused by the presence of liquid water containing dissolved gases, salts, and acids. Much of the corrosion is caused by the presence of acids, which bring the pH into the acidic range.

Water-soluble alkalis such as $NaOH, Na_2CO_3$, and NH_4OH have been used extensively for corrosion control. Low-molecular-weight amines are also used as neutralizers. The cost of neutralizing chemicals is high because it is proportional to the amount of neutralization required. Good control must be exercised to maintain a pH range such that scaling does not occur.

Film-forming corrosion inhibitors are also used extensively. Their chemical structure consists of a polar portion, which contains nitrogen, sulfur, oxygen, or another atom that has an unshared electron pair to permit chemisorption to an active metal surface, as well as a nonpolar extremity.

It is thought that the nonpolar end is attracted to the hydrocarbon and the inhibitor is chemisorbed onto the surface, forming a film that is water-repellent. Such neutralizing inhibitors are not required in stoichiometric amounts to accomplish neutralization. However, a certain minimum amount of inhibitor is required to ensure formation of a continuous protective film on the metal surface.

An effective treatment procedure is to use a combination of a chemical neutralizer such as an amine and a film-forming inhibitor such as a neutralizing amine. The amount of film-forming inhibitor should be closely controlled to avoid emulsion or foaming problems at liquid-liquid or gas-liquid interfaces.

(g) Fouling in gas streams

The combustion of fossil fuels can produce particulate and condensable materials in the gaseous products. These materials deposit on heat transfer surfaces, where they inhibit the transfer of heat. A major problem is encountered under conditions where fly ash is deposited on furnace walls or temperatures become low enough for acids to condense. The combination of condensable (or molten) materials and solid particles is worse than either of them separately. Liquids wet the particles, and they adhere more firmly to the heat transfer surface. Coatings of significant thickness can be formed. In recent years, emphasis has been on energy recovery from hot dirty gas streams such as diesel exhausts which contain carbon particles.

The subject of gas-side fouling was discussed extensively at a recent workshop [90, 91]. Before interest developed in heat recovery from dirty gases, the major gas-side fouling problem occurred in fossil-fueled furnaces. Wynnyckyj and Rhodes [92] proposed a mechanism for furnace fouling. Deposits in coal-tired furnaces do not grow evenly but produce a very rough surface. The growth of the deposit is postulated to be a dynamic process involving three types of particles. One type is fly ash particles 5-20 μm in diameter, which are hollow spheres (cenospheres). The cenospheres appear to fuse and agglomerate to form larger, relatively dense particles (nodules) in the size range 0.1-l .O mm. These particles are large and heavy enough to penetrate the boundary layer and impinge on the furnace wall. Large lumps (pyroclasts) several centimeters in diameter are formed on the furnace wall from the agglomeration of nodules. This hypothesis is based on visual and circumstantial evidence and physical measurements by heat flux probes [93].

Magnesium oxide has been used successfully to minimize fouling of coal-fired boilers, but the amount required, 0.4-3% of the fuel burned, made the practice uneconomical. However, Radway and Boyce [94] reported that the use of magnesia dispersions of tine particle size at a rate of 0.015% of the fuel yielded a reduction in fouling. Further investigation of this phenomenon is warranted.

A good survey of the use of fire-side additives to control fouling in utility boilers has been presented by Locklin et al. [95]. For oil-fired boilers, additives are used to control SO_3-related problems, high-temperature fouling, high-temperature corrosion, superheater temperature, and stack plume color. For coal-fired boilers, additives are used to control fly ash conditioning for electrostatic precipitation, convective tube fouling, coal-ash slag, SO_3-related problems, and superheat control. In many cases, evaluation of the effect of additives is qualitative in nature and more fundamental information is needed.

Heat recovery systems usually have extended surfaces to remove heat from the gas. Protos and Sharon [96] studied the effect of spacing and arrangement of finned tubes on fouling from air containing gypsum particles. The in-line arrangement had a small relative

©1984 Hemisphere Publishing Corporation

Table 8 Design parameters for extended surfaces in fossil fuel flue gases[a]

Type of flue gas	Fouling resistance, m^2 K/W (h ft^2 °F/Btu)	Fin spacing, m (in)	Gas velocity m/s (ft/s)
Clean gas (cleaning devices not required)			
Natural gas	8.8 x 10^{-5}-5.3 x 10^{-4} (0.000 S-0.003)	1.3 x 10^{-3}-3.0 x 10^{-3} (0.050-0.118)	31-37 (100-120)
Propane	1.8 x 10^{-4}-5.3 X 10^{-4} (0.001-0.003)	1.8 x 10-s (0.070)	
Butane	1.8 x 10^{-4}-5.3 x 10^{-4} (0.001-0.003)	1.8 x 10^{-3} (0.070)	
Average gas (provisions for future installation of cleaning device)			
No. 2 oil	3.5 x 10^{-4}-7.0 x 10^{-4} (0.002-0.004)	3.0 x 10-s-3.8 x 10-s (0.120-0.151)	26-31 (85-100)
Diesel engine	5.3 x 10^{-4} (0.003)		
Dirty gas (cleaning devices required)			
No. 6 oil	5.3 x 10-4-1.2 x 10^{-3} (0.003-0.007)	4.6 x 10^{-3}-5.8 x 10-s (0.180-0.228)	18-24 (60-80)
Crude oil	7.0 x 10^{-4}-2.6 x 10-s (0.004-0.015)	5.1 x 10-s (0.200)	
Residual oil	8.8 x 10^{-4}-3.5 x 10-s (0.005-0.02)	5.1 x 10-s (0.200)	
Coal	8.8 x 10-4-8.8 x 10^{-3} (0.005-0.05)	5.9 x 10^{-3}-8.6 x 10^{-3} (0.231-0.340)	15-21 (50-70)

From Weierman [90].

tendency for fouling except for very close transverse spacing. The relative fouling tendency was primarily dependent on spacing ratios and only slightly affected by gas velocity.

Silvestrini [97] investigated fouling of finned surfaces exposed to diesel exhausts at various plant sites utilizing heat recovery systems. Fin type (plain or serrated) did not affect fouling rate. Fins of greater density showed worse fouling in terms of flow area reduction. Fin bridging occurs through soot buildup from the base tube surface. There is a significant relationship between sulfuric acid concentration and fouling.

Weierman [90] discussed some factors involved in the design of extended surface heat exchangers for fossil fuel gases and showed examples of severe bridging across serrated fins. Table 8 gives a range of suggested design parameters.

In the cement industry, exhaust gases in the temperature range 300-l 900° F are suitable for heat recovery but are dusty and heavily laden with alkalis, sulfates, and chlorides [98]. Because of the nature of the gases, particulate fouling, chemical reaction fouling, and corrosion fouling occur. A more thorough knowledge of the mechanism of gas-side fouling is needed before successful heat recovery from such gases can be accomplished.

References for Section 3. I 7. 4 appear at the end of Section 3. I 7. 7.

© 1984 Hemisphere P iblishing Corporation

3.17.5
Cleaning of heat exchangers

James G. Knudsen

■ If design and fluid treatment do not accomplish significant mitigation of fouling and serious reduction in capacity results, it is necessary to take the heat exchanger out of service and clean it. If there is no spare exchanger to take its place, a complete plant shutdown may be necessary. This is a costly occurrence and should be avoided if possible. Most industrial plants shut down for periodic maintenance, and heat exchanger cleaning should coincide with these planned shutdowns.

Excessive fouling can occur for the following reasons [37]:

1. Changes in flow rates and temperatures
2. Plant failures and excursions from normal operations
3. Ingress of air, bacteria, and corrosive chemicals (from process fluid leaks)
4. Changes in fluid composition or product quality
5. Corrosion in remote parts of the system
6. Difficulty in monitoring and dosing treatment additives

A. Mechanical cleaning

(a) On-line mechanical cleaning

On-line mechanical cleaning equipment can significantly improve heat exchanger performance and increase times between shutdowns for cleaning. On-line techniques generally work best if the deposits are soft and friable with a low removal resistance. A wide variety of on-line mechanical techniques are available.

For gases, soot blowers are used most extensively. There are two types: sonic soot blowers and jet soot blowers. Sonic soot blowers are used in the cooler part of furnaces, where soft deposits are present. They can withstand temperatures up to 1 050° C (1900°F). They emit sound for 15-30 s every 10-30 min. Jet soot blowers emit pulses of steam or air at regular intervals. They remove harder deposits than do sonic soot blowers, but do not remove glossy deposits.

On-line cleaning is also performed with scrapers, chains, and thermal shock. A number of scraped surface heat exchangers for special applications are described in the patent literature.

The two main on-line systems for mitigating fouling in liquid systems are the Amertap system (Amertap Corporation, Woodbury, N.Y.) and the MAN system (Machinenfabrik Augsburg-Niirnburg, Nuremburg, West Germany). The Amertap recirculating sponge ball system uses sponge rubber balls (sometimes coated with abrasive) which circulate through the heat exchanger. The balls are slightly compressed as they pass through the tubes. A ball passes through a tube about once every 5 min. Balls leaving the exchanger are separated by a strainer and returned to the inlet. The MAN system uses brushes that fit the tubes and move through them under the force of the flowing fluid. A special retainer is placed on each end of each tube, and under normal operation the brushes are retained at the exit end. When flow is reversed the brushes are moved to the other end of the tubes, removing deposited material. Operation is returned to normal and the brushes move through the tubes again to be retained at the tube exit.

© 1984 Hemisphere Publishing Corporation

Table 1 Typical deposits removed by chemical cleaning[a]

Organic	Inorganic
Oil	Rust
Grease	Magnetite
Fats	Calcium carbonate
Waxes	Calcium sulfate
Soft carbon	Magnesium hydroxide
Tars	Calcium phosphate
Silt	Silica
Vegetation	Magnesium silicate
Biological matter	Copper, copper oxides
Polymers	Alumina
Resins	Nickel oxide
Paints	

From French [37].

Both of these systems are claimed to maintain nearly zero fouling resistances in heat exchangers where they have been used.

(b) Off-line mechanical techniques

In many cases, even though fluid treatment and on-line cleaning are used, heat exchangers require cleaning during shutdown. Off-line mechanical cleaning usually requires disassembly of the heat exchanger.

In mechanical cleaning the deposit is removed by drilling, chipping, or high-pressure water. High-pressure water jets are most frequently used. Occasionally, sand is injected with the water to remove hard adherent scale. High-pressure water is effective in removing deposits from the inside and outside of tubes, but it can erode the tube surface and remove protective films that inhibit corrosion. Another device is the lance, which may be equipped with various cleaning and cutting heads that rotate on its end. Mechanical means such as drilling out tubes or chipping off the scale are labor-intensive and can seriously damage the surface. If it is expected that the shell side of a heat exchanger will require cleaning, it is necessary to use a square-pitch tube layout.

Table 2 Deposits not normally removed by chemical cleaning

Glasses	Inert plastics (e.g., polythene)
Ceramics	Vulcanized rubber
Hard carbon	Rubber latex

From French[37].

Off-line techniques for gas-side deposits include baking, hydroblasting, dissolving the deposit with a solvent, and thermal shock. The deposit may be burned off if it is combustible. It is important in cleaning gas-side surfaces to match the cleaning technique to the nature of the deposit and the mechanism of attachment [91].

B. Chemical cleaning

French [37] presented a good discussion of chemical cleaning in practice, including several case studies. The advantages of chemical cleaning are:

1. It is relatively rapid.
2. It is effective.
3. Heat transfer surfaces are not damaged mechanically.
4. Chemical solutions usually reach otherwise inaccessible areas.
5. Complete surface treatment is achieved.
6. It is not as labor-intensive as mechanical cleaning.
7. Cleaning can be performed in situ.

Table 1 lists deposits that can be removed by chemical cleaning, and Table 2 lists deposits that are not susceptible to chemical cleaning. Table 3 is a list of typical chemicals used for in situ chemical cleaning.

When acids are used as cleaning chemicals, it is important to use an inhibitor so that the acid will remove the deposit and not dissolve the heat transfer surface. Modern inhibitors can be used under extremes of temperature and flow rate, and metal losses are less than 2.5 μm for a 6-h contact time.

Table 3 Common types of chemicals utilized for in situ chemical cleaning

Acids	Alkalis	Complexing agents	Oxidants	Solvents	Others
Hydrochloric	Caustic soda	EDTA	Potassium permanganate	Aromatic	Inhibitors
Nitric	Ammonia	Gluconates	Sodium bromate	Aliphatic	Surfactants
Sulfuric	Trisodium phosphate		Sodium nitrite	Chlorinated	Antifoams
Hydrofluoric	Sodium metasilicate		Sodium hypochlorite	Solvent emulsifiers	Biocides
Citric	Soda ash		Ammonium persulfate	Dewatering formulations	Dispersants
Formic					Hydrazinc bifluoride
Sulfamic					

From French [37].

©1984 Hemisphere Publishing Corporation

Chemical cleaning operations generally involve a circulation technique to ensure that the chemicals are always well mixed and that fresh chemical contacts the heat transfer surfaces. With this technique the deposits are dissolved as well as removed by mechanical scouring.

On-stream cleaning is often carried out when biofouling occurs, and biocide is added periodically as a shock treatment to kill the biological growth. Biocide does not necessarily remove the biofilm. Miller and Bott [38] investigated the removal of biological films with sodium hypochlorite solutions. A concentration of 4 ppm free chlorine resulted in an initial film removal rate four to six times greater than that achieved with 2.5 ppm free chlorine. The film thickness was reduced by 80% but the film recovered rapidly after treatment. The effectiveness of the biocide was greater at high velocities.

References for Section 3. I 7.5 appear at the end of Section 3.17.7.

©1984 Hemisphere Publishing Corporation

3.17.6
Measurement of fouling resistances

James G. Knudsen

■ There are many different types of fouling and the overall process is very complex. Heat, mass, and momentum transfer and chemical reactions occur simultaneously. In order to understand the fouling mechanism, it is necessary to study the individual processes that occur during fouling. However, regardless of the individual processes, the overall result is an increase in the resistance to heat transfer. Hence, a variety of monitors have been developed to measure the thermal resistance of fouling deposits as they are laid down on a heat transfer surface.

As a heat exchanger surface becomes fouled, the overall fouling resistance can be expressed by the simple relationship

$$R_{f1} + R_{f2}\frac{A_1}{A_2} = R_f = \frac{1}{U_F} - \frac{1}{U_C} \qquad (1)$$

provided the change from U_C, the overall heat transfer coefficient under clean conditions, to U_F, the overall heat transfer coefficient under fouled conditions, is due *only* to the fouling. The overall coefficients are based on A_1. In an operating heat exchanger this is not always the case. Therefore, the determination of accurate fouling factors on full-scale equipment is difficult. A good summary of techniques for measuring fouling factors has been given by Epstein [4]. Knudsen [22] described the characteristics of several generic types of test sections. The various types are listed in Table 1.

The use of fouling monitors with a liquid as the heating mechanism has disadvantages. One advantage is that the surface cannot overheat. Most operating heat exchangers are similarly limited. However, most fouling monitors are electrically heated. The most common configurations are 1 and 2b in Table 1. Configuration 1 was developed by Heat Transfer Research Incorporated and consists of an annular duct with a concentric core, a portion of which is electrically heated. Configuration 2a consists of a thick-walled tube that is electrically heated. Fetkovich et al. [99,100] utilized this configuration and a transient cooling technique to determine fouling factors for biofilms formed from contact with seawater. Characklis et al. [101] developed a fouling monitoring device based on configuration 2b. It is electrically heated and operated under steady-state conditions. Heat flux is determined from the radial temperature gradient in the thick-walled test section.

There is always a question of whether a fouling monitor actually simulates the thermal hydraulic condi-

Table 1 Types of fouling test devices[a]

Configuration	Description
1	Annular geometry, indirect electric heating
2a	Thin-walled tube, indirect electric heating
2b	Thick-walled tube, indirect electric heating
2c	Thick-walled tube, transient technique
3	Circular tube geometry, thermoelectric heating or cooling
4	Annular or circular tube geometry, direct electric heating
5	Annular or circular tube geometry, sensible heat of fluids
6	Annular or circular tube geometry, condensing vapor
7	Complex geometries
8	Electrically heated wires and coils

From Knudsen [22].

©1984 Hemisphere Publishing Corporation

tions in a heat exchanger. Test sections of well-defined geometry (annular ducts or circular tubes) can probably simulate the thermal hydraulic conditions inside the tube of a heat exchanger.

Fetisoff et al. [102] compared two probes with widely different configurations. One was similar to configuration 1. The other was a coiled hot wire probe made of 0.14-mm-diameter wire with a coil diameter of 1.1 mm. In a flowing system with heptane containing small amounts of styrene, both probes gave essentially the same results. The fouling studied was due to a chemical reaction (polymerization of styrene) and the probes might behave differently with other types of fouling.

Although it is possible to develop devices to simulate the thermal hydraulic conditions in a heat exchanger, it is difficult to simulate the actual fluid whose fouling characteristics are to be determined. One of the earliest and most sophisticated devices was the HTRI portable fouling unit, in which the fluid being tested flowed in annular duct with an electrically heated central core [103]. Other test devices with varying degrees of sophistication have been developed for use in the field [23,104]. These utilize a small side stream of the fluid to be tested. All the test sections are similar to configuration 1 (Table 1). Ling and Lund [105] employed a test section similar to configuration 1 but with direct resistance heating of the concentric core of the annulus. This apparatus was used to study fouling of heated surfaces by biological fluids. Direct resistance heating probes may cause unwanted corrosion if the fluid is an electrolyte. Other devices include the ASTM-CRC fuel coker (manufactured by Erdco Engineering Co.), a kinetic device developed by Taylor [106], and the UOP (Universal Oil Products) [107] miniaturized probe.

It is important that fouling resistances be measured under constant conditions of temperature, flow rate, and quality of the fluid being tested.

In addition to measuring fouling resistances, it is important that chemical composition of the deposit be determined as well as the physical characteristics of the scale such as thermal conductivity, bulk density, porosity, adhesion strength, and crystalline form. Scanning electron micrographs of the scale surface and microprobe analyses can yield valuable information on the deposition process.

A. Constant heat flux devices

A constant heat flux measuring device can be based on either indirect electrical heating or direct resistance heating, using the material of the heat transfer surface itself. Electrically heated devices have the advantage that the local heat flux may be determined, permitting determination of local heat transfer coefficients and fouling resistance. For most electrically heated devices equipped with wall temperature sensors, the fouling resistance can be calculated from

$$R_f = \frac{T_{wF} - T_{wC}}{\dot{q}} \qquad (2)$$

provided the fluid velocity, bulk temperature, and heat flux remain constant during the test period. Here T_{wC} is the wall temperature under clean conditions, T_{wF} is the wall temperature under fouled conditions, and $\dot{q}$ is the heat flux. This equation assumes no change in the heat transfer coefficient of the fluid being tested for the duration of the test.

The use of indirect electrical heating (e.g., with cartridge heaters inside a tube) is the preferred method since it does not restrict the type of material of the heat transfer surface. Heat fluxes up to 380 000 W/m^2 (120 000 Btu/h ft) are possible and power requirements are 2-4 kW. The test section area can range from 3.2 X 10^{-3} to 6.4 X 10^{-3} m^2 (5-10 in^2).

Direct electrical resistance heating is convenient, but the materials of the heat transfer test section are limited to those with high resistivities such as stainless steel and nichrome. The wall thickness must be very uniform or the heat flux will vary over the surface.

B. Constant wall temperature devices

Test devices that make use of a boiling liquid or condensing vapor to transfer heat to or from a test fluid are essentially constant wall temperature devices. As fouling proceeds, the wall temperature remains constant and the heat flux decreases. Even though the wall temperature may be known, the local heat flux cannot be determined and hence only average fouling resistances over the heat transfer section can be determined. In addition, condensing and boiling heat transfer coefficients are variable with time, resulting in a large band of uncertainty on the value of the measured fouling resistances.

C. Liquid-liquid devices

The fluid being tested may be heated or cooled by another fluid, which should be nonfouling in nature. This fluid should be passed through the test section at a high mass rate to minimize its temperature change. These devices are limited to low heat fluxes, and a condition somewhere between constant heat flux and constant wall temperature is achieved. Liquid-liquid devices are best suited to studying fouling with complex surfaces and complex geometries.

Nomenclature for Section 3. I 7. 6 appears at the beginning of Part 3. References appear at the end of Section 3.1 7.7.

© 1984 Hemisphere Publishing Corporation

3.17.7
Recommended fouling resistances for design

James G. Knudsen

■ Ultimately, the designer must decide how much additional surface must be included in the heat exchanger to account for the fouling that occurs during operation. Despite the extensive research that is under way, there has emerged no clear-cut correlation by which accurate fouling resistances may be predicted. The ultimate fouling that occurs in a heat exchanger is highly dependent on the operation of the equipment. As listed in Sec. 3.17.5, various conditions can contribute to excessive fouling over which the designer has no control.

In specifying the additional surface necessary to account for fouling, the following items should be considered:

1. Nature of the fluids and any past operating experience
2. Treatments available to mitigate fouling
3. Nature of any potential deposit
4. Possible geometries that will reduce the potential for deposition
5. Effects on operation of specifying more heat transfer surface than is needed

The result of specifying a fouling resistance in design is to provide excess surface over that needed for the clean heat exchanger. Figure 1 shows the relation between fouling resistance R_f and overall coefficient for the clean exchanger U_C for various percentages of excess surface. For example, 100% excess surface means that the heat exchanger has twice as much surface as needed when it is clean. Therefore, modifications must be made in the operating conditions to achieve the heat duty for which the exchanger was designed.

Table 3.17.3(1) indicates that an increase in velocity and reduction in surface temperature cause a reduction in the asymptotic fouling resistance for several types of fouling. This behavior is shown schematically in Fig. 2. Such a plot cannot yet be expressed qualitatively for any type of fouling, but Fig. 2 serves to illustrate the problem. Point A represents the design velocity and surface temperature and the corresponding fouling resistance, which was used for one fluid assuming that the other fluid is nonfouling. At start-up, there is too much area in the exchanger for the required heat duty. Operating conditions must then be adjusted to point B,

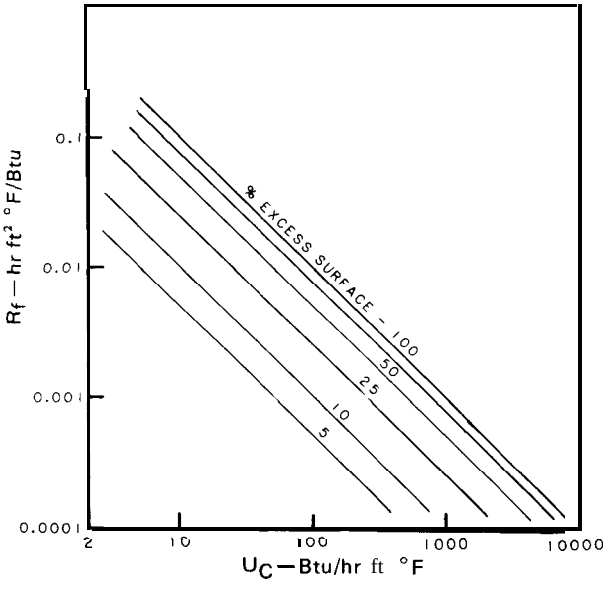

Figure 1 Relation between fouling resistance, overall coefficient for clean exchanger, and percent of excess surface.

© 1984 Hemisphere Publishing Corporation

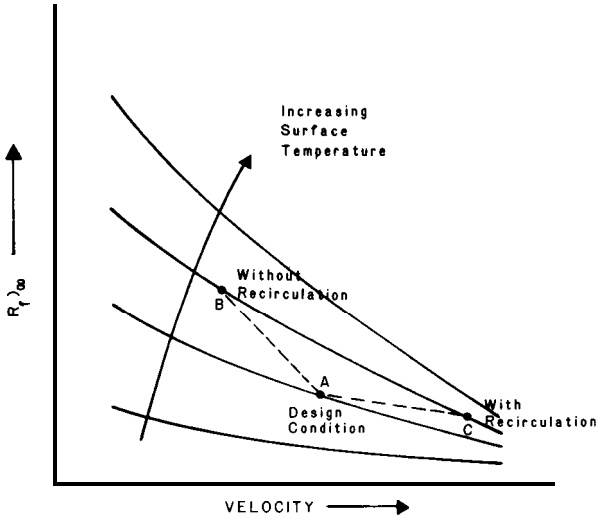

Figure 2 Effect of velocity and surface temperature on the asymptotic fouling resistance.

corresponding to a lower than design velocity and higher than design surface temperature. This is a region of higher fouling resistance than was used in the design, so conditions exist for this higher fouling resistance to develop.

As fouling proceeds at constant heat duty, the velocity of the fluid must be increased and its outlet temperature decreased. If fouling proceeds beyond the design value of the fouling resistance, the velocity of the fouling fluid must continue to increase, resulting in a significant friction loss penalty.

It would be desirable if, during the initial operating period, the velocity could be maintained at a value equal to or greater than the design value. This can be accomplished by recirculation of the fouling fluid so that initial start-up conditions correspond to point C in Fig. 2. With recirculation the exchanger can be operated at or above the design velocity, with the result that the average bulk temperature of the fouling fluid is increased. At high recirculation rates there is a cost penalty for additional friction loss.

Unfortunately, the quantitative effect of velocity and surface temperature on fouling are not well enough known that firm economic analyses can be made.

A. Recommended fouling resistances

(a) Cooling water

With the treatment techniques available, the asymptotic fouling resistance for cooling water should not be greater than 1.7 X 10^{-4} m^2 K/W (0.001 h ft^2 °F/Btu) and certainly not greater than 3.5 X 10^{-4} m^2 K/W (0.002 h ft^2 °F/Btu). If possible, water velocity in the tube side should be at least 2 m/s (6.6 ft/s) if erosion is not a problem. Power condensers with stainless steel or titanium tubes can tolerate 3-5 m/s (10-16 ft/s). If a well-defined, well-controlled treatment program is used, an excess surface of not more than 25% should be specified.

Regardless of how much excess area is specified, the designer must determine the initial operating conditions of the heat exchanger to meet the design heat duty and determine whether those conditions are such that excessive fouling will occur. For cooling waters from which calcium carbonate may be deposited, a heat transfer surface temperature above 60° C (140° F) should be avoided.

If it is known that cooling water scales at a certain temperature and the asymptotic fouling resistance is known, the effect of surface temperature may be determined from the relationship

$$R_f^* \approx C \exp\left(\frac{-E}{\tilde{R}T_s}\right) \qquad (1)$$

where E is the activation energy. The value of E has been found to be in the range 4.7 X 10 to 9.3 X 10 J/kmol (20 000-40 000 Btu/lb mol) [33]. A conservative approach would be to use E = 2.3 X 10 J/kmol (10 000 Btu/lb mol) if the wall temperature is being lowered and 4.7 X 10 J/kmol (20 000 Btu/lb mol) if it is being raised.

If a fouling resistance-time relationship is desired, it might be developed in the form

$$R_f = R_f^*(1 - e^{Bt}) \qquad (2)$$

If two points on the curve are known-for example, t_1, $(R_f)_1$ and t_2, $(R_f)_2$ -the constants in the equations may be determined. Zanker [108] developed a nomograph with which the constants R_f^* and B can be readily determined.

Initial deposition rates have been shown by Watkinson [109] to be related to the Langelier saturation index, but further testing of the model is required. Watkinson also reported the effect of fluid velocity on the asymptotic fouling resistance as follows:

1. Calcium carbonate scaling, constant surface temperature and composition:

$$R_f^* = \frac{0.101}{V^{1.33}D^{0.23}}$$

2. Gas oil fouling, fixed heat flux:

$$R_f^* = \frac{0.55}{V^2}$$

3. Sand deposition from water, fixed heat flux

$$R_f^* = \frac{0.015}{V^{1.2}}$$

© 1984 Hemisphere Publishing Corporation

where R_f^* = asymptotic fouling resistance, m^2 K/kW
V = fluid velocity, m/s
D = tube diameter, m

In the case of biofouling in the absence of other types of fouling, a significant resistance to heat transfer can occur. Biofilms have essentially the same thermal conductivity as water; thus a biofilm 125 μm (0.005 in) thick has a fouling resistance of approximately 1.7 X 10^{-4} m^2 K/W (0.001 h ft^2°F/Btu).

(b) Boiling and evaporation

A wide range of fouling resistances may be encountered in boiling and evaporation operations. If hard adherent deposits are formed, sufficient surface should be specified that a reasonable operating time is obtained between shutdowns for cleaning.

For spent alkaline pulping liquors, fouling resistances appear to be in the range 7 X 10^{-4} to 1.4 X 10^{-3} m^2 K/W (0.004-0.008 h ft^2°F/Btu) before cleaning [46, 47].

Fredrick and Grace [24,110] indicate that water-soluble scales (mainly Na_2SO_4-Na_2CO_3 and $CaCO_3$) account for over 80% of the evaporator fouling problems in alkaline pulp mills. The calcium carbonate scales have a much greater impact on evaporator capacity. From experiments with calcium carbonate [110] they conclude that deposition rate is doubled for a 3.1 K (5.5°F) increase in liquor temperature, scaling rate is not strongly dependent on liquor solids concentration, and calcium carbonate addition to the black liquor (seeding) reduces fouling tendency.

For desalination plants, typical fouling resistances range from 1.5 X 10^{-4} to 7.6 X 10^{-5} m^2 K/W (0.000 85-0.000 43 h ft^2°F/Btu)[84].

In steam boilers and boiling-water nuclear reactors, in situ corrosion can occur as well as deposition of iron oxides that are present in the boiling liquid. There has been considerable study of the deposition of iron oxide onto surfaces on which water is boiling. Lister [111] presented Charlesworth s model [112] for deposition of iron oxide from water dosed with ammonia. The mass of deposited iron oxide M, is given by

$$M = 0.025\, \dot{q}^2 c[1 - \exp(-0.01\, t)] \quad (3)$$

where M = mass deposited, kg/cm^2
$\dot{q}$ = heat flux, W/cm^2
c = concentration, kg/kg
t = time, h

Charlesworth found that the deposition was reversible, reached a steady state in time, was proportional to the total iron concentration, and was not greatly influenced by the chemistry of the coolant or mode of heat transfer (boiling or nonboiling).

Table 1 Values of *a* and *b* in Eq. (4)

q, W/cm²	*c*, mg/kg	*P*, kg/cm²	a	*b*
IO-60	O-5	l-180	2	1
25-140	O-2.5	70	l-5	1
O-35	O-2.5	1	1	1
10-30	o-3	1	1	1

The dependence of the deposition rate of iron oxide on heat flux and concentration has been determined by various workers. The results were summarized by Asakura et al. [113] as shown in Table 1, based on the equation

$$\frac{dM}{dt} = k\dot{q}^a c^b \quad (4)$$

Asakura et al. derived the following equation based on their experimental data:

$$\frac{dM}{dt} = \frac{K\dot{q}c}{\lambda} \quad (5)$$

where λ is the latent heat of vaporization. The deposition rate constant K was determined from a theoretical analysis and compares well with experimental values, as shown in Fig. 3. At constant pressure Eq. (5) will not give a value of the asymptotic fouling resistance, as shown by Charlesworth [112], and it is probably applicable only in the early deposition period.

Palmer [81] indicates that the best method of controlling iron oxide is by use of a dispersant that

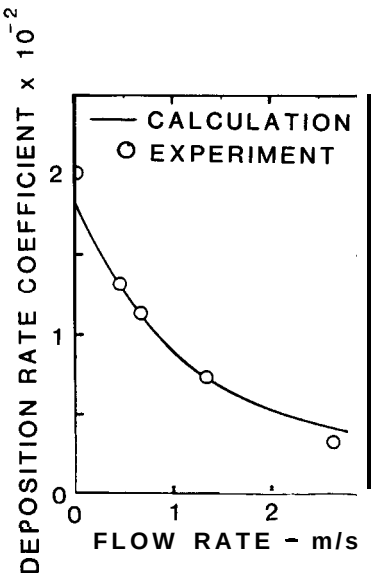

Figure 3 Deposition rate constant for iron oxide. From Asakura et al. [113].

©1984 Hemisphere Publishing Corporation

interacts with the iron oxide in the feedwater. Maximum benefit from the clispersant treatment is obtained when iron levels are reduced in the feedwater by amine treatment and filtration.

Phosphate conditioning of boiler feedwater may cause phosphates to precipitate if alkaline earth metal ions are present. A common contaminant of phosphate-treated boilers is calcium hydroxyapatite. Kelen and Gustafsson [114] investigated the kinetics of deposition of this material in a boiler. The deposition rate constant k (m/s) is defined by

$$\frac{dM}{dt} = kc \qquad (6)$$

where M = mass deposited, kg/m^2
t = time, s
c = concentration of phosphate in the water, kg/m^3

They obtained the following results: the range of k was 0.1-100 m/s; steam content did not influence deposition rate in the nucleate boiling regime; k was proportional to $\dot{q}^{2-3}$; k was larger at higher temperatures; and sodium polyacrylate showed a strong inhibiting effect on deposition.

Table 2a TEMA fouling resistances for water

Temperature of heating medium	≤ 240° F		240°-400° F[a]	
Temperature of water	≤125° F		> 125° F	
	Water velocity, ft/s		Water velocity, ft/s	
Types of water	≤3	>3	≤3	>3
Seawater	**0.000 5**	**0.000 5**	0.001	0.001
Brackish water	**0.002**	**0.00 1**	**0.003**	**0.002**
Cooling tower and artificial spray pond				
Treated makeup	0.001	0.001	**0.002**	**0.002**
Untreated	**0.003**	**0.003**	**0.005**	**0.004**
City or well water (such as Great Lakes)	0.001	0.001	**0.002**	**0.002**
River water				
Minimum	**0.002**	0.001	**0.003**	**0.002**
Average	**0.003**	**0.002**	**0.004**	**0.003**
Muddy or silty	**0.003**	**0.002**	**0.004**	**0.003**
Hard (over 15 grains/gal)	**0.003**	**0.003**	**0.005**	**0.005**
Engine jacket	0.001	0.001	0.001	0.001
Distilled or closed cycle condensate	**0.000 5**	**0.000 5**	**0.000 5**	**0.000 5**
Treated boiler feedwater	0.001	0.000 5	0.001	0.001
Boiler blowdown	**0.002**	**0.002**	**0.002**	**0.002**

[a] Ratings in the third and fourth columns are based on a temperature of the heating medium of 240 -400° F. If the heating medium temperature is over 400° F and the cooling medium is known to scale, these ratings should be modified accordingly.

Table 2b TEMA fouling resistances for industrial fluids

Oils	
Fuel oil	**0.005**
Transformer oil	0.001
Engine lube oil	0.001
Quench oil	**0.004**
Gases and vapors	
Manufactured gas	0.01
Engine exhaust gas	0.01
Steam (non-oil bearing)	**0.000 5**
Exhaust steam (oil bearing)	0.001
Refrigerant vapors (oil bearing)	**0.002**
Compressed air	**0.002**
Industrial organic heat transfer media	0.001
Liquids	
Refrigerant liquids	0.001
Hydraulic fluid	0.001
Industrial organic heat transfer media	0.001
Molten heat transfer salts	**0.000 5**

(c) Hydrocarbons

As indicated previously, hydrocarbons cannot usually be prevented from fouling, but additives can reduce the rate of fouling and extend the operating time between shutdowns. An approximate fouling resistance for reformer feed-effluent heat exchangers is obtained from data presented by Dugan et al. [87]. In 6 mo, with no additive, the overall coefficient changed from 204 to 102 W/m^2 K (36-18 Btu/h ft^2 F), indicating a fouling resistance of 5.3 X 10^{-3} m^2 K/W (0.03 h ft^2 °F/Btu). In the same period, with additive, the overall coefficient changed from 204 to 165 W/m^2 K (36-29 Btu/h (ft^2 °F), indicating a fouling resistance of 1.2 X 10^{-3} m^2 K/W (0.007 h ft^2 °F/Btu). These are rather large fouling resistances; however, the overall coefficients are low. For a clean coefficient of 204 W/m^2 K (36 Btu/h ft^2 °F) and a fouling resistance of 1.7 X 10^3 m^2 K/W (0.01 h ft^2 °F/Btu), the excess surface is 36%.

Table 2c TEMA fouling resistances for chemical processing streams

Gases and vapors	
Acid gas	0.001
Solvent vapors	0.001
Stable overhead products	0.001
Liquids	
MEA and DEA solutions	**0.002**
DEG and TEG solutions	**0.002**
Stable side draw and bottom product	0.001
Caustic solutions	**0.002**
Vegetable oils	**0.003**

©1984 Hemisphere Publishing Corporation

Table 2d TEMA fouling resistances for natural gas-gasoline processing streams

Gases and vapors	
Natural gas	0.001
Overhead products	0.001
Liquids	
Lean oil	0.002
Rich oil	0.001
Natural gasoline and liquefied petroleum gases	0.001

(d) Gases

The fouling resistances of deposits from dirty gas streams are difficult to predict. Table 3.17.4(8) indicates the range of fouling resistances that might be expected.

B. TEMA fouling resistances

In some cases, design engineers have a reasonable background of experience on which to base estimates of fouling resistances to be used in Eq. 3.17.1(l). In addition, the fouling resistances for a number of specific services may be estimated from the Tubular Exchanger Manufacturers Association (TEMA) standards [66], which are based on experience values collected for many years. These are shown in Table 2.

Table 2e TEMA fouling resistances for oil refinery streams

Crude and vacuum unit gases and vapors						
Atmospheric tower overhead vapors						0.001
Light naphthas						0.001
Vacuum overhead vapors						0.002
Crude and vacuum liquids						
Crude oil						
	Velocity, ft/s					
	T = O-199° F			T = 200°-299° F		
	<2	2-4	⩾4	<2	2-4	⩾4
Dry salt[a]	0.003	0.002	0.002	0.003	0.002	0.002
	0.003	0.002	0.002	0.005	0.004	0.004
	T = 300°-499° F			T = ⩾500° F		
	0.004	0.003	0.002	0.005	0.004	0.003
	0.006	0.005	0.004	0.007	0.006	0.005
Gasoline						0.001
Naphtha and light distillates						0.001
Kerosene						0.001
Light gas oil						0.002
Heavy gas oil						0.003
Heavy fuel oils						0.005
Asphalt and residuum						0.010
Cracking and coking unit streams						
Overhead vapors						0.002
Light cycle oil						0.002
Heavy cycle oil						0.003
Light coker gas oil						0.003
Heavy coker gas oil						0.004
Bottoms slurry oil ($4\frac{1}{2}$ ft/s minimum)						0.003
Light liquid products						0.002
Catalytic reforming, hydrocracking, and hydrodesulfurization streams						
Reformer charge						0.002
Reformer effluent						0.001
Hydroaacker charge and effluent[b]						0.002
Recycle gas						0.001
Hydrodesulfurization charge and effluent[b]						0.002
Overhead vapors						0.001
Liquid product over 50° A.P.I.						0.001
Liquid product 30°-50° A.P.I.						0.002
Light ends processing streams						
Overhead vapors and gases						0.001
Liquid products						0.001
Absorption oils						0.002
Alkylation trace acid streams						0.002
Reboiler streams						0.003
Lube oil processing streams						
Feed stock						0.002
Solvent feed mix						0.002
Solvent						0.001
Ex tract[c]						0.003
Raftinate						0.001
Asphalt						0.005
Wax slurries[c]						0.003
Refined lube oil						0.001

[a] Normally desalted below this temperature range (applies to 200°-299°F, 300°-499°F, 500° F and over).

[b] Depending on charge characteristics and storage history, charge resistance may be many times this value.

[c] Precautions must be taken to prevent wax deposition on cold tube walls.

The fouling resistances recommended by TEMA should not be considered as constant or asymptotic values that will be attained in a heat exchanger after a period of operation. If they were true asymptotic values that represented maximum attainable values of the fouling resistance, the designer could specify the heat exchanger to account for this resistance and the heat exchanger would never need to be shut down for cleaning.

The TEMA standard fouling resistances have several limitations: (1) they do not recognize the time-dependent behavior of fouling, (2) they are not related to specific design and operational characteristics of particular heat exchangers, and (3) information is available only for a number of fluids.

The use of TEMA fouling resistances allows oversizing of the heat exchanger such that it will meet

© 1984 Hemisphere I blishing Corporation

performance requirements with reasonable intervals between shutdowns for cleaning. The goal is to select an optimal design that will result in a minimum of the sum of fixed costs and shutdown and cleaning costs.

Nomenclature for Section 3.17.7 appears at the beginning of Part 3.

REFERENCES FOR SECTIONS 3.17.1-3.17.7

1. Taborek, J., et al., Fouling: The Major Unresolved Problem in Heat Transfer, *Chem. Eng. Prog.*, vol. 68, no. 2, p. 59, 1972.
2. Taborek, J., et al., Predictive Methods for Fouling Behavior, *Chem. Eng. Prog.*, vol. 68, no. 7, p. 69, 1972.
3. Epstein, N., Fouling: Technical Aspects, in ***Fouling of Heat Transfer Equipment,*** eds. E. F. C. Somerscales and J. G. Knudsen, p. 31, Hemisphere, Washington, D.C., 1981.
4. Epstein, N., Fouling in Heat Exchangers, in ***Fouling of Heat Transfer Equipment,*** eds. E. F. C. Somerscales and J. G. Knudsen, p. 701, Hemisphere, Washington, D.C., 1981.
5. Hasson, D., ***Heat Exchanger Fouling,*** Chemical Engineering Research Group, Council for Scientific and Industrial Research, CSIR Rept. CENF 339, August 1980.
6. Knudsen, J. G., and Roy, B. V., Influence of Fouling on Heat Transfer, ***Proc. 7th Int. Heat Transfer Conf.,*** Munich, West Germany, September 6-10, 1982, vol. 1, p. 269, Hemisphere, Washington, D.C., 1982.
7. Thackery, P. A., The Cost of Fouling in Heat Exchange Plant, in ***Fouling-Science or Art,*** ed. A. M. Pritchard, Proceedings of a Conference at the University of Surrey, Guildford, U.K., March 27-28, 1979, p. 1.
8. Bridgwater, J., Crystallisation Fouling-A Review of Fundamentals, in ***Fouling-Science or Art,*** ed. A. M. Pritchard, Proceedings of a Conference at the University of Surrey, Guildford, U.K., March 27-28, 1979, p. 82.
9. Bott, T. R., Biological Fouling of Heat Transfer Surfaces, in ***Fouling-Science or Art,*** ed. A. M. Pritchard, Proceedings of a Conference at the University of Surrey, Guildford, U.K., March 27-28, 1979, p. 117.
10. Van Nostrand, W. L., Leach, S. H., and Haluska, J. L., Economic Penalties Associated with the Fouling of Refinery Heat Transfer Equipment, in ***Fouling of Heat Transfer Equipment,*** eds E. F. C. Somerscales and J. G. Knudsen, p. 619, Hemisphere, Washington, D.C., 1981.
11. Crittenden, B. D., and Khater, E. H., Economic Fouling Resistance Selection, in ***Fouling of Heat Transfer Equipment,*** eds E. F. C. Somerscales and J, G. Knudsen, p. 645, Hemisphere, Washington, D.C., 1981.
12. Epstein, N., Optimum Evaporator Cycles with Scale Formation, in ***Fouling of Heat Transfer Equipment,*** eds. E. F. C. Somerscales and J. G. Knudsen, p. 653, Hemisphere, Washington, D.C., 1981.
13. Hasson, D., Precipitation Fouling, in ***Fouling of Heat Transfer Equipment,*** eds. E. F. C. Somerscales and J. G. Knudsen, p. 527, Hemisphere, Washington, D.C., 1981.
14. Bott, T. R., Fouling due to Liquid Solidification, in ***Fouling of Heat Transfer Equipment,*** eds E. F. C. Somerscales and J. G. Knudsen, p. 201, Hemisphere, Washington, D.C., 1981.
15. Gudmundsson, J. S., Particulate Fouling, in ***Fouling of Heat Transfer Equipment,*** eds. E. F. C. Somerscales and J. G. Knudsen, p. 357, Hemisphere, Washington, D.C., 1981.
16. Froment, G. F., Fouling of Heat Transfer Surfaces by Coke Formation in Petrochemical Reactors, in ***Fouling of Heat Transfer Equipment,*** eds. E. F. C. Somerscales and J. G. Knudsen, p. 411, Hemisphere, Washington, D.C., 1981.
17. Lund, D., and Sandu, C., Chemical Reaction Fouling due to Foodstuffs, in ***Fouling of Heat Transfer Equipment,*** eds. E. F. C. Somerscales and J. G. Knudsen, p. 437, Hemisphere, Washington, D.C., 1981.
18. Lister, D. H., Corrosion Products in Power Generating Systems, in ***Fouling of Heat Transfer Equipment,*** eds. E. F. C. Somerscales and J. G. Knudsen, p. 135, Hemisphere, Washington, D.C., 1981.
19. Characklis, W. G., Microbial Fouling: A Process Analysis, in ***Fouling of Heat Transfer Equipment,*** eds E. F. C. Somerscales and J. G. Knudsen, p. 251, Hemisphere, Washington, D.C., 1981.
20. Somerscales, E. F. C., Introduction and Summary: The Fouling of Heat Transfer Equipment, in ***Fouling of Heat Transfer Equipment,*** eds. E. F. C. Somerscales and J. G. Knudsen, p. 1, Hemisphere, Washington, D.C., 1981.
21. Baier, R. E., Early Events of Micro-Biofouling of All Heat Transfer Equipment, in ***Fouling of Heat Transfer Equipment,*** eds. E. F. C. Somerscales and J. G. Knudsen, p. 293, Hemisphere, Washington, D.C., 1981.
22. Knudsen, J. G., Apparatus and Techniques for Measurement of Fouling of Heat Transfer Surfaces, in ***Fouling of Heat Transfer Equipment,*** eds. E. F. C. Somerscales and J. G. Knudsen, p. 57, Hemisphere, Washington, DC., 1981.
23. Oberhofer, A. W., and Fulks, K. E., A Cooling Water Evaluation Unit, in ***Fouling of Heat Transfer Equipment,*** eds. E. F. C. Somerscales and J. G. Knudsen, p. 95, Hemisphere, Washington, D.C., 1981.
24. Fredrick, W. J., and Grace, T. M., Scaling in Alkaline Spent Pulping Liquor Evaporators, in ***Fouling of Heat Transfer Equipment,*** eds. E. F. C. Somerscales and J. G. Knudsen, p. 587, Hemisphere, Washington, D.C., 1981.
25. Rice, J. K., Chlorine Minimization-An Overview, in ***Condenser Biofouling Control,*** ed. J. Garey, p. 295, Ann Arbor Science, Ann Arbor, Mich., 1980.
26. Waite, T. D., and Fagan, J. R., Summary of Biofouling Control Alternatives, in ***Condenser Biofouling Control,*** ed. J. Garey, p. 441, Ann Arbor Science, Ann Arbor, Mich., 1980.
27. Marto, P. J., and Nunn, R. H. (eds), ***Power Condenser Heat Transfer Technology,*** pp. 375-443, Hemisphere, Washington, D.C., 1981.
28. Ritter, R. B., Suitor, J. W., and Cypher, G. A., Thermal Fouling Rates for 90: 10 Copper-Nickel and Titanium in Seawater Service, in ***OTEC Biofouling and Corrosion,*** PNL-SA-7115, ed. R. H. Gray, p. 353, Battelle Pacific Northwest Laboratory, Richland, Wash, 1978.

© 1984 Hemisphere Publishing Corporation

29. DePalma, V. A., and Baier, R. E. Microfouling of Metallic and Coated Metallic Flow Surfaces in Model Heat Exchange Cells, in ***OTEC Biofouling and Corrosion,*** PNL-SA-7115, ed. R. H. Gray, p. 89, Battelle Pacific Northwest Laboratory, Richland, Wash., 1978.
30. Pinhiero, J. deD. R. S., Fouling of Heat Exchangers: Discussion of a Model, in ***Heat Exchangers: Theory and Practice,*** eds. J. Taborek, G. F. Hewitt, and N. H. Afghan, Hemisphere, Washington, D.C., 1983.
31. Klaren, D. G., Fluid Bed Heat Exchanger: The Ultimate Solution to Fouling in Heat Transfer, ***in Heat Exchangers: Theory and Practice,*** eds. J. Taborek, G. F. Hewitt, and N. H. Afghan, Hemisphere, Washington, D.C., 1983.
32. Novak, L., Fouling in Plate Heat Exchangers and Its Reduction by Proper Design, in ***Heat Exchangers: Theory and Practice,*** eds. J. Taborek, G. F. Hewitt, and N. H. Afghan, Hemisphere, Washington, D.C., 1983.
33. Knudsen, J. G., and Lahm, L., Jr., Precipitation Fouling of Cooling Water, in ***Heat Exchangers: Theory and Practice,*** eds. J. Taborek, G. F. Hewitt, and N. H. Afghan, Hemisphere, Washington, D.C., 1983.
34. Curlett, P. L., and Impagliazzo, M., The Impact of Condenser Tube Fouling on Power Plant Design Economics, ***in Fouling in Heat Exchange Equipment,*** eds. J. M. Chenoweth and M. Impagliazzo, ASME HTD, vol. 17, p. 45, 1981.
35. Somerscales, E. F. C., Corrosion Fouling, in ***Fouling in Heat Exchange Equipment,*** eds. J. M. Chenoweth and M. Impagliazzo, ASME HTD, vol. 17, p. 17, 1981.
36. Baier, R. E., DePalma, V. A., Meyer, A. E., King, R. W., and Formalik, M. S., Control of Heat Exchanger Surface Microfouling by Material and Process Variation, in ***Fouling in Heat Exchanger Equipment,*** eds. J. M. Chenoweth and M. lmpagliazzo, ASME HTD, vol, 17, p. 97, 1981.
37. French, M. A., Chemical Cleaning in Practice, in ***Progress in the Prevention of Fouling in Industrial Plant,*** ed. A. M. Pritchard, Proceedings of a Conference at Nottingham University, April l-3, 1981, p. 68.
38. Miller, P. C., and Bott, T. R., The Removal of Biological Films using Sodium Hypochlorite Solutions, in ***Progress in the Prevention of Fouling in Industrial Plant,*** ed. A. M. Pritchard, Proceedings of a Conference at Nottingham University, April l-3, 1981, p. 121.
39. Bryers, R. W. (ed.), ***Fouling of Heat Exchanger Surfaces,*** Proceedings of an Engineering Foundation Conference, October 31-November 5, 1982, White Haven, Pa., Engineering Foundation, New York, 1983.
40. Wright, K. H. R., What Have Turbulent Bursts to do with Fouling, ***Fouling Prev. Res Dig.,*** vol. 4, no. 2, p. iii, 1982.
41. Cousins, L. B., and Pritchard, A. M., Fouling Resistance and the Designer, ***Fouling Prev. Res Dig.,*** vol. 2, no. 3, p. iv, 1980.
42. Mansfield, G. H., OPERCOW Systems, ***Fouling Prev. Res Dig.,*** vol. 4, no. 3, p. ii, 1982.
43. Parry, D. J., Scaling-The Options Available, ***Fouling Prev. Res Dig.,*** vol. 3, no. 1, p. iv, 1981.
44. Troup, D. H., and Richardson, J. A., Scale Nucleation on a Heat Transfer Surface and Its Prevention, ***Chem Eng. Commun,*** vol. 2, pp. 167-180, 1978.
45. ***Drew Principles of Industrial Water Treatment,*** 1st ed., Drew Chemical, Boonton, N.J., 1977.
46. Institute of Paper Chemistry, Appleton, Wis., A Survey of Evaporator Scaling in the Alkaline Pulp Industry, Rept 1, Project 3234, September 22, 1975.
47. Institute of Paper Chemistry, Appleton, Wis., Study of Evaporator Scaling Soluble Carbonate-Sulfate Scales, Rept. 2, Project 3234, January 25, 1977.
48. Fassbender, L. L., in ***Proceedings*** of ***PNL Workshop,*** December 21, 1982, Seattle, Wash., PNL-4871, Battelle Pacific Northwest Laboratories, Richland, Wash., September 1983.
49. Garrett-Price, B. A., Watts, R. L., Smith, S. A., and Knudsen, J. G., in Industrial Fouling: Problem Characterization, Economic Assessment and Review of Prevention, Mitigation and Accommodation Techniques, PNL-4883, Battelle Pacific Northwest Laboratories, Richland, Wash., September 1983.
50. Epstein, N., Thinking about Heat Transfer Fouling: A 5 X 5 Matrix, ***Heat Transfer Eng.,*** vol. 4, no. 1, p. 43, 1983.
51. Kern, D. Q., and Seaton, R. E., Heat Exchanger Design for Fouling Surfaces, ***Chem Eng. Prog.,*** vol. 62, no. 7, p. 51, 1966.
52. Kern, D. Q., and Seaton, R. E., A Theoretical Analysis of Thermal Surface Fouling, ***Chem Eng. Prog.,*** vol. 55, no. 6, p. 71, 1959.
53. Morse, R. W., and Knudsen, J. G., Effect of Alkalinity on the Scaling of Simulated Cooling Tower Water, ***Can J. Chem Eng.,*** vol. 55, p. 272, 1977.
54. Pinheiro, J. deD. R. S., Fouling of Heat Transfer Surfaces, in ***Heat Exchangers-Thermal Hydraulic Fundamentalsand Design,*** eds. S. Kakac, A. E. Bergles, and F. Mayinger, pp. 1013-1035, Hemisphere, Washington, D.C., 1981.
55. Langelier, W. F., The Analytical Control of Anticorrosion Water Treatment, ***J. Am Water Works Assoc.,*** vol. 28, p. 1500, 1966.
56. Ryznar, J. W., A New Index for Determining the Amount of Calcium Carbonate Formed by Water, ***J. Am Water Works Assoc.,*** vol. 36, p. 472, 1944.
57. Bodnar, Yu, F., Selecting a Criterion to Estimate the Scale Forming Properties of Cooling Water, ***Thermal Eng.,*** no. 2667, p. 434, 1979.
58. Ingle, S. E., Schuldt, M. D., and Schultz, D. W., A Users Guide for REDEQL EPA: A Computer Program for Chemical Equilibrium in Aqueous Systems, Rept. EPA-600/3-78-024, Environmental Research Laboratory, Office of Research and Development, U.S. Environmental Protection Agency, Corvallis, Oreg., 1978.
59. Baier, R. E., Substrate Influences on Adhesion of Microorganisms and Their Resultant New Surface Properties, ***in Adsorption of Micro-organisms to Surfaces,*** eds. G. Britton and K. C. Marshall, p. 59, Wiley, New York, 1980.
60. Bowen, B. D., and Epstein, N., Fine Particle Deposition in Smooth Parallel-Plate Channels, ***J. Colloid Interface Sci,*** vol. 72, p. 81, 1979.
61. Grocki, J. M., and Westergren, L., ***Tubec-A Different Approach to Scale Control,*** in Corrosion 81, p. 263, National Association of Corrosion Engineers, Houston, Texas, 1981.
62. Watkinson, A. P., Louis, L., and Brent, R., Scaling of Enhanced Heat Exchanger Tubes, ***Can J. Chem Eng.,*** vol. 52, p. 558, 1974.
63. Epstein, N., Fouling of Heat Exchangers, in ***Heat Exchangers: Theory and Practice,*** eds. J. Taborek, G. F. Hewitt, and N. Afgan, pp. 795-815, Hemisphere, Washington, D.C., 1981.
64. Moore, J. A., Fin Tubes Foil Fouling for Scaling Services, *Chem.* Process, vol. 37, no. 8, pp. 8–10, August 1974.
65. Copper, A., et al., Cooling Water Fouling in Plate Heat Exchangers, ***Heat Transfer Eng., vol.*** 1, no. 3, pp. 50-55, 1980.

© 1984 Hemisphere Publishing Corporation

66. ***Standards of the Tubular Exchanger Manufacturers Association,*** 6th ed., TEMA, New York, 1978.

67. **Gilmour,** C. H., No Fooling-No Fouling, ***Chem Eng. Prog.,*** **vol.** 6, no. 7, p. 49, 1965.

68. Lord, R. C., **Minton,** P. E., and **Slusser,** R. P., Guide to **Trouble-Free** Heat Exchangers, ***Chem Eng.,*** **vol.** ***77, no. 12,*** **p.** ***153,*** 1970.

69. **Small,** W. M., and Young, R. K., The ROD Baffle Heat Exchanger, ***Heat Transfer Eng.,*** **vol.** 1, no. 2, p. 21, 1979.

70. Smyth, R., A Comparative Assessment of ROD Baffle Shell and Tube Heat Exchanger, ***Heat Transfer Eng.,*** **vol. 2,** nos. 3-4, p. 90, 1981.

71. Krisher, Raw Water Treatment in the CPI, Chem ***Eng.,*** vol. 85, no. 19, p. 79, August 28, 1978.

72. ***Betz Handbook of Industrial Water Conditioning,*** 7th ed., Betz Laboratories, Trevose, Pa., 1976.

73. ***Nalco Water Handbook, Nalco Chemical Company,*** 1st ed., McGraw-Hill, New York, 1979.

74. Troup, D. H., and Richardson, J. A., Scale Nucleation on a Heat Transfer Surface and Its Prevention, ***Chem Eng. Commun.,*** **vol.** 2, pp. 167-180, 1978.

75. Donohue, J. M., ***Cooling Water Treatment- Where Do We Stand?, Mater. Prot. Perform,*** vol. 11, pp. 19-22, June 1972.

76. Schieber, J. R., Control of Cooling Water Treatment, ***Combustion,*** **vol. 49,** no. 11, p. 25, May 1978.

77. Midkiff, W. S., and Foyt, H. P., Silica **Scale** Technology and Water Conservation, ***Mater. Perform.,*** vol. 18, pp. 39-42, August 1979.

78. Kumar, **J.,** and Fairfax, J. P., Rating Alternatives to Chromates in Cooling Water Treatment, ***Chem. Eng.,*** **vol.** 83, no. 9, p. 111, April 26, 1976.

79. Simon, D. E., II, Feedwater Quality in Modern Industrial Boilers: A Consensus of Proper Current Operating Practices, 36th Annu. Int. Water Conf., Pittsburgh, Pa., November 1975.

80. Herman, K. W., Causes and Cures of Waterside Problems in Industrial Boiler Systems, ***Combustion,*** vol. 50, no. 2, p. 9, August 1978.

Palmer, M. L., Controlling Iron Oxide Deposits in Boiler Systems, ***Power Eng.,*** vol. 84, p. 50, January 1980.

81. Palmer, M. L., Controlling Iron Oxide Deposits in **Boiler** Systems, ***Power Eng.,*** p. 50, January 1980.

82. **Elliot,** M. N., The Present State of Scale Control in Sea Water Evaporators, ***Desalination,*** **vol.** 6, p. 87, 1969.

83. Morse, J. W., de **Kanel,** J., and Craig, H. L., Jr., A Literature Review of the Saturation State of Seawater with Respect to Calcium Carbonate and Its Possible Significance for Scale Formation on OTEC Heat Exchangers, Rept. PNL-2605, UC-64, Battelle Pacific Northwest Laboratories, Richland, Wash, **April** 5, 1978.

84. Wade, N. M., A Review of Scale Control Methods, ***Desalination,*** **vol.** 31, p. 309, 1979.

85. Sexsmith, D. R., and Petrey, E. Q., The Use of Polyelectrolytes for Scale Control in Sea Water Evaporators, ***Desalination, vol.*** 13, p. 87, 1973.

86. Bhargava, A,, Chou, J. S. C., and Kihara, D. H., A Review of Problems on Scaling and Corrosion in Geothermal Plants, Rept. NSF-RA-N-75-364, NTIS no. PB-262 708, National Science Foundation, Washington, D.C., June 1975.

87. Dugan, C. F., Van Nostrand, W. L., and Haluska, J. L., How Antifoulants Reduce the Energy Consumption of Refineries, ***Chem Eng. Prog.,*** vol. 74, no. 5, p. 53, 1978.

88. Van der Wee, P., and Tritsmans, P. A., What to Do about Crude Unit Preheat Exchanger Fouling, ***Hydrocarbon Process,*** vol. 45, no. 8, p. 141, 1966.

89. Nathan, C. C., Use of Chemicals for Solution of Refinery Corrosion and Related Problems, Materials Protection Performance, **vol.** 9, no. 11, 1970.

90. Weierman, R. C., Design of Heat Transfer Equipment for Gas-Side Fouling Service, in ***Workshop on an Assessment of Gas-Side Fouling in Fossil Fuel Environments,*** Boulder, 1981, eds. W. J. Marner and R. L. Webb, Rept. DOE/ID 12138-1, UC **95f,** JPL **Publ. 82-67,** p. 4-15, July 1982.

91. Chenoweth, J. M., Operation and Cleaning of Heat Transfer Equipment in Dirty Gas Environments, in ***Workshop on an Assessment of Gas-Side Fouling in Fossil Fuel Environments,*** Boulder, Colo., October 8-9, 1981, eds W. J. Marner and R. L. Webb, Rept. DOE/ID 12138-1, UC **95f,** JPL Publ. 82-67, p. 6-17, July 1982.

92. **Wynnyckyj,** J. R., and Rhodes, E., Mechanisms of Furnace Fouling, ***in Heat Exchangers: Theory and Practice,*** eds. J. Taborek, G. F. Hewitt, and N. **Afgan,** pp. 817-831, Hemisphere, Washington, D.C., 1981.

93. Chambers, A. K., et **al.,** Development of a Monitoring System for Ash Deposits on Boiler Tube Surfaces, ***Can J. Chem Eng.,*** **vol.** 59, pp. 230-235, 1981.

94. Radway, J. E., and Boyce, T., Reduction of Coal Ash Deposits with Magnesia Treatment, ***Combustion, vol. 49,*** no. 10, pp. 24-30, April 1978.

Locklin, D. W., Fireside Additive Trials in Utility Boilers-Overview of an **EPRI** Survey, *Combustion,* ***vol.*** 51, no, 8, pp. 26-33, February 1980.

95. Locklin, D. W., Fireside Additive Trials in Utility Boilers-Overview of an EPRI Survey, ***Combustion,*** pp. 26-33, February 1980.

96. Protos, P., and Sharon, H. N., Effect of Tube Spacing and Arrangement upon the Fouling Characteristics of Banks of Tubes, ***Sulzer Tech. Rev.,*** no. 4, 1960.

97. Silvestrini, R., Waste Heat Recovery: Heat Exchanger Fouling and Corrosion, ***Chem Eng. Prog.,*** **vol.** 75, no. 12, pp. 29-35, 1979.

98. Marner, W. J., An Assessment of Gas-Side Fouling in Cement Plants, JPL **Publ.** 82-83, Rept. DOE/ID 12138-2, UC **95F,** September 1982.

99. Fetkovich, J. ***G.,*** et **al.,** ***A Novel Method of Measuring Heat Transfer Coefficients with High Precision,*** **Proc.** 12th Southeast. Seminar on Thermal Science, pp. 1-6, Charlottesville, Va., 1976.

100. Fetkovich, J. G., et **al.,** Studies of Biofouling in Ocean Thermal Energy Conversion Plants, **Proc.** 4th Annu. Conf. Ocean Thermal Energy Conversion, Univ. of New Orleans, New Orleans, La, March 22-24, 1977.

101. Characklis, W. G., Influence of Fouling **Biofilms** on Heat Transfer, ***Heat Transfer Eng.,*** **vol. 3, no.** 1, pp. 23-37, 1981.

102. Fetissoff, P. E., Watkinson, A. P., and Epstein, N., Comparison of Two Heat Transfer Fouling Probes, in ***Heat Transfer 1982: Proceedings of the Seventh International Heat Transfer Conference, München, Federal Republic of Germany,*** September 1982, pp. 391-401, Hemisphere, Washington, D.C., 1982.

© 1984 Hemisphere Publishing Corporation

103. Fisher, P., Suitor, J. W., and Ritter, R. B., Fouling Measurement Techniques, ***Chem Eng. Bog.,*** vol. 71, no. 7, p. 66, 1975.
104. Herman, K. W., and Knudsen, J. G., The Use of a Novel Portable Fouling and Corrosion Monitor in Industrial Cooling Water Systems, ***Proc. 40th Znt. Water Conf.,*** pp. 293-299, October 30-November 1, 1979.
105. Ling, A. C., and Lund, D. B., Apparatus for Studying Fouling of Heated Surfaces by Biological Fluids, ***J. Food Sci,*** vol. 43, pp. 390-393, 1978.
106. Taylor, W. F., Deposit Formation from Deoxygenated Hydrocarbons, ***Znd. Eng. Chem Process Des Dev.,*** vol. 13, no. 2, p. 133, 1974.
107. Braun, R., and Hausler, R. H., Instrument Measures Process Fouling, Helps Plan Prevention, ***Oil Gas J.,*** February 14, 1977.
108. Braun, R., and Hausler, R. H., Instrument Measures Process Fouling, Helps Plan Prevention, ***Oil Gas J.,*** vol. 75, February 14, 1977.
109. Zanker, A., Predict Fouling by Nomograph, ***Hydrocarbon Process,*** vol. 57, no. 3, p. 145, March 1978.
110. Fredrick, W. J., and Grace, T. M., Analysis of Scaling in a Black Liquor Evaporator, ***Chem Eng. Prog. Symp. Ser.,*** vol. 184, no. 75, pp. 95-101, 1979.
111. Lister, D. H., The Mechanisms of Corrosion Product Transport and Their Investigation in High Temperature Water Loops, ***Corrosion-NACE, vol, 35,*** no. 3, p. 89096, 1979.
112. Charlesworth, D. H., The Deposition of Corrosion Products in Boiling Water Systems, ***Chem Eng. Prog. Symp. Ser.,*** vol. 66, no. 104, p. 21, 1970.
113. Asakura, Y., et al., Deposition of Iron Oxide on Heated Surfaces in Boiling Water, ***Nucl. Sci Eng.,*** vol. ***67, pp.*** 1–7, 1978.
114. Kelen, T., and Gustafsson, R., The Deposition Kinetics of Calcium Hydroxy Apatite on Heat Transfer Surfaces at Boiling, AE-498, Aktiebolaget Atomenergi, Studsvik, Nykoping, Sweden, 1974.

© 1984 Hemisphere Publishing Corporation

INDEX

A

Absorption of thermal radiation:
  in gases, 2.9.5-1/2.9.5-12
    gas mixtures, 2.9.5-11/2.9.5-12
    measurement, 2.9.5-2/2.9.5-4
    molecular, 2.9.5-8/2.9.5-11
  in solids, 2.9.2-2/2.9.2-3
    characteristics, 2.9.2-1/2.9.2-2
    measurement, 2.9.2-3
Absorption coefficient, 2.9.5-2
Absorption spectra in gases, 2.9.5-4/2.9.5-8
Absorptivity:
  of particles, 2.9.5-l
  of surfaces: definition, 2.9.2-l
    measurement of, 2.9.2-3
Acentric factor:
  definition, 5.1.1-1, 5.2.1-3
  in hydrocarbons, 5.2.1-3/5.2.1-4
Acetic acid saturation properties, 5.5.1-27
Acetone saturation properties, 5.5.1-27
Acetylene saturation properties, 5.5.1-15
Ackerman correction factor in condensation, 2.6.3-6
Acoustic vibration of heat exchangers, 4.6.4-3/4.6.4-4
Active systems for augmentation of heat transfer:
  in condensation, 2.6.6-1/2.6.6-3
  definition, 2.5.1 l-3
  in forced convection, 2.5.11-4/2.5.11-9
  in free convection, 2.5.1 1-8/2.5.11-9
Additives:
  effect on friction factor, 2.2.2-7
  use in heat transfer augmentation, 2.5.11-2, 2.7.9-4
Adiabatic flows, compressible, in duct, 2.2.2-13
Advanced models for furnaces, 3.11.7-1/3.1 1.7-5
Aggregative fluidization, 2.2.6-l
Agitated beds, heat transfer to, 2.8.34

A slash between two page numbers (e.g., 2.7.3-22/2.7.3-26) indicates a range of those pages.

Agitated vessels, 3.14.1-1
  approximate overall heat transfer coefficients in, 2.1.2-5
  equipment used in, 3.14.2-1/3.14.2-4
    gas sparging, 3.14.2-1/3.14.2-2
    mechanical agitators, 3.14.2-1
    vessel internals, 3.14.2-2/3.14.2-4
  heat exchanger, description of, 3.1.2-5/3.1.2-6
  heat transfer correlations for, 3.14.3-l/3.14.3-8
    with anchors and helical ribbons, 3.14.3-1/3.14.3-4
    with nonproximity agitators, 3.14.3-1/3.14.3-3
    scraped-wall pipe and related equipment, 3.14.3-4/3.14.3-6
Ahmad scaling method for critical heat flux in flow boiling of nonaqueous fluids, 2.7.3-8
Air:
  properties of dry and saturated, 3.12.2-6
  saturated liquid/vapor properties, 5.5.1-29
  superheated gaseous, thermodynamic properties, 5.5.2-8/5.5.2-9
Air-activated gravity conveyor, 2.3.3-2
Air-cooled heat exchangers:
  comparison of air and water as coolants, 3.8.1-1
  cooling air supply: by fans, 3.8.7-1/3.8.7-3
    by natural draft, 3.8.8-l
  costing, 4.8.3-1/4.8.3-3
  custom built, 3.8.2-1/3.8.2-2
  description, 3.1.2-4/3.1.2-5
  finned tube bundles for, 3.8.4-1/3.8.4-2
  finned tube systems for, 3.8.3-1/3.8.3-3
  mechanical design, 4.4.1-1/4.4.1-7
    for cold climates and viscous fluid, 4.4.1-7
    components, 4.4.1-2/4.4.1-6
    nomenclature for, 4.4.1-2
    structural design factors, 4.4.1-6/4.4.1-7
  special features, 3.8.9-1/3.8.9-4
    sound emission from, 3.8.9-l
  thermal rating, 3.8.5-1/3.8.5-5
  tubeside flow arrangements, 3.8.6-l
Albedo for single scatter in radiation, 2.9.7-2
Aluminum, spectral characteristics of anodized surfaces, 2.9.2-16
Ammonia, saturated properties of, 5.5.1-29

© 1983 Hemisphere Publishing Corporation

AMTD (see Arithmetic mean temperature difference)
Analogy between heat and mass and momentum transfer, 1.2.3-6/1.2.3-7, 2.1.5-1/2.1.5-4
Analytic solutions for heat exchangers, 1.3.1-1/1.3.2-l
Analytical solution of groups, for calculation of thermodynamic properties of nonhydrocarbons, 5.2.2-3/5.2.2-9
  tables of constants for, 5.5.4-1/5.5.4-6
Anchor agitators:
  description, 3.14.2-1/3.14.2-2
  heat transfer with, 3.14.3-3/3.14.3-4
Andrade equation for variation of viscosity with temperature, 5.1.4-3
Anelasticity, 5.4.5-5
Angled tubes, use in increasing flooding rate in reflux condensation, 2.6.2-8/2.6.2-9
Aniline, saturation properties, 5.5.1-26
Anisotropy of elastic properties, 5.4.5-4/5.4.5-5
Annular dispersed flow (see Annular flow)
Annular distributor in shell-and-tube heat exchangers, 3.3.5-11
Annular ducts:
  critical heat flux In flow in, 2.7.3-20
  forced convective heat transfer in single phase flow:
    laminar flow, 2.5.1-3/2.5.1-4
    with liquid metals, 2.5.13-1/2.5.13-2
    turbulent heat transfer in, 2.5.1-6, 2.5.1-10/2.5.1-11
  free convective heat transfer m closedend: horizontal, 2.5.8-14/2.5.8-16
    vertical (heated on vertical curved surfaces), 2.5.8-13/2.5.8-14
  single phase flow and pressure drop in, 2.2.2-7/2.2.2-10
    Iaminar flow, 2.2.2-7/2.2.2-9
    turbulent flow, 2.2.2-9/2.2.2-10
Annular fins, efficiency, 2.5.3-9
Annular flow:
  critical heat flux in, 2.7.3-22/2.7.3-30
  hydrodynamics in horizontal tubes, 2.3.2-25/2.3.2-26
  hydrodynamics in vertical tubes, 2.3.2-19/2.3.2-21
    deposition and entrainment correlations, 2.3.2-2 1
    interfacial roughness relationship, 2.3.2-20
    triangular relationship for, 2.3.2-10
  regimes of occurrence of: in horizontal flow, 2.3.2-3/2.3.2-4
    in inclined tubes, 2.3.2-4/2.3.2-5
    in systems with phase change, 2.3.2-6/2.3.2-7
Annuli (see Annular ducts)
Arc welding of tubes into tube sheets:
  on Inner face, 4.2.6-10
  on outer face, 4.2.6-8
Archimedes number, 2.2.1-11
Area of tube outside surface in shell-and-tube heat exchangers: charts for, 3.1.4-6, 3.3.10-5
Argon, saturated properties, 5.5.1-30
Arithmetic mean temperature difference, definition, 3.1.4-2
Armstrong, Robert C., 2.2.8-1/2.2.8-13, 2.5.12-1/2.5.12-16
ASME VIII code, for mechanical design of shell-and-tube heat exchangers:
  description, 4.3.1-1/4.3.1-2
  index to, 4.3.2-1/4.3.2-11
ASOG (see Analytical solution of groups)
Assisted convection:
  around immersed bodies, 2.5.9-1/2.5.9-4
  in vertical channels, 2.5.9-2/2.5.9-6
Asymmetric loading, in heat exchangers, 4.1.2-2/4.1.2-9
Augmentation of heat transfer, 2.5.1 l-112.5.1 1-12, 2.6.6-1/2.6.6-4, 2.7.9-1/2.7.9-5
  active systems for: definition, 2.5.1 l-3
    in forced convection, 2.5.11-8/2.5.11-9
    in free convection, 2.5.114
  compound systems for, 2.5.11-9
  in boiling, 2.7.9-1/2.7.9-5
    pool boiling, 2.7.9-1/2.7.9-2
    within tubes, 2.7.9-3/2.7.9-4
  in condensation, 2.6.6-1/2.6.6-4
    in forced convection, 2.6.6-2/2.6.6-3
    in vapor space, 2.6.6-1/2.6.6-2
  in kettle reboilers, 3.6.26
  in she&and-tube heat exchangers using low finned tubes, 3.3.1 l-213.3.1 l-3
  passive systems for: definition, 2.5.1 l-112.5.1 l-3
    in forced convection, 2.5.11-4/2.5.11-8
    in free convection, 2.5 .11-3
  performance evaluation criteria for, 2.5.1 l-9/2.5.1 l-10
Austenitic chromium-nickel steels, as material of construction, 4.5.24
Average phase velocity in multiphase flows, 2.3.14

B

Baffle leakage in shell-and-tube heat exchangers:
  numerical methods for predictions of, 1.4.2-3
  recommended design procedures for accounting for, 3.3.1-1/3.3.11-5
Baffle pipes in agitated vessels, 3.14.2-3/3.14.2-4
Baffles in shell-and-tube heat exchangers:
  constructional features affecting thermal design:
    clearances, 4.2.5-7
    cross type, 4.2.5-4/4.2.5-5
    longitudinal type, 4.2.5-8
    maximum pitch, 4.2.5-7
    support type, 4.2.5-5/4.2.5-6
    thickness, 4.2.5 -7
  disk-and-doughnut, 3.3.1 l-2
  double segmental, 3.3.1 l-2
  leakage effects associated with (see Baffle leakage, Leakage effects)
  number of, calculation of, 3.3.64
  segmental, recommended characteristics of, 3.3.5-7/3.3.5-10
Baker flow regime map for horizontal gas-liquid flow, 2.3.2-3
Balance equation (applied to complete equipment), 1.2.4-1/1.2.4-7
  average interaction coefficients and driving forces for, 1.2.4-2/1.2.4-3
  conventional representations of heat exchanger performance by, 1.2.4-4/1.2.4-5
  differential form of, 1.2.5-1/1.2.5-3
    for enthalpy, temperature and concentration, 1.2.5-1/1.2.5-3
    solution and closure, 1.2.5-2/1.2.5-3
  for enthalpy, temperature and concentration changes, 1.2.4-1/1.2.4-2
  NTU and effectiveness in, 1.2.4-3/1.2.4-4
Band dryer:
  description, 3.13.24
  practical design, 3.13.7-1/3.13.7-2
Banks of tubes (see Tube banks)
Barrels for shell-and-tube heat exchangers (see Shells)
Basket-type evaporator, 3.5.2-1/3.5.2-3
Bauer, R., 2.8.1-1/2.8.1-14, 2.8.2-1/2.8.2-8
Bayonet tube heat exchangers, constructional features of, 4.2.3-9/4.2.3-10

© 1983 Hemisphere Publishing Corporation

Beer-Lambert law, 2.9.5-5
Bell, Kenneth J., 3.1.1-1/3.1.4-9
Bell-Delaware method for shell-side heat transfer and pressure drop in shell-and-tube heat exchangers, 3.3.2-5/3.3.2-6
modified form as basis for recommended procedure, 3.3.3-1/3.3.11-5
Bell and Ghaly method for calculation of multicomponent systems:
condensation, 2.6.3-4/2.6.3-5
evaporation, 2.7.8-5
Bellows, expansion, for shell-and-tube heat exchangers:
analytic basis for codes for, 4.3.3-2
constructional features, 4.2.6-10/4.2.6-11
index to U.S., U.K., and F.R.G. codes for, 4.3.2-1014.3.2-l 1
Benard cells in free convection in horizontal fluid layers, 2.5.8-1/2.5.8-3
Bends:
boiling heat transfer in tubes with, 2.7.4-4/2.7.4-6
dryout in tubes with, 2.7.4-2/2.7.4-4
enhancement of condensation in, 2.6.6-3
multiphase pressure loss in: gas-liquid systems, 2.3.2-17
solid-gas systems, 2.3.3-7
solid-liquid systems, 2.3.44
single-phase fluid flow and pressure drop in, 2.2.2-16/2.2.2-17
loss coefficients for, 2.2.2-16
use of vaned bends, 2.2.2-16/2.2.2-17
Benedict-Webb-Rubin equation of state, 5.2.2-3
Benzene saturation properties, 5.5.1-12
Berenson equation for pool film boiling from a horizontal surface, 2.7.2-14
Bergles, Arthur E., 2.5.11-1/2.5.11-12, 2.6.6-1/2.6.6-4, 2.7.9-1/2.7.9-5
Bernoulli equation, application to flow across cylinders, 2.2.4-l
Bimetal tubes, use of in shell-and-tube heat exchangers, 4.2.5-2
Binary mixtures:
bubble growth in, 2.7.6-5/2.7.6-7
bubble nucleation in, 2.7.6-5
condensation of 2.1.6-2/2.1.6-3, 2.6.3-7
condensers for, 3.4.4-1/3.4.4-2
constants for, for use in calculation of multicomponent systems, 5.5.4-1/5.5.4-9
diffusion and mass transfer in, 2.1.5-1/2.1.5-4
forced convection boiling of, 2.7.8-1/2.7.8-10
combined heat and mass transfer in, 2.7.8-3/2.7.8-6
critical heat flux in, 2.7.8-6/2.7.8-7
saturated nucleate, 2.7.8-1/2.7.8-2
two-phase forced convective, 2.7.8-2/2.7.8-3
phase equilibria in, 2.7.6-1/2.7.6-3
pool boiling of, 2.7.7-1/2.7.7-7
critical heat flux, 2.7.7-4/2.7.7-5
film boiling, 2.7.7-6
minimum heat flux, 2.7.7-5/2.7.7-6
nucleate boiling, 2.7.7-1/2.7.7-4
transition boiling, 2.7.7-5
Bingham fluid (non-Newtonian), 2.2.8-7
Biot number:
in conduction, 2.4.3-2
in melting and solidification, 2.4.4-1/2.4.4-2
Black surface:
heat transfer between gas and, 2.9.6-1/2.9.6-2
spectral characteristics of reflectance from selective, 2.9.2-17
Blackbody radiation, 2.9.1-3/2.9.1-5
Blake-Carmen-Kozeny equation, 2.2.5-2
Blasius equation for friction factor, 2.2.2-3
Block-type heat exchanger, 4.4.44
Blowing (see Injection)
Blunt bodies, drag coefficients for, 2.2.3-7
Boilers:
combustion systems for firing, 3.11.2-2/3.11.2-3
as type of heat exchanger, 1.1.5-2
(*See also* Reboilers)
Boiling:
augmentation of heat transfer in, 2.7.9-1/2.7.9-5
pool boiling, 2.7.9-1/2.7.9-2
within tubes, 2.7.9-3/2.7.9-5
in axial flow reboilers, 3.6.2-6
basic processes, 2.7.1-1/2.7.1-9
bubble detachment and frequency, 2.7.1-7/2.7.1-8
bubble growth, 2.7.1-6/2.7.1-7
evaporation, 2.7.1-2
heterogeneous nucleation, 2.7.1-3/2.7.1-5
homogeneous nucleation, 2.7.1-2/2.7.1-3
sizing of active nucleation sites, 2.7.1-5/2.7.1-6
vapor formation, 2.7.1-1/2.7.1-2
of binary and multicomponent mixtures:
basic process in, 2.7.6-1/2.7.6-7
forced convective boiling, 2.7.8-1/2.7.8-10
pool boiling, 2.7.7-1/2.7.7-7
in evaporators, 3.5.7-2/3.5.7-3
in horizontal tubes, 2.7.4-1/2.7.4-7
dryout in (including bends and coils), 2.7.4-1/2.7.4-4
heat transfer rates in, 2.7.4-4/2.7.4-6
in kettle and horizontal thermosiphon reboilers, 3.6.2-1/3.6.2-6
pool boiling, 2.7.2-1/2.7.2-17
boiling curve for, 2.7.1-1
critical heat flux in, 2.7.2-9/2.7.2-13
film boiling in, 2.7.2-14/2.7.2-15
minimum heat flux in, 2.7.2-13/2.7.2-14
nucleate boiling in, 2.7.2-3/2.7.2-9
onset of nucleate boiling in, 2.7.2-2/2.7.2-3
transition boiling in, 2.7.2-13
outside tubes and tube bundles, 2.7.5-1/2.7.5-7
single tube in crossflow, 2.7.5-1/2.7.5-4
tube bundles, 2.7.5-4/2.7.5-7
in vertical tubes, 2.7.3-1/2.7.3-37
critical heat flux, 2.7.3-12/2.7.3-30
heat transfer in the region where critical heat flux has been exceeded, 2.7.3-30/2.7.3-34
regimes of flow and heat transfer in, 2.7.3-1/2.7.3-5
saturated boiling, 2.7.3-10/2.7.3-12
subcooled boiling, 2.7.3-5/2.7.3-10
Boiling curve:
in binary mixtures, 2.7.7-l
in pool boiling, 2.7.2-l
effect of surface finish on, 2.7.2-3
for single horizontal tube in crossflow, 2.7.5-l
for tube banks, 2.7.5-4
Boiling length:
definition, 2.7.3-15
quality/boiling length correlations, 2.7.3-15
application of nonuniform heating cases, 2.7.3-19
Boiling number, definition, 2.7.4-5
Boiling point, normal, 5.1.3-1
of commonly used fluids, 5.5.1-1/5.5.1-40
Boiling range (in multicomponent mixtures), influence on selection of reboilers, 3.6.1-6
very wide, effect on reboiler design, 3.6.4-3
Boiling surface in boiling in vertical tubes, 2.7.34
Bolted channel head in shell-and-tube exchanger, 4.2.4-l
Bolted cone head in shell-and-tube heat exchanger, 4.2.4-2

© 1983 Hemisphere Publishing Corporation

Bolting of flanges in shell-and-tube heat exchangers, 4.2.6-4/4.2.6-5
Boltzmann s constant, 2.9.1-3
Bonnet head, in shell-and-tube heat exchanger, 4.2.4-1/4.2.4-2
Borishanski, V. M., 2.5.13-1/2.5.13-4
Borishanski correlation for nucleate pool boiling, 2.7.2-5
Botterill, J. S. M., 2.8.4-1/2.8.4-8
Boundary layer:
in combined free and forced convection heat transfer to immersed bodies, 2.5.9-1/2.5.9-3
concept, 2.2.1-16/2.2.1-17
equations, 2.2.1-17/2.2.1-18
continuity, 2.2.1-17
internal energy, 2.2.1-18
internal forms of, 2.2.1-20
Levy-Lees transformation of, 2.2.1-18/2.2.1-20
mean kinetic energy, 2.2.1-17
momentum, 2.2.1-17
solutions of, 2.2.1-20/2.2.1-22
turbulent **kinetic energy,** 2.2.1-18
on flat plate, 2.2.1-22/2.2.1-30
in flow over cylinders, 2.2.3-312.2.3-s
in flow over immersed bodies, 2.2.3-1/2.2.3-2
in heat transfer to flat plates: laminar boundary layer, 2.5.2-1/2.5.2-2
turbulent, 25.2-2
theory, 2.2.1-16/2.2.1-30
as example of theory of models, 2.2.1-13
Thickness of (displacement, momentum, energy, density, temperature); 2.2.1-20
Turbulent: prediction methods for, 2.2.1-26/2.2.1-29
universal laws for, 2.2.1-25/2.2.1-26
Boussinesq approximations:
application in free convective flows, 2.5.7-l
for gravity effect, 2.2.1-10
application to laminar flow in circular duct, 2.2.2-5
Boussinesq number, definition, 2.5.7-2
Bowring correlations for critical heat flux, 2.7.3-16/2.7.3-18
Bracket supports for heat exchangers, index to U.S., U.K., and F.R.G. codes for, 4.3.2-7
Branches, mechanical design aspects, 4.1.8-1/4.1.8-2
Brazing in plate fin heat exchanger construction, 4.4.3-3/4.4.3-4
Bricks, drying of, 3.13.5-2/3.13.5-5
Brinkman number, 2.5.126
British Standards Institute code for mechanical design of heat exchangers (see BS 1500 code)
Bromley equation for film boiling from horizontal cylinders, 2.7.2-14
BS 1500 code for mechanical design of shell-and-tube heat exchangers:
description, 4.3.1-1/4.3.1-3
index to, 4.3.2-1/4.3.2-11
Bubble crowding as mechanism of critical heat flux, 2.7.3-22
Bubble flow:
drift flux model for, in vertical flow, 2.3.2-18/2.3.2-19
regions of occurrence: in horizontal flow, 2.3.2-2/2.3.2-4
in inclined tubes, 2.3.2-4/2.3.2-5
in shell-and-tube heat exchangers, 2.3.2-5/2.3.2-6
in systems with phase change, 2.3.2-6/2.3.2-7
in vertical flow, 2.3.2-1/2.3.2-2
Bubbles:
in boiling of binary mixtures: growth, 2.7.6-5/2.7.6-7
nucleation, 2.7.6-5
in boiling of single components: detachment and frequency, 2.7.1-7/2.7.1-8
growth, 2.7.1-6/2.7.1-7
nucleation, 2.7.1-1/2.7.1-6
in fluidized beds, 2.2.6-412.2.6-l
coalescence, 2.2.6-5/2.2.6-6
single bubbles, 2.2.6-4/2.2.6-5
spatial distribution, 2.2.6-6/2.2.6-7
in gas-liquid flow: horizontal tubes, 2.3.2-2/2.3.2-4
vertical tubes, 2.3.1-1/2.3.2-2, 2.3.2-18/2.3.2-19
rise velocity of gas bubbles in liquid, 2.3.2-18/2.3.2-19
Buffer layer in duct flow, 2.2.2-l
Bulk viscosity, 2.2.1-2
Bundle-induced convection in kettle reboilers, 3.6.2-2/3.6.2-3
Buoyancy effects:
on developing flows in ducts, 2.2.2-l 1
on flows, 2.2.1-10/2.2.1-11
inducing flow in channels, free convection heat transfer with, 2.5.7-19/2.5.7-20
on laminar flow over flat plate, 2.2.1-24
Buoyancy-induced flow in channels, free convective heat transfer with, 2.5.7-19/2.5.7-20
Burnout (see Critical heat flux)
1,2-Butadiene saturation properties, 5.5.1-16
1,3-Butadiene saturation properties, 5 5.1-l 7
Butane saturation properties, 5.5.1-7
Butanol saturation properties, 5.5.1-19
Butterworth, D., 2.6.1-1/2.6.3-10
t-Butyl alcohol saturation properties, 5.5.1-20
By pass (shell-to-tube bundle):
clearances in shell-and-tube heat exchangers, 3.3.5-14
heat transfer and pressure drop correction factors for, 3.3.6-8/3.3.6-9
BWR equation of state (see Benedict-Webb-Rubin equation of state)

C

Cabin heater, 3.11.2-2
Calorically perfect gas, 2.2.1-8
Carbon dioxide:
emissivity of gaseous, 5.5.5-2
saturation properties, 5.5.1-30
superheated gaseous, thermodynamic properties, 5.5.2-2
Carbon monoxide saturation properties, 5 .5.1-3 1
Carbon steel as material of construction, 4.5.2-2/4.5.2-3
Carbon tetrachloride saturation properties, 5.5.1-31
Carmen-Kozeny equation (see Blake-Carmen Kozeny equation)
Carrean fluid (non-Newtonian), 2.2.8-7
Carryover of solids in fluidized beds, 2.2.6-3
Cavitation as source of damage in heat exchangers, 4.5.3-l
Centrifugal dryer, 3.13.24
Ceramics, spectral characteristics of reflectance from, 2.9.2-18
Certification of heat exchangers, 4.7.7-l
Channel emissivity, 2.9.7-11/2.9.7-12
Channel flow, heat and mass transfer in, 2.1.7-1/2.1.7-2
Chapman-Rubescin formula for viscosity variation with temperature, 2.2.1-9
Chemical formulas of commonly used fluids, 5 .5.1-1/5.5.1-40
Chemical reactions, numerical calculation of flows involving, 1.4.3-2/1.4.3-3
Chen correlation for forced convective boiling, 2.7.3-11/2.7.3-13
Chenoweth, J. M., 4.6.1-1/4.6.6-3
Chevron troughs as corrugation design in plate heat exchangers, 3.7.1-1, 3.7.3-1/3.7.3-2, 3.7.6-2
CHF (see Critical heat flux)
Chillers, construction features of, 4.2.3-9

© 1983 Hemisphere Publishing Corporation

Chilton-Colburn analogy, 1.2.3-6
Chisholm, D., 2.6.7-1/2.6.7-4, 3.10.1-1/3.10.7-9, 4.8.1-1
Chlsholm correlations:
for frictional pressure drop in straight channels, 2.3.2-l 1
for pressure drop in singularities, 2.3.2-15/2.3.2-18
Chlorine, saturation properties, 5.5 .1-32
Chloroform, saturation properties, 5.5.1-26
Choice of heat transfer equipment (see Selection of heat transfer equipment)
Chugging flow (gas-liquid), in shell-and-tube heat exchangers, 2.3.2-5/2.3.2-6
Churchill, S. W., 2.5.7-1/2.5.10-12
Churchill and Chu correlations for free convective heat transfer:
horizontal cylinders, 2.5.7-21
vertical plates: laminar flow, 2.5.7-3
turbulent flow, 2.5.7-4
Churn flow, *regions* of occurrence of, 2.3.2-1/2.3.2-2
Circles, radiative heat transfer shape factors between parallel coaxial, 2.9.3-3
Circular cylinders (see Cylinders)
Circulation, modes of in free convection: in enclosures heated from below, 2.5.8-6
CISE correlations for void fractions, 2.3.2-14/2.3.2-15
Clapeyron-Clausius relationship (see Clausius-Clapeyron relationship)
Clausius-Clapeyron relationship:
application in evaporation, 2.7.1-2
in homogeneous nucleation, 2.7.1-3
Cleaning of shell-and-tube heat exchangers, 3.3.4-5
Climbing film evaporator, 3.5.2-4
Closed distillation process, 2.1.7-8
Coalescence of bubbles in fluidized beds, 2.2.6-5/2.2.6-6
Coatings for corrosion protection, 4.5.2-5/4.5.2-6
Cocurrent flow:
F-factor chart for, 1.5.2-3
heat exchangers, 1.1.1-1/1.1.1-2
single-phase temperature pattern in, 1.1.3-l
solutionsfor, 1.3.1-1/1.3.1-4
θ-NTU chart for, 1.5.2-3
Codes, mechanical design:
analytic basis of code rules, 4.3.3-1/4.3.3-2
comparison of principal codes, 4.3.4-1/4.3.4-3
cylinders: external pressure, 4.3.4-1/4.3.4-2
flanges, 4.3.4-2/4.3.4-3
nozzles, 4.3.4-3
stresses, 4.3.4-l
tubesheets, 4.3.4-2
example of applications, 4.3.6-1/4.3.6-23
guides to national practice in application of, 4.3.5-1/4.3.5-9
France (SNCT), 4.3.5-6
Germany (Merkblatter), 4.3.54
Holland (Stoomwesen), 4.3.5-S
Italy (ANCC), 4.3.5-7
Japan: high pressure, 4.5.3-9
standard, JIS-B8243, 4.3.5-8
U.K. (BS1500), 4.3.5-3
U.S. (ASME VIII), 4.3.5-2
index to U.S., U.K., and F.R.G. codes, 4.3.2-114.3.2-l 1
conical shell, 4.3.2-3/4.3.2-4
cylindrical shell and channel, 4.3.2-2/4.3.2-3
dished head, 4.3.24
flanges, 4.3.2-5/4.3.2-7
flat head, 4.3.2-4/4.3.2-5
floating head, 4.3.2-S
nozzles, 4.3.2-9/4.3.2-10
shell bellows, 4.3.2-10/4.3.2-11
supports, 4.3.2-7
tubes, 4.3.2-3
tubesheets, 4.3.2-714.3.2-g
introduction, 4.3.1-1/4.3.1-3
Coiled tubes (see Helical coils, Curved ducts)
Coiled wire inserts for enhancement of heat transfer in boiling, 2.7.9-3
Colburn and Drew method for binary vapor condensation, 2.6.3-7
Colburn and Hougen method for condensation in presence of noncondensable gases, 2.6.3-6
Colburn equation for single-phase heat transfer outside tube banks, 3.3.2-l
Colburn j factor:
application in heat exchangers, 3.3.1-2
defmition, 2.1.3-4
for flow over tube banks, 3.3.7-1/3.3.7-4
in plate fin exchangers, 3.9.4-1/3.9.6-2
values of heat transfer in tubes, 2.1.3-7
Colebrook-White equation for friction factor in rough circular pipe, 2.2.2-3
Coles, law of the wake, 2.2.1-26
Collier, J. G., 2.7.1-1/2.7.8-10
Column internal reboiler (see Internal reboilers)
Combined conductive, convective, and radiative heat transfer, 2.9.8-1/2.9.8-10
Combined free and forced convection heat transfer:
in channels, 2.5.10-1/2.5.10-10
horizontal channels, 2.5.10-7/2.5.10-12
vertical channels: laminar assisted convection, 2.5.10-2/2.5.10-6
laminar opposing convection, 2.5.10-6
turbulent, 2.5.10-6/2.5.10-7
around immersed bodies, 2.5.9-l/2.5.9-6
creeping flow regime (assisting convection), 2.5.9-3
horizontal plates (transverse flow), 2.5.9-4/2.5.9-6
immersed bodies (transverse flow), 2.5.9-6
opposing convection, 2.5.9-4
slightly inertial flow regime (assisting convection), 2.5.9-3/2.5.9-4
thin boundary layer regime (assisting convection), 2.5.9-1/2.5.9-3
turbulent regime (assisting convection), 2.5.9-4
Combined heat and mass transfer, 2.1.6-1/2.1.6-4
in condensation of mixtures, 2.1.6-2/2.1.6-4
in drying, 2.1.6-1/2.1.6-2
in evaporation of binary and multicomponent mixtures, 2.7.8-2/2.7.8-6
in heat exchangers, 1.1.2-1, 1.2.2-3/1.2.2-4
in single-phase free convection, 2.5.7-12/2.5.7-13
Combining flow, loss coefficients in, 2.2.2-20
Combustion chambers (see Furnaces)
Combustion model for furnaces, 3.11.7-3/3.11.7-4
Compact heat exchangers (see Plate fin heat exchangers)
Compartment dryers, 3.13.2-3
Compound systems for augmentation of heat transfer, 2.5.1 l-9
Compressible flow:
in ducts, 2.2.2-12/2.2.2-14
adiabatic (Fanno) flow, 2.2.2-13
basic equations for, 2.2.2-12/2.2.2-13
with constant heat transfer, 2.2.2-12/2.2.2-13
over cylinders, 2.2.3-6
inviscid flow with heat addition, 2.2.2-13
low density effect in, 2.2.2-13
Computer methods for heat exchanger design:
discussion of, 3.3.10-1/3.3.10-2
logic of, 3.1.3-3/3.1.3-4

© 1983 Hemisphere F blishing Corporation

Computer methods for heat exchanger design, logic of (*Cont.*):
design, 3.1.3-3/3.1.3-4
rating, 3.1.3-3
plate exchangers, 3.7.104
Computer program for Monte Carlo calculations of radiative heat transfer, 2.9.4-4/2.9.4-5
Concentration, choice of evaporator type for, 3.5.5-1/3.5.5-2
Concentric spheres, free convective heat transfer in, 2.5.8-16
Concurrency corrections in plate heat exchangers, 3.7.8-1/3.7.8-2
Condensation:
combined heat and mass transfer in, 2.1.6-2/2.1.6-4
dropwise, 2.6.5-1/2.6.5-4
calculation of heat transfer in, 2.6.5-2/2.6.5-3
introduction to, 2.1.7-6
mechanism of, 2.6.5-1/2.6.5-2
order of magnitude heat transfer coefficient in, 2.6.5-l
promoters for, 2.6.5-3/2.6.5-4
fii, introduction to, 2.1.7-4/2.1.7-6
filmwise, of pure vapor, 2.6.2-1/2.6.2-19
outside horizontal and inclined tubes, 2.6.2-9/2.6.2-12, 3.4.6-3
inside horizontal tubes, 2.6.2-12/2.6.2-15, 3.4.6-2
interfacial resistance in, 2.6.2-15
liquid metals, 2.6.2-15/2.6.2-16
on vertical surfaces, 2.6.2-2/2.6.2-9, 3.4.6-3
on firmed tubes, 3.4.6-3
fogging in, 2.6.7-1/2.6.7-4
conditions producing supersaturation, 2.6.7-2/2.6.7-3
design to minimize, 2.6.7-3
effects of, 2.6.7-3
nuclei formation, 2.6.7-1/2.6.7-2
supersaturation, 2.6.7-l
in horizontal tubes, flow regimes in, 2.3.2-7
in plate exchangers, 3.7.12-1
in plate fin heat exchangers, 3.9.13-1/3.9.13-2
introduction to, 2.6.1-1
heat transfer resistances in, 2.6.1-2
modes of, 2.6.1-1/2.6.1-2
of vapor mixture, 2.6.3-1/2.6.3-10, 3.4.64
approximate method, 2.6.3-2/2.6.3-5
binary vapor mixtures, 2.6.3-7
multicomponent mixtures, 2.6.3-7/2.6.3-9
single vapor with noncondensable gas, 2.6.3-5/2.6.3-7
of vapor mixtures forming immiscible liquids, 2.6.4-1/2.6.4-7
eutectic mixtures, 2.6.4-2/2.6.4-3
with incondensable gases, 2.6.4-5/2.6.4-7
non-eutectic mixtures, 2.6.4-3/2.6.4-5
Condensation curves:
description, 2.6.3-1/2.6.3-2
differential, 2.6.3-4/2.6.3-5
integral, 2.6.3-3/2.6.3-5
Condensers:
approximate overall heat transfer coefficients in, 2.1.2-3
design procedures for, 3.4.9-1/3.4.9-4
overall, 3.4.9-1/3.4.9-2
inside tubes, 3.4.9-2/3.4.9-3
outside tubes, 3.4.9-3/3.4.9-4
discussion of types of, 3.4.3-1/3.4.3-6
horizontal m-tube, 3.4.3-3/3.4.3-4
horizontal, outside tube, 3.4.3-4/3.4.3-6
vertical m-tube, downflow, 3.4.3-1/3.4.3-2
vertical in-tube, upflow, 3.4.3-2/3.4.3-3
vertical, outside tube, 3.4.36
fogging in, 2.6.7-1/2.6.7-4, 3.4.5-2
heat transfer in, 3.4.6-1/3.4.6-4
finned tubes, 3.4.6-3
outside horizontal tubes, 3.4.6-3
with mixtures, 3.4.6-4
subcooling in, 3.4.64
inside tubes, 3.4.6-1/3.4.6-2
outside vertical tubes, 3.4.6-3/3.4.6-4
introduction to, 3.4.1-l
mean temperature difference in, 3.4.8-1/3.4.8-3
operational problems in, 3.4.5-1/3.4.5-2
fogging, 3.4.5-2
due to limited vapor load, 3.4.5-1/3.4.5-2
pressure control, 3.4.5-l
venting, 3.4.5-2
pressure drop in, 3.4.7-1/3.4.7-2
selection of type of, 3.4.2-1/3.4.2-4
temperature patterns in, 1.1.3-1/1.1.3-2
as type of heat exchanger, 1.1.5-2
for use in association with evaporators, 3.5.4-2
for vapor mixtures, 3.4.3-1/3.4.4-2
(See also Condensation)
Conduction, heat:
basic equations for, 2.4.1-1/2.4.1-2
in melting and solidification, 2.4.4-1/2.4.4-3
periodic change of temperature in, 2.4.5-1/2.4.5-4
steady state, 2.4.2-1/2.4.2-3
in bodies with internal heat sources, 2.4.2-3
plane, cylindrical and spherical shells without internal heat sources, 2.4.2-1/2.4.2-3
thermal contact resistance in, 2.4.6-1/2.4.6-2
transient response to a step change in temperature, 2.4.3-1/2.4.3-12
one-dimensional systems, 2.4.3-1/2.4.3-10
multidimensional systems, 2.4.3-10/2.4.3-l 1
Conductors, thermal conductivity of, 5.4.3-2/5.4.3-3
Cones, vertical:
free convective heat transfer from, 2.5.7-24
Conical shells, mechanical design of:
analytic basis for codes, 4.3.3-l
basic principles of, 4.1.3-2
index to U.K., U.S., and F.R.G. codes for, 4.3.2-3/4.3.2-4
Connors equation for fluid elastic instability, 4.6.4-2
Conservation equations:
for chemical species, 1.2.1-3
in differential form, 2.2.1-5/2.2.1-7
in duct flow, 2.2.1-3/2.2.1-5
in furnaces, 3.11.7-1/3.11.7-2
for gas-liquid flows, 2.3.2-8/2.3.2-9
homogeneous model, 2.3.2-8
separated flow model, 2.3.2-8/2.3.2-9
in integral form, 2.2.1-2/2.2.1-5
for multiphase flows, 2.3.1-4/2.3.1-7
homogeneous model for, 2.3.1-4/2.3.1-7
separated flow model for, 2.3.1-6/2.3.1-7
for turbulent flows, 2.2.1-13/2.2.1-14
Construction elements of heat exchangers, 4.1.1-2/4.1.2-3
Contact angle, 2.3.1-2
influence in nucleate boiling, 2.7.1-5, 2.7.2-2
Contact resistance:
influence on particle-to-wall heat transfer in packed beds, 2.8.3-3
thermal, 2.4.6-1/2.4.6-4
Continuity equation:
applications in heat exchanger calculations, 1.2.6-5
in boundary layer, 2.2.1-17
in compressible duct flows, 2.2.2-12
differential form in single phase flow, 2.2.1-5/2.2.1-7

© 1983 Hemisphere Publishing Corporation

Continuity equation (Cont.):
in gas-liquid flows, 2.3.2-8/2.3.2-9
integral form in single phase flow, 2.2.2-2
in multiphase flows: homogeneous, 2.3.1-5
separated flow, 2.3.1-25
in turbulent flow, 2.2.1-14
Continuum model, for fluids, 2.2.1-1
Continuum theories, for non-Newtonian fluids, 2.2.8-6/2.2.8-9
Lodge s rubber-like liquid, 2.2.8-8
Maxwell model, 2.2.8-7
Oldroyd eight constant model, 2.2.8-8
White-Metzner model, 2.2.8-8
Contraction, sudden, pressure drop in: single-phase flow, 2.2.2-20
two-phase gas-liquid flow, 2.3.2-16/2.3.2-17
two-phase gas-liquid flow, 2.3.2-16/2.3.2-17
Control:
of heat pipes, 3.10.7-1/3.10.7-2
of reboilers, 3.6.4-2
Convection effects, on heat transfer in kettle reboilers:
bundle induced, 3.6.2-2/3.6.2-3
externally induced, 3.6.2-3
Convective boiling (see Boiling)
Convective heat transfer, single phase:
around immersed bodies: single bodies, 2.5.2-3/2.5.2-8
smooth flat plates, 2.5.2-1/2.5.2-3
augmentation of, 2.5.11-1/2.5.11-12
in combined free and forced convection (see Combined free and forced convection)
channel flows, 2.5.10-1/2.5.10-12
immersed bodies, 2.5.9-1/2.5.9-7
effect of radiation on, 2.9.8-1/2.9.8-10
in fixed beds, 2.8.2-1/2.8.2-8, 2.8.3-1/2.8.3-3
in flow over tube banks, 2.5.3-1/2.5.3-16
finned tubes, 2.5.3-6/2.5.3-16
plain tubes, 2.5.3-1/2.5.3-6
forced convection in ducts, 2.5.1-1/2.5.1-13
laminar flow, 2.5.1-2/2.5.1-5
turbulent flow, 2.5.1-5/2.5.1-13
in free convection: immersed bodies, 2.5.7-1/2.5.7-3 1
layers and enclosures, 2.5.8-1/2.5.8-25
with impingingjets, 2.5.6-1/2.5.6-10
in liquid metal systems, 2.5.13-1/2.5.13-4
with non-Newtonian fluids, 2.5.12-1/2.5.12-16
in channels with viscous heating, 2.5.12-10/2.5.12-14
in channels without viscous heating, 2.5.12-6/2.5.12-10
with dilute polymer solution, 2.5.12-14/2.5.12-15
in packed and agitated beds, 2.8.3-1/2.8.3-9
Conversion factors, for physical properties, 5 5 .1-3
Conveyor, gravity:
air activated, 2.3.3-2
fluidized bed, 2.3.3-7/2.3.3-9
Cooling towers:
effect of variation in atmospheric pressure on, 3.12.6-2/3.12.6-3
hybrid, 3.12.5-1/3.12.5-5
assisted draft, 3.12.5-3/3.12.5-4
closed-circuit evaporative coolers, 3.12.5-4/3.12.5-5
dry, 3.12.5-1/3.12.5-2
wet-dry, 3.12.5-2/3.12.5-3
introduction to, 3.12.1-1
mechanical draft, 3.12.4-1/3.12.4-4
natural draft: dry, 3.8.2-1/3.8.2-2,3.8.8-l
wet, structural design, 3.12.3-6/3.12.3-7
wet, thermal design, 3.12.3-1/3.12.3-6
main features of, 3.12.4-1/3.12.4-2
thermal performance and design, 3.12.2-4/3.12.4-4
packing region in, 3.12.2-1/3.12.2-13
departures from uniform counter flow in, 3.12.2-12/3.12.2-13
heat and mass transfer in, 3.12.2-1/3.12.2-3
packings in, 3.12.2-8/3.12.2-11
state of air leaving, 3.12.2-11/3.12.2-12
theory of thermal design of, 3.12.2-3/3.12.2-8
testing and acceptance of, 3.12.6-1/3.12.6-2
as type of heat exchanger, 1.1.5-2
water loss from, 3.12.6-2
Cooper, Anthony, 3.7.1-1/3.7.12-2
Copper-base alloys, as material of construction, 4.5.2-4/4.5.2-5
Correlation, general nature of, 1.2.3-5/1.2.3-6
Correspondence principle, in physical properties, 5.1.1-1
Corrosion:
associated with phase separation, 4.5.3-5
associated with welds, 4.5.3-5/4.5.3-6
erosion/corrosion, 4.5.3-1/4.5.3-2
fretting, 4.5.3-2
gas-vapor phase, 4.5.3-6/4.5.3-7
materials of construction to avoid, 4.5.2-2/4.5.2-6
in shell-and-tube heat exchangers, 3.3.4-5
vapor blanketing as cause, 4.5.34
in various equipment: reboilers, 45.3-5
waste heat boilers, 4.5.34
Corrugation design, for plate heat exchangers, 3.7.3-1/3.7.3-2, 4.4.2-3/4.4.2-4
Costing of heat exchangers:
an-cooled, 4.8.3-1/4.8.3-3
introduction to, 4.8.1-l
plate, 4.8.4-1/4.8.4-2
shell-and-tube, 4.8.2-1/4.8.2-5
Countercurrent flow:
critical heat flux in, 2.7.3-26
gas-liquid, in vertical channels, 2.3.2-21/2.3.2-22
heat exchangers, 1.1.1-1
temperature pattern for in single-phase flow, 1.1.3-1
θ-NTU chart for, 1.5.2-2
Counterflow (see Countercurrent flow)
Coupled thermal fields, in transient conduction, 2.4.3-12
Cowie, R. C., 4.8.2-1/4.8.2-5
Creeping flow, in combined free and forced convection around immersed bodies, 2.5.9-3
Critical density, of commonly used fluids, 5.5.1-1/5.5.1-40
Critical flow, in gas-liquid systems, 2.3.2-26/2.3.2-29
Henry-Fauske model for, 2.3.2-28/2.3.2-29
homogeneous models for, 2.3.2-28
Critical heat flux:
in axial flow reboilers, 3.6.2-7/3.6.2-8
in counter-current flow, 2.7.3-26
enhancement of, in boiling in tubes, 2.7.9-3/2.7.9-4
pool boiling, 2.7.9-1/2.7.9-2
in evaporators, 3.5.7-3
in flow in vertical annuli, 2.7.3-20/2.7.3-21
in flow in vertical tubes, 2.7.3-13/2.7.3-30
nomenclature for, 2.7.3-13
with non-uniform heat flux, 2.7.3-18/2.7.3-20
with uniform heat flux, 2.7.3-13/2.7.3-18
in forced convective boiling of binary and multicomponent mixtures, 2.7.8-6/2.7.8-7
departure from nucleate boiling, 2.7.8-6/2.7.8-7
dryout, 2.7.8-7
in kettle reboilers, 3.6.2-4/3.6.2-5
mechanisms of, 2.7.3-22/2.7.3-26
annular flow prediction methods for, 2.7.3-23/2.7.3-26

© 1983 Hemisphere Publishing Corporation

Critical heat flux (Cont.):
with nonaqueous fluids, 2.7.3-26/2.7.3-30
in pool boiling, 2.7.2-9/2.7.2-13
geometric effects in, 2.7.2-10/2.7.2-11
liquid viscosity effects on, 2.7.2-12
subcooling effects on, 2.7.2-12/2.7.2-13
surface condition effects on, 2.7.2-13
Zuber analysis for, 2.7.2-9/2.7.2-10
in pool boiling of binary and multicomponent mixtures, 2.7.7-4/2.7.7-5
in rectangular channels, 2.7.3-20
in rod bundles, 2.7.3-21/2.7.3-22
outside single tubes in crossflow, 2.7.5-2/2.7.5-3
outside tubes in tube banks, 2.7.5-5/2.7.5-7
correlations for, 2.7.5-6/2.7.5-7
mechanisms of, 2.7.5-5/2.7.5-6
Critical pressure:
of commonly used fluids, 5 .5.1-1/5 5.140
in hydrocarbon mixtures, 5.2.1-3
Kesler and Lee equation for, 5.2.1-6
in pure fluids, 5.1.1-2
Critical Rayleigh number, in free convection, 2.5.8-2/2.5.8-3, 2.5.8-3/2.5.8-6
Critical temperature:
of commonly used fluids, 5.5.1-1/5.5.1-40
in hydrocarbon mixtures, 5.2.1-3
Kesler and Lee equation for, 5.2.1-5
in pure fluids, 5.1.1-1/5.1.1-2
Critical velocity, in stratification in bends and horizontal tubes, 2.7.4-1/2.7.4-3
Critical volume, 5.1.1-2
Crocco s integral, application to boundary layer equations, 2.2.1-19
Cross counter flow heat exchangers, 1.1.1-2
solutions for, 1.3.1-1/1.3.1-4
Crossflow:
in air-cooled heat exchangers, 3.8.5-1/3.8.5-5
boiling in over horizontal tubes and tube banks, 2.7.5-1/2.7.5-4
in cooling towers, 3.12.2-12/3.12.2-13
over cylinders (see Cylinders)
flow induced vibration in, 4.6.1-1/4.6.6-3
heat exchangers: definition of, 1 .1 .l-2
solutions for heat transfer in, 1.2.64, 1.3.14
pressure drop in gas-liquid, 2.3.2-12
in shell-and-tube heat exchangers, 3.3.6-3/3.3.6-4
temperature difference correction (F-correction) and θ-NTU charts for various configurations of, 1.5.3-1/1.5.3-13
with both streams mixed, 1.5.3-3
one tube row, unmixed, 1.5.34
four tube rows, four passes, unmixed, 1.5.3-11
four tube rows, two passes, mixed, 1.5.3-12
three tube rows, one pass, unmixed, 1.5.3-6
three tube rows, three passes, unmixed, 1.5.3-10
two tube rows, one pass, unmixed, 1.5.3-5
two tube rows, two passes, unmixed, 1.5.3-9
over tube banks (see Tube banks)
Crossflow shells (see X-shells)
Crystallization, choice of evaporator type for, 3.5.5-2
Curved ducts:
dryout in evaporative heat transfer in, 2.7.4-2/2.7.4-4
single-phase fluid flow and pressure drop in, 2.2.2-14/2.2.2-16
flow characteristics in, 2.2.2-14/2.2.2-15
laminar flow in, 2.2.2-15/2.2.2-16
turbulent flow in, 2.2.2-16
Cut-and-twist factor, in enhancement of heat transfer in double pipe heat exchangers, 3.2.3-l
Cyclohexane, saturation properties of, 5.5.1-I 1
Cyclopentane, saturation properties of, 5.5.1-11
Cylinders:
banks of cylinders (see Tube banks)
boiling from outside horizontal in crossflow, 2.7.5-1/2.7.5-4
characteristics of as packings for fixed beds, 2.2.5-2
combined free and forced convective heat transfer from, 2.5.9-1/2.5.9-6
fixed beds of, heat transfer in, 2.8.1-1/2.8.1-14, 2.8.2-1/2.8.2-8
flow across, 2.2.3-3/2.2.3-7
circular, 2.2.2-3/2.2.2-6
noncircular, 2.2.3-6/2.2.3-7
pressure coefficient in, 2.2.4-2
free convective heat transfer from, 2.5.7-20/2.5.7-24
horizontal, 2.5.7-20/2.5.7-23
vertical and inclined, 2.5.7-23/2.5.7-24
free convective heat transfer inside horizontal, 2.5.8-14
hollow, radiation and conduction around, 2.9.8-6/2.9.8-7
pool boiling from, 2.7.2-1/2.7.2-15
critical heat flux in, 2.7.2-9/2.7.2-12
radiative heat transfer on nonisothermal gas in, 2.9.7-3
steady-state thermal conduction in, 2.4.2-1/2.4.2-3
transient conduction in, 2.4.3-1/2.4.3-10
numerical methods for, 2.4.3-8/2.4.3-10
series solution for, 2.4.3-1/2.4.3-7
single-phase heat transfer in flow over, 2.5.2-4/2.5.2-5
solution using internal heat transfer coefficient, 2.4.3-7/2.4.3-8
under external pressure, comparison of mechanical design codes for, 4.3.4-1/4.3.4-2

D

Damage, sources of in heat exchangers, 4.5.3-1/4.5.3-7, 4.6.1-1/4.6.1-2
Damköhler number:
definition, 2.2.1-11
modified form for compressible flows with heat transfer, 2.2.2-12
Damping:
capacity, anelasticity, and, 5.4.5-5
of flow-induced vibration, 4.6.24
Davis and Anderson criterion, for onset of nucleate boiling, 2.7.3-6
Decane, saturation properties of, 5.5.1-10
Degradation temperature, of polymers, 25.12-1
Del operator (see Differential vector operators)
Delaware method, for shell-side heat transfer and pressure drop, (see Bell-Delaware method)
Dengler and Addoms correlation, for forced convective heat transfer in two-phase flow, 2.7.3-8
Density:
defmition, 2.2.1-1
fluid with constant, 2.2.1-8/2.2.1-9
fluid with small variations of, 2.2.1-8
of Liquid water, 5.5.3-2
of multicomponent liquid mixtures, 5.2.3-1/5.2.3-2
relation with viscosity for gases, 2.2.1-9
of saturated liquids and vapors, 5.5.1-1/5.5.1-40
of solids, 5.4.1-1/5.4.1-2
graphite and carbon, 5.4.1-1

© 1983 Hemisphere Publishing Corporation

Density, of solids (Cont.):
metal alloys, 5.4.1-1
organics, 5.4.1-2
refractories, 5.4.1-1/5.4.1-2
Deposition of droplets in annular flow, 2.3.2-21, 2.7.3-24
Design of heat exchangers, introduction, 3.1.1-1/3.1.4-9
Design procedures, for segmentally baffled heat exchangers, 3.3.10-1/3.3.10-8
Desuperheaters for use in association with evaporators, 3.5.4-2
Developing flow in ducts:
single-phase flow and pressure drop in, 2.2.2-10/2.2.2-11
hydrodynamic entrance region in, 2.2.2-10/2.2.2-11
various forms and effects on, 2.2.2-11
Diathermanous fluid, 2.9.1-1
Differential condensation:
calculation of condensation curves, 2.6.34
description, 2.6.3-1/2.6.3-3
Differential formulations for nonisothermal gas radiation, 2.9.7-5/2.9.7-8
embedding, 2.9.7-7/2.9.7-8
multiflex methods, 2.9.7-6/2.9.7-7
radiation diffusion, 2.9.7-5/2.9.7-6
Differential resistance term in heat exchanger design, 3.3.9-2
Differential vector operators in heat conduction, 2.4.1-2
Diffraction models for radiative heat transfer from surfaces, 2.9.4-7/2.9.4-8
Diffuse surfaces, radiative heat transfer between, 2.9.3-1/2.9.3-17
Diffuse wall passages, radiative heat transfer in, 2.9.3-13/2.9.3-16
Diffusers, single-phase flow and pressure drop in, 2.2.2-17/2.2.2-19
effect of inlet conditions, 2.2.2-18/2.2.2-19
with free discharge, 2.2.2-17/2.2.2-18
methods of improving performance in, 2.2.2-19
performance, 2.2.2-17
Diffusion coefficients:
in gases, 5.2.5-3/5.2.5-4
in liquids, 5.2.5-1/5.2.5-3
Dimensional analysis:
pi theorem for, 2.2.1-11/2.2.1-12
and theory of similarity, 2.2.1-10/2.2.1-13
Dimensionless groups:
equivalent groups in heat and mass transfer, 2.1.5-2
in fluidization, 2.2.6-2/2.2.6-3
in free convective heat transfer to immersed bodies, 2.5.7-2/2.5.7-3
table of, 2.2.1-11
Dimensionless numbers (see Dimensionless groups)
Dimensionless time (see Fourier number)
Dimethyl propane saturated properties, 5 .5 .l-6
Direct contact condensation:
introduction, 2.6.1-1
mechanical construction, 4.4.4-6/4.4.4-7
Direct contact cooling, 4.4.4-8
Direct contact evaporation, 4.4.4-7
Dirt (see Fouling)
Discretization in numerical analysis:
for cases where flow patterns must be calculated, 1.4.2-1
in design of heat exchangers with prescribed flow patterns, 1.4.1-1/1.4.1-6
effect of fineness, 1.4.1-5/1.4.1-6
subdivision of space, 1.4.1-1/1.4.1-2
subdivision of time, 1.4.1-2/1.4.1-3
Disk-and-doughnut baffled heat exchangers, 3.3.11-2
Disk turbine agitator, 3.14.2-1/3.14.2-2
heat transfer in vessel agitated by, 3.14.3-1
Disks, free convective heat transfer from inclined, 2.5.7-25
Dispersed bubble flow (see Bubble flow)
Dissipation of turbulent energy, 2.2.1-20
Distillation, closed distillation process, 2.1.7-8
Distribution:
annular, in shell-and-tube heat exchangers, 3.3.5-l 1
design in fluidized beds, 2.2.6-7/2.2.6-8
Dittus-Boelter equation, for single-phase forced convective heat transfer, 2.7.3-5
Dividing flow, loss coefficients in, 2.2.2-19
DNB (departure from nucleate boiling) (see Critical heat flux)
Donohue method, for shell-side heat transfer in shell-and-tube heat exchangers, 3.3.2-2
Double-pipe heat exchanger:
approximate overall heat transfer coefficients, 2.1.2-3
description, 3.1.2-1/3.1.2-2
design, 3.2.1-1/3.2.6-2
applications of, 3.2.2-l
construction/mechanical design, 3.2.5-1/3.2.5-2, 4.4.4-1/4.4.4-2
design parameters for, 3.2.3-1/3.2.3-6
introduction, 3.2.1-1
operational advantages of, 3.2.6-1/3.2.6-2
types available, 3.2.4-1/3.2.4-2
Double segmental baffled heat exchangers, 3.3.11-2
Downward facing surfaces, free convective heat transfer from, 2.5.7-13/2.5.7-15
Downward flow in vertical tubes, flow patterns in gas/liquid, 2.3.2-2
Dowtherm A saturation properties, 5.5.1-28
Dowtherm J saturation properties, 5.5.1-28
Drag coefficient:
for circular cylinder, 2.2.3-3/2.2.3-4
definition, 2.2.3-2
in fluidized beds, 2.2.6-2
for sphere, 2.2.3-3
on tube in tube bank, 2.2.4-3/2.2.4-5
Drag force:
on immersed bodies, 2.2.3-2/2.2.3-4
on tube in tube bank, 2.2.4-3/2.2.4-5
Drag reduction, 2.2.8-11/2.2.8-12
effect on heat transfer, 2.5.12-14/2.5.12-15
Drift flux model for two-phase flows, 2.3.1-7/2.3.1-9
Droplets:
deposition and entrainment of, in annular flow, 2.3.2-21
nucleation of in supersaturated vapors, 2.6.7-1/2.6.7-2
use in augmentation of heat transfer, 2.5.11-8
Dropwise condensation:
calculation of heat transfer in, 2.6.5-2/2.6.5-3
introduction, 2.1.7-6,2.6.1-l, 2.6.5-l
mechanisms of, 2.6.5-1/2.6.5-2
order of magnitude heat transfer coefficient in, 2.6.5-l
promotors for, 2.6.5-3/2.6.5-4
Dry cooling towers, 3.8.2-1/3.8.2-2, 3.8.8-1, 3.12.5-1/3.12.5-2
Dry-wall convection, in evaporation (see Postdryout heat transfer)
Dryers:
classification and selection, 3.13.2-1/3.13.2-4
introduction, 3.13.1-1/3.13.1-2
layout and performance data, 3.13.3-1/3.13.3-5
description of drying process in the Mollier chart, 3.13.3-4/3.13.3-5
energy and mass balances, 3.13.3-1/3.13.3-2
Mollier chart, 3.13.3-1
wet bulb temperature in, 3.13.3-2/3.13.3-4
practical design, 3.13.7-1/3.13.7-3
band dryers, 3.13.7-1/3.13.7-2

© 1983 Hemisphere Publishing Corporation

Dryers, practical design (Cont.):
fluid bed dryers, 3.13.7-2
pneumatical conveying dryers, 3.13.7-2
rotary dryers, 3.13.7-2
spray dryers, 3.13.7-2/3.13.7-3
prediction of drying rates in, 3.13.4-1/3.13.4-5
prediction of residence time in: with nonprescribed material flow, 3.13.6-l
with prescribed material flow, 3.13.5-1/3.15.5-5
as type of heat exchange equipment, 1.1.5-3
Drying, combined heat and mass transfer in, 2.1.6-1/2.1.6-2
Drying loft, 3.13.2-3
Drying plant (see Dryers)
Drying rates, prediction of, 3.13.4-1/3.13.4-5
Dryout:
introduction, 2.7.3-2
as mechanism for critical heat flux: of liquid film, 2.7.3-22/2.7.3-30
under a vapor clot, 2.7.3-22
(See *also* Critical heat flux)
Ductile fracture as failure mode of heat exchanger, 4.1.1-3
Ducts, single-phase fluid flow and pressure drop in, 2.2.2-1/2.2.2-25
circular pipes, fully developed flow, 2.2.2-1/2.2.2-7
compressible flow in, 2.2.2-12/2.2.2-14
curved ducts, 2.2.2-14/2.2.2-17
developing flow in, 2.2.2-10/2.2.2-11
losses in piping components in, 2.2.2-14/2.2.2-20
noncircular ducts, fully developed flow, 2.2.2-7/2.2.2-10
unstead flow in, 2.2.2-14
Durand correlation for heterogeneous conveyance in solid/liquid flow, 2.3.4-6

E

E-type shells in shell-and-tube heat exchangers:
recommended calculation methods for pressure drop and heat transfer in, 3.3.1-1/3.3.10-8
temperature difference correction (F) and θ-NTU charts for, 1.5.2-5/1.5.2-10
Eckert number, 2.2.1-11
Eddy viscosity:
definition, 2.2.2-2
relation to mixing length, 22.24
Edwards, D. K., 2.9.1-1/2.9.8-12, 5.5.5-1/5.5.5-4
EEC code for thermal design of heat exchangers, 4.3.1-3
Effective thermal conductivity of fixed beds, 2.8.1-1/2.8.1-14, 2.8.2-2/2.8.2-5
Effective tube length in shell-and-tube heat exchangers, 3.3.5-17
Effectiveness of a heat exchanger, definition, 1.2.4-3, 2.1.2-2
Efficiency of fins, 2.5.3-6/2.5.3-7
Elastic analysis, in mechanical design, 4.1.2-l 1
Elastic properties of solids:
anelasticitydamping capacity, 5.4.5-5
anisotropy, 5.4.5-4/5.4.5-5
introduction to, 5.4.5-l
isotropic materials, 5.4.5-3/5.4.5-4
static and dynamic properties, 5.4.5-2
stress-strain curve, 5.4.5-2/5.4.5-3
tables of, 5.5.8-1/5.5.8-3
Electric fields, effect on properties of rheologically complex materials, 5.3.8-1/5.3.8-2
Electromagnetic theory of radiation, 2.9.2-7/2.9.2-10
Electrostatic fields in augmentation of heat transfer, 2.5.11-3/2.5.11-4, 2.5.11-8/2.5.11-9, 2.7.9-4
Elhadidy relation between heat and momentum transfer, 1.2.3-6
Embedding methods for radiative heat transfer in nonisothermal gases, 2.9.7-7/2.9.7-8
Emission of thermal radiation, in solids, 2.9.2-1/2.9.2-3
characteristics of, 2.9.2-1/2.9.2-2
measurement of, 2.9.2-3
Emissivity:
of gaseous combustion products, 3.11.34
of gases, 2.9.5-1/2.9.5-13
table, 5.5.5-1/5.5.5-4
of solids, 5.4.4-1/5.4.4-6
of surfaces: definition, 2.9.2-l
measurement of, 2.9.2-3
tables, 5.5.7-1/5.5.7-3
total, of solids, table, 3.11.3-6
EMTD (effective mean temperature difference) in air-cooled heat exchangers, 3.8.5-4/3.8.5-5
Enclosures:
annuli, free convective heat transfer in: horizontal, 2.5.8-14/2.5.8-16
vertical (heated on vertical curved surfaces), 2.5.8-13/2.5.8-14
concentric spheres, free convective heat transfer in, 2.5.8-16
free convection heat transfer in, when heated from below, 2.5.8-3/2.5.8-6
critical Rayleigh number, 2.5.8-3/2.5.8-6
heat transfer rates, 2.5.8-6
modes of circulation, 2.5.8-6
honeycombs, free convective heat transfer in, 2.5.8-20/2.5.8-23
horizontal cylinders, free convective heat transfer inside, 2.5.8-14
inclined, free convective heat transfer in, 2.5.8-17/2.5.8-20
large aspect ratios, 2.5.8-17/2.5.8-19
moderate aspect ratios, 2.5.8-20
rectangular, free convective heat transfer in, when heated from the sides, 2.5.8-6/2.5.8-13
flow patterns in, 2.5.8-6/2.5.8-8
large aspect ratios, 2.5.8-8/2.5.8-10
with local heating, 2.5.8-13
low aspect ratios, 2.5.8-10/2.5.8-13
Energy, internal (see Specific internal energy)
Energy equation:
in boundary layers, 2.2.1-18
in compressible duct flow, 2.2.2-12
differential form in single-phase flow, 2.2.1-5/2.2.1-7
in gas-liquid flows, 2.3.2-8/2.3.2-9
homogeneous flow, 2.3.2-8
separated flow, 2.3.2-812.3.2-g
in heat exchangers, 1.2.6-2/1.2.6-3
integral form in single-phase flow, 2.2.1-3
in multiphase flows: homogeneous, 2.3.1-5/2.3.1-6
separated flow, 2.3.1-7
in non-Newtonian flow, 2.5.12-5
in turbulent flow, 2.2.1-14
Enhancement devices:
for condensation, 2.6.6-1/2.6.6-4
for single-phase heat transfer, 2.5.11-1/2.5.11-12
Enhancement of heat transfer (see Augmentation)
Enlargements in pipes:
single-phase flow and pressure drop in, 2.2.2-17/2.2.2-19
diffusers, 2.2.2-17/2.2.2-19
sudden enlargements, 2.2.2-19

© 1983 Hemisphere Publishing Corporation

Enlargements in pipes (Cont.):
two-phase flow and pressure drop in, 2.3.2-15/2.3.2-16
slow change, 2.3.2-15/2.3.2-16
sudden enlargement, 2.3.2-16
Enthalpy:
changes in streams in heat exchangers, 1.2.4-1/1.2.4-2
of saturated liquids and vapors, 5.5.1-1/5.5.1-40
(See *also* Specific enthalpy)
Enthalpy balance equations for cooling towers, 3.12.2-5
Entrainment in annular gas-liquid flow, 2.3.2-l 1, 2.7.3-24
Entrance effects in heat and mass transfer:
comparison of laminar and turbulent flows, 2.1.7-1/2.1.7-2
in turbulent flow heat transfer, 2.5.1-7
Entrance lengths, hydrodynamic in pipe flow, 2.2.2-10/2.2.2-l 1
Entrance losses for tube inlet in shell-and-tube heat exchanger, 2.2.7-7/2.2.7-8
Entropy (see Specific entropy)
Eötvos number:
in bubble departure, 2.7.1-8
definition, 2.3.2-19
Equations of state:
Benedict-Webb-Rubin, 5.2.2-3
Peng-Robinson, 5.1.24
Redlich-Kwong, 5.1.24
Redlich-Kwong-Soave, 5.1.24
van der Waals, 5.1.2-3/5.1.2-4
Equilibrium interphase:
in binary and multicomponent mixture, 2.7.6-1/2.7.6-4, 5.2.1-l/5.2.1-8
hydrocarbon phase behavior, 5.2.1-3/5.2.1-5
in mixtures of undefined components, 5.2.1-5/5.2.1-8
nonhydrocarbon phase behavior, 5.2.1-5
vapor-liquid, 5.2.1-2/5.2.1-3
introduction, 1.2.1-3
metastable and stable, 2.7.1-1
Equilibrium vapor nucleus, 2.7.1-3
Equivalent sand roughness, 2.2.1-29/2.2.1-30
Ergun equation, for pressure drop in fixed beds, 2.2.5-2
Ethane:
saturation properties, 5.5.1-5
superheated gaseous, thermodynamic properties of, 5.5.2-2
Ethanol:
critical heat flux table for flow boiling of in vertical tube, 2.7.3-29
saturation properties of, 5.5.1-18
Ethyl acetate saturation properties, 5 5.1-25
Ethyl benzene saturation properties, 55.1-14
Ethyl ether saturation properties, 55.1-23
Ethylene:
saturation properties of, 5.5.1-15
superheated gaseous, thermodynamic properties, 5.5.2-3
Ethylene oxide saturation properties, 5.5.1-24
Euler number:
definition, 2.2.1-11
effect of roughness on, in flow over tube banks, 2.2.4-14/2.2.4-15
in flow over tube banks, 2.2.4-5/2.2.4-12
European Economic Community (see EEC code for thermal design of heat exchangers)
Eutectic mixtures, condensation of forming immiscible liquids, 2.6.4-2/2.6.4-3
Evaporation:
flow regimes in, 2.3.2-6/2.3.2-7
at an interface, 2.7.1-2
interfacial resistance in, 2.1.7-8
introduction to, 2.1.7-6/2.1.7-8
in plate fin heat exchangers, 3.9.13-1/3.9.13-2
in plate heat exchangers, 3.7.12-1
(See *also* Boiling)
Evaporative coolers, 3.12.5-4/3.12.5-5
Evaporators:
arrangements for, 3.5.3-1/3.5.3-2
flash evaporation, 3.5.3-2
multiple effect, 3.5.3-1/3.5.3-2
vapor recompression, 3.5.3-2
choice of type of, 3.5.5-1/3.5.5-2
concentration, 3.5.5-1/3.5.5-2
crystallization, 3.5.5-2
vaporization, 3.5.5-l
design aspects, 3.5.4-1/3.5.4-2
condensers for, 3.5.4-2
desuperheaters for, 3.5.4-2
hot fluid space in, 3.5.4-l
separators for, 3.5.4-l/3.5.4-2
estimation of heat transfer coefficients in, 3.5.7-1/3.5.7-3
estimation of pressure drop and circulation in, 35.6-l
estimation of surface area in, 3.5.8-1
introduction to, 3.5.1-l
as type of heat exchanger, 1.1.5-2
types, 3.5.2-1/3.5.2-7
basket type, 3.5.2-1/3.5.2-3
climbing film, 3.5.24
falling film, 3.5.2-4/3.5.2-5
horizontal shell side, 3.5.2-l
horizontal tube side, 3.5.2-5/3.5.2-6
long-tube vertical, 3.5.2-3/3.5.2-4
plate-type, 3.5.2-6
short-tube vertical, 3.5.2-l
Exit losses for tubes in shell-and-tube exchanger, 2.2.7-8
Expansion joints, mechanical design of:
basic principles of, 4.1.6-l
constructional details of, 4.2.6-10/4.2.6-11
Expansion of tubes into tube sheets:
explosive, 4.2.6-7
roller, 4.2.6-6/4.2.6-7
Explosive welding of tubes into tube sheets, 4.2.6-8/4.2.6-10
Extended surfaces (see Fins)
Externally induced convection, in kettle reboilers, 3.6.2-3
Extinction coefficient, 2.9.5-l
Extinction efficiency, 2.9.5-l
Extruders, heat transfer in, 3.14.3-5/3.14.3-6
Eyring fluid (non-Newtonian), 2.2.8-7

F

F-correction method:
application to single-pass cocurrent and countercurrent flow exchangers, 1.3.1-2/1.3.1-4, 1.5.2-1/1.5.2-2
F-factor charts and equations for various heat exchanger configurations, 1.5.2-2/1.5.3-12
crossflow (both streams mixed), 1.5.3-3
four tube rows, four passes, unmixed, 1.5.3-11
four tube rows, one pass, unmixed, 1.5.3-7
four tube rows, two passes, **mixed, 1.5.3-12**
one tube row, unmixed, 1.5.34
three tube rows, one pass, unmixed, 1.5.3-6
three tube rows, three passes, unmixed, 1.5.3-10

© 1983 Hemisphere Publishing Corporation

F-correction method, F-factor charts and equations for various heat exchanger configurations, crossflow (Cont.):
two tube rows, one pass, unmixed, 15.3-5
two tube rows, two tube passes, unmixed, 1.5.3-9
double-pipe heat exchangers, 3.2.3-4/3.2.3-5
E-shell with even number of passes, 15.2-5
five E-shells in series, 1.5.2-9
four E-shells in series, 15.2-8
Gshell, even number of tube passes, 1.5.2-l 3
J-shell, even number of tube passes, 1.5.2-12
J-shell, one tube pass, 1.5.2-l 1
single pass cocurrent, 1.5.2-3
six E-shells in series, 1.5.2-10
three E-shells in series, 1.5.2-7
two E-shells in series, 1.5.2-6
for calculation of heat exchangers, 1.2.44, 1.5.1-1/1.5.3-12
F-factor method:
for temperature difference (see F-correction method)
tong, for critical heat flux with non-uniform heat flux, 2.7.3-19/2.7.3-20
F-type shells:
calculation of heat transfer and pressure drop in, 3.3.11-2
discussion of, 3.3.4-3
thermal leakage in, 1.5.2-14/1.5.2-15
Failure modes of heat exchangers, 4.1.1-3/4.1.1-5
corrosion and other damage mechanisms, 4.5.3-1/4.5.3-7
ductile fracture, 4.1.1-3
high strain fatigue, 4.1.1-5
incremental collapse, 4.1.1-3/4.1.1-5
Falling film evaporator:
description of, 3.5.2-4/3.5.2-5
mass transfer in, 2.1.7-8
Fanning friction factor (see Friction factor)
Fanno flow, 2.2.2-13
Fans in air-cooled heat exchangers:
drive design, 3.8.7-2, 4.4.1-4/4.4.1-6
noise emission, 3.8.9-l
power consumption, 3.8.7-1/3.8.7-2
selection and sizing, 3.8.7-l
Fatigue as failure mode of a heat exchanger, 4.1.1-5, 4.5.3-2/4.5.3-3, 4.6.1-2
Ferritic stainless steels, as material of construction, 4.5.2-3/4.5.2-4
Fick s Jaw for diffusion, 2.1.1-2
extensions to multicomponent system, 2.1.5-l
limitations in, 2.1.1-1/2.1.1-4
Film boiling:
in axial flow reboilers, 3.6.2-9
in cross flow over single cylinder, 2.7.5-3/2.7.5-4
in forced convective boiling on vertical surfaces, 2.7.3-30/2.7.3-31
vertical flat plate, 2.7.3-30/2.7.3-31
vertical rod, 2.7.3-31
in kettle reboilers, 3.6.2-5
in pool boiling, 2.7.2-14/2.7.2-15
Film cooler, approximate overall heat transfer coefficients in, 2.1.24
Film temperature, definition of for turbulent flow over flat plate, 2.2.1-29
Films in heat exchangers, 1.1.4-2
Filmwise condensation:
description of, 2.6.1-1
of pure vapors, 2.6.2-1/2.6.2-19
inside horizontal tubes, 2.6.2-12/2.6.2-15
outside horizontal tubes, 2.6.2-9/2.6.2-12
interfacial resistance in, 2.6.2-15
with liquid metals, 2.6.2-15/2.6.2-16
on vertical surfaces, 2.6.2-2, 2.6.2-9
Finite difference equations:
application to natural convection in enclosures, 2.5.8-8
for flow pattern calculation, 1.4.2-1/1.4.2-4
for heat exchangers, 1.4.1-3/1.4.1-4
Finned-tube banks (see Tube banks finned)
Fins:
application in enhancement of boiling heat transfer, 2.7.9-1/2.7.9-4
as augmentation devices, 2.5.1 l-2
in condensation, 2.6.6-2/2.6.6-3
internally finned tubes, 2.5.11-5/2.5.11-6, 2.6.6-2/2.6.6-3
in natural convection, 2.5.11-3/2.5.11-4
on cylinders in tube banks: pressure drop in, 2.2.4-13/2.2.4-14
effect on flow over cylinders, 2.2.3-6/2.2.3-7
free convective heat transfer from, 2.5.7-25
longitudinal (straight): application in double-pipe heat exchangers, 3.2.1-1/3.2.6-2
efficiency of, 2.5.3-9, 3.2.1-1/3.2.6-2
low finned tubes: applications in shell-and-tube heat exchangers, 3.3.1 l-2/3.3.1 1-4
correlation for single-phase heat transfer in flow over, 2.5.3-12/2.5.3-13
use in boiling augmentation, 2.7.9-1/2.7.9-2
radiating, 2.9.8-4/2.9.8-6
single-phase forced convective heat transfer to banks of tubes with, 2.5.3-6/2.5.3-16
efficiency of fins in, 2.5.3-6/2.5.3-11
experimental data compared with correlations for, 2.5.3-13/2.5.3-15
heat transfer correlations for high fins, 2.5.3-11/2.5.3-12
heat transfer correlations for low fins, 2.5.3-12/2.5.3-13
types, in heat exchangers, 1.1.4-1
types used in air-cooled heat exchangers, 3.8.3-l/3.8.3-3
Fire-tube boiler, 3.11.2-3
Fired heaters, 3.11.2-1/3.11.2-2
Firsova, E. V., 2.5.13-1/2.5.13-4
Fittings, pipe (see Piping components)
Fixed beds:
characteristics of packings in, 2.25-2
heat transfer in, with gas flowing through, 2.8.2-1/2.8.2-7, 2.8.3-1/2.8.3-3
contact area resistance in, 2.8.3-2
effective thermal conductivity in, 2.8.2-2/2.8.2-5
fluid-to-particle heat transfer in, 2.5.4-1/2.5.4-6
heat transfer from walls of, 2.8.2-5/2.8.2-7, 2.8.3-1/2.8.3-3
molecular gas conduction influence in, 2.8.3-1/2.8.3-2
onedimensional temperature field in, 2.8.2-7
radiative heat transfer in, 2.8.3-2
twodimensional temperature field in, 2.8.2-1/2.8.2-2
heat transfer in stagnant (with no flow through), 2.8.1-1/2.8.1-14
effective thermal conductivity of, 2.8.1-3/2.8.1-5
heat transfer coefficient from walls to, 2.8.1-5/2.8.1-10
one-dimensional temperature field in, 2.8.1-10/2.8.1-14
twodimensional temperature field in, 2.8.1-1/2.8.1-2
non-uniform heat transfer in, 2.1.4-3/2.1.4-4
single-phase flow and pressure drop in, 2.2.5-l/2.2.5-5
voidage in, 2.2.5-l
Fixed tubesheet, shell-and-tube exchangers:
comparison of codes, 4.3.4-2
mechanical features, 4.2.3-1/4.2.3-4
Flanges, mechanical design of in heat exchangers:
basic principles, 4.1.7-1/4.1.7-2

© 1983 Hemisphere Publishing Corporation

Flanges, mechanical design of in heat exchangers (Cont.):
comparison of codes, 4.3.4-2/4.3.4-3
constructional features, 4.2.6-3/4.2.6-5
index to U.S., U.K., and F.R.G. codes, 4.3.2-514.3.2-l
Flash evaporation, 3.5.3-2
Flat absorber of thermal radiation, 2.9.2-15
Flat plate:
free convective heat transfer on: inclined and horizontal plates, 2.5.7-13/2.5.7-19
vertical plates, 2.5 .7-2/2.5.7-13
laminar flow along, 2.2.1-22/2.2.1-24
effect of buoyancy forces, 2.2.1-24
effect of density-viscosity function, 2.2.1-22
effect of Mach number, 2.2.1-23
effect of Prandtl number, 2.2.1-23
effect of suction or injection, 2.2.1-23
effect of wall temperature, 2.2.1-22
effect of wall temperature distribution, 2.2.1-23/2.2.1-24
higher order effects, 2.2.1-24
reference temperature, 2.2.1-23
single-phase forced convective heat transfer in, 2.5.2-1/2.5.2-3
transition flow along, 2.2.1-24/2.2.1-25
effect of outer flow turbulence, 2.2.1-24
effect of pressure gradient, 2.2.1-24
heat transfer in, 2.2.1-25
suction on blowing effect, 2.2.1-25
surface roughness, 2.2.1-25
turbulent flow along, 2.2.1-29/2.2.1-30
effect of suction or injection, 2.2.1-30
heat transfer on, 2.2.1-29/2.2.1-30
Mach number effect on, 2.2.1-30
skin friction on, 2.2.1-29
Flat *reflector* of thermal radiation, 2.9.2-14
Floating head designs for shell-and-tube heat exchangers:
analytical basis for codes for, 4.3.3-l
comparison of codes for, 4.3.4-2
detailed constructional features, 4.2.3-4/4.2.3-7
outside packed type, 4.2.3-7
packed-lantern ring type, 4.2.3-5/4.2.3-6
pull through type, 4.2.3-5
split backing ring type, 4.2.3-4/4.2.3-5
discussion, 3.3.5-12/3.3.5-13
example of calculation of heat exchanger mechanical design with, 4.3.6-1/4.3.6-23
flanges in, 4.2.6-3
mechanical design of: basic principles of, 4.1.4-2/4.1.4-4
Flooding phenomena:
in gas-liquid flow in vertical tubes, 2.3.2-21/2.3.2-23
in reflux condensation, 2.6.2-7/2.6.2-9, 3.4.3-2/3.4.3-3
Pushkina and Sorokin correlation for, 2.3.2-22
as source of critical heat flux limitation in countercurrent flow: in tube banks, 2.7.5-5/2.7.5-6
in tubes, 2.7.3-26
Wallis correlation for, 2.3.2-22, 2.6.2-8
Flow distribution in plate heat exchangers, 3.7.6-2, 3.7.8-3/3.7.8-4, 4.4.3-3
Flow-induced vibration, 4.6.1-1/4.6.6-3
design considerations, 4.6.6-1/4.6.6-3
introduction, 4.6.1-1/4.6.1-2
sources of damage by, 4.6.1-1/4.6.1-2
prediction procedure, 4.6.5-1/4.6.5-2
shell-side velocities causing, 4.6.3-l
tube bundle vibration characteristics, 4.6.2-1/4.6.2-4
amplitude of vibration, 4.6.24
damping, 4.6.24
finned-tube natural frequencies, 4.6.2-3
span lengths, 4.6.2-3
straight tube natural frequencies, 4.6.2-1/4.6.2-3
U-bend tube natural frequencies, 4.6.2-3
vibration phenomena, 4.6.4-1/4.6.4-4
acoustic vibration, 4.6.4-3/4.6.4-4
combined phenomena, 4.6.44
fluid elastic whirling, 4.6.4-2
parallel flow eddy formation, 4.6.4-3
turbulent buffeting, 4.6.4-2
vortex shedding, 4.6.4-1/4.6.4-2
Flow patterns (see Flow regimes)
Flow quality (see Quality)
Flow regimes:
in combined free and forced convection in channels:
circular pipes, 2.5.10-1/2.5.10-2
rectangular channels, 2.5.1 0- 11
in combined free and forced convection around immersed bodies, 2.5.9-1/2.5.9-4
in condensation forming immiscible liquids, 2.6.4-2
in fixed beds, 2.8.2-2
in fluidized beds, 2.2.6-1, 2.2.6-3
in gas-liquid flow, 2.3.2-1/2.3.2-7
horizontal tubes, 2.3.2-2/2.3.2-4
inclined tubes, 2.3.2-4/2.3.2-5
shell-and-tube heat exchangers, 2.3.2-5/2.3.2-6, 3.4.7-2
systems with phase change, 2.3.2-612.3.2-l
vertical tubes, 2.3.2-1/2.3.2-2
influence of free convection on, in horizontal pipe flow, *2.2.2-6*
in natural convection in enclosures, 2.5.8-6/2.5.8-8
in single-phase flow in tube banks, 2.2.4-1/2.2.4-3
in single-phase flow over immersed bodies:
boundary layer regime, 2.2.3-1/2.2.3-2
over circular cylinders, 2.2.3-3
over noncircular cylinders, 2.2.3-6/2.2.3-7
in solid-gas flow, 2.3.3-2
Fluid elastic instability as source of flow-induced vibration, *4.6.4-2*
Fluid elastic whirling (see Fluid elastic instability as a source of flow induced vibration)
Fluid mechanics, Eulerian formulation for, 2.2.1-l
Fluid-to-particle heat transfer in fluidized beds, 2.5.5-1/2.5.5-6
Fluidized bed dryer:
description, 3.13.24
practical design, 3.13.7-2
Fluidized bed gravity conveyors, 2.3.3-7/2.3.3-9
Fluidized beds:
bed-to-immersed tube heat transfer in, 2.8.4-6/2.8.4-7
bed-to-wall heat transfer in, 2.8.4-1/2.8.4-8
interphase gas convective *component, 2.8.4-3*
particle convective component, 2.8.4-2/2.8.4-3
predictive methods for, 2.8.4-4/2.8.4-6
radiative component, 2.8.4-3
fluid-to-particle heat transfer in, 2.5.5-1/2.5.5-6
introduction, 2.5.1-1/2.5.5-2
low Peclet numbers, 2.5.3-3/2.5.3-6
recommended equations, 2.5.5-2/2.5.5-3
single-phase fluid flow and pressure drop in, 2.2.6-1/2.2.6-9
local structure in, 2.2.6-6/2.2.6-8
minimum velocity for fluidization in, 2.2.6-2/2.2.6-3
pressure drop, 2.2.6-2
state diagram for, 2.2.6-2/2.2.6-3
types of fluidization, 2.2.6-1/2.2.6-2
use in augmentation of heat transfer, 2.5.11-S
Fluids:
models for, 2.2.1-7/2.2.1-10

© 1983 Hemisphere I blishing Corporation

Fluids, models for (Cont.):
calorifically perfect, 2.2.1-8
constant density, 2.2.1-8/2.2.1-9
continuum, 2.2.1-1
perfect gas (ideal gas), 2.2.1-7/2.2.1-8
small density variation, 2.2.1-8
physical properties: mixtures of fluids, 5.2.1-1/5.2.5-5
pure fluids, 5.1.1-1/5.1.5-3
rheologically complex, 5.3.1-1/5.3.8-3
tables, 5.5.1-1/5.5.5-4
Fluorine saturation properties, 5.5.1-32
Fluted tubes, application in evaporators, 2.7.9-3
Flux method, for modeling radiation in furnaces, 3.11.7-5
Flux relationships in heat exchangers, 1.2.2-1/1.2.2-4
Fog formation (see Fogging in condensation)
Fogging in condensation, 2.6.7-1/2.6.7-4
design to minimize, 2.6.7-3, 3.4.5-2
effects of, 2.6.7-3, 3.4.5-2
nuclei formation, 2.6.7-1/2.6.7-2
supersaturation, 2.6.7-1/2.6.7-3
Forced convection heat transfer, single-phase (see Convection heat transfer)
Forced convective boiling (see Boiling)
Forced flow reboilers:
characteristics, advantages, and disadvantages of, 3.6.1-5
heat transfer characteristics of, 3.6.2-6/3.6.2-10
Forster and Zuber correlation for nucleate boiling, 2.7.24
Fouling:
in double-pipe heat exchangers, 3.2.6-l
in evaporators, 3.5.7-1/3.5.7-2
influence in selection of reboiler type, 3.6.1-6
numerical methods in the prediction of, 1.4.24
in plate heat exchangers, 3.7.9-l
in reboiler design, 3.6.4-1/3.6.4-2
fouling resistances in reboilers, 3.6.4-2
in shell-and-tube heat exchangers, 3.3.4-5, 3.3.5-14/3.3.5-15
as limiting factor in design, 3.3.10-7/3.3.10-8
as source of damage, 4.5.3-S
Four phase flows, examples, 2.3.1-2
Fourier law for conduction, 2.1.1-2,2.4.1-l
limitations in, 2.1.1-1/2.1.1-4
Fourier number (Fo):
defmition, 1.2.3-5, 2.1.3-2
in packed beds, 2.8.3-1/2.8.3-3
in solidification and melting, 2.4.4-1/2.4.4-2
in transient conduction, 2.4.3-1/2.4.3-7
Frames for plate heat exchangers, 4.4.2-5/4.4.2-7
France, guide to national practice for mechanical design, 4.3.5-6
Free convection:
augmentation of heat transfer in: active systems for, 2.5.114
passive systems for, 2.5.1 1-3
combined with forced convection (see Combined free and forced convection)
effect on laminar flow heat transfer in channels, 2.5.1-4/2.5.1-5
effect of, on single-phase flow in vertical ducts, 2.2.2-l 1
heat transfer around immersed bodies, 2.5.7-1/2.5.7-3 1
generalized solutions for, 2.5.7-25/2.5.7-28
horizontal cylinders, 2.5.7-20/2.5.7-23
inclined and horizontal surfaces, 2.5.7-13/2.5.7-19
open ended channels, 2.5.7-19/2.5.7-20
other shapes, 2.5.7-25
spheres, 2.5.7-24/2.5.7-25
vertical cones, 2.5.7-24
vertical and inclined cylinders, 2.5.7-23/2.5.7-24
vertical plates, 2.5.7-2/2.5.7-13
influence on friction factor in circular pipe flow, 2.2.2-512.2.2-I
in layers and enclosures, 2.5.8-1/2.5.8-25
circular vertical annuli heated and cooled on vertical curved surfaces, 2.5.8-13/2.5.8-14
concentric spheres, 2.5.8-16
enclosures heated from below, 2.5.8-3
honeycombs, 2.5.8-20/2.5.8-23
horizontal annuli, 2.5.8-14/2.5.8-16
horizontal cylinders, 2.5.8-14
inclined enclosures, 2.5.8-17/2.5.8-20
infinite horizontal layers, 2.5.8-1/2.5.8-3
rectangular enclosures heated and cooled on the sides, 2.5.8-6/2.5.8-13
occurrence in flow in horizontal circular pipe, Metais and Eckert diagram for, 2.2.2-6
Free-fall velocity of particles, 2.3.3-3
Free molecule conditions, maximum shear stress, heat flux, and mass flux in, 2.1.1-2
Free-stream turbulence, effect on flow over cylinders, 2.2.36
Freeze protection of air-cooled heat exchangers, 4.4.1-1/4.4.1-2, 4.4.1-7
Fresnel relations in reflection of radiation, 2.9.2-9
Fretting corrosion, 4.5.3-2
Friction coefficient (see Friction factor)
Friction factor:
in circular pipe flow, 2.2.2-1/2.2.2-2
definition, 2.2.2-l
Moody chart for, 1.2.3-3, 2.2.2-2
definition, 1.2.3-2
in fixed beds, 2.2.5-3
in flow over tube banks, 3.3.7-1/3.3.7-4
interfacial, 2.3.2-21/2.6.2-6
liquid film, 2.3.2-10
in plate fin exchangers, 3.9.4-1/3.9.6-2
in plate heat exchangers, 3.7.4-1/3.7.4-2
on the shell side of double-pipe heat exchangers, 3.2.3-5/3.2.3-6
of solid in solid gas flow, 2.3.3-5/2.3.3-7
definition, 2.3.3-5
in horizontal pneumatic conveyance, 2.3.3-5/2.3.3-6
in vertical pneumatic conveyance, 2.3.3-5
in systems with heat transfer augmentation: coiled tubes, 2.5.11-7
internally finned tubes, 2.5.11-6
roughened surfaces, 2.5.1 l-2/2.5.11-5
twisted tape systems, 2.5.11-7
Friction multipliers in gas-liquid flow:
correlation for: in singularities, 2.3.2-15/2.3.2-18
in straight channels, 2.3.2-9/2.3.2-12
definition, 2.3.2-9
Friction velocity definition, 2.2.1-25
Frictional pressure drop (see Pressure drop)
Friedel correlation for frictional pressure gradient in straight channels, 2.3.2-11
Froude number:
definition, 1.2.3-5, 2.2.1-11
in fluidized beds, 2.2.6-2/2.2.6-3
Fuels, properties of, 3.11.3-2/3.11.3-3
Fugacity, 5.2.1-2
Furnaces:
advanced models for, 3.11.7-l/3.11.7-6
in boilers, 3.11.2-2/3.11.2-3
heat transfer in, 3.11.3-6
heat sink, 3.11.3-3/3.11.3-6
heat source, 3.11.3-1/3.11.3-3

© 1983 Hemisphere Publishing Corporation

Furnaces, heat transfer in (Cont.):
heat transfer of the sink, 3.11.3-6
refractory surfaces, 3.11.3-6
introduction, 3.11.1-1
multizone model for, 3.11.6-1/3.11.6-4
plug flow model for, 3.11.5-1/3.11.5-2
in process heaters, 3.11.2-1/3.11.2-2
radiation characteristics of row of cylinders backed by refractory wall in, 2.9.3-12/2.9.3-13
stirred reactor model for, 3.11.4-1/3.1 1.4-6
as type of heat exchange equipment, 1.1.5-3

G

G-type shells in shell-and-tube heat exchangers:
description, 3.3.4-3
temperature difference correction factor (F) and θ-NTU chart for, 1.5.2-13
Galileo number, 2.2.1-11
in bubble rise in liquids, 2.3.2-19
Gas heater, approximate overall heat transfer coefficients in, 2.1.2-3
Gas-liquid flows:
applications of one-dimensional equations, 2.3.2-7/2.3.2-18
conservation equations, 2.3.2-812.3.2-p
correlation for void fraction, 2.3.2-13/2.3.2-15
frictional pressure drop in straight channels, 2.3.2-9/2.3.2-12
pressure changes across singularities, 2.3.2-15/2.3.2-18
pressure drop in heat exchangers, 2.3.2-12/2.3.2-13
critical two-phase flow, 2.3.2-26/2.3.2-29
flow patterns in, 2.3.2-1/2.3.2-7
horizontal tubes, 2.3.2-2/2.3.2-4
shell-and-tube heat exchangers, 2.3.2-5/2.3.2-6
in systems with phase change, 2.3.2-6/2.3.2-7
inclined tubes, 2.3.2-4/2.3.2-5
vertical tubes, 2.3.2-1/2.3.2-2
hydrodynamics of specific flow regimes (horizontal), 2.3.2-23/2.3.2-26
annular flow, 2.3.2-25/2.3.2-26
slug flow, 2.3.2-24/2.3.2-25
stratified flow, 2.3.2-23/2.3.2-24
hydrodynamics of specific flow regimes (vertical), 2.3.2-18/2.3.2-23
annular flow, 2.3.2-19/2.3.2-21
bubble flow, 2.3.2-18/2.3.2-19
counter-current flow and flooding, 2.3.2-21/2.3.2-23
plug-slug flow, 2.3.2-19
in plate heat exchangers, 3.7.12-1
Gas-solid flow (see Solid-gas flow)
Gas sparging, for agitation of vessels:
description, 3.14.2-1/3.14.2-2
heat transfer with, 3.14.3-3
Gaseous fuels, properties of, 3.11.3-2
Gases:
as constituent of multiphase flows, 2.3.1-2
combined radiative and convective heat transfer to, 2.9.8-7/2.9.8-10
diffusion coefficients in, 5.2.5-3/5.2.5-4
emissivity of, 2.9.5-1/2.9.5-13
table of, 5.5.5-1/5.5.5-4
emissivity of combustion product mixtures of, 3.11.34, 5.5.5-3/5.5.5-4
isothermal, radiative heat transfer in, 2.9.6-1/2.9.6-9
nonisothermal, radiative heat transfer in, 2.9.7-1/2.9.7-13
P-$\tilde{V}$-T relationships for, 5.1.2-1/5.1.2-4
radiation properties, 2.9.5-1/2.9.5-12
equation of transfer for, 2.9.5-1/2.9.5-2
gas mixtures, 2.9.5-11/2.9.5-12
measurement of, 2.9.5-2/2.9.5-4
molecular, 2.9.5-8/2.9.5-11
physics of, 2.9.54
spectral, band and total property definition, 2.9.5-4/2.9.5-8
superheated, thermodynamic properties of, tables, 5.5.2-1/5.5.2-11
thermodynamic properties, 5.1.3-1/5.1.3-7
transport properties, 5.1.3-1/5.1.3-7
Gasketed plate heat exchangers (see Plate heat exchangers)
Gaskets:
for flanges in shell-and-tube heat exchangers, 4.2.6-3/4.2.6-4
for graphite block exchangers, 4.4.44
in plate heat exchangers, design and properties, 4.4.2-414.4.2-S
Geometric optics models for radiative heat transfer from surfaces, 2.9.4-8
Germany, Federal Republic of, mechanical design of heat exchangers in:
guide to national practice, 4.3.5-4
index to Merkblatter code, 4.3.2-1/4.3.2-11
Gersten, K., 2.2.1-1/2.2.3-P
Gibbs phase rule, 5.2.1-1
Girth flanges, in shell-and-tube heat exchangers:
analytical basis for code for, 4.3.3-2
constructional details of, 4.2.6-3
Gn (heat generation number), 2.5.126
Gnielinski, V., 2.5.1-1/2.5.4-6
Goodness factor, as a basis for comparison of plate fin heat exchanger surfaces, 3.9.7-1/3.9.7-3
Goody narrow band model for gas radiation properties, 2.9.5-5
Graetz number:
definition, 1.2.3-5, 2.1.3-2
in non-Newtonian flows, 2.5.12-6/2.5.12-7
Graetz problem (see Nusselt-Graetz problem)
Graphite, density of, 5.4.1-1
Graphite block heat exchanger, 4.4.44
Grashof number, 1.2.34, 2.2.1-11, 2.2.2-6
in free convection over immersed bodies, 2.5.7-2
Gravitational acceleration, effect in pool boiling, 2.7.2-9
Gravity conveyor:
air-activated, 2.3.3-2
fluidized bed, 2.3.3-712.3.3-p
Gregorig effect in enhancement of condensation, 2.6.6-1/2.6.6-2
Griffith, P., 2.6.5-1/2.6.5-4
Groeneveld correlation for postdryout heat transfer, 2.7.3-3 1
Groeneveld and Delorme correlation for postdryout heat transfer, 2.7.3-32/2.7.3-33
Group contribution parameters tables, 5.5.4-10
Guerrieri and Talty correlations for forced convective heat transfer in two-phase flow, 2.7.3-8
Guldberg's rule for critical temperature, 5.1.1-1
Guy, A. R., 3.2.1-1/3.2.6-2

H

Hagen-Poseville law, 2.1.1-2,2.2.2-l, 2.2.2-3
Hagen-Rubens relation, between electrical and optical constants, 2.9.2-10

© 1983 Hemisphere I blishing Corporation

Hampson coils (see Helical coils)
Handley and Heggs equation for fixed bed pressure drop, 2.2.5-3
Harris, D., 4.3.6-1/4.3.6-23
Hausen equation for developing laminar flow, 2.5 .1-2
Headers in shell-and-tube heat exchangers, 2.2.7-1/2.2.7-2
  inlet distribution header, 2.2.7-5/2.2.7-6
  outlet combining headers, 2.2.7-6/2.2.7-7
  tube entry/exit pressure loss, 2.2.7-7/2.2.7-8
Heads, in heat exchangers:
  analytic basis for codes, 4.3.3-l
  constructional features of affecting mechanical design, 4.2.6-1/4.2.6-2
  index of U.K., U.S.A., and F.R.G. codes for, 4.3.2414.3.2-s
  mechanical design of, 4.1.8-1
  types of, in shell-and-tube exchangers, 4.2.4-1/4.2.4-2
    bolted channel, 4.2.4-l
    bolted cone, 4.2.4-2
    Bonnett type, 4.2.4-1/4.2.4-2
    high pressure, 4.2.4-2/4.2.4-3
    welded channel, 4.2.4-l
Heat and mass transfer:
  combined, 2.1.6-1/2.1.6-4
    in condensation, 2.1.6-2/2.1.6-4
    in cooling towers, 3.12.2-1/3.12.2-3
    in drying, 2.1.6-1/2.1.6-2
    in heat exchangers, 1.1.2-1, 1.2.2-3/1.2.2-4
    in single-phase free convection, 2.5.7-12/2.5.7-13
  relations between, 1.2.3-6/1.2.3-7
  state of the art, 2.1.7-1/2.1.7-8
Heat capacity (see Specific heat capacity)
Heat conduction (see Conduction, heat)
Heat exchanger design, introduction, 3.1.1-1/3.1.4-9
  approximate sizing of shell-and-tube heat exchangers, 3.1.4-1/3.1.4-9
    basic design equation, 3.1.4-1
    estimation of heat load, 3.1.4-1/3.1.4-2
    estimation of mean temperature difference, 3.1.4-2/3.1.4-3
    estimation of overall heat transfer coefficient, 3.1.4-3/3.1.4-6
    estimation of surface area, 3.1.4-6/3.1.4-7
    example, 3.1.4-7/3.1.4-9
  fundamental concepts, 3.1.1-1/3.1.1-3
    basic design equation, 3.1.1-2
    heat transfer coefficients, 3.1.1-1
    mean temperature difference, 3.1.1-2/3.1.1-3
  logic of the design process, 3.1.3-1/3.1.3-4
    criteria for successful design, 3.1.3-1/3.1.3-2
    relationship among selection rating and design, 3.1.3-2/3.1.3-4
    simplified example of design modification algorithm for computer, 3.1.3-3/3.1.3-4
  types of heat exchangers and their applications, 3.1.2-1/3.1.2-6
    air-cooled, 3.1.2-4/3.1.2-5
    double-pipe, 3.1.2-1/3.1.2-2
    mechanically aided, 3.1.2-5
    plate fin or matrix, 3.1.2-5
    plate heat, 3.1.2-3/3.1.2-4
    shell-and-tube, 3.1.2-2/3.1.2-3
Heat exchangers:
  agitated vessels, 3.14.1-1/3.14.3-8
  air-cooled, thermal design, 3.8.1-1/3.8.9-4
  condensers, 3.4.1-1/3.4.9-5
  corrosion and other damage, 4.5.3-1/4.5.3-7
  costing, 4.8.1-1/4.8.4-2
    air-cooled, 4.8.3-1/4.8.3-3
    plate, 4.8.4-1/4.8.4-2
    shell-and-tube, 4.8.2-1/4.8.2-5
  definitions and quantitative relationships, 1.2.0-1/1.2.6-7
    balance equations for equipment, 1.2.4-1/1.2.4-7
    differential equations for streams in, 1.2.5-1/1.2.5-3
    flux relationships, 1.2.2-1/1.2.2-4
    partial differential equations for interpenetrating continua in, 1.2.6-1/1.2.6-7
    thermodynamic concepts, 1.2.1-1/1.2.1-3
    transfer coefficient dependences, 1.2.3-1/1.2.3-7
  description of, 1.1.0-1/1.1.6-1
    equipment forms, 1.1.5-1/1.1.5-3
    interactions between streams in, 1.1.2-1/1.1.2-2
    interfaces between streams in, 1.1.4-1/1.1.4-2
    temperature change patterns, 1.1.3-1/1.1.3-2
    types of flow configuration, 1.1.1-1/1.1.1-4
    unsteady operation, 1.1.6-1
  design, 3.1.1-1/3.1.4-9
  double pipe, 3.2.1-1/3.2.6-2
    application of, 3.2.2-l
    construction/mechanical design, 3.2.5-1/3.2.5-2, 4.4.4-1/4.4.4-2
    design parameters, 3.2.3-1/3.2.3-6
    introduction, 3.2.1-1
    operational advantages, 3.2.6-1/3.2.6-2
    types available, 3.2.4-1/3.2.4-2
  F-correction method for, 1.2.44, 1.3.1-2/1.3.1-4
  F-factor charts for, 1.5.2-3/1.5.3-12
  gas-liquid pressure drop in, 2.3.2-12/2.3.2-13
  liquid metal heat transfer in, 2.5.13-8/2.5.13-4
  materials of construction, 4.5.2-1/4.5.2-6
  mechanical design: air-cooled, 4.4.1-1/4.4.1-7
    basic principles, 4.1.1-1/4.1.8-3
    block type, 4.4.44
    direct contact, 4.4.4-6/4.4.4-8
    double-pipe, 3.2.5-1/3.2.5-2, 4.4.4-1/4.4.4-2
    example of design, 4.3.6-1/4.3.6-23
    heat pipes, 4.4.4-9/4.4.4-11
    helical (Hampson) coils, 4.4.4-8/4.4.4-9
    jacketed heaters, 4.4.4-3/4.4.4-4
    plate tin heat exchangers, 4.4.3-1/4.4.3-P
    plate heat exchangers, 4.4.2-1/4.4.2-8
    scraped surface, 4.4.4-5/4.4.4-6
    shell-and-tube (codes), 4.3.1-1/4.3.5-l
    shell-and-tube (construction), 4.2.1-1/4.2.6-13
    spiral plate, 4.4.4-5
    tubular and panel immersion, 4.4.4-2/4.4.4-3
  numerical solution methods for: with calculation of flow pattern, 1.4.2-1/1.4.2-4
    with prescribed flow patterns, 1.4.1-1/1.4.1-6
  plate fin, 3.9.1-1/3.9.13-4
  plate, thermal design of, 3.7.1-1/3.7.12-2
  P-NTU method for, 1.2.4-4/1.2.4-5, 1.3.1-2
  pressure drop in headers, nozzles, and turnarounds, 2.2.7-l
  radiant, 2.9.84
  representation as interpenetrating continua, 1.2.6-1/1.2.6-7
  shell-and-tube (single phase), thermal design of, 3.3.1-1/3.3.11-5
  θ method chart for, 1.5.2-1/1.5.3-12
  θ method for, 1.2.4-5, 1.3.1-2/1.3.1-4
Heat generation number (Gn), 2.3.12-6
Heating media, for reboilers, 3.6.2-10
Heat of vaporization, 5.1.3-2/5.1.3-4
  of commonly used fluids, 5.5.1-1/5.5.1-40

© 1983 Hemisphere I blishing Corporation

Heat pipes:
axial heat transfer and operational envelope for, 3.10.4-I
characteristics of wicks for, 3.10.6-1/3.10.6-2
circulation and axial heat transfer in, 3.10-2-1/3.10.2-3
introduction to, 3.10.1-1/3.10.1-2
mechanical design of exchangers using, 4.4.4-9/4.4.4-l 1
selection of working fluid for, 3.10.5-1/3.10.5-2
start-up and control of, 3.10.7-1/3.10.7-2
temperature distribution and radial heat flux in, 3.10.3-1/3.10.3-2
Heat transfer:
analogy with mass transfer, 2.1.5-1/2.1.5-4
augmentation of (see Augmentation of heat transfer)
in cooling towers, 3.12.2-1/3.12.2-2
enhancement of, (see Augmentation of heat transfer)
in fluidized beds, fluid-to-particle, 2.5 .5-2/2.5.5-6
in non-uniform systems, 2.1.4-1/2.1.4-4
in packed beds, 2.1.4-3/2.1.4-4
in shell-and-tube heat exchangers, 2.1.4-1/2.1.4-3
single phase convective (see Convective heat transfer, single phase)
in transition flow over flat plate, 2.2.1-25
in tubes: Colburnj-factor (laminar and turbulent), 2.1.3-7
correlations for, 2.5.1-1/2.5.1-11
Nusselt numbers for (laminar and turbulent), 2.1.3-6
in turbulent flow over flat plates, 2.2.1-29/2.2.1-30
by radiation (see Radiative heat transfer)
Heat transfer coefficient:
in agitated vessels, 3.14.3-1/3.14.3-8
in air-cooled heat exchangers, 3.8.5-1/3.8.5-5
average and overall values for, discussion, 1.2.4-2/1.2.4-3
in bed-to-wall heat transfer in fluidized beds, 2.8.4-1/2.8.4-7
in boiling in a vertical tube, 2.7.3-1/2.7.3-37
variation with quality of, 2.7.3-3
in boiling in horizontal tubes, bends, and coils, 2.7.4-1/2.7.4-7
in boiling of binary and multicomponent mixtures: forced convective, 2.7.8-1/2.7.8-10
pool boiling, 2.7.7-1/2.7.7-7
in boiling on outside of single tubes and tube banks, 2.7.5-1/2.7.5-7
in combined free and forced convection: in channels, 2.5.10-1/2.5.10-10
over immersed bodies, 2.5.9-1/2.5.9-6
in condensation, 2.6.1-2
in double-pipe exchangers, 3.2.3-3/3.2.3-3
in evaporators, 3.5.6-1/3.5.7-3
in fixed beds: between wall and bed, stagnant (no flow) conditions, 2.8.1-5/2.8.1-10
particle-to-fluid, 2.5.4-1, 2.8.3-1/2.8.3-3
in flow over tube banks, 2.5.3-1/2.5.3-8
in fluidized beds: particle-to-fluid heat transfer, 2.5.5-1/2.5.5-6
in free convection: in layers and enclosures, 2.5.8-1/2.5.8-25
over immersed bodies, 2.5.7-1/2.5.7-31
individual, definition of, 1.2.2-1/1.2.2-2, 2.1.2-6
typical values of, 2.1.2-6
internal, use in transient conduction calculations, 2.4.3-7/2.4.3-8
with liquid metals, 2.5.13-1/2.5.13-4
local, definition, 2.5.1-1
mean, along duct, 25.1-l
in moving, agitated, and vibrated beds of particles, 2.8.3-312.8.3-g
in non-Newtonian flows, 2.5.12-1/2.5.12-16
numerical calculation of, 1.4.3-3/1.4.3-4
overall definition of, 1.2.2-1/1.2.2-2, 2.1.2-1, 3.1.1-I
in various heat exchangers, 2.1.2-3/2.1.2-4
in plate fin exchangers, 3.9.4-1/3.9.6-2
in plate heat exchangers, 3.7.5-l
in pool boiling, 2.7.2-1/2.7.2-17
radiation, 2.9.8-2
in reboilers, 3.6.2-1/3.6.2-10
on the shell side in shell-and-tube heat exchangers, 3.3.1-1/3.3.11-5
in single-phase flow in ducts: laminar flow, 2.5.1-3/2.5.1-4
turbulent flow, 2.5.1-5/2.5.1-11
volumetric, 1.1.2-2
Heat transfer regimes:
in boiling in a vertical tube, 2.7.3-2
in free and forced single-phase convection, 2.5.10-2
Heated cavity reflectometer, 2.9.2-7
Heggs, P. J., 2.2.5-1/2.2.5-5
Helical coils:
in agitated vessels, 3.14.2-2/3.14.2-3
heat transfer to, 3.14.3-1/3.14.3-2
augmentation of boiling heat transfer using, 2.7.9-4
convective boiling in, 2.7.4-5/2.7.4-6
cooler, approximate overall heat transfer coefficients in, 2.1.24
dryout in evaporative heat transfer in, 2.7.4-3/2.7.4-4
Hampson-type for heat exchangers, 4.4.4-8/4.4.4-9
single-phase flow and pressure drop in, 2.2.2-14/2.2.2-16, 2.5.11-6/2.5.11-7
single-phase heat transfer in, 2.5.11-6/2.5.11-7
Helical inserts, for enhancement of heat transfer in boiling, 2.7.9-3
Helical ribbon agitator:
description, 3.14.2-1/3.14.2-2
heat transfer with, 3.14.3-3/3.14.3-4
Helium:
saturation properties, 5.5.1-33
superheated, thermodynamic properties, 5.5.2-1/5.5.2-2
Helmholtz reciprocity principle, in radiative heat transfer, 2.9.2-6
Henry, J. A. R., 2.2.7-1/2.2.7-11
Henry-Fauske model, for critical two-phase flow, 2.3.2-28/2.3.2-29
Henry s law, for partial pressure, 2.7.6-l
Heptane saturation properties, 5.5.1-9
Heterogeneous conveyance in horizontal pipes, 2.3.4-3/2.3.4-6
Heterogeneous nucleation in boiling, 2.7.1-3/2.7.1-5
Hewitt, Geoffrey F., 2.3.1-1/2.3.2-33
Hexagonal cells, in free convection, 2.5.8-2
Hexane saturation properties, 5.5 .1-8
Hicks equation, for fixed-bed pressure drop, 2.2.5-3
High firmed tubes, correlations for single-phase heat transfer in flow over, 2.5.3-11/2.5.3-12
Hohlraum cavity, 2.9.1-3
Holland, guide to national practice for mechanical design of heat exchangers, 4.3.5-5
Homogeneous condensation (fog formation), 2.6.1-1
effects, 2.6.7-3
nuclei formation, 2.6.7-1/2.6.7-2
supersaturation, 2.6.7-1/2.6.7-3
Homogeneous model:
conservation equations for, in multiphase flows, 2.3.1-4/2.3.1-7
in gas-liquid flows: conservation equations, 2.3.2-8
critical flow estimation by, 2.3.2-28
frictional pressure drop correlations based on, 2.3.2-10
pressure drop in singularities calculated by, 2.3.2-15/2.3.2-18

© 1983 Hemisphere Publishing Corporation

Homogeneous model (Cont.):
in solid-liquid flow, 2.3.4-2/2.3.4-3
Homogeneous nucleation:
of droplets in supersaturated vapor, 2.6.7-1/2.6.7-2
of vapor bubbles in liquids, 2.7.1-2/2.7.1-3
table of values of temperature for various substances, 2.7.1-4
Honeycombs:
free convective heat transfer in, 2.5.8-20/2.5.8-23
loss coefficients in, 2.2.2-20
Horizontal cylinders:
free convective heat transfer inside, 2.5.8-14
(See *also* Cylinders, Horizontal tubes)
Horizontal layers, of fluid, free convection heat transfer in, 2.5.8-1/2.5.8-3
Horizontal pipes:
hydraulic conveyance in, 2.3.4-1/2.3.4-6
pneumatic conveyance in, 2.3.3-1/2.3.3-2
(See *also* Pipes, circular; Horizontal tubes)
Horizontal plates (see Horizontal surfaces; Flat plates)
Horizontal shell-side evaporator, 3.5.2-l
Horizontal surfaces:
combined free and forced convection in transverse flow *over,* 2.5.9-4/2.5.9-6
free convective heat transfer from, 2.5.7-13/2.5.7-18
downward facing surfaces, 2.5.7-13/2.5.7-15
upward facing surfaces, 2.5.7-15/2.5.7-18
pool boiling from, 2.7.2-1/2.7.2-15
Horizontal thermosiphon reboilers:
calculation procedures for, 3.6.5-2/3.6.5-3
characteristics, advantages and disadvantages of, 3.6.1-3
thermal design, 3.6.2-1/3.6.2-6
bubble-induced convection effects, 3.6.2-2/3.6.2-3
critical heat flux and film boiling, 3.6.2-4/3.6.2-5
effective mean temperature difference, 3.6.24
externally induced convection effects, 3.6.2-3
finned tubes in, 3.6.2-6
flow distribution and hydraulics of, 3.6.26
mixture effects, 3.6.2-3/3.6.2-4
single tube nucleate boiling, 3.6.2-1/3.6.2-2
vapor liquid disengagement in, 3.6.2-6
Horizontal tube-side evaporator, 3.5.2-5/3.5.2-6
Horizontal tubes:
boiling outside with crossflow, 2.7.5-1/2.7.5-4
combined free and forced convection in, 2.5.10-7/2.5.10-11
with uniform heat flux, 2.5.10-7/2.5.10-11
with uniform wall temperature, 2.5.10-7
combined free and forced convective heat transfer from outside, 2.5.9-1/2.5.9-6
condensation on inside, 2.6.2-12/2.6.2-15, 3.4.6-1/3.4.6-2
annular flow, 2.6.2-15
flow regimes, 2.6.2-12/2.6.2-13, 3.4.6-2
stratifying flow, 2.6.2-13/2.6.2-14, 3.4.6-2
condensation on outside of, 2.6.2-9/2.6.2-12, 3.4.6-3
in bundles, 2.6.2-10/2.6.2-12
effect of vapor shear, single tube, 2.6.2-9/2.6.2-10
laminar flow, single tube, 2.6.2-9
condensers with condensation inside, 3.4.3-3/3.4.3-4, 3.4.9-3
condensers with condensation outside, 3.4.3-5/3.4.3-6, 3.4.9-3/3.4.9-4
convective boiling in, 2.7.4-1/2.7.4-7
dryout in, 2.7.4-1/2.7.4-4
heat transfer in, 2.7.4-4/2.7.4-6
flow regimes in gas-liquid flow in, 2.3.2-2/2.3.2-4
free convective heat transfer from outside of, 2.5.7-20/2.5.7-23
heat transfer to, in fluidized beds, 2.8.4-6/2.8.4-7
hydrodynamics of various two-phase flow regimes In, 2.3.2-23/2.3.2-26
annular flow, 2.3.2-25/2.3.2-26
slug flow, 2.3.2-24/2.3.2-25
stratified flow, 2.3.2-23/2.3.2-24
pool boiling from, 2.7.2-1/2.7.2-15
(See *also* Horizontal pipes; Pipes, circular)
Hottel s rule, in absorption of radiation by gases, 2.9.5-7
Hsu criterion, for onset of nucleate boiling, 2.7.2-2
Hybrid cooling towers, 3.12.5-1/3.12.5-5
assisted draft towers, 3.12.5-3/3.12.5-4
closed circuit evaporative coolers, 3.12.5-4/3.12.5-5
wet-dry towers, 3.12.5-2/3.12.5-3
Hydraulic conveyance:
homogeneous and pseudohomogeneous, 2.3.4-2/2.3.4-3
in horizontal tubes: flow regimes in, 2.3.4-1/2.3.4-2
heterogeneous conveyance in, 2.3.4-3/2.3.4-6
Hydraulically smooth surface, 2.2.2-l
Hydrocarbons:
phase behavior, 5.2.1-3/5.2.1-4
thermodynamic properties, 5.2.2-1/5.2.2-9
Hydrodynamic entrance length, in single-phase flow in ducts, 2.2.2-10/2.2.2-11
Hydrogen:
saturated properties, 5.5.1-33
supersaturated gaseous, thermodynamic properties, 5 5.24
Hydrogen chloride saturation properties, 5 .5.1-34
Hydrogen fluoride saturation properties, 5.5.1-34
Hydrogen sulfide saturation properties, 5.5 .l-35
Hydrostatic testing of shell-and-tube heat exchangers, 4.2.6-11/4.2.6-13
Hysteresis: in boiling curve, 2.7.2-8
reduction of, using porous surfaces, 2.7.9-3

I

Ideal gas law, 2.2.1-7
Ideal gas, velocity of sound in, 2.2.1-8
Illingworth, A., 4.7.1-1/4.7.10-l
Immersed bodies:
combined free and forced convection around, 2.5.9-1/2.5.9-6
creeping flow regime (assisting convection), 2.5.9-3
opposing convection, 2.5.94
slightly inertial regime (assisting convection), 2.5.9-3/2.5.9-4
thin boundary layer regime (assisting convection), 2.5.9-1/2.5.9-3
transverse flow, 2.5.9-4/2.5.9-6
turbulent regime (assisting convection), 2.5.9-4
free convective heat transfer to, 2.5.7-1/2.5.7-3 1
generalized solutions for, 2.5.7-25/2.5.7-28
horizontal cylinders, 2.5.7-20/2.5.7-23
inclined and horizontal surfaces, 2.5.7-l 3/2.5.7-19
open-ended channels, 2.5.7-19/2.5.7-20
other shapes, 2.5.7-25
spheres, 2.5.7-24/2.5.7-25
vertical cones, 2.5.7-24
vertical and Inclined cylinders, 2.5.7-23/2.5.7-24
vertical plates, 2.5.7-2/2.5.7-13
single-phase flow over, 2.2.3-1/2.2.3-9
circular cylinder, 2.2.3-3/2.2.3-6
flow regimes in, 2.2.3-1/2.2.3-2
forces exerted on, in, 2.2.3-2/2.2.3-3

© 1983 Hemisphere Publishing Corporation

Immersed bodies (Conk):
noncircular cylinders, 2.2.3-6/2.2.3-7
single-phase forced convective heat transfer to: flat plates, 2.5.2-1/2.5.2-3
single bodies, 2.5.2-3/2.5.2-8
Immersed tubes, heat transfer to, in fluidized beds, 2.8.4-6/2.8.4-7
Immersion exchangers, 4.4.4-2/4.4.4-3
Immersion heaters, 4.4.4-2/4.4.4-3
Immiscible liquids, condensation of vapors producing, 2.6.4-112.6.4-l
description, 2.6.1-1, 2.6.4-l
eutectic mixtures, 2.6.4-2/2.6.4-3
Imperfectly diffuse surfaces:
definition, 2.9.4-l
radiative heat transfer between specular surfaces and, 2.9.4-1/2.9.4-11
Impingement damage in heat exchangers, 4.5.3-l
Impingement plate:
constructional features of, 4.2.5-7/4.2.5-8
effect on inlet pressure drop in shell-and-tube heat exchangers, 2.2.7-4/2.2.7-5
in condensers, 3.4.3-5
(See also Impingement protection)
Impingement protection, in shell-and-tube heat exchangers, 3.3.5-10/3.3.5-11
with condensation, 3.4.3-5
Impinging jets:
single-phase heat transfer in, 2.5.6-1/2.5.6-10
average coefficients in, 2.5.6-3/2.5.6-4
local coefficients in, 2.5.6-2/2.5.6-3
Inclined cylinders (see Inclined pipes; Cylinders)
Inclined enclosures, free convective heat transfer in, 2.5.8-17/2.5.8-20
large aspect ratios, 2.5.8-17/2.5.8-19
moderate aspect ratios, 2.5.8-20
Inclined flow, effect of on heat transfer to cylinders, 2.5.2-4/2.5.2-5
Inclined pipes:
flow regimes in gas-liquid flow in, 2.3.2-4/2.3.2-5
free convection heat transfer on outside of, 2.5.7-23/2.5.7-24
pneumatic conveying (solid/gas flow) in, 2.3.3-2
(See also Pipes, circular)
Inclined plates (see Inclined surfaces; Flat plates)
Inclined surfaces, free convective heat transfer from, 2.5.7-13/2.5.7-18
downward facing surfaces, 2.5.7-13/2.5.7-15
upward facing surfaces, 2.5.7-15/2.5.7-18
Inclined tubes (see Pipes, circular; Pipes, noncircular; Inclined Pipes; Cylinders)
Incondensables (see Noncondensables)
Inconel, spectral characteristics of reflectance from oxidized surface of, 2.9.2-15
Incremental collapse, as failure mode in heat exchanger, 4.1.1-3/4.1.1-5
Inert gases, effect on condensation, 2.1.6-3/2.1.6-4
Injection:
effect in transition flow over flat plate, 2.2.1-25
effect in turbulent flow over flate plates, 2.2.1-30
effect on laminar flow on flat plate, 2.2.1-23
use in augmentation of heat transfer, 2.5.11-3/2.5.11-9
Inlet effects in shell-and-tube heat exchangers, 3.3.6-9/3.3.6-10
In-life flow, bundles of tubes (see Tube banks)
In-line tube banks:
correction for heat transfer in, 2.5.3-1/2.5.3-16
finned tubes, 2.5.3-l 1
plain tubes, 2.5.3-2
drag coefficients for tubes in, 2.2.44
pressure drop in with finned tubes, 2.2.4-14
pressure drop in with plain tubes, 2.2.4-7/2.2.4-8
correction factors for small number of tube rows, 2.2.4-10
effect of yawing on, 2.2.4-12
Inspection (see Testing and inspection)
Insulators, thermal conductivity of, 5.4.3-1/5.4.3-2
Integral condensation:
calculation of condensation curves for, 2.6.3-3/2.6.3-4
description, 2.6.3-1/2.6.3-3
Integral finned tubes:
as augmentation device in natural convection, 2.5.11-3
use in shell-and-tube heat exchangers, 4.25-3
Interaction coefficients in heat exchangers, 1.1.2-1/1.1.2-2
Interaction parameters for binary systems, tables, 5.5.4-8/5.5.4-9
Interfacial resistance, in condensation, 2.6.2-15
Interfacial roughness, relationships for, in annular gas-liquid flow, 2.3.2-20/2.3.2-21
Interfacial shear stress, effect on filmwise condensation:
on vertical surface, 2.6.2-5/2.6.2-7
Interfacial tension (see Surface tension)
Intermating troughs, as corrugation design in plate heat exchangers, 3.7.1-1, 3.7.3-1/3.7.3-2, 3.7.6-l
Intermittent flows:
gas liquid, in horizontal and inclined flows, 2.3.2-2/2.3.2-5
plug flow, in vertical pipes, 2.3.2-19
slug flow, in horizontal pipes, 2.3.2-24/2.3.2-25
Internal energy (see specific internal energy)
Internal heat sources, temperature distribution in bodies with, 2.4.2-3
Internal heat transfer coefficient, use in transient conduction calculations, 2.4.3-7/2.4.3-8
Internal reboilers (in distillation columns), characteristics, advantages and disadvantages of, 3.6.1-2/3.6.1-3
Internally finned tubes, heat transfer and pressure drop in, 2.5.11-5/2.5.11-6
International Standards Organization (see ISO)
Interpenetrating continua (as representation of heat exchangers):
partial differential equations for, 1.2.6-1/1.2.6-7
porosity in, 1.2.6-2
Intertube velocity, in tube banks, 2.2.4-3
Inviscid flow, compressible, with heat addition, 2.2.2-13/2.2.2-14
Irvine, T. F., Jr., 2.4.6-1/2.4.6-4
ISO codes for mechanical design of heat exchangers, 4.3.1-3
Isobutane saturated properties, 5.5.1-6
Isopentane saturation properties, 5.5 .1-7
Isothermal flow, compressible, in ducts, 2.2.2-13
Isothermal gas, radiation heat transfer to walls from, 2.9.6-1/2.9.6-9
Isotropic materials, elastic properties, 5.4.5-3/5.4.5-4
Isotropic scattering, 2.9.5-2
Italy, guide to national practice for heat exchanger mechanical design, 4.3.5-7

J

J-type shells, in shell-and-tube heat exchangers:
calculation of heat transfer and pressure drop in, 3.3 .1 l-l
description of, 3.3.4-3
temperature difference correction (F) and θ-NTU charts for, 1.5.2-11/1.5.2-12
Jadcet-type heaters, 4.4.4-3/4.4.4-4

© 1983 Hemisphere P ishing Corporation

Jacob number, 2.7.1-8
Japan, guide to national practice for heat exchanger mechanical design:
high-pressure gas control law, 4.3.5-9
standard construction (JISB8243), 4.358
Jayatillaka relation, between heat and momentum transfer, 1.2.3-6
Jens and Lottes correlation for subcooled forced convective boiling of water, 2.7.3-8
Jet impingement dryer, 3.13.2-4
Jets, impinging (see Impinging jets)

K

Kapitza number, 2.1.7-4/2.1.7-5
Kern method, for shell-side heat transfer in shell-and-tube heat exchangers, 3.3.2-2
Kesler and Lee equations, for critical temperature, critical pressure, acentric factor and molecular weight, 5.2.1-615.2.1-g
Kettle reboilers:
calculation procedures for, 3.6.5-l/3.6.5-2
characteristics, advantages and disadvantages of, 3.6.1-2
constructional features of, 4.2.3-7/4.2.3-8
thermal design, 3.6.2-l/3.6.2-6
bubble-induced convection effects, 3.6.2-2/3.6.2-3
critical heat flux and film boiling, 3.6.2-4/3.6.2-5
effective mean temperature difference, 3.6.24
externally induced convection effects, 3.6.2-3
finned tubes in, 3.6.2-6
flow distribution and hydraulics, 3.6.2-6
mixture effects, 3.6.2-3/3.6.2-4
single tube nucleate boiling, 3.6.2-l/3.6.2-2
vapor-liquid disengagement in, 3.6.2-6
Kirchoff's law, in radiative heat transfer, 2.9.2-2
Knudsen number, 2.2.1-11
K-values, in phase equilibrium, 5.2.1-3

L

Lamella heat exchangers, 3.1.2-3/3.1.2-4
Laminar boundary layers (see Boundary layers)
Laminar flow:
combined free and forced convective heat transfer in, 2.5.10-1/2.5.10-11
condensation in vertical surfaces, 2.6.2-2/2.6.2-4
heat transfer in ducts in, 2.5.1-2/2.5.1-5
augmentation of, 2.5 .1 l-412.5.11-8
in concentric annular ducts, 2.5.1-3
free convection effects in, 2.5.1-4/2.5.1-5
with liquid metals, 2.5.13-1/2.5.13-2
between parallel plates, 2.5 .l-3
in straight circular pipes, 2.5.1-2
heat transfer in free convection on a vertical surface in, 2.5.7-3
heat transfer in tube bundles in, 2.5.13-2/2.5.13-3
in circular pipes, 2.2.2-1/2.2.2-2
in ducts, characteristic of plate fin heat exchangers, 3.9.5-1/3.9.5-3
in noncircular pipes, 2.2.2-7/2.2.2-9
Laminar flow control, of boundary layers, 2.2.1-25
Laminar sublayer (see Viscous sublayer)
Lancaster, J. F., 4.5.1-1/4.5.3-7
Large eddy simulation, in prediction of turbulent boundary layers, 2.2.1-29
Latent heat (see Heat of vaporization)
Laws for turbulent flows:
of the wake, 2.2.1-26
of the wall, 2.2.1-25
velocity defect, 2.2.1-26
Layers of fluid, free convection heat transfer in, 2.5.8-l/2.5.8-3
Le Fevre equations for free convective heat transfer, 2.5.7-3
Leakage between streams, in shell-and-tube heat exchangers, 3.3.4-4/3.3.4-5, 4.6.1-2
Leakage effects, on heat transfer and pressure drop in shell-and-tube heat exchangers, 3.3.1-1/3.3.11-5
shell-to-baffle: correction factors, 3.3.6-613.3.6-g
leakage area, 3.3.6-4/3.3.6-5
tubes-to-baffle: correction factors, 3.3.6-6/3.3.6-8
leakage area, 3.3.6-5
Lessing rings, characteristic of, as packings for fixed beds, 2.2.5-2
Lienhard and Dhir analysis of critical heat flux in pool boiling, 2.7.2-10/2.7.2-12
Lienhard and Eichhorn criterion, for transition in critical heat flux mechanism in crossflow over single tube, 2.7.5-3
Lift force:
in flow in tube banks, 2.2.4-16
in flow over immersed bodies, 2.2.3-3
Liley, P. E., 5.5.6-1/5.5.7-3
Liquid fuels, properties of, 3.11.3-3
Liquid hold-up, 2.3.1-3
Liquid metals:
heat transfer in, 2.5.13-1/2.5.13-4
in channel flows, 2.5.13-1/2.5.13-4
condensation of, 2.6.2-15/2.6.2-16
in heat exchangers, 2.5.13-3
Liquid-solid flow (see Solid-liquid flow)
Liquids:
as constituent in multiphase flows, 2.3.1-1/2.3.1-2
physical properties of:
in multicomponent mixtures, 5.2.3-1/5.2.4-4
rheologically complex, 5.3.1-1/5.3.8-3
saturated property tables for, 5.5.1-1/5.5.1-40
specific heat capacity, 5 .1.3-7
specific volume, 5.1.2-1/5.1.2-2
surface tension, 5.1.5-1/5.1.5-3
thermal conductivity, 5.1.4-6/5.1.4-7
thermal expansion coefficient, 5.1.2-2
viscosity, 5.1.4-1/5.1.4-5
LMTD (see Logarithmic mean temperature difference)
Loads, types of in heat exchangers, 4.1.1-l
Local conditions hypothesis, for critical heat flux in flow boiling, 2.7.3-18/2.7.3-19
Lockhart and Martinelli correlations:
for frictional pressure gradient, 2.3.2-10
for void fraction, 2.3.2-17
Lodge s rubber-like liquid (non-Newtonian), 2.2.8-8
Logarithmic driving force. in mass transfer, 2.1.5-3
Logarithmic law region, 2.2.2-l
Logarithmic Mean Temperature Difference, 1.2.4-2/1.2.4-3, 2.1.2-2, 2.5.1-1, 3.1.1-2
Longitudinal fins (see Straight fins)
Long-tube vertical evaporator, 3.5.2-3/3.5.2-4
Loss coefficient, 2.2.2-14
for bends, 2.2.2-16
in combining and dividing flow, 2.2.2-19/2.2.2-20
for diffusers, 2.2.2-17/2.2.2-18
values for various fittings, 2.2.2-19/2.2.2-20

© 1983 Hemisphere Publishing Corporation

Louvered fins, in plate fin exchangers, 3.9.3-l
Low-ahoy steels, as material of construction, 4.5.2-3
Low-finned tubes:
application in shell-and-tube heat exchangers 3.3.11-2/3.3.11-3
correlations for single phase heat transfer in flow over, 2.5.3-12/2.5.3-11
use in boiling augmentation, 2.7.9-1/2.7.9-2
Lubricants, physical properties of:
classification, 5.3.2-l
lubricant-cooling liquids, 5.3.5-1/5.3.5-2
oils, 5.3.3-1/5.3.3-2
plastic lubricants, 5.3.4-1/5.3.4-2
Ludwieg-Tillmann formula, for skin friction, 2.2.1-26
Lydersen's incremental method, for critical parameters, 5.1.1-1/5.1.1-2

M

Macdonald equation, for fixed-bed pressure drop, 2.2.5-3
Mach number, 2.2.1-11
effect on turbulent flow over flat plate, 2.2.1-30
incompressible duct flows with heat transfer, 2.2.2-12
Maddox, R. N., 5.2.1-1/5.2.5-5, 5.5.1-1/5.5.2-11, 5.5.4-1/5.5.4-9
Magnetic fields, effect on properties of rheologically complex materials, 5.3.8-1/5.3.8-2
Manifolds (see Headers)
Martin, H., 2.4.1-1/2.4.5-4, 2.5.5-1/2.5.6-10
Martinelli and Boelter equations for combined free and forced convection, 2.5.10-2/2.5.10-3
Martinelli and Nelson correlations:
for frictional pressure gradient, 2.3.2-10/2.3.2-11
for void fraction, 2.3.2-14
Mass absorption coefficient, 2.9.5-2
Mass and heat transfer, combined:
in condensation, 2.1.6-2/2.1.6-4
in drying, 2.1.6-1/2.1.6-2
Mass extinction coefficient, 2.9.5-2
Mass fraction, in multicomponent mixtures, 1.2.1-2
Mass scattering coefficient, 2.9.5-2
Mass transfer:
analogy with heat transfer, 2.1.5-1/2.1.5-4
in cooling towers, 3.12.2-2/3.12.2-3
in condensation: in multicomponent mixtures, 2.6.3-7/2.6.3-8
of binary mixtures, 2.6.3-7
of single vapor with noncondensables, 2.6.3-5/2.6.3-7
with impinging jets, 2.5.6-1/2.5.6-10
in fixed beds, 2.5.4-2/2.5.2-6
in fluidized beds, 2.5.5-3/2.5.5-6
in nonuniform systems, 2.1.4-1/2.1.4-4
volumetric coefficient for, 1.1.2-2
Mass transfer coefficient:
in fixed beds, 2.5.4-1/2.5.4-6
individual definition of, 1.2.2-2/1.2.2-3, 2.1.5-2/2.1.5-3
Matovosian, Robert, 5.5.5-1/5.5.5-4
Materials of construction, for heat exchangers, 4.5.1-1/4.5.3-7
materials for corrosive service, 4.5.2-2/4.5.2-6
austenitic stainless steels, 4.5.24
carbon steel, 4.5.2-2/4.5.2-3
coatings, 4.5.2-5/4.5.2-6
copper base alloys, 4.5.2-4/4.5.2-5
ferritic chromium stainless steels, 4.5.2-3
low alloy steels, 4.5.2-3
nickel based alloys, 4.5.2-5
non-metallic materials, 4.5.2-6
titanium, 4.5.2-5
materials for noncorrosive service, 4.5.2-2
product forms, 4.5.2-1/4.5.2-2
shells, channels, covers, and bonnets, 4.5.2-1/4.5.2-2
tubes, 4.5.2-l
tubesheets, 45.2-1
testing and inspection of, 4.7.2-l
Matrix heat exchangers (see Plate fin heat exchangers)
Matrix inversion techniques, in radiative heat transfer, 2.9.3-7/2.9.3-8
Maximum bed-to-surface heat transfer, in fluidized beds, 2.8.4-4/2.8.4-5
Maximum heat flux:
by conduction in solids, 2.1.1-2
in condensation, 2.1.7-4/2.1.7-6
under free molecule conditions in gases, 2.1.1-2
Maximum mass flux:
in condensation, 2.1.7-4/2.1.7-6
under free molecule conditions, 2.1.1-2
Maximum shear stress, under free molecule conditions, 2.1.1-2
Maximum velocities (in shelf-and-tube heat exchangers), 3.3.5-15, 4.5.3-3
Maxwell model, for non-Newtonian fluid, 2.2.8-7
Maxwell velocity of a vapor, as limiting phenomenon in condensation, 2.1.7-4/2.1.7-6
Maxwell s equations, for electromagnetic radiation, 2.9.2-7/2.9.2-8
Mean-beam-length concept, in radiative heat transfer:
tables of geometric mean beam lengths, 2.9.6-5
theory of, 2.9.6-2/2.9.3
theory of, 2.9.6-2/2.9.6-3
Mean equivalent temperature, of a surface in combined convective and radiative heat transfer, 2.9.8-2
Mean phase content, 2.3.1-3
Mean temperature difference:
application in shell-and-tube heat exchangers, 3.3.5-17
concept of, 3.1.1-2/3.1.1-3
effective, in kettle reboilers, 3.6.24
in condensers, 3.4.8-1/3.4.8-3
(See *also* Logarithmic mean temperature difference, Arithmetic mean temperature difference)
Mechanical agitators, for agitated vessels, 3.14.2-1/3.14.2-2
heat transfer correlations for, 3.14.3-1/3.14.3-6
Mechanical design of heat exchangers:
air cooled heat exchangers, 4.4.1-1/4.4.1-7
basic principles, 4.1.1-1/4.1.8-3
expansion joints, 4.1.6-1
flanges, 4.1.7-1/4.1.7-2
heads, openings and branches, 4.1.8-1/4.1.8-2
introduction to, 4.1.1-1/4.1.1-5
methods of analysis, 4.1.2-1/4.1.2-9
shells, 4.1.3-1/4.1.3-3
tube plates, 4.1.4-1/4.1.4-3
tubes, 4.1.5-1
block type, 4.4.44
direct contact, 4.4.4-6/4.4.4-8
double-pipe exchangers, 3.2.5-1/3.2.5-2, 4.4.4-1/4.4.4-2
heat pipes, 4.4.4-914.4.4-l 1
helical (Hampson) coils, 4.4.4-8/4.4.4-9
jacketed heaters, 4.4.4-3/4.4.4-4
plate fin heat exchangers, 4.4.3-1/4.4.3-9
plate heat exchangers, 4.4.2-1/4.4.2-8
shell-and-tube exchangers: constructional features, 4.2.1-1/4.2.6-13

© 1983 Hemisphere I blishing Corporation

Mechanical design of heat exchangers, shell-and-tube exchangers:
constructional features (Cont.):
design codes for, 4.3.1-1/4.3.5-1
example of design, 4.3.1-6/4.3.6-23
scraped surface, 4.4.4-5 /4.4.4-7
spiral plate, 4.4.4-5
tubular and panel immersion, 4.4.4-2/4.4.4-3
Mechanical draft cooling towers, 3.12.4-1/3.12.4-2
thermal performance and design, 3.12.4-2/3.12.4-4
Mechanical draft fan coolers (see Air-cooled heat exchangers)
Melting, thermal conduction in, 2.4.4-1/2.4.4-2
Melting point of commonly used substances, 5.5.1-1/5.5.1-40
Mercury:
saturation properties, 5.5 .1-35
superheated gaseous, thermodynamic properties of, 5.5.2-4/5.5.2-5
Merkblatter (German) code, for mechanical design of heat exchangers, 4.3.1-3
index to, 4.3.2-1/4.3.2-4
Merkel s equation, in cooling tower design, 3.12.2-3
Metais and Eckert diagrams, for regimes of convection:
in horizontal pipes, 2.2.6-6, 2.5.10-1/2.5.10-2
in vertical pipes, 2.5.10-2
Metastable equilibrium, of vapor and Liquid, 2.7.1-1
Methane saturation properties, 5 .5.1-4
Methanol saturation properties, 5.5.1-17
Methyl acetate saturation properties, 5.5 .l-25
Methyl-*t*-butyl ether saturation properties, 5.5 .1-23
Metals:
condensation of, 2.6.2-15/2.6.2-16
density, 5.4.1-1
liquid, single-phase heat transfer in, 2.5.13-1/2.5.13-4
spectral absorptivity, 2.9.2-11/2.9.2-12
Microlayer evaporation, in boiling of binary mixtures, 2.7.6-7
Minimum heat flux in pool boiling:
of binary and multicomponent mixtures, 2.7.7-5/2.7.7-6
of pure components, 2.7.2-13/2.7.2-14
Minimum tubeside velocity, in shell-and-tube heat exchangers, 3.3.5-16
Minimum velocity for fluidization, 2.2.6-2
Minimum wetting rate, for binary mixtures, 2.7.8-7
Mirror-image concept, in radiative heat transfer, 2.9.4-1/2.9.4-2
Mirrors, spectral characteristics of reflectance from, 2.9.2-17
Mist flow:
in axial flow reboilers, 3.6.2-9
heat transfer in (see Post-dryout heat transfer)
onset, as mechanism for critical heat flux in reboilers, 3.6.2-812.6.2-g
Mixed convection, occurrence in horizontal circular pipe, Metais and Eckert diagram for, 2.2.2-6
Mixing length, 2.2.24
table of turbulent flow in circular pipes, 2.2.2-3
Mixing vessel (see Agitated vessel)
Mixtures:
of gases, radiation properties, 2.9.5-l l/2.9.5-12
condensers for, 3.4.4-1/3.4.4-2
(See *also* Binary mixtures, Multicomponent mixtures)
Models, theory of, 2.2.1-12/2.2.1-13
Modes of heat transfer, Nusselt description, 2.1.0-2
Molecular gas radiation properties, 2.9.5-8/2.9.5-11
Molecular weight:
of commonly used fluids, 5.5.1-1/5.5.1-40
Kesler and Lee equation for estimation of in hydrocarbon mixtures, 5.2.1-7
Molerus, O., 2.2.6-1/2.2.6-9
Mollier chart, for humid air, 3.13.1-1
description of drying processes in terms of, 3.13.3-4/3.13.3-5
Momentum equation:
in boundary layer, 2.2.1-17
in compressible duct flow, 2.2.1-12
differential form for single-phase flow, 2.2.1-5/2.2.1-7
in gas-liquid flows, 2.3.2-812.3.2-g
homogeneous model, 2.3.2-8
separated flow model, 2.3.2-8/2.3.2-9
in heat exchanger calculations, 1.2.6-5/1.2.6-7
integral form for single-phase flow, 2.2.1-2/2.2.1-3
in multiphase flows: homogeneous flow, 2.3.1-5
separated flow, 2.3.1-7
in non-Newtonian flow, 2.5.12-5
in turbulent flow, 2.2.1-14
Monte Carlo methods, in radiative heat transfer, 2.9.4-2/2.9.4-5
for radiative heat transfer with an isothermal gas, 2.9.6-812.9.6-g
Moody chart:
for critical two-phase flow, 2.3.2-28
for single-phase friction factor in circular pipes, 1.2.3-3, 2.2.2-2
Morcos and Bergles equation, for influence of free convection of friction factor, 2.2.2-6
Morris, M., 4.3.1-1/4.3.5-11
Mostinski correlations:
for critical heat flux, 3.6.2-5
for nucleate boiling, 2.7.2-6
application to kettle reboilers, 3.6.2-l
Moving bed, heat transfer to, 2.8.3-3/2.8.3-4
Moving belt, heat transfer to, 2.1.3-2/2.1.3-3
Muchowski, E., 2.8.3-1/2.8.3-9
Mueller, A. C., 3.4.1-1/3.4.9-5
Multicomponent mixtures:
air-cooled condensers for, 3.8.9-2/3.8.9-4
boiling of, in kettle reboilers, 3.6.2-3/3.6.2-4
condensation of, 2.6.3-7/2.6.3-9, 2.6.4-1/2.6.4-7
condensers for, 3.4.4-1/3.4.4-2
diffusion in, 2.1.5-1/2.1.5-4
forced convective boiling of, 2.7.8-1/2.7.8-10
combined heat and mass transfer in, 2.7.8-3/2.7.8-6
critical heat flux in, 2.7.8-6/2.7.8-7
saturated nucleate, 2.7.8-1/2.7.8-2
two-phase forced convective, 2.7.8-2/2.7.8-3
of gases, radiation properties of, 2.9.5-11/2.9.5-12
phase equilibria in, 2.7.6-3/2.7.6-5
physical properties of, 5.2.1-1/5.2.5-5
diffusion coefficients, 5.2.5-1/5.2.5-5
equilibria, 5.2.1-1/5.2.1-8
interfacial tension, 5.2.4-1/5.2.4-3
thermodynamic properties, 5.2.2-1/5.2.2-9
thermophysical properties, 5.2.3-1/5.2.3-9
pool boiling of, 2.7.7-1/2.7.7-7
critical heat flux, 2.7.7-4/2.7.7-5
film boiling, 2.7.7-6
minimum heat flux, 2.7.7-5/2.7.7-6
nucleate boiling, 2.7.7-1/2.7.7-4
transition boiling, 2.7.7-5
Multidimensional systems, heat conduction in, 2.4.3-10/2.4.3-12
Multiflux methods, for radiative heat transfer in non-isothermal gases, 2.9.7-612.9.7-l
Multipass shell-and-tube heat exchangers, 1.1.1-2
Multiphase fluid flow and pressure drop:
introduction and fundamentals, 2.3.1-1/2.3.1-10

© 1983 Hemisphere Publishing Corporation

Multiphase fluid flow and pressure drop, introduction and fundamentals (Cont.):
classification of multiphase flows, 2.3.1-1/2.3.1-2
conservation equations for, 2.3.1-3/2.3.1-7
design parameters in, 2.3.1-2/2.3.1-3
drift flux models for, 2.3.1-7/2.3.1-10
solid-gas flow, 2.3.3-1/2.3.3-10
flow patterns in, 2.3.3-2
pressure drop in, 2.3.3-2, 2.3.3-4/2.3.3-8
principles of pneumatic conveyance, 2.3.3-1/2.3.3-2
solid-liquid flow, 2.3.4-1/2.3.4-7
flow regimes in, 2.3.4-1/2.3.4-2
pressure drop in, 2.3.4-3/2.3.4-6
Multiple effect evaporation, 3.5.3-1/3.5.3-2
Multirod clusters (see Rod bundles)
Multizone model, for furnaces, 3.11.6-1/3.11.6-4
Murray, I., 4.4.4-1/4.4.4-11

N

"Nabla" operator (see Differential vector operators)
Nahme-Griffith number, 2.5 .12-6
National practice, in mechanical design, guide to, 4.3.5-1/4.3.5-9
Natural convection:
as precursor to nucleate boiling, 2.7.2-1/2.7.2-2
(See also Free convection)
Natural draft cooling towers:
dry, 3.8.2-1/3.8.2-2, 3.8.8-1, 3.12.5-1/3.12.5-2
main features of, 3.12.3-1/3.12.3-2
structural design, 3.12.3-6/3.12.3-7
thermal performance and design of, 3.12.3-2/3.12.3-6
design optimization of, 3.12.3-5/3.12.3-6
performance away from design point, 3.12.3-6
pressure losses in, 3.12.3-3/3.12.3-5
thermal design equation, 3.12.3-2/3.12.3-3
Natural draft heat exchangers (see Ah cooled heat exchangers, Cooling towers)
Natural frequency of tube vibration in heat exchangers, 4.6.2-1/4.6.2-4
Navier-Stokes equation, 2.2.1-5
Neon saturation properties, 5.5 .1-36
Neopentane saturated properties, 5.5 .1-6
Net free area, in double-pipe heat exchangers, 3.2.3-l
Netherlands, guide to national mechanical design practice, 4.3.5-5
Newton s law, for momentum transfer, 2.1.1-2
limitations in, 2.1.1-1/2.1.1-4
NFA (see Net free area)
Nickel-base alloys, as material of construction, 4.5.2-5
Nitrogen:
critical heat flux table for flow boiling of in vertical tube, 2.7.3-29
saturation properties, 5.5 .1-36
superheated gaseous, thermodynamic properties, 5.5.2-5
Noise, in air-cooled heat exchangers, 3.8.9-l
Nonane saturation properties, 5 .5.1-10
Nonaqueous fluids, critical heat flux in, 2.7.3-6/2.7.3-30
Noncircular cylinders (see Cylinders)
Nonwndensables:
in boiling, 2.7.2-8
in condensation, 2.1.6-2, 2.6.1-2, 2.6.3-5/2.6.3-7, 2.6.4-5 /2.6.4-6, 2.6.5-2/2.6.5-3
Nondestructive testing, of heat exchangers, 4.7.6-1/4.7.6-2
Nonmetallic materials, for heat exchangers, 4.5.2-6
Non-Newtonian flow:
free convective heat transfer from: spheres, 2.5.7-25
vertical plates, 2.5.7-10/2.5.7-11
properties of rheologically complex fluids in, 5.3.1-1/5.3.8-3
single-phase fluid flow and pressure drop in, 2.2.8-1/2.2.8-13
experimental characterization of non-Newtonian fluids, 2.2.8-1/2.2.8-6
models for non-Newtonian fluids, 2.2.8-612.2.8-g
turbulent flow of non-Newtonian fluids, 2.2.8-l 1
volume flow rate/pressure drop relations, 2.2.8-9/2.2.8-11
single-phase forced convective heat transfer with, 2.5.12-1/2.5.12-16
in channel flows, 2.5.12-6/2.5.12-15
equations and dimensionless groups for, 2.5.12-5/2.5.12-6
governing physical properties in, 2.5.12-2/2.5.12-5
Non-uniform heat flux, critical heat flux with, 2.7.3-18/2.7.3-22
North, C., 4.8.3-1/4.8.3-3
No-tubes-in-window shells, calculation of heat transfer and pressure drop in, 3.3.1 l-1/3.3.1 1-3
Nozzles:
analytic basis for codes for, 4.3.3-2
comparison of codes for, 4.3.4-2
impinging jets from, heat transfer in, 2.5.6-1/2.5.6-10
arrays of nozzles, 2.5.6-5/2.5.6-6
optical spatial arrangement, 2.5.6-6/2.5.6-9
single nozzles, 2.5.6-4/2.5.6-5
in shell-and-tube heat exchangers: constructional features of, 4.2.5-12, 4.2.6-2/4.2.6-3
description of, 2.2.7-l
impingement protection for, 3.3.5-10/3.3.5-11
pressure change across inlet nozzle, 2.2.7-2/2.2.7-3
pressure change across outlet nozzle, 2.2.7-3/2.2.7-4
index to U.S., U.K., and F.R.G. codes for, 4.3.2-9/4.3.2-10
loss coefficients in, 2.2.2-20
NTU (see Number of transfer units)
Nuclear fuel suspensions, properties of, 5.3.1-2/5.3.1-3
Nucleate boiling:
augmentation of, 2.7.9-1/2.7.9-4
in axial flow reboilers, 3.6.2-6/3.6.2-7
in evaporators, 3.5.7-2/3.5.7-3
in forced convective boiling of binary and multicomponent mixtures, 2.7.8-1/2.7.8-2
in forced convective heat transfer in vertical tubes, 2.7.3-1/2.7.3-12
in horizontal tubes, 2.7.4-1/2.7.4-7
in kettle reboilers, 3.6.2-1/3.6.2-4
outside tubes and tube bundles in crossflow, 2.7.5-1/2.7.5-7
in pool boiling of binary and multicomponent mixtures, 2.7.7-1/2.7.7-4
in pool boiling systems, 2.7.2-3/2.7.3-9
correlations for, 2.7.2-3/2.7.3-7
hysteresis in, 2.7.2-8
influence of dissolved gases on, 2.7.2-8
influence of gravitational acceleration on, 2.7.2-9
influence of liquid subcooling on, 2.7.2-9
influence of size and orientation of surface on, 2.7.2-8/2.7.2-9
influence of surface conditions on, 2.7.2-7/2.7.2-8
influence of system pressure on, 2.7.2-7
influence of wettability of surface on, 2.7.2-9
Nucleation:
augmentation devices for, 2.7.9-1/2.7.9-2
in binary systems, 2.7.6-5
heterogeneous, in boiling, 2.7.1-3/2.7.1-4
homogeneous, of vapor bubble in liquid, 2.7.1-2/2.7.1-3
in supersaturated vapor, 2.6.7-1/2.6.7-2

© 1983 Hemisphere Publishing Corporation

Nucleation sites:
critical size for nucleation: in pool boiling, 2.7.2-2/2.7.2-3
in subcooled forced convective boiling, 2.7.3-6
enhancement of number and activity of, 2.7.9-1/2.7.9-2
size in binary mixtures, 2.7.6-5
sizing of active, 2.7.1-5/2.7.1-6
Nuclei, formation in supersaturated vapor, 2.6.7-1/2.6.7-2
Number of transfer units (NTU):
in air-cooled heat exchangers, 3.8.5-1/3.8.5-5
average value in nonuniform heat transfer in shell-and-tube heat exchangers, 2.1.4-1/2.1.4-3
as basis for design of plate heat exchangers, 3.7.2-l
rating in, 3.7.7-l
in cooling of slab, 2.1.3-1/2.1.3-2
in cooling towers, 3.12.2-4/3.12.2-5
in heat exchangers, 1.2.4-3
in particle-to-fluid heat transfer in fluidized beds, 2.5.5-2/2.5.5-3
in transient heat transfer, defmition of, 2.1.2-2/2.1.3-7
(See also θ or θ-NTU method)
Numerical methods:
application in furnace prediction, 3.11.7-5
for cases in which flow patterns must be calculated, 1.4.2-1/1.4.2-2
applications, 1.4.2-3/1.4.2-4
discretization, 1.4.2-1
finite difference equations for, 1.4.2-1/1.4.2-2
solution procedure, 1.4.2-2/1.4.2-3
for the solution of heat exchangers with a prescribed flow pattern, 1.4.1-1/1.4.1-6
discretization, 1.4.1-1/1.4.1-3
finite difference equations for, 1.4.1-3/1.4.1-4
influence of fineness of discretization, 1.4.1-5/1.4.1-6
special applications of, 1.4.3-1/1.4.3-6
calculations of heat transfer coefficients, 1.4.3-3/1.4.3-4
flows with chemical reactions, 1.4.3-2/1.4.3-3
flows with radiation, 1.4.3-3
turbulent flow in empty spaces, 1.4.3-2
two-phase flows, 1.4.3-1
in transient conduction calculations, 2.4.3-8/2.4.3-10
Nusselt:
description of modes of heat transfer, 2.1.9-2
equations for condensation: inside horizontal tube, 2.6.2-13
outside horizontal tube, 2.6.2-9
vertical surface, 2.6.2-2
Nusselt-Graetz problem, in laminar heat transfer in ducts, 2.5.1-2
Nusselt number:
in combined and free and forced convection: around immersed bodies, 2.5.9-1/2.5.9-6
in channels, 2.5.10-2/2.5.10-11
definition, 1.2.3-2
in finned tube banks, 25.3-11
in flow over tube banks, 2.5.3-1/2.5.3-6
forms of correlation for, 2.1.34
in free convection over immersed bodies, 25.7-2
for heat transfer in tubes, 2.1.3-6
in laminar flow in ducts, 2.5.1-2/2.5.1-5
in liquid metal flow, 2.5.13-1/2.5.13-4
in non-Newtonian flows, 2.5.12-7/2.5.12-16
in nonuniform heat transfer in packed beds, 2.1.4-3/2.1.4-4
in particle to fluid heat transfer in fiied beds, 25.4-l
in plate heat exchangers, 3.7.5-l
in single-phase flow over immersed bodies, 2.5.2-1/2.5.2-8
in systems with heat transfer augmentation, 2.5.11-1/2.5.11-12
in turbulent flow in ducts, 2.5.1-5/2.5.1-11

O

Oblate spheroids, free convective heat transfer from, 2.5.7-25
Octane saturation properties, 5.5.1-9
Oldroyd eight constant model, for non-Newtonian fluid, 2.2.8-8
ONB (onset of nucleate boiling):
in pool boiling, 2.7.2-12
in subcooled boiling in vertical tubes, 2.7.3-5/2.7.3-7
One equation models, for turbulent boundary layers, 2.2.1-28
Openings, mechanical design aspects, 4.1.8-1/4.1.8-2
Operational envelope of a heat pipe, 3.10.4-l
Opposed convection:
around immersed bodies, 2.5.9-11
in vertical tubes, 2.5.10-6
Optimization methods, for heat exchanger design, 3.3.4-2
Organic solids, density, 5.4.1-2
Orifices:
loss coefficients in, 2.2.2-21
two-phase gas liquid flow, 2.3.2-17/2.3.2-18
OTL (see Outer tube limit)
Outer tube limit, in shell-and-tube heat exchangers, 4.2.5-9
Outlet effects, in shell-and-tube heat exchangers, 3.3.6-9/3.3.6-10
Overall heat transfer coefficient, 2.1.2-1
approximate values: in shell-and-tube exchangers, 3.1.4-4/3.1.4-5
in liquid metal heat exchangers, 2.5.13-3
in various heat exchangers, 2.1.2-3/2.1.2-4
in air-cooled heat exchangers, 3.8.5-1/3.8.5-5
Overall power hypothesis, for critical heat flux in flow boiling, 2.7.3-19
Oxygen:
saturation properties, 5.5.1-37
superheated gaseous, thermodynamic properties of, 5.5.2-6

P

Packed beds (see Fixed beds)
Packing relationship, in cooling tower design, 3.12.2-3/3.12.2-4
Packings, for cooling towers, 3.12.2-8/3.12.2-10
Packings, for fixed beds:
characteristics, 2.2.5-2
effective conductivity of various in fixed beds: beds with gas flow, 2.8.2-2/2.8.2-5
stagnant beds, 2.8.1-3/2.8.1-5
Paikert, P., 3.8.1-1/3.8.9-4
Paints, spectral characteristics of reflectance of surfaces treated with, 2.9.2-14/2.9.2-17
Palen and Small correlation, for critical heat flux in tube banks, 2.7.5-6
Palen, J. W., 3.6.1-1/3.6.5-6
Panel immersion exchangers, 4.4.4-2/4.4.4-3
Parallel flow (see Cocurrent flow)
Parallel plates, (see Plates)
Partial boiling in subcooled forced convective heat transfer, 2.7.3-812.7.3-g
Particle convective component, in heat transfer from fluidized beds, 2.8.4-2/2.8.4-3
Particle emissivity, 2.9.7-2
Particle Reynolds number in fixed beds, 2.2.5-2
Particles:
fluid-to-particle heat transfer in fluidized beds, 2.5.5-1/2.5.5-6
free fall velocity of, 2.3.3-3

© 1983 Hemisphere Publishing Corporation

Particles (*Cont.*):
particle-to-wall heat transfer in fluidized beds, 2.8.4-1/2.8.4-8
Particulate fluidization, 2.2.6-l
Pass arrangements, in plate heat exchangers, 3.7.8-1/3.7.8-3
Passes, tube side, 4.2.5-3/4.2.5-4
boxed in" 4.2.5-4
number of, 4.2.5-3/4.2.5-4
partition plates between, 4.2.5-3
Passive methods, for augmentation of heat transfer, 2.5.11-1/2.5.11-3
in condensation, 2.6.6-1/2.6.6-4
in forced convection, 2.5.11-4/2.5.11-8
in free convection, 2.5 .11-3
Pearson number, 2.5.12-6
Peclet number, 1.2.3-2/1.2.3-3, 2.1.5-2
heat and mass transfer at low, in fluidized beds, 2.5.5-312.5.5-s
in heat transfer in liquid metal systems, 2.5.13-1/2.5.13-4
in non-Newtonian flow, 2.5.12-6
Peng-Robinson equation of state, 5.1.24
application to hydrocarbons, 5.2.2-2
Penner s rule, in absorption of radiation by gases, 2.9.5-7
Pentane:
normal, critical heat flux for flow boiling of in vertical tube, 2.7.3-29
saturation properties of, 5.5.1-8
Perfect gas (see Ideal gas)
Perforated fins, in plate fin heat exchangers, 3.9.3-I
Perforated plates, loss coefficients in, 2.2.2-20
Periodic variations in temperature, thermal conduction in bodies with, 2.4.5-1/2.4.5-4
Petroleum properties, 5.3.1-3
Phase change number, 2.4.4-l
Phase envelope, for natural gas mixture, 5.2.1-4
Phase equilibrium:
in binary mixtures, 2.7.6-1/2.7.6-3
in multicomponent mixtures, 2.7.6-3/2.7.6-4
(See also Equilibrium, phase)
Phase rule (Gibbs), 5.2. l-l
Phase separation, as source of corrosion problems, 4.5.3-5
PHE (see Plate heat exchanger)
Phenol saturation properties, 5.5 .l-20
Phonons, in thermal conductivity of solids, 5.4.3-1/5.4.3-3
Physical properties:
of mixtures of fluids, 5.2.1-1/5.2.5-5
of pure fluids, 5.1.1-1/5.1.5-3
of rheologically complex media, 5.3.1-1/5.3.8-3
of solids, 5.4.0-1/5.4.5-5
tables of, 5.5.1-1/5.5.8-3
variation with temperature: effect in developing flow, 2.2.2-11
effect on flow in tube banks, 2.2.4-10/2.2.4-12
effect on flow over cylinder, 2.2.3-6
effect on friction factor in circular pipe flow, 2.2.2-7/2.2.2-8
effect in heat transfer of flat plates, 2.5.2-2/2.5.2-3
effect in laminar flow heat transfer in channels, 2.5.1-4
effect in turbulent flow heat transfer in channels, 2.5.1-6/2.5.1-7
nature of variation, 2.2.1-9
in polymers, 2.5.12-2/2.5.12-4
Pin fins (see Spine fins)
Pi theorum, in dimensional analysis, 2.2.1-11
Pipe fittings (see Piping components)
Pipes, circular:
augmentation of heat transfer in, 2.5.11-4/2.5.11-9
internally finned for, 2.5.11-5/2.5.11-6
boiling of binary and multicomponent mixtures in, 2.7.8-1/2.7.8-7
critical heat flux, 2.7.8-6/2.7.8-7
forced convective (including mass transfer effects), 2.7.8-2/2.7.8-6
nucleate boiling, 2.7.8-1/2.7.8-2
combined free and forced convection in, 2.5.10-1/2.5.10-12
in condensers, 3.4.1-1/3.4.9-5
horizontal channels, 2.5.10-7/2.5.10-11
vertical pipes, 2.5.10-2/2.5.10-7
flow boiling in: horizontal pipes, 2.7.4-1/2.7.4-7
vertical pipes, 2.7.3-1/2.7.3-37
free convective heat transfer from outside of, 2.5.7-20/2.5.7-24
horizontal, 2.5.7-20/2.5.7-23
vertical and inclined, 2.5.7-23/2.5.7-24
heat transfer to, in fluidized beds, 2.8.4-6/2.8.4-7
heat transfer to liquid metals in, 2.5 .13-1
laminar heat transfer in, 2.5 .l-2
in hydrodynamically developed flow, 2.5.1-1
in thermally and hydrodynamically developing flow, 2.5.1-2
pneumatic conveyance (gas solids flow) in, 2.3.3-1/2.3.3-2
radiative heat transfer along, 2.9.3-15/2.9.3-16
roughened surface, radiative heat transfer along, 2.9.4-9/2.9.4-10
single-phase fluid flow and pressure drop in fully developed flow in, 2.2.2-1/2.2.2-7
effect of free convection on, 2.2.2-5/2.2.2-7
effect of temperature dependent fluid properties on, 2.2.2-7
friction factor, 2.2.2-1/2.2.2-2
influence of additives on, 2.2.2-7
turbulence characteristics in, 2.2.2-1/2.2.2-5
turbulent heat transfer in, 2.5.1-5/2.5.1-9
two-phase gas-liquid flow in, 2.3.2-1/2.3.2-33
flow regimes in, 2.3.2-1/2.3.2-5
hydrodynamics of flow in, 2.3.2-7/2.3.2-26
use in shell-and-tube heat exchangers for single-phase flow, 3.3.1-1/3.3.11-5
Pipes, noncircular:
triangular ducts: single-phase fluid flow and pressure drop in, 2.2.2-7/2.2.2-10
laminar flow, 2.2.2-7/2.2.2-8
turbulent flow, 2.2.2-9/2.2.2-10
(See also Rectangular ducts, Square ducts)
Piping components:
gas-liquid flow and pressure drop in, 2.3.2-15/2.3.2-18
bends, 2.3.2-17
open valves, 2.3.2-18
orifice plates, 2.3.2-17/2.3.2-18
slow changes in cross section, 2.3.2-15/2.3.2-16
sudden contractions, 2.3.2-16/2.3.2-17
sudden enlargements, 2.3.2-16
single-phase fluid flow and pressure drop In, 2.2.2-14/2.2.2-20
curved ducts, 2.2.2-14/2.2.2-17
enlargements, 2.2.2-17/2.2.2-19
miscellaneous fittings, 2.2.2-19/2.2.2-20
Plain tube banks (see Tube banks, plain)
Planck s constant, 2.9.1-3
Planck s law, for spectral distribution of blackbody radiation, 2.9.1-3
Plane shells: steady-state thermal conduction in, 2.4.2-1/2.4.2-3

© 1983 Hemisphere Publishing Corporation

Plastic analysis, in mechanical design, 4.1.2-1/4.1.2-2
Plate-and-frame heat exchangers (see Plate heat exchangers)
Plate coil baffles, in agitated vessels, 3.14.2-3/3.14.2-4
Plate fin heat exchangers, 1.1.4-2, 3.9.1-1/3.9.1-2
approximate overall heat transfer coefficients in, 2.1.24
calculation procedure for a rating problem, 3.9.9-I
correlation of heat transfer and friction data for, 3.9.6-1/3.9.6-2
definition of geometric terms for, 3.9.2-l
description of, 3.1.2-5
goodness factor comparisons for, 3.9.7-1/3.9.7-3
laminar flow surfaces, 3.9.5-1/3.9.5-3
mechanical design, 4.4.3-1/4.4.3-9
brazing, 4.4.3-3/4.4.3-4
construction, 4.4.3-1/4.4.3-3
flow distributors, 4.4.3-3
materials, 4.4.3-7/4.4.3-8
plate fin-tube construction, 4.4.3-5/4.4.3-7
multifluid service in, 3.9.12-1/3.9.12-2
pressure drop calculation in, 3.9.10-1/3.9.10-2
procedures for the thermal sizing problems in, 3.9.11-1/3.9.11-2
recent theory and data on vaporization and condensation in, 3.9.13-1/3.9.13-4
specifications of sizing and rating problems in, 3.9.8-1/3.9.8-2
surface geometries for, 3.9.3-l
surface performance data for, 3.9.4-1/3.9.4-2
Plate fins, efficiency of, 2.5.3-9/2.5.3-10
Plate heat exchangers:
approximate overall heat transfer coefficients in, 2.1.24
construction and operation of, 3.7.1-1/3.7.1-3
corrugation design, 3.7.3-1/3.7.3-2
costing, 4.8.4-1/4.8.4-2
description, 3.1.2-3/3.1.2-4
gasketed plate, 3.1.2-3
lamella (Ramen), 3.1.2-3/3.1.2-4
spiral plate, 3.1.2-3
factors affecting plate design, 3.7.6-1/3.7.6-2
corrugation geometry, 3.7.6-1/3.7.6-2
distribution, 3.7.6-2
factors governing plate specification, 3.7.2-l
fouling, 3.7.9-1
friction factor correlations, 3.7.4-1/3.7.4-2
heat transfer correlations, 3.7.5-1/3.7.5-2
mechanical design, 4.4.2-1/4.4.2-8
frame design, 4.4.2-5/4.4.2-7
gasket design and properties, 4.4.2414.4.2-s
plate arrangements, 4.4.2-l
plate construction features, 4.4.2-1/4.4.2-2
plate design features, 4.4.2-3/4.4.2-4
methods of surface area calculation, 3.7.10-1/3.7.10-4
overall plate design for, 3.7.7-l /3.7.7-2
plate arrangements and correction factors for, 3.7.8-1/3.7.8-4
concurrency corrections, 3.7.8-1/3.7.8-2
distribution along port manifolds, 3.7.8-3/3.7.8-4
end effects, 3.7.8-2/3.7.8-3
types of pass arrangements, 3.7.8-l
thermal mixing in, 3.7.11-1/3.7.11-2
two-phase flow applications, 3.7.12-1
Plates:
characteristic of, as packings for fixed beds, 2.2.5-2
parallel, laminar heat transfer in flow between, 2.5 .1-3
in hydrodynamically developed flow, 2.5.1-3
in thermally and hydrodynamically developing flow, 2.5.1-3
Plate-type evaporator, 3.5.2-6
Plug flow:
regions of occurrence of: in horizontal flow, 2.3.2-2/2.3.2-4
in inclined tubes, 2.3.2412.3.2-s
in systems with phase change, 2.3.2-6/2.3.2-7
in vertical flow, 2.3.2-1/2.3.2-2
in vertical channels, 2.3.2-19
bubble rise velocity in, 2.3.2-19
Plug flow model, for furnaces, 3.11.5-1/3.11.5-2
Pneumatic conveyance, 2.3.3-1/2.3.3-2
in horizontal pipes, 2.3.3-1/2.3.3-3
in inclined pipes, 2.3.3-2
in vertical pipes, 2.3.3-l
Pneumatic conveying dryer, 3.13.7-2
P-NTU method:
application to single pass exchangers, 1.3.1-2/1.3.1-4
for calculation of heat exchangers, 1.2.4-4/1.2.4-5
Poiseuille law (see Hagen Poiseuille law)
Polarization, of thermal radiation, 2.9.2-12/2.9.2-14
Polymers:
degradation temperature, 2.5.12-1
physical properties, 2.5.12-2/2.5.12-4, 5.3.6-1/5.3.7-2
specific heat capacity, 2.5.12-3
thermal conductivity, 2.5.12-2
viscosity, 2.5.12-2/2.5.12-4
non-Newtonian heat transfer to, 2.5.12-1/2.5.12-15
Pool boiling, 2.1.7-6/2.1.7-8
augmentation of heat transfer in, 2.7.9-1/2.7.9-2
boiling curve for, 2.7.2-1/2.7.2-2
critical heat flux in, 2.7.2-9/2.7.2-13
geometric effects on, 2.7.2-11/2.7.2-12
liquid viscosity effect on, 2.7.2-12
subcooling effects on, 2.7.2-12/2.7.2-13
surface condition effects on, 2.7.2-13
film boiling in, 2.7.2-14/2.7.2-15
minimum heat flux in, 2.7.2-13/2.7.2-14
nucleate boiling, 2.7.2-312.7.3-y
correlations for, 2.7.2-3/2.7.3-7
hysteresis in, 2.7.2-8
influence of dissolved gas on, 2.7.2-8
influence of gravitational acceleration on, 2.7.2-Y
influence of liquid subcooling on, 2.7.2-9
influence of size and orientation of surface on, 2.7.2-8/2.7.2-9
influence of surface conditions on, 2.7.2-712.7.2-g
influence of system pressure on, 2.7.2-7
influence of wettability of surface on, 2.7.2-9
of binary and multiwmponent mixtures, 2.7.7-1/2.7.7-7
critical heat flux, 2.7.7-4/2.7.7-5
fiim boiling, 2.7.7-6
minimum heat flux, 2.7.7-5/2.7.7-6
nucleate boiling, 2.7.7-1/2.7.7-2
transition boiling, 2.7.7-5
onset of nucleate boiling in, 2.7.2-2/2.7.2-3
transition boiling in, 2.7.2-13
Porous surfaces, for enhancement of boiling heat transfer, 2.7.9-1
Post-burnout heat transfer (see Postdryout heat transfer, Transition boiling, Film boiling)
Postdryout heat transfer:
correlations for in vertical tubes, 2.7.3-31/2.7.3-34
with departure from thermodynamic equilibrium, 2.7.3-32/2.7.3-33
empirical correlations, 2.7.3-31/2.7.3-32
semi-theoretical, 2.7.3-33/2.7.3-34
in evaporators, 3.5.7-3

© 1983 Hemisphere Publishing Corporation

Powders:
classification of types of, in fluidized beds, 2.2.6-3/2.2.6-4
thermal conductivity under vacuum, 2.1.1-2
Power law fluid (non-Newtonian), 2.2.8-7
forced convective heat transfer to, 2.5.12-1/2.5.12-16
free convective heat transfer to bodies immersed in, 2.5.7-10, 2.5.7-25
Prandtlnumber, 1.2.3-4, 2.1.3-3
effect on laminar flow over flat plate, 2.2.1-23
formulas for, 5.1.4-7
of liquid water, 5.5.34
of saturated vapors and liquids, 5.5.1-1/5.5.5.1-40
shell-side, in shell-and-tube heat exchangers, 3.3.5-17
turbulent, 2.2.1-19
Pressure coefficient:
for flow over single cylinder, 2.2.4-2
for flow over tube in tube bank, 2.2.4-2
Pressure control of condensers, 3.4.5-l
Pressure drop:
in condensers, 3.4.7-1/3.4.7-2
in double-pipe heat exchangers, 3.2.3-5/3.2.3-6
in evaporators, 3.5.6-l
in fluidized beds, 2.2.6-2
in gas-liquid flow, 2.3.2-7/2.3.2-18
frictional, in straight pipes, 2.3.2-9/2.3.2-12
in shell-and-tube heat exchangers, 2.3.2-12/2.3.2-13
in singularities, 2.3.2-15/2.3.2-18
in stratified flow, 2.3.2-23/2.3.2-24
in vertical annular flow, 2.3.2-19
in headers, nozzles and turnarounds in shell-and-tube heat exchangers, 2.2.7-1/2.2.7-11
in internally finned tubes, 2.5.11-5/2.5.11-6
in multiphase systems, 2.3.1-1/2.3.1-10
in gas-solid flow, 2.3.3-2, 2.3.3-4/2.3.3-7
overall, in cooling towers, 3.12.3-3/3.12.3-5
in the packings of cooling towers, 3.12.2-10/3.12.2-11
in plate fin heat exchangers, 3.9.10-1/3.9.10-2
in plate heat exchangers, 3.7.4-1/3.7.4-2
and pumping power in heat exchangers, 1.2.4-5/1.2.4-6
in reboilers, 3.6.3-l
on the shell side of shell-and-tube heat exchangers, 3.3.1-1/3.3.11-5
as limitation in design, 3.3.10-6
in single phase systems: in ducts and fittings, 2.2.2-1/2.2.2-25
in fixed beds, 2.2.5-1/2.2.5-5
introduction and fundamentals, 2.2.1-1/2.2.1-35
in non-Newtonian fluid flow, 2.2.8-9/2.2.8-11
in tube banks, 2.2.4-1/2.2.4-17, 3.3.7-1/3.3.7-4
in vertical tubes with subcooled boiling, 2.7.3-9/2.7.3-10
Pressure gradient:
effect in transition boundary layer flow over flat plate, 2.2.1-24
(See also Pressure drop)
Process heaters, fired, 3.11.2-1/3.11.2-2
Prolate spheroids, free convective heat transfer from, *2.5.7-25*
Promoters, for dropwise condensation, 2.6.5-3/2.6.5-4
Propane:
saturation properties, 5.5.1-5
superheated gaseous, thermodynamic properties of, *5.5.2-6/5.5.2-7*
1-Propanol saturation properties, 5.5.1-18
2-Propanol saturation properties, 5.5.1-19
Propeller agitator, 3.13.2-1/3.14.2-2
heat transfer in agitated vessels with, 3.14.3-1
Propylene:
saturation properties, 5.5.1-6
superheated gaseous, thermodynamic properties, 5.5.2-7
Propylene oxide saturation properties, 5 .5.1-24
Proximity agitators, 3.14.2-1
heat transfer in agitated vessels with, 3.14.3-3/3.14.3-6
Pugh, S. F., 5.4.5-1/5.4.5-5, 5.5.8-1/5.5.8-3
Pulsations, use in augmentation of heat transfer, 2.5 .ll-8
Pushkina and Sorokin correlation, for flooding in vertical tubes, *2.3.2-22*
P-V̄-T correlations, for pure fluids, 5.1.2-1/5.1.2-4
Pyramid, free convective heat transfer from, 2.5.7-25

Q

Quality, in multiphase flows:
flow quality, 1.2.1-1, 2.3.14,2.7.3-l
static quality, 1.2.1-1, 2.3.1-4

R

Radiant heat exchanger, 2.9.8-4
Radiating fin, 2.9.8-4/2.9.8-6
Radiation:
diffusion method, for calculation of nonisothermal gas radiation, 2.9.7-5/2.9.7-6
effect in film boiling, 2.7.2-15
effect on heat transfer in packed beds, 2.8.3-2
heat transfer coefficient, 2.9.8-2
in heat transfer from fluidized beds, 2.8.4-3, 2.8.4-6/2.8.4-7
models for, in furnaces, 3.11.7-4/3.11.7-5
networks, 2.9.3-8/2.9.3-10
with a gas, 2.9.64
numerical calculation of flows involving, 1.4.3-3
(See *also* Radiative heat transfer)
Radiation shields, in radiation heat transfer, 2.9.3-12/2.9.3-13
Radiative heat transfer:
acting with conduction and convection, 2.9.8-1/2.9.8-10
combined phenomena in, 2.9.8-l
around hollow cylinder, 2.9.8-6/2.9.8-7
in molecular gas convection, 2.9.8-7/2.9.8-10
in radiant heat exchanger, 2.9.84
from radiating tin, 2.9.8-4/2.9.8-6
radiation coupled transient heating or cooling, 2.9.8-3/2.9.8-4
thermal network analysis of, 2.9.8-1/2.9.8-3
gas radiation properties, 2.9.5-1/2.9.5-13
equation of transfer for, 2.9.5-1/2.9.5-2
gas mixtures, 2.9.5-11/2.9.5-12
measurement of, 2.9.5-2/2.9.5-4
molecular, 2.9.5-8/2.9.5-11
physics, of, 2.9.5-4
spectral, band and total property definitions, 2.9.5-4/2.9.5-8
in furnaces, 3.11.3-1/3.11.7-6
introduction to, 2.9.1-1/2.9.1-5
blackbody radiation, 2.9.1-3/2.9.1-5
radiant intensity and flux, 2.9.1-2/2.9.1-3
thermodynamic surfaces and surface systems, 2.9.1-1/2.9.1-2
nonisothermal gas radiation, 2.9.7-1/2.9.7-13

© 1983 Hemisphere Publishing Corporation

Radiative heat transfer, nonisothermal gas radiation (Cont.):
differential formulations for, 2.9.7-5/2.9.7-8
equation of transfer for, 2.9.7-1/2.9.7-2
geometric considerations, 2.9.7-2/2.9.7-3
molecular gas radiation in, 2.9.7-10/2.9.7-13
slab geometry, 2.9.7-312.9.7-s
spectral considerations and scaling approximations in, 2.9.7-8/2.9.7-10
radiation transfer between perfectly diffuse surfaces, 2.9.3-1/2.9.3-17
diffuse-walled passages, 2.9.3-13/2.9.3-16
radiation network, 2.9.3-8/2.9.3-10
radiosity-irradiation formulations, 2.9.3-4/2.9.3-8
refractory surfaces, 2.9.3-8
selected working relations for, 2.9.3-10/2.9.3-13
shape factors for, 2.9.3-1/2.9.3-4
radiation transfer between specular and imperfectly diffuse surfaces, 2.9.4-1/2.9.4-1 1
mirror-image concept, 2.9.4-1/2.9.4-2
Monte Carlo algorithms, 2.9.4-212.9.4-s
rough walled passages, 2.9.4-9/2.9.4-10
specular and imperfectly diffuse surfaces, 2.9.4-1
specular walled passages, 2.9.4-5/2.9.4-7
surface models, 2.9.4-712.9.4-y
surface radiation characteristics, 2.9.2-1/2.9.2-20
absorption and emission characteristics, 2.9.2-1/2.9.2-3
approximations, 2.9.2-10/2.9.2-12
electromagnetic theory and the Fresnel relations, 2.9.2-7/2.9.2-10
polarization, 2.9.2-12/2.9.2-15
radiation characteristics in thermal design, 2.9.2-15/2.9.2-20
reflection and transmission characteristics, 2.9.2-3/2.9.2-7
between surfaces and isothermal gas, 2.9.6-1/2.9.6-9
calculation of, 2.9.6-4/2.9.6-8
heat transfer at black wall, 2.9.6-l
mean beam length concept for, 2.9.6-2/2.9.6-3
Monte Carlo solutions for, 2.9.6-8/2.9.6-9
radiation network in, 2.9.6-4
radiosity-irradiation formulation for gas filled enclosure wall, 2.9.6-3/2.9.6-4
wall layer transmission in, 2.9.6-3
Radiators, automotive, construction, 4.4.3-5/4.4.3-7
Radiometers, application in gas radiation property measurement, 2.9.5-3
Radiosity, Stephan s law for, 2.9.1-3
Radiosity-irradiation formulations in radiative heat transfer, 2.9.3-4/2.9.3-8
for gas-filled enclosure wall, 2.9.6-3/2.9.6-4
Ramen heat exchanger (see Lamella heat exchanger)
Raoult s law for partial pressure, 2.7.6-l
Rating of heat exchangers, 3.1.3-2, 3.3.4-l
computer program structure for, 3.1.3-3
Rayleigh instability, in free convection, 2.5.8-2
Rayleigh number, 1.2.3-4, 2.2.1-16, 2.2.2-6
critical, for instability in free convection: in enclosures heated from below, 2.5.8-3/2.5.8-6
in horizontal layers, 2.5.8-2/2.5.8-3
in free convection over immersed bodies, 2.5.7-3
Reay, D., 3.13.7-1/3.13.7-3
Reboilers:
approximate overall coefficients in, 2.1.2-3
shell-and-tube, 3.6.1-1/3.6.5-6
calculation procedures for, 3.6.5-1/3.6.5-6
pressure drop in, 3.6.3-l
special design considerations for, 3.6.4-1/3.6.4-4
thermal design of, 3.6.2-1/3.6.2-10
as type of heat exchanger, 1.1.5-2
(See also Boilers)
Reciprocal mode integrating sphere, for reflection and transmission measurements in radiation, 2.9.2-7
Rectangles:
closed form solutions for mean beam lengths between, 2.9.64
radiative heat transfer shape factors for opposite and adjacent, 2.9.3-3
table of mean beam lengths, 2.9.6-5
Rectangular ducts:
combined free and forced convective heat transfer in, 2.5.10-11, 3.9.5-1/3.9.3-3
critical heat flux in flow boiling in, 2.7.3-20
laminar flow in, 2.2.2-7/2.2.2-9
radiative heat transfer along, 2.9.3-16/2.9.3-17
turbulent flow in, 2.2.2-10
Rectangular enclosures, free convective heat transfer in:
when heated and cooled on vertical sides, 2.5.8-6/2.5.8-13
when heated from below, 2.5.8-3/2.5.8-6
Rectangular fins, for plate fin exchangers, 3.9.3-l
Redlich-Kwong and Redlich-Kwong-Soave equations of state, 5.1.24
application to hydrocarbons, 5.2.2-1/5.2.2-2
Reduced pressure, correlations for pool boiling using, 2.7.2-5/2.7.2-7
Reentrance cavities, for enhancement of boiling, 2.7.9-1/2.7.9-2
Reference temperature:
in calculation of friction factor in circular duct, 2.2.2-7
for laminar flow over flat plates, 2.2.1-23
for turbulent flow over flat plates, 2.2.1-29
Reflectance (see Reflectivity)
Reflection, of thermal radiation, from solid surfaces:
characteristics of, 2.9.2-3/2.9.2-6
measurement of, 2.9.2-6/2.9.2-7
Reflectivity, of solid surfaces, 2.9.2-3
measurement of, 2.9.2-6/2.9.2-7
Reflectometer, heated cavity, 2.9.2-7
Reflux condensers, 3.4.3-2
flooding phenomena in, 2.6.2-9, 3.4.3-2/3.4.3-3
Refractories, density of, 5.4.1-1/5.4.1-2
Refractory services, 2.9.3-8
in furnaces, 3.11.3-6
heat transfer by radiation between source, sink and, 2.9.3-l l/2.9.3-12
Refrigerant 12:
critical heat flux table for flow of in vertical tube, 2.7.3-29
saturation properties, 3.5.1-21
Refrigerant 13 saturation properties, 5.5 .1-2 1
Refrigerant 21 saturation properties, 5.5.1-22
Refrigerant 22 saturation properties, 5.5.1-22
Regenerative heat exchangers, 1.1.1-3/1.1.1-4
periodic operation of, 1 .1.6-1
Regimes of heat transfer, in ducts, single phase flow, 2.5.1-1
Relaminarization, of turbulent flow, 2.2.1-16
Residence times, in dryers:
with non-prescribed material flow, 3.13.6-1
with prescribed material flow, 3.13.5-1/3.13.5-2
Retrograde behavior, in phase envelope for natural gas, 5.2.1-4/5.2.1-5
Reynolds number, 2.1.1-3
as limiting criteria for applicability of molecular flux relationship, 2.1.1-3

© 1983 Hemisphere Publishing Corporation

Reynolds number (Cont.):
bubble, 2.3.2-19
definition of, 1.2.3-2/1.2.3-3
in finned tube bundles, 2.5.3-11
in condensation on vertical surface, 2.6.2-3
in cross flow over tube banks, 2.2.4-1/2.2.4-12, 2.5.3-1/2.5.3-8, 3.3.7-1/3.3.7-4
particle, fixed beds, 2.2.5-2
fluidized beds, 2.2.6-2
shell-side, in shell-and-tube heat exchangers, 3.3.5-16
in two-phase gas-liquid flow, 2.3.2-10
Rheologically complex materials, properties of:
disperse compositions, 5.3.1-1/5.3.1-3
nuclear fuel suspensions, 5.3.1-2/5.3.1-3
petroleum, 5.3.1-3
two-component compositions, 5.3.1-1/5.3.1-2
effect of external electric and magnetic fields on, 5.3.8-1/5.3.8-2
lubricants: classification of, 5.3.2-l
lubricant-cooling liquids, 5.3.5-1/5.3.5-2
oils, 5.3.3-1/5.3.3-2
polymers, 5.3.6-1/5.3.7-2
Rheology, shear flow experiments used in, 2.2.8-3
Richardson number, 2.2.1-11
Ring cells, in free convection, 2.5.8-2
Ring stiffness, in shell-and-tube heat exchangers, 4.1.2-8/4.1.2-9
Rod bundles:
critical heat flux in flow in, 2.7.3-21/2.7.3-22
turbulent longitudinal flow in, 2.2.2-10
Rohsenow correlation, for nucleate boiling, 2.7.24
application in forced convection boiling in vertical tubes, 2.7.3-7/2.7.3-8
Roll cells, in free convection, 2.5.8-2
Roller expansion, of tubes into tube sheets, 4.2.6-6/4.2.6-7
Room, thermal network for combined radiation and convection in, 2.9.8-3
Rossby number, 2.2.1-11
Rotary dryer, 3.13.24
practical design of, 3.13.7-2
Rotating drums, heat transfer to particle bed in, 2.8.3-4/2.8.3-5
Rotation, as device for heat transfer augmentation, 2.5.11-4, 2.5.11-8
Roughness, surface:
in augmentation of condensation, 2.6.6-1/2.6.6-2
in augmentation of heat transfer, 2.5.11-2, 2.5.11-3/2.5.11-4
as enhancement device in boiling, 2.7.9-2
completely rough surface, 2.2.2-2
effect in flow in fixed beds, 2.2.5-4
effect on flow over cylinders, 2.2.3-6
effect in pool boiling: critical heat flux, 2.7.2-13
nucleate boiling, 2.7.2-312.7.2-S
effect on pressure drop in tube banks, 2.2.4-14/2.2.4-15
effect on skin friction in turbulent flow over flat plate, 2.2.1-29
effect in transition flow over flat plate, 2.2.1-25
radiative heat transfer from, 2.9.4-7/2.9.4-10
values for commercial surfaces, 2.2.24
Rough walled passages, radiative heat transfer down, 2.9.4-9/2.9.4-10
Ruiz, C., 4.1.1-1/4.1.8-3

S

Saddle supports, for heat exchangers, as source of assymetric loading, 4.1.2-2/4.1.2-9
Sand roughness, equivalent, 2.2.1-29/2.2.1-30
Sardesai, R. G., 2.6.4-1/2.6.4-7
Saturated boiling:
in pool boiling, 2.7.2-1/2.7.2-17
in vertical tubes, 2.7.3-10/2.7.3-12
nucleate, 2.7.3-10/2.7.3-11
two-phase forced convective, 2.7.3-11/2.7.3-12
Saturated fluids, tables of physical properties, 5.5.1-1/5.5.1-40
Saturation pressure, 2.7.1-1
Saturation temperature, 2.7.1-1
Saunders, E. A. D., 4.2.1-1/4.2.6-13
Scaling approximations, in nonisothermal gas radiation, 2.9.7-8/2.9.7-10
narrow band scaling: the Curtis Godson approximation, 2.9.7-812.9.7-y
wide-band scaling, 2.9.7-9/2.9.7-10
Scattering bed models, for radiative heat transfer from surfaces, 2.9.4-812.9.4-y
Scattering coefficient, 2.9.5-2
Schack wide-band model, for gas radiation properties, 2.9.5-6
Schlünder, E. U., 2.1.1-1/2.1.7-8, 3.13.1-1/3.13.6-1
Schlünder equations:
for developing laminar flow, 2.5.1-2
for gas conduction in packed beds, 2.8.3-l
Schmidt number, 1.2.34
Schrock and Grossman correlations, for forced convective heat transfer in two-phase flow, 2.7.3-8
Schunk, M., 5.1.1-1/5.1.5-3, 5.4.1-1/5.4.4-6
Schwier, K., 5.5.3-1/5.5.3-5
Scraped surfaces:
in augmentation of heat transfer, 2.5 .11-3
heat exchangers, description of, 3.1.2-6
in heat exchangers, 1.1.4-2
heat transfer coefficients with, 3.14.3-4/3.14.3-6
mechanical design for, 4.4.4-5/4.4.4-6
Scaling devices, in shell-and-tube heat exchangers, 4.2.5-8/4.2.5-9
Seider-Tate equation, for heat transfer in heat exchangers, 3.3.2-2
Selection of heat transfer equipment:
for condensation duty, 3.4.2-1/3.4.2-4
dryers, 3.13.2-1/3.13.2-4
for evaporation, 3.5.5-1/3.5.5-2
general introduction to, 3.1.2-1/3.1.2-6
reboilers, 3.6.1-2/3.6.1-6
selection table, 3.6.1-6
Semiconductors, thermal conductivity, 5.4.3-3
Separated flow model:
application to stratified flow prediction, 2.3.2-23/2.3.2-24
conservation equations for: in gas-liquid flow, 2.3.2-812.3.2-y
in multiphase flows, 2.3.1-6/2.3.1-7
Separators for use in association with evaporators, 3.5.4-1/3.5.4-2
Series solutions, for one-dimensional transient conduction, 2.4.3-1/2.4.3-7
Serrated fms, in plate fm heat exchangers, 3.9.3-1
Shah correlation, for boiling in horizontal tubes, 2.7.4-5
Shape factor, in radiative heat transfer between diffuse surfaces, 2.9.3-1/2.9.3-4
Shear flow, of non-Newtonian fluids, 2.2.8-1/2.2.8-3
Shear free flow, of non-Newtonian fluids, 2.2.8-3/2.2.8-6
Shear rate, in fluid, 2.2.8-l
Shear stress:
distribution of wall, in flow over single cylinder, 2.2.3-5
interfacial effect on filmwise condensation: on vertical surfaces, 2.6.2-5/2.6.2-7
turbulent, in pipe flow, 2.2.2-5
Shelf dryer, 3.13.24

© 1983 Hemisphere Publishing Corporation

Shell-and-tube heat exchanger:
application of low-fin tubes in, 3.3.11-2/3.3.11-3
approximate overall coefficient in, 2.1.2-3
approximate sizing of, 3.1.4-1/3.1.4-9
basic design equation for, 3.1.4-9
estimation of heat load, 3.1.4-1/3.1.4-2
estimation of mean temperature difference, 3.1.4-2/3.1.4-3
estimation of overall heat transfer coefficient, 3.1.4-3/3.1.4-6
estimation of surface area, 3.1.4-6/3.1.4-7
example of, 3.1.4-7/3.1.4-9
baffle leakage in, numerical calculation of, 1.4.2-3
condensation in, 3.4.1-1/3.4.1-5
corrosion and other damage of, 4.5.3-1/4.5.3-7
description of 3.1.2-2/3.1.2-3
F-factor and θ-NTU charts for, 1.5.2-1/1.5.2-15
E-shell with even number of passes, 1.5.2-5
five E-shells in series, 1.5.2-g
four E-shells in series, 1.5.2-8
G-shell, even number of tube passes, 1.5.2-13
J-shell, even number of tube passes, 1.5.2-12
J-shell, one tube pass, 1.5.2-l 1
six E-shells in series, 1.5.2-10
three E-shells in series, 1.5.2-7
two E-shells in series, 1.5.2-6
F-type shells, thermal leakage in, 1.5.2-14/1.5.2-15
introduction to design features, 1.1.5-1/1.1.5-2
materials of construction, 4.5.2-1/4.5.2-6
mechanical design: basic principles, 4.1.1-1/4.1.8-3
constructional features of, 4.2.1-1/4.2.6-13
design codes for, 4.3.1-1/4.3.5-11
example of calculations, 4.3.6-1/4.3.6-23
multipass, 1.1.1-2
non-uniform heat transfer in, 2.1.4-1/2.1.4-3
numerical solutions for: with flow pattern calculation, 1.4.2-1/1.4.2-4
with prescribed flow patterns, 1.4.1-1/1.4.1-6
pressure drop in headers, nozzles and turnarounds in, 2.2.7-112.2.7-l 1
thermal design, 3.3.1-1/3.3.11-5
auxiliary calculations, 3.3.6-1/3.3.6-11
calculation of shell-side heat transfer coefficient and pressure drop, 3.3.8-1/3.3.8-3
extension to other shell, baffle and tube bundle geometries, 3.3.11-1/3.3.11-3
ideal tube-bank correlations for, 3.3.7-1/3.3.7-4
input data and recommended practices, 3.3.5-1/3.3.5-17
objectives and background, 3.3.1-1/3.3.1-2
performance evaluation when geometry specified, 3.3.9-1/3.3.9-6
practices of design, 3.3.4-1/3.3.4-5
procedures for segmentally baffled exchangers, 3.3.10-1/3.3.10-8
recommended method: principles and limitations, 3.3.3-1/3.3.3-5
survey of shell-side flow correlations, 3.3.2-1/3.3.2-6
Shells, for shell-and-tube heat exchangers:
costing, 4.8.2-1/4.8.2-5
inside diameter: metric practice for, 3.3.5-3
U.S. practice for, 3.3.5-3
materials of construction, 4.5.2-1/4.5.2-2
mechanical design: analytical basis for codes, 4.3.3-l
basic principles, 4.1.3-1
constructional features of, 4.2.6-l
index to U.S., U.K., and F.R.G. codes for, 4.3.2-2/4.3.2-3
Shell-to-baffle clearance, in shell-and-tube heat exchangers, 3.3.5-13/3.3.5-14
Sherwood number, 1.2.3-2, 2.1.5-2
in particle-to-fluid mass transfer in fixed beds, 2.5.4-1/2.5.4-6
Shipes, K. V., 4.4.1-1/4.4.1-7
Short-tube vertical evaporator, 3.5.2-1
Shulman, Z. P., 5.3.1-1/5.3.8-3
Silver method, for calculation of multiwmponent condensation, 2.6.3-4/2.6.3-5
Similarity, theory of, 2.2.1-10/2.2.1-13
Simultaneous heat and mass transfer (see Heat and mass transfer, combined)
Singham, J. R., 3.12.1-1/3.12.6-4
Single-phase convective heat transfer (see Convective heat transfer, single-phase)
Single-phase fluid flow:
in ducts and fittings, 2.2.2-1/2.2.2-25
in fixed beds, 2.2.5-1/2.2.5-5
over immersed bodies, 2.2.3-1/2.2.3-9
introduction and fundamentals, 2.2.1-1/2.2.1-35
in headers, nozzles and turnarounds, 2.2.7-1/2.2.7-11
in tube banks, 2.2.4-1/2.2.4-17
Singularities, two-phase gas-liquid pressure drop across, 2.3.2-15/2.3.2-18
bends, 2.3.2-17
open valves, 2.3.2-18
orifice plates, 2.3.2-17/2.3.2-18
slow changes in cross section, 2.3.2-15/2.3.2-16
sudden contraction, 2.3.2-16/2.3.2-17
sudden enlargement, 2.3.2-16
Sink, in radiation:
heat transfer between source, refractory and, 2.9.3-11/2.9.3-12
heat transfer from source to, 2.9.3-10/2.9.3-11
Skin friction coefficient, 2.2.1-20
in flow over cylinders, 2.2.3-5
in flow over tube banks, 2.2.4-3/2.2.4-5
Ludwieg-Tillman formula for, 2.2.1-26
Stratford formulas for, in boundary layers, 2.2.1-21
in turbulent flow over flat plates, 2.2.1-29
Slab:
heat transfer in cooling of, 2.1.3-1/2.1.3-2
leaching process in, 2.1.5-2
radiative heat transfer in non-isothermal gas in, 2.9.7-3/2.9.7-5, 2.9.7-10/2.9.7-13
transient conduction in, 2.4.3-1/2.4.3-10
numerical methods for, 2.4.3-8/2.4.3-10
series solution for, 2.4.3-1/2.4.3-7
solution using internal heat transfer coefficient, 2.4.3-7/2.4.3-8
Slip ratio (see Velocity ratio)
Slot, radiative heat transfer along, 2.9.3-15/2.9.3-16
Slug flow:
hydrodynamics of, 2.3.2-24/2.3.2-25
mechanism of critical heat flux in, 2.7.3-22
regions of occurrence of, in gas-liquid flow in horizontal tubes, 2.3.2-1/2.3.2-5
Slugging, in fluidized beds, 2.2.6-l
Smith, R. A., 3.5.1-1/3.5.8-3
Smoluchowski effect, 2.1.1-2
Snell's law, in radiation, 2.9.2-9
Solar absorber, 2.9.2-15/2.9.2-16
Solar reflector, 2.9.2-16
Soldered fins, in double pipe exchangers, 3.2.5-l
Solid fuels, properties of, 3.11.3-3

© 1983 Hemisphere Publishing Corporation

Solid-gas flow:
flow patterns in, 2.3.3-2
free-fall velocity in, 2.3.3-3
pressure drop in, 2.3.3-2, 2.3.3412.3.3-g
principles of pneumatic conveyance by, 2.3.3-1/2.3.3-2
horizontal pipes, 2.3.3-1/2.3.3-2
inclined pipes, 2.3.3-2
vertical pipes, 2.3.3-l
velocity ratio in, 2.3.34
Solidification, heat conduction in, 2.4.4-1/2.4.4-2
Solid-liquid flow:
flow patterns in, 2.3.4-1/2.3.4-2
pressure drop in, 2.3.4-2/2.3.4-6
principles of hydraulic conveyance, 2.3.4-l
Solids:
as constituents in multiphase flows, 2.3.1-1
physical properties, 5.4.1-1/5.4.5-5
density, 5.4.1-1/5.4.1-2
elastic properties, 5.4.5-1/5.4.5-5
emissivity, 5.4.4-1/5.4.4-4
specific heat, 5.4.2-1/5.4.2-2
thermal conductivity, 5.4.3-1/5.4.3-3
total emissivities, 3.11.3-6
Solids circulation, in fluidized beds, 2.2.6-6/2.2.6-7
Sound velocity:
in ideal gas, 2.2.1-8
in two-phase gas-liquid flow, 2.3.2-27
Source, in radiation:
radiative heat transfer between refractory, sink and, 2.9.3-11/2.9.3-12
radiative heat transfer between sink and, 2.9.3-10/2.9.3-l 1
Spacers, in shell-and-tube heat exchangers, 4.2.5-814.2.5-g
Spalding, D. B., 1.1.1-1/1.4.3-6
sparging:
for agitation of vessels, 3.1.4-2
of reboilers, 3.6.4-3
Specific enthalpy, 1.2.1-1
of saturated liquids and vapors, 5 .5.1-1/5.5.1-40
of superheated gases, 5.5.2-115.5.2-l 1
Specific entropy, of superheated gases, tables of, 5.5.2-115.5.2-l 1
Specific heat (see Specific heat capacity)
Specific heat capacity, 1.2.1-2/1.2.1-3
in polymers, 2.5.12-8, 5.3.6-2
in pure fluids, 5.1.3-4/5.1.3-7
of liquid water, 5.5.3-2
of multicomponent mixtures, 5.2.3-815.2.3-g
of saturated liquids and vapors, 5.5.1-1/5.5.1-5
of solids, 5.4.2-1/5.4.2-2
Specific internal energy, 1.2.1-1
Specific volume:
of polymers, 5.3.6-2
of superheated gas, tables of, 5.5.2-1/5.5.2-1 1
of the gas phase, 5.1.2-2/5.1.2-3
of the liquid phase, 5.1.2-1
Spectral absorptivity:
in gases, 2.9.5-S
of metals at room temperatures, 2.9.2-l 1/2.9.2-12
Spectral emissivity, in gases, 2.9.5-5
Specular surface, 2.9.4-l
radiative heat transfer between imperfectly diffuse surfaces and, 2.9.4-1/2.9.4-11
Specular-walled passages, radiative heat transfer in, 2.9.4-5/2.9.4-7
with adiabatic sides, 2.9.4-6/2.9.4-7
with isothermal sides, 2.9.4-5/2.9.4-6
with non-isothermal sides, 2.9.4-6
Spheres:
characteristics of, as packings for fixed beds, 2.2.5-2
combined free and forced convective heat transfer fr ---, 2.5.9-1/2.5.9-6
in transverse flow, 2.5.9-6
in vertical flow, 2.5.9-1/2.5.9-4
concentric, free convective heat transfer in, 2.5.8-16
drag coefficients for, 2.2.3-2
fixed beds of, heat transfer in, 2.8.1-1/2.8.1-14, 2.8.2-1/2.8.2-8, 2.5.4-1/2.5.4-7
free convective heat transfer from, 2.5.7-24/2.5.7-25
heat transfer to beds of moving, agitated and vibrated, 2.8.3-3/2.8.3-8
single-phase forced convection heat transfer to, 2.5.2-5/2.5.2-8,2.5.4-l
combined correlation for, 2.5.2-5,2.5.4-l
in restricted channel, 2.5.2-5
transient conduction in, 2.4.3-1/2.4.3-10
numerical methods for, 2.4.3-8/2.4.3-10
series solutions for, 2.4.3-1/2.4.3-7
solutions using internal heat transfer coefficient, 2.4.3-7/2.4.3-8
Spherical shells:
mechanical design, of, 4.1.3-1/4.1.3-2
steady-state thermal conduction in, 2.4.2-1/2.4.2-3
Spheroids (oblate and prolate), free convective heat transfer from, 2.5.7-25
Spine fins:
efficiency, 2.5.3-9
in plate fin exchangers, 3.9.3-l
Spiral heat exchanger:
approximate overall heat transfer wefficients in, 2.1.24
description of, 3.1.2-3/3.1.2-4
mechanical design of, 4.4.4-4/4.4.4-5
Spray dryers, 3.13.7-2/3.13.7-3
Sprays, in heat exchangers, 1.1.4-2
Square ducts:
laminar flow in, 2.2.2-712.2.2-g
roughened wall, radiative heat transfer along, 2.9.4-9/2.9.4-10
Stable equilibrium, of vapor and liquid, 2.7.1-1
Staggered tube banks:
application in shell-and-tube heat exchangers, 3.3.5-5
correlations for heat transfer in, 2.5.3-1/2.5.3-16
finned tubes, 2.5.3-11
plain tubes, 2.5.3-2
drag coefficients for tubes in, 2.2.44
pressure drop in, with plain tubes, 2.2.4-8/2.2.4-9
correction factors for overall number of tube rows, 2.2.4-10
effect of yawing on, 2.2.4-12
pressure drop with tinned tubes, 2.2.4-13/2.2.4-14
Stagnant packed beds (see Fixed beds)
Stainless steels:
as materials of construction, 4.5.2-3/4.5.2-4
austenitic, 4.5.24
ferritic, 4.5.2-3/4.5.2-4
spectral characteristics of reflectance from oxidized surface of, 2.9.2-15
Stanton number, 1.2.3-1, 2.2.1-11
startup:
of heat pumps, 3.10.7-1/3.10.7-2
of reboilers, 3.6.4-2
State diagram, for fluidized beds, 2.2.6-2
Static mixer inserts, as enhancement device in condensation, 2.6.6-3
Static quality (see Quality)

© 1983 Hemisphere Publishing Corporation

Steels, as material of construction, 4.5.2-2/4.5.2-4
austenitic stainless, 4.5.24
carbon steel, 4.5.2-2/4.5.2-3
ferritic stainless, 4.5.2-3/4.5.2-4
low alloy steels, 4.5.2-3
Stefan-Boltzmann constant, 2.9.1-3
Stefan s law, for blackbody radiation, 2.9.1-3
Stegmaier, W., 2.3.3-1/2.3.3-10
Stephan and Korner correlation, for boiling of binary mixtures, 2.7.7-2
Stephan-Maxwell equations for diffusion, 2.1.5-1
Stirred beds, heat transfer to, 2.8.34
Stirred reactor model, for furnaces, 3.11.4-1/3.11.4-6
Stirred tanks (see Agitated vessels)
Straight fins (longitudinal fms)
application in double-pipe heat exchangers, 3.2.1-1/3.2.6-2
efficiency of, 2.5.3-9, 3.2.3-1/3.2.3-3
Stratfords method, for solution of boundary layer equations, 2.2.1-21
Stratification, in gas-liquid flow (see Stratified flow)
Stratified flow:
as source of dryout in evaporative heat transfer, 2.7.4-1/2.7.4-4
in bends, 2.7.4-2/2.7.4-3
in helical coils, 2.7.4-3/2.7.4-4
in horizontal tubes, 2.7.4-1/2.7.4-2
prediction of, in horizontal and inclined tubes, 2.3.2-23/2.3.2-24
regions of occurrence of: in condensation, 2.3.2-7
in horizontal tubes, 2.3.2-2/2.3.2-4
in inclined tubes, 2.3.2-4/2.3.2-5
in shell-and-tube heat exchangers, 2.3.2-5/2.3.2-6
Stream analysis methods, for shell-side heat transfer and pressure drop in shell-and-tube heat exchangers, 3.3.2-3/3.3.2-6
Stress equation models, for turbulent boundary layers, 2.2.1-29
Stresses:
allowable, comparison of codes for, in mechanical design of heat exchangers, 4.3.4-l
types of, in heat exchangers, 4.1.1-1/4.1.1-2
Stress tensor:
in non-Newtonian fluids, 2.2.8-2
in single phase fluid flow, 2.2.1-2
in turbulent flow, 2.2.1-15
Stress-strain curve, for solids, 5.4.5-2/5.4.5-3
Strouhal number, 2.2.3-3
values for: banks of tubes, 2.2.4-15/2.2.4-16
flow over blunt bodies, 2.2.3-7
flow over single cylinders, 2.2.34,2.2.4-l
in vortex shedding as source of tube vibration, 4.6.4-1/4.6.4-2
Subchannel analysis, for critical heat flux in rod bundles, 2.7.3-21
Subcooled boiling:
in pool boiling, 2.7.2-1/2.7.2-17
in vertical tubes, 2.7.3-5/2.7.3-10
fully developed, 2.7.3-7/2.7.3-8
onset of, 2.7.3-5/2.7.3-7
partial, 2.7.3-812.7.3-g
single phase convection, 2.7.3-5
void fraction in, 2.7.3-9/2.7.3-10
Subcooling:
in condensers, 3.4.6-4
of liquid: effect on critical heat flux, 2.7.3-13
effect on forced convective boiling, 2.7.3-5/2.7.3-10
effect on pool boiling: critical heat flux, 2.7.2-12/2.7.2-13
nucleate boiling, 2.7.2-9
of vapor in condensation, 2.6.7- 1
Sublayer, viscous, 2.2.2-l
Suction:
effect in transition flow over flat plate, 2.2.1-25
effect in turbulent flow over flat plate, 2.2.1-30
effect on laminar flow over flat plate, 2.2.1-23
use in augmentation of heat transfer, 2.5 .11-3, 2.5.11-9
Sudden contractions (see Contraction)
Sudden enlargements (see Enlargement)
Superficial velocity, in multiphase flow, 2.3.14
Superheated liquid, in metastable state, 2.7.1-1
Superheated gases, thermodynamic properties of, 5.5.2-1/5.5.2-11
Superheated vapor, condensation of, on vertical surface, 2.6.2-3
Supersaturation, as cause of fogging in condensers:
conditions producing, 2.6.7-2/2.6.7-3
description of, 2.6.7-l
Supports, for heat exchangers (see Saddle supports, Bracket supports)
Suppression of nucleate boiling, 2.7.3-10/2.7.3-11
Surface condensers, 3.4.3-5
Surface finish:
effect in pool boiling:
critical heat flux, 2.7.2-13
nucleate boiling, 2.7.2-3/2.7.2-8
(See also Roughness, surface)
Surface, hydraulically smooth, 2.2.2-l
Surface models, in radiative heat transfer, 2.9.4-7/2.9.4-9
diffraction models, 2.9.4-7/2.9.4-8
geometric optics models, 2.9.4-8
scattering bed models, 2.9.4-812.9.4-g
Surface roughness (see Roughness, surface)
Surface tension:
devices depending on, for heat transfer augmentation, 2.5.11-2
methods of estimating, 5.1.5-1/5.1.5-2
in mixtures of fluids, 5.2.4-1/5.2.4-3
tables of, for saturated fluids, 5.5.1-1/5.5.1-40
Sutherland formula, for viscosity variation with temperature, 2.2.1-9
Sutterby fluid (non-Newtonian), free convective heat transfer to, 2.5.7-11
Swirling flow, in augmentation of heat transfer, 2.5.11-2

T

Taborek, J., 1.5.2-1/1.5.3-12, 3.3.1-1/3.3.11-5
Taitel and Dukler flow regime map, for horizontal and inclined gas-liquid flows, 2.3.2-3/2.3.2-4
Tapes, twisted (see Twisted tapes)
Teflon, use in heat transfer enhancement:
in boiling, 2.7.9-l
in condensation, 2.6.6-l
TEMA (Tubular Exchanger Manufacturers Association):
example of calculation of mechanical design of TEMA type AJS, 4.3.6-1/4.3.6-23
mechanical design standards, 4.3.1-2/4.3.1-3
index to, 4.3.2-114.3.2-l 1
recommended baffle characteristics in segmentally baffled exchangers, 3.3.5-8
specification sheet for exchanger, 3.3.4-2
standards, 3.3.1-1
type designation system, 4.2.2-1/4.2.2-3
Temperature-dependent physical properties (see Physical properties, variation with temperature)

© 1983 Hemisphere Publishing Corporation

Temperature distribution:
in condensation, 2.6.1-2
in fixed beds: in stagnant conditions, 2.8.1-1/2.8.1-2, 2.8.1-10/2.8.1-14
with flow-through bed, 2.8.2-1/2.8.2-2, 2.8.2-7
series solutions for, in transient conduction, 2.4.3-1/2.4.3-7
Ternary mixtures, diffusion and mass transfer in, 2.154
Testing and inspection of heat exchangers:
certification, 4.7.7-l
cleanliness and storage, 4.7.9-l
constructions, 4.7.5-l
fittings, 4.7.8-l
materials, 4.7.2-l
nondestructive testing, 4.7.6-1/4.7.6-2
objectives of, 4.7.1-1/4.7.1-2
preparation and dispatch, 4.7.10-l
stages of inspection, 4.7.4-l
welding, 4.7.3-l
Thermal conduction (see Conduction, heat)
Thermal conductivity:
effective, in fixed beds: with flow, 2.8.2-212.8.2-s
with no flow (stagnant), 2.8.1-1/2.8.1-14
effective, of wicks in heat pipes, 3.10.3-l
of liquid water, 5.5.3-3
of multicomponent mixtures, 5.2.3-7/5.2.3-8
of polymers, 2.5.12-2
of pure fluids, 5.1.4-5/5.1.4-7
gases, 5.1.4-5/5.1.4-6
liquids, 5.1.4-7
of rheologically complex materials, 5.3.1-1/5.3.2-3
of saturated vapors and liquids, 5.5.1-1/5.5.1-40
of solids, 5.4.3-1/5.4.3-3
electrical conductors, 5.4.3-2/5.4.3-3
electrical insulators, 5.4.3-1/5.4.3-2
semiconductors, 5.4.3-3
tables of, 5.5.6-1/5.5.6-4
of typical tube materials in heat exchangers, 3.3.5-5
Thermal contact resistance, 2.4.6-1/2.4.6-4
Thermal design, constructional features affecting, in shell-and-tube heat exchangers, 3.1.1-1/3.1.4-9, 4.2.5-1/4.2.5-23
Thermal diffusivity of liquid water, 5 .5.3-5
Thermal expansion, effect of, in shell-and-tube heat exchangers, 3.3.44
Thermal expansion coefficient:
in gases, 5 .1.2-3
of liquid water, 5.5.3-3
in liquids, 5.1.2-2
in saturated liquids, tables of, 5.5.1-1/5.5.1-40
Thermal leakage in F-type shell-and-tube heat exchangers, 1.5.2-14/1.5.2-15
Thermal mixing in plate heat exchangers, 3.7.11-1/3.7.11-2
Thermal network analysis of radiation acting with conduction and convection, 2.9.8-1/2.9.8-3
Thermal stress:
in heat exchanger shells, 4.1.3-2
numerical methods in the production of, 1.4.24
in tube plates, 4.1.4-4
Thermodynamic properties:
of saturated fluids, 5.5.1-1/5.5.1-40
of superheated gases, 5.5.2-1/5.5.2-4
Thermodynamic surface in radiative heat transfer, 2.9.1-1/2.9.1-2
Thermoexel surface, for enhancement of boiling, 2.7.9-1/2.7.9-2
Thermosiphon, as form of heat pipe, 3.10.1-l
Thermosiphon reboilers (see Vertical thermosiphon reboilers, Horizontal thermosiphon reboilers)
θ-NTU method:
application to single pass counter and cocurrent flow exchangers, 1.3.1-2/1.3.1-4, 1.5.2-1/1.5.2-2
charts and equations for heat exchanger design, 1.5.2-2/1.5.3-12
for counter flow, 1.5.2-2
cross flow (both streams mixed), 1.5.3-3
four tube rows, four passes, unmixed, 1.5.3-l 1
four tube rows, two passes, mixed, 1.5.3-12
one tube row, unmixed, 1.5.3-4
three tube rows, one pass, unmixed, 1.5.3-6
three tube rows, three passes, unmixed, 1.5.3-10
two tube rows, one pass, unmixed, 1.5.3-5
two tube rows, two tube passes, unmixed, 1.5.3-9
E-shell with even number of passes, 1.5.2-S
five E-shells in series, 1.5.2-g
four E-shells in series, 1.5.2-8
G-shell, even number of tube passes, 1.5.2-13
J-shell, even number of tube passes, 15.2-12
J-shell, one tube pass, 15.2-l 1
single pass cocunent, 1.5.2-3
six E-shells in series, 1.5.2-10
three E-shells in series, 1.5.2-7
two E-shells in series, 1.5.2-6
for calculation of heat exchangers, 1.2.4-5, 1.5.2-1/1.5.3-12
Thickness of boundary layers (displacement, momentum, energy, density, temperature), 2.2.1-20
Three-phase flows:
classification, 2.3.1-2
gas-liquid-liquid, 2.3.1-2
gasliquid-solid, 2.3.1-2
solid-liquid-liquid, 2.3.1-2
Thwaites method for solution of boundary layer equations, 2.2.1-21
Tie rods in shell-and-tube heat exchangers, 4.2.5-814.2.5-g
Tinker method for shell-side heat transfer in shell-and-tube heat exchangers, 3.3.2-3/3.3.2-6
Titanium as material of construction, 4.5.2-5
T-junctions, loss coefficients in, 2.2.2-20
Toluene saturation properties, 5.5.1-12
Tong F-factor method, for critical heat flux with nonuniform heating, 2.7.3-19/2.7.3-20
Toroidal shells, mechanical design, 4.1.3-2
Total emissivity in gases, 2.9.5-5
Transcendental equations in transient conduction, 2.4.34
Transient behavior:
in free convective heat transfer on vertical plates, 2.5.7-9/2.5.7-10
of heat exchangers, 1.1.6-1
in radiation-coupled heating or cooling, 2.9.8-3/2.9.8-4
Transition boiling:
in binary and forced convective boiling, 2.7.7-5
in forced convection over vertical surfaces, 2.7.3-30
in pool boiling, 2.7.2-13
Transition flow, heat transfer in free convective flow over vertical surfaces in, 2.5.7-4/2.5.7-5
Transmission of thermal radiation in solids:
characteristics, 2.9.2-3/2.9.2-6
measurement, 2.9.2-6/2.9.2-7
Transmissivity of solids:
definition, 2.9.2-3
measurement, 2.9.2-6/2.9.2-7
Transport phenomena, approximate model for in dilute gases, 2.1.1-1

© 1983 Hemisphere Publishing Corporation

Transport properties:
of pure fluids, 5.1.4-1/5.1.4-7
turbulent, 2.1.1-3
Transverse flow, combined free and forced convection in, 2.5.9-4/2.5.9-6
Treated surfaces, for augmentation of heat transfer, 25 .11-1
Triangular duct:
laminar flow in, 2.2.2-9
laminar heat transfer in, 3.9.5-1/3.9.5-3
Triangular fins, in plate tin exchangers, 3.9.3-l
Triangular relationship, in annular gas-liquid flow, 2.3.2-20
Triple interface (gas/solid/liquid), 2.3.1-2
Trouton s rule, for heat of vaporization, 5.1.3-3
Truelove, J. S., 3.11.1-1/3.11.7-6
True temperature difference, in double pipe exchangers, 3.2.34
Tube-baffle damage, in heat exchangers, 4.5.3-3
Tube banks, finned:
application in kettle reboilers, 3.6.2-6
mechanical design, in air cooled heat exchangers, 4.4.1-2/4.4.1-5
single-phase flow and pressure drop in, 2.2.4-13/2.2.4-15
correlation for pressure drop for staggered banks with annular (ring shaped) fins, 2.2.4-13/2.2.4-14
correlation for staggered banks with helical fins, 2.2.4-14
single-phase heat transfer in, 2.5.3-6/2.5.3-16
comparison of experimental data and correlations for, 2.5.3-13/2.5.3-15
fin efficiency in, 2.5.3-612.5.3-l 1
heat transfer correlations for, with high-finned tubes, 2.5.3-11/2.5.3-12
heat transfer correlations for, with low-finned tubes, 2.5.3-12/2.5.3-13
types used in air-cooled heat exchangers, 3.8.4-1/3.8.4-2
Tube banks, plain:
boiling on outside of tubes within, 2.7.5-4/2.7.5-7
critical heat flux in, 2.7.5-5/2.7.5-7
heat transfer coefficients in, 2.7.5-4/2.7.5-5
condensation in horizontal, 2.6.2-10/2.6.2-12
condensation in vertical, 2.6.2-2/2.6.2-10
flow induced vibration in, 4.6.1-1/4.6.6-3
single-phase flow and pressure drop in, 2.2.4-1/2.2.4-12, 3.3.7-1/3.3.7-4
description of, 2.2.4-1/2.2.4-3
drag and pressure drop in, 2.2.4-3/2.2.4-12, 3.3.7-1/3.3.7-4
Strouhal numbers in, 2.2.4-15/2.2.4-16
single-phase heat transfer to, 2.5.3-1/2.5.3-8
with liquid metals, 25.13-2
single row of tubes, 2.5.3-1/2.5.3-2, 2.5.3-3
tube banks, 2.5.3-2/2.5.3-8, 3.3.7-1/3.3.7-4
Tube banks, roughened tubes, effect of roughness on Euler number in, 2.2.4-14/2.2.4-15
Tube bundles:
characteristics of in shell-and-tube heat exchangers, 3.3.4-3/3.3.4-4
(See *also* Rod bundles, Tube banks)
Tube counts, in shell-and-tube heat exchangers:
constructional features affecting, 4.2.5-9/4.2.5-12
simplified equations for, 3.3.5-11/3.3.5-12
tables of, 4.2.5-13/4.2.5-23
Tube end attachment, in shell-and-tube heat exchangers:
arc welding: on inner face, 4.2.6-10
on outer face, 4.2.6-8
explosive expansion, 4.2.6-7/4.2.6-8
explosive welding, 4.2.6-8/4.2.6-10
roller expansion, 4.2.6-6/4.2.6-7
Tubein-plate extended surface configurations, fin efficiency of, 2.5.3-10
Tube plates, in shell-and-tube heat exchangers:
analytic basis for codes for, 4.3.3-2
basic mechanical principles of design of, 4.1.4-1/4.1.4-4
equivalent plates, 4.1.4-1
perforated, stresses in, 4.1.4-3/4.1.4-4
plates connected by tubes, 4.1.4-2
stresses and edge rotation of unperforated, 4.1.4-1/4.1.4-2
thermal stresses, 4.1.44
comparison of codes for, 4.3.4-2
constructional features of, 4.2.6-5/4.2.6-6, 4.5.3-3
double, constructional features of, 4.2.3-1014.2.3-l 1
index to U.S., U.K., and F.R.G. codes for, 4.3.2-714.3.2-g
materials of construction for, 4.5.2-1
Tubes:
characteristics of, in shell-and-tube heat exchangers, 4.2.5-1/4.2.5-3
bimetal, 4.2.5-2
diameter and thickness, 4.2.5-l
integrally finned, 4.2.5-3
length, 4.2.5-1/4.2.5-2
pitch, 4.2.5-2
circular (see Pipes, circular)
codes for mechanical design of:
analytical basis of, 4.3.3-l
index to U.S., U.K., and F.R.G. codes, 4.3.2-3
flow-induced vibration of, 4.6.2-1/4.6.6-3
natural frequency of, 4.6.2-1/4.6.2-4
materials of construction for, 4.5.2-l
mechanical design characteristics of, 4.15-1
noncircular (see Pipes, noncircular)
recommended dimensions of, in shell-and-tube heat exchangers, 3.3.5413.3.5-s
thermal conductivity of typical materials for, 3.3.5-5
Tubesheets, in shell-and-tube heat exchangers (see Tube plates)
Tube-side passes (see Passes, tubsside)
Tubular Exchanger Manufacturers Association (see TEMA)
Tubular immersion exchangers, 4.4.4-2/4.4.4-3
Tubular reactor, nonuniform heat and mass transfer in, 2.1.4-3/2.1.4-4
Tunnel dryer, 3.13.2-4
Turbine agitators:
axial flow, 3.14.2-2
disk, 3.14.2-1/3.14.2-2
flat blade, 3.14.2-1/3.14.2-2
glass coated, 3.14.2-1
heat transfer in vessels agitated by, 3.14.3-1
pitched blade, 3.14.2-1
Turbine exhaust condensers, air cooled, 3.8.9-2
Turbulence:
characteristics in circular pipe flow, 2.2.2-1/2.2.2-5
effect in film condensation, 2.6.2-4/2.6.2-5
integral scale of, 2.2.1
limitation of phenomenological transport laws by, 2.1.1-3/2.1.1-4
modeling of, 2.2.1-14/2.2.1-16
in furnace prediction, 3.11.7-2/3.11.7-3
origin of, 2.2.1-16
relaminarization of, 2.2.1-16
Turbulent boundary layers:
differential methods for, 2.2.1-28/2.2.1-29
large-eddy simulations, 2.2.1-29
one-equation models, 2.2.1-28
stressequation models, 2.2.1-29

© 1983 Hemisphere Publishing Corporation

Turbulent boundary layers: differential methods for (Cont.):
two-equation models, 2.2.1-28
zero-equation models, 2.2.1-28
integral methods for, 2.2.1-26/2.2.1-27
Turbulent buffeting, as source of tube vibration, 4.6.4-2
Turbulent energy, integral equation for, 2.2.1-20
dissipation of, 2.2.1-20
production of, 2.2.1-20
Turbulent flow:
in boundary layers, 2.2.1-18
in circular pipes, 2.2.2-1/2.2.2-5
combined free and forced convective heat transfer in channels in, 2.5.10-6/2.5.10-11
combined radiative and convective heat transfer to, 2.9.8-7/2.9.8-10
in condensation, on vertical surfaces, 2.6.2-4/2.6.2-5
conservation equations for, 2.2.1-13/2.2.1-14
averaging in, 2.2.1-13
in empty spaces, numerical calculation of, 1.4.3-2
fundamentals of, 2.2.1-13/2.2.1-16
heat transfer in free convective flow over vertical surfaces in, 2.5.74
modeling of, 2.2.1-14/2.2.1-16
of non-Newtonian fluids, 2.2.8-11/2.2.8-12
in noncircular pipes, 2.2.2-9/2.2.2-10
in plate heat exchangers, 3.7.10-2/3.7.10-3
relaminarization in, 2.2.1-16
single-phase heat transfer in ducts in, 2.5.1-5/2.5.1-13
augmentation of, 2.5.11-4/2.5.11-9
concentricammli, 2.5.1-10/2.5.1-11
in liquid metal systems, 2.5.13-1/2.5.13-2
smooth tubes, 2.5.1-5/2.5.1-9
Turbulent transport properties, 2.1.1-3
Turnarounds, in heat exchangers, 2.2.7-l
pressure losses in, 2.2.7-8/2.2.7-9
Twisted tapes:
enhancement of boiling heat transfer by, 2.7.9-3/2.7.9-4
enhancement of condensation by, 2.6.6-3
as inserts for augmentation of heat transfer, 2.5.11-7/2.5.11-8
Two-equation models, for turbulent boundary layers, 2.2.1-28
Two-phase flows:
classification of, 2.3.1-2
liquid-liquid flows, 2.3.1-2
numerical calculation of, 1.4.3-1
(See also Gas-liquid flow, Solid-gas flow, Solid-liquid flow)
Two-shell pas exchanger (see F-shells)

U

$\bar{U}$-$\bar{\alpha}$ method, 2.1.2-5
$\bar{U}$ method, 2.1.2-7/2.1.2-9
Ulinskas, R., 2.2.4-1/2.2.4-17
Unequal baffle spacing, correction factor for, 3.3.6-l 1
UNIFAC method, for estimation of thermodynamic properties of mixtures, 5.2.2-6/5.2.2-9
tables of constants for use with, 5 .5.4-6/5.5.4-7
Uniform heat flux:
combined free and forced convection in channels with:
horizontal channels, 2.5.10-7/2.5.10-11
vertical channels, 2.5.10-4/2.5.10-7
critical heat flux in vertical tubes with, 2.7.3-12/2.7.3-18
solutions and correlations for free convective heat transfer within: horizontal and inclined plates, 2.5.7-18
vertical plates, 2.5.7-6/2.5.7-9
Uniform wall temperature, combined forced and free convection in channels with:
horizontal channels, 2.5.10-7
vertical channels, 2.5.10-3/2.5.10-4
Uniheads, as form of double-pipe heat exchanger, 3.2.4-l
United Kingdom, mechanical design of heat exchangers in:
guide to national practice, 4.3.5-3
index to BS1500 code, 4.3.2-1/4.3.2-11
United States of America (see U.S.)
Universal laws, for turbulent boundary layers, 2.2.1-25/2.2.1-26
law of the wake of D. Coles, 2.2.1-26
law of the wall, 2.2.1-25
table of, 2.2.1-27
universal velocity profile, 2.2.1-26
velocity defect law of von Karman, 2.2.1-26
Universal velocity profile, 2.2.1-26
Universal velocity defect law, 2.2.2-2
Unsteady flows:
in ducts, 2.2.2-14
over cylinders, 2.2.3-6
Upward facing surfaces, free convective heat transfer from, 2.5.7-15/2.5.7-18
U.S., mechanical design of heat exchangers in:
guide to national practice, 4.3.5-2
index to ASME VIII code and TEMA standards, 4.3.2-1/4.3.2-11
Usher, J. Dennis, 3.7.1-1/3.7.12-2, 4.4.2-1/4.4.2-8, 4.8.4-1/4.8.4-2
U.S.S.R. Academy of Sciences, tables of critical heat flux data for water, 2.7.3-17/2.7.3-18
U-tube bundles, for shell-and-tube heat exchangers, 3.3.5-12/3.3.5-13, 4.2.3-4
vibration of, natural frequencies in, 4.6.2-3

V

Vacuum condensers, air cooled, 3.8.9-2
Vacuum operation, of reboilers, 3.6.4-3
Valves:
loss coefficients in, 2.2.2-20
open, two-phase gasliquid flow pressure losses in, 2.3.2-18
van der Waals equation of state, 5.1.2-3/5.1.2-4
Vaned bends, single-phase flow and pressure drop in, 2.2.2-16/2.2.2-17
Vapor belt, in condensers, 3.4.3-5
Vapor blanketing, as mechanism of critical heat flux, 2.7.3-22
in kettle reboilers, 3.6.2-5
as source of accelerated corrosion, 4.5.34
Vapor injection, effect of on boiling heat transfer in tube bundles bundles, 2.7.5-5
Vaporization, choice of evaporator type for, 3.5.5-l
in plate-fin heat exchangers, 3.9.13-1/3.9.13-2
Vaporization, heat of (see Heat of vaporization)
Vaporizer, double bundle, constructional features, 4.2.3-9
Vapor-liquid disengagement, in kettle reboilers, 3.6.2-6
Vapor-liquid separation, for evaporators, 3.5.4-1/3.5.4-2
3.5.4-1/3.5.4-2
Vapor pressure, variation with temperature, 5.1.3-1/5.1.3-2
Vapor recompression, in evaporation, 3.5.3-2

© 1983 Hemisphere Publishing Corporation

Velocity defect law:
for turbulent boundary layers, 2.2.1-26
universal, 2.2.2-2
Velocity distribution:
in circular pipe flow, 2.2.2-3
distorted inlet, effect on single phase flow and pressure drop, 2.2.2-l 1
Velocity fluctuations, in turbulent pipe flow, 2.2.2-4/2.2.2-5
Velocity ratio (slip ratio):
in gas-liquid flow, 2.3.2-13
In solid-gas flow, 2.3.3-4
Venting of condensers, 3.4.5-2
Vertical cones (see Cones, vertical)
Vertical cylinders (see Cylinders, Vertical pipes, Pipes, circular)
Vertical cylindrical fired heater, 3.11.2-1
Vertical pipes:
annular flow in, 2.3.2-19/2.3.2-21
boiling in, 2.7.3-1/2.7.3-37
critical heat flux, 2.7.3-12/2.7.3-30
heat transfer in region where critical heat flux has been exceeded, 2.7.3-30/2.7.3-34
regimes of flow and heat transfer in, 2.7.3-1/2.7.3-5
saturated boiling, 2.7.3-10/2.7.3-12
subcooled boiling, 2.7.3-5/2.7.3-10
bubble flow in, 2.3.2-18/2.3.2-19
combined free and forced convective heat transfer in:
laminar flow (assisting convection), 2.5 .10-2/2.5.10-6
laminar flow (opposing convection), 2.5.10-6
regimes in, 2.5.10-2
turbulent convection, 2.5.10-6
condensation in, 2.6.2-2/2.6.2-9
effect of interfacial shear, 2.6.2-5/2.6.2-7
effect of waves and turbulence, 2.6.2-4/2.6.2-5
laminar flow, 2.6.2-2/2.6.2-4
reflux condensation, 2.6.2-7/2.6.2-9
condensers with condensation inside, 3.4.3-1/3.4.3-3
downflow, 3.4.3-1/3.4.3-2, 3.4.9-2/3.4.9-3
upflow, 3.4.3-2/3.4.3-3, 3.4.9-3
condensers with condensation outside, 3.4.3-6, 3.4.94
flooding in: in gas liquid vertical flow, 2.3.2-21/2.3.2-23
in reflux condensation, 2.6.2-7/2.6.2-9
flow regimes in gas-liquid flow in, 2.3.2-1/2.3.2-2
free convective heat transfer from outside of, 2.5.7-23/2.5.7-24
hydraulic conveyance in, 2.3.4-1/2.3.4-3
plug (or slug) flow In, 2.3.2-19
pneumatic conveyance in, 2.3.3-l
(See *also* Pipes, circular; Pipes, noncircular)
Vertical plates (see Vertical surfaces)
Vertical surfaces:
combined free and forced convective heat transfer to, 2.5.9-1/2.5.9-4
wmbined heat and mass transfer on, 2.5.7-12
film boiling in forced convection on, 2.7.3-30/2.7.3-31
filmwise condensation on, 2.6.2-2/2.6.2-9
free convective heat transfer from, 2.5.7-2/2.5.7-13
combined equation for uniform wall temperature case, 2.5.7-5/2.5.7-6
dimensionless groupings for, 2.5.7-2/2.5.7-3
laminar flow with uniform wall temperature, 2.5.7-3/2.5.7-4
non-Newtonian, 2.5.7-1012.5.7-l 1
solution for uniform heat flux, 2.5.7-6/2.5.7-9
transient behavior of, 2.5.7-9/2.5.7-11
transition flow with uniform wall temperature, 2.5.7-4/2.5.7-5
turbulent flow with uniform wall temperature, 2.5.7-4/2.5.7-5
free convective mass transfer to, 2.5.7-11/2.5.7-12
pool boiling, from 2.7.2-1/2.7.2-15
Vertical thermosiphon reboilers:
calculation procedures for, 3.6.5-3/3.6.5-4
heat transfer characteristics of, 3.6.2-6/3.6.2-10
convective and nucleate boiling, 3.6.2-6/3.6.2-7
film boiling in, 3.6.2-9
heat flux limitations in, 3.6.2-7/3.6.2-9
mist flow, 3.6.2-9
temperature profiles in, 3.6.2-9/3.6.2-10
shell-side characteristics, advantages and disadvantages, 3.6.1-5
tube-side characteristics, advantages and disadvantages, 3.6.1-313.6-l-5
Vertical tubes (see Vertical pipes)
Vibrated beds, heat transfer to, 2.8.3-5/2.8.3-6
Vibration:
in augmentation of heat transfer, 2.5 .11-3, 2.5.11-4, 2.5.11-8, 2.7.9-4
numerical methods for prediction of occurrence of, 1.4.2-4
(See *also* Flow-induced vibration)
Viscometric functions (non-Newtonian flow), methods of determining, 2.2.84
Viscosity:
liquid, effect on critical heat flux in pool boiling, 2.7.2-12
of liquid water, 5 5.34
of multicomponent mixtures, 5.2.3-2/5.2.3-6
non-Newtonian, 2.2.8-2
of pure fluids, 5.1.3-1
gases, 5.1.4-1
liquids, 5.1.4-1/5.1.4-5
relation with density for gases, 2.2.1-9
of saturated liquids and vapors, 5.5.1-1/5.5.1-40
small variations in, 2.2.1-9/2.2.1-10
variation with temperature:
Chapman-Rubescin formula for, 2.2.1-9
Sutherland formula for, 2.2.1-9
Viscosity number (Vi), 2.3.2-19
Viscous dissipation, influence on heat transfer in non-Newtonian flows, 2.5.12-10/2.5.12-14
Viscous sublayer, in duct flow, 2.2.2-l
Voidage, in fixed beds, definition, 2.2.5-l
Void fraction, 2.3.1-3
correlations for in gas-liquid flow, 2.3.2-13/2.3.2-15
CISE correlations for, 2.3.2-14/2.3.2-15
drift flux models for, 2.3.2-13/2.3.2-14
homogeneous, 2.3.2-13
Martinelli correlations for, 2.3.2-14
models for in gas-liquid flow :
horizontal stratified flow, 2.3.2-23/2.3.2-24
vertical bubble flow, 2.3.2-18/2.3.2-19
vertical plug flow, 2.3.2-19
in subwoled boiling, 2.7.3-9/2.7.3-10
Volumetric heat transfer coefficient, 1.1.2-2
Volumetric mass transfer coefficient, 1.1.2-2
von Karman friction factor equation for fully rough surface, 2.2.2-3
von Karman velocity defect law, 2.2.1-26
Vortex shedding:
from single cylinders, 2.2.3-3
as source of tube vibration, 4.6.4-1/4.6.4-2
in tube banks, 2.2.4-15/2.2.4-16

© 1983 Hemisphere Publishing Corporation

Votator, agitator, 3.14.2-1
heat transfer with, 3.14.3-6

W

Wallis correlations:
for flooding, 2.3.2-22
application in reflux condensation, 2.6.2-8
for interfacial friction factor, 2.3.2-21
Wallis criterion, for transition from-stratified to annular flow, applications in condensation, 3.4.6-2
Wall baffles, in agitated vessels, 3.14.2-2
Wall layer transmissivity, 2.9.7-12/2.9.7-13
Wall temperature:
effect in laminar flow along flat plate, 2.2.1-22
effect of distribution of, in laminar flow along flat plate, 2.2.1-23/2.2.1-24
Wake, Coleslaw of the, 2.2.1-26
Waste heat boilers, corrosion and failure in, 4.5.3-4/4.5.3-5
Water:
critical heat flux values for, in tubes (table), 2.7.3-17/2.7.3-18
emissivity of gaseous, 5.5.5-1/5.5.5-2
liquid, properties of, 5.5.3-1/5.5.3-5
pool boiling curve for, at atmospheric pressure, 2.7.2-l
saturated properties: (0°-50°C), 3.12.2-6
(O-647 K), 5.5.1-37
superheated gaseous, thermodynamic properties of, 5.5.2-9/5.5.2-11
Water loss, from cooling towers, 3.12.6-2
Water tube boiler, 3.11.2-3
Wavelengths, of blackbody radiation, 2.9.1-4/2.9.1-5
Waves, interfacial, effect on film condensation on vertical surface, 2.6.2-4/2.6.2-5
Wavy fins, in plate fin exchangers, 3.9.3-l
Webb, R. L., 3.9.1-1/3.9.134,4.4.3-l/4.4.3-9
Weber, M., 2.3.3-1/2.3.4-7
Weber number, 1.2.3-5
Welded channel head, in shell-and-tube heat exchanger, 4.2.4-l
Welded fins, in double pipe exchangers, 3.2.5-l
Welding:
testing and inspection of, 4.7.3-l
of tubes into tube sheets: arc, 4.2.6-8, 4.2.6-10
explosive, 4.2.6-8/4.2.6-10
Welds, corrosion of, 4.5.3-5/4.5.3-6
Wentz and Thodos equation, for fixed-bed pressure drop, 2.2.5-3
Wet-bulb temperature, 3.13.3-2/3.13.3-4
Wettability, of surface, effect on pool boiling, 2.7.2-9
Whalley and Hewitt correlations:
for entrainment, 2.3.2-22
for interfacial roughness, 2.3.2-21
White-Metzner model, for non-Newtonian fluid, 2.2.8-8
Wicking, in enhancement of heat transfer, 2.5.1 l-2
Wicks, for heat pipes:
characteristics of, 3.10.6-1/3.10.6-2
effective thermal conductivity of, 3.10.3-l
Window zone, in shell-and-tube heat exchangers:
calculation of effective areas of, for flow through, 3.3.6-1/3.3.6-2
pressure drop in gas-liquid flow in, 2.3.2-12/2.3.2-13
Winter, H. H., 2.5.12-1/2.5.12-16
Wire inserts, coiled, for enhancement of heat transfer in boiling, 2.7.9-3
Wispy annular flow, regions of occurrence of, 2.3.2-1/2.3.2-2
Working fluid, selection of for heat pipe, 3.10.5-1/3.10.5-2

X

m-Xylene saturation properties, 5.5.1-13
o-Xylene saturation properties, 55.1-13
p-Xylene saturation properties, 5.5.1-14
X-type shells (cross flow shells):
application in condensers, 3.4.9-3
description of, 3.3.4-3

Y

Yawed tube banks, pressure drop in, 2.2.4-12
Youngs modulus, 5.4.5-3
table of values of, 5.5.8-2

Z

Zero equation models, for turbulent boundary layers, 2.2.1-28
Zivi equation, for void fraction, 2.6.2-14
Zone model, for furnaces (see Multizone model)
Zuber-Findlay model, for two-phase flows, 2.3.1-9/2.3.1-10
Zuber theory, for critical heat flux in pool boiling, 2.7.2-10
Žukauskas, A., 2.2.4-1/2.2.4-17, 2.5.3-1/2.5.3-16

© 1983 Hemisphere F blishing Corporation